

**Linear Conjugated Molecular Wires:  
Organic Materials and Single-Molecule Electronics**

Jeffrey S. Meisner

Submitted in partial fulfillment of the requirements  
for the degree of Doctor of Philosophy in the  
Graduate School of Arts and Sciences

COLUMBIA UNIVERSITY

2013

© 2013  
Jeffrey S. Meisner  
All Rights Reserved



## Abstract

### **Linear Conjugated Molecular Wires: Organic Materials and Single-Molecule Electronics**

Jeffrey S. Meisner

In this work, the synthesis and properties of different families of molecule wires are described. These families are made up of collections of linear conjugated oligomers, such as oligoenes and phenylenevinylenes and their derivatives. The bulk properties of each system were examined in order to establish structure-performance relationship between the intrinsic molecular properties of the bridging organic wire and the performance of their single-molecule junctions. The electrical as well as mechanical characteristics of single-molecular junctions were measured using the scanning tunneling-based break junction (STM-BJ) and atomic force microscope-based break junction (AFM-BJ) techniques. In addition, stilbene molecular wires and their derivatives are ideal model compounds for both of these oligomeric families and have helped to isolate and quantify some of the factors that govern charge transport through linear conjugated molecules.

After an introduction of molecular electronics, a highly tunable class of oligoenes, the  $\alpha,\omega$ -diphenyl- $\mu,\nu$ -dicyano-oligoenes (DPDC) is described in the second chapter. They range from three to eleven linear C=C double bonds in length. Their synthesis is reported while their bulk solution properties show novel electronic structures, as well as broad optical absorptions and high extinction coefficients. Theoretical investigation using DFT calculations as well as strategies for functionalizing DPDCs are described. We have found that functionalization of these intractable materials has opened new doors for their

material applications. We envisioned functionalized oligoenes as molecular building blocks (i.e. conducting wires or rigid connectors) in the bottom up construction of new materials and devices.

Their prototypical structure and variable length would make DPDCs ideal candidates for molecular wires especially in the field of single-molecule electronics. Molecular junctions of the form metal-oligoene-metal were formed using the STM-BJ method and their charge transport characteristics were quantified in Chapter 2. In addition, we utilize long DPDC oligomers ( $n > 5$ ) as variable resistance single-molecule potentiometers.

In chapter 3, we synthesize and employ our oligoene model compounds, the stilbenes, to differentiate the mechanical from electrical properties in molecular junctions. This enabled the development of new tools for uncovering the transport mechanisms in other molecules. One example is demonstrated in chapter 4, where stilbenes proved useful as mono-functionalized molecular wires. Together with extended oligoenes, stilbene molecular wires helped us to understand how current flows through a conjugated scaffold having only one electrode binding functional group (chapter 5). We observed a  $\pi$ -Au interaction that is weak, however strong enough to couple electronically to the electrode and complete the molecular circuit.

In the last chapter, we showcase a variety of new chemical structures that were prepared to probe the IV characteristics of organic single-molecule wires. A series of end-functionalized (p-phenylenevinylene) (PPV) oligomers and DPDC molecular wires were prepared. Exotic end-groups were important modifications for PPV's, since they increase oligomer solubility; the single-molecule STM-BJ measurements would not be

possible on these otherwise insoluble compounds. PPV materials are very stable and can be further functionalized along their main-chains, however due to shorter effective conjugations lengths (smaller than that of the oligoenes), the range of electronic tunability is smaller in these materials. In addition to this family of symmetric molecules other asymmetric oligoene molecules were synthesized as candidates for single-molecule rectification. These molecules allow different electronic coupling to the right and left electrodes, which may modulate their IV characteristics.

## Table of Contents

### Chapter 1. Introduction on Molecular Electronics

- 1.1 Introduction
- 1.2 Molecular Electronics
- 1.3 Measuring Single-molecular Properties
- 1.4 Single-molecule Devices
- 1.5 Linker Effects
- 1.6 Challenges and Frontiers
- 1.7 Addressing Future Challenges
- 1.8 References

### Chapter 2. Functionalizing Molecular Wires: A Tunable Class of $\alpha,\omega$ -diphenyl- $\mu,\nu$ -dicyano-oligoenes

- 2.1 Motivations
  - 2.1.1 From Polyacetylene to Oligoenes
  - 2.1.2 Naturally Occurring Oligoenes
  - 2.1.3 Rational Design Toward Cyano-functionalized Oligoenes
- 2.2  $\alpha,\omega$ -diphenyl- $\mu,\nu$ -dicyano-oligoenes
  - 2.2.1 Synthetic Approach
  - 2.2.2 Solid-state Structure
  - 2.2.3 Control Group:  $\alpha,\omega$ -diphenyl-oligoenes
  - 2.2.4 Band Gap Modulation
  - 2.2.5 Electrochemical Studies
  - 2.2.6 Theoretical Band Gap
- 2.3 End-functionalized DPDC Derivatives
  - 2.3.1 Tuning the Electronic Properties of Oligoenes
  - 2.3.2 Solubility Enhancements
  - 2.3.3 Tuning the Solid-state Assembly through End-functionalization
- 2.4 Materials Applications

2.4.1 Self-assembly of Oligoenes on Semiconducting Surfaces

2.5 Conclusions and Future Outlook

2.6 References and Footnotes

**Chapter 3.** Oligoenes in Single-molecule Electronics

3.1 Motivations

3.1.1 Oligoenes Molecular Wires

3.1.2 Scanning Tunneling Microscope Break Junctions (STM-BJs)

3.1.3 End-Functionalized DPDC Molecular Wires

3.2 Charge-transport Properties

3.2.1 Conductance Histograms

3.2.2 Conductance-Displacement Histograms

3.2.3 Control Molecules

3.2.4 Theoretical investigations

3.3 Single-molecule Potentiometer

3.3.1 Variable and Reversible Resistance

3.3.2 Control Experiments

3.4 Conclusion

3.5 References and Footnotes

**Chapter 4.** Stilbene Single-molecule Wires: Dissecting the Electrical and Mechanical Contributions in Molecular Junctions

4.1 Background and Motivations

4.2 Independent Measure of Force and Conductance

4.3 Data Analysis

4.4 Stilbene Molecular Junctions

4.5 Theoretical Analysis

4.6 Conclusions

4.7 References

**Chapter 5.** Direct Metal- $\pi$  Bonding in Single-molecule Junctions

- 5.1 Introduction
- 5.2 Experimental Methods
  - 5.2.1 Molecular Wire Synthesis
  - 5.2.2 STM and AFM-BJ Measurements
  - 5.2.3 Theoretical Methods
- 5.3 Results and Discussion
  - 5.3.1 Single-molecule Conductance: General Substitution Effects
  - 5.3.2 Single-molecule Rupture Force: General Substitution Effects
  - 5.3.3 Length-dependent Molecular Conductance
  - 5.3.4 Molecular Junction Evolution
  - 5.3.5 Deciphering Electronic from Mechanical Contributions Using Amine Derivatives
- 5.4 Theoretical Analysis
- 5.5 Conclusion
- 5.6 References and Footnotes

**Chapter 6.** Promising Molecular Wires for Current-Voltage Measurements of Molecular Junctions

- 6.1 Background and Motivation
- 6.2 PPV Molecular Wire Design
- 6.3 Synthesis of PPV Molecular Wires
- 6.4 Synthesis of Asymmetric Oligoene Wires
- 6.5 STM-Break Junctions
- 6.6 Theoretical Methods
- 6.7 Conclusions and Future Outlook
- 6.8 References and Footnotes

**Appendix A.** Functionalizing Molecular Wires: A Tunable Class of  $\alpha,\omega$ -diphenyl- $\mu,\nu$ -dicyano-oligoenes

**Part 1:**

- A1 List of Compounds

- A2 Synthetic Details
- A3 UV-Vis Absorption Spectroscopy
- A4 Cyclic Voltammetry
- A5 Particle in a Box: A simple Model for Electron Confinement
- A6 Nanoparticle Synthetic Details and SAM Preparation
- A7 Theoretical Methods and Details
- A8 Comparison of **DPDCn** Band Gaps from Various Methods
- A9 References

**Part 2:** DFT Summary for Oligoene Molecular Wires

**Part 3:** NMR Spectra

## **Appendix B.** Oligoenes in Single-molecule Electronics

- B1 General Information
- B2 Modified STM Break Junction Studies
- B3 Variable Resistance Measurements and Controls
- B4 Theoretical Methods and Details
- B5 References

## **Appendix C.** Stilbene Single-molecule Wires: Dissecting the Electrical and Mechanical Contributions in Molecular Junctions

- C1 Synthetic Details
- C2 NMR Spectra
- C3 Optical Absorption Spectroscopy
- C4 AFM-based Single-molecule Break Junction Studies
- C5 Theoretical Methods and Details
- C6 References

## **Appendix D.** Direct Metal-p Bonding in Single-molecule Junctions

- D1 General Information
- D2 Synthetic Experimentals
- D3 Optical Absorption Spectroscopy

D4 Single-Molecule Conductance and Force Measurement and Analysis

D5 Theoretical Methods and Details

D6 References

**Appendix E.** Promising Molecular Wires for Current-Voltage Measurements of  
Molecular Junctions

E1 Synthetic Experimentals

E2 NMR Spectra

E3 Optical Absorption Spectroscopy

E4 STM and AFM-BJ Measurement and Analysis

E5 Theoretical Methods and Details

E6 References



## Acknowledgements

Prof. Colin Nuckolls has been instrumental to my academic and experimental career. His informal advising style has given me the opportunity to find my own interests in organic materials, empowering me to launch into new research directions, especially when they involve collaborations with scientists outside my field.

Of these, I especially thank Prof. Latha Venkataraman for her patience in teaching a synthetic chemist a little bit about applied physics. There have been many students in her group that I've had the pleasure of working with and learning from, such as Masha Kamenetska, Eek Huisman, Sriharsha Aradhya, Arunabh Batra, Jonathan Widawsky, and Radha Parameswaran. These scientists are responsible for the measurements and data analysis of much of the STM and AFM-BJ experiments in this dissertation.

Other collaborators have been essential to my projects in the last five years; Darcy Peterka, Prof. William Wilson, and Prof. Rafa Yuste for their interest in tailoring oligoene SHG properties as voltage sensors. Also, Prof. Christopher Murray and Jun Chan for collaborations in oligoene self-assembly and ligand exchange on metal oxide surfaces, as well as Luis Campos for his genuine insights in polymeric materials.

The members of the Nuckolls group have been an ongoing source of ideas and input, of the many I especially acknowledge Danielle Sedbrook, Matthew Carnes, Noah Tremblay, Kyle Plunkett, Tracy Chen, Seokhoon Ahn, Bryce Boardman and two undergraduate researchers, Markrete Krikorian and Carmen del Valle. Michael Steigerwald has been a unique influence. Often I've thought of him as my second advisor, who has the enchanting ability to turn devastating result into the fitting answer for a different, nonetheless exciting, question. His "lemons-to-lemonade" trick is evidence of his vast understanding and childlike amazement of the world around us.

Lastly, I recognize the many individuals outside of the world of science that have all made lasting impressions throughout my time at Columbia. They are my parents, Teresa and Dwight Meisner, my grandparents, Donna and Robert Colclessner, my sisters, Laurie and Merry, and my friends Andress Barnes, Joseph Parks, Bryan Handyside, Nili Ostrov, Jamison Heldrich, Andy Miller, Uma, Bella, Cassandra Simon, Alain Rostain, Carolyn Morrison, Jennifer Glenn, Janet Linnell, Petra Ornstein, Courtney Hopen, Grady Turner, NY Tribe, Brandon Robinson, Shea, Hacienda Group, Evan Kushin and Andrew Cray.

*This work is dedicated to Donna and Robert Colclessor, my grandparents.*

## Preface

Before beginning, it is important that the reader is informed that much of the work in this dissertation was collaborative and many of the concepts, experiments and analysis carried out by others. The most influential collaboration has been that with the Venkataraman group here in Columbia's Applied Engineering and Mathematics Department. Many graduate and undergraduate students, post-docs and Prof. Venkataraman herself have guided my understanding of single-molecule electronics and preformed the STM and AFM-BJ experiments for Chapters 3 through 5. Following is a chapter-by-chapter account describing how each individual contributed to the work in this dissertation.

In chapter 2, Danielle F. Sedbrook, and I synthesized all oligoene compounds, with assistance from Markrete Krikorian, while collaborators at University of Pennsylvania synthesized and characterized the nanoparticles. Danielle Sedbrook prepared monolayer devices and preformed SEM studies. Michael Steigerwald ran and analyzed the DFT calculations. Aaron Sattler in the Parkin Group, carried out single-crystal X-ray diffraction characterization on the oligoene molecules.

The molecules in chapter 3 were synthesized by myself with the assistance of Markrete Krikorian and the single-molecule STM-BJ measurements were preformed by Maria Kamenetska. DFT calculations were preformed by Michael Steigerwald.

In chapter 4, the synthesis was carried out by Markrete Krikorian and myself, while the STM-BJ measurements were preformed by Seokhoon Ahn, Radha Parameswaran and Sriharsha Aradhya. AFM-BJ studies were preformed by Sriharsha Aradhya. DFT calculations were run and analyzed by Michael Steigerwald.

STM-BJ measurements in chapter 5 were also preformed by Seokhoon Ahn with the assistance of Radha Parameswaran and Sriharsha Aradhya. AFM-BJ studies and analysis were done by Sriharsha Aradhya. Both Sri and Seokhoon are responsible for the

statistical analysis of variation. Molecules were synthesized by Markrete Krikorian and myself. Michael Steigerwald and myself ran the DFT calculations.

Finally in chapter 6, all molecules were synthesized by myself, while physical investigations were performed by Eek Huisman, Jonathan Widawsky and Arun Batra. Collaborators from University of California Berkeley in Prof. Jeff Neaton's group, Pierre Darancet are responsible for modeling and calculations. Other DFT calculations were run by Michael Steigerwald and myself.

# Chapter 1. Introduction on Molecular Electronics

## 1.1. Introduction

This dissertation is centered on the construction and design of organic molecules that when placed in metal-molecule-metal junctions provide insight into the molecular effects that govern junction behavior. In other words, the focus is on the “molecule” portion of these single-molecule junctions. Here, the charge transport through molecular junctions is understood, and ultimately controlled, by making rational modifications to the chemical structure of the bridging molecule. Changes in their atomically defined structures lead to differences in junction performance and character. Identifying such effects enable us to outline structure-performance relationships that guide the design and fabrication of functional devices with tailored or enhanced properties. In this chapter, we will inspect a few reports in the literature to contextualize what types of molecules have been studied since the introduction of modern single-molecular measurement techniques, of which the most relevant is the break junction method.

There are many factors that govern the charge transport properties through a molecular junction. Some of these factors are: the length of the conductance path; Fermi energy ( $E_F$ ) of the electrode materials; as well as the alignment of the  $E_F$  with the molecular orbitals of the bridging molecule,<sup>8</sup> and the strength of the metal-molecule contact. To no surprise, the way in which molecules contact the electrode surface is critical. Not only does this contact determine electronic coupling between the molecule and electrodes but also plays major roles in the mechanical dynamics of the junction. In

the following chapters, several systems of molecules are showcased that enable the decoupling of these two factors including the novel systems having multiple conductance pathways, variable resistivity, quantum interference pathways and asymmetric chemical structures. These results, combined with those already present in the literature, paint a clear picture showing that inside a metal-molecule-metal junction, the molecule is not simply “just a molecule,” but may instead be a critical component be used to control the transport properties of the junction.

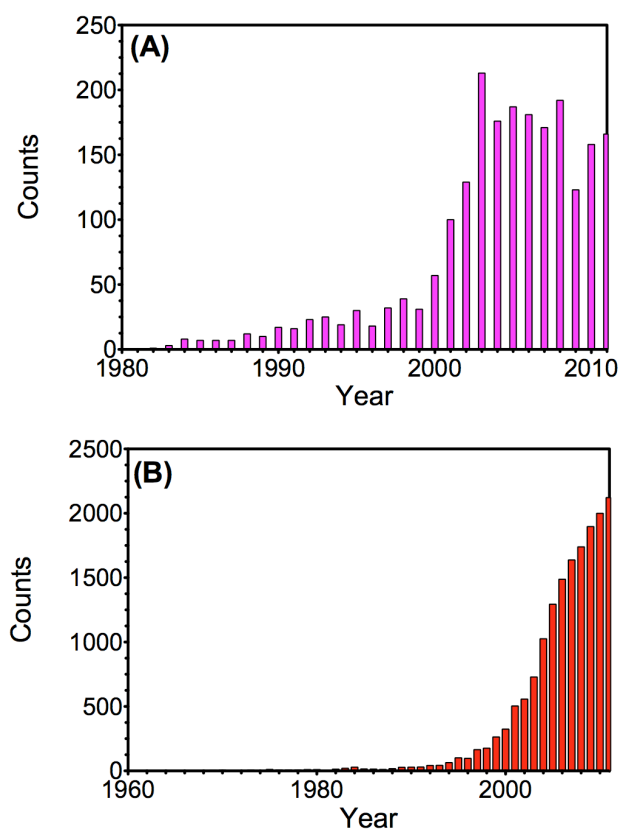


**Figure 1.1:** The increase in the number of publications containing the phrase (A) “molecular electronics” and (B) “single-molecule.”

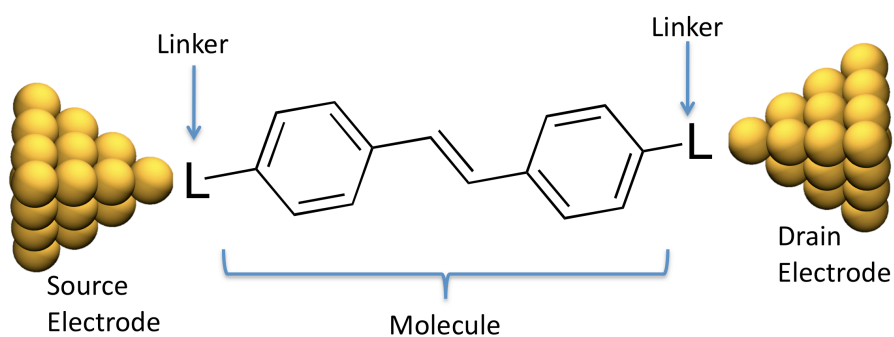
## 1.2. Molecular Electronics

Molecular electronics is a highly interdisciplinary field drawing from many natural and applied disciplines, such as engineering, physics, materials science and chemistry. Together they pursue a common interest to develop and utilize molecular-sized components in the fabrication of electrical devices. The essential goal is to control charge transport across atomically precise systems. This is an appealing goal not only because of the small size of such devices, but also because the great diversity of chemical structure that is available through synthetic chemistry can be used to tailor junction properties for specific applications. In fact, the term “molecular electronics” itself is poorly defined. Some authors include “molecular-based” materials referring to thin-film and liquid crystalline-based devices. Others define it more specifically to mean strictly single-molecule-based or single-molecule-thick applications, such is the type found in molecular wires or arrays of self-assembling monolayers. Here, the latter is accepted, since this work discusses the electronic properties of single metal-molecule-metal junctions (Figure 1.2).

Until a few decades ago tools to study systems at the single-molecule level were unavailable and thus fabrication of molecular-sized and single-molecule devices were unrealistic. Since then the amount of scientific research in this area has burgeoned. For historical context Figure 2 illustrates the number of peer-reviewed articles and patents published on this topic.<sup>1</sup> In order to progress the field, knowledge of how to make, handle and study molecular-scaled devices is required.

## 1.3. Measuring Single-molecular Properties

Special techniques are needed in order to measure the transport characteristics of a single molecule, of which a handful of strategies have been developed. Most take advantage of the ability for molecules to self-assemble on metal surfaces or into molecular-sized gaps. For example, self-assembled monolayers (SAMs)<sup>2</sup> on conductive surfaces, such as silver or gold, orient molecular wires away from the substrate. Since these molecules are bound to the conductive substrate they are already attached to the bottom contact of a device. To make a second contact, another electrode is either deposited or brought into contact with the top of the monolayer.<sup>3</sup> One popular method utilizes a gold conducting probe atomic force microscope (CP-AFM) tip and gold substrate as the source and drain electrodes.<sup>4</sup> Even though this method does not usually measure the charge transport through a single molecules it is worth mentioning since many accomplishments in molecular electronics have been made employing the SAM-based method.





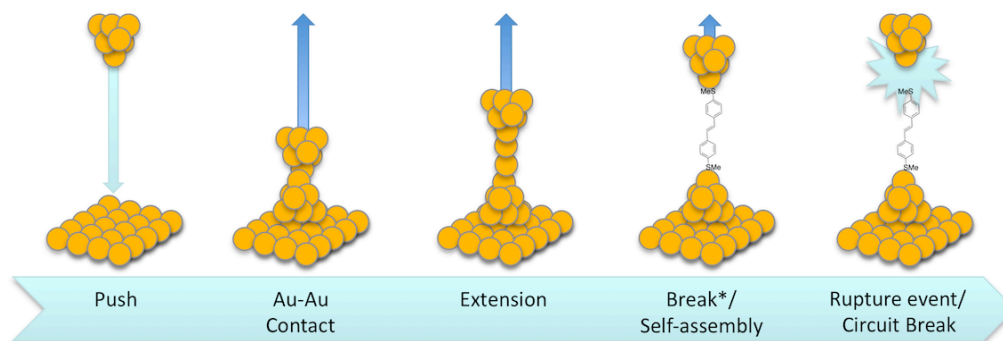


**Figure 1.2:** (top) A single-molecule junction. (bottom) Procedure for forming junctions using the STM-BJ method.

Another method that is more relevant to this dissertation relies on the mechanical stretching of nanometer-sized gold wires, and is called the mechanical break junction (BJ) technique. When stretched, the gold wire extends in length while thinning down to an atomically thick string of atoms before breaking. When performed in solutions of molecular wires, the bridging molecules self-assemble between the insipient nanoscale gap. Here, each end of the gap functions as the source and drain electrodes. Variations upon this principal have been made that utilize substrate bending<sup>5</sup> and electromigration.<sup>6</sup> A breakthrough was pioneered by Tao and coworkers that utilized a scanning tunneling microscope (STM) with a gold tip and gold substrate.<sup>7</sup> This method, the STM-BJ method, has grown in popularity since thousands of reliable measurements to be carried out in a matter of hours. The tip may be repeatedly smashed into the gold surface and drawn away each time making fresh electrodes, from which a new molecule junction may be formed and measured. This process is depicted in the bottom of Figure 1.2. Due to the quantity of measurements, statistical interpretations on the conductance of molecular junctions are therefore possible. To compare different molecular systems we primarily use this method

in the following chapters to quantify the charge transport through oligoene and oligo-phenylenevinylene molecules.

#### 1.4. Single-molecule Devices

The simplest single-molecule device can be seen in Figure 1.2. Comprised of a molecule bound between two electrodes, it represents a metal-molecule-metal junction. Gold is a popular electrode material owing to its oxidative stability and malleability. Electrodes are an important consideration, since the work function differences will effect the alignment of the Fermi energy ( $E_F$ ) with the molecular levels.<sup>8</sup>

Molecules of many different types may be bound into the device. This is the most varied portion of the junction in the literature. Changes in atomic constitution determine the intrinsic attributes of the bridging molecule, such as the level of conjugation, energy of the molecular orbitals, strength and character of molecule-electrode interactions, even the length of the molecule. Each of these plays major roles in device performance. For instance, the conductance of unsaturated vs. saturated molecular junctions, such as 1,4-diminobutane and 1,4-diamiobenzene, has been compared.<sup>9,11</sup> Both are linked through primary amines and are four carbons in length, but perform very differently. The aromatic molecule has a significantly lower HOMO-LUMO difference and its frontier orbitals align more closely with the  $E_F$  of the electrodes. Thus, conductance of the benzene derivative ( $6.4 \times 10^{-3} G_0$ ) is higher than the alkane ( $1 \times 10^{-3} G_0$ ).

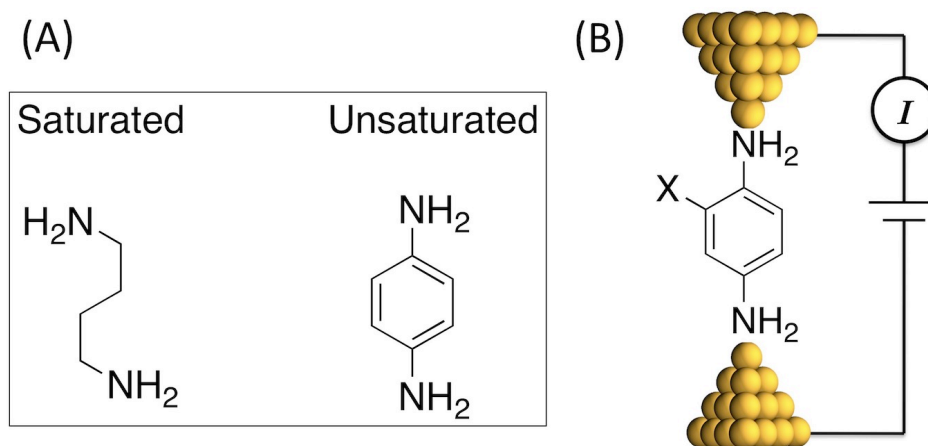


**Figure 1.3:** The atomic constitution of the molecule in molecular junction can modulate the junction conductance. (A) Saturated alkanes are less conductive than aromatic molecules of similar length. (B) Slight changes in the electronic structure of aromatic molecules through installation of chemical substituents affects junction conductance.

Molecular structures can be further modified by decoration functional groups. In 2007 functionalized 1,4-diaminobenzene, with electron-donating and electron-withdrawing groups.<sup>9</sup> A schematic of these junctions are given in Figure 1.3. Both the number and type of substituents were varied. Here in conjugated molecule such effects are easier to see since they are less resistive than aliphatic molecules. Similarly, our group has previously demonstrated how functionalization of biphenyls controls the conformational twist about the aryl-aryl bond. The bulkier the substituent, the more twisted the molecule becomes, thus changing the degree conjugation and ultimately the molecular conductance.

In summary, there is interplay between electrode material, chemical structure and linker constitution. Together they determine the charge transport properties of the

junction. However, the greatest possibility for variation belongs to the molecular portion. Here a wide variety of structure can be made with a variety of properties and functions, such as the level of conjugation, energy of the molecular orbitals, strength and character of molecule-electrode interactions, even the simple length of the molecule. Each of these plays major roles in device performance.

In order to deconvolute the many factors mentioned above, and quantify them individually, it is necessary to use sets of rationally designed molecular architectures that allow for simple comparisons and deductions to be made. These “molecular toolboxes” would contain sets of atomically precise molecular variations, each of which would be tailored to modulate one (or a few) of the many contributing factors. Since organic synthetic chemistry possesses the know-how to synthesize new molecules and their variations, it is central to overcoming these challenges in molecular electronics.

### **1.5. Linker effects**

A design requirement for single-molecule electrical devices is that the molecule must be both structurally and electrically connected to the metallic electrodes, even if only weakly so. Therefore, just as much emphasis is placed on the functional groups that attach the bridging molecules to the electrodes as the design of their interiors. We name the chemical functional groups that anchor the molecules into the molecular junction as linkers. Since gold leads are used in our STM-BJ setup, aurophilic functional groups are used to form Au-molecule-Au junctions. To date many different linkers have been employed, such as -SH,<sup>6,10</sup> -NH<sub>2</sub>, -SMe, -PR<sub>2</sub>, -COOH, -SCN, -NO<sub>2</sub>, and others.<sup>11,12</sup> Even

strained aromatic groups act as linkers, such as in oligo(para[2.2]cyclophanes)<sup>13</sup> and buckminsterfullerene.<sup>14</sup>

Linker choice is very important, since linkers affect the level of electronic coupling between the molecule and the electrode, as well as junction mechanics. Each of these factors attenuates the junction performance (see Figure 1.4A). Other junction properties can also be affected by the type of linker, such as conductance step-lengths and rupture forces.<sup>15</sup> For example, Vekataraman and coworkers measured three analogous series of alkanes functionalized at each end with a linker group (either primary amines, methylsulfides, or dimethylphosphines).<sup>12</sup> Each series was systematically elongated and measured using the STM-BJ method. Fitting the conductance vs. length data (Figure 1.4B) gave similar decay constants for each series, which is expected since the atomic constitution of the molecular backbone was identical. Although the decay parameters were identical, the overall resistivity between each series varied. This was the result of differences in the effective contact resistance, or the resistivity attributed to the metal-molecule interfaces. It was found to depend systematically on the linker type and ranged from 370 k $\Omega$  for amines to 270 k $\Omega$  and 130 k $\Omega$  for the methylsulfides and phosphines, respectively.

Linker groups also result in differences in the molecular conductance step lengths, called step lengths for short. As the electrodes are pulled apart, the step-length is the distance between electrodes just before the circuit breaks. It is the maximal junction length and correlates to the molecular length. Figure 1.4C, shows how dramatic linker effects are in the step length of difunctionalized n-butane molecules. For NH<sub>2</sub> linkers

(green line) a step-length of  $\sim 0.8$  Å is observed, while for SMe (red line) and PMe<sub>2</sub> (blue line) step-lengths are 1.7 Å and 3.2 Å.

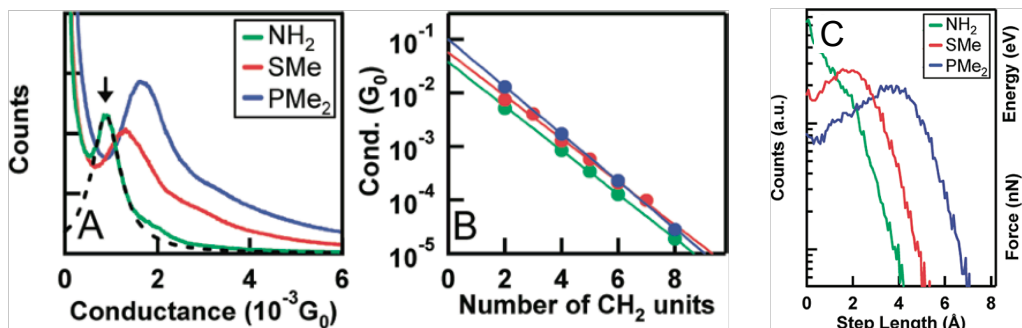


**Figure 1:** Linker effects in oligo-alkanes. (A) Step-length differences in a set of three butane molecules each functionalized with different linkers. Figures were adapted from a previously published article.<sup>12</sup>

## 1.6. Challenges and Frontiers

Despite the many accomplishments in single-molecular electronics, future goals seek to harness molecular components in molecule-based integrated circuitry; these goals are far from met. First, expansion into measurements on more exotic molecular designs will push our current understanding of molecular electronics. Such materials present many obstacles (i.e. low band gap and photooxidative materials), since they are more difficult to synthesize, store and measure. More complex structures may also establish bridging components with multiple conductance pathways, which will inevitably convolute their analysis. Secondly, there is more to make than simple resistors; the most well understood property of organic single-molecule wires is their resistivity. How do we use that to make devices with higher functions? Lastly, conductance is the primary means

of understanding single-molecular junctions. Therefore, it is difficult to quantify junction performance in low and non-conductive systems. Such molecules include cross-conjugated and quantum interfered systems or molecules of sufficient length to conduct below the sensitivity of our instrumentation. In these cases, it is difficult to quantify the electron transport through these structures, let alone prove that a junction has formed at all. Only systems that are electrically conductive within our detection limits can be measured properly. Therefore it is necessary to enable the measure of alternative quantities (such as force). This would open established techniques to molecules of greater length and even polymeric materials, cross-conjugated molecules and systems having pathways dominated by quantum interference.

### **1.7. Addressing Future Challenges**

In this dissertation we seek to meet these challenges by synthesizing novel molecular tools, such as those discussed in chapter 2 and 6, to expand our understanding of the role that intrinsic molecular properties play in the transport of single-molecule junctions. In chapter 4 we use a new technique, developed by the Venkataraman Group, to measure simple systems exhibiting quantum interference; a phenomenon that up until now could not be studied with previous single-molecular methods. We target not only the electronic performance of rationally designed molecules, but also investigate the interplay between mechanical factors and charge transport (chapter 5). In chapter 6 we describe the unusual IV and mechanical characteristics of a family of conjugated oligomers. In doing so we have gone beyond the simple resistor to create new electrical

components, such as potentiometers (chapter 3) and rectifiers (chapter 7), on the molecular scale.

## 1.8. References

---

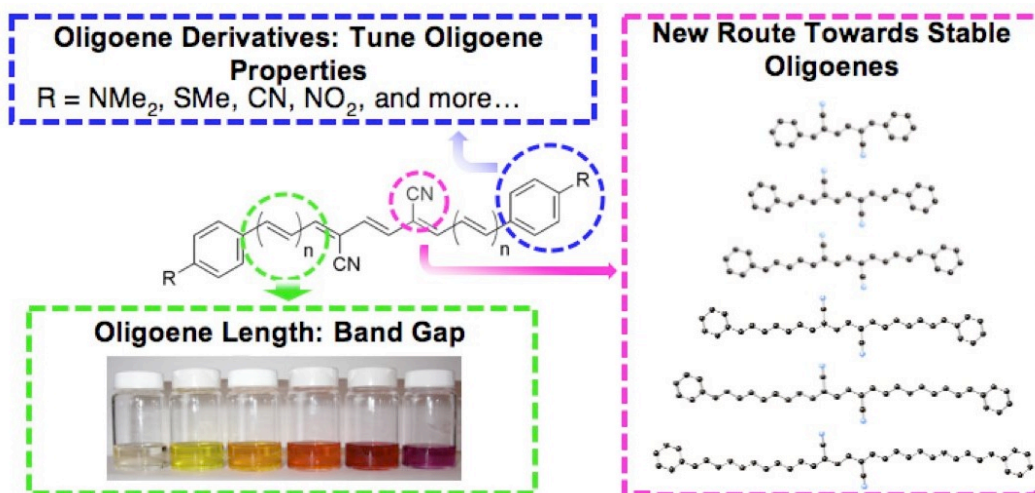
1. Scifinder search was input with the search phrase, “single-molecule” and “molecular electronics.”
2. Dibenedetto, S. A.; Facchetti, A.; Ratner, M. A.; Marks, T. J., *Adv. Mat.*, **2009**, *21*, 1407-1433.
3. (a) Wold, D. J.; Frisbie, C. D., *J. Am. Chem. Soc.*, **2000**, *122*, 2970-2971. (b) Holmlin, R. E.; Haag, R.; Chabinyo, M. L.; Ismagilov, R. F.; Cohen, A.; Terfort, A.; Rampi, M. A.; Whitesides, G. M., *J. Am. Chem. Soc.*, **2001**, *123*, 5075-5085; (c) Selzer, Y.; Salomon, A.; Cahen, D., *J. Phys. Chem. B*, **2002**, *106*, 10432; (d) Slowinski, K.; Fong, H. K. Y.; Majda, M., *J. Am. Chem. Soc.*, **1999**, *121*, 7257-7261.
4. (a) Choi, S. H.; Risko, C.; Delgado, M. C. R.; Kim, B.; Bredas, J.-L.; Frisbie, C. D., *J. Am. Chem. Soc.*, **2010**, *132*, 4358–4368; (b) Salomon, A.; Cahen, D.; Lindsay, S.; Tomfohr, J.; Engelkes, V.B.; Frisbie, C. D., *Adv. Mater.*, **2003**, *15*, 22, 1881-1890, and references therein.
5. Reed, M. A.; Zhou, C.; Muller, C. J.; Burgin, T. P., Tour, J. M. *Science*, **1997**, *278*, 252– 253.
6. (a) Park, J.; Pasupathy, A. N.; Goldsmith, J. I.; Chang, C.; Yaish, Y.; Petta, J.; Rinkoski, M.; Sethna, J. P.; Abrun, H. D.; McEuen, P. L.; Ralph, D. C. *Nature*, **2002**, *417*, 722–725; (b) Kubatkin, S.; Danilov, A.; Hjort, M.; Cornil, J.; Bredas, J.-L.; Stuhr-Hansen, N.; Hedegard, P.; Bjørnholm, T. *Nature*, **2003**, *425*, 698–701.
7. Xu, B. Q.; Tao, N. J. *Science*, **2003**, *301*, 1221–1223
8. Kim, B. S.; Choi, S.-H.; Frisbie, C. D. *J. Am. Chem. Soc.*, **2011**, *133*, 19864-19877.
9. Venkataraman, L.; Park, Y. S.; Whalley, A. C.; Nuckolls, C.; Hybertsen, M. S.; Steigerwald, M. L. *Nano Lett.*, **2007**, *7*, 502–506.
10. (a) Reichert, J.; Ochs, R.; Beckmann, D.; Weber, H. B.; Mayor, M.; Loehneysen, H. *v. Phys. Rev. Lett.*, **2002**, *88*, 176804; (b) Beebe, J. M.; Engelkes, V. B.; Miller, L. L.;



- 
- Frisbie, C. D. *J. Am. Chem. Soc.*, **2002**, *124*, 11268-11269; (c) Ulrich, J.; Esrail, D.; Pontius, W.; Venkataraman, L.; Millar, D.; Doerrer, L. H., *J. Phys. Chem. B*, **2006**, *110*, 2462-2466; (d) Li, C.; Pobelov, I.; Wandlowski, T.; Bagrets, A.; Arnold, A.; Evers, F. *J. Am. Chem. Soc.*, **2008**, *130*, 318-326; (f) Chen, F.; Li, X. L.; Hihath, J.; Huang, Z. F.; Tao, N. J. *J. Am. Chem. Soc.*, **2006**, *128*, 15874-15881.
11. Mischenko, A.; Zotti, L. A.; Vonlanthen, D.; Bürkle, M.; Pauly, F.; Cuevas, J. C.; Mayor, M.; Wandlowski, T., *J. Am. Chem. Soc.*, **2011**, *133*, 184–187, and references therein.
  12. Park, Y. S.; Whalley, A. C.; Kamenetska, M.; Steigerwald, M. L.; Hybertsen, M. S.; Nuckolls, C.; Venkataraman, L., *J. Am. Chem. Soc.*, **2007**, *129*, 15768-15769;
  13. Schneebeli, S., Kamenetska, M.; Cheng, Z.; Skouta, R.; Friesner, R. A.; Venkataraman, L.; Breslow, R. *J. Am. Chem. Soc.*, **2011**, *133*, 2136–2139.
  14. Park, H.; Park, J.; Lim, A.; Anderson, E.; Alivisatos, A.; McEuen, P. *Nature*, **2000**, *407*, 57–60.
  15. Frei, M.; Aradhya, S. V.; Koentopp, M.; Hybertsen, M. S.; Venkataraman, L. *Nano Lett.*, **2011**, *11*, 1518–1523.

## Chapter 2. Functionalizing Molecular Wires: A Tunable Class of $\alpha,\omega$ -diphenyl- $\mu,\nu$ -dicyano-oligoenes<sup>†</sup>

*All molecules in Chapter 2 were synthesized by Danielle Sedbrook and I with assistance from Markrete Krikorian. Our collaborators at University of Pennsylvania synthesized and characterized the nanoparticles. Danielle Sedbrook did the SEM studies. Michael Steigerwald with assistance from myself ran the DFT calculations.*



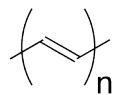
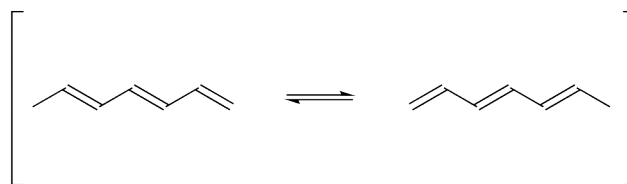
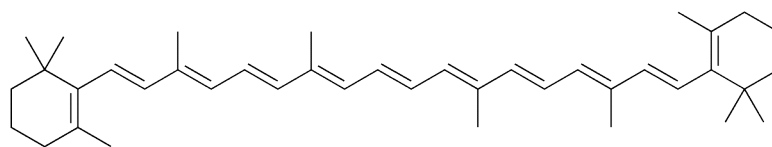
### 2.1. Motivations

Molecules with linear conjugated structures are ideal candidates as molecular wires and connectors in molecular-sized devices. Oligomers having well defined, atomically precise fragments enable the systematic study of their length-dependent properties and yield insight into the assembly and electronics of their polymer analogues. In this chapter we explore the electronic and physical properties of a new class of oligoene materials and their derivatives.

<sup>†</sup>Parts of Chapter 2 were reproduced or adapted with permission from the authors: Meisner, J. S.; Sedbrook, D. F.; Krikorian, M.; Chen, J.; Sattler, A.; Carnes, M. E.; Murray, C. B.; Steigerwald, M.L.; Nuckolls, C., *Chem. Sci.*, **2012**, 3, 1007–1014. Copyright 2012 Royal Chemical Society.

### 2.1.1. From Polyacetylene to Oligoenes

Of the many classes of conjugated materials, oligo-olefins are of particular importance owing to their prototypical chemical structure; they are monodisperse vinylogues of the classic electronic polymer, polyacetylene (PA, Figure 2.1a). The simplest conjugated hydrocarbon polymer, PA is made up of alternating C-C single and C=C double bonds. Its ground electronic state is doubly degenerate (Figure 2.1b) allowing for delocalization of the  $\pi$ -electrons along the conjugated backbone. It is a semiconductor, however, is highly conductive when doped.<sup>1</sup> In fact, depending on the type and concentration of the dopant, the conductivity of PA may be increased by over eight orders of magnitude ( $I_2$  doping) reaching conductivity values similar to silver metal. Additionally, PA has a low band gap and shows large nonlinear optical susceptibilities.<sup>2</sup> Since the fully conjugated high polymer is electrically conductive, we believe that well-defined oligomers, hereafter referred to as oligoenes, should be useful molecular conductors in nanoscale situations. In addition, naturally occurring terpenoid-based oligoenes, such as carotenoids (Figure 2.1c), have been made into electrical devices and are known to have useful optical properties.<sup>3</sup> Although, nature provides a limited number of structures that are often difficult to functionalize further, thus preventing their use in widespread applications.

(a) Polyacetylene (**PA**)(b) Degenerate ground State of **PA**(c)  $\beta$ -carotene

**Figure 2.1:** Structure of Polyacetylene (**PA**). **PA** has a doubly-degenerate ground state. (c) carotenoids are tetraterpenoids that naturally occurring oligoenes.  $\beta$ -carotene is a widely known example of a carotenoid.

The synthesis and study of conjugated oligomers has flourished over the past 20 years, however oligoene systems remain understudied. Three major challenges have hampered the development of oligoenes as electronic materials: (1) The most thoroughly studied examples of PA oligomers have been obtained inefficiently through the painstaking isolation of individual oligomers from polymerization reactions terminated at low monomer conversion.<sup>4</sup> (2) Previous preparative methods have not supported diverse functionalization to incorporate them into electronic devices. (3) Oligomers of PA are chemically impractical because they are nearly insoluble and oxidatively unstable. Using the new synthetic strategy detailed below for the  $\alpha,\omega$ -diphenyl- $\mu,\nu$ -dicyano oligoenes.<sup>5</sup>

(DPDC, Figure 2.2b) we have overcome these challenges. The key to this synthesis is the use of sterically innocent yet electronically stabilizing cyano groups bound directly to the oligoene chain while protecting the reactive terminal olefins with bulky phenyl groups.<sup>6</sup> These phenyl end-groups can easily be modified with a diverse range of functional groups to reveal a wide variety of compounds that can be produced through our synthetic method. We also highlight the versatility and adaptability of these new electronic materials by using appropriately functionalized oligoenes as electrical conduits that connect magnetic nanoparticles to a semiconductor surface.

Other methods have been used to stabilize oligoenes. Several approaches protect the highly reactive terminal olefins with bulky end-groups such as phenyl (DPO, Figure 2.2a)<sup>6</sup> or *tert*-butyl.<sup>7,8</sup> Other than such hydrocarbon-end-capped oligoenes, however, there are few other examples of non-terpenoid  $\alpha,\omega$ -disubstituted oligoenes longer than pentaenes.<sup>9,10</sup>

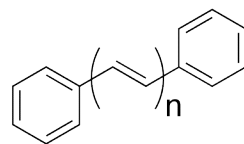
### 2.1.2. Naturally Occurring Oligoenes

Nature provides its own methods of oligoene stabilization: terpenoid-based biomolecules such as carotenoids (Figure 2.1c). Carotenoids are the most studied class of oligoenes, of which the most well-known member is  $\beta$ -carotene. They play essential roles in many biological processes such as vision (retinal), cell differentiation (retinol) and photosynthesis and pigmentation.<sup>11</sup> Built from terpene subunits, methyl groups decorate the oligoene backbones and contribute to both the solubility and stability. However, they also create allylic-1,3-strain along the poly-olefin backbone, which cause the molecules to bend. Torsional distortions reduce the conjugation and increase the energy difference

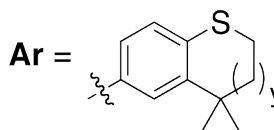
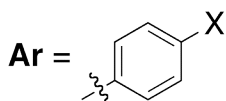
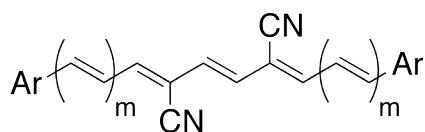
between the highest occupied molecular orbital (HOMO) and lowest unoccupied molecular orbital (LUMO), and shifts the electronic absorptions to higher energies.

### 2.1.3. Rational Design Toward Cyano-functionalized Oligoenes

In order to use oligoenes in optical devices, it is desirable to have a family of light-harvesters that cover the entire visible and near-infrared spectral regions. Therefore, we sought small and synthetically available substituents that could confer stability while maintaining the bathochromic absorption shifts expected for longer oligoenes. Cyano groups, shown in Figure 2.3, fulfill these requirements: they are  $\pi$ -electron withdrawing groups with a linear geometry and are not bulky enough to disrupt molecular planarity. The A-value of a cyano group has been determined to be 0.19 kcal/mol in contrast to that of a bulkier methyl group (1.74 Kcal/mol).<sup>12</sup> They have been used to alter the band gaps of a variety of aromatic molecules and conjugated polymer materials.<sup>13</sup> Cyano groups are known as strong electron-withdrawing groups as evidenced by their high Hammett substituent coefficient ( $\sigma_p = 0.66$ )<sup>14</sup> and because of their electron-withdrawing ability they are expected to lower the energies of the frontier orbitals, thus stabilizing the system toward oxidative decomposition. As an ultimate benefit they are easily installed and enable an economical synthesis that allows for diverse end-group functionalization.

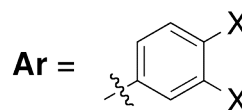
(a)  $\alpha,\omega$ -Diphenyl-oligoene (DPO)

n = 3, **DPO3**  
 n = 5, **DPO5**  
 n = 7, **DPO7**

(b)  $\alpha,\omega$ -diaryl- $\mu,\nu$ -dicyano-oligoenes (DPDC)

X = H, **DPDCn**  
 F, **DPDCn-F**  
 Br, **DPDCn-Br**  
 CO<sub>2</sub>H, **DPDCn-CO<sub>2</sub>H**  
 CO<sub>2</sub>Et, **DPDCn-CO<sub>2</sub>Et**  
 NO<sub>2</sub>, **DPDCn-NO<sub>2</sub>**  
 CN, **DPDCn-CN**  
 C≡C-C<sub>6</sub>H<sub>13</sub>, **DPDCn-C<sub>8</sub>H<sub>13</sub>**  
 SMe, **DPDCn-SMe**  
 NMe<sub>2</sub>, **DPDCn-NMe<sub>2</sub>**  
 NPh<sub>2</sub>, **DPDCn-NPh<sub>2</sub>**

y = 0, **DPDCn-SC<sub>4</sub>H<sub>8</sub>**  
 1, **DPDCn-SC<sub>5</sub>H<sub>10</sub>**



X = OC<sub>6</sub>H<sub>13</sub>, **DPDCn-OC<sub>6</sub>H<sub>13</sub>**  
 OC<sub>10</sub>H<sub>21</sub>, **DPDCn-OC<sub>10</sub>H<sub>21</sub>**  
 OC<sub>14</sub>H<sub>29</sub>, **DPDCn-OC<sub>14</sub>H<sub>29</sub>**

**Figure 2.2:** (top) Structure of  $\alpha,\omega$ -diphenyl-oligoenes (DPO), which we regard as control molecules for comparison with (bottom) cyano-functionalized  $\alpha,\omega$ -diphenyl-oligoenes (DPDC). We identify the oligoene molecules according to the length of their linear conjugated backbone ( $n$ ) and aryl end-group ( $X$ ), **DPDCn-X**. For instance, 1,10-di-(4-bromophenyl)-4,7-dicyano-deca-1,3,5,7,9-pentaene is denoted as **DPDC5-Br**. See Appendix A for a complete list of molecules.

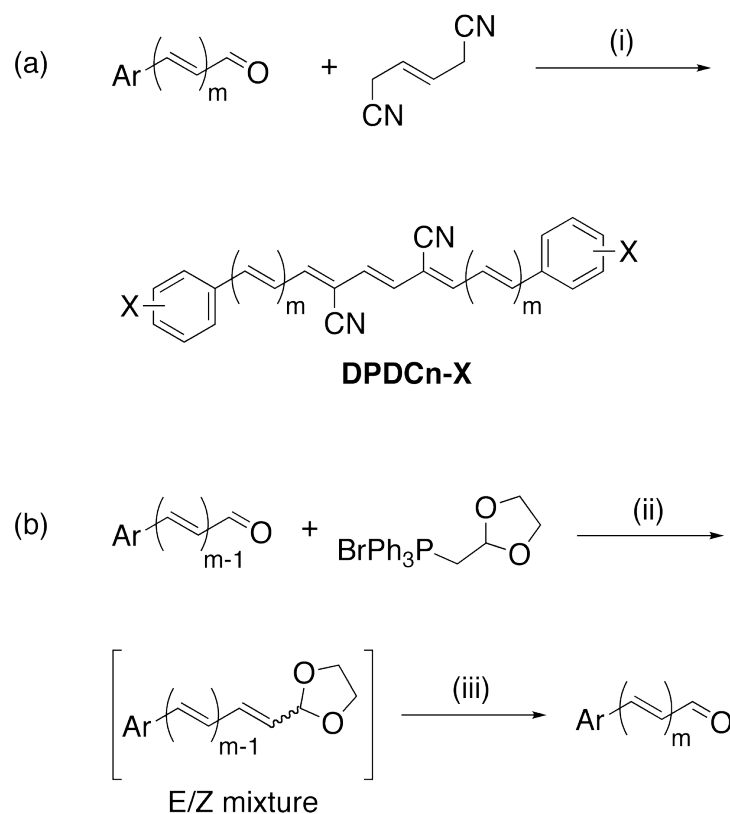
## 2.2. $\alpha,\omega$ -diphenyl- $\mu,\nu$ -dicyano-oligoenes

### 2.2.1. Synthetic Approach

A convergent synthetic pathway was necessary to allow easy access to multiple oligomeric lengths while avoiding unique synthetic routes to each individual member of the series. The Knoevenagel condensation reaction was first published in 1898,<sup>15</sup> where one equivalent of benzaldehyde reacted with malonic acid under basic conditions. A bronsted base first deprotonates the acidic  $\alpha$ -proton, subsequently attacking the electrophilic carbonyl center on the aldehyde. From the tetrahedral intermediate proton transfer to the incipient hydroxyl generates a good leaving group, water.

The key step in our synthesis, a double Knoevenagel condensation between 1,4-dicyano-2-butene and two equivalents of the appropriate aryl-enal (Scheme 2.1a) sews together the oligoene backbone while simultaneously installing two central cyano groups. We prepare the aryl-oligoenals starting from the analogous benzaldehyde or *trans*-cinnamaldehyde via iterative Wittig homologations<sup>16</sup> and subsequent acidic hydrolysis of the intermediate acetal. The conditions for both reactions tolerate a wide variety of functionality and give access to a range of derivatives. Figure 2.2b shows those derivatives that we prepared for this study via this method. They are made in a small number of steps from commercially available starting materials.





**Scheme 2.1:** Synthesis of DPDCs via (a) Double-Knoevenagel condensation reaction and (b) Wittig reaction. (i) DBU, MeOH, 25° C, 6-12 h, (60-10%, for **DPDCn** series; from  $m = 0$  to 5); (ii) LiOMe, THF, 75° C, 12-24 h. (iii); 10% aq. HCl, 25° C, 2 h (70-98%). For instance, if  $m = 1$ , then the intermediate acetal leads to the product (2*E*,4*E*)-5-phenylpenta-2,4-dienal. A list of all compounds is provided in Appendix A.

In general, the Knoevenagel condensations give moderate yields, which decrease with increasing molecular length producing the **DPDCn** series in 10–60% isolated yields, shown in Table 2.1. Despite moderate yields, the condensation reaction is operationally simple: (1) A common base, such as sodium methoxide (NaOMe) or the non-nucleophilic organic base 1,8-Diazabicyclo[5.4.0]undec-7-ene (DBU), is the only reagent, of which the later can be stored under normal laboratory conditions; (2) anhydrous solvents are not necessary and (3) isolation does not require chromatography. This reaction joins two

fragments together; more than doubling the length of the starting aryl-oligoenals. The products precipitate from the reaction mixture and are easily isolated by filtration. When necessary the crude products are purified by recrystallization from CH<sub>2</sub>Cl<sub>2</sub> by adding MeOH. With this approach, the synthesis of **DPDC13** (one of the longest oligoenes prepared to date) is straightforward and involves only five steps. It is also important to mention that the sequence shown in Scheme 2.1 is scalable; we tested members of the **DPDCn** series on the gram-scale with no loss in their isolated yields.

**Table 2.1:** Double Knoevenagel Condensation Yields for the **DPDCn** Series.

<b>Oligoene</b>	<b>Oligomeric</b>	<b>Isolated Yield (%)</b>
<b>DPDC3</b>	3	55
<b>DPDC5</b>	5	60
<b>DPDC7</b>	7	54
<b>DPDC9</b>	9	45
<b>DPDC11</b>	11	40
<b>DPDC13</b>	13	10

All of the compounds have exclusively *trans*-stereochemistry in their double bonds. The stereochemistry of the double bonds in the each aryl-oligoenal starting material can be identified by the coupling constants of the olefinic doublet of doublets near 6.5 ppm (this signal belongs to the  $\beta$ -proton of the aryl-enal). This resonance is coupled to the aldehyde and a *trans*-olefin (-CH=) proton, and resides in an isolated region of the spectra allowing for stereochemical characterization throughout the growth of the aryl-oligoenals.

Wittig conditions (Scheme 2.1b) produce an *E/Z*-mixture of stereoisomers, however acid hydrolysis of the intermediate acetals exclusively produces the *trans*-product. Cleavage of the acetal is carried out before separation, however to further understand our method we tracked the stereoisomeric transformations throughout the extension of *trans*-cinnamaldehyde to (2*E*,4*E*)-5-phenylpenta-2,4-dienal. In this case performing the Wittig reaction on *trans*-cinnamaldehyde produces the (*E*)- and (*Z*)-4-phenylpenta-2,4-dienyl acetals in 16% and 60% yield, respectively. We separated each product by column chromatography; coupling constants from <sup>1</sup>H-NMR spectra identified each stereoisomer. Acid hydrolysis of either stereoisomer, *E* or *Z*, by addition of 10% aq. hydrochloric acid to a solution of acetal in tetrahydrofuran generates the same product, (2*E*,4*E*)-5-phenylpenta-2,4-dienal, in quantitative yields.

Many Wittig homologations are carried out with potassium or sodium *tert*-butoxide (i.e. <sup>t</sup>BuOK), however significant reduction in the yields of our aryl-oligoenals were observed with these bases. The difference in yield is due to the base-induced disproportionation of the aldehyde starting material. First reported in 1853 by Stanislaw Cannizzaro this reaction is called the Cannizzaro reaction.<sup>17</sup> In the Wittig homologation starting from *trans*-cinnamaldehyde and instead using potassium *tert*-butoxide the cinnamyl alcohol was isolated in 20% yield.

### 2.2.2. Solid-state Structure

We have grown crystals of each member of the **DPDC<sub>n</sub>** family (from *n* = 3 to 13) and determined the molecular structure of each crystallographically. Shown in Figure 2.3, each oligoene occurs exclusively in the all-*trans* form. **DPDC13** is the longest oligoene

thus far characterized by XRD, longer even than the natural product, rhodopin glucoside,<sup>18</sup> which contains 11 linear conjugated C=C bonds. Although some of the shorter vinylogues have been previously reported in the resin dye patent literature,<sup>19</sup> a systematic characterization has been heretofore unavailable. Only a few non-terpenoid structures having more than six conjugated C=C bonds have been previously reported, and none having more than nine.<sup>20</sup>

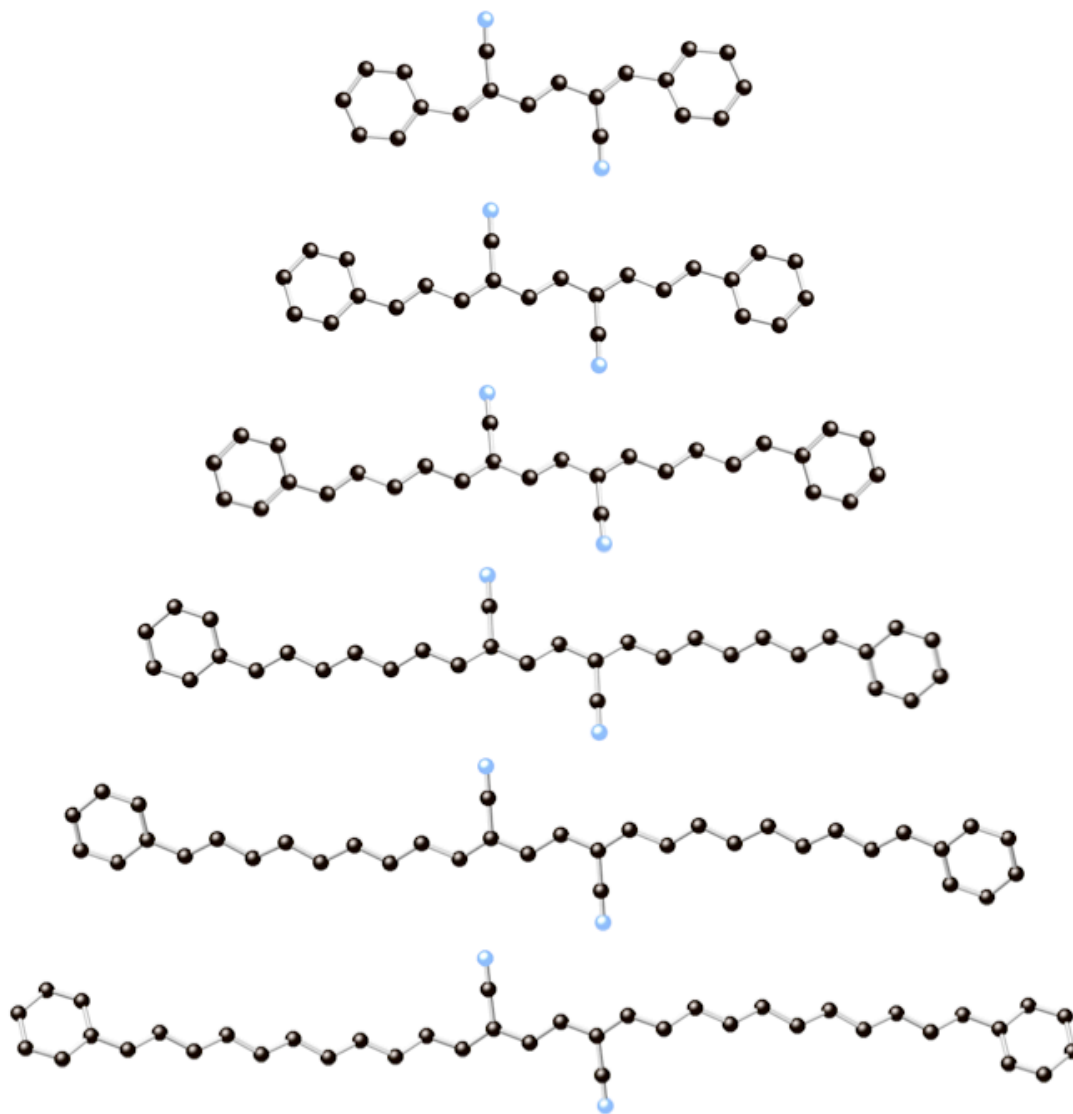


**Figure 2.3:** Crystal structures of **DPDCn** series were determined by single crystal X-ray diffraction.

We observe different packing structures within the parent series of **DPDC<sub>n</sub>** oligomers. The shortest vinylogues, **DPDC3** and **DPDC5**, are planar and stack in a herringbone pattern, indicating that the cyano groups do not significantly interact with allylic hydrogens (Figure 2.4). The longer oligomers, **DPDC7-DPDC13**, co-crystallize with one solvent molecule per unit cell and are not fully planar. The central dicyano-butene moiety is planar and to either side out-of-plane bending of the conjugated backbone is accompanied by a slight twist. DFT calculations at the B3LYP/6-31G\*\* level predict fully planar conformations, however the incorporation of solvent as well as bending is common in crystal structures of oligoenes having more than six C=C bonds.<sup>7,8</sup>

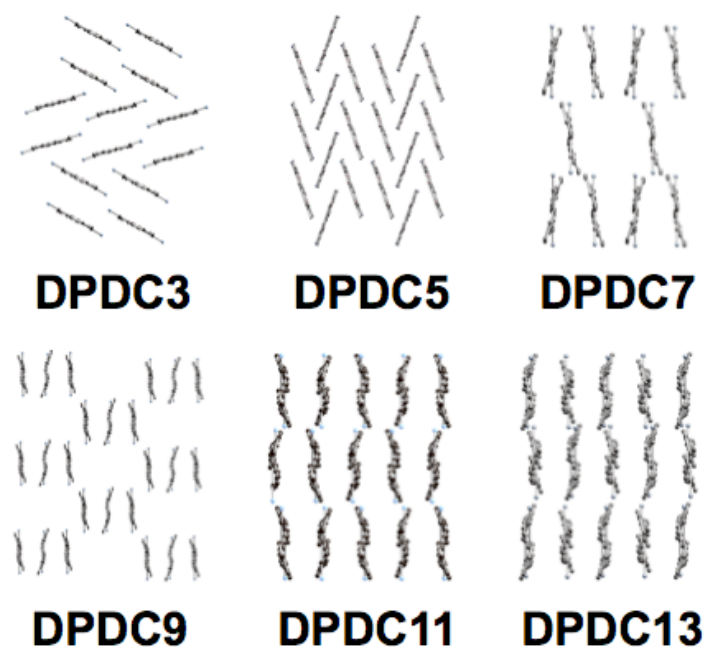


**Figure 2.4:** Packing structures of **DPDC3-DPDC13**. Solid-state packing morphs from herringbone-type to aligned stacks of oligoenes as oligoene length increases. For **DPDC7-DPDC13** solvent molecules were omitted for clarity.

There exists a dearth of solid-state structural information on oligoenes especially for those having more than 5 linear conjugated C=C bonds. For instance, the Cambridge Structural Database (CSD) provides only two non-terpenoid (such as carotenoids) oligoene structures containing 9 or more linear conjugated C=C double bonds. Both structures belong to the cyclic oligomer, [18]-annulene.<sup>20</sup> Other search results show: 6 structures for  $n = 8$ ; 10 for  $n = 7$ ; and 13 for  $n = 6$ .

We were concerned that the cyano groups would disturb the local structure of the oligoene backbone and minimize the degree of conjugation. Despite the observed bending, the central alkene unit (that having doubly allylic cyano groups) remains planar for each member of the series with a dihedral angle of  $180.0^\circ$ . This suggests that deviations from planarity may be attributed to co-crystallization with solvent molecules and not the result of cyano-functionalization.

### 2.2.3. Control Group: $\alpha,\omega$ -diphenyl-oligoenes (DPO)

In order to verify the practical value of cyano substitution, we have also prepared the unsubstituted  $\alpha,\omega$ -diphenyl-oligoenes (DPO) of the corresponding lengths, **DPO3**, **DPO5** and **DPO7**. We synthesized these molecules lacking the cyano groups via the Horner-Wadsworth-Emmons reaction<sup>21</sup> as described by Spangler and coworkers.<sup>10</sup> Dicyano-oligoenes are less reactive toward ambient oxidation, intermolecular oligomerization or intramolecular decomposition than their unsubstituted relatives; we can conveniently study them under normal aerobic laboratory conditions for extended periods.<sup>22</sup> The thermal stability of these dicyano-oligoenes (**DPDC3-DPDC13**) is similar to that of the  $\alpha,\alpha,\omega,\omega$ -tetrakis-*t*-butyl-functionalized oligoenes reported by Hopf and

coworkers<sup>8</sup> and far higher than that of the methyl and unfunctionalized analogs.<sup>23</sup> Differential scanning calorimetry shows that under an inert atmosphere all members of the parent series **DPDC3-DPDC13** are thermally stable up to  $\sim 250^\circ$  C. For a direct comparison between cyano-functionalized and unfunctionalized oligoenes, we photooxidatively decomposed both **DPO5** and **DPDC5** in a side-by-side experiment. We monitored the oligoene starting materials with UV-vis spectroscopy and found that the unsubstituted material decomposes four times faster than the cyano-functionalized material.<sup>24</sup>

#### 2.2.4. Band-gap Modulation

In order to realize what kind of effect the cyano groups have on the electronic properties we first consider the derivatives that have unsubstituted phenyl groups, the parent **DPDCn** series. Despite providing stabilization to the oligoene core, the cyano groups do not fundamentally alter the "polyacetylene-like" electronic behavior of oligoenes in the sense that the HOMO-LUMO gap decreases as the length of the oligoene increases, which is typical of other vinylogous series.<sup>25</sup> The optical absorptions of the **DPDCn** series for n between 3 and 13 span the entire visible spectrum (Figure 2.5a). The absorptions are also quite intense with molar extinction coefficients ( $\epsilon$ ) that exceed  $10^5$   $\text{M}^{-1}\text{cm}^{-1}$ . We estimate the solution-phase optical band gap ( $E_{\text{og}}$ ) for **DPDC11** and **DPDC13** to be 1.81 eV and 1.77 eV, respectively. These values approach the band gap observed for PA itself.<sup>26</sup> Similarly, we can analyze this series using the quantum mechanical "particle in a box" model, which is often used to describe optical absorptions in one-dimensional systems. This model holds that the excitation energies in a simple

system vary with the inverse square of the dimensional length. Fitting the excitation energies in the **DPDCn** series with such an inverse-square expression (see Figure 2.5c) leads to an effective mass of  $2.15 \times 10^{-45}$  kg. Extrapolation of the wavelength for the strongest absorption ( $\lambda_{max}$ ) and optical band gap ( $E_{og}$ ) to an infinite "box" length estimates values of 577 nm and 1.59 eV, respectively. This is within the reported range of band gaps (1.4-1.6 eV) for *trans*-PA.<sup>1,26</sup> Our extrapolations were carried out as simple linear regression analyses; the Meier correction<sup>27</sup> didn't provide any benefit in this case because the effective conjugation length (ECL) of the series had not been reached. The ECL of oligoenes is higher than other poly-conjugated systems<sup>25</sup> and has been estimated to lie between 15 and 20 repeat units.<sup>4,28</sup> We estimate the ECL of the **DPDCn** series by selecting the point in our three extrapolations where a change in oligomeric length of one repeat unit corresponds to a negligible energy difference of less than 0.01 eV. In each case, the emergence of size-independent electronic properties ( $\lambda_{max}$ ,  $E_{og}$  and  $E_{cv}$ ) is predicted to occur at lengths  $\geq 19$  alkene repeat units.



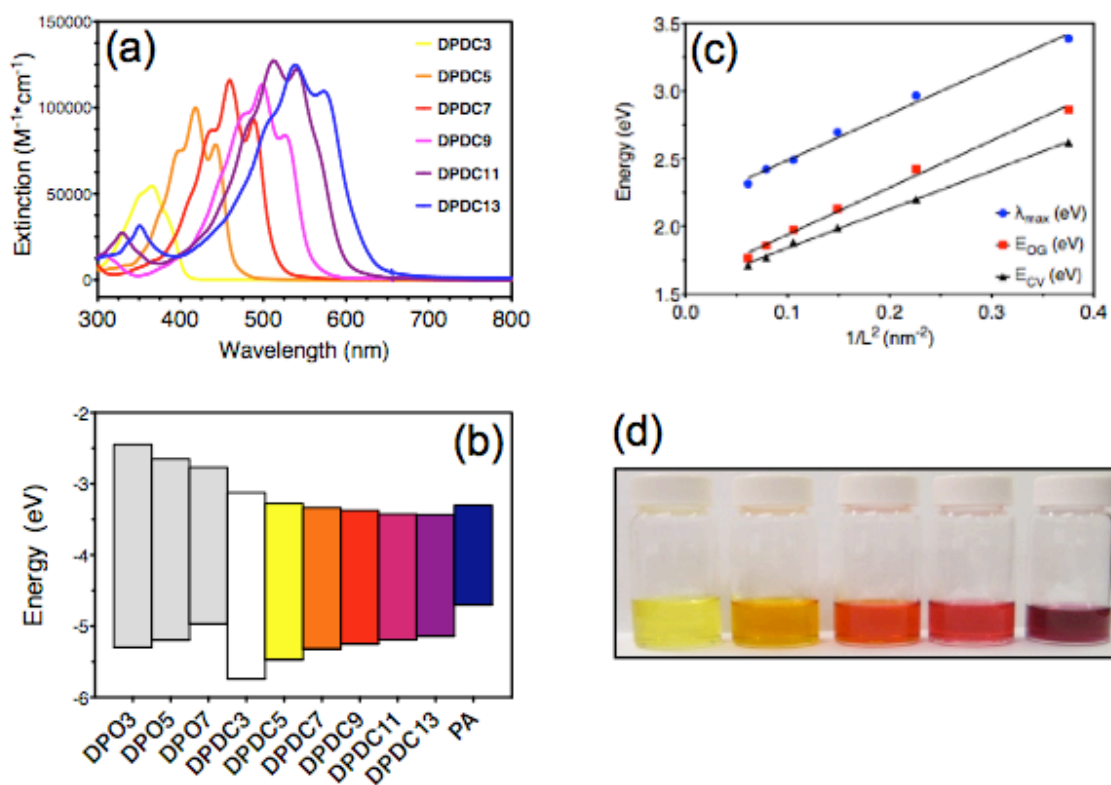


**Figure 2.5:** (a) UV-vis absorption spectra of the parent oligoene series (**DPDCn**) in  $CH_2Cl_2$ . The wavelength of strongest absorption,  $\lambda_{max}$ , (from left to right) at 363, 418, 459, 499, 513, and 536 nm; increasing the oligomeric length tunes the optical absorptions over a range of 350 nm. (b) Effect of the cyano groups on the HOMO and LUMO energies of diphenyl-oligoenes determined by cyclic voltammetry (CV). Redox gap of **DPO3**, **DPO5**, **DPO7** (grey) and the cyano-functionalized series, **DPDCn**. CVs were obtained in DMF solution with 0.1 M  $(n-Bu)_4N^+ \cdot PF_6^-$ . Ferrocene was used as an internal standard for electrochemical measurements. Experimentally determined values for PA (blue) are included for reference.<sup>26</sup> (c)  $\lambda_{max}$ , the optical band gap ( $E_{og}$ ) and the redox band gap ( $E_{cv}$ ) for the **DPDCn** series are fit using “particle in a box” energies. Extrapolative analysis estimates the analogous values for an oligomer of infinite length (polymer) of 577 nm, 1.59 eV and 1.55 eV, respectively. Predicted values agree with experimentally determined values for PA.

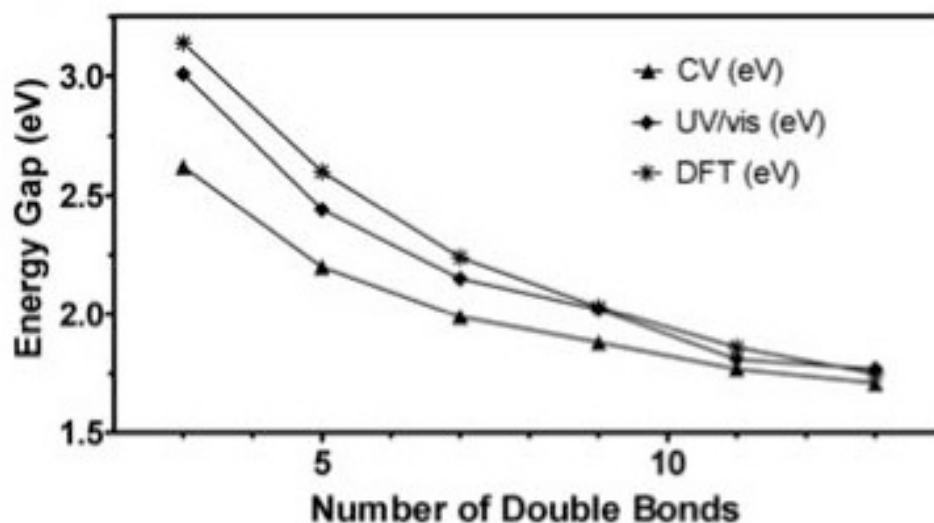
### 2.2.5. Electrochemical Studies

Since cyano groups are strongly electron withdrawing, their presence should lower the energies of the frontier orbitals with respect to those of the unfunctionalized DPOs. The redox potentials determined by cyclic voltammetry were used to estimate the energies of the HOMOs and LUMOs of the **DPDCn** series. We found that installation of two cyano groups onto the oligoene core stabilizes the HOMO and LUMO by as much as 0.44 eV and 0.68 eV with respect to the corresponding unsubstituted **DPOn** molecules (Figure 2.5b). This is consistent with UV-vis absorption spectroscopy, in which we observe a bathochromic shift of up to 35 nm between **DPOn** and **DPDCn** series. The electrochemically determined energy gap,  $E_{cv}$ , for **DPDCn** molecules can also be extrapolated to predict the band gap of the homologous polymer. In Figure 2.5c we again use simple “particle in a box” energies to predict the band gap for the polymer to be 1.55 eV. Both the  $E_{cv}$  and the  $E_{og}$  converge to similar values.

### 2.2.6. Theoretical Band Gap

To gain further insight into the electronic structure of the parent **DPDCn** series, as well as the **DPOn** series, we performed density functional theory (DFT) calculations on each member of the series. All electronic structure calculations used Jaguar (version 7.7, Schrodinger LLC, New York, NY, 2010) using the B3LYP hybrid functional and the 6-31G\*\* basis sets. The geometries of **DPDCn** and **DPOn** were fully optimized before calculation of its molecular orbitals. The final geometries, total energies, bond angles, bond distances and molecular orbital energies can be found in Appendix A.

DFT was used as an a third way to estimate the band gap of the **DPDC<sub>n</sub>** series. In Figure 2.6, DFT band gaps are smaller than those found by solution-based techniques, however as oligomeric length increases the various methods converge to similar values.

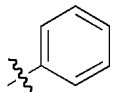
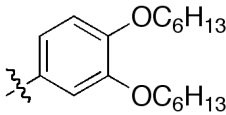
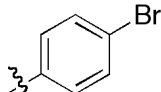
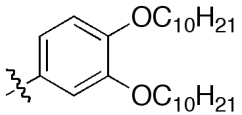
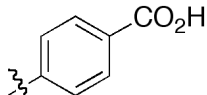
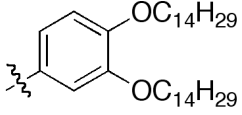
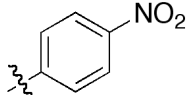
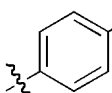
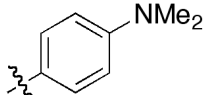
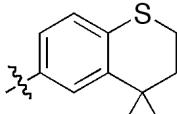


**Figure 2.6:** Comparison of band gap estimations from CV, UV-Vis and DFT. Greater variation between methods is seen for the shorter oligomers while values converge as molecular length increases.

### 2.3. End-functionalized DPDC Derivatives.

Substitution on the terminal phenyl groups offers another opportunity to tailor the electrical and physical properties of oligoenes. We synthesized a family of derivatives of **DPDC5** (Table 2.2), whose phenyl-substituents varied from strongly electron-withdrawing ( $\text{NO}_2$ ) to electron-donating ( $\text{NMe}_2$ ). We found *para*-substitution to be most effective, apparently since it is strongly resonance-coupled to the oligoene backbone and at the same time sterically remote (Appendix A). Spangler and coworkers reported

similar results for non-cyano DPOs having the *para*-substituents NO<sub>2</sub>, Cl, SMe, OMe, and NMe<sub>2</sub>.<sup>9</sup> Examples of the effect of aryl-functionalization on the optical absorption are displayed in Figure 2.7a.

entry	R group	$\lambda_{\max}$ (nm/eV) <sup>a</sup>	entry	R group	$\lambda_{\max}$ (nm/eV) <sup>a</sup>
1		418/2.97	6		454/2.73
	<b>DPDC5</b>			<b>DPDC5-OC<sub>6</sub>H<sub>13</sub></b>	
2		426/2.91	7		453/2.74
	<b>DPDC5-Br</b>			<b>DPDC5-OC<sub>10</sub>H<sub>21</sub></b>	
3		426 <sup>b</sup> /2.91	8		455/2.73
	<b>DPDC5-CO<sub>2</sub>H</b>			<b>DPDC5-OC<sub>14</sub>H<sub>29</sub></b>	
4		449/2.76	9		453/2.74
	<b>DPDC5-NO<sub>2</sub></b>			<b>DPDC5-SMe</b>	
5		523/2.37	10		465/2.67
	<b>DPDC5-NMe<sub>2</sub></b>			<b>DPDC5-SC<sub>5</sub>H<sub>10</sub></b>	

**Table 2.2:** Comparison of selected **DPDC5** derivatives and their UV-vis strongest-wavelength absorptions. <sup>a</sup>The strongest wavelength absorption is taken at the global  $\lambda_{\max}$  and is not indicative of HOMO-LUMO gap energies,  $E_{og}$ .

### 2.3.1. Tuning the Solid-state Assembly through End-functionalization

Strong electron-donating groups give the largest bathochromic shifts and broadened absorption peaks. Functionalization of the **DPDC5** scaffold with *p*-NMe<sub>2</sub> groups shifts the longest-wavelength absorption from 490 nm to 640 nm, and this shift is accompanied by the loss of vibronic fine-structure.<sup>29</sup> These electronic differences indicate topological changes in the frontier orbitals due to a transformation from an oligoene  $\pi$ - $\pi^*$  excitation to a “push-pull”  $n$ - $\pi^*$  transition; giving rise to an intramolecular charge transfer (ICT).<sup>30</sup> We performed time-dependent density functional theory (TD-DFT)<sup>31</sup> calculations at the B3LYP/6-31\*\* level on **DPDC5** and **DPDC5-NMe<sub>2</sub>** to investigate their excited states and the topologies of relevant molecular orbitals. In each case we found that the lowest-energy excitation is predominantly promotion of an electron from the HOMO to the LUMO, and in each case this transition is strongly allowed. We show these frontier orbitals for each molecule in Figure 2.7c and 2.7d, respectively. The LUMOs of **DPDC5** and **DPDC5-NMe<sub>2</sub>** are remarkably similar: each is primarily the expected, lowest-energy  $\pi^*$ -orbital of a conjugated polyene. However, the HOMOs of the two molecules differ. While the HOMO of **DPDC5** is primarily the expected, highest-energy  $\pi$ -orbital of the polyene, in **DPDC5-NMe<sub>2</sub>** there is significant electron density on the terminal aryl groups and the nitrogen lone pairs. A similar trend in the frontier orbitals is predicted even when the cyano groups are removed from the oligoene core (see Appendix A) implying that the cyano groups contribute less to the intramolecular charge transfer (ICT) than do the NMe<sub>2</sub> groups. Thus while the HOMO-LUMO excitation in **DPDC5** is largely  $\pi$ - $\pi^*$ , that in **DPDC5-NMe<sub>2</sub>** has a significant component of  $n$ - $\pi^*$  character. This may be considered ICT.<sup>29</sup>

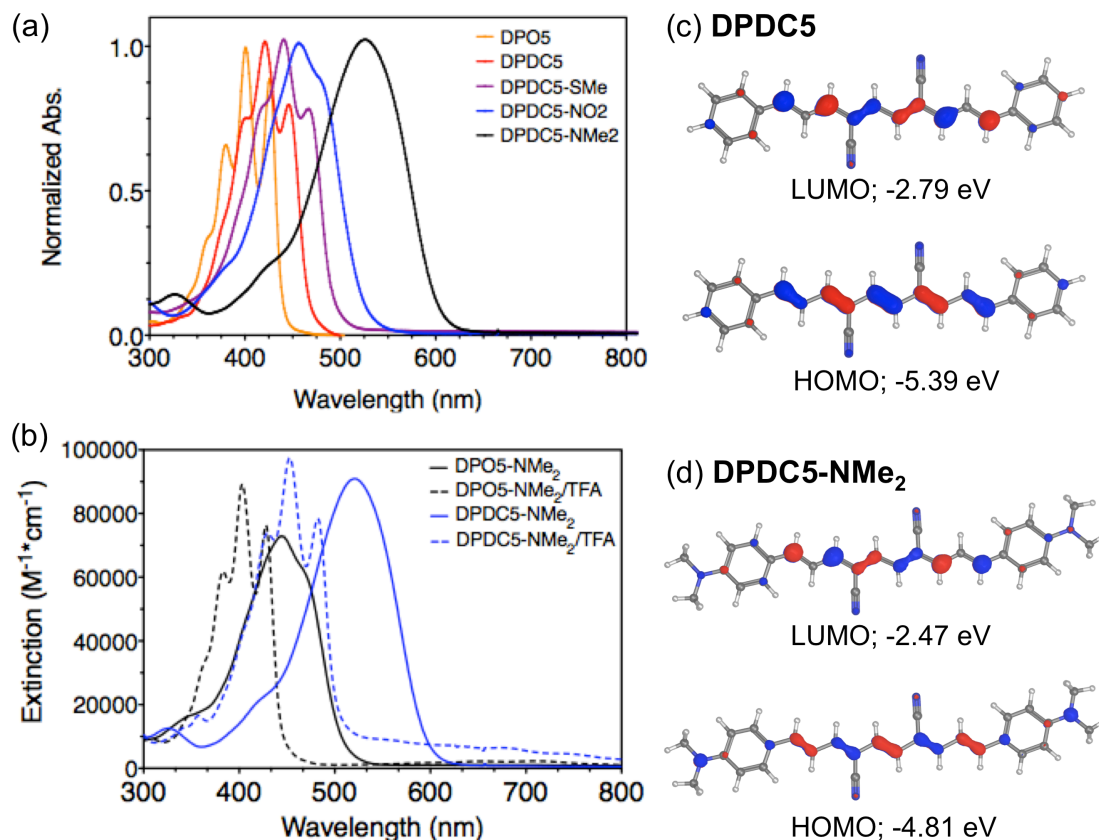


**Figure 2.7:** (a) UV-vis absorption spectra of oligoene derivatives in CH<sub>2</sub>Cl<sub>2</sub>; **DPO5** (orange), **DPDC5** (red), **DPDC5-SMe** (purple), **DPDC5-NO<sub>2</sub>** (blue) and **DPDC5-NMe<sub>2</sub>** (black). For easy comparison absorptions have been normalized to 1. (b) Absorption spectra of protonated (solid line) and deprotonated (dashed line) forms of **DPDC5-NMe<sub>2</sub>** (black) and **DPO5-NMe<sub>2</sub>** (blue) in CH<sub>2</sub>Cl<sub>2</sub>. TD-DFT calculations compare the LUMO and HOMO of (c) **DPDC5** and (d) **DPDC5-NMe<sub>2</sub>**.

Since the HOMO-LUMO transition in **DPDC5-NMe<sub>2</sub>** is due, at least in part, to n- $\pi^*$  promotion, protonation of the nitrogens should remove the nitrogen lone pair from participation in the HOMO and therefore quench any ICT, leaving behind the  $\pi$ - $\pi^*$  absorptions of the oligoene. Indeed, addition of trifluoroacetic acid to solutions of **DPDC5-NMe<sub>2</sub>** and **DPO5-NMe<sub>2</sub>** resulted in a hypsochromic shift and resolution of the

vibronic fine-structure as seen in Figure 2.7b. The effect is reversible; when we neutralize the erstwhile acidic solutions with triethylamine, absorption is again shifted to the red and the vibronic structure is lost.

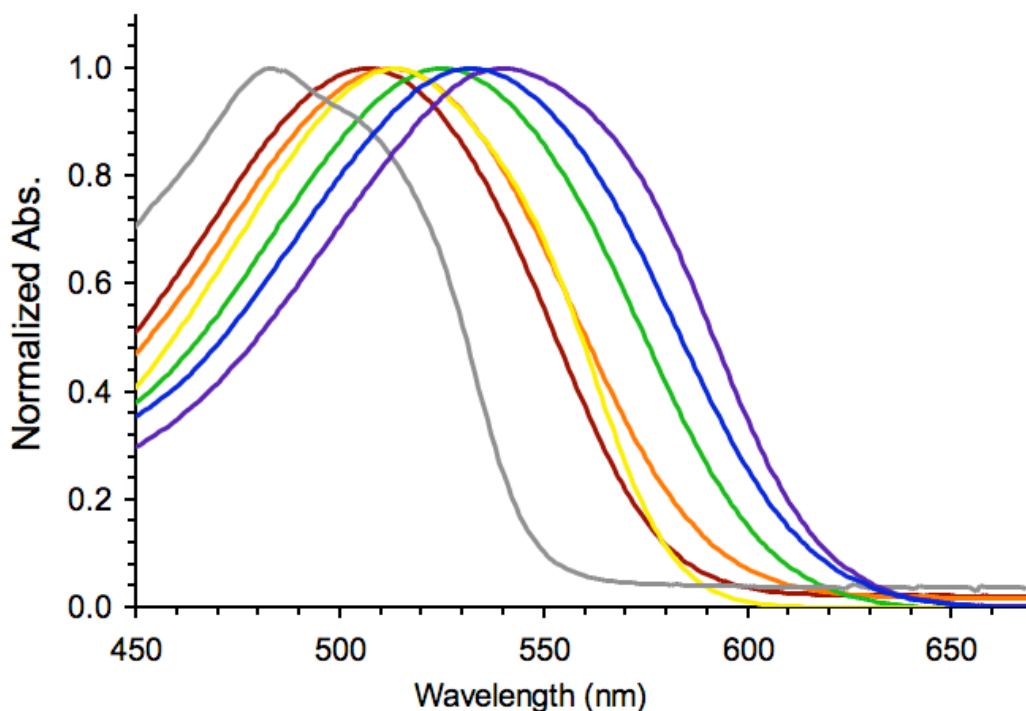


**Figure 2.8.** Solvatochromic behavior of **DPDC5-NMe<sub>2</sub>** selected solvents; heptane (grey) ethyl acetate (red), acetone (orange), toluene (yellow), chlorobenzene (green), DMSO (blue), and nitrobenzene (purple). Spectra are normalized to 1.0 abs. Absorption data from 15 different solvents is tabulated in Appendix A.

Solvatochromism may be used to assess the amount of ICT behavior in conjugated push-pull systems, since the polarizability of  $\pi$ -electrons partially depends on the environment provided by the solvent, such as solvent polarizability and cavity size.<sup>29</sup> The absorption behavior of **DPDC5-NMe<sub>2</sub>** was surveyed throughout fifteen organic

solvents. In figure 2.8, the  $\lambda_{max}$  was observed to shift 55 nm from solutions of heptane to nitrobenzene, while the longest-wavelength absorption shifted 70 nm from heptane to dimethyl sulfoxide (DMSO). Absorption data for all solvents has been placed in Appendix A.

### 2.3.2. Solubility Enhancements

The rigid structure of conjugated oligoenes leaves them sparingly soluble in organic solvents and hinders solution-based processing techniques such as spin-casting or inkjet printing. This is an important obstacle for promising organic electronic materials to overcome for application in film-based technologies. Again, we take advantage of the facile functionalization of phenyl end-groups in order to enhance oligoene solubility. Long alkoxy groups and bulky thioethers (Table 2.2, entries 6-10) tune the solubility over a wide range while maintaining consonant electronic properties (based on UV-vis absorption, as well as  $^1\text{H}$ - and  $^{13}\text{C}$ -NMR spectra; Appendix A). For example, **DPDC5-OC<sub>14</sub>H<sub>29</sub>** and **DPDC5-SC<sub>5</sub>H<sub>10</sub>** reach molarities up to  $\sim 0.10$  M in chloroform at room temperature; increasing the solubility from  $\sim 10^{-4}$  M for **DPDC5**. These derivatives are also soluble in other common organic solvents such as toluene, tetrahydrofuran, and benzene. Using this synthetic approach, longer alkoxy chains or even polymeric attachments are presumed to be possible.

### 2.3.3. Tuning the Solid-state Assembly through End-functionalization

The molecular organization in the solid state changes when we functionalize the DPDCs with carboxylate groups. Unlike the pentaene of the parent series (**DPDC5**),



crystals of **DPDC5-CO<sub>2</sub>H** contain two molecules of solvent, dimethylformamide (DMF), per oligoene and do not organize in a herringbone structure. In Figure 2.9c we show that hydrogen bonding with DMF facilitates the assembly of the carboxylic acids into  $\pi$ -stacked sheets of oligoenes. The lack of solvent between oligoenes allows for the intermolecular distances to decrease to 3.38 Å between  $\pi$ -faces of neighboring molecules. These values approach the interplanar distances found for the classic carbon allotrope, graphite; 3.35 Å.<sup>33</sup> **DPDC5-CO<sub>2</sub>H** stacks in an oblique alignment with six close neighbors oriented in a hexagonal pattern when viewed down the length of the molecule.<sup>34</sup> All molecules in the crystal are aligned in the same direction and overlap with neighboring molecules through  $\pi$ -stacking interactions. This is an ideal geometry for charge transport through a single crystal.

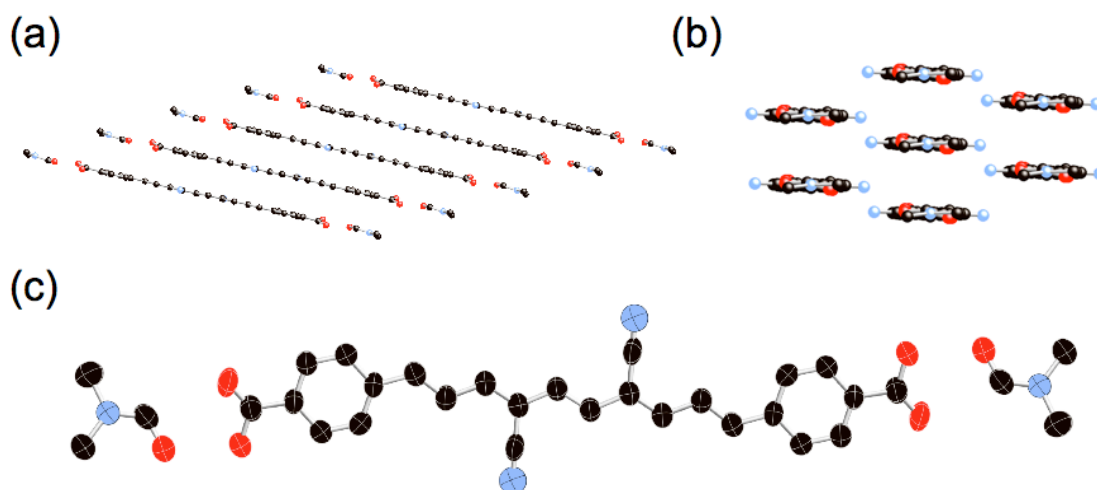


**Figure 2.9:** Packing structure of **DPDC5-CO<sub>2</sub>H•2DMF** (a) viewed from the side and (b) down the length of oligoene chain. (c) Ellipsoids represent 50% probability levels. Hydrogen atoms have been omitted.

## 2.4. Material Applications

Despite the unique electronic properties of oligoenes, such as large extinction coefficients, broad absorptions and low band gaps, they have not made particularly useful electronic materials. Not only has solubility and instability, but other factors, such as control over their assembly, have hindered applications as thin-film materials in organic photovoltaics (OPV's) and organic field-effect transistors (OFET's) and also in liquid crystalline arrays. However, oligoenes are not predicted to be useful as organic light-emitting diodes (OLED's), since they have low fluorescent quantum yields.

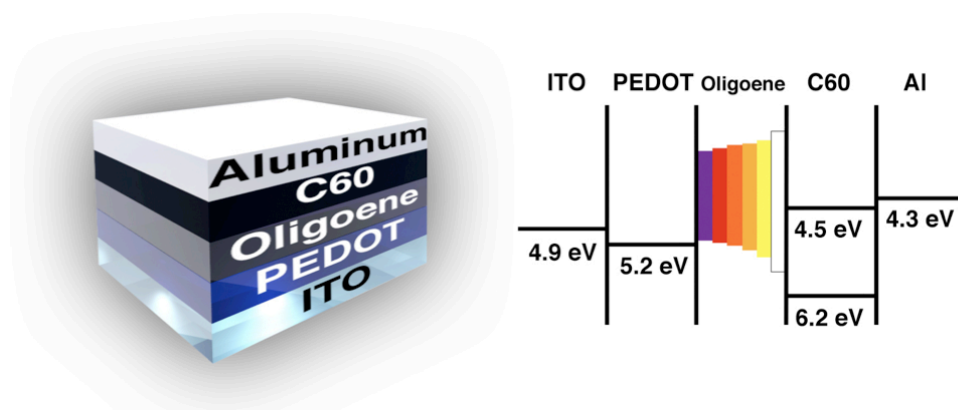


**Figure 2.10:** OPV device architecture. (left) Donor-acceptor bilayer device using indium tin oxide (ITO) as the transparent cathode and thermally deposited aluminum as the anode. (right) Band gap alignment diagram, demonstrates how to tune the energies of the MO's to align with other elements of the device (i.e. the work functions of the metal electrodes and the orbitals of the acceptor material) simply by changing the length of the oligoene donor.

To investigate potential in photovoltaics, bilayer OPV's of **DPDC5-DPDC9** were prepared by thermal deposition of the donor layer (oligoene) atop an acceptor ( $C_{60}$ ) layer over ITO/PEDOT. The schematic of the device architecture is displayed in Figure 2.10.

Efficiencies for these devices were low, reaching  $\sim 0.5\%$  under 1 sun (AM1.5G) standard solar illumination in air for **DPDC9**. Similarly, OFET devices constructed by spin-coating hot solutions of **DPDC11** in THF onto silicon oxide surfaces yielded devices with low performance. Even though device performance was poor, conductance values doubled after devices were exposed to iodine vapor for twenty minutes and could be the result of  $I_2$ -doped oligoene films.

#### 2.4.1. Self-assembly of Oligoenes on Semiconducting Surfaces

As a demonstration of how end-functionalized oligoenes allow for their incorporation as molecular wires into molecular architectures, we used carboxylic acid-functionalized oligoenes (**DPDC3-CO<sub>2</sub>H**) to assemble monolayers of magnetic nanoparticles on GaAs substrates. It has been shown previously that carboxylic acids bind to GaAs<sup>35</sup> and Fe<sub>3</sub>O<sub>4</sub> through known ligand exchange procedures.<sup>36</sup> In fact, preliminary ligand exchange studies found that the addition of **DPDC3-CO<sub>2</sub>H** solutions to solutions of 10-nm and 5-nm magnetite nanoparticles in DMF lead to the immediate formation of an insoluble dark grey solid, which could not be characterized. Therefore, we presumed that our carboxylates readily undergo ligand exchange at the nanoparticle surface.

To form a self-assembled monolayers (SAMs) atop a GaAs surface, the native oxide layer of the GaAs substrates were removed through submersion in aqueous ammonium hydroxide (NH<sub>4</sub>OH). After rinsing with ethanol they were submerged in a 1.5 mM solution of oligoene (**DPDC3-CO<sub>2</sub>H**) in DMSO. They were then removed from solution, again rinsed with ethanol, and submerged for 1 hour in a solution of 10-nm

$\text{Fe}_2\text{O}_4$  nanoparticles in DMF. Scanning electron microscopy (SEM) analysis of these films shows clear formation of nanoparticle monolayers as shown in Figure 2.11a. At low concentration of oligoene coverage was complete; yielding a compact monolayer of nanoparticles that coats the entire surface with long-range uniformity. Nanoparticle coverage was found to be dependent upon the concentration (1.5 mM, 3.0 mM, or 6.0 mM) of the oligoene solution. When solutions of 3.0 mM (Figure 2.11b) and higher were used, multilayer coverage was observed. As a control, no monolayer formation was observed when only DMSO without oligoene was used or upon the direct submersion of the GaAs substrate into the nanoparticle solution (see Appendix A).

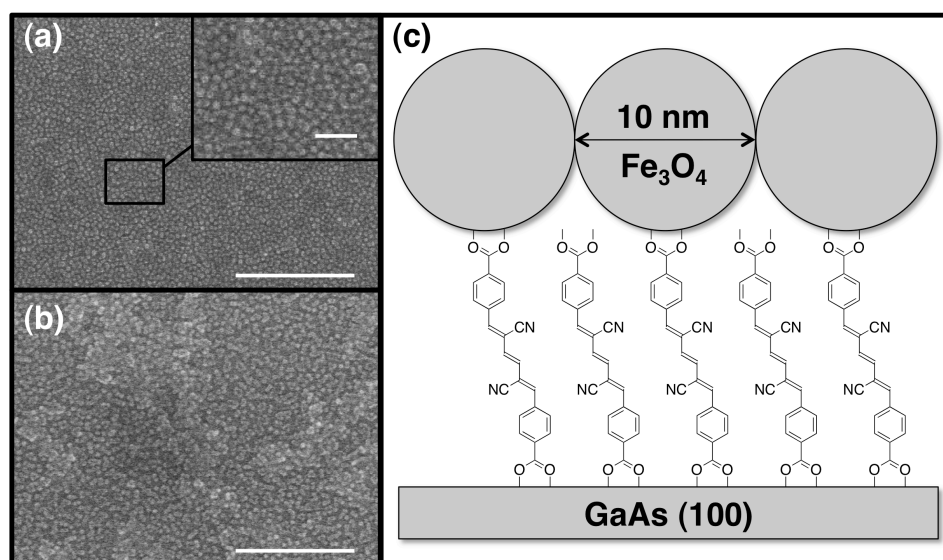


**Figure 2.11:** Scanning electron micrographs (SEM) of 10-nm  $\text{Fe}_3\text{O}_4$  nanoparticle SAMs made using (a) 1.5 mM and (b) 3.0 mM solution of **DPDC3-CO<sub>2</sub>H**, show monolayer coverage at low concentrations and the presence of multilayers at higher concentration. Scale bars are set to 500 nm, while insert scale bar is set to 50 nm. (c) Schematic of oligoene- $\text{Fe}_3\text{O}_4$  composite monolayer.

## 2.5. Conclusions and Future Outlook

We have developed a new method to synthesize cyano-substituted oligoenes with up to thirteen all-*trans* conjugated C=C bonds, and have demonstrated its utility in the synthesis of a wide variety of aryl-functionalized oligoenes. These materials are highly tunable summarized in Figure 2.12. Cyano groups decrease the band gap of oligoenes and stabilize them for study under normal laboratory conditions while preserving the conjugation along the poly-olefin backbone. Derivatization of the terminal phenyl groups allows us to fine-tune the electronic structure and physical properties. We can access practically any energy within the visible spectral region by pairing the appropriate oligoene length with the appropriate aryl end-group.

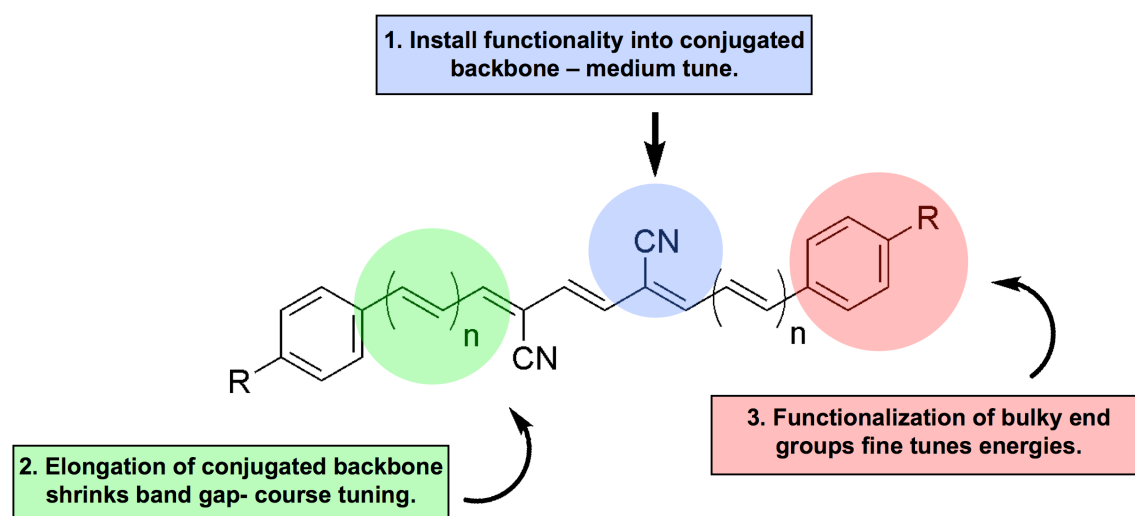


**Figure 2.12:** Three ways to tune the band gap of oligoene materials: (1) main-chain cyano groups lower the energies of the frontier orbitals relative to unfunctionalized conjugated backbones; (2) the length-dependent properties greatly effect the band gap, while (3) end-functionalization can fine-tune the gap amongst each oligomeric length.

Functionalized oligoenes are ideal structures for nanoscale electronic and structural components and can be used to guide oligoene self-assembly and the construction of heterogeneous materials. Furthermore, the utility of these materials in photovoltaics is an obvious application since their band gaps are easily tuned, their absorptions are broad and cover the visible spectrum, and their extinctions coefficients are large. DPDC molecules are also predicted to be useful in singlet fission,<sup>37</sup> since their first excited triplet state is ( $T_1$ ) is well positioned (energetically) to undergo such a process. We are currently building devices that utilized singlet-fission for use in photodetection and photovoltaics.

## 2.6. References and Footnotes

1. (a) C. K. Chiang, M. A. Druy, S. C. Gau, A. J. Heeger, E. J. Louis, A. G. MacDiarmid, Y. W. Park, H. Shiraka, *J. Am. Chem. Soc.*, **1978**, *100*, 3, 1013–1015. (b) Y. W. Park, A. J. Heeger, M. A. Druy, A. G. MacDiarmid, *J. Chem. Phys.*, **1980**, *73*, 946–957.
2. (a) F. Kajzar, S. Etemad, G. L. Baker, J. Messier, *Solid State Comm.*, **1987**, *63*, 1113–1117. (b) W. S. Fann, S. Benson, J. M. J. Madey, S. Etemad, G. L. Baker, F. Kajzar, *Phys. Rev. Lett.*, **1989**, *62*, 1492–1495.
3. (a) R. R. Burch, Y. Dong, C. Fincher, M. Goldfinger, P. E. Rouviere, *Synth. Metals*, **2004**, *126*, 43–46. (b) J. He, F. Chen, J. Li, O. F. Sankey, Y. Terazono, C. Herrero, D. Gust, T. A. Moore, A. L. Moore, S. M. Lindsay, *J. Am. Chem. Soc.*, **2005**, *127*, 5, 1384–1385. (c) I. Visoly-Fisher, K. Daie, Y. Terazono, C. Herrero, F. Fungo, L. Otero, E. Durantini, J. J. Silber, L. Sereno, D. Gust, T. A. Moore, L. A. Moore, S. M. Lindsay, *Proc. Natl Acad. Sci. USA*, **2006**, *103*, 23, 8686–8690.
4. (a) K. Knoll, K. A. Krouse, R. R. Schrock, *J. Am. Chem. Soc.*, **1988**, *110*, 4424–4425. (b) K. Knoll, R. R. Schrock, *J. Am. Chem. Soc.*, **1989**, *111*, 7989–8004. (c) C. Scriban, B. S. Amagai, E. A. Stemmler, R. L. Christensen, R. R. Schrock, *J. Am. Chem. Soc.*, **2009**, *131*, 13441–13452.

5. The symbols,  $\mu$  and  $\nu$ , are used to designate central positions along the oligoene main chain, because they are the middle letters in the Greek alphabet. This nomenclature is unprecedented, but serves to distinguish central locations from the terminal locations,  $\alpha$  and  $\omega$ .
6. R. Kuhn, *Angew. Chem.*, **1937**, *50*, 703–718.
7. A. Kiehl, A. Eberhardt, K. Müllen, *Lieb. Ann. Chem.*, **1995**, 223–230.
8. D. Klein, P. Kiliçkiran, C. Mlynek, H. Hopf, I. Dix, P. G. Jones, *Chem. Euro. J.*, **2010**, *16*, 34, 10507–10522.
9. (a) C. W. Spangler, R. K. McCoy, A. A. Dembek, L. S. Sapochak, B. D. Gates, *J. Chem. Soc., Perkin Trans. 1*, **1989**, 151–154. (b) C. W. Spangler, P. K. Liu, A. A. Dembek, K. Havelka, *J. Chem. Soc., Perkin Trans. 1*, **1991**, 799–802.
10. (a) L. Duhatuel, P. Duhamel, *Tetrahedron*, **1993**, *34*, 7399–7400. (b) W. Froehlich, H. J. Dewey, H. Deger, B. Dick, K. A. Klingensmith, W. Puettmann, E. Vogel, G. Hohlneicher, J. Michl, *J. Am. Chem. Soc.*, **1983**, *105*, 6211–6220.
11. (a) H. Nakamichi, T. Okada, *Angew. Chem. Int. Ed.*, **2006**, *45*, 4270–4273. (b) G. Duester, *Cell*, **2008**, *134*, 921–931. (c) T. Polí'vka, H. A. Frank, *Acc. Chem. Res.*, **2010**, *43*, 1125–1134. (d) For general carotenoid reference see: H. A. Frank, G. Britton, A. J. Young, A. Young, R. J. Cogdell, in *The Photochemistry of Carotenoids*, Springer-Verlag. New York, **2000**.
12. (a) H. J. Schneider, V. Hoppen, *J. Org. Chem.*, **1978**, *43*, 3866–3873. (b) H. Booth, J. R. Everette, *J. Chem. Soc., Chem. Comm.*, **1976**, 278–279.
13. (a) O. W. Webster, *J. Polym. Sci., Part A: Polym. Chem.*, **2002**, *40*, 210–221. (b) M. S. Liu, X. Jiang, S. Liu, P. Herguth, A. K.-Y. Jen, *Macromolecules*, **2002**, *35*, 3532–3538. (c) Y.-F. Lim, Y. Shu, S. R. Parkin, J. E. Anthony, G. G. Malliaras, *J. Mat. Chem.*, **2009**, *19*, 3049. (d) M. L. Kaplan, R. C. Haddon, F. B. Bramwell, F. Wudl, J. H. Marshall, D. O. Cowan, S. Gronowitz, *J. Phys. Chem.*, **1980**, *84*, 427–431. (e) M. J. Ahrens, M. J. Fuller, M. R. Wasielewski, *J. Mat. Chem.*, **2003**, *15*, 2684–2686.
14. C. Hansch, A. Leo, R. W. Taft, *Chem. Rev.*, **1991**, *91*, 165–195.
15. E. Knoevenagel, *Chem. Ber.*, **1898**, *31*, 2596–2619.
16. (a) G. Wittig, U. Schoellkopf, *Chem. Ber.*, **1954**, *87*, 1318–1330. (b) G. Wittig, W. Haag, *Chem. Ber.*, **1955**, *88*, 1654–1666.

17. The Cannizzaro reaction is a Aldehyde disproportionation reaction beginning with nucleophilic attack on the electrophilic carbonyl center from a hydroxide anion, therefore forming the tetrahedral intermediate. Hydride transfer occurs as the newly charged species attack a second aldehyde forming an alkoxide and acid anion, which exchange a final proton, resulting in an alcohol and carboxylate. See, Cannizzaro, S., *Liebigs Annalen*, **1853**, 88, 129–130.
18. G. McDermott, S. M. Prince, A. A. Freer, A. M. Hawthornthwaite-Lawless, M. Z. Papiz, R. J. Cogdell, N. W. Isaacs, *Nature*, **1995**, 374, 517–521.
19. (a) J. G. J. Kok, R. Van Moorselaar, A. Noordermeer, *Verfahren zum Faerben synthetischer Harze und gefaerbte Harze*, June 23 1972, DE 2230783. (b) C. M. Langkammerer, *Reaction products of 3-hexenedinitrile and certain aldehydes*, February 22 1949, US 2462407.
20. S. Gorter, E. Rutten-Keulemans, M. Krever, C. Romers, D. W. J. Cruickshank, *Acta Cryst.*, **1995**, B51, 1036–1045.
21. W. S. Wadsworth, *Org. React.*, **1977**, 25, 73.
22. Stability of **DPDCn series** was observed by <sup>1</sup>H-NMR and thin layer chromatography over the duration of 6 months. When stored at 0° C in the absence of light **DPDCn** and **DPOn** series showed no signs of degradation. When stored on the bench top in ambient conditions **DPDC3-DPDC7** also did not degrade. However, the degradation of **DPDC9-DPDC13** were observed and increased with increased molecular length. Broadened peaks were found in their <sup>1</sup>H-NMR spectra and **DPDC13** was observed to lighten in color. At short lengths (n = 3 to 7) **DPDCn** and **DPOn** series are stable in ambient conditions. Further comparisons between the each series were limited, since we were unable to synthesize/characterize longer **DPOn** molecules due to very low solubility.
23. (a) F. Bohlmann, H. J. Mannhardt, *Chem. Ber.*, **1956**, 89, 1307–1315. (b) P. Nayler, M. C. Whiting, *J. Chem. Soc.*, **1955**, 3037–3047. (c) F. Sondheimer, D. A. Ben-Efraim, R. Wolovsky, *J. Am. Chem. Soc.*, **1961**, 83, 1675–1681. (d) F. Sondheimer; D. A. Ben-Efraim, Y. Gaoni, *J. Am. Chem. Soc.*, **1961**, 83, 1682–1685.
24. Dilute solutions (~10<sup>-4</sup> M) of **DPO5** and **DPDC5** were prepared and irradiated with a 450 W ACE mercury lamp (#7825-34) at room temperature. This procedure was



carried out under both aerobic and anaerobic conditions. We observed degradation of **DPO5** and **DPDC5** through the loss of their longest-wavelength absorbance by UV-vis spectrometry.

25. Y. Geerts, G. Klaerner, K. Muellen, in *Electronic materials: The Oligomeric Approach*, Ed. K. Muellen, G. Wegner, Wiley-VHC, New York, **1998**, p. 3–25, 360 and 406–410, and references therein.
26. Reported experimental values for polyacetylene cover a wide range owing to different methods of polymer and film preparation. See the following and references therein: (a) H. Fujimoto, K. Kamiya, J. Tanaka, *Synth. Metals*, **1985**, *10*, 367–375. (b) K. A. O. Starzewki, G. M. Bayer, *Angew. Chem. Int. Ed.*, **1991**, *30*, 961–962. (c) F. Krausz, P. Lásztity, J. S. Bakos, *Appl. Phys. B*, **1988**, *45*, 21–25.
27. Meier, H.; Stalmach, U.; Kolshorn, H. *Acta Polym.* **1997**, *48*, 379–384.
28. (a) M. Rumi, A. Kiehl, G. Zerbi, *Chem. Phys. Lett.*, **1994**, *231*, 70–74. (b) V. Hernandez, C. Castiglioni, M. Del Zoppo, G. Zerbi, *Phys. Rev B*, **1994**, *50*, 9815. (c) J. L. Brédas, R. Silbey, D. S. Boudreaux, R. R. Chance, *J. Am. Chem. Soc.*, **1983**, *105*, 6555–6559.
29. (a) B. E. Kohler, *J. Chem. Phys.*, **1988**, *88*, 2788–2792. (b) B. E. Kohler, C. Spangler, C. Westerfield. *J. Chem. Phys.*, **1988**, *89*, 5422–5428.
30. (a) B. Breiten, Y.-L. Wu, P. D. Jarowski, J.-P. Gisselbrecht, C. Boudon, M. Griesser, C. Onitsch, G. Gescheidt, W. B. Schweizer, N. Langer, C. Lennartz, F. Diederich, *Chem. Science*, **2011**, *2*, 88. (b) L.-O. Pålsson, C. Wang, A. S. Batsanov, S. M. King, A. Beeby, A. P. Monkman, M. R. Bryce, *Chem. Euro. J.*, **2010**, *16*, 1470–1479.
31. DFT calculations were run in the gas phase using *Jaguar* (version 7.7, Schrodinger LLC, New York, NY, **2010**).
32. (a) F. Bures, O. Pytela, F. Diederich, *J. Phys. Org. Chem.*, **2011**, *24*, 274–281. (b) F. Bovey, S. Yanari, *Nature*, **1960**, *186*, 1042–1044.
33. Y. Baskin, L. Meyer, *Phys. Rev.*, **1955**, *100*, 544.
34. The oblique packing structures of **DPDC7-DPDC13** and **DPDC5-COOH** differ from the herringbone-type structure found in polyacetylene, which more closely resemble structures for **DPDC3** and **DPDC5**. See: C. R. Fincher, C.-E. Chen, A. J. Heeger, A. G. MacDiarmid, J. B. Hastings, *Phys. Rev. Lett.*, 1985, **48**, *2*, 100–104. The closest

oligomeric approximation of the structure of polyacetylene can be made with *trans*-1,3,5,7-octatetraene, see: R. H. Baughman, B. E. Kohler, I. J. Levy, C. Spangler, *Synth. Metals*, **1985**, *11*, 37–52.

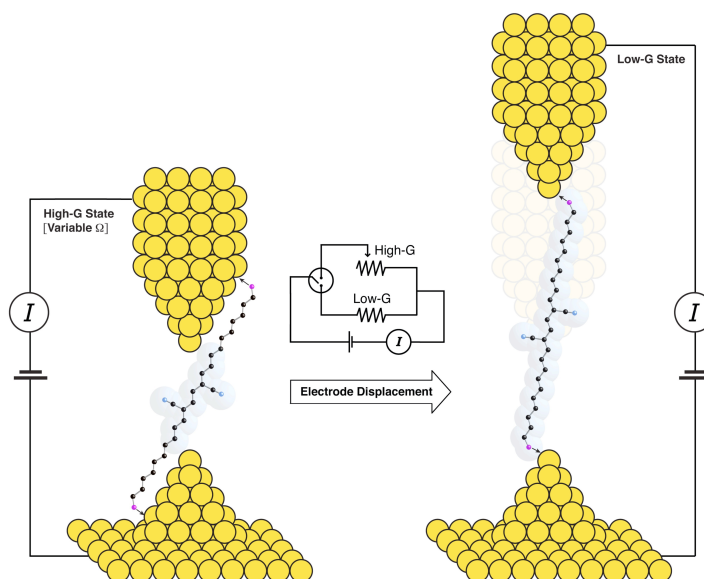
35. J. Martz, L. Zuppiroli, F. Nüesch, *Langmuir*, **2004**, *20*, 11428–11432.

36. A. Dong, X. Ye, J. Chen, Y. Kang, T. Gordon, J. M. Kikkawa, C. B. Murray, *J. Am. Chem. Soc.*, **2011**, *133*, 998–1006.

37. B. M. Smith, J. Michl, *Chem. Rev.*, **2010**, *110*, 6891–6936.

## Chapter 3. Oligoenes in Single-molecule Electronics<sup>†</sup>

*The molecules in Chapter 3 were synthesized by myself with the assistance of Markrete Krikorian. The single-molecule STM-BJ measurements were performed by Maria Kamenetska. DFT calculations were performed by Michael Steigerwald.*



### 3.1. Motivations

Understanding and controlling charge transport through molecular devices is critical, not only to the realization of molecular sized devices, but also in advancing the performance of organic based electronics.<sup>1,2</sup> For such devices, it is insufficient simply to ascertain that certain molecular backbones can conduct; one must predict, and ultimately control, molecular conductance. In this chapter a new type of single-molecule electronic device is described, which we are able to predictably adjust the conductance of the individual molecular circuit over a well-defined range.<sup>3</sup> In doing so, the length-dependent

<sup>†</sup> Parts of Chapter 3 were reproduced with permission from the authors: Meisner, J. S.; Kamenetska, M.; Krikorian, M.; Steigerwald, M. L.; Venkataraman, L.; Nuckolls, C., *Nano Lett.*, **2011**, 11 (4), 1575–1579; Copyright 2011 American Chemical Society.

charge-transport properties through a series systematically elongated oligoenes (**An** and **Bn**) that have been end-functionalized were quantified.

### 3.1.1. Oligoene Single-molecule Wires

Very few reports of molecular junctions formed from oligoenes has been reported. Oligoenes that require specific end-functionalizations can be difficult to synthesize. Also, STM-BJ measurements are often carried out in air under normal conditions, which may lead to oligoene decomposition, especially in terminal oligoenes. The first reported oligoene single-molecular junction appeared in 2003, where Lindsay and coworkers<sup>4</sup> synthesized a terpenoid-based linear nonaene terminated with benzyl thiols. Known to interact strongly with gold, the dithiol was embedding into a docosanyl thiol monolayer, from which a bottom chemicontact to a gold substrate was established. Steric congestion oriented the molecule like the docosanes and away from the surface. Gold nanoparticles were bound to the second thiol and used as top contacts. Electrical measurements were then made by contacting those nanoparticles with a gold-coated AFM probe tip. Because only one compound was measured they were unable to obtain information about the electrical decay constants ( $\beta$ ). It was not until their later reports, where two similar families of oligo-terpenoids we measured: (1) a series of three pyridyl and (2) four benzyl thiol end-functionalized carotenoids.<sup>5</sup> Differences in the effective contact resistance due to atomic constitution of the electrode binding groups (pyridyl vs.  $\text{ArCH}_2\text{SH}$ ) can be observed between each series. The decay constants, however, were in closer agreement with one another ( $\beta_{\text{pyr}} = 0.17 \pm 0.03 \text{ \AA}^{-1}$  and  $\beta_{\text{thiol}} = 0.22 \pm 0.04 \text{ \AA}^{-1}$ ).

Outside of the conducting probe AFM/nanoparticle technique oligoenes have not been studied further, nor have any non-terpenoid oligoenes, which are predicted to be better suited for electronic transport because they do not contain main-chain methyl groups that distort the planar structure due to allylic-1,3-strain.<sup>6</sup> Here, we investigate the charge transport properties of two families of non-terpenoid oligoenes using the STM-BJ technique. Each family contains five oligomeric vinylogues that range from the triene to the undecene.

### 3.1.2. Scanning Tunneling Microscope Break Junctions (STM-BJ's)

Using a custom-built STM, cut or etched gold STM tips and Au (011) surfaces are used as the macroscopic bottom and top contacts. Current is continually measured allowing us to monitor junction formation and rupture processes, as well as record the current that flows through single-molecule junctions. A step-by-step schematic of this process is given in Figure 3.1A. The STM begins in the open position with the tip-displaced from the surface. Then each is brought into contact via piezoelectric controls forming Au-Au bonds. Next, the tip is displaced from the surface and, as this occurs, the Au-Au chemicontacts begin thinning down until the bridging metal becomes as thick as a single Au atom. These pre-electrodes are referred to as gold atomic point-contacts, which have a conductance equal to the quantum of conductance ( $G_0 = 2e^2/h$ ) and is highlighted by a dashed arrow in Figure 3.1B. Further displacement ruptures the point contacts, breaking the circuit and leaving under-coordinated Au-atoms at the surface of the tip and substrate. When these point contacts are broken in a solution of molecular wires, we are able to trap individual molecules (sometimes multiple molecules) between the electrodes.

Three sample traces are shown in Figure 3.1B. Point contact rupture is clearly visible by a large drop in conductance (after the dashed arrow), to a lower conductance plateau (solid arrow) signifying the formation of a molecular junction. When we elongate further, the junction ruptures and conductance ceases.

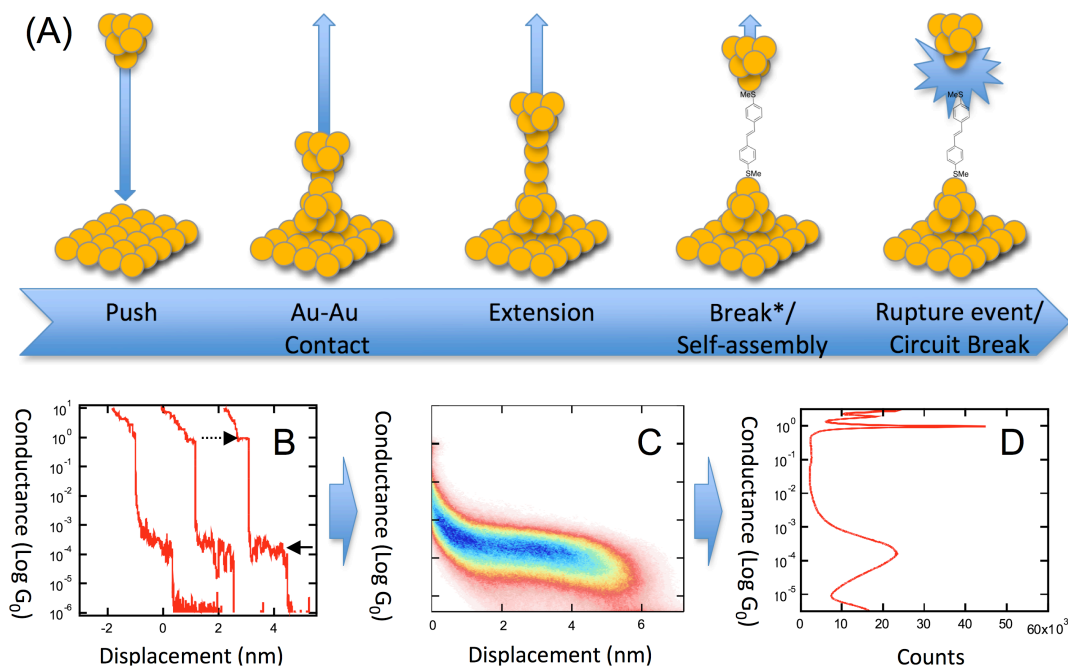


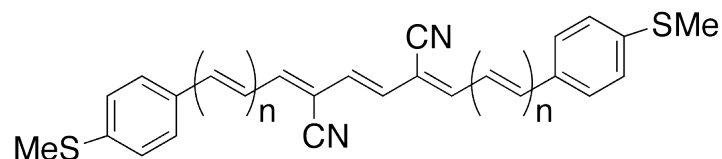
**Figure 3.1:** STM-BJ method. (A) Step-by-step visualization of STM-BJ formation and rupture. (B) Examples of individual conductance-displacement traces measured from a single-molecule junction using the STM-BJ technique. By combining thousands of these traces together histographical analysis containing statistically relevant data can be viewed as (C) 2D conductance-displacement or (D) 1D conductance histograms.

Junction-to-junction variance is observed when measuring single-molecules. Therefore, we run thousands of measurement and generate thousands of traces, which we compile into histograms giving statistically relevant data. Generally, we use unselected

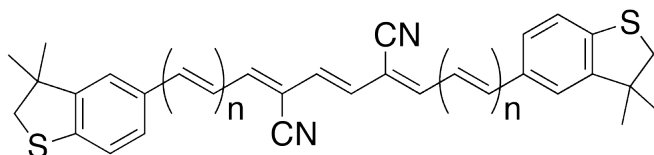
data to construct our histograms without the refinement of choice data to give an accurate account of our junctions.

### 3.1.3. End-Functionalized DPDC Molecular Wires

The design of the molecular wires is shown in Figure 3.1A. They are  $\alpha,\omega$ -diphenyl- $\mu,\nu$ -dicyano-oligoenes (DPDC), which have been end-functionalized with methylsulfide (Ar-SMe)<sup>7</sup> or cyclic alkylsulfide (Ar-SR, where R completes a 3,3-dimethyl-2,3-dihydrobenzo[*b*]thiophene) end-group. These end-groups are localized, two-electron donor and are *aurephilic*, meaning that they readily interact with Au (*aurophilic*), forming dynamic donor-acceptor bonds. These end-groups are important and referred to as linkers, since they act as terminal contacts, which serves as the physical anchor linking the molecule to the electrodes in a molecular junction. Secondly, the electrical variable-contact is the set of alternating  $\pi$ -bonds that form the conjugated  $\pi$ -space of a linear oligoene. During the conductance measurement, electronic coupling of the electrodes to the terminal contacts results in a low fixed junction conductance, while additional direct coupling through the  $\pi$ -space leads to higher tunable junction conductance. Basically, as the contact moves along the molecular  $\pi$ -space (over a distance of more than 1 nm), the device conductance changes continuously. This sampled distance can be controlled easily via our piezoelectronic cantilever controls. Thus, the conductance for the molecule can be *a priori* simply by selecting the appropriate inter-electrode spacing. These experiments form the basis for a new type of tunable molecular electronic device, a single-molecule potentiometer.



**An**;  $n = 0, 1, 2, 3, \& 4$



**Bn**,  $n = 0, 1, 2, 3, \& 4$

**Figure 3.2:** Chemical structure of oligoene molecular wires, **An** and **Bn**. Each series is composed of systematically elongated members ranging in length from 3 to 11 C=C double bonds. Oligoenes are end-functionalized with (**An**) methylsulfide or (**Bn**) cyclic alkyldisulfide linkers.

For this study, we designed and synthesized two series of molecular wires that are atomically defined segments of polyacetylene,<sup>8,9</sup> each with different terminal anchor groups (**An** and **Bn** in Figure 3.2). A simple synthesis was developed that affords molecules longer than 4 nm. This synthesis also tolerates a diversity of end-groups while the cyano-groups on the molecular backbone enhance molecular stability due to lowered HOMO and LUMO energies relative to vacuum (see Appendix B). The crystallographically determined molecular structures of the parent series oligomers (**DPDCn** series) show an ideal path of conjugation with alternating single and double bonds exclusively in the *trans* configuration (see Ch.2, Figure 2.3). In each series above, the color of these compounds is a strong function of the molecular length, indicating that



the HOMO-LUMO gap in these molecules decreases with increasing molecular length (see Appendix B and Ch. 2, Figure 2.5B).

### 3.2. Charge-transport Properties

We first demonstrate that these oligoenes behave as molecular wires by measuring their electrical properties using a STM-BJ method.<sup>10</sup> STM-BJ's are formed in dilute solutions of oligoene (10 mM in 1,2,4-trichlorobenzene), allowing for effective trapping of individual oligoenes between the electrodes.<sup>11</sup> We apply a constant bias voltage (between 200 and 750 mV)<sup>12</sup> and measure the current that passes between the electrodes. When oligoenes bridge the broken point-contacts we measure the conductance of these metal-oligoene-metal junctions as a function of the distance between the two electrodes. The data are recorded in the form of individual conductance traces, of which thousands are measured and compiled into histograms without any data selection to reveal statistically significant conductance values.

Oligoenes that bind to under-coordinated Au through their alkylsulfide linkers. Differences are observed between the two oligoene series (**An** and **Bn**); **An** is functionalized with methylsulfide linkers and shows a broader conductance distribution than the cyclic analogues, **Bn**.<sup>12</sup> This difference is due to the rotational freedom around the aryl-sulfur bond in the former set, which broadens the electronic coupling between the electrode and p-orbital. However, the general trends within and between the two sets are similar – incorporation of the linking sulfur atom into the five-membered ring does not significantly alter the fundamental physics, however it does simplify the analysis.

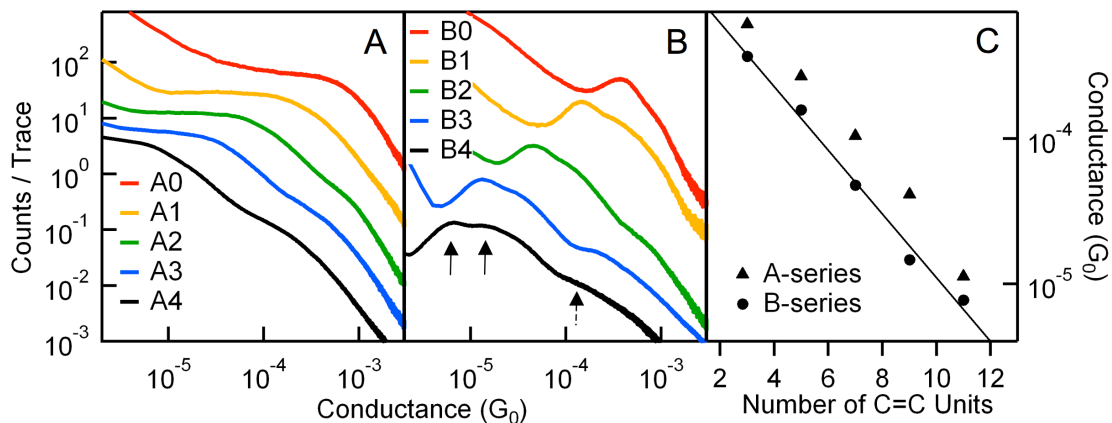


**Figure 3.3:** Linear histograms generated without data selection from >5000 conductance traces collected in the presence of each of the (A)  $A_n$  and (B)  $B_n$  molecules. The  $B_n$  series show clear peaks at molecule-specific conductance values, indicated by the solid arrow for  $B_4$ . In the longer molecules, a shoulder at higher conductance is visible, indicated by the dashed arrow for  $B_4$ . (C) Peak positions of the single-molecule conductance peaks observed for the  $A_n$  and  $B_n$  series as a function of the total number of oligoene units. For the  $A_n$  series the peak position was taken from the logarithmic histograms (see Appendix B). A linear fit to the data on the semi-log plots reveals that in both cases, conductance decays exponentially with a decay factor,  $\beta = 0.22/\text{\AA}$ .

### 3.2.1. Conductance Histograms

Within each series, the peak in the conductance histograms (Figure 3.3A and 2.3B) decays exponentially with increasing length, following the expected relation,  $G \sim e^{-\beta n}$  (Figure 3.3C). Fitting the conductance data in accordance with this relationship allows us to extract the non-resonant tunneling decay constant,  $\beta$ . The decay constant was determined to be  $\beta = 0.22/\text{\AA}$  for the  $B_n$  series, in agreement with previously published values for conjugated molecules.<sup>5</sup> Typically, histograms show a single conductance peak; however, for  $n > 1$  in  $A_n$  and  $B_n$ , in addition to the conductance peaks indicated by

arrows in Figure 3.3B, we see a second broad increase in counts at significantly higher conductance values (dashed arrow).

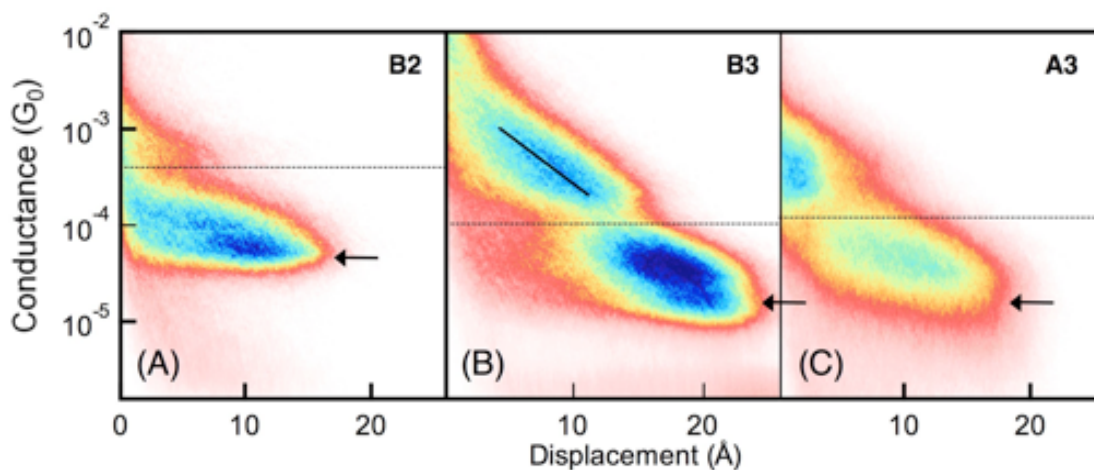


**Figure 3.4:** 2D conductance-displacement histograms preserve displacement information for (A) **B2**, (B) **B3** and (C) **A3** respectively. Comparing (A) and (B), within the same linker-family, longer molecules are able to sustain more junction elongation while remaining bound in the junction. All three molecules show a higher conductance shoulder in the region above the dashed line, corresponding to a junction geometry that forms immediately after rupture of the Au point contact. The average slope of this high conductance shoulder (solid line) reveals that conductance in this geometry decays with  $\beta \sim 0.2/\text{\AA}$  as the junction is stretched, in agreement with the decay constant shown in Figure 3.3C. Arrows indicate the corresponding peak conductance positions appearing in the 1D conductance histograms in Figure 3.3B.

### 3.2.2. Conductance-Displacement Histograms

To elucidate the two conductance regions found in the 1D histograms, we examined two-dimensional conductance histograms<sup>14,15</sup> that preserve displacement information during junction elongation. In Figure 3.4, we show 2D conductance-displacement histograms for **B2**, **B3** and **A3**, where two regions with increased counts are clearly seen, a high- and low-conductance regime (separated by the dashed line for clarity). The higher region forms immediately following the breaking of the Au point contact (at zero-displacement in this 2D histogram). The extent to which this high-conductance state persists as the junction extends depends on **n**, as well as the terminal group (see Appendix B). In Figure 3.4B, we see also that the high-conductance value decreases almost exponentially as the gap widens. Furthermore, this high-conductance region is absent in the shortest molecules.

One possibility for the two different conductance regimes is that these all-*trans* oligoenes may access two different conformations: the *s-cis* and *s-trans*. As the junction is elongated, oligoenes undergo rotations around the C-C single bonds. However, the two conformers are expected to have similar conductance; thus, rotational isomerization cannot explain this finding.<sup>16</sup>

We postulate instead that there are two independent conductance pathways. In the higher conductance state the tunneling path originates at one electrode, passes directly to the olefin backbone, thence via the sulfide to the second electrode, as illustrated in Figure 3.5A. In the lower conductance state, which occurs only when inter-electrode distances are sufficiently large, the tunneling path switches from electrode-olefin-sulfide-electrode to the more typical electrode-sulfide-olefin-sulfide-electrode.

For the shortest molecules in our study, the length of the olefin chain is comparable to the distance between electrodes upon Au-Au point-contact rupture (6-7 Å).<sup>17,18</sup> Thus, direct contact between the electrode and the backbone is rarely accommodated. As a result, no clear high-conductance peak is seen in the 1D conductance histograms of Figure 3.3A and 3.3B (see Appendix B). Other factors such as steric hindrance and the electron-withdrawing properties of the nitriles may result in only one conductance value.

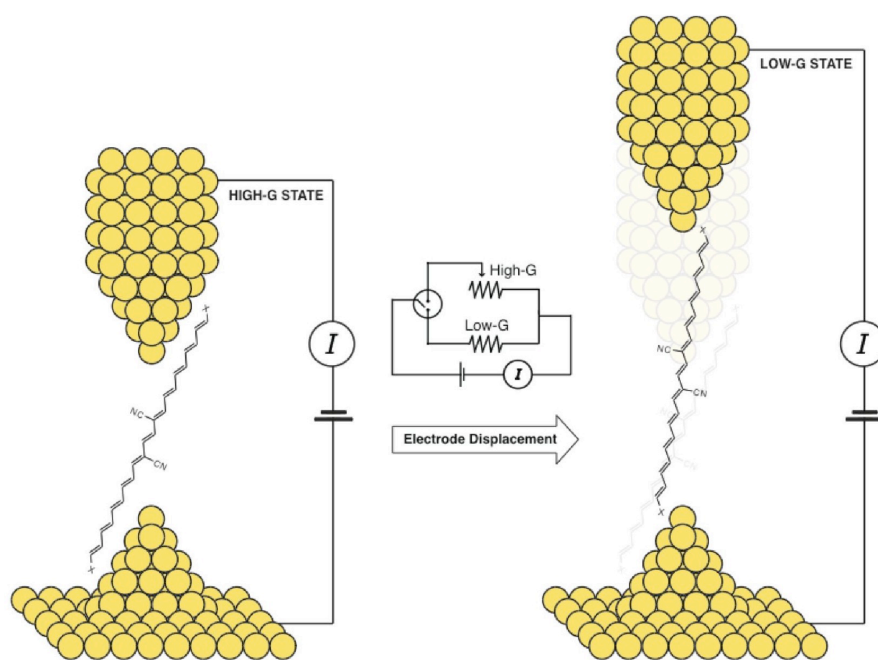


**Figure 3.5:** Schematic depiction of an oligoene break junction. Both the polyolefin chain and the end-groups, X, may act as electrical contacts. Oligoenes behave as a resistive potentiometer as the tip displaces along the olefin backbone, while the alkylthio end-groups stabilize the junction.

For the longer molecules, the initial electrode separation distance is significantly shorter than the length of our oligoenes. Although both terminal alkylthio groups anchor the oligoene to the electrodes, close proximity of the electrode to the olefin backbone results in a low-resistance pathway directly from the electrode to the olefin backbone (Figure 3.5A). As the junction is extended further, it slides up the backbone until an abrupt change in conductance is observed. Once fully extended, the oligoene is bound at the apex of each electrode, where Au atoms are no longer in proximity to the polyolefin chain, and the high-conductance state turns off. The lower conductance at this stage corresponds to the conductance through the entire molecule, and follows an exponential decay with increasing molecule length. Extending the junction further breaks the molecular circuit, and conductance is lost.

### 3.2.3. Control Molecules

One group has reported the use of nitriles as linker groups to gold electrodes.<sup>19</sup> In order to dismiss the possibility that cyano groups in the DPDC's were establishing an electrical contact to the electrode, we synthesized an oligoene analogous to **A1**, but lacking nitriles. For this molecule we observe the two-conductance states as well, indicating that the nitriles are not responsible for this two-state behavior (see Appendix B). In fact, the enhanced high-conductance state in this molecule compared to **A1** suggests that the absence of cyano groups facilitates greater coupling of the olefin to the electrode by removing some steric hindrance, as well as making the olefin more electron rich. Other dinitriles were also measured, such as the central dinitrile moiety of the **An**

and **Bn**, 1,4-dicyano-2-butene and the unfunctionalized **DPDCn** series, also do not conduct.

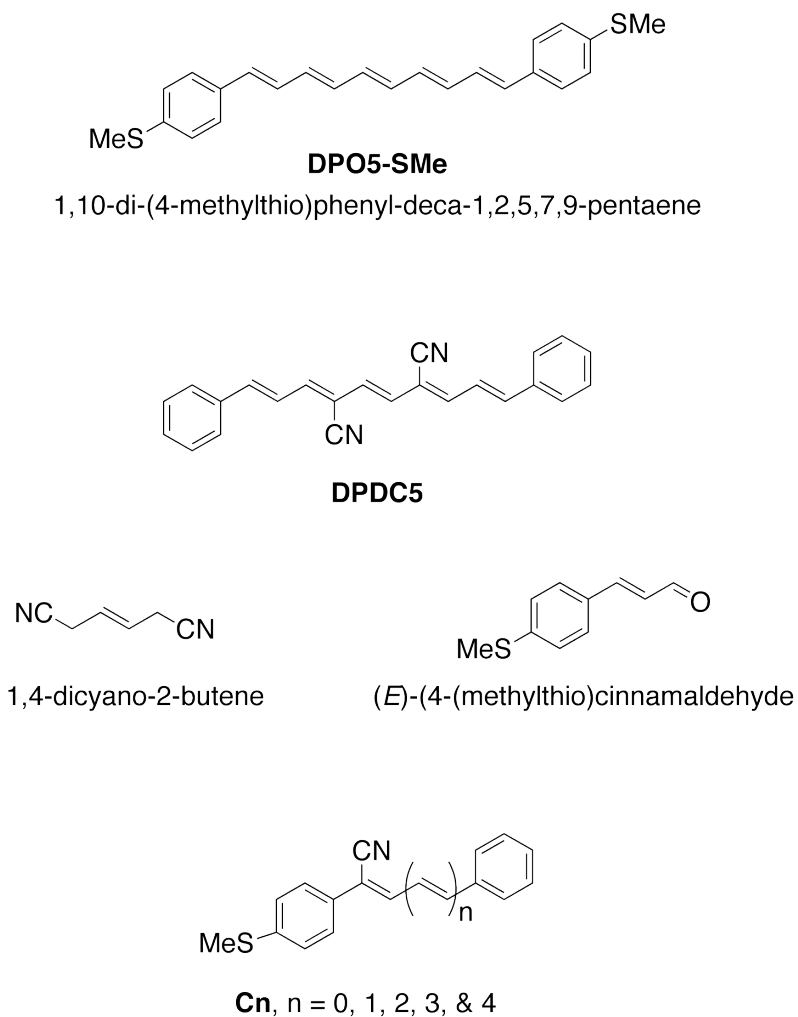


**Figure 3.6:** (A) Control molecules (from top to bottom) **DPO5-SMe**, **DPDC5**, as well as the starting materials for the Knoevenagel condensation in the preparation of **A1**, 1,4-dicyano-2-butene and *(E)*-(4-(methylthio)cinnamaldehyde). Asymmetric oligoenes (bottom) containing only one linker group were synthesized.

While both S-Au and olefin-Au bonds form, it is clear that the former is stronger than the latter. We demonstrate the importance of this with a series of asymmetric

oligoenes, each having only one methylsulfide (**Cn**), and with the parent DPDC series that lacks sulfides entirely (**DPDCn**) (see Appendix B). None of the **DPDCn** examples that we tested showed a measurable conductance, while the **Cn** series showed measurable conductance, albeit quite low. Moreover, the absolute height of the peak in the conductance histogram for **Cn** is quite low, suggesting that the formation of an Au-**Cn**-Au junction is a lower probability event. Thus, the  $\pi$ -complex is not strong enough to hold the mechanical circuit together alone, but if the molecule is held in the junction by at least one strong structural element, the  $\pi$ -complex link is strong enough to complete the electrical circuit.

#### 3.2.4. Theoretical investigations

To further explore this unusual mode of electrode-molecule coupling, we turned to computation. Density functional theory (DFT) calculations (B3LYP/6-31G\*\*) on **A1** allowed us to clearly visualize the molecular orbitals (MO's) pertinent to molecular junction formation (see Appendix B).<sup>20</sup> We modeled this as a two-step process; the molecule first binds to one electrode, and then this electrode-molecule complex binds to the second electrode. This model helps us to understand junction formation, after the first terminal has been contacted and elucidates the different binding modes to the second electrode that are available to the molecule as the gap between the two electrodes changes. For conceptual, as well as computational simplicity, we chose to model the Au electrode with a homonuclear diatomic gold cluster. The Au<sub>2</sub> is the simplest model and offers the empty orbital space (Lewis acidity), into which the S-lone pair can delocalize, to form the donor-acceptor bond that initiates the molecular-bridge-forming process. This



avoids many of the pitfalls of using atomic Au since it contains one unpaired s-electron, further complicating the analysis. The Los Alamos core valence potential (LACVP) basis set was used for calculations on complexes containing Au<sub>2</sub> clusters, since 6-31G basis set isn't large enough to accommodate the additional orbitals in gold.

In Figure 3.7A, we show the HOMO of Au<sub>2</sub>-**A1**, in which the Au<sub>2</sub> unit is bound to one of the terminal sulfides. Examination of these MO's suggests that oligoenes contain two potential electrode-binding locations; not only at the distal sulfurs, but also along to the  $\pi$ -system of the polyolefin backbone. Both binding locations have ample precedent in homogeneous organometallic chemistry<sup>21</sup> and would result in different electron tunneling pathways. Thus these calculations are consistent with our observations that **An** and **Bn** show two conductance channels. Previous reports reveal that it is common for transition metals to interact with oligoenes. In addition to the numerous weak and dynamic interactions between transition metals and alkenes, stable inorganic complexes have been isolated, in which Pd and Ru interact directly with oligoenes through the  $\pi$ -system.<sup>22-24</sup>

For comparison, in Figure 3.7B we show the HOMO for Au<sub>2</sub>-**C4**. This orbital is entirely localized in the  $\pi$ -space of the oligoene. Thus the channel for electrical conduction is present in **C4**, and it is quite similar to the channel in the **An** and **Bn** series. The difference in the conductances of **A1** (and **B1**) versus **C4** lies in the capability of the alkylsulfide linker to mechanically stabilize the oligoene close to the electrode surface, rather than in the electronic structure of the molecular conductor.

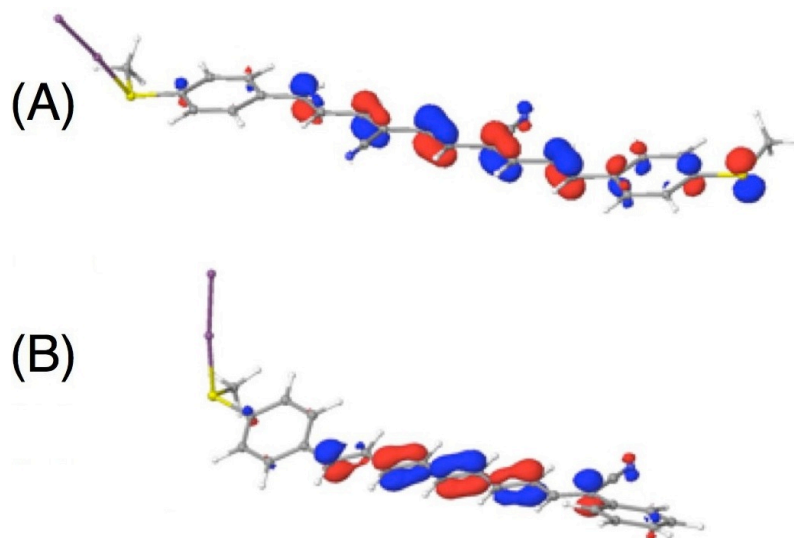


**Figure 3.7:** DFT calculations produce the HOMO of (A) Au<sub>2</sub>-A1 and (B) Au<sub>2</sub>-C4 complexes. The HOMO shows significant electron density both along the polyolefin chain and at the terminal methylsulfide functional group, we consider both spots to be available for interactions with the Au electrodes.

### 3.3. Single-molecule Potentiometer

#### 3.3.1. Variable And Reversible Resistance

If we indeed have a direct conduction path from the electrode through the olefin backbone, it should be possible to change the conductance by modulating the electrode position and generating a single-molecule circuit that functions as a potentiometer. This is shown in Figure 3.8. Here, conductance is measured in a solution of **B4** while applying a modified ramp to our piezoelectric actuator, which controls the substrate position relative to the fixed tip<sup>25</sup> (dashed trace in Figure 3.8A). Of the 3000 traces measured with this ramp, over 50% of the traces show a molecule in the high conductance regime at the start of the zigzag ramp, as determined by an automated algorithm. A sample of selected

traces is shown in Figure 3.8A, and all selected traces were used to construct the 2D conductance-time histogram on a semi-log scale, shown in Figure 3.8B.

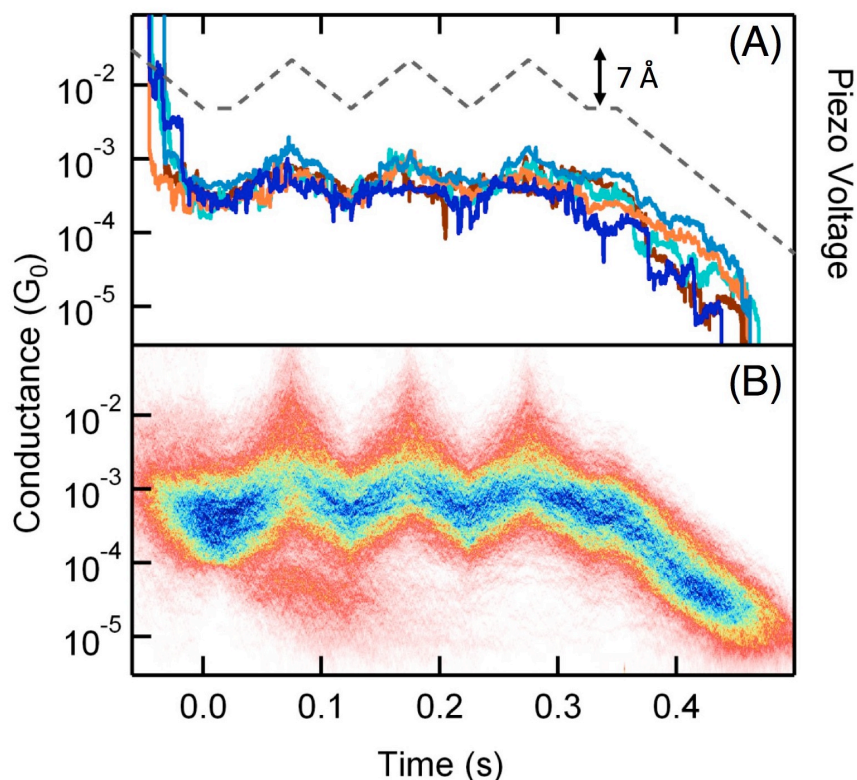


**Figure 3.8:** (A) Sample traces collected in the presence of **B4**, showing conductance changing continuously and reversibly as piezo voltage is modulated along the dashed line repeatedly stretching and compressing the junction. (B) 2D histogram constructed from selected traces, for which the average conductance during the initial hold section fell within the high-conductance range; > 50% of the 3000 traces collected met the selection criteria. Fitting the average slope of the different sections of the ramp shows that the conductance grows and decays exponentially with a factor of  $0.2/\text{\AA}$  throughout the measurement, emphasizing the reproducibility of the potentiometer behavior.

The conductance follows a zigzag pattern, as the tip-sample distance is modulated by 7 Å, with an average change in conductance from  $\sim 4 \times 10^{-4} G_0$  to  $\sim 2 \times 10^{-3} G_0$ . This range is similar to that of the high conductance peak for this molecule, and has an exponential dependence on separation ( $e^{-0.2/\text{Å}}$ ;  $\beta = 0.2 \text{ Å}^{-1}$ ). This exponential dependence of conductance on electrode distance suggests that, while the contact resistance does not change, the length of the backbone through which transport occurs varies as the junction is compressed or elongated.

### 3.3.2. Controls Experiments

Control experiments with alkanes show no modulation of conductance (see Appendix B for 1D conductance histograms). Throughout the zigzag ramp traces collected in pure solvent show changes in conductance between  $10^{-6} G_0$  to  $10^{-1} G_0$ . These intense changes would be expected for tunneling through a gap without molecules. The ability to change the conductance of the junction continuously in this high-conductance state with an exponential decay of  $0.2/\text{Å}$  can only be explained if the contact to the molecule is through direct  $\pi$ -coupling to the electrodes.

### 3.4. Conclusion

In conclusion, we experimentally demonstrate transport through single-molecule junctions where direct electronic coupling between the molecular  $\pi$ -conjugated backbone and Au electrode is achieved. Furthermore, this coupling is enabled by an auxiliary terminal chemical linker that provides mechanical support for the junction. Conductance through the molecular backbone can be tuned continuously and reversibly by changing

the electrode separation. Thus, this system provides a new class of molecular scale devices that perform as a resistive potentiometer.

### 3.5. References and Footnotes

1. Nitzan, A.; Ratner, M. A. *Science*, **2003**, 300, (5624), 1384-1389.
2. Joachim, C.; Ratner, M. A. *Proceedings of the National Academy of Sciences of the United States of America*, **2005**, 102, (25), 8800-8800.
3. Lafferentz, L.; Ample, F.; Yu, H.; Hecht, S.; Joachim, C.; Grill, L. *Science*, **2009**, 323, (5918), 1193-1197.
4. Ganesh K., Ramachandran, John K. Tomfohr, Jun Li, Otto F. Sankey, Xristo Zarate, Alex Primak, Yuichi Terazono, Thomas A. Moore, Ana L. Moore, Devens Gust, Larry A. Nagahara, and Stuart M. Lindsay, *J. Phys. Chem. B*, **2003**, 107, 6162-6169.
5. (a) He, J.; Chen, F.; Li, J.; Sankey, O. F.; Terazono, Y.; Herrero, C.; Gust, D.; Moore, T. A.; Moore, A. L.; Lindsay, S. M. *Journal of the American Chemical Society*, **2005**, 127, (5), 1384-1385. (b) Iris Visoly-Fisher, Kayvon Daie, Yuichi Terazono, Christian Herrero, Fernando Fungo, Luis Otero, Edgardo Durantini, Juana J. Silber, Leonides Sereno, Devens Gust, Thomas A. Moore, Ana L. Moore, and Stuart M. Lindsay, *Proc. Natl. Acad. Sci.*, 2006, 103, 23, 8686-8690.
6. Park, Y. S.; Whalley, A. C.; Kamenetska, M.; Steigerwald, M. L.; Hybertsen, M. S.; Nuckolls, C.; Venkataraman, L. *Journal of the American Chemical Society*, **2007**, 129, (51), 15768-15769.
7. Knoll, K.; Krouse, S. A.; Schrock, R. R. *Journal of the American Chemical Society*, **1988**, 110, (13), 4424-4425.
8. Developed by Gerd Binnig and Heinrich Rohrer at IBM Zürich in 1989, the STM functions upon the concepts of quantum tunneling. Its inventors later won the Nobel Prize in Physics in 1986 (see, Binnig, G., Rohrer, H., *IBM J. Res. Dev.*, 1986, **30**, 4.). It can be run in air or under ultra-high vacuum conditions, in aqueous or organic media. When a conducting tip is brought very near to the surface an applied bias facilitates the tunneling of electrons through the vacuum between them. These tunneling electrons create current, which is a function of tip position, applied voltage,

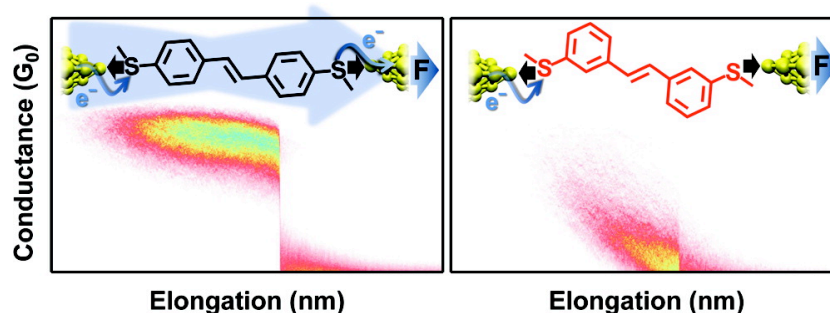
and the local density of states of the sample. Extremely clean and stable surfaces, sharp tips, excellent vibration control, and sophisticated electronics are all required to gain high resolution with an STM.

9. Catalan, J.; Hopf, H.; Mlynek, C.; Klein, D.; Kilickiran, P. *Chemistry-a European Journal*, **2005**, 11, (13), 3915-3920.
10. Xu, B. Q.; Tao, N. J. *Science*, **2003**, 301, (5637), 1221-1223.
11. Venkataraman, L.; Klare, J. E.; Nuckolls, C.; Hybertsen, M. S.; Steigerwald, M. L. *Nature*, **2006**, 442, (7105), 904-907.
12. This bias range was required to measure conductances down to  $10^{-6}$  G<sub>0</sub>. No bias dependence was found within this bias range.
13. Park, Y. S.; Widawsky, J. R.; Kamenetska, M.; Steigerwald, M. L.; Hybertsen, M. S.; Nuckolls, C.; Venkataraman, L. *Journal of the American Chemical Society*, **2009**, 131, (31), 10820-10821.
14. Quek, S. Y.; Kamenetska, M.; Steigerwald, M. L.; Choi, H. J.; Louie, S. G.; Hybertsen, M. S.; Neaton, J. B.; Venkataraman, L. *Nature Nanotechnology*, **2009**, 4, (4), 230-234.
15. Martin, C. A.; Ding, D.; Sorensen, J. K.; Bjornholm, T.; van Ruitenbeek, J. M.; van der Zant, H. S. J. *Journal of the American Chemical Society*, **2008**, 130, (40), 13198-13199.
16. The rotational barrier about the single bond in a conjugated diene is ~6 kcal/mol, where the local minima of the *s-cis* conformer lies ~2 kcal/mol higher in energy (see Carriera, L. A. *J. Chem. Phys.*, **1975**, 62 (10), 3851-3854). Time-dependent DFT calculations on a **D3** (all *s-trans*) estimates the rotation about the a single bond at 4 kcal/mol. Calculations suggest that orbitals energies of these conformers are similar and also that molecular length is does not change significantly before and after rotation The *s-trans/s-cis* conformers are not expected to account for the dramatic difference between the high- and low-conductance states in our break junction measurements, but may contribute to peak broadening.
17. Yanson, A. I.; Bollinger, G. R.; van den Brom, H. E.; Agrait, N.; van Ruitenbeek, J. M. *Nature*, **1998**, 395, (6704), 783-785.

18. Kamenetska, M.; Koentopp, M.; Whalley, A.; Park, Y. S.; Steigerwald, M.; Nuckolls, C.; Hybertsen, M.; Venkataraman, L. *Physical Review Letters*, **2009**, 102, (12), 126803.
19. Mishchenko, A.; Zotti, L. A.; Vonlanthen, D.; Bürkle, M.; Paul, F.; Cuevas, J. C.; Mayor, M.; Wandlowski, T. *J. Am. Chem. Soc.*, **2011**, 133 (2), 184-187.
20. DFT calculations were run using Jaguar version 7.7, Schrodinger LLC, New York, 2010. All calculations were run in the gas phase.
21. Collman, J. P.; Hegedus, L. S.; Norton, J. R.; Finke, R. G. *Principles and Applications of Organotransition Metal Chemistry*. University Science Books: 1987.
22. Fukumoto, H.; Mashima, K., *Organometallics*, **2005**, 24, (16), 3932-3938.
23. Fukumoto, H.; Mashima, K. *European Journal of Inorganic Chemistry*, **2006**, (24), 5006-5011.
24. Murahashi, T.; Mochizuki, E.; Kai, Y.; Kurosawa, H. *J. Am. Chem. Soc.*, **1999**, 121, (45), 10660-10661.
25. Xia, J. L.; Diez-Perez, I.; Tao, N. J. *Nano Letters*, **2008**, 8, (7), 1960-1964.

## Chapter 4. Stilbene Single-molecule Wires: Dissecting the Electrical and Mechanical Contributions in Molecular Junctions<sup>†</sup>

*In Chapter 4, the synthesis was carried out by myself with the assistance of Markrete Krikorian. STM-BJ measurements were performed by Seokhoon Ahn and Radha Parameswaran. AFM-BJ studies and analysis were done by Sriharsha Aradhya. DFT calculations were run and analyzed by Michael Steigerwald.*



### 4.1. Background and Motivations

Understanding and controlling the electronic properties of molecular wires is fundamentally important for molecular electronics.<sup>1,2</sup> The scanning tunneling microscope (STM) based break junction approach gives a deep insight into the structure-conductance relationship in single-molecule junctions because it provides a statistical interpretation over an ensemble of measurements.<sup>3-5</sup> However, in these studies only one physical property, the junction conductance, is measured. This limits the interpretation of the results in junctions where the conductance is either very small or ill-defined. Theory predicts that there will be large modulations in single molecule conductance for systems

<sup>†</sup> Chapter 4 was reprinted with permission from the authors: Aradhya, S. V; Meisner, J. S.; Krikorian, M.; Ahn, S.; Parameswaran, R.; Steigerwald, M. L.; Nuckolls, C.; Venkataraman, L. *Nano Lett.*, **2012**, *12*, 1643–1647. Copyright 2012 American Chemical Society.



exhibiting quantum interference, such as variously substituted aromatic molecules and cross-conjugated molecular wires.<sup>6-12</sup> For example, theoretical calculations have predicted that a benzene ring bound to metal electrodes with linker groups at the 1 and 3 positions (meta to each other) should have a conductance that is five orders of magnitude lower than that of a 1,4-linked benzene.<sup>6</sup> To determine, from low-bias conductance measurements alone, whether such effects are present is difficult because the conductance of the *meta*-substituted molecules is often below the experimental noise limit of the instruments. At high biases, non-equilibrium effects, junction heating, and inelastic processes cannot be ruled out.<sup>13-15</sup> Furthermore, a statistical approach is needed to demonstrate the robustness of interference phenomenon by rigorously accounting for experimental details such as junction formation probability, binding strength, junction-to-junction variation and junction structure.

In this manuscript, we overcome these critical challenges by simultaneously measuring force and conductance across single molecule junctions using a conducting atomic force microscope setup.<sup>16,17</sup> We study three molecular backbones: 4,4'-di(methylthio)stilbene (**1**), 1,2-bis(4-(methylthio)phenyl)ethane (**2**), and 3,3'-di(methylthio)stilbene (**3**). These molecules are chosen for three reasons: (1) stilbenes are model compounds for understanding single-molecule electronic properties of longer extended oligoenes; (2) since the longer stilbene backbones, rather than benzene backbones discussed above, form molecular junctions more frequently and (3) the thiomethyl (SMe) terminal groups provide reliable mechanical and electrical contacts to the Au electrodes.<sup>18,19</sup> We exploit the high binding probabilities and reliable contact properties to acquire and analyze large data sets comprised of thousands of individual

junctions to probe the robustness of interference effects, in each case. The *para*-positioned linker groups in **1** effectively couple across the  $\pi$ -system and provide a conducting single-molecule junction. In **2**, the mechanical linkages between the metal and the molecule are the same as in **1**, but conjugation is broken due to the saturated bridge, which results in lower junction conductance. In **3**, the mechanical linkers are moved to the *meta*-positions but the conjugated bridge is retained, as in **1**. There is no measurable single-molecule conductance feature in **3**. We use the simultaneously measured force data to independently obtain signatures of junction formation and rupture. We quantitatively determine the elongation length and rupture force for each of the three molecules, irrespective of their conductance. In contrast to the conductance, we find that the rupture force is insensitive to the linker group placement. We are able to demonstrate, for the first time, that the meta-substituted **3** forms mechanically stable Au–molecule–Au junctions but does not show a measurable conductance, and theoretical calculations point to quantum mechanical interference as the origin of this behavior. These measurements enable us not only to investigate junctions of non-conducting molecules, but more generally allow us to deconvolute electronic effects from mechanical evolution in single-molecule junctions.

## 4.2 Independent Measure of Force and Conductance

Simultaneous measurements of single-molecule conductance and force are carried out using a custom-built conductive atomic force microscope (AFM), which has been described in detail previously.<sup>17</sup> Molecular junctions are formed between an Au-coated AFM cantilever and an Au-on-mica substrate schematically represented in Figure 4.1a.

Conductance is determined by measuring current through the junction at an applied bias of 75 mV. Simultaneous measurements of cantilever deflection relate to the force applied across the junction. The AFM is operated in ambient conditions at room temperature. Dilute solutions (0.1 mM) of the target molecules (**1–3**, Figure 4.1b) in 1,2,4-trichlorobenzene are deposited on the substrate. For each measurement, the tip is brought into contact with the substrate until a conductance greater than  $5 G_0$  ( $G_0 = 2e^2/h$ , the quantum of conductance) is achieved and then retracted at a constant velocity of 18 nm/s while both conductance and cantilever deflection are continuously recorded. During this elongation, the Au contact thins down to a single atom point contact, clearly identified by a conductance plateau of  $1 G_0$ . In the absence of molecules the Au contact ruptures to a broken junction when elongated further. However, in a solution of molecules, molecular junctions are frequently formed after the rupture of the  $1 G_0$  plateau.

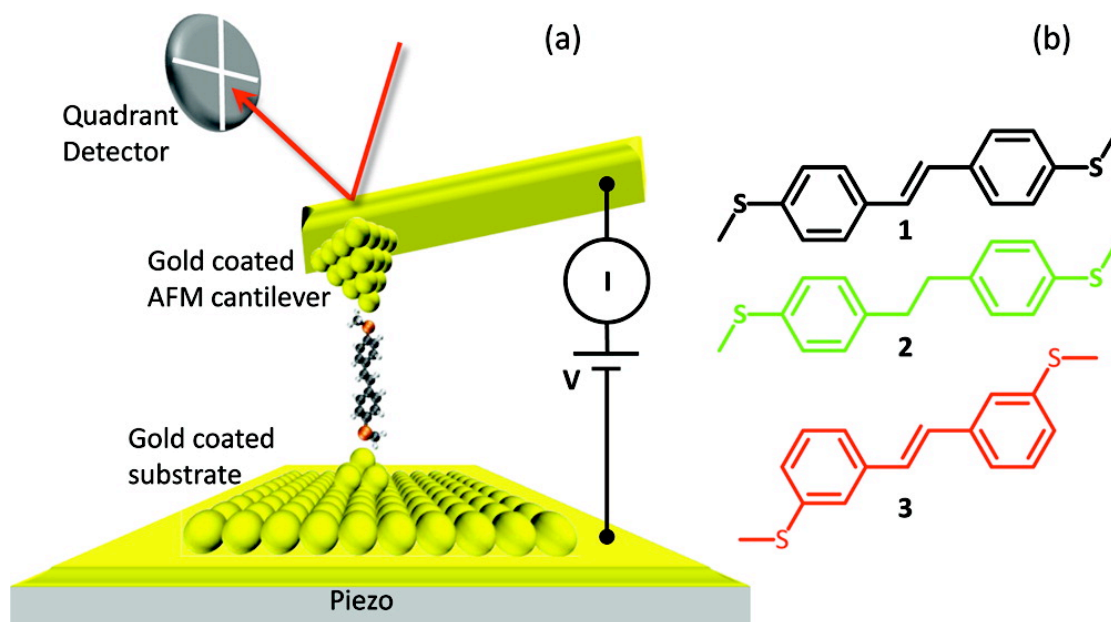


**Figure 4.1:** (a) Schematic of AFM apparatus and (b) chemical structures of molecules **1–3**.

Figure 4.2 displays simultaneously measured force and conductance traces obtained while breaking Au point contacts without molecules (Figure 4.2a) or with **1** and **3** (Figure 4.2b and 4.2c, respectively). We see a stepwise decrease in conductance (red) while the simultaneously measured force (blue) has a characteristic sawtooth pattern with alternating linear ramps (elastic loading) and abrupt drops (structural rearrangement or bond rupture) in force.<sup>17,20</sup> After the rupture of the Au single-atom contact in the absence of molecules (identified by its characteristic  $1 G_0$  conductance plateau), no further features are seen in either conductance or force. The conductance drops below the measurable level ( $\sim 10^{-5} G_0$ ), and the force stays constant because there is no more a load on the cantilever, as seen in Figure 4.2a. When an Au point contact is broken in the presence of **1** or **2**, a single-molecule junction with a characteristic conductance feature is formed  $\sim 90\%$  of the time.<sup>18,19</sup> This additional plateau is seen in the conductance traces immediately following the rupture of the Au contact, as illustrated in Figure 4.2b (red trace) for an individual measurement with **1**. The simultaneously acquired force traces (blue) also show additional sawtooth features. In this trace, we see that the  $1 G_0$  ruptures at  $\sim 0.5$  nm along the displacement axis and the molecular junction ruptures after an additional elongation of about 0.6 nm. Once this molecular junction has ruptured, no more conductance or force features are seen in measurements with **1** or **2**. In contrast, measurements with **3** do not exhibit any well-defined conductance plateau, however a majority of the measured traces show multiple force features after the rupture of the Au-contact as illustrated in Figure 4.2c. Such force features are similar in magnitude to those seen in measurements of **1** and **2**.

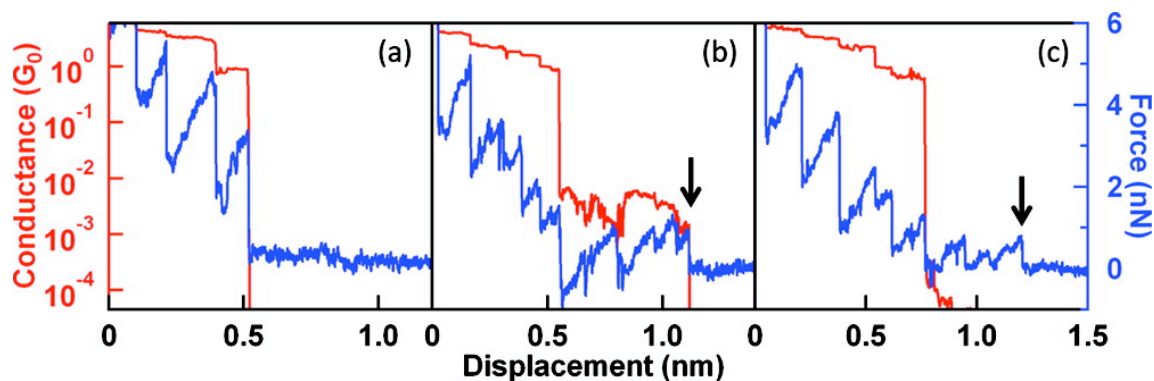


**Figure 4.2:** Sample traces of simultaneously measured conductance (red, left axis) and force (blue, right axis) for (a) Au–Au junctions (b) Au–**1**–Au and (c) Au–**3**–Au single molecule junctions. Downward arrows indicate the final force event identifying junction rupture.

### 4.3. Data Analysis

For each molecule (**1–3**), we analyze 7000 simultaneously measured conductance and force traces using an automated algorithm detailed in the Appendix C document. We use these large data sets to obtain statistically significant information because the atomic-scale structure varies from junction to junction. We begin by locating the displacement when the Au point contact ruptures in the conductance traces. This is the point in the trace when conductance drops below  $1 G_0$ . Focusing on the simultaneously acquired force trace, we analyze a 1 nm long segment of this trace ( $\sim$ S–S distance for the three molecules) beyond the  $1 G_0$  rupture point to locate the final junction rupture event, that is, the last abrupt force drop. The distance between the  $1 G_0$  rupture location and this final force event defines the molecular junction elongation length. For conducting molecules (Figure 4.2b), we observe that molecular junctions form immediately after the rupture of the Au point contacts and therefore junction elongation length is equivalent to the conductance plateau length, which has been used in previous studies to characterize

single-molecule junction mechanics.<sup>16,18,21</sup> It is important to note that we are able to identify molecular junction rupture events through force data and do not require a well-defined conductance plateau to obtain the elongation length.

Two-dimensional conductance and force histograms are now generated using the location of the final force event as the origin along the displacement axis.<sup>18</sup> For conductance, individual traces are offset laterally such that the rupture location is the origin of the displacement axis. The 2D conductance histograms have linear bins along the displacement axis ( $x$ -axis, 500 bins/nm) and logarithmic bins along the conductance axis ( $y$ -axis, 200 bins/decade).<sup>22</sup> For force data, individual traces are offset both laterally as above and vertically such that the force value at the origin is zero. The 2D force histograms have linear bins along displacement ( $x$ , 500 bins/nm) and force ( $y$ , 12.5 bins/nN) axes. Every vertical section of this 2D force histogram is fit with a Gaussian and its peak is used to determine a statistically averaged force profile for the entire data set.<sup>17</sup> Since there is no selection based on conductance, every trace with a significant force event after Au rupture (>85% of measured traces in each case) is analyzed.

#### 4.4. Stilbene Molecular Junctions

In Figure 4.2b, we display a sample force and conductance measurement with **1**. We see a clear conductance plateau after the rupture of Au point contacts. The simultaneously acquired force traces shows several sawtooth features indicating multiple structural changes in the junction; ultimately rupturing after  $\sim 0.6$  nm of elongation.<sup>23</sup> The final force event (downward arrow in Figure 4.2b) occurs at exactly the same displacement as the conductance drop. Figure 4.3a shows the 2D conductance histogram

for **1** representing 6788 of the 7000 individual traces for which a significant force event was found after  $1 G_0$  rupture. Although only force data was used to identify and set the zero displacement at the molecular junction rupture point, we observe that the conductance also drops sharply to the instrument noise level at zero-displacement, demonstrating the reliability of this force-based alignment procedure. A conductance profile of this histogram shows a clear peak at  $1.3 \times 10^{-3} G_0$  (Figure 4.3d, black trace), which compares well with the 1D conductance histograms created from all the measured traces (see Appendix C). We see that the para-linked molecule **1** forms junctions with relatively high, well-defined conductance, as observed for other fully conjugated molecular wires. The 2D force histogram created from the simultaneously acquired force traces is shown in Figure 4.4, along with the statistically averaged force profile. This force profile shows an abrupt drop of 0.5 nN at zero displacement, corresponding to the force required to rupture this junction.<sup>17</sup>

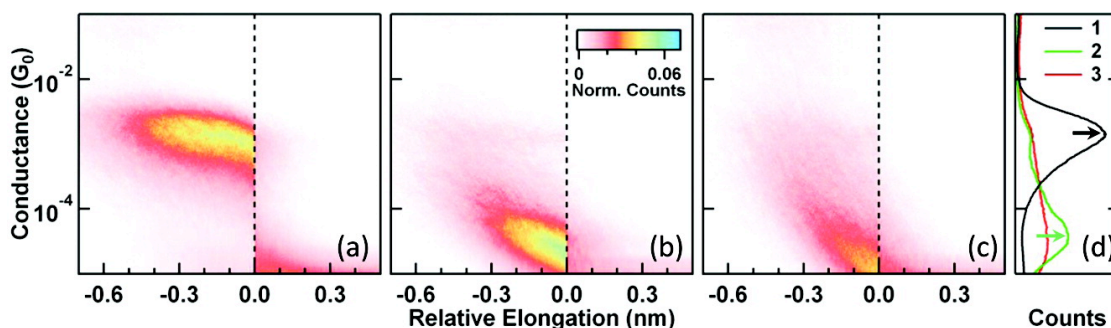


**Figure 4.3:** Displacement-preserving 2D conductance histograms (a, b, c) for **1**, **2**, and **3**, respectively, and profiles of conductance before rupture (d). The histograms represent more than 85% of the 7000 measured traces that show a significant force event beyond Au rupture in each case. The abrupt jump in conductance at the displacement origin (dashed vertical lines provided as a visual guide) for **1** and **2** shows that bond rupture

coincides with conductance drops. Arrows indicate the most frequently measured conductance value from the conductance profiles of **1** and **2**.

Molecule **2** shows similar behavior in conductance and force. The 2D conductance histogram (Figure 4.3b, from > 6000 traces) shows a clear conductance feature at a significantly lower value of  $3.2 \times 10^{-5}G_0$ . This result is intuitively understood as arising from the lowered communication between the aromatic rings due to the ethane bridge at the center, even though the para-positions of the linkers is identical to **1**. The 2D force histogram created from the simultaneously acquired force traces is shown in Appendix C. From the statistically averaged force profile (inset, Figure 4.4, green trace), we find that these junctions also rupture at a force of 0.5 nN and show a loading and rupture behavior similar to **1**.

Qualitatively different behavior is found in junctions of **3**. We do not see clear conductance plateaus in individual traces, as shown in Figure 4.2c. Individual force traces, however, do show sawtooth signatures typical of junction structure evolution and bond rupture and are analogous to force measurements of **1** and **2**. This is representative of the loading and rupture event of the molecular junction in individual traces. The 2D conductance histogram (Figure 4.3c), constructed from all traces that show a clear bond rupture event in the force data, shows a broad conductance feature slightly above the noise level as seen in the profile in Figure 4.3d (red trace). This can be ascribed to the small, but nonzero contribution to conductance from the sigma channel, through-space tunneling between the electrodes and possibly dispersive interactions between the molecular  $\pi$ -orbitals and the Au electrodes.<sup>9,24</sup> The 2D force histogram for this molecule is shown in Appendix C. The averaged force profile centered at the rupture event



generated from 5965 traces is shown in the inset of Figure 4.4 (red trace). Clearly, there are a statistically significant number of traces that have rupture events after the  $G_0$  plateau, a fraction similar to **1** and **2**, which could not be identified by conductance data alone. The bond rupture force for these junctions is also 0.5 nN. Therefore, we conclude that single-molecule junctions of **3** are formed but do not show clear conductance plateaus and have a significantly lower conductance, confirming the theoretical predictions of a low conductance due to interference effects. It is important to note that the character of the conductance we observe for **3** is qualitatively very different from that seen in **1** or **2**, as is further evidenced in the conventional linear and log binned 1D conductance histograms shown in Appendix C.

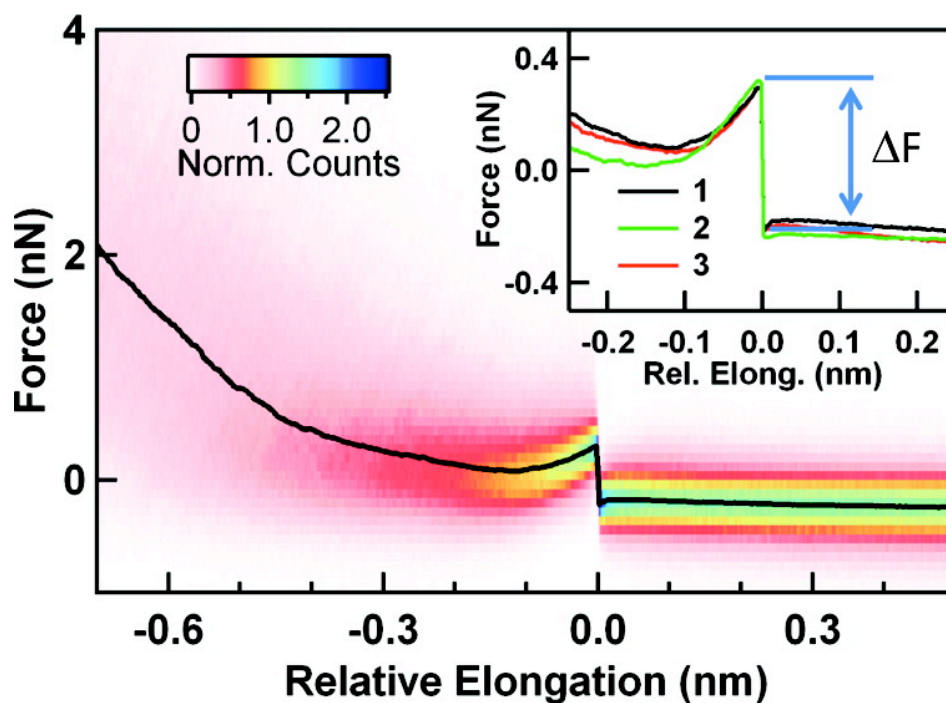


**Figure 4.4:** The 2D force histogram for molecule **1** with the averaged force profile overlaid. (Inset) Statistically averaged force profiles for molecular junctions of **1**, **2**, and **3** in black, green, and red, respectively.

Taken together, the force profiles for **1**, **2**, and **3** illustrate that bond rupture forces are approximately the same for all three molecular junctions, independent of the linker position. The rupture force depends on the specific interaction of the Au-SMe donor-acceptor bond in each molecule, and the apparent insensitivity of the rupture force to the linker position, within our experimental resolution, can be explained by the similar local structure near the Au-SMe bonds for **1–3**.

The independent analysis of force and conductance allows us to study the mechanical aspects of junction evolution even in the absence of conductance plateaus. In particular, the amount of elongation sustained by the junction before rupture, the junction elongation length, gives information about the geometry of the Au-molecule-Au junction. In general, the molecule in the junction can sample multiple binding sites during elongation before achieving the idealized vertical Au-molecule-Au junction geometry.<sup>18</sup> The junction elongation length scales with the molecular S-S distance but is smaller than the molecule length, because of a nonzero gap that is opened when the Au point contact is broken.<sup>22</sup> Histograms of elongation lengths are constructed from individual traces and have a Gaussian distribution (Appendix C). The peak values obtained from these distributions for **1–3** are presented in Table 4.1. The plateau lengths of **1** and **3** are in accordance with their respective S-S distances. However, a relatively smaller plateau length is observed for **2**. This could be due to nonplanar configurations accessible to the ethane bridge in **2**, which are not allowed in either **1** or **3** due to the central C=C double bond. These measured elongation lengths give us further confirmation of the junction formation, independent of conductance.<sup>3,25</sup>

**Table 4.1.** Conductance, Elongation Length, and Rupture Force for Single Molecule Junctions with Molecules **1–3**.

	experimental measurements			DFT
	molecule conductance ( $G_0$ )	elongation (nm)	length rupture (nN)	force S–S distance (nm) <sup>a</sup>
<b>1</b>	$1.3 \times 10^{-3}$	0.42	0.5	1.31
<b>2</b>	$3.2 \times 10^{-5}$	0.32	0.5	1.29
<b>3<sup>b</sup></b>		0.31	0.5	1.17

<sup>a</sup>B3LYP/6-31G\*\* level of theory.

<sup>b</sup>Nonconductive molecule did not show well-defined peak in conductance profiles.

Having established the similar mechanical stability for **1–3**, we are able to make direct comparisons between the chemical structures and the corresponding conductance values. We can unambiguously conclude that **2** is less conducting than **1** due to broken conjugation, while **3** forms mechanically stable yet electrically insulating junctions. Molecular backbones **1** and **3** are essentially planar structures with all sp<sup>2</sup>-carbon atoms and with similar molecular lengths; however, the meta-positioned linker groups effectively turn off the conductance.

#### 4.5. Theoretical Analysis

To better understand these results, we have examined the electronic structures of the organic molecules bonded to an Au dimer (which represents one of the Au electrodes) through an Au–S donor–acceptor bond. We use a dimer of Au atoms to avoid

complications attendant to the unpaired spin occupying the valence 6s orbital of a single Au atom. We attach the candidate organic molecule to just one “electrode” in order to appreciate what the second electrode sees as it encounters the metal-bound organic. In effect, this is a simplified model for the chemical state of the system prior to the charge transfer. We performed DFT calculations of the electronic structures of these model systems at the B3LYP/6-31G\*\* level.<sup>26</sup> The highest occupied molecular orbital (HOMO) from the geometry-optimized structures, Au<sub>2</sub>-**1**, Au<sub>2</sub>-**2**, and Au<sub>2</sub>-**3**, are shown in Figure 4.5. The HOMO of **1** extends across the entire  $\pi$ -space of the molecule in contrast to that of **2** and **3**. Significantly, in **1** the HOMO connects both the terminal sulfur atoms and provides a clear electronic conduit between the sulfur groups. In contrast, in **2** one side of the molecule does not communicate with the other, which is a direct result of the saturated ethane bridge. In addition, rotation around these sp<sup>3</sup>-carbons increases the conformational freedom in the molecular junction. Therefore, a broad peak is expected in the conductance histograms without retarding the rupture force. In **3**, we observe that although the HOMO extends across the bridge, it does not have significant amplitude on the sulfur atom at the meta-position. This finding is consistent with observations from various related approaches, such as organic reaction kinetics,<sup>27,28</sup> Hammett coefficients,<sup>29</sup> and even classic organic arrow-pushing conventions, which predict a node at the meta-position.<sup>30</sup> For direct experimental evidence, Daub and co-workers electrochemically quantified the charge-transport kinetics between meta- and para-(styryl)stilbenes.<sup>31</sup> However, this area has recently received more theoretical attention due to the possibility of studying these effects at the single-molecule level.<sup>6-12</sup>

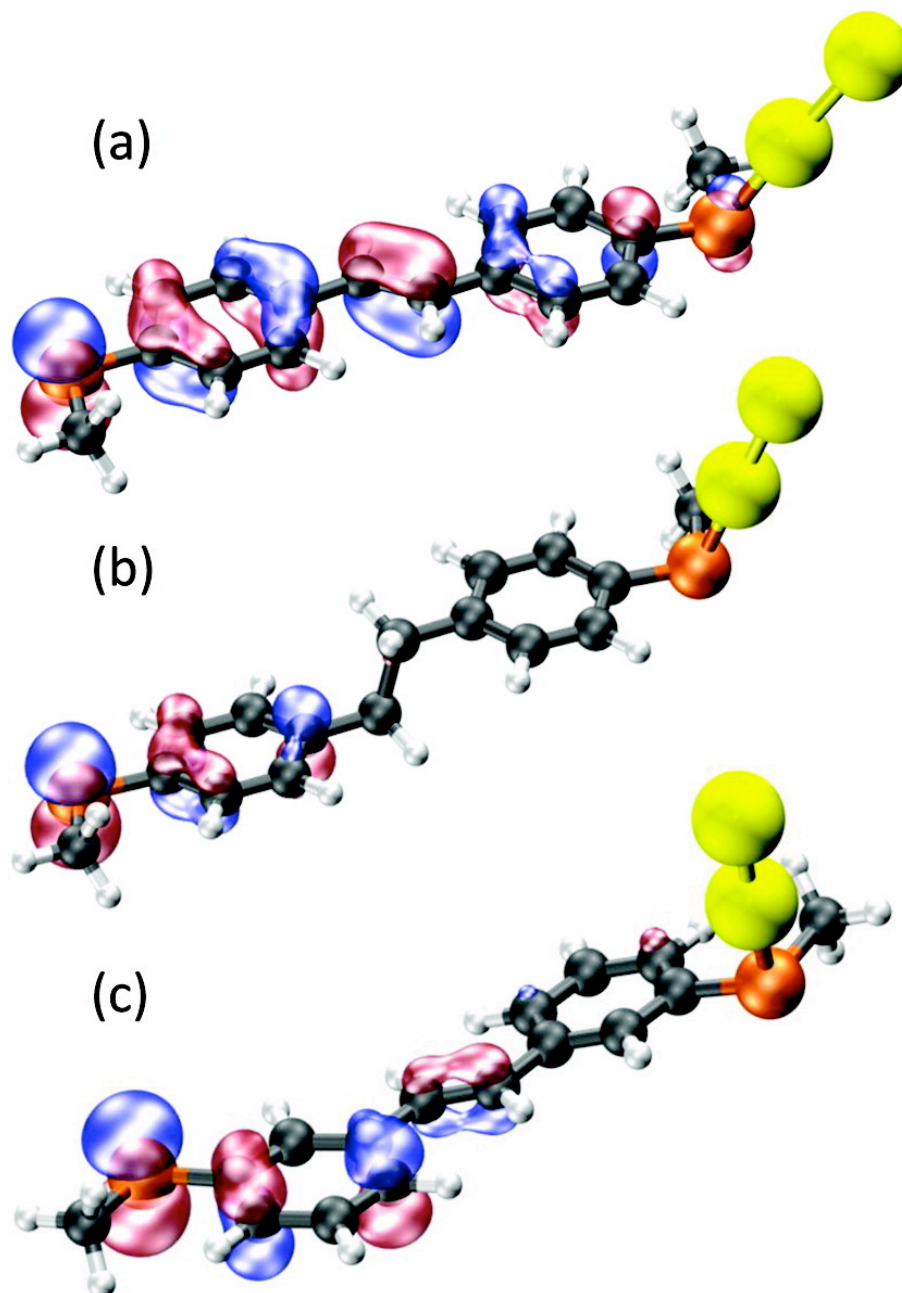


**Figure 4.5.** DFT optimized structures and isosurface plots of the HOMO of (a) Au<sub>2</sub>-1, (b) Au<sub>2</sub>-2, and (c) Au<sub>2</sub>-3.

#### 4.6. Conclusions

Single-molecule junctions of stilbene derivatives with para and meta-linked stilbenes have been formed using a conducting-AFM approach that allows for

measurements of single-molecule mechanics through force, independent of conductance. We have found that despite great differences in their conductance values, each molecule assembles into single-molecule junctions that are mechanically stable. Our results show that both para- and meta-linkers provide similar mechanical stability to the junctions yet radically change the conductance. For these reasons the para-linker groups behave as typical electro-mechano contacts, while meta-linkers disrupt the conduction acting primarily as mechanical contacts. By quantitatively accounting for the contact mechanics, these results represent the first direct proof that quantum interference is an inherent property arising from the molecular structure and is not quenched by microscopic junction-to-junction variations. This two-property measurement capability extends our understanding of single-molecule junction properties to such low-conductive and insulating systems as simple molecular connectors and dielectrics materials. Moreover, this approach provides a means to design and study new molecular switches and devices that utilize quantum interference.

#### 4.7. Reference

1. Nitzan, A.; Ratner, M. A., *Science*, **2003**, 300 (5624), 1384–1389.
2. Joachim, C.; Gimzewski, J. K.; Aviram, A., *Nature*, **2000**, 408 (6812), 541–548.
3. Xu, B.; Tao, N. J., *Science* **2003**, 301 (5637), 1221–1223.
4. Venkataraman, L.; Klare, J. E.; Tam, I. W.; Nuckolls, C.; Hybertsen, M. S.; Steigerwald, M. L., *Nano Lett.*, **2006**, 6 (3), 458–462.
5. Li, C.; Pobelov, I.; Wandlowski, T.; Bagrets, A.; Arnold, A.; Evers, F., *J. Am. Chem. Soc.*, **2007**, 130 (1), 318–326.
6. Solomon, G. C.; Andrews, D. Q.; Hansen, T.; Goldsmith, R. H.; Wasielewski, M. R.; Dwyne, R. P. V.; Ratner, M. A., *J. Chem. Phys.*, **2008**, 129 (5), 054701.

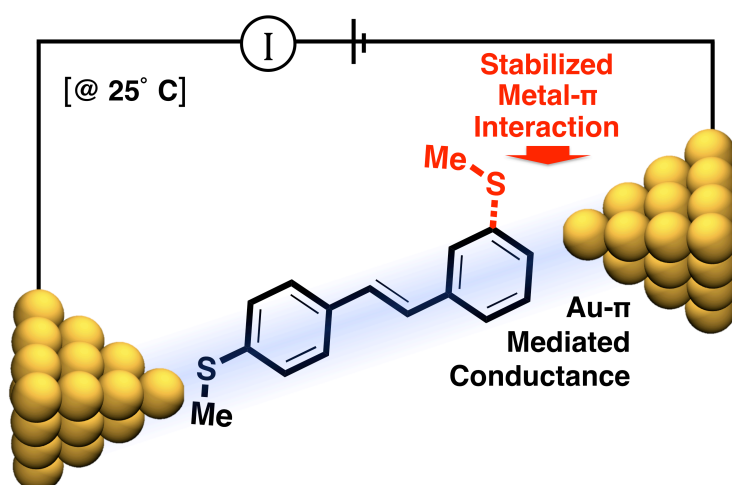
7. Markussen, T.; Stadler, R.; Thygesen, K. S., *Nano Lett.*, **2010**, 10 (10), 4260–4265.
8. Tsuji, Y.; Staykov, A.; Yoshizawa, K., *J. Am. Chem. Soc.*, **2011**, 133 (15), 5955–5965.
9. Ke, S.-H.; Yang, W.; Baranger, H. U., *Nano Lett.*, **2008**, 8 (10), 3257–3261.
10. Cardamone, D. M.; Stafford, C. A.; Mazumdar, S., *Nano Lett.*, **2006**, 6 (11), 2422–2426.
11. Markussen, T.; Stadler, R.; Thygesen, K. S., *Phys. Chem. Chem. Phys.*, **2011**, 13 (32), 14311–14317.
12. Ernzerhof, M., *J. Chem. Phys.*, **2011**, 135 (1), 014104.
13. Mayor, M.; Weber, H. B.; Reichert, J.; Elbing, M.; von Hanisch, C.; Beckmann, D.; Fischer, M., *Angew. Chem., Int Ed.*, **2003**, 42 (47), 5834–5838.
14. Taniguchi, M.; Tsutsui, M.; Mogi, R.; Sugawara, T.; Tsuji, Y.; Yoshizawa, K.; Kawai, T., *J. Am. Chem. Soc.*, **2011**, 133 (30), 11426–11429.
15. Fracasso, D.; Valkenier, H.; Hummelen, J. C.; Solomon, G. C.; Chiechi, R. C., *J. Am. Chem. Soc.*, **2011**, 133 (24), 9556–9563.
16. Xu, B. Q.; Xiao, X. Y.; Tao, N. J., *J. Am. Chem. Soc.*, **2003**, 125 (52), 16164–16165.
17. Frei, M.; Aradhya, S. V.; Koentopp, M.; Hybertsen, M. S.; Venkataraman, L., *Nano Lett.* **2011**, 11 (4), 1518–1523.
18. Kamenetska, M.; Koentopp, M.; Whalley, A.; Park, Y.; Steigerwald, M.; Nuckolls, C.; Hybertsen, M.; Venkataraman, L., *Phys. Rev. Lett.*, **2009**, 102 (12), 126803.
19. Park, Y. S.; Whalley, A. C.; Kamenetska, M.; Steigerwald, M. L.; Hybertsen, M. S.; Nuckolls, C.; Venkataraman, L., *J. Am. Chem. Soc.*, **2007**, 129 (51), 15768–15769.
20. Rubio, G.; Agraït, N.; Vieira, S., *Phys. Rev. Lett.*, **1996**, 76 (13), 2302–2305.
21. Yanson, A. I.; Bollinger, G. R.; van den Brom, H. E.; Agraït, N.; van Ruitenbeek, J. M., *Nature*, **1998**, 395 (6704), 783–785.
22. Quek, S. Y.; Kamenetska, M.; Steigerwald, M. L.; Choi, H. J.; Louie, S. G.; Hybertsen, M. S.; Neaton, J. B.; Venkataraman, L., *Nat. Nanotechnol.*, **2009**, 4 (4), 230–234.
23. Park, Y. S.; Widawsky, J. R.; Kamenetska, M.; Steigerwald, M. L.; Hybertsen, M. S.; Nuckolls, C.; Venkataraman, L., *J. Am. Chem. Soc.*, **2009**, 131 (31), 10820–10821.

24. Meisner, J. S.; Kamenetska, M.; Krikorian, M.; Steigerwald, M. L.; Venkataraman, L.; Nuckolls, C., *Nano Lett.*, **2011**, 11 (4), 1575–1579.
25. Chen, F.; Hihath, J.; Huang, Z.; Li, X.; Tao, N. J., *Annu. Rev. Phys. Chem.*, **2007**, 58, 535–564.
26. *Jaguar*, v7.8; Schrödinger, LLC: New York, **2011**.
27. King, B. T.; Kroulik, J.; Robertson, C. R.; Rempala, P.; Hilton, C. L.; Korinek, J. D.; Gortari, L. M. J., *Org. Chem.*, **2007**, 72 (7), 2279–2288.
28. Michinobu, T.; Boudon, C.; Gisselbrecht, J. P.; Seiler, P.; Frank, B.; Moonen, N. N. P.; Gross, M.; Diederich, F., *Chem.—Eur. J.*, **2006**, 12 (7), 1889–1905.
29. Hansch, C.; Leo, A.; Taft, R. W., *Chem. Rev.*, **1991**, 91 (2), 165–195.
30. Pauling, L., “*The Nature of the Chemical Bond and the Structure of Molecules and Crystals: An Introduction to Modern Structural Chemistry*,” 3rd ed.; Cornell University Press, Ithaca, NY, **1960**.
31. Mayor, M.; Buschel, M.; Fromm, K. M.; Lehn, J. M.; Daub, J., *Ann. N.Y. Acad. Sci.*, **2002**, 960, 16–28.



## Chapter 5. Direct Metal- $\pi$ Bonding in Conjugated Single-molecule Junctions<sup>†</sup>

*STM-BJ measurements in Chapter 5 were performed by Seokhoon Ahn with the assistance of Radha Parameswaran. AFM-BJ studies and analysis were done by Sriharsha Aradhya. Molecules were synthesized by Markrete Krikorian and myself. DFT calculations were run by Michael Steigerwald and myself.*



### 5.1. Introduction

This study describes the mechanism of conduction through asymmetric molecular junctions containing conjugated molecules having only one electrode-binding “linker” group.<sup>1</sup> Linker groups are aurophilic functional groups that bind the molecule between Au electrodes, such as thiols (-SH), primary amines (-NH<sub>2</sub>) and methylsulfides (-SMe).<sup>2</sup> Typical molecules employed in single-molecule electronics are conjugated or short aliphatic molecules that are functionalized at each end with linker groups. Here,

<sup>†</sup> Chapter 5 was reproduced with permission from the authors: Meisner, J. S.; Ahn, S.; Aradhya, S. V.; Krikorian, M.; Parameswaran, R.; Steigerwald, M. L.; Venkataraman, L.; Nuckolls, C.; *J. Am. Chem. Soc.*, **2012**, Accepted on Nov. 21, 2012. Copyright 2012 American Chemical Society.

conjugated olefins of varying lengths are end-functionalized with methylsulfide and amine linkers at one or both terminal phenyl rings. To explore quantum mechanical effects<sup>3</sup> we vary the position of these linkers between the *meta* or *para* positions. The conductance and rupture forces of single-molecule junctions formed from these molecules are measured using the break-junction (BJ) technique with a scanning tunneling microscope (STM)<sup>2a</sup> and an atomic force microscope (AFM).<sup>4</sup> We find that for measurable conductivity to occur, at least one of the rings must have a linker *para* to the olefin providing strong electronic coupling to the electrode. We measure both the highest conductivity and the narrowest distribution of conductance for olefins with two *para* linkers. When one of these *para* linkers is replaced with a *meta* linker, the conductance decreases by almost an order of magnitude, due to a reduction in the Au-molecule-Au coupling. If this mechanical contact, the *meta* linker, is removed leaving only a single *para* linker, the conductance decreases even further. We show that the conductance of our molecular wires that have at least one *para* linker decay exponentially with increasing oligomeric length and that they have step lengths corresponding to their molecular length. Both of these results indicate that we are probing the conductance of single-molecule junctions, as opposed to junctions formed by overlapping or interdigitated molecular dyads. That is, these measurements allow us to conclude that mono-functionalized stilbene molecules do not readily form junctions where molecules conduct via intermolecular carrier transfer (i.e.  $\pi$ - $\pi$ -stacking interactions).<sup>5</sup>

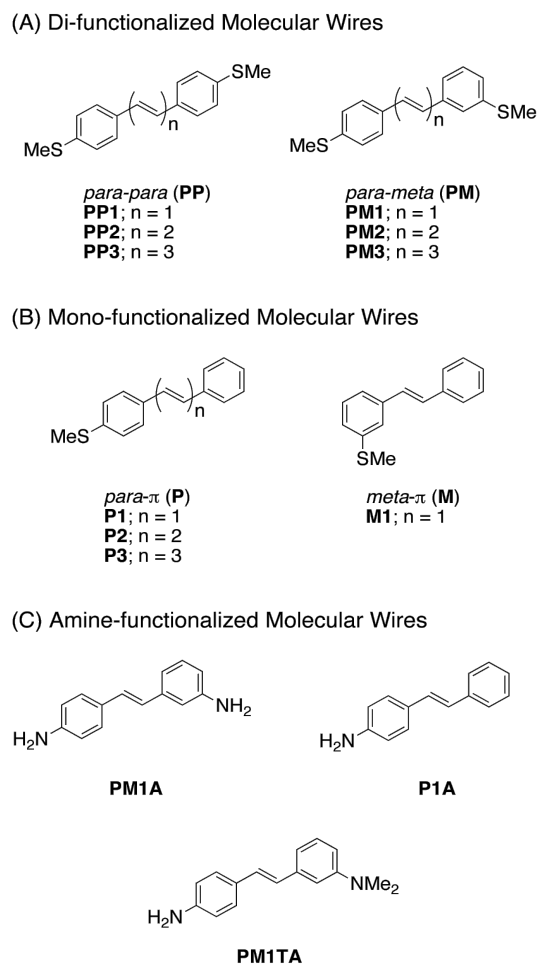


**Figure 5.1:** Chemical structures of *trans*-stilbene and all-*trans*-oligoene molecular wires: (A) difunctionalized series, having only *para*-positioned linker groups (**PP<sub>n</sub>**) or a mixture of *para* and *meta* linkers (**PM<sub>n</sub>**); (B) mono-functionalized wires **P<sub>n</sub>** and **M1** contain either one *meta* or one *para* linker. (C) Stilbene derivatives end-functionalized with primary and tertiary amines.

## 5.2. Experimental Methods

**5.2.1. Molecular Wire Synthesis.** For this study we synthesized three different vinylogous series of methylsulfide functionalized *trans*- $\alpha,\omega$ -diphenyl-oligoenes as well as 3-(methylthio)stilbene. Each series ranges in length from the stilbene (n = 1) to the triene (n = 3) and is displayed in Figure 5.1A and 5.1B. Convenient shorthand is used to

name these compounds (**PPn**, **PMn**, **Pn**, and **M1**), which includes the linker substitution (P = *para*, M = *meta*) and the length of the oligomer (n). As examples, **PP2** denotes *para-para'*-dithiomethyl-diphenylbutadiene and **PM3** denotes *para-meta'*-dithiomethyl-diphenylhexatriene. Both difunctionalized (**PPn** and **PMn**) and mono-functionalized (**Pn** and **M1**) molecules were synthesized through Wittig<sup>6</sup> and Horner-Wadsworth-Emmons reactions (see Appendix D for synthetic details and characterization).<sup>7</sup>

A set of three additional stilbene derivatives bearing amine linkers were synthesized in order to deconvolute the electronic and mechanical contributions in molecular junctions; (*E*)-3,4'-diaminostilbene (**PM1A**) and (*E*)-4-amino-stilbene (**P1A**) as analogous compounds to the conducting (*E*)-(methylthio)stilbenes above, as well as (*E*)-3-dimethylamino-4'-aminostilbene (**PM1TA**); where A = amine and TA = tertiary amine.

**5.2.2. STM and AFM-BJ Measurements.** STM-BJ measurements<sup>2a,2b</sup> were performed in dilute solutions ( $1 \pm 0.1$  mM in 1,2,4-trichlorobenzene) of molecular wires using a gold-on-mica substrate and a gold STM tip (cut Au wire, 0.25 mm diameter, 99.998%, Alfa Aesar). Gold atomic point contacts were repeatedly formed and broken in the solution of molecules under a 500 mV voltage applied to the junction with a 100 k $\Omega$  resistor in series. As the point contacts are broken, one or a few molecules may bind to bridge the gap between the broken Au contact, thereby forming molecular junctions. The electrodes are then pulled farther apart until the junction is broken. Conductance (current/voltage) is measured as a function of piezo displacement yielding individual conductance traces. In doing so, our STM-BJ method does not take consecutive measurements on a single junction. Instead, at the end of each measurement the junction is destroyed. Then, before forming a new junction the tip and substrate are smashed

together and pulled apart forming fresh electrodes and thus a new junction. For each molecule, over 5000 traces are collected and analyzed by creating one-dimensional (1D) conductance and two-dimensional (2D) conductance-displacement histograms<sup>2d,8</sup> that reveal statistically relevant information on junction conductance, as well its evolution under junction elongation.

Molecular conductance step lengths<sup>9</sup> and the slopes of the conductance features ( $\beta_s$ ) in the 2D histograms were determined by fitting the average conductance profile; both procedures are outlined in detail in Appendix D.

Simultaneous conductance and force measurements were obtained using a custom built conducting AFM set-up.<sup>4a</sup> Single-molecule junctions were formed between a gold-coated commercial AFM cantilever (NanoAndMore, Inc) and a gold-on-mica substrate. Conductance is measured across the tip/sample junction at a bias of 75 mV. The force is measured simultaneously by monitoring the deflection of a laser focused on the back of the cantilever. AFM-BJ measurements are carried out on **PP1**, **PM1** and **P1**. In each case 2D force-displacement histograms are constructed from measurements on over 8000 junctions.

**5.2.3. Theoretical Methods.** Density functional theory (DFT) electronic structure calculations examined shape and energy differences amongst the most relevant molecular orbitals (MO's) for molecular conductance. All calculations were performed using Jaguar<sup>10</sup> with the B3LYP hybrid functional and the 6-31G\*\* basis sets. The molecular geometries were fully optimized. The final geometries, total energies and MO energies for each molecule in this study are given provided in the Appendix D.

### 5.3. Results and Discussion

**5.3.1. Single-molecule Conductance: General Substitution Effects.** We begin by comparing the conductance and rupture forces of molecular junctions of four stilbene derivatives having either one or two methylsulfide linkers in either the *meta* or *para* positions (**PP1**, **PM1**, **P1**, and **M1**). Their 1D logarithmically binned conductance histograms are obtained from STM-BJ measurements and are compared in Figure 5.2A. The histogram for **PP1** shows a clear molecular conductance peak, indicating that reproducible single-molecule junctions are formed throughout thousands of measurements. The sharpest peak at  $10^{-3} G_0$  is characteristic of a conjugated stilbene having two *para*-linkers, as has been shown before.<sup>3d,11</sup> A characteristic conductance signature (peak in the histogram) appears for **P1** even though it contains only one linker. The peak conductance for **P1** is almost two orders of magnitude lower than that for **PP1**, therefore electronic coupling across the **P1** junction is weaker than with **PP1**. From the width of the peak, we conclude that the junction conductance varies significantly more than in the case of **PP1**, which has two linkers. We quantify the peak width for all junctions in Table 5.1 using the half width at half-maximum. We next compare **P1** with **M1**, which also has only one linker, but now at the *meta*-position; we see no peak in this histogram indicating that junctions with a conductance above our instrument noise ( $\sim 10^{-7} G_0$ ) are not formed with **M1**. This trend is expected since *meta*-linkers do not provide strong electronic coupling into the  $\pi$ -system.<sup>3a</sup> Nonetheless, they do provide a mechanical link as we have previously shown.<sup>3d</sup> Indeed, we see with **PM1** that the additional mechanical stability provided by the *meta* linker yields both a higher conductance and a

narrower distribution compared with **P1**. Conductance values for each compound are given in Table 5.1.

**5.3.2. Single-molecule Rupture Forces: General Substitution Effects.** We confirm the mechanical enhancement provided by the *meta* linker by measuring force in AFM-BJ's of **PP1**, **PM1** and **P1**. The rupture forces are measured by pulling the junction apart until it breaks and (to a first order approximation) establish an upper limit on the strength of the weakest Au-molecule interaction. Stilbenes with two methylsulfide linkers (regardless of their position on the phenyl rings) are stabilized in the junction and give rupture forces of 0.5 nN, as is the case with **PP1**<sup>3d</sup> and **PM1** (Figure 5.2C). In contrast, we found that the rupture force for **P1** is smaller than 0.3 nN (twice the instrumental noise). Our rupture force results for each stilbene are overlaid in Figure 5.2C (inset). Consequently, the interaction between the Au electrode and unsubstituted phenyl ring does not contribute much to the mechanical stability of the junction at room temperature. Since linkers in the *meta*-position behave as typical mechanical contacts (albeit without providing electrical coupling), we postulate that the conductance modulation found between the **PMn** and **Pn** series is the result of a strengthened Au- $\pi$  interaction, where the tunneling pathway is coupling directly into the  $\pi$ -space of the second ring while the *meta*-linker secures that end to the electrode surface. Similar metal- $\pi$  (Pt or Ag) interactions have been used to rationalize the conductance mechanism through symmetric metal-benzene-metal junctions at low temperature,<sup>12</sup> as well as molecular junctions of C<sub>60</sub> and stacked oligomers of paracyclophane using Au electrodes at room temperature.<sup>13</sup>

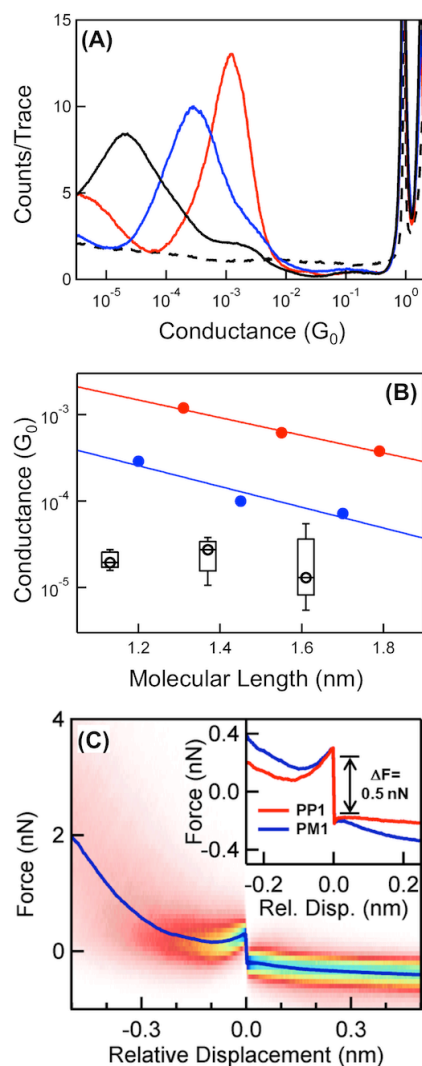


**Figure 5.2:** (A) 1D conductance histograms constructed using logarithm bins for junctions of **PP1** (red), **PM1** (blue), **P1** (black) and **M1** (dashed). **M1** does not form conductive junctions. Histograms were generated from over 5000 traces without data selection, using 100 bins/decade. (B) Plot of molecular length vs. conductance for *para-para* series (**PPn**; red) and *para-meta* series (**PMn**; blue). Exponential decay constants were found to be  $\beta = 0.23 \pm 0.03 \text{ \AA}^{-1}$  and  $0.27 \pm 0.08 \text{ \AA}^{-1}$ , respectively. The effective contact resistance for **PPn** is 520 kW and for **PMn** is 1820 kW. Conductance for **Pn** (black) is represented with the mean peak conductance (black circles) within a distribution of the inner 50<sup>th</sup> percentile (black boxes) and the inner 80<sup>th</sup> percentile (bars). Due to junction-to-junction variations larger samples sizes were used for **Pn** (over 30,000 individual conductance traces). (C) The 2D force histogram of **PM1** junctions compiled



from ~8000 traces. Colored contours represent the normalized histogram counts. (Inset): Average force profiles of **PP1** and **PM1** are overlaid yielding rupture forces of 0.5 nN for each.

**5.3.3. Length-dependent Molecular Conductance.** To understand the conduction mechanism in greater detail it is necessary to verify that conductance occurs through the molecular backbone of a single molecule. Therefore, we measured the length-dependence of conductance through a series of oligomers **PPn**, **PMn** and **Pn**, with  $n = 1, 2,$  and  $3$ . The peak conductance of each oligomer is given in Table 5.1. In Figure 5.2B, we plot the conductance histogram peaks against the molecular length for each series. The *para-para* bound series, **PPn**, is especially useful as a control group representing typical linear  $\alpha,\omega$ -diphenyl-oligoenes.<sup>14</sup> The decay constant ( $\beta$ ), which describes the exponential decrease of conductance with increasing molecular length is found to be  $\beta = 0.23 \pm 0.02 \text{ \AA}^{-1}$ , in good agreement with published results.<sup>15</sup> For the **PMn** series, we also find an exponentially decreasing conductance with a decay constant of  $\beta = 0.27 \pm 0.08 \text{ \AA}^{-1}$ , which is similar to that of **PPn**. This indicates that conduction is through the  $\pi$ -system of a single molecule and not by any other mechanism, such as  $\pi$ - $\pi$ -stacking between dimers.<sup>5</sup> When measuring conductance of the **Pn** series, we found that conductance peak values shifted within half of an order of magnitude over the course of the experiment (thousands of consecutive traces). This junction-to-junction variation in conductance is illustrated by the error bars in Figure 5.2B. The variability increased with molecular length (**P1** < **P2** < **P3**) making it impossible to determine a decay constant with precision.<sup>16</sup> Outside of the mono-substituted **Pn** series, the variation during and between different experimental runs (changing tip and substrate) caused insignificant variations in

the most frequently measured conductance. This is typically the result obtained with methylsulfide linkers.<sup>17</sup>

**5.3.4. Molecular Junction Evolution.** In order to further understand junction evolution, we show how the conductance changes during elongation. By constructing 2D conductance-displacement histograms, we can determine the maximal junction length, or step length, as well as trends in the molecule-electrode coupling. Figure 5.3A-C displays the 2D histograms<sup>18</sup> of the stilbenes junctions, **PP1**, **PM1** and **P1** (all others are given in Appendix D). Their molecular conductance features extend about 0.6 nm. The step lengths are summarized in Table 5.1. We note that they are  $\sim 0.7$  nm shorter than the molecular lengths, which is common in STM-BJ's due to snapback relaxations at the Au electrodes.<sup>19</sup> The fact that all three molecules have step lengths corresponding to their molecular length indicates that in each case molecular junctions are formed with a single molecule. We quantify the step length for each molecule as detailed in Appendix D and summarize them in Table 5.1. For each oligomeric series, the step length increases linearly with molecular backbone length (Figure 5.3D).<sup>2c</sup> The step lengths of **Pn** are slightly longer (0.02-0.04 nm) than those of **PPn**. We attribute the difference to changes in the linker group<sup>2c</sup> (*para*-SMe vs. Au- $\pi$ ) and not the formation of  $\pi$ - $\pi$ -stacked dimers, since significantly larger step lengths would then be expected.

The 2D histograms also show that the slope of the conductance-versus-displacement curves change significantly between each series in the order, **PPn** > **PMn** > **Pn**. The white lines overlaid in Figure 5.3A-C represent the statistically averaged decreasing conductance, whose slopes are tabulated in Table 5.1 for all our molecules. Steeper

slopes correspond to junctions that are more sensitive to elongation. For example, the largest change in slope is observed between **PPn** and **PMn** and can be attributed to more geometrically demanding coupling in the **PMn** and **Pn** series. Since the *meta*-SMe linker improves the mechanical stabilization of the junction, the slope of **PMn** is shallower than **Pn**. It is important to note that the numerical value of the slope depends on several factors, such as mechanical stability, structural evolution during pulling, and competing tunneling current. Therefore, while our systematic approach allows us to qualitatively understand the differences between each series at this point, quantitative comparisons will require further, more-detailed experiments combined with significant theoretical efforts.

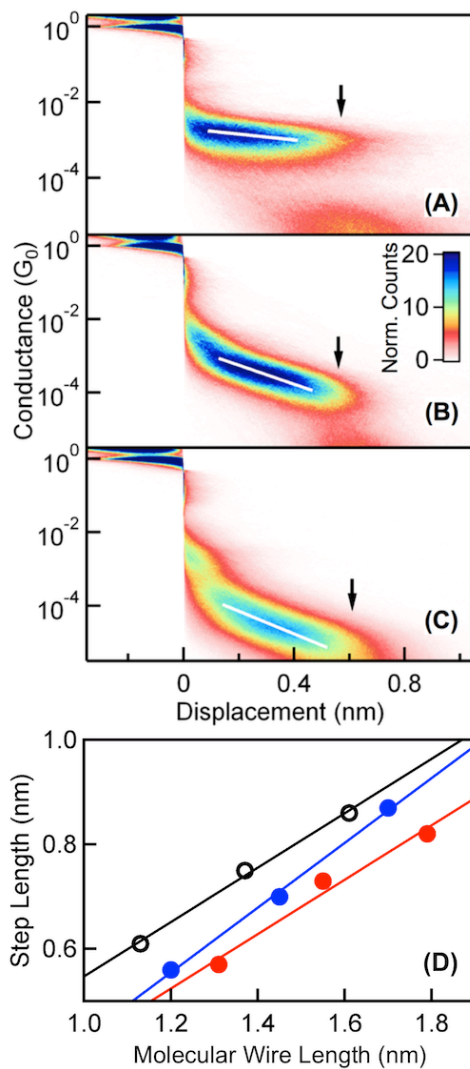


**Figure 5.3:** 2D conductance-displacement histograms are generated from over 5000 individual measurements on (A) **PP1**, (B) **PM1** and (C) **P1** single-molecule junctions. Colored contour represents the number of counts  $\times 1000$ . Step lengths are marked by black arrows, representing the 90<sup>th</sup> percentile of conductance, at 0.57, 0.56 and 0.61 nm, respectively. (D) Plot of the step lengths vs. molecular wire lengths of **PPn** (red), **PMn** (blue) and **Pn** (black) series, with slopes of 0.52, 0.62 and 0.52, respectively. Molecular wire lengths were determined by DFT calculations.

**Table 5.1:** Tabulation of Conductance Parameters from STM-BJ Measurements.

Molecule	1D Conductance Peak ( $G_0$ )	Conductance Peak Width <sup>e</sup>	Slope $\beta_s$ ( $\text{\AA}^{-1}$ )	Step Length (nm)	Molecule Length <sup>a</sup> (nm)
PP1	$1.2 \times 10^{-3}$	0.42	0.18	0.57	1.31 <sup>c</sup>
PP2	$6.2 \times 10^{-4}$	0.44	0.12	0.73	1.55 <sup>c</sup>
PP3	$3.8 \times 10^{-4}$	0.44	0.12	0.82	1.79 <sup>c</sup>
PM1	$2.9 \times 10^{-4}$	0.63	0.58	0.56	1.20 <sup>c</sup>
PM2	$1.0 \times 10^{-4}$	0.69	0.35	0.70	1.45 <sup>c</sup>
PM3	$7.2 \times 10^{-5}$	0.74	0.35	0.87	1.70 <sup>c</sup>
P1	$2.1 \times 10^{-5}$	0.90	0.67	0.61	1.13 <sup>d</sup>
P2	$2.6 \times 10^{-5}$	0.94	0.54	0.75	1.37 <sup>d</sup>
P3	$1.7 \times 10^{-5}$	1.02	0.46	0.86	1.61 <sup>d</sup>
M1	n/a <sup>b</sup>	n/a <sup>b</sup>	n/a <sup>b</sup>	n/a <sup>b</sup>	1.00 <sup>d</sup>
PM1A	$2.2 \times 10^{-4}$	0.83	0.67	0.63	1.14 <sup>c</sup>
P1A	$2.8 \times 10^{-5}$	0.98	0.70	0.67	1.09 <sup>d</sup>
PM1TA	$2.8 \times 10^{-5}$	1.03	0.89	0.66	1.09 <sup>d</sup>

<sup>a</sup>Molecular length is taken from DFT optimized structures. <sup>b</sup>Molecules do not form conductive junctions. <sup>c</sup>Length refers to the through-space distance between terminal linker group heteroatoms. <sup>d</sup>Length refers to the through-space distance from the *para*-linker group heteroatom to most distant carbon atom. <sup>e</sup>Conductance peak widths are determined using the half width at half-maximum on the high-conductance side of the peak, since low-conductance half-maxima are sometimes lost in the experimental noise.

**5.3.5. Deciphering Electronic from Mechanical Contributions Using Amine Derivatives.** Since the conductance of the **PPn** series is systematically higher than the

corresponding **PMn** series, and since *meta*-substitution appears to be non-conductive, our data suggest that conduction in **PMn** junctions occurs through the combination of an Au-S interaction in the *para*-substituted ring and a direct Au- $\pi$  interaction in the *meta*-substituted ring. To verify these effects, we employed a series of amine-terminated stilbenes where, in contrast to the methylsulfide stilbenes, we are able to retain electronic effects while disrupting the mechanical coupling at the *meta*-linker (**PM1A** and **PM1TA** from Figure 5.1C). Molecules terminated with primary amines (RNH<sub>2</sub>) bind to the Au electrodes forming molecular junctions in the STM-BJ set-up. However, when primary amines are methylated to form tertiary amines (RNMe<sub>2</sub>), they do not bind to Au.<sup>2b</sup> In this way, the linker group's electron-donating contributions to the MO's are preserved, while arresting additional mechanical stabilization.

Conductance histograms of **PM1A**, **P1A** and **PM1TA** junctions are compared in Figure 5.4. The conductance peak for the *para-meta* bound junction (**PM1A**) is almost an order of magnitude higher than that of the *para*- $\pi$  bound junction (**P1A**), similar to what was observed for the methylsulfide analogues (**PM1** vs. **P1**). However, when the *meta*-NH<sub>2</sub> of **PM1A** is replaced by *meta*-NMe<sub>2</sub>, the conductance of the resulting **PM1TA** drops by an order of magnitude, overlapping the conductance of mono-functionalized **P1A**. With these direct structural comparisons we conclude that the electrical pathway in the *para-meta*-bound series is through an Au- $\pi$  interaction and that the *meta* linker serves as a mechanical stabilizer that enhances the electronic coupling between the terminal phenyl group and Au electrode.

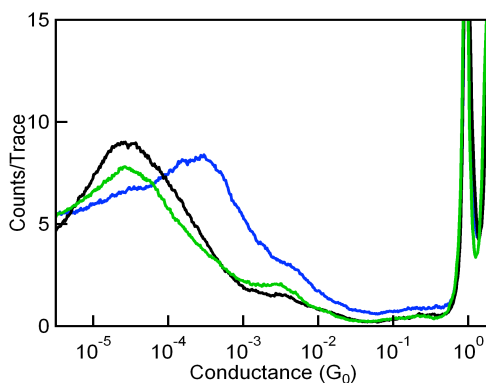


**Figure 5.4:** Log-binned conductance histograms of amine-functionalized stilbene molecular wires: *para-meta* **PM1A** (blue), *para- $\pi$*  **P1A** (green), and methylated *para-meta* **PM1TA** (black) were generated from 5000 individual conductance traces.

#### 5.4. Theoretical Analysis

To gain insight into the electronic structure of our molecular junctions, DFT calculations were carried out to examine the shape of MO's. The methylsulfide-functionalized stilbenes (**PP1**, **PM1**, and **P1**) are considered. The most relevant MOs are those nearest to the Fermi level of the electrodes. Since these junctions are generally HOMO conducting,<sup>20</sup> we examine the HOMO, HOMO-1 and HOMO-2 of **PP1** and **PM1**, which contain the p- $\pi$  orbitals of sulfur and the olefin (C=C), as well as the HOMO and HOMO-1 for compounds **P1**. Since other MO's are much lower in energy their contributions become negligible.

First, we inspect the results of the *para-para* case (**PP1**), which are shown in Figure 5.5A. We see that the orbitals are strongly coupled across the molecular backbone and include both sulfur lone pairs ( $S_{LP}$ ). In contrast, the two  $S_{LP}$ 's in the *para-meta* compound (**PM1**; Figure 5.5B) are decoupled. In fact, the energy cost to mix these orbitals and establish a conduction pathway (through each  $S_{LP}$ ) is roughly equal to the energetic cost ( $\sim 0.85$  eV) required to disrupt that in the previous case (**PP1**). In light of this, it would be

reasonable to expect **PM1** to not conduct at all. However, upon deeper inspection we find density located on the phenyl ring opposite the *para*-linker and propose this as an alternative conduction pathway. This secondary path is also predicted to exist in **PP1**; however, since it is expected to be more resistive, it may not be experimentally distinguishable in **PP1**. In the special case of **PM1**, the secondary path may be the only available conductance pathway.



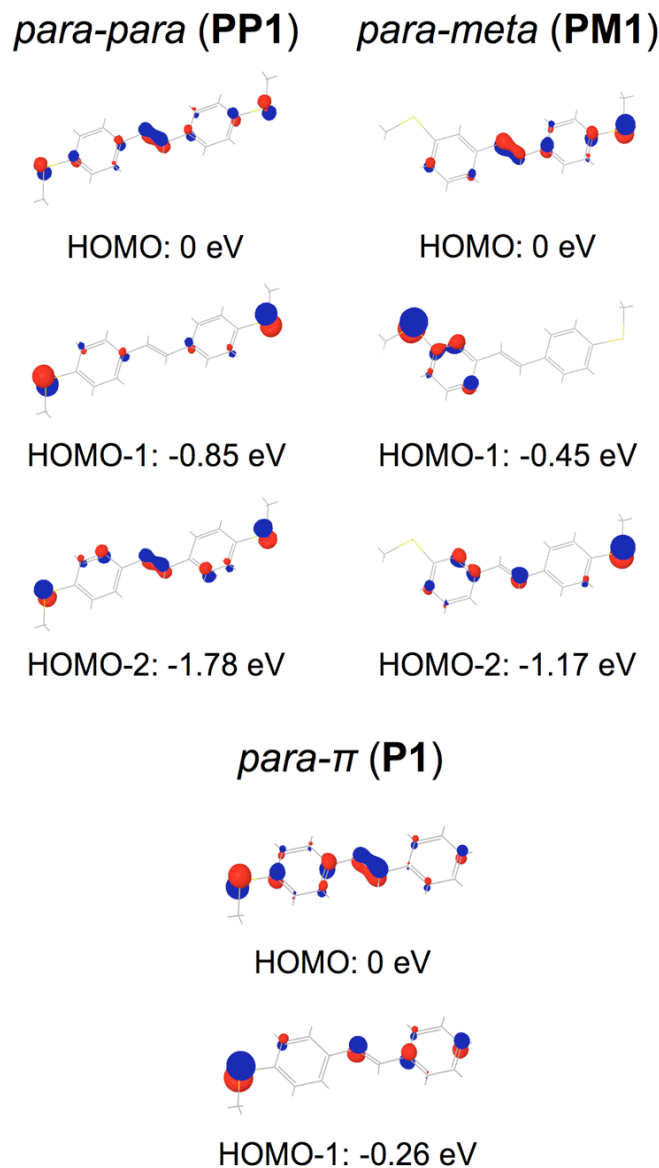


**Figure 5.5:** DFT calculated isosurfaces of MO's relevant in single-molecule conductance. Geometries of **PP1**, **PM1** and **P1** were optimized and MOs calculated at the B3LYP/6-31\*\* level of theory in the gas phase. HOMO energies were normalized to 0 eV for easy comparison. Contour values set at 0.75.

For the *para- $\pi$*  bound molecule (**P1**; Figure 5.5C) the ring systems and  $S_{LP}$  are strongly coupled to one another. Due to the lack of a second linker, a single conductance pathway

exists in **P1**, which closely resembles that of the secondary path found in **PM1**, leading to conducting junctions, despite lacking in the mechanical stability provided by a second linker. This MO interpretation helps to identify relationships linking the intrinsic properties of the bridging molecule with the conductance mechanism and overall device performance. Further studies that include the mapping of the density of states and couplings of the Au electrodes are beyond the scope of this study. Our theoretical results agree with our experimental findings and give weight to a dominant secondary pathway in **PM1** that is similar to that found in **P1**.

## 5.5. Conclusion

The mechanism of conductance through mono-functionalized single-molecule wires was determined by measuring the electrical and mechanical properties in single-molecule junctions. By using a combination of rational molecular design, STM- and AFM-BJ techniques, we showed that mono and difunctionalized molecular wires conduct through the backbone of a single molecule rather than through  $\pi$ - $\pi$ -stacked dimers. The conductance mechanism differs between the *para-para* bound (**PPn**) and *para- $\pi$*  bound molecules (**Pn**, **P1A** and **P1TA**). Since the **Pn** series is functionalized with only one linker, a mechanically weak, yet electronically coupled, Au- $\pi$  interaction completes the molecular circuit. The limited strength of this new interaction causes significant variability in junction-to-junction conductance. However, installing a second linker at the *meta* position stabilizes this interaction by securing the terminal phenyl group to the electrode surface, such as for the *para-meta* compounds (**PMn** and **PM1A**). *Meta* linkers result in quantum electronic interference effects, but the position of the linkers (*meta* vs.

*para*) does not significantly alter their mechanical attachment to the Au electrodes. By exploiting this attribute we strengthen a direct molecule-metal interaction that dominates in the charge transport of mono-functionalized molecular junctions, in turn enabling us to quantify the charge transport properties arising from Au- $\pi$  interactions. This strategy may prove useful in future molecular-scale device architectures for the positioning of molecules onto electrode surfaces while mediating their electronic couplings, such as is needed for advancement in single-molecule rectification.<sup>21</sup>

## 5.6. References and Footnotes

1. (a) Diez-Perez, I.; Hihath, J.; Lee, Y.; Yu, L.; Adamska, L.; Kozhushner, M. A.; Oleynik, II; Tao, N. *Nature Chem.*, **2009**, *1*, 635; (b) Kim, B.; Choi, S. H.; Zhu, X. Y.; Frisbie, C. D. *J. Am. Chem. Soc.*, **2011**, *133*, 19864; (c) Holmlin, R. E.; Haag, R.; Chabinye, M. L.; Ismagilov, R. F.; Cohen, A. E.; Terfort, A.; Rampi, M. A.; Whitesides, G. M. *J. Am. Chem. Soc.*, **2001**, *123*, 5075.
2. (a) Xu, B. Q.; Tao, N. *J. Science*, **2003**, *301*, 1221; (b) Venkataraman, L.; Klare, J. E.; Tam, I. W.; Nuckolls, C.; Hybertsen, M. S.; Steigerwald, M. L. *Nano Lett.*, **2006**, *6*, 458 ; (c) Park, Y. S.; Whalley, A. C.; Kamenetska, M.; Steigerwald, M. L.; Hybertsen, M. S.; Nuckolls, C.; Venkataraman, L. *J. Am. Chem. Soc.*, **2007**, *129*, 15768; (d) Martin, C. A.; Ding, D.; Sorensen, J. K.; Bjornholm, T.; van Ruitenbeek, J. M.; van der Zant, H. S. J. *J. Am. Chem. Soc.*, **2008**, *130*, 13198; (e) Hong, W.; Manrique, D. Z.; Moreno-García, P.; Gulcur, M.; Mishchenko, A.; Lambert, C. J.; Bryce, M. R.; Wandlowski, T. *J. Am. Chem. Soc.*, **2011**, *134*, 2292.
3. (a) Mayor, M.; Weber, H. B.; Reichert, J.; Elbing, M.; von Hanisch, C.; Beckmann, D.; Fischer, M. *Angew, Chem. Int. Ed.*, **2003**, *42*, 5834; (b) Solomon, G. C.; Andrews, D. Q.; Hansen, T.; Goldsmith, R. H.; Wasielewski, M. R.; Van Duyne, R. P.; Ratner, M.

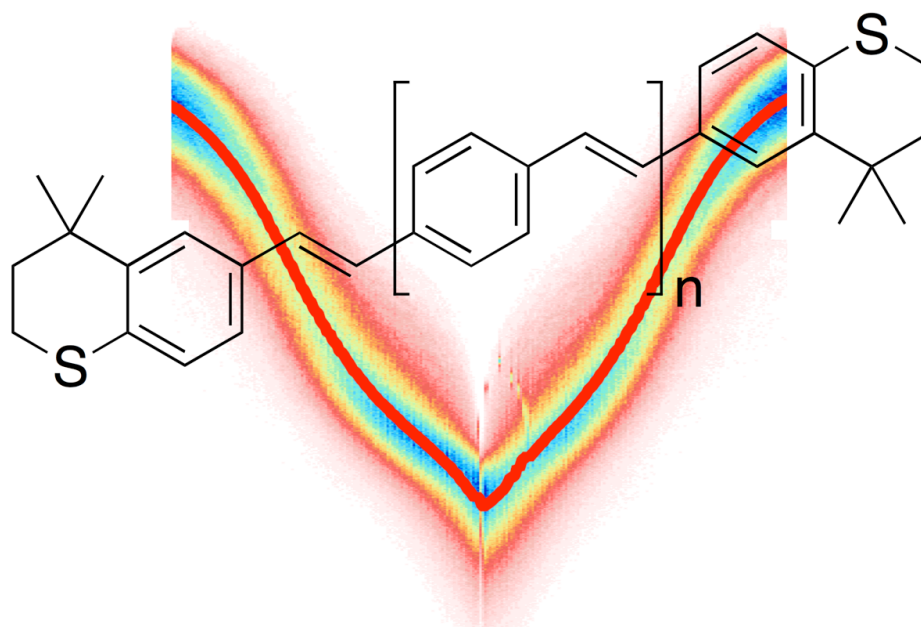
- A. *J. Chem. Phys.*, **2008**, *129*; (c) Ke, S. H.; Yang, W. T.; Baranger, H. U. *Nano Lett.* **2008**, *8*, 3257; (d) Aradhya, S. V.; Meisner, J. S.; Krikorian, M.; Ahn, S.; Parameswaran, R.; Steigerwald, M. L.; Nuckolls, C.; Venkataraman, L. *Nano Lett.*, **2012**, *12*, 1643; (e) Guedon, C. M.; Valkenier, H.; Markussen, T.; Thygesen, K. S.; Hummelen, J. C.; van der Molen, S. J. *Nat. Nanotechnol.*, **2012**, *7*, 305.
4. (a) Frei, M.; Aradhya, S. V.; Koentopp, M.; Hybertsen, M. S.; Venkataraman, L. *Nano Lett.*, **2011**, *11*, 1518; (b) Xu, B. Q.; Xiao, X. Y.; Tao, N. J. *J. Am. Chem. Soc.*, **2003**, *125*, 16164.
5.  $\pi$ - $\pi$ -stacking in STM-BJ's has been previously reported, however many experimental factors were different from our study including the structure of their bridging molecules, longer molecular lengths and different solvent system during their STM-BJ measurements. See: Wu, S. M.; Gonzalez, M. T.; Huber, R.; Grunder, S.; Mayor, M.; Schonenberger, C.; Calame, M. *Nat. Nanotechnol.*, **2008**, *3*, 569.
6. Wittig, G.; Schollkopf, U. *Chem. Ber.*, **1954**, *87*, 1318.
7. Wadsworth, W. S. In *Org. React.*; John Wiley & Sons, Inc.: 1977; Vol. 25, p 73.
8. Kamenetska, M.; Koentopp, M.; Whalley, A.; Park, Y. S.; Steigerwald, M.; Nuckolls, C.; Hybertsen, M.; Venkataraman, L. *Phys. Rev. Lett.*, **2009**, *102*, 126803.
9. Parameswaran, R.; Widawsky, J. R.; Vazquez, H.; Park, Y. S.; Boardman, B. M.; Nuckolls, C.; Steigerwald, M. L.; Hybertsen, M. S.; Venkataraman, L. *J. Phys. Chem. Lett.*, **2010**, *1*, 2114–2119.
10. *Jaguar* (version 7.8, Schrodinger LLC, New York, NY, 2011).
11. Widawsky, J. R.; Kamenetska, M.; Klare, J.; Nuckolls, C.; Steigerwald, M. L.; Hybertsen, M. S.; Venkataraman, L. *Nanotechnology*, **2009**, *20*, 434009.
12. (a) Kiguchi, M.; Tal, O.; Wohlthat, S.; Pauly, F.; Krieger, M.; Djukic, D.; Cuevas, J. C.; van Ruitenbeek, J. M. *Phys. Rev. Lett.*, **2008**, *101*, 046801; (b) Kiguchi, M.; Miura, S.; Takahashi, T.; Hara, K.; Sawamura, M.; Murakoshi, K. *J. Phys. Chem. Cm*, **2008**, *112*, 13349.
13. (A) Schneebeli, S.; Kamenetska, M.; Cheng, Z.; Skouta, R.; Friesner, R. A.; Venkataraman, L.; Breslow, R. *J. Am. Chem. Soc.*, **2011**, *133*, 2136–2139; (b) Park, H.; Park, J.; Lim, A.; Anderson, E.; Alivisatos, A.; McEuen, P. *Nature*, **2000**, *407*, 57–60; (c) Schull, G.; Frederiksen, T.; Arnau, A.; Sanchez-Portal, D.; Berndt, R.

- Nature Nanotechnology*, **2011**, *6*, 23–27; (d) Neel, N.; Kroeger, J.; Limot, L.; Palotas, K.; Hofer, W. A.; Berndt, R. *Phys. Rev. Lett.*, **2007**, *98*, 016801.
14. **PPn**, **PMn** and **Pn** represent the first oligoene series having no main-chain functionalizations to be studied in STM-BJs or other single-molecule methods. Other oligoene systems studied are based on carotenoid or  $\alpha,\omega$ -diphenyl- $\mu,\nu$ -dicyano structures, which are decorated with methyl or cyano groups along the conjugated backbone (see: reference 13).
  15. (a) Meisner, J. S.; Kamenetska, M.; Krikorian, M.; Steigerwald, M. L.; Venkataraman, L.; Nuckolls, C. *Nano Lett.*, **2011**, *11*, 1575; (b) He, J.; Chen, F.; Li, J.; Sankey, O. F.; Terazono, Y.; Herrero, C.; Gust, D.; Moore, T. A.; Moore, A. L.; Lindsay, S. M. *J. Am. Chem. Soc.*, **2005**, *127*, 1384.
  16. Large variability in the junction conductance of the **Pn** series results in a range in the estimation of the decay constant ( $0 > \beta > 0.46 \text{ \AA}^{-1}$ ).
  17. Venkataraman, L.; Klare, J. E.; Tam, I. W.; Nuckolls, C.; Hybertsen, M. S.; Steigerwald, M. *Nano Lett.*, **2006**, *6*, 458–462.
  18. 2D histograms are generated using an automated algorithm with the added requirement that a  $G_0$  break is clearly identifiable in the trace (more than 80% of the traces that start with a conductance greater than  $1 G_0$  and successfully break, satisfy this requirement). In 2D histograms the conductance is binned logarithmically with 200 bins per decade in conductance (y-axis), while displacement is binned linearly (x-axis).
  19. Immediately after the formation of gold point contact electrodes, surface adatoms quickly reorganize, thus widening the distance between the electrodes. We refer to this as the "snapback" distance. This was first discovered during measurements at 4 K: (a) Yanson, A. I.; Bollinger, G. R.; van den Brom, H. E.; Agrait, N.; van Ruitenbeek, J. M. *Nature*, **1998**, *395*, 783; For room temperature: (b) Quek, S. Y.; Kamenetska, M.; Steigerwald, M. L.; Choi, H. J.; Louie, S. G.; Hybertsen, M. S.; Neaton, J. B.; Venkataraman, L. *Nat. Nanotechnol.*, **2009**, *4*, 230.
  20. (a) Venkataraman, L.; Park, Y. S.; Whalley, A. C.; Nuckolls, C.; Hybertsen, M. S.; Steigerwald, M. L. *Nano Lett.*, **2007**, *7*, 502; (b) Ma, G. H.; Sun, L. L.; Zhang, R. X.; Shen, Z. Y.; Hou, S. M. *Chem. Phys.*, **2010**, *375*, 67; (c) Li, Z.; Kosov, D. S. *Phys.*

- Rev. B*, **2007**, *76*, 035415; (d) Quek, S. Y.; Venkataraman, L.; Choi, H. J.; Loule, S. G.; Hybertsen, M. S.; Neaton, J. B. *Nano Lett.*, **2007**, *7*, 3477.
21. Aviram, A.; Ratner, M. A. *Chem. Phys. Lett.*, **1974**, *29*, 277–283.

## Chapter 6. Promising Molecular Wires for Current-Voltage Measurements of Molecular Junctions

*In this chapter, molecules were synthesized by myself, while the physical investigations were performed by Eek Huisman and Jonathan Widawsky. Pierre Darancet is responsible for modeling and calculations. Other DFT calculations were run by Michael Steigerwald and myself.*



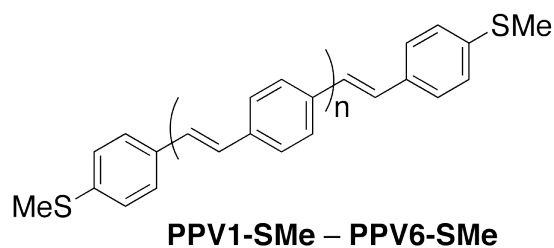
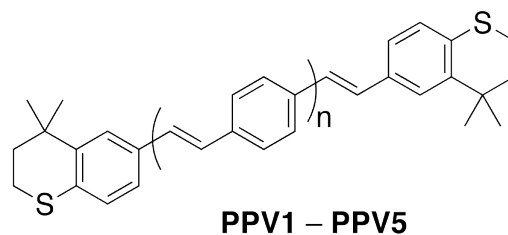
### 6.1. Background and Motivation

The electronic properties of molecular junctions have been studied using a variety of linear chemical structures and it is commonly found for organic molecules that the through-molecule current decays exponentially as the length of the molecules increase.<sup>1</sup> This decrease is a result of the longer tunneling barriers in the molecules of increased

length. The other parameters that govern zero-bias conductance in the Landauer-Büttiker model,<sup>2</sup> are the energy of the conducting orbitals and their coupling to the metal electrodes.<sup>3</sup> In fact, it is often found that a single molecular orbital dominates the charge transport properties.<sup>4</sup> The molecular level broadens, due to its interaction with the electrodes, resulting in a finite conductance at the Fermi energy. However, the relationship between broadening and conductance decay as the molecular length is systemically changed is not well understood.

In this chapter, we outline the synthesis of two families of conjugated molecules that show promise for understanding the current-voltage (IV) characteristics of single-molecule junctions, which may aid in understanding the relationship between junction conductance and molecular level broadening. A series of symmetric molecules, oligo(p-phenylenevinylene)<sup>5</sup> (PPV) derivatives (Figure 6.1A), as well as a series of asymmetric oligoene derivatives (Figure 6.1C) are prepared and range in length from 1.2 to 4.0 nm. Their prototypical molecular wire structures are linear and fully conjugated. We believe these molecules to have promising current-voltage (IV) characteristics.



(A) Oligo(p-phenylenevinylene) (**PPVn**) Derivatives

## (B) Asymmetric 3,4-Methylthio-diphenyl-Oligoenes

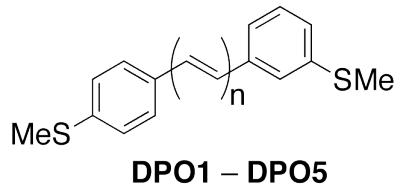


**Figure 6.1:** Two different families of oligo(p-phenylenevinylene) derivatives, the **PPVn** series was synthesized while the **PPVn-SMe** derivatives comprise our theoretical control group. Asymmetric oligoene were synthesized from the stilbene to the diphenyl pentene and are end-functionalized with one *meta*- and one *para*-methylsulfide linker group.

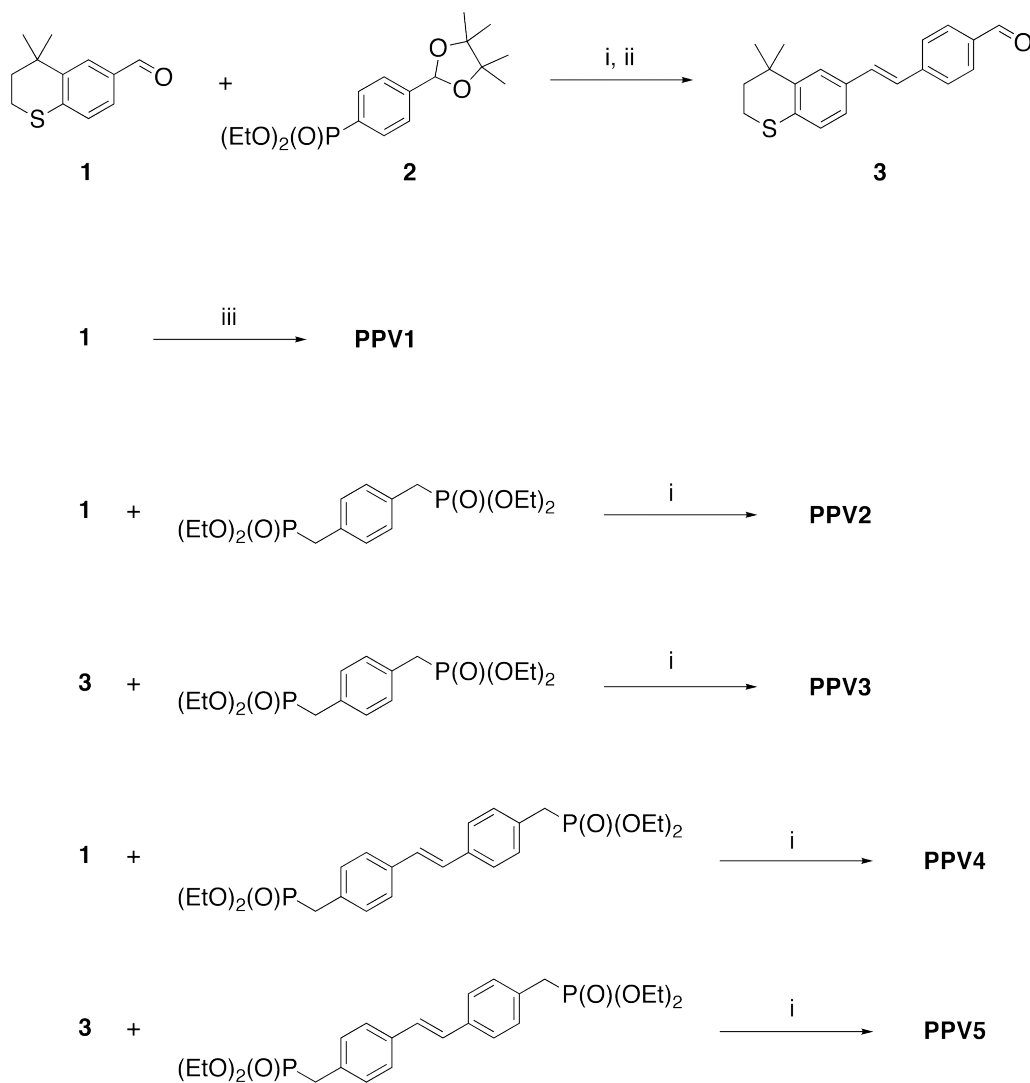
## 6.2. PPV Molecular Wire Design

A series of five PPV molecular wires (**PPV1-PPV5**, Figure 6.1A) and studied their charge transport characteristics using the scanning tunneling microscopy (STM) break-junction technique.<sup>6,7</sup> The molecular wires are terminated with alkylsulfide linker groups, which bind to the electrodes through the formation of a donor-acceptor bond between the sulfur lone pairs and under-coordinated Au surface atoms. Alkylsulfide linkers are embedded inside a six-membered ring locking the orientation of the sulfur lone pair with respect to the  $\pi$ -system.<sup>8</sup> The two protruding methyl groups added to this ring simplify the synthesis<sup>9</sup> as well as endows these otherwise unfunctionalized PPV's with superior solubility by disrupting intermolecular  $\pi$ - $\pi$  stacking interactions; without these specially designed end-groups **PPVn** molecules, where  $n > 2$  are too insoluble to measure using our STM-BJ method.

## 6.3. Synthesis of PPV Molecular Wires

Shown in Scheme 6.1A, each member of the **PPVn** series was synthesized in one step from the end-functionalized benzaldehyde (**1**; see also Ch. 1 and Appendix A) or extended (*E*)-4-styrylbenzaldehyde (**3**). Compound **3** is also prepared from compound **1** through Hörner-Wadsworth-Emmons (H.W.E.)<sup>10</sup> chemistry from the acetal-protected phosphonate (**2**). The smallest homologue, **PPV1**, was synthesized by McMurray coupling<sup>11</sup> from two molar equivalents of **1**. Similarly, **PPV2** and **PPV4** were also prepared from two molar equivalents of **1**, however through H.W.E. conditions with the appropriate bisphosphonate. Using the same conditions, the longer odd-numbered oligomers, **PPV3** and **PPV5**, were obtained from compound **2**. Each compound was

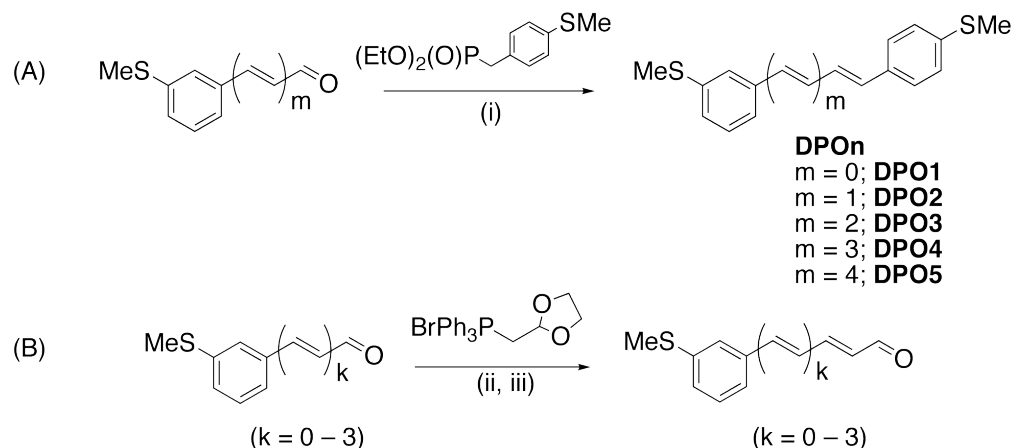
characterized by mass spectrometry, and UV-vis absorption spectroscopy,  $^1\text{H}$ - and  $^{13}\text{C}$ -, as well as  $^{31}\text{P}$ -NMR (when applicable).



**Scheme 6.1:** Synthetic route to end-functionalized oligo(p-phenylenevinylene) molecular wires (**PPVn**). (i) H.W.E. reaction: tBuOK, THF, 0° C to 25° C, 16 h; (ii) conc. HCl, THF, 25° C, 3 h; (iii) McMurray coupling: Zn powder, TiCl<sub>4</sub>, THF, reflux, 16 h. Cyclic thioethers are more soluble than the MeS-terminated analogues due to the disruption of intermolecular attractive forces by distal out-of-plane methyl groups. For a comparison, **PPV5** and the smaller methylthio derivative, 1,4-bis(4-(4-(methylthio)styryl)styryl)-benzene (**PPV2-SMe**), have comparable solubilities in chlorinated organic solvents.

## 6.4. Synthesis of Asymmetric Oligoene Wires

A family of oligoene rectifier candidates bearing one *meta*- and one *para*-methylsulfide linker were prepared from the appropriate oligoenals and dimethyl 4-(methylthio)benzylphosphonate through a Horner-Wadsworth-Emmons olefination using potassium *tert*-butoxide as a base. Oligoenals were extended through iterative Wittig homologation cycles (see Chapter 2) starting from 3-(methylthio)benzaldehyde.



**Scheme 7.1:** Synthetic route to asymmetric oligoene rectifier candidates. (i) Horner-Wadsworth-Emmons reaction: *t*BuOK, THF, 0° to 25° C over 12 h; (ii) Wittig Homologation reaction: LiOMe, THF, reflux, 16 h; (iii) Acidolysis: 10% aq. HCl, THF, 60 min.

## 6.5. STM-break Junctions

We plan to carry out STM-BJ experiments to measure the conductance as a function of voltage of these oligomers. This procedure is similar to that described in the

previous chapters. For each experiment on PPV molecules a point-contact between a gold tip and substrate will be broken repeatedly (typically 5000 times) in a dilute molecular solution in 1,2,4-trichlorobenzene. The conductance of our PPV molecules was found to be concentration dependent. Because of this we measured them at the lower limit of concentration (10  $\mu\text{M}$ ); below this concentration the formation of molecular junctions was not observed. Conductance (current/voltage) traces are recorded while the tip is retracted with a constant speed of 16 nm/s over a distance of 5-8 nm at a bias of 250-700 mV.

## 6.6. Theoretical Methods

To determine the molecular length and HOMO-LUMO energy gaps of the **PPV $n$**  series, electronic structure calculations<sup>12</sup> using the B3LYP hybrid functional and the 6-31G\*\* basis sets. Besides the **PPV $n$**  series, we also ran calculations of their *para*-methylthio analogues (**MeS-PPV $n$** ) as a reference. The geometries of both series were fully optimized. The final geometries, total energies, bond distances, bond angles and torsional angles may be found in the Appendix D. Below in Table 6.1 is a summary of the HOMO-LUMO energy differences (band gap) results of our calculations on our **PPV $n$**  series (from  $n = 1$  to 5) and our reference molecules (**MeS-PPV $n$** ;  $n = 1$  to 6). As expected, molecular band gaps converge as oligomer length ( $n$ ) increases (Figure 6.2). Previous experimental studies on oligo(*p*-phenylenevinylene) compounds have predicted the saturation of the electronic properties at oligomeric lengths of  $n \approx 10$ .<sup>13,14</sup> Geometry optimizations of the longer **PPV $n$**  molecules (**PPV3**, **PPV4** and **PPV5**) were found to

converge on a distribution of geometries, all of which were energetically similar. The geometries differed from each other by small degrees of twists and bends along the conjugated backbone. Incorporation of even the smallest distortions gave large variations in the molecular length (i.e. S-S distance). **MeS-PPV $n$**  molecules, however, converged on reliable linear geometries, which are expected for fully elongated break junction. In such cases, sulfur-to-sulfur (S-S) distances were taken from the **MeS-PPV $n$**  calculations and not from those of the **PPV $n$**  molecules.

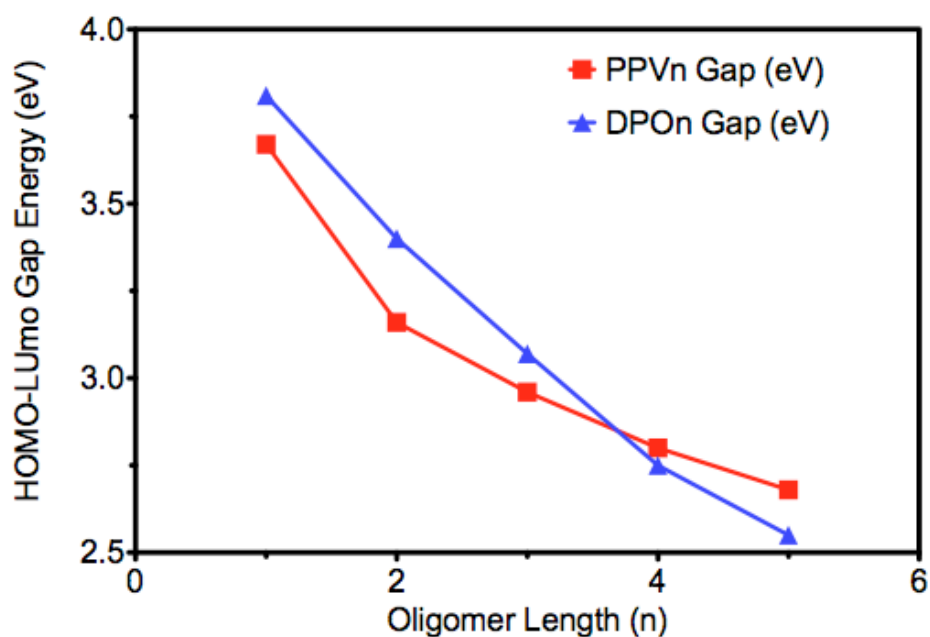


**Figure 6.2:** DFT estimations of the molecular band gap of **PPV $n$**  and asymmetric **DPO $n$**  series.

<b>PPV<sub>n</sub></b>	S-S Length <sup>b</sup> (nm)	HOMO (eV)	LUMO (eV)	HOMO- LUMO gap
<b>PPV1</b>	1.30	-4.90	-1.23	3.67
<b>PPV2</b>	1.97	-4.84	-1.68	3.16
<b>PPV3<sup>a</sup></b>	2.65 <sup>a</sup>	-4.82	-1.86	2.96
<b>PPV4<sup>a</sup></b>	3.31 <sup>a</sup>	-4.86	-2.06	2.80
<b>PPV5<sup>a</sup></b>	3.99 <sup>a</sup>	-4.79	-2.11	2.68
<b>DPO<sub>n</sub></b>				
<b>DPO1</b>	1.20	-5.22	-1.41	3.81
<b>DPO2</b>	1.42	-5.06	-1.66	3.40
<b>DPO3</b>	1.70	-4.93	-1.86	3.07
<b>DPO4</b>	1.95	-4.70	-1.95	2.75
<b>DPO5</b>	2.17	-4.62	-2.07	2.55

**Table 6.1:** DFT calculation results on **PPV<sub>n</sub>** and **DPO<sub>n</sub>** series. <sup>a</sup>Due to unreliable convergence in the geometry optimization, sulfur-to-sulfur (S-S) distances for the longer oligomers, **PPV3-PPV5**, were estimated from DFT calculations performed on the model series **MeS-PPV** (see Appendix E). <sup>b</sup>Through-space sulfur-to-sulfur distance.

## 6.7. Conclusions and Future Outlook

A set of oligo(p-phenylenevinylene) oligomers (**PPV<sub>n</sub>**) was end-functionalized with cyclic alkylsulfides making them soluble for STM-BJ studies. This is a work in progress and we are currently investigating the single-molecule conductance and IV curves for **PPV<sub>n</sub>** molecular junctions. Future studies include modeling the electronic properties (i.e. the IV and transmission characteristics) of **PPV<sub>n</sub>** junctions in greater detail.

The asymmetric end-functionalization of oligoene molecular wires (**DPOn**) is also a significant achievement since they may lead to large rectification ratios<sup>15</sup> as a result of asymmetric electronic coupling between the electrodes and molecule. As gap energies decrease (molecular length increases) more asymmetric transmission profiles may be accessed in the scanned bias window, resulting in asymmetric IV properties. We are currently investigating the IV characteristics of the single-molecule junctions of these molecules.

Molecular rectification<sup>16</sup> is definitely one of the basic steps toward controlling molecular electronics, since electronic components are essential in the construction of logic switches. Such rectifiers are rare due to the difficulties in building and orienting them between electrical leads. Additionally, contact asymmetry can be adapted to molecules outside of oligoenes. It is also compatible with other molecular rectification strategies such as those employed in donor-acceptor designs and may aid in the generation of high-performance single-molecule rectifiers in the future.

## 6.8. References and Footnotes

---

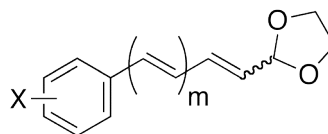
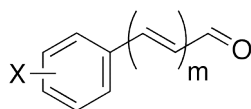
1. Salomon, A.; Cahen, D.; Lindsay, S.; Tomfohr, J.; Engelkes, V.B.; Frisbie, C.D., *Adv. Mat.*, **2003**, *15*, 1881–1890.
2. (a) Büttiker, M.; Imry, Y.; Landauer, R.; Pinhas, S. *Phys. Rev. B*, **1985**, *31*, 6207–6215; (b) Datta, S. *Electronic Transport in Mesoscopic Systems* (Cambridge University Press, **1995**).
3. Datta, S. *Quantum transport: Atom to Transistor* (Cambridge University Press, Cambridge, **2005**).



- 
4. (a) Zotti, L. A.; Kirchner, T.; Cuevas, J.-C.; Pauly, F.; Huhn, T.; Scheer, E.; Erbe, A. *Small*, **2010**, *6*, 1529–1535; (b) Yee, S. K.; Sun, J.; Darancet, P.; Tilley, T. D.; Majumdar, A.; Neaton, J. B.; Segalman, R. A. *ACS Nano*, **2011**, *5*, 9256–9263.
  5. (a) Davis, W. B.; Svec, W. A.; Ratner, M. A.; Wasielewski, M. R. *Nature*, **1998**, *396*, 60–63; (b) Kushmerick, J. G.; Holt, D. B.; Pollack, S. K.; Ratner, M. A.; Yang, J. C.; Schull, T. L.; Naciri, J.; Moore, M. H.; Shashidhar, R. *J. Am. Chem. Soc.*, **2002**, *124*, 10654–10655; (c) Kubatkin, S.; Danilov, A.; Hjort, M.; Cornil, J.; Bredas, J.-L.; Stuhr-Hansen, N.; Hedegård, P.; Bjørnholm, T. *Nature*, **2003**, *425*, 698–701; (c) Huber, R.; González, M. T.; Wu, S.; Langer, M.; Grunder, S.; Horhoiu, V.; Mayor, M.; Bryce, M. R.; Wang, C.; Jitchati, R.; Schönenberger, C.; Calame. *J. Am. Chem. Soc.*, **2008**, *130*, 1080–1084; (d) Osorio, E. A.; O’Neill, K.; Stuhr-Hansen, N.; Nielsen, O. F.; Bjørnholm, T.; van der Zant, H. S. J. *Adv. Mat.*, **2007**, *19*, 281–285.
  6. Xu, B. Q.; Tao, N. J. *J. Science*, **2003**, *301*, 1221–1223.
  7. Venkataraman, L.; Klare, J. E.; Tam, I. W.; Nuckolls, C.; Hybertsen, M. S.; Steigerwald, M. L. *Nano Lett.*, **2006**, *6*, 458–462.
  8. Park, Y. S.; Widawsky, J. R.; Kamenetska, M.; Steigerwald, M. L.; Hybertsen, M. S.; Nuckolls, C.; Venkataraman, L. *J. Am. Chem. Soc.*, **2009**, *131*, 10820–10821.
  9. Schneebeli, S.; Kamenetska, M.; Foss, F.; Vazquez, H.; Skouta, R.; Hybertsen, M.; Venkataraman, L.; Breslow, R. *Org. Lett.*, **2010**, *12*, 4114–4117.
  10. Wadsworth, W. S. *Org. React.*, **1977**, *25*, 73.
  11. McMurry, J. E.; Fleming, M. P. *J. Am. Chem. Soc.*, **1974**, *96*, 4708–4709.
  12. *Jaguar* (version 7.8, Schrodinger LLC, New York, NY, 2011).
  13. Geerts, Y., Klaerner, G. & Muellen, K. *Electronic materials: The Oligomeric Approach* (eds. Muellen, K. & Wegner, G.) (Wiley-VHC, New York, 1998).
  14. Meier, H., Stalmach, U. & Kolshorn, H. *Acta Polym.*, **1997**, *48*, 379–384.
  15. Metzger, R. M. *J. Mat. Chem.*, **2008**, *18*, 4364–4369.
  16. Aviram, A.; Ratner, M. A. *Chem. Phys. Lett.* **1974**, *29*, 277–283.

## Appendix A (Part 1)

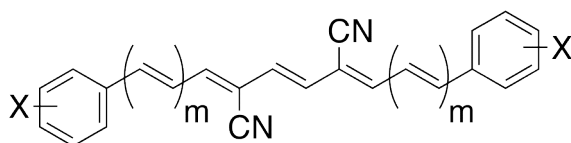
## A1. List of Compounds



X	m	Molecule
H	2	<b>1a</b>
H	3	<b>1b</b>
H	4	<b>1c</b>
H	5	<b>1d</b>
4-SMe	1	<b>2a</b>
4-SMe	2	<b>2b</b>
4-SMe	3	<b>2c4</b>
4-SMe	4	<b>2d</b>
4-SC <sub>4</sub> H <sub>8</sub>	0	<b>3a</b>
4-SC <sub>4</sub> H <sub>8</sub>	1	<b>3b</b>
4-SC <sub>4</sub> H <sub>8</sub>	2	<b>3c</b>
4-SC <sub>4</sub> H <sub>8</sub>	3	<b>3d</b>
4-SC <sub>4</sub> H <sub>8</sub>	4	<b>3e</b>
4-SC <sub>5</sub> H <sub>10</sub>	0	<b>4a</b>
4-SC <sub>5</sub> H <sub>10</sub>	1	<b>4b</b>
4-SC <sub>5</sub> H <sub>10</sub>	2	<b>4c</b>
4-SC <sub>5</sub> H <sub>10</sub>	3	<b>4d</b>
4-SC <sub>5</sub> H <sub>10</sub>	4	<b>4e</b>
4-SC <sub>5</sub> H <sub>10</sub>	5	<b>4f</b>
4-Me <sub>2</sub> N	2	<b>5a</b>
4-Ph <sub>2</sub> N	1	<b>6a</b>
4-Br	1	<b>7a</b>
4-Br	2	<b>7b</b>
4-Br	3	<b>7c</b>
4-CO <sub>2</sub> H	0	<b>8a</b>
4-CO <sub>2</sub> H	1	<b>8b</b>

X	m	E/Z	Molecule
H	2	<i>E</i>	<b><i>E</i>-1e</b>
H	2	<i>Z</i>	<b><i>Z</i>-1e</b>
Br	1	<i>E</i>	<b><i>E</i>-7d</b>
Br	1	<i>Z</i>	<b><i>Z</i>-7d</b>
Br	2	<i>E</i>	<b><i>E</i>-7e</b>
Br	2	<i>Z</i>	<b><i>Z</i>-7e</b>

4-CO <sub>2</sub> H	2	<b>8c</b>
4-CO <sub>2</sub> Et	0	<b>9a</b>
4-CO <sub>2</sub> Et	1	<b>9b</b>
4-CO <sub>2</sub> Et	2	<b>9c</b>
3,5-OC <sub>6</sub> H <sub>13</sub>	0	<b>10a</b>
3,5-OC <sub>6</sub> H <sub>13</sub>	1	<b>10b</b>
3,5-OC <sub>6</sub> H <sub>13</sub>	2	<b>10c</b>
3,5-OC <sub>10</sub> H <sub>21</sub>	0	<b>11a</b>
3,5-OC <sub>10</sub> H <sub>21</sub>	1	<b>11b</b>
3,5-OC <sub>10</sub> H <sub>21</sub>	2	<b>11c</b>
3,5-OC <sub>14</sub> H <sub>29</sub>	0	<b>12a</b>
3,5-OC <sub>14</sub> H <sub>29</sub>	1	<b>12b</b>
4-C≡C-C <sub>6</sub> H <sub>13</sub>	0	<b>13a</b>
4-C≡C-C <sub>6</sub> H <sub>13</sub>	1	<b>13b</b>
4-C≡C-C <sub>6</sub> H <sub>13</sub>	2	<b>13c</b>
4-CN	1	<b>14a</b>



### DPDCn-X

X	m	Total n	Molecule
H	0	3	<b>DPDC3</b>
H	1	5	<b>DPDC5</b>
H	2	7	<b>DPDC7</b>
H	3	9	<b>DPDC9</b>
H	4	11	<b>DPDC11</b>
H	5	13	<b>DPDC13</b>
4-SMe	0	3	<b>DPDC3-SMe</b>
4-SMe	1	5	<b>DPDC5-SMe</b>
4-SMe	2	7	<b>DPDC7-SMe</b>
4-SMe	3	9	<b>DPDC9-SMe</b>
4-SMe	4	11	<b>DPDC11-SMe</b>
4-SC <sub>4</sub> H <sub>8</sub>	0	3	<b>DPDC3-SC<sub>4</sub>H<sub>8</sub></b>

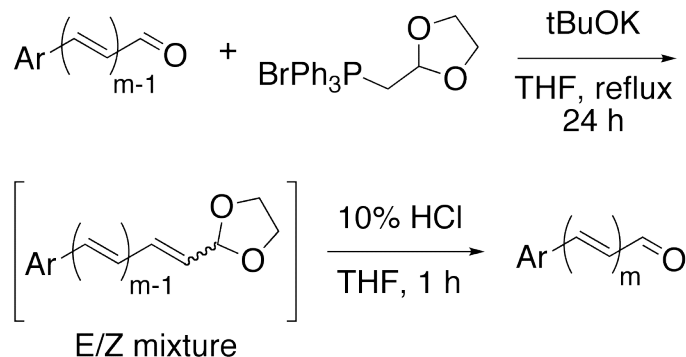
4-SC <sub>4</sub> H <sub>8</sub>	1	5	<b>DPDC5-SC<sub>4</sub>H<sub>8</sub></b>
4-SC <sub>4</sub> H <sub>8</sub>	2	7	<b>DPDC7-SC<sub>4</sub>H<sub>8</sub></b>
4-SC <sub>4</sub> H <sub>8</sub>	3	9	<b>DPDC9-SC<sub>4</sub>H<sub>8</sub></b>
4-SC <sub>4</sub> H <sub>8</sub>	4	11	<b>DPDC11-SC<sub>4</sub>H<sub>8</sub></b>
4-SC <sub>5</sub> H <sub>10</sub>	0	3	<b>DPDC3-SC<sub>5</sub>H<sub>10</sub></b>
4-SC <sub>5</sub> H <sub>10</sub>	1	5	<b>DPDC5-SC<sub>5</sub>H<sub>10</sub></b>
4-SC <sub>5</sub> H <sub>10</sub>	2	7	<b>DPDC7-SC<sub>5</sub>H<sub>10</sub></b>
4-SC <sub>5</sub> H <sub>10</sub>	3	9	<b>DPDC9-SC<sub>5</sub>H<sub>10</sub></b>
4-SC <sub>5</sub> H <sub>10</sub>	4	11	<b>DPDC11-SC<sub>5</sub>H<sub>10</sub></b>
4-SC <sub>5</sub> H <sub>10</sub>	5	13	<b>DPDC13-SC<sub>5</sub>H<sub>10</sub></b>
4-Me <sub>2</sub> N	0	3	<b>DPDC3-NMe<sub>2</sub></b>
4-Me <sub>2</sub> N	1	5	<b>DPDC5-NMe<sub>2</sub></b>
4-Me <sub>2</sub> N	2	7	<b>DPDC7-NMe<sub>2</sub></b>
4-Ph <sub>2</sub> N	0	3	<b>DPDC3-NPh<sub>2</sub></b>
4-Ph <sub>2</sub> N	1	5	<b>DPDC5-NPh<sub>2</sub></b>
4-Br	0	3	<b>DPDC3-Br</b>
4-Br	1	5	<b>DPDC5-Br</b>
4-Br	2	7	<b>DPDC7-Br</b>
4-Br	3	9	<b>DPDC9-Br</b>
4-CO <sub>2</sub> H	0	3	<b>DPDC3-CO<sub>2</sub>H</b>
4-CO <sub>2</sub> H	1	5	<b>DPDC5-CO<sub>2</sub>H</b>
4-CO <sub>2</sub> H	2	7	<b>DPDC7-CO<sub>2</sub>H</b>
4-CO <sub>2</sub> Et	0	3	<b>DPDC3-CO<sub>2</sub>Et</b>
4-CO <sub>2</sub> Et	1	5	<b>DPDC5-CO<sub>2</sub>Et</b>
4-CO <sub>2</sub> Et	2	7	<b>DPDC7-CO<sub>2</sub>Et</b>
3,5-OC <sub>6</sub> H <sub>13</sub>	0	3	<b>DPDC3-OC<sub>6</sub>H<sub>13</sub></b>
3,5-OC <sub>6</sub> H <sub>13</sub>	1	5	<b>DPDC5-OC<sub>6</sub>H<sub>13</sub></b>
3,5-OC <sub>6</sub> H <sub>13</sub>	2	7	<b>DPDC7-OC<sub>6</sub>H<sub>13</sub></b>
3,5-OC <sub>10</sub> H <sub>21</sub>	0	3	<b>DPDC3-OC<sub>10</sub>H<sub>21</sub></b>
3,5-OC <sub>10</sub> H <sub>21</sub>	1	5	<b>DPDC5-OC<sub>10</sub>H<sub>21</sub></b>
3,5-OC <sub>10</sub> H <sub>21</sub>	2	7	<b>DPDC7-OC<sub>10</sub>H<sub>21</sub></b>
3,5-OC <sub>14</sub> H <sub>29</sub>	0	3	<b>DPDC3-OC<sub>14</sub>H<sub>29</sub></b>
3,5-OC <sub>14</sub> H <sub>29</sub>	1	5	<b>DPDC5-OC<sub>14</sub>H<sub>29</sub></b>
4-C≡C-C <sub>6</sub> H <sub>13</sub>	0	3	<b>DPDC3-C<sub>8</sub>H<sub>13</sub></b>
4-C≡C-C <sub>6</sub> H <sub>13</sub>	1	5	<b>DPDC5-C<sub>8</sub>H<sub>13</sub></b>

4-C≡C-C <sub>6</sub> H <sub>13</sub>	2	7	<b>DPDC7-C<sub>8</sub>H<sub>13</sub></b>
4-CN	0	3	<b>DPDC3-CN</b>
4-CN	1	5	<b>DPDC5-CN</b>
2-Br	0	3	<i>ortho</i> - <b>DPDC3-Br</b>
3-Br	0	3	<i>meta</i> - <b>DPDC3-Br</b>
2-OMe	0	3	<i>ortho</i> - <b>DPDC3-OMe</b>
3-OMe	0	3	<i>meta</i> - <b>DPDC3-OMe</b>
4-OMe	0	3	<b>DPDC3-OMe</b>
3-NO <sub>2</sub>	0	3	<i>meta</i> - <b>DPDC3-NO<sub>2</sub></b>
4-NO <sub>2</sub>	0	3	<b>DPDC3-NO<sub>2</sub></b>
4-NO <sub>2</sub>	0	5	<b>DPDC5-NO<sub>2</sub></b>
4-F	0	5	<b>DPDC5-NO<sub>2</sub></b>

## A2. Synthetic Details

### General Information:

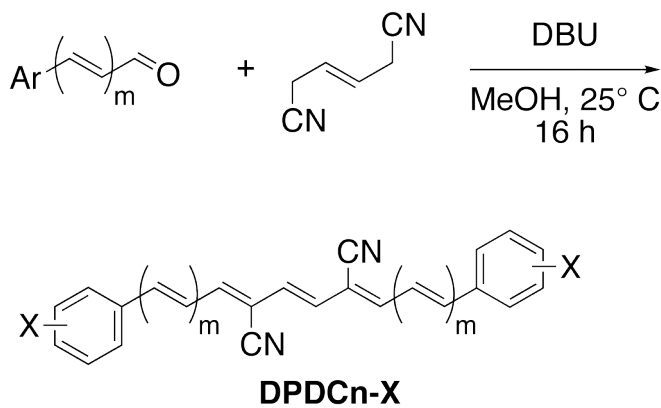
(1,3-dioxolan-2-yl)methyl-triphenylphosphonium bromide was purchased from TCI America and stored in a desiccator. Benzaldehyde, 4-bromobenzaldehyde, 3-bromobenzaldehyde, 2-bromobenzaldehyde, 4-methoxybenzaldehyde, 3-methoxybenzaldehyde, 2-methoxybenzaldehyde, 4-(methylthio)-benzaldehyde, 4-(dimethylamino)-benzaldehyde, 4-formal benzoic acid, 4-fluorobenzaldehyde, 4-nitrobenzaldehyde, 3-nitrobenzaldehyde, 4-cyanobenzaldehyde, *trans*-cinnamaldehyde, *trans*-(4-dimethylamino)cinnamaldehyde and *trans*-(4-nitro)cinnamaldehyde, 1,4-dicyano-2-butene, 1,2-epoxy-2-methylpropane, 1,8-diazabicyclo[5.4.0]undec-7-ene (DBU), 3,3-dimethylallyl bromide and all other reagents were purchased from Sigma-Aldrich Chemical. Alkoxybenzaldehydes,<sup>1</sup>  $\alpha,\omega$ -diphenyl-oligoenes (**DPOn**) and  $\alpha,\omega$ -(4-dimethylamino)phenyl-deca-pentaene<sup>2</sup> (**DPO-NMe<sub>2</sub>**) were synthesized according to the literature. All reactions were carried out under nitrogen unless otherwise noted. All chromatography was performed on a Teledyne ISCO Combiflash RF using Redisep RF silica columns. <sup>1</sup>H and <sup>13</sup>C NMRs were recorded on a Bruker DRX300 (300MHz), DRX400 (400MHz) or Bruker DMX500 (500MHz). In general, mass spectrometry for the oligoenes was difficult to interpret. <sup>1</sup>H and <sup>13</sup>C NMR spectra for the compounds prepared here are contained at the end of the Supporting Information.



**General Procedure for Wittig Homologation of Aldehydes:** As an example, lithium methoxide (0.149 g, 3.93 mmol, 2.6 eq.) was added to a stirring solution of (1,3-dioxolan-2-yl)methyl-triphenylphosphonium bromide (1.62 g, 3.78 mmol, 2.5 eq.) in 50 mL of anhydrous tetrahydrofuran (THF) in a 100-mL round-bottom flask. The suspension was heated to reflux stirred for 30 minutes, changing color from off-white to light orange/pink. *trans*-cinnamaldehyde (0.200 g, 1.51 mmol, 1.0 eq.) in 20 mL of dry THF solution was added dropwise over 30-60 min. The suspension was refluxed for 24 h. The reaction suspension was then cooled to room temperature, at which point 10% aqueous hydrochloric acid (HCl) was added. Stirring was continued for 1 hour in order to hydrolyze the intermediate acetals (mixture of *E*- and *Z*-stereoisomers) to the all-*trans* configuration. The organic layer was extracted with CH<sub>2</sub>Cl<sub>2</sub> (25 mL x3) and the combined fractions were washed with water, sat. aqueous sodium bicarbonate solution and brine, and then dried over MgSO<sub>4</sub>. Solvent was removed by rotary evaporation and the product was purified via column chromatography using an eluent gradient from 0% to 10% ethyl acetate in hexanes over 25 column volumes. The product, in this case (2*E*,4*E*)-5-phenylpenta-2,4-dienal, was obtained in 92% yield (0.199 g) as a yellow oil. This reaction was typically carried out on 0.200 g of starting aldehyde for quick work up and

separation, but can easily be scaled up to multi-gram quantities. We have attempted this reaction on a 5.00 g scale without significant loss in yield (~3.7%).

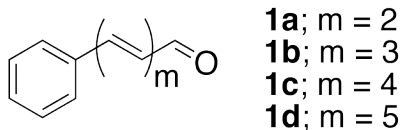
Alternatively, the (*E*)- and (*Z*)-acetals may be isolated by column chromatography. As in the reaction above, *trans*-cinnamaldehyde is reacted with the triphenylphosphonium salt. After refluxing for 24 h the reaction was cooled to room temperature, diluted with water, extracted with CH<sub>2</sub>Cl<sub>2</sub> (3x) and dried over MgSO<sub>4</sub>. The organic solvent was removed by rotary evaporation. The (*E*)- and (*Z*)-diene-acetals were isolated by column chromatography 5% ethyl acetate in hexanes ( $R_{fE}/R_{fZ} = 0.2/0.1$ ) in 16.6% and 70.8%, respectively. (*Z*)-isomer is produced in 14:3 ratio compared with the (*E*)-isomer. When 10% aq. HCl solution is added to a solution of either stereoisomer or a mixture of isomers only the *E*-enal, the desired product, is obtained (see <sup>1</sup>H and <sup>13</sup>C NMR for compound **1a**). In the route to most DPDC's we did not isolate the intermediate acetals. In few circumstances it was synthetically necessary to isolate these acetals in order to synthesize the carboxylic acid polyenals for our DPDCn-CO<sub>2</sub>H series (see **7e** and **7d**).





**General Procedure for Double Knoevenagel Condensation:** The appropriate oligoenal (150 mg) and 1,4-dicyano-2-butene (0.75 eq.) were dissolved in wet methanol (25-50 mL) in a 100-mL round-bottomed flask (anhydrous solvents do not effect isolated yield). In some cases, the aryl-oligoenals were insoluble in methanol and a methanol/tetrahydrofuran mixture was used instead. The flask was sealed with a rubber septum and purged by bubbling nitrogen through the reaction solution for 10 minutes. 1,8-diazabicyclo[5.4.0]undec-7-ene (DBU; 1.0 eq.) were added via syringe and the solution was left stirring for 16 hours, over which the product usually precipitated out. The crude product was filtered off and washed with methanol and then purified either by recrystallization from dichloromethane/methanol or by flash column chromatography using dichloromethane/hexanes (1:1) as eluent. To test whether this procedure was scalable we prepared **DPDC5** on gram quantities without a significant loss in yield (~4%).

### Synthetic Experimentals and Characterization:



*(2E,4E)*-5-phenylpenta-2,4-dienal (**1a**; m = 2): General Wittig homologation procedure.

The product was prepared from *trans*-cinnamaldehyde and isolated as a yellow oil in 92.0% yield. This compound is known and agrees with spectroscopic data in literature.<sup>3</sup>

<sup>1</sup>H NMR (400 MHz, CDCl<sub>3</sub>): δ 9.63 (d, *J* = 8.1 Hz, 1H), 7.51 (d, *J* = 8.4 Hz, 2H), 7.34 (m, 4H), 7.07-7.10 (m, 2H), 6.30 (dd, *J* = 7.9 Hz, 15.2 Hz, 1H); <sup>13</sup>C NMR (400 MHz, CD<sub>2</sub>Cl<sub>2</sub>): δ 194.1, 152.6, 142.9, 136.0, 132.0, 130.1, 129.4, 128.0, 126.6.

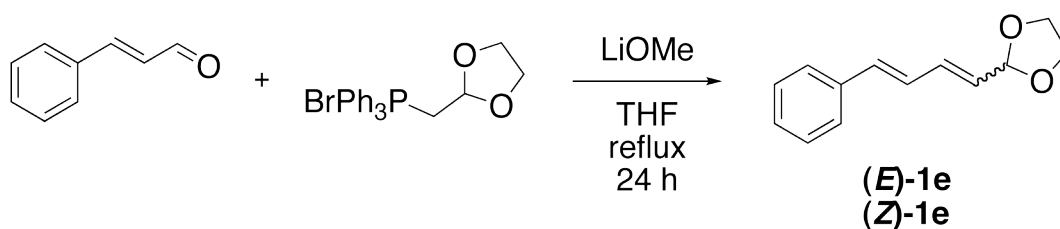
*(2E,4E,6E)*-7-phenylhepta-2,4,6-trienal (**1b**; m = 3): General Wittig homologation procedure. The product was prepared from **1a** and isolated as a dark yellow solid in 88.0% yield. This compound is known and agrees with spectroscopic data in literature.<sup>4,5</sup>

<sup>1</sup>H NMR (400 MHz, CDCl<sub>3</sub>): δ 9.62 (d, *J* = 8.0 Hz, 1H), 7.49 (d, *J* = 8.2 Hz, 2H), 7.40-7.28 (m, 3H), 7.23 (dd, *J* = 11.6 Hz, 15.2 Hz, 1H), 6.96-6.86 (m, 3H), 6.61 (dd, *J* = 11.2 Hz, 14.0 Hz, 1H), 6.22 (dd, *J* = 8.0 Hz, 15.2 Hz, 1H); <sup>13</sup>C NMR (400 MHz, CDCl<sub>3</sub>): δ 193.45, 151.67, 142.71, 138.34, 136.36, 131.23, 130.15, 128.85, 128.83, 127.72, 127.02.

*(2E,4E,6E,8E)*-9-phenylnona-2,4,6,8-tetraenal (**1c**; m = 4): General Wittig homologation procedure. The product was prepared from **1b** and isolated as an orange solid in 70.0% yield. This compound is known and agrees with spectroscopic data in literature.<sup>4,5</sup> <sup>1</sup>H NMR (300 MHz, CDCl<sub>3</sub>): δ 9.59 (d, *J* = 8.1 Hz, 1H), 7.45 (d, *J* = 7.2 Hz, 2H), 7.37-7.24

(m, 3H), 7.17 (dd,  $J = 11.4$  Hz, 15.0 Hz, 1H), 6.90 (dd,  $J = 10.8$  Hz, 15.3 Hz, 1H), 6.82-6.42 (m, 5H), 6.19 (dd,  $J = 8.1$  Hz, 15.0 Hz, 1H);  $^{13}\text{C}$  NMR (300 MHz,  $\text{CDCl}_3$ ):  $\delta$  193.45, 151.72, 142.61, 138.93, 136.76, 136.06, 131.86, 131.02, 129.98, 128.78, 128.36, 128.35, 126.77.

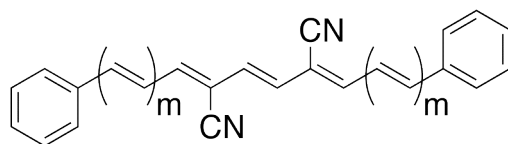
(2*E*,4*E*,6*E*,8*E*,10*E*)-11-phenylundeca-2,4,6,8,10-pentaenal (**1d**;  $m = 5$ ): General Wittig homologation procedure. The product was prepared from **1c** and isolated as a dark orange solid in 55.0% yield. This compound is known and agrees with spectroscopic data in literature.<sup>4,6</sup>  $^1\text{H}$  NMR (300 MHz,  $\text{CDCl}_3$ ):  $\delta$  9.61 (d,  $J = 7.2$  Hz, 1H), 7.46 (d,  $J = 7.5$  Hz, 2H), 7.35 (t,  $J = 8.1$  Hz, 2H), 7.27 (t,  $J = 6.5$  Hz, 1H), 7.18 (dd,  $J = 11.2$  Hz, 15.1 Hz, 1H), 6.90 (dd,  $J = 10.8$  Hz, 15.4 Hz, 1H), 6.77 (dd,  $J = 11.4$  Hz, 14.6 Hz, 1H), 6.68 (d,  $J = 15.6$  Hz, 1H), 6.64-6.30 (m, 5H), 6.18 (dd,  $J = 8.1$  Hz, 15.0 Hz, 1H);  $^{13}\text{C}$  NMR (300 MHz,  $\text{CDCl}_3$ ):  $\delta$  193.44, 151.72, 142.67, 138.83, 137.00, 136.76, 134.78, 132.63, 131.75, 130.92, 129.93, 128.73, 128.71, 128.05, 126.61.



2-((1*E*,3*E*)-4-phenylbuta-1,3-dienyl)-1,3-dioxolane (**E-1e**) and 2-((1*Z*,3*E*)-4-phenylbuta-1,3-dienyl)-1,3-dioxolane (**Z-1e**): Using the modified general Wittig homologation procedure outlined above (pp. S6-S7) The (*E*)- and (*Z*)-products were prepared from *trans*-cinnamaldehyde and isolated by column chromatography 5% ethyl acetate in

hexanes ( $R_{fE}/R_{fZ} = 0.2/0.1$ ) in 16.6% and 70.8% yield, respectively. The (*Z*)-isomer is selectively formed in a 14:3 ratio compared with the (*E*)-isomer. **E-1e** was isolated as a pale yellow oil in 16.6% yield.  $^1\text{H}$  NMR (500 MHz,  $\text{CDCl}_3$ ):  $\delta$  7.41 (d,  $J = 7.4$  Hz, 2H), 7.31 (t,  $J = 7.8$  Hz, 2H), 7.23 (t,  $J = 7.5$  Hz, 1H), 6.79 (dd,  $J = 11.6$  Hz, 15.2 Hz, 1H), 6.62 (d,  $J = 15.7$  Hz, 1H), 6.52 (dd,  $J = 15.5$  Hz, 10.6 Hz, 1H), 5.75 (dd,  $J = 15.5$  Hz, 4.9 Hz, 1H), 4.90 (dd,  $J = 4.9$  Hz, 0.7 Hz, 1H), 3.35 (s, 4H);  $^{13}\text{C}$  NMR (500 MHz,  $\text{CDCl}_3$ ):  $\delta$  137.0, 134.7, 133.9, 129.4, 128.6, 127.8, 127.7, 126.5, 102.6, 52.6. **Z-1e** was isolated as a pale yellow oil in 70.8% yield.  $^1\text{H}$  NMR (500 MHz,  $\text{CDCl}_3$ ):  $\delta$  7.42 (d,  $J = 7.4$  Hz, 2H), 7.29 (t,  $J = 7.8$  Hz, 2H), 7.23 (t,  $J = 7.3$  Hz, 1H), 7.14 (ddd,  $J = 15.5$  Hz, 11.3 Hz, 0.9 Hz, 1H), 6.60 (d,  $J = 15.6$  Hz, 1H), 6.34 (t,  $J = 11.2$  Hz, 1H), 5.48 (dd,  $J = 11.1$  Hz, 5.9 Hz, 1H), 5.32 (dd,  $J = 5.9$  Hz, 1.2 Hz, 1H), 3.34 (s, 4H);  $^{13}\text{C}$  NMR (500 MHz,  $\text{CDCl}_3$ ):  $\delta$  136.9, 135.5, 132.5, 128.7, 128.1, 127.4, 126.7, 123.9, 99.8, 52.2.

---



**DPDC<sub>n</sub>**;  $m = 0, 1, 2, 3, 4, 5$

(1*Z*,3*E*,5*Z*)-2,5-dicyano-1,6-diphenyl-hexa-1,3,5-triene (**DPDC3**;  $m = 0$ ): General double Knoevenagel condensation procedure. The product was prepared from benzaldehyde and isolated as a yellow crystalline solid in 55.0% yield.  $^1\text{H}$  NMR (300 MHz,  $\text{C}_2\text{D}_2\text{Cl}_4$ ):  $\delta$  7.87-7.84 (m, 4H), 7.47 (m, 6H), 7.22 (s, 2H), 6.87 (s, 2H);  $^{13}\text{C}$  NMR (300 MHz, 350 K,  $\text{C}_2\text{D}_2\text{Cl}_4$ ):  $\delta$  145.60, 133.12, 131.07, 130.08, 129.29, 129.02, 116.02, 109.31.

(1*E*,3*Z*,5*E*,7*Z*,9*E*)-4,7-dicyano-1,10-diphenyl-deca-1,3,5,7,9-pentaene (**DPDC5**;  $m = 1$ ): General double Knoevenagel condensation procedure. The product was prepared from *trans*-cinnamaldehyde and isolated as an orange crystalline solid in 60.1% yield.  $^1\text{H}$  NMR (300 MHz,  $\text{C}_2\text{D}_2\text{Cl}_4$ ):  $\delta$  7.59 (d,  $J = 6.6$  Hz, 4H), 7.44-7.28 (m, 8H), 7.08-7.01 (m, 4H), 6.76 (s, 2H);  $^{13}\text{C}$  NMR (300 MHz, 350 K,  $\text{C}_2\text{D}_2\text{Cl}_4$ ):  $\delta$  145.0, 142.0, 135.6, 129.7, 129.0, 128.8, 127.5, 124.7, 114.8, 111.9.

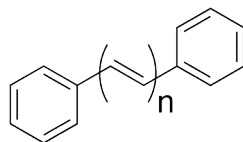
(1*E*,3*E*,5*Z*,7*E*,9*Z*,11*E*,13*E*)-6,9-dicyano-1,14-diphenyl-tetradeca-1,3,5,7,9,11,13-heptaene (**DPDC7**;  $m = 2$ ): General double Knoevenagel condensation procedure was run at 55° C. The product was prepared from **1a** and isolated as a red solid in 53.8% yield.  $^1\text{H}$  NMR (400 MHz, 350 K,  $\text{DMSO}-d_6$ ):  $\delta$  7.59 (d,  $J = 7.6$  Hz, 4H), 7.44-7.30 (m, 8H), 7.24 (dd,  $J = 10.8$  Hz, 15.6 Hz, 2H), 7.04-6.95 (m, 4H), 6.84 (dd,  $J = 11.6$  Hz, 14.0 Hz, 2H), 6.75 (s, 2H);  $^{13}\text{C}$  NMR (300 MHz, 370 K,  $\text{DMSO}-d_6$ ):  $\delta$  146.22, 143.44, 138.76, 137.06, 129.23, 129.18, 129.16, 129.13, 127.59, 115.49, 111.03.

*(1E,3E,5E,7Z,9E,11Z,13E,15E,17E)-8,11-dicyano-1,18-diphenyl-octadeca-1,3,5,7,9,11,13,15,17-nonaene* (**DPDC9**;  $m = 3$ ): General double Knoevenagel condensation procedure was run at 55° C. The product was prepared from **1b** and isolated as a dark purple solid in 45.4% yield.  $^1\text{H}$  NMR (400 MHz, 350 K, DMSO- $d_6$ ):  $\delta$  7.53 (d,  $J = 7.6$  Hz, 4H), 7.39-7.27 (m, 8H), 7.10-6.68 (m, 14H);  $^{13}\text{C}$  NMR (300 MHz, 380 K, DMSO- $d_6$ ):  $\delta$  146.25, 143.50, 140.26, 140.00, 137.79, 136.63, 133.42, 129.81, 129.53, 129.27, 128.98, 127.58, 115.86, 111.27.

*(1E,3E,5E,7E,9Z,11E,13Z,15E,17E,19E,21E)-10,13-dicyano-1,22-diphenyl-docosa-1,3,5,7,9,11,13,15,17,19,21-undecaene* (**DPDC11**;  $m = 4$ ): General double Knoevenagel condensation procedure was run at 55° C. The product was prepared from **1c** and isolated as a lustrous dark purple-black solid in 40.4% yield.  $^1\text{H}$  NMR (400 MHz, 350 K,  $\text{C}_2\text{H}_2\text{Cl}_4$ ):  $\delta$  7.47 (d,  $J = 7.6$  Hz, 4H), 7.37 (t,  $J = 7.2$  Hz, 4H), 7.28 (t,  $J = 7.2$  Hz, 2H), 6.95-6.47 (m, 20H);  $^{13}\text{C}$  NMR (400 MHz, 350 K,  $\text{C}_2\text{D}_2\text{Cl}_4$ ):  $\delta$  144.0, 141.6, 136.6, 136.4, 134.4, 132.3, 131.7, 128.6, 128.4, 128.2, 127.5, 126.1; due to insolubility four carbon signals were not observed (see crystal structure in supporting information).

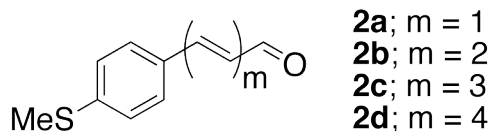
*(1E,3E,5E,7E,9E,11Z,13E,15Z,17E,19E,21E,23E,25E)-12,15-dicyano-1,26-diphenyl-hexacos-1,3,5,7,9,11,13,15,17,19,21,23,25-tridecaene* (**DPDC13**;  $m = 5$ ): General double Knoevenagel condensation procedure was run at 55° C. The product was prepared from **1d** and isolated as a lustrous dark black solid in 10.0% yield;  $^1\text{H}$  and  $^{13}\text{H}$  NMR data unavailable due to insolubility (see crystal structure in supporting information).

---



**DPO<sub>n</sub>**; n = 3, 5, 7

*(1E,3E,5E)*-1,6-diphenyl-hexa-1,3,5-triene (**DPO3**; n = 3), *(1E,3E,5E,7E,9E)*-1,10-diphenyl-deca-1,3,5,7,9-pentaene (**DPO5**; n = 5), and *(1E,3E,5E,7E,9E,11E,13E)*-1,14-diphenyl-tetradeca-1,3,5,7,9,11,13-heptaene (**DPO7**; n = 7) were prepared according to the procedure reported by Spangler and coworkers.<sup>2</sup> Longer **DPO<sub>n</sub>** molecules, where n > 7, were insoluble and difficult to characterize.



*trans*-4-(methylthio)cinnamaldehyde (**2a**; m = 1): General Wittig homologation procedure. The product was prepared from (4-methylthio)benzaldehyde and isolated as a pale yellow oil in 96.0% yield. The molecule is known, however specific characterizations have not been reported.<sup>7</sup> <sup>1</sup>H NMR (300 MHz, CDCl<sub>3</sub>): δ 9.70 (d, *J* = 7.6 Hz, 1H), 7.49 (d, *J* = 8.4 Hz, 2H), 7.45 (d, *J* = 16.0 Hz, 1H), 7.28 (d, *J* = 8.4 Hz, 2H), 6.69 (dd, *J* = 7.6 Hz, 15.6 Hz, 1H), 2.53 (s, 3H); <sup>13</sup>C NMR (300 MHz, CDCl<sub>3</sub>): δ 193.9, 152.2, 144.0, 130.8, 129.2, 128.0, 126.3, 15.4.

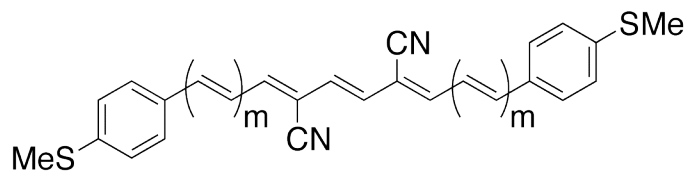
(2*E*,4*E*)-5-(4-(methylthio)phenyl)penta-2,4-dienal (**2b**; m = 2): General Wittig homologation procedure. The product was prepared from **2a** and isolated as a yellow solid in 99.0% yield. <sup>1</sup>H NMR (300 MHz, CDCl<sub>3</sub>): δ 9.62 (d, *J* = 7.8 Hz, 1H), 7.43 (d, *J* = 8.5 Hz, 2H), 7.26 (m, 3H), 6.95 (m, 2H), 6.27 (dd, *J* = 8.1 Hz, 15.0 Hz, 1H), 2.50 (s, 3H); <sup>13</sup>C NMR (300 MHz, CDCl<sub>3</sub>): δ 193.8, 152.1, 143.2, 140.3, 138.1, 131.4, 130.2, 127.7, 127.4, 126.8, 15.8.

(2*E*,4*E*,6*E*)-7-(4-(methylthio)phenyl)hepta-2,4,6-trienal (**2c**; m = 3): General Wittig homologation procedure. The product was prepared from **2b** and isolated as an orange solid in 73.0% yield. <sup>1</sup>H NMR (300 MHz, CDCl<sub>3</sub>): δ 9.60 (d, *J* = 8.1 Hz, 1H), 7.38 (d, *J* = 8.4 Hz, 2H), 7.19 (m, 3H), 6.83 (m, 3H), 6.55 (dd, *J* = 11.1 Hz, 15.3 Hz, 1H), 6.19 (dd, *J* = 8.1 Hz, 15.3 Hz, 1H), 2.50 (s, 3H). <sup>13</sup>C NMR (300 MHz, CDCl<sub>3</sub>): δ 193.48, 151.78, 142.83, 139.88, 137.78, 133.10, 131.05, 129.85, 127.37, 127.01, 126.35, 15.45.



*(2E,4E,6E,8E)-9-(4-(methylthio)phenyl)nona-2,4,6,8-tetraenal* (**2d**; m = 4): General Wittig homologation procedure. The product was prepared from **2c** and isolated as an orange-red solid in 70.0% yield. <sup>1</sup>H NMR (400 MHz, CDCl<sub>3</sub>): δ 9.57 (d, *J* = 8.0 Hz, 1H), 7.35 (d, *J* = 8.4 Hz, 2H), 7.20 (d, *J* = 8.5 Hz, 2H), 7.16 (dd, *J* = 12.0 Hz, 15.9 Hz, 1H), 6.84 (dd, *J* = 10.8 Hz, 15.4 Hz, 1H), 6.76 (dd, *J* = 11.2 Hz, 14.5 Hz, 1H), 6.70-6.58 (m, 2H), 6.47 (m, 2H), 6.17 (dd, *J* = 7.9 Hz, 15.1 Hz, 1H), 2.50 (s, 3H). <sup>13</sup>C NMR (300 MHz, CDCl<sub>3</sub>), 400 MHz: δ 193.9, 152.2, 143.1, 139.4, 135.9, 134.6, 134.0, 132.0, 131.3, 130.3, 128.1, 127.5, 126.9, 16.0.

---



**DPDCn-SMe**;  $m = 0, 1, 2, 3, 4$

*(1Z,3E,5Z)-2,5-dicyano-1,6-di-(4-(methylthio)phenyl)-hexa-1,3,5-triene* (**DPDC3-SMe**;  $m = 0$ ): General double Knoevenagel condensation procedure. The product was prepared from (4-methylthio)benzaldehyde and isolated as a lemon yellow solid in 70.0% yield.  $^1\text{H}$  NMR (300 MHz,  $\text{C}_2\text{D}_2\text{Cl}_3$ ):  $\delta$  7.78 (d,  $J = 8.3$  Hz, 4H), 7.34 (d,  $J = 8.3$  Hz, 4H), 7.18 (s, 2H), 6.86 (s, 2H), 2.58 (s, 6H);  $^{13}\text{C}$  NMR (300 MHz, 350 K,  $\text{C}_2\text{D}_2\text{Cl}_4$ ):  $\delta$  144.3, 143.3, 129.9, 129.8, 129.5, 126.1, 116.0, 108.5, 15.0.

*(1E,3Z,5E,7Z,9E)-4,7-dicyano-1,10-di-(4-(methylthio)phenyl)-deca-1,3,5,7,9-pentaene* (**DPDC5-SMe**;  $m = 1$ ): General double Knoevenagel condensation procedure. The product was prepared from **2a** and isolated as a red solid in 45.0% yield.  $^1\text{H}$  NMR (300 MHz,  $\text{CDCl}_3$ ):  $\delta$  7.85 (d,  $J = 8.4$  Hz, 4H), 7.26-7.18 (m, 6H), 7.00 (d,  $J = 11.4$  Hz, 2H), 6.94 (d,  $J = 15.0$  Hz, 2H), 6.68 (s, 2H), 2.52 (s, 6H);  $^{13}\text{C}$  NMR (300 MHz, 350 K,  $\text{C}_2\text{D}_2\text{Cl}_4$ ):  $\delta$  145.0, 141.4, 141.2, 132.5, 128.8, 127.9, 126.5, 124.1, 115.0, 111.4, 15.3.

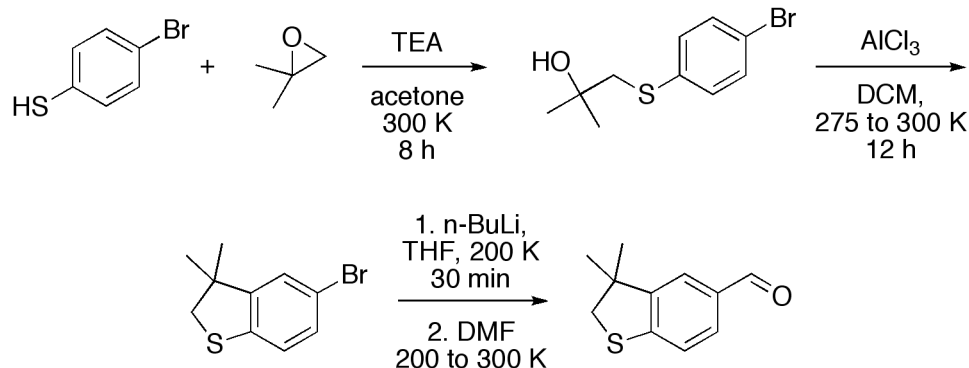
*(1E,3E,5Z,7E,9Z,11E,13E)-6,9-dicyano-1,14-di-(4-(methylthio)phenyl)-tetradeca-1,3,5,7,9,11,13-heptaene* (**DPDC7-SMe**;  $m = 2$ ): General double Knoevenagel condensation procedure. The product was prepared from **2b** and isolated as a purple crystalline solid in 20.3% yield.  $^1\text{H}$  NMR (400 MHz,  $\text{C}_2\text{D}_2\text{Cl}_4$ ):  $\delta$  7.41 (d,  $J = 8.4$  Hz, 4H), 7.23 (d,  $J = 8.4$  Hz, 4H), 6.99-6.89 (m, 4H), 6.82-6.67 (m, 6H), 6.64 (s, 2H), 2.52 (s,

6H);  $^{13}\text{C}$  NMR (300 MHz, 350 K,  $\text{C}_2\text{D}_2\text{Cl}_4$ ):  $\delta$  144.21, 142.39, 139.47, 137.47, 132.76, 128.06, 128.5, 127.00, 126.96, 114.76, 110.63, 15.01.

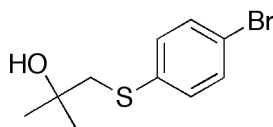
*(1E,3E,5E,7Z,9E,11Z,13E,15E,17E)-8,11-dicyano-1,18-di-(4-(methylthio)phenyl)-octadeca-1,3,5,7,9,11,13,15,17-nonaene (DPDC9-SMe; m = 3)*: General Double Knoevenagel Condensation Procedure was carried out at 55° C. The product was prepared from **2c** and isolated as a dark purple-black solid in 40.5% yield.  $^1\text{H}$  NMR (500 MHz,  $\text{C}_2\text{D}_2\text{Cl}_4$ ):  $\delta$  7.40 (d,  $J = 8.5$  Hz, 4H), 7.29 (d,  $J = 8.5$  Hz, 4H), 7.13-6.34 (m, 16H), 2.54 (s, 6H).  $^{13}\text{C}$  NMR could not be obtained due to insolubility.

*(1E,3E,5E,7E,9Z,11E,13Z,15E,17E,19E,21E)-10,13-dicyano-1,22-di-(4-(methylthio)phenyl)-docosa-1,3,5,7,9,11,13,15,17,19,21-undecaene (DPDC11-SMe; m = 4)*: General double Knoevenagel condensation procedure. The product was prepared from **2d** and isolated as a lustrous dark black solid in 10.0% yield.  $^1\text{H}$  NMR (500 MHz,  $\text{CD}_2\text{Cl}_2$ ):  $\delta$  7.37 (d,  $J = 8.0$  Hz, 4H), 7.22 (d,  $J = 8.0$  Hz, 4H), 6.92-6.45 (m, 16H), 6.49 (m, 4H), 2.51 (s, 6H);  $^{13}\text{C}$  NMR could not be obtained due to compound insolubility.

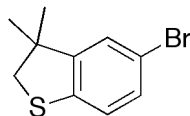
---



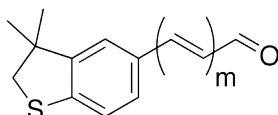
**Scheme S1.** Synthesis of 3,3-dimethyl-2,3-dihydrobenzo[*b*]thiophene-5-carbaldehyde from 4-bromothiophenol.



*4-bromophenylthio 2-methylpropan-2-ol*: 4-bromothiophenol (1.0 g, 5.3 mmol) and 1,2-Epoxy-2-methylpropane (0.76 g, 10.5 mmol) were added to a 100-mL round-bottom flask with magnetic stir bar. The reaction flask was then charged with 50 mL of acetone (from drum) and nitrogen was bubbled through for 20 min. Triethylamine (3 mL) was added to reaction via syringe. The reaction was stirred overnight at room temperature. The organic solvent was removed by rotary evaporation. The product was isolated by column chromatography (20% ethyl acetate in hexanes) and 1.28 g (93%) of clear oil was isolated.  $^1\text{H}$  NMR (300 MHz,  $\text{CDCl}_3$ ):  $\delta$  7.40 (d,  $J = 8.7$  Hz, 2H), 7.28 (d,  $J = 8.7$  Hz, 2H), 3.08 (s, 2H), 2.14 (bs, 1H), 1.30 (s, 6H);  $^{13}\text{C}$  NMR (300 MHz,  $\text{CDCl}_3$ ):  $\delta$  136.8, 132.4, 131.3, 120.4, 71.2, 48.9, 29.1.



*5-bromo-3,3-dimethyl-2,3-dihydrobenzo[b]thiophene*: A solution of 4-bromophenylthio 2-methyl-propan-2-ol (0.36 g, 1.39 mmol) in  $\text{CH}_2\text{Cl}_2$  was added to a stirring suspension of aluminum chloride (0.20 g, 1.53 mmol) in  $\text{CH}_2\text{Cl}_2$  cooled in an ice bath. The suspension was left to stir overnight while warming to room temperature. Water was added to quench unreacted  $\text{AlCl}_3$ . The organic layer was washed with water and then sat. aqueous sodium chloride solution before drying over  $\text{MgSO}_4$ . The product was isolated by column chromatography (100% hexanes) and 1.90 g (57%) of clear oil was isolated.  $^1\text{H}$  NMR (300 MHz,  $\text{CDCl}_3$ ):  $\delta$  7.23 (dd,  $J = 1.8$  Hz, 8.4 Hz, 1H), 7.14 (d,  $J = 1.8$  Hz, 1H), 7.05 (d,  $J = 8.4$  Hz, 1H), 3.18 (s, 2H), 1.36 (s, 6H);  $^{13}\text{C}$  NMR (300 MHz,  $\text{CDCl}_3$ ):  $\delta$  150.7, 140.1, 130.6, 126.4, 124.1, 118.2, 47.9, 47.8, 27.6.



**3a**;  $m = 1$   
**3b**;  $m = 2$   
**3c**;  $m = 3$   
**3d**;  $m = 4$

*3,3-dimethyl-2,3-dihydrobenzo[b]thiophene-5-carbaldehyde (3a;  $m = 0$ )*: A 100-mL round-bottom flask was flame dried and charged with 5-bromo-3,3-dimethyl-2,3-dihydrobenzo[b]thiophene (0.310 g, 1.20 mmol) and anhydrous THF (25 mL). The reaction flask was cooled to  $-78^\circ\text{C}$  in an acetone/dry ice bath for 40 min. 0.9 mL of *n*-BuLi (1.6 M in hexanes) was dripped into the reaction slowly over 5 minutes. The reaction was allowed to stir at  $-78^\circ\text{C}$  for 30 min before dry DMF (1 mL) was added dropwise. This reaction was allowed to warm to room temperature overnight. The reaction was then quenched with water, left to stir for 10 min and extracted with ether.

The organic layers were combined and washed with sat. sodium chloride solution and then dried over MgSO<sub>4</sub>. Product was isolated by column chromatography to yield 0.203 g (94 %) of a colorless oil. NOTE: yields varied. <sup>1</sup>H NMR (300 MHz, CDCl<sub>3</sub>): δ 9.88 (s, 1H), 7.62 (dd, *J* = 1.8 Hz, 8.1 Hz, 1H), 7.55 (d, *J* = 1.8 Hz, 1H), 7.29 (d, *J* = 8.1 Hz, 1H), 3.24 (s, 2H), 1.41 (s, 6H); <sup>13</sup>C NMR (300 MHz, CDCl<sub>3</sub>): δ 191.6, 150.5, 149.6, 134.1, 131.1, 123.0, 122.9, 47.8, 47.3, 27.9.

*(E)*-3-(3,3-dimethyl-2,3-dihydrobenzo[*b*]thiophen-5-yl)acrylaldehyde (**3b**; *m* = 1): General Wittig homologation procedure. The product was prepared from **3a** and isolated as a pale yellow solid in 94.0% yield. <sup>1</sup>H NMR (300 MHz, CDCl<sub>3</sub>): δ 9.68 (d, *J* = 8.0 Hz, 1H), 7.44 (d, *J* = 15.8 Hz, 1H), 7.32 (dd, *J* = 1.4 Hz, 8.0 Hz, 1H), 7.22 (m, 2H), 6.68 (dd, *J* = 7.8 Hz, 15.8 Hz, 1H), 3.21 (s, 2H), 1.39 (s, 6H); <sup>13</sup>C NMR (300 MHz, CDCl<sub>3</sub>): δ 193.6, 152.8, 149.1, 145.9, 130.7, 128.3, 127.0, 122.8, 122.4, 47.5, 47.1, 27.5.

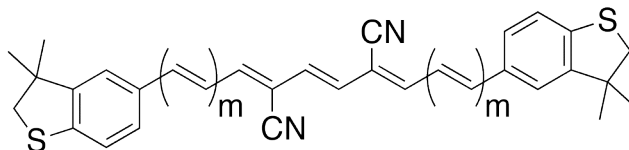
*(2E,4E)*-5-(3,3-dimethyl-2,3-dihydrobenzo[*b*]thiophen-5-yl)penta-2,4-dienal (**3c**; *m* = 2): General Wittig homologation procedure. The product was prepared from **3b** and isolated as a yellow solid in 92.0% yield. <sup>1</sup>H NMR (400 MHz, CDCl<sub>3</sub>): δ 9.61 (d, *J* = 8.0 Hz, 1H), 7.26-7.16 (m, 2H), 6.96 (m, 2H), 6.26 (dd, *J* = 8.0 Hz, 15.2 Hz, 1H), 3.22 (s, 2H), 1.40 (s, 6H); <sup>13</sup>C NMR (400 MHz, CDCl<sub>3</sub>): δ 193.81, 152.80, 149.30, 143.94, 142.88, 132.73, 131.23, 127.77, 125.10, 123.07, 121.80, 47.82, 47.46, 27.80.

*(2E,4E,6E)*-7-(3,3-dimethyl-2,3-dihydrobenzo[*b*]thiophen-5-yl)hepta-2,4,6-trienal (**3d**; *m* = 3): General Wittig homologation procedure. The product was prepared from **3c** and

isolated as an orange solid in 90.0% yield.  $^1\text{H}$  NMR (300 MHz,  $\text{CDCl}_3$ ):  $\delta$  9.87 (d,  $J = 7.8$  Hz, 1H), 7.16 (m, 4H), 6.80 (m, 3H), 6.50 (dt,  $J = 2.7$  Hz, 11.1 Hz, 1H), 6.12 (dd,  $J = 8.1$  Hz, 15.0 Hz, 1H), 3.16 (s, 2H), 1.35 (s, 6H);  $^{13}\text{C}$  NMR (300 MHz,  $\text{CDCl}_3$ ):  $\delta$  193.78, 152.27, 149.17, 143.44, 142.71, 138.77, 133.49, 131.21, 129.86, 127.10, 126.72, 123.04, 121.37, 47.84, 47.48, 27.81.

*(2E,4E,6E,8E)-9-(3,3-dimethyl-2,3-dihydrobenzo[b]thiophen-5-yl)nona-2,4,6,8-tetraenal* (**3e**;  $m = 4$ ): General Wittig homologation procedure. The product was prepared from **3d** and isolated as a red-orange solid in 63.0% yield.  $^1\text{H}$  NMR (500 MHz,  $\text{CDCl}_3$ ):  $\delta$  9.55 (d,  $J = 8.1$  Hz, 1H), 7.18-7.07 (m, 4H), 6.85-6.56 (m, 4H), 6.48 (d,  $J = 11.1$  Hz, 1H), 6.41 (dd,  $J = 8.1$  Hz, 11.7 Hz, 1H), 6.14 (dd,  $J = 8.1$  Hz, 15.3 Hz, 1H), 3.16 (s, 2H), 1.36 (s, 6H);  $^{13}\text{C}$  NMR (300 MHz,  $\text{CDCl}_3$ ):  $\delta$  193.9, 152.4, 149.1, 143.3, 142.0, 139.7, 136.5, 133.9, 131.6, 131.2, 130.0, 127.4, 126.9, 123.0, 121.1, 47.8, 47.5, 27.8.

---



**DPDC $n$ -SC $_4$ H $_8$ ;  $m = 0, 1, 2, 3, 4$**

*(1Z,3E,5Z)*-2,5-dicyano-1,6-di-(3,3-dimethyl-2,3-dihydrobenzo[*b*]thiophene)-hexa-1,3,5-triene (**DPDC3-SC $_4$ H $_8$** ;  $m = 0$ ): General double Knoevenagel condensation procedure. This molecule was prepared from **3a** and isolated as a lemon yellow solid in 41.9% yield.  $^1\text{H}$  NMR (300 MHz, CDCl $_3$ ):  $\delta$  7.61 (d,  $J = 1.7$  Hz, 2H), 7.57 (dd,  $J = 1.7$  Hz, 8.2 Hz, 2H), 7.25 (d,  $J = 8.3$  Hz, 2H), 7.12 (s, 2H), 6.79 (s, 2H), 3.24 (s, 4H), 1.42 (s, 12H);  $^{13}\text{C}$  NMR (300 MHz, CDCl $_3$ ):  $\delta$  149.13, 145.70, 144.91, 130.13, 129.79, 129.39, 123.18, 122.75, 116.58, 107.63, 47.52, 47.22, 27.46.

*(1E,3Z,5E,7Z,9E)*-4,7-dicyano-1,10-di-(3,3-dimethyl-2,3-dihydrobenzo[*b*]thiophene)-deca-1,3,5,7,9-pentaene (**DPDC5-SC $_4$ H $_8$** ;  $m = 1$ ): General double Knoevenagel condensation procedure. The product was prepared from **3b** and isolated as a red solid in 30.0% yield.  $^1\text{H}$  NMR (300 MHz, CD $_2$ Cl $_2$ ):  $\delta$  7.33 (dd,  $J = 1.5$  Hz, 8.1 Hz, 2H), 7.28-7.19 (m, 6H), 7.05 (d,  $J = 11.4$  Hz, 2H), 6.98 (d,  $J = 15.3$  Hz, 2H), 6.70 (s, 2H), 3.24 (s, 4H), 1.41 (s, 12H);  $^{13}\text{C}$  NMR (300 MHz, CDCl $_3$ ):  $\delta$  149.7, 146.0, 144.2, 142.2, 132.9, 129.3, 127.9, 123.8, 123.1, 122.0, 115.8, 111.3, 47.5, 47.0, 26.6.

*(1E,3E,5Z,7E,9Z,11E,13E)*-6,9-dicyano-1,14-di-(3,3-dimethyl-2,3-dihydrobenzo[*b*]thiophene)-tetradeca-1,3,5,7,9,11,13-heptaene (**DPDC7-SC $_4$ H $_8$** ;  $m = 2$ ): General double Knoevenagel condensation procedure. The product was prepared from **3c** and isolated as a purple solid in 17.0% yield.  $^1\text{H}$  NMR (300 MHz, CD $_2$ Cl $_2$ ):  $\delta$  7.12 (m,

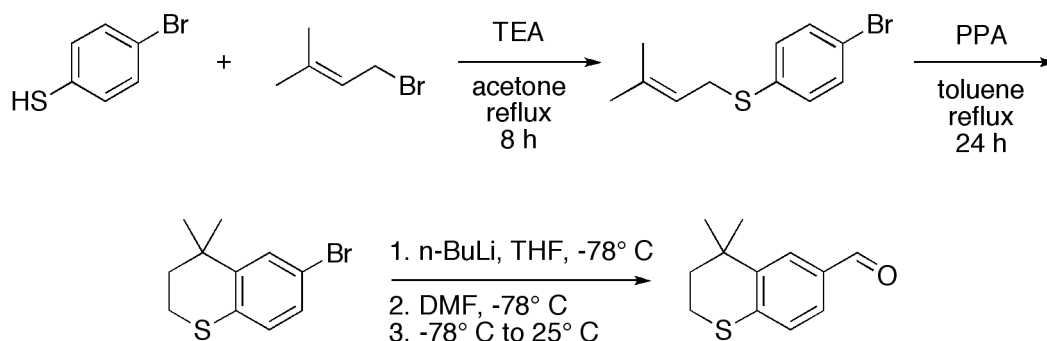


6H), 7.05-6.77 (m, 10H), 6.67 (s, 2H), 3.23 (s, 4H), 1.41 (s, 12H);  $^{13}\text{C}$  NMR (300 MHz,  $\text{CDCl}_3$ ):  $\delta$  149.22, 145.17, 142.88, 142.87, 138.94, 133.57, 129.34, 128.73, 127.37, 127.14, 123.09, 121.29, 115.80, 111.35, 47.87, 47.50, 27.81.

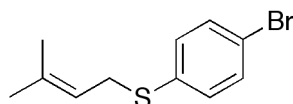
*(1E,3E,5E,7Z,9E,11Z,13E,15E,17E)-8,11-dicyano-1,18-di-(3,3-dimethyl-2,3-dihydrobenzo[b]thiophene)-octadeca-1,3,5,7,9,11,13,15,17-nonaene (DPDC9-SC<sub>4</sub>H<sub>8</sub>; m = 3)*: General double Knoevenagel condensation procedure. The product was prepared from **3d** and isolated as a dark purple solid in 10.5% yield.  $^1\text{H}$  NMR (300 MHz,  $\text{CD}_2\text{Cl}_2$ ):  $\delta$  7.44 (d,  $J = 11.9$  Hz, 2H), 7.35 (s, 2H), 7.31 (d,  $J = 8.4$  Hz, 2H), 7.20 (d,  $J = 6.6$  Hz, 2H), 7.09 (dd,  $J = 12.3$  Hz, 17.2 Hz, 2H), 6.93 (dd,  $J = 13.5$  Hz, 16.9 Hz, 2H), 6.85-6.62 (m, 12H), 3.22 (s, 4H), 2.08 (s, 12H);  $^{13}\text{C}$  NMR (300 MHz,  $\text{CDCl}_3$ ):  $\delta$  149.10, 145.00, 142.62, 142.07, 139.94, 136.72, 133.96, 132.09, 129.42, 128.86, 127.59, 126.95, 123.01, 121.14, 115.79, 111.33, 47.85, 47.49, 27.80.

*(1E,3E,5E,7E,9Z,11E,13Z,15E,17E,19E,21E)-10,13-dicyano-1,22-di-(3,3-dimethyl-2,3-dihydrobenzo[b]thiophene)-phenyl)-docosa-1,3,5,7,9,11,13,15,17,19,21-undecaene (DPDC11-SC<sub>4</sub>H<sub>8</sub>; m = 4)*: General double Knoevenagel condensation procedure. The product was prepared from **3e** and isolated as a dark purple-black solid in 8.0% yield.  $^1\text{H}$  NMR (300 MHz,  $\text{CD}_2\text{Cl}_2$ ):  $\delta$  7.22-7.11 (m, 6H), 6.90-6.48 (m, 20H), 3.21 (s, 4H), 1.40 (s, 12H);  $^{13}\text{C}$  NMR (500 MHz,  $\text{CD}_2\text{Cl}_2$ ):  $\delta$  148.2, 144.0, 141.6, 140.7, 138.7, 136.7, 134.4, 133.4, 131.7, 128.6, 128.0, 127.1, 125.7, 122.0, 120.2, 114.8, 110.4, 47.0, 46.5, 26.9; one  $\text{sp}^2$  carbon signal not observed.

---

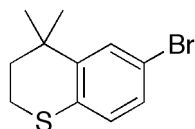


**Scheme S2.** Synthesis of 4,4-dimethylthiochroman-6-carbaldehyde.

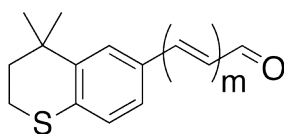


1-bromo-4-[(3-methyl-2-buten-1-yl)thio]benzene: This compound is known<sup>8</sup> in the literature and has been prepared in poor yields by Fe-catalyzed sulfenylation of 4-bromothiophenol with isobutyl 1,1-dimethylprop-2-enyl hydrogen carbonate. We chose a different method for our preparation. 4-bromothiophenol (5.00 g, 26.4 mmol) and 3,3-dimethylallyl bromide (7.88 g, 52.9 mmol) was added to a 250-mL round-bottom flask with magnetic stir bar. The reaction flask was then charged with 200 mL of acetone and nitrogen was bubbled through for 25 min. 5 mL of triethylamine was added to reaction via syringe and the a white precipitate crashed out immediately. The reaction was stirred overnight at room temperature before filtering off the white solid and washing with acetone. Solvent was removed from the organic layer by rotary evaporation and then loaded onto a silica gel loading column. Column chromatography (100% hexanes) was

used to isolate the product in quantitative yields.  $^1\text{H}$  NMR (300 MHz,  $\text{CD}_2\text{Cl}_2$ ): 7.39 (d,  $J = 8.7$ , 2H), 7.20 (d,  $J = 8.6$  Hz, 2H), 5.27 (m, 1H), 3.50 (d,  $J = 7.7$  Hz, 2H), 1.71 (s, 3H), 1.59 (s, 3H);  $^{13}\text{C}$  NMR (300 MHz,  $\text{CDCl}_3$ ): 150.7, 140.1, 130.6, 126.4, 124.1, 118.1, 53.8, 47.9, 47.8, 27.6.



*6-bromo-4,4-dimethylthiochroman*: This compound is known, however NMR characterization was provided.<sup>9</sup> (4-bromophenyl)(3-methylbut-2-enyl)sulfane (2.72 g, 10.58 mmol) was in a 100-mL round-bottom flask and dissolved in a minimal amount of toluene (not dry). Polyphosphonic acid (5-10 mL) was added and the mixture was refluxed for 24 hours. The reaction was cooled to room temperature and toluene was decanted off. The remaining mixture was dissolved in water and extracted with toluene. Organics were combined, washed with sat. aqueous sodium chloride solution and dried over  $\text{MgSO}_4$ . After column chromatography in 100% hexanes the product was isolated in 2.37 g (87%) as a white powder.  $^1\text{H}$  NMR (300 MHz,  $\text{CDCl}_3$ ): 7.45 (d,  $J = 1.5$  Hz, 1H), 7.14 (dd,  $J = 1.5$  Hz, 6.3 Hz, 1H), 6.95 (d,  $J = 6.3$  Hz, 1H), 3.01 (m, 2H), 1.92 (m, 2H), 1.31 (s, 6H);  $^{13}\text{C}$  NMR (300 MHz,  $\text{CDCl}_3$ ): 144.5, 131.5, 129.8, 129.4, 128.4, 117.7, 37.5, 33.6, 30.4, 23.4.



**4a**;  $m = 0$   
**4b**;  $m = 1$   
**4c**;  $m = 2$   
**4d**;  $m = 3$   
**4e**;  $m = 4$   
**4f**;  $m = 5$

*4,4-dimethylthiochroman-6-carbaldehyde* (**4a**;  $m = 0$ ): This compound is known, however NMR characterization was provided.<sup>9</sup> A 100-mL round-bottom flask was flame dried and charged with 6-bromo-4,4-dimethylthiochroman (1.00 g, 3.89 mmol) and anhydrous THF (50 mL). The reaction flask was cooled to  $-78^{\circ}\text{C}$  in an acetone/dry ice bath for 40 min. 2.67 mL of n-BuLi (1.6 M in hexanes) solution was dripped into the reaction very slowly over 10 minutes. The reaction was allowed to stir at  $-78^{\circ}\text{C}$  for 30 min before dry DMF (1 mL) was added dropwise. This reaction was allowed to warm to room temperature overnight. Reaction was quenched with water, allowed to stir for 10 min and extracted with ether. The organic layers were combined and washed with sat. sodium chloride solution and then dried over  $\text{MgSO}_4$ . Product was isolated by column chromatography to yield 0.686 g (86 %) of a colorless oil.  $^1\text{H}$  NMR (300 MHz,  $\text{CDCl}_3$ ): 9.87 (s, 1H), 7.85 (d,  $J = 1.8$  Hz, 1H), 7.52 (dd,  $J = 1.8$  Hz, 8.1 Hz, 1H), 7.23 (d,  $J = 8.1$  Hz, 1H), 3.08 (m, 2H), 1.97 (m, 2H), 1.37 (s, 6H);  $^{13}\text{C}$  NMR (500 MHz,  $\text{CDCl}_3$ ): 191.5, 142.4, 141.7, 132.7, 127.6, 127.0, 126.9, 36.7, 33.1, 29.8, 23.3.

*(E)-3-(4,4-dimethylthiochroman-6-carbaldehyde)acrylaldehyde* (**4b**;  $m = 1$ ): General Wittig homologation procedure. The product was prepared from **4a** and isolated as a pale yellow solid in 92.0% yield.  $^1\text{H}$  NMR (300 MHz,  $\text{CDCl}_3$ ):  $\delta$  9.64 (d,  $J = 7.5$  Hz, 1H), 7.54 (d,  $J = 1.8$  Hz, 1H), 7.42 (d,  $J = 15.6$  Hz, 1H), 7.24 (dd,  $J = 1.8$  Hz, 8.1 Hz, 1H), 7.12 (d,  $J = 8.1$  Hz, 1H), 6.63 (dd,  $J = 7.5$  Hz, 15.9 Hz, 1H), 3.05 (m, 2H), 1.94 (m, 2H), 1.33 (s, 6H);  $^{13}\text{C}$  NMR (300 MHz,  $\text{CDCl}_3$ ):  $\delta$  193.34, 153.81, 144.14, 138.88, 131.80, 128.94, 128.88, 128.85, 127.36, 41.45, 37.51, 34.28, 28.13.

*(2E,4E)-5-(4,4-dimethylthiochroman-6-carbaldehyde)penta-2,4-dienal* (**4c**;  $m = 2$ ):

General Wittig homologation procedure. The product was prepared from **4b** and isolated as a yellow solid in 92.7% yield.  $^1\text{H}$  NMR (300 MHz,  $\text{CDCl}_3$ ):  $\delta$  9.62 (d,  $J = 7.5$  Hz, 1H), 7.46 (d,  $J = 1.8$  Hz, 1H), 7.19-7.30 (m, 2H), 7.11 (d,  $J = 8.1$  Hz, 1H), 6.97-6.99 (m, 2H), 6.29 (dd,  $J = 7.8$  Hz, 15.0 Hz, 1H), 3.06 (m, 2H), 1.97 (m, 2H), 1.36 (s, 6H);  $^{13}\text{C}$  NMR (300 MHz,  $\text{CDCl}_3$ ):  $\delta$  193.9, 152.9, 143.1, 142.8, 135.4, 131.9, 131.2, 127.5, 126.5, 125.1, 125.0, 37.6, 33.4, 30.4, 23.6.

*(2E,4E,6E)-7-(4,4-dimethylthiochroman-6-carbaldehyde)hepta-2,4,6-trienal* (**4d**;  $m = 3$ ):

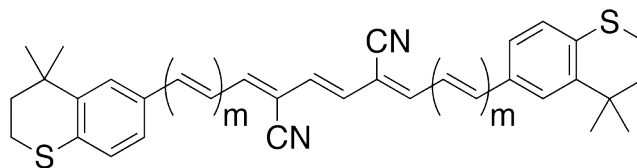
General Wittig homologation procedure. The product was prepared from **4c** and isolated as a golden solid in 71.0% yield.  $^1\text{H}$  NMR (300 MHz,  $\text{CDCl}_3$ ):  $\delta$  9.55 (d,  $J = 7.8$  Hz, 1H), 7.38 (d,  $J = 1.2$  Hz, 1H), 7.17-7.01 (m, 3H), 6.82-6.67 (m, 3H), 6.52 (m, 1H), 6.16 (dd,  $J = 7.8$  Hz, 15.0 Hz, 1H), 3.00 (m, 2H), 1.91 (m, 2H), 1.31 (s, 6H);  $^{13}\text{C}$  NMR (300 MHz,  $\text{CDCl}_3$ ):  $\delta$  193.6, 152.3, 143.5, 142.7, 138.9, 134.0, 132.7, 131.1, 129.8, 127.3, 126.6, 126.0, 124.5, 37.7, 33.3, 30.3, 23.6.

*(2E,4E,6E,8E)-9-(4,4-dimethylthiochroman-6-carbaldehyde)nona-2,4,6,8-tetraenal* (**4e**;

$m = 4$ ): General Wittig homologation procedure. The product was prepared from **4d** and isolated as an orange solid in 59.4% yield.  $^1\text{H}$  NMR (300 MHz,  $\text{CDCl}_3$ ):  $\delta$  9.55 (d,  $J = 8.1$  Hz, 1H), 7.34 (d,  $J = 1.8$  Hz, 1H), 7.20-7.08 (m, 2H), 7.03 (d,  $J = 8.4$  Hz, 1H), 6.83-6.56 (m, 4H), 6.48-6.36 (m, 2H), 6.17 (dd,  $J = 8.1$  Hz, 15.0 Hz, 1H), 3.01 (m, 2H), 1.93 (m, 2H), 1.31 (s, 6H);  $^{13}\text{C}$  NMR (500 MHz,  $\text{CDCl}_3$ ):  $\delta$  193.42, 151.86, 142.87, 142.23,

139.29, 136.25, 132.90, 132.75, 131.10, 130.75, 129.52, 126.95, 126.88, 125.30, 123.97, 37.43, 33.00, 30.06, 23.20.

*(2E,4E,6E,8E,10E)-9-(4,4-dimethylthiochroman-6-carbaldehyde)undeca-2,4,6,8,10-pentaenal* (**4f**;  $m = 5$ ): General Wittig homologation procedure. The product was prepared from **4e** and isolated as an orange solid in 41.3% yield.  $^1\text{H}$  NMR (300 MHz,  $\text{CDCl}_3$ ):  $\delta$  9.60 (d,  $J = 7.8$  Hz, 1H), 7.43 (d,  $J = 1.8$  Hz, 1H), 7.25-7.15 (m, 2H), 7.06 (d,  $J = 8.1$  Hz, 1H), 6.92-6.77 (m, 2H), 6.69-6.40 (m, 6H), 6.20 (dd,  $J = 8.1$  Hz, 15.3 Hz, 1H), 3.07 (m, 2H), 1.98 (m, 2H), 1.37 (s, 6H);  $^{13}\text{C}$  NMR (300 MHz,  $\text{CDCl}_3$ ):  $\delta$  193.7, 152.1, 143.0, 142.7, 139.3, 137.3, 135.1, 133.4, 132.9, 132.4, 131.9, 131.1, 130.1, 127.7, 127.1, 125.6, 124.1, 37.8, 33.3, 30.2, 23.6.



**DPDCn-SC<sub>8</sub>H<sub>10</sub>**; m = 0, 1, 2, 3, 4, 5

*(1Z,3E,5Z)*-2,5-dicyano-1,6-di-(4,4-dimethylthiochroman)-hexa-1,3,5-triene (**DPDC3-SC<sub>5</sub>H<sub>10</sub>**; m = 0): General double Knoevenagel condensation procedure. The product was prepared from **4a** and isolated as a lemon yellow solid in 43.0% yield. <sup>1</sup>H NMR (300 MHz, CDCl<sub>3</sub>): δ 7.92 (d, *J* = 1.8 Hz, 2H), 7.50 (dd, *J* = 2.1 Hz, 8.4 Hz, 2H), 7.16 (d, *J* = 8.1 Hz, 2H), 7.09 (s, 2H), 6.79 (s, 2H), 3.07 (m, 4H), 1.98 (m, 4H), 1.38 (s, 12H); <sup>13</sup>C NMR (300 MHz, CD<sub>2</sub>Cl<sub>2</sub>): δ 145.3, 143.0, 137.6, 130.0, 129.8, 127.9, 127.2, 127.1, 116.9, 108.0, 37.3, 33.5, 30.0, 23.7.

*(1E,3Z,5E,7Z,9E)*-4,7-dicyano-1,10-di-(4,4-dimethylthiochroman)-deca-1,3,5,7,9-pentaene (**DPDC5-SC<sub>5</sub>H<sub>10</sub>**; m = 1): General double Knoevenagel condensation procedure. The product was prepared from **4b** and isolated as a bright red solid in 34.8% yield. <sup>1</sup>H NMR (300 MHz, CD<sub>2</sub>Cl<sub>2</sub>): δ 7.50 (d, *J* = 1.5 Hz, 2H), 7.32 (dd, *J* = 1.2 Hz, 8.4 Hz, 2H), 7.23 (dd, *J* = 11.4 Hz, 15.0 Hz, 2H), 7.12 (d, *J* = 8.1 Hz, 2H), 7.06 (d, *J* = 11.7 Hz, 2H), 6.97 (d, *J* = 15.3 Hz, 2H), 6.71 (s, 2H), 3.09 (m, 4H), 1.98 (m, 4H), 1.37 (s, 12H); <sup>13</sup>C NMR (300 MHz, CDCl<sub>3</sub>): δ 145.7, 143.0, 142.4, 135.7, 132.1, 129.2, 127.3, 126.8, 124.8, 123.6, 115.5, 111.2, 37.6, 33.3, 30.0, 23.6.

*(1E,3E,5Z,7E,9Z,11E,13E)*-6,9-dicyano-1,14-di-(4,4-dimethylthiochroman)-tetradeca-1,3,5,7,9,11,13-heptaene (**DPDC7-SC<sub>5</sub>H<sub>10</sub>**; m = 2): General double Knoevenagel condensation procedure. The product was prepared from **4c** and isolated as a red-purple

solid in 23.2%.  $^1\text{H}$  NMR (300 MHz,  $\text{CD}_2\text{Cl}_2$ ):  $\delta$  7.43 (d,  $J = 1.8$  Hz, 2H), 7.17 (dd,  $J = 1.8$  Hz, 8.4 Hz, 2H), 7.04 (d,  $J = 8.1$  Hz, 2H), 6.95-6.71 (m, 10H), 6.63 (s, 2H), 3.03 (m, 4H), 1.94 (m, 4H), 1.32 (s, 12H);  $^{13}\text{C}$  NMR (300 MHz,  $\text{CDCl}_3$ ):  $\delta$  146.7, 144.4, 144.2, 140.6, 135.5, 134.1, 130.5, 129.9, 128.8, 128.4, 127.4, 126.1, 117.4, 112.4, 38.9, 34.7, 31.8, 25.1.

*(1E,3E,5E,7Z,9E,11Z,13E,15E,17E)-8,11-dicyano-1,18-di-(4,4-dimethylthiochroman)-octadeca-1,3,5,7,9,11,13,15,17-nonaene (DPDC9-SC<sub>5</sub>H<sub>10</sub>; m = 3)*: General double Knoevenagel condensation procedure. The product was prepared from **4d** and isolated as a dark purple solid in 15.5% yield.  $^1\text{H}$  NMR (300 MHz,  $\text{CDCl}_3$ ):  $\delta$  7.39 (s, 2H), 7.19 (d,  $J = 9.0$  Hz, 2H), 7.07 (d,  $J = 8.4$  Hz, 2H), 6.91-6.62 (m, 14H), 6.55-6.47 (m, 2H), 3.07 (m, 4H), 1.97 (m, 4H), 1.34 (s, 12H);  $^{13}\text{C}$  NMR (300 MHz,  $\text{CDCl}_3$ ):  $\delta$  144.6, 142.3, 142.2, 139.5, 136.4, 132.8, 132.6, 131.5, 128.7, 128.2, 127.0, 126.8, 125.3, 123.9, 115.4, 110.5, 37.1, 32.8, 29.9, 23.1.

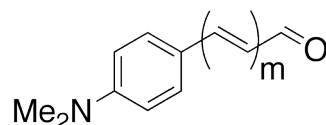
*(1E,3E,5E,7E,9Z,11E,13Z,15E,17E,19E,21E)-10,13-dicyano-1,22-di-(4,4-dimethylthiochroman)-docosa-1,3,5,7,9,11,13,15,17,19,21-undecaene (DPDC11-SC<sub>5</sub>H<sub>10</sub>; m = 4)*: General double Knoevenagel condensation procedure. The product was prepared from **4e** and isolated as a lustrous blue-black solid in 6.0% yield.  $^1\text{H}$  NMR (300 MHz,  $\text{CD}_2\text{Cl}_2$ ):  $\delta$  7.41 (d,  $J = 1.2$  Hz, 2H), 7.18 (bd,  $J = 8.0$  Hz, 2H), 7.10 (d,  $J = 8.2$  Hz, 2H), 6.92-6.45 (m, 20H), 3.08 (m, 4H), 2.01 (m, 4H), 1.40 (s, 12H);  $^{13}\text{C}$  NMR (400 MHz,  $\text{CDCl}_3$ ):  $\delta$  144.49, 142.19, 142.14, 139.32, 137.34, 135.09, 133.04, 133.02, 132.48,



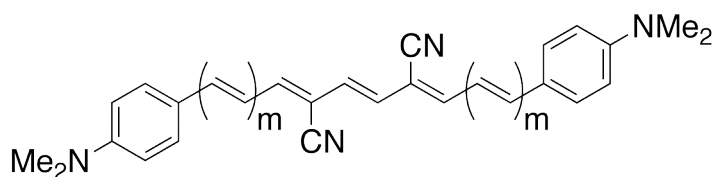
132.21, 129.06, 128.61, 127.38, 126.93, 125.14, 123.92, 115.40, 110.93, 37.49, 33.00, 30.07, 23.20.

*(1E,3E,5E,7E,9E,11Z,13E,15Z,17E,19E,21E,23E,25E)-12,15-dicyano-1,26-di-(4,4-dimethylthiochroman)-hexacos-1,3,5,7,9,11,13,15,17,19,21,23,25-tridecaene*

**(DPDC13-SC<sub>5</sub>H<sub>10</sub>; m = 5)**: General double Knoevenagel condensation procedure. The product was prepared from **4f** and isolated as a lustrous blue-black solid in 5.1% yield%. <sup>1</sup>H NMR (400 MHz, C<sub>2</sub>D<sub>2</sub>Cl<sub>4</sub>): δ 7.38 (bs, 2H), 7.27-7.14 (m, 6H), 7.03 (d, *J* = 8.2 Hz, 2H), 6.88 (m, 2H), 6.82 (dd, *J* = 10.4 Hz, 15.3 Hz, 2H), 6.72-6.38 (m, 16H), 3.05 (m, 4H), 1.95 (m, 4H), 1.34 (s, 12H); <sup>13</sup>C NMR could not be obtained due to insolubility of product.



(*2E,4E*)-5-(4-(dimethylamino)phenyl)penta-2,4-dienal (**5a**;  $m = 2$ ): Compound is known.<sup>10</sup> General Wittig homologation procedure. The product was prepared from *trans*-(4-dimethylamino)cinnamaldehyde and isolated as a golden-orange solid in 91.1% yield. <sup>1</sup>H NMR (300 MHz, CDCl<sub>3</sub>):  $\delta$  9.57 (d,  $J = 8.1$  Hz, 1H), 7.41 (d,  $J = 8.9$  Hz, 2H), 7.29 (dd,  $J = 7.5$  Hz, 15.3 Hz, 1H), 6.97-6.73 (m, 2H), 6.71 (d,  $J = 8.9$  Hz, 2H), 6.21 (dd,  $J = 8.1$  Hz, 15.0 Hz, 1H), 3.02 (s, 6H); <sup>13</sup>C NMR (300 MHz, CDCl<sub>3</sub>):  $\delta$  194.0, 154.1, 151.8, 143.9, 129.6, 129.5, 124.0, 122.0, 112.4, 40.6.



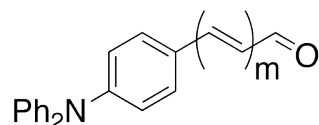
**DPDCn-NMe<sub>2</sub>**;  $m = 0, 1, 2$

(*1Z,3E,5Z*)-2,5-dicyano-1,6-di-(4-(dimethylamino)phenyl)-hexa-1,3,5-triene (**DPDC3-NMe<sub>2</sub>**;  $m = 0$ ): General double Knoevenagel condensation procedure. The product was prepared from (4-dimethylamino)benzaldehyde and isolated as an orange-red solid in 8.1% yield. <sup>1</sup>H NMR (300 MHz, C<sub>2</sub>D<sub>2</sub>Cl<sub>4</sub>):  $\delta$  7.78 (d,  $J = 8.7$  Hz, 4H), 7.02 (s, 2H), 6.72 (d,  $J = 8.7$  Hz, 4H), 6.66 (s, 2H), 3.06 (s, 12H); <sup>13</sup>C NMR (500 MHz, C<sub>2</sub>D<sub>2</sub>Cl<sub>4</sub>):  $\delta$  151.2, 143.7, 130.7, 127.7, 121.1, 117.1, 111.2, 102.9, 39.4.

(*1E,3Z,5E,7Z,9E*)-4,7-dicyano-1,10-di-(4-(dimethylamino)phenyl)-deca-1,3,5,7,9-pentaene (**DPDC5-NMe<sub>2</sub>**;  $m = 1$ ): General double Knoevenagel condensation procedure.

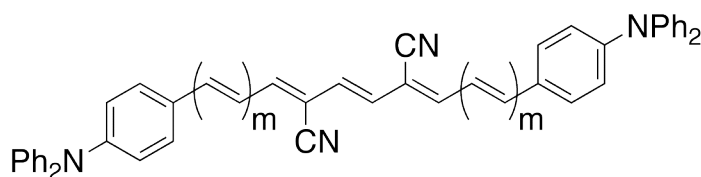
The product was prepared from *trans*-(4-dimethylamino)cinnamaldehyde and isolated as a lustrous blue-black solid in 30.1% yield.  $^1\text{H}$  NMR (500 MHz,  $\text{C}_2\text{D}_2\text{Cl}_4$ ):  $\delta$  7.46 (d,  $J$  = 7.0 Hz, 4H), 7.17-6.83 (m, 6H), 6.73 (d,  $J$  = 7.0 Hz, 4H), 6.64 (s, 2H), 3.06 (s, 12H);  $^{13}\text{C}$  NMR was not obtained due to insolubility.

*(1E,3E,5Z,7E,9Z,11E,13E)*-6,9-dicyano-1,14-di-(4-(dimethylamino)phenyl)-tetradeca-1,3,5,7,9,11,13-heptaene (**DPDC7-NMe<sub>2</sub>**;  $m = 2$ ): General double Knoevenagel condensation procedure. The product was prepared from **5a** and isolated as a black lustrous solid in 23.3% yield.  $^1\text{H}$  NMR (300 MHz,  $\text{C}_2\text{D}_2\text{Cl}_4$ ):  $\delta$  7.40 (d,  $J$  = 8.7 Hz, 4H), 6.97-6.66 (m, 14H), 6.61 (s, 2H), 3.05 (s, 12H);  $^{13}\text{C}$  NMR was not obtained due to limited solubility.



*(E)*-3-(4-(diphenylamino)phenyl)acrylaldehyde (**6a**;  $m = 1$ ): Compound is known.<sup>11</sup>

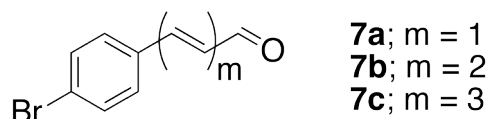
General Wittig homologation procedure. The product was prepared from 4-diphenylamino)benzaldehyde and isolated as a pale yellow solid in 55.3% yield. <sup>1</sup>H NMR (300 MHz, CD<sub>2</sub>Cl<sub>2</sub>):  $\delta$  9.65 (d,  $J = 7.8$  Hz, 1H), 7.41 (d,  $J = 8.5$  Hz, 2H), 7.35-7.25 (m, 5H), 7.15-7.09 (m, 6H), 7.02 (d,  $J = 8.7$  Hz, 2H), 6.62 (dd,  $J = 7.8$  Hz, 15.6 Hz, 1H); <sup>13</sup>C NMR (300 MHz, CDCl<sub>3</sub>):  $\delta$  194.0, 153.0, 151.2, 147.0, 130.2, 130.0, 127.1, 126.5, 126.1, 124.9, 121.4.



**DPDCn-NPh<sub>2</sub>**;  $m = 0, 1$

*(1Z,3E,5Z)*-2,5-dicyano-1,6-di-(4-(diphenylamino)phenyl)-hexa-1,3,5-triene (**DPDC3-NPh<sub>2</sub>**;  $m = 0$ ): General double Knoevenagel condensation procedure. The product was prepared from 4-diphenylamino)benzaldehyde and isolated as a orange-red solid in 16.3% yield. <sup>1</sup>H NMR (300 MHz, C<sub>2</sub>D<sub>2</sub>Cl<sub>4</sub>):  $\delta$  7.76 (d,  $J = 8.8$  Hz, 4H), 7.40-7.38 (m, 8H), 7.21-7.11 (m, 14H), 7.03 (d,  $J = 8.8$  Hz, 4H), 6.79 (s, 2H); <sup>13</sup>C NMR (300 MHz, CDCl<sub>3</sub>):  $\delta$  150.60, 146.87, 144.36, 131.06, 129.95, 129.61, 126.62, 126.27, 124.96, 120.84, 117.17, 106.53.

*(1E,3Z,5E,7Z,9E)-4,7-dicyano-1,10-di-(4-(diphenylamino)phenyl)-deca-1,3,5,7,9-pentaene (DPDC5-NPh<sub>2</sub>; m = 1)*: General double Knoevenagel condensation procedure. The product was prepared from **6a** and isolated as a dark purple solid in 51.6% yield. <sup>1</sup>H NMR (500 MHz, CDCl<sub>3</sub>): δ 7.37 (d, *J* = 8.3 Hz, 4H), 7.29 (t, *J* = 7.5 Hz, 8H), 7.14-7.08 (m, 14H), 7.00 (d, *J* = 8.3 Hz, 4H), 6.95 (d, *J* = 11.5 Hz, 2H), 6.89 (d, *J* = 15.2 Hz, 2H), 6.63 (s, 2H); <sup>13</sup>C NMR (500 MHz, CDCl<sub>3</sub>): δ 149.44, 146.87, 145.38, 141.52, 129.50, 128.95, 128.83, 128.57, 125.37, 124.04, 122.69, 121.88, 115.64, 110.21.

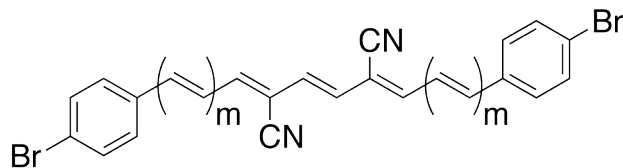


*4-bromocinnamaldehyde (7a; m = 1)*: General Wittig homologation procedure. The product was prepared from 4-bromobenzaldehyde and isolated by column chromatograph (15% ethyl acetate in hexanes) as a white solid in 91.5% yield. This compound is known and matches the reported spectroscopic data.<sup>12</sup> <sup>1</sup>H NMR (400 MHz, CDCl<sub>3</sub>): δ 9.69 (d, *J* = 7.6 Hz, 1H), 7.56 (d, *J* = 8.4 Hz, 2H), 7.43-7.38 (m, 3H), 6.69 (dd, *J* = 7.6 Hz, 16.0 Hz, 1H); <sup>13</sup>C NMR (300 MHz, CDCl<sub>3</sub>): δ 193.4, 151.2, 133.1, 132.5, 129.9, 129.2, 125.8.

*(2E,4E)-5-(4-bromophenyl)penta-2,4-dienal (7b; m = 2)*: General Wittig homologation procedure. The product was prepared from **7a** and isolated by column chromatography (15% ethyl acetate in hexanes) as a yellow solid in 96.0% yield. This compound is known and matches the reported spectroscopic data.<sup>13</sup> <sup>1</sup>H NMR (400 MHz, CDCl<sub>3</sub>): δ 9.62 (d, *J* = 7.6 Hz, 1H), 7.51 (d, *J* = 8.8 Hz, 2H), 7.36 (d, *J* = 8.8 Hz, 2H), 7.27-7.21 (dd, *J* = 9.6 Hz, 15 Hz, 1H), 7.02-6.91 (m, 2H), 6.31-6.25 (dd, *J* = 8.0 Hz, 15.0 Hz, 1H); <sup>13</sup>C NMR (400 MHz, CDCl<sub>3</sub>): δ 193.5, 151.5, 140.9, 134.5, 132.1, 132.0, 128.9, 126.8, 123.8.

*(2E,4E,6E)-7-(4-bromophenyl)hepta-2,4,6-trienal (7c; m = 3)*: General Wittig homologation procedure. The product prepared from **7b** and was isolated by column chromatograph (15% ethyl acetate in hexanes) as a orange-yellow solid in 73.7% yield. <sup>1</sup>H NMR (400 MHz, CDCl<sub>3</sub>): δ 9.60 (d, *J* = 7.6 Hz, 1H), 7.48 (d, *J* = 8.4 Hz, 2H), 7.31 (d, *J* = 8.4 Hz, 2H), 7.18 (dd, *J* = 11.0 Hz, 15.0 Hz, 1H), 6.92-6.72 (m, 3H), 6.58 (dd, *J* = 11.0 Hz, 14.0 Hz, 1H), 6.21, (dd, *J* = 7.6 Hz, 15.0 Hz, 1H); <sup>13</sup>C NMR (400 MHz,

$\text{CDCl}_3$ ):  $\delta$  193.4, 151.3, 142.1, 136.8 135.3, 132.0, 131.4, 130.6, 128.3(4), 128.3(2),  
122.7.



**DPDCn-Br**;  $m = 0, 1, 2, 3$

*(1Z,3E,5Z)*-2,5-dicyano-1,6-di-(4-bromophenyl)-hexa-1,3,5-triene (**DPDC3-Br**): General double Knoevenagel condensation procedure. The product was prepared from 4-bromobenzaldehyde and isolated as a yellow solid in 35.6% yield.  $^1\text{H}$  NMR (400 MHz,  $\text{C}_2\text{D}_2\text{Cl}_4$ ):  $\delta$  7.72 (d,  $J = 8.4$  Hz, 4H), 7.62 (d,  $J = 8.4$  Hz, 4H), 7.19 (s, 2H), 6.86 (s, 2H);  $^{13}\text{C}$  NMR (400 MHz,  $\text{DMSO-}d_6$ ): 7.81 (d,  $J = 8.4$  Hz, 4H), 7.76 (s, 2H), 7.74 (d,  $J = 8.4$  Hz, 4H), 6.97 (s, 2H);  $^{13}\text{C}$  NMR (400 MHz,  $\text{DMSO-}d_6$ ):  $\delta$  145.7, 133.2, 132.6, 131.4, 130.6, 124.8, 116.1, 110.2.

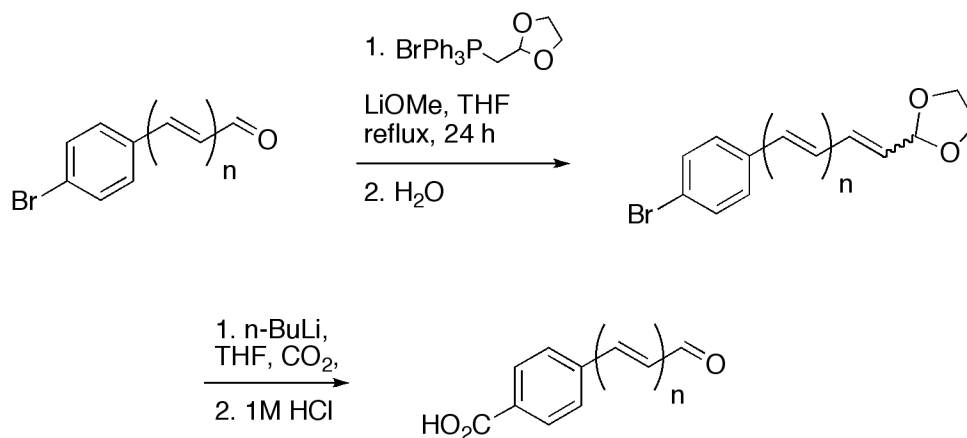
*(1E,3Z,5E,7Z,9E)*-4,7-dicyano-1,10-di-(4-bromophenyl)-deca-1,3,5,7,9-pentaene (**DPDC5-Br**): General double Knoevenagel condensation procedure. The product was prepared from **7a** and isolated as a peach-orange solid in 33.4% yield.  $^1\text{H}$  NMR (400 MHz,  $\text{C}_2\text{D}_2\text{Cl}_4$ ):  $\delta$  7.58 (d,  $J = 8.4$  Hz, 4H), 7.44 (d,  $J = 8.4$  Hz, 4H), 7.28 (dd,  $J = 12.0$  Hz, 15.0 Hz, 2H), 7.05 (d,  $J = 12.0$  Hz, 2H), 6.97 (d,  $J = 15.0$  Hz, 2H), 6.75 (s, 2H);  $^{13}\text{C}$  NMR (500 MHz,  $\text{C}_2\text{D}_2\text{Cl}_4$ ):  $\delta$  146.2, 142.0, 136.2, 133.6, 130.8, 130.3, 126.8, 125.4, 116.2, 114.0

*(1E,3E,5Z,7E,9Z,11E,13E)*-6,9-dicyano-1,14-di-(4-bromophenyl)-tetradeca-1,3,5,7,9,11,13-heptaene (**DPDC7-Br**): General double Knoevenagel condensation procedure. The product was prepared from **7b** and isolated as a red solid in 15.5% yield.  $^1\text{H}$  NMR (500 MHz,  $\text{C}_2\text{D}_2\text{Cl}_4$ ):  $\delta$  7.54 (d,  $J = 8.5$  Hz, 4H), 7.36 (d,  $J = 8.5$  Hz, 4H), 6.98-

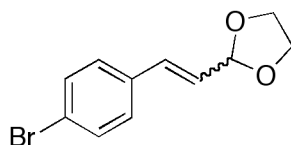


6.64 (m, 12H);  $^{13}\text{C}$  NMR (500 MHz,  $\text{C}_2\text{D}_2\text{Cl}_4$ ):  $\delta$  145.8, 143.5, 143.1, 138.6, 138.3, 133.5, 130.7, 130.2, 129.8, 124.2, 116.3, 113.4.

*(1E,3E,5E,7Z,9E,11Z,13E,15E,17E)-8,11-dicyano-1,18-di-(4-bromophenyl)-octadeca-1,3,5,7,9,11,13,15,17-nonaene (DPDC9-Br)*: General double Knoevenagel condensation procedure. The product was prepared from **7c** and isolated as a red-purple solid in 7.6% yield.  $^1\text{H}$  NMR (500 MHz,  $\text{C}_2\text{D}_2\text{Cl}_4$ ):  $\delta$  7.52 (d,  $J = 8.4$  Hz, 4H), 7.33 (d,  $J = 8.4$  Hz, 4H), 6.99-6.55 (m, 16H); Limited solubility prevented acquisition of  $^{13}\text{C}$  NMR.

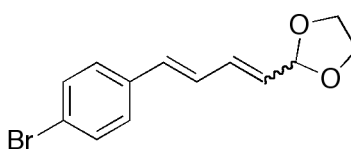


**Scheme S3.** General route to the synthesis of carboxylic acid aryl-enals through Wittig reaction and concomitant lithium-halogen exchange and carboxylation.



*(E)*-2-(4-bromostyryl)-1,3-dioxolane (**E-7d**): Compound is known.<sup>14</sup> The product was synthesized from 4-bromobenzaldehyde using the general Wittig homologation procedure without acidic hydrolysis. Water was added to quench the reaction solution and the product was isolated by column chromatography (15% ethyl acetate in hexanes) as a white solid in 36.3% yield (both stereoisomers in overall 80.5% yield).  $^1\text{H}$  NMR (400 MHz,  $\text{CDCl}_3$ ):  $\delta$  7.44 (d,  $J = 8.8$  Hz, 2H), 7.27 (d,  $J = 8.8$  Hz, 2H), 6.73 (d,  $J = 16.0$  Hz, 1H), 6.15 (dd,  $J = 6.0$  Hz, 16.0 Hz, 1H), 5.41 (d,  $J = 6.0$  Hz, 1H), 4.09-3.19 (m, 4H);  $^{13}\text{C}$  NMR (400 MHz,  $\text{CDCl}_3$ ):  $\delta$  134.8, 133.5, 131.7, 128.4, 125.9, 122.3, 103.6, 65.1.

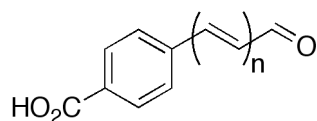
*(Z)*-2-(4-bromostyryl)-1,3-dioxolane (**Z-7d**): Compound is known.<sup>14</sup> The product was synthesized from 4-bromobenzaldehyde using the general Wittig homologation procedure without acidic hydrolysis. The product was isolated by column chromatography (15% ethyl acetate in hexanes) as a colorless oil in 44.2% yield (both stereoisomers in overall 80.5% yield). <sup>1</sup>H NMR (300 MHz, CDCl<sub>3</sub>): δ 7.45 (d, *J* = 8.4 Hz, 2H), 7.23 (d, *J* = 8.4 Hz, 2H), 6.70 (d, *J* = 11.7 Hz, 1H), 5.73 (dd, *J* = 7.5 Hz, 11.7 Hz, 1H), 5.44 (d, *J* = 7.5 Hz, 1H), 4.09-3.84 (m, 4H); <sup>13</sup>C NMR (300 MHz, CDCl<sub>3</sub>): δ 135.0, 134.7, 131.8, 131.0, 129.0, 122.4, 99.9, 65.6.



2-((1*E*,3*E*)-4-(4-bromophenyl)buta-1,3-dienyl)-1,3-dioxolane (**E-7e**): Acetals were synthesized from **7a** using the general Wittig homologation procedure without acidic hydrolysis. The product was isolated by column chromatography (15% ethyl acetate in hexanes) as a pale yellow solid in 36.4% yield (both stereoisomers in overall 93.5% yield). <sup>1</sup>H NMR (400 MHz, CDCl<sub>3</sub>): δ 7.44 (d, *J* = 8.4 Hz, 2H), 7.26 (d, *J* = 8.4 Hz, 2H), 6.77 (dd, *J* = 10.8 Hz, 15.6 Hz, 1H), 6.54 (m, 2H), 5.78 (dd, *J* = 6.0 Hz, 15.2 Hz, 1H), 5.35 (d, *J* = 6.0 Hz, 1H), 4.04-3.88 (m, 4H); <sup>13</sup>C NMR (400 MHz, CDCl<sub>3</sub>): δ 135.7, 135.5, 133.5, 131.8, 131.8, 129.4, 121.7, 103.4, 65.0; one sp<sup>2</sup>-carbon signal not observed due to overlapping signals.

2-((1*Z*,3*E*)-4-(4-bromophenyl)buta-1,3-dienyl)-1,3-dioxolane (**Z-7e**): Acetals were synthesized from **7a** using the general Wittig homologation procedure without acidic

hydrolysis. The product was isolated by column chromatography (15% ethyl acetate in hexanes) as a pale yellow solid in 93.5% yield (both stereoisomers in overall 80.5% yield).  $^1\text{H}$  NMR (400 MHz,  $\text{CDCl}_3$ ):  $\delta$  7.44 (d,  $J = 8.4$  Hz, 2H), 7.28 (d,  $J = 8.4$  Hz, 2H), 7.14 (dd,  $J = 11.2$  Hz, 15.2 Hz, 1H), 6.55 (d,  $J = 15.0$  Hz, 1H), 6.40 (t,  $J = 11.0$  Hz, 1H), 5.78 (d,  $J = 6.4$  Hz, 1H), 5.54 (dd,  $J = 4.4$  Hz, 11.0 Hz, 1H), 4.10-3.91 (m, 4H);  $^{13}\text{C}$  NMR (400 MHz,  $\text{CDCl}_3$ ):  $\delta$  135.8, 134.6, 134.1, 131.8, 128.2, 127.2, 124.0, 121.9, 99.5, 65.1.

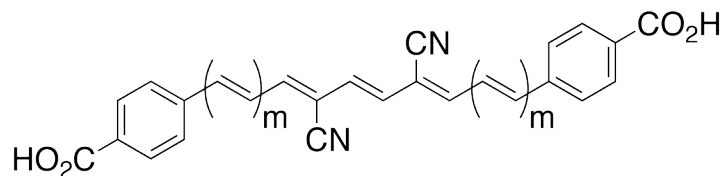


(*E*)-4-(3-oxoprop-1-enyl)benzoic acid (**8a**;  $m = 1$ ): This compound has been previously prepared by the saponification of methyl 4-(3-Oxo-1-propenyl)benzoate using sodium hydroxide.<sup>15</sup> In our method, a three-neck round-bottomed flask was charged with acetal protected polyenal (either **E-7d** or **Z-7d**, 1.0 eq.) in dry THF and cooled to  $-78^\circ\text{C}$ . *n*-butyl lithium (1.6 M in hexanes, 1.1 eq.) was added dropwise and the yellow solution was stirred for 15 minutes. Carbon dioxide gas ( $\text{CO}_2$  tank, Matheson Tri-Gas; Product Grade) was bubbled into the solution until the yellow color disappeared, and then the reaction was left to warm to room temperature. The solution was diluted with diethyl ether, and then extracted (3x) with water. 1 M aq. hydrochloric acid was added to the aqueous layer and stirred for 1 h, during which time a precipitate formed. This was collected by vacuum filtration to yield pure product ( $\text{C}_{10}\text{O}_2\text{H}_8$ ) as a white solid in 89.4% yield. [**Note**: When the *Z*-alkene is used, acetal hydrolysis may remain incomplete. In that event, the precipitate is dissolved in tetrahydrofuran before adding 1 M aq. hydrochloric acid. After stirring for 1 h, the solution was diluted with water and extracted (3x) with ethyl acetate.

The organic layer was washed with brine, dried over magnesium sulfate, and concentrated to yield the all-*trans* product. It is important to note that both the (*E*)- and (*Z*)-acetals yield the same all-*trans*-product. Therefore, the *E/Z* mixture can be used as the starting material for **8a**.] <sup>1</sup>H NMR (300 MHz, Acetone-*d*<sub>6</sub>): δ 11.39 (bs, 1H), 9.76 (d, *J* = 7.5 Hz, 1H), 8.10 (d, *J* = 8.4 Hz, 2H), 7.86 (d, *J* = 8.4 Hz, 2H), 7.77 (d, *J* = 16.2 Hz, 1H), 6.88 (dd, *J* = 7.5 Hz, 16.2 Hz, 1H); <sup>13</sup>C NMR (300 MHz, Acetone-*d*<sub>6</sub>): δ 193.5, 166.4, 151.1, 139.0, 132.8, 130.9, 130.6, 128.9.

4-((1*E*,3*E*)-5-oxopenta-1,3-dienyl)benzoic acid (**8b**; *m* = 2): A three-neck round-bottomed flask was charged with acetal protected polyenal (either *E*-**7e** or *Z*-**7e**, 1.0 eq.) in dry THF and cooled to -78° C. *n*-butyl lithium (1.6 M in hexanes, 1.1 eq.) was added dropwise and the yellow solution was stirred for 15 minutes. Carbon dioxide gas (CO<sub>2</sub> tank, Matheson Tri-Gas; Product Grade) was bubbled into the solution until the yellow color disappeared, and then the reaction was left to warm to room temperature. The solution was diluted with diethyl ether, and then extracted (3x) with water. To the water layer was added 1 M aq. hydrochloric acid and this was stirred for one hour during which time a precipitate formed. This was collected by vacuum filtration to yield pure product (C<sub>12</sub>O<sub>2</sub>H<sub>10</sub>) as a yellow solid in 90.7% yield. [**Note**: When the *Z*-alkene is used, acetal hydrolysis may remain incomplete. In that event, the precipitate is dissolved in tetrahydrofuran before adding 1 M aq. hydrochloric acid. After stirring for 1 h, the solution was diluted with water and extracted (3x) with ethyl acetate. The organic layer was washed with brine, dried over magnesium sulfate, and concentrated to yield the all-*trans* product. It is important to note that both the (*E*)- and (*Z*)-acetals yield the same all-

*trans*-product. Therefore, the *E/Z* mixture can be used as the starting material.]  $^1\text{H}$  NMR (400 MHz, Acetone- $d_6$ ):  $\delta$  11.39 (bs, 1H), 9.68 (d,  $J = 8.0$  Hz, 1H), 8.07 (d,  $J = 8.4$  Hz, 2H), 7.76 (d,  $J = 8.4$  Hz, 2H), 7.51 (dd,  $J = 10.8$  Hz, 14.8 Hz, 1H), 7.43-7.36 (m, 1H), 7.26 (d,  $J = 15.6$  Hz, 1H), 6.35 (dd,  $J = 8.0$  Hz, 15.2 Hz, 1H);  $^{13}\text{C}$  NMR (400 MHz, Acetone- $d_6$ ):  $\delta$  193.0, 166.3, 151.2, 137.3, 132.8, 130.8, 130.1, 129.0, 127.4, 125.2.



**DPDCn-CO<sub>2</sub>H**; m = 0, 1, 2

(1Z,3E,5Z)-2,5-dicyano-1,6-di-(4-(carboxy)phenyl)-hexa-1,3,5-triene (**DPDC3-CO<sub>2</sub>H**; m = 0): A round-bottomed flask is charged with 4-formylbenzoic acid (1.0 eq.) and *trans*-1,4-dicyano-2-butene (1.0 eq.) in methanol under a nitrogen atmosphere. Sodium metal (>6.0 eq.) is dissolved in methanol and this is added directly to reaction solution. The reaction is stirred for 12 hours during which time a colored precipitate forms. The precipitate is collected by vacuum filtration, then suspended in methanol, and excess 1 M aq. hydrochloric acid is added. The reaction mixture is left to sit for one hour while the solid settles and is again collected by vacuum filtration. The yellow solid is pure product; 19.8% yield. <sup>1</sup>H NMR (400 MHz, DMSO-*d*<sub>6</sub>): δ 13.22 (bs, 2H), 8.05 (d, *J* = 8.4 Hz, 4H), 7.94 (m, 6H), 7.04 (s, 2H); <sup>13</sup>C NMR (400 MHz, DMSO-*d*<sub>6</sub>): δ 167.0, 146.2, 137.8, 132.9, 131.1, 130.4, 129.7, 116.1, 111.2.

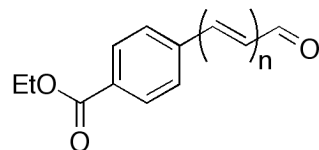
(1E,3Z,5E,7Z,9E)-4,7-dicyano-1,10-di-(4-(carboxy)phenyl)-deca-1,3,5,7,9-pentaene (**DPDC5-CO<sub>2</sub>H**; m = 1): A round-bottomed flask is charged with **8a** acid (1.0 eq.) and *trans*-1,4-dicyano-2-butene (1.0 eq.) in methanol under a nitrogen atmosphere. Sodium metal (>6.0 eq.) is dissolved in methanol and this is added directly to reaction solution. The reaction is stirred for 12 hours during which time a colored precipitate forms. The precipitate is collected by vacuum filtration, then suspended in methanol, and excess 1 M aq. hydrochloric acid is added. The reaction mixture is left to sit for one hour while the solid settles and is again collected by vacuum filtration. The dark orange solid is pure

product; 14.4% yield.  $^1\text{H}$  NMR (400 MHz,  $\text{DMSO-}d_6$ ):  $\delta$  13.00 (bs, 2H) 7.95 (d,  $J = 8.0$  Hz, 4H), 7.75 (d,  $J = 8.0$  Hz, 4H), 7.61 (d,  $J = 10.4$  Hz, 2H), 7.33-7.21 (m, 4H), 6.86 (s, 2H);  $^{13}\text{C}$  NMR (400 MHz,  $\text{DMSO-}d_6$ ):  $\delta$  167.3, 146.7, 141.5, 139.9, 131.8, 130.4, 129.8, 128.2, 127.0, 115.2, 112.7.

*(1E,3E,5Z,7E,9Z,11E,13E)-6,9-dicyano-1,14-di-(4-(carboxy)phenyl)-tetradeca-*

*1,3,5,7,9,11,13-heptaene (DPDC7-CO<sub>2</sub>H; m = 2)*: A round-bottomed flask is charged with **8b** (1.0 eq.) and *trans*-1,4-dicyano-2-butene (1.0 eq.) in methanol under a nitrogen atmosphere. Sodium metal (>6.0 eq.) is dissolved in methanol and this is added directly to reaction solution. The reaction is stirred for 12 hours during which time a colored precipitate forms. The precipitate is collected by vacuum filtration, then suspended in methanol, and excess 1 M aq. hydrochloric acid is added. The reaction mixture is left to sit for one hour while the solid settles and is again collected by vacuum filtration. The dark red solid is pure product; 18.1% yield.  $^1\text{H}$  NMR (400 MHz,  $\text{DMSO-}d_6$ ):  $\delta$  13.00 (bs, 2H), 7.91 (d,  $J = 8.4$  Hz, 4H), 7.68 (d,  $J = 8.4$  Hz, 4H), 7.51 (d,  $J = 11.6$  Hz, 2H), 7.42 (dd,  $J = 11.0$  Hz, 15.4 Hz, 2H), 7.04-7.00 (m, 4H), 6.87 (dd,  $J = 11.6$  Hz, 14.8 Hz, 2H), 6.78 (s, 2H); Limited solubility prevented acquisition of  $^{13}\text{C}$  NMR.



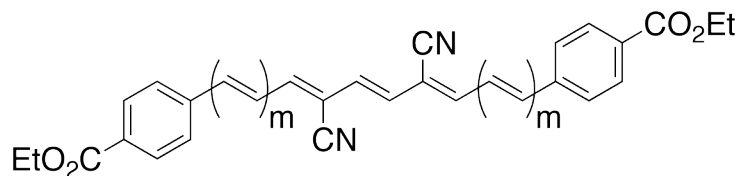


*ethyl 4-formylbenzoate (9a; m = 0)*: Product prepared from reaction of 4-formylbenzoic acid with 1-bromoethane in the presence of base. Detailed preparation and characterization has been previously reported.<sup>16</sup>

*(E)-ethyl 4-(3-oxoprop-1-enyl)benzoate (9b; m = 1)*: Product was prepared via Heck reaction involving ethyl 4-bromo-benzoate and acrolein diethyl acetal. Detailed preparation and characterization have been previously reported.<sup>17</sup> Yield: 85.1%. <sup>1</sup>H NMR (400 MHz, CDCl<sub>3</sub>): δ 9.73 (d, *J* = 7.6 Hz, 1H), 8.09 (d, *J* = 8.4 Hz, 2H), 7.62 (d, *J* = 8.4, 2H), 7.50 (d, *J* = 16.0 Hz, 1H), 6.77 (dd, *J* = 7.6 Hz, 16.0 Hz, 1H), 4.39 (q, *J* = 6.8 Hz, 2H), 1.38 (t, *J* = 6.8 Hz, 3H); <sup>13</sup>C NMR (400 MHz, CDCl<sub>3</sub>): δ 193.3, 165.8, 150.9, 138.0, 132.6, 130.3, 130.2, 128.3, 61.3, 14.3.

*ethyl 4-((1E,3E)-5-oxopenta-1,3-dienyl)benzoate (9c; m = 2)*: General Wittig homologation procedure was modified by using 3.0 eq. of (1,3-dioxolan-2-yl)methyl-triphenylphosphonium bromide and 3.3 eq. of LiOMe. The product was isolated by column chromatograph (15% ethyl acetate in hexanes) as a pale yellow solid in 64.6% yield. <sup>1</sup>H NMR (500 MHz, CDCl<sub>3</sub>): δ 9.64 (d, *J* = 8.0 Hz, 1H), 8.05 (d, *J* = 8.0 Hz, 2H), 7.56 (d, *J* = 8.0 Hz, 2H), 7.28 (dd, *J* = 9.5 Hz, 15.5 Hz, 1H), 7.07 (m, 2H), 6.32 (dd, *J* = 7.5 Hz, 15.5 Hz, 1H), 4.39 (q, *J* = 7.5 Hz, 2H), 1.41 (t, *J* = 7.5 Hz, 3H); <sup>13</sup>C NMR (500 MHz, CDCl<sub>3</sub>): 193.4 166.0, 151.0, 140.8, 139.7, 132.7, 131.1, 130.1, 128.3, 127.3, 61.2, 14.3.





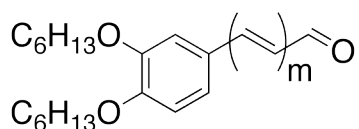
**DPDCn-CO<sub>2</sub>Et; m = 0, 1, 2**

*(1Z,3E,5Z)-2,5-dicyano-1,6-di-(4-(diethylbenzoate))-hexa-1,3,5-triene* (**DPDC3-CO<sub>2</sub>Et**; m = 0): General double Knoevenagel condensation procedure was modified by employing sodium methoxide as base; instead of DBU. The product was prepared from **9a** and was isolated as a bright yellow solid in 33.4% yield and was very insoluble. <sup>1</sup>H NMR (300 MHz, 355 K, C<sub>2</sub>D<sub>2</sub>Cl<sub>4</sub>): δ 8.12 (bs, 4H), 7.92 (bs, 4H), 7.31 (bs, 2H), 6.94 (bs, 2H), 4.04 (bs, 4H), 1.42 (bs, 6H); <sup>13</sup>C NMR (400 MHz, C<sub>2</sub>D<sub>2</sub>Cl<sub>4</sub>): δ 167.2, 145.9, 138.5, 134.0, 132.5, 131.5, 130.6, 116.7, 113.2, 62.7, 15.6.

*(1E,3Z,5E,7Z,9E)-4,7-dicyano-1,10-di-(4-(diethylbenzoate))-deca-1,3,5,7,9-pentaene* (**DPDC5-CO<sub>2</sub>Et**; m = 1): General double Knoevenagel condensation procedure. The product was prepared from **9b** and isolated as an orange solid in 32.4% yield. <sup>1</sup>H NMR (300 MHz, C<sub>2</sub>D<sub>2</sub>Cl<sub>4</sub>): δ 8.06 (d, *J* = 8.1 Hz, 4H), 7.62 (d, *J* = 8.1 Hz, 4H), 7.35 (dd, *J* = 11.5 Hz, 15.3 Hz, 2H), 7.08 (d, *J* = 11.5 Hz, 2H), 7.04 (d, *J* = 15.3 Hz, 2H), 6.75 (s, 2H), 4.39 (q, *J* = 7.2 Hz, 4H), 1.41 (t, *J* = 7.2 Hz, 6H); <sup>13</sup>C NMR (400 MHz, C<sub>2</sub>D<sub>2</sub>Cl<sub>4</sub>): δ 165.49, 144.61, 140.36, 139.09, 130.58, 129.58, 129.08, 127.00, 126.15, 114.44, 112.45, 60.82, 13.86.

*(1E,3E,5Z,7E,9Z,11E,13E)-6,9-dicyano-1,14-di-(4-(diethylbenzoate))-tetradeca-1,3,5,7,9,11,13-heptaene* (**DPDC7-CO<sub>2</sub>Et**; m = 2): General double Knoevenagel condensation procedure. The product was prepared from **9c** and isolated as a red solid in

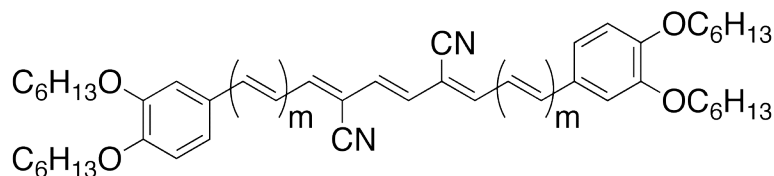
14.6% yield.  $^1\text{H}$  NMR (400 MHz,  $\text{DMSO-}d_6$ ):  $\delta$  8.04 (d,  $J = 8.0$  Hz, 4H), 7.54 (d,  $J = 8.0$  Hz, 4H), 7.11-6.72 (m, 12H), 4.41 (q,  $J = 7.0$  Hz, 4H), 1.43 (t,  $J = 7.0$  Hz, 6H);  $^1\text{H}$  NMR (500 MHz,  $\text{C}_2\text{D}_2\text{Cl}_4$ ):  $\delta$  8.03 (d,  $J = 8.2$  Hz, 4H), 7.53 (d,  $J = 8.2$  Hz, 4H), 7.08 (dd,  $J = 10.5$  Hz, 15.3 Hz, 2H), 6.97-6.80 (m, 8H), 6.68 (s, 2H), 4.38 (q,  $J = 7.1$  Hz, 4H), 1.40 (t,  $J = 7.1$  Hz, 6H);  $^{13}\text{C}$  NMR (500 MHz,  $\text{C}_2\text{D}_2\text{Cl}_4$ ):  $\delta$  165.64, 144.26, 141.34, 140.05, 136.69, 129.76, 129.62, 129.59, 129.53, 128.84, 126.39, 114.65, 111.51, 60.71, 13.89.



*3,4-bis(hexyloxy)benzaldehyde* (**10a**;  $m = 0$ ): This product was prepared by reaction of 3,4-dihydroxybenzaldehyde with 1-bromodecane under basic conditions. Detailed preparation and characterization has been reported by Binnemanns and coworkers.<sup>1</sup>

*(E)-3-(3,4-bis(hexyloxy)phenyl)acrylaldehyde* (**10b**;  $m = 1$ ): General Wittig Homologation procedure. The product was prepared from **10a** and isolated as a pale yellow solid in 91.1% yield. <sup>1</sup>H NMR (300 MHz, CDCl<sub>3</sub>):  $\delta$  9.68 (d,  $J = 7.8$  Hz, 1H), 7.44 (d,  $J = 15.9$  Hz, 1H), 7.16 (dd,  $J = 1.8$  Hz, 8.4 Hz, 1H), 7.11 (d,  $J = 1.8$  Hz, 1H), 6.92 (d,  $J = 8.1$  Hz, 1H), 6.62 (dd,  $J = 7.8$  Hz, 15.9 Hz, 1H), 4.04 (m, 4H), 1.84 (m, 4H), 1.51 (m, 4H), 1.39 (m, 8H), 0.95 (m, 6H); <sup>13</sup>C NMR (300 MHz, CDCl<sub>3</sub>):  $\delta$  194.1, 153.6, 152.7, 149.6, 127.2, 126.8, 123.9, 113.1, 112.7, 69.7, 69.4, 32.0, 31.9, 29.5, 29.4, 26.1, 26.0, 23.0, 22.9, 14.4 (2 -CH<sub>3</sub> carbon signals).

*(2E,4E)-5-(3,4-bis(hexyloxy)phenyl)penta-2,4-dienal* (**10c**;  $m = 2$ ): General Wittig procedure. The product was prepared from **10b** and isolated as a lemon yellow solid in 42.0% yield. <sup>1</sup>H NMR (300 MHz, CD<sub>2</sub>Cl<sub>2</sub>):  $\delta$  9.62 (d,  $J = 8.1$  Hz, 1H), 7.32 (dd,  $J = 10.2$  Hz, 15.3 Hz, 1H), 7.10-6.88 (m, 5H), 6.25 (dd,  $J = 7.8$  Hz, 15.0 Hz, 1H), 4.06 (m, 4H), 1.86 (m, 4H), 1.50 (m, 4H), 1.37 (m, 8H), 0.93 (m, 6H); <sup>13</sup>C NMR (300 MHz, CDCl<sub>3</sub>):  $\delta$  195.73, 154.96, 152.97, 151.07, 144.77, 132.05, 130.25, 125.79, 124.04, 115.28, 114.24, 71.36, 70.96, 33.36, 33.33, 31.07, 30.94, 27.49, 27.46, 24.45, 24.43, 15.9 (2 -CH<sub>3</sub> signals).



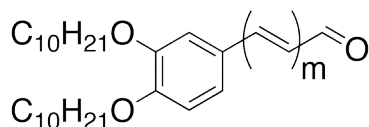
**DPDCn-OC<sub>6</sub>H<sub>13</sub>**; m = 0, 1, 2

(*1Z,3E,5Z*)-2,5-dicyano-1,6-di-(3,4-bis(hexyloxy)phenyl)-hexa-1,3,5-triene (**DPDC3-OC<sub>6</sub>H<sub>13</sub>**; m = 0): General double Knoevenagel condensation procedure. The product was prepared from **10a** and isolated as a lemon yellow solid in 7.8% yield. <sup>1</sup>H NMR (300 MHz, CDCl<sub>3</sub>): δ 7.61 (d, *J* = 2.1 Hz, 2H), 7.32 (dd, *J* = 1.8 Hz, 8.4 Hz, 2H), 7.09 (s, 2H), 6.92 (d, *J* = 8.4 Hz, 2H), 6.77 (s, 2H), 4.06 (m, 8H), 1.86 (m, 8H), 1.52 (m, 8H), 1.37 (m, 16H), 0.94 (m, 12H); <sup>13</sup>C NMR (300 MHz, CDCl<sub>3</sub>): δ 152.2, 149.4, 145.4, 139.3, 129.8, 126.8, 125.0, 113.1, 113.0, 107.0, 69.6, 69.4, 32.0, 31.9, 30.1, 29.6, 29.5, 26.1, 26.0, 23.0, 14.4 (2 -CH<sub>3</sub> carbon signals).

(*1E,3Z,5E,7Z,9E*)-4,7-dicyano-1,10-di-(3,4-bis(hexyloxy)phenyl)-deca-1,3,5,7,9-pentaene (**DPDC5-OC<sub>6</sub>H<sub>13</sub>**; m = 1): General double Knoevenagel condensation procedure. The product was prepared from **10b** and isolated as a dark red solid in 13.0% yield. <sup>1</sup>H NMR (300 MHz, CDCl<sub>3</sub>): δ 7.28 (s, 2H), 7.17-7.07 (m, 6H), 7.00-6.86 (m, 6H), 6.67 (s, 2H), 4.09 (m, 8H), 1.87 (m, 8H), 1.52 (m, 8H), 1.38 (m, 16H), 0.93 (m, 12H); <sup>13</sup>C NMR (300 MHz, CDCl<sub>3</sub>): δ 151.6, 149.7, 145.9, 142.6, 129.1, 129.0, 123.0, 122.7, 116.0, 113.4, 112.1, 110.7, 69.8, 69.5, 32.0, 31.9, 29.6, 29.5, 26.1, 26.0, 23.0 (2 -CH<sub>2</sub>- signals), 14.4 (2 -CH<sub>3</sub> carbon signals).

(*1E,3E,5Z,7E,9Z,11E,13E*)-6,9-dicyano-1,14-di-(3,4-bis(hexyloxy)phenyl)-tetradeca-1,3,5,7,9,11,13-heptaene (**DPDC7-OC<sub>6</sub>H<sub>13</sub>**; m = 2): General double Knoevenagel

condensation procedure. The product was prepared from **10c** and isolated as a dark purple solid in 20.1% yield.  $^1\text{H}$  NMR (300 MHz,  $\text{CDCl}_3$ ):  $\delta$  7.04 (d,  $J = 1.8$  Hz, 2H), 7.01 (dd,  $J = 2.1$  Hz,  $J = 8.7$  Hz, 2H), 6.95-6.75 (m, 12H), 6.65 (s, 2H), 4.04 (m, 8H), 1.87 (m, 8H), 1.51 (m, 8H), 1.37 (m, 16H), 0.93 (m, 12H);  $^{13}\text{C}$  NMR ( $\text{CDCl}_3$ );  $\delta$  300 MHz: 150.76, 149.67, 145.22, 142.99, 139.08, 129.21, 128.32, 126.53, 121.77, 115.88, 115.00, 113.65, 111.70, 111.06, 69.68, 69.54, 32.00, 31.98, 29.63, 29.54, 26.11, 26.08, 23.03, 23.02, 14.45, 14.43.



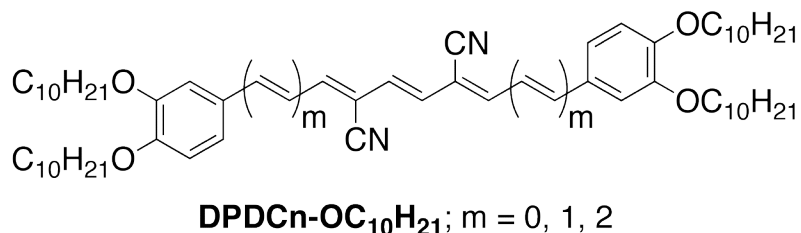
*3,4-bis(decyloxy)benzaldehyde* (**11a**;  $m = 0$ ): This product was prepared by reaction of 3,4-dihydroxybenzaldehyde with 1-bromohexane under basic conditions. Detailed preparation and characterization has been reported by Binnemanns and coworkers.<sup>1</sup>

*(E)-3,4-bis(decyloxy)cinnamaldehyde* (**11b**;  $m = 1$ ): General Wittig homologation procedure. The product was prepared from **11a** and isolated as a pale yellow solid in 98.8% yield. <sup>1</sup>H NMR (400 MHz, CDCl<sub>3</sub>):  $\delta$  9.68 (d,  $J = 8.0$  Hz, 1H), 7.41 (d,  $J = 15.6$  Hz, 1H), 7.13 (dd,  $J = 2.0$  Hz, 8.4 Hz, 1H), 7.09 (d,  $J = 1.6$  Hz, 1H), 6.89 (d,  $J = 8.4$  Hz, 1H), 6.60 (dd,  $J = 8.0$  Hz, 16 Hz, 1H), 4.04 (m, 4H), 1.84 (m, 4H), 1.48 (m, 4H), 1.36-1.28 (m, 24H), 0.88 (t,  $J = 6.4$  Hz, 6H); <sup>13</sup>C NMR (500 MHz, CDCl<sub>3</sub>):  $\delta$  193.57, 153.06, 152.34, 149.34, 126.88, 126.52, 123.44, 112.93, 112.54, 69.43, 69.12, 31.91, 29.62, 29.60, 29.58, 29.40, 29.37, 29.35, 29.22, 29.20, 26.01, 25.98, 22.68 (2 -CH<sub>2</sub>- carbon signals), 14.10 (2 -CH<sub>3</sub> carbon signals); three other aliphatic carbon signals not observed due to overlapping shifts.

*(2E,4E)-5-(3,4-bis(decyloxy)phenyl)penta-2,4-dienal* (**11c**;  $m = 2$ ): General Wittig homologation procedure. The product was prepared from **11b** and isolated as a yellow solid in 96.4% yield. <sup>1</sup>H NMR (500 MHz, CDCl<sub>3</sub>):  $\delta$  9.58 (d,  $J = 8.1$  Hz, 1H), 7.25 (dd,  $J = 10.4$  Hz, 15.1 Hz, 1H), 7.05 (d,  $J = 1.9$  Hz, 1H), 7.03 (dd,  $J = 1.9$  Hz, 8.1 Hz, 1H), 6.97 (d,  $J = 15.4$  Hz, 1H), 6.88-6.67 (m, 2H), 6.87-6.83 (m, 2H), 6.26 (d,  $J = 8.1$  Hz, 15.3 Hz, 1H), 4.03 (m, 4H), 1.82 (m, 4H), 1.48 (m, 4H), 1.41-1.16 (m, 24H), 0.88 (t,  $J = 6.9$  Hz,



6H);  $^{13}\text{C}$  NMR (500 MHz,  $\text{CDCl}_3$ ):  $\delta$  193.54, 152.62, 151.10, 149.35, 142.72, 130.53, 128.60, 124.06, 122.05, 113.23, 112.02, 69.46, 69.16, 31.92, 29.63, 29.62, 29.59, 29.57, 29.43, 29.35, 29.34, 29.30, 29.18, 26.05, 26.013, 22.69 (2  $-\text{CH}_2-$  carbon signals), 14.10 (2  $-\text{CH}_3$  carbon signals); two other aliphatic carbon signals not observed due to overlapping shifts.

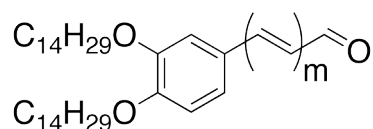


*(1Z,3E,5Z)*-2,5-dicyano-1,6-di-(3,4-bis(decyloxy)phenyl)-hexa-1,3,5-triene (**DPDC3-OC $_{10}$ H $_{21}$** ;  $m = 0$ ): General double Knoevenagel condensation procedure. The product was prepared from **11a**. Reaction took longer than other double Knoevenagel condensations and was stirred for 48 h at 50° C. The product was isolated as a lemon yellow solid in 18.7% yield.  $^1\text{H}$  NMR (400 MHz,  $\text{CDCl}_3$ ):  $\delta$  7.59 (d,  $J = 1.6$  Hz, 2H), 7.30 (dd,  $J = 1.6$  Hz,  $J = 8.4$  Hz, 2H), 7.08 (s, 2H), 6.90 (d,  $J = 8.4$  Hz, 2H), 6.76 (s, 2H), 4.07 (m, 8H), 1.85 (m, 8H), 1.49 (m, 8H), 1.40-1.20 (m, 48H), 0.88 (t,  $J = 6.4$  Hz, 12H);  $^{13}\text{C}$  NMR (300 MHz,  $\text{CDCl}_3$ ):  $\delta$  152.17, 149.46, 145.32, 129.75, 126.77, 124.97, 117.24, 113.33, 113.11, 106.99, 69.64, 69.47, 32.32, 30.11, 30.03, 30.01, 29.99, 29.77, 29.54, 29.46, 28.77, 26.44, 26.37, 26.18, 23.10, 22.57, 14.52 (2 -CH $_3$  carbon signals); two aliphatic carbon signals were not observed due to overlapping chemical shifts.

*(1E,3Z,5E,7Z,9E)*-4,7-dicyano-1,10-di-(3,4-bis(decyloxy)phenyl)-deca-1,3,5,7,9-pentaene (**DPDC5-OC $_{10}$ H $_{21}$** ;  $m = 1$ ): General double Knoevenagel condensation procedure. The product was prepared from **11b**. Reaction took longer than other double Knoevenagel condensations and was run for 48 h at 50° C. The product was isolated as a purple solid in 9.6% yield.  $^1\text{H}$  NMR (300 MHz,  $\text{CDCl}_3$ ):  $\delta$  7.16-7.04 (m, 6H), 6.97-6.84 (m, 6H), 6.52 (s, 2H), 4.04 (m, 8H), 1.86 (m, 8H), 1.50 (m, 8H), 1.38 (m, 48H), 0.88 (m, 12H);  $^{13}\text{C}$  NMR (400 MHz,  $\text{CDCl}_3$ ):  $\delta$  151.27, 149.42, 145.49, 142.20, 128.71, 128.63, 122.68,

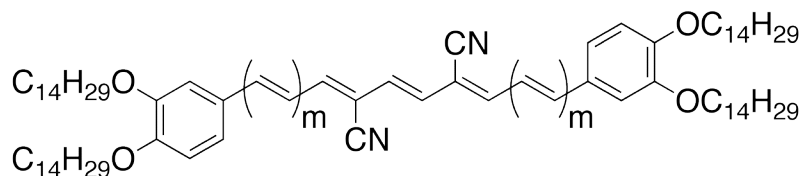
122.31, 115.59, 113.21, 111.99, 110.32, 69.48, 69.15, 31.92, 29.63, 29.61, 29.58, 29.44, 29.40, 29.36, 29.34, 29.32, 29.17, 26.05, 26.00, 22.69 (2 -CH<sub>2</sub>- carbon signals), 14.10 (2 -CH<sub>3</sub> carbon signals); two aliphatic carbon signals were not observed due to overlapping chemical shifts.

*(1E,3E,5Z,7E,9Z,11E,13E)-6,9-dicyano-1,14-di-(3,4-bis(decyloxy)phenyl)-tetradeca-1,3,5,7,9,11,13-heptaene* (**DPDC7-OC<sub>10</sub>H<sub>21</sub>**; m = 2): General double Knoevenagel condensation procedure. The product was prepared from **11c**. Reaction took longer than other double Knoevenagel condensations and was run for 48 h at 50° C. The product was isolated as a purple solid in 25.6% yield. <sup>1</sup>H NMR (300 MHz, CDCl<sub>3</sub>): δ 7.03-6.65 (m, 18H), 4.05 (m, 8H), 1.86 (m, 8H), 1.51 (m, 8H), 1.30 (m, 48H), 0.91 (t, *J* = 6.4 Hz, 12H); <sup>13</sup>C NMR (300 MHz, CDCl<sub>3</sub>): δ 150.1, 149.7, 145.2, 143.0, 139.1, 129.9, 129.2, 128.3, 126.5, 121.8, 115.9, 113.7, 111.8, 111.1, 69.7, 69.6, 32.3, 30.0 2 -CH<sub>3</sub> carbon signals, 29.8 (2 -CH<sub>3</sub> carbon signals), 29.7, 29.6, 26.4 (2 -CH<sub>3</sub> carbon signals), 23.1, 14.5 (2 -CH<sub>3</sub> carbon signals); five aliphatic carbon signals were not observed due to overlapping chemical shifts.



*3,4-bis(tetradecyloxy)benzaldehyde* (**12a**;  $m = 0$ ): This product was prepared by reaction of 3,4-dihydroxybenzaldehyde with 1-bromotetradecane under basic conditions. Detailed preparation and characterization has been reported by Binnemanns and coworkers.<sup>1</sup>

*3,4-bis(tetradecyloxy)cinnamaldehyde* (**12b**;  $m = 1$ ): General Wittig homologation procedure. The product was prepared from **12a** and isolated by column chromatography (5% ethylacetate in hexanes) as a light yellow solid in 53.4% yield. <sup>1</sup>H NMR (400 MHz, CDCl<sub>3</sub>):  $\delta$  9.66 (d,  $J = 7.8$  Hz, 1H), 7.40 (d,  $J = 15.9$  Hz, 1H), 7.13 (dd,  $J = 2.1$  Hz, 8.1 Hz, 1H), 7.08 (d,  $J = 1.8$  Hz, 1H), 6.89 (d,  $J = 8.1$  Hz, 1H), 6.63 (dd,  $J = 7.8$  Hz, 15.9 Hz, 1H), 4.04 (m, 4H), 1.84 (m, 4H), 1.78-1.02 (m, 44H), 0.88 (t,  $J = 6.9$  Hz, 6H); <sup>13</sup>C NMR (300 MHz, CDCl<sub>3</sub>):  $\delta$  193.79, 153.31, 152.75, 149.78, 127.31, 126.93, 123.78, 113.32, 123.96, 69.81, 69.50, 35.06, 34.91, 32.33, 31.98, 30.11, 29.81, 29.77, 29.63, 29.51, 29.45, 26.42, 26.39, 25.66, 23.07, 23.03, 21.03 (2 -CH<sub>2</sub>- carbon signals), 14.43 (2 -CH<sub>3</sub> carbon signals); seven aliphatic peaks not observed due to overlapping chemical shifts.



**DPDCn-OC<sub>14</sub>H<sub>29</sub>; m = 0, 1**

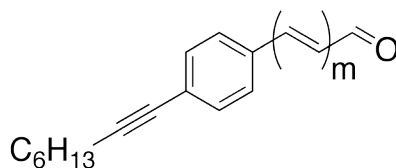
*(1Z,3E,5Z)-2,5-dicyano-1,6-di-(3,4-bis(tetradecyloxy)phenyl)-hexa-1,3,5-triene*

**(DPDC3-OC<sub>14</sub>H<sub>29</sub>; m = 0):** General double Knoevenagel condensation procedure. The product was prepared from **12a**. Reaction took longer than other double Knoevenagel condensations and was run for 36 h at 60° C. The product was isolated as a lemon yellow solid in 15.9% yield with a small amount of starting material as impurity. <sup>1</sup>H NMR (300 MHz, CDCl<sub>3</sub>): δ 7.60 (d, *J* = 1.8 Hz, 2H), 7.33 (dd, *J* = 1.8 Hz, 8.4 Hz, 2H), 7.09 (s, 2H), 6.92 (d, *J* = 8.4 Hz, 2H), 6.78 (s, 2H), 4.08 (m, 8H), 1.86 (m, 8H), 1.49 (m, 8H), 1.28 (m, 80H), 0.90 (t, *J* = 6.9 Hz, 12H); <sup>13</sup>C NMR (300 MHz, CDCl<sub>3</sub>): δ 151.96, 149.26, 144.83, 129.40, 126.51, 124.52, 116.73, 113.43, 113.08, 106.73, 69.41, 69.20, 31.89, 29.67, 29.62, 29.59, 29.57, 29.38, 29.34, 29.31, 29.19, 29.12, 26.03, 25.96, 22.63 (2 -CH<sub>2</sub>-signals), 14.01 (2 -CH<sub>3</sub> signals); ten carbon signals not observed due to overlapping chemical shifts.

*(1E,3Z,5E,7Z,9E)-4,7-dicyano-1,10-di-(3,4-bis(tetradecyloxy)phenyl)-deca-1,3,5,7,9-*

*pentaene (DPDC5-OC<sub>14</sub>H<sub>29</sub>; m = 1):* General double Knoevenagel condensation procedure. The product was prepared from **12b**. Reaction took longer than other double Knoevenagel condensations and was run for 36 h at 60° C. The product was isolated as a purple solid in 24.5% yield. <sup>1</sup>H NMR (300 MHz, CDCl<sub>3</sub>): δ 7.16 (dd, *J* = 11.4 Hz, 15.0 Hz, 2H), 7.07 (m, 4H), 6.98-6.84 (m, 6H), 6.65 (s, 2H), 4.04 (m, 8H), 1.84 (m, 8H), 1.50 (m, 8H), 1.42-1.18 (m, 80H), 0.88 (m, 12H); <sup>13</sup>C NMR (400 MHz, CDCl<sub>3</sub>): δ 151.27,

149.42, 145.49, 142.19, 128.71, 128.63, 122.67, 122.31, 115.59, 113.21, 111.99, 110.33, 69.48, 69.15, 31.93, 29.72, 29.67, 29.64, 29.62, 29.45, 29.40, 29.37, 29.32, 29.18, 26.05, 26.01, 22.69 (2 -CH<sub>2</sub>- signals), 14.11 (2 -CH<sub>3</sub> signals); ten carbon signals not observed due to overlapping chemical shifts.



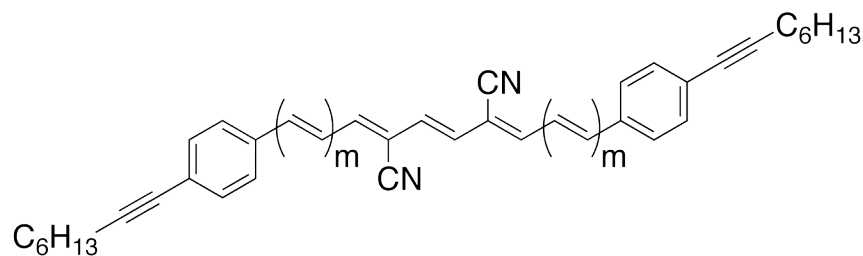
*4-(oct-1-ynyl)benzaldehyde* (**13a**;  $m = 0$ ): This compound was prepared by modifying the reported procedure.<sup>18</sup> 4-bromobenzaldehyde (1.0 g, 5.4 mmol), PPh<sub>3</sub> (10 mol%), PdCl<sub>2</sub>(PPh<sub>3</sub>)<sub>2</sub> (5 mol%) and 25 mL of THF combined into a flame dried 100-mL round-bottomed flask to make a yellow suspension. The suspension was degassed with nitrogen gas for 10 min before copper(I) iodide (10 mol%) was added and the suspension was further degassed for another 10 min. During this time the suspended solid dissolved into an orange solution. 1-octyne was added via syringe and the reaction was heated at 40° C for 16 h. The resulting brown solution was cooled to room temperature and diluted with diethyl ether, washed with water and dried over MgSO<sub>4</sub>. After removing the solvent under reduced pressure the product was isolated by flash column chromatography in hexanes/ethyl acetate (3:1), yielding a crude product as a light brown/yellow oil (99.0%). Spectroscopic data agrees with the literature. This product was not purified further but used in the next step as is. <sup>1</sup>H NMR (300 MHz, CDCl<sub>3</sub>): δ 9.97 (s, 1H), 7.80 (d,  $J = 8.4$  Hz, 2H), 7.53 (d,  $J = 8.4$  Hz, 2H), 2.43 (t,  $J = 7.2$  Hz, 2H), 1.60 (m, 2H), 1.45 (m, 2H), 1.30 (m, 4H), 0.91 (t,  $J = 6.9$  Hz, 3H); <sup>13</sup>C NMR (CDCl<sub>3</sub>): δ 191.7, 135.4, 132.4, 131.0, 129.8, 95.7, 80.5, 31.7, 29.0, 28.9, 22.9, 19.9, 14.5.

*(E)-(4-(oct-1-ynyl)phenyl)acrylaldehyde* (**13b**;  $m = 1$ ): General Wittig homologation procedure. The product was prepared from **13a** and isolated by column chromatography (10% ethyl acetate in hexanes) as an orange oil in 31.6% yield. <sup>1</sup>H NMR (300 MHz, CDCl<sub>3</sub>): δ 9.73 (d,  $J = 7.8$  Hz, 1H), 7.52-7.43 (m, 5H), 6.72 (dd,  $J = 7.8$  Hz, 15.9 Hz,

1H), 2.44 (t,  $J = 7.2$  Hz, 2H), 1.63 (m, 2H), 1.46 (m, 2H), 1.34 (m, 4H), 0.92 (t,  $J = 6.9$  Hz, 3H);  $^{13}\text{C}$  NMR ( $\text{CDCl}_3$ ):  $\delta$  193.9, 152.3, 133.3, 132.5, 129.0, 128.7, 127.6, 94.3, 80.7, 31.7, 29.0, 28.9, 23.0, 19.9, 14.5.

*(2E,4E)-5-(4-(oct-1-ynyl)phenyl)penta-2,4-dienal* (**13c**;  $m = 2$ ): General Wittig homologation procedure. The product was prepared from **13b** and isolated by column chromatography (10% ethyl acetate in hexanes) as a dark orange oil in 74.1% yield.  $^1\text{H}$  NMR (300 MHz,  $\text{CDCl}_3$ ):  $\delta$  9.65 (d,  $J = 8.1$  Hz, 1H), 7.45-7.38 (m, 4H), 7.31-7.22 (ddd,  $J = 4.8$  Hz, 6.7 Hz, 10.3 Hz, 1H), 6.99 (m, 2H), 6.31 (dd,  $J = 7.8$  Hz, 15.3 Hz, 1H), 2.44 (t,  $J = 6.9$  Hz, 2H), 1.63 (m, 2H), 1.47 (m, 2H), 1.33 (m, 4H), 0.93 (t,  $J = 7.2$  Hz, 3H);  $^{13}\text{C}$  NMR (300 MHz,  $\text{CDCl}_3$ ):  $\delta$  193.8, 152.1, 142.0, 135.0, 132.4, 132.1, 127.7, 126.9, 125.9, 93.5, 80.8, 31.7, 29.1, 29.0, 22.9, 19.9, 14.4.



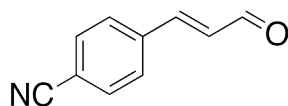


**DPDCn-C<sub>8</sub>H<sub>13</sub>**; m = 0, 1, 2

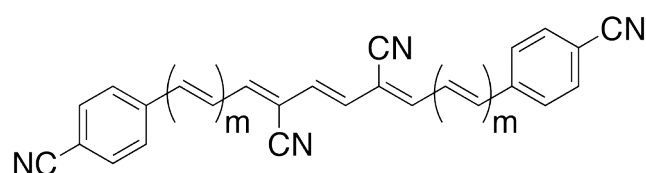
*(1Z,3E,5Z)*-2,5-dicyano-1,6-di-(4-(oct-1-ynyl)phenyl)-hexa-1,3,5-triene (**DPDC3-C<sub>8</sub>H<sub>13</sub>**; m = 0): General double Knoevenagel condensation procedure. The product was prepared from **13a** and isolated as a lemon yellow solid in 45.6% yield. <sup>1</sup>H NMR (300 MHz, CDCl<sub>3</sub>): δ 7.79 (d, *J* = 8.4 Hz, 4H), 7.46 (d, *J* = 8.1 Hz, 4H), 7.15 (s, 2H), 6.84 (s, 2H), 2.44 (d, *J* = 6.6 Hz, 4H), 1.62 (m, 4H), 1.49 (m, 4H), 1.34 (m, 8H), 0.91 (t, *J* = 6.9 Hz, 6H); <sup>13</sup>C NMR (300 MHz, CDCl<sub>3</sub>): δ 145.1, 132.6, 132.5, 130.9, 129.7, 127.5, 116.4, 109.9, 94.8, 80.8, 31.7, 29.0, 28.9, 22.9, 20.0, 14.4.

*(1E,3Z,5E,7Z,9E)*-4,7-dicyano-1,10-di-(4-(oct-1-ynyl)phenyl)-deca-1,3,5,7,9-pentaene (**DPDC5-C<sub>8</sub>H<sub>13</sub>**; m = 1): General double Knoevenagel condensation procedure. The product was prepared from **13b** and isolated as an orange-red solid in 7.6% yield. <sup>1</sup>H NMR (300 MHz, CDCl<sub>3</sub>): δ 7.48 (d, *J* = 8.1 Hz, 4H), 7.42 (d, *J* = 8.4 Hz, 4H), 7.31 (dd, *J* = 11.7 Hz, 15.3 Hz, 2H), 7.02 (d, *J* = 15.6 Hz, 2H), 6.98 (d, *J* = 15.3 Hz, 2H), 6.71 (s, 2H), 2.45 (d, *J* = 6.9 Hz, 4H), 1.64 (m, 4H), 1.47 (m, 4H), 1.35 (m, 8H), 0.93 (t, *J* = 6.9 Hz, 6H); <sup>13</sup>C NMR (300 MHz, CDCl<sub>3</sub>): δ 145.56, 141.77, 135.04, 132.48, 129.64, 127.90, 126.13, 125.39, 115.52, 112.41, 93.79, 80.92, 31.75, 29.03, 29.02, 22.94, 19.98, 14.44.

*(1E,3E,5Z,7E,9Z,11E,13E)-6,9-dicyano-1,14-di-(4-(oct-1-ynyl)phenyl)-tetradeca-1,3,5,7,9,11,13-heptaene* (**DPDC7-C<sub>8</sub>H<sub>13</sub>**; *m* = 2): General double Knoevenagel condensation procedure. The product was prepared from **13c** and isolated as a purple solid in 48.9% yield. <sup>1</sup>H NMR (300 MHz, CDCl<sub>3</sub>): δ 7.37 (s, 8H), 6.98-6.75 (m, 10H), 6.65 (s, 2H), 2.42 (d, *J* = 6.6 Hz, 4H), 1.63 (m, 4H), 1.47 (m, 4H), 1.33 (m, 8H), 0.91 (t, *J* = 6.6 Hz, 6H); <sup>13</sup>C NMR (300 MHz, CDCl<sub>3</sub>): δ 145.1, 142.5, 138.3, 135.9, 132.4, 129.6, 129.5, 128.8, 127.3, 125.1, 115.6, 112.0, 93.1, 81.0, 31.7, 29.1, 29.0, 22.9, 20.0, 14.4.



*trans*-4-cyanocinnamaldehyde (**14a**): General Wittig homologation procedure. The product was prepared from 4-cyanobenzaldehyde and isolated by column chromatography (15% ethyl acetate in hexanes) as a dark orange oil in 98.0% yield.  $^1\text{H}$  NMR (300 MHz,  $\text{CDCl}_3$ ):  $\delta$  9.78 (d,  $J = 8.4$  Hz, 1H), 7.75 (d,  $J = 8.4$  Hz, 2H), 7.69 (d,  $J = 8.4$  Hz, 2H), 7.52 (d,  $J = 16.2$  Hz, 1H), 6.82 (dd,  $J = 7.8$  Hz, 15.9 Hz, 1H);  $^{13}\text{C}$  NMR (300 MHz,  $\text{CDCl}_3$ ):  $\delta$  193.3, 149.8, 138.6, 133.2, 131.6, 129.1, 118.5, 114.7.



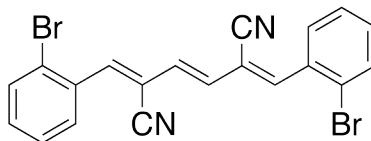
**DPDCn-CN**;  $m = 0, 1$

(1*Z*,3*E*,5*Z*)-2,5-dicyano-1,6-di-(4-cyanophenyl)-hexa-1,3,5-triene (**DPDC3-CN**;  $m = 0$ ): General double Knoevenagel condensation procedure. The product was prepared from 4-cyanobenzaldehyde and isolated as a dull yellow solid in 21.8% yield.  $^1\text{H}$  NMR (300 MHz, 355 K,  $\text{DMSO-}d_6$ ):  $\delta$  8.01 (d,  $J = 7.8$  Hz, 4H), 7.94 (d,  $J = 7.8$  Hz, 4H), 7.85 (s, 2H), 7.06 (s, 2H);  $^{13}\text{C}$  NMR (300 MHz, 355 K,  $\text{DMSO-}d_6$ ):  $\delta$  145.7, 138.4, 133.5, 131.9, 130.6, 113.9, 113.1, 104.5, 106.0.

(1*E*,3*Z*,5*E*,7*Z*,9*E*)-4,7-dicyano-1,10-di-(4-cyanophenyl)-deca-1,3,5,7,9-pentaene

(**DPDC5-CN**;  $m = 1$ ): General double Knoevenagel condensation procedure. The product was prepared from **14a** and isolated as an insoluble bright-orange solid in 25.8% yield.

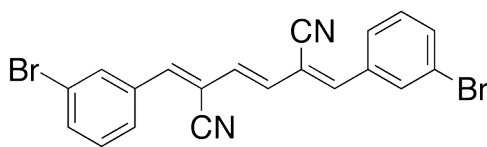
$^1\text{H}$  NMR (400 MHz, 355 K,  $\text{DMF-}d_7$ ):  $\delta$  8.05 (m, 8H), 7.81 (bd, 2H), 7.64 (bt, 2H), 7.53 (bd, 2H), 7.14 (bs, 2H);  $^{13}\text{C}$  NMR was not obtained do to insolubility.



***ortho*-DPDC3-Br**

*(1Z,3E,5Z)*-2,5-dicyano-1,6-di-(2-bromophenyl)-hexa-1,3,5-triene (***ortho*-DPDC3-Br**):

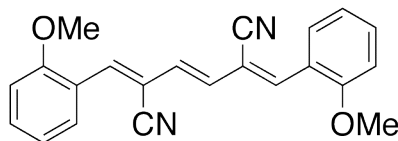
General double Knoevenagel condensation procedure. The product was prepared from 2-bromobenzaldehyde and isolated as a pale yellow solid in 33.9% yield.  $^1\text{H}$  NMR (300 MHz,  $\text{CDCl}_3$ ):  $\delta$  8.10 (dd,  $J = 1.5$  Hz, 7.8 Hz, 2H), 7.70 (dd,  $J = 1.2$  Hz, 8.1 Hz, 2H), 7.58 (s, 2H), 7.47 (td,  $J = 1.2$  Hz, 7.8 Hz, 2H), 7.33 (td,  $J = 1.5$  Hz, 7.8 Hz, 2H), 6.98 (s, 2H);  $^{13}\text{C}$  NMR (300 MHz, 350 K,  $\text{C}_2\text{D}_2\text{Cl}_4$ ):  $\delta$  144.5, 133.3, 133.2, 131.7, 130.7, 129.3, 127.7, 125.2, 115.0, 112.6.



***meta*-DPDC3-Br**

*(1Z,3E,5Z)*-2,5-dicyano-1,6-di-(3-bromophenyl)-hexa-1,3,5-triene (***meta*-DPDC3-Br**):

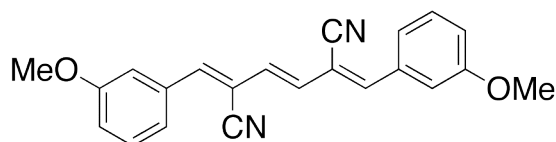
General double Knoevenagel condensation procedure. The product was prepared from 3-bromobenzaldehyde and isolated as a yellow solid in 24.9% yield.  $^1\text{H}$  NMR (300 MHz,  $\text{CDCl}_3$ ):  $\delta$  7.93 (dd,  $J = 1.7$  Hz, 2H), 7.83 (d,  $J = 8.1$  Hz, 2H), 7.58 (d,  $J = 8.1$  Hz, 2H), 7.92 (t,  $J = 7.9$  Hz, 2H), 7.15 (s, 2H), 6.88 (s, 2H);  $^{13}\text{C}$  NMR (300 MHz, 350 K,  $\text{C}_2\text{D}_2\text{Cl}_4$ ):  $\delta$  143.3, 134.8, 133.3, 131.6, 130.2, 130.0, 127.1, 122.6, 114.7, 110.7.



***ortho*-DPDC3-OMe**

*(1Z,3E,5Z)*-2,5-dicyano-1,6-di-(2-methoxyphenyl)-hexa-1,3,5-triene (***ortho*-DPDC3-**

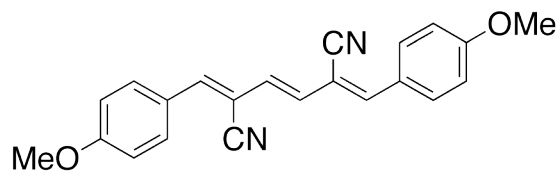
**OMe**): General double Knoevenagel condensation procedure. The product was prepared from 2-methoxybenzaldehyde and isolated as a yellow solid in 8.5% yield.  $^1\text{H}$  NMR (400 MHz,  $\text{CDCl}_3$ ):  $\delta$  8.17 (dd,  $J = 1.4$  Hz, 7.8 Hz, 2H), 7.66 (s, 2H), 7.43-7.39 (m, 2H), 7.04 (t,  $J = 7.6$  Hz, 2H), 6.94 (d,  $J = 8.3$  Hz, 2H), 6.88 (s, 2H), 3.90 (s, 6H);  $^{13}\text{C}$  NMR (400 MHz,  $\text{CDCl}_3$ ):  $\delta$  157.99, 140.11, 132.44, 130.28, 128.34, 122.69, 120.88, 116.47, 110.89, 109.46, 55.67.



***meta*-DPDC3-OMe**

*(1Z,3E,5Z)*-2,5-dicyano-1,6-di-(3-methoxyphenyl)-hexa-1,3,5-triene (***meta*-DPDC3-**

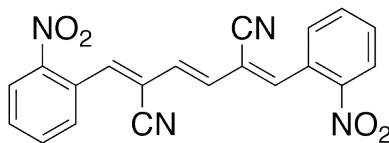
**OMe**): General double Knoevenagel condensation procedure. The product was prepared from 3-methoxybenzaldehyde and isolated as a neon yellow solid in 9.2% yield.  $^1\text{H}$  NMR (400 MHz,  $\text{CDCl}_3$ ):  $\delta$  7.46 (m, 2H), 7.40-7.33 (m, 4H), 7.19 (s, 2H), 7.00 (dt,  $J = 2.5$  Hz, 6.6 Hz, 2H), 6.86 (s, 2H), 3.87 (s, 6H);  $^{13}\text{C}$  NMR (400 MHz,  $\text{CDCl}_3$ ):  $\delta$  159.94, 145.60, 134.57, 130.42, 130.08, 122.52, 117.66, 116.06, 113.53, 109.76, 55.43.



***para*-DPDC3-OMe**

*(1Z,3E,5Z)*-2,5-dicyano-1,6-di-(4-methoxyphenyl)-hexa-1,3,5-triene      (***para*-DPDC3-**

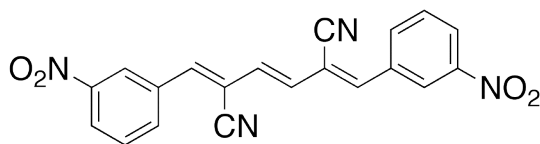
**OMe**): General double Knoevenagel condensation procedure. The product was prepared from 4-methoxybenzaldehyde and isolated as a yellow solid in 11.4% yield. <sup>1</sup>H NMR (400 MHz, DMSO-*d*<sub>6</sub>): δ 7.83 (d, *J* = 8.4, 4H), 7.57 (s, 2H), 7.06 (d, *J* = 8.4, 4H), 6.82 (s, 2H), 3.85 (s, 6H); <sup>13</sup>C NMR (400 MHz, DMSO-*d*<sub>6</sub>): δ 161.1, 144.7, 130.6, 128.5, 125.9, 115.8, 114.3, 105.8, 55.1.



***ortho*-DPDC3-NO<sub>2</sub>**

(1Z,3E,5Z)-2,5-dicyano-1,6-di-(2-nitrophenyl)-hexa-1,3,5-triene (***ortho*-DPDC3-NO<sub>2</sub>**):

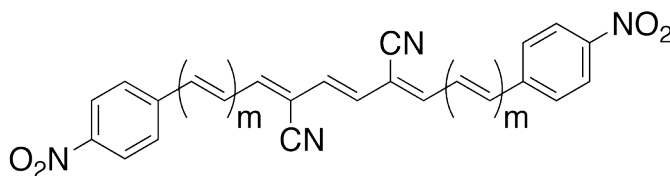
This product could not be synthesized from 2-nitrobenzaldehyde using our method.



***meta*-DPDC3-NO<sub>2</sub>**

(1Z,3E,5Z)-2,5-dicyano-1,6-di-(3-nitrophenyl)-hexa-1,3,5-triene (***meta*-DPDC3-NO<sub>2</sub>**):

General double Knoevenagel condensation procedure was modified. The base, DBU, was substituted with catalytic amounts sodium methoxide. The product was prepared from 3-nitrobenzaldehyde and isolated as a yellow solid in 10.9% yield. <sup>1</sup>H NMR (500 MHz, C<sub>2</sub>D<sub>2</sub>C<sub>14</sub>): δ 8.67 (s, 2H), 8.33 (d, *J* = 8.2 Hz, 2H), 8.22 (d, *J* = 7.8 Hz, 2H), 7.71 (t, *J* = 8.0 Hz, 2H), 7.37 (s, 2H), 6.99 (s, 2H); <sup>13</sup>C NMR (500 MHz, C<sub>2</sub>D<sub>2</sub>C<sub>14</sub>): δ 149.9, 144.7, 136.0, 135.9, 132.6, 131.8, 126.8, 125.4, 116.5, 113.8.



**DPDC<sub>n</sub>-NO<sub>2</sub>; m = 0, 1**

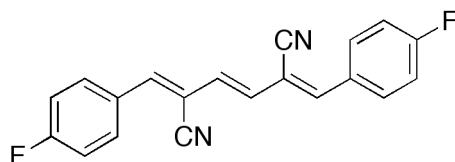


*(1Z,3E,5Z)-2,5-dicyano-1,6-di-(4-nitrophenyl)-hexa-1,3,5-triene* (**DPDC3-NO<sub>2</sub>**; m = 0):

General double Knoevenagel condensation procedure was modified. The base, DBU, was substituted with catalytic amounts sodium methoxide. The product was prepared from 4-nitrobenzaldehyde and isolated as a yellow solid in 24.0% yield. <sup>1</sup>H NMR (500 MHz, C<sub>2</sub>D<sub>2</sub>C<sub>14</sub>): δ 8.33 (d, *J* = 8.5 Hz, 4H), 8.02 (d, *J* = 8.5 Hz, 4H), 7.36 (s, 2H), 7.00 (s, 2H); <sup>13</sup>C NMR (500 MHz, C<sub>2</sub>D<sub>2</sub>C<sub>14</sub>): δ 147.89, 142.98, 138.37, 131.22, 129.65, 123.78, 114.51, 112.67.

*(1E,3Z,5E,7Z,9E)-4,7-dicyano-1,10-di-(4-nitrophenyl)-deca-1,3,5,7,9-pentaene*

(**DPDC5-NO<sub>2</sub>**; m = 1): General double Knoevenagel condensation procedure was modified. The base, DBU, was substituted with catalytic amounts sodium methoxide. The product was prepared from *trans*-4-nitrocinnamaldehyde and isolated as a dark orange solid in 11.4% yield. <sup>1</sup>H NMR (400 MHz, 350 K, C<sub>2</sub>D<sub>2</sub>C<sub>14</sub>): δ 8.26 (d, *J* = 8.0 Hz, 4H), 7.71 (d, *J* = 8.0 Hz, 4H), 7.48-7.33 (m, 2H), 7.18-6.80 (m, 6H); <sup>1</sup>H NMR (400 MHz, 373 K, DMSO-*d*<sub>6</sub>): δ 8.26 (d, *J* = 8.3 Hz, 4H), 7.93 (d, *J* = 8.3 Hz, 4H), 7.64 (d, *J* = 10.8 Hz, 2H), 7.44-7.32 (m, 4H), 6.94 (s, 2H); <sup>13</sup>C NMR could not be obtained due to limited solubility.



*(1Z,3E,5Z)*-2,5-dicyano-1,6-di-(4-fluorophenyl)-hexa-1,3,5-triene (**DPDC3-F**): General double Knoevenagel condensation procedure. The product was prepared from 4-fluorobenzaldehyde and isolated as a pale yellow solid in 33.4% yield.  $^1\text{H}$  NMR (300 MHz,  $\text{DMSO-}d_6$ ):  $\delta$  7.92 (bs, 4H), 7.75 (s, 2H), 7.35 (bs, 2H), 6.93 (s, 2H);  $^1\text{H}$  NMR (500 MHz,  $\text{C}_2\text{D}_2\text{Cl}_4$ ):  $\delta$  7.92 (m, 4H), 7.18 (m, 6H), 6.84 (s, 2H);  $^{13}\text{C}$  NMR (400 MHz,  $\text{C}_2\text{D}_2\text{Cl}_4$ ):  $\delta$  165.0, 143.4, 131.0, 130.9, 129.7, 115.8, 115.6, 109.1;  $^{19}\text{F}$  NMR (400 MHz,  $\text{C}_2\text{D}_2\text{Cl}_4$ ):  $\delta$  106.2.

### **A3. UV-Vis Absorption Spectroscopy**

**General Procedure and Instrumentation:** Absorption spectra were taken on an Agilent Technologies 8453 UV-Vis spectrophotometer. Solutions of oligoenes were prepared in dichloromethane solution at a concentration between  $10^{-5}$  and  $10^{-6}$  M. A quartz cuvette with path length equal to 1.0 cm was used in the collection of each spectrum.

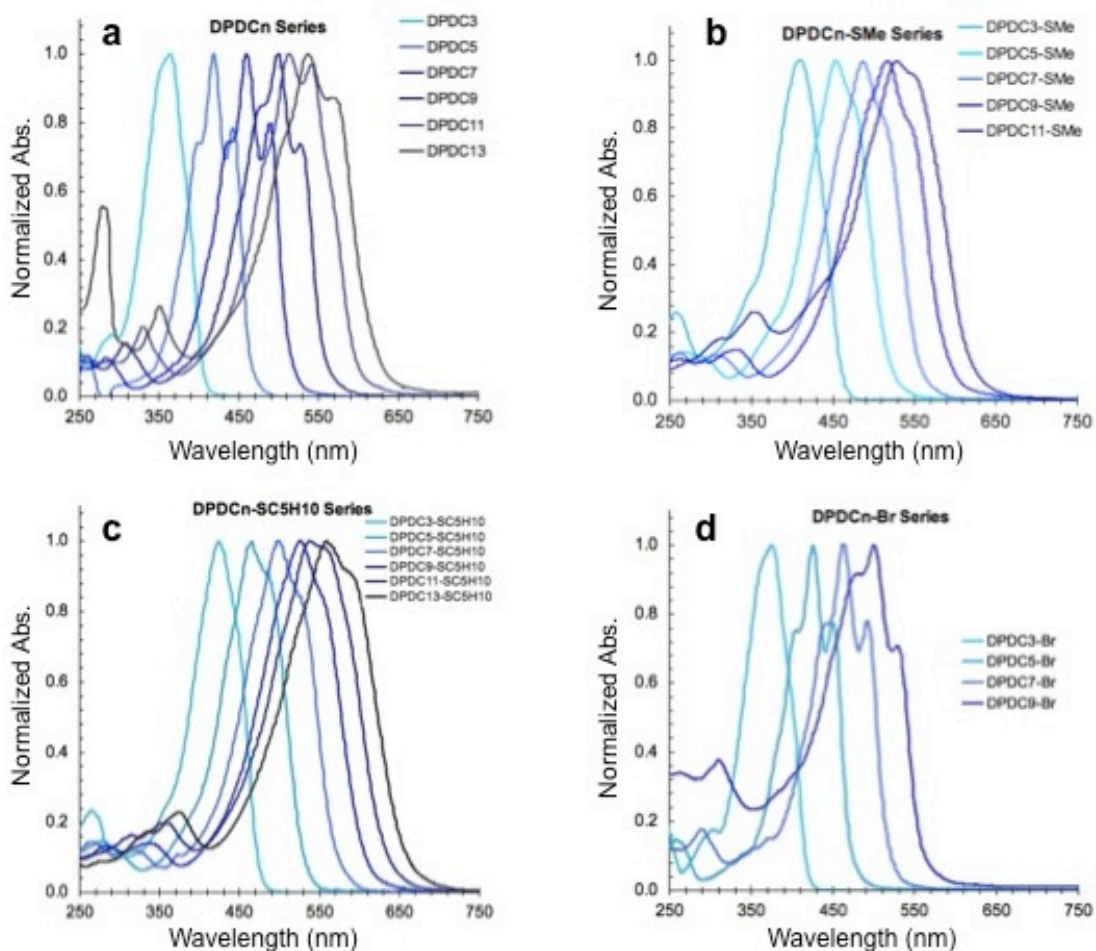


**Figure A1:** Optical absorption spectra of different families of  $\alpha,\omega$ -diphenyl- $\mu,\nu$ -dicyano-oligoenes: (a) the unfunctionalized **DPDC $n$**  series ( $n = 3$  to 13), (b) **DPDC $n$ -SMe** ( $n = 3$  to 11), (c) **DPDC $n$ -SC $_5$ H $_{10}$**  ( $n = 3$  to 13) and (d) **DPDC $n$ -Br** ( $n = 3$  to 9). In all cases the spectra shift towards the red with increasing oligoene length ( $n$ ). All spectra obtained in dichloromethane.

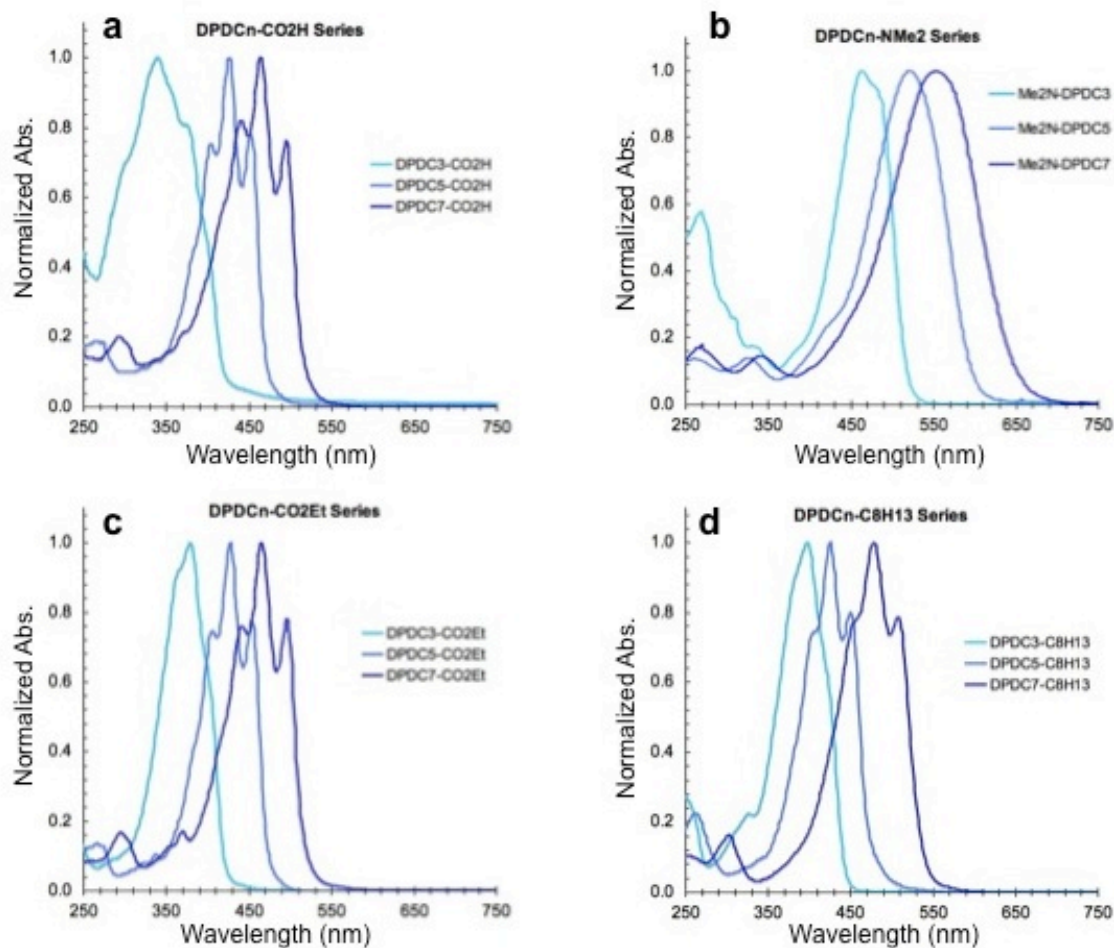


**Figure A2:** Optical absorption spectra of the (a) **DPDC<sub>n</sub>-CO<sub>2</sub>H** series ( $n = 3, 5$  and  $7$ ) in tetrahydrofuran solutions, as well as (b) **DPDC<sub>n</sub>-NMe<sub>2</sub>** ( $n = 3, 5$  and  $7$ ), (c) **DPDC<sub>n</sub>-CO<sub>2</sub>Et** ( $n = 3, 5$  and  $7$ ) and (d) **DPDC<sub>n</sub>-C<sub>8</sub>H<sub>13</sub>** ( $n = 3, 5$  and  $7$ ) in dichloromethane solutions. In all cases the spectra shift towards the red with increasing oligoene length ( $n$ ).

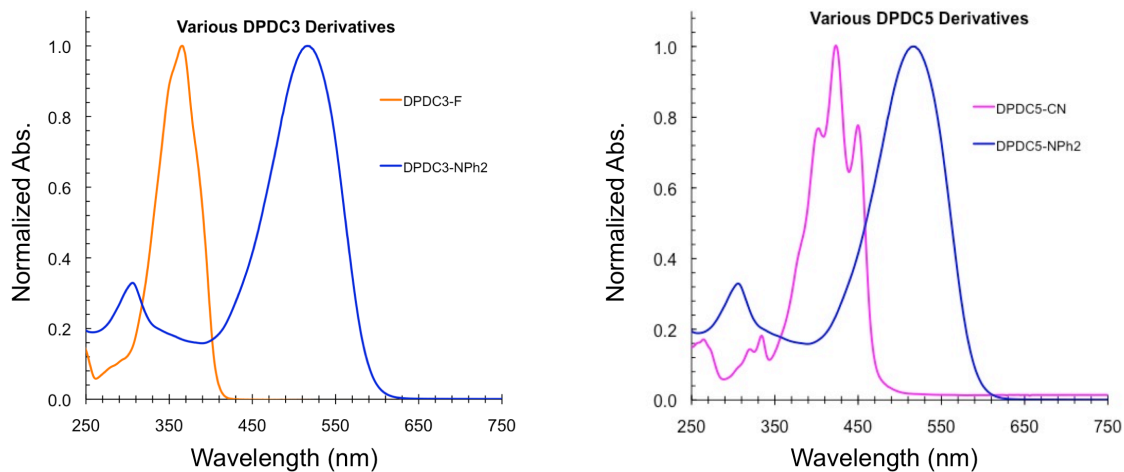


**Figure A3:** Optical absorption spectra of various (a) **DPDC3-X** derivatives, where  $X = \mathbf{F}$  (orange line) and  $\mathbf{NPh}_2$  (blue line); and (b) **DPDC5-X** derivatives, where  $X = \mathbf{CN}$  (purple line) and  $\mathbf{NPh}_2$  (dark blue line). All spectra obtained in dichloromethane solutions.

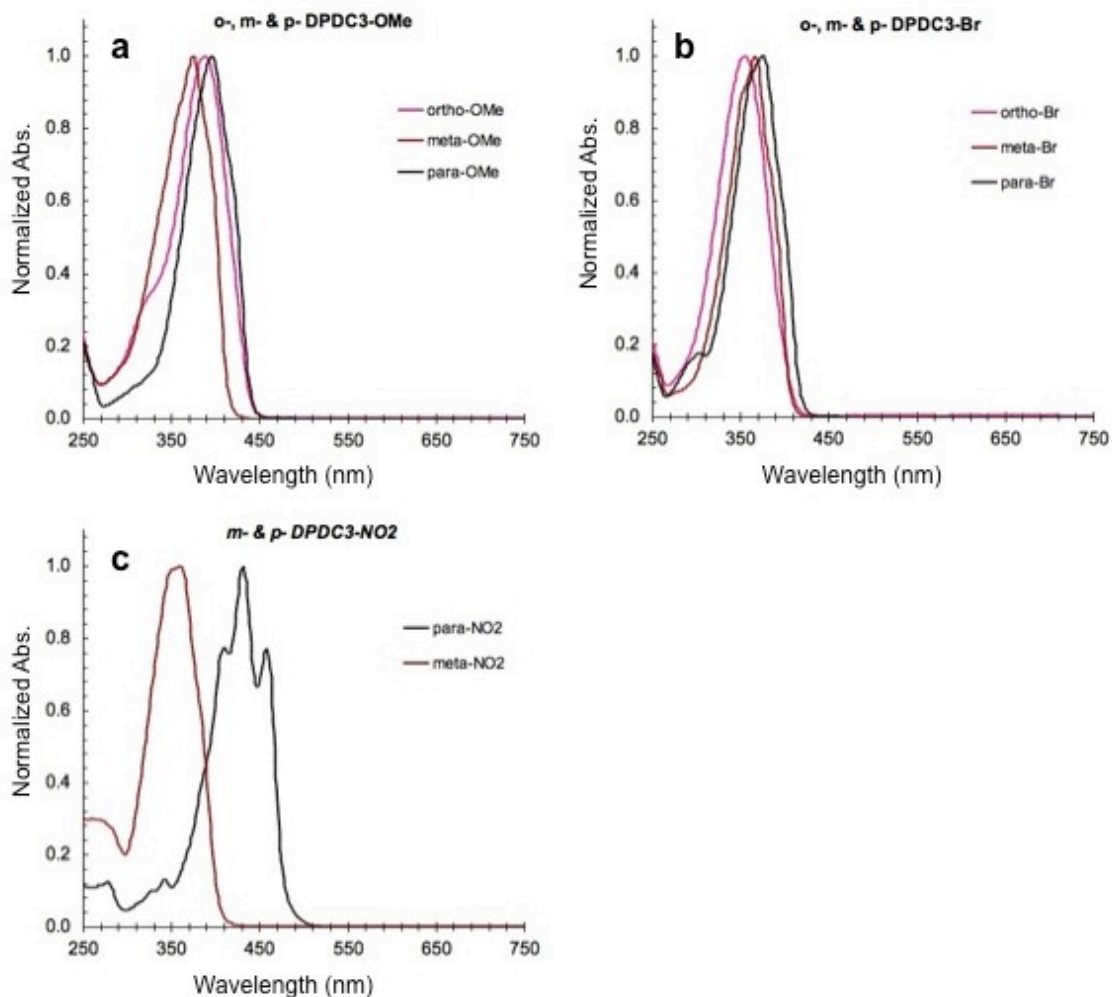


**Figure A4:** Effects on the substitution pattern of electron-donating and electron-withdrawing groups were investigated. UV-Vis absorption spectra (a) **DPDC3-OMe**, (b) **DPDC3-Br** and (c) **DPDC3-NO<sub>2</sub>** derivatives were taken in dichloromethane solutions. Our observations agree well with Hammett coefficients suggesting that *para*-substitutions are most strongly coupled to the  $\pi$ -conjugated oligoene backbone.

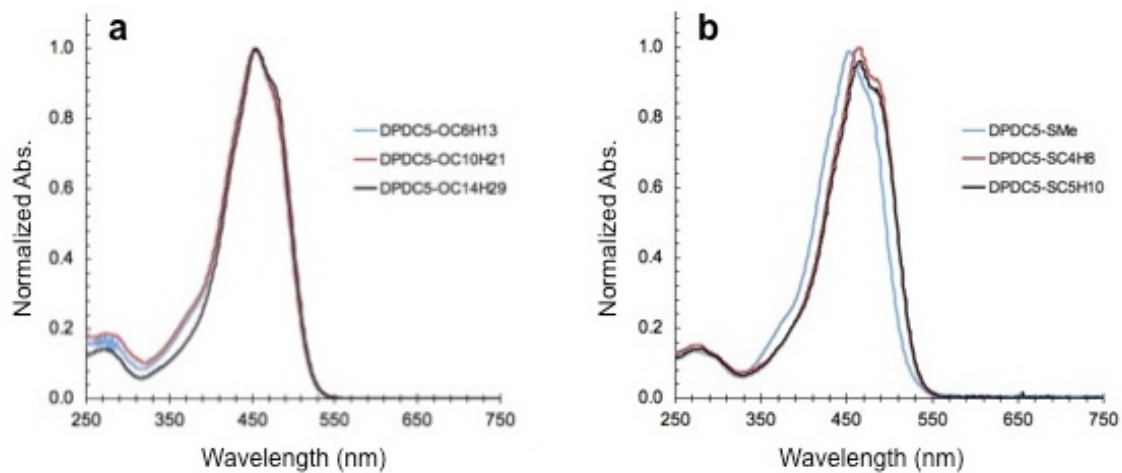


**Figure A5:** The physical properties can be tuned independently from the electronic structure as shown in the following collections of **DPDC5** derivatives: (a) **DPDC5-OC<sub>6</sub>H<sub>13</sub>**, **DPDC5-OC<sub>10</sub>H<sub>21</sub>**, **DPDC5-OC<sub>14</sub>H<sub>29</sub>**; and (b) **DPDC5-SMe**, **DPDC5-SC<sub>4</sub>H<sub>8</sub>**, **DPDC5-SC<sub>5</sub>H<sub>10</sub>**. Spectra obtained in dichloromethane solutions.



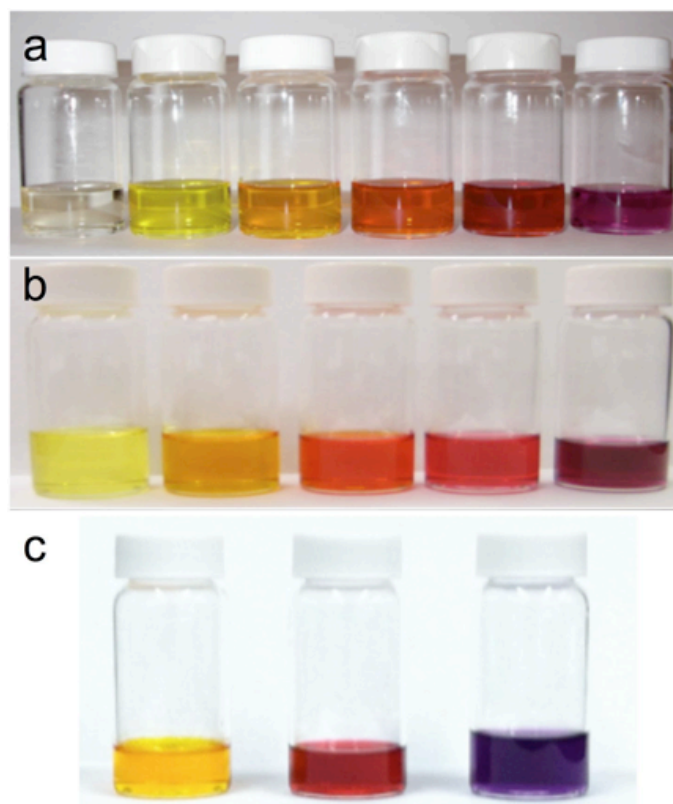


**Figure A6:** Photograph of dilute solutions ( $\sim 10^{-4}$  M) of oligoene series (a) **DPDCn** (b) **DPDCn-SMe** and (c) **DPDCn-NMe<sub>2</sub>** in dichloromethane.

### Extinction Coefficient Values for DPDCn's and Their Derivatives:

Molecule	Wavelength (nm)	Extinction ( $\text{cm}^{-1} \cdot \text{mol}^{-1}$ )
DPDC3	353 <sup>a</sup>	$5.00 \times 10^4$
	366	$5.44 \times 10^4$
	383 <sup>a</sup>	$3.78 \times 10^4$
DPDC5	399 <sup>a</sup>	$7.51 \times 10^4$
	418	$1.00 \times 10^5$
	442	$7.85 \times 10^4$
DPDC7	284	$1.34 \times 10^4$
	438	$8.69 \times 10^4$
	460	$1.16 \times 10^5$
	489	$1.02 \times 10^5$
DPDC9	307	$1.54 \times 10^4$
	480	$9.69 \times 10^4$
	498	$1.13 \times 10^5$
	526	$8.40 \times 10^4$
DPDC11	330	$2.73 \times 10^4$
	485 <sup>a</sup>	$9.36 \times 10^4$
	512	$1.27 \times 10^5$
	540	$1.22 \times 10^5$
DPDC13 <sup>c</sup>	351	$3.14 \times 10^4$
	510 <sup>a</sup>	$9.45 \times 10^4$
	536	$1.24 \times 10^5$
	572	$1.09 \times 10^5$
DPDC3-SMe	225	$1.45 \times 10^4$
	412	$7.33 \times 10^4$
DPDC5-SMe	267	$1.18 \times 10^4$
	453	$8.25 \times 10^4$
	476 <sup>a</sup>	$7.11 \times 10^4$
DPDC7-SMe	263	$1.44 \times 10^4$
	309	$1.46 \times 10^4$
	487	$1.04 \times 10^5$
	513 <sup>a</sup>	$8.59 \times 10^4$
DPDC9-SMe <sup>c</sup>	308	$2.34 \times 10^4$
	476 <sup>a</sup>	$1.22 \times 10^5$
	498	$1.41 \times 10^5$
	526	$1.03 \times 10^5$
DPDC11-SMe <sup>c</sup>	312 <sup>a</sup>	$1.93 \times 10^4$
	350	$2.57 \times 10^4$
	497 <sup>a</sup>	$7.10 \times 10^4$
	527	$9.00 \times 10^4$
	555 <sup>a</sup>	$8.12 \times 10^4$

<b>DPDC3-SC<sub>4</sub>H<sub>8</sub></b>	263	$3.87 \times 10^4$
	382	$5.62 \times 10^4$
	485 <sup>a</sup>	$4.74 \times 10^4$
<b>DPDC5-SC<sub>4</sub>H<sub>8</sub></b>	280	$1.41 \times 10^4$
	463	$9.61 \times 10^4$
	485 <sup>a</sup>	$8.57 \times 10^4$
<b>DPDC7-SC<sub>4</sub>H<sub>8</sub></b>	274	$5.38 \times 10^4$
	497	$1.24 \times 10^5$
	525 <sup>a</sup>	$1.03 \times 10^5$
<b>DPDC9-SC<sub>4</sub>H<sub>8</sub></b>	336	$2.23 \times 10^4$
	523	$1.07 \times 10^5$
	552 <sup>a</sup>	$8.82 \times 10^4$
<b>DPDC11-SC<sub>4</sub>H<sub>8</sub></b>	353	$2.52 \times 10^4$
	359	$2.52 \times 10^4$
	537	$1.22 \times 10^5$
	557	$1.18 \times 10^5$
<b>DPDC3-SC<sub>5</sub>H<sub>10</sub></b>	264	$1.19 \times 10^4$
	424	$6.72 \times 10^4$
	447 <sup>a</sup>	$5.29 \times 10^4$
<b>DPDC5-SC<sub>5</sub>H<sub>10</sub></b>	280	$1.18 \times 10^4$
	463	$7.62 \times 10^4$
	484 <sup>a</sup>	$6.91 \times 10^4$
<b>DPDC7-SC<sub>5</sub>H<sub>10</sub></b>	271	$1.41 \times 10^4$
	317	$1.32 \times 10^4$
	498	$1.04 \times 10^5$
	526 <sup>a</sup>	$8.75 \times 10^4$
<b>DPDC9-SC<sub>5</sub>H<sub>10</sub></b>	284	$1.27 \times 10^4$
	339	$1.38 \times 10^4$
	526	$9.23 \times 10^4$
	555 <sup>a</sup>	$7.71 \times 10^4$
<b>DPDC11-SC<sub>5</sub>H<sub>10</sub></b>	353	$2.50 \times 10^4$
	360	$2.54 \times 10^4$
	539	$1.28 \times 10^5$
	558 <sup>a</sup>	$1.26 \times 10^5$
<b>DPDC13-SC<sub>5</sub>H<sub>10</sub></b>	336	$2.39 \times 10^4$
	375	$3.12 \times 10^4$
	658	$1.27 \times 10^5$
	589 <sup>a</sup>	$1.13 \times 10^5$
<b>DPDC3-NMe<sub>2</sub></b>	264	$6.82 \times 10^3$
	383 <sup>a</sup>	$3.55 \times 10^4$
	464	$3.19 \times 10^4$
	485 <sup>a</sup>	$7.38 \times 10^3$

<b>DPDC5-NMe<sub>2</sub></b>	264	1.33 x 10 <sup>4</sup>
	325	1.14 x 10 <sup>4</sup>
	521	8.82 x 10 <sup>4</sup>
<b>DPDC7-NMe<sub>2</sub></b>	328	1.25 x 10 <sup>4</sup>
	426 <sup>a</sup>	2.26 x 10 <sup>4</sup>
	521	9.09 x 10 <sup>4</sup>
<b>DPDC3-NPh<sub>2</sub></b>	303	2.03 x 10 <sup>4</sup>
	476	4.84 x 10 <sup>4</sup>
<b>DPDC5-NPh<sub>2</sub></b>	306	2.80 x 10 <sup>4</sup>
	516	8.45 x 10 <sup>4</sup>
<b>DPDC3-Br</b>	242	1.08 x 10 <sup>4</sup>
	359 <sup>a</sup>	5.59 x 10 <sup>4</sup>
	377	6.49 x 10 <sup>4</sup>
	396 <sup>a</sup>	4.31 x 10 <sup>4</sup>
<b>DPDC5-Br</b>	258	1.37 x 10 <sup>4</sup>
	404 <sup>a</sup>	7.67 x 10 <sup>4</sup>
	425	1.03 x 10 <sup>5</sup>
	450	8.00 x 10 <sup>4</sup>
<b>DPDC7-Br</b>	290	1.46 x 10 <sup>4</sup>
	371 <sup>a</sup>	1.32 x 10 <sup>4</sup>
	441	7.58 x 10 <sup>4</sup>
	463	9.88 x 10 <sup>4</sup>
	492	7.76 x 10 <sup>4</sup>
<b>DPDC9-Br<sup>c</sup></b>	311	1.24 x 10 <sup>4</sup>
	477 <sup>a</sup>	6.01 x 10 <sup>4</sup>
	501	6.98 x 10 <sup>4</sup>
	529	5.08 x 10 <sup>4</sup>
<b>DPDC3-CO<sub>2</sub>H<sup>b</sup></b>	368 <sup>a</sup>	5.13 x 10 <sup>4</sup>
	383	5.60 x 10 <sup>4</sup>
	404 <sup>a</sup>	3.62 x 10 <sup>4</sup>
<b>DPDC5-CO<sub>2</sub>H<sup>b</sup></b>	343 <sup>a</sup>	6.16 x 10 <sup>3</sup>
	384 <sup>a</sup>	1.91 x 10 <sup>4</sup>
	411 <sup>a</sup>	3.90 x 10 <sup>4</sup>
	434	5.17 x 10 <sup>4</sup>
	460	4.06 x 10 <sup>4</sup>
<b>DPDC7-CO<sub>2</sub>H<sup>b</sup></b>	296	1.27 x 10 <sup>4</sup>
	450	4.84 x 10 <sup>4</sup>
	474	6.19 x 10 <sup>4</sup>
	505	4.93 x 10 <sup>4</sup>
<b>DPDC3-CO<sub>2</sub>Et</b>	362 <sup>a</sup>	5.70 x 10 <sup>4</sup>
	378	6.18 x 10 <sup>4</sup>
	398 <sup>a</sup>	3.94 x 10 <sup>4</sup>

<b>DPDC5-CO<sub>2</sub>Et</b>	266	$1.37 \times 10^4$
	337	$1.38 \times 10^4$
	405	$8.24 \times 10^4$
	427	$1.10 \times 10^5$
	453	$8.48 \times 10^4$
<b>DPDC7-CO<sub>2</sub>Et<sup>c</sup></b>	295	$8.94 \times 10^3$
	370	$9.18 \times 10^3$
	441	$4.32 \times 10^4$
	465	$5.68 \times 10^4$
	496	$4.43 \times 10^4$
<b>DPDC3-OC<sub>6</sub>H<sub>13</sub></b>	258	$1.33 \times 10^4$
	411	$6.40 \times 10^4$
	432 <sup>a</sup>	$5.03 \times 10^4$
<b>DPDC5-OC<sub>6</sub>H<sub>13</sub></b>	276	$9.53 \times 10^3$
	427 <sup>a</sup>	$5.27 \times 10^4$
	454	$7.50 \times 10^4$
	476 <sup>a</sup>	$6.69 \times 10^4$
<b>DPDC7-OC<sub>6</sub>H<sub>13</sub></b>	271	$9.73 \times 10^3$
	305	$9.20 \times 10^3$
	493	$8.58 \times 10^4$
	521 <sup>a</sup>	$7.10 \times 10^4$
<b>DPDC3-OC<sub>10</sub>H<sub>21</sub></b>	247	$1.47 \times 10^4$
	411	$3.47 \times 10^4$
	431 <sup>a</sup>	$2.73 \times 10^4$
<b>DPDC5-OC<sub>10</sub>H<sub>21</sub></b>	278	$1.38 \times 10^4$
	454	$8.20 \times 10^4$
	474 <sup>a</sup>	$7.28 \times 10^4$
<b>DPDC7-OC<sub>10</sub>H<sub>21</sub></b>	300	$1.45 \times 10^4$
	492	$4.96 \times 10^4$
	519 <sup>a</sup>	$4.14 \times 10^4$
<b>DPDC3-C<sub>8</sub>H<sub>13</sub></b>	249	$1.37 \times 10^4$
	379 <sup>a</sup>	$5.85 \times 10^4$
	399	$7.16 \times 10^4$
	423 <sup>a</sup>	$4.64 \times 10^4$
<b>DPDC5-C<sub>8</sub>H<sub>13</sub></b>	279	$1.34 \times 10^4$
	420 <sup>a</sup>	$6.89 \times 10^4$
	443	$9.08 \times 10^4$
	470	$6.97 \times 10^4$
<b>DPDC7-C<sub>8</sub>H<sub>13</sub></b>	303	$2.36 \times 10^4$
	453 <sup>a</sup>	$1.10 \times 10^5$
	478	$1.43 \times 10^5$
	508	$1.13 \times 10^5$
<b>DPDC3-CN</b>	238	$1.34 \times 10^4$

	361 <sup>a</sup>	5.29 x 10 <sup>4</sup>
	376	5.68 x 10 <sup>4</sup>
	395 <sup>a</sup>	3.74 x 10 <sup>4</sup>
<b>DPDC5-CN</b>	264	1.51 x 10 <sup>4</sup>
	402	7.61 x 10 <sup>4</sup>
	424	1.03 x 10 <sup>5</sup>
	450	8.12 x 10 <sup>4</sup>
<b>ortho-DPDC3-Br</b>	230	9.26 x 10 <sup>3</sup>
	355	3.79 x 10 <sup>4</sup>
<b>meta-DPDC3-Br</b>	240	9.92 x 10 <sup>3</sup>
	352 <sup>a</sup>	4.96 x 10 <sup>4</sup>
	367	5.52 x 10 <sup>4</sup>
	385 <sup>a</sup>	3.66 x 10 <sup>4</sup>
<b>ortho-DPDC3-OMe</b>	242	8.57 x 10 <sup>3</sup>
	321 <sup>a</sup>	1.10 x 10 <sup>4</sup>
	389	3.60 x 10 <sup>4</sup>
<b>meta-DPDC3-OMe</b>	229	1.20 x 10 <sup>4</sup>
	374	4.76 x 10 <sup>4</sup>
<b>para-DPDC3-OMe</b>	249	1.14 x 10 <sup>4</sup>
	396	5.72 x 10 <sup>4</sup>
<b>meta-DPDC3-NO<sub>2</sub><sup>c</sup></b>	281	1.81 x 10 <sup>3</sup>
	359	3.09 x 10 <sup>3</sup>
<b>DPDC3-NO<sub>2</sub></b>	236	7.29 x 10 <sup>3</sup>
	267	6.69 x 10 <sup>3</sup>
	390	4.59 x 10 <sup>4</sup>
	414 <sup>a</sup>	2.89 x 10 <sup>4</sup>
<b>DPDC5-NO<sub>2</sub></b>	228	3.21 x 10 <sup>4</sup>
	415 <sup>a</sup>	5.20 x 10 <sup>4</sup>
	437	6.77 x 10 <sup>4</sup>
	462	5.20 x 10 <sup>4</sup>
<b>DPDC3-F</b>	236	1.18 x 10 <sup>4</sup>
	367	5.60 x 10 <sup>4</sup>
	382 <sup>a</sup>	4.27 x 10 <sup>4</sup>

**Table A1:** UV-vis spectra were obtained in dichloromethane solutions. <sup>a</sup>Peaks were not well-defined; absorption shoulder. <sup>b</sup>Spectra were obtained in DMSO due to limited solubility. <sup>c</sup>There is more error in these values due to their extreme insolubility.

#	Solvent	$\lambda_{\text{max}}$ (nm)
1	nitrobenzene	539
2	dimethyl sulfoxide	533
3	1,1',2,2'-Tetrachloroethane	529
4	dimethylformamide	523
5	chlorobenzene	523
6	methylene chloride	520
7	chloroform	518
8	tetrahydrofuran	514
9	acetonitrile	512
10	acetone	512
11	benzene	511
12	toluene	511
13	ethyl acetate	506
14	diethyl ether	500
15	n-heptane	484

**Table A2:** Solvatochromism survey in the UV-vis absorption maxima for **DPDC-NMe<sub>2</sub>**.

#### A4. Cyclic Voltammetry

**General Procedure and Data Analysis:** Cyclic voltammetry (CV) was performed using a CHI600c potentiometer. All electrodes were purchased from Bioanalytical Systems, Inc; working electrode was a glass carbon electrode (MF-2070), reference electrode was Ag/AgCl (MF-2062), and auxiliary electrode was a platinum electrode (MW-4130). All measurements were carried out under argon in dimethylformamide (DMF) solution with tetrabutylammonium hexafluorophosphate electrolyte (0.1 M) and oligoene (350  $\mu\text{M}$ ). Ferrocene was used as an internal standard. To assure that the addition of the internal standard did not affect the redox chemistry of the analyte, oligoene solutions were first measured without the presence of ferrocene and then again with the internal standard. Ionization potentials were then set relative to that of ferrocene at  $E^0 = -4.8$  eV.



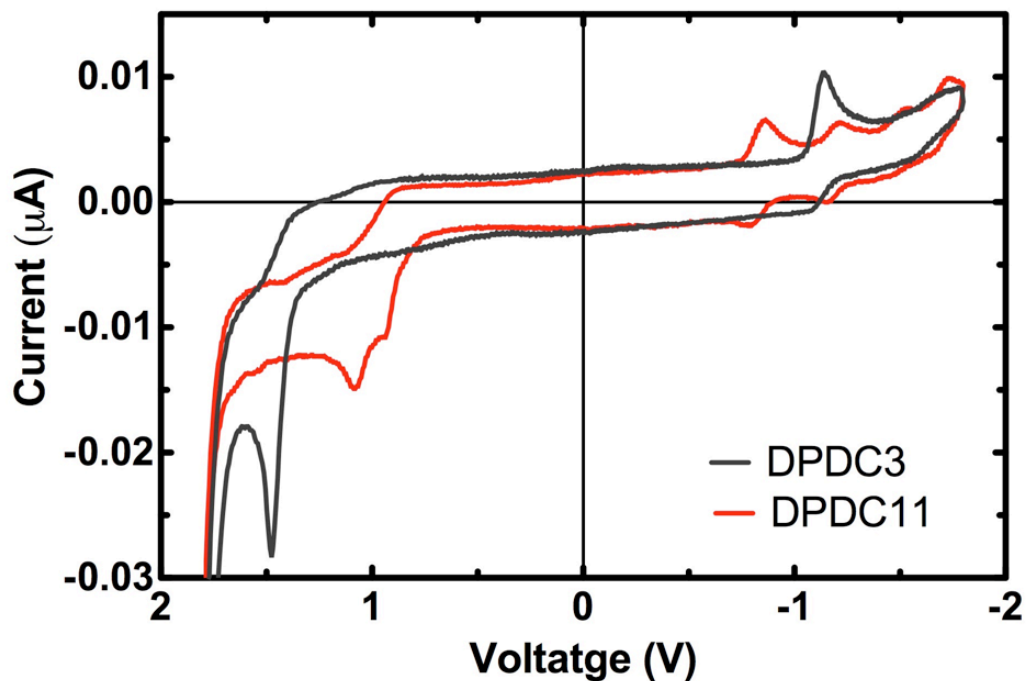


**Figure A8:** Comparison of ionization potentials obtained from cyclic voltammetry (CV). As a general trend, reductions become more reversible as the molecular length increases. Oxidations, on the other hand, are generally unstable, where apparent deposition of the oxidized material is observed on the electrode surface. The irreversibility of the oxidations does not change if the CV was stopped before reaching the solvent oxidation. Ferrocene was used as an internal standard.

**Tabulated DPDCn Redox Potentials:**

Molecule	Reductions								Oxidations			
	$E_1$	$E^0_1$	$E_2$	$E^0_2$	$E_3$	$E^0_3$	$E_4$	$E^0_4$	$E_1$	$E^0_1$	$E_2$	$E^0_2$
<b>DPDC3</b>	-3.09	-3.13	-	-	-	-	-	-	-5.74	-	-	-
<b>DPDC5</b>	-3.25	-3.28	-	-	-	-	-	-	-5.47	-	-	-
<b>DPDC7</b>	-3.29	-3.34	-2.85	-2.90	-2.51	-	-	-	-5.32	-	-5.57	-
<b>DPDC9</b>	-3.33	-3.38	-2.97	-3.02	-2.90	-2.76	-	-	-5.25	-	-5.42	-
<b>DPDC11</b>	-3.37	-3.43	-3.03	-3.07	-2.97	-2.84	-2.49	-	-5.19	-	-5.34	-
<b>DPDC13</b>	-3.38	-3.44	-3.06	-3.11	-3.06	-2.94	-2.59	-	-5.14	-	-5.27	-

**Table A3.** Ionization potentials obtained by CV. Oligoene solutions (350  $\mu\text{M}$ ) were prepared in DMF with tetrabutylammonium hexafluorophosphate electrolyte (0.1 M). All value are relative to ferrocene ( $E^0 = -4.8$  eV) as internal standard.

<b>DPDCn</b>	<b>DPDC3</b>	<b>DPDC5</b>	<b>DPDC7</b>	<b>DPDC9</b>	<b>DPDC11</b>	<b>DPDC13</b>
LUMO	-3.125	-3.275	-3.335	-3.375	-3.425	-3.435
HOMO	-5.740	-5.470	-5.320	-5.250	-5.190	-5.140
<b>DPOn</b>	<b>DPO3</b>	<b>DPO5</b>	<b>DPO7</b>			
LUMO	-2.448	-2.650	-2.770			
HOMO	-5.298	-5.193	-4.969			
Difference in LUMO	0.677	0.625	0.565			
Difference in HOMO	0.442	0.277	0.351			

**Table A4:** Redox potentials estimate the HOMO and LUMO energy differences between series **DPDCn** and **DPOn**. The installation of nitriles lowers the energy of both the LUMO (up to 0.68 eV) and the HOMO (up to 0.44 eV) and shrinks the molecular band gap,  $E_{cv}$ , as much as 0.24 eV. Longer **DPOn** oligomers could not be synthesized/characterized due to their high insolubility.

### A5. Particle in a Box: A Simple Model for Electron Confinement in DPDCn Series

As a simple model for small-scale confinement, the energies of a one-dimensional “particle in a box” were found to relate the optical absorptions and electrochemical redox potential gaps,  $E_{cv}$ , of the **DPDCn** series.

$$E_n = \frac{n^2 \hbar^2 \pi^2}{2m^* L^2} = \frac{n^2 h^2}{8m^* L^2} \quad (\text{eq. A1})$$

where  $L$  is the molecular length, which was obtained directly from the crystal structures and measured between the *para*-positioned hydrogens at each end of the molecule (see Table S5). The strongest wavelength absorption ( $\lambda_{\text{max}}$ ), solution optical band gap ( $E_{og}$ ), and the electrochemical band gap ( $E_{CV}$ ) can be described with this model. Linear regression analysis yielded fitted lines with  $R^2$  values  $> 0.99$ . Simple extrapolative analysis to oligomers of infinite lengths predicts values that agree well with those obtained experimentally for the polymer, polyacetylene.

L (nm)	$1/L^2$ (nm <sup>-2</sup> )	$\lambda_{\text{max}}$ (eV)	$E_{OG}$ (eV)	$E_{CV}$ (eV)
1.633	0.3752	3.39	2.86	2.62
2.104	0.2259	2.97	2.42	2.20
2.591	0.1490	2.70	2.13	1.99
3.077	0.1056	2.49	1.97	1.88
3.555	0.0791	2.42	1.86	1.77
4.043	0.0612	2.31	1.76	1.71
Extrapolation Results				
slope	n/a	3.40	3.47	2.86

y-intercept	n/a	2.15	1.59	1.55
-------------	-----	------	------	------

**Table A5:** Values used for particle in a box modeling of **DPDCn** series. Molecular length (L) was obtained from crystal structures and measured between the *para*-positioned carbons at each end of the molecule. The values for the slope and y-intercept obtained from our simple extrapolative analysis are also tabulated.

In order to calculate the resulting effective mass, data was converted to standard units of energy (erg), time (s), mass (g) and length (cm). Given the equation above the slope obtained from our linear regression would have units [erg x s].

$$\text{slope} = \frac{h^2}{8m^*} \quad (\text{eq. A2})$$

Thus, the appropriate value for Planck's constant was chosen,  $6.626 \times 10^{-27}$  erg x s, providing mass in grams.

$$[\text{erg}] \times [\text{cm}^2] = \frac{[\text{erg} \times \text{s}]^2}{m^*}$$

$$[\text{erg}] = \frac{[\text{g} \times \text{cm}^2]}{\text{s}^2}$$

$$m^* = [\text{g}]$$

A sample calculation gives an effective mass; To a first order approximation the exciton behaves as a spatially confined quantum mechanical particle relative to the length of the molecule.

$$m^* = \frac{h^2}{8 \times (\text{slope})}$$

$$m^* = \frac{(6.626 \times 10^{-27} \text{ erg} \cdot \text{s})^2}{8 \cdot (2.551 \times 10^{-12} \text{ erg} \times \text{cm}^2)} = 2.151 \times 10^{-42} \text{ g} = 2.151 \times 10^{-45} \text{ kg}$$

## A6. Nanoparticle Synthetic Details and SAM Preparation

**General information:** Gallium Arsenide (100) single crystalline wafer was purchased from Sigma-Aldrich. Ammonium Hydroxide, 30% in water (NH<sub>4</sub>OH) and Ethanol, 200 proof (EtOH) were purchased from Fischer Scientific. Dimethyl Sulfoxide (DMSO) 99% anhydrous was purchased from Sigma-Aldrich. EtOH and DMSO were degassed over several (three or greater) freeze pump thaw cycles before use. Iron (III) chloride 97%, and oleic acid 90% were purchased from Sigma-Aldrich. Sodium oleate 97% was purchased from TCI. 1-octadecene 90% was purchased from Acros Organics. Hexane was purchased from Fischer Scientific. Monolayer formation was observed using a Hitachi S-4700 FE-SEM.

**Nanoparticle Synthesis.** Fe<sub>3</sub>O<sub>4</sub> nanoparticles were prepared using the method developed by Hyeon *et al.*<sup>19</sup> Iron oleate precursor was made by adding 10.8 g of iron (III) chloride and 36.5 g of sodium oleate into a mixed solvent of 30 mL of ethanol, 40 mL of DI water and 70 mL of hexane. The reaction was kept at 60 °C for 4 hours and the product was purified with DI water and then dried under vacuum. The 10 nm Fe<sub>3</sub>O<sub>4</sub> nanoparticles were synthesized by mixing 3.6 g of iron oleate, 1.28 mL of oleic acid and 20 mL of 1-octadecene into a three neck flask, and the solution was heated to 320 °C at a heating rate of 200 °C/hr and kept at 320 °C for 30 minutes. After the reaction mixture was cooled to room temperature, ethanol was added as anti-solvent to precipitate the nanoparticles by centrifugation. The precipitated nanoparticles were re-dispersed in hexane.

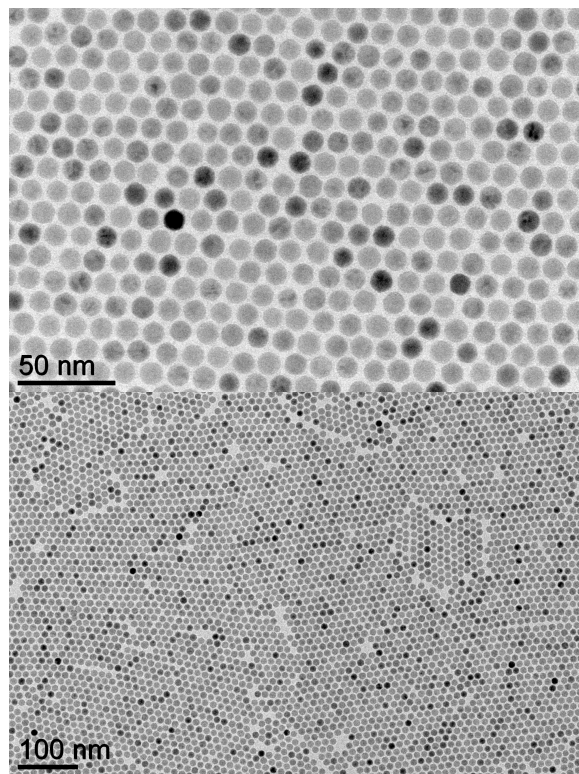


**Figure A9:** TEM images of as-synthesized 10-nm Fe<sub>3</sub>O<sub>4</sub> nanoparticles.



**Monolayer Formation Procedure.** Gallium Arsenide crystal was cut into several 0.75-1.0 cm square wafers using a diamond scribe. The wafers were submerged in  $\text{NH}_4\text{OH}$  and allowed to stand covered for 10 minutes. Upon removal from the  $\text{NH}_4\text{OH}$ , a wafer is rinsed with ethanol, dried under an argon stream, rinsed and dried a second time, then immediately submerged in a 1.5 mM solution of **DPDC3-CO<sub>2</sub>H** in dimethyl sulfoxide (DMSO). The solution is transferred to a nitrogen glove box and allowed to stand for 16 hours. After removal from the glove box, the wafer is removed from the solution, rinsed thoroughly with ethanol and dried under an argon stream. It is immediately submerged into a solution of 10-nm iron oxide ( $\text{Fe}_3\text{O}_4$ ) nanoparticles in dimethylformamide, and allowed to stand 1-2 hours. Upon removal from the nanoparticle solution, the wafer is rinsed with ethanol and dried under an argon stream, at which point they are ready for microscopy (Figure S12a).

**Controls.** In order to probe the dependence of monolayer formation on oligoene concentration in DMSO, the above procedure was carried out using both 3.0 and 6.0 mM solutions. It was found that nanoparticle coverage increased with increasing concentration of **DPDC3-CO<sub>2</sub>H** (Figure S12b and S12c).

We verified that monolayer formation is initiated by the oligoene connectors. Two controls were carried out: First, to eliminate the possibility that DMSO was acting as an inter-particle connector the above procedure was carried out using pure DMSO in place of the oligoene solution; secondly, in order to eliminate the possibility that submersion

into the nanoparticle solution was sufficient to generate monolayers, a wafer was placed into the nanoparticle solution directly after cleaning. No monolayer formation was observed in either case as seen in Figure S12c and S12d.

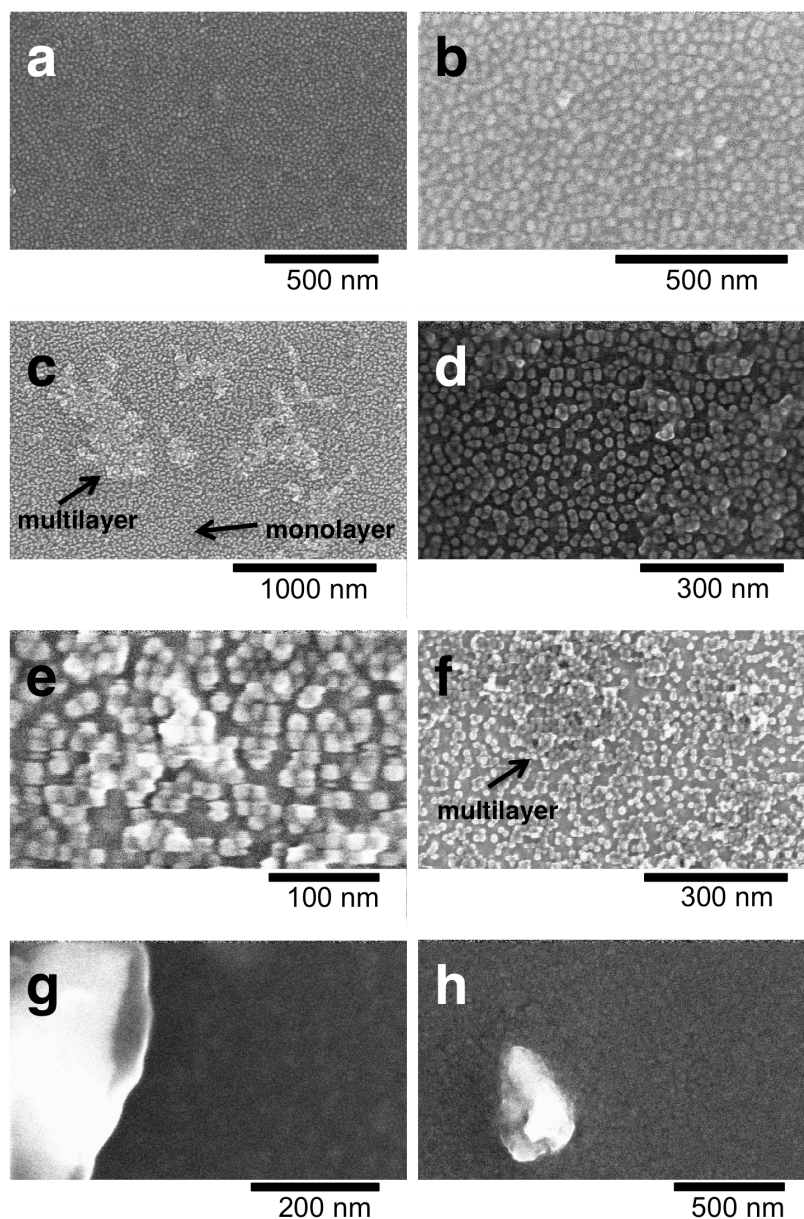


**Figure A10:** SEM images of monolayers of  $\text{Fe}_3\text{O}_4$  nanoparticles formed after carrying out the above procedure using: (a) 1.5 mM **DPDC3-CO<sub>2</sub>H**, where the scale bar represents a distance of 500 nm; (b) 1.5 mM **DPDC3-CO<sub>2</sub>H**, where the scale bar represents a distance of 300 nm; (c) 3.0 mM **DPDC3-CO<sub>2</sub>H**, where the scale bar represents a distance of 1  $\mu\text{m}$ ; (d) 3.0 mM **DPDC3-CO<sub>2</sub>H**, where the scale bar represents a distance of 300 nm; (e) 6.0 mM **DPDC3-CO<sub>2</sub>H**, where the scale bar represents a distance of 100 nm; (f) 6.0 mM **DPDC3-CO<sub>2</sub>H**, where the scale bar represents a distance of at 300 nm; (g) DMSO only; (h) DMF only.

### **A7. Theoretical Methods and Details.**

All electronic structure calculations used Jaguar (version 7.0, Schrodinger LLC, New York, NY, 2007) using the B3LYP hybrid functional and the 6-31G\*\* basis sets. The geometries of **DPDCn** and **DPOn** were fully optimized. The final geometries, total energies, bond angles and bond distances can be found in a separate supporting information file. Below is a summary the results of our calculations on selected **DPDC5** and **DPO5** derivatives.

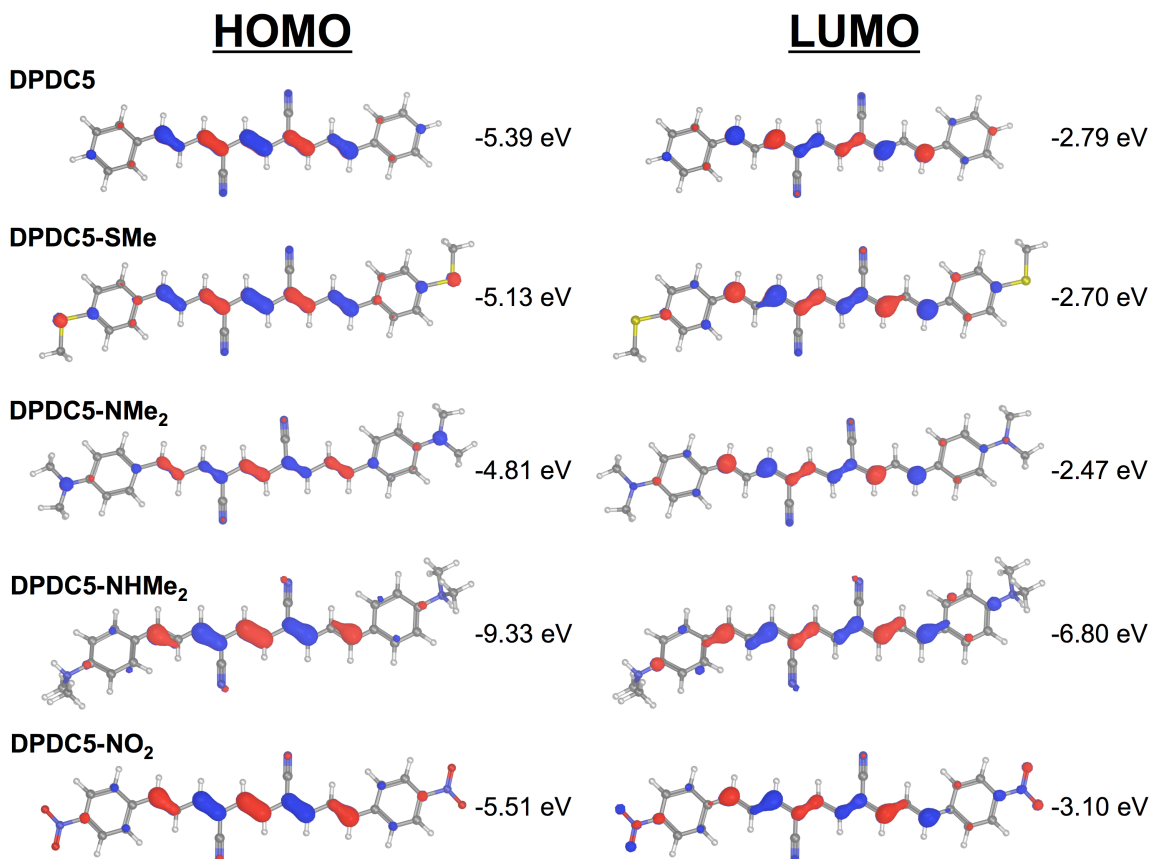


**Figure A11:** HOMO and LUMO topologies of selected **DPDC5** derivatives predicted by DFT B3LYP 6-31G\*\* (gas phase).

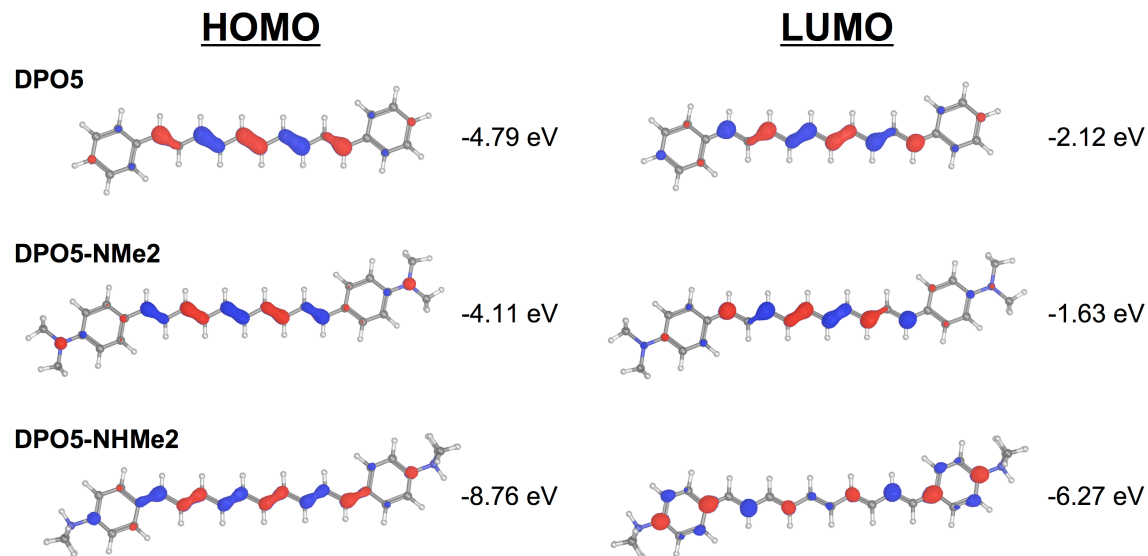


**Figure A12:** HOMO and LUMO topologies of selected **DPO5** derivatives predicted by DFT B3LYP 6-31G\*\* (gas phase).

Molecule	lone pair sigma/pi	E(S1), nm	Oscillator strength
DPO5	-	413	4.3
DPDC5	-	431	3.8
DPO5- NH <sub>2</sub>	sigma	418	4.5
DPO5- NH <sub>2</sub>	pi	442	4.5
DPDC5- NH <sub>2</sub>	sigma	437	3.9
DPDC5-NH <sub>2</sub>	pi	471	4.1
DPO5-SMe	sigma	432	4.7
DPO5-SMe	pi	451	4.6
DPDC5-SMe	sigma	446	4.2
DPDC5-SMe	pi	482	4.0
DPO5-NO <sub>2</sub>	sigma	-	-
DPO5-NO <sub>2</sub>	pi	-	-
DPDC5-NO <sub>2</sub>	sigma	436	4.0
DPDC5-NO <sub>2</sub>	pi	474	3.7
DPO5-NMe <sub>2</sub>	sigma	422	4.6
DPO5-NMe <sub>2</sub>	pi	463	4.5
DPDC5-NMe <sub>2</sub>	sigma	440	4.1
DPDC5-NMe <sub>2</sub>	pi	498	4.2

**Table A6.** TD-DFT calculations results on the energy and character of the energy of the first excited state, E(S1), of selected DPOs and DPDCs.

**A8. Comparison of DPDCn Band Gaps from Various Methods**

<b># of Double Bonds</b>	<b>UV-Vis Eg (eV)†</b>	<b>CV Eg (eV)</b>	<b>DFT (eV)</b>
3	3.01	2.62	3.14
5	2.44	2.20	2.60
7	2.15	1.99	2.24
9	2.02	1.88	2.03
11	1.81	1.77	1.86
13	1.77	1.71	1.75

**Table A7:** Bad Gap Estimations from various methods.



## A9. References

1. T. Cardineals, J. Ramaekers, P. Nockmann, K. Driesen, K. Van Hecke, L. Van Meervelt, S. Lei, S. de Feyter, D. Guillon, B. Donnio, K. Binnemanns, *Chem. Mater.*, **2008**, *20*, 1278–1291.
2. C. W. Spangler, R. K. McCoy, A. A. Dembek, L. S. Sapochak, B. D. Gates, *J. Chem. Soc., Perkin Trans. 1*, **1989**, *1*, 151–154.
3. X.-Y. Tang, M. Shi, *Tetrahedron*, **2009**, *65*, 8863–8868.
4. D. Soullez, G. Ple, L. Duhamel, *J. Chem. Soc., Perkin Trans. 1*, **1997**, *11*, 1639–1646.
5. G. V. Kryshnal, G. M. Zhdankina, N. V. Ignat'ev, M. Schulte, S. G. Zlotin, *Tetrahedron*, **2011**, *67*, 173–178.
6. **1d** has previously been characterized by mp and UV-vis: (a) J. F. Thomas, G. Branch, *J. Am. Chem. Soc.*, **1953**, *75*, 479034802; (b) R. Kuhn, K. Wallenfels, *Ber.*, **1937**, *70*, 1331; (c) C. Gansser, L. Zechmeister, *J. Am. Chem. Soc.*, **1957**, *79*, 3854–3858; (d) Mp, UV-vis and IR: A. Ishida, T. Mukaiyama, *Bull. Chem. Soc. Jap.* **1977**, *50*, 1161–1168; (e) <sup>1</sup>H and <sup>13</sup>C NMR in reference 3.
7. V. Cadierno, J. Francos, J. Gimeno, *Tetrahedron Lett.*, **2009**, *50*, 4773–4776.
8. M. S. Holzwarth, W. Frey, B. Plietker, *Chem. Comm.*, **2011**, *47*, 11113–11115.
9. M. E. Garst, L. J. Dolby, N. A. Fedoruk, *Process for preparing 4,4-dialkyl-6-halochromans or -thiochromans useful as pharmaceutical intermediates using regioselective electrophilic halogenation as key step*, May 30 1995, US 5420295.
10. C. W. Spangler, R. K. McCoy, *Syn. Comm.*, **1988**, *18*, 51–59.
11. P. Hrobárik, I. Sigmundová, P. Zahradník, P. Kasák, V. Arion, E. Franz, K. Clays, *J. Phys. Chem. C*, **2010**, *114*, 22289–22302.
12. H. Dong, M. Shen, J. E. Redford, B. J. Stokes, A. L. Pumphrey, T. G.; Driver, *Org. Lett.*, **2007**, *9*, 5191–5194.
13. L.-X. Shao, J. Li, B.-Y. Wang, M. Shi, *Euro. J. Org. Chem.*, **2010**, *33*, 6448–6453.
14. L. Huang, K. Cheng, B. Yao, J. Zhao, Y. Zhang, *Synth.*, **2009**, *20*, 3504–3510.
15. H. Fu, J. Park, D. Pei, *Biochemistry*. **2002**, *41*, 10700–10709.
16. I.-H. Kim, C. Morisseau, T. Watanabe, B. D. Hammock, *J. Med. Chem.*, **2004**, *47*, 2110–2122.

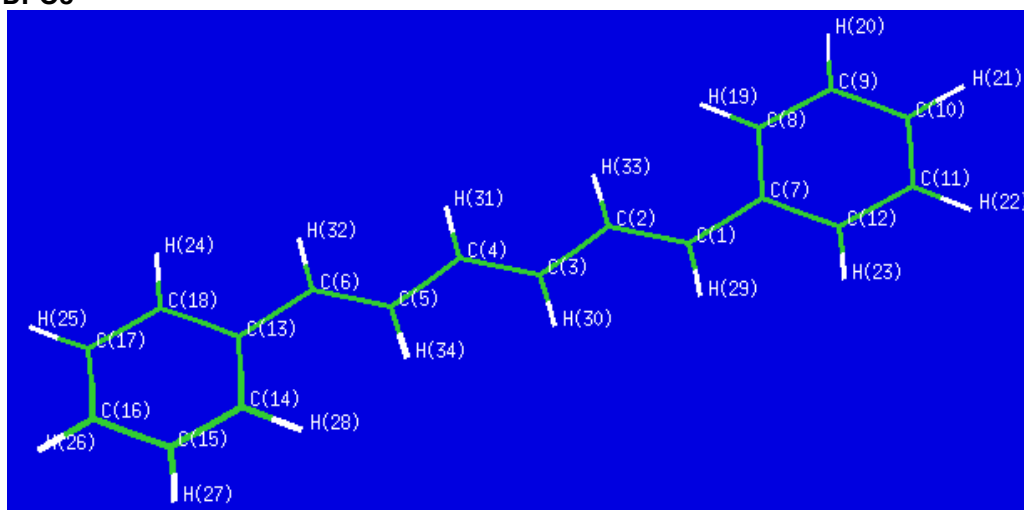
- 
17. G. Battistuzzi, S. Cacchi, G. Fabrizi, *Org. Lett.*, **2003**, *5*, 777–780.
18. N. T. Lucas, E. G. A. Notaras, M. P. Cifuentes, M. G. Humphrey, *Organometallics*, **2003**, *22*, 284–301.
19. (a) A. Dong, X. Ye, J. Chen, Y. Kang, T. Gordon, J. M. Kikkawa, C. B. Murray, *J. Am. Chem. Soc.*, **2011**, *133*, 998–1006. (b) J. Park, K. J. An, Y. S. Hwang, J. G. Park, H. J. Noh, J. Y. Kim, J. H. Park, N. M Hwang, T. Hyeon, *Nature Mater.*, **2004**, *3*, 891–895.

## Appendix A (Part 2)

### Density Functional Theory (DFT) Calculation Summary for DPDCn and DPOn

#### $\alpha,\omega$ -diphenyl-oligoene Series (DPOn):

##### DPO3



final geometry:

atom	x	y	z
C1	0.2639357739	-0.0045845578	-0.1806805468
C2	0.2807805026	-0.0019002222	1.1736092721
C3	1.4859075458	-0.0030603202	1.9566268003
C4	1.5181685464	-0.0001035078	3.3149372916
C5	2.7257553496	-0.0023191867	4.0940227597
C6	2.7510621393	0.0013705327	5.4479611439
C7	-0.9020386405	-0.0043846758	-1.0599649108
C8	-2.2319192227	-0.0016965938	-0.5920006510
C9	-3.2997549733	-0.0019110874	-1.4819850414
C10	-3.0750592389	-0.0047430685	-2.8618802365
C11	-1.7661961674	-0.0073228581	-3.3431798079
C12	-0.6962302123	-0.0071434489	-2.4529630024
C13	3.9253244806	-0.0013419265	6.3162972632
C14	5.2501270585	-0.0220463788	5.8346313761
C15	6.3274346958	-0.0234093366	6.7130483384
C16	6.1175451577	-0.0043629054	8.0951435668
C17	4.8138423461	0.0157874421	8.5900361479
C18	3.7343764119	0.0169534844	7.7112196326
H19	-2.4320654598	0.0005350516	0.4748481869
H20	-4.3164389799	0.0001402303	-1.0992188937
H21	-3.9129806966	-0.0049246081	-3.5527442902
H22	-1.5777007740	-0.0095027827	-4.4130677389
H23	0.3220220560	-0.0091726496	-2.8342280505
H24	2.7203423893	0.0326874053	8.1031689595

H25	4.6368098472	0.0304530146	9.6617738445
H26	6.9628209884	-0.0057327910	8.7770103887
H27	7.3398909800	-0.0399805421	6.3194891628
H28	5.4390349315	-0.0383040764	4.7658532635
H29	1.2252448105	-0.0073250412	-0.6936723388
H30	2.4300908700	-0.0068609272	1.4111814987
H31	0.5749260229	0.0039297217	3.8618834552
H32	1.7935082482	0.0080716467	5.9685092754
H33	-0.6556647085	0.0010842712	1.7290221234
H34	3.6594724525	-0.0067635386	3.5339054746

Final total energy: -695.549672

HOMO energy: -0.18543

LUMO energy: -0.06770

bond lengths (angstroms):

C1	-C2	:	1.354397	C1	-C7	:	1.460355
C1	-H29	:	1.089625	C2	-C3	:	1.437167
C2	-H33	:	1.088771	C3	-C4	:	1.358697
C3	-H30	:	1.090416	C4	-C5	:	1.437096
C4	-H31	:	1.090354	C5	-C6	:	1.354180
C5	-H34	:	1.088843	C6	-C13	:	1.460448
C6	-H32	:	1.089920	C7	-C8	:	1.409816
C7	-C12	:	1.408122	C8	-C9	:	1.390088
C8	-H19	:	1.085463	C9	-C10	:	1.398073
C9	-H20	:	1.086352	C10	-C11	:	1.394553
C10	-H21	:	1.086004	C11	-C12	:	1.391874
C11	-H22	:	1.086368	C12	-H23	:	1.087292
C13	-C14	:	1.409799	C13	-C18	:	1.408050
C14	-C15	:	1.390040	C14	-H28	:	1.085466
C15	-C16	:	1.398071	C15	-H27	:	1.086384
C16	-C17	:	1.394620	C16	-H26	:	1.086018
C17	-C18	:	1.391965	C17	-H25	:	1.086360
C18	-H24	:	1.087261				

bond angles:

C7	-C1	-C2	:	127.733172	H29	-C1	-C2	:	117.373669
H29	-C1	-C7	:	114.893158	C3	-C2	-C1	:	123.725750
H33	-C2	-C1	:	119.960065	H33	-C2	-C3	:	116.314184
C4	-C3	-C2	:	124.373676	H30	-C3	-C2	:	116.972059
H30	-C3	-C4	:	118.654263	C5	-C4	-C3	:	124.188644
H31	-C4	-C3	:	118.747289	H31	-C4	-C5	:	117.064064
C6	-C5	-C4	:	123.898774	H34	-C5	-C4	:	116.213026
H34	-C5	-C6	:	119.888193	C13	-C6	-C5	:	127.552151
H32	-C6	-C5	:	117.459115	H32	-C6	-C13	:	114.988708
C8	-C7	-C1	:	123.593104	C12	-C7	-C1	:	118.616229
C12	-C7	-C8	:	117.790667	C9	-C8	-C7	:	120.804331
H19	-C8	-C7	:	120.011776	H19	-C8	-C9	:	119.183894
C10	-C9	-C8	:	120.560756	H20	-C9	-C8	:	119.559915
H20	-C9	-C10	:	119.879329	C11	-C10	-C9	:	119.438386
H21	-C10	-C9	:	120.256840	H21	-C10	-C11	:	120.304774
C12	-C11	-C10	:	120.049653	H22	-C11	-C10	:	120.181742
H22	-C11	-C12	:	119.768605	C11	-C12	-C7	:	121.356206
H23	-C12	-C7	:	118.931935	H23	-C12	-C11	:	119.711859
C14	-C13	-C6	:	123.535731	C18	-C13	-C6	:	118.683018
C18	-C13	-C14	:	117.781244	C15	-C14	-C13	:	120.824052
H28	-C14	-C13	:	120.010880	H28	-C14	-C15	:	119.165033
C16	-C15	-C14	:	120.553983	H27	-C15	-C14	:	119.562054
H27	-C15	-C16	:	119.883955	C17	-C16	-C15	:	119.428754
H26	-C16	-C15	:	120.252998	H26	-C16	-C17	:	120.318242

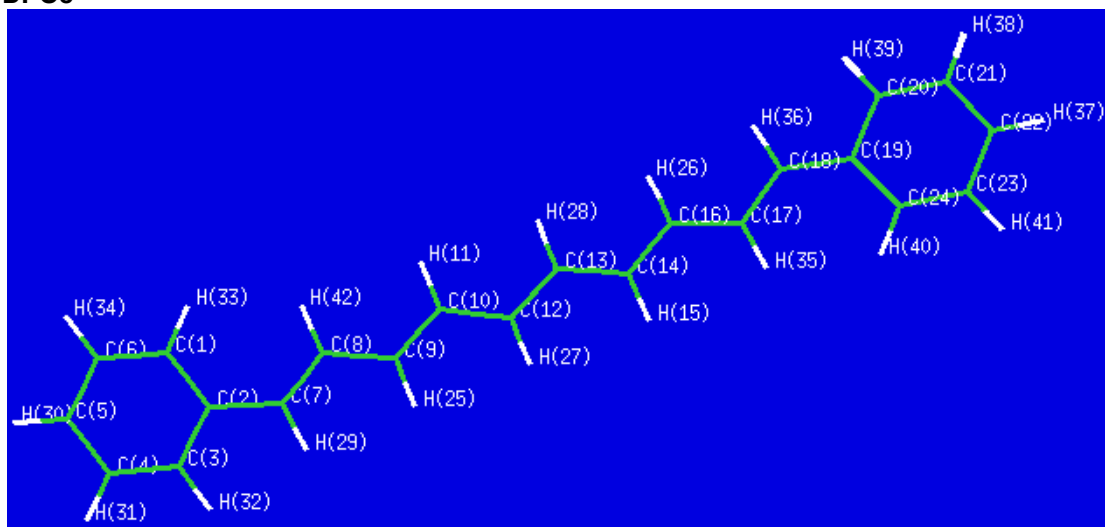
C18 -C17 -C16 : 120.060518 H25 -C17 -C16 : 120.173020  
 H25 -C17 -C18 : 119.766461 C17 -C18 -C13 : 121.351433  
 H24 -C18 -C13 : 118.933732 H24 -C18 -C17 : 119.714830

torsional angles:

C1 -C2 -C3 -C4 : 179.984705  
 C1 -C2 -C3 -H30 : -0.033129  
 C1 -C7 -C8 -C9 : -179.987721  
 C1 -C7 -C8 -H19 : 0.009784  
 C1 -C7 -C12 -C11 : 179.989576  
 C1 -C7 -C12 -H23 : -0.010047  
 C2 -C1 -C7 -C8 : -0.023714  
 C2 -C1 -C7 -C12 : 179.982498  
 C2 -C3 -C4 -C5 : 179.949833  
 C2 -C3 -C4 -H31 : -0.032006  
 C3 -C2 -C1 -C7 : 179.966372  
 C3 -C2 -C1 -H29 : -0.027938  
 C3 -C4 -C5 -C6 : 179.963304  
 C3 -C4 -C5 -H34 : -0.006437  
 C4 -C3 -C2 -H33 : -0.030365  
 C4 -C5 -C6 -C13 : 179.957084  
 C4 -C5 -C6 -H32 : -0.104545  
 C5 -C4 -C3 -H30 : -0.032055  
 C5 -C6 -C13 -C14 : -0.660280  
 C5 -C6 -C13 -C18 : 179.371863  
 C6 -C5 -C4 -H31 : -0.054576  
 C6 -C13 -C14 -C15 : 179.993369  
 C6 -C13 -C14 -H28 : -0.074970  
 C6 -C13 -C18 -C17 : -179.981163  
 C6 -C13 -C18 -H24 : -0.007252  
 C7 -C1 -C2 -H33 : -0.018036  
 C7 -C8 -C9 -C10 : -0.002898  
 C7 -C8 -C9 -H20 : 179.996933  
 C7 -C12 -C11 -C10 : -0.000229  
 C7 -C12 -C11 -H22 : -179.998727  
 C8 -C7 -C1 -H29 : 179.970717  
 C8 -C7 -C12 -C11 : -0.004574  
 C8 -C7 -C12 -H23 : 179.995802  
 C8 -C9 -C10 -C11 : -0.002057  
 C8 -C9 -C10 -H21 : 179.998351  
 C9 -C8 -C7 -C12 : 0.006114  
 C9 -C10 -C11 -C12 : 0.003601  
 C9 -C10 -C11 -H22 : -179.997907  
 C10 -C9 -C8 -H19 : 179.999576  
 C10 -C11 -C12 -H23 : 179.999391  
 C11 -C10 -C9 -H20 : 179.998114  
 C12 -C7 -C1 -H29 : -0.023071  
 C12 -C7 -C8 -H19 : -179.996380  
 C12 -C11 -C10 -H21 : -179.996807  
 C13 -C6 -C5 -H34 : -0.074228  
 C13 -C14 -C15 -C16 : 0.006762  
 C13 -C14 -C15 -H27 : 179.973441

C13	-C18	-C17	-C16	:	-0.027729
C13	-C18	-C17	-H25	:	179.982494
C14	-C13	-C6	-H32	:	179.400053
C14	-C13	-C18	-C17	:	0.049120
C14	-C13	-C18	-H24	:	-179.976968
C14	-C15	-C16	-C17	:	0.015867
C14	-C15	-C16	-H26	:	179.987082
C15	-C14	-C13	-C18	:	-0.038503
C15	-C16	-C17	-C18	:	-0.005519
C15	-C16	-C17	-H25	:	179.984216
C16	-C15	-C14	-H28	:	-179.925469
C16	-C17	-C18	-H24	:	179.998560
C17	-C16	-C15	-H27	:	-179.950705
C18	-C13	-C6	-H32	:	-0.567804
C18	-C13	-C14	-H28	:	179.893157
C18	-C17	-C16	-H26	:	-179.976714
H19	-C8	-C9	-H20	:	-0.000594
H20	-C9	-C10	-H21	:	-0.001478
H21	-C10	-C11	-H22	:	0.001685
H22	-C11	-C12	-H23	:	0.000894
H24	-C18	-C17	-H25	:	0.008784
H25	-C17	-C16	-H26	:	0.013020
H26	-C16	-C15	-H27	:	0.020509
H27	-C15	-C14	-H28	:	0.041210
H29	-C1	-C2	-H33	:	179.987653
H30	-C3	-C2	-H33	:	179.951802
H30	-C3	-C4	-H31	:	179.986106
H31	-C4	-C5	-H34	:	179.975683
H32	-C6	-C5	-H34	:	179.864144

## DPO5



final geometry:

atom	x	y	z	angstroms
C1	0.0163039242	0.1219747686	-0.0673436152	
C2	-0.0085225022	0.0327573420	1.3394044852	
C3	1.2281652926	0.0277622743	2.0151536824	
C4	2.4340563544	0.1067926781	1.3260253541	
C5	2.4386373964	0.1949561000	-0.0664502972	
C6	1.2221635666	0.2016768150	-0.7560710395	
C7	-1.2273925745	-0.0458213317	2.1394122170	
C8	-2.5220745548	-0.0755638252	1.7330084304	
C9	-3.6172353688	-0.1302657674	2.6633129539	
C10	-4.9394996950	-0.1484464518	2.3406592999	
H11	-5.2259598542	-0.1329738331	1.2888015646	
C12	-5.9969997976	-0.1691722514	3.3089618126	
C13	-7.3236911053	-0.1670426561	3.0018602554	
C14	-8.3990347696	-0.1501244239	3.9509391929	
H15	-8.1404595019	-0.1449038033	5.0098093437	
C16	-9.7086465941	-0.1271896249	3.5811443959	
C17	-10.8526826619	-0.0752358489	4.4519640030	
C18	-12.1171930038	-0.0409162234	3.9599415262	
C19	-13.3925375702	0.0365112569	4.6655798476	
C20	-14.5725403118	0.0353519105	3.8947235862	
C21	-15.8284975173	0.1147893073	4.4872461346	
C22	-15.9409912943	0.1990059155	5.8753939020	
C23	-14.7823096266	0.2020903106	6.6579105658	
C24	-13.5264523406	0.1217647553	6.0657110556	
H25	-3.3502400723	-0.1490357981	3.7208598062	
H26	-9.9307884880	-0.1366332309	2.5131983006	
H27	-5.7048785956	-0.1761414153	4.3596010925	
H28	-7.6070501723	-0.1637118598	1.9485975437	
H29	-1.0553408716	-0.0805637198	3.2153609162	
H30	3.3766516813	0.2581255376	-0.6098741162	
H31	3.3705438937	0.1005141580	1.8766062495	
H32	1.2329036894	-0.0391237539	3.1002994805	



H33	-0.9152428914	0.1314672898	-0.6252853745
H34	1.2153398055	0.2707070232	-1.8402835395
H35	-10.6703758260	-0.0570809794	5.5257378770
H36	-12.2148203007	-0.0684199026	2.8744718254
H37	-16.9183749240	0.2626086644	6.3443190664
H38	-16.7191992849	0.1120465674	3.8652480157
H39	-14.4921871411	-0.0281680882	2.8123028671
H40	-12.6406998495	0.1294266602	6.6937112609
H41	-14.8602594194	0.2690742759	7.7394202869
H42	-2.7681299376	-0.0480118771	0.6721011399

Final total energy..... -850.37013

HOMO energy: -0.17577

LUMO energy: -0.07707

bond lengths (angstroms):

C1	-C2	:	1.409793	C1	-C6	:	1.390969
C1	-H33	:	1.085895	C2	-C3	:	1.409276
C2	-C7	:	1.460079	C3	-C4	:	1.391157
C3	-H32	:	1.087216	C4	-C5	:	1.395271
C4	-H31	:	1.086364	C5	-C6	:	1.398367
C5	-H30	:	1.085896	C6	-H34	:	1.086429
C7	-C8	:	1.357295	C7	-H29	:	1.090172
C8	-C9	:	1.437997	C8	-H42	:	1.089416
C9	-C10	:	1.361183	C9	-H25	:	1.090891
C10	-H11	:	1.090277	C10	-C12	:	1.433996
C12	-C13	:	1.361773	C12	-H27	:	1.090517
C13	-C14	:	1.434364	C13	-H28	:	1.090718
C14	-H15	:	1.089997	C14	-C16	:	1.361013
C16	-C17	:	1.438695	C16	-H26	:	1.090846
C17	-C18	:	1.357295	C17	-H35	:	1.089291
C18	-C19	:	1.459597	C18	-H36	:	1.090198
C19	-C20	:	1.409478	C19	-C24	:	1.409102
C20	-C21	:	1.390979	C20	-H39	:	1.087256
C21	-C22	:	1.395242	C21	-H38	:	1.086388
C22	-C23	:	1.398172	C22	-H37	:	1.085917
C23	-C24	:	1.390802	C23	-H41	:	1.086382
C24	-H40	:	1.085818				

bond angles:

C6	-C1	-C2	:	120.861549	H33	-C1	-C2	:	119.877325
H33	-C1	-C6	:	119.260952	C3	-C2	-C1	:	117.596138
C7	-C2	-C1	:	124.391456	C7	-C2	-C3	:	118.011177
C4	-C3	-C2	:	121.529732	H32	-C3	-C2	:	118.857363
H32	-C3	-C4	:	119.612898	C5	-C4	-C3	:	120.053380
H31	-C4	-C3	:	119.726044	H31	-C4	-C5	:	120.220549
C6	-C5	-C4	:	119.315660	H30	-C5	-C4	:	120.394253
H30	-C5	-C6	:	120.290083	C5	-C6	-C1	:	120.643514
H34	-C6	-C1	:	119.493678	H34	-C6	-C5	:	119.862781
C8	-C7	-C2	:	129.301951	H29	-C7	-C2	:	114.251271
H29	-C7	-C8	:	116.446206	C9	-C8	-C7	:	122.247604
H42	-C8	-C7	:	120.429185	H42	-C8	-C9	:	117.320335
C10	-C9	-C8	:	125.942238	H25	-C9	-C8	:	116.194906
H25	-C9	-C10	:	117.860197	H11	-C10	-C9	:	118.928998
C12	-C10	-C9	:	123.813927	C12	-C10	-H11	:	117.251696
C13	-C12	-C10	:	124.482180	H27	-C12	-C10	:	116.943021
H27	-C12	-C13	:	118.571345	C14	-C13	-C12	:	125.534122
H28	-C13	-C12	:	118.091119	H28	-C13	-C14	:	116.368879
H15	-C14	-C13	:	117.709251	C16	-C14	-C13	:	122.806618
C16	-C14	-H15	:	119.480800	C17	-C16	-C14	:	126.963589
H26	-C16	-C14	:	117.503747	H26	-C16	-C17	:	115.528263

C18	-C17	-C16	: 121.488463	H35	-C17	-C16	: 117.657055
H35	-C17	-C18	: 120.853091	C19	-C18	-C17	: 129.801114
H36	-C18	-C17	: 116.341500	H36	-C18	-C19	: 113.856231
C20	-C19	-C18	: 117.843819	C24	-C19	-C18	: 124.514697
C24	-C19	-C20	: 117.639972	C21	-C20	-C19	: 121.527589
H39	-C20	-C19	: 118.858795	H39	-C20	-C21	: 119.613578
C22	-C21	-C20	: 120.003746	H38	-C21	-C20	: 119.752780
H38	-C21	-C22	: 120.243440	C23	-C22	-C21	: 119.349930
H37	-C22	-C21	: 120.379968	H37	-C22	-C23	: 120.270072
C24	-C23	-C22	: 120.655236	H41	-C23	-C22	: 119.856907
H41	-C23	-C24	: 119.487810	C23	-C24	-C19	: 120.823507
H40	-C24	-C19	: 119.840416	H40	-C24	-C23	: 119.335561

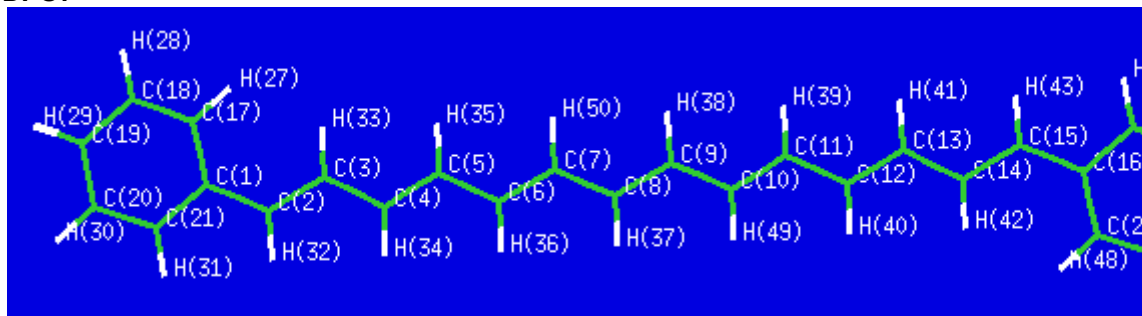
torsional angles:

C1	-C2	-C3	-C4	: -0.042043
C1	-C2	-C3	-H32	: 179.927330
C1	-C2	-C7	-C8	: 1.384365
C1	-C2	-C7	-H29	: -178.327221
C1	-C6	-C5	-C4	: 0.018483
C1	-C6	-C5	-H30	: -179.958080
C2	-C1	-C6	-C5	: 0.002891
C2	-C1	-C6	-H34	: -179.936435
C2	-C3	-C4	-C5	: 0.064369
C2	-C3	-C4	-H31	: -179.995337
C2	-C7	-C8	-C9	: -178.826512
C2	-C7	-C8	-H42	: 0.539868
C3	-C2	-C1	-C6	: 0.008349
C3	-C2	-C1	-H33	: -179.838947
C3	-C2	-C7	-C8	: -179.029471
C3	-C2	-C7	-H29	: 1.258943
C3	-C4	-C5	-C6	: -0.051498
C3	-C4	-C5	-H30	: 179.925040
C4	-C3	-C2	-C7	: -179.656709
C4	-C5	-C6	-H34	: 179.957586
C5	-C4	-C3	-H32	: -179.904777
C5	-C6	-C1	-H33	: 179.851117
C6	-C1	-C2	-C7	: 179.596091
C6	-C5	-C4	-H31	: -179.991494
C7	-C2	-C1	-H33	: -0.251206
C7	-C2	-C3	-H32	: 0.312664
C7	-C8	-C9	-C10	: 179.255058
C7	-C8	-C9	-H25	: -0.135986
C8	-C9	-C10	-H11	: 0.785725
C8	-C9	-C10	-C12	: -178.346206
C9	-C8	-C7	-H29	: 0.879791
C9	-C10	-C12	-C13	: 178.955998
C9	-C10	-C12	-H27	: -0.356292
C10	-C9	-C8	-H42	: -0.130006
C10	-C12	-C13	-C14	: -178.167295
C10	-C12	-C13	-H28	: 0.915711
H11	-C10	-C9	-H25	: -179.832328
H11	-C10	-C12	-C13	: -0.189394

H11	-C10	-C12	-H27	:-179.501683
C12	-C10	-C9	-H25	: 1.035741
C12	-C13	-C14	-H15	: -0.417548
C12	-C13	-C14	-C16	: 178.914270
C13	-C14	-C16	-C17	:-178.318199
C13	-C14	-C16	-H26	: 0.880440
C14	-C13	-C12	-H27	: 1.134629
C14	-C16	-C17	-C18	: 179.219199
C14	-C16	-C17	-H35	: -0.355131
H15	-C14	-C13	-H28	:-179.514631
H15	-C14	-C16	-C17	: 1.002260
H15	-C14	-C16	-H26	:-179.799101
C16	-C14	-C13	-H28	: -0.182814
C16	-C17	-C18	-C19	:-178.788659
C16	-C17	-C18	-H36	: 0.792026
C17	-C18	-C19	-C20	:-178.986299
C17	-C18	-C19	-C24	: 1.472817
C18	-C17	-C16	-H26	: 0.006890
C18	-C19	-C20	-C21	:-179.593741
C18	-C19	-C20	-H39	: 0.334465
C18	-C19	-C24	-C23	: 179.518797
C18	-C19	-C24	-H40	: -0.218031
C19	-C18	-C17	-H35	: 0.772156
C19	-C20	-C21	-C22	: 0.041580
C19	-C20	-C21	-H38	: 179.974324
C19	-C24	-C23	-C22	: 0.046119
C19	-C24	-C23	-H41	:-179.874742
C20	-C19	-C18	-H36	: 1.424581
C20	-C19	-C24	-C23	: -0.022945
C20	-C19	-C24	-H40	:-179.759773
C20	-C21	-C22	-C23	: -0.018287
C20	-C21	-C22	-H37	: 179.918673
C21	-C20	-C19	-C24	: -0.020777
C21	-C22	-C23	-C24	: -0.025087
C21	-C22	-C23	-H41	: 179.895483
C22	-C21	-C20	-H39	:-179.886095
C22	-C23	-C24	-H40	: 179.784260
C23	-C22	-C21	-H38	:-179.950698
C24	-C19	-C18	-H36	:-178.116302
C24	-C19	-C20	-H39	: 179.907429
C24	-C23	-C22	-H37	:-179.962118
H25	-C9	-C8	-H42	:-179.521051
H26	-C16	-C17	-H35	:-179.567440
H27	-C12	-C13	-H28	:-179.782365
H29	-C7	-C8	-H42	:-179.753829
H30	-C5	-C4	-H31	: -0.014956
H30	-C5	-C6	-H34	: -0.018977
H31	-C4	-C3	-H32	: 0.035517
H33	-C1	-C6	-H34	: -0.088209
H35	-C17	-C18	-H36	:-179.647159
H37	-C22	-C21	-H38	: -0.013738
H37	-C22	-C23	-H41	: -0.041548
H38	-C21	-C20	-H39	: 0.046650

H40 -C24 -C23 -H41 : -0.136601

## DPO7



final geometry:

atom	angstroms			z
	x	y		
C1	-0.0704590910	0.1452901882		-0.0068445096
C2	-0.0892360394	0.0524084180		1.4492038362
C3	0.9726244166	-0.0225477331		2.2885196922
C4	0.8602944166	-0.0937659836		3.7166856229
C5	1.9252863220	-0.1463176660		4.5637558553
C6	1.8300036493	-0.1894787560		5.9900293113
C7	2.9067206997	-0.2089696859		6.8268423335
C8	2.8276132845	-0.2178701129		8.2531535101
C9	3.9121344308	-0.2003639910		9.0806793071
C10	3.8412435818	-0.1739951647		10.5070598868
C11	4.9263876852	-0.1204794662		11.3313665480
C12	4.8508813506	-0.0625892426		12.7583596638
C13	5.9278430399	0.0206982727		13.5878215699
C14	5.8353556035	0.1021121246		15.0172338255
C15	6.9060927478	0.2035869671		15.8417952335
C16	6.9012486201	0.3046939259		17.2973523779
C17	1.1131410930	0.1743027414		-0.7720322386
C18	1.0651330732	0.2682554979		-2.1582450492
C19	-0.1630392986	0.3362684977		-2.8232956090
C20	-1.3443851323	0.3089168549		-2.0818377362
C21	-1.2969321458	0.2146166759		-0.6946507366
C22	8.1337202332	0.3976194058		17.9717583160
C23	8.1957196138	0.4989194523		19.3575082667
C24	7.0222388935	0.5099841926		20.1107632407
C25	5.7872756478	0.4196819675		19.4613401753
C26	5.7252257297	0.3185742349		18.0759903726
H27	2.0786210173	0.1239717704		-0.2785946417
H28	1.9908676914	0.2892964054		-2.7265554132
H29	-0.1952943621	0.4100105104		-3.9064239371
H30	-2.3057517234	0.3615339151		-2.5848699724
H31	-2.2218953510	0.1940330402		-0.1237467205
H32	-1.0831837221	0.0489699528		1.8958001695
H33	1.9839685905	-0.0223917760		1.8852256990
H34	-0.1459519923	-0.0950986165		4.1366108218
H35	2.9290729432	-0.1426260725		4.1375530824
H36	0.8290978641	-0.1937703304		6.4226831890
H37	1.8317013482	-0.2250794616		8.6971129127
H38	4.9063745490	-0.1903081841		8.6328491185
H39	5.9201447670	-0.1074128043		10.8825625750

H40	3.8552962962	-0.0759690220	13.2031552485
H41	6.9256198423	0.0366533704	13.1484549316
H42	4.8305994290	0.0850378659	15.4364582022
H43	7.8941974253	0.2163005801	15.3819652360
H44	9.0526769862	0.3891352889	17.3915167921
H45	9.1614014057	0.5694874335	19.8500324212
H46	7.0653367351	0.5887023764	21.1930172657
H47	4.8684099006	0.4291422614	20.0412425083
H48	4.7546497406	0.2508291931	17.5940957588
H49	2.8479033937	-0.1842303044	10.9563047251
H50	3.9047514114	-0.2020405922	6.3878273811

Final total energy: -1005.193166 hartrees

HOMO energy: -0.17018

LUMO energy: -0.08455

bond lengths (angstroms):

C1	-C2	:	1.459129	C1	-C17	:	1.409703
C1	-C21	:	1.407878	C2	-C3	:	1.355587
C2	-H32	:	1.089675	C3	-C4	:	1.434346
C3	-H33	:	1.088790	C4	-C5	:	1.361799
C4	-H34	:	1.090354	C5	-C6	:	1.430104
C5	-H35	:	1.090527	C6	-C7	:	1.363802
C6	-H36	:	1.090422	C7	-C8	:	1.428531
C7	-H50	:	1.090343	C8	-C9	:	1.364292
C8	-H37	:	1.090409	C9	-C10	:	1.428385
C9	-H38	:	1.090489	C10	-C11	:	1.363775
C10	-H49	:	1.090252	C11	-C12	:	1.430161
C11	-H39	:	1.090481	C12	-C13	:	1.361907
C12	-H40	:	1.090510	C13	-C14	:	1.434713
C13	-H41	:	1.090347	C14	-C15	:	1.355240
C14	-H42	:	1.088841	C15	-C16	:	1.459073
C15	-H43	:	1.089934	C16	-C22	:	1.407993
C16	-C26	:	1.410496	C17	-C18	:	1.390222
C17	-H27	:	1.085433	C18	-C19	:	1.398329
C18	-H28	:	1.086464	C19	-C20	:	1.395022
C19	-H29	:	1.086115	C20	-C21	:	1.391198
C20	-H30	:	1.086294	C21	-H31	:	1.087158
C22	-C23	:	1.390830	C22	-H44	:	1.086846
C23	-C24	:	1.394479	C23	-H45	:	1.086325
C24	-C25	:	1.398227	C24	-H46	:	1.085969
C25	-C26	:	1.390420	C25	-H47	:	1.086596
C26	-H48	:	1.085739				

bond angles:

C17	-C1	-C2	:	123.625992	C21	-C1	-C2	:	118.648433
C21	-C1	-C17	:	117.725246	C3	-C2	-C1	:	127.682502
H32	-C2	-C1	:	114.892513	H32	-C2	-C3	:	117.424316
C4	-C3	-C2	:	123.909682	H33	-C3	-C2	:	119.884814
H33	-C3	-C4	:	116.203516	C5	-C4	-C3	:	124.056714
H34	-C4	-C3	:	117.116573	H34	-C4	-C5	:	118.823767
C6	-C5	-C4	:	124.709534	H35	-C5	-C4	:	118.464370
H35	-C5	-C6	:	116.821013	C7	-C6	-C5	:	124.040232
H36	-C6	-C5	:	117.193006	H36	-C6	-C7	:	118.761886
C8	-C7	-C6	:	124.680817	H50	-C7	-C6	:	118.392532
H50	-C7	-C8	:	116.919724	C9	-C8	-C7	:	124.160806
H37	-C8	-C7	:	117.202421	H37	-C8	-C9	:	118.630998
C10	-C9	-C8	:	124.506108	H38	-C9	-C8	:	118.411028
H38	-C9	-C10	:	117.076025	C11	-C10	-C9	:	124.389526
H49	-C10	-C9	:	117.162961	H49	-C10	-C11	:	118.442201



C12	-C11	-C10	: 124.240666	H39	-C11	-C10	: 118.478086
H39	-C11	-C12	: 117.276246	C13	-C12	-C11	: 124.640204
H40	-C12	-C11	: 117.044239	H40	-C12	-C13	: 118.312155
C14	-C13	-C12	: 124.006574	H41	-C13	-C12	: 118.627448
H41	-C13	-C14	: 117.363388	C15	-C14	-C13	: 124.020823
H42	-C14	-C13	: 116.243841	H42	-C14	-C15	: 119.734270
C16	-C15	-C14	: 127.555096	H43	-C15	-C14	: 117.415769
H43	-C15	-C16	: 115.028750	C22	-C16	-C15	: 118.652558
C26	-C16	-C15	: 123.652274	C26	-C16	-C22	: 117.694949
C18	-C17	-C1	: 120.906063	H27	-C17	-C1	: 119.941222
H27	-C17	-C18	: 119.152686	C19	-C18	-C17	: 120.520693
H28	-C18	-C17	: 119.568177	H28	-C18	-C19	: 119.911123
C20	-C19	-C18	: 119.343479	H29	-C19	-C18	: 120.243905
H29	-C19	-C20	: 120.412612	C21	-C20	-C19	: 120.159865
H30	-C20	-C19	: 120.156760	H30	-C20	-C21	: 119.683371
C20	-C21	-C1	: 121.344651	H31	-C21	-C1	: 118.927337
H31	-C21	-C20	: 119.728005	C23	-C22	-C16	: 121.403476
H44	-C22	-C16	: 118.939703	H44	-C22	-C23	: 119.656817
C24	-C23	-C22	: 120.083503	H45	-C23	-C22	: 119.741503
H45	-C23	-C24	: 120.174993	C25	-C24	-C23	: 119.462814
H46	-C24	-C23	: 120.364567	H46	-C24	-C25	: 120.172607
C26	-C25	-C24	: 120.456261	H47	-C25	-C24	: 119.897952
H47	-C25	-C26	: 119.645771	C25	-C26	-C16	: 120.898962
H48	-C26	-C16	: 119.980228	H48	-C26	-C25	: 119.120777

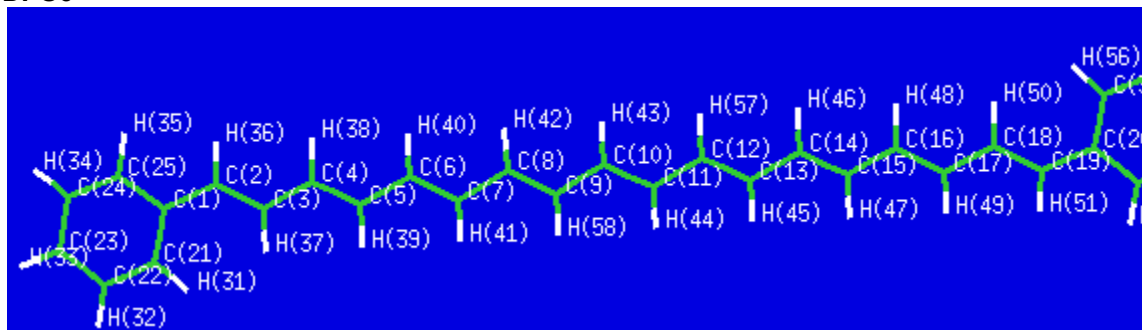
torsional angles:

C1	-C2	-C3	-C4	: 179.135057
C1	-C2	-C3	-H33	: -0.332030
C1	-C17	-C18	-C19	: 0.008663
C1	-C17	-C18	-H28	: 179.977364
C1	-C21	-C20	-C19	: 0.019513
C1	-C21	-C20	-H30	: -179.957195
C2	-C1	-C17	-C18	: -179.788420
C2	-C1	-C17	-H27	: 0.149586
C2	-C1	-C21	-C20	: 179.785178
C2	-C1	-C21	-H31	: -0.184464
C2	-C3	-C4	-C5	: -178.839000
C2	-C3	-C4	-H34	: 0.527756
C3	-C2	-C1	-C17	: -0.177000
C3	-C2	-C1	-C21	: -179.963552
C3	-C4	-C5	-C6	: 178.631355
C3	-C4	-C5	-H35	: -0.520531
C4	-C3	-C2	-H32	: -0.550441
C4	-C5	-C6	-C7	: -178.327235
C4	-C5	-C6	-H36	: 0.857520
C5	-C4	-C3	-H33	: 0.646026
C5	-C6	-C7	-C8	: 178.333526
C5	-C6	-C7	-H50	: -0.677341
C6	-C5	-C4	-H34	: -0.725300
C6	-C7	-C8	-C9	: -178.120372
C6	-C7	-C8	-H37	: 0.991238
C7	-C6	-C5	-H35	: 0.837298

C7	-C8	-C9	-C10	: 178.291347
C7	-C8	-C9	-H38	: -0.727429
C8	-C7	-C6	-H36	: -0.839283
C8	-C9	-C10	-C11	: -178.163739
C8	-C9	-C10	-H49	: 0.982483
C9	-C8	-C7	-H50	: 0.903732
C9	-C10	-C11	-C12	: 178.466427
C9	-C10	-C11	-H39	: -0.696244
C10	-C9	-C8	-H37	: -0.808447
C10	-C11	-C12	-C13	: -178.482504
C10	-C11	-C12	-H40	: 0.833080
C11	-C10	-C9	-H38	: 0.866992
C11	-C12	-C13	-C14	: 178.837662
C11	-C12	-C13	-H41	: -0.560410
C12	-C11	-C10	-H49	: -0.669682
C12	-C13	-C14	-C15	: -179.049518
C12	-C13	-C14	-H42	: 0.572779
C13	-C12	-C11	-H39	: 0.689408
C13	-C14	-C15	-C16	: 179.314902
C13	-C14	-C15	-H43	: -0.446966
C14	-C13	-C12	-H40	: -0.469930
C14	-C15	-C16	-C22	: 179.780095
C14	-C15	-C16	-C26	: -0.394369
C15	-C14	-C13	-H41	: 0.355573
C15	-C16	-C22	-C23	: 179.877009
C15	-C16	-C22	-H44	: -0.144260
C15	-C16	-C26	-C25	: -179.875822
C15	-C16	-C26	-H48	: 0.058368
C16	-C15	-C14	-H42	: -0.294961
C16	-C22	-C23	-C24	: 0.009294
C16	-C22	-C23	-H45	: -179.980411
C16	-C26	-C25	-C24	: 0.006431
C16	-C26	-C25	-H47	: 179.960809
C17	-C1	-C2	-H32	: 179.515252
C17	-C1	-C21	-C20	: -0.014038
C17	-C1	-C21	-H31	: -179.983680
C17	-C18	-C19	-C20	: -0.003393
C17	-C18	-C19	-H29	: 179.973725
C18	-C17	-C1	-C21	: -0.000033
C18	-C19	-C20	-C21	: -0.010522
C18	-C19	-C20	-H30	: 179.966075
C19	-C18	-C17	-H27	: -179.929825
C19	-C20	-C21	-H31	: 179.988916
C20	-C19	-C18	-H28	: -179.971987
C21	-C1	-C2	-H32	: -0.271300
C21	-C1	-C17	-H27	: 179.937973
C21	-C20	-C19	-H29	: -179.987601
C22	-C16	-C15	-H43	: -0.453200
C22	-C16	-C26	-C25	: -0.048731
C22	-C16	-C26	-H48	: 179.885459
C22	-C23	-C24	-C25	: -0.052735
C22	-C23	-C24	-H46	: 179.987692
C23	-C22	-C16	-C26	: 0.041026

C23	-C24	-C25	-C26	:	0.045048
C23	-C24	-C25	-H47	:	-179.909214
C24	-C23	-C22	-H44	:	-179.969287
C24	-C25	-C26	-H48	:	-179.928316
C25	-C24	-C23	-H45	:	179.936925
C26	-C16	-C15	-H43	:	179.372337
C26	-C16	-C22	-H44	:	-179.980243
C26	-C25	-C24	-H46	:	-179.995300
H27	-C17	-C18	-H28	:	0.038876
H28	-C18	-C19	-H29	:	0.005131
H29	-C19	-C20	-H30	:	-0.011003
H30	-C20	-C21	-H31	:	0.012207
H32	-C2	-C3	-H33	:	179.982472
H33	-C3	-C4	-H34	:	-179.987218
H34	-C4	-C5	-H35	:	-179.877186
H35	-C5	-C6	-H36	:	-179.977947
H36	-C6	-C7	-H50	:	-179.850150
H37	-C8	-C7	-H50	:	-179.984658
H37	-C8	-C9	-H38	:	-179.827224
H38	-C9	-C10	-H49	:	-179.986786
H39	-C11	-C10	-H49	:	-179.832354
H39	-C11	-C12	-H40	:	-179.995009
H40	-C12	-C13	-H41	:	-179.868002
H41	-C13	-C14	-H42	:	179.977870
H42	-C14	-C15	-H43	:	179.943171
H44	-C22	-C23	-H45	:	0.041008
H45	-C23	-C24	-H46	:	-0.022648
H46	-C24	-C25	-H47	:	0.050437
H47	-C25	-C26	-H48	:	0.026061

## DPO9



final geometry:

atom	angstroms		
	x	y	z
C1	-0.0011750393	-0.0296692541	-0.0023206387
C2	0.0195664490	-0.0076153987	1.4567000657
C3	1.1027336347	0.0159595469	2.2730233735
C4	1.0160377858	0.0447841354	3.7043307128
C5	2.0875533231	0.0637296577	4.5460251669
C6	1.9839581628	0.1000069001	5.9717434570
C7	3.0443129384	0.1140803612	6.8307609130
C8	2.9195726497	0.1559833125	8.2530619674
C9	3.9689814355	0.1637529965	9.1266730763
C10	3.8312883212	0.2092779491	10.5470242125
C11	4.8775018859	0.2106306659	11.4251161593
C12	4.7431798391	0.2581776619	12.8456397580
C13	5.7966360309	0.2542486184	13.7143570917
C14	5.6820929427	0.3030232019	15.1372055210
C15	6.7498657140	0.2955521292	15.9869917755
C16	6.6629583190	0.3459898471	17.4133389085
C17	7.7459833659	0.3375158701	18.2402660329
C18	7.6852303851	0.3911052724	19.6722526655
C19	8.7856016795	0.3820168689	20.4654789955
C20	8.8449450110	0.4370829410	21.9221958955
C21	1.1606889238	0.0153446751	-0.7997591468
C22	1.0748722891	-0.0054195780	-2.1868371762
C23	-0.1694653403	-0.0718408047	-2.8205675042
C24	-1.3302062220	-0.1170374911	-2.0484056260
C25	-1.2452854713	-0.0952974338	-0.6596295597
C26	10.1074355381	0.4003970213	22.5459952585
C27	10.2326100497	0.4517765437	23.9307906359
C28	9.0946141171	0.5419913327	24.7322425282
C29	7.8324737175	0.5796369416	24.1322804725
C30	7.7065117002	0.5281380950	22.7489197749
H31	2.1382126179	0.0715230848	-0.3306459522
H32	1.9838345440	0.0323427065	-2.7807166342
H33	-0.2308579302	-0.0872377588	-3.9047246236
H34	-2.3032879906	-0.1682560012	-2.5285775110
H35	-2.1537591931	-0.1299175866	-0.0634487534
H36	-0.9624751341	-0.0120717812	1.9297099499
H37	2.1046890279	0.0134694675	1.8474055483
H38	0.0154946650	0.0540807689	4.1377073211

H39	3.0904153233	0.0519233639	4.1182122398
H40	0.9780435557	0.1189308158	6.3923301678
H41	4.0530504970	0.0923674841	6.4174163589
H42	1.9079934674	0.1841794662	8.6593154381
H43	2.8175066888	0.2454256687	10.9469069829
H44	5.8910251442	0.1723372327	11.0245741367
H45	6.8052202881	0.2105544857	13.3019565759
H46	4.6775602453	0.3496340646	15.5584686875
H47	7.7506343368	0.2480879434	15.5563949927
H48	5.6666555644	0.3955301950	17.8534004164
H49	8.7386655165	0.2876202016	17.7917464623
H50	6.6927456697	0.4422972102	20.1166960844
H51	9.7550670049	0.3272684696	19.9709017445
H52	10.9980788616	0.3309534206	21.9263566110
H53	11.2190809096	0.4221132459	24.3847567754
H54	9.1872338780	0.5827731353	25.8135018469
H55	6.9414140229	0.6511476902	24.7496309660
H56	6.7160463692	0.5611198927	22.3054104158
H57	3.7320255105	0.3004031460	13.2513194011
H58	4.9822098553	0.1329330755	8.7249613190

Final total energy: -1160.015207 hartrees

HOMO energy: -0.16589

LUMO energy: -0.08866

bond lengths (angstroms):

C1	-C2	:	1.459335	C1	-C21	:	1.409916
C1	-C25	:	1.408607	C2	-C3	:	1.356536
C2	-H36	:	1.090029	C3	-C4	:	1.434220
C3	-H37	:	1.088610	C4	-C5	:	1.362701
C4	-H38	:	1.090407	C5	-C6	:	1.429937
C5	-H39	:	1.090365	C6	-C7	:	1.364720
C6	-H40	:	1.090466	C7	-C8	:	1.428375
C7	-H41	:	1.090356	C8	-C9	:	1.365473
C8	-H42	:	1.090472	C9	-C10	:	1.427736
C9	-H58	:	1.090392	C10	-C11	:	1.365873
C10	-H43	:	1.090397	C11	-C12	:	1.427652
C11	-H44	:	1.090472	C12	-C13	:	1.365451
C12	-H57	:	1.090317	C13	-C14	:	1.428285
C13	-H45	:	1.090516	C14	-C15	:	1.364673
C14	-H46	:	1.090285	C15	-C16	:	1.429882
C15	-H47	:	1.090506	C16	-C17	:	1.362653
C16	-H48	:	1.090288	C17	-C18	:	1.434276
C17	-H49	:	1.090448	C18	-C19	:	1.356506
C18	-H50	:	1.088658	C19	-C20	:	1.458965
C19	-H51	:	1.089710	C20	-C26	:	1.408671
C20	-C30	:	1.409891	C21	-C22	:	1.389885
C21	-H31	:	1.085714	C22	-C23	:	1.397999
C22	-H32	:	1.086430	C23	-C24	:	1.394846
C23	-H33	:	1.086003	C24	-C25	:	1.391540
C24	-H34	:	1.086313	C25	-H35	:	1.087177
C26	-C27	:	1.391390	C26	-H52	:	1.087207
C27	-C28	:	1.394811	C27	-H53	:	1.086319
C28	-C29	:	1.397988	C28	-H54	:	1.085985
C29	-C30	:	1.390038	C29	-H55	:	1.086381
C30	-H56	:	1.085730				

bond angles:

C21	-C1	-C2	:	123.592079	C25	-C1	-C2	:	118.671982
C25	-C1	-C21	:	117.735644	C3	-C2	-C1	:	127.825035
H36	-C2	-C1	:	114.896618	H36	-C2	-C3	:	117.278311
C4	-C3	-C2	:	123.547688	H37	-C3	-C2	:	119.973812
H37	-C3	-C4	:	116.478500	C5	-C4	-C3	:	124.691659
H38	-C4	-C3	:	116.889749	H38	-C4	-C5	:	118.418458
C6	-C5	-C4	:	124.002562	H39	-C5	-C4	:	118.732312
H39	-C5	-C6	:	117.265089	C7	-C6	-C5	:	124.859112
H40	-C6	-C5	:	116.860955	H40	-C6	-C7	:	118.279879
C8	-C7	-C6	:	124.001742	H41	-C7	-C6	:	118.684918
H41	-C7	-C8	:	117.313340	C9	-C8	-C7	:	124.758368
H42	-C8	-C7	:	116.919266	H42	-C8	-C9	:	118.322355
C10	-C9	-C8	:	124.231674	H58	-C9	-C8	:	118.573143

H58	-C9	-C10	: 117.195175	C11	-C10	-C9	: 124.451947
H43	-C10	-C9	: 117.100763	H43	-C10	-C11	: 118.447289
C12	-C11	-C10	: 124.585522	H44	-C11	-C10	: 118.407881
H44	-C11	-C12	: 117.006587	C13	-C12	-C11	: 124.080167
H57	-C12	-C11	: 117.307225	H57	-C12	-C13	: 118.612604
C14	-C13	-C12	: 124.877320	H45	-C13	-C12	: 118.233263
H45	-C13	-C14	: 116.889415	C15	-C14	-C13	: 123.876025
H46	-C14	-C13	: 117.403696	H46	-C14	-C15	: 118.720258
C16	-C15	-C14	: 124.988684	H47	-C15	-C14	: 118.190839
H47	-C15	-C16	: 116.820472	C17	-C16	-C15	: 123.836452
H48	-C16	-C15	: 117.371918	H48	-C16	-C17	: 118.791553
C18	-C17	-C16	: 124.888689	H49	-C17	-C16	: 118.307907
H49	-C17	-C18	: 116.803367	C19	-C18	-C17	: 123.313062
H50	-C18	-C17	: 116.613519	H50	-C18	-C19	: 120.073377
C20	-C19	-C18	: 128.068130	H51	-C19	-C18	: 117.168487
H51	-C19	-C20	: 114.763383	C26	-C20	-C19	: 118.529889
C30	-C20	-C19	: 123.715180	C30	-C20	-C26	: 117.754806
C22	-C21	-C1	: 120.870061	H31	-C21	-C1	: 119.948432
H31	-C21	-C22	: 119.180936	C23	-C22	-C21	: 120.534936
H32	-C22	-C21	: 119.561167	H32	-C22	-C23	: 119.903789
C24	-C23	-C22	: 119.425424	H33	-C23	-C22	: 120.233989
H33	-C23	-C24	: 120.340568	C25	-C24	-C23	: 120.078915
H34	-C24	-C23	: 120.149451	H34	-C24	-C25	: 119.771603
C24	-C25	-C1	: 121.354964	H35	-C25	-C1	: 118.922974
H35	-C25	-C24	: 119.722054	C27	-C26	-C20	: 121.358795
H52	-C26	-C20	: 118.912425	H52	-C26	-C27	: 119.728773
C28	-C27	-C26	: 120.056966	H53	-C27	-C26	: 119.775272
H53	-C27	-C28	: 120.167747	C29	-C28	-C27	: 119.455277
H54	-C28	-C27	: 120.327399	H54	-C28	-C29	: 120.217324
C30	-C29	-C28	: 120.524982	H55	-C29	-C28	: 119.894383
H55	-C29	-C30	: 119.580575	C29	-C30	-C20	: 120.849171
H56	-C30	-C20	: 119.936976	H56	-C30	-C29	: 119.213707

torsional angles:

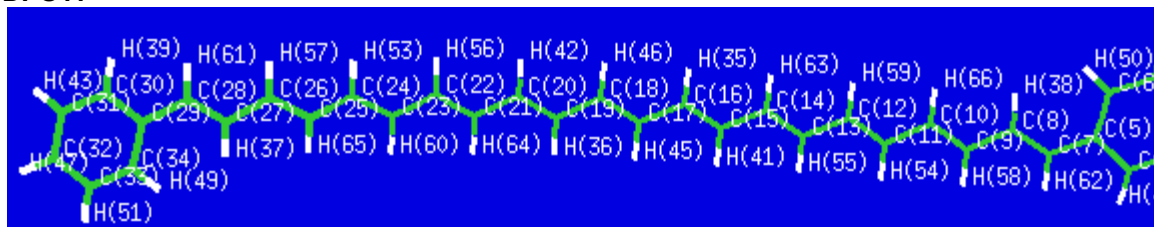
C1	-C2	-C3	-C4	: 179.601638
C1	-C2	-C3	-H37	: -0.402522
C1	-C21	-C22	-C23	: -0.012759
C1	-C21	-C22	-H32	: 179.867686
C1	-C25	-C24	-C23	: -0.083447
C1	-C25	-C24	-H34	: 179.980376
C2	-C1	-C21	-C22	: -179.836086
C2	-C1	-C21	-H31	: -0.113291
C2	-C1	-C25	-C24	: 179.894440
C2	-C1	-C25	-H35	: -0.136760
C2	-C3	-C4	-C5	: 179.740458
C2	-C3	-C4	-H38	: -0.395053
C3	-C2	-C1	-C21	: -2.184076
C3	-C2	-C1	-C25	: 178.018246
C3	-C4	-C5	-C6	: 179.632943
C3	-C4	-C5	-H39	: -0.295193
C4	-C3	-C2	-H36	: -0.471597
C4	-C5	-C6	-C7	: 179.727153

C4	-C5	-C6	-H40	:	-0.358811
C5	-C4	-C3	-H37	:	-0.255517
C5	-C6	-C7	-C8	:	179.730856
C5	-C6	-C7	-H41	:	-0.264071
C6	-C5	-C4	-H38	:	-0.229639
C6	-C7	-C8	-C9	:	179.651357
C6	-C7	-C8	-H42	:	-0.387165
C7	-C6	-C5	-H39	:	-0.343740
C7	-C8	-C9	-C10	:	179.831656
C7	-C8	-C9	-H58	:	-0.202070
C8	-C7	-C6	-H40	:	-0.182062
C8	-C9	-C10	-C11	:	179.663958
C8	-C9	-C10	-H43	:	-0.350249
C9	-C8	-C7	-H41	:	-0.353653
C9	-C10	-C11	-C12	:	179.897863
C9	-C10	-C11	-H44	:	-0.141655
C10	-C9	-C8	-H42	:	-0.129325
C10	-C11	-C12	-C13	:	179.756500
C10	-C11	-C12	-H57	:	-0.265510
C11	-C10	-C9	-H58	:	-0.302742
C11	-C12	-C13	-C14	:	179.915431
C11	-C12	-C13	-H45	:	-0.101846
C12	-C11	-C10	-H43	:	-0.087753
C12	-C13	-C14	-C15	:	179.873231
C12	-C13	-C14	-H46	:	-0.180125
C13	-C12	-C11	-H44	:	-0.204487
C13	-C14	-C15	-C16	:	179.880657
C13	-C14	-C15	-H47	:	-0.094158
C14	-C13	-C12	-H57	:	-0.062292
C14	-C15	-C16	-C17	:	-179.986352
C14	-C15	-C16	-H48	:	-0.087928
C15	-C14	-C13	-H45	:	-0.109702
C15	-C16	-C17	-C18	:	179.813487
C15	-C16	-C17	-H49	:	-0.113998
C16	-C15	-C14	-H46	:	-0.065329
C16	-C17	-C18	-C19	:	-179.939026
C16	-C17	-C18	-H50	:	-0.013704
C17	-C16	-C15	-H47	:	-0.011225
C17	-C18	-C19	-C20	:	179.766174
C17	-C18	-C19	-H51	:	-0.224907
C18	-C17	-C16	-H48	:	-0.083585
C18	-C19	-C20	-C26	:	179.306112
C18	-C19	-C20	-C30	:	-0.825647
C19	-C18	-C17	-H49	:	-0.010553
C19	-C20	-C26	-C27	:	179.885359
C19	-C20	-C26	-H52	:	-0.084199
C19	-C20	-C30	-C29	:	-179.867897
C19	-C20	-C30	-H56	:	-0.008096
C20	-C19	-C18	-H50	:	-0.156674
C20	-C26	-C27	-C28	:	-0.020516
C20	-C26	-C27	-H53	:	-179.976165
C20	-C30	-C29	-C28	:	-0.000480
C20	-C30	-C29	-H55	:	179.910281



C21	-C1	-C2	-H36	: 177.887684
C21	-C1	-C25	-C24	: 0.084851
C21	-C1	-C25	-H35	:-179.946349
C21	-C22	-C23	-C24	: 0.015945
C21	-C22	-C23	-H33	: 179.965590
C22	-C21	-C1	-C25	: -0.036642
C22	-C23	-C24	-C25	: 0.031537
C22	-C23	-C24	-H34	: 179.967471
C23	-C22	-C21	-H31	:-179.737652
C23	-C24	-C25	-H35	: 179.947998
C24	-C23	-C22	-H32	:-179.864091
C25	-C1	-C2	-H36	: -1.909995
C25	-C1	-C21	-H31	: 179.686153
C25	-C24	-C23	-H33	:-179.918053
C26	-C20	-C19	-H51	: -0.702626
C26	-C20	-C30	-C29	: 0.001294
C26	-C20	-C30	-H56	: 179.861095
C26	-C27	-C28	-C29	: 0.020974
C26	-C27	-C28	-H54	:-179.975079
C27	-C26	-C20	-C30	: 0.009206
C27	-C28	-C29	-C30	: -0.010654
C27	-C28	-C29	-H55	:-179.921135
C28	-C27	-C26	-H52	: 179.948797
C28	-C29	-C30	-H56	:-179.861281
C29	-C28	-C27	-H53	: 179.976447
C30	-C20	-C19	-H51	: 179.165615
C30	-C20	-C26	-H52	:-179.960352
C30	-C29	-C28	-H54	: 179.985403
H31	-C21	-C22	-H32	: 0.142793
H32	-C22	-C23	-H33	: 0.085554
H33	-C23	-C24	-H34	: 0.017881
H34	-C24	-C25	-H35	: 0.011821
H36	-C2	-C3	-H37	: 179.524243
H37	-C3	-C4	-H38	: 179.608973
H38	-C4	-C5	-H39	: 179.842225
H39	-C5	-C6	-H40	: 179.570297
H40	-C6	-C7	-H41	: 179.823012
H41	-C7	-C8	-H42	: 179.607825
H42	-C8	-C9	-H58	: 179.836949
H43	-C10	-C9	-H58	: 179.683050
H43	-C10	-C11	-H44	: 179.872730
H44	-C11	-C12	-H57	: 179.773503
H45	-C13	-C12	-H57	: 179.920431
H45	-C13	-C14	-H46	: 179.836942
H46	-C14	-C15	-H47	: 179.959856
H47	-C15	-C16	-H48	: 179.887199
H48	-C16	-C17	-H49	: 179.988930
H49	-C17	-C18	-H50	: 179.914768
H50	-C18	-C19	-H51	: 179.852245
H52	-C26	-C27	-H53	: -0.006852
H53	-C27	-C28	-H54	: -0.019606
H54	-C28	-C29	-H55	: 0.074923
H55	-C29	-C30	-H56	: 0.049479

## DPO11



final geometry:

atom	angstroms		
	x	y	z
C1	0.1757747976	0.0217251870	0.2552688024
C2	0.2576219401	0.0121502934	1.6508916533
C3	1.5102908262	-0.0033722528	2.2641768354
C4	2.6658835273	-0.0090838996	1.4888016257
C5	2.6041565511	0.0004473396	0.0815873958
C6	1.3290191918	0.0159556639	-0.5203531192
C7	3.8524422865	-0.0058511114	-0.6739313406
C8	4.0032592174	0.0012925273	-2.0216296948
C9	5.2742169521	-0.0048643486	-2.6855481590
C10	5.4280303640	0.0024257364	-4.0393860504
C11	6.6869690376	-0.0027516707	-4.7157636854
C12	6.8269729299	0.0049894049	-6.0735017445
C13	8.0785414436	0.0007708704	-6.7589559862
C14	8.2134125663	0.0090070072	-8.1185104875
C15	9.4652293643	0.0055822710	-8.8014254579
C16	9.6119272284	0.0142475205	-10.1604335094
C17	10.8744575902	0.0113435593	-10.8229207066
C18	11.0513480433	0.0202395563	-12.1783490825
C19	12.3307956873	0.0176290296	-12.8082062718
C20	12.5446599038	0.0265576491	-14.1579157437
C21	13.8409290954	0.0241631669	-14.7540317383
C22	14.0865200293	0.0330024289	-16.0976780991
C23	15.3960125468	0.0307825206	-16.6665774958
C24	15.6666534011	0.0393918999	-18.0042554448
C25	16.9873504257	0.0373202362	-18.5520000821
C26	17.2768487941	0.0455222626	-19.8834523751
C27	18.6088145633	0.0434798834	-20.4159197978
C28	18.8947903575	0.0511641694	-21.7415963629
C29	20.2119619185	0.0498010325	-22.3702128890
C30	20.2894538006	0.0584113385	-23.7765967890
C31	21.5158114198	0.0575269520	-24.4343183757
C32	22.7023896506	0.0479462929	-23.7012470333
C33	22.6464805158	0.0393061599	-22.3044622108
C34	21.4221556621	0.0401434079	-21.6467302194
H35	8.7171205313	0.0244313829	-10.7831081449
H36	13.2007358762	0.0078560359	-12.1510099811
H37	19.4180581748	0.0352035379	-19.6876361109
H38	3.1247158495	0.0128355200	-2.6643784668
H39	19.3681424127	0.0659625265	-24.3538362132
H40	3.6396541083	-0.0211655754	1.9723434766
H41	10.3646666036	-0.0046376134	-8.1855134092
H42	11.6831973014	0.0363655562	-14.8260147563

H43	21.5451835828	0.0643348425	-25.5202159935
H44	1.5878433442	-0.0109937011	3.3477432183
H45	11.7617140304	0.0013257729	-10.1894132946
H46	10.1719054315	0.0302805376	-12.8225488566
H47	23.6616391962	0.0472064310	-24.2103213799
H48	-0.6468733913	0.0167675974	2.2518784775
H49	21.4048406347	0.0333386332	-20.5612094140
H50	1.2397074251	0.0234954267	-1.6021384198
H51	23.5657469261	0.0318476494	-21.7255337129
H52	-0.7962454480	0.0337791226	-0.2297090451
H53	14.8332029445	0.0485471329	-18.7070708018
H54	7.5851022393	-0.0135647090	-4.0982672758
H55	8.9808957963	-0.0096850950	-6.1475137909
H56	13.2403925507	0.0425586246	-16.7851083212
H57	16.4540387217	0.0542180615	-20.5987548625
H58	6.1644103279	-0.0161227070	-2.0566321761
H59	5.9260149676	0.0156211743	-6.6870237419
H60	16.2354013234	0.0215985837	-15.9704690442
H61	18.0546950673	0.0593231903	-22.4355185348
H62	4.7576330904	-0.0176521768	-0.0673937559
H63	7.3113475223	0.0193492644	-8.7302769469
H64	14.6943763802	0.0146587384	-14.0751911440
H65	17.8150295174	0.0285588165	-17.8419935837
H66	4.5335856429	0.0134613936	-4.6624300315

Final total energy: -1314.837227 hartrees

HOMO energy: -0.16343

LUMO energy: -0.09254

bond lengths (angstroms):

C1	-C2	:	1.398054	C1	-C6	:	1.389818
C1	-H52	:	1.086357	C2	-C3	:	1.394826
C2	-H48	:	1.085964	C3	-C4	:	1.391630
C3	-H44	:	1.086365	C4	-C5	:	1.408600
C4	-H40	:	1.087285	C5	-C6	:	1.410159
C5	-C7	:	1.459132	C6	-H50	:	1.085492
C7	-C8	:	1.356130	C7	-H62	:	1.089678
C8	-C9	:	1.433931	C8	-H38	:	1.088622
C9	-C10	:	1.362567	C9	-H58	:	1.090003
C10	-C11	:	1.429140	C10	-H66	:	1.090109
C11	-C12	:	1.364959	C11	-H54	:	1.089983
C12	-C13	:	1.426986	C12	-H59	:	1.090068
C13	-C14	:	1.366253	C13	-H55	:	1.090052
C14	-C15	:	1.425984	C14	-H63	:	1.089994
C15	-C16	:	1.366930	C15	-H41	:	1.090156
C16	-C17	:	1.425791	C16	-H35	:	1.090186
C17	-C18	:	1.366951	C17	-H45	:	1.090255
C18	-C19	:	1.426083	C18	-H46	:	1.090190
C19	-C20	:	1.366577	C19	-H36	:	1.090320
C20	-C21	:	1.426770	C20	-H42	:	1.090216
C21	-C22	:	1.365935	C21	-H64	:	1.090544
C22	-C23	:	1.427733	C22	-H56	:	1.090222
C23	-C24	:	1.364809	C23	-H60	:	1.090516
C24	-C25	:	1.429779	C24	-H53	:	1.090263
C25	-C26	:	1.362586	C25	-H65	:	1.090522
C26	-C27	:	1.434454	C26	-H57	:	1.090298
C27	-C28	:	1.356193	C27	-H37	:	1.088734
C28	-C29	:	1.459487	C28	-H61	:	1.089658
C29	-C30	:	1.408544	C29	-C34	:	1.409996
C30	-C31	:	1.391600	C30	-H39	:	1.087234
C31	-C32	:	1.394795	C31	-H43	:	1.086316
C32	-C33	:	1.397930	C32	-H47	:	1.085964
C33	-C34	:	1.389814	C33	-H51	:	1.086400
C34	-H49	:	1.085680				

bond angles:

C6	-C1	-C2	:	120.563779	H52	-C1	-C2	:	119.874877
H52	-C1	-C6	:	119.561343	C3	-C2	-C1	:	119.444131
H48	-C2	-C1	:	120.242509	H48	-C2	-C3	:	120.313360
C4	-C3	-C2	:	120.054443	H44	-C3	-C2	:	120.181635
H44	-C3	-C4	:	119.763922	C5	-C4	-C3	:	121.346065
H40	-C4	-C3	:	119.732587	H40	-C4	-C5	:	118.921348
C6	-C5	-C4	:	117.784044	C7	-C5	-C4	:	118.669648

C7	-C5	-C6	: 123.546306	C5	-C6	-C1	: 120.807536
H50	-C6	-C1	: 119.200503	H50	-C6	-C5	: 119.991961
C8	-C7	-C5	: 127.566784	H62	-C7	-C5	: 114.992230
H62	-C7	-C8	: 117.440986	C9	-C8	-C7	: 123.964290
H38	-C8	-C7	: 119.805629	H38	-C8	-C9	: 116.230075
C10	-C9	-C8	: 124.060754	H58	-C9	-C8	: 117.178543
H58	-C9	-C10	: 118.760703	C11	-C10	-C9	: 124.726933
H66	-C10	-C9	: 118.379692	H66	-C10	-C11	: 116.893369
C12	-C11	-C10	: 124.132345	H54	-C11	-C10	: 117.243487
H54	-C11	-C12	: 118.624168	C13	-C12	-C11	: 124.593773
H59	-C12	-C11	: 118.367898	H59	-C12	-C13	: 117.038323
C14	-C13	-C12	: 124.371695	H55	-C13	-C12	: 117.170008
H55	-C13	-C14	: 118.458297	C15	-C14	-C13	: 124.277711
H63	-C14	-C13	: 118.480928	H63	-C14	-C15	: 117.241355
C16	-C15	-C14	: 124.773142	H41	-C15	-C14	: 116.983525
H41	-C15	-C16	: 118.243332	C17	-C16	-C15	: 123.846516
H35	-C16	-C15	: 118.674080	H35	-C16	-C17	: 117.479399
C18	-C17	-C16	: 125.120841	H45	-C17	-C16	: 116.785482
H45	-C17	-C18	: 118.093677	C19	-C18	-C17	: 123.644170
H46	-C18	-C17	: 118.789660	H46	-C18	-C19	: 117.566166
C20	-C19	-C18	: 125.212495	H36	-C19	-C18	: 116.720137
H36	-C19	-C20	: 118.067367	C21	-C20	-C19	: 123.698461
H42	-C20	-C19	: 118.793140	H42	-C20	-C21	: 117.508397
C22	-C21	-C20	: 125.052800	H64	-C21	-C20	: 116.804397
H64	-C21	-C22	: 118.142802	C23	-C22	-C21	: 123.838788
H56	-C22	-C21	: 118.735577	H56	-C22	-C23	: 117.425633
C24	-C23	-C22	: 124.918418	H60	-C23	-C22	: 116.848543
H60	-C23	-C24	: 118.233039	C25	-C24	-C23	: 123.962020
H53	-C24	-C23	: 118.703558	H53	-C24	-C25	: 117.334422
C26	-C25	-C24	: 124.791242	H65	-C25	-C24	: 116.850162
H65	-C25	-C26	: 118.358596	C27	-C26	-C25	: 124.055169
H57	-C26	-C25	: 118.736418	H57	-C26	-C27	: 117.208412
C28	-C27	-C26	: 123.961707	H37	-C27	-C26	: 116.224442
H37	-C27	-C28	: 119.813850	C29	-C28	-C27	: 127.684909
H61	-C28	-C27	: 117.384937	H61	-C28	-C29	: 114.930155
C30	-C29	-C28	: 118.665524	C34	-C29	-C28	: 123.614859
C34	-C29	-C30	: 117.719616	C31	-C30	-C29	: 121.358496
H39	-C30	-C29	: 118.916444	H39	-C30	-C31	: 119.725059
C32	-C31	-C30	: 120.086009	H43	-C31	-C30	: 119.754091
H43	-C31	-C32	: 120.159901	C33	-C32	-C31	: 119.417146
H47	-C32	-C31	: 120.336703	H47	-C32	-C33	: 120.246151
C34	-C33	-C32	: 120.536845	H51	-C33	-C32	: 119.910829
H51	-C33	-C34	: 119.552326	C33	-C34	-C29	: 120.881889
H49	-C34	-C29	: 119.959563	H49	-C34	-C33	: 119.158548

torsional angles:

C1	-C2	-C3	-C4	: 0.006580
C1	-C2	-C3	-H44	: -179.996509
C1	-C6	-C5	-C4	: 0.007405
C1	-C6	-C5	-C7	: -179.977759
C2	-C1	-C6	-C5	: -0.004375
C2	-C1	-C6	-H50	: 179.992663

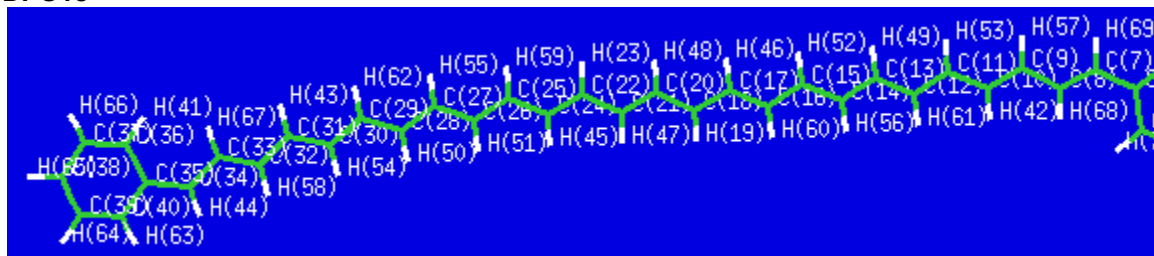
C2	-C3	-C4	-C5	:	-0.003419
C2	-C3	-C4	-H40	:	179.998269
C3	-C2	-C1	-C6	:	-0.002732
C3	-C2	-C1	-H52	:	179.997059
C3	-C4	-C5	-C6	:	-0.003536
C3	-C4	-C5	-C7	:	179.982372
C4	-C3	-C2	-H48	:	-179.993350
C4	-C5	-C6	-H50	:	-179.989610
C4	-C5	-C7	-C8	:	179.993909
C4	-C5	-C7	-H62	:	-0.007775
C5	-C4	-C3	-H44	:	179.999658
C5	-C6	-C1	-H52	:	179.995833
C5	-C7	-C8	-C9	:	179.955748
C5	-C7	-C8	-H38	:	-0.016921
C6	-C1	-C2	-H48	:	179.997198
C6	-C5	-C4	-H40	:	179.994790
C6	-C5	-C7	-C8	:	-0.021051
C6	-C5	-C7	-H62	:	179.977266
C7	-C5	-C4	-H40	:	-0.019303
C7	-C5	-C6	-H50	:	0.025226
C7	-C8	-C9	-C10	:	-179.993271
C7	-C8	-C9	-H58	:	0.009314
C8	-C9	-C10	-C11	:	179.960831
C8	-C9	-C10	-H66	:	-0.010544
C9	-C8	-C7	-H62	:	-0.042533
C9	-C10	-C11	-C12	:	-179.983588
C9	-C10	-C11	-H54	:	0.015586
C10	-C9	-C8	-H38	:	-0.019709
C10	-C11	-C12	-C13	:	179.958835
C10	-C11	-C12	-H59	:	-0.011405
C11	-C10	-C9	-H58	:	-0.041792
C11	-C12	-C13	-C14	:	-179.977234
C11	-C12	-C13	-H55	:	0.019269
C12	-C11	-C10	-H66	:	-0.011827
C12	-C13	-C14	-C15	:	179.960483
C12	-C13	-C14	-H63	:	-0.010348
C13	-C12	-C11	-H54	:	-0.040328
C13	-C14	-C15	-C16	:	-179.974063
C13	-C14	-C15	-H41	:	0.020903
C14	-C13	-C12	-H59	:	-0.006635
C14	-C15	-C16	-C17	:	179.964374
C14	-C15	-C16	-H35	:	-0.008310
C15	-C14	-C13	-H55	:	-0.035978
C15	-C16	-C17	-C18	:	-179.977628
C15	-C16	-C17	-H45	:	0.015250
C16	-C15	-C14	-H63	:	-0.002901
C16	-C17	-C18	-C19	:	179.969203
C16	-C17	-C18	-H46	:	-0.007698
C17	-C16	-C15	-H41	:	-0.030534
C17	-C18	-C19	-C20	:	-179.985496
C17	-C18	-C19	-H36	:	0.004465
C18	-C17	-C16	-H35	:	-0.004642
C18	-C19	-C20	-C21	:	179.972652

C18	-C19	-C20	-H42	: -0.010139
C19	-C18	-C17	-H45	: -0.023591
C19	-C20	-C21	-C22	:-179.993691
C19	-C20	-C21	-H64	: -0.003194
C20	-C19	-C18	-H46	: -0.008333
C20	-C21	-C22	-C23	: 179.978239
C20	-C21	-C22	-H56	: -0.008127
C21	-C20	-C19	-H36	: -0.017186
C21	-C22	-C23	-C24	: 179.996860
C21	-C22	-C23	-H60	: -0.010386
C22	-C21	-C20	-H42	: -0.010695
C22	-C23	-C24	-C25	: 179.982576
C22	-C23	-C24	-H53	: -0.010327
C23	-C22	-C21	-H64	: -0.012142
C23	-C24	-C25	-C26	: 179.985960
C23	-C24	-C25	-H65	: -0.017764
C24	-C23	-C22	-H56	: -0.016609
C24	-C25	-C26	-C27	: 179.990863
C24	-C25	-C26	-H57	: -0.008668
C25	-C24	-C23	-H60	: -0.010086
C25	-C26	-C27	-C28	: 179.974936
C25	-C26	-C27	-H37	: -0.026080
C26	-C25	-C24	-H53	: -0.021048
C26	-C27	-C28	-C29	:-179.998619
C26	-C27	-C28	-H61	: -0.002027
C27	-C26	-C25	-H65	: -0.005361
C27	-C28	-C29	-C30	: 179.976866
C27	-C28	-C29	-C34	: -0.015888
C28	-C27	-C26	-H57	: -0.025526
C28	-C29	-C30	-C31	:-179.996384
C28	-C29	-C30	-H39	: 0.008673
C28	-C29	-C34	-C33	: 179.997860
C28	-C29	-C34	-H49	: -0.008330
C29	-C28	-C27	-H37	: 0.002431
C29	-C30	-C31	-C32	: 0.001393
C29	-C30	-C31	-H43	:-179.997935
C29	-C34	-C33	-C32	: -0.005115
C29	-C34	-C33	-H51	: 179.995984
C30	-C29	-C28	-H61	: -0.019797
C30	-C29	-C34	-C33	: 0.005042
C30	-C29	-C34	-H49	: 179.998852
C30	-C31	-C32	-C33	: -0.001297
C30	-C31	-C32	-H47	: 179.999159
C31	-C30	-C29	-C34	: -0.003201
C31	-C32	-C33	-C34	: 0.003154
C31	-C32	-C33	-H51	:-179.997949
C32	-C31	-C30	-H39	: 179.996295
C32	-C33	-C34	-H49	:-179.998973
C33	-C32	-C31	-H43	: 179.998028
C34	-C29	-C28	-H61	: 179.987449
C34	-C29	-C30	-H39	:-179.998144
C34	-C33	-C32	-H47	:-179.997302
H35	-C16	-C15	-H41	: 179.996782

H35	-C16	-C17	-H45	: 179.988237
H36	-C19	-C18	-H46	: 179.981628
H36	-C19	-C20	-H42	: -179.999977
H37	-C27	-C26	-H57	: 179.973458
H37	-C27	-C28	-H61	: 179.999023
H38	-C8	-C7	-H62	: 179.984798
H38	-C8	-C9	-H58	: 179.982875
H39	-C30	-C31	-H43	: -0.003032
H40	-C4	-C3	-H44	: 0.001346
H41	-C15	-C14	-H63	: 179.992066
H42	-C20	-C21	-H64	: 179.979802
H43	-C31	-C32	-H47	: -0.001516
H44	-C3	-C2	-H48	: 0.003560
H45	-C17	-C18	-H46	: 179.999508
H47	-C32	-C33	-H51	: 0.001595
H48	-C2	-C1	-H52	: -0.003010
H49	-C34	-C33	-H51	: 0.002125
H50	-C6	-C1	-H52	: -0.007129
H53	-C24	-C23	-H60	: 179.997011
H53	-C24	-C25	-H65	: 179.975228
H54	-C11	-C10	-H66	: 179.987347
H54	-C11	-C12	-H59	: 179.989432
H55	-C13	-C12	-H59	: 179.989869
H55	-C13	-C14	-H63	: 179.993191
H56	-C22	-C21	-H64	: -179.998508
H56	-C22	-C23	-H60	: 179.976145
H57	-C26	-C25	-H65	: 179.995108
H58	-C9	-C10	-H66	: 179.986833



## DPO13



final geometry:

atom	angstroms			
	x	y	z	
C1	-0.1161583897	-0.0359749208	0.0993952798	
C2	-0.0402995352	-0.2581481179	1.4901240851	
C3	1.2388222534	-0.4116724682	2.0583393024	
C4	2.3897718455	-0.3475352727	1.2776915117	
C5	2.2942524481	-0.1273489406	-0.0964877558	
C6	1.0328220662	0.0277590310	-0.6788480655	
C7	-1.2153745734	-0.3319321445	2.3539814952	
C8	-2.5093100390	-0.2084799292	1.9689249812	
C9	-3.6438985927	-0.2788970108	2.8422467855	
C10	-4.9234194712	-0.1363655647	2.3965202049	
C11	-6.1011263881	-0.1858668685	3.2021928018	
C12	-7.3582525476	-0.0253992236	2.6951678288	
C13	-8.5606564874	-0.0610049960	3.4596671079	
C14	-9.8087760332	0.1079731023	2.9300643579	
C15	-11.0109560227	0.0739583806	3.6933645566	
C16	-12.2673331405	0.2390315482	3.1816761547	
C17	-13.4498067103	0.1931961624	3.9743918292	
C18	-14.7225327513	0.3419299341	3.5006442040	
H19	-14.8715928850	0.5150071503	2.4347595809	
C20	-15.8813525132	0.2740035646	4.3263741874	
C21	-17.1657857724	0.3969033915	3.8786835970	
C22	-18.3171037943	0.3018304515	4.7128519401	
H23	-18.1523373660	0.1320496166	5.7769697453	
C24	-19.5994366052	0.3937829787	4.2528890385	
C25	-20.7712682554	0.2710797760	5.0547900268	
C26	-22.0333177138	0.3318843796	4.5372702324	
C27	-23.2481501947	0.1838043517	5.2679803297	
C28	-24.4720458161	0.2164751605	4.6638590422	
C29	-25.7349197866	0.0464785161	5.3037340732	
C30	-26.9117747462	0.0562292172	4.6129239551	
C31	-28.2123020470	-0.1316153042	5.1706189694	
C32	-29.3495859461	-0.1395157642	4.4199759610	
C33	-30.6719936032	-0.3420507834	4.9309281295	
C34	-31.7778040949	-0.3603223271	4.1456420770	
C35	-33.1612811848	-0.5668286044	4.5561644993	
C36	-33.5533393002	-0.7812770955	5.8937257467	
C37	-34.8904518369	-0.9747572831	6.2193954458	
C38	-35.8732879884	-0.9605850218	5.2251143791	
C39	-35.5038362917	-0.7496172484	3.8968434067	
C40	-34.1659876929	-0.5554575504	3.5688643305	
H41	-32.8073258752	-0.7967393585	6.6821657232	
H42	-5.0740326974	0.0354617016	1.3300765918	

H43	-28.2862973634	-0.2842622935	6.2469867729
H44	-31.6341678447	-0.2068107654	3.0763547188
H45	-19.7520466737	0.5603329286	3.1859442180
H46	-13.3179614527	0.0192155342	5.0428065011
H47	-17.3340781922	0.5677318728	2.8150279888
H48	-15.7195334439	0.1008831855	5.3907017917
H49	-8.4690119871	-0.2331006775	4.5322817546
H50	-24.4978804448	0.3738680122	3.5848325374
H51	-22.1333594025	0.4936107415	3.4632734620
H52	-10.9111729317	-0.0991996604	4.7652780183
H53	-5.9802666521	-0.3574274907	4.2717757360
H54	-26.8658881210	0.2102829469	3.5344496450
H55	-23.1854489103	0.0239283376	6.3441858447
H56	-9.9004889675	0.2805023749	1.8573891154
H57	-3.4630808002	-0.4498007171	3.9034293401
H58	-29.2581665561	0.0121726014	3.3442853886
H59	-20.6417585275	0.1060886548	6.1243972955
H60	-12.3815391119	0.4123491022	2.1114433840
H61	-7.4612152858	0.1466301766	1.6232601369
H62	-25.7488347450	-0.1093020137	6.3822790143
H63	-33.8826604705	-0.3915445285	2.5320630653
H64	-36.2584834570	-0.7362912675	3.1156488936
H65	-36.9164033426	-1.1127914426	5.4858883223
H66	-35.1715722608	-1.1384848727	7.2558439553
H67	-30.7630600782	-0.4914556811	6.0053314998
H68	-2.7375218034	-0.0381172958	0.9179129043
H69	-1.0103042745	-0.5015259144	3.4109109331
H70	1.3224005749	-0.5833099405	3.1287799324
H71	3.3633903047	-0.4695228610	1.7439098586
H72	3.1900307245	-0.0762259868	-0.7079991208
H73	0.9464280609	0.2005162330	-1.7479517332
H74	-1.0826784888	0.0892434543	-0.3784042661

Final total energy: -1469.658033 hartrees

HOMO energy: -0.16068

LUMO energy: -0.09420

bond lengths (angstroms):

C1	-C2	:	1.410405	C1	-C6	:	1.389202
C1	-H74	:	1.085418	C2	-C3	:	1.408045
C2	-C7	:	1.460306	C3	-C4	:	1.392196
C3	-H70	:	1.087331	C4	-C5	:	1.394982
C4	-H71	:	1.086358	C5	-C6	:	1.398002
C5	-H72	:	1.085808	C6	-H73	:	1.086412
C7	-C8	:	1.355647	C7	-H69	:	1.089915
C8	-C9	:	1.433506	C8	-H68	:	1.088912
C9	-C10	:	1.362410	C9	-H57	:	1.089959
C10	-C11	:	1.427779	C10	-H42	:	1.090647
C11	-C12	:	1.364987	C11	-H53	:	1.089976
C12	-C13	:	1.425308	C12	-H61	:	1.090496
C13	-C14	:	1.366322	C13	-H49	:	1.090192
C14	-C15	:	1.424437	C14	-H56	:	1.090326
C15	-C16	:	1.366586	C15	-H52	:	1.090385
C16	-C17	:	1.424339	C16	-H60	:	1.090174
C17	-C18	:	1.366159	C17	-H46	:	1.090487
C18	-H19	:	1.090085	C18	-C20	:	1.424538
C20	-C21	:	1.365760	C20	-H48	:	1.090390
C21	-C22	:	1.424924	C21	-H47	:	1.090352
C22	-H23	:	1.090101	C22	-C24	:	1.365430
C24	-C25	:	1.425234	C24	-H45	:	1.090596
C25	-C26	:	1.365391	C25	-H59	:	1.089979
C26	-C27	:	1.425371	C26	-H51	:	1.090703
C27	-C28	:	1.365266	C27	-H55	:	1.089821
C28	-C29	:	1.425900	C28	-H50	:	1.090751
C29	-C30	:	1.364662	C29	-H62	:	1.089826
C30	-C31	:	1.427473	C30	-H54	:	1.090388
C31	-C32	:	1.362697	C31	-H43	:	1.089653
C32	-C33	:	1.432081	C32	-H58	:	1.090173
C33	-C34	:	1.356401	C33	-H67	:	1.088558
C34	-C35	:	1.457801	C34	-H44	:	1.089758
C35	-C36	:	1.410237	C35	-C40	:	1.408661
C36	-C37	:	1.389736	C36	-H41	:	1.085547
C37	-C38	:	1.398128	C37	-H66	:	1.086306
C38	-C39	:	1.394742	C38	-H65	:	1.085937
C39	-C40	:	1.391081	C39	-H64	:	1.086248
C40	-H63	:	1.087244				

bond angles:

C6	-C1	-C2	:	121.006553	H74	-C1	-C2	:	120.008173
H74	-C1	-C6	:	118.985243	C3	-C2	-C1	:	117.642625
C7	-C2	-C1	:	123.228938	C7	-C2	-C3	:	119.128315

C4	-C3	-C2	: 121.313069	H70	-C3	-C2	: 118.967889
H70	-C3	-C4	: 119.719041	C5	-C4	-C3	: 120.200854
H71	-C4	-C3	: 119.676732	H71	-C4	-C5	: 120.122411
C6	-C5	-C4	: 119.317650	H72	-C5	-C4	: 120.379753
H72	-C5	-C6	: 120.302586	C5	-C6	-C1	: 120.519240
H73	-C6	-C1	: 119.525311	H73	-C6	-C5	: 119.955427
C8	-C7	-C2	: 126.542564	H69	-C7	-C2	: 115.474900
H69	-C7	-C8	: 117.982385	C9	-C8	-C7	: 125.305271
H68	-C8	-C7	: 119.237935	H68	-C8	-C9	: 115.456487
C10	-C9	-C8	: 122.606906	H57	-C9	-C8	: 118.004247
H57	-C9	-C10	: 119.388415	C11	-C10	-C9	: 125.904076
H42	-C10	-C9	: 117.779862	H42	-C10	-C11	: 116.315604
C12	-C11	-C10	: 123.092582	H53	-C11	-C10	: 117.886483
H53	-C11	-C12	: 119.020683	C13	-C12	-C11	: 125.083854
H61	-C12	-C11	: 118.074645	H61	-C12	-C13	: 116.841288
C14	-C13	-C12	: 124.030451	H49	-C13	-C12	: 117.435791
H49	-C13	-C14	: 118.533722	C15	-C14	-C13	: 124.076293
H56	-C14	-C13	: 118.538248	H56	-C14	-C15	: 117.385456
C16	-C15	-C14	: 124.916381	H52	-C15	-C14	: 116.958336
H52	-C15	-C16	: 118.125182	C17	-C16	-C15	: 123.433220
H60	-C16	-C15	: 118.887663	H60	-C16	-C17	: 117.678838
C18	-C17	-C16	: 125.233729	H46	-C17	-C16	: 116.746544
H46	-C17	-C18	: 118.018724	H19	-C18	-C17	: 118.930650
C20	-C18	-C17	: 123.479536	C20	-C18	-H19	: 117.588286
C21	-C20	-C18	: 124.801442	H48	-C20	-C18	: 116.913249
H48	-C20	-C21	: 118.282291	C22	-C21	-C20	: 124.192331
H47	-C21	-C20	: 118.621709	H47	-C21	-C22	: 117.182252
H23	-C22	-C21	: 117.369379	C24	-C22	-C21	: 123.856597
C24	-C22	-H23	: 118.768489	C25	-C24	-C22	: 125.228138
H45	-C24	-C22	: 118.116031	H45	-C24	-C25	: 116.649925
C26	-C25	-C24	: 122.880043	H59	-C25	-C24	: 117.870092
H59	-C25	-C26	: 119.242647	C27	-C26	-C25	: 126.075603
H51	-C26	-C25	: 117.684634	H51	-C26	-C27	: 116.233066
C28	-C27	-C26	: 122.324301	H55	-C27	-C26	: 118.193177
H55	-C27	-C28	: 119.475537	C29	-C28	-C27	: 126.337222
H50	-C28	-C27	: 117.543557	H50	-C28	-C29	: 116.113718
C30	-C29	-C28	: 122.395825	H62	-C29	-C28	: 118.193871
H62	-C29	-C30	: 119.405281	C31	-C30	-C29	: 125.942674
H54	-C30	-C29	: 117.736171	H54	-C30	-C31	: 116.317851
C32	-C31	-C30	: 123.087279	H43	-C31	-C30	: 117.789599
H43	-C31	-C32	: 119.120541	C33	-C32	-C31	: 125.096149
H58	-C32	-C31	: 118.212333	H58	-C32	-C33	: 116.690083
C34	-C33	-C32	: 123.240929	H67	-C33	-C32	: 116.667551
H67	-C33	-C34	: 120.090613	C35	-C34	-C33	: 127.775052
H44	-C34	-C33	: 117.304559	H44	-C34	-C35	: 114.920141
C36	-C35	-C34	: 123.536469	C40	-C35	-C34	: 118.578241
C40	-C35	-C36	: 117.885173	C37	-C36	-C35	: 120.724813
H41	-C36	-C35	: 119.999253	H41	-C36	-C37	: 119.275933
C38	-C37	-C36	: 120.549693	H66	-C37	-C36	: 119.574435
H66	-C37	-C38	: 119.875869	C39	-C38	-C37	: 119.510606
H65	-C38	-C37	: 120.202050	H65	-C38	-C39	: 120.287344
C40	-C39	-C38	: 120.026502	H64	-C39	-C38	: 120.180328
H64	-C39	-C40	: 119.793171	C39	-C40	-C35	: 121.303204

H63 -C40 -C35 : 118.928307 H63 -C40 -C39 : 119.768483

torsional angles:

C1 -C2 -C3 -C4 : -0.027014  
 C1 -C2 -C3 -H70 : 179.962255  
 C1 -C2 -C7 -C8 : 0.256782  
 C1 -C2 -C7 -H69 :-179.597848  
 C1 -C6 -C5 -C4 : 0.003488  
 C1 -C6 -C5 -H72 :-179.958581  
 C2 -C1 -C6 -C5 : -0.021742  
 C2 -C1 -C6 -H73 :-179.967910  
 C2 -C3 -C4 -C5 : 0.009801  
 C2 -C3 -C4 -H71 : 179.991135  
 C2 -C7 -C8 -C9 :-179.669557  
 C2 -C7 -C8 -H68 : 0.119440  
 C3 -C2 -C1 -C6 : 0.032906  
 C3 -C2 -C1 -H74 :-179.903378  
 C3 -C2 -C7 -C8 :-179.873384  
 C3 -C2 -C7 -H69 : 0.271987  
 C3 -C4 -C5 -C6 : 0.002456  
 C3 -C4 -C5 -H72 : 179.964495  
 C4 -C3 -C2 -C7 :-179.904103  
 C4 -C5 -C6 -H73 : 179.949425  
 C5 -C4 -C3 -H70 :-179.979388  
 C5 -C6 -C1 -H74 : 179.915183  
 C6 -C1 -C2 -C7 : 179.904552  
 C6 -C5 -C4 -H71 :-179.978794  
 C7 -C2 -C1 -H74 : -0.031732  
 C7 -C2 -C3 -H70 : 0.085166  
 C7 -C8 -C9 -C10 : 179.463820  
 C7 -C8 -C9 -H57 : -0.295481  
 C8 -C9 -C10 -C11 :-179.611520  
 C8 -C9 -C10 -H42 : 0.132282  
 C9 -C8 -C7 -H69 : 0.181832  
 C9 -C10 -C11 -C12 : 179.497236  
 C9 -C10 -C11 -H53 : -0.317739  
 C10 -C9 -C8 -H68 : -0.332261  
 C10 -C11 -C12 -C13 :-179.715535  
 C10 -C11 -C12 -H61 : 0.111031  
 C11 -C10 -C9 -H57 : 0.144575  
 C11 -C12 -C13 -C14 : 179.715765  
 C11 -C12 -C13 -H49 : -0.214134  
 C12 -C11 -C10 -H42 : -0.249888  
 C12 -C13 -C14 -C15 :-179.932024  
 C12 -C13 -C14 -H56 : 0.046081  
 C13 -C12 -C11 -H53 : 0.097443  
 C13 -C14 -C15 -C16 :-179.913634  
 C13 -C14 -C15 -H52 : -0.032217  
 C14 -C13 -C12 -H61 : -0.112731  
 C14 -C15 -C16 -C17 : 179.716959  
 C14 -C15 -C16 -H60 : -0.086528  
 C15 -C14 -C13 -H49 : -0.002843

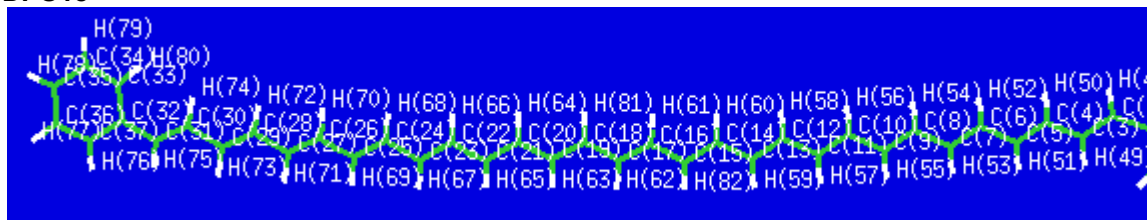
C15	-C16	-C17	-C18	:-179.420764
C15	-C16	-C17	-H46	: 0.206143
C16	-C15	-C14	-H56	: 0.108028
C16	-C17	-C18	-H19	:-0.287080
C16	-C17	-C18	-C20	: 179.251946
C17	-C16	-C15	-H52	:-0.163192
C17	-C18	-C20	-C21	:-178.877903
C17	-C18	-C20	-H48	: 0.477169
C18	-C17	-C16	-H60	: 0.384941
C18	-C20	-C21	-C22	: 178.770478
C18	-C20	-C21	-H47	:-0.508054
H19	-C18	-C17	-H46	:-179.909672
H19	-C18	-C20	-C21	: 0.666892
H19	-C18	-C20	-H48	:-179.978035
C20	-C18	-C17	-H46	:-0.370646
C20	-C21	-C22	-H23	: 0.771133
C20	-C21	-C22	-C24	:-178.360627
C21	-C22	-C24	-C25	: 178.409391
C21	-C22	-C24	-H45	:-0.674349
C22	-C21	-C20	-H48	:-0.576488
C22	-C24	-C25	-C26	:-177.996525
C22	-C24	-C25	-H59	: 1.017547
H23	-C22	-C21	-H47	:-179.940799
H23	-C22	-C24	-C25	:-0.710987
H23	-C22	-C24	-H45	:-179.794728
C24	-C22	-C21	-H47	: 0.927441
C24	-C25	-C26	-C27	: 178.279267
C24	-C25	-C26	-H51	:-0.739968
C25	-C26	-C27	-C28	:-177.870196
C25	-C26	-C27	-H55	: 1.162487
C26	-C25	-C24	-H45	: 1.099281
C26	-C27	-C28	-C29	: 178.404186
C26	-C27	-C28	-H50	:-0.705468
C27	-C26	-C25	-H59	:-0.721865
C27	-C28	-C29	-C30	:-178.068710
C27	-C28	-C29	-H62	: 1.110425
C28	-C27	-C26	-H51	: 1.161598
C28	-C29	-C30	-C31	: 178.724222
C28	-C29	-C30	-H54	:-0.587617
C29	-C28	-C27	-H55	:-0.616502
C29	-C30	-C31	-C32	:-178.525040
C29	-C30	-C31	-H43	: 0.884553
C30	-C29	-C28	-H50	: 1.052112
C30	-C31	-C32	-C33	: 179.100371
C30	-C31	-C32	-H58	:-0.448263
C31	-C30	-C29	-H62	:-0.445315
C31	-C32	-C33	-C34	:-179.087364
C31	-C32	-C33	-H67	: 0.565847
C32	-C31	-C30	-H54	: 0.795436
C32	-C33	-C34	-C35	: 179.505675
C32	-C33	-C34	-H44	:-0.303040
C33	-C32	-C31	-H43	:-0.301741
C33	-C34	-C35	-C36	: 0.243757

C33	-C34	-C35	-C40	:-179.629042
C34	-C33	-C32	-H58	: 0.467458
C34	-C35	-C36	-C37	:-179.859464
C34	-C35	-C36	-H41	: 0.127178
C34	-C35	-C40	-C39	: 179.851437
C34	-C35	-C40	-H63	:-0.121175
C35	-C34	-C33	-H67	:-0.136156
C35	-C36	-C37	-C38	: 0.012259
C35	-C36	-C37	-H66	: 179.991873
C35	-C40	-C39	-C38	: 0.016542
C35	-C40	-C39	-H64	:-179.984220
C36	-C35	-C34	-H44	:-179.943664
C36	-C35	-C40	-C39	:-0.028608
C36	-C35	-C40	-H63	: 179.998780
C36	-C37	-C38	-C39	:-0.024815
C36	-C37	-C38	-H65	: 179.974909
C37	-C36	-C35	-C40	: 0.014159
C37	-C38	-C39	-C40	: 0.010497
C37	-C38	-C39	-H64	:-179.988738
C38	-C37	-C36	-H41	:-179.974478
C38	-C39	-C40	-H63	: 179.988928
C39	-C38	-C37	-H66	: 179.995633
C40	-C35	-C34	-H44	: 0.183536
C40	-C35	-C36	-H41	:-179.999199
C40	-C39	-C38	-H65	:-179.989228
H41	-C36	-C37	-H66	: 0.005135
H42	-C10	-C9	-H57	: 179.888378
H42	-C10	-C11	-H53	: 179.935137
H43	-C31	-C30	-H54	:-179.794972
H43	-C31	-C32	-H58	:-179.850375
H44	-C34	-C33	-H67	:-179.944871
H45	-C24	-C25	-H59	:-179.886646
H46	-C17	-C16	-H60	:-179.988152
H47	-C21	-C20	-H48	:-179.855020
H49	-C13	-C12	-H61	: 179.957371
H49	-C13	-C14	-H56	: 179.975263
H50	-C28	-C27	-H55	:-179.726155
H50	-C28	-C29	-H62	:-179.768753
H51	-C26	-C25	-H59	:-179.741100
H51	-C26	-C27	-H55	:-179.805720
H52	-C15	-C14	-H56	: 179.989445
H52	-C15	-C16	-H60	:-179.966679
H53	-C11	-C12	-H61	: 179.924010
H54	-C30	-C29	-H62	:-179.757155
H57	-C9	-C8	-H68	: 179.908438
H58	-C32	-C33	-H67	:-179.879331
H63	-C40	-C39	-H64	:-0.011834
H64	-C39	-C38	-H65	: 0.011537
H65	-C38	-C37	-H66	:-0.004643
H68	-C8	-C7	-H69	: 179.970829
H70	-C3	-C4	-H71	: 0.001945
H71	-C4	-C5	-H72	:-0.016755
H72	-C5	-C6	-H73	:-0.012644

H73 -C6 -C1 -H74 : -0.030986



## DPO15



final geometry:

atom	angstroms		
	x	y	z
C1	-0.0510348764	-0.0076449271	0.0400482352
C2	-0.0718001018	-0.0102797611	1.5000061528
C3	0.9897367409	-0.0178112697	2.3450309810
C4	0.8754699505	-0.0170924628	3.7752798248
C6	1.8359030298	-0.0184659793	6.0550066774
C5	1.9381407375	-0.0213884184	4.6289865952
C7	2.9057256452	-0.0188769752	6.9036139604
C8	2.8079617401	-0.0144261712	8.3278460600
C9	3.8781696884	-0.0107232689	9.1778793312
C10	3.7751918478	-0.0052031250	10.6003673066
C11	4.8392259620	0.0027114946	11.4591946784
C12	4.7172376759	0.0093148006	12.8793635345
C13	5.7645044182	0.0213674672	13.7590436820
C14	5.6078407131	0.0295597673	15.1761146088
C15	6.6312474522	0.0454861803	16.0839004942
C16	6.4384600882	0.0557739699	17.4964231596
C17	7.4407263632	0.0748817260	18.4276740321
C18	7.2192808532	0.0880565885	19.8359215402
C19	8.2042593200	0.1096415923	20.7852704590
C20	7.9589556015	0.1260051468	22.1894681362
C21	8.9289638955	0.1498404751	23.1532846254
C22	8.6642011165	0.1694430715	24.5538509181
C23	9.6221480550	0.1944789785	25.5290493829
C24	9.3393671963	0.2168089633	26.9266511705
C25	10.2824802302	0.2418345548	27.9152621781
C26	9.9756074108	0.2662835595	29.3091359370
C27	10.8992504973	0.2910548975	30.3138888506
C28	10.5647644506	0.3171897450	31.7034548254
C29	11.4669558177	0.3417893427	32.7242203123
C30	11.1026185188	0.3692327627	34.1111702942
C31	11.9926269462	0.3937907050	35.1342807372
C32	11.6988971888	0.4233987020	36.5640907960
C33	10.3905808884	0.4247999103	37.0906449735
C34	10.1739986458	0.4551937092	38.4630235769
C35	11.2524375471	0.4851997872	39.3519515992
C36	12.5537954065	0.4836081868	38.8500642983
C37	12.7720391355	0.4531212367	37.4759136055
C38	1.1341726391	-0.0105846534	-0.7239192545
C39	1.0887856019	-0.0069128446	-2.1129955372
C40	-0.1378795134	0.0003553839	-2.7833012438
C41	-1.3211730051	0.0033045006	-2.0447640019
C42	-1.2765836594	-0.0006569336	-0.6538795472

H43	-2.2030941155	0.0019639672	-0.0850441720
H44	-2.2811677508	0.0087758476	-2.5530837050
H45	-0.1681013785	0.0034720559	-3.8688509418
H46	2.0158257993	-0.0095108329	-2.6794947732
H47	2.0989717436	-0.0153707153	-0.2270350962
H48	-1.0665881870	-0.0050550836	1.9455717917
H49	2.0015493294	-0.0236360957	1.9432433844
H50	-0.1315699711	-0.0118500269	4.1932669255
H51	2.9431186004	-0.0258143247	4.2065302270
H52	0.8325340223	-0.0147794899	6.4816909257
H53	3.9083323064	-0.0213805910	6.4749770400
H54	1.8052483996	-0.0129788454	8.7561947305
H55	4.8810611616	-0.0108431564	8.7508126025
H56	2.7702281738	-0.0065605852	11.0234901253
H57	5.8461816762	0.0050438498	11.0419932102
H58	3.7057468494	0.0050513504	13.2860147623
H59	6.7804869045	0.0257547084	13.3635197034
H60	4.5860679904	0.0229968229	15.5567830161
H61	5.4076830115	0.0481957881	17.8519374079
H62	8.4746397801	0.0807207686	18.0821649305
H63	9.2439424307	0.1149778996	20.4575378615
H64	6.9162803689	0.1199561131	22.5077949772
H65	9.9732977818	0.1545081658	22.8412997560
H66	7.6173498027	0.1652276687	24.8589474131
H67	10.6704061455	0.1979284431	25.2305338588
H68	8.2884162090	0.2149240116	27.2173379337
H69	11.3356857959	0.2436226568	27.6335223014
H70	8.9195300571	0.2664987132	29.5807667409
H71	11.9575435497	0.2912779578	30.0529120213
H72	9.5031748944	0.3188482858	31.9530223220
H73	12.5306839844	0.3407517791	32.4862266499
H74	10.0350356643	0.3714429471	34.3246257884
H75	13.0525779974	0.3921092864	34.8798678942
H76	13.7891332898	0.4521818239	37.0915363904
H77	13.4008644133	0.5060914540	39.5298478788
H78	11.0775949952	0.5092212736	40.4234616487
H79	9.1570692042	0.4553306746	38.8452106106
H80	9.5367856000	0.4011108391	36.4212204792
H81	6.1820611585	0.0808689908	20.1709918222
H82	7.6573031265	0.0511375516	15.7161067494

Final total energy: -1624.481322 hartrees

HOMO energy: -0.15985

LUMO energy: -0.09683

bond lengths (angstroms):

C1	-C2	:	1.460108	C1	-C38	:	1.410096
C1	-C42	:	1.408387	C2	-C3	:	1.356829
C2	-H48	:	1.090027	C3	-C4	:	1.434806
C3	-H49	:	1.088684	C4	-C5	:	1.363122
C4	-H50	:	1.090353	C5	-C6	:	1.429683
C5	-H51	:	1.090169	C6	-C7	:	1.365524
C6	-H52	:	1.090331	C7	-C8	:	1.427591
C7	-H53	:	1.090393	C8	-C9	:	1.366717
C8	-H54	:	1.090375	C9	-C10	:	1.426221
C9	-H55	:	1.090035	C10	-C11	:	1.367412
C10	-H56	:	1.090407	C11	-C12	:	1.425414
C11	-H57	:	1.089964	C12	-C13	:	1.367754
C12	-H58	:	1.090182	C13	-C14	:	1.425728
C13	-H59	:	1.090266	C14	-C15	:	1.368097
C14	-H60	:	1.090399	C15	-C16	:	1.425655
C15	-H82	:	1.089997	C16	-C17	:	1.368258
C16	-H61	:	1.090389	C17	-C18	:	1.425613
C17	-H62	:	1.090132	C18	-C19	:	1.368178
C18	-H81	:	1.090022	C19	-C20	:	1.425557
C19	-H63	:	1.090128	C20	-C21	:	1.367635
C20	-H64	:	1.090202	C21	-C22	:	1.425507
C21	-H65	:	1.089949	C22	-C23	:	1.367224
C22	-H66	:	1.090412	C23	-C24	:	1.426098
C23	-H67	:	1.089940	C24	-C25	:	1.366543
C24	-H68	:	1.090413	C25	-C26	:	1.427464
C25	-H69	:	1.090240	C26	-C27	:	1.365012
C26	-H70	:	1.090451	C27	-C28	:	1.429496
C27	-H71	:	1.089997	C28	-C29	:	1.362540
C28	-H72	:	1.090532	C29	-C30	:	1.434268
C29	-H73	:	1.090027	C30	-C31	:	1.356272
C30	-H74	:	1.088715	C31	-C32	:	1.459969
C31	-H75	:	1.090057	C32	-C33	:	1.410302
C32	-C37	:	1.408523	C33	-C34	:	1.389696
C33	-H80	:	1.085199	C34	-C35	:	1.397900
C34	-H79	:	1.086376	C35	-C36	:	1.394785
C35	-H78	:	1.085947	C36	-C37	:	1.391708
C36	-H77	:	1.086341	C37	-H76	:	1.087303
C38	-C39	:	1.389822	C38	-H47	:	1.085244
C39	-C40	:	1.397880	C39	-H46	:	1.086431
C40	-C41	:	1.394858	C40	-H45	:	1.085975
C41	-C42	:	1.391605	C41	-H44	:	1.086282
C42	-H43	:	1.087199				

bond angles:

C38	-C1	-C2	: 123.619707	C42	-C1	-C2	: 118.704595
C42	-C1	-C38	: 117.675676	C3	-C2	-C1	: 127.706259
H48	-C2	-C1	: 114.941587	H48	-C2	-C3	: 117.352148
C4	-C3	-C2	: 123.952543	H49	-C3	-C2	: 119.821953
H49	-C3	-C4	: 116.225461	C5	-C4	-C3	: 124.208854
H50	-C4	-C3	: 117.109269	H50	-C4	-C5	: 118.681853
C6	-C5	-C4	: 124.675488	H51	-C5	-C4	: 118.423311
H51	-C5	-C6	: 116.901130	C7	-C6	-C5	: 124.321341
H52	-C6	-C5	: 117.138688	H52	-C6	-C7	: 118.539948
C8	-C7	-C6	: 124.495173	H53	-C7	-C6	: 118.429924
H53	-C7	-C8	: 117.074848	C9	-C8	-C7	: 124.532479
H54	-C8	-C7	: 117.058574	H54	-C8	-C9	: 118.408921
C10	-C9	-C8	: 124.318750	H55	-C9	-C8	: 118.474807
H55	-C9	-C10	: 117.206407	C11	-C10	-C9	: 124.768502
H56	-C10	-C9	: 116.972722	H56	-C10	-C11	: 118.258752
C12	-C11	-C10	: 123.999786	H57	-C11	-C10	: 118.586548
H57	-C11	-C12	: 117.413644	C13	-C12	-C11	: 125.120868
H58	-C12	-C11	: 116.809475	H58	-C12	-C13	: 118.069642
C14	-C13	-C12	: 123.722171	H59	-C13	-C12	: 118.700291
H59	-C13	-C14	: 117.577523	C15	-C14	-C13	: 125.266368
H60	-C14	-C13	: 116.738696	H60	-C14	-C15	: 117.994928
C16	-C15	-C14	: 123.804014	H82	-C15	-C14	: 118.707193
H82	-C15	-C16	: 117.488788	C17	-C16	-C15	: 125.126670
H61	-C16	-C15	: 116.796565	H61	-C16	-C17	: 118.076757
C18	-C17	-C16	: 123.963531	H62	-C17	-C16	: 118.626440
H62	-C17	-C18	: 117.410028	C19	-C18	-C17	: 125.011720
H81	-C18	-C17	: 116.833617	H81	-C18	-C19	: 118.154651
C20	-C19	-C18	: 124.040723	H63	-C19	-C18	: 118.559951
H63	-C19	-C20	: 117.399325	C21	-C20	-C19	: 124.912634
H64	-C20	-C19	: 116.880068	H64	-C20	-C21	: 118.207264
C22	-C21	-C20	: 124.118711	H65	-C21	-C20	: 118.550281
H65	-C21	-C22	: 117.331007	C23	-C22	-C21	: 124.813566
H66	-C22	-C21	: 116.946814	H66	-C22	-C23	: 118.239573
C24	-C23	-C22	: 124.081483	H67	-C23	-C22	: 118.591573
H67	-C23	-C24	: 117.326944	C25	-C24	-C23	: 124.919268
H68	-C24	-C23	: 116.894181	H68	-C24	-C25	: 118.186496
C26	-C25	-C24	: 123.942716	H69	-C25	-C24	: 118.671065
H69	-C25	-C26	: 117.386219	C27	-C26	-C25	: 125.001670
H70	-C26	-C25	: 116.836267	H70	-C26	-C27	: 118.161993
C28	-C27	-C26	: 123.884287	H71	-C27	-C26	: 118.733742
H71	-C27	-C28	: 117.381970	C29	-C28	-C27	: 125.004040
H72	-C28	-C27	: 116.760610	H72	-C28	-C29	: 118.235279
C30	-C29	-C28	: 123.820607	H73	-C29	-C28	: 118.853787
H73	-C29	-C30	: 117.325606	C31	-C30	-C29	: 124.271856
H74	-C30	-C29	: 116.022543	H74	-C30	-C31	: 119.705523
C32	-C31	-C30	: 127.381229	H75	-C31	-C30	: 117.516431
H75	-C31	-C32	: 115.102333	C33	-C32	-C31	: 123.525634
C37	-C32	-C31	: 118.759343	C37	-C32	-C33	: 117.715011
C34	-C33	-C32	: 120.884576	H80	-C33	-C32	: 119.969032
H80	-C33	-C34	: 119.146372	C35	-C34	-C33	: 120.545017
H79	-C34	-C33	: 119.558041	H79	-C34	-C35	: 119.896941
C36	-C35	-C34	: 119.403242	H78	-C35	-C34	: 120.245960
H78	-C35	-C36	: 120.350796	C37	-C36	-C35	: 120.107896

H77	-C36	-C35	: 120.153951	H77	-C36	-C37	: 119.738153
C36	-C37	-C32	: 121.344239	H76	-C37	-C32	: 118.935553
H76	-C37	-C36	: 119.720208	C39	-C38	-C1	: 120.933245
H47	-C38	-C1	: 119.945917	H47	-C38	-C39	: 119.120833
C40	-C39	-C38	: 120.525973	H46	-C39	-C38	: 119.556372
H46	-C39	-C40	: 119.917654	C41	-C40	-C39	: 119.376200
H45	-C40	-C39	: 120.249314	H45	-C40	-C41	: 120.374485
C42	-C41	-C40	: 120.133030	H44	-C41	-C40	: 120.129062
H44	-C41	-C42	: 119.737908	C41	-C42	-C1	: 121.355871
H43	-C42	-C1	: 118.932944	H43	-C42	-C41	: 119.711182

torsional angles:

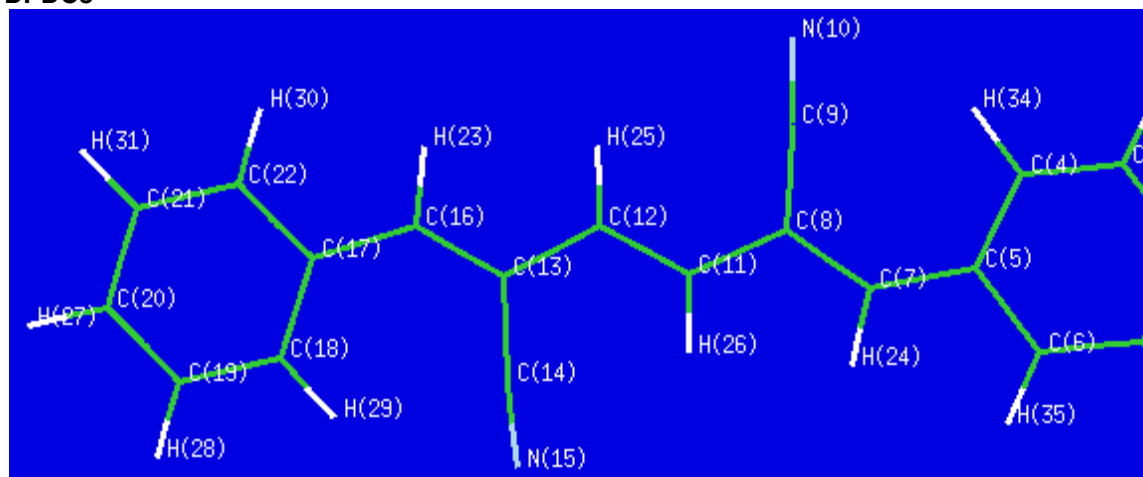
C1	-C2	-C3	-C4	: 179.866435
C1	-C2	-C3	-H49	: -0.055862
C1	-C38	-C39	-C40	: 0.026616
C1	-C38	-C39	-H46	: -179.986622
C1	-C42	-C41	-C40	: 0.001221
C1	-C42	-C41	-H44	: -179.994338
C2	-C1	-C38	-C39	: -179.955528
C2	-C1	-C38	-H47	: 0.019218
C2	-C1	-C42	-C41	: 179.944439
C2	-C1	-C42	-H43	: -0.037118
C2	-C3	-C4	-C5	: -179.835121
C2	-C3	-C4	-H50	: 0.107954
C3	-C2	-C1	-C38	: -0.109877
C3	-C2	-C1	-C42	: 179.945436
C3	-C4	-C5	-C6	: 179.890131
C3	-C4	-C5	-H51	: -0.009300
C4	-C3	-C2	-H48	: -0.104065
C4	-C5	-C6	-C7	: -179.800244
C4	-C5	-C6	-H52	: 0.142939
C5	-C4	-C3	-H49	: 0.089730
C5	-C6	-C7	-C8	: 179.924993
C5	-C6	-C7	-H53	: 0.013323
C6	-C5	-C4	-H50	: -0.052110
C6	-C7	-C8	-C9	: -179.790811
C6	-C7	-C8	-H54	: 0.149520
C7	-C6	-C5	-H51	: 0.100579
C7	-C8	-C9	-C10	: 179.947481
C7	-C8	-C9	-H55	: 0.018652
C8	-C7	-C6	-H52	: -0.017451
C8	-C9	-C10	-C11	: -179.786811
C8	-C9	-C10	-H56	: 0.156324
C9	-C8	-C7	-H53	: 0.121952
C9	-C10	-C11	-C12	: 179.943265
C9	-C10	-C11	-H57	: -0.001343
C10	-C9	-C8	-H54	: 0.007894
C10	-C11	-C12	-C13	: -179.790397
C10	-C11	-C12	-H58	: 0.164206
C11	-C10	-C9	-H55	: 0.142845
C11	-C12	-C13	-C14	: 179.910560
C11	-C12	-C13	-H59	: -0.044186

C12	-C11	-C10	-H56	:	0.000802
C12	-C13	-C14	-C15	:	-179.803164
C12	-C13	-C14	-H60	:	0.164734
C13	-C12	-C11	-H57	:	0.154810
C13	-C14	-C15	-C16	:	179.880554
C13	-C14	-C15	-H82	:	-0.095037
C14	-C13	-C12	-H58	:	-0.043522
C14	-C15	-C16	-C17	:	-179.838422
C14	-C15	-C16	-H61	:	0.129073
C15	-C14	-C13	-H59	:	0.152054
C15	-C16	-C17	-C18	:	179.843142
C15	-C16	-C17	-H62	:	-0.144493
C16	-C15	-C14	-H60	:	-0.086978
C16	-C17	-C18	-C19	:	-179.875325
C16	-C17	-C18	-H81	:	0.083206
C17	-C16	-C15	-H82	:	0.137445
C17	-C18	-C19	-C20	:	179.830215
C17	-C18	-C19	-H63	:	-0.159426
C18	-C17	-C16	-H61	:	-0.123974
C18	-C19	-C20	-C21	:	-179.887850
C18	-C19	-C20	-H64	:	0.043236
C19	-C18	-C17	-H62	:	0.112449
C19	-C20	-C21	-C22	:	179.829916
C19	-C20	-C21	-H65	:	-0.158903
C20	-C19	-C18	-H81	:	-0.127816
C20	-C21	-C22	-C23	:	-179.942318
C20	-C21	-C22	-H66	:	-0.023346
C21	-C20	-C19	-H63	:	0.101902
C21	-C22	-C23	-C24	:	179.856728
C21	-C22	-C23	-H67	:	-0.135240
C22	-C21	-C20	-H64	:	-0.100332
C22	-C23	-C24	-C25	:	179.993588
C22	-C23	-C24	-H68	:	-0.093685
C23	-C22	-C21	-H65	:	0.046626
C23	-C24	-C25	-C26	:	179.884909
C23	-C24	-C25	-H69	:	-0.105051
C24	-C23	-C22	-H66	:	-0.061284
C24	-C25	-C26	-C27	:	179.977867
C24	-C25	-C26	-H70	:	-0.120494
C25	-C24	-C23	-H67	:	-0.014351
C25	-C26	-C27	-C28	:	179.906367
C25	-C26	-C27	-H71	:	-0.086777
C26	-C25	-C24	-H68	:	-0.026785
C26	-C27	-C28	-C29	:	179.980280
C26	-C27	-C28	-H72	:	-0.118379
C27	-C26	-C25	-H69	:	-0.032054
C27	-C28	-C29	-C30	:	179.927831
C27	-C28	-C29	-H73	:	-0.077817
C28	-C27	-C26	-H70	:	0.005920
C28	-C29	-C30	-C31	:	179.997723
C28	-C29	-C30	-H74	:	-0.104866
C29	-C28	-C27	-H71	:	-0.026490
C29	-C30	-C31	-C32	:	179.950043

C29	-C30	-C31	-H75	:	-0.020412
C30	-C29	-C28	-H72	:	0.027820
C30	-C31	-C32	-C33	:	0.283783
C30	-C31	-C32	-C37	:	-179.676287
C31	-C30	-C29	-H73	:	0.003291
C31	-C32	-C33	-C34	:	-179.929993
C31	-C32	-C33	-H80	:	0.120508
C31	-C32	-C37	-C36	:	179.928647
C31	-C32	-C37	-H76	:	-0.063110
C32	-C31	-C30	-H74	:	0.056180
C32	-C33	-C34	-C35	:	0.005388
C32	-C33	-C34	-H79	:	-179.980827
C32	-C37	-C36	-C35	:	0.001031
C32	-C37	-C36	-H77	:	179.997450
C33	-C32	-C31	-H75	:	-179.745153
C33	-C32	-C37	-C36	:	-0.033751
C33	-C32	-C37	-H76	:	179.974491
C33	-C34	-C35	-C36	:	-0.038869
C33	-C34	-C35	-H78	:	179.979266
C34	-C33	-C32	-C37	:	0.030466
C34	-C35	-C36	-C37	:	0.035597
C34	-C35	-C36	-H77	:	-179.960807
C35	-C34	-C33	-H80	:	179.955297
C35	-C36	-C37	-H76	:	179.992725
C36	-C35	-C34	-H79	:	179.947299
C37	-C32	-C31	-H75	:	0.294777
C37	-C32	-C33	-H80	:	-179.919034
C37	-C36	-C35	-H78	:	-179.982558
C38	-C1	-C2	-H48	:	179.861226
C38	-C1	-C42	-C41	:	-0.003550
C38	-C1	-C42	-H43	:	-179.985107
C38	-C39	-C40	-C41	:	-0.028621
C38	-C39	-C40	-H45	:	179.983441
C39	-C38	-C1	-C42	:	-0.010310
C39	-C40	-C41	-C42	:	0.014771
C39	-C40	-C41	-H44	:	-179.989687
C40	-C39	-C38	-H47	:	-179.948334
C40	-C41	-C42	-H43	:	179.982637
C41	-C40	-C39	-H46	:	179.984664
C42	-C1	-C2	-H48	:	-0.083462
C42	-C1	-C38	-H47	:	179.964435
C42	-C41	-C40	-H45	:	-179.997307
H43	-C42	-C41	-H44	:	-0.012923
H44	-C41	-C40	-H45	:	-0.001765
H45	-C40	-C39	-H46	:	-0.003274
H46	-C39	-C38	-H47	:	0.038428
H48	-C2	-C3	-H49	:	179.973638
H49	-C3	-C4	-H50	:	-179.967195
H50	-C4	-C5	-H51	:	-179.951542
H51	-C5	-C6	-H52	:	-179.956238
H52	-C6	-C7	-H53	:	-179.929121
H53	-C7	-C8	-H54	:	-179.937718
H54	-C8	-C9	-H55	:	-179.920934

H55	-C9	-C10	-H56	:-179.914020
H56	-C10	-C11	-H57	:-179.943806
H57	-C11	-C12	-H58	:-179.890587
H58	-C12	-C13	-H59	:-179.998268
H59	-C13	-C14	-H60	:-179.880048
H60	-C14	-C15	-H82	: 179.937431
H61	-C16	-C15	-H82	:-179.895060
H61	-C16	-C17	-H62	: 179.888391
H62	-C17	-C18	-H81	:-179.929020
H63	-C19	-C18	-H81	: 179.882544
H63	-C19	-C20	-H64	:-179.967013
H64	-C20	-C21	-H65	: 179.910850
H65	-C21	-C22	-H66	: 179.965598
H66	-C22	-C23	-H67	: 179.946748
H67	-C23	-C24	-H68	: 179.898376
H68	-C24	-C25	-H69	: 179.983255
H69	-C25	-C26	-H70	: 179.869585
H70	-C26	-C27	-H71	:-179.987224
H71	-C27	-C28	-H72	: 179.874851
H72	-C28	-C29	-H73	:-179.977827
H73	-C29	-C30	-H74	: 179.900701
H74	-C30	-C31	-H75	:-179.914275
H76	-C37	-C36	-H77	: -0.010856
H77	-C36	-C35	-H78	: 0.021038
H78	-C35	-C34	-H79	: -0.034565
H79	-C34	-C33	-H80	: -0.030918



**$\alpha,\omega$ -diphenyl- $\mu,\nu$ -dicyano-oligoene (DPDCn) Series:****DPDC3**

final geometry:

atom	angstroms		
	x	y	z
C1	0.0381824916	-0.1227603836	-0.2673295124
C2	-0.2117708504	-0.6567283298	0.9975668046
C3	0.8459437885	-0.8475952316	1.8909054414
C4	2.1475446870	-0.5114388428	1.5347028258
C5	2.4182916768	0.0291818696	0.2593850383
C6	1.3362597060	0.2145640979	-0.6287728769
C7	3.7295080231	0.4183500785	-0.2316873774
C8	4.9798793012	0.3898709402	0.3206839049
C9	5.2494922254	-0.0870492097	1.6447285370
N10	5.5276665244	-0.4619501885	2.7110929237
C11	6.1152606212	0.8622925178	-0.4568587258
C12	7.4081776482	0.9023809817	-0.0653453624
C13	8.4928584952	1.3910825136	-0.9093782547
C14	8.1050839066	1.8418707965	-2.2153216392
N15	7.7128822233	2.1902684475	-3.2543543146
C16	9.7883969479	1.4163822232	-0.4757024823
C17	11.0205697875	1.8492569924	-1.1218434294
C18	11.1194781809	2.3458119328	-2.4398994431
C19	12.3500002450	2.7322988710	-2.9580994685
C20	13.5106560124	2.6370557537	-2.1868494556
C21	13.4332011212	2.1474417956	-0.8824679209
C22	12.2051938427	1.7589988316	-0.3596609423
H23	9.9297509456	1.0476423746	0.5385878616
H24	3.7084729765	0.8120977016	-1.2461391016
H25	7.6929352388	0.5591145947	0.9262003426
H26	5.8603420128	1.2122263831	-1.4541124432
H27	14.4676714308	2.9414896019	-2.6000853122
H28	12.4031549256	3.1112564405	-3.9742670771
H29	10.2401366793	2.4309301300	-3.0631843680
H30	12.1501325940	1.3778835930	0.6569136791
H31	14.3286351384	2.0680884280	-0.2732973270
H32	-1.2239867829	-0.9230947522	1.2872675723

H33	0.6538467648	-1.2629739733	2.8756649088
H34	2.9496325789	-0.6689066653	2.2451647884
H35	1.5294538228	0.6301711788	-1.6142993694
H36	-0.7763419456	0.0297764742	-0.9689999963

Final total energy: -880.026574 hartrees

HOMO energy: -0.21161

LUMO energy: -0.09611

bond lengths (angstroms):

C1	-C2	:	1.395550	C1	-C6	:	1.389041
C1	-H36	:	1.085845	C2	-C3	:	1.397585
C2	-H32	:	1.086029	C3	-C4	:	1.390700
C3	-H33	:	1.085906	C4	-C5	:	1.411386
C4	-H34	:	1.083004	C5	-C6	:	1.412085
C5	-C7	:	1.453235	C6	-H35	:	1.086883
C7	-C8	:	1.367243	C7	-H24	:	1.088390
C8	-C9	:	1.432912	C8	-C11	:	1.454938
C9	-N10	:	1.164072	C11	-C12	:	1.351490
C11	-H26	:	1.087176	C12	-C13	:	1.458682
C12	-H25	:	1.087236	C13	-C14	:	1.434945
C13	-C16	:	1.366431	C14	-N15	:	1.163955
C16	-C17	:	1.457096	C16	-H23	:	1.088455
C17	-C18	:	1.411957	C17	-C22	:	1.411525
C18	-C19	:	1.389996	C18	-H29	:	1.081189
C19	-C20	:	1.396789	C19	-H28	:	1.085832
C20	-C21	:	1.395397	C20	-H27	:	1.085966
C21	-C22	:	1.390042	C21	-H31	:	1.085904
C22	-H30	:	1.087062				

bond angles:

C6	-C1	-C2	:	119.745360	H36	-C1	-C2	:	120.337691
H36	-C1	-C6	:	119.916948	C3	-C2	-C1	:	119.739757
H32	-C2	-C1	:	120.169308	H32	-C2	-C3	:	120.090935
C4	-C3	-C2	:	120.770286	H33	-C3	-C2	:	119.869253
H33	-C3	-C4	:	119.360461	C5	-C4	-C3	:	120.236295
H34	-C4	-C3	:	119.340178	H34	-C4	-C5	:	120.423526
C6	-C5	-C4	:	118.139862	C7	-C5	-C4	:	125.520866
C7	-C5	-C6	:	116.339268	C5	-C6	-C1	:	121.368431
H35	-C6	-C1	:	119.664220	H35	-C6	-C5	:	118.967349
C8	-C7	-C5	:	133.082454	H24	-C7	-C5	:	113.228750
H24	-C7	-C8	:	113.688794	C9	-C8	-C7	:	123.525998
C11	-C8	-C7	:	119.405603	C11	-C8	-C9	:	117.068372
N10	-C9	-C8	:	176.989041	C12	-C11	-C8	:	126.967346
H26	-C11	-C8	:	114.314742	H26	-C11	-C12	:	118.717896
C13	-C12	-C11	:	123.620621	H25	-C12	-C11	:	120.357081
H25	-C12	-C13	:	116.022286	C14	-C13	-C12	:	115.525276
C16	-C13	-C12	:	121.842313	C16	-C13	-C14	:	122.632304
N15	-C14	-C13	:	175.957874	C17	-C16	-C13	:	131.799332
H23	-C16	-C13	:	114.368857	H23	-C16	-C17	:	113.831743
C18	-C17	-C16	:	125.286671	C22	-C17	-C16	:	116.824397
C22	-C17	-C18	:	117.888887	C19	-C18	-C17	:	120.518161
H29	-C18	-C17	:	120.587670	H29	-C18	-C19	:	118.894142

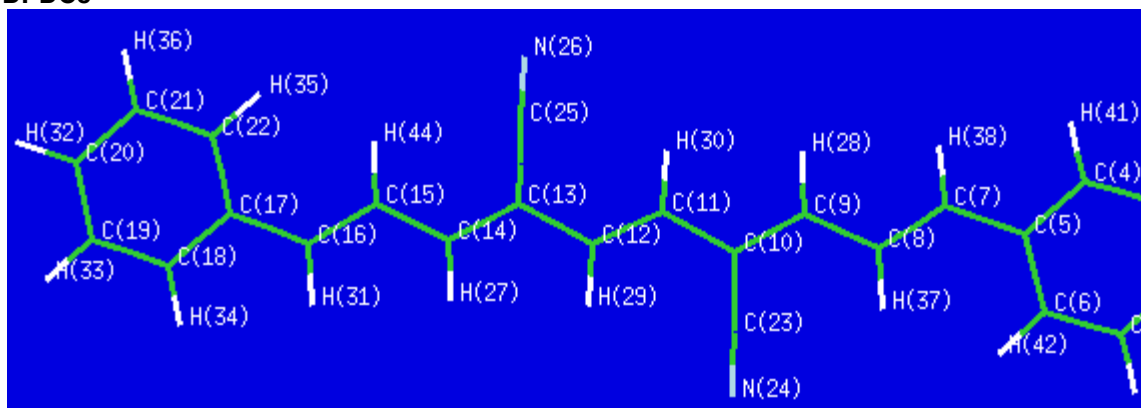
C20	-C19	-C18	: 120.717360	H28	-C19	-C18	: 119.292274
H28	-C19	-C20	: 119.990363	C21	-C20	-C19	: 119.600285
H27	-C20	-C19	: 120.202118	H27	-C20	-C21	: 120.197581
C22	-C21	-C20	: 119.911762	H31	-C21	-C20	: 120.282198
H31	-C21	-C22	: 119.806038	C21	-C22	-C17	: 121.363413
H30	-C22	-C17	: 119.003748	H30	-C22	-C21	: 119.632820

torsional angles:

C1	-C2	-C3	-C4	: -0.000219
C1	-C2	-C3	-H33	: -179.997425
C1	-C6	-C5	-C4	: -0.017565
C1	-C6	-C5	-C7	: 179.960127
C2	-C1	-C6	-C5	: -0.006699
C2	-C1	-C6	-H35	: 179.989223
C2	-C3	-C4	-C5	: -0.024626
C2	-C3	-C4	-H34	: 179.987319
C3	-C2	-C1	-C6	: 0.015819
C3	-C2	-C1	-H36	: -179.990527
C3	-C4	-C5	-C6	: 0.032998
C3	-C4	-C5	-C7	: -179.942439
C4	-C3	-C2	-H32	: -179.998206
C4	-C5	-C6	-H35	: 179.986485
C4	-C5	-C7	-C8	: -0.030917
C4	-C5	-C7	-H24	: 179.955720
C5	-C4	-C3	-H33	: 179.972594
C5	-C6	-C1	-H36	: 179.999621
C5	-C7	-C8	-C9	: -0.042298
C5	-C7	-C8	-C11	: 179.896028
C6	-C1	-C2	-H32	: -179.986195
C6	-C5	-C4	-H34	: -179.979078
C6	-C5	-C7	-C8	: 179.993251
C6	-C5	-C7	-H24	: -0.020111
C7	-C5	-C4	-H34	: 0.045485
C7	-C5	-C6	-H35	: -0.035823
C7	-C8	-C9	-N10	: -179.949241
C7	-C8	-C11	-C12	: -179.978082
C7	-C8	-C11	-H26	: -0.025894
C8	-C11	-C12	-C13	: 179.909171
C8	-C11	-C12	-H25	: -0.050135
C9	-C8	-C7	-H24	: 179.971111
C9	-C8	-C11	-C12	: -0.035821
C9	-C8	-C11	-H26	: 179.916368
N10	-C9	-C8	-C11	: 0.111096
C11	-C8	-C7	-H24	: -0.090563
C11	-C12	-C13	-C14	: 0.062118
C11	-C12	-C13	-C16	: 179.945939
C12	-C13	-C14	-N15	: 1.360596
C12	-C13	-C16	-C17	: 179.942251
C12	-C13	-C16	-H23	: -0.160563
C13	-C12	-C11	-H26	: -0.041148
C13	-C16	-C17	-C18	: -1.248127
C13	-C16	-C17	-C22	: 178.831136

C14	-C13	-C12	-H25	:-179.976958
C14	-C13	-C16	-C17	: -0.182238
C14	-C13	-C16	-H23	: 179.714947
N15	-C14	-C13	-C16	:-178.522211
C16	-C13	-C12	-H25	: -0.093137
C16	-C17	-C18	-C19	: 179.976028
C16	-C17	-C18	-H29	: -0.083873
C16	-C17	-C22	-C21	:-179.938052
C16	-C17	-C22	-H30	: 0.010966
C17	-C18	-C19	-C20	: 0.011914
C17	-C18	-C19	-H28	: 179.991092
C17	-C22	-C21	-C20	: -0.072942
C17	-C22	-C21	-H31	: 179.943250
C18	-C17	-C16	-H23	: 178.854257
C18	-C17	-C22	-C21	: 0.135150
C18	-C17	-C22	-H30	:-179.915832
C18	-C19	-C20	-C21	: 0.053432
C18	-C19	-C20	-H27	:-179.993012
C19	-C18	-C17	-C22	: -0.104001
C19	-C20	-C21	-C22	: -0.023155
C19	-C20	-C21	-H31	: 179.960575
C20	-C19	-C18	-H29	:-179.929188
C20	-C21	-C22	-H30	: 179.978356
C21	-C20	-C19	-H28	:-179.925601
C22	-C17	-C16	-H23	: -1.066480
C22	-C17	-C18	-H29	: 179.836099
C22	-C21	-C20	-H27	:-179.976714
H25	-C12	-C11	-H26	: 179.999546
H27	-C20	-C19	-H28	: 0.027955
H27	-C20	-C21	-H31	: 0.007017
H28	-C19	-C18	-H29	: 0.049990
H30	-C22	-C21	-H31	: -0.005453
H32	-C2	-C1	-H36	: 0.007458
H32	-C2	-C3	-H33	: 0.004588
H33	-C3	-C4	-H34	: -0.015461
H35	-C6	-C1	-H36	: -0.004457

## DPDC5



final geometry:

atom	angstroms		
	x	y	z
C1	-0.1162094820	-0.0069872294	0.0075163409
C2	-0.0971985878	0.0551256162	1.4043488578
C3	1.1240553839	0.1004591200	2.0769409569
C4	2.3145713883	0.0838401412	1.3573900706
C5	2.3153503036	0.0218035298	-0.0498604949
C6	1.0716494531	-0.0236013473	-0.7129172555
C7	3.5961934258	0.0084899811	-0.7437397582
C8	3.8160788025	-0.0425768383	-2.0833050998
C9	5.1321719836	-0.0471446615	-2.6403519872
C10	5.4473262951	-0.0953593792	-3.9762893570
C11	6.8163323676	-0.0917403839	-4.4464336255
C12	7.1972279364	-0.1338986058	-5.7470852309
C13	8.5693978625	-0.1259842123	-6.2079260596
C14	8.9030445836	-0.1689513257	-7.5393040282
C15	10.2298178425	-0.1623663843	-8.0702239561
C16	10.4844024034	-0.2085424413	-9.4032722639
C17	11.7861634243	-0.2037394032	-10.0578137895
C18	11.8332372278	-0.2764519445	-11.4634862502
C19	13.0464418358	-0.2775817909	-12.1445604870
C20	14.2446453825	-0.2043562558	-11.4342009295
C21	14.2176642251	-0.1304677267	-10.0382588868
C22	13.0072780005	-0.1302707711	-9.3564651336
C23	4.3955218310	-0.1505472314	-4.9509694692
N24	3.5540482242	-0.1966854697	-5.7541516885
C25	9.6110730655	-0.0707111669	-5.2219269690
N26	10.4438745279	-0.0252934473	-4.4098672882
H27	8.0799789576	-0.2133159652	-8.2504122342
H28	5.9669642668	-0.0073327401	-1.9424402754
H29	6.4382401775	-0.1762378124	-6.5251467709
H30	7.5779565851	-0.0501786756	-3.6708158762
H31	9.6294346747	-0.2589597250	-10.0772067483
H32	15.1937345768	-0.2042497639	-11.9617497767
H33	13.0572219538	-0.3353392913	-13.2288788118
H34	10.9015384182	-0.3335477252	-12.0204068243
H35	13.0099184544	-0.0715733850	-8.2726988053
H36	15.1475334032	-0.0723760513	-9.4803697847

H37	2.9814102474	-0.0798848027	-2.7782705864
H38	4.4705502530	0.0456153114	-0.0946658394
H39	-1.0288392745	0.0678339467	1.9619880112
H40	1.1488472140	0.1487768212	3.1615009654
H41	3.2646135822	0.1195135516	1.8843673351
H42	1.0343280881	-0.0723702119	-1.7965716567
H43	-1.0644270195	-0.0426095752	-0.5205492836
H44	11.0480052084	-0.1138829669	-7.3569537537

Final total energy: -1034.854828 hartrees

HOMO energy: -0.19793

LUMO energy: -0.10237

bond lengths (angstroms):

C1	-C2	:	1.398342	C1	-C6	:	1.389356
C1	-H43	:	1.085928	C2	-C3	:	1.394954
C2	-H39	:	1.085853	C3	-C4	:	1.391171
C3	-H40	:	1.085919	C4	-C5	:	1.408618
C4	-H41	:	1.086995	C5	-C6	:	1.410141
C5	-C7	:	1.456779	C6	-H42	:	1.085393
C7	-C8	:	1.358452	C7	-H38	:	1.089576
C8	-C9	:	1.429134	C8	-H37	:	1.086757
C9	-C10	:	1.373454	C9	-H28	:	1.088827
C10	-C11	:	1.447490	C10	-C23	:	1.435040
C11	-C12	:	1.355933	C11	-H30	:	1.087833
C12	-C13	:	1.447511	C12	-H29	:	1.087766
C13	-C14	:	1.373220	C13	-C25	:	1.435387
C14	-C15	:	1.429072	C14	-H27	:	1.088614
C15	-C16	:	1.357926	C15	-H44	:	1.086525
C16	-C17	:	1.457062	C16	-H31	:	1.089816
C17	-C18	:	1.408339	C17	-C22	:	1.410109
C18	-C19	:	1.391305	C18	-H34	:	1.086960
C19	-C20	:	1.394871	C19	-H33	:	1.085909
C20	-C21	:	1.398157	C20	-H32	:	1.085854
C21	-C22	:	1.389200	C21	-H36	:	1.085943
C22	-H35	:	1.085358	C23	-N24	:	1.164177
C25	-N26	:	1.164071				

bond angles:

C6	-C1	-C2	:	120.456608	H43	-C1	-C2	:	119.939422
H43	-C1	-C6	:	119.603969	C3	-C2	-C1	:	119.668843
H39	-C2	-C1	:	120.122487	H39	-C2	-C3	:	120.208670
C4	-C3	-C2	:	119.962325	H40	-C3	-C2	:	120.198076
H40	-C3	-C4	:	119.839599	C5	-C4	-C3	:	121.179705
H41	-C4	-C3	:	119.788582	H41	-C4	-C5	:	119.031709
C6	-C5	-C4	:	118.078450	C7	-C5	-C4	:	118.472511
C7	-C5	-C6	:	123.449033	C5	-C6	-C1	:	120.654066
H42	-C6	-C1	:	119.264778	H42	-C6	-C5	:	120.081154
C8	-C7	-C5	:	127.759477	H38	-C7	-C5	:	114.929567
H38	-C7	-C8	:	117.310914	C9	-C8	-C7	:	122.245080
H37	-C8	-C7	:	120.501929	H37	-C8	-C9	:	117.252873
C10	-C9	-C8	:	126.196473	H28	-C9	-C8	:	117.135124
H28	-C9	-C10	:	116.668347	C11	-C10	-C9	:	122.198869
C23	-C10	-C9	:	119.591692	C23	-C10	-C11	:	118.209424
C12	-C11	-C10	:	125.250989	H30	-C11	-C10	:	115.510951
H30	-C11	-C12	:	119.238019	C13	-C12	-C11	:	124.855413
H29	-C12	-C11	:	119.427852	H29	-C12	-C13	:	115.716703



C14	-C13	-C12	: 122.603119	C25	-C13	-C12	: 117.998910
C25	-C13	-C14	: 119.397970	C15	-C14	-C13	: 125.847062
H27	-C14	-C13	: 116.801164	H27	-C14	-C15	: 117.351717
C16	-C15	-C14	: 122.589108	H44	-C15	-C14	: 117.093556
H44	-C15	-C16	: 120.316840	C17	-C16	-C15	: 127.472165
H31	-C16	-C15	: 117.487631	H31	-C16	-C17	: 115.039803
C18	-C17	-C16	: 118.558897	C22	-C17	-C16	: 123.395441
C22	-C17	-C18	: 118.045658	C19	-C18	-C17	: 121.183687
H34	-C18	-C17	: 119.042381	H34	-C18	-C19	: 119.773901
C20	-C19	-C18	: 119.980591	H33	-C19	-C18	: 119.835042
H33	-C19	-C20	: 120.184366	C21	-C20	-C19	: 119.647092
H32	-C20	-C19	: 120.225111	H32	-C20	-C21	: 120.127791
C22	-C21	-C20	: 120.452597	H36	-C21	-C20	: 119.948825
H36	-C21	-C22	: 119.598574	C21	-C22	-C17	: 120.690329
H35	-C22	-C17	: 120.103719	H35	-C22	-C21	: 119.205915
N24	-C23	-C10	: 179.152182	N26	-C25	-C13	: 179.149764

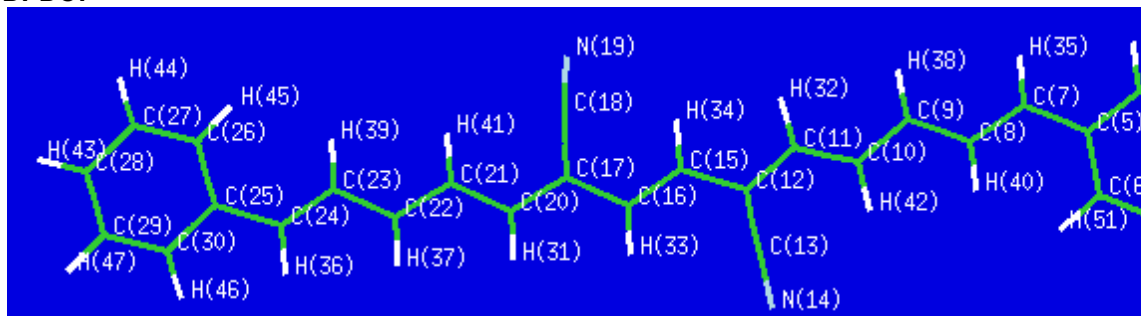
torsional angles:

C1	-C2	-C3	-C4	: 0.004838
C1	-C2	-C3	-H40	:-179.997744
C1	-C6	-C5	-C4	: 0.014070
C1	-C6	-C5	-C7	:-179.956406
C2	-C1	-C6	-C5	: -0.001078
C2	-C1	-C6	-H42	: 179.982384
C2	-C3	-C4	-C5	: 0.008622
C2	-C3	-C4	-H41	: 179.985348
C3	-C2	-C1	-C6	: -0.008586
C3	-C2	-C1	-H43	: 179.989954
C3	-C4	-C5	-C6	: -0.017896
C3	-C4	-C5	-C7	: 179.954080
C4	-C3	-C2	-H39	: 179.996583
C4	-C5	-C6	-H42	:-179.969257
C4	-C5	-C7	-C8	:-179.731967
C4	-C5	-C7	-H38	: 0.190537
C5	-C4	-C3	-H40	:-179.988805
C5	-C6	-C1	-H43	:-179.999623
C5	-C7	-C8	-C9	: 179.863616
C5	-C7	-C8	-H37	: -0.008116
C6	-C1	-C2	-H39	: 179.999663
C6	-C5	-C4	-H41	:-179.994795
C6	-C5	-C7	-C8	: 0.238400
C6	-C5	-C7	-H38	:-179.839097
C7	-C5	-C4	-H41	: -0.022818
C7	-C5	-C6	-H42	: 0.060267
C7	-C8	-C9	-C10	:-179.927227
C7	-C8	-C9	-H28	: -0.016851
C8	-C9	-C10	-C11	: 179.808953
C8	-C9	-C10	-C23	: -0.146896
C9	-C8	-C7	-H38	: -0.057292
C9	-C10	-C11	-C12	:-179.815392
C9	-C10	-C11	-H30	: 0.110056
C9	-C10	-C23	-N24	:-176.491045

C10	-C9	-C8	-H37	:	-0.051544
C10	-C11	-C12	-C13	:	179.811853
C10	-C11	-C12	-H29	:	-0.121229
C11	-C10	-C9	-H28	:	-0.101792
C11	-C10	-C23	-N24	:	3.551351
C11	-C12	-C13	-C14	:	-179.939335
C11	-C12	-C13	-C25	:	0.056896
C12	-C11	-C10	-C23	:	0.141041
C12	-C13	-C14	-C15	:	179.897512
C12	-C13	-C14	-H27	:	-0.192045
C12	-C13	-C25	-N26	:	-1.164141
C13	-C12	-C11	-H30	:	-0.111040
C13	-C14	-C15	-C16	:	179.921159
C13	-C14	-C15	-H44	:	-0.334685
C14	-C13	-C12	-H29	:	-0.004027
C14	-C13	-C25	-N26	:	178.832214
C14	-C15	-C16	-C17	:	179.827182
C14	-C15	-C16	-H31	:	-0.415836
C15	-C14	-C13	-C25	:	-0.098667
C15	-C16	-C17	-C18	:	179.127671
C15	-C16	-C17	-C22	:	-0.852543
C16	-C15	-C14	-H27	:	0.011157
C16	-C17	-C18	-C19	:	-179.910704
C16	-C17	-C18	-H34	:	0.025305
C16	-C17	-C22	-C21	:	179.960496
C16	-C17	-C22	-H35	:	-0.109410
C17	-C16	-C15	-H44	:	0.091033
C17	-C18	-C19	-C20	:	-0.069786
C17	-C18	-C19	-H33	:	179.943137
C17	-C22	-C21	-C20	:	-0.031528
C17	-C22	-C21	-H36	:	179.946527
C18	-C17	-C16	-H31	:	-0.634382
C18	-C17	-C22	-C21	:	-0.019813
C18	-C17	-C22	-H35	:	179.910281
C18	-C19	-C20	-C21	:	0.016888
C18	-C19	-C20	-H32	:	-179.956852
C19	-C18	-C17	-C22	:	0.070579
C19	-C20	-C21	-C22	:	0.033350
C19	-C20	-C21	-H36	:	-179.944629
C20	-C19	-C18	-H34	:	179.994666
C20	-C21	-C22	-H35	:	-179.962243
C21	-C20	-C19	-H33	:	-179.996081
C22	-C17	-C16	-H31	:	179.385404
C22	-C17	-C18	-H34	:	-179.993411
C22	-C21	-C20	-H32	:	-179.992885
C23	-C10	-C9	-H28	:	179.942359
C23	-C10	-C11	-H30	:	-179.933511
C25	-C13	-C12	-H29	:	179.992204
C25	-C13	-C14	-H27	:	179.811775
H27	-C14	-C15	-H44	:	179.755313
H28	-C9	-C8	-H37	:	179.858832
H29	-C12	-C11	-H30	:	179.955878
H31	-C16	-C15	-H44	:	179.848016

H32	-C20	-C19	-H33	:	0.030179
H32	-C20	-C21	-H36	:	0.029137
H33	-C19	-C18	-H34	:	0.007590
H35	-C22	-C21	-H36	:	0.015812
H37	-C8	-C7	-H38	:	-179.929024
H39	-C2	-C1	-H43	:	-0.001797
H39	-C2	-C3	-H40	:	-0.005999
H40	-C3	-C4	-H41	:	-0.012079
H42	-C6	-C1	-H43	:	-0.016161

## DPDC7



final geometry:

atom	angstroms		
	x	y	z
C1	0.0758788280	-0.0963861364	-0.1259788144
C2	-0.0010154487	-0.1261026227	1.2691602386
C3	1.1715276728	-0.0953052956	2.0234684011
C4	2.4106114462	-0.0361143624	1.3908297581
C5	2.5070182105	-0.0052728190	-0.0118206090
C6	1.3090832837	-0.0368575468	-0.7567592075
C7	3.8177626736	0.0478662714	-0.6504145160
C8	4.0077008268	0.0844900955	-1.9910243664
C9	5.2477631261	0.1104392573	-2.6968638262
C10	5.2529066684	0.1223500341	-4.0617289000
C11	6.4117517755	0.1147927644	-4.8752304006
C12	6.4118759274	0.1022248826	-6.2529128979
C13	5.1633648911	0.1127970051	-6.9577744888
N14	4.1369937483	0.1218181781	-7.5076247676
C15	7.6541347974	0.0674140456	-6.9742741256
C16	7.8519345917	0.0403046056	-8.3161981898
C17	9.1785863179	-0.0011965258	-8.8892561238
C18	10.2758951120	-0.0232050524	-7.9629024707
N19	11.1329879155	-0.0419034352	-7.1756901390
C20	9.4464635203	-0.0182985792	-10.2370344449
C21	10.7538989871	-0.0457944348	-10.8025034664
C22	10.9984852476	-0.0485910648	-12.1431265934
C23	12.3064019178	-0.0563923320	-12.7273097480
C24	12.4993415940	-0.0447949656	-14.0700319766
C25	13.7536129439	-0.0349691506	-14.8106351404
C26	15.0277077250	-0.0382114769	-14.2066158174
C27	16.1788618750	-0.0230967302	-14.9859326027
C28	16.0924252165	-0.0042749374	-16.3815178882
C29	14.8398553387	-0.0012424228	-16.9951107542
C30	13.6873138685	-0.0166098988	-16.2174965040
H31	8.5964043583	-0.0032649747	-10.9167757062
H32	7.3822315259	0.1065337226	-4.3839162652
H33	7.0117396999	0.0483591698	-9.0058581491
H34	8.5318832618	0.0583134866	-6.3336937345
H35	4.6825023331	0.0509709734	0.0113840405
H36	11.6062899897	-0.0359339287	-14.6944155544
H37	10.1517321381	-0.0364290332	-12.8299320659
H38	6.1842634225	0.1073386954	-2.1406389854

H39	13.1539790211	-0.0652811078	-12.0451897306
H40	3.1333798866	0.0847426368	-2.6362908565
H41	11.5978783058	-0.0575651724	-10.1159027669
H42	4.2921052200	0.1245128870	-4.5724540265
H43	16.9961191052	0.0077294511	-16.9835750433
H44	17.1526150450	-0.0256876346	-14.5047968688
H45	15.1166993436	-0.0516310944	-13.1247310177
H46	12.7121147903	-0.0133386367	-16.6978271791
H47	14.7612730485	0.0132559366	-18.0782833274
H48	-0.9673785229	-0.1733307534	1.7621393935
H49	1.1213532040	-0.1181465813	3.1081767838
H50	3.3204316703	-0.0137153235	1.9849285082
H51	1.3373876195	-0.0176080699	-1.8402973007
H52	-0.8315412700	-0.1208032974	-0.7222925819

Final total energy: -1189.672379 hartrees

HOMO energy: -0.18875

LUMO energy: -0.10648

bond lengths (angstroms):

C1	-C2	:	1.397572	C1	-C6	:	1.386442
C1	-H52	:	1.086093	C2	-C3	:	1.394556
C2	-H48	:	1.085871	C3	-C4	:	1.392503
C3	-H49	:	1.086108	C4	-C5	:	1.406298
C4	-H50	:	1.086843	C5	-C6	:	1.411021
C5	-C7	:	1.458999	C6	-H51	:	1.084079
C7	-C8	:	1.354493	C7	-H35	:	1.088927
C8	-C9	:	1.427108	C8	-H40	:	1.086649
C9	-C10	:	1.364927	C9	-H38	:	1.089233
C10	-C11	:	1.415897	C10	-H42	:	1.088110
C11	-C12	:	1.377740	C11	-H32	:	1.087791
C12	-C13	:	1.433779	C12	-C15	:	1.436935
C13	-N14	:	1.164412	C15	-C16	:	1.356694
C15	-H34	:	1.086678	C16	-C17	:	1.445726
C16	-H33	:	1.087025	C17	-C18	:	1.436211
C17	-C20	:	1.374248	C18	-N19	:	1.163899
C20	-C21	:	1.424745	C20	-H31	:	1.088520
C21	-C22	:	1.362755	C21	-H41	:	1.088053
C22	-C23	:	1.432472	C22	-H37	:	1.090340
C23	-C24	:	1.356563	C23	-H39	:	1.088004
C24	-C25	:	1.456635	C24	-H36	:	1.089713
C25	-C26	:	1.410024	C25	-C30	:	1.408542
C26	-C27	:	1.390223	C26	-H45	:	1.085622
C27	-C28	:	1.398386	C27	-H44	:	1.086137
C28	-C29	:	1.394789	C28	-H43	:	1.085946
C29	-C30	:	1.390421	C29	-H47	:	1.086116
C30	-H46	:	1.087079				

bond angles:

C6	-C1	-C2	:	120.266522	H52	-C1	-C2	:	120.108718
H52	-C1	-C6	:	119.624735	C3	-C2	-C1	:	119.552623
H48	-C2	-C1	:	120.204839	H48	-C2	-C3	:	120.242532
C4	-C3	-C2	:	120.222927	H49	-C3	-C2	:	120.058971
H49	-C3	-C4	:	119.718088	C5	-C4	-C3	:	121.002287
H50	-C4	-C3	:	119.829811	H50	-C4	-C5	:	119.167894
C6	-C5	-C4	:	117.896896	C7	-C5	-C4	:	119.930189
C7	-C5	-C6	:	122.171439	C5	-C6	-C1	:	121.058729
H51	-C6	-C1	:	118.601995	H51	-C6	-C5	:	120.339063
C8	-C7	-C5	:	124.067610	H35	-C7	-C5	:	116.584802
H35	-C7	-C8	:	119.346384	C9	-C8	-C7	:	127.724500
H40	-C8	-C7	:	118.353155	H40	-C8	-C9	:	113.919066
C10	-C9	-C8	:	119.868104	H38	-C9	-C8	:	119.634909
H38	-C9	-C10	:	120.492074	C11	-C10	-C9	:	125.279128

H42	-C10	-C9	: 117.777389	H42	-C10	-C11	: 116.938217
C12	-C11	-C10	: 125.074923	H32	-C11	-C10	: 118.081492
H32	-C11	-C12	: 116.839572	C13	-C12	-C11	: 119.435598
C15	-C12	-C11	: 120.151752	C15	-C12	-C13	: 120.410575
N14	-C13	-C12	: 178.731407	C16	-C15	-C12	: 128.541084
H34	-C15	-C12	: 113.739375	H34	-C15	-C16	: 117.719019
C17	-C16	-C15	: 121.764311	H33	-C16	-C15	: 120.977551
H33	-C16	-C17	: 117.258124	C18	-C17	-C16	: 116.479505
C20	-C17	-C16	: 124.609144	C20	-C17	-C18	: 118.911267
N19	-C18	-C17	: 177.604665	C21	-C20	-C17	: 124.636197
H31	-C20	-C17	: 117.389695	H31	-C20	-C21	: 117.972898
C22	-C21	-C20	: 123.723577	H41	-C21	-C20	: 117.488274
H41	-C21	-C22	: 118.786502	C23	-C22	-C21	: 124.407571
H37	-C22	-C21	: 118.702706	H37	-C22	-C23	: 116.887985
C24	-C23	-C22	: 122.240021	H39	-C23	-C22	: 117.106744
H39	-C23	-C24	: 120.651952	C25	-C24	-C23	: 128.738894
H36	-C24	-C23	: 116.785027	H36	-C24	-C25	: 114.475129
C26	-C25	-C24	: 124.073020	C30	-C25	-C24	: 117.864697
C30	-C25	-C26	: 118.061933	C27	-C26	-C25	: 120.534182
H45	-C26	-C25	: 120.066165	H45	-C26	-C27	: 119.399627
C28	-C27	-C26	: 120.558045	H44	-C27	-C26	: 119.604591
H44	-C27	-C28	: 119.837362	C29	-C28	-C27	: 119.641747
H43	-C28	-C27	: 120.132949	H43	-C28	-C29	: 120.225303
C30	-C29	-C28	: 119.890253	H47	-C29	-C28	: 120.247026
H47	-C29	-C30	: 119.862721	C29	-C30	-C25	: 121.313827
H46	-C30	-C25	: 118.920212	H46	-C30	-C29	: 119.765922

torsional angles:

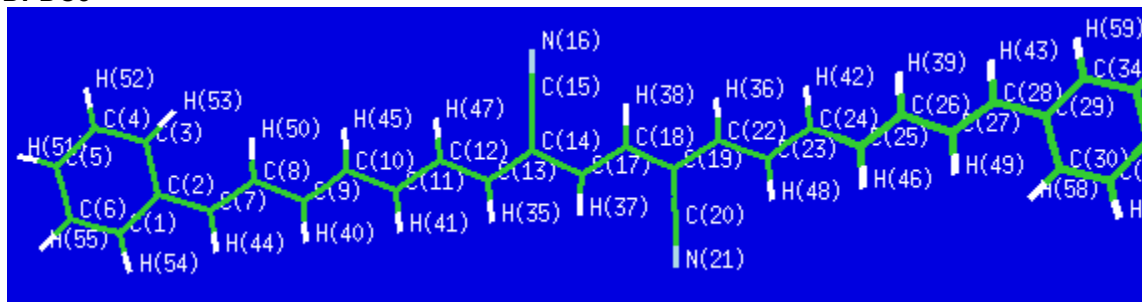
C1	-C2	-C3	-C4	: -0.036450
C1	-C2	-C3	-H49	: -179.993428
C1	-C6	-C5	-C4	: 0.001399
C1	-C6	-C5	-C7	: 179.558875
C2	-C1	-C6	-C5	: 0.009508
C2	-C1	-C6	-H51	: 179.842328
C2	-C3	-C4	-C5	: 0.048095
C2	-C3	-C4	-H50	: -179.919025
C3	-C2	-C1	-C6	: 0.007933
C3	-C2	-C1	-H52	: 179.949783
C3	-C4	-C5	-C6	: -0.030138
C3	-C4	-C5	-C7	: -179.597915
C4	-C3	-C2	-H48	: 179.934535
C4	-C5	-C6	-H51	: -179.828531
C4	-C5	-C7	-C8	: -179.789335
C4	-C5	-C7	-H35	: 0.613572
C5	-C4	-C3	-H49	: -179.994780
C5	-C6	-C1	-H52	: -179.932623
C5	-C7	-C8	-C9	: -178.646533
C5	-C7	-C8	-H40	: 0.651019
C6	-C1	-C2	-H48	: -179.963063
C6	-C5	-C4	-H50	: 179.937197
C6	-C5	-C7	-C8	: 0.661951
C6	-C5	-C7	-H35	: -178.935143

C7	-C5	-C4	-H50	:	0.369419
C7	-C5	-C6	-H51	:	-0.271055
C7	-C8	-C9	-C10	:	178.825274
C7	-C8	-C9	-H38	:	-0.372525
C8	-C9	-C10	-C11	:	-178.357280
C8	-C9	-C10	-H42	:	0.779686
C9	-C8	-C7	-H35	:	0.940114
C9	-C10	-C11	-C12	:	178.747225
C9	-C10	-C11	-H32	:	-0.498956
C10	-C9	-C8	-H40	:	-0.498470
C10	-C11	-C12	-C13	:	0.773403
C10	-C11	-C12	-C15	:	-178.704898
C11	-C10	-C9	-H38	:	0.833541
C11	-C12	-C13	-N14	:	0.133552
C11	-C12	-C15	-C16	:	179.439957
C11	-C12	-C15	-H34	:	-0.288193
C12	-C11	-C10	-H42	:	-0.396258
C12	-C15	-C16	-C17	:	-179.636845
C12	-C15	-C16	-H33	:	0.320003
C13	-C12	-C11	-H32	:	-179.971972
C13	-C12	-C15	-C16	:	-0.033209
C13	-C12	-C15	-H34	:	-179.761359
N14	-C13	-C12	-C15	:	179.610475
C15	-C12	-C11	-H32	:	0.549727
C15	-C16	-C17	-C18	:	0.490015
C15	-C16	-C17	-C20	:	-179.402853
C16	-C17	-C18	-N19	:	2.435192
C16	-C17	-C20	-C21	:	179.344865
C16	-C17	-C20	-H31	:	-0.245736
C17	-C16	-C15	-H34	:	0.082047
C17	-C20	-C21	-C22	:	-179.300356
C17	-C20	-C21	-H41	:	0.226215
C18	-C17	-C16	-H33	:	-179.468365
C18	-C17	-C20	-C21	:	-0.545590
C18	-C17	-C20	-H31	:	179.863809
N19	-C18	-C17	-C20	:	-177.665536
C20	-C17	-C16	-H33	:	0.638766
C20	-C21	-C22	-C23	:	179.046608
C20	-C21	-C22	-H37	:	-0.458030
C21	-C22	-C23	-C24	:	-179.295248
C21	-C22	-C23	-H39	:	0.294942
C22	-C21	-C20	-H31	:	0.288053
C22	-C23	-C24	-C25	:	179.219577
C22	-C23	-C24	-H36	:	-0.403248
C23	-C22	-C21	-H41	:	-0.474191
C23	-C24	-C25	-C26	:	0.102562
C23	-C24	-C25	-C30	:	-179.677470
C24	-C23	-C22	-H37	:	0.217593
C24	-C25	-C26	-C27	:	-179.754754
C24	-C25	-C26	-H45	:	0.186395
C24	-C25	-C30	-C29	:	179.755420
C24	-C25	-C30	-H46	:	-0.173281
C25	-C24	-C23	-H39	:	-0.356379



C25	-C26	-C27	-C28	:	0.007381
C25	-C26	-C27	-H44	:	179.990738
C25	-C30	-C29	-C28	:	0.018776
C25	-C30	-C29	-H47	:	-179.970558
C26	-C25	-C24	-H36	:	179.732614
C26	-C25	-C30	-C29	:	-0.038102
C26	-C25	-C30	-H46	:	-179.966802
C26	-C27	-C28	-C29	:	-0.027425
C26	-C27	-C28	-H43	:	179.983385
C27	-C26	-C25	-C30	:	0.024876
C27	-C28	-C29	-C30	:	0.014396
C27	-C28	-C29	-H47	:	-179.996312
C28	-C27	-C26	-H45	:	-179.934157
C28	-C29	-C30	-H46	:	179.946882
C29	-C28	-C27	-H44	:	179.989258
C30	-C25	-C24	-H36	:	-0.047418
C30	-C25	-C26	-H45	:	179.966025
C30	-C29	-C28	-H43	:	-179.996424
H31	-C20	-C21	-H41	:	179.814623
H32	-C11	-C10	-H42	:	-179.642438
H33	-C16	-C15	-H34	:	-179.961105
H35	-C7	-C8	-H40	:	-179.762334
H36	-C24	-C23	-H39	:	-179.979204
H37	-C22	-C21	-H41	:	-179.978828
H37	-C22	-C23	-H39	:	179.807782
H38	-C9	-C8	-H40	:	-179.696269
H38	-C9	-C10	-H42	:	179.970508
H43	-C28	-C27	-H44	:	0.000067
H43	-C28	-C29	-H47	:	-0.007131
H44	-C27	-C26	-H45	:	0.049199
H46	-C30	-C29	-H47	:	-0.042452
H48	-C2	-C1	-H52	:	-0.021213
H48	-C2	-C3	-H49	:	-0.022443
H49	-C3	-C4	-H50	:	0.038100
H51	-C6	-C1	-H52	:	-0.099803

## DPDC9



final geometry:

atom	angstroms			
	x	y	z	
C1	0.1960386397	0.2858460312	0.3519596121	
C2	0.1948422846	0.2390581649	1.6992741428	
C3	1.3814750432	0.0789003086	2.5024865347	
C4	1.3966531730	0.0465999345	3.8622464284	
C5	2.5888453871	-0.0943257407	4.6415591165	
C6	2.6271119244	-0.1016665843	6.0067373826	
C7	3.8367461520	-0.2154273783	6.7498529646	
C8	3.9541249676	-0.1948233960	8.1215082920	
C9	5.2297405595	-0.2827936665	8.7948134666	
C10	5.4077420935	-0.2148811336	10.1394099157	
C11	6.6833477181	-0.2694344571	10.8158013080	
C12	6.7994744236	-0.1426954576	12.1818078799	
C13	8.0102577153	-0.1542718794	12.9312956106	
C14	8.0469062065	0.0081139443	14.2869742143	
C15	9.2429339321	0.0245794738	15.0728105109	
C16	9.2604002158	0.2070774818	16.4207645875	
C17	10.4548191019	0.2389596172	17.2278642124	
C18	10.4602096186	0.4296149020	18.5624408184	
C19	2.7755291655	-0.0633001522	8.9283110972	
N20	1.8311337202	0.0418608332	9.6009917298	
C21	7.8622584985	-0.4465250334	10.0186992416	
N22	8.8066247366	-0.5920683319	9.3535126823	
H23	1.1496330358	0.1935718346	-0.1692860668	
H24	-0.7522343985	0.3312623256	2.2311314888	
H25	2.3272284393	-0.0152865567	1.9684943321	
H26	0.4555401022	0.1421391391	4.4026651345	
H27	3.5270212914	-0.1914045917	4.0948496798	
H28	1.6965569216	-0.0026298301	6.5622034637	
H29	4.7611600885	-0.3153213683	6.1840700533	
H30	6.0967345684	-0.3963504788	8.1482865572	
H31	4.5399879694	-0.0941670936	10.7836318637	
H32	5.8727485697	-0.0091257388	12.7370074855	
H33	8.9439631252	-0.2881115986	12.3885543471	
H34	7.1051168010	0.1438079096	14.8191124658	
H35	10.1872660610	-0.1116308041	14.5469451301	
H36	8.3119231340	0.3443954500	16.9403955855	
H37	11.4038303187	0.1010499365	16.7095339265	
H38	9.5049772081	0.5674876821	19.0704713763	
C39	-1.0171136675	0.4599419857	-0.5056506262	
C40	11.6838331619	0.4711819400	19.4223889894	

H41	11.6471442329	-0.3022209700	20.2007610103
H42	12.5957730128	0.3225537373	18.8369833781
H43	11.7665729300	1.4324295628	19.9463817690
H44	-0.9370012829	1.3624919050	-1.1257393132
H45	-1.1348073930	-0.3818050830	-1.2002412954
H46	-1.9285660189	0.5381220628	0.0936880158

Final total energy: -1344.499258 hartrees

HOMO energy: -0.18270

LUMO energy: -0.10794

bond lengths (angstroms):

C1	-C2	:	1.408511	C1	-C6	:	1.391560
C1	-H54	:	1.087115	C2	-C3	:	1.409929
C2	-C7	:	1.458727	C3	-C4	:	1.389495
C3	-H53	:	1.085541	C4	-C5	:	1.398020
C4	-H52	:	1.086203	C5	-C6	:	1.394816
C5	-H51	:	1.085911	C6	-H55	:	1.086127
C7	-C8	:	1.356858	C7	-H44	:	1.089934
C8	-C9	:	1.432842	C8	-H50	:	1.088248
C9	-C10	:	1.363835	C9	-H40	:	1.090260
C10	-C11	:	1.427048	C10	-H45	:	1.089792
C11	-C12	:	1.367455	C11	-H41	:	1.090297
C12	-C13	:	1.421442	C12	-H47	:	1.088593
C13	-C14	:	1.378091	C13	-H35	:	1.088721
C14	-C15	:	1.433976	C14	-C17	:	1.442605
C15	-N16	:	1.164277	C17	-C18	:	1.359086
C17	-H37	:	1.087392	C18	-C19	:	1.442340
C18	-H38	:	1.087331	C19	-C20	:	1.433747
C19	-C22	:	1.378110	C20	-N21	:	1.164284
C22	-C23	:	1.421302	C22	-H36	:	1.088367
C23	-C24	:	1.367629	C23	-H48	:	1.088486
C24	-C25	:	1.426817	C24	-H42	:	1.090333
C25	-C26	:	1.363929	C25	-H46	:	1.089704
C26	-C27	:	1.432685	C26	-H39	:	1.090287
C27	-C28	:	1.356947	C27	-H49	:	1.088163
C28	-C29	:	1.458657	C28	-H43	:	1.089968
C29	-C30	:	1.410014	C29	-C34	:	1.408471
C30	-C31	:	1.389410	C30	-H58	:	1.085497
C31	-C32	:	1.398066	C31	-H57	:	1.086200
C32	-C33	:	1.394959	C32	-H56	:	1.085934
C33	-C34	:	1.391533	C33	-H60	:	1.086126
C34	-H59	:	1.087107				

bond angles:

C6	-C1	-C2	:	121.264169	H54	-C1	-C2	:	118.981327
H54	-C1	-C6	:	119.754442	C3	-C2	-C1	:	117.873161
C7	-C2	-C1	:	118.653843	C7	-C2	-C3	:	123.472629
C4	-C3	-C2	:	120.808088	H53	-C3	-C2	:	120.025099
H53	-C3	-C4	:	119.166179	C5	-C4	-C3	:	120.482266
H52	-C4	-C3	:	119.588901	H52	-C4	-C5	:	119.928728
C6	-C5	-C4	:	119.532881	H51	-C5	-C4	:	120.185174
H51	-C5	-C6	:	120.281878	C5	-C6	-C1	:	120.039203
H55	-C6	-C1	:	119.797964	H55	-C6	-C5	:	120.162813
C8	-C7	-C2	:	127.556195	H44	-C7	-C2	:	115.050316
H44	-C7	-C8	:	117.393455	C9	-C8	-C7	:	123.655814

H50	-C8	-C7	: 119.961475	H50	-C8	-C9	: 116.382552
C10	-C9	-C8	: 124.044894	H40	-C9	-C8	: 117.244831
H40	-C9	-C10	: 118.709764	C11	-C10	-C9	: 124.239425
H45	-C10	-C9	: 118.656146	H45	-C10	-C11	: 117.103436
C12	-C11	-C10	: 123.933483	H41	-C11	-C10	: 117.332399
H41	-C11	-C12	: 118.733597	C13	-C12	-C11	: 123.522667
H47	-C12	-C11	: 118.772448	H47	-C12	-C13	: 117.704115
C14	-C13	-C12	: 125.731810	H35	-C13	-C12	: 117.540532
H35	-C13	-C14	: 116.727262	C15	-C14	-C13	: 119.330151
C17	-C14	-C13	: 122.746641	C17	-C14	-C15	: 117.922926
N16	-C15	-C14	: 179.009352	C18	-C17	-C14	: 124.947265
H37	-C17	-C14	: 115.762094	H37	-C17	-C18	: 119.290437
C19	-C18	-C17	: 125.194249	H38	-C18	-C17	: 119.187140
H38	-C18	-C19	: 115.618508	C20	-C19	-C18	: 118.064843
C22	-C19	-C18	: 122.505155	C22	-C19	-C20	: 119.429876
N21	-C20	-C19	: 179.036825	C23	-C22	-C19	: 126.060107
H36	-C22	-C19	: 116.580401	H36	-C22	-C23	: 117.359492
C24	-C23	-C22	: 123.205697	H48	-C23	-C22	: 117.871314
H48	-C23	-C24	: 118.922987	C25	-C24	-C23	: 124.194042
H42	-C24	-C23	: 118.601397	H42	-C24	-C25	: 117.204528
C26	-C25	-C24	: 124.077612	H46	-C25	-C24	: 117.226171
H46	-C25	-C26	: 118.696199	C27	-C26	-C25	: 124.129346
H39	-C26	-C25	: 118.668221	H39	-C26	-C27	: 117.202378
C28	-C27	-C26	: 123.622760	H49	-C27	-C26	: 116.394620
H49	-C27	-C28	: 119.982519	C29	-C28	-C27	: 127.557420
H43	-C28	-C27	: 117.399569	H43	-C28	-C29	: 115.042794
C30	-C29	-C28	: 123.450201	C34	-C29	-C28	: 118.672163
C34	-C29	-C30	: 117.877631	C31	-C30	-C29	: 120.814875
H58	-C30	-C29	: 120.018476	H58	-C30	-C31	: 119.166617
C32	-C31	-C30	: 120.472210	H57	-C31	-C30	: 119.593762
H57	-C31	-C32	: 119.934023	C33	-C32	-C31	: 119.537109
H56	-C32	-C31	: 120.181675	H56	-C32	-C33	: 120.281202
C34	-C33	-C32	: 120.040148	H60	-C33	-C32	: 120.165280
H60	-C33	-C34	: 119.794571	C33	-C34	-C29	: 121.257967
H59	-C34	-C29	: 119.002630	H59	-C34	-C33	: 119.739342

torsional angles:

C1	-C2	-C3	-C4	: -0.141430
C1	-C2	-C3	-H53	: 179.566456
C1	-C2	-C7	-C8	: 177.585710
C1	-C2	-C7	-H44	: -2.345640
C1	-C6	-C5	-C4	: -0.007551
C1	-C6	-C5	-H51	: -179.913692
C2	-C1	-C6	-C5	: -0.112548
C2	-C1	-C6	-H55	: 179.937955
C2	-C3	-C4	-C5	: 0.026832
C2	-C3	-C4	-H52	: 179.908394
C2	-C7	-C8	-C9	: 179.413216
C2	-C7	-C8	-H50	: -0.436644
C3	-C2	-C1	-C6	: 0.184739
C3	-C2	-C1	-H54	: -179.905788
C3	-C2	-C7	-C8	: -2.639488

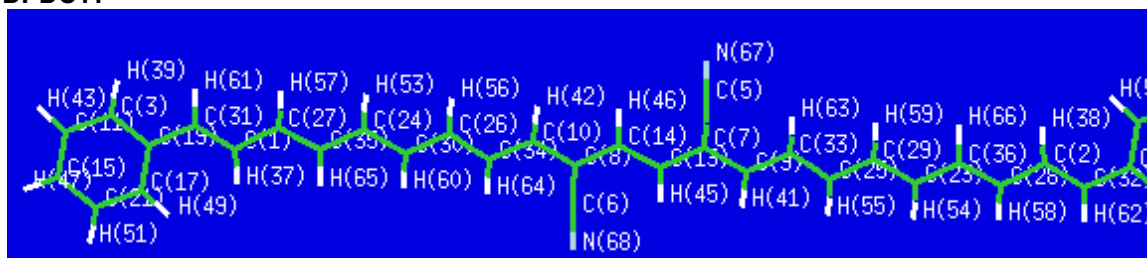
C3	-C2	-C7	-H44	: 177.429162
C3	-C4	-C5	-C6	: 0.049891
C3	-C4	-C5	-H51	: 179.956125
C4	-C3	-C2	-C7	:-179.917875
C4	-C5	-C6	-H55	: 179.941761
C5	-C4	-C3	-H53	:-179.683530
C5	-C6	-C1	-H54	: 179.978669
C6	-C1	-C2	-C7	: 179.972236
C6	-C5	-C4	-H52	:-179.831268
C7	-C2	-C1	-H54	: -0.118291
C7	-C2	-C3	-H53	: -0.209990
C7	-C8	-C9	-C10	:-179.997636
C7	-C8	-C9	-H40	: -0.262029
C8	-C9	-C10	-C11	: 179.267036
C8	-C9	-C10	-H45	: -0.359238
C9	-C8	-C7	-H44	: -0.656831
C9	-C10	-C11	-C12	:-179.805215
C9	-C10	-C11	-H41	: -0.071585
C10	-C9	-C8	-H50	: -0.142835
C10	-C11	-C12	-C13	: 179.278258
C10	-C11	-C12	-H47	: -0.394824
C11	-C10	-C9	-H40	: -0.464955
C11	-C12	-C13	-C14	:-179.902654
C11	-C12	-C13	-H35	: -0.139990
C12	-C11	-C10	-H45	: -0.173621
C12	-C13	-C14	-C15	: -0.443454
C12	-C13	-C14	-C17	: 179.359180
C13	-C12	-C11	-H41	: -0.451881
C13	-C14	-C15	-N16	:-177.614471
C13	-C14	-C17	-C18	:-179.897468
C13	-C14	-C17	-H37	: -0.063459
C14	-C13	-C12	-H47	: -0.226315
C14	-C17	-C18	-C19	: 179.650129
C14	-C17	-C18	-H38	: -0.227782
C15	-C14	-C13	-H35	: 179.792162
C15	-C14	-C17	-C18	: -0.092206
C15	-C14	-C17	-H37	: 179.741803
N16	-C15	-C14	-C17	: 2.573400
C17	-C14	-C13	-H35	: -0.405204
C17	-C18	-C19	-C20	: -0.253039
C17	-C18	-C19	-C22	: 179.877121
C18	-C19	-C20	-N21	: -2.826718
C18	-C19	-C22	-C23	: 179.897335
C18	-C19	-C22	-H36	: -0.111398
C19	-C18	-C17	-H37	: -0.178464
C19	-C22	-C23	-C24	: 179.893146
C19	-C22	-C23	-H48	: -0.088892
C20	-C19	-C18	-H38	: 179.628752
C20	-C19	-C22	-C23	: 0.029207
C20	-C19	-C22	-H36	:-179.979525
N21	-C20	-C19	-C22	: 177.047248
C22	-C19	-C18	-H38	: -0.241088
C22	-C23	-C24	-C25	:-179.984494

C22	-C23	-C24	-H42	:	-0.053030
C23	-C24	-C25	-C26	:	179.781045
C23	-C24	-C25	-H46	:	-0.169508
C24	-C23	-C22	-H36	:	-0.098061
C24	-C25	-C26	-C27	:	-179.929179
C24	-C25	-C26	-H39	:	-0.016551
C25	-C24	-C23	-H48	:	-0.002636
C25	-C26	-C27	-C28	:	179.759877
C25	-C26	-C27	-H49	:	-0.124100
C26	-C25	-C24	-H42	:	-0.151298
C26	-C27	-C28	-C29	:	-179.946290
C26	-C27	-C28	-H43	:	-0.125066
C27	-C26	-C25	-H46	:	0.020695
C27	-C28	-C29	-C30	:	-1.150121
C27	-C28	-C29	-C34	:	178.822516
C28	-C27	-C26	-H39	:	-0.153929
C28	-C29	-C30	-C31	:	179.908996
C28	-C29	-C30	-H58	:	-0.156794
C28	-C29	-C34	-C33	:	-179.880783
C28	-C29	-C34	-H59	:	0.029413
C29	-C28	-C27	-H49	:	-0.066275
C29	-C30	-C31	-C32	:	0.002440
C29	-C30	-C31	-H57	:	179.977929
C29	-C34	-C33	-C32	:	-0.061138
C29	-C34	-C33	-H60	:	179.953428
C30	-C29	-C28	-H43	:	179.025069
C30	-C29	-C34	-C33	:	0.093389
C30	-C29	-C34	-H59	:	-179.996415
C30	-C31	-C32	-C33	:	0.031946
C30	-C31	-C32	-H56	:	179.989142
C31	-C30	-C29	-C34	:	-0.063845
C31	-C32	-C33	-C34	:	-0.002912
C31	-C32	-C33	-H60	:	179.982468
C32	-C31	-C30	-H58	:	-179.932323
C32	-C33	-C34	-H59	:	-179.970682
C33	-C32	-C31	-H57	:	-179.943460
C34	-C29	-C28	-H43	:	-1.002294
C34	-C29	-C30	-H58	:	179.870365
C34	-C33	-C32	-H56	:	-179.960065
H35	-C13	-C12	-H47	:	179.536349
H36	-C22	-C23	-H48	:	179.919902
H37	-C17	-C18	-H38	:	179.943625
H39	-C26	-C25	-H46	:	179.933323
H39	-C26	-C27	-H49	:	179.962094
H40	-C9	-C8	-H50	:	179.592772
H40	-C9	-C10	-H45	:	179.908771
H41	-C11	-C10	-H45	:	179.560009
H41	-C11	-C12	-H47	:	179.875037
H42	-C24	-C23	-H48	:	179.928828
H42	-C24	-C25	-H46	:	179.898149
H43	-C28	-C27	-H49	:	179.754949
H44	-C7	-C8	-H50	:	179.493309
H51	-C5	-C4	-H52	:	0.074965

H51	-C5	-C6	-H55	:	0.035619
H52	-C4	-C3	-H53	:	0.198032
H54	-C1	-C6	-H55	:	0.029172
H56	-C32	-C31	-H57	:	0.013736
H56	-C32	-C33	-H60	:	0.025315
H57	-C31	-C30	-H58	:	0.043166
H59	-C34	-C33	-H60	:	0.043884



## DPDC11



final geometry:

atom	angstroms			
	x	y	z	
C1	-11.5596556375	2.1321136710	-0.2237190568	
C2	11.5596556375	-2.1321136710	0.2237190568	
C3	-15.2992366101	1.9754701035	0.0970934069	
C4	15.2992366101	-1.9754701035	-0.0970934069	
C5	1.5983947691	-1.8906199282	0.7889341316	
C6	-1.5983947691	1.8906199282	-0.7889341316	
C7	1.8045681034	-0.6150266305	0.1671700931	
C8	-1.8045681034	0.6150266305	-0.1671700931	
C9	3.0906744061	-0.2038817456	-0.1179974105	
C10	-3.0906744061	0.2038817456	0.1179974105	
C11	-16.4884936245	2.6555731434	-0.1475192009	
C12	16.4884936245	-2.6555731434	0.1475192009	
C13	0.6420620873	0.1825237890	-0.1313851967	
C14	-0.6420620873	-0.1825237890	0.1313851967	
C15	-16.4626435737	3.9144054140	-0.7478133337	
C16	16.4626435737	-3.9144054140	0.7478133337	
C17	-14.0475176641	3.8059882283	-0.8560762681	
C18	14.0475176641	-3.8059882283	0.8560762681	
C19	-14.0532133857	2.5326867686	-0.2503326080	
C20	14.0532133857	-2.5326867686	0.2503326080	
C21	-15.2355095994	4.4841352260	-1.0999210370	
C22	15.2355095994	-4.4841352260	1.0999210370	
C23	7.9844319544	-0.8897732044	-0.1265253567	
C24	-7.9844319544	0.8897732044	0.1265253567	
C25	5.5363462480	-0.5172763993	-0.1377170203	
C26	-5.5363462480	0.5172763993	0.1377170203	
C27	-10.4215986368	1.3175063719	0.0860354048	
C28	10.4215986368	-1.3175063719	-0.0860354048	
C29	6.7043116764	-1.2830689953	0.1446240491	
C30	-6.7043116764	1.2830689953	-0.1446240491	
C31	-12.8418065074	1.7698518783	0.0317354907	
C32	12.8418065074	-1.7698518783	-0.0317354907	
C33	4.2693566754	-0.9475364588	0.1529603761	
C34	-4.2693566754	0.9475364588	-0.1529603761	
C35	-9.1337616286	1.6834870334	-0.1712502808	
C36	9.1337616286	-1.6834870334	0.1712502808	
H37	-11.3509797636	3.0924395275	-0.6913630857	
H38	11.3509797636	-3.0924395275	0.6913630857	
H39	-15.3253122360	0.9945862552	0.5651668455	
H40	15.3253122360	-0.9945862552	-0.5651668455	

H41	3.2019836857	0.7712267454	-0.5890478363
H42	-3.2019836857	-0.7712267454	0.5890478363
H43	-17.4358750117	2.2028248269	0.1304456489
H44	17.4358750117	-2.2028248269	-0.1304456489
H45	0.8353397389	1.1437756659	-0.6021179099
H46	-0.8353397389	-1.1437756659	0.6021179099
H47	-17.3881945520	4.4486801451	-0.9406202819
H48	17.3881945520	-4.4486801451	0.9406202819
H49	-13.1070664958	4.2688933316	-1.1383974234
H50	13.1070664958	-4.2688933316	1.1383974234
H51	-15.2072376137	5.4640448473	-1.5678152572
H52	15.2072376137	-5.4640448473	1.5678152572
H53	-8.1495174303	-0.0804388403	0.5946226210
H54	8.1495174303	0.0804388403	-0.5946226210
H55	5.6693918655	0.4573369989	-0.6076996863
H56	-5.6693918655	-0.4573369989	0.6076996863
H57	-10.6106902461	0.3514641743	0.5537529104
H58	10.6106902461	-0.3514641743	-0.5537529104
H59	6.5520566702	-2.2548761648	0.6132331594
H60	-6.5520566702	2.2548761648	-0.6132331594
H61	-13.0058522699	0.8000849720	0.5013870966
H62	13.0058522699	-0.8000849720	-0.5013870966
H63	4.1501484730	-1.9219259191	0.6227514052
H64	-4.1501484730	1.9219259191	-0.6227514052
H65	-8.9544283439	2.6512209802	-0.6391930066
H66	8.9544283439	-2.6512209802	0.6391930066
N67	1.4102674640	-2.9226237176	1.2937235252
N68	-1.4102674640	2.9226237176	-1.2937235252

Final total energy: -1499.321022 hartrees

HOMO energy: -0.17812

LUMO energy: -0.10982

bond lengths (angstroms):

C1	-C27	: 1.433425	C1	-C31	: 1.356614
C1	-H37	: 1.088330	C2	-C28	: 1.433425
C2	-C32	: 1.356614	C2	-H38	: 1.088330
C3	-C11	: 1.391656	C3	-C19	: 1.408463
C3	-H39	: 1.087155	C4	-C12	: 1.391656
C4	-C20	: 1.408463	C4	-H40	: 1.087155
C5	-C7	: 1.433958	C5	-N67	: 1.164146
C6	-C8	: 1.433958	C6	-N68	: 1.164146
C7	-C9	: 1.380011	C7	-C13	: 1.441056
C8	-C10	: 1.380011	C8	-C14	: 1.441056
C9	-C33	: 1.419765	C9	-H41	: 1.088630
C10	-C34	: 1.419765	C10	-H42	: 1.088630
C11	-C15	: 1.394876	C11	-H43	: 1.086175
C12	-C16	: 1.394876	C12	-H44	: 1.086175
C13	-C14	: 1.360619	C13	-H45	: 1.087635
C14	-H46	: 1.087635	C15	-C21	: 1.398009
C15	-H47	: 1.085941	C16	-C22	: 1.398009
C16	-H48	: 1.085941	C17	-C19	: 1.410055
C17	-C21	: 1.389485	C17	-H49	: 1.085557
C18	-C20	: 1.410055	C18	-C22	: 1.389485
C18	-H50	: 1.085557	C19	-C31	: 1.459105
C20	-C32	: 1.459105	C21	-H51	: 1.086254
C22	-H52	: 1.086254	C23	-C29	: 1.366350
C23	-C36	: 1.428149	C23	-H54	: 1.089807
C24	-C30	: 1.366350	C24	-C35	: 1.428149
C24	-H53	: 1.089807	C25	-C29	: 1.424885
C25	-C33	: 1.369262	C25	-H55	: 1.090163
C26	-C30	: 1.424885	C26	-C34	: 1.369262
C26	-H56	: 1.090163	C27	-C35	: 1.363328
C27	-H57	: 1.089841	C28	-C36	: 1.363328
C28	-H58	: 1.089841	C29	-H59	: 1.089580
C30	-H60	: 1.089580	C31	-H61	: 1.089923
C32	-H62	: 1.089923	C33	-H63	: 1.088278
C34	-H64	: 1.088278	C35	-H65	: 1.089789
C36	-H66	: 1.089789			

bond angles:

C31	-C1	-C27	: 123.912001	H37	-C1	-C27	: 116.236508
H37	-C1	-C31	: 119.851486	C32	-C2	-C28	: 123.912001
H38	-C2	-C28	: 116.236508	H38	-C2	-C32	: 119.851486
C19	-C3	-C11	: 121.285783	H39	-C3	-C11	: 119.742989
H39	-C3	-C19	: 118.971228	C20	-C4	-C12	: 121.285783
H40	-C4	-C12	: 119.742989	H40	-C4	-C20	: 118.971228
N67	-C5	-C7	: 178.963814	N68	-C6	-C8	: 178.963814

C9	-C7	-C5	: 119.249986	C13	-C7	-C5	: 117.786061
C13	-C7	-C9	: 122.963950	C10	-C8	-C6	: 119.249986
C14	-C8	-C6	: 117.786061	C14	-C8	-C10	: 122.963950
C33	-C9	-C7	: 125.325131	H41	-C9	-C7	: 116.844100
H41	-C9	-C33	: 117.830769	C34	-C10	-C8	: 125.325131
H42	-C10	-C8	: 116.844100	H42	-C10	-C34	: 117.830769
C15	-C11	-C3	: 120.055859	H43	-C11	-C3	: 119.780492
H43	-C11	-C15	: 120.163649	C16	-C12	-C4	: 120.055859
H44	-C12	-C4	: 119.780492	H44	-C12	-C16	: 120.163649
C14	-C13	-C7	: 124.949348	H45	-C13	-C7	: 115.813950
H45	-C13	-C14	: 119.236701	C13	-C14	-C8	: 124.949348
H46	-C14	-C8	: 115.813950	H46	-C14	-C13	: 119.236701
C21	-C15	-C11	: 119.501128	H47	-C15	-C11	: 120.306240
H47	-C15	-C21	: 120.192632	C22	-C16	-C12	: 119.501128
H48	-C16	-C12	: 120.306240	H48	-C16	-C22	: 120.192632
C21	-C17	-C19	: 120.841088	H49	-C17	-C19	: 120.019058
H49	-C17	-C21	: 119.139855	C22	-C18	-C20	: 120.841088
H50	-C18	-C20	: 120.019058	H50	-C18	-C22	: 119.139855
C17	-C19	-C3	: 117.826229	C31	-C19	-C3	: 118.683280
C31	-C19	-C17	: 123.490489	C18	-C20	-C4	: 117.826229
C32	-C20	-C4	: 118.683280	C32	-C20	-C18	: 123.490489
C17	-C21	-C15	: 120.489914	H51	-C21	-C15	: 119.931627
H51	-C21	-C17	: 119.578460	C18	-C22	-C16	: 120.489914
H52	-C22	-C16	: 119.931627	H52	-C22	-C18	: 119.578460
C36	-C23	-C29	: 123.547589	H54	-C23	-C29	: 118.908725
H54	-C23	-C36	: 117.543671	C35	-C24	-C30	: 123.547589
H53	-C24	-C30	: 118.908725	H53	-C24	-C35	: 117.543671
C33	-C25	-C29	: 123.197231	H55	-C25	-C29	: 117.766196
H55	-C25	-C33	: 119.036567	C34	-C26	-C30	: 123.197231
H56	-C26	-C30	: 117.766196	H56	-C26	-C34	: 119.036567
C35	-C27	-C1	: 123.823919	H57	-C27	-C1	: 117.304997
H57	-C27	-C35	: 118.871075	C36	-C28	-C2	: 123.823919
H58	-C28	-C2	: 117.304997	H58	-C28	-C36	: 118.871075
C25	-C29	-C23	: 125.025350	H59	-C29	-C23	: 118.229114
H59	-C29	-C25	: 116.745528	C26	-C30	-C24	: 125.025350
H60	-C30	-C24	: 118.229114	H60	-C30	-C26	: 116.745528
C19	-C31	-C1	: 127.492599	H61	-C31	-C1	: 117.450735
H61	-C31	-C19	: 115.056663	C20	-C32	-C2	: 127.492599
H62	-C32	-C2	: 117.450735	H62	-C32	-C20	: 115.056663
C25	-C33	-C9	: 124.269322	H63	-C33	-C9	: 117.414205
H63	-C33	-C25	: 118.316469	C26	-C34	-C10	: 124.269322
H64	-C34	-C10	: 117.414205	H64	-C34	-C26	: 118.316469
C27	-C35	-C24	: 124.866413	H65	-C35	-C24	: 116.783310
H65	-C35	-C27	: 118.350271	C28	-C36	-C23	: 124.866413
H66	-C36	-C23	: 116.783310	H66	-C36	-C28	: 118.350271

torsional angles:

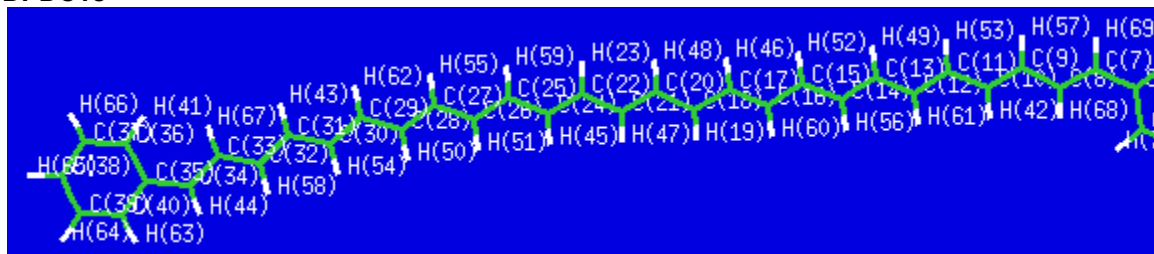
C1	-C27	-C35	-C24	: -179.939193
C1	-C27	-C35	-H65	: 0.031077
C1	-C31	-C19	-C3	: -179.916516
C1	-C31	-C19	-C17	: 0.100215
C2	-C28	-C36	-C23	: 179.939193

C2	-C28	-C36	-H66	:	-0.031077
C2	-C32	-C20	-C4	:	179.916516
C2	-C32	-C20	-C18	:	-0.100215
C3	-C11	-C15	-C21	:	-0.003874
C3	-C11	-C15	-H47	:	179.996266
C3	-C19	-C17	-C21	:	-0.004260
C3	-C19	-C17	-H49	:	179.998234
C3	-C19	-C31	-H61	:	0.104602
C4	-C12	-C16	-C22	:	0.003874
C4	-C12	-C16	-H48	:	-179.996266
C4	-C20	-C18	-C22	:	0.004260
C4	-C20	-C18	-H50	:	-179.998234
C4	-C20	-C32	-H62	:	-0.104602
C5	-C7	-C9	-C33	:	0.055898
C5	-C7	-C9	-H41	:	-179.945230
C5	-C7	-C13	-C14	:	-0.033837
C5	-C7	-C13	-H45	:	179.975781
C6	-C8	-C10	-C34	:	-0.055898
C6	-C8	-C10	-H42	:	179.945230
C6	-C8	-C14	-C13	:	0.033837
C6	-C8	-C14	-H46	:	-179.975781
C7	-C9	-C33	-C25	:	-179.897942
C7	-C9	-C33	-H63	:	0.077435
C7	-C13	-C14	-C8	:	180.000000
C7	-C13	-C14	-H46	:	0.009922
C8	-C10	-C34	-C26	:	179.897942
C8	-C10	-C34	-H64	:	-0.077435
C8	-C14	-C13	-H45	:	-0.009922
C9	-C7	-C5	-N67	:	179.322019
C9	-C7	-C13	-C14	:	179.984942
C9	-C7	-C13	-H45	:	-0.005441
C9	-C33	-C25	-C29	:	179.992632
C9	-C33	-C25	-H55	:	0.021957
C10	-C8	-C6	-N68	:	-179.322019
C10	-C8	-C14	-C13	:	-179.984942
C10	-C8	-C14	-H46	:	0.005441
C10	-C34	-C26	-C30	:	-179.992632
C10	-C34	-C26	-H56	:	-0.021957
C11	-C3	-C19	-C17	:	0.000871
C11	-C3	-C19	-C31	:	-179.983351
C11	-C15	-C21	-C17	:	0.000508
C11	-C15	-C21	-H51	:	179.996185
C12	-C4	-C20	-C18	:	-0.000871
C12	-C4	-C20	-C32	:	179.983351
C12	-C16	-C22	-C18	:	-0.000508
C12	-C16	-C22	-H52	:	-179.996185
C13	-C7	-C5	-N67	:	-0.659923
C13	-C7	-C9	-C33	:	-179.963143
C13	-C7	-C9	-H41	:	0.035729
C14	-C8	-C6	-N68	:	0.659923
C14	-C8	-C10	-C34	:	179.963143
C14	-C8	-C10	-H42	:	-0.035729
C15	-C11	-C3	-C19	:	0.003182

C15	-C11	-C3	-H39	:-179.996191
C15	-C21	-C17	-C19	: 0.003624
C15	-C21	-C17	-H49	:-179.998849
C16	-C12	-C4	-C20	: -0.003182
C16	-C12	-C4	-H40	: 179.996191
C16	-C22	-C18	-C20	: -0.003624
C16	-C22	-C18	-H50	: 179.998849
C17	-C19	-C3	-H39	:-179.999752
C17	-C19	-C31	-H61	:-179.878666
C17	-C21	-C15	-H47	:-179.999631
C18	-C20	-C4	-H40	: 179.999752
C18	-C20	-C32	-H62	: 179.878666
C18	-C22	-C16	-H48	: 179.999631
C19	-C3	-C11	-H43	: 179.998960
C19	-C17	-C21	-H51	:-179.992068
C19	-C31	-C1	-C27	:-179.929021
C19	-C31	-C1	-H37	: 0.047025
C20	-C4	-C12	-H44	:-179.998960
C20	-C18	-C22	-H52	: 179.992068
C20	-C32	-C2	-C28	: 179.929021
C20	-C32	-C2	-H38	: -0.047025
C21	-C15	-C11	-H43	:-179.999636
C21	-C17	-C19	-C31	: 179.979142
C22	-C16	-C12	-H44	: 179.999636
C22	-C18	-C20	-C32	:-179.979142
C23	-C29	-C25	-C33	:-179.864634
C23	-C29	-C25	-H55	: 0.106391
C23	-C36	-C28	-H58	: -0.025922
C24	-C30	-C26	-C34	: 179.864634
C24	-C30	-C26	-H56	: -0.106391
C24	-C35	-C27	-H57	: 0.025922
C25	-C29	-C23	-C36	: 179.955124
C25	-C29	-C23	-H54	: -0.001167
C25	-C33	-C9	-H41	: 0.103197
C26	-C30	-C24	-C35	:-179.955124
C26	-C30	-C24	-H53	: 0.001167
C26	-C34	-C10	-H42	: -0.103197
C27	-C1	-C31	-H61	: 0.049421
C27	-C35	-C24	-C30	: 179.931173
C27	-C35	-C24	-H53	: -0.025674
C28	-C2	-C32	-H62	: -0.049421
C28	-C36	-C23	-C29	:-179.931173
C28	-C36	-C23	-H54	: 0.025674
C29	-C23	-C36	-H66	: 0.039519
C29	-C25	-C33	-H63	: 0.017461
C30	-C24	-C35	-H65	: -0.039519
C30	-C26	-C34	-H64	: -0.017461
C31	-C1	-C27	-C35	:-179.986337
C31	-C1	-C27	-H57	: 0.048043
C31	-C19	-C3	-H39	: 0.016026
C31	-C19	-C17	-H49	: -0.018364
C32	-C2	-C28	-C36	: 179.986337
C32	-C2	-C28	-H58	: -0.048043

C32	-C20	-C4	-H40	:	-0.016026
C32	-C20	-C18	-H50	:	0.018364
C33	-C25	-C29	-H59	:	0.101179
C34	-C26	-C30	-H60	:	-0.101179
C35	-C24	-C30	-H60	:	0.010226
C35	-C27	-C1	-H37	:	0.036824
C36	-C23	-C29	-H59	:	-0.010226
C36	-C28	-C2	-H38	:	-0.036824
H37	-C1	-C27	-H57	:	-179.928796
H37	-C1	-C31	-H61	:	-179.974533
H38	-C2	-C28	-H58	:	179.928796
H38	-C2	-C32	-H62	:	179.974533
H39	-C3	-C11	-H43	:	-0.000412
H40	-C4	-C12	-H44	:	0.000412
H41	-C9	-C33	-H63	:	-179.921426
H42	-C10	-C34	-H64	:	179.921426
H43	-C11	-C15	-H47	:	0.000503
H44	-C12	-C16	-H48	:	-0.000503
H45	-C13	-C14	-H46	:	180.000000
H47	-C15	-C21	-H51	:	-0.003954
H48	-C16	-C22	-H52	:	0.003954
H49	-C17	-C21	-H51	:	0.005459
H50	-C18	-C22	-H52	:	-0.005459
H53	-C24	-C30	-H60	:	179.966516
H53	-C24	-C35	-H65	:	-179.996366
H54	-C23	-C29	-H59	:	-179.966516
H54	-C23	-C36	-H66	:	179.996366
H55	-C25	-C29	-H59	:	-179.927796
H55	-C25	-C33	-H63	:	-179.953214
H56	-C26	-C30	-H60	:	179.927796
H56	-C26	-C34	-H64	:	179.953214
H57	-C27	-C35	-H65	:	179.996192
H58	-C28	-C36	-H66	:	-179.996192

## DPDC13



final geometry:

atom	angstroms			
	x	y	z	
H1	0.1242624540	0.0150421899	0.5865098031	
C2	0.3850863448	0.0250929874	1.6402352085	
C3	1.7396168862	0.0329418828	2.0318719685	
C4	2.8508643276	0.0287933485	1.0878793636	
C5	2.7911169950	0.0186572859	-0.2667712591	
C6	3.9537327364	0.0151470650	-1.1041124963	
C7	3.9303071067	0.0065608895	-2.4672861728	
C8	5.1040714492	0.0032495473	-3.2804754163	
C9	5.1114488082	-0.0034655099	-4.6468614969	
C10	6.3064057372	-0.0063338274	-5.4241778506	
C11	6.3608905734	-0.0108904201	-6.7914597214	
C12	7.5847002125	-0.0131631903	-7.5184897030	
C13	7.6968144209	-0.0152948449	-8.8844424189	
C14	8.9548457411	-0.0170783218	-9.5417705311	
C15	9.1802653906	-0.0168742075	-10.9036605620	
C16	10.5138611047	-0.0183447485	-11.4505621737	
C17	10.8343736617	-0.0151752019	-12.7723080024	
C18	12.1807252979	-0.0160263006	-13.2882620706	
C19	12.4677303978	-0.0090254524	-14.6382762487	
C20	13.7697663125	-0.0083757132	-15.2038836318	
C21	14.0222212360	0.0017101588	-16.5503309271	
C22	15.3344236483	0.0036015386	-17.1043138010	
C23	15.6141236702	0.0162742451	-18.4431385758	
C24	16.9355246616	0.0191405779	-18.9804864866	
C25	17.2301103182	0.0340946143	-20.3142291251	
C26	18.5588291531	0.0377992166	-20.8403193241	
C27	18.8648646870	0.0546502776	-22.1686956473	
C28	20.2028826653	0.0590496104	-22.6846008122	
C29	20.5029597499	0.0774153291	-24.0069253245	
C30	21.8277895077	0.0837172452	-24.6194129957	
C31	8.0671223050	-0.0154098135	-11.8070504246	
N32	7.1735759637	-0.0142832887	-12.5536775094	
C33	13.2625644502	-0.0237301017	-12.3457395004	
N34	14.1286076973	-0.0298127726	-11.5675885368	
H35	19.3768872159	0.0267165538	-20.1199023690	
H36	2.9670613203	0.0015086118	-2.9763732436	
H37	3.8408936490	0.0352413781	1.5428514767	
H38	9.8416208745	-0.0183276713	-8.9103138109	
H39	11.6184749817	-0.0037419973	-15.3193538636	
H40	11.3172828141	-0.0219917590	-10.7175987718	
H41	10.0391382471	-0.0118716965	-13.5138877841	



H42	14.7846839025	0.0245291335	-19.1501864536
H43	7.2487417876	-0.0040182194	-4.8757690434
H44	8.5033703935	-0.0125345349	-6.9312713214
H45	13.1803293693	0.0085084092	-17.2429850149
H46	16.4080893468	0.0436738402	-21.0300804767
H47	6.0625857369	0.0070709656	-2.7614048088
H48	5.4305110136	-0.0133401830	-7.3583358152
H49	16.1681183091	-0.0050787035	-16.4024831994
H50	18.0501469521	0.0653507604	-22.8933150787
H51	4.9214762027	0.0203594998	-0.6023075016
H52	6.7948816566	-0.0161534140	-9.4931768626
H53	14.6160695512	-0.0155783421	-14.5197710290
H54	17.7607879165	0.0091647666	-18.2684979497
H55	4.1603256306	-0.0072575384	-5.1787292911
C56	-0.6285729693	0.0298331104	2.5905957180
C57	-0.3233536112	0.0425436466	3.9546503764
C58	1.0109571620	0.0503940621	4.3602802150
C59	2.0267117889	0.0455543140	3.4103918563
H60	3.0655784264	0.0517195343	3.7308904329
H61	1.2601892458	0.0602918914	5.4174918503
H62	-1.1196207648	0.0462458914	4.6930310020
H63	-1.6657762329	0.0235620060	2.2680805844
H64	1.8262640341	0.0122715197	-0.7699861521
H65	21.0043358502	0.0472498064	-21.9484500438
H66	19.6705725904	0.0886034971	-24.7099626625
C67	21.9222574169	0.1049098322	-26.0249210560
C68	23.1570655385	0.1120322585	-26.6675832122
C69	24.3346599261	0.0979372552	-25.9193023435
C70	24.2603743322	0.0766042548	-24.5229240838
C71	23.0280980037	0.0695687295	-23.8798414949
H72	21.0082216227	0.1156729900	-26.6137562199
H73	23.1996291224	0.1285689307	-27.7529154758
H74	25.2999830298	0.1034798874	-26.4162335614
H75	25.1721064445	0.0654034509	-23.9326750767
H76	22.9970329887	0.0526643376	-22.7949100974

Final total energy: -1654.143389 hartrees

HOMO energy: -0.17442

LUMO energy: -0.10994

bond lengths (angstroms):

H1	-C2	:	1.085572	C2	-C3	:	1.410033
C2	-C56	:	1.389501	C3	-C4	:	1.458084
C3	-C59	:	1.408155	C4	-C5	:	1.356005
C4	-H37	:	1.089587	C5	-C6	:	1.432769
C5	-H64	:	1.088213	C6	-C7	:	1.363402
C6	-H51	:	1.090121	C7	-C8	:	1.427939
C7	-H36	:	1.089513	C8	-C9	:	1.366422
C8	-H47	:	1.090045	C9	-C10	:	1.425535
C9	-H55	:	1.089740	C10	-C11	:	1.368375
C10	-H43	:	1.090300	C11	-C12	:	1.423477
C11	-H48	:	1.089477	C12	-C13	:	1.370548
C12	-H44	:	1.090312	C13	-C14	:	1.419411
C13	-H52	:	1.088137	C14	-C15	:	1.380420
C14	-H38	:	1.088627	C15	-C16	:	1.441382
C15	-C31	:	1.433598	C16	-C17	:	1.360055
C16	-H40	:	1.087536	C17	-C18	:	1.441829
C17	-H41	:	1.087360	C18	-C19	:	1.380203
C18	-C33	:	1.434846	C19	-C20	:	1.419581
C19	-H39	:	1.088636	C20	-C21	:	1.369947
C20	-H53	:	1.088251	C21	-C22	:	1.424351
C21	-H45	:	1.090228	C22	-C23	:	1.367788
C22	-H49	:	1.089811	C23	-C24	:	1.426482
C23	-H42	:	1.089934	C24	-C25	:	1.365970
C24	-H54	:	1.089994	C25	-C26	:	1.429083
C25	-H46	:	1.090070	C26	-C27	:	1.363277
C26	-H35	:	1.090111	C27	-C28	:	1.434040
C27	-H50	:	1.090391	C28	-C29	:	1.356070
C28	-H65	:	1.088294	C29	-C30	:	1.459573
C29	-H66	:	1.089612	C30	-C67	:	1.408839
C30	-C71	:	1.409931	C31	-N32	:	1.164422
C33	-N34	:	1.164297	C56	-C57	:	1.397843
C56	-H63	:	1.086207	C57	-C58	:	1.394626
C57	-H62	:	1.085938	C58	-C59	:	1.390708
C58	-H61	:	1.086237	C59	-H60	:	1.087199
C67	-C68	:	1.392055	C67	-H72	:	1.087338
C68	-C69	:	1.395296	C68	-H73	:	1.086292
C69	-C70	:	1.398516	C69	-H74	:	1.085735
C70	-C71	:	1.390003	C70	-H75	:	1.086174
C71	-H76	:	1.085508				

bond angles:

C3	-C2	-H1	:	120.030425	C56	-C2	-H1	:	119.251827
C56	-C2	-C3	:	120.717747	C4	-C3	-C2	:	123.524411

C59	-C3	-C2	: 117.892202	C59	-C3	-C4	: 118.583388
C5	-C4	-C3	: 127.822245	H37	-C4	-C3	: 114.969478
H37	-C4	-C5	: 117.208269	C6	-C5	-C4	: 123.236936
H64	-C5	-C4	: 120.070918	H64	-C5	-C6	: 116.692140
C7	-C6	-C5	: 124.777915	H51	-C6	-C5	: 116.828433
H51	-C6	-C7	: 118.393642	C8	-C7	-C6	: 123.730027
H36	-C7	-C6	: 118.842449	H36	-C7	-C8	: 117.427519
C9	-C8	-C7	: 125.023944	H47	-C8	-C7	: 116.847661
H47	-C8	-C9	: 118.128383	C10	-C9	-C8	: 123.353390
H55	-C9	-C8	: 118.905106	H55	-C9	-C10	: 117.741499
C11	-C10	-C9	: 125.326033	H43	-C10	-C9	: 116.757698
H43	-C10	-C11	: 117.916256	C12	-C11	-C10	: 122.995407
H48	-C11	-C10	: 119.072025	H48	-C11	-C12	: 117.932563
C13	-C12	-C11	: 125.405584	H44	-C12	-C11	: 116.699666
H44	-C12	-C13	: 117.894739	C14	-C13	-C12	: 122.279555
H52	-C13	-C12	: 119.324133	H52	-C13	-C14	: 118.396305
C15	-C14	-C13	: 126.985632	H38	-C14	-C13	: 116.958753
H38	-C14	-C15	: 116.055610	C16	-C15	-C14	: 121.696656
C31	-C15	-C14	: 119.663256	C31	-C15	-C16	: 118.640088
C17	-C16	-C15	: 125.928663	H40	-C16	-C15	: 115.327470
H40	-C16	-C17	: 118.743864	C18	-C17	-C16	: 124.598466
H41	-C17	-C16	: 119.369992	H41	-C17	-C18	: 116.031541
C19	-C18	-C17	: 122.969395	C33	-C18	-C17	: 117.968626
C33	-C18	-C19	: 119.061968	C20	-C19	-C18	: 125.481930
H39	-C19	-C18	: 116.727386	H39	-C19	-C20	: 117.790683
C21	-C20	-C19	: 124.098908	H53	-C20	-C19	: 117.568429
H53	-C20	-C21	: 118.332645	C22	-C21	-C20	: 123.507500
H45	-C21	-C20	: 118.827376	H45	-C21	-C22	: 117.665122
C23	-C22	-C21	: 124.687720	H49	-C22	-C21	: 117.018234
H49	-C22	-C23	: 118.294033	C24	-C23	-C22	: 123.928881
H42	-C23	-C22	: 118.647748	H42	-C23	-C24	: 117.423370
C25	-C24	-C23	: 124.583243	H54	-C24	-C23	: 117.082715
H54	-C24	-C25	: 118.334033	C26	-C25	-C24	: 124.055038
H46	-C25	-C24	: 118.598921	H46	-C25	-C26	: 117.346040
C27	-C26	-C25	: 124.573185	H35	-C26	-C25	: 117.027677
H35	-C26	-C27	: 118.399132	C28	-C27	-C26	: 124.058445
H50	-C27	-C26	: 118.680672	H50	-C27	-C28	: 117.260882
C29	-C28	-C27	: 123.870183	H65	-C28	-C27	: 116.342626
H65	-C28	-C29	: 119.787181	C30	-C29	-C28	: 127.597218
H66	-C29	-C28	: 117.403574	H66	-C29	-C30	: 114.999204
C67	-C30	-C29	: 118.657397	C71	-C30	-C29	: 123.543633
C71	-C30	-C67	: 117.798970	N32	-C31	-C15	: 179.180262
N34	-C33	-C18	: 179.122984	C57	-C56	-C2	: 120.541829
H63	-C56	-C2	: 119.571011	H63	-C56	-C57	: 119.887160
C58	-C57	-C56	: 119.523443	H62	-C57	-C56	: 120.227642
H62	-C57	-C58	: 120.248915	C59	-C58	-C57	: 120.007925
H61	-C58	-C57	: 120.175717	H61	-C58	-C59	: 119.816358
C58	-C59	-C3	: 121.316853	H60	-C59	-C3	: 118.911390
H60	-C59	-C58	: 119.771756	C68	-C67	-C30	: 121.340928
H72	-C67	-C30	: 118.949618	H72	-C67	-C68	: 119.709453
C69	-C68	-C67	: 120.066326	H73	-C68	-C67	: 119.741694
H73	-C68	-C69	: 120.191980	C70	-C69	-C68	: 119.392711
H74	-C69	-C68	: 120.322650	H74	-C69	-C70	: 120.284638

C71 -C70 -C69 : 120.604462 H75 -C70 -C69 : 119.878359  
 H75 -C70 -C71 : 119.517179 C70 -C71 -C30 : 120.796601  
 H76 -C71 -C30 : 120.003899 H76 -C71 -C70 : 119.199497

torsional angles:

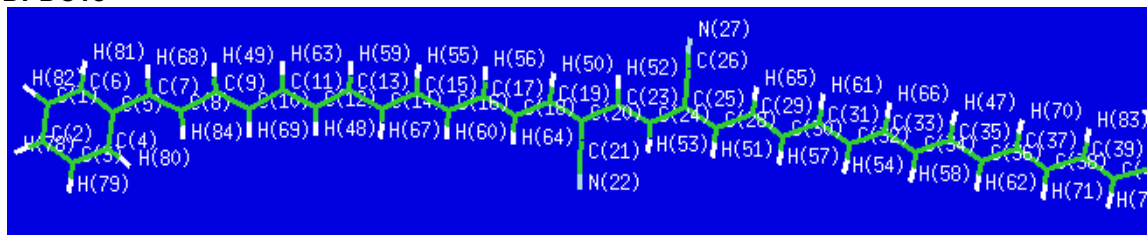
H1 -C2 -C3 -C4 : 0.021524  
 H1 -C2 -C3 -C59 :-179.983458  
 H1 -C2 -C56 -C57 : 179.991052  
 H1 -C2 -C56 -H63 : -0.007301  
 C2 -C3 -C4 -C5 : 0.074942  
 C2 -C3 -C4 -H37 :-179.959362  
 C2 -C3 -C59 -C58 : -0.010401  
 C2 -C3 -C59 -H60 : 179.998515  
 C2 -C56 -C57 -C58 : -0.004849  
 C2 -C56 -C57 -H62 : 179.997030  
 C3 -C2 -C56 -C57 : 0.002467  
 C3 -C2 -C56 -H63 :-179.995886  
 C3 -C4 -C5 -C6 :-179.986724  
 C3 -C4 -C5 -H64 : -0.014430  
 C3 -C59 -C58 -C57 : 0.008214  
 C3 -C59 -C58 -H61 :-179.991919  
 C4 -C3 -C2 -C56 :-179.989979  
 C4 -C3 -C59 -C58 : 179.984869  
 C4 -C3 -C59 -H60 : -0.006215  
 C4 -C5 -C6 -C7 :-179.921754  
 C4 -C5 -C6 -H51 : 0.042062  
 C5 -C4 -C3 -C59 :-179.920044  
 C5 -C6 -C7 -C8 : 179.998520  
 C5 -C6 -C7 -H36 : -0.024930  
 C6 -C5 -C4 -H37 : 0.048242  
 C6 -C7 -C8 -C9 :-179.905567  
 C6 -C7 -C8 -H47 : 0.052765  
 C7 -C6 -C5 -H64 : 0.105083  
 C7 -C8 -C9 -C10 : 179.987769  
 C7 -C8 -C9 -H55 : -0.037195  
 C8 -C7 -C6 -H51 : 0.035225  
 C8 -C9 -C10 -C11 :-179.890933  
 C8 -C9 -C10 -H43 : 0.066803  
 C9 -C8 -C7 -H36 : 0.117576  
 C9 -C10 -C11 -C12 : 179.979108  
 C9 -C10 -C11 -H48 : -0.047419  
 C10 -C9 -C8 -H47 : 0.029925  
 C10 -C11 -C12 -C13 :-179.876224  
 C10 -C11 -C12 -H44 : 0.085095  
 C11 -C10 -C9 -H55 : 0.133759  
 C11 -C12 -C13 -C14 : 179.979968  
 C11 -C12 -C13 -H52 : -0.050687  
 C12 -C11 -C10 -H43 : 0.021816  
 C12 -C13 -C14 -C15 :-179.875244  
 C12 -C13 -C14 -H38 : 0.097084  
 C13 -C12 -C11 -H48 : 0.150018  
 C13 -C14 -C15 -C16 : 179.977427

C13	-C14	-C15	-C31	:	-0.033979
C14	-C13	-C12	-H44	:	0.019067
C14	-C15	-C16	-C17	:	-179.838798
C14	-C15	-C16	-H40	:	0.138852
C14	-C15	-C31	-N32	:	-179.807630
C15	-C14	-C13	-H52	:	0.155139
C15	-C16	-C17	-C18	:	179.964248
C15	-C16	-C17	-H41	:	-0.044350
C16	-C15	-C14	-H38	:	0.004883
C16	-C15	-C31	-N32	:	0.181312
C16	-C17	-C18	-C19	:	-179.817194
C16	-C17	-C18	-C33	:	0.144806
C17	-C16	-C15	-C31	:	0.172495
C17	-C18	-C19	-C20	:	179.946130
C17	-C18	-C19	-H39	:	-0.063832
C17	-C18	-C33	-N34	:	-0.664552
C18	-C17	-C16	-H40	:	-0.012711
C18	-C19	-C20	-C21	:	-179.846551
C18	-C19	-C20	-H53	:	0.103272
C19	-C18	-C17	-H41	:	0.191145
C19	-C18	-C33	-N34	:	179.298975
C19	-C20	-C21	-C22	:	179.934114
C19	-C20	-C21	-H45	:	-0.078269
C20	-C19	-C18	-C33	:	-0.015473
C20	-C21	-C22	-C23	:	-179.862582
C20	-C21	-C22	-H49	:	0.095537
C21	-C20	-C19	-H39	:	0.163508
C21	-C22	-C23	-C24	:	179.943466
C21	-C22	-C23	-H42	:	-0.070415
C22	-C21	-C20	-H53	:	-0.015352
C22	-C23	-C24	-C25	:	-179.879836
C22	-C23	-C24	-H54	:	0.085495
C23	-C22	-C21	-H45	:	0.149667
C23	-C24	-C25	-C26	:	179.952084
C23	-C24	-C25	-H46	:	-0.061112
C24	-C23	-C22	-H49	:	-0.014161
C24	-C25	-C26	-C27	:	-179.898941
C24	-C25	-C26	-H35	:	0.072992
C25	-C24	-C23	-H42	:	0.133888
C25	-C26	-C27	-C28	:	179.958887
C25	-C26	-C27	-H50	:	-0.054223
C26	-C25	-C24	-H54	:	-0.012847
C26	-C27	-C28	-C29	:	-179.919433
C26	-C27	-C28	-H65	:	0.044221
C27	-C26	-C25	-H46	:	0.114102
C27	-C28	-C29	-C30	:	179.976141
C27	-C28	-C29	-H66	:	-0.048772
C28	-C27	-C26	-H35	:	-0.012690
C28	-C29	-C30	-C67	:	-179.941882
C28	-C29	-C30	-C71	:	0.064975
C29	-C28	-C27	-H50	:	0.093506
C29	-C30	-C67	-C68	:	179.992522
C29	-C30	-C67	-H72	:	-0.017736

C29	-C30	-C71	-C70	:-179.997691
C29	-C30	-C71	-H76	: 0.020329
C30	-C29	-C28	-H65	: 0.013671
C30	-C67	-C68	-C69	: 0.007889
C30	-C67	-C68	-H73	:-179.993544
C30	-C71	-C70	-C69	: 0.001708
C30	-C71	-C70	-H75	:-179.999035
C31	-C15	-C14	-H38	: 179.993477
C31	-C15	-C16	-H40	:-179.849855
C33	-C18	-C17	-H41	:-179.846856
C33	-C18	-C19	-H39	: 179.974564
H35	-C26	-C25	-H46	:-179.913965
H35	-C26	-C27	-H50	: 179.974199
H36	-C7	-C6	-H51	:-179.988225
H36	-C7	-C8	-H47	:-179.924093
H37	-C4	-C3	-C59	: 0.045652
H37	-C4	-C5	-H64	:-179.979464
H38	-C14	-C13	-H52	:-179.872534
H39	-C19	-C20	-H53	:-179.886670
H40	-C16	-C17	-H41	: 179.978691
H42	-C23	-C22	-H49	: 179.971958
H42	-C23	-C24	-H54	:-179.900781
H43	-C10	-C9	-H55	:-179.908505
H43	-C10	-C11	-H48	: 179.995289
H44	-C12	-C11	-H48	:-179.888663
H44	-C12	-C13	-H52	: 179.988412
H45	-C21	-C20	-H53	: 179.972264
H45	-C21	-C22	-H49	:-179.892214
H46	-C25	-C24	-H54	: 179.973957
H47	-C8	-C9	-H55	:-179.995039
H50	-C27	-C28	-H65	:-179.942840
H51	-C6	-C5	-H64	:-179.931101
C56	-C2	-C3	-C59	: 0.005038
C56	-C57	-C58	-C59	: -0.000441
C56	-C57	-C58	-H61	: 179.999693
C57	-C58	-C59	-H60	: 179.999223
C58	-C57	-C56	-H63	: 179.993499
C59	-C58	-C57	-H62	: 179.997680
H60	-C59	-C58	-H61	: -0.000910
H61	-C58	-C57	-H62	: -0.002187
H62	-C57	-C56	-H63	: -0.004622
H65	-C28	-C29	-H66	: 179.988758
H66	-C29	-C30	-C67	: 0.082521
H66	-C29	-C30	-C71	:-179.910622
C67	-C30	-C71	-C70	: 0.009111
C67	-C30	-C71	-H76	:-179.972869
C67	-C68	-C69	-C70	: 0.003293
C67	-C68	-C69	-H74	:-179.996416
C68	-C67	-C30	-C71	: -0.013938
C68	-C69	-C70	-C71	: -0.008052
C68	-C69	-C70	-H75	: 179.992694
C69	-C68	-C67	-H72	:-179.981776
C69	-C70	-C71	-H76	: 179.983831

C70	-C69	-C68	-H73	:-179.995268
C71	-C30	-C67	-H72	: 179.975804
C71	-C70	-C69	-H74	: 179.991656
H72	-C67	-C68	-H73	: 0.016791
H73	-C68	-C69	-H74	: 0.005024
H74	-C69	-C70	-H75	: -0.007598
H75	-C70	-C71	-H76	: -0.016912

## DPDC15



final geometry:

atom	x	y	z	angstroms
C1	0.0073500156	0.0047503020	-0.0006584579	
C2	0.0086184680	0.0038894649	1.3945911631	
C3	1.2276598240	0.0041060930	2.0794162974	
C4	2.4297248283	0.0050837280	1.3820581493	
C5	2.4489977482	0.0060203897	-0.0276970055	
C6	1.2110167620	0.0059421132	-0.6999343693	
C7	3.6763532591	0.0071987370	-0.8181254438	
C8	4.9542547086	0.0013413434	-0.3627867723	
C9	6.1079483170	0.0049499252	-1.2152200082	
C10	7.3920582237	-0.0014454812	-0.7582132057	
C11	8.5559246359	0.0035782093	-1.5879591414	
C12	9.8324100370	-0.0044059632	-1.1026147599	
C13	11.0142176653	0.0013568950	-1.9019562962	
C14	12.2785448708	-0.0098907329	-1.3811202626	
C15	13.4811758974	-0.0041049335	-2.1454994314	
C16	14.7305306142	-0.0203793515	-1.5860435925	
C17	15.9531473417	-0.0152059436	-2.3143465320	
C18	17.1861732252	-0.0382654854	-1.7153087855	
C19	18.4171147435	-0.0340755637	-2.4212245848	
C20	19.6710488826	-0.0646928264	-1.8425396110	
C21	19.7789292821	-0.1055443696	-0.4121018522	
N22	19.8854384364	-0.1386923223	0.7468736445	
C23	20.8909743748	-0.0603482652	-2.6096248690	
C24	22.1424390981	-0.1008239056	-2.0764620686	
C25	23.3717649400	-0.1017219497	-2.8267822626	
C26	23.2921006393	-0.0442286500	-4.2569609854	
N27	23.2103586155	0.0044148728	-5.4174303238	
C28	24.6098999218	-0.1559179760	-2.2180632633	
C29	25.8651377903	-0.1662182933	-2.8782703102	
C30	27.0649077365	-0.2209714727	-2.2174191954	
C31	28.3321115495	-0.2348836984	-2.8636308226	
C32	29.5318572012	-0.2875561316	-2.2066050705	
C33	30.7998528521	-0.3031920355	-2.8558248921	
C34	32.0007589522	-0.3534724785	-2.2038456254	
C35	33.2691234676	-0.3703627342	-2.8566534694	
C36	34.4688985696	-0.4188715899	-2.2060208195	
C37	35.7415172814	-0.4369713452	-2.8562043628	
C38	36.9346648385	-0.4847438000	-2.1988298436	
C39	38.2182334628	-0.5044120441	-2.8380425528	
C40	39.3893495615	-0.5520724739	-2.1545722381	
C41	40.7439688765	-0.5771483762	-2.6957936498	



C42	41.0344019199	-0.5605714273	-4.0751820655
C43	42.3482422248	-0.5871265493	-4.5273490511
C44	43.4102261182	-0.6311240392	-3.6194408323
C45	43.1428048958	-0.6482032477	-2.2507162961
C46	41.8276727942	-0.6216005111	-1.7970137604
H47	33.2683087943	-0.3426974507	-3.9464315965
H48	9.9709068872	-0.0164435681	-0.0212571011
H49	5.9331435442	0.0136377185	-2.2913320768
H50	18.3783531861	-0.0056786598	-3.5089776549
H51	24.6149304734	-0.1954097295	-1.1300850184
H52	20.7724309035	-0.0234723420	-3.6903168184
H53	22.2527575614	-0.1391417329	-0.9949429498
H54	29.5267339031	-0.3196781072	-1.1167182035
H55	13.3908950595	0.0135520839	-3.2318290018
H56	15.8952026296	0.0073460416	-3.4028880618
H57	27.0577604953	-0.2563358296	-1.1276425539
H58	31.9997915854	-0.3827489835	-1.1138659837
H59	10.8914921776	0.0150680283	-2.9850841081
H60	14.8060676851	-0.0398261415	-0.4988001225
H61	28.3366257014	-0.2012100425	-3.9528686414
H62	34.4679079385	-0.4460308512	-1.1159712601
H63	8.4040174038	0.0143439221	-2.6674124115
H64	17.2311563344	-0.0628017844	-0.6276246343
H65	25.8673839220	-0.1291645967	-3.9662177646
H66	30.8013599175	-0.2728770389	-3.9454191131
H67	12.3861729477	-0.0251753517	-0.2963359487
H68	3.5280855166	0.0135712896	-1.8980389550
H69	7.5569860272	-0.0110362488	0.3195432887
H70	35.7444375883	-0.4110990509	-3.9460830988
H71	36.9263173992	-0.5104882763	-1.1087691597
H72	39.3305609791	-0.5749516344	-1.0662897432
H73	44.4350393301	-0.6520066881	-3.9779631268
H74	42.5481500360	-0.5737874586	-5.5950534299
H75	40.2259424666	-0.5275012104	-4.7984563085
H76	41.6253656432	-0.6354438898	-0.7289211182
H77	43.9594886034	-0.6824568962	-1.5354434123
H78	-0.9278704925	0.0031173125	1.9441549479
H79	1.2387093356	0.0036270407	3.1656305779
H80	3.3626231030	0.0058086777	1.9371898024
H81	1.2023455993	0.0067306820	-1.7871878016
H82	-0.9323219276	0.0046615801	-0.5457818862
H83	38.2218526904	-0.4793193766	-3.9266254332
H84	5.1468286064	-0.0064916566	0.7088391469

Final total energy: -1808.965556 hartrees

HOMO energy: -0.17184

LUMO energy: -0.11123

bond lengths (angstroms):

C1	-C2	:	1.395250	C1	-C6	:	1.392050
C1	-H82	:	1.086344	C2	-C3	:	1.398230
C2	-H78	:	1.085833	C3	-C4	:	1.389701
C3	-H79	:	1.086271	C4	-C5	:	1.409887
C4	-H80	:	1.085574	C5	-C6	:	1.408723
C5	-C7	:	1.459856	C6	-H81	:	1.087288
C7	-C8	:	1.356613	C7	-H68	:	1.090063
C8	-C9	:	1.434456	C8	-H84	:	1.088820
C9	-C10	:	1.363024	C9	-H49	:	1.090252
C10	-C11	:	1.429366	C10	-H69	:	1.090345
C11	-C12	:	1.365664	C11	-H63	:	1.090143
C12	-C13	:	1.426762	C12	-H48	:	1.090257
C13	-C14	:	1.367450	C13	-H59	:	1.090145
C14	-C15	:	1.425002	C14	-H67	:	1.090218
C15	-C16	:	1.368993	C15	-H55	:	1.090218
C16	-C17	:	1.423111	C16	-H60	:	1.090038
C17	-C18	:	1.371033	C17	-H56	:	1.090316
C18	-C19	:	1.418997	C18	-H64	:	1.088890
C19	-C20	:	1.381363	C19	-H50	:	1.088814
C20	-C21	:	1.435082	C20	-C23	:	1.441061
C21	-N22	:	1.164331	C23	-C24	:	1.360906
C23	-H52	:	1.087799	C24	-C25	:	1.440216
C24	-H53	:	1.087806	C25	-C26	:	1.433549
C25	-C28	:	1.380744	C26	-N27	:	1.164361
C28	-C29	:	1.418309	C28	-H51	:	1.088706
C29	-C30	:	1.370828	C29	-H65	:	1.088581
C30	-C31	:	1.422529	C30	-H57	:	1.090374
C31	-C32	:	1.368885	C31	-H61	:	1.089768
C32	-C33	:	1.424621	C32	-H54	:	1.090372
C33	-C34	:	1.367399	C33	-H66	:	1.090017
C34	-C35	:	1.426602	C34	-H58	:	1.090373
C35	-C36	:	1.365700	C35	-H47	:	1.090130
C36	-C37	:	1.429204	C36	-H62	:	1.090388
C37	-C38	:	1.363094	C37	-H70	:	1.090190
C38	-C39	:	1.434060	C38	-H71	:	1.090397
C39	-C40	:	1.356804	C39	-H83	:	1.088878
C40	-C41	:	1.458953	C40	-H72	:	1.090109
C41	-C42	:	1.409730	C41	-C46	:	1.408615
C42	-C43	:	1.389725	C42	-H75	:	1.085277
C43	-C44	:	1.397871	C43	-H74	:	1.086340
C44	-C45	:	1.394709	C44	-H73	:	1.085917
C45	-C46	:	1.391447	C45	-H77	:	1.086168
C46	-H76	:	1.087171				

## bond angles:

C6	-C1	-C2	: 120.102577	H82	-C1	-C2	: 120.171000
H82	-C1	-C6	: 119.726423	C3	-C2	-C1	: 119.378199
H78	-C2	-C1	: 120.353795	H78	-C2	-C3	: 120.268005
C4	-C3	-C2	: 120.554420	H79	-C3	-C2	: 119.908936
H79	-C3	-C4	: 119.536644	C5	-C4	-C3	: 120.902719
H80	-C4	-C3	: 119.125321	H80	-C4	-C5	: 119.971947
C6	-C5	-C4	: 117.719192	C7	-C5	-C4	: 123.565179
C7	-C5	-C6	: 118.715629	C5	-C6	-C1	: 121.342891
H81	-C6	-C1	: 119.697729	H81	-C6	-C5	: 118.959379
C8	-C7	-C5	: 127.605534	H68	-C7	-C5	: 114.964147
H68	-C7	-C8	: 117.430320	C9	-C8	-C7	: 123.927195
H84	-C8	-C7	: 119.800234	H84	-C8	-C9	: 116.272571
C10	-C9	-C8	: 123.948607	H49	-C9	-C8	: 117.233367
H49	-C9	-C10	: 118.818024	C11	-C10	-C9	: 124.921924
H69	-C10	-C9	: 118.291893	H69	-C10	-C11	: 116.786182
C12	-C11	-C10	: 123.694021	H63	-C11	-C10	: 117.476102
H63	-C11	-C12	: 118.829877	C13	-C12	-C11	: 125.106242
H48	-C12	-C11	: 118.118100	H48	-C12	-C13	: 116.775655
C14	-C13	-C12	: 123.533730	H59	-C13	-C12	: 117.609571
H59	-C13	-C14	: 118.856694	C15	-C14	-C13	: 125.167292
H67	-C14	-C13	: 118.058648	H67	-C14	-C15	: 116.774048
C16	-C15	-C14	: 123.431470	H55	-C15	-C14	: 117.688935
H55	-C15	-C16	: 118.879581	C17	-C16	-C15	: 125.089310
H60	-C16	-C15	: 118.103664	H60	-C16	-C17	: 116.806999
C18	-C17	-C16	: 123.296568	H56	-C17	-C16	: 117.733075
H56	-C17	-C18	: 118.970331	C19	-C18	-C17	: 124.245868
H64	-C18	-C17	: 118.292443	H64	-C18	-C19	: 117.461635
C20	-C19	-C18	: 125.378862	H50	-C19	-C18	: 117.786989
H50	-C19	-C20	: 116.834106	C21	-C20	-C19	: 119.106692
C23	-C20	-C19	: 123.051437	C23	-C20	-C21	: 117.841753
N22	-C21	-C20	: 179.062635	C24	-C23	-C20	: 124.738918
H52	-C23	-C20	: 115.892070	H52	-C23	-C24	: 119.368909
C25	-C24	-C23	: 125.509849	H53	-C24	-C23	: 118.934679
H53	-C24	-C25	: 115.555217	C26	-C25	-C24	: 118.183273
C28	-C25	-C24	: 122.395107	C28	-C25	-C26	: 119.421618
N27	-C26	-C25	: 179.154282	C29	-C28	-C25	: 126.063624
H51	-C28	-C25	: 116.496004	H51	-C28	-C29	: 117.440329
C30	-C29	-C28	: 123.399477	H65	-C29	-C28	: 117.826578
H65	-C29	-C30	: 118.773932	C31	-C30	-C29	: 124.128216
H57	-C30	-C29	: 118.514176	H57	-C30	-C31	: 117.357608
C32	-C31	-C30	: 124.269197	H61	-C31	-C30	: 117.221818
H61	-C31	-C32	: 118.508985	C33	-C32	-C31	: 124.178662
H54	-C32	-C31	: 118.474867	H54	-C32	-C33	: 117.346470
C34	-C33	-C32	: 124.388671	H66	-C33	-C32	: 117.159095
H66	-C33	-C34	: 118.452233	C35	-C34	-C33	: 124.269054
H58	-C34	-C33	: 118.479121	H58	-C34	-C35	: 117.251824
C36	-C35	-C34	: 124.296803	H47	-C35	-C34	: 117.160464
H47	-C35	-C36	: 118.542730	C37	-C36	-C35	: 124.469930
H62	-C36	-C35	: 118.447171	H62	-C36	-C37	: 117.082899
C38	-C37	-C36	: 124.088267	H70	-C37	-C36	: 117.186085
H70	-C37	-C38	: 118.725641	C39	-C38	-C37	: 124.679338

H71	-C38	-C37	: 118.440409	H71	-C38	-C39	: 116.880251
C40	-C39	-C38	: 123.265053	H83	-C39	-C38	: 116.633031
H83	-C39	-C40	: 120.101913	C41	-C40	-C39	: 127.963036
H72	-C40	-C39	: 117.198856	H72	-C40	-C41	: 114.838109
C42	-C41	-C40	: 123.646451	C46	-C41	-C40	: 118.565753
C46	-C41	-C42	: 117.787773	C43	-C42	-C41	: 120.857693
H75	-C42	-C41	: 119.932879	H75	-C42	-C43	: 119.209408
C44	-C43	-C42	: 120.498178	H74	-C43	-C42	: 119.572183
H74	-C43	-C44	: 119.929637	C45	-C44	-C43	: 119.479421
H73	-C44	-C43	: 120.207787	H73	-C44	-C45	: 120.312791
C46	-C45	-C44	: 120.064850	H77	-C45	-C44	: 120.164083
H77	-C45	-C46	: 119.771066	C45	-C46	-C41	: 121.312084
H76	-C46	-C41	: 118.953567	H76	-C46	-C45	: 119.734347

torsional angles:

C1	-C2	-C3	-C4	: -0.003999
C1	-C2	-C3	-H79	: 179.988692
C1	-C6	-C5	-C4	: -0.010825
C1	-C6	-C5	-C7	: 179.995492
C2	-C1	-C6	-C5	: 0.013726
C2	-C1	-C6	-H81	: -179.992562
C2	-C3	-C4	-C5	: 0.006751
C2	-C3	-C4	-H80	: 179.965171
C3	-C2	-C1	-C6	: -0.006120
C3	-C2	-C1	-H82	: -179.995875
C3	-C4	-C5	-C6	: 0.000595
C3	-C4	-C5	-C7	: 179.993947
C4	-C3	-C2	-H78	: 179.999571
C4	-C5	-C6	-H81	: 179.995418
C4	-C5	-C7	-C8	: 0.332891
C4	-C5	-C7	-H68	: -179.667051
C5	-C4	-C3	-H79	: -179.985967
C5	-C6	-C1	-H82	: -179.996473
C5	-C7	-C8	-C9	: -179.908807
C5	-C7	-C8	-H84	: 0.084397
C6	-C1	-C2	-H78	: 179.990307
C6	-C5	-C4	-H80	: -179.957476
C6	-C5	-C7	-C8	: -179.673819
C6	-C5	-C7	-H68	: 0.326239
C7	-C5	-C4	-H80	: 0.035876
C7	-C5	-C6	-H81	: 0.001734
C7	-C8	-C9	-C10	: -179.973986
C7	-C8	-C9	-H49	: 0.044209
C8	-C9	-C10	-C11	: -179.921440
C8	-C9	-C10	-H69	: 0.072912
C9	-C8	-C7	-H68	: 0.091134
C9	-C10	-C11	-C12	: -179.931593
C9	-C10	-C11	-H63	: 0.064574
C10	-C9	-C8	-H84	: 0.032591
C10	-C11	-C12	-C13	: -179.947015
C10	-C11	-C12	-H48	: 0.072889
C11	-C10	-C9	-H49	: 0.060095

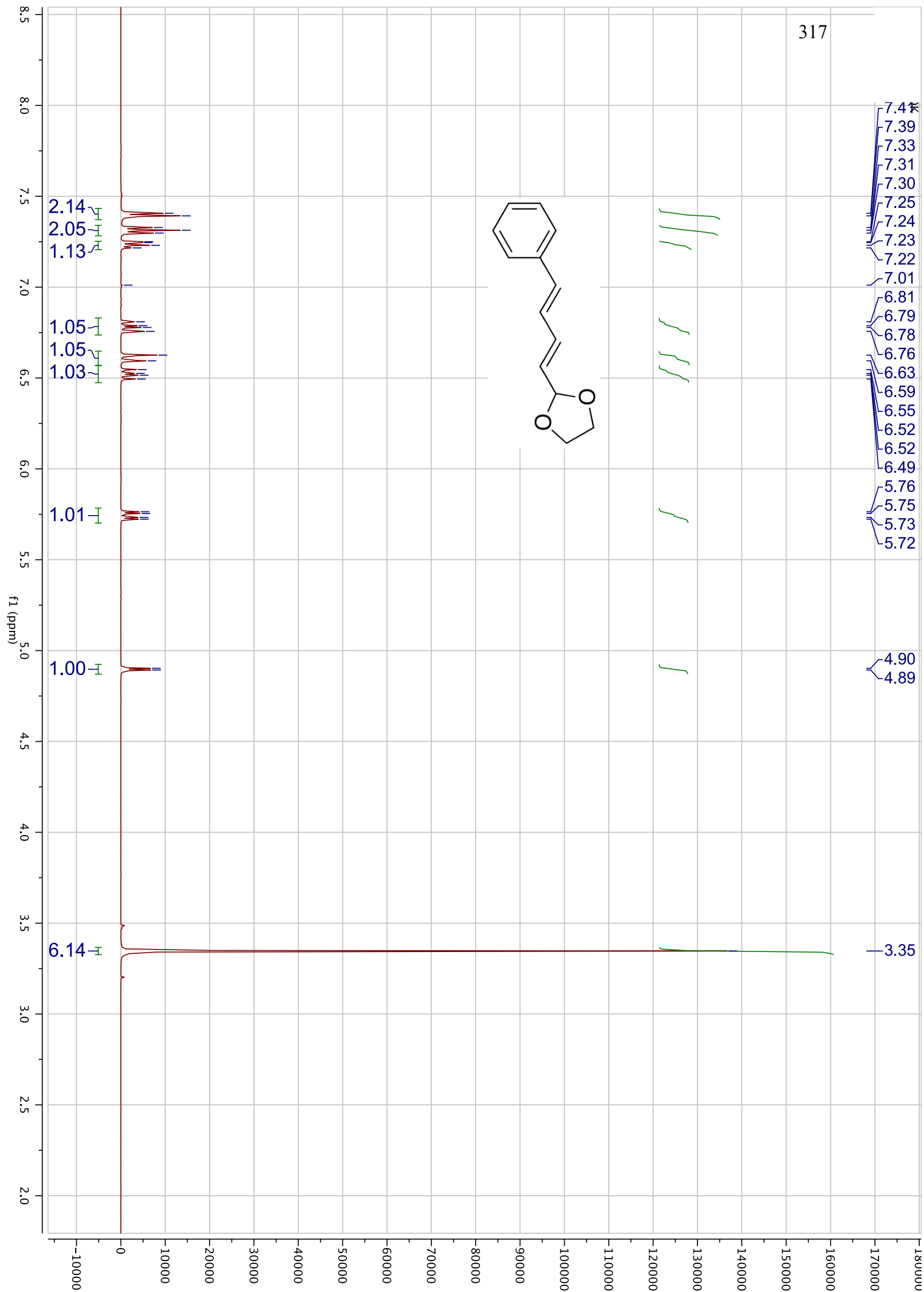
C11	-C12	-C13	-C14	:-179.853388
C11	-C12	-C13	-H59	: 0.120066
C12	-C11	-C10	-H69	: 0.073978
C12	-C13	-C14	-C15	:-179.973340
C12	-C13	-C14	-H67	: 0.069107
C13	-C12	-C11	-H63	: 0.056867
C13	-C14	-C15	-C16	:-179.770637
C13	-C14	-C15	-H55	: 0.185504
C14	-C13	-C12	-H48	: 0.126949
C14	-C15	-C16	-C17	:-179.995348
C14	-C15	-C16	-H60	: 0.066670
C15	-C14	-C13	-H59	: 0.053519
C15	-C16	-C17	-C18	:-179.688945
C15	-C16	-C17	-H56	: 0.250712
C16	-C15	-C14	-H67	: 0.187406
C16	-C17	-C18	-C19	:179.978569
C16	-C17	-C18	-H64	: 0.065400
C17	-C16	-C15	-H55	: 0.049005
C17	-C18	-C19	-C20	:-179.603127
C17	-C18	-C19	-H50	: 0.319089
C18	-C17	-C16	-H60	: 0.249763
C18	-C19	-C20	-C21	: 0.050450
C18	-C19	-C20	-C23	:179.923095
C19	-C18	-C17	-H56	: 0.039620
C19	-C20	-C21	-N22	:-179.478778
C19	-C20	-C23	-C24	:-179.433707
C19	-C20	-C23	-H52	: 0.447915
C20	-C19	-C18	-H64	: 0.310706
C20	-C23	-C24	-C25	:179.780029
C20	-C23	-C24	-H53	: -0.027837
C21	-C20	-C19	-H50	:-179.872431
C21	-C20	-C23	-C24	: 0.440454
C21	-C20	-C23	-H52	:-179.677924
N22	-C21	-C20	-C23	: 0.641943
C23	-C20	-C19	-H50	: 0.000214
C23	-C24	-C25	-C26	: 0.558648
C23	-C24	-C25	-C28	:-179.426669
C24	-C25	-C26	-N27	: 5.251597
C24	-C25	-C28	-C29	:179.738115
C24	-C25	-C28	-H51	: -0.183641
C25	-C24	-C23	-H52	: -0.097770
C25	-C28	-C29	-C30	:179.987754
C25	-C28	-C29	-H65	: -0.054203
C26	-C25	-C24	-H53	:-179.627736
C26	-C25	-C28	-C29	: -0.247027
C26	-C25	-C28	-H51	:179.831217
N27	-C26	-C25	-C28	:-174.762636
C28	-C25	-C24	-H53	: 0.386947
C28	-C29	-C30	-C31	:179.863480
C28	-C29	-C30	-H57	: -0.139129
C29	-C30	-C31	-C32	:179.901069
C29	-C30	-C31	-H61	: -0.105709
C30	-C29	-C28	-H51	: -0.091149

C30	-C31	-C32	-C33	: 179.912759
C30	-C31	-C32	-H54	: -0.099762
C31	-C30	-C29	-H65	: -0.094187
C31	-C32	-C33	-C34	: 179.884649
C31	-C32	-C33	-H66	: -0.124413
C32	-C31	-C30	-H57	: -0.096350
C32	-C33	-C34	-C35	: 179.934684
C32	-C33	-C34	-H58	: -0.072710
C33	-C32	-C31	-H61	: -0.080382
C33	-C34	-C35	-C36	: 179.913506
C33	-C34	-C35	-H47	: -0.104957
C34	-C33	-C32	-H54	: -0.102960
C34	-C35	-C36	-C37	: 179.949979
C34	-C35	-C36	-H62	: -0.046455
C35	-C34	-C33	-H66	: -0.056145
C35	-C36	-C37	-C38	: 179.963195
C35	-C36	-C37	-H70	: -0.069142
C36	-C35	-C34	-H58	: -0.079183
C36	-C37	-C38	-C39	: 179.950961
C36	-C37	-C38	-H71	: -0.031968
C37	-C36	-C35	-H47	: -0.031321
C37	-C38	-C39	-C40	: 179.993398
C37	-C38	-C39	-H83	: -0.027005
C38	-C37	-C36	-H62	: -0.040326
C38	-C39	-C40	-C41	: 179.940757
C38	-C39	-C40	-H72	: -0.062801
C39	-C38	-C37	-H70	: -0.016238
C39	-C40	-C41	-C42	: -0.319824
C39	-C40	-C41	-C46	: 179.738003
C40	-C39	-C38	-H71	: -0.023431
C40	-C41	-C42	-C43	: -179.953450
C40	-C41	-C42	-H75	: -0.004678
C40	-C41	-C46	-C45	: 179.954533
C40	-C41	-C46	-H76	: -0.029703
C41	-C40	-C39	-H83	: -0.038160
C41	-C42	-C43	-C44	: 0.009111
C41	-C42	-C43	-H74	: 179.991165
C41	-C46	-C45	-C44	: -0.005211
C41	-C46	-C45	-H77	: -179.994989
C42	-C41	-C40	-H72	: 179.683664
C42	-C41	-C46	-C45	: 0.008947
C42	-C41	-C46	-H76	: -179.975288
C42	-C43	-C44	-C45	: -0.005039
C42	-C43	-C44	-H73	: 179.983378
C43	-C42	-C41	-C46	: -0.010858
C43	-C44	-C45	-C46	: 0.003078
C43	-C44	-C45	-H77	: 179.992816
C44	-C43	-C42	-H75	: -179.940027
C44	-C45	-C46	-H76	: 179.978904
C45	-C44	-C43	-H74	: -179.987028
C46	-C41	-C40	-H72	: -0.258509
C46	-C41	-C42	-H75	: 179.937914
C46	-C45	-C44	-H73	: -179.985327

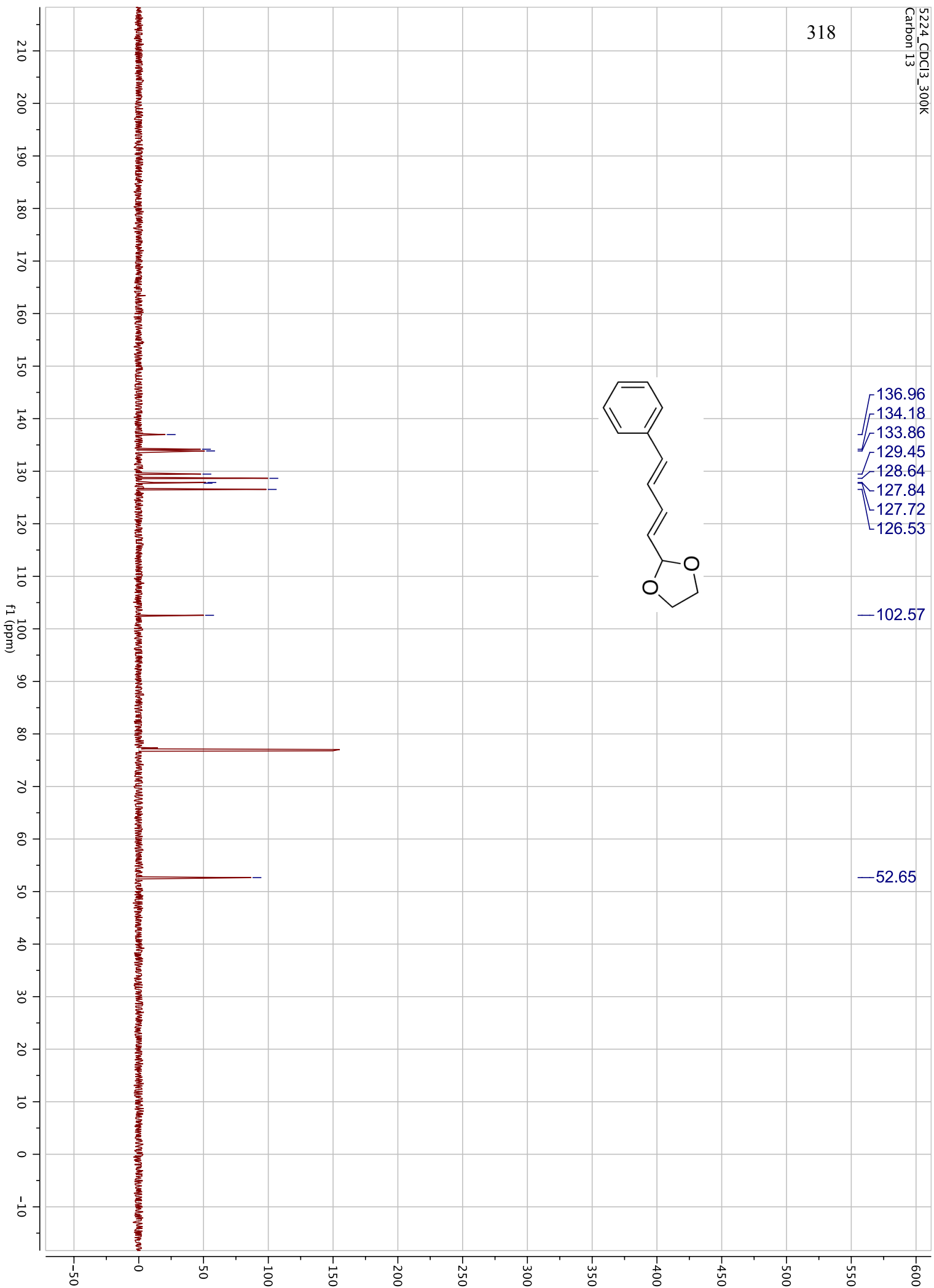
H47	-C35	-C34	-H58	: 179.902354
H47	-C35	-C36	-H62	: 179.972244
H48	-C12	-C11	-H63	:-179.923229
H48	-C12	-C13	-H59	:-179.899598
H49	-C9	-C8	-H84	:-179.949214
H49	-C9	-C10	-H69	:-179.945553
H50	-C19	-C18	-H64	:-179.767078
H51	-C28	-C29	-H65	: 179.866893
H52	-C23	-C24	-H53	:-179.905637
H54	-C32	-C31	-H61	: 179.907097
H54	-C32	-C33	-H66	: 179.887978
H55	-C15	-C14	-H67	:-179.856453
H55	-C15	-C16	-H60	:-179.888978
H56	-C17	-C16	-H60	:-179.810580
H56	-C17	-C18	-H64	:-179.873550
H57	-C30	-C29	-H65	: 179.903204
H57	-C30	-C31	-H61	: 179.896872
H58	-C34	-C33	-H66	: 179.936461
H59	-C13	-C14	-H67	:-179.904034
H62	-C36	-C37	-H70	: 179.927337
H63	-C11	-C10	-H69	:-179.929855
H68	-C7	-C8	-H84	:-179.915662
H70	-C37	-C38	-H71	:-179.999167
H71	-C38	-C39	-H83	: 179.956165
H72	-C40	-C39	-H83	: 179.958281
H73	-C44	-C43	-H74	: 0.001389
H73	-C44	-C45	-H77	: 0.004411
H74	-C43	-C42	-H75	: 0.042026
H76	-C46	-C45	-H77	: -0.010875
H78	-C2	-C1	-H82	: 0.000552
H78	-C2	-C3	-H79	: -0.007738
H79	-C3	-C4	-H80	: -0.027546
H81	-C6	-C1	-H82	: -0.002761

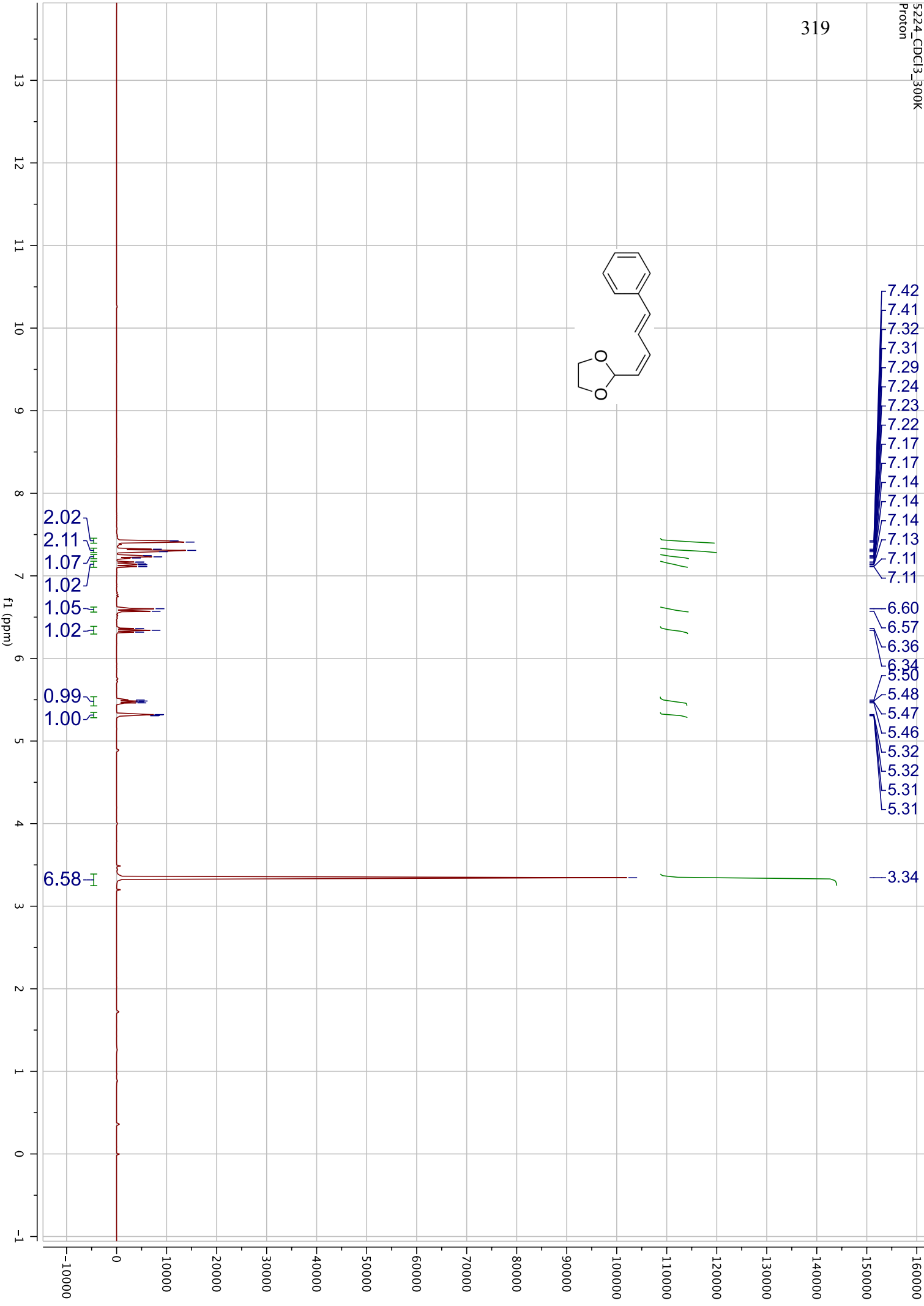
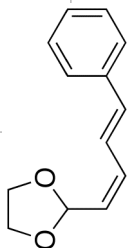
**Appendix A (Part 3)** **$^1\text{H}$ -NMR and  $^{13}\text{C}$ -NMR Spectra:**



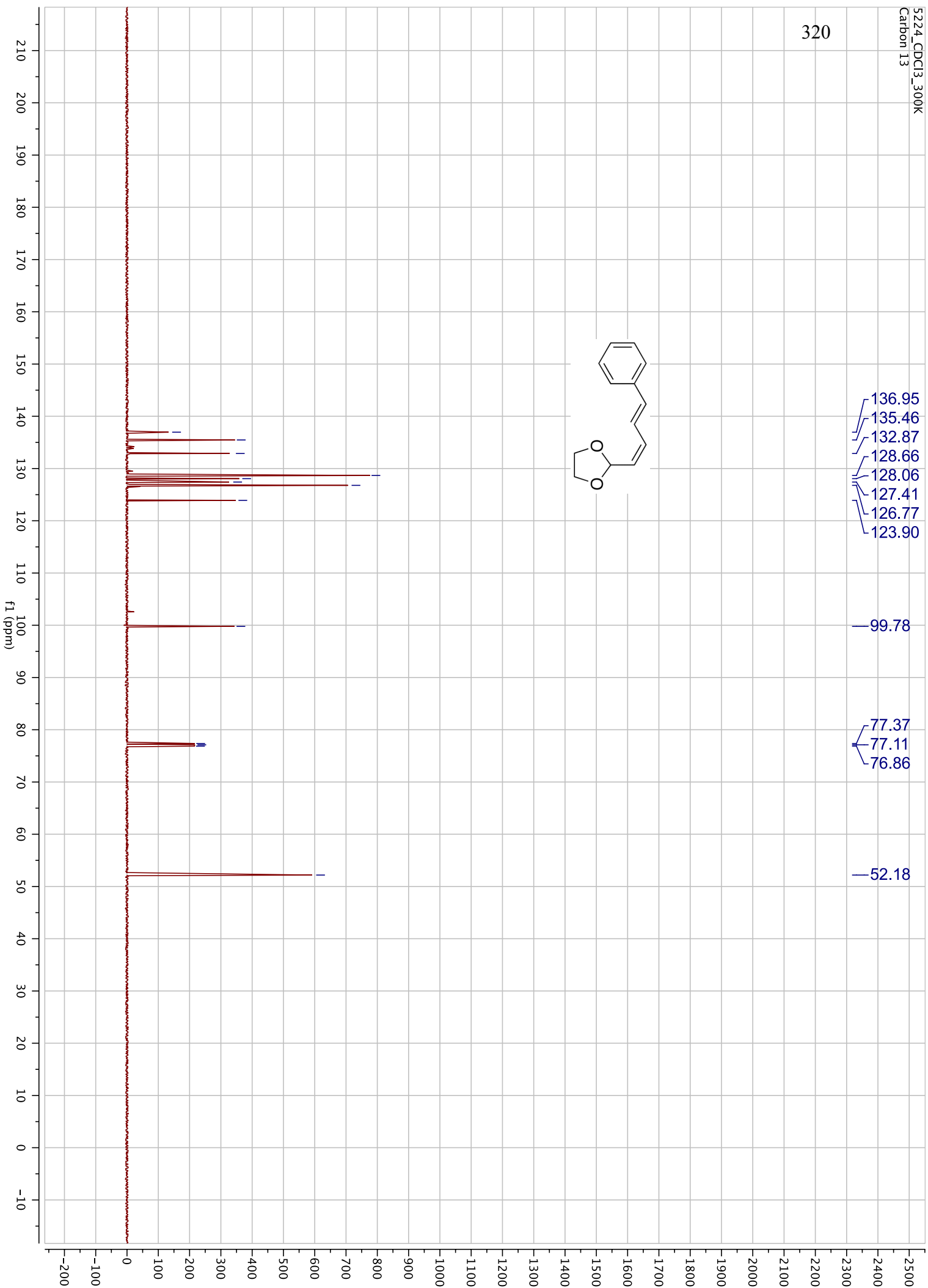


318

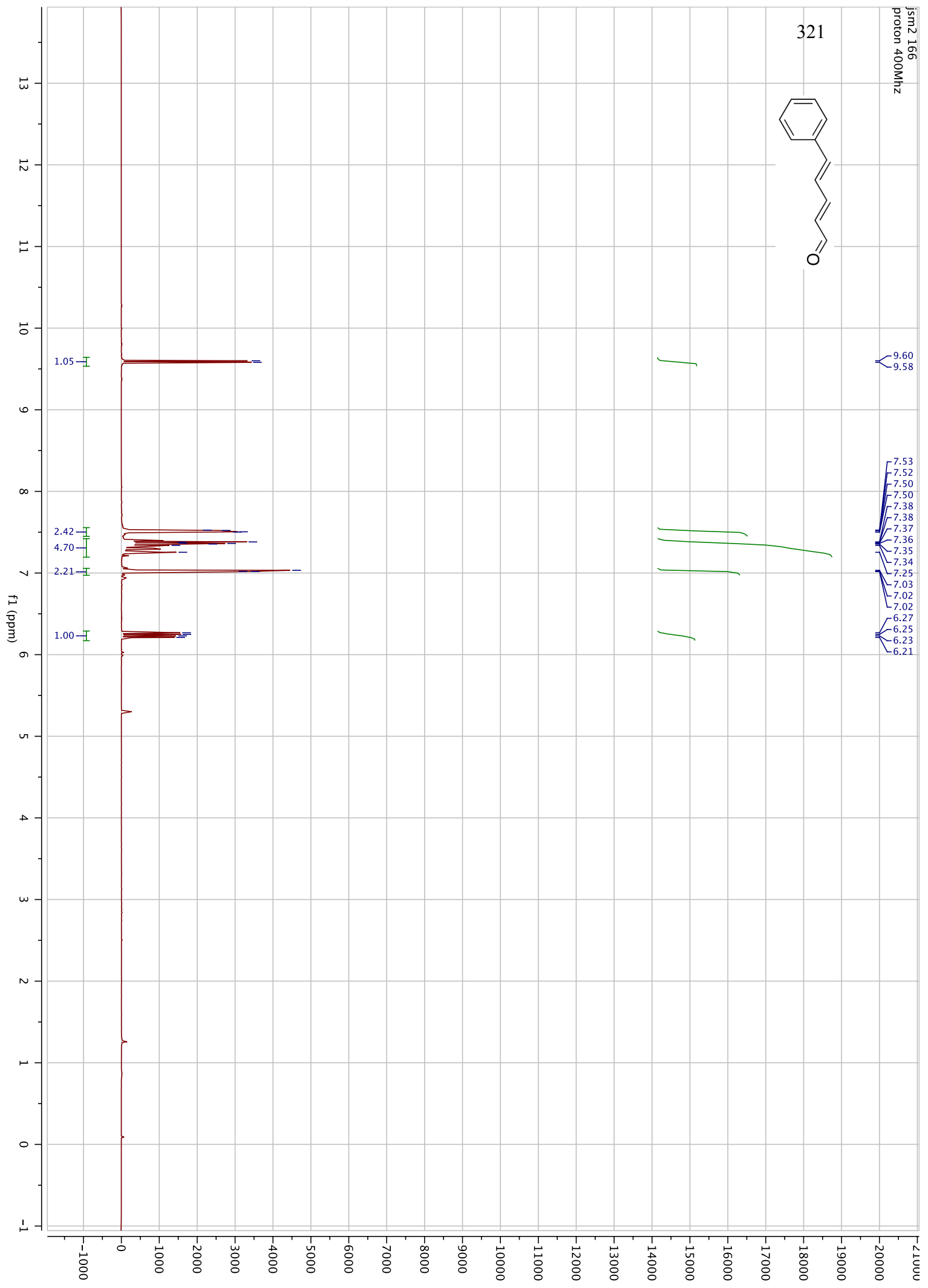
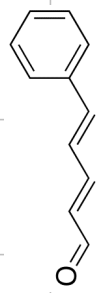


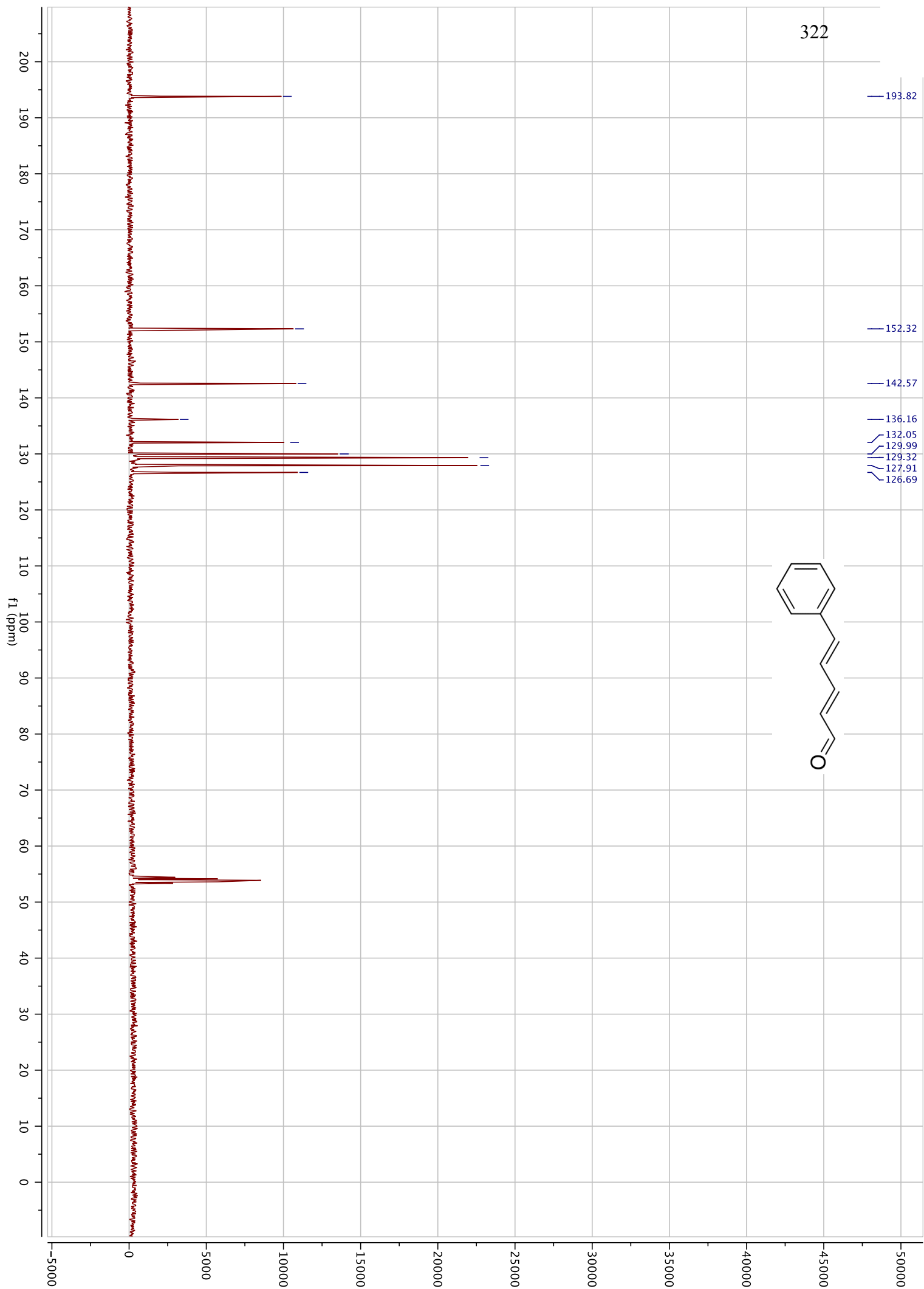


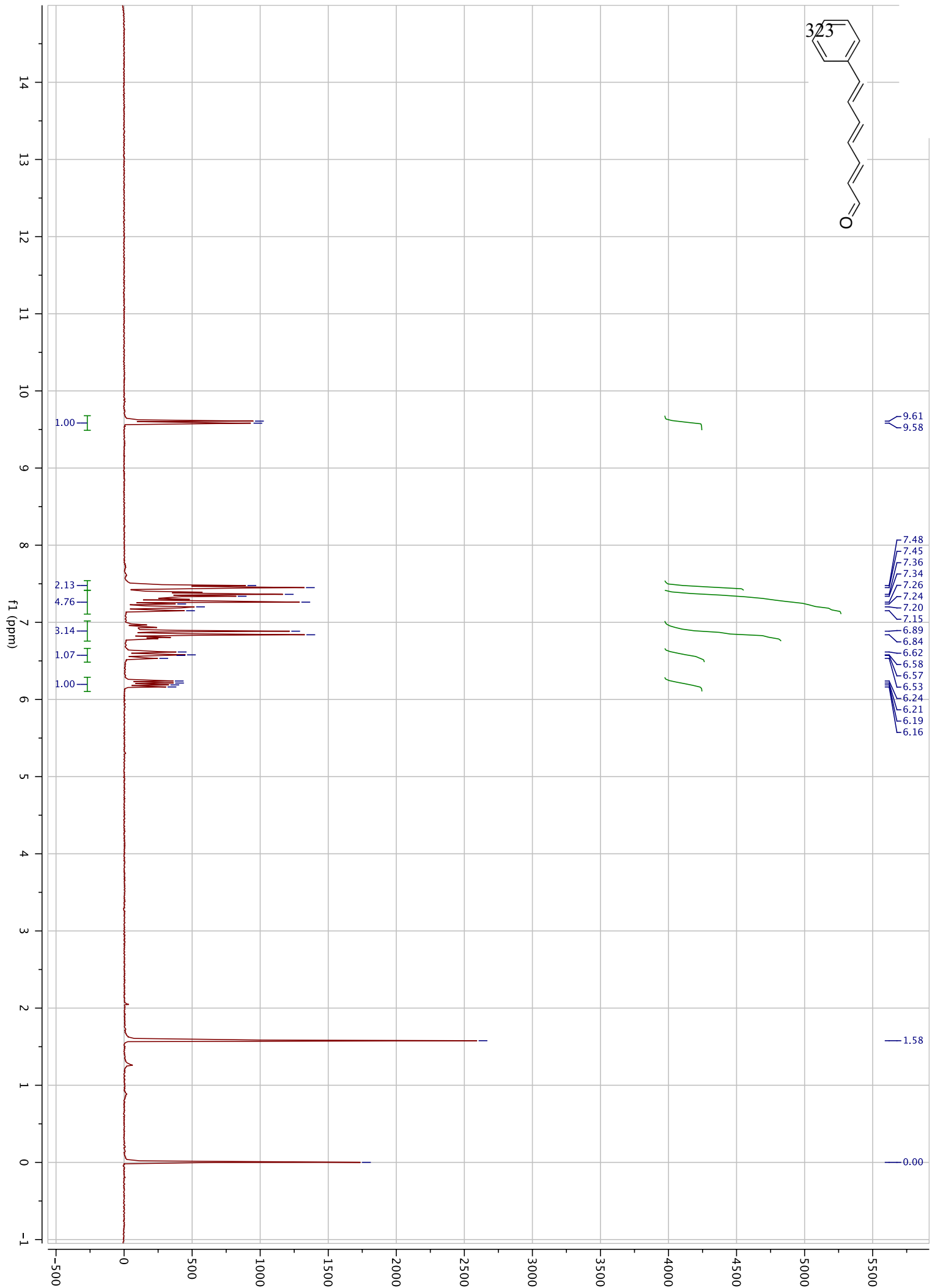
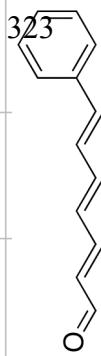
320

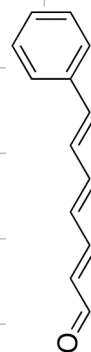


321









— 193.45

— 151.67

— 142.71

— 138.34

— 136.36

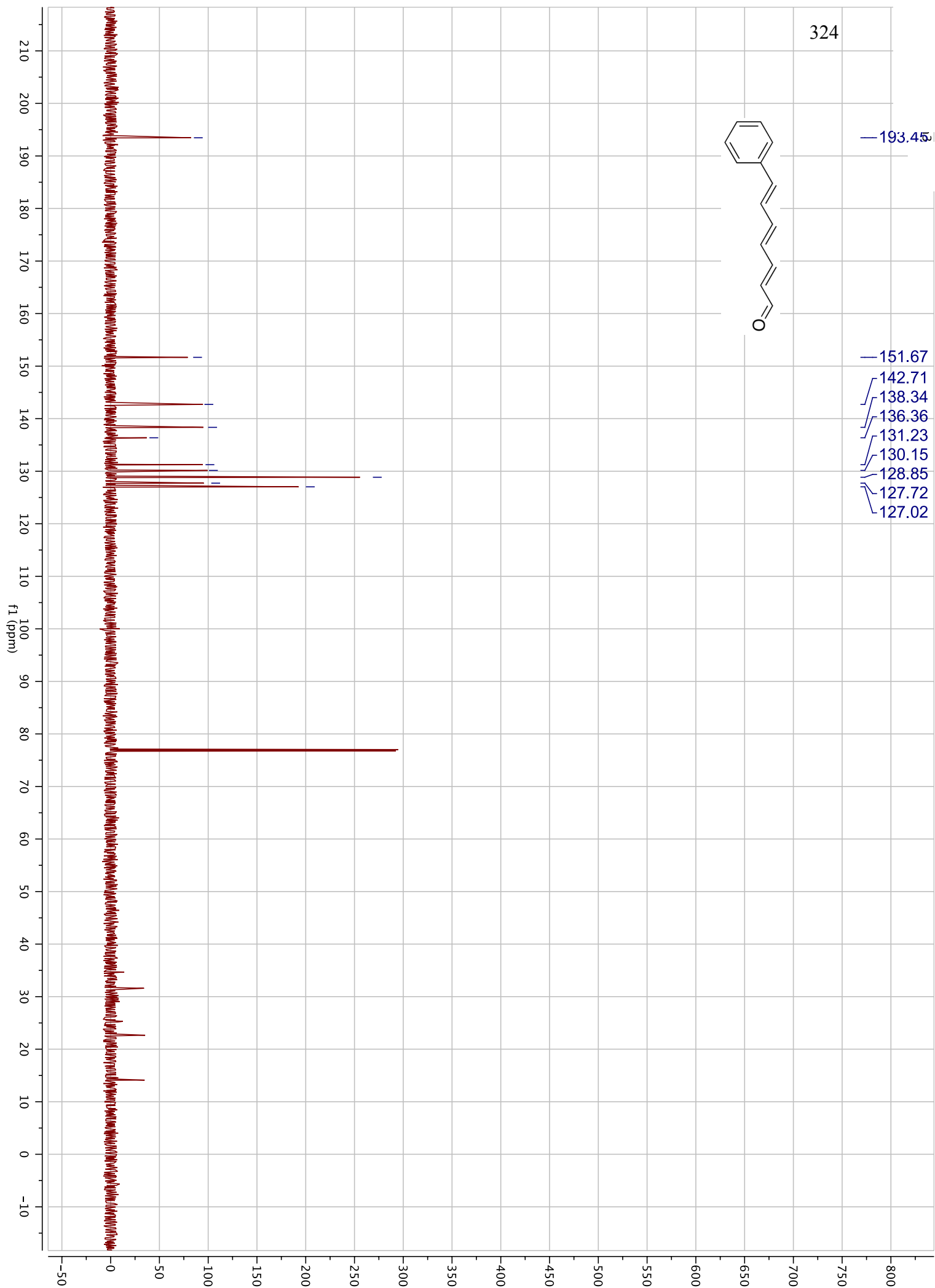
— 131.23

— 130.15

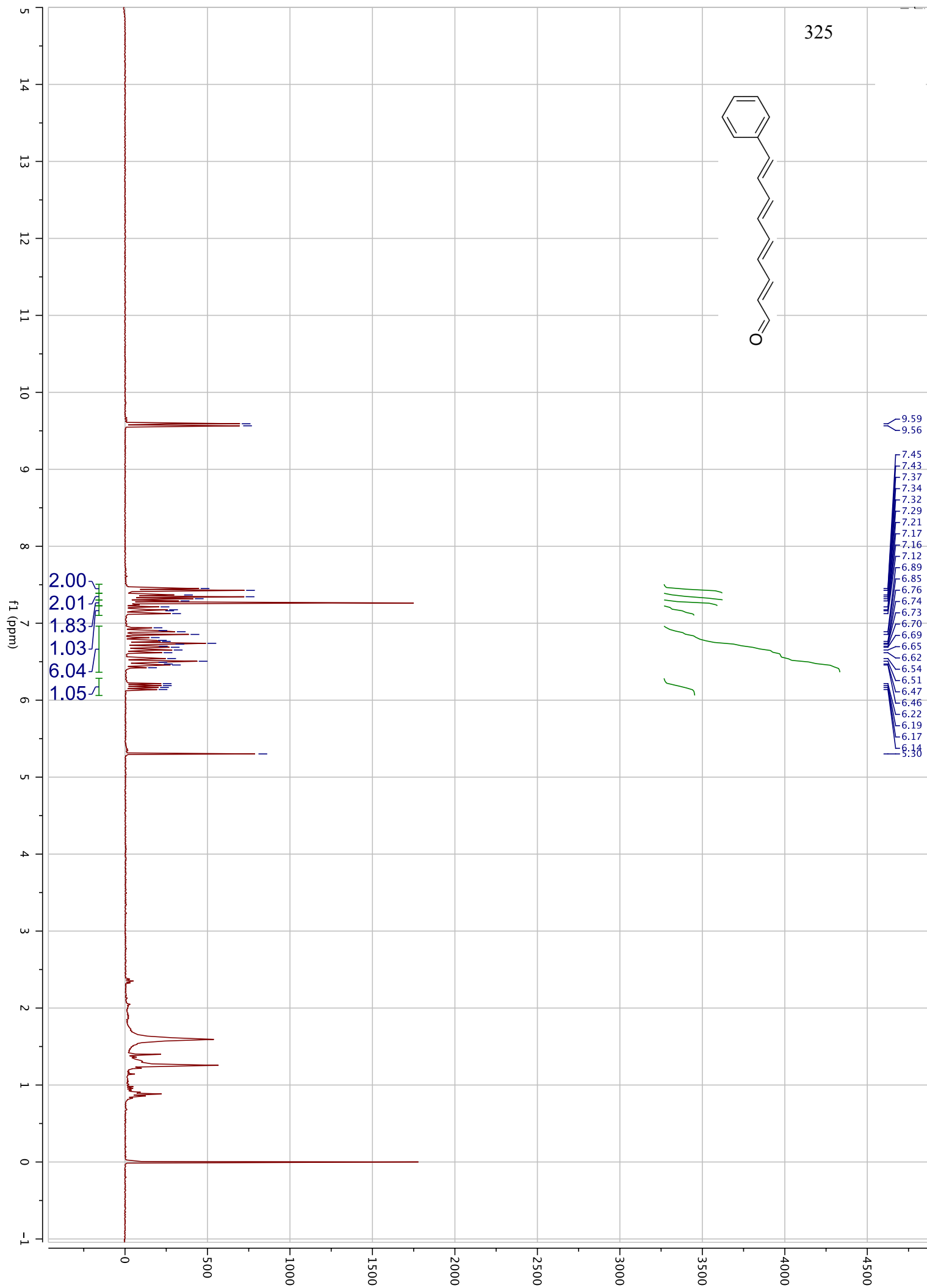
— 128.85

— 127.72

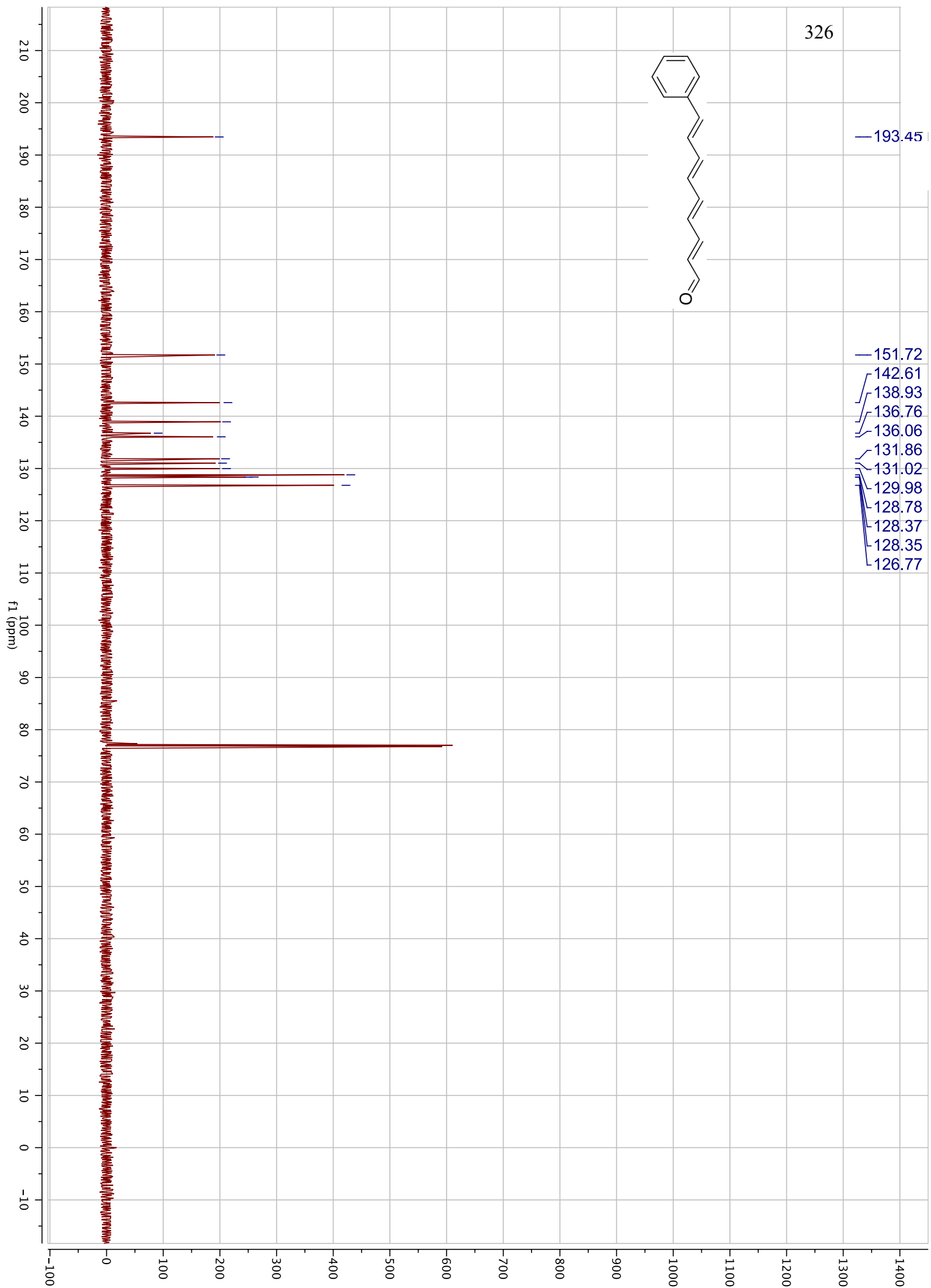
— 127.02







326



phenyl pent-2-enal  
proton standard

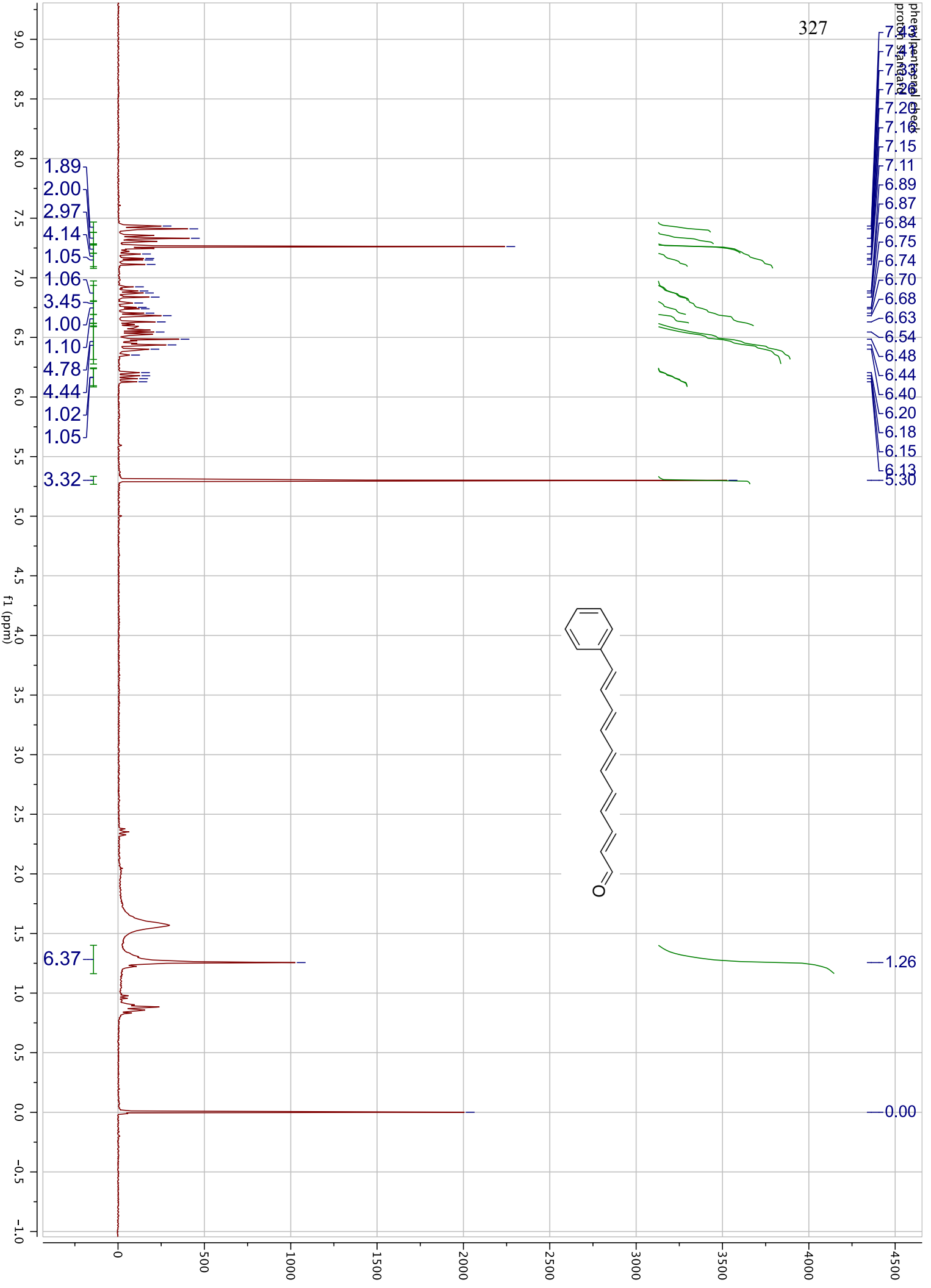
- 7.19
- 7.15
- 7.11
- 6.89
- 6.87
- 6.84
- 6.75
- 6.74
- 6.70
- 6.68
- 6.63
- 6.54
- 6.48
- 6.44
- 6.40
- 6.20
- 6.18
- 6.15
- 5.30

- 1.89
- 2.00
- 2.97
- 4.14
- 1.05
- 1.06
- 3.45
- 1.00
- 1.10
- 4.78
- 4.44
- 1.02
- 1.05

6.37

1.26

0.00



328

— 193.44

— 151.72

— 142.67

— 138.83

— 137.01

— 136.76

— 134.78

— 132.63

— 131.75

— 130.92

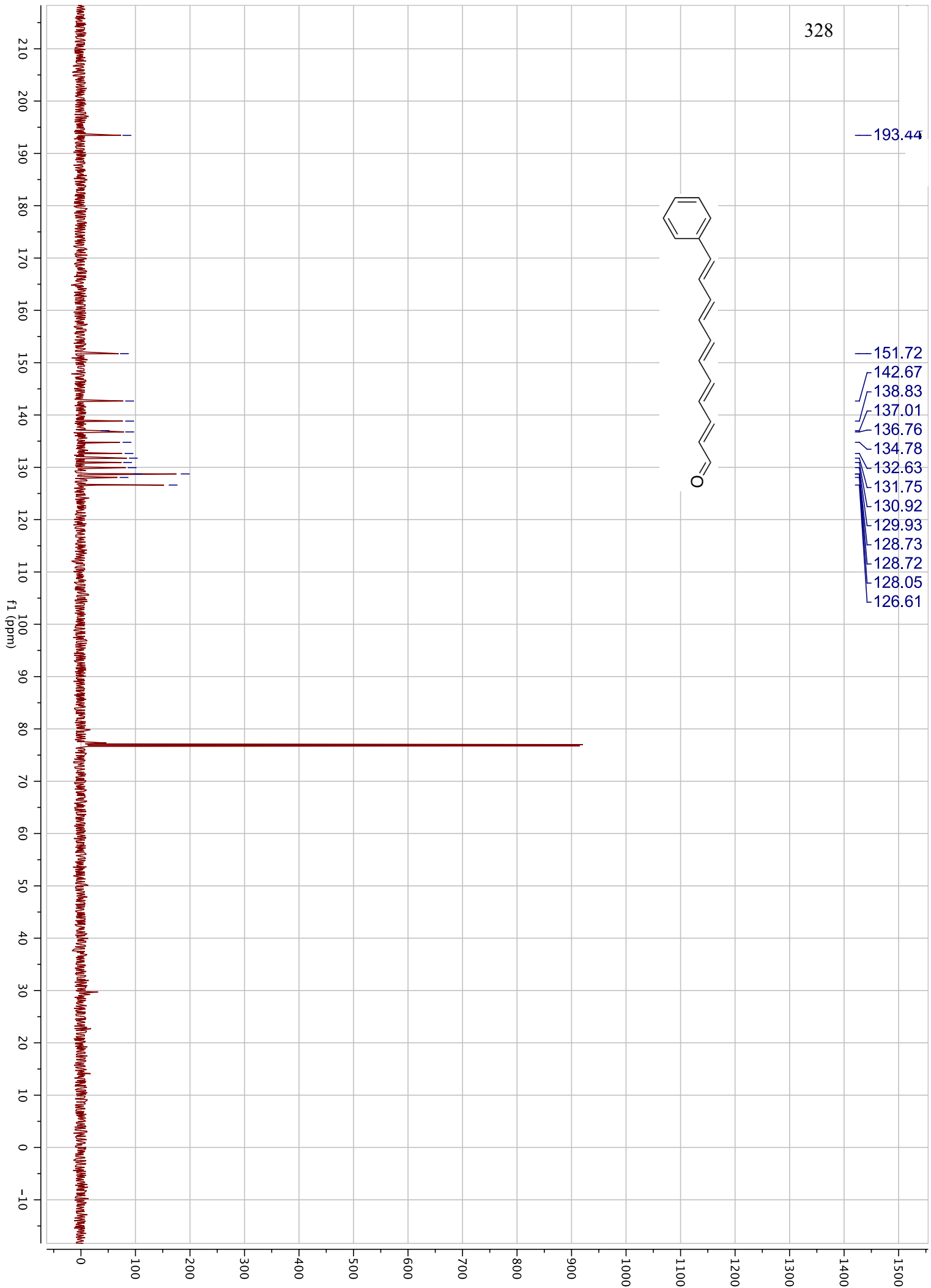
— 129.93

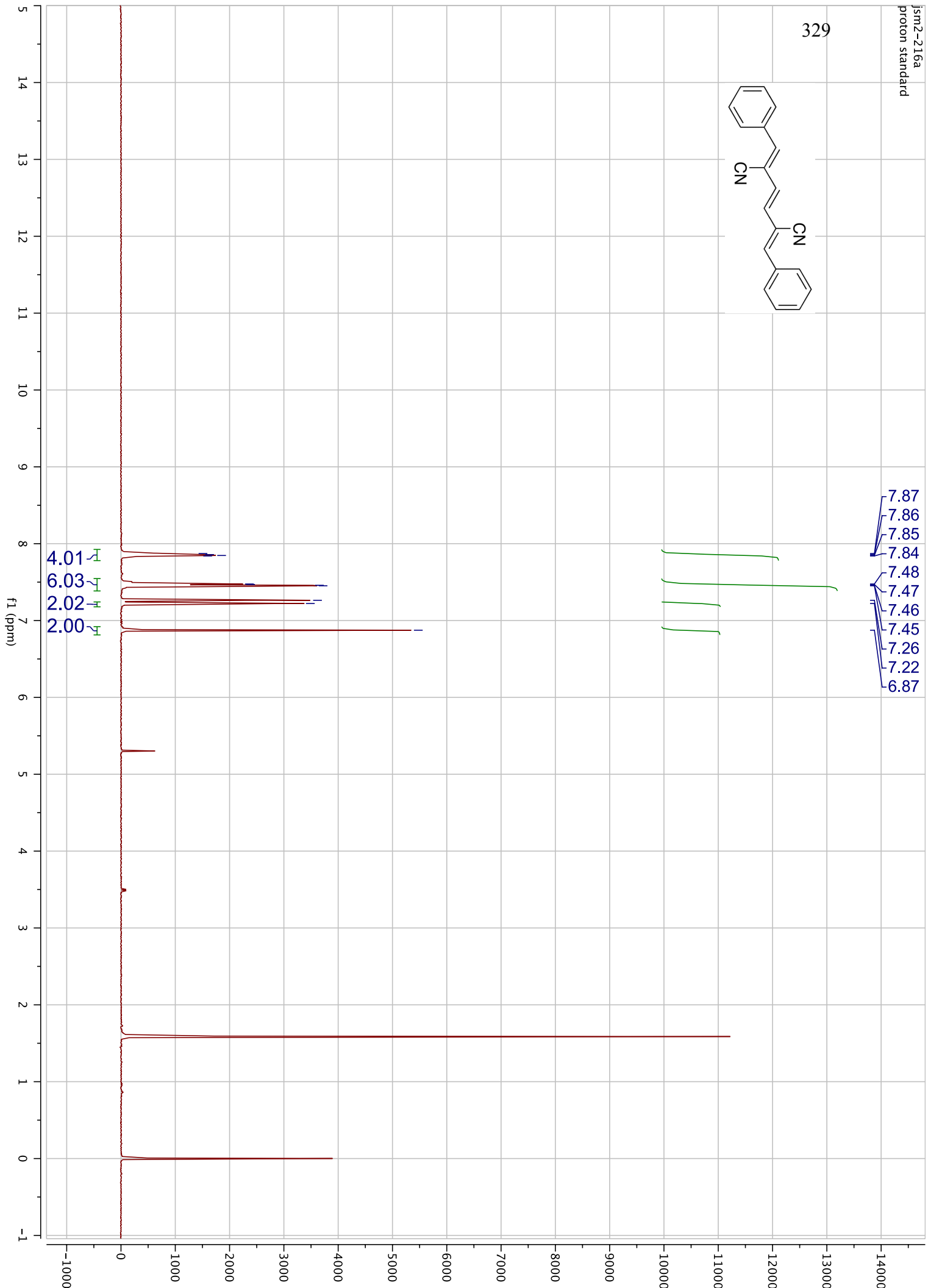
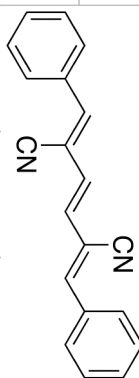
— 128.73

— 128.72

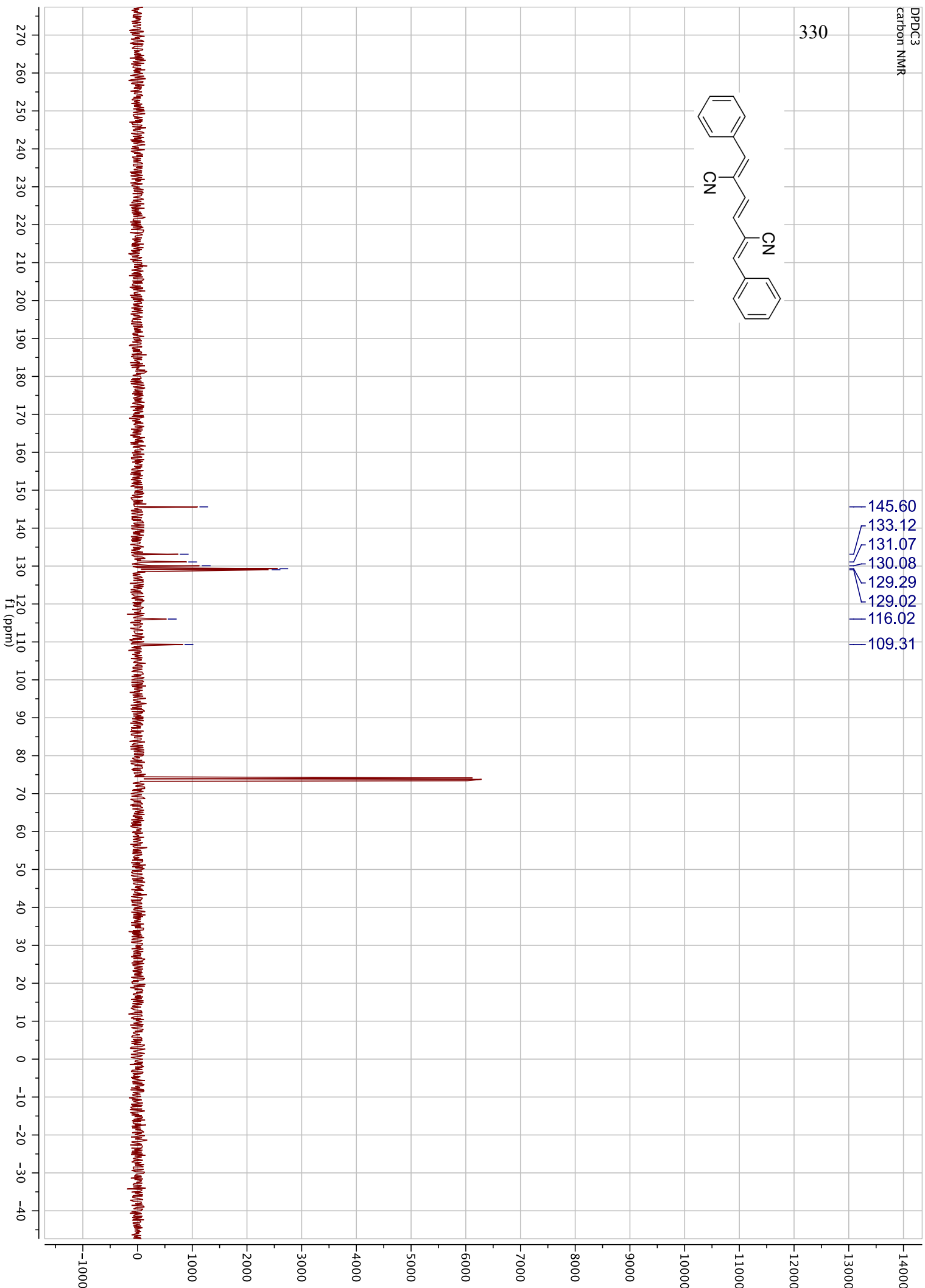
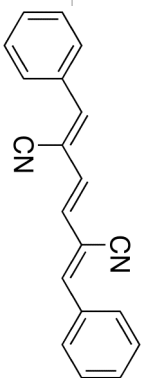
— 128.05

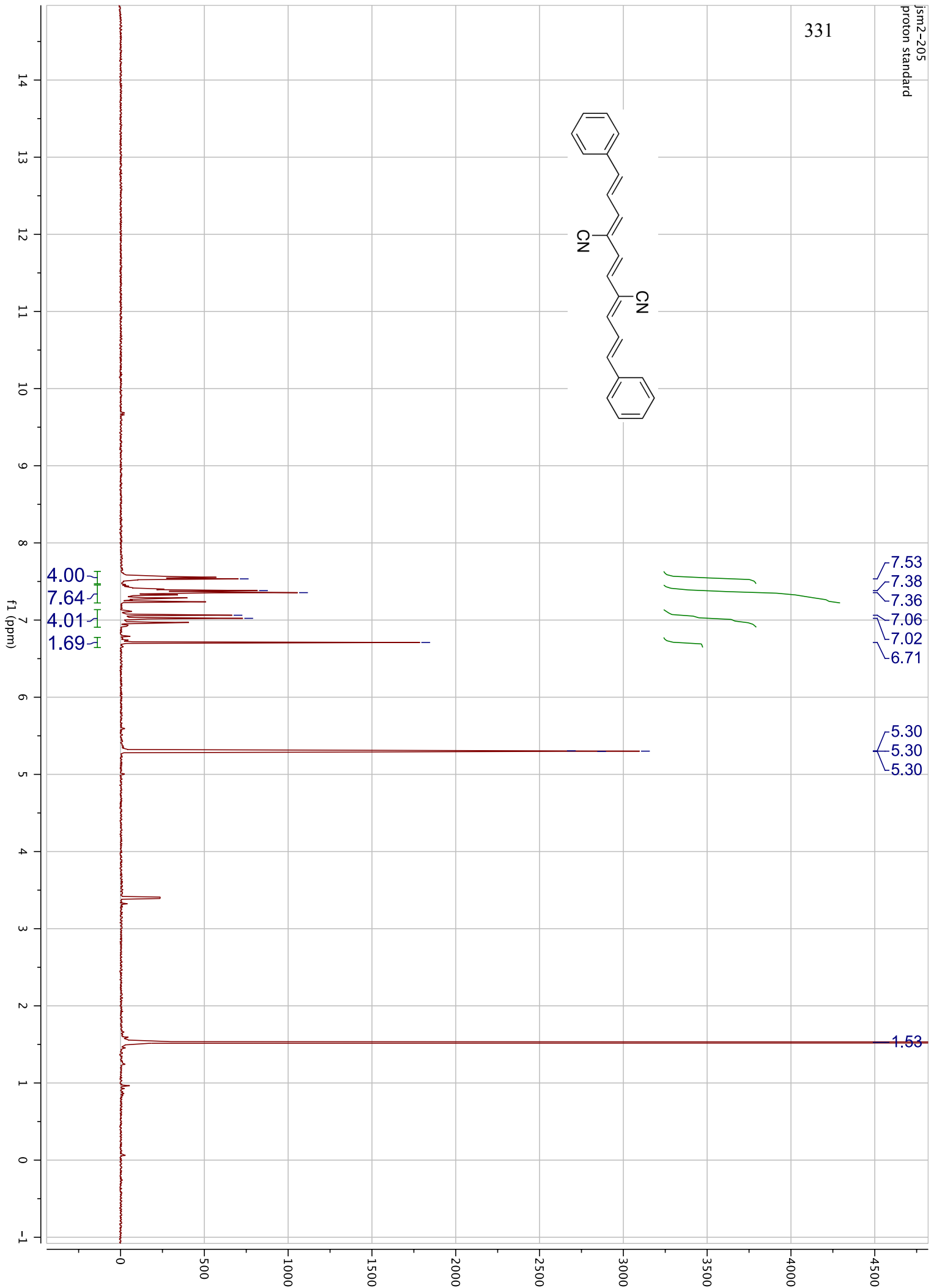
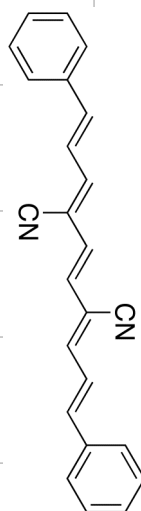
— 126.61



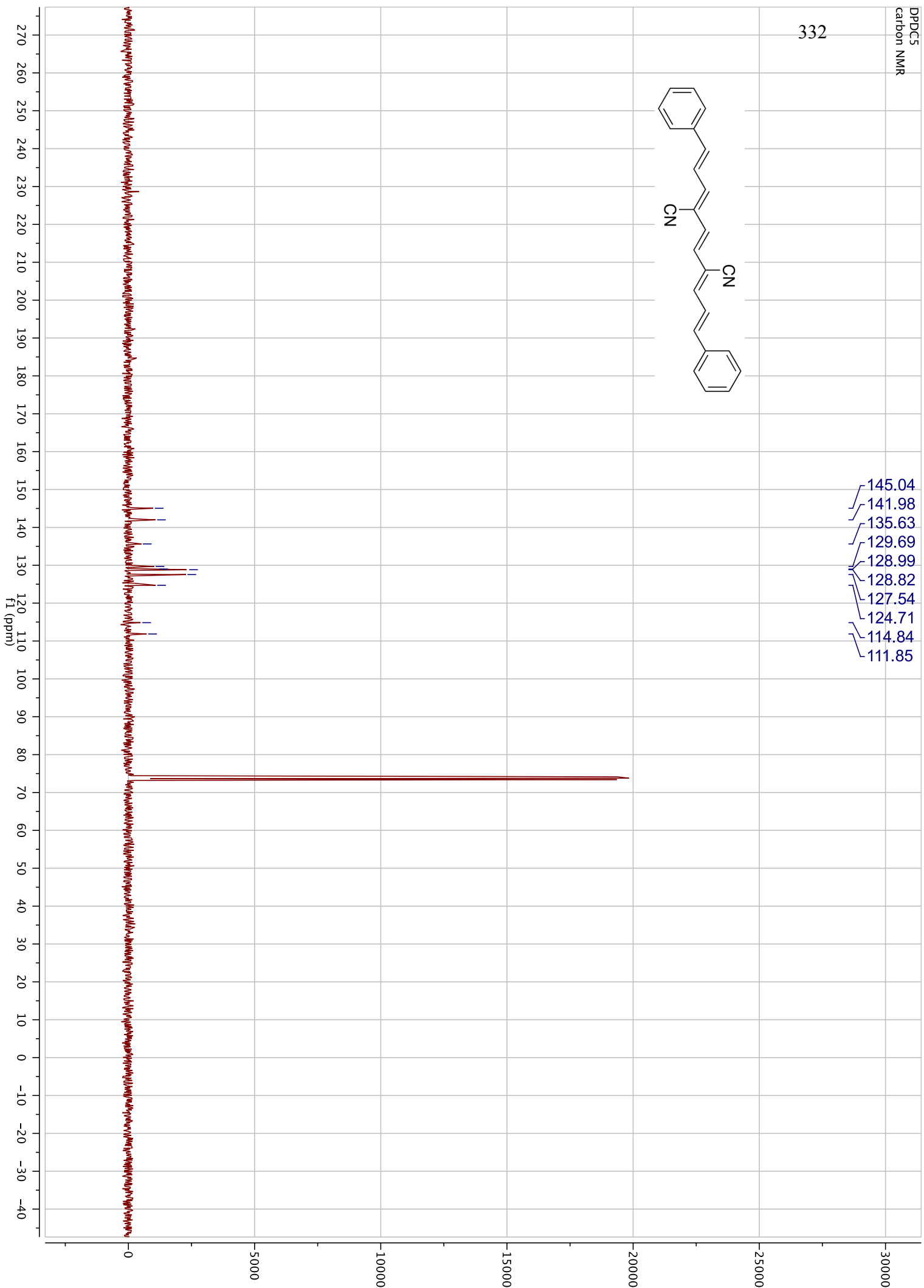
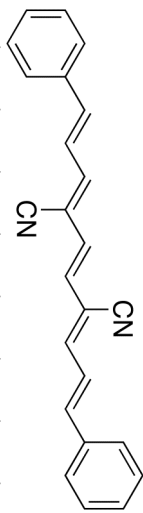


330

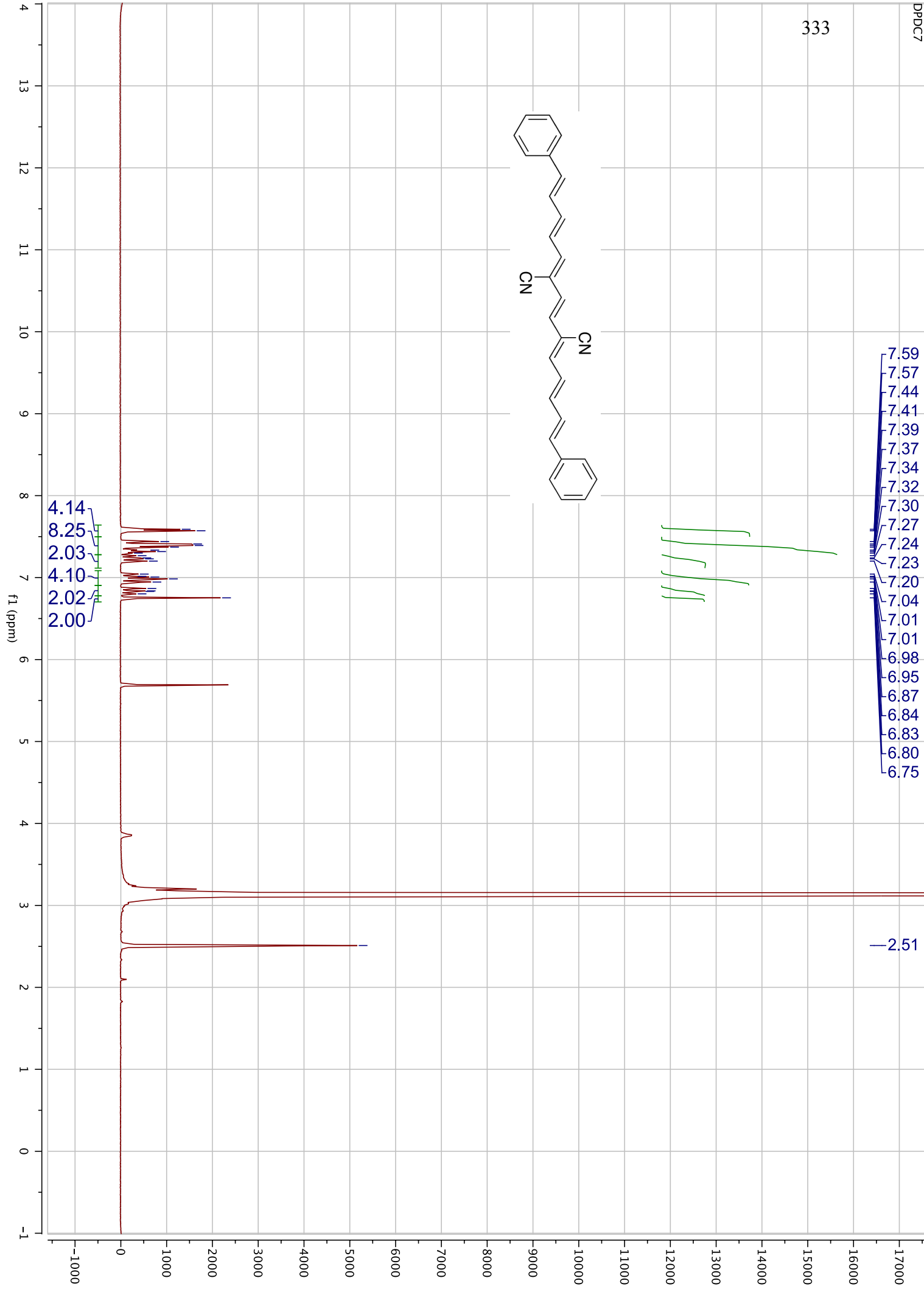
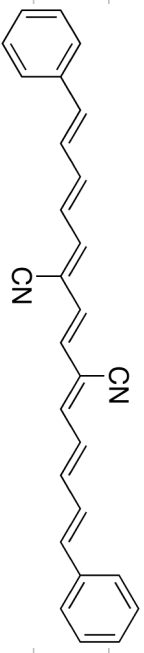




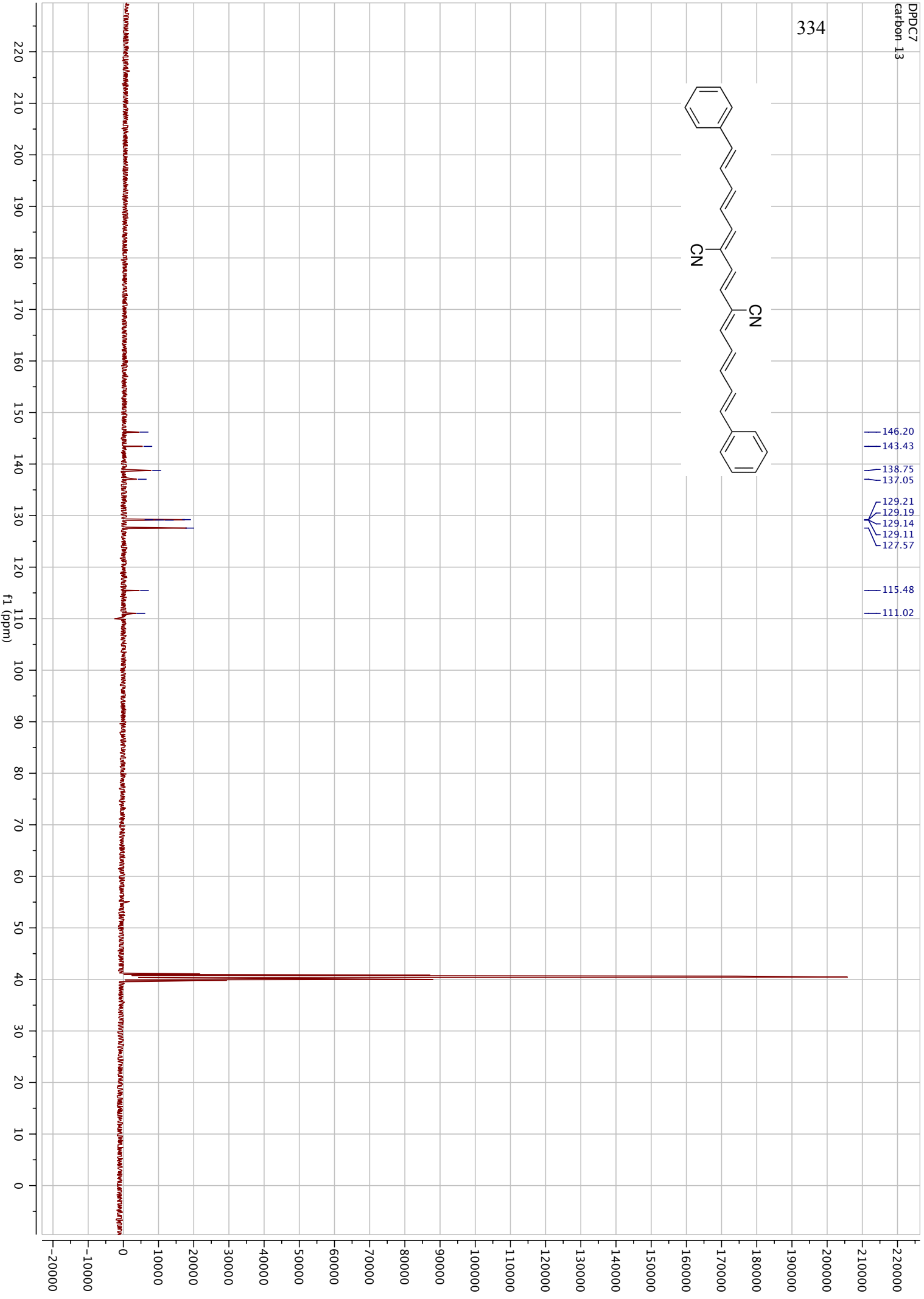
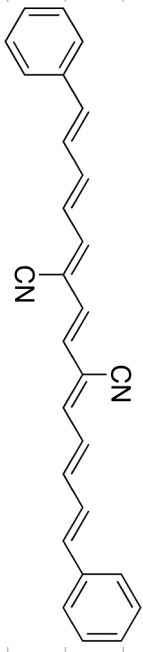
332



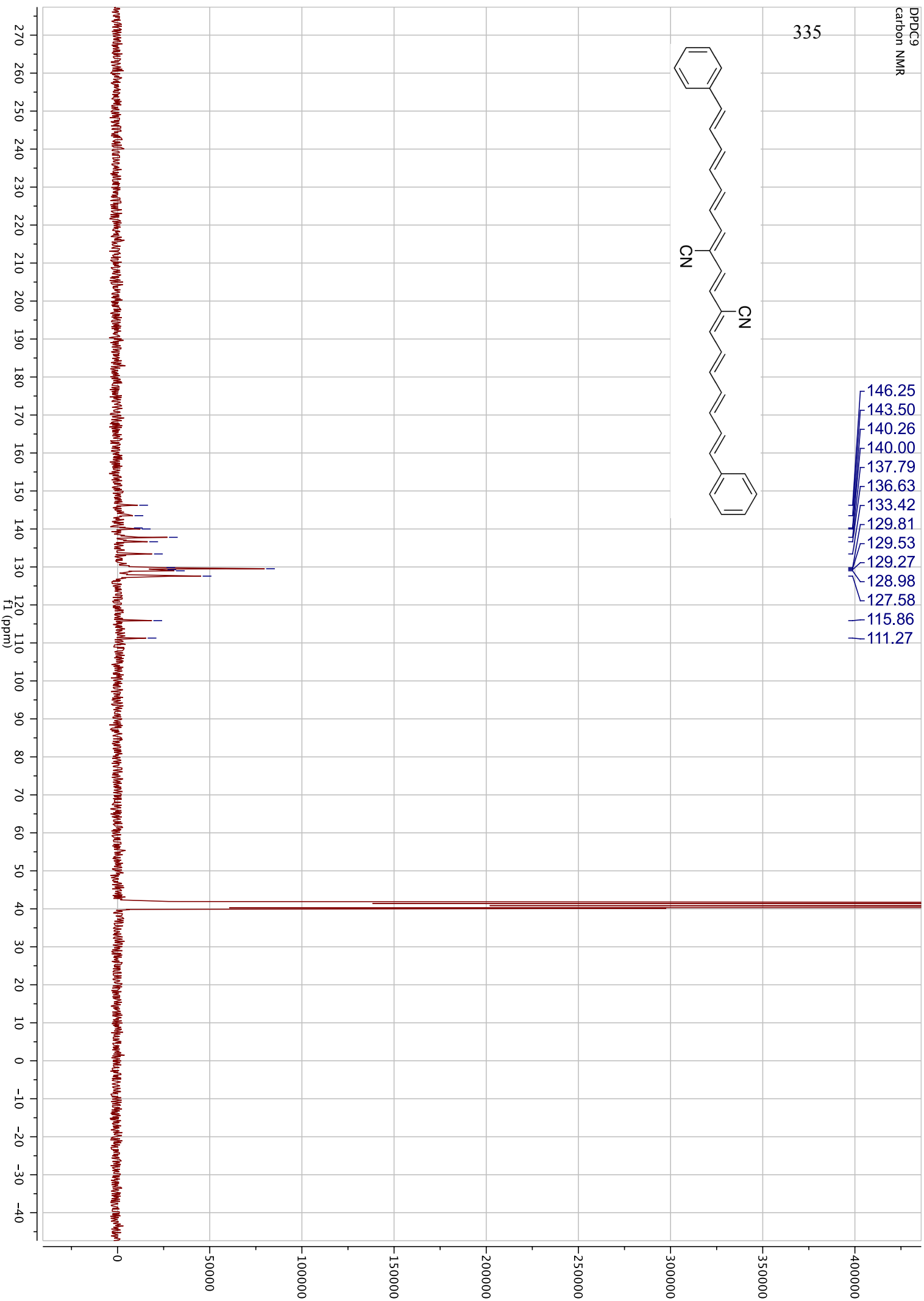
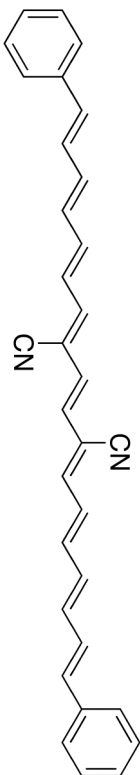


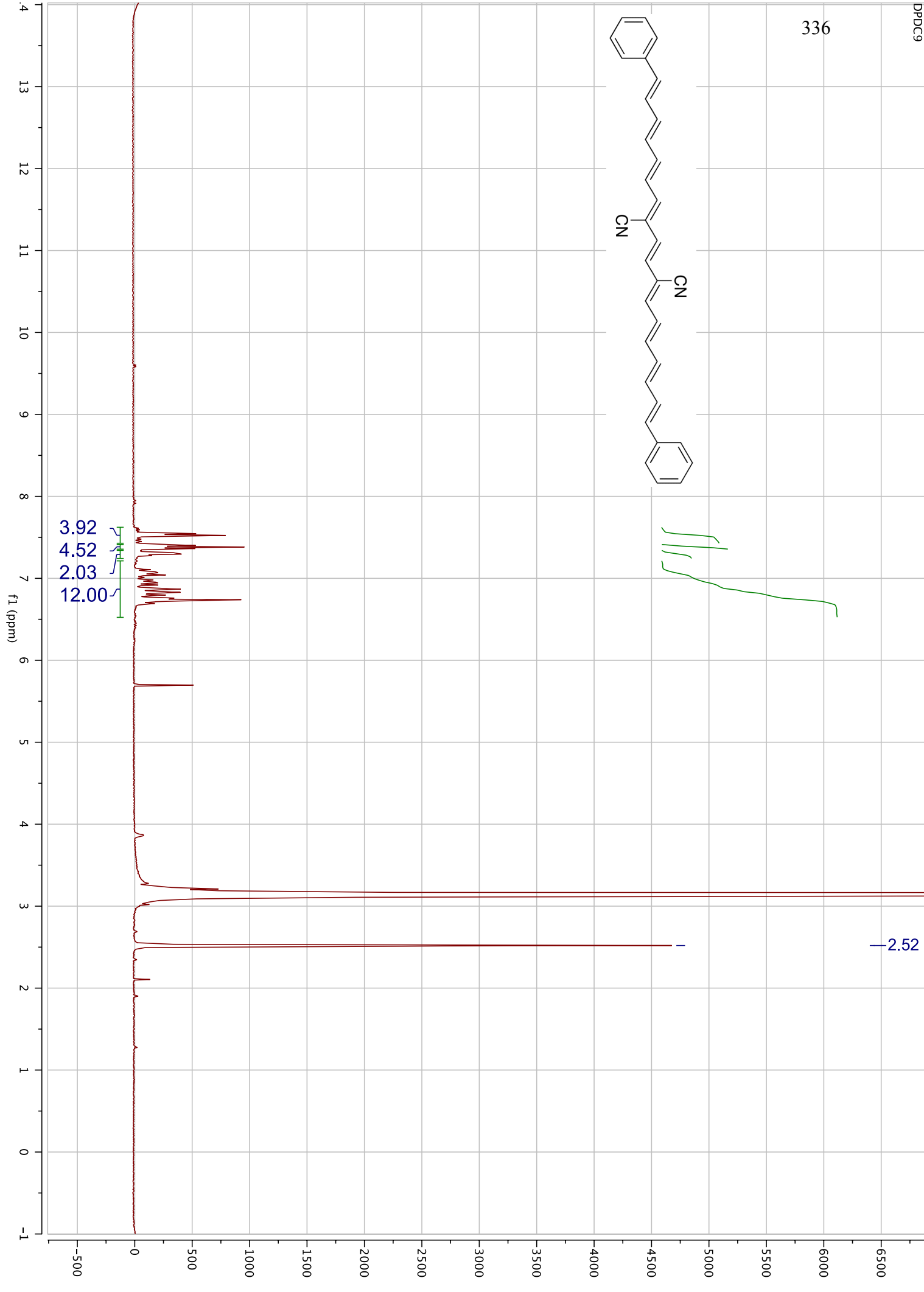
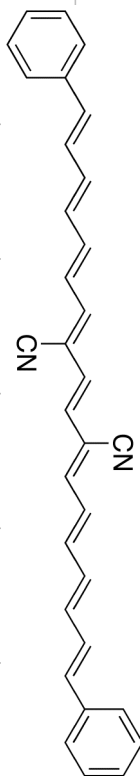


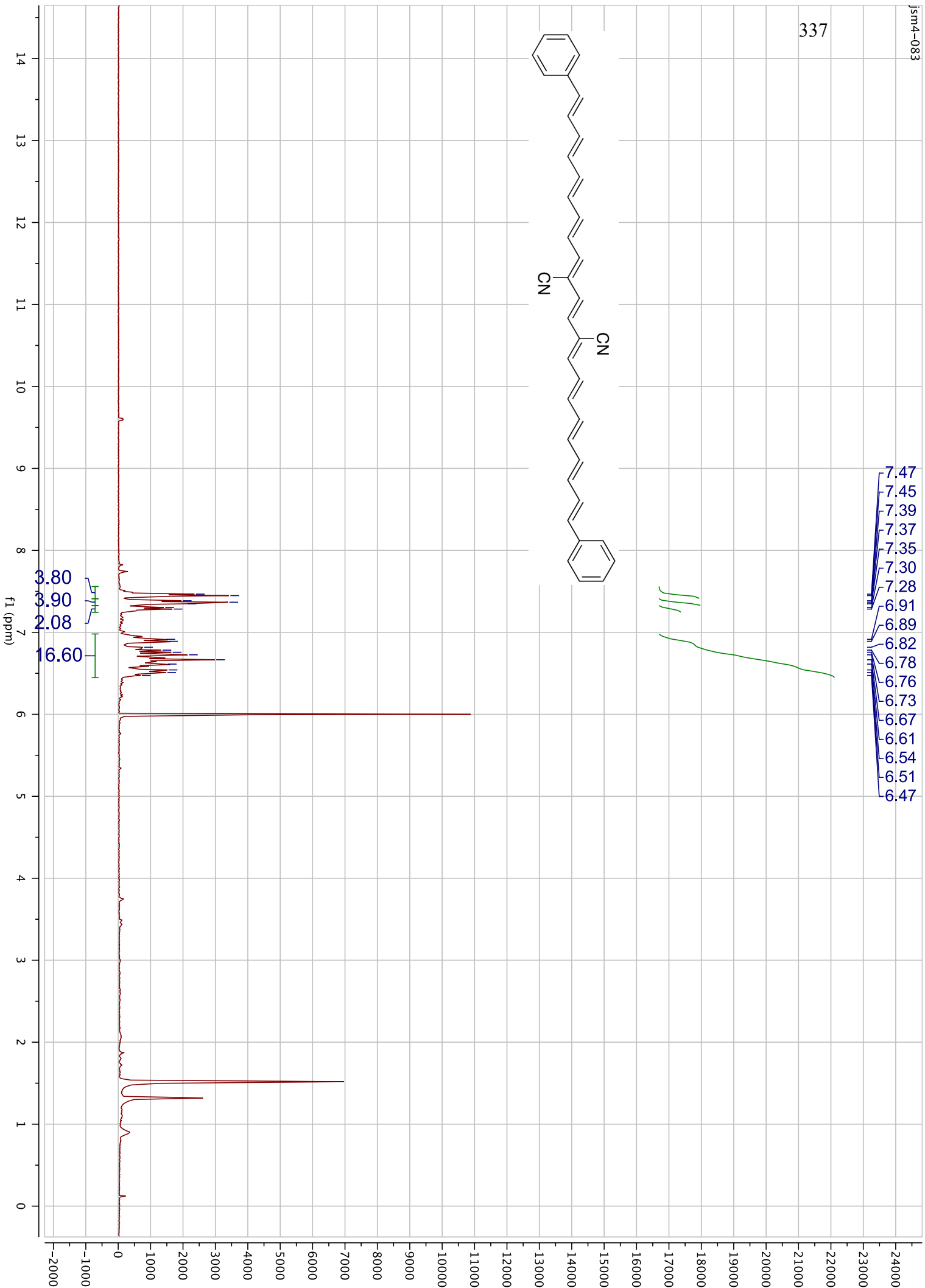
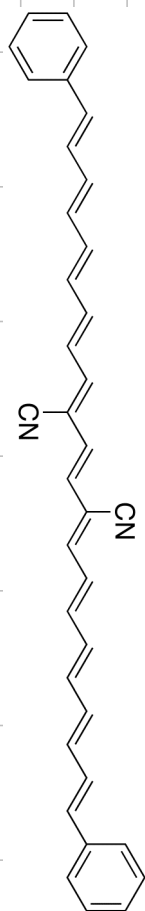
334

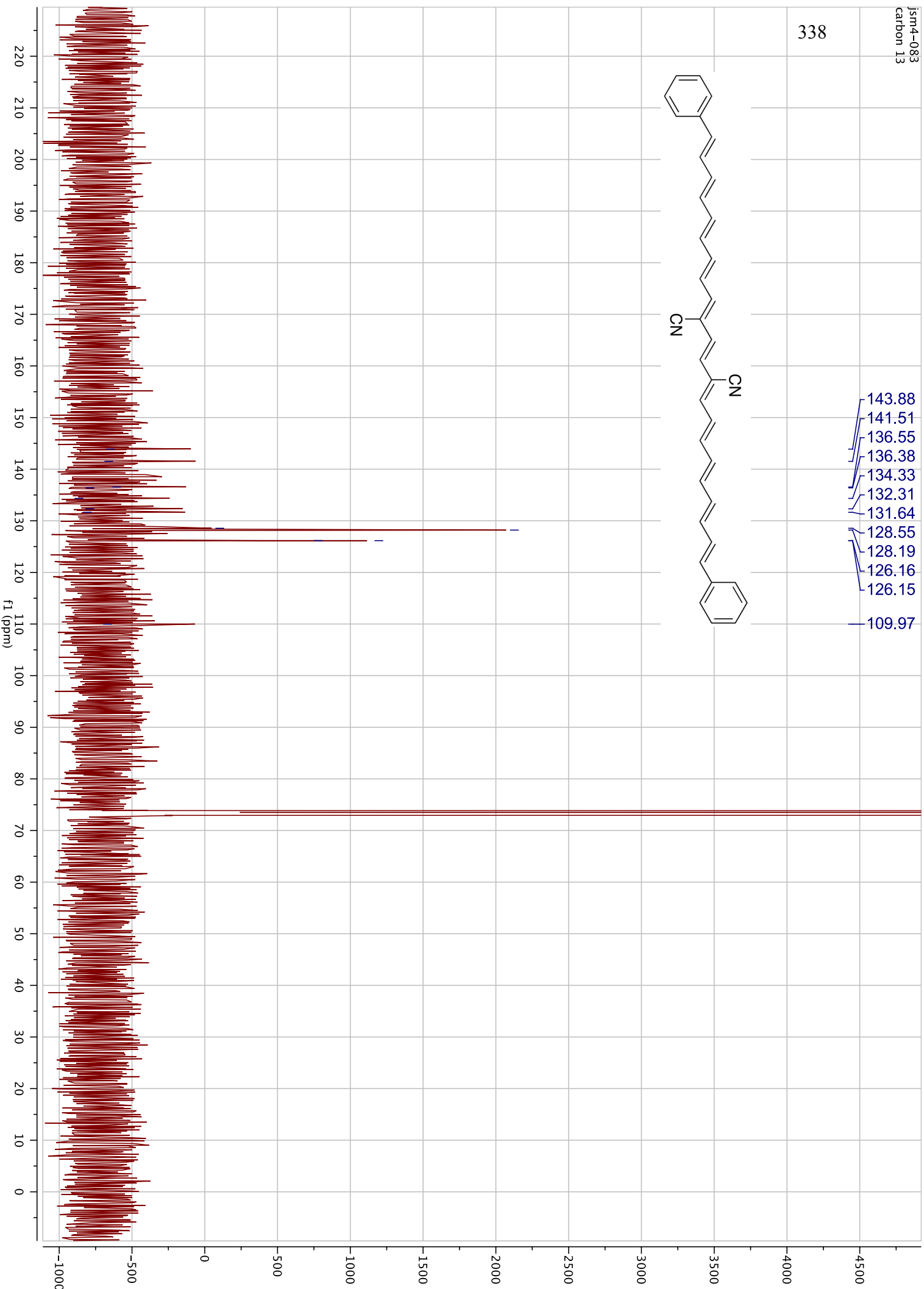


335

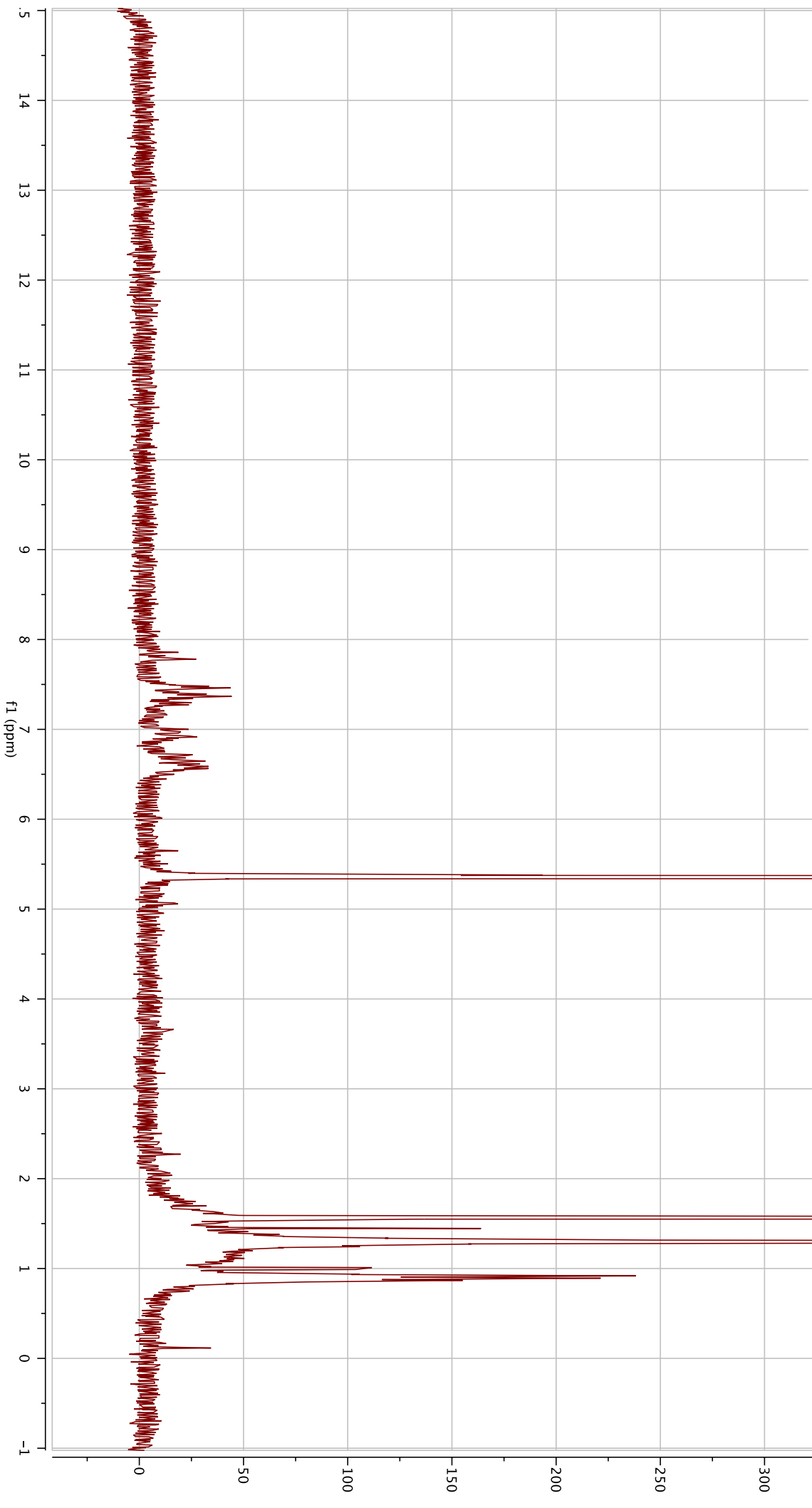
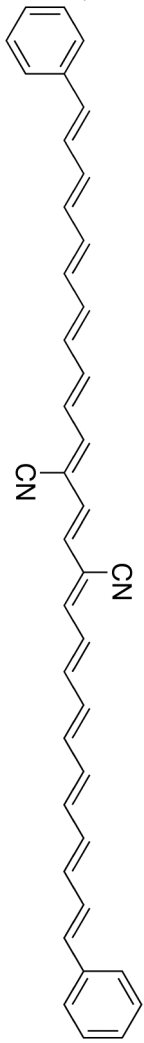




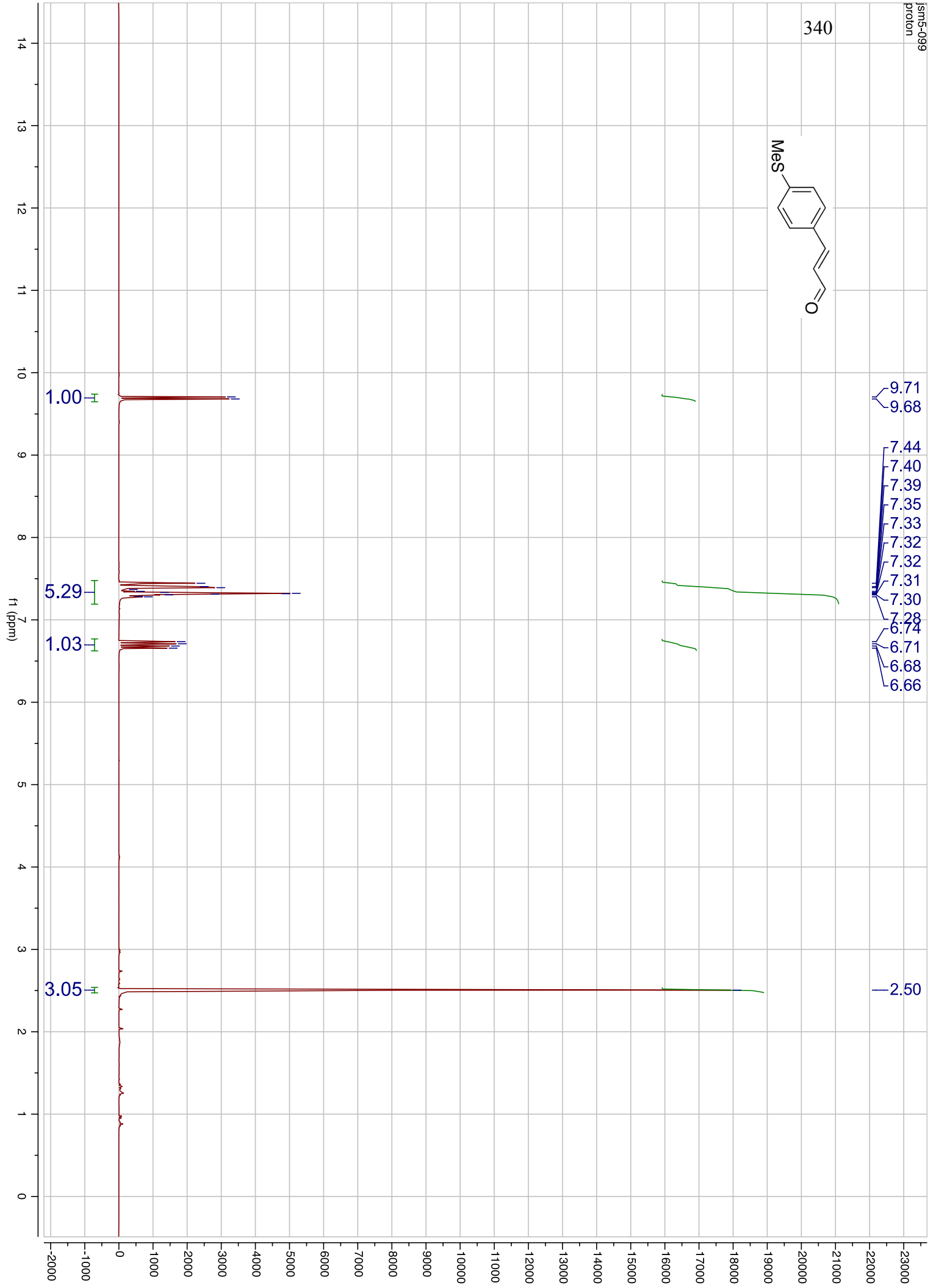
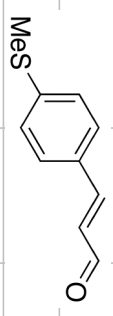




339

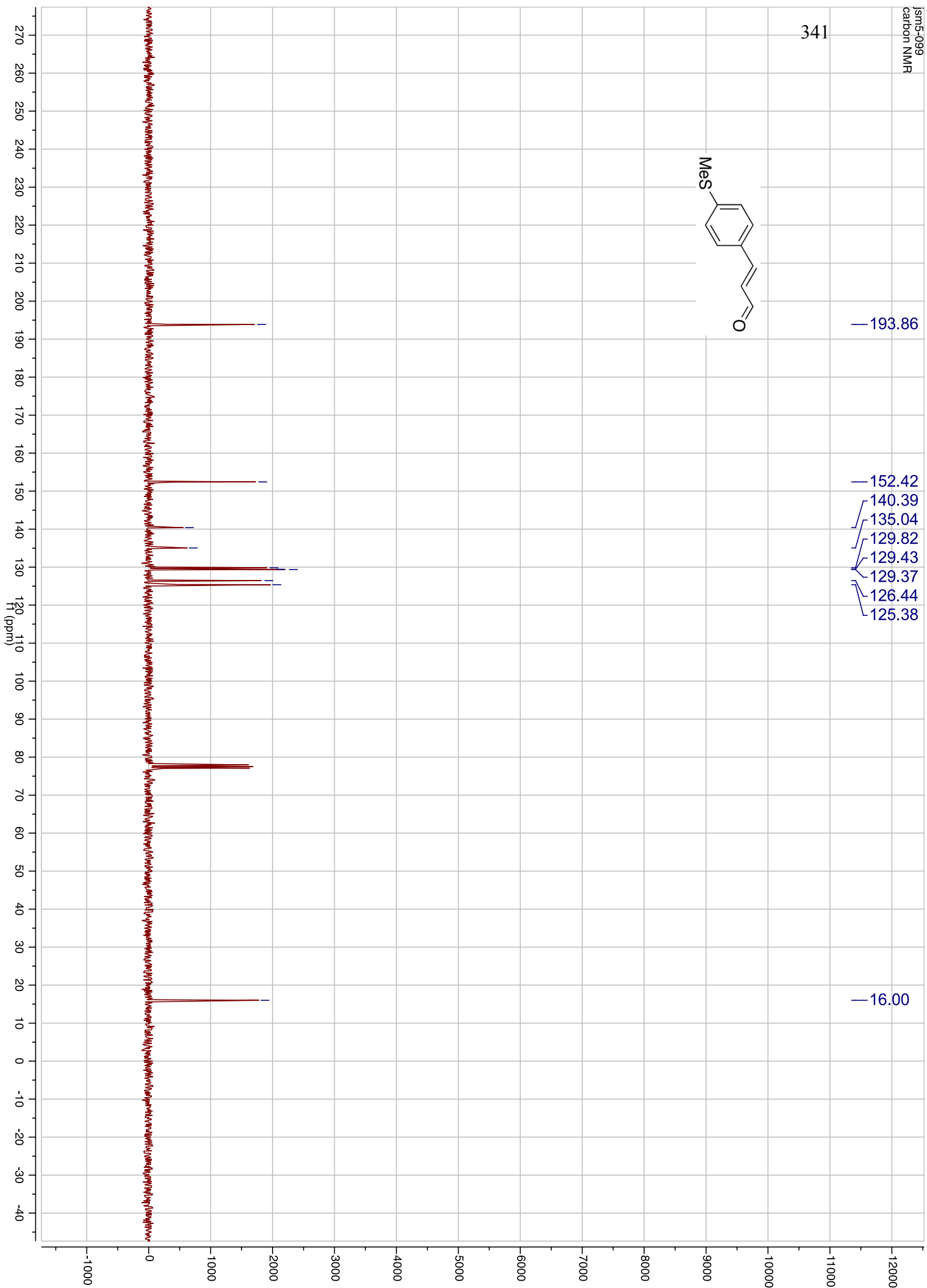
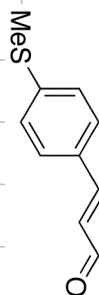


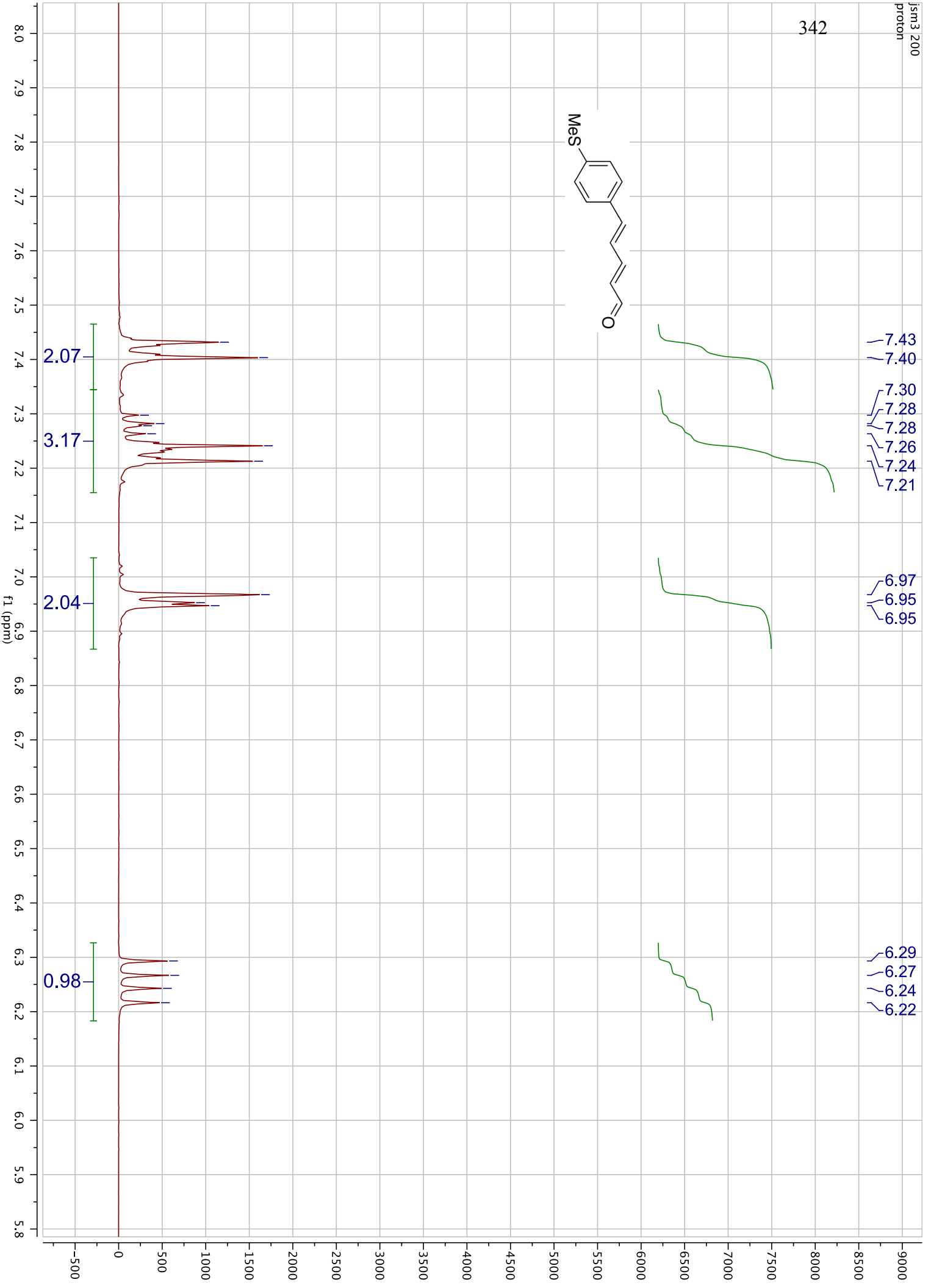
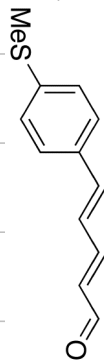
340



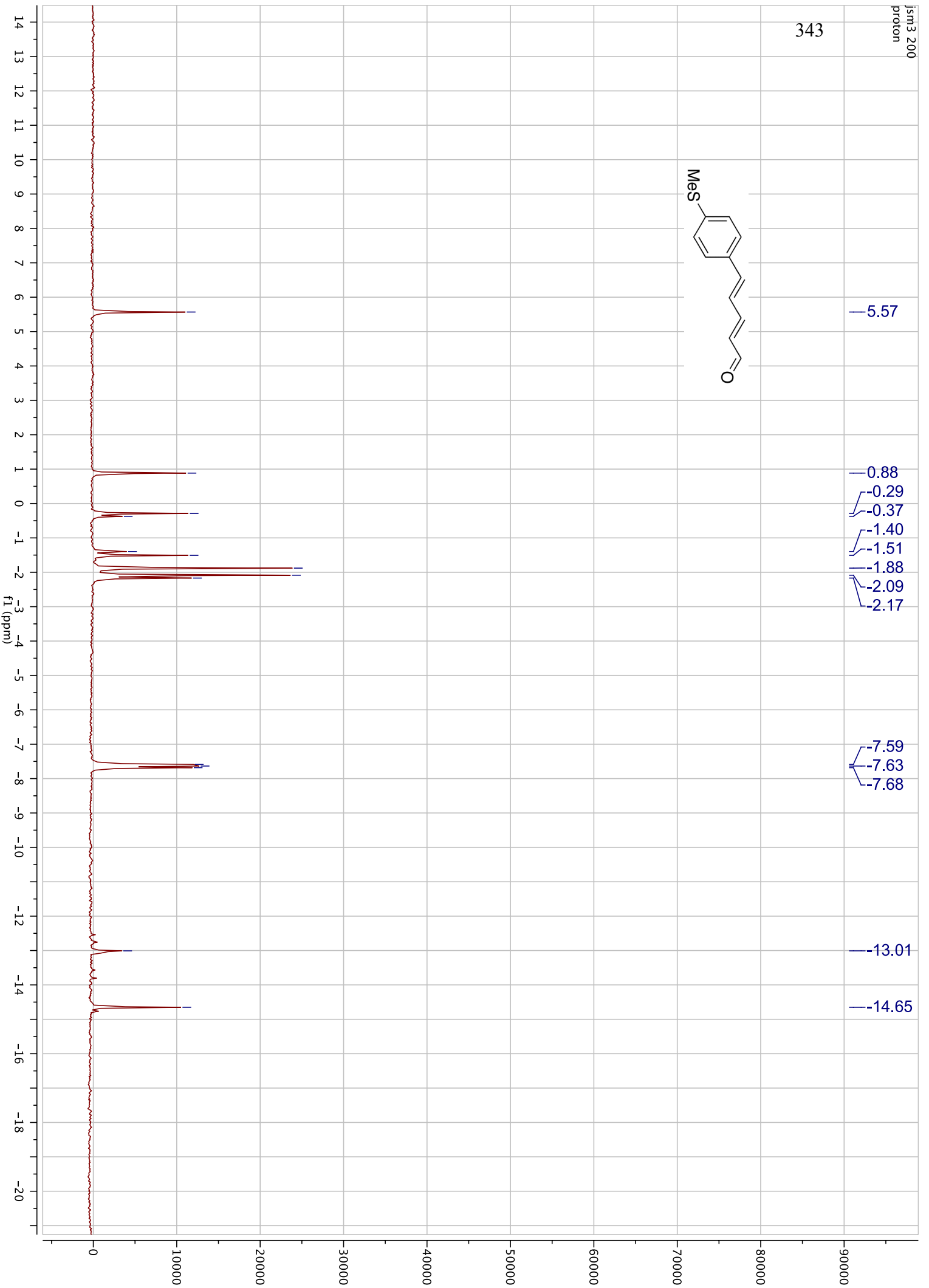
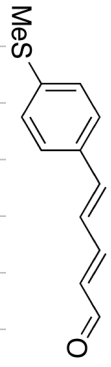


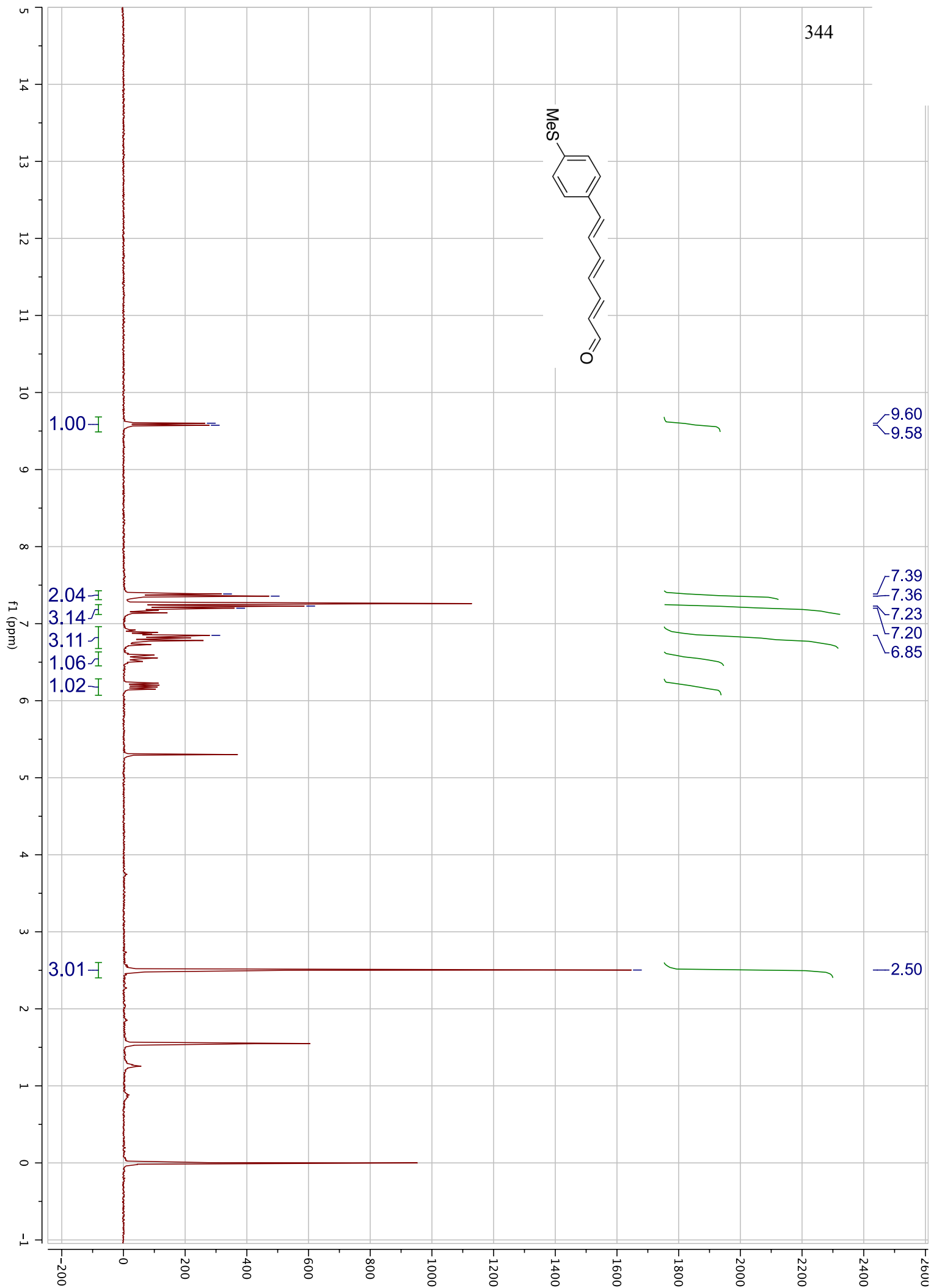
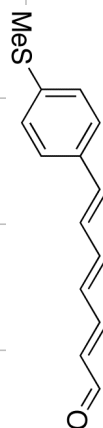
341



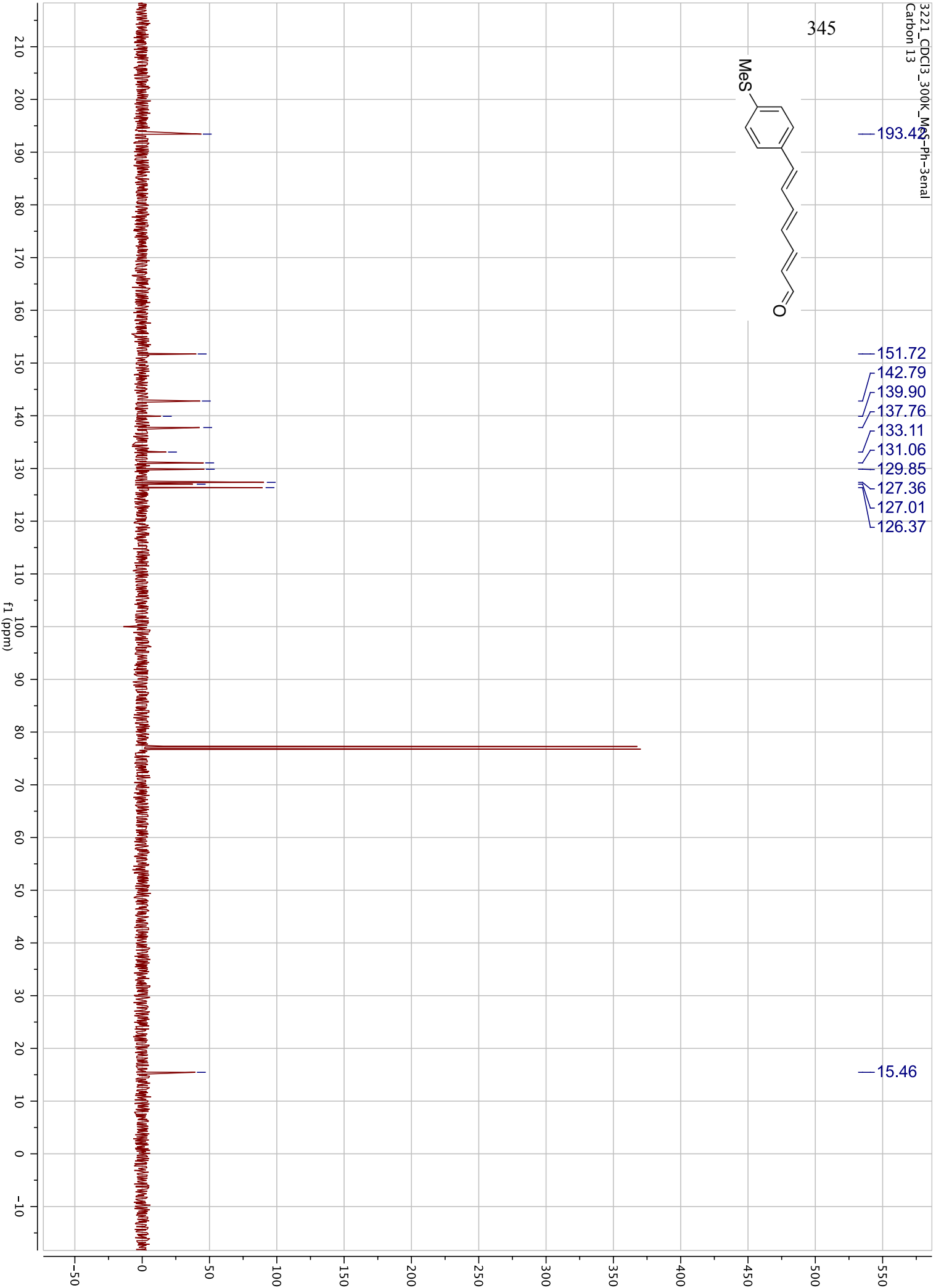
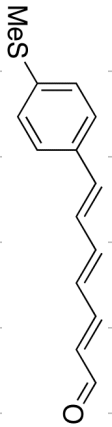


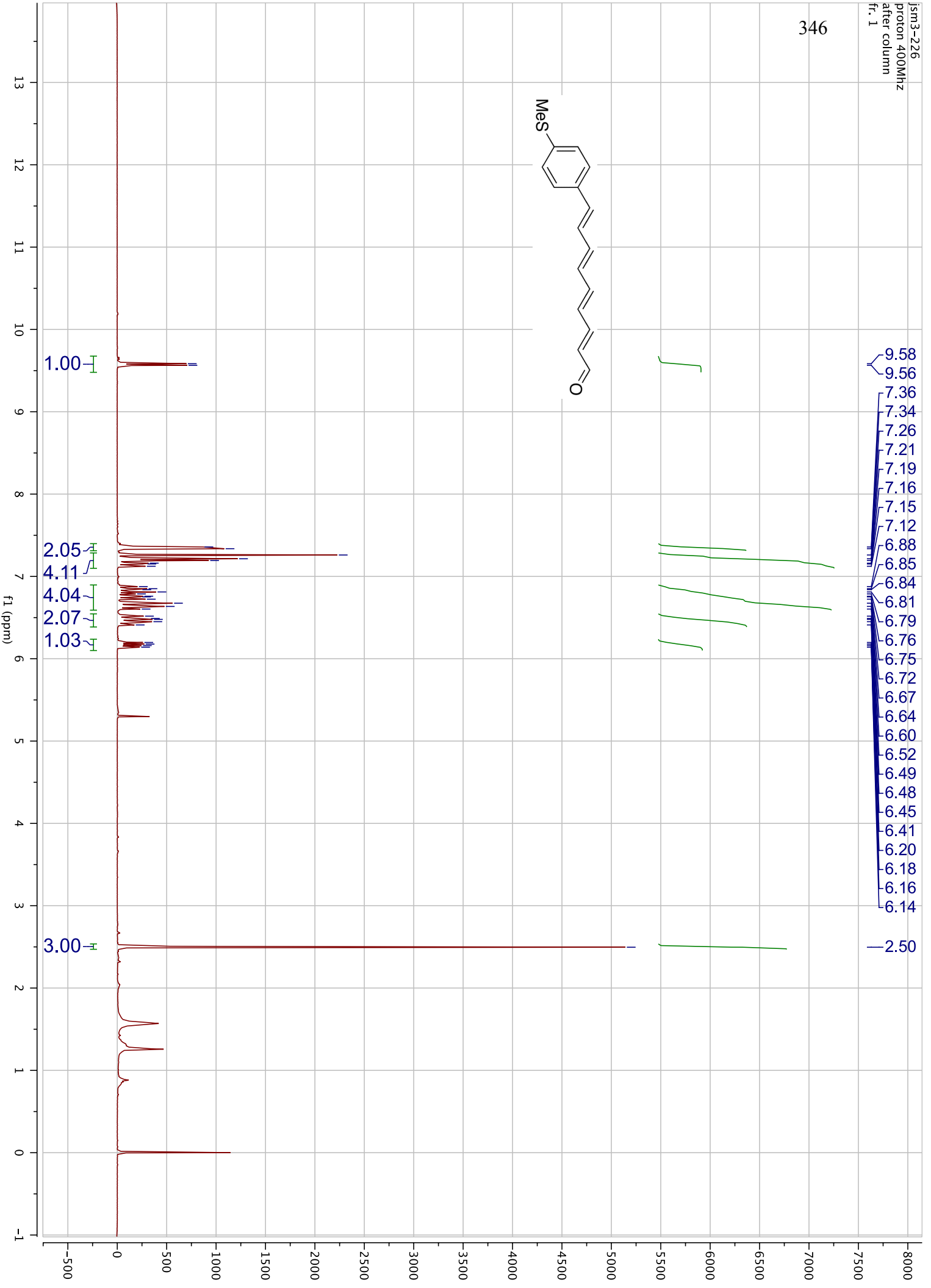
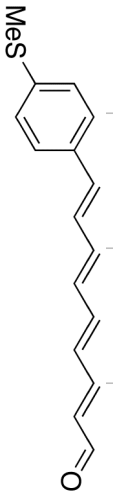
343



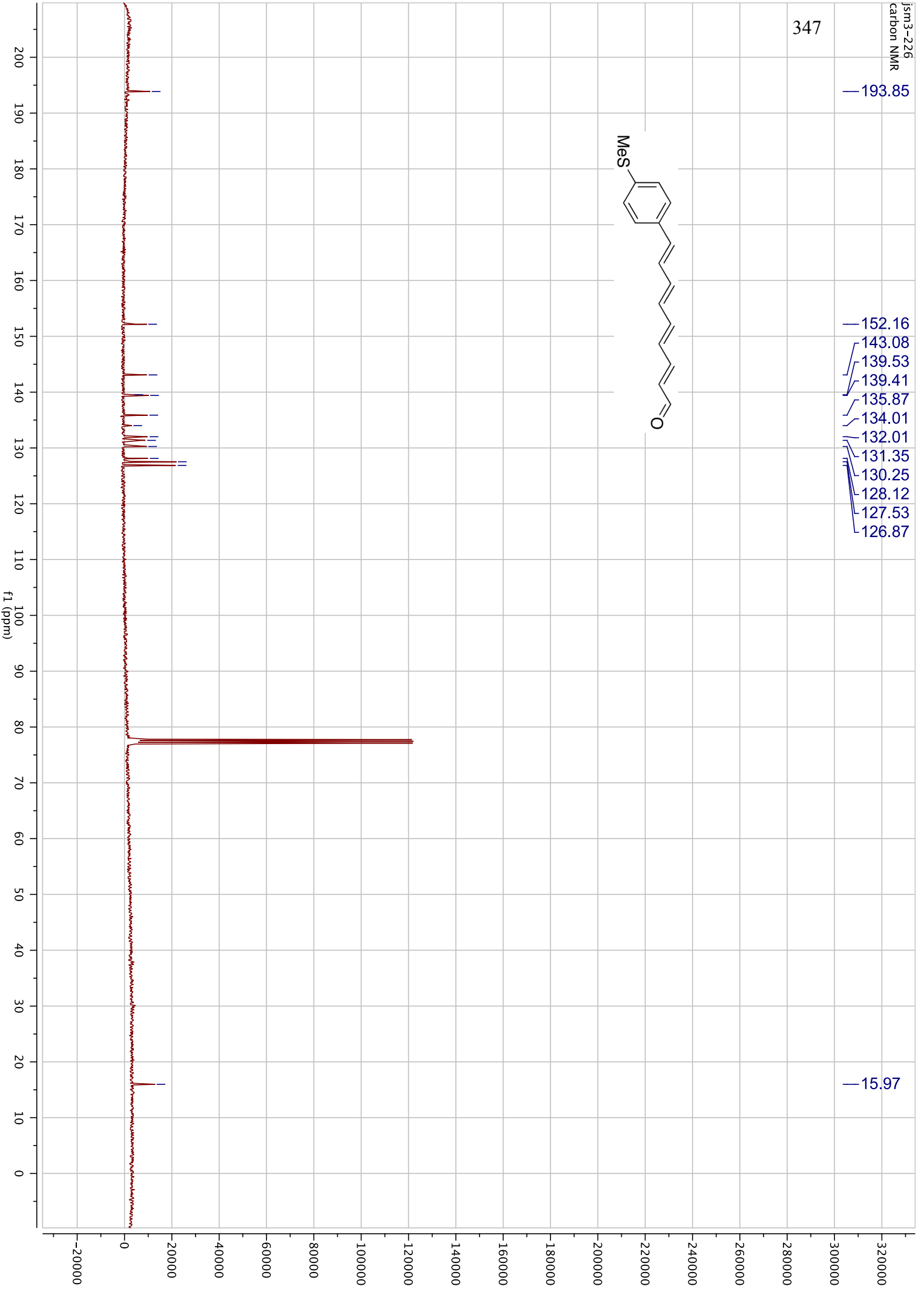
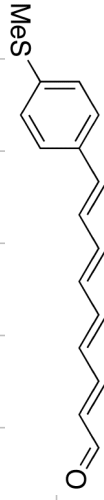


345

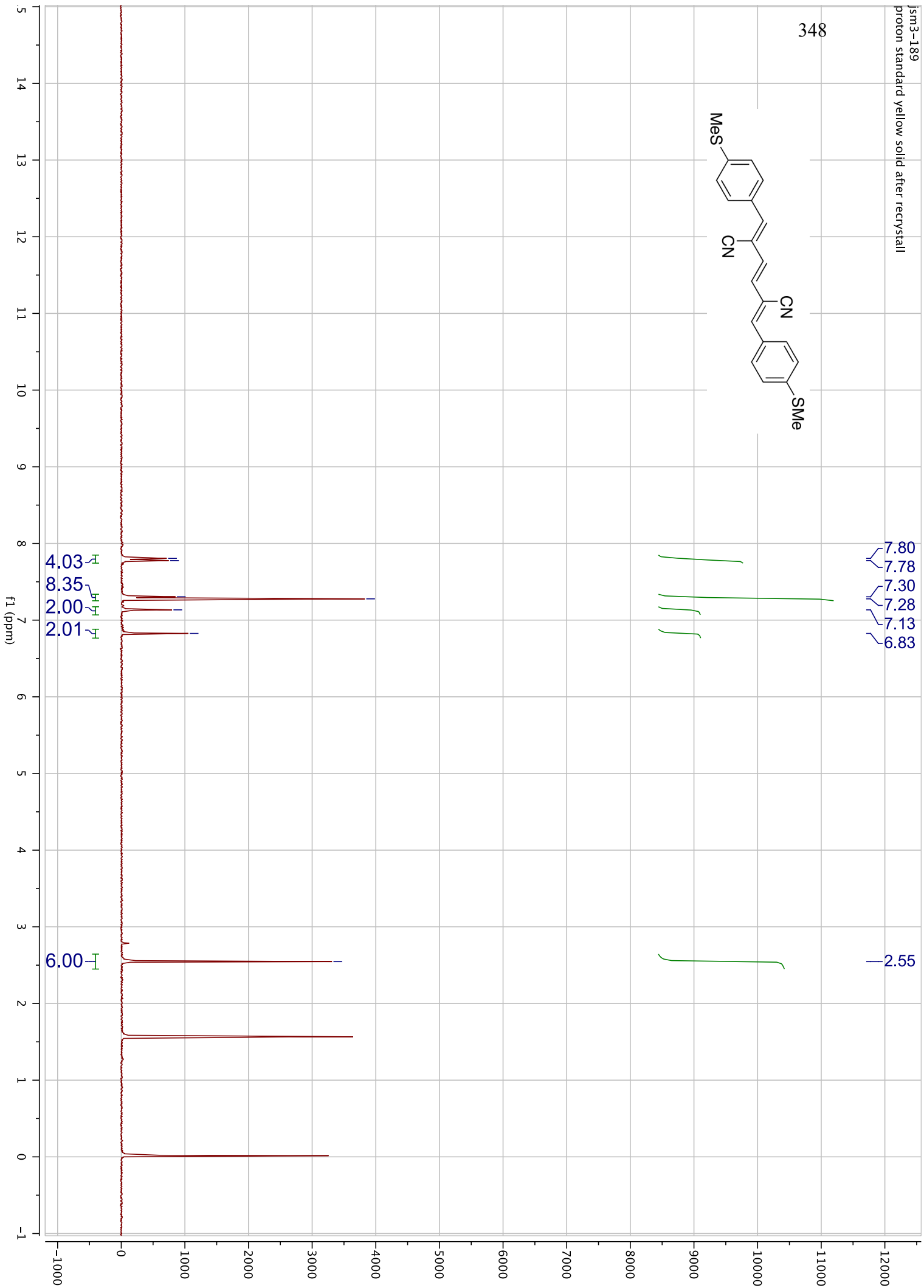
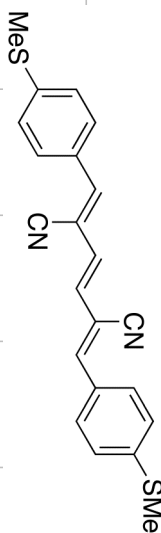




347

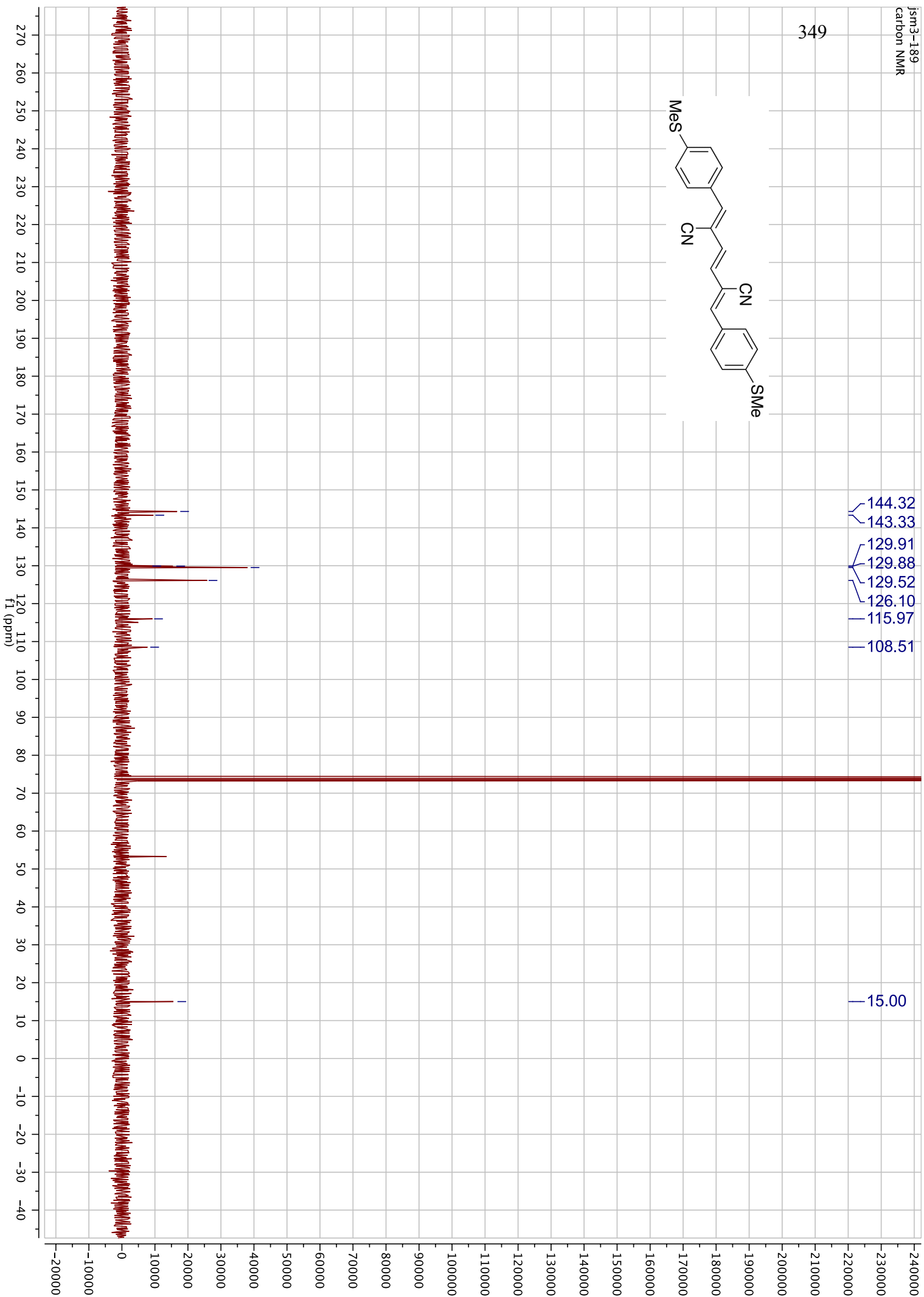
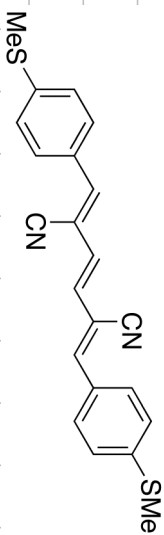


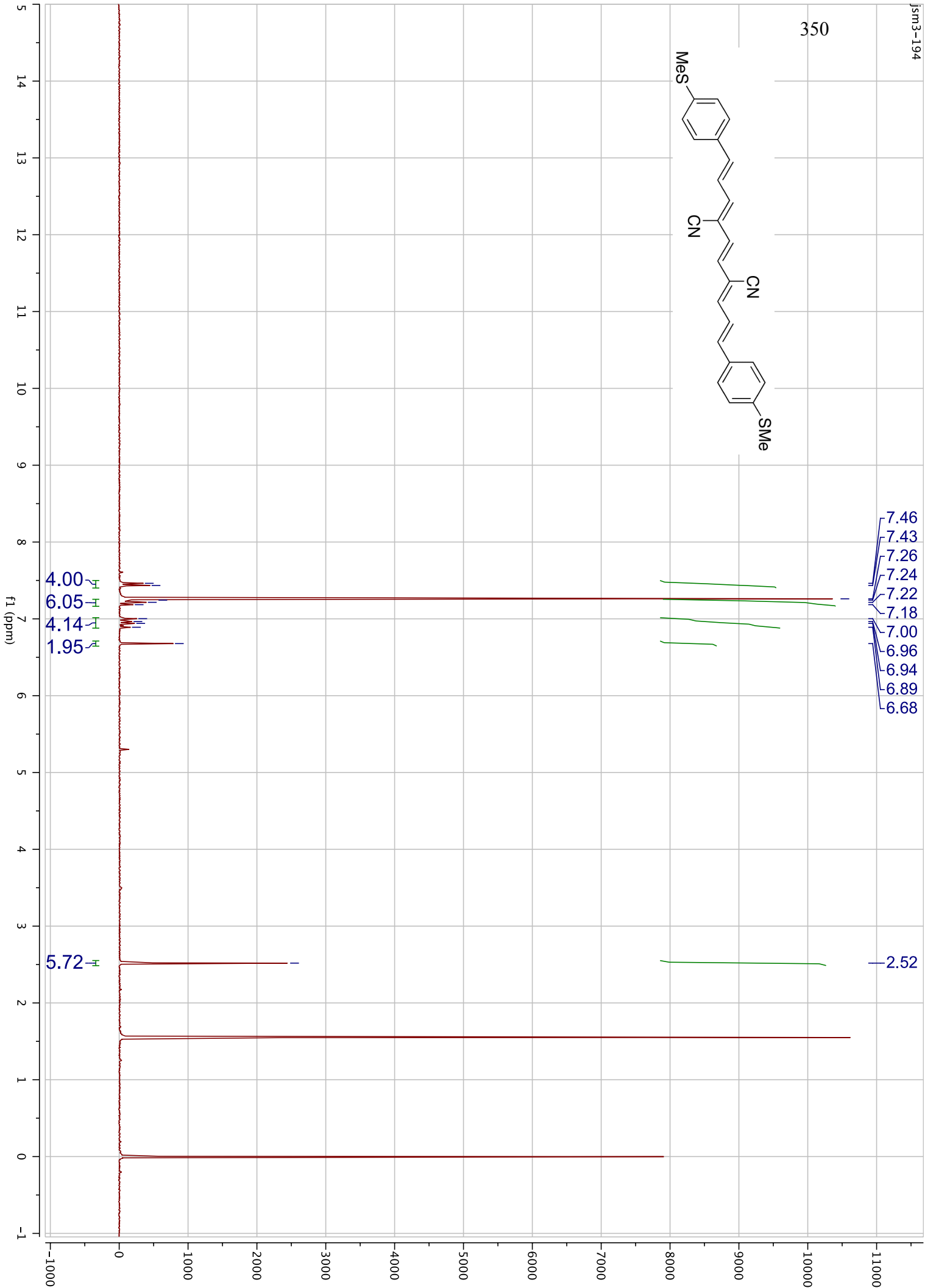
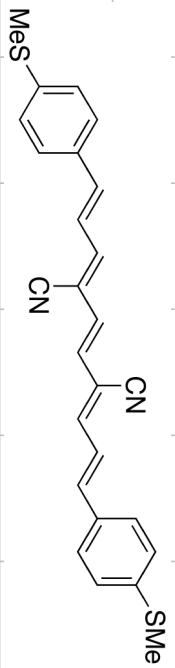
348



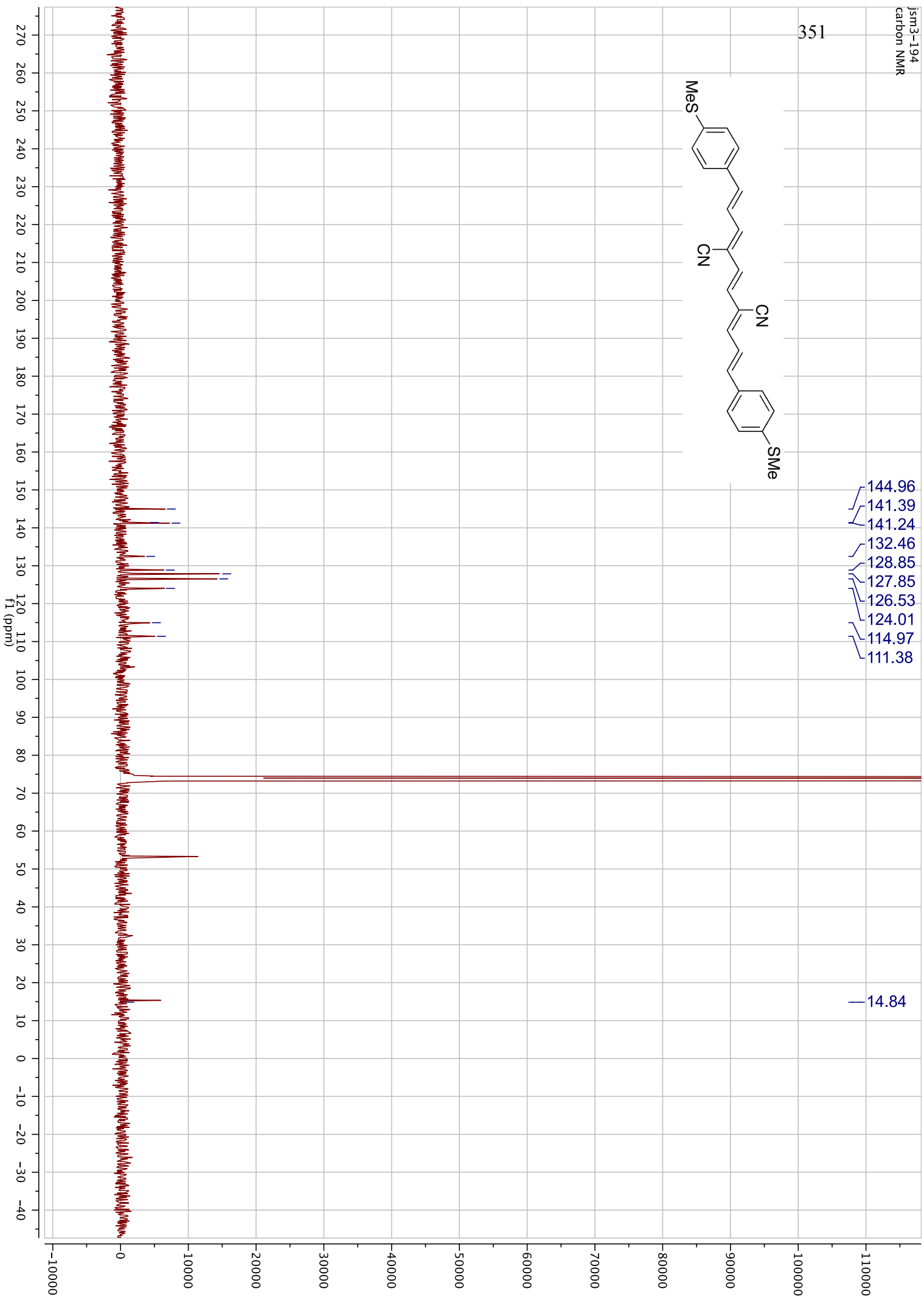
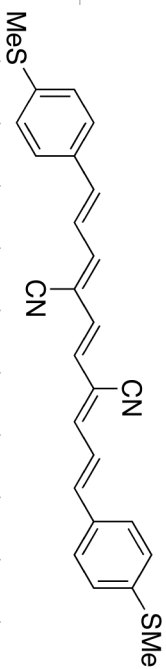


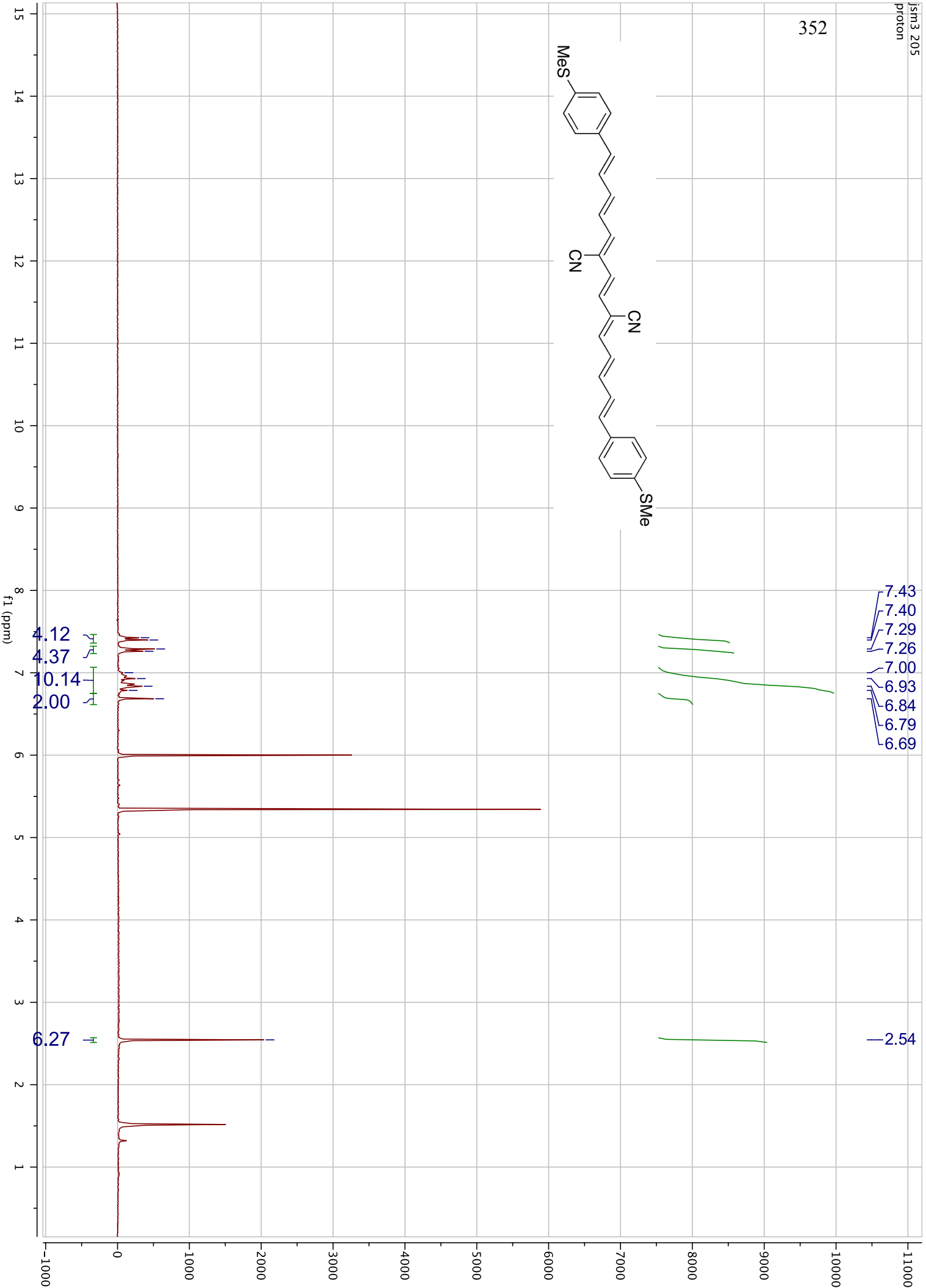
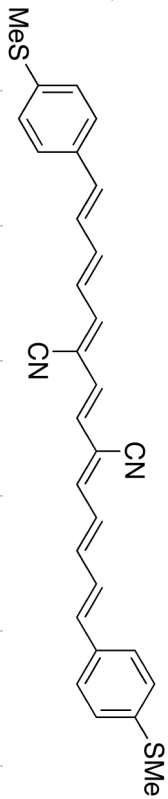
349

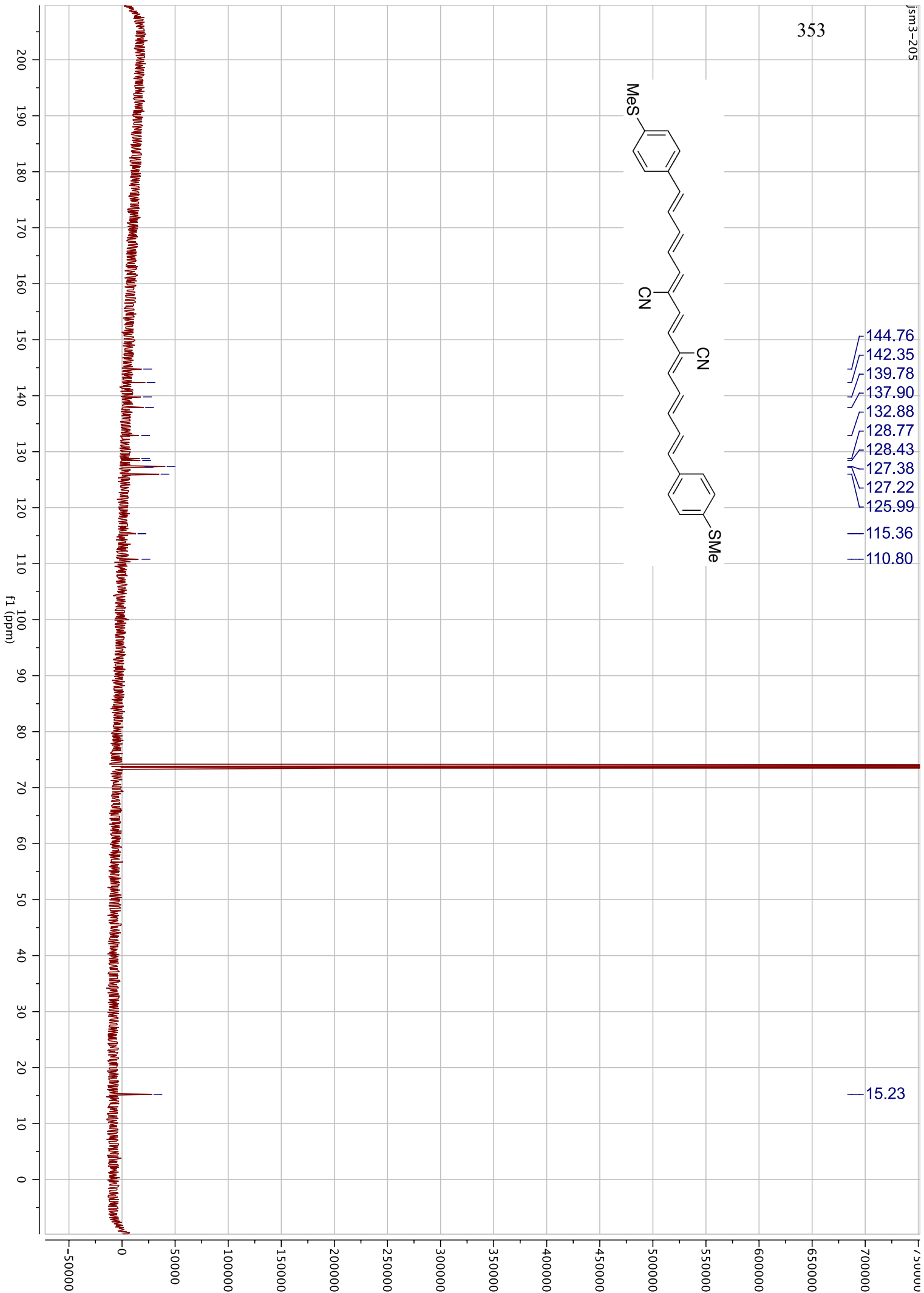
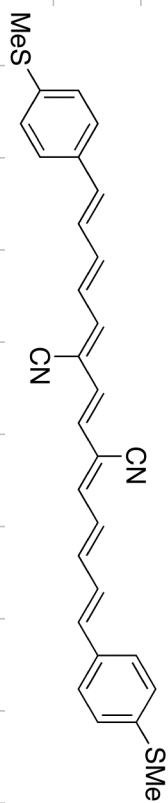


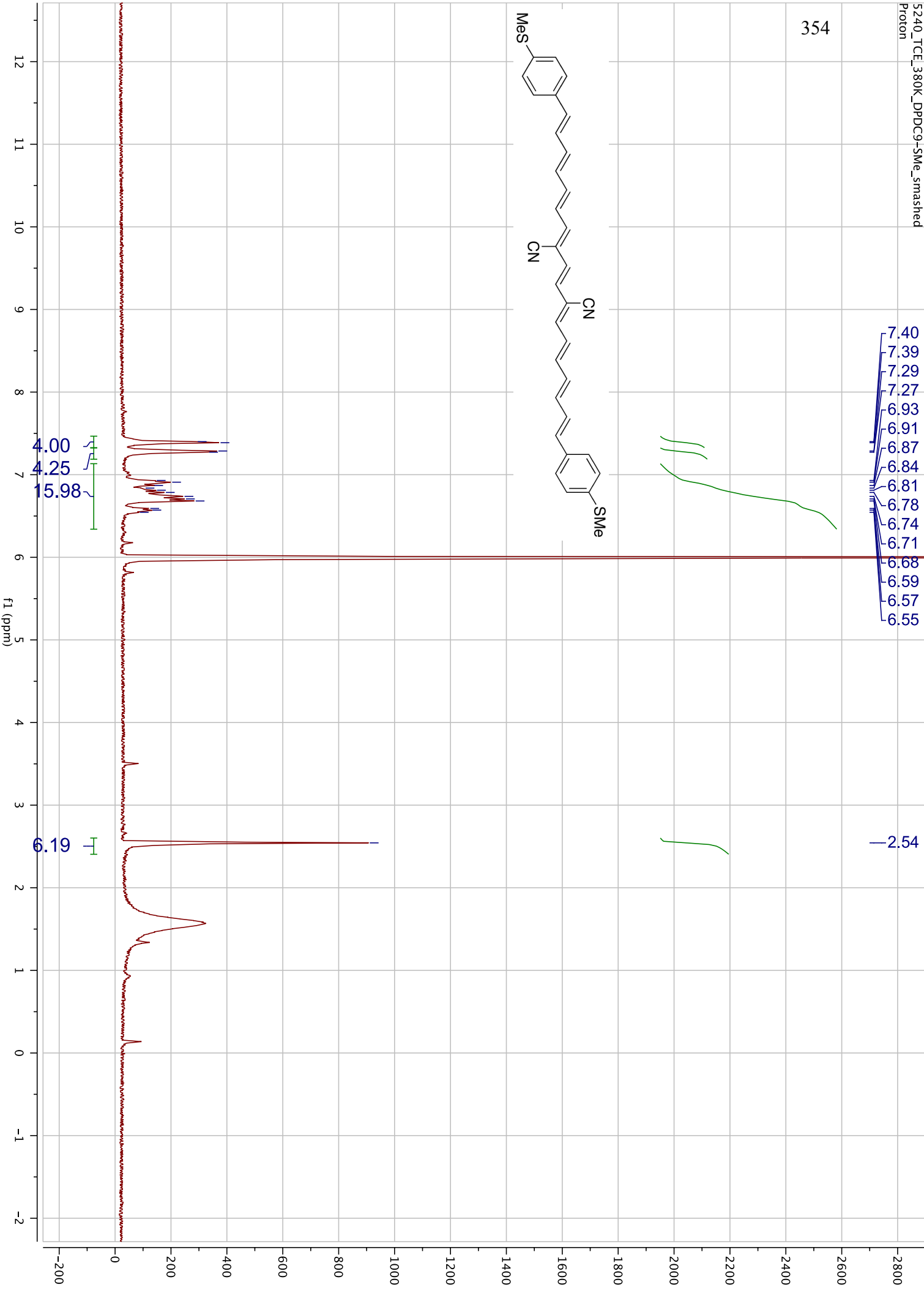
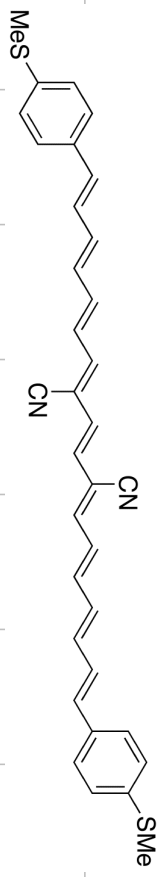


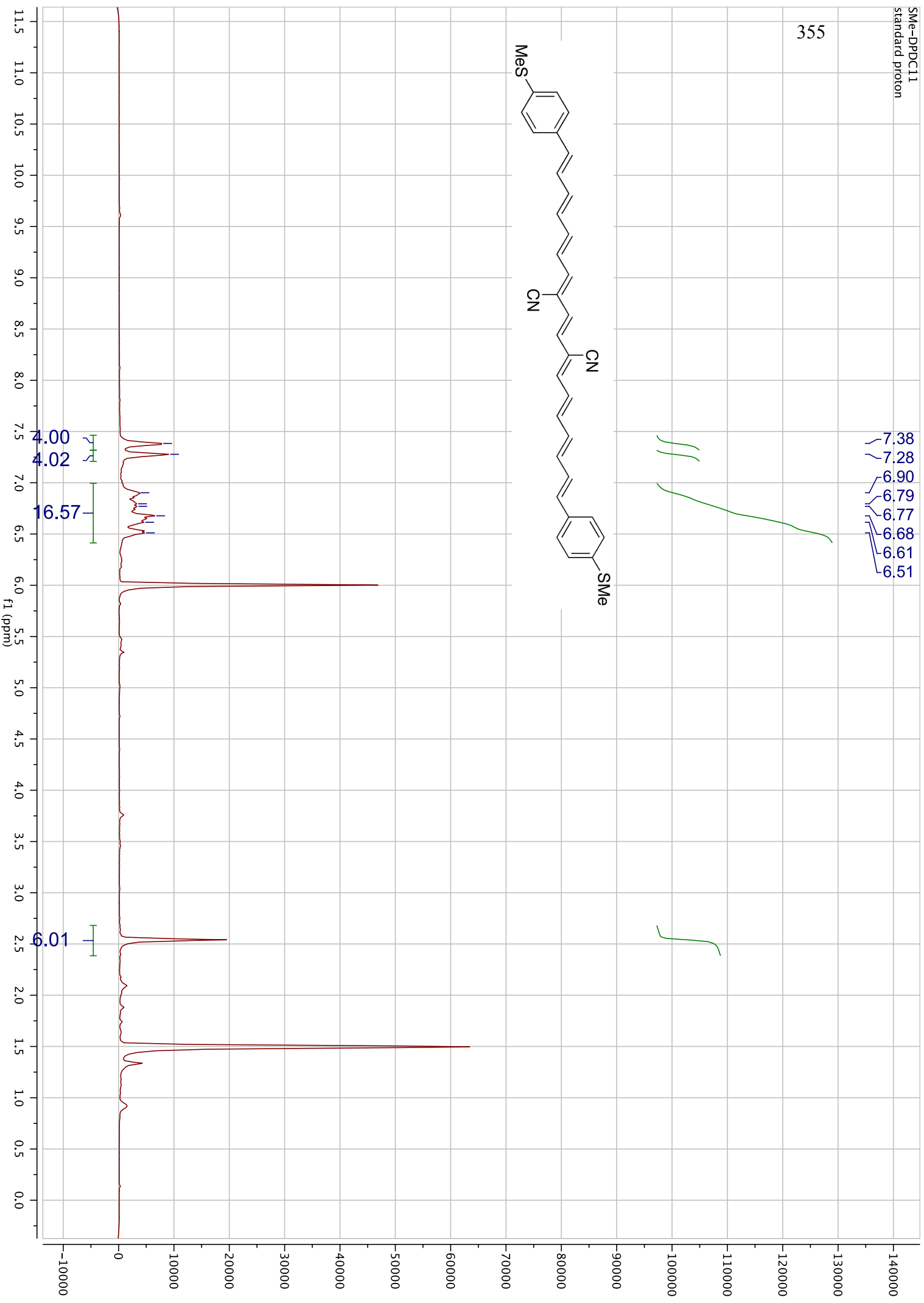
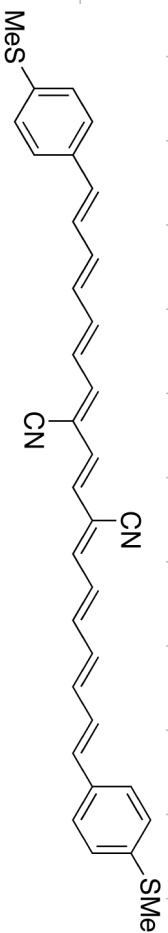
351

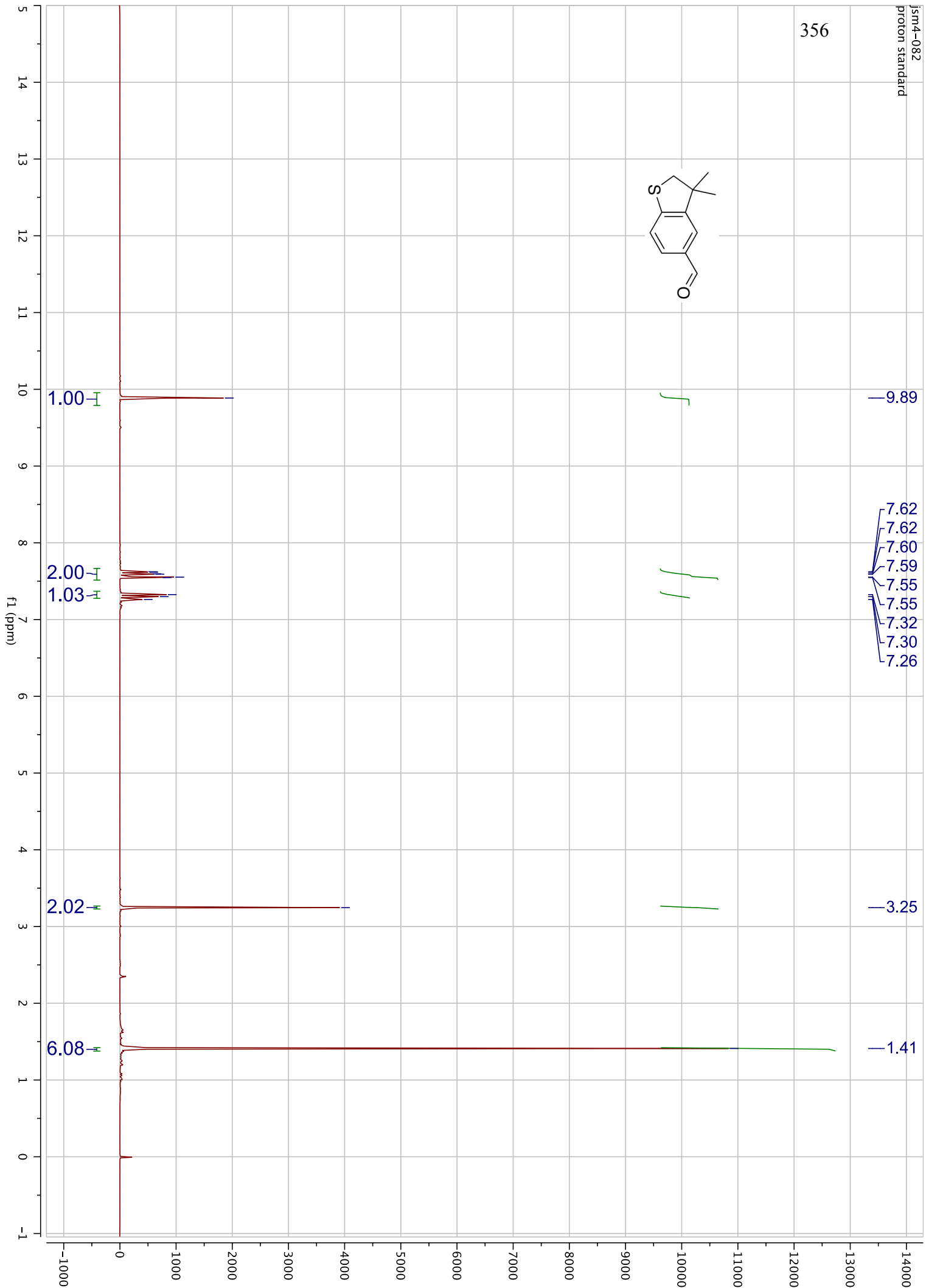
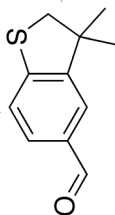




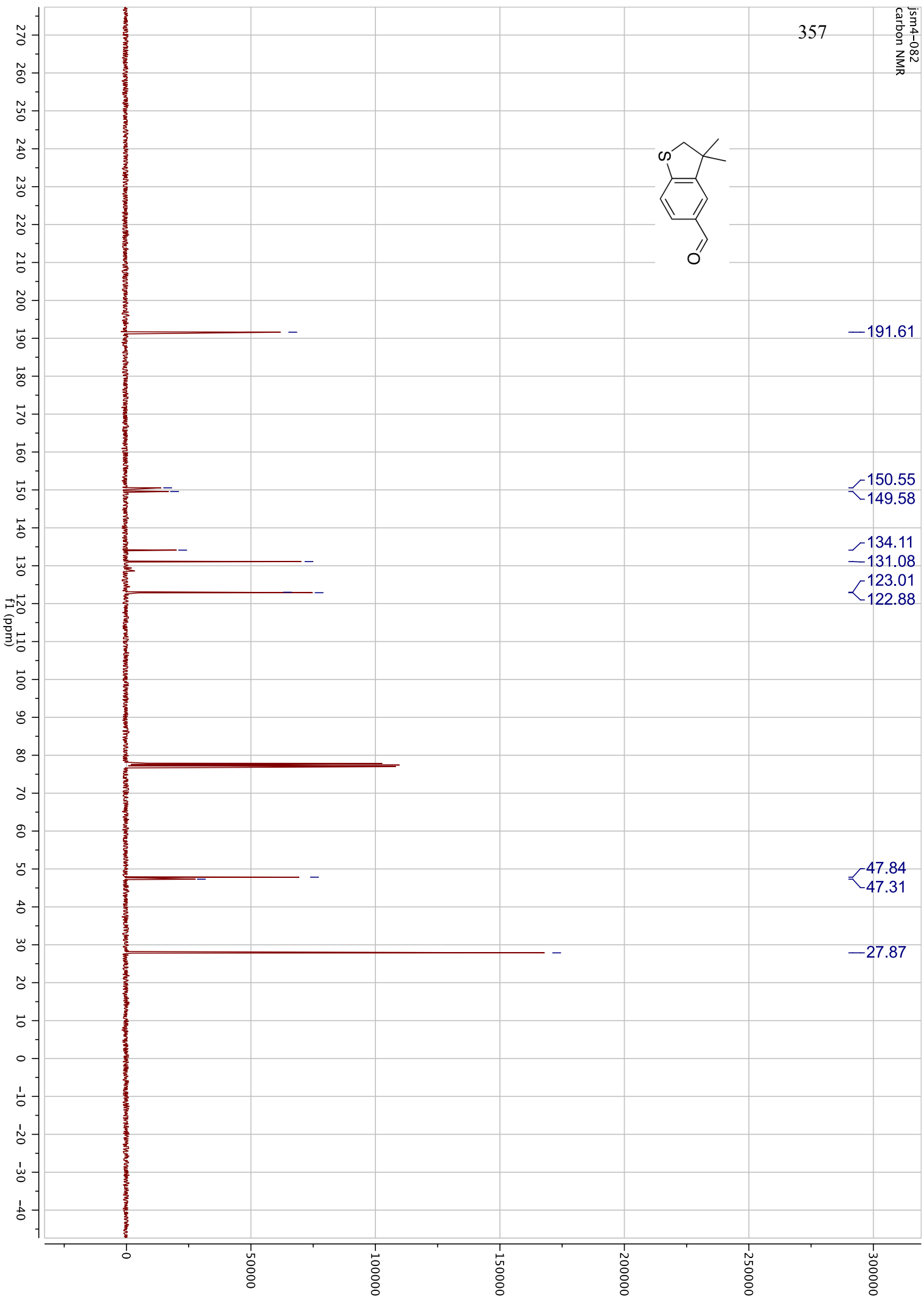
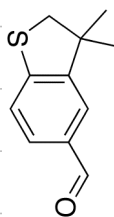


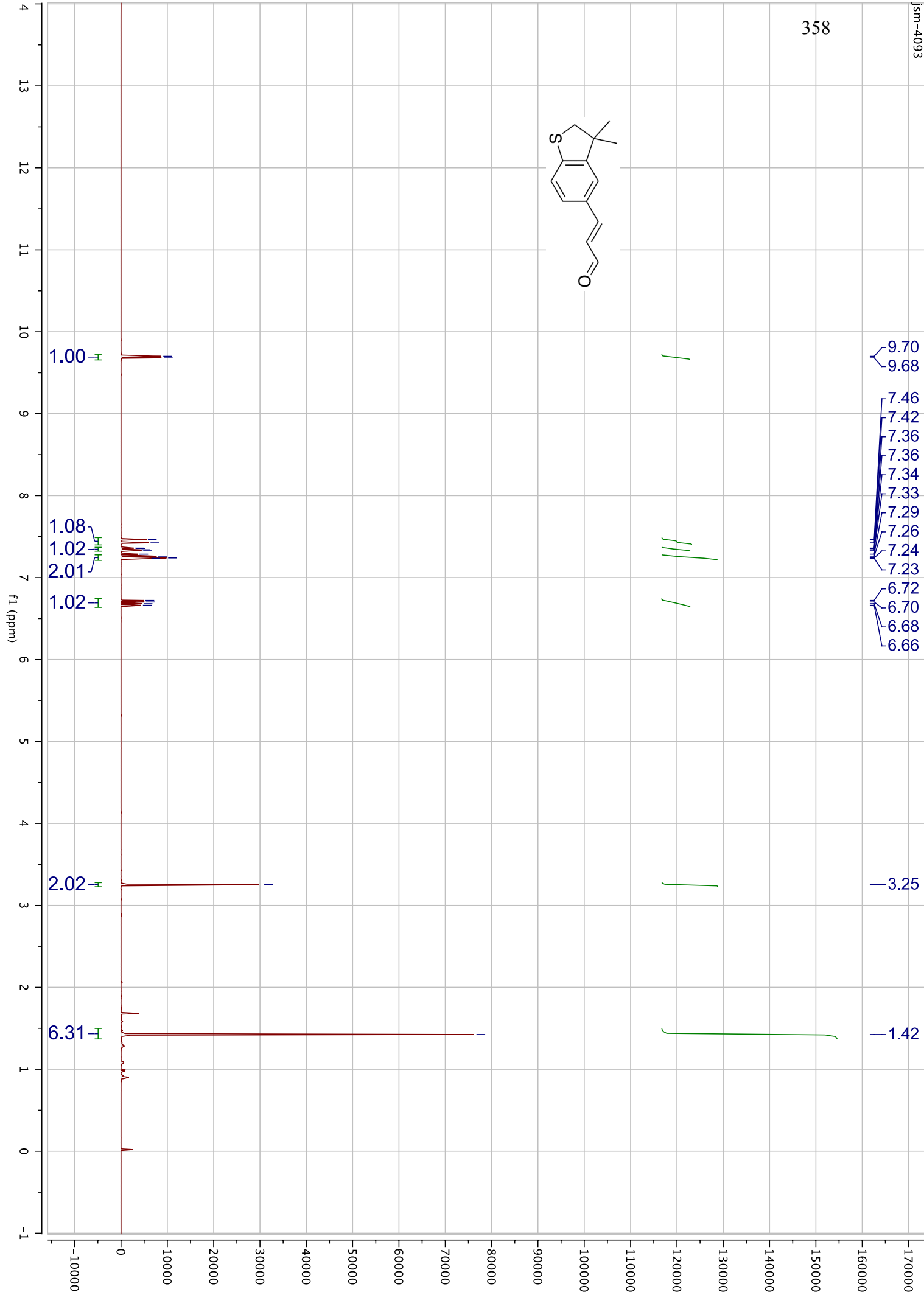
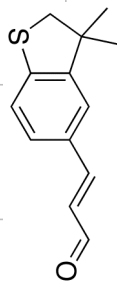


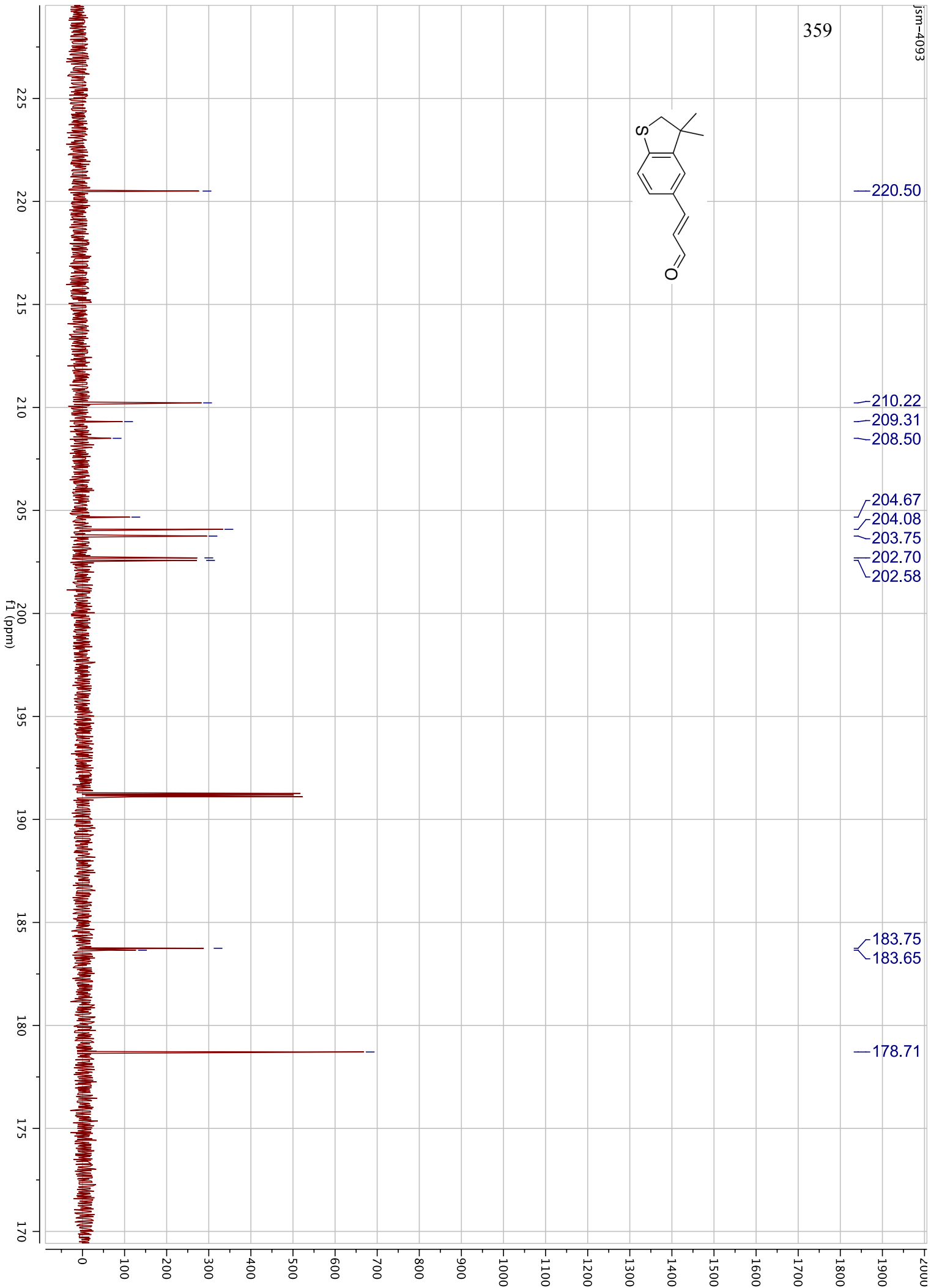
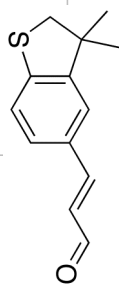


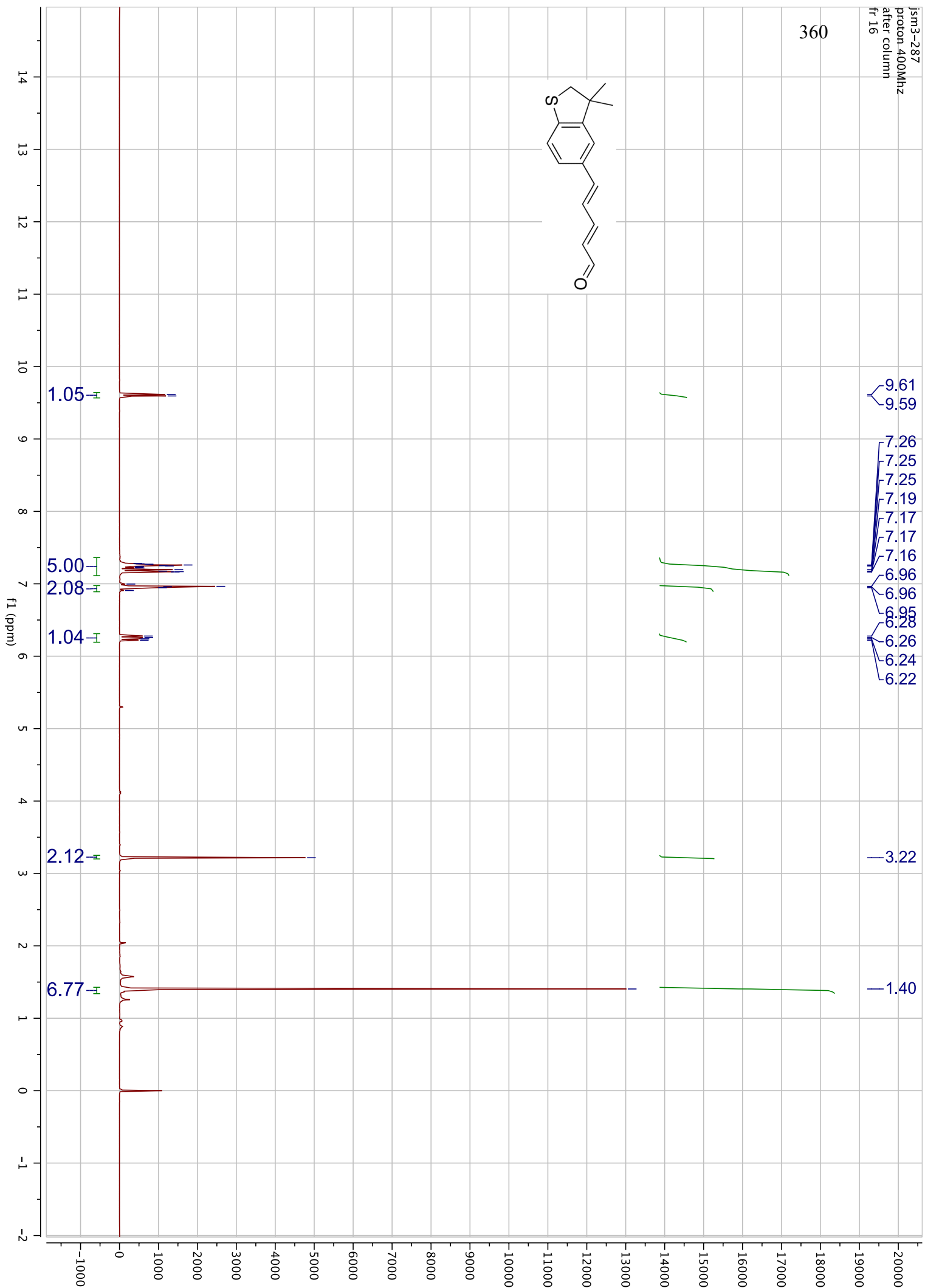
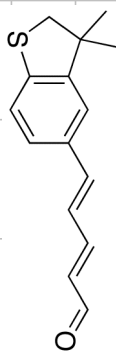


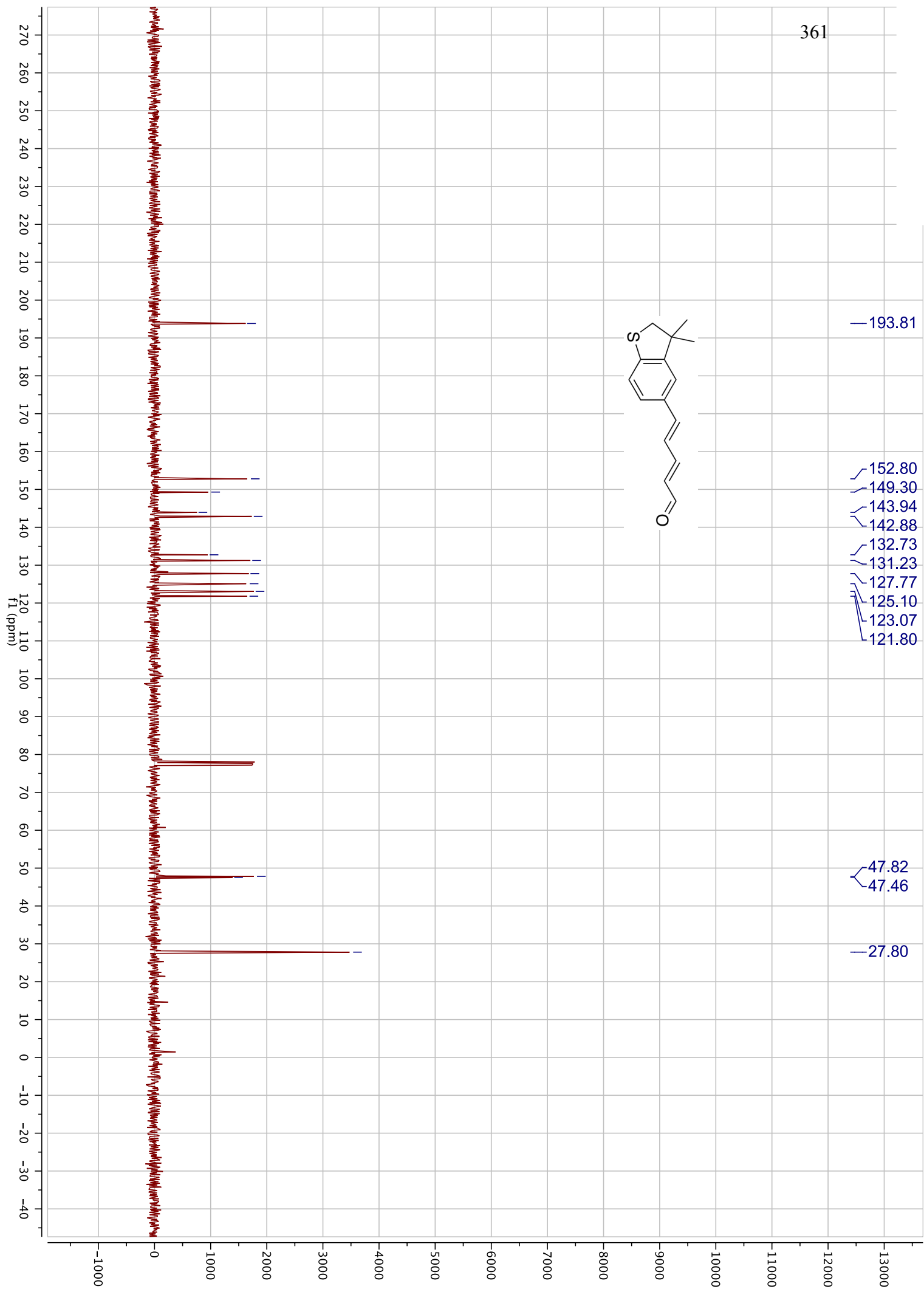


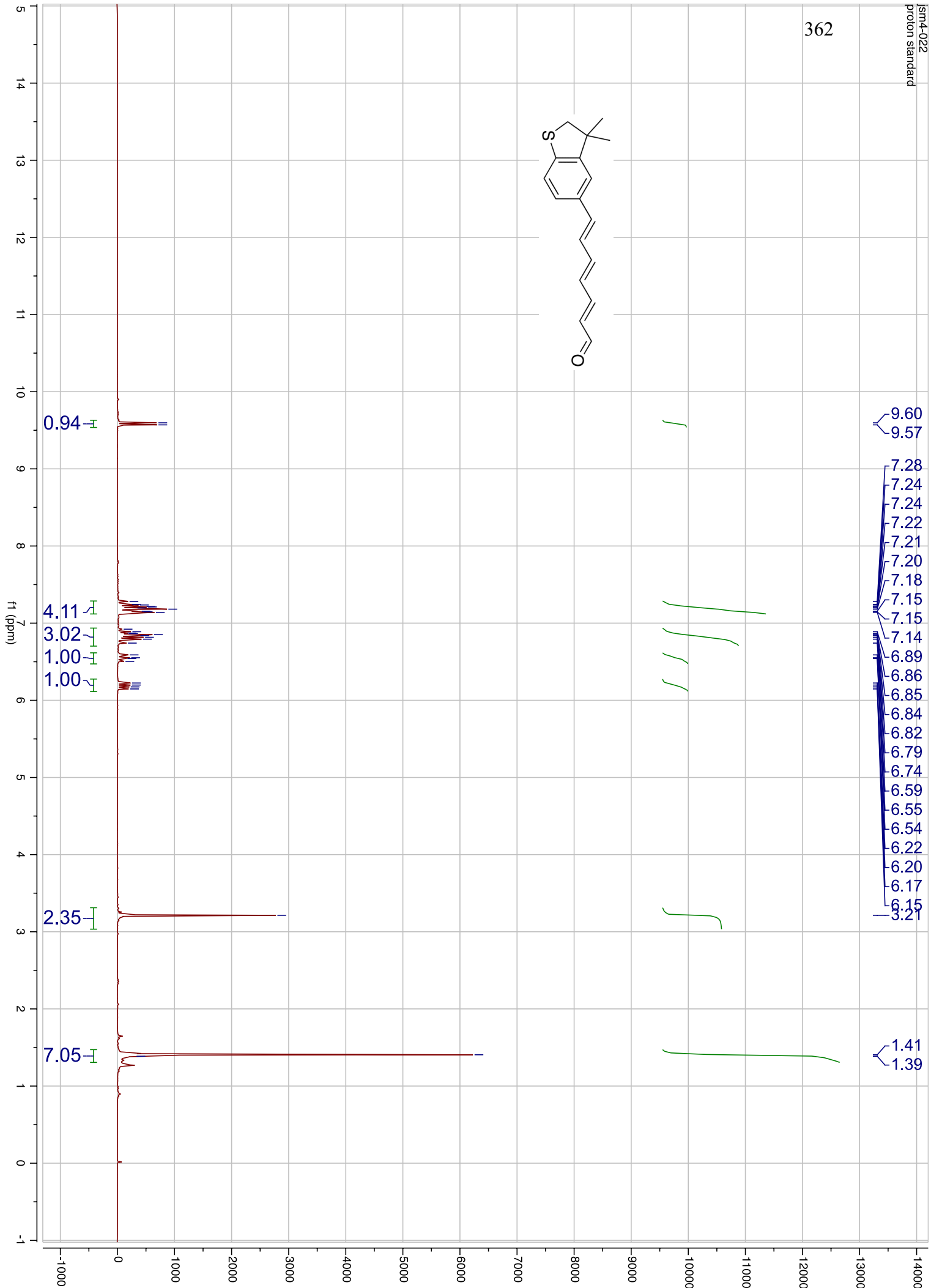
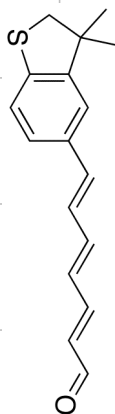


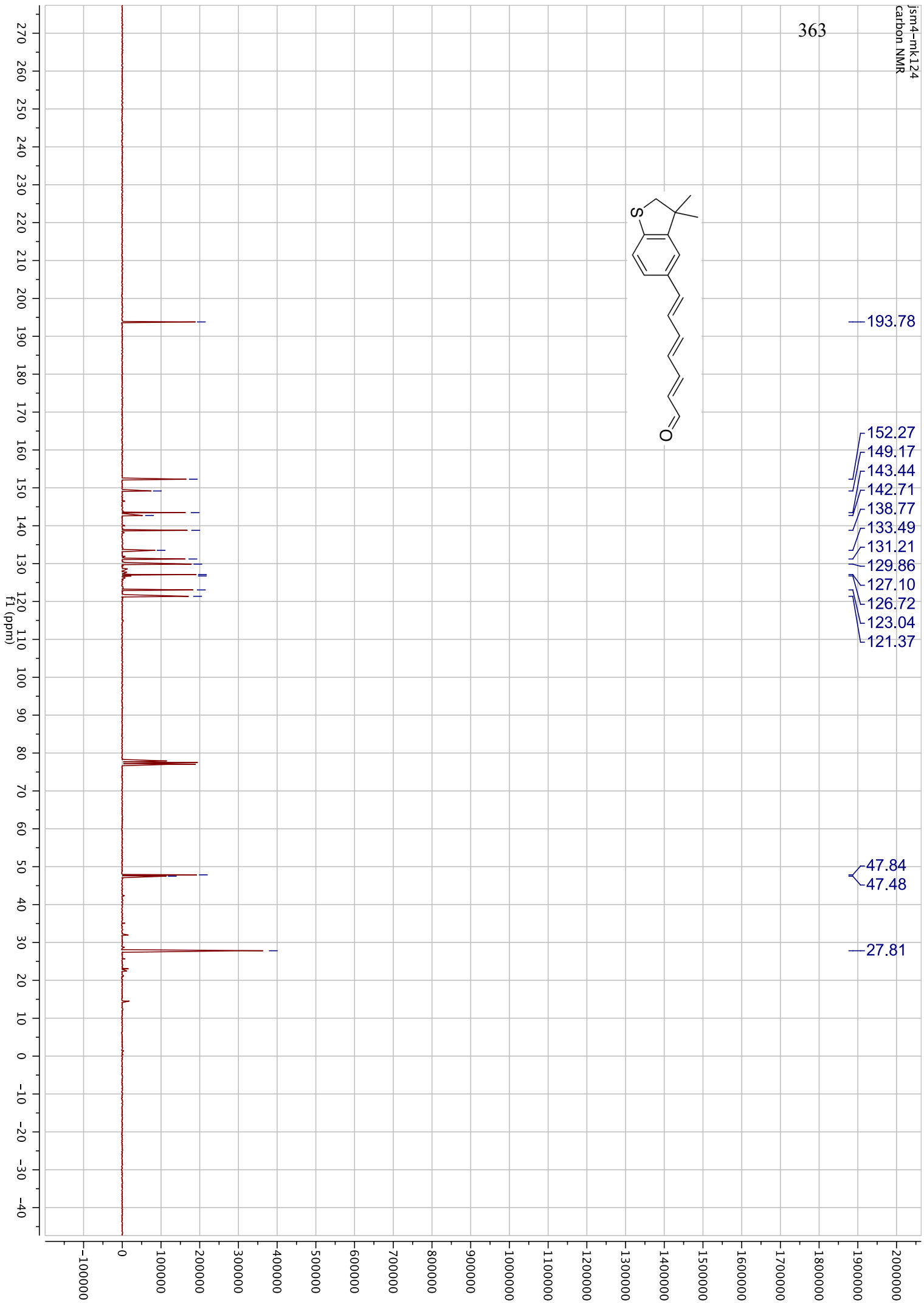
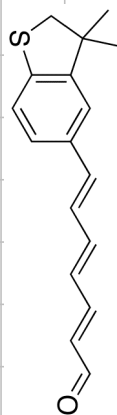




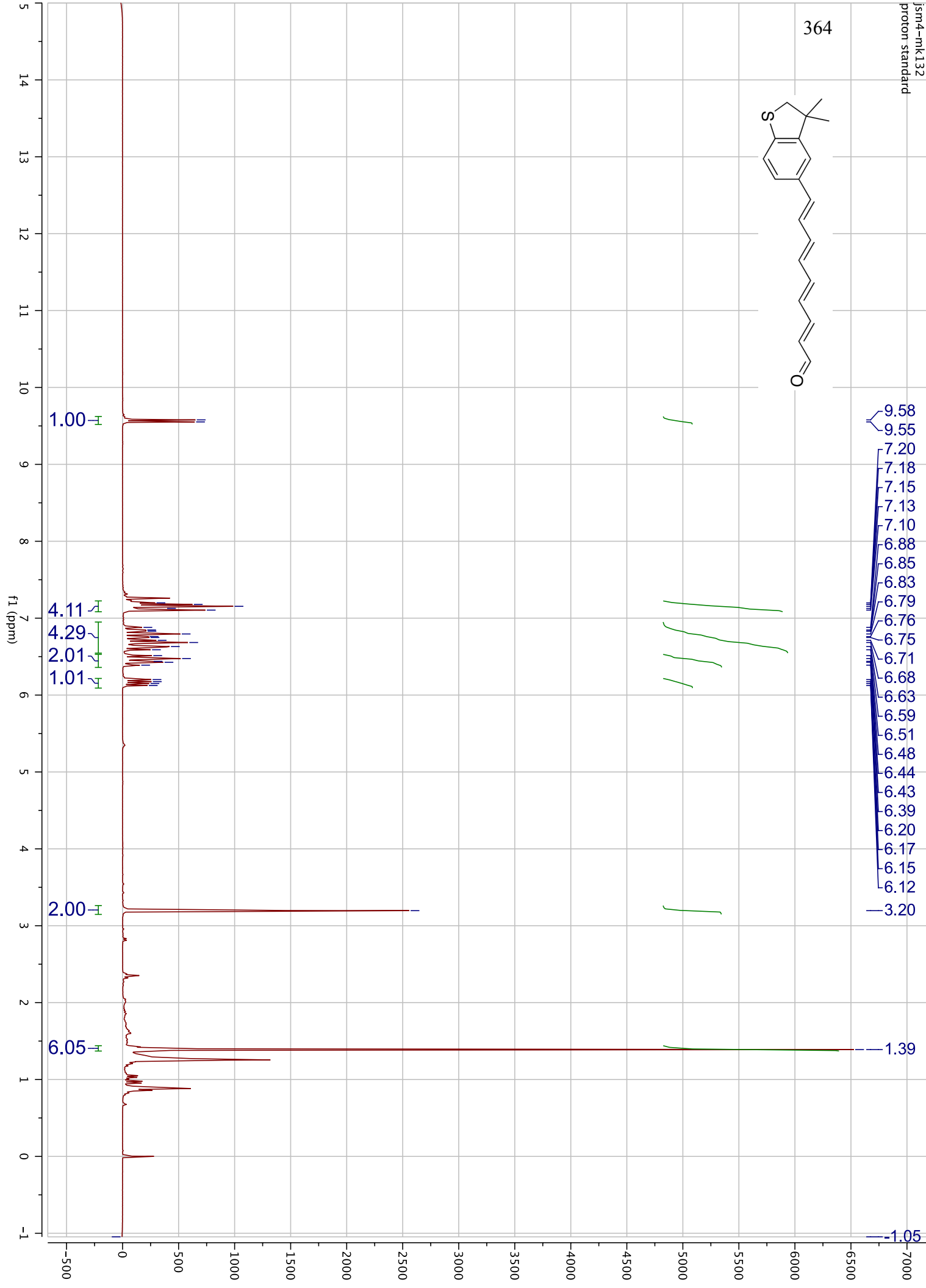
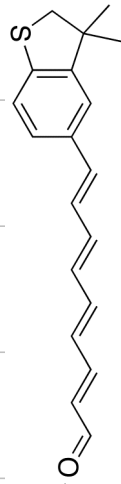






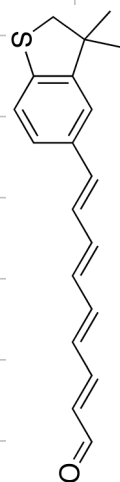


364





365

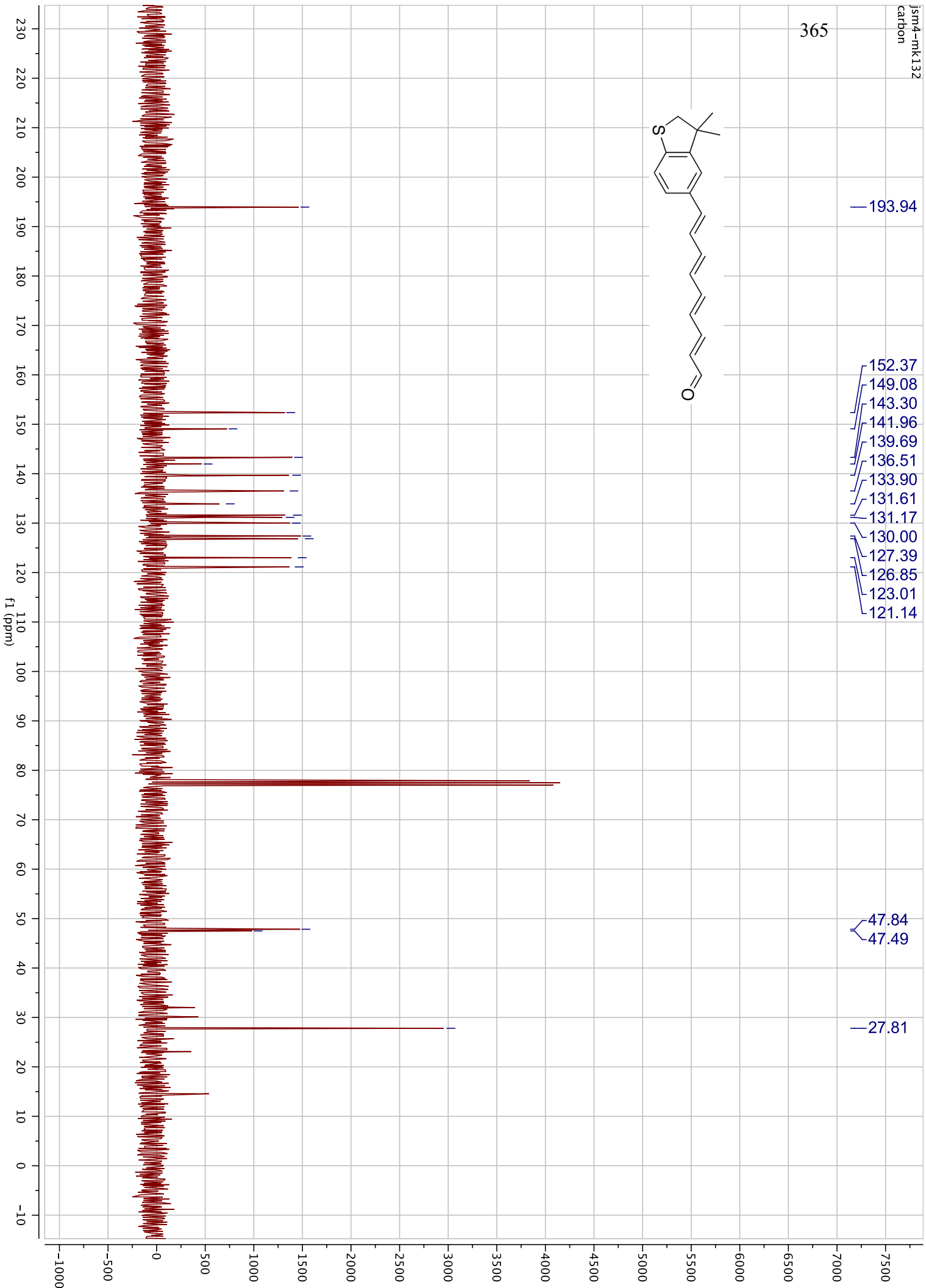


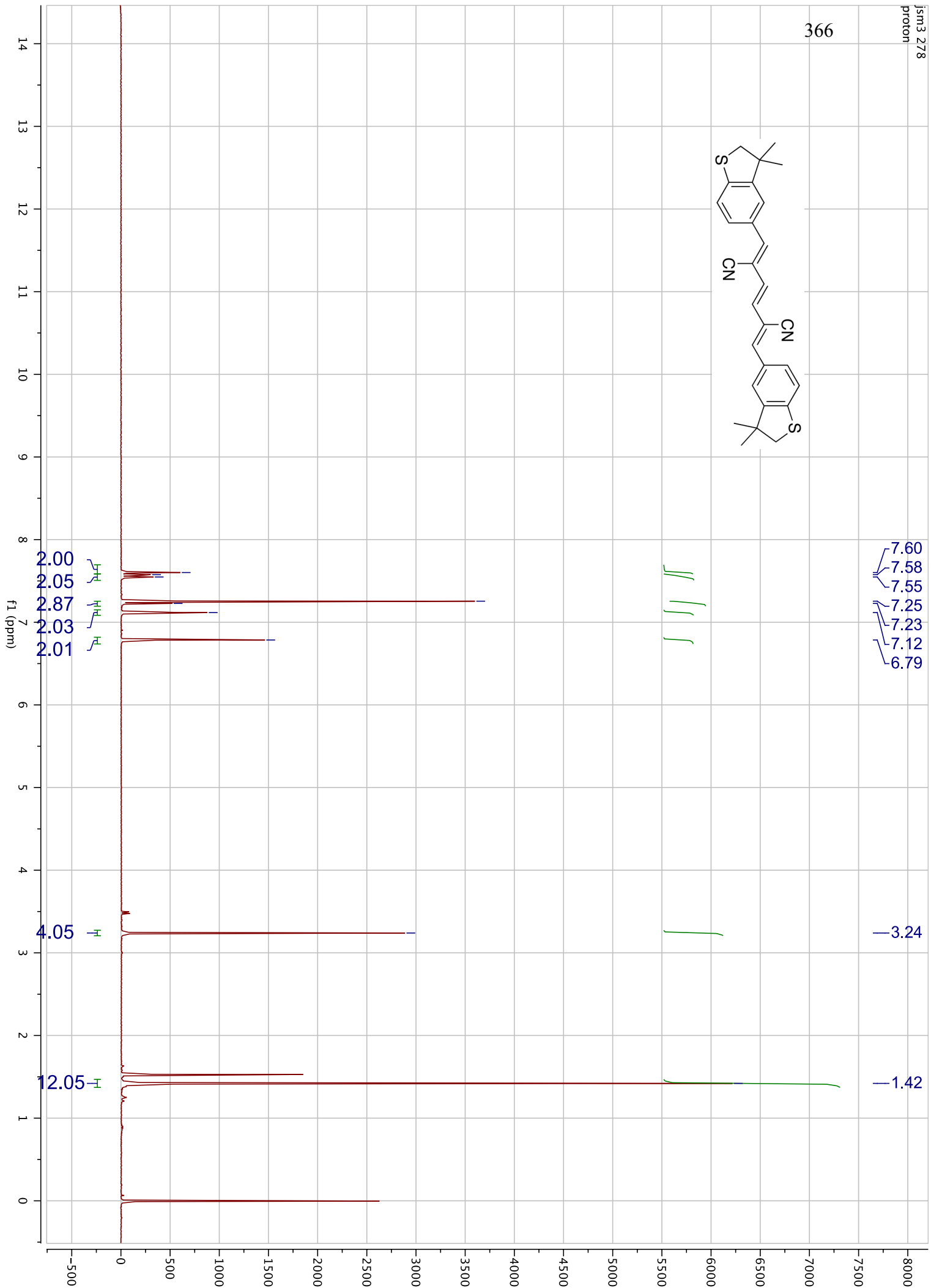
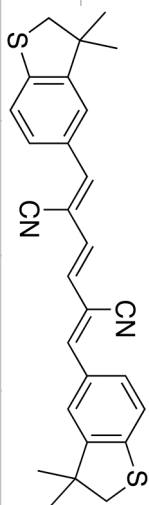
— 193.94

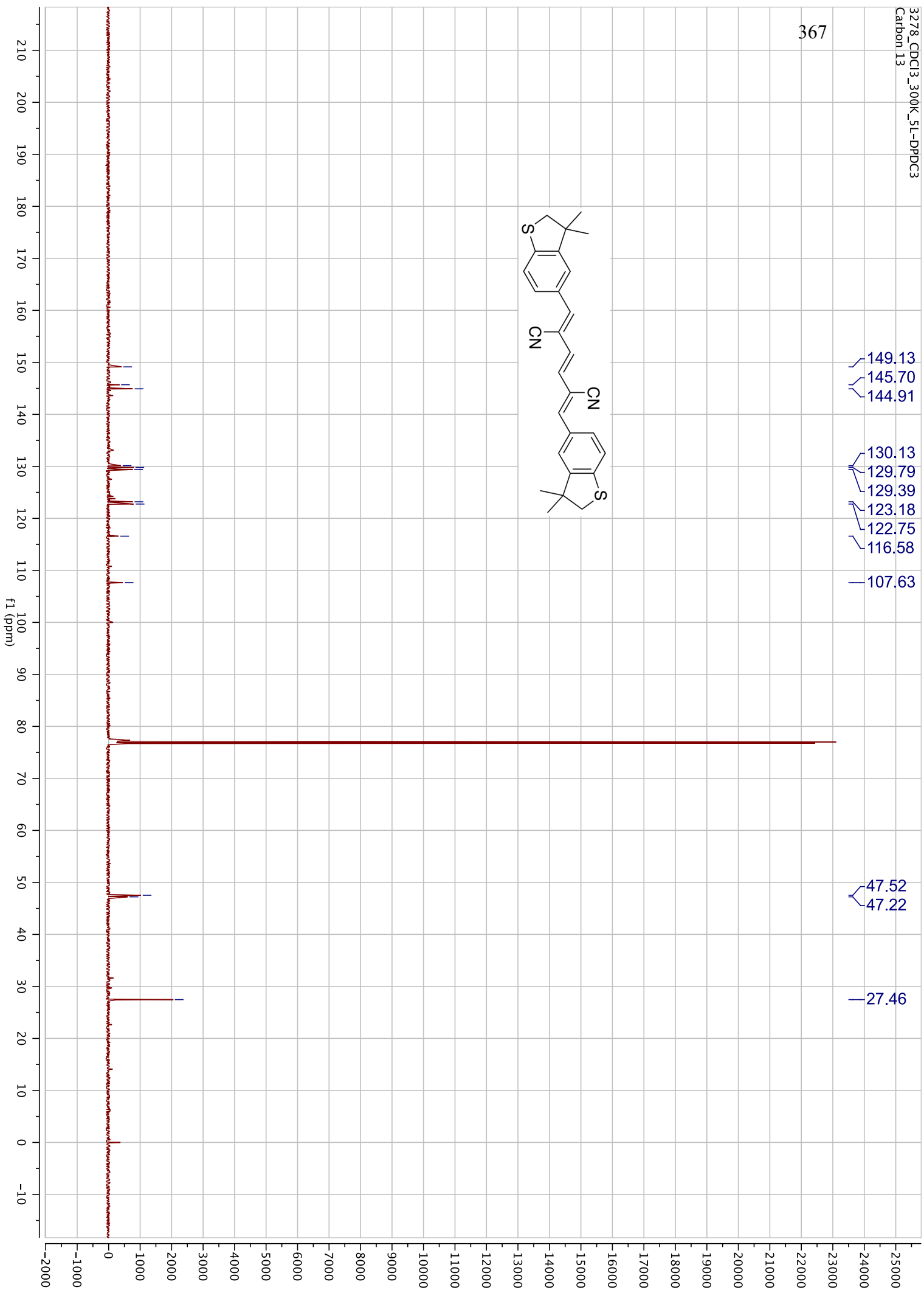
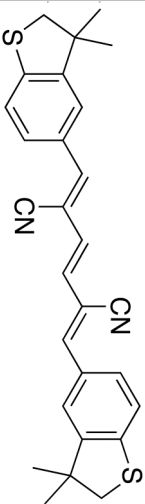
- 152.37
- 149.08
- 143.30
- 141.96
- 139.69
- 136.51
- 133.90
- 131.61
- 131.17
- 130.00
- 127.39
- 126.85
- 123.01
- 121.14

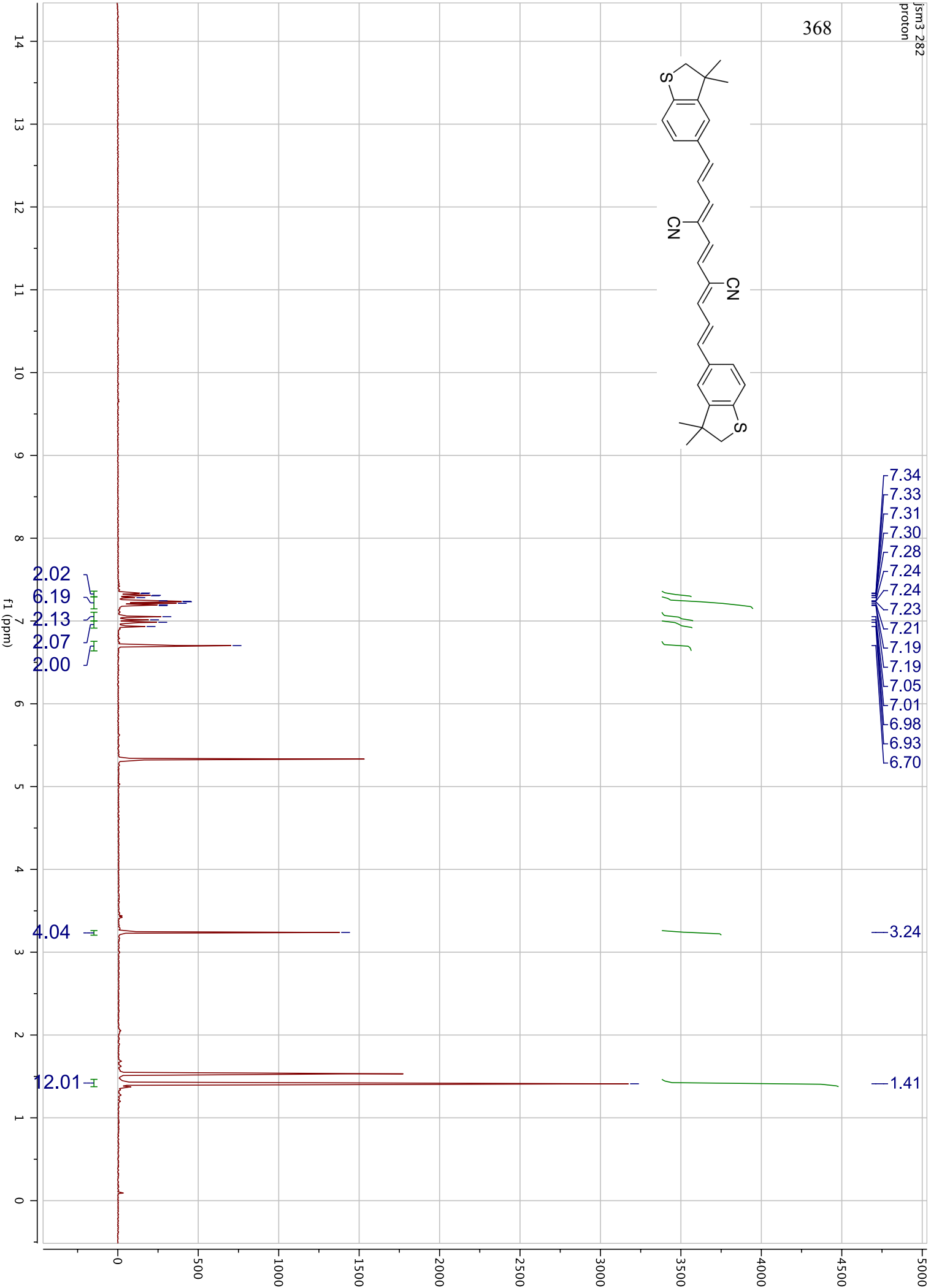
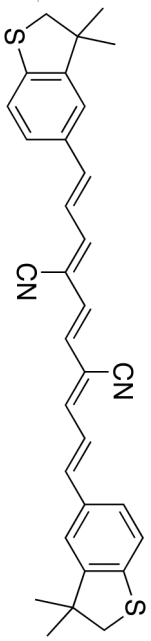
47.84  
47.49

— 27.81

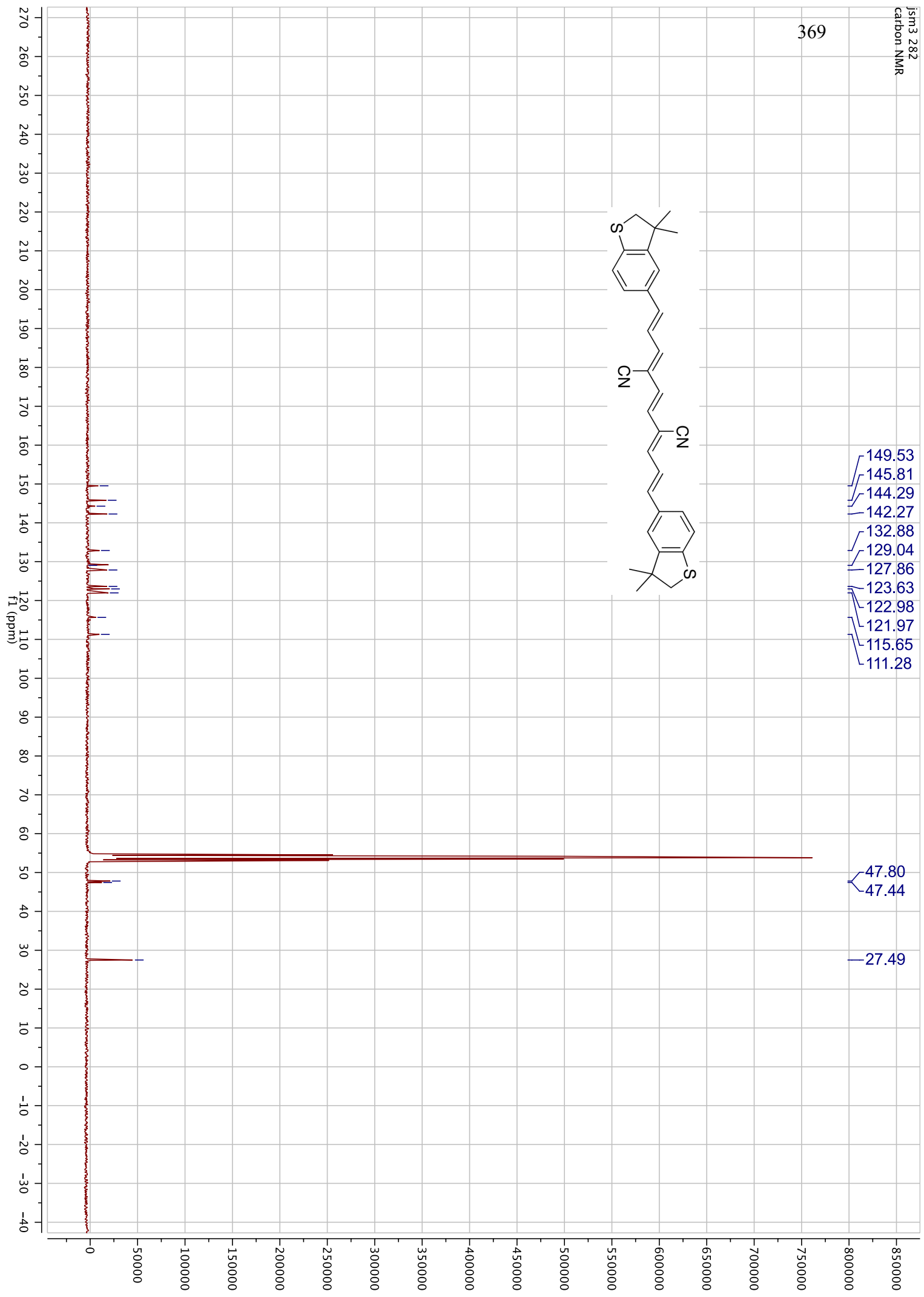
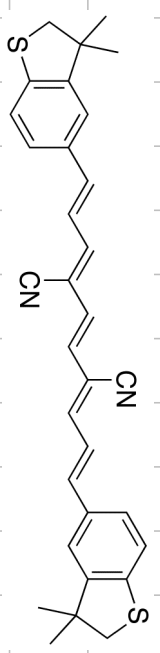


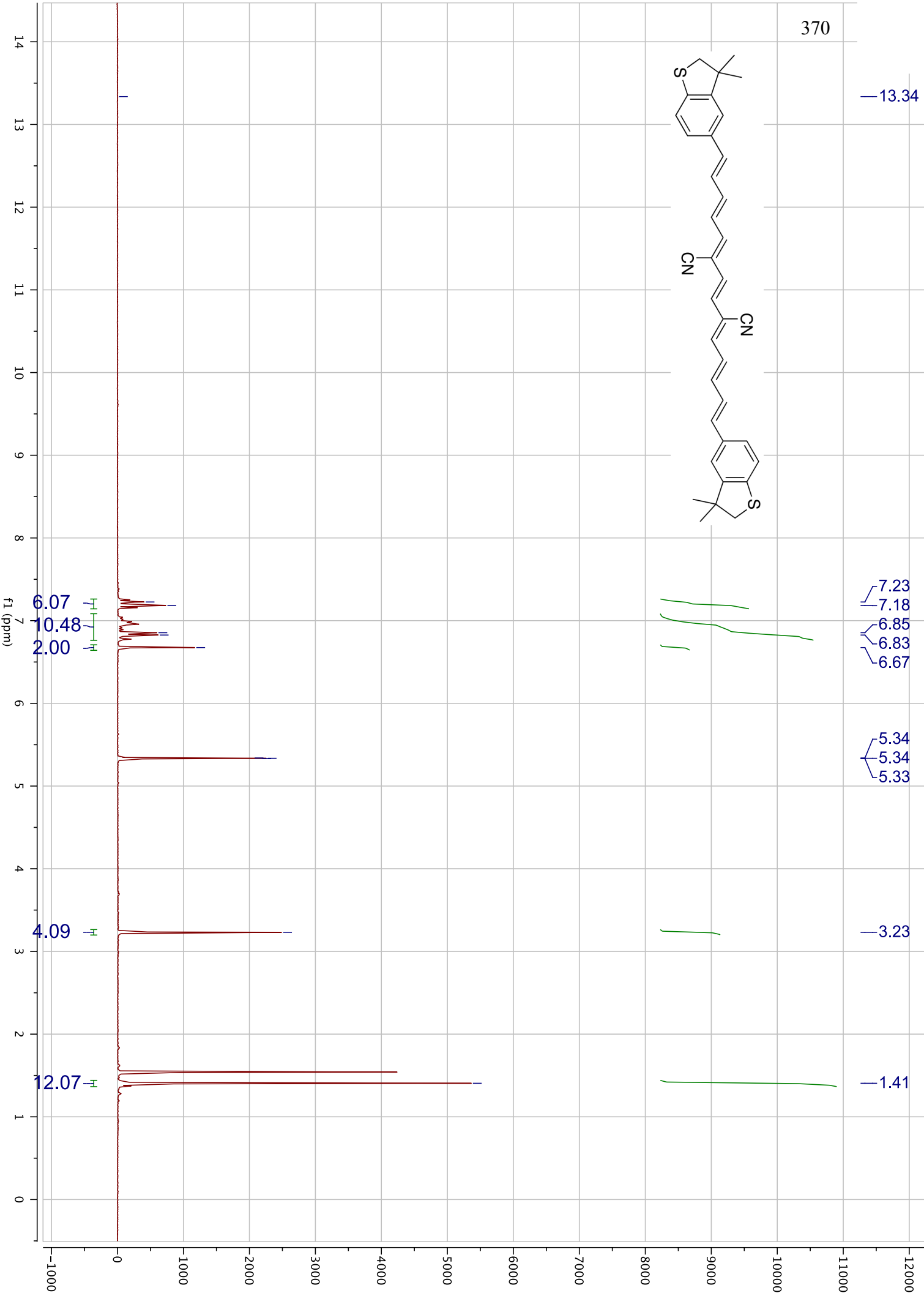




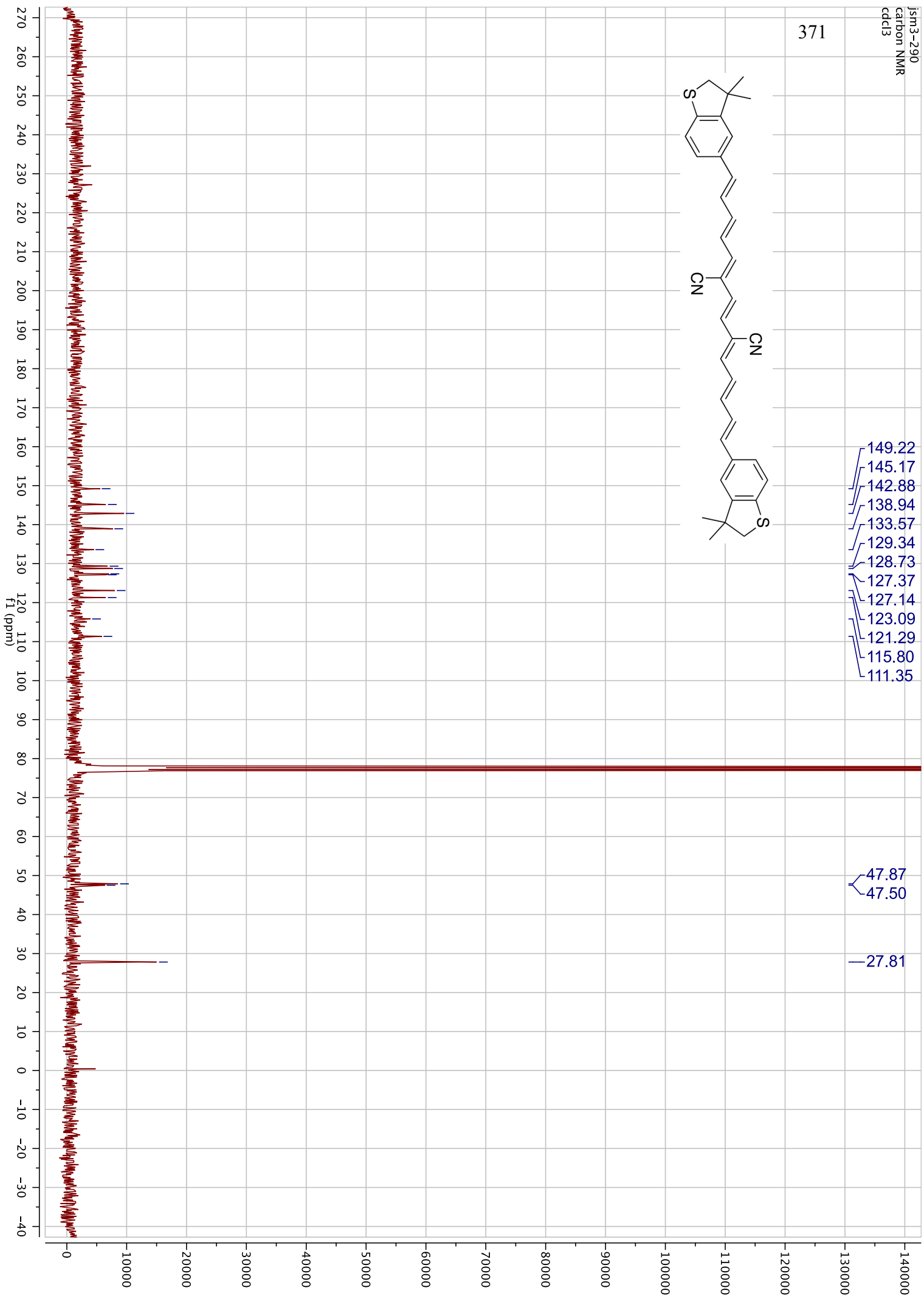
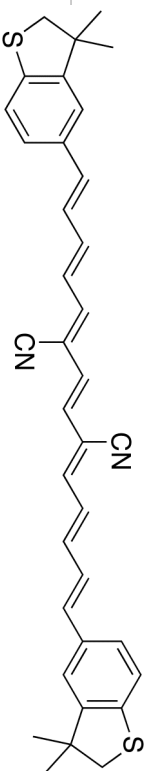


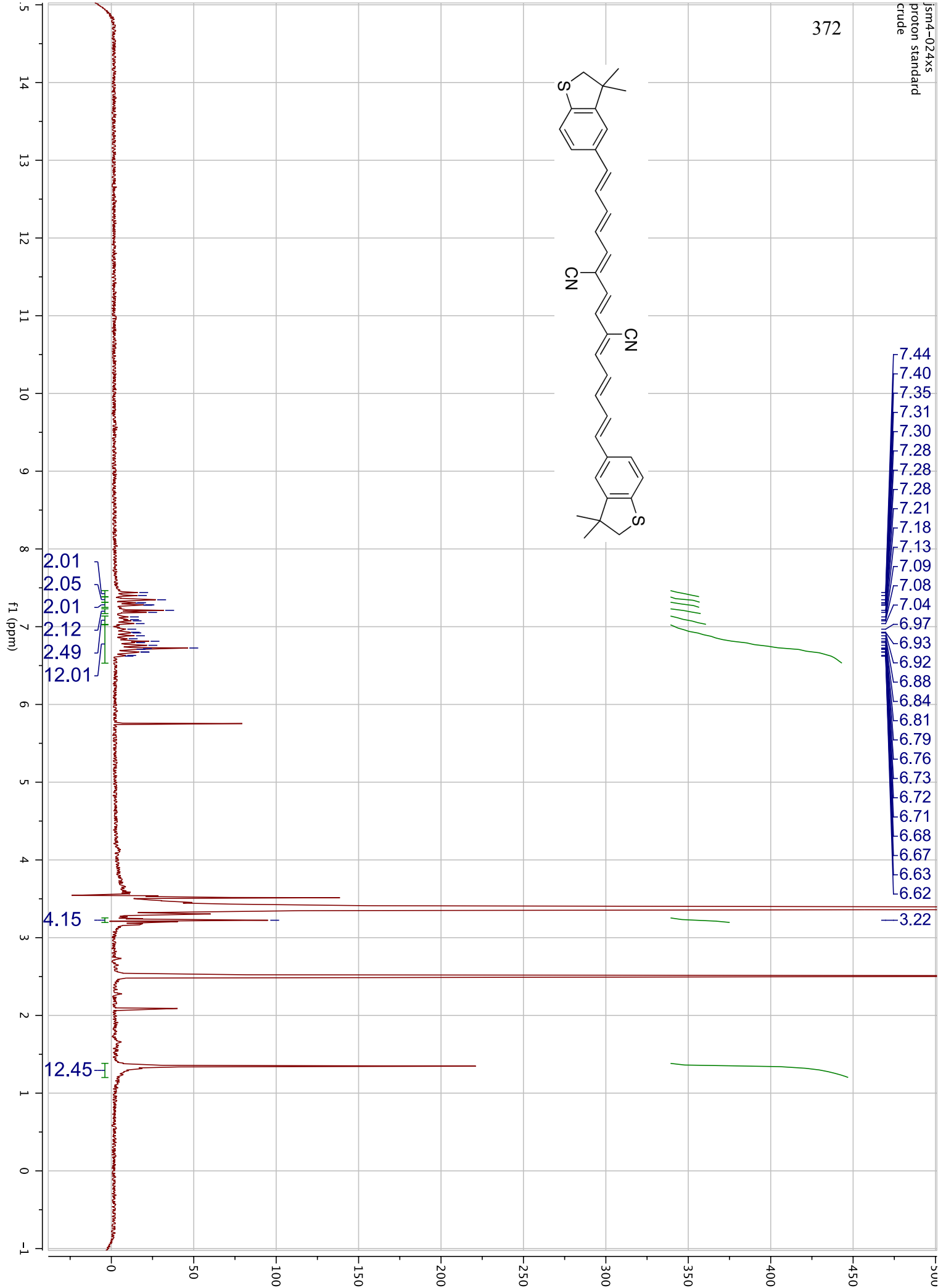
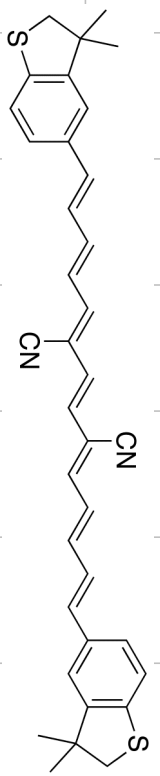
369





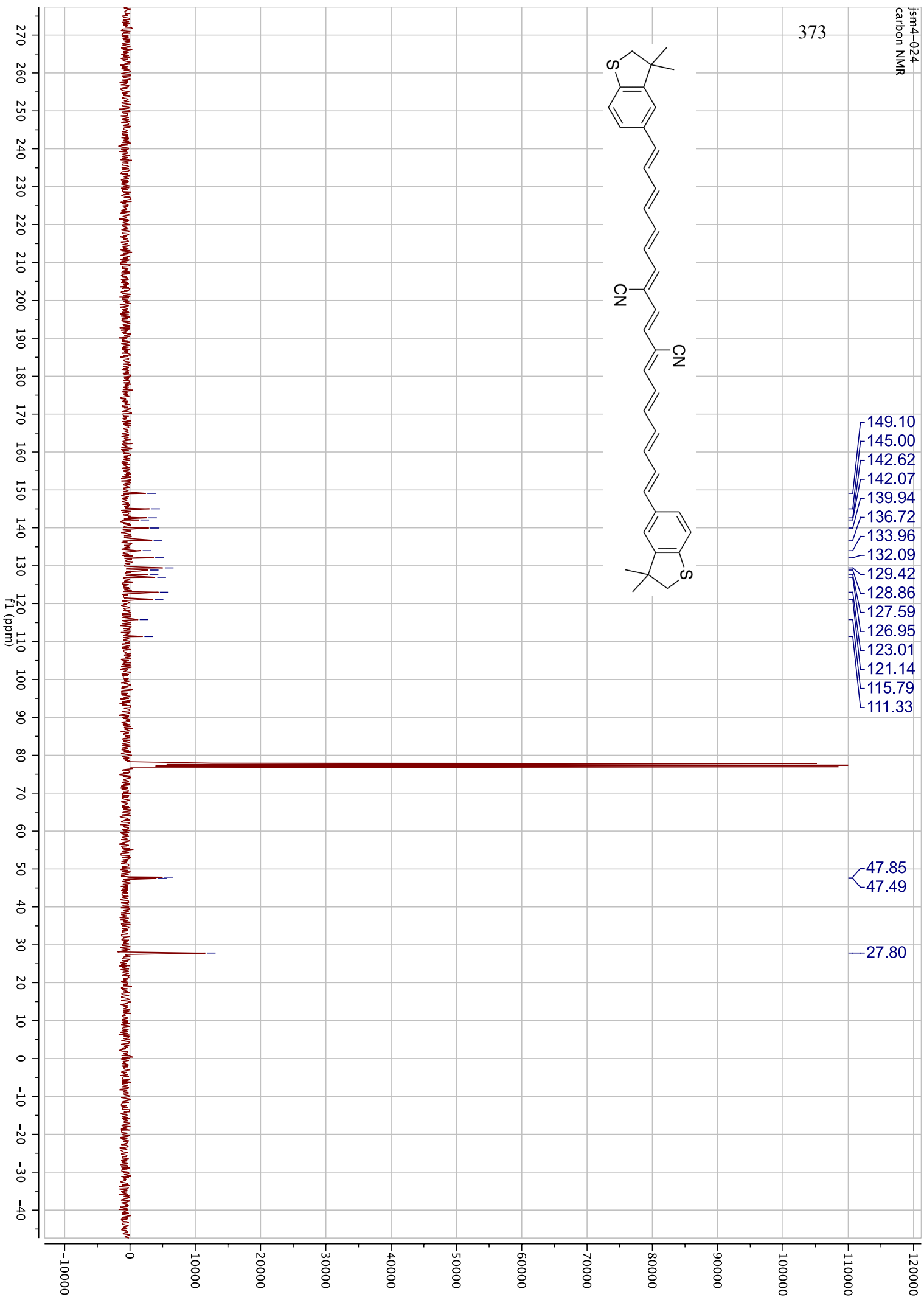
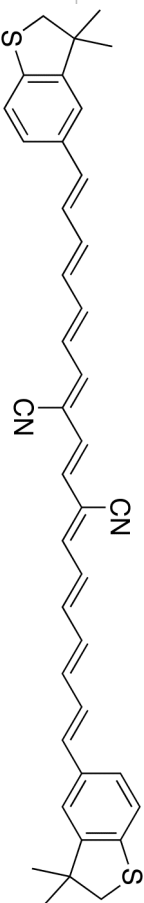
371

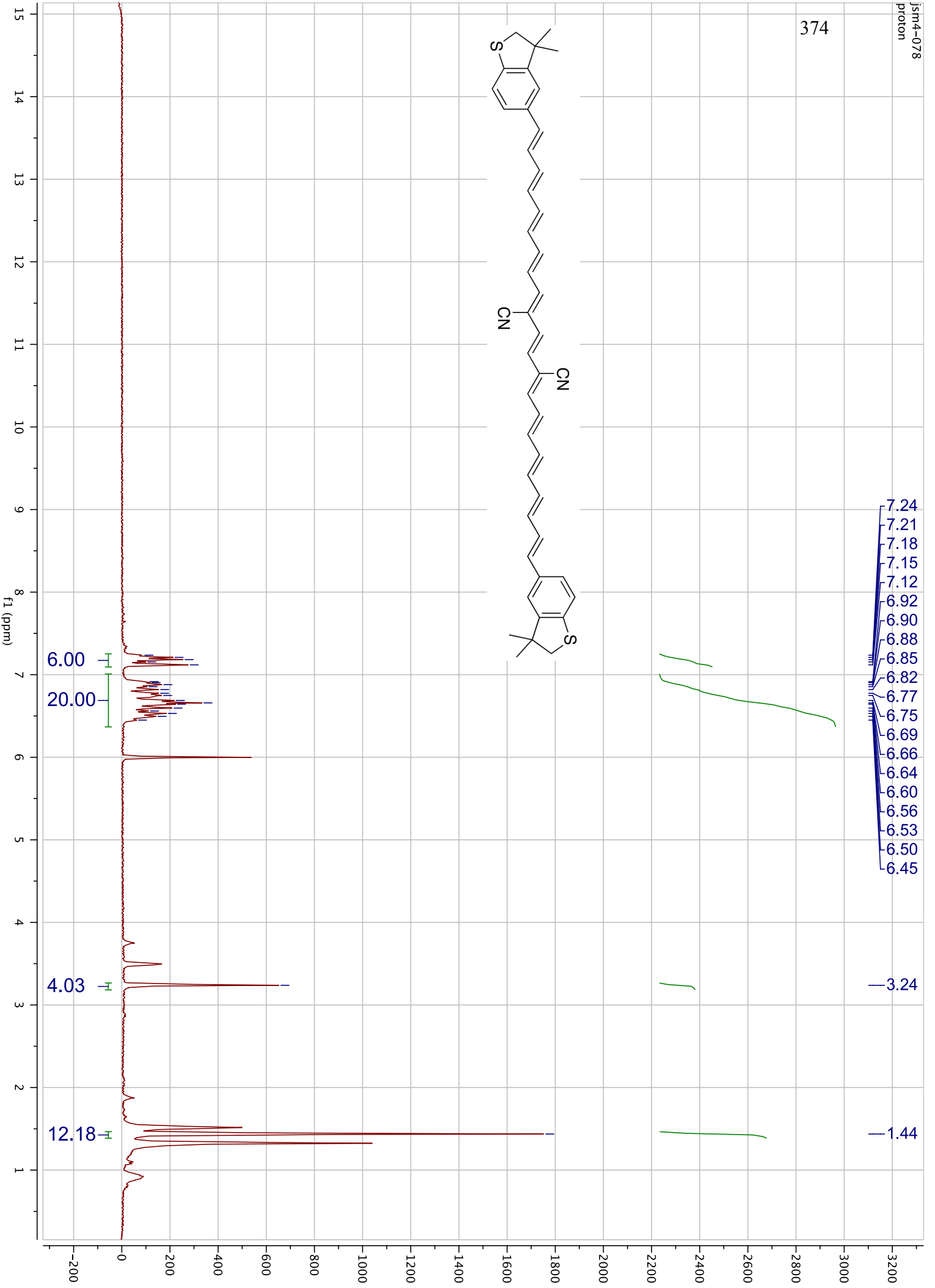


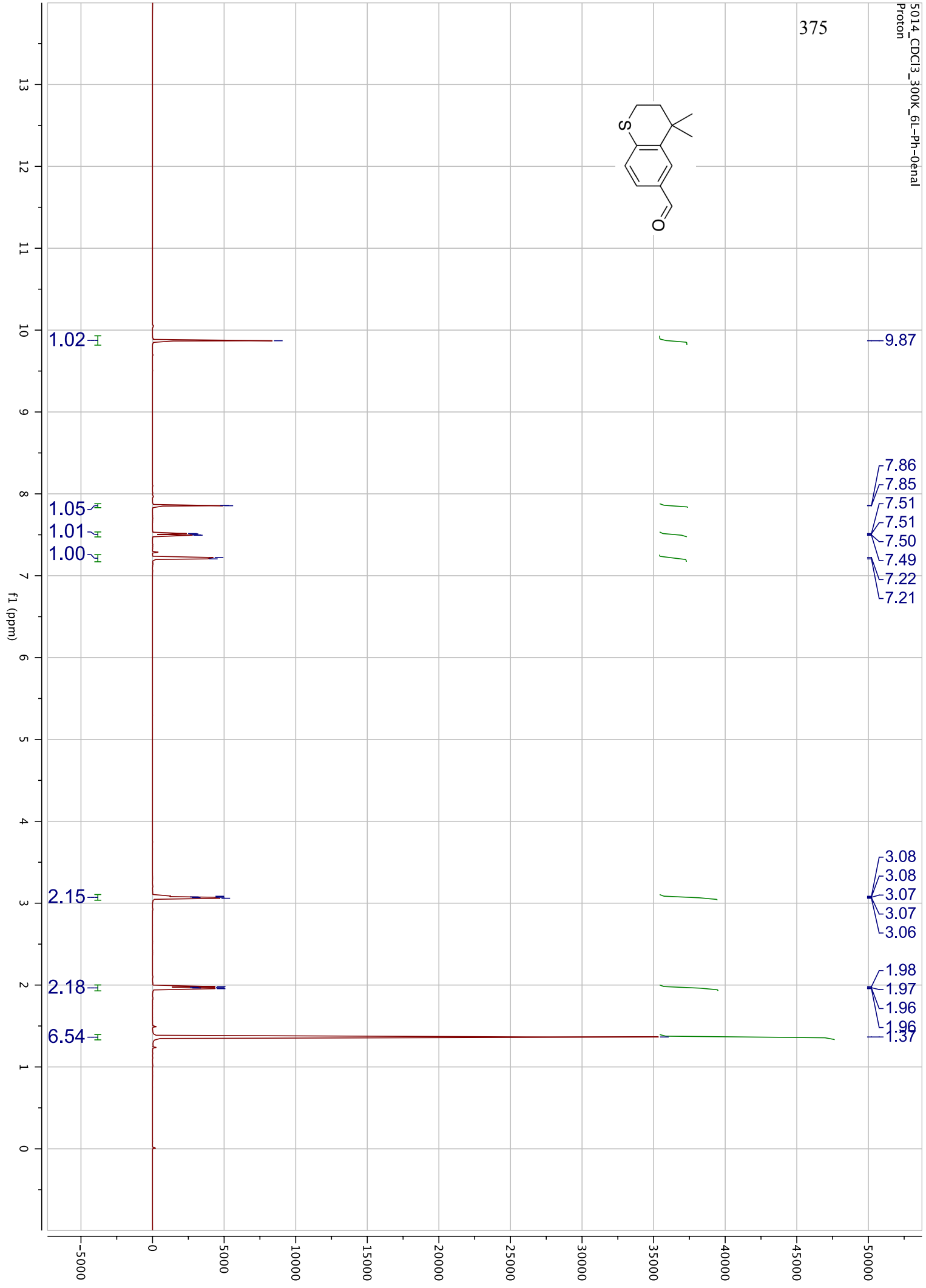
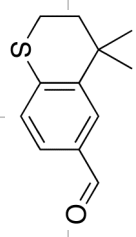




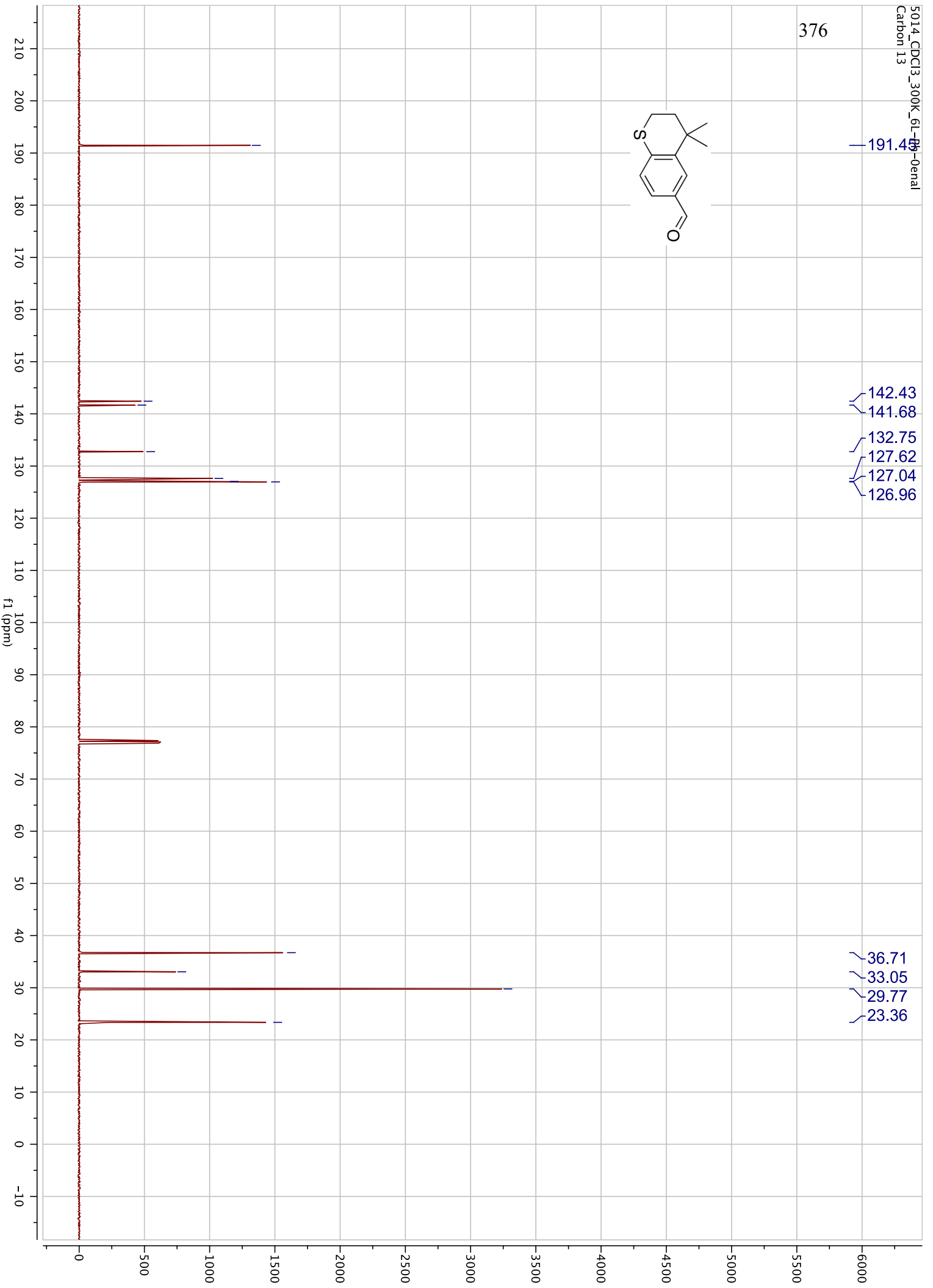
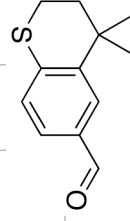
373

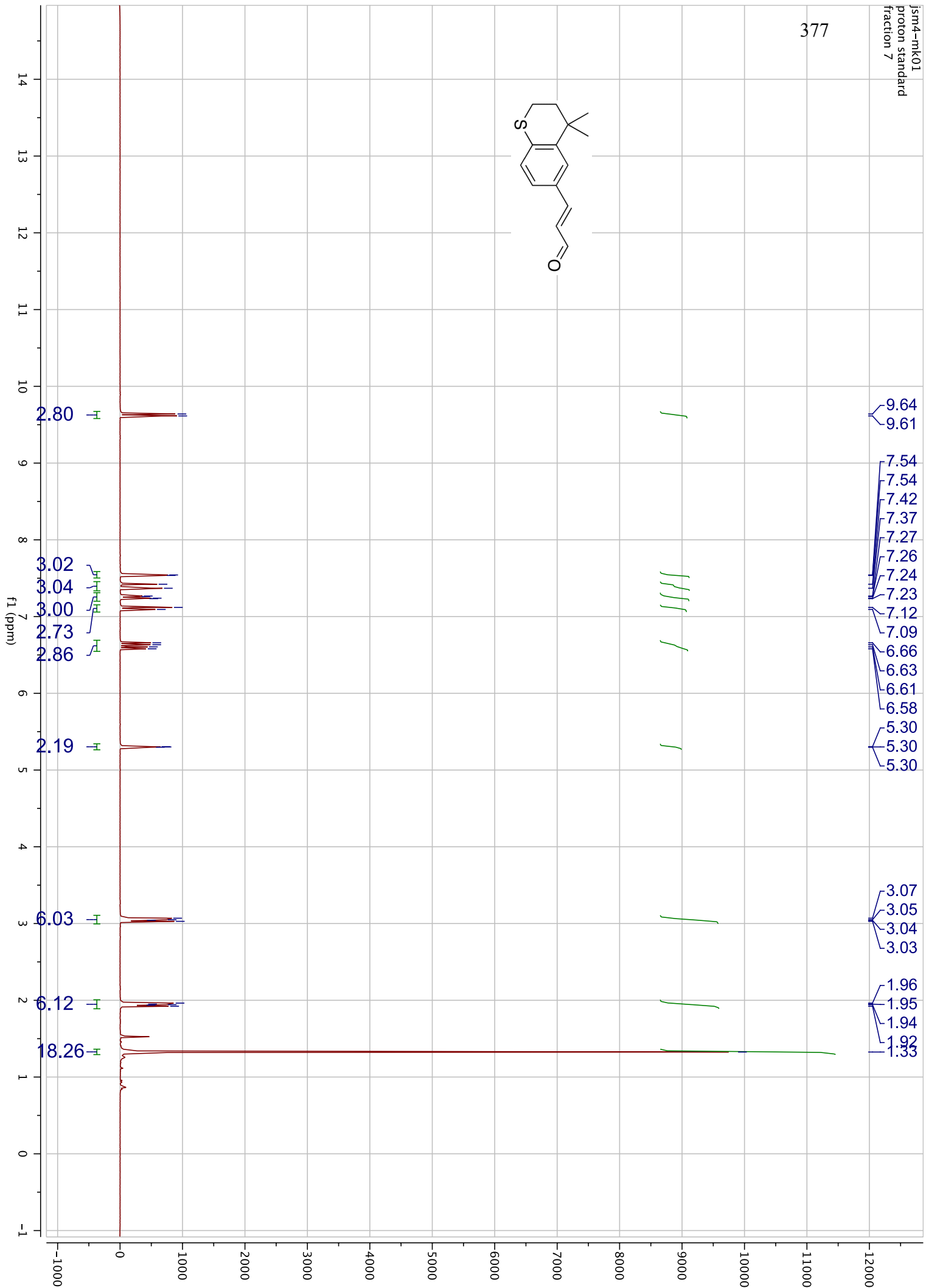
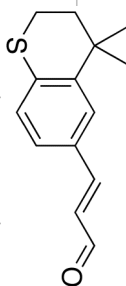




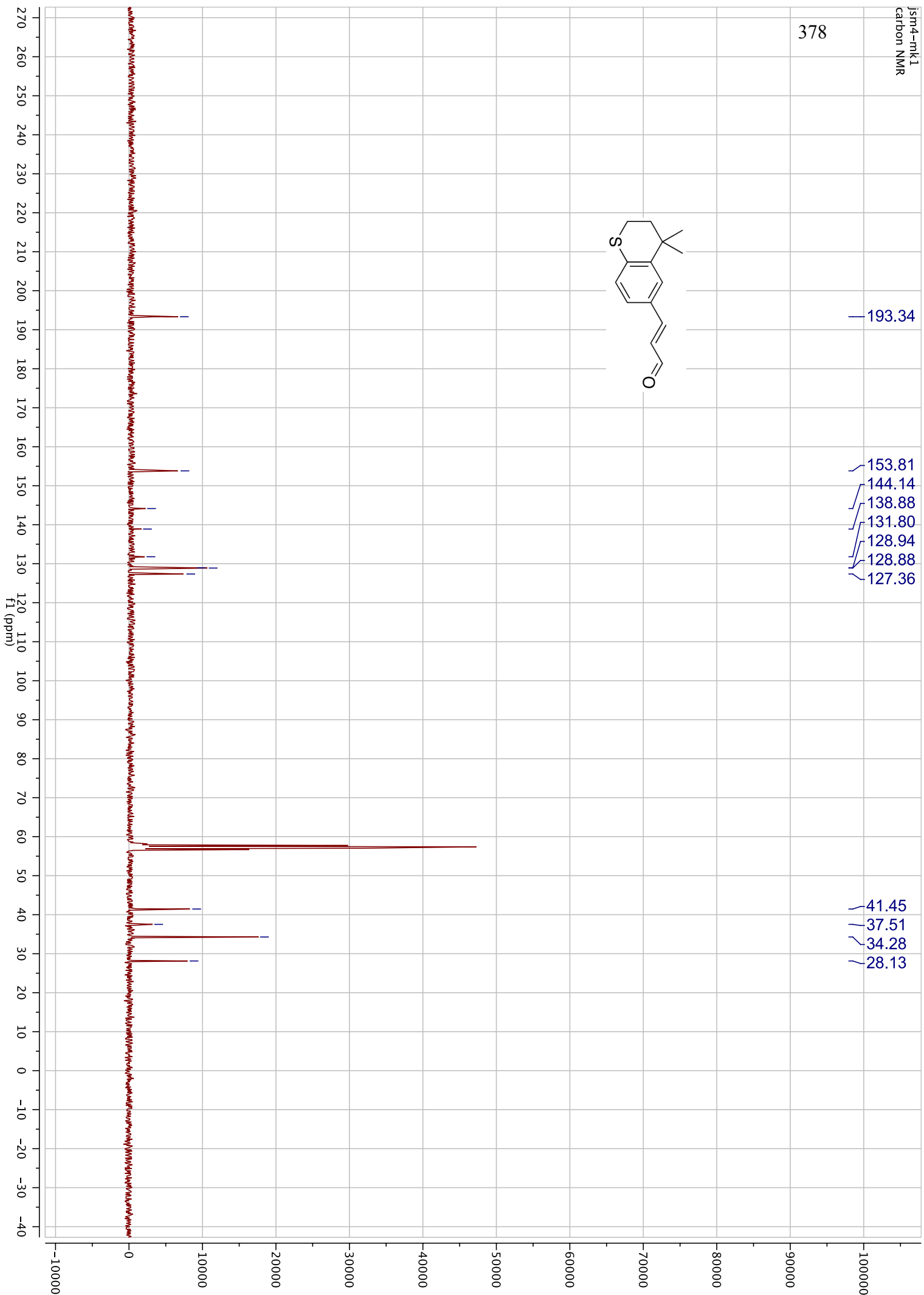
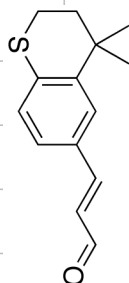


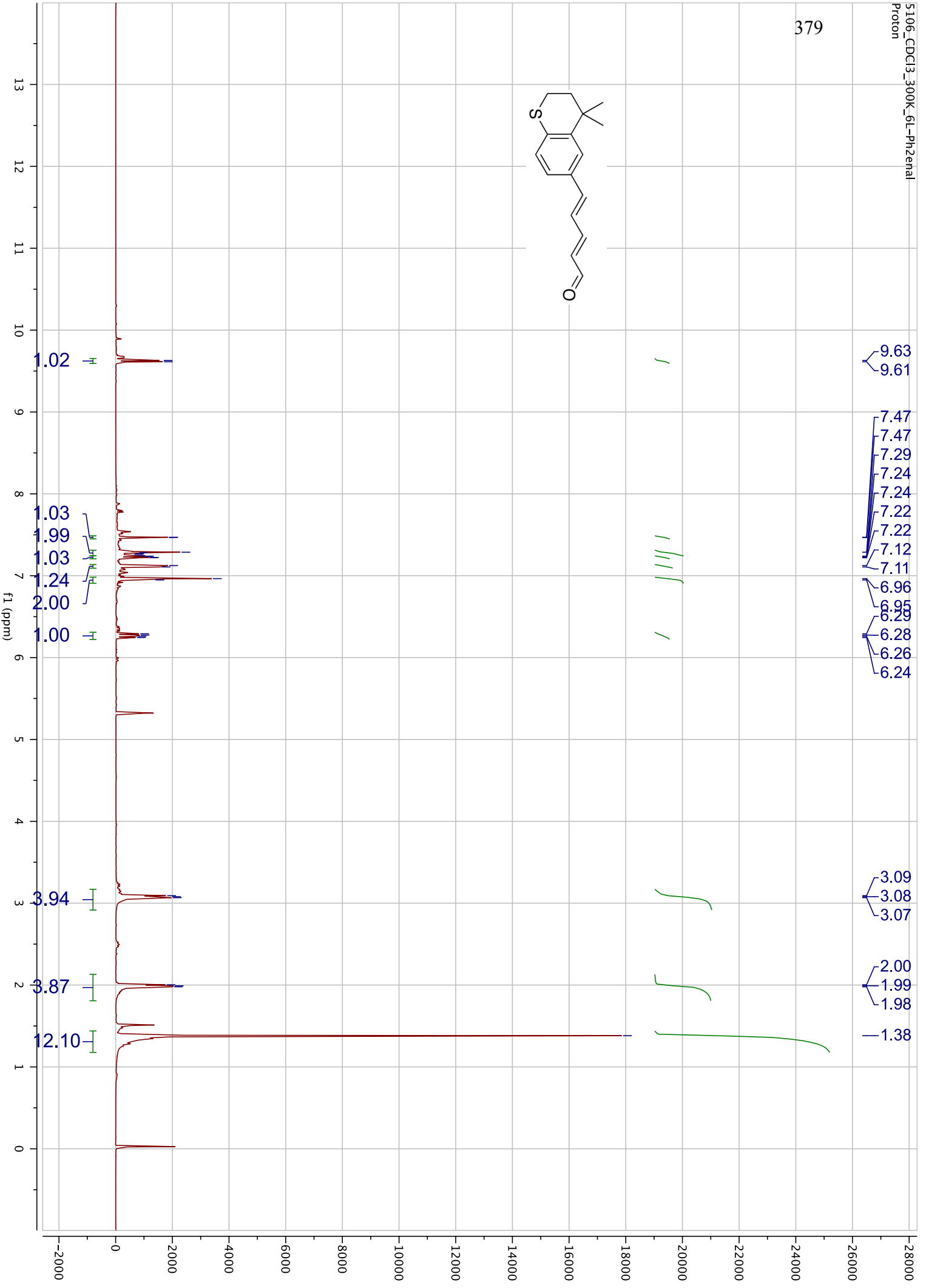
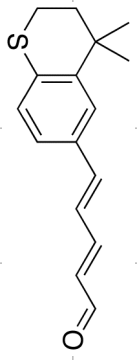
376



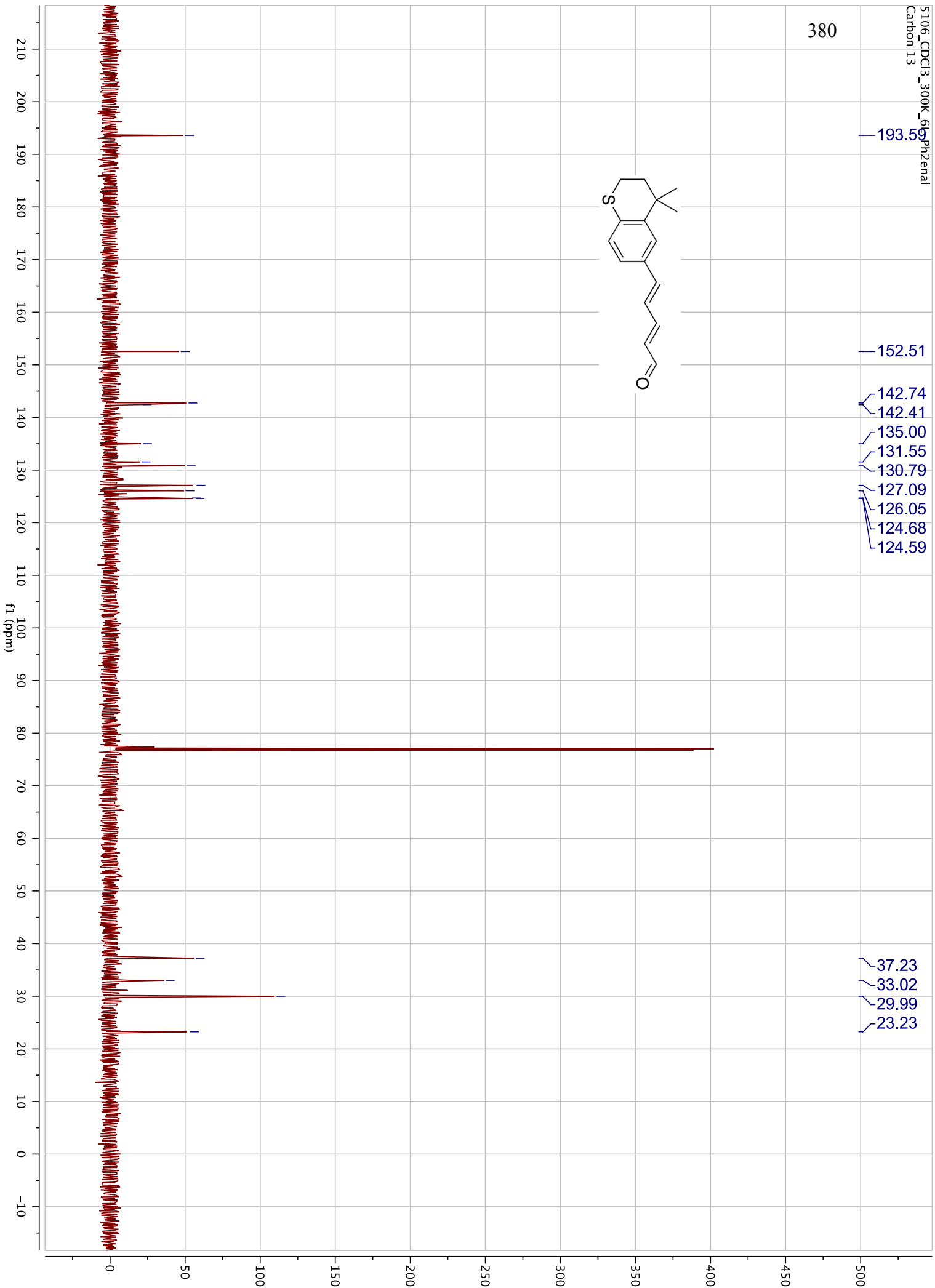
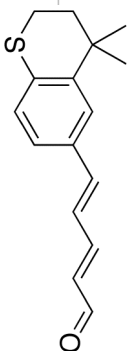


378

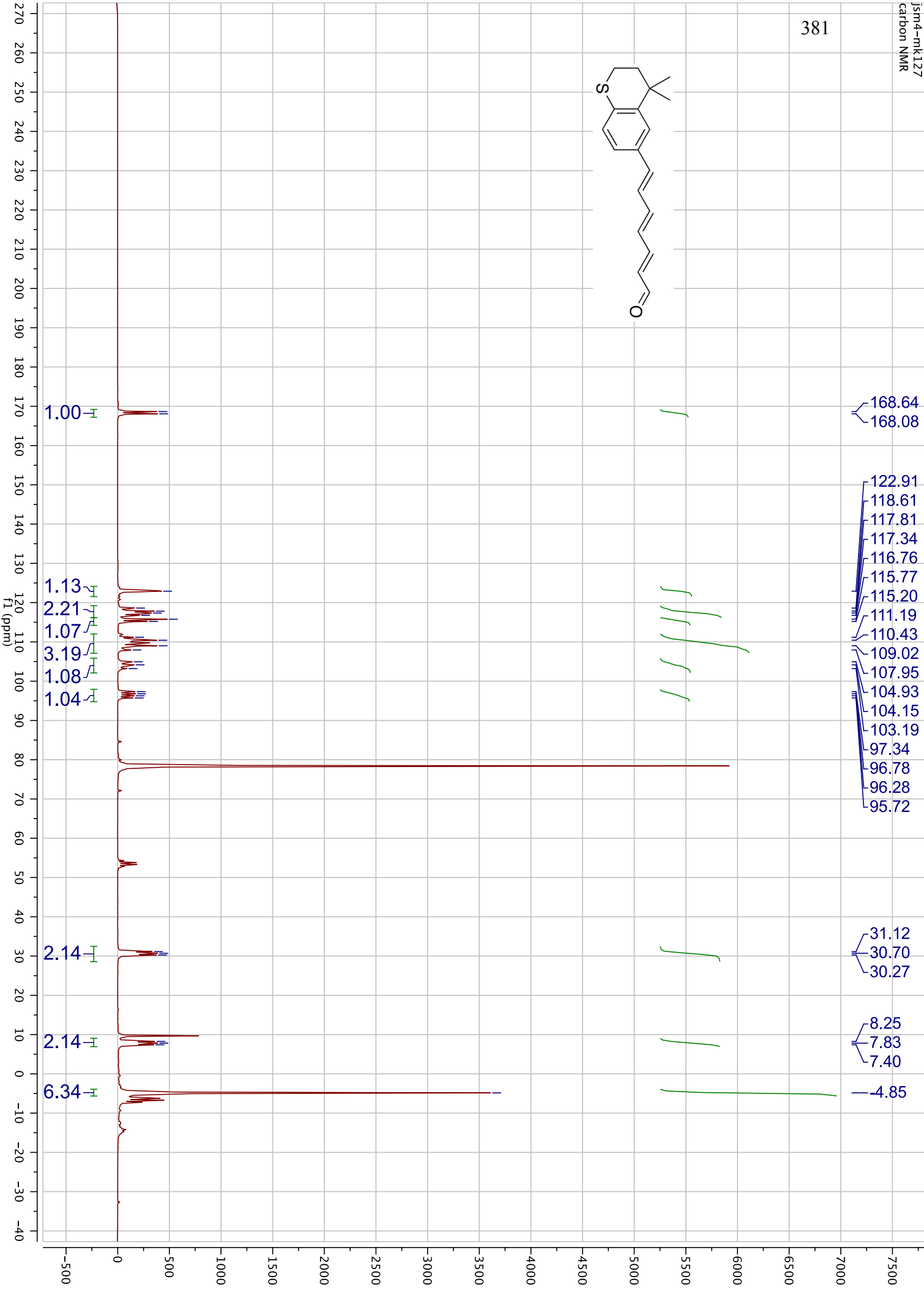
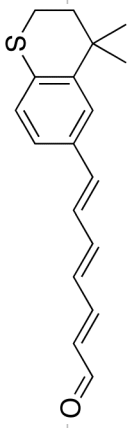




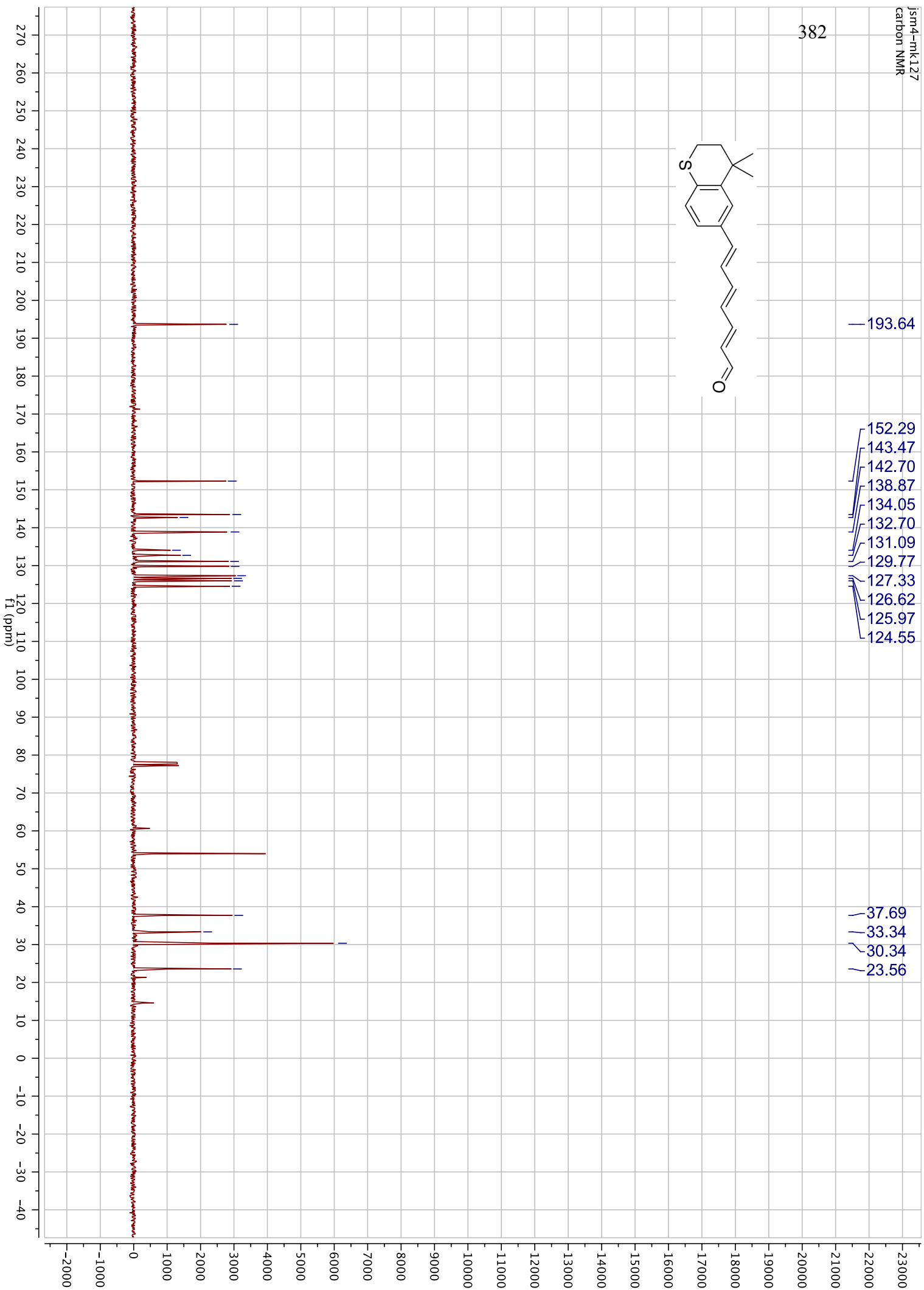
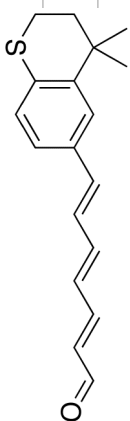
380

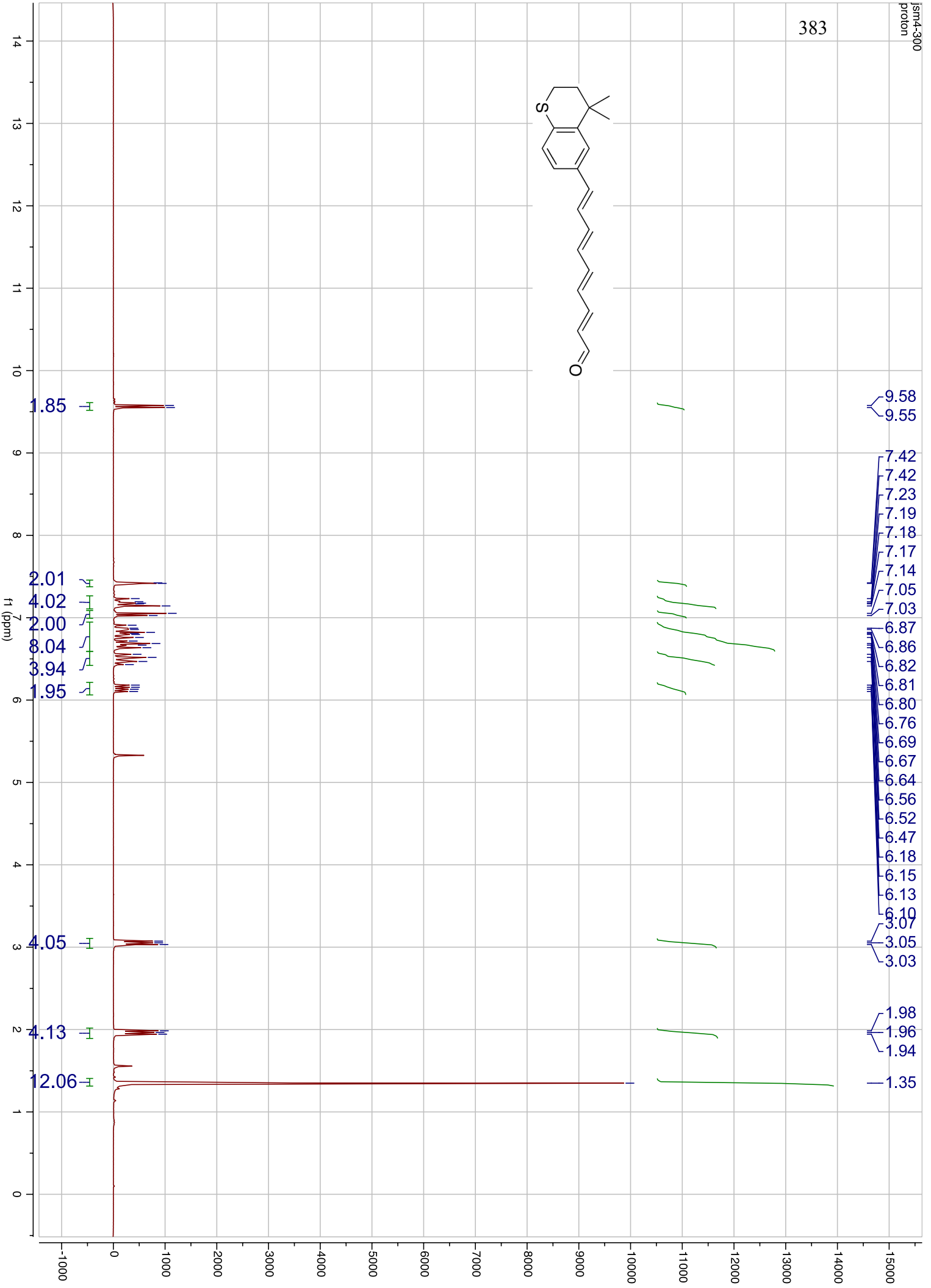
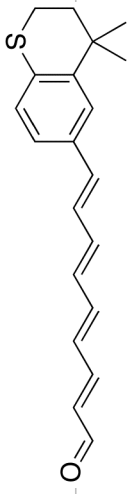




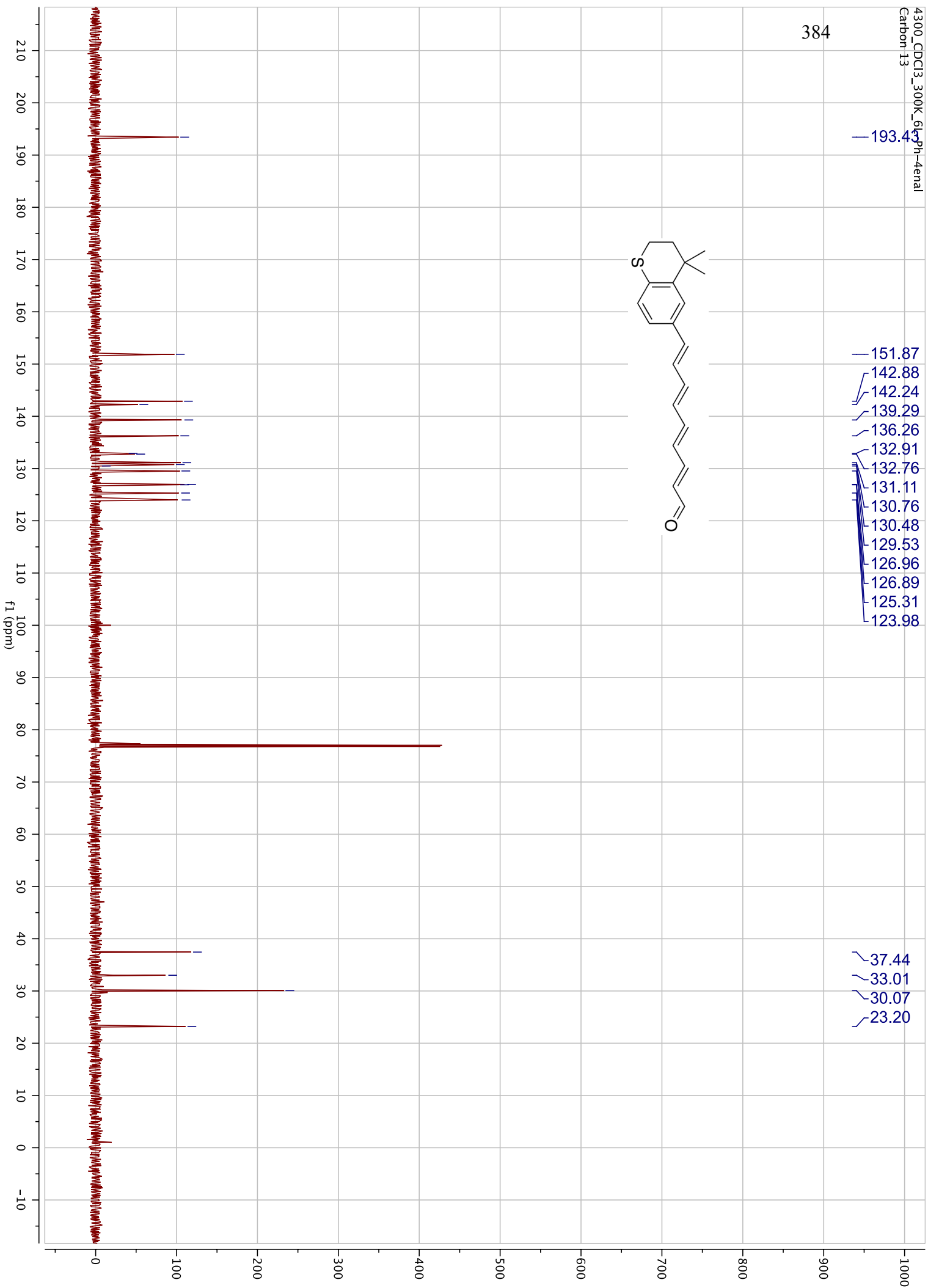
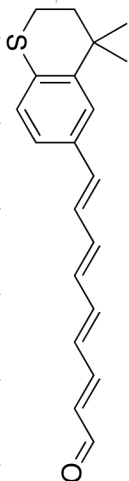


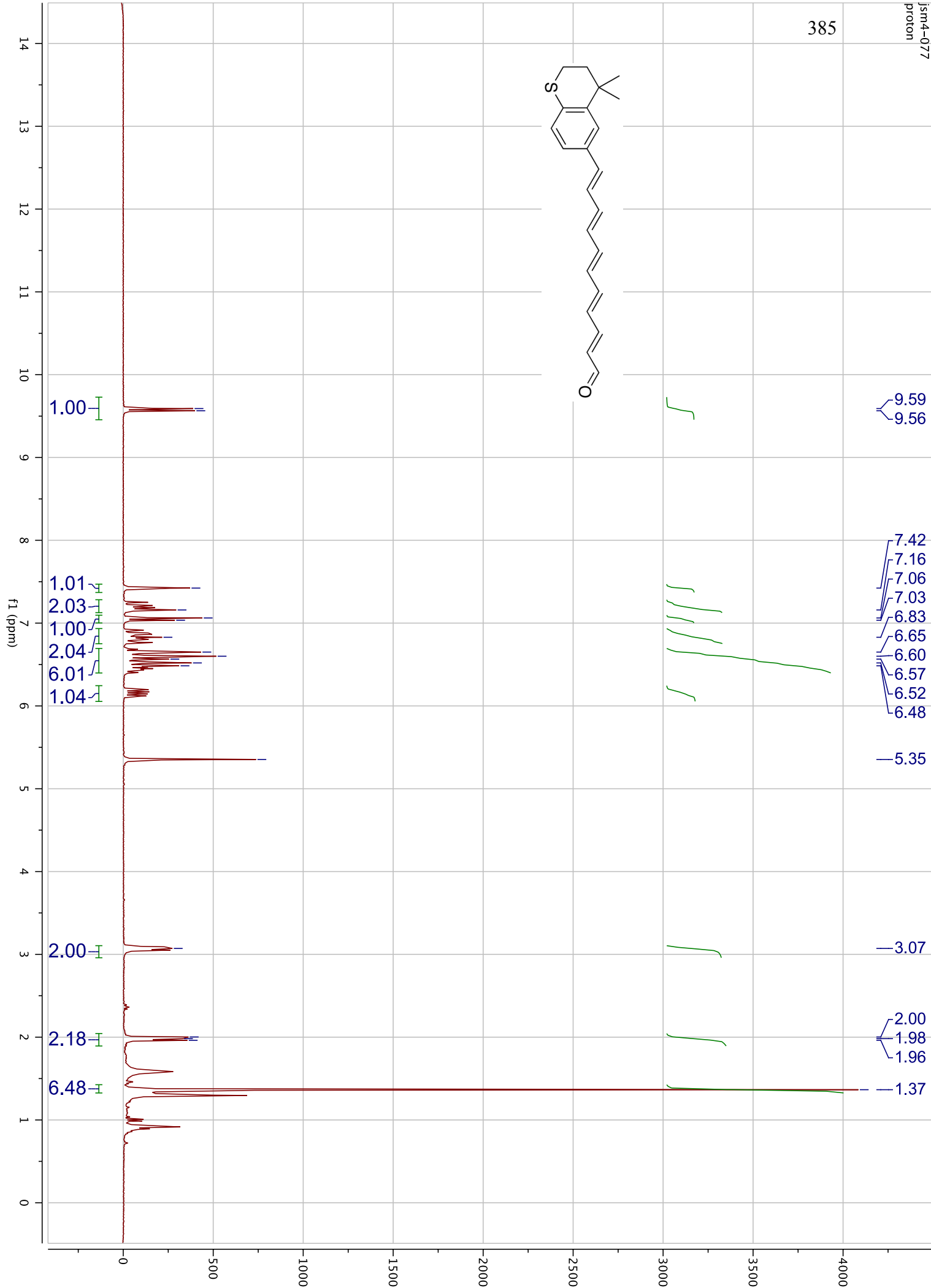
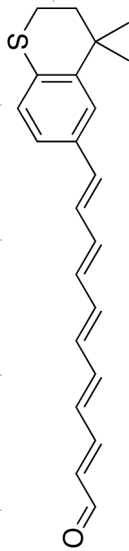
382



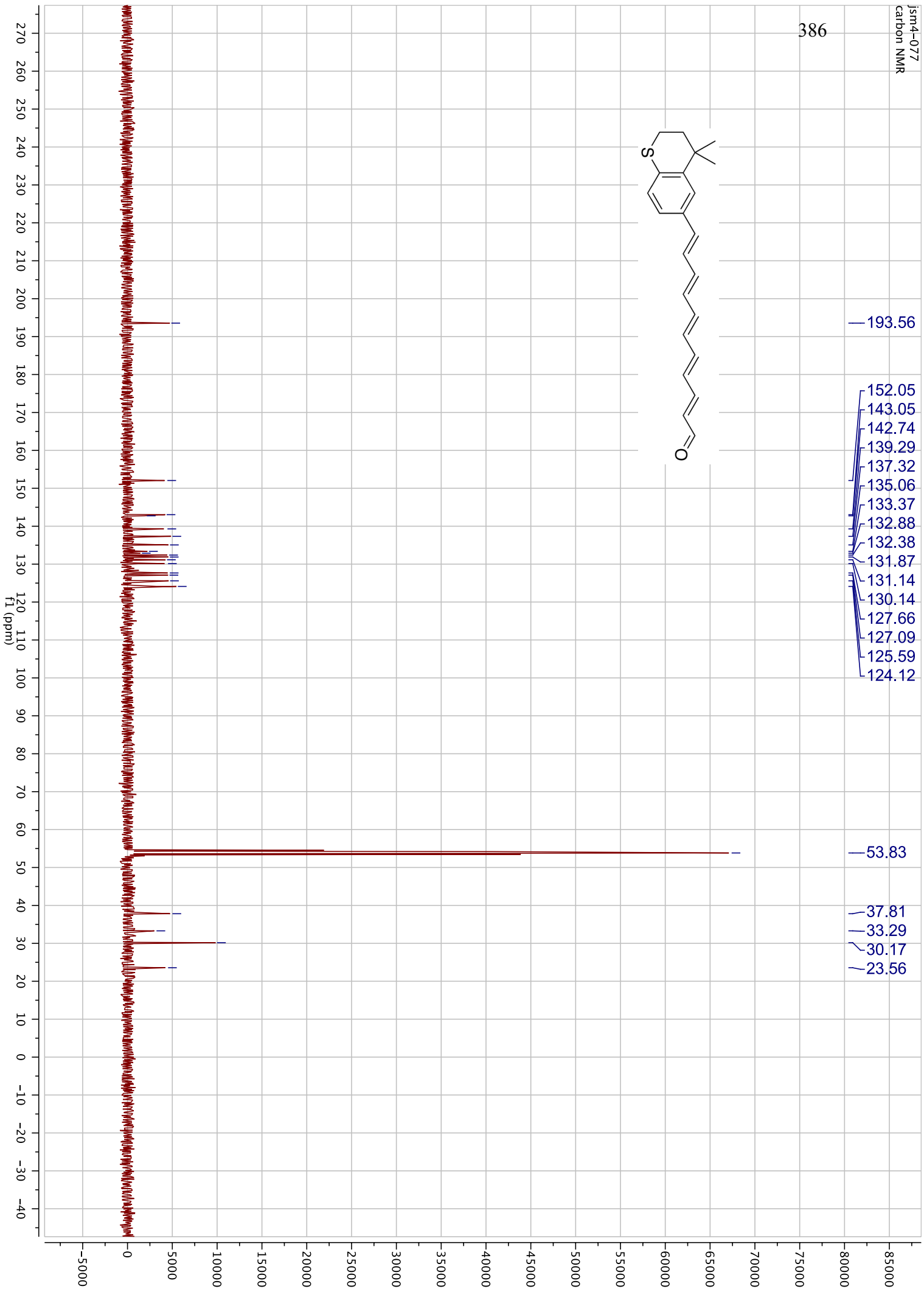
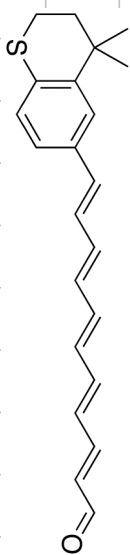


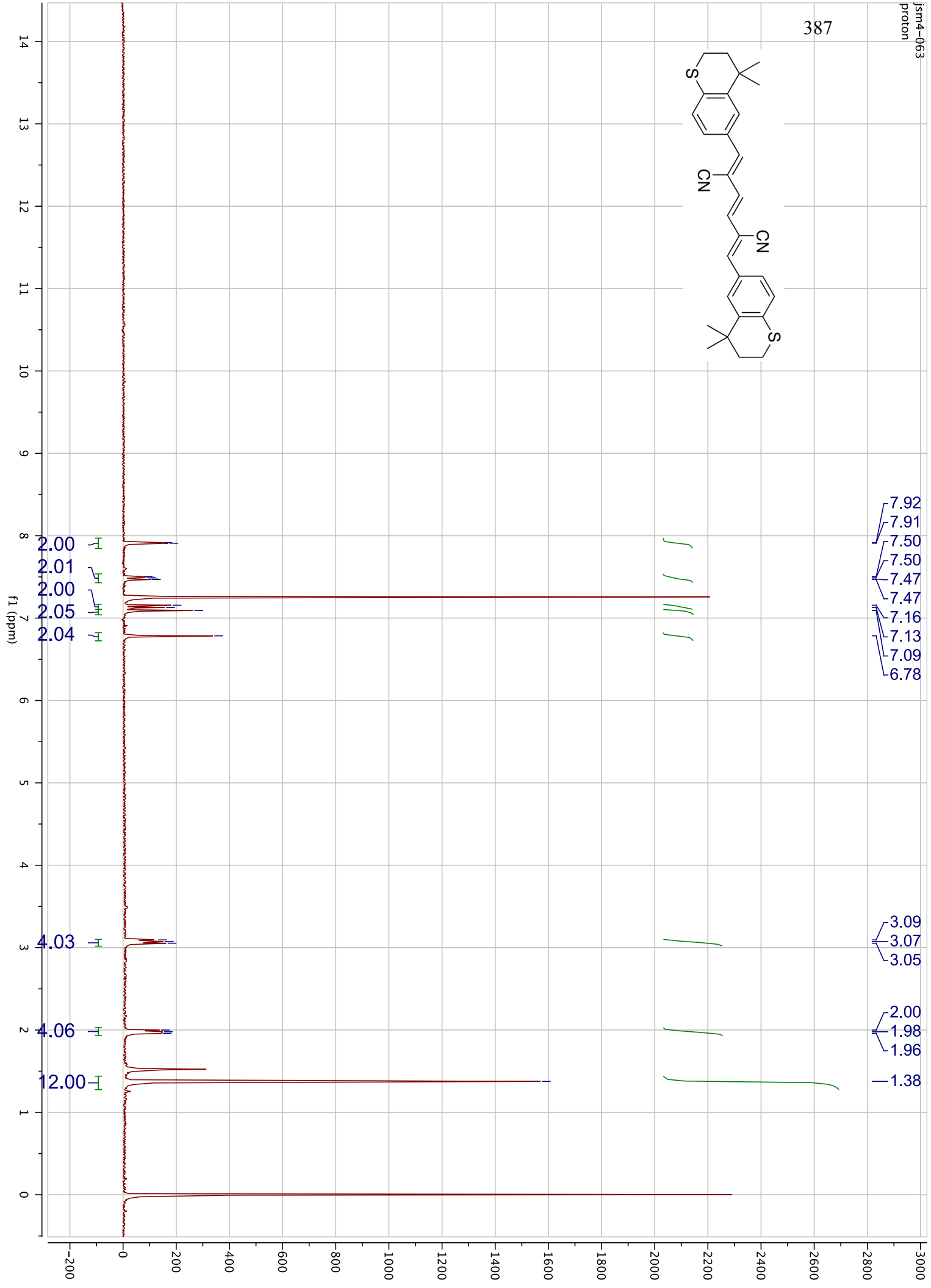
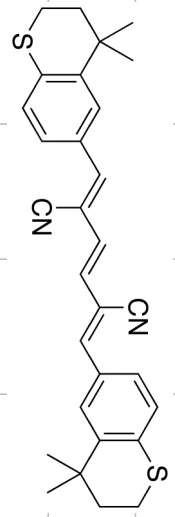
384



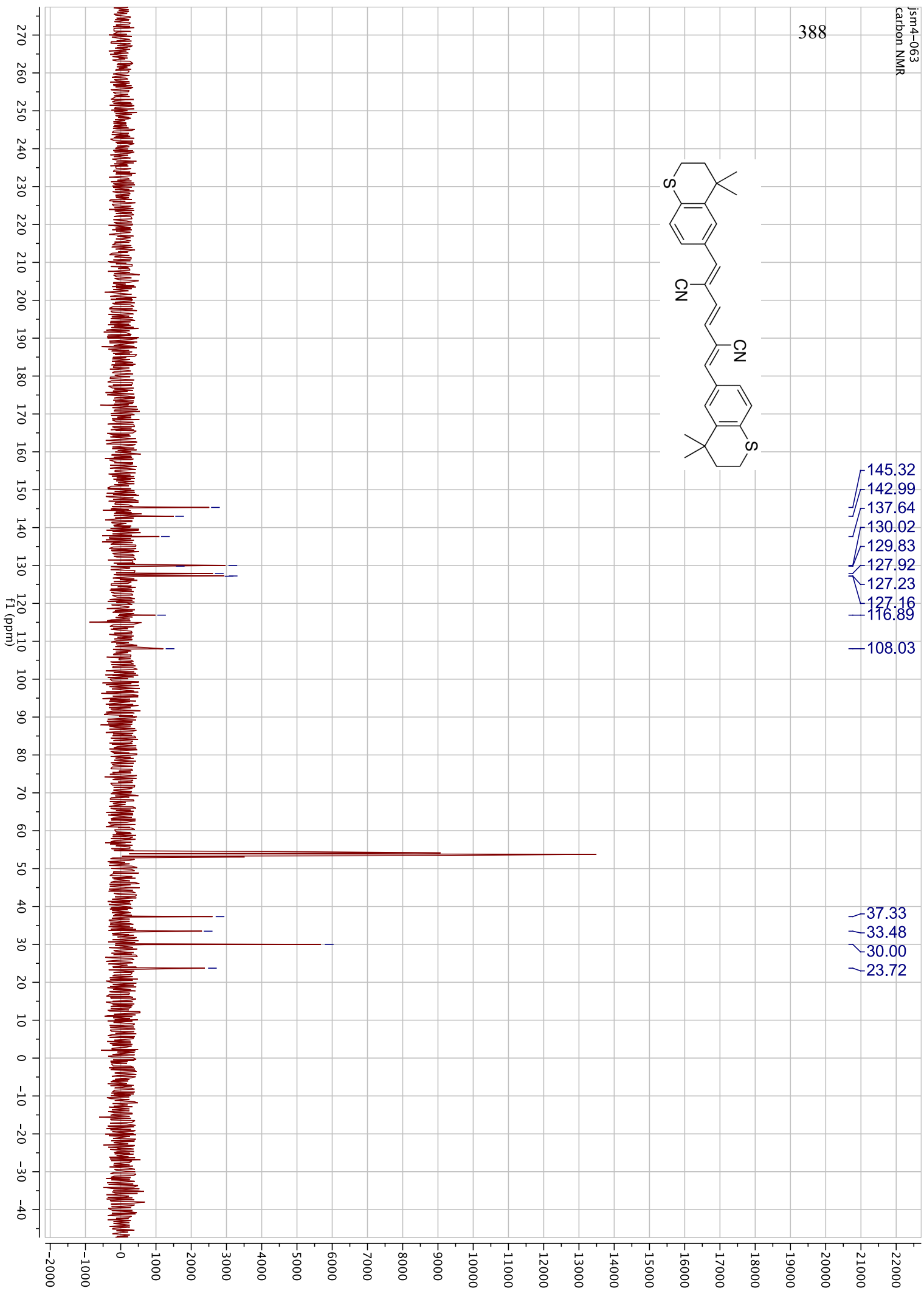
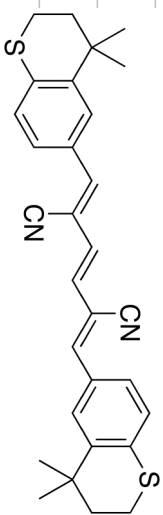


386



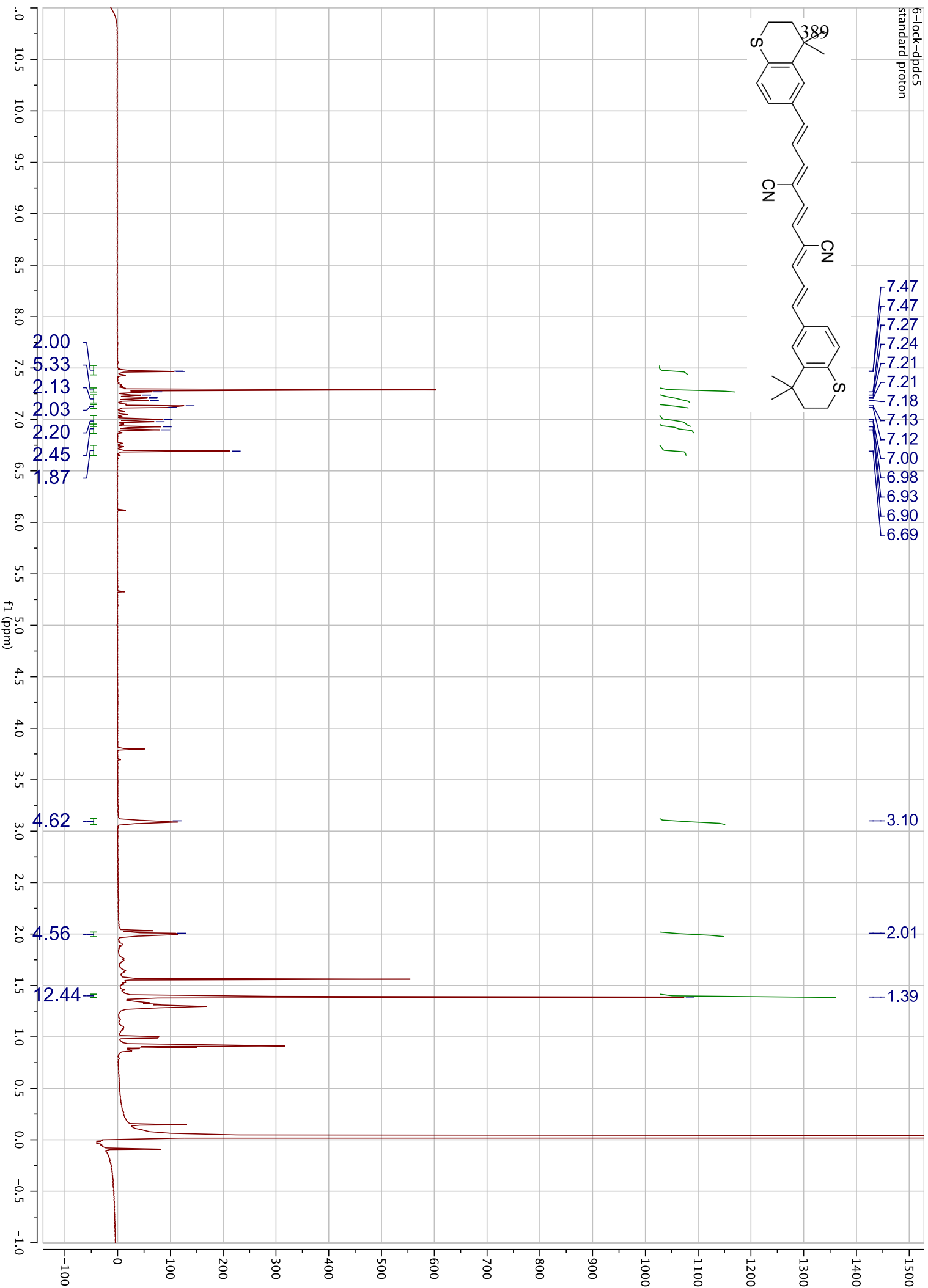
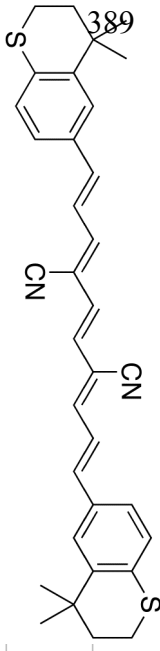


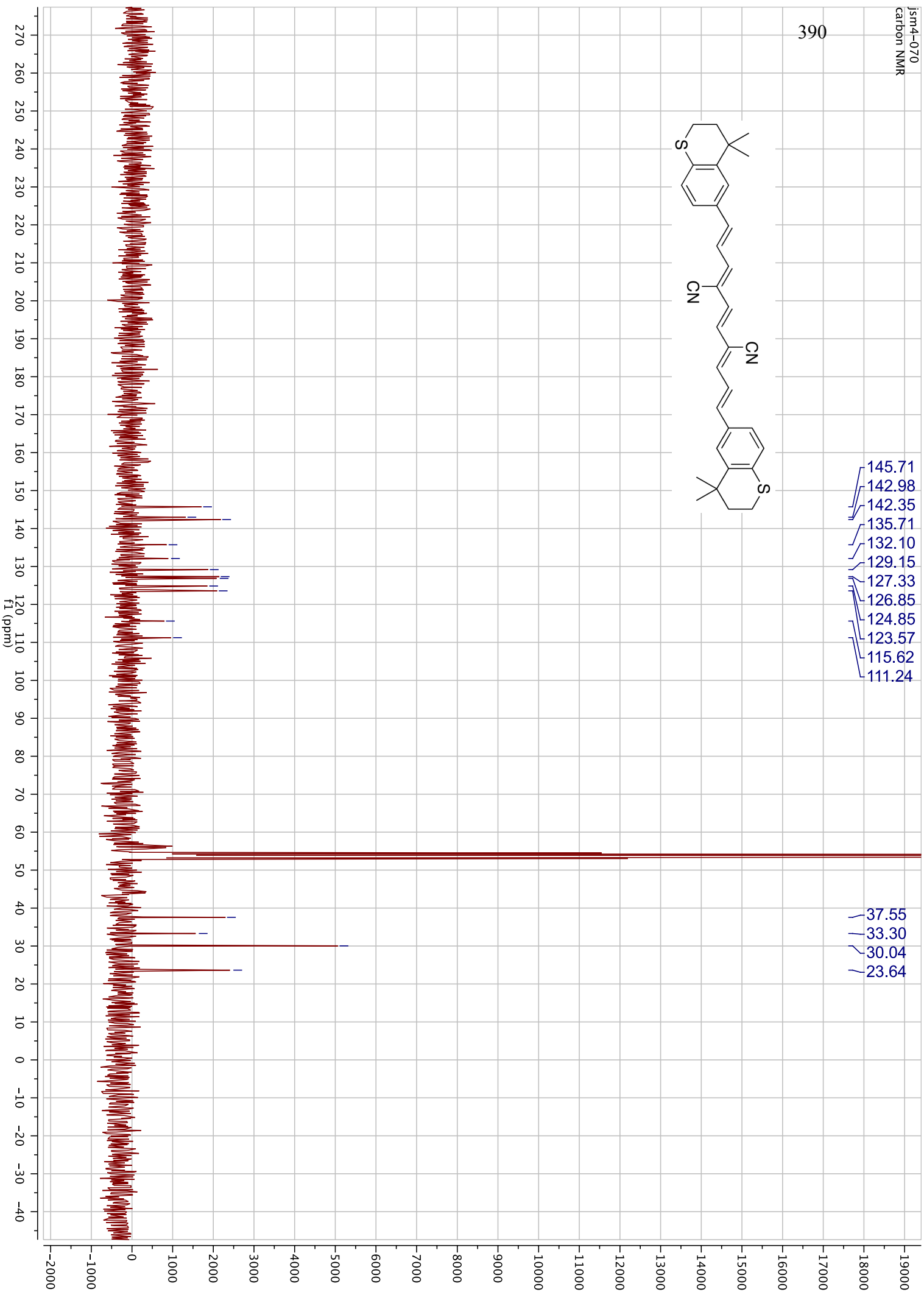
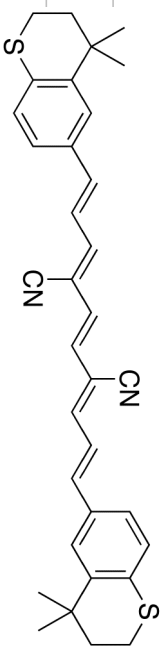
388

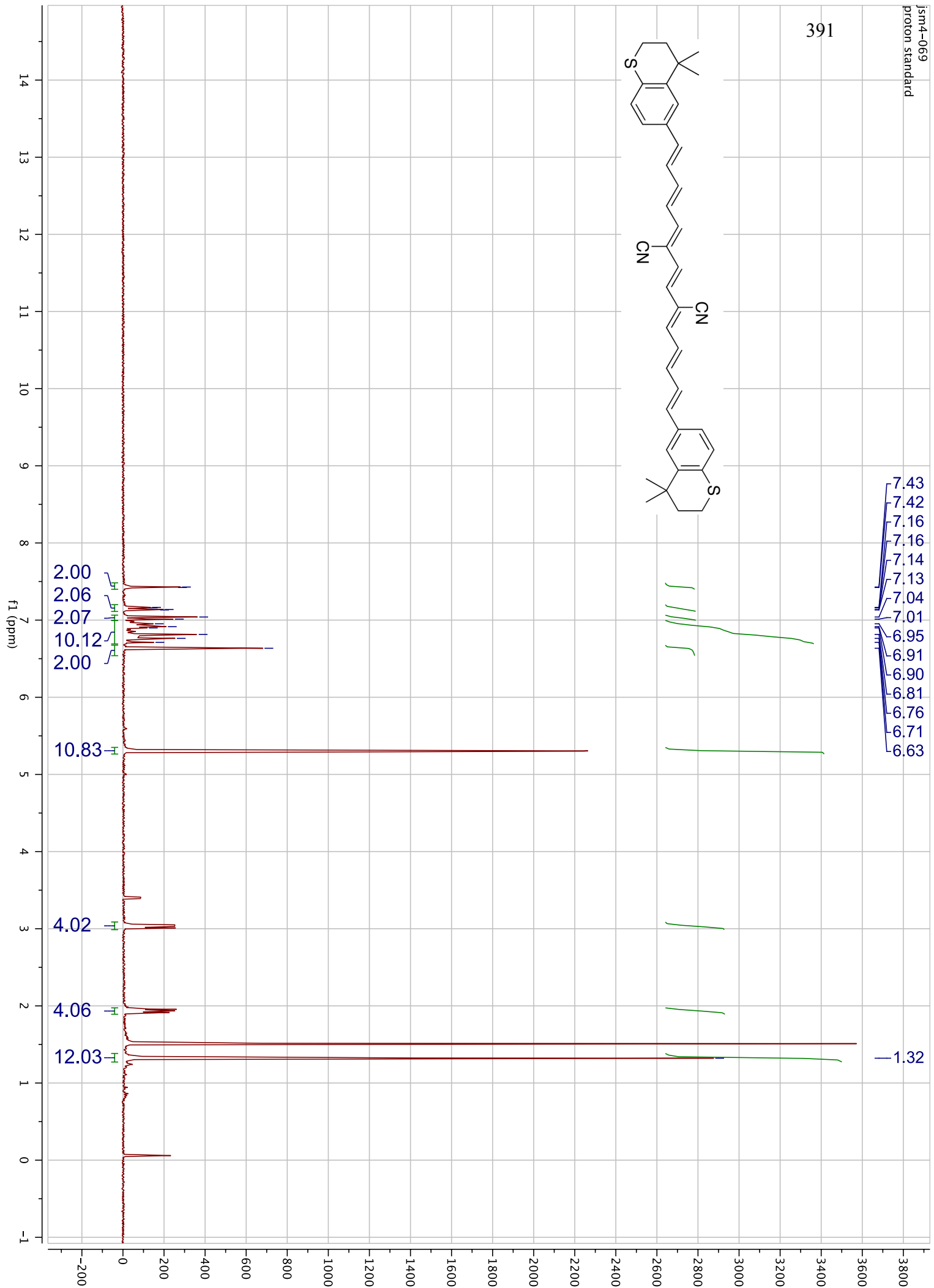
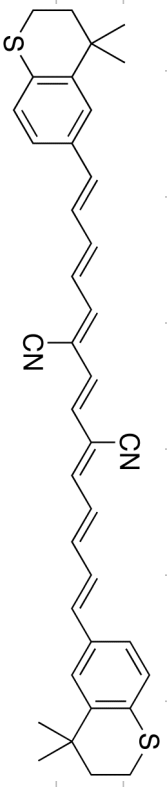




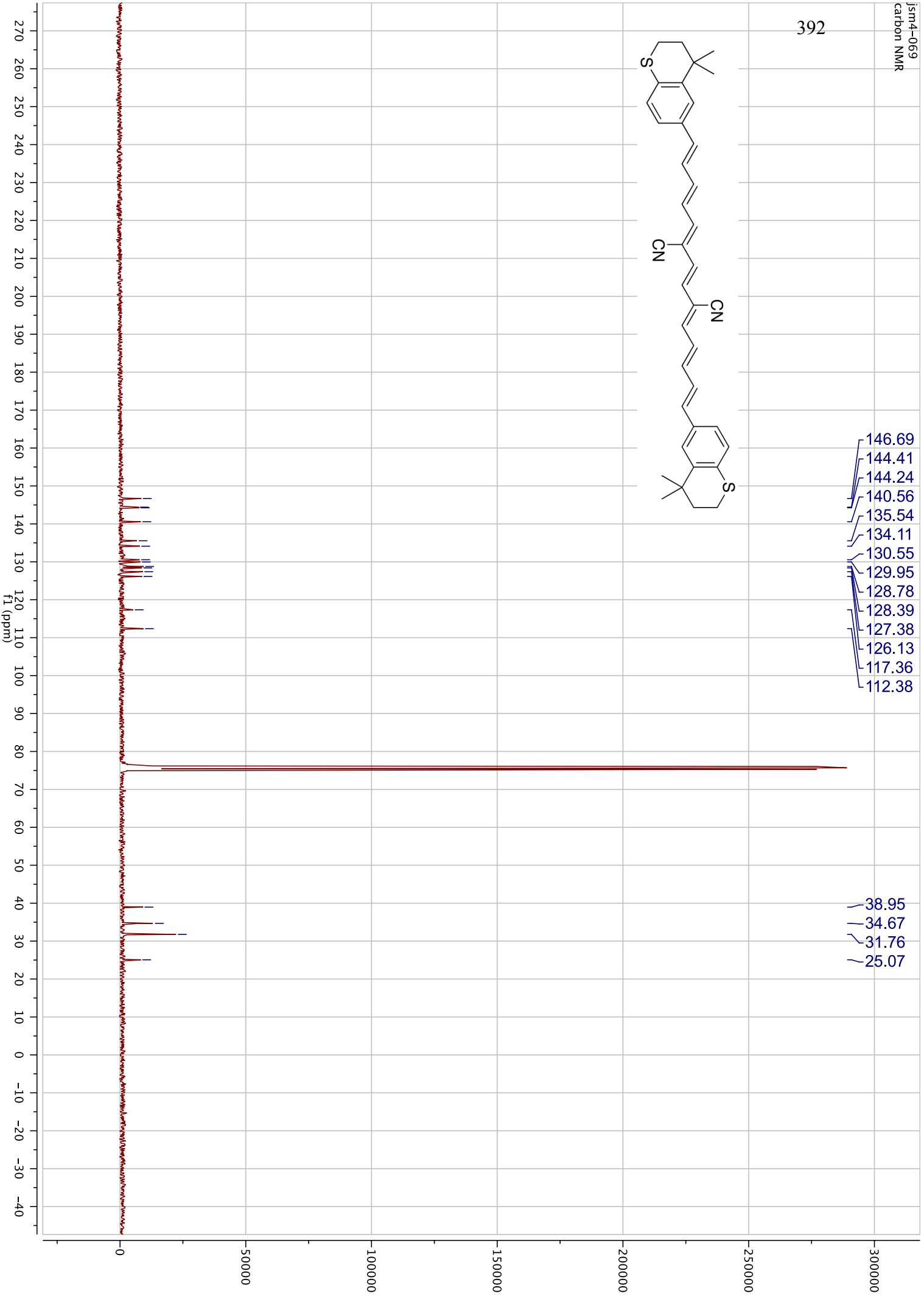
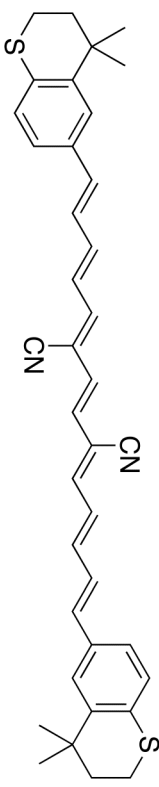
6-lock-dpdcs  
standard proton

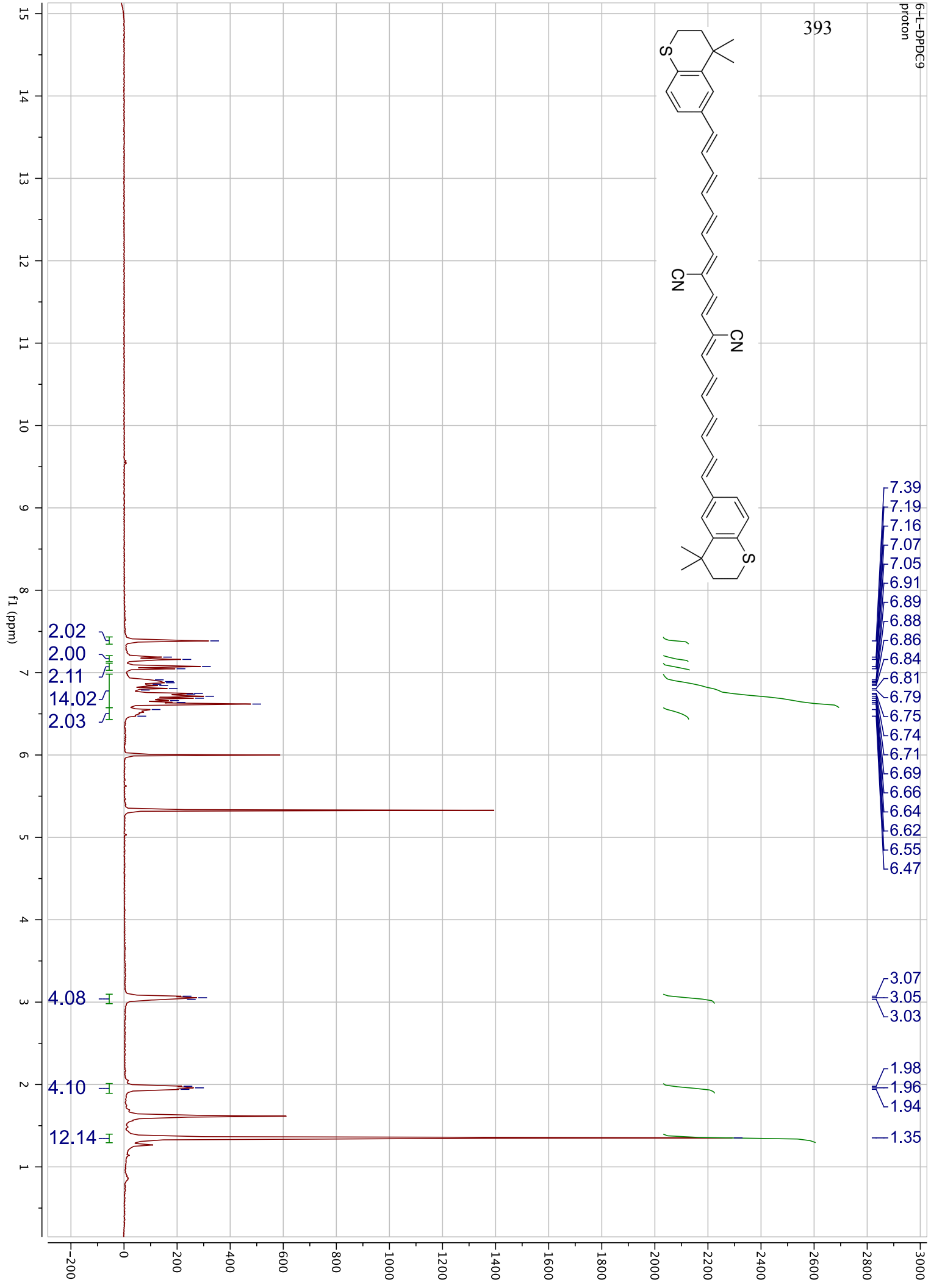
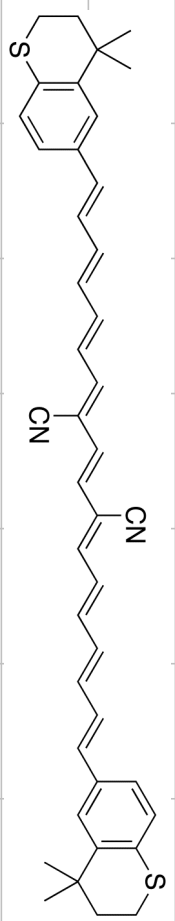




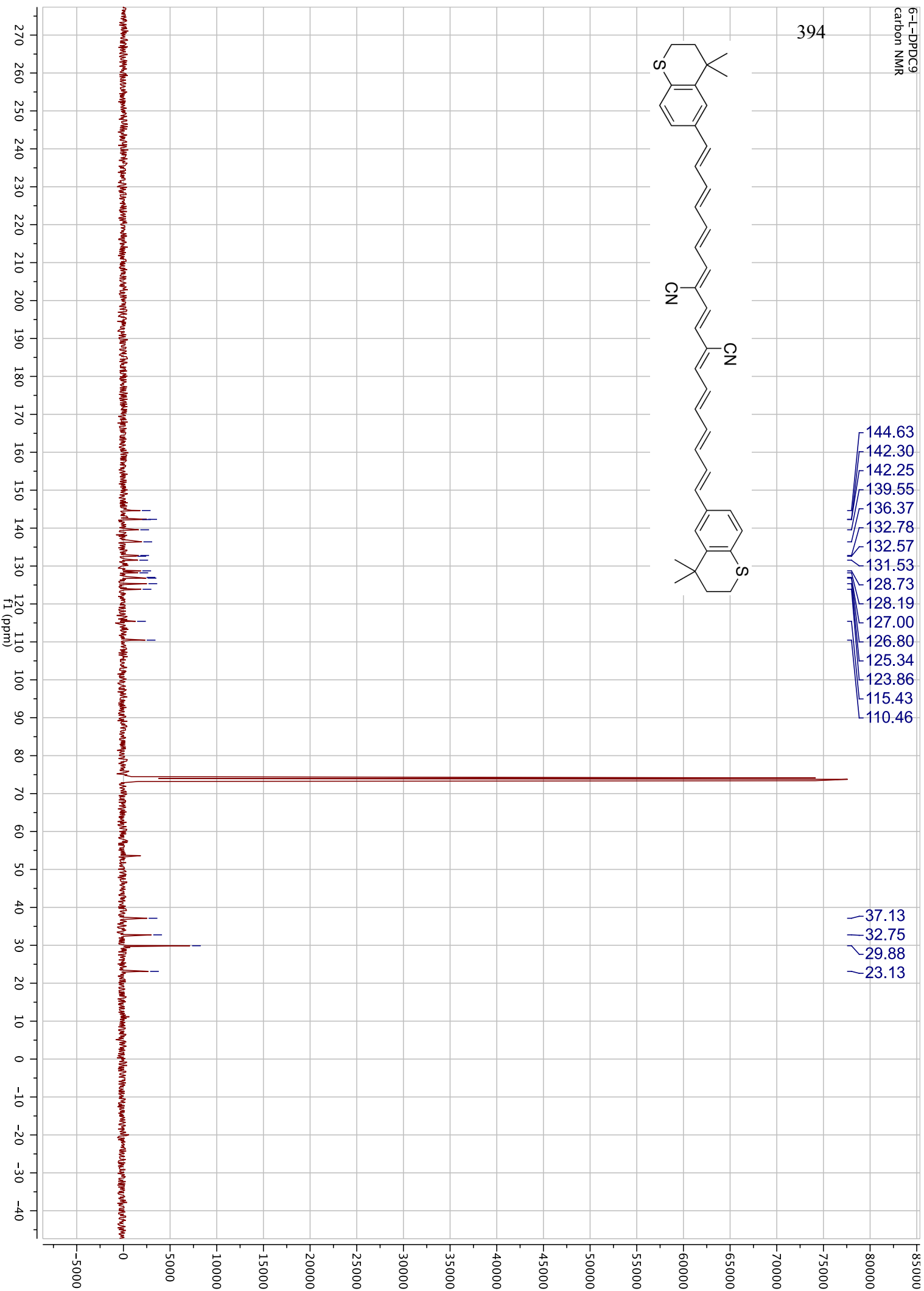
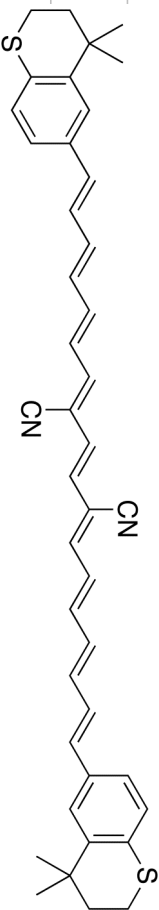


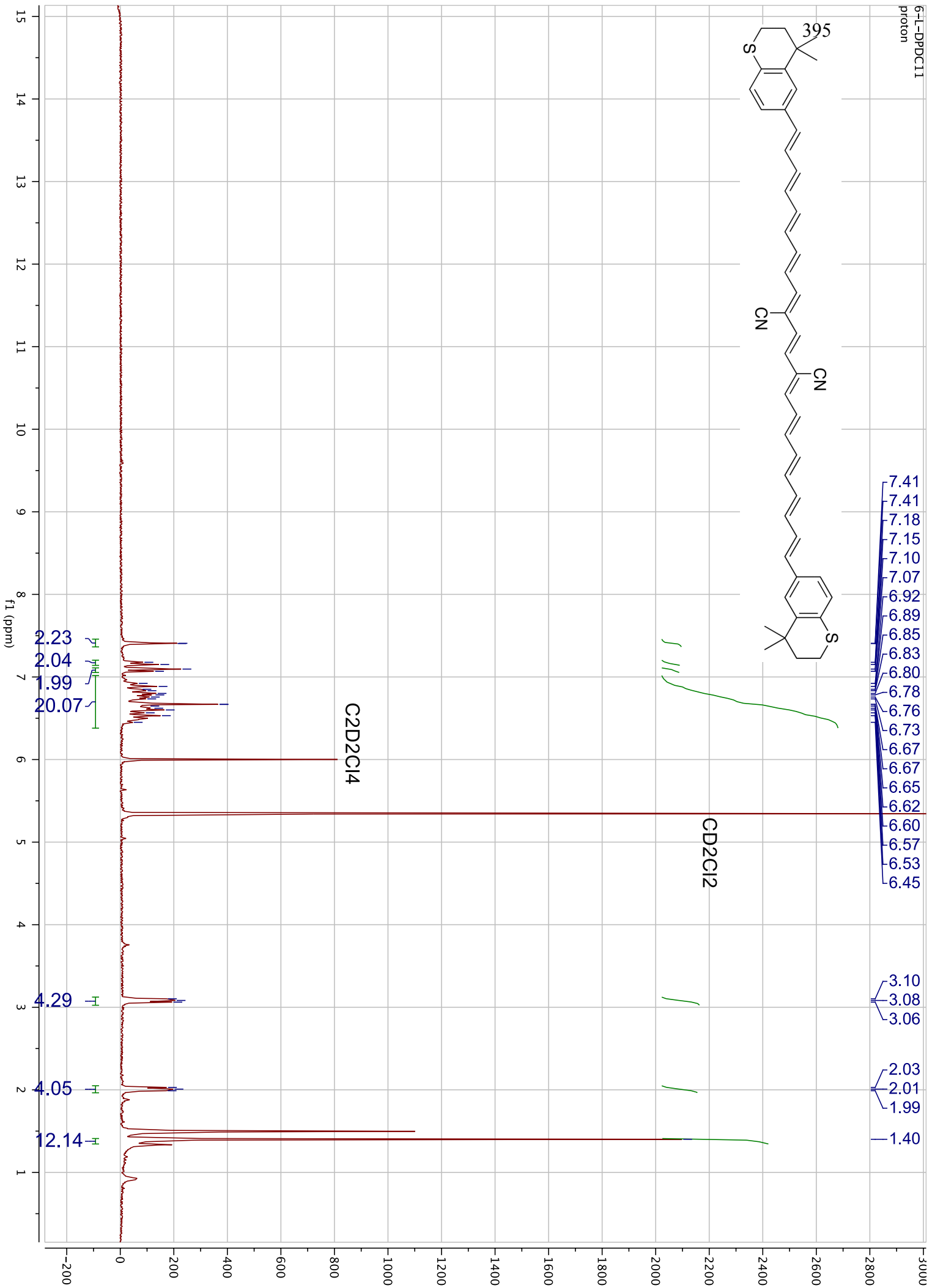
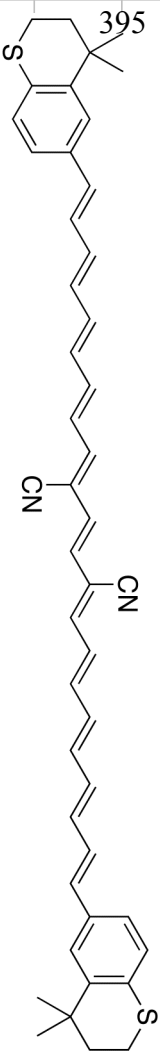
392



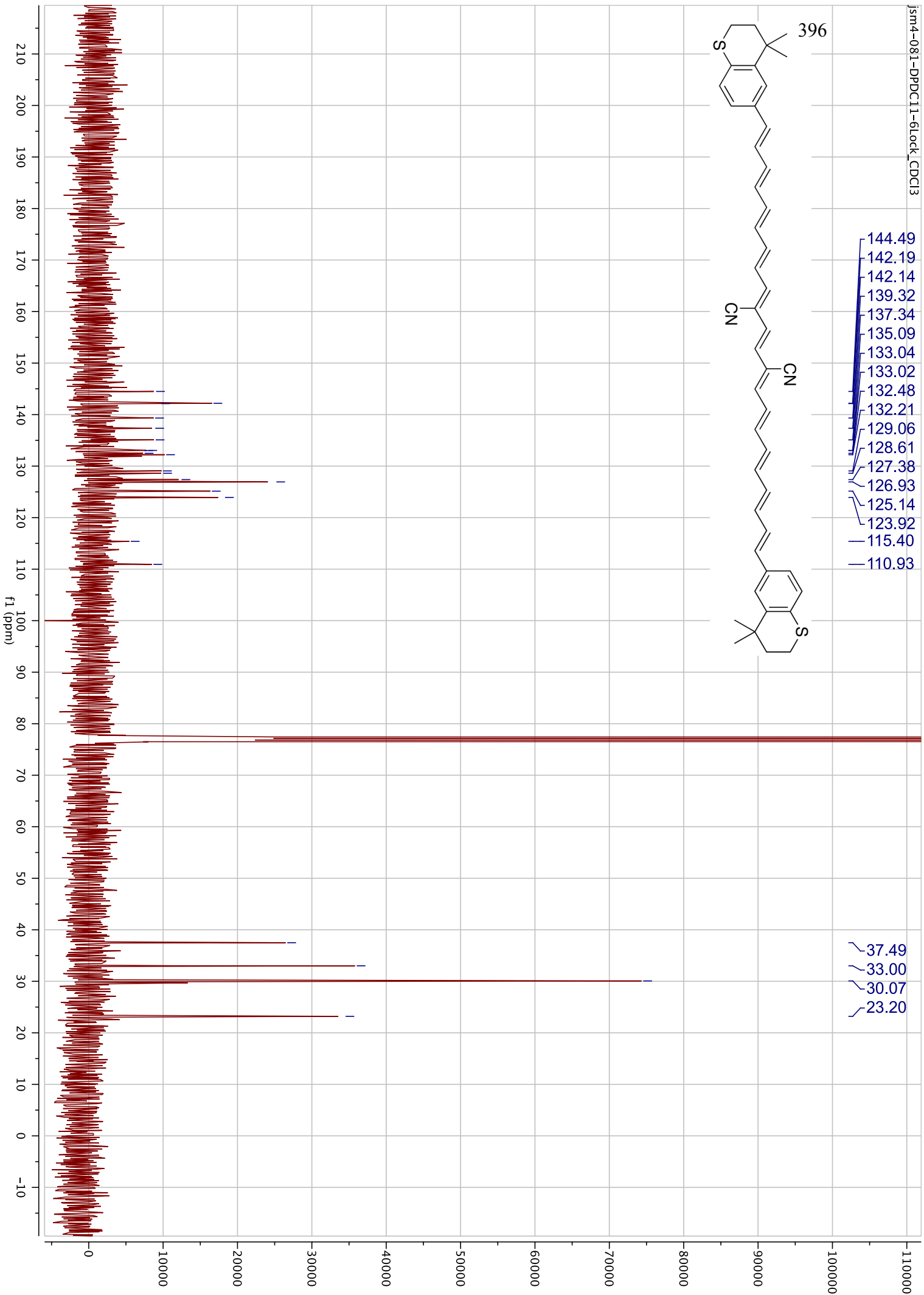
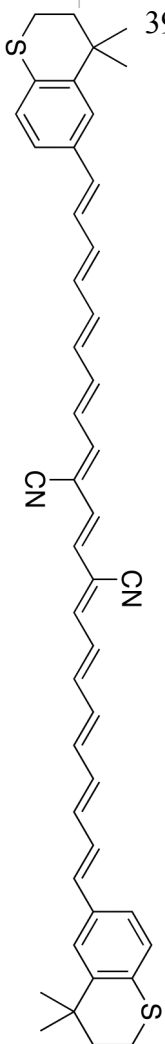


394

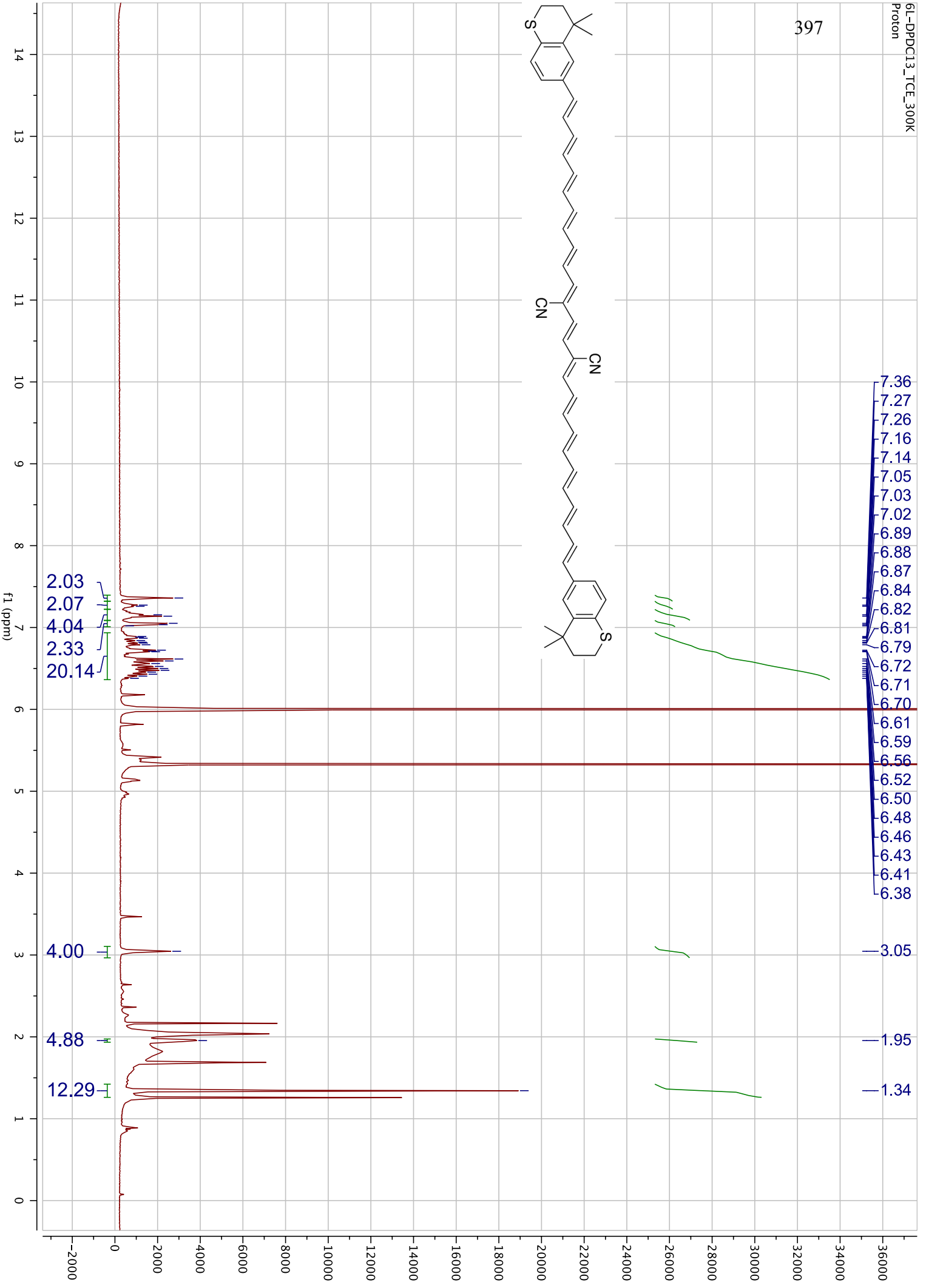
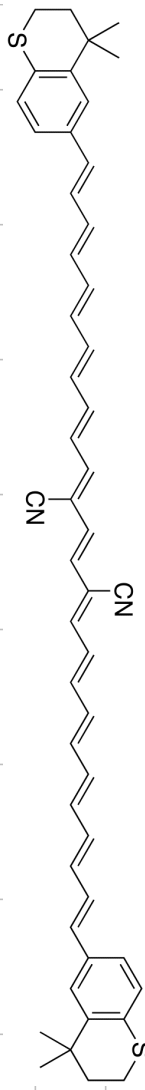


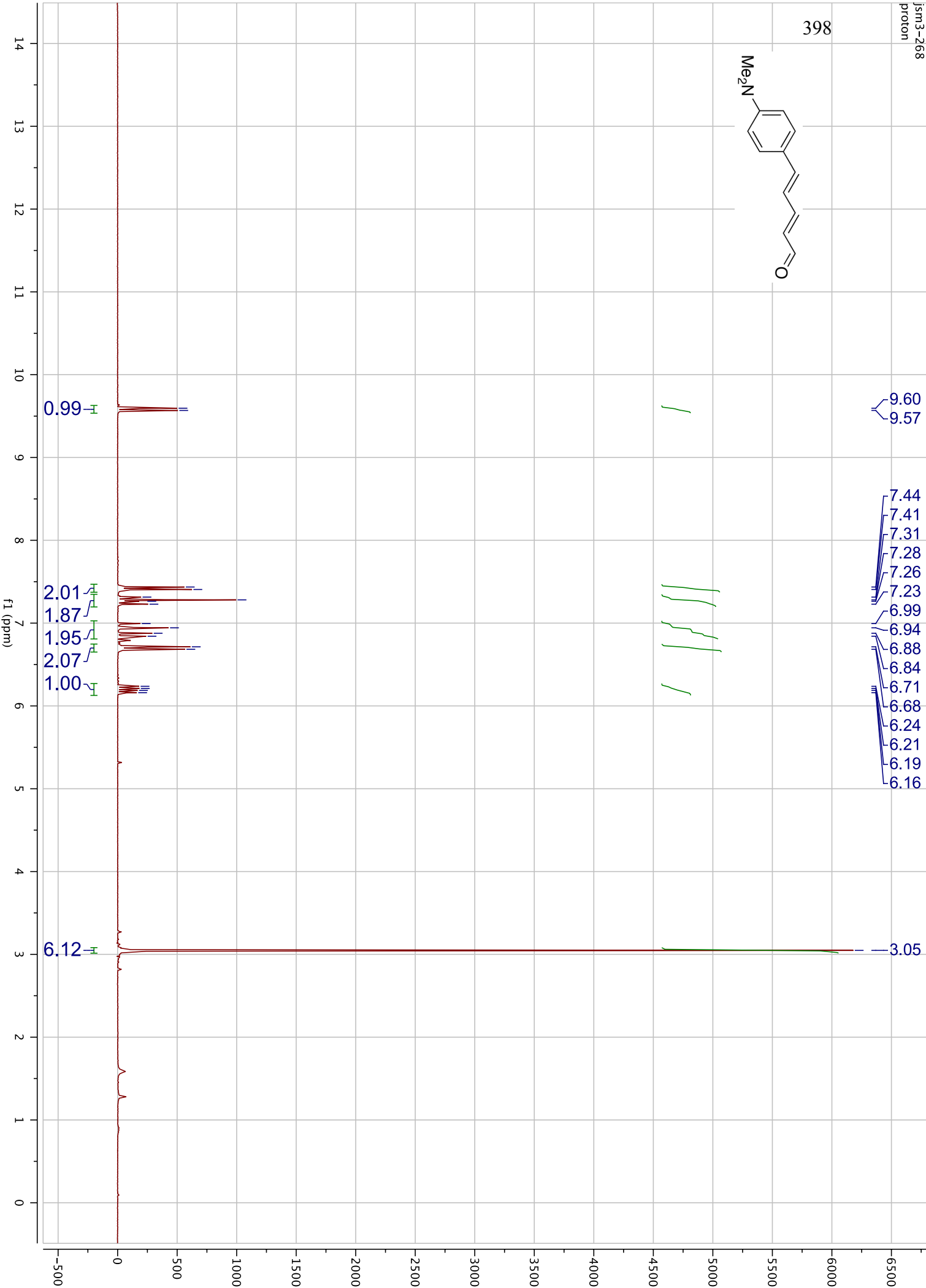
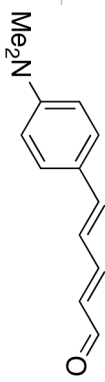


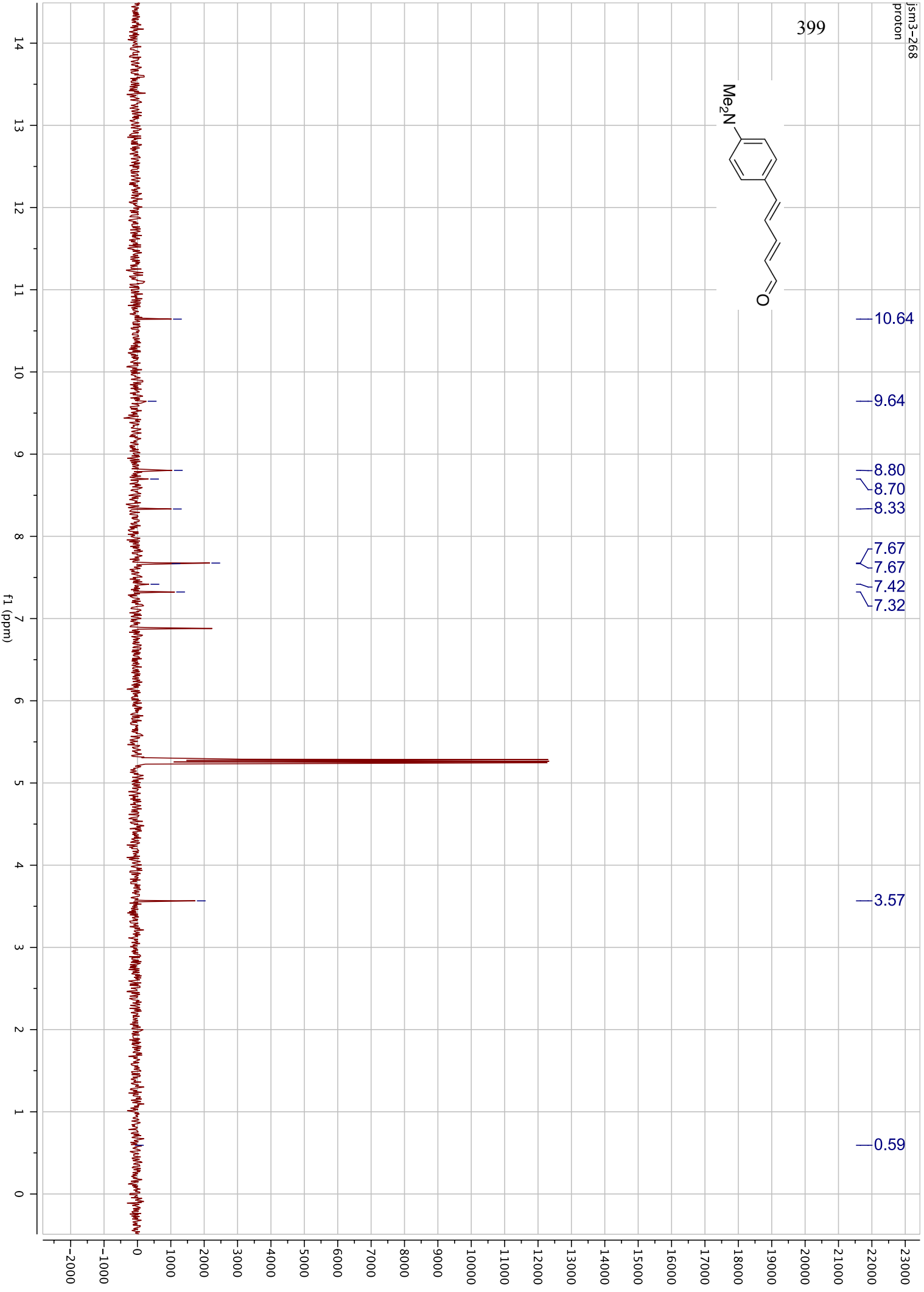
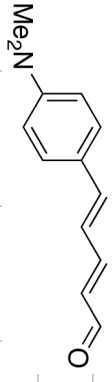
396



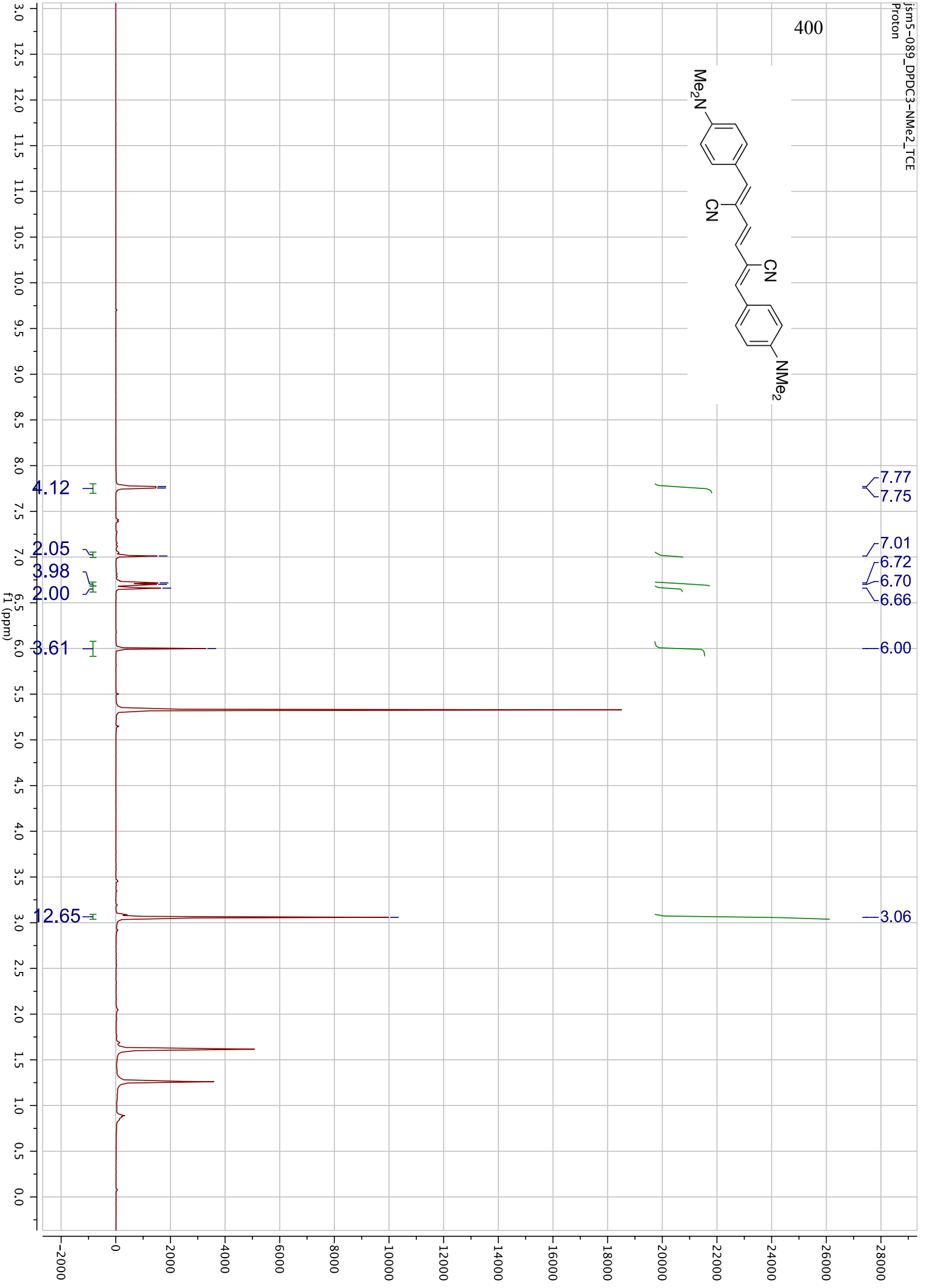
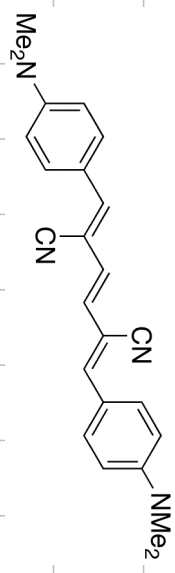




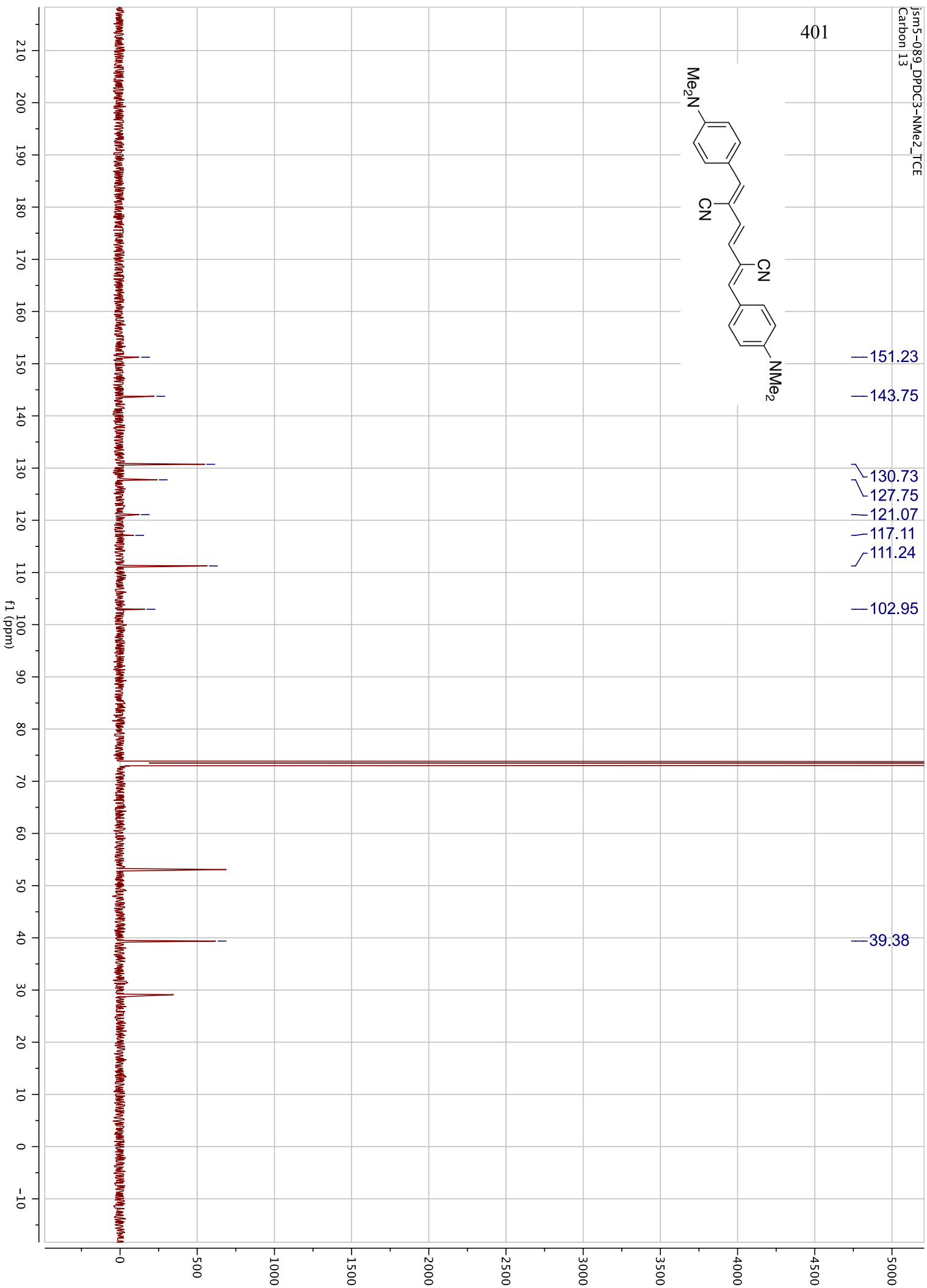
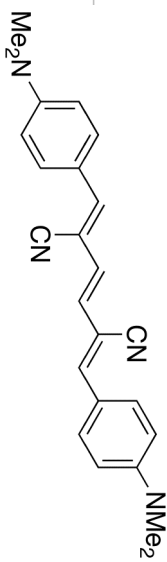


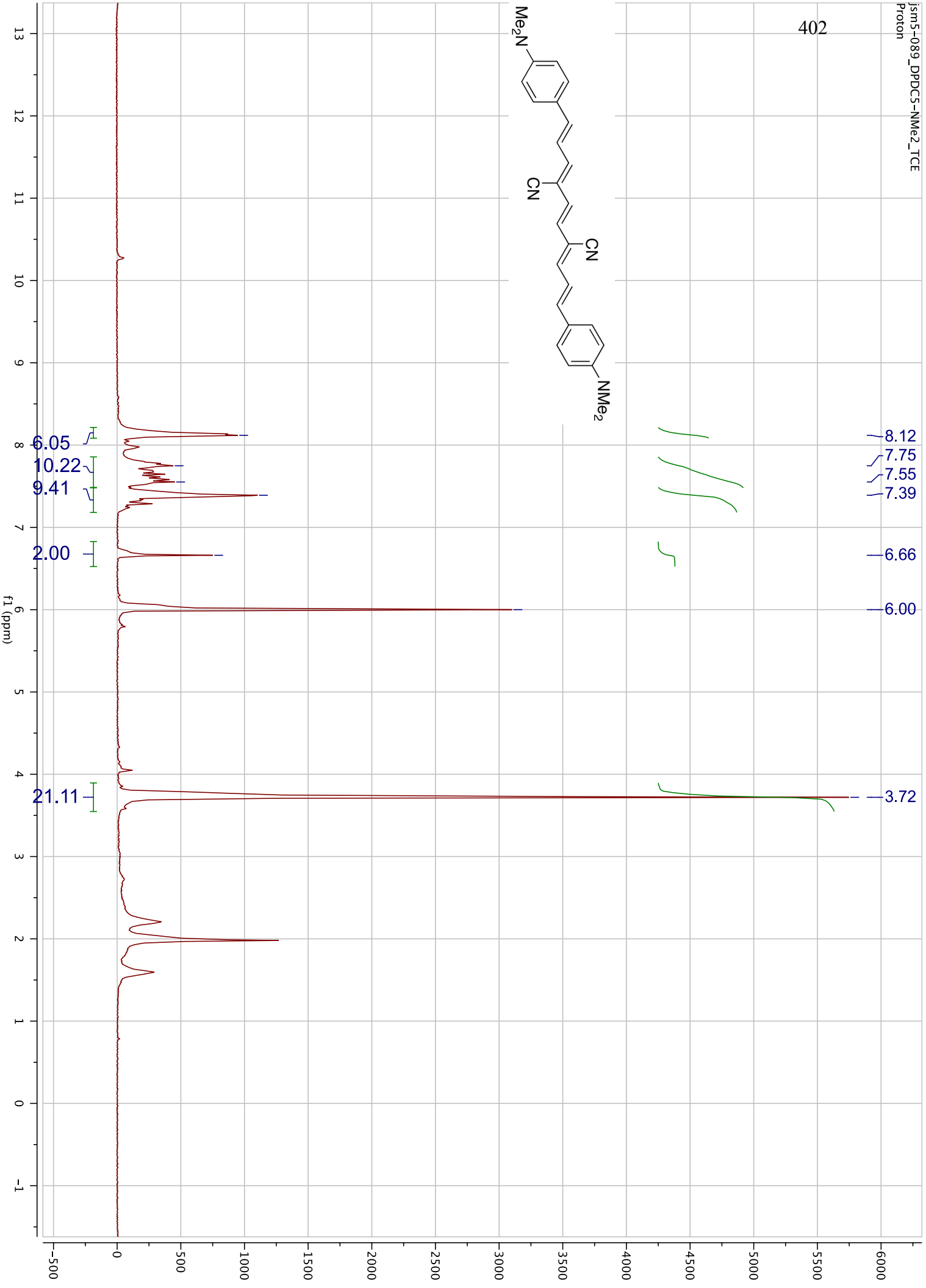
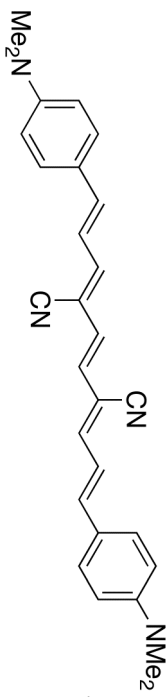


400

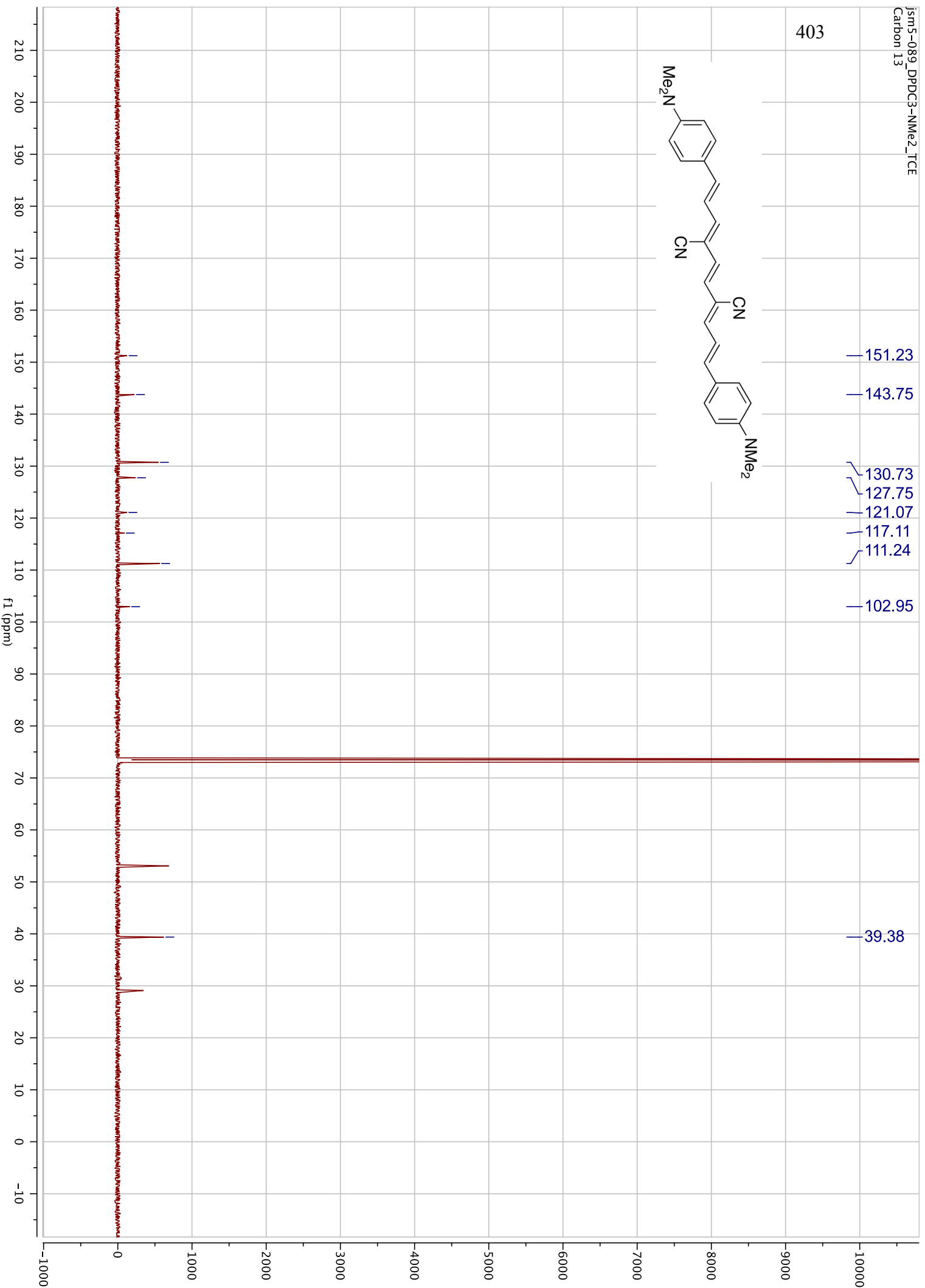
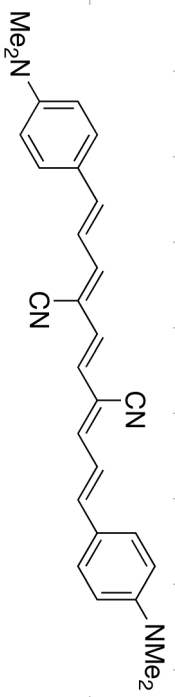


401

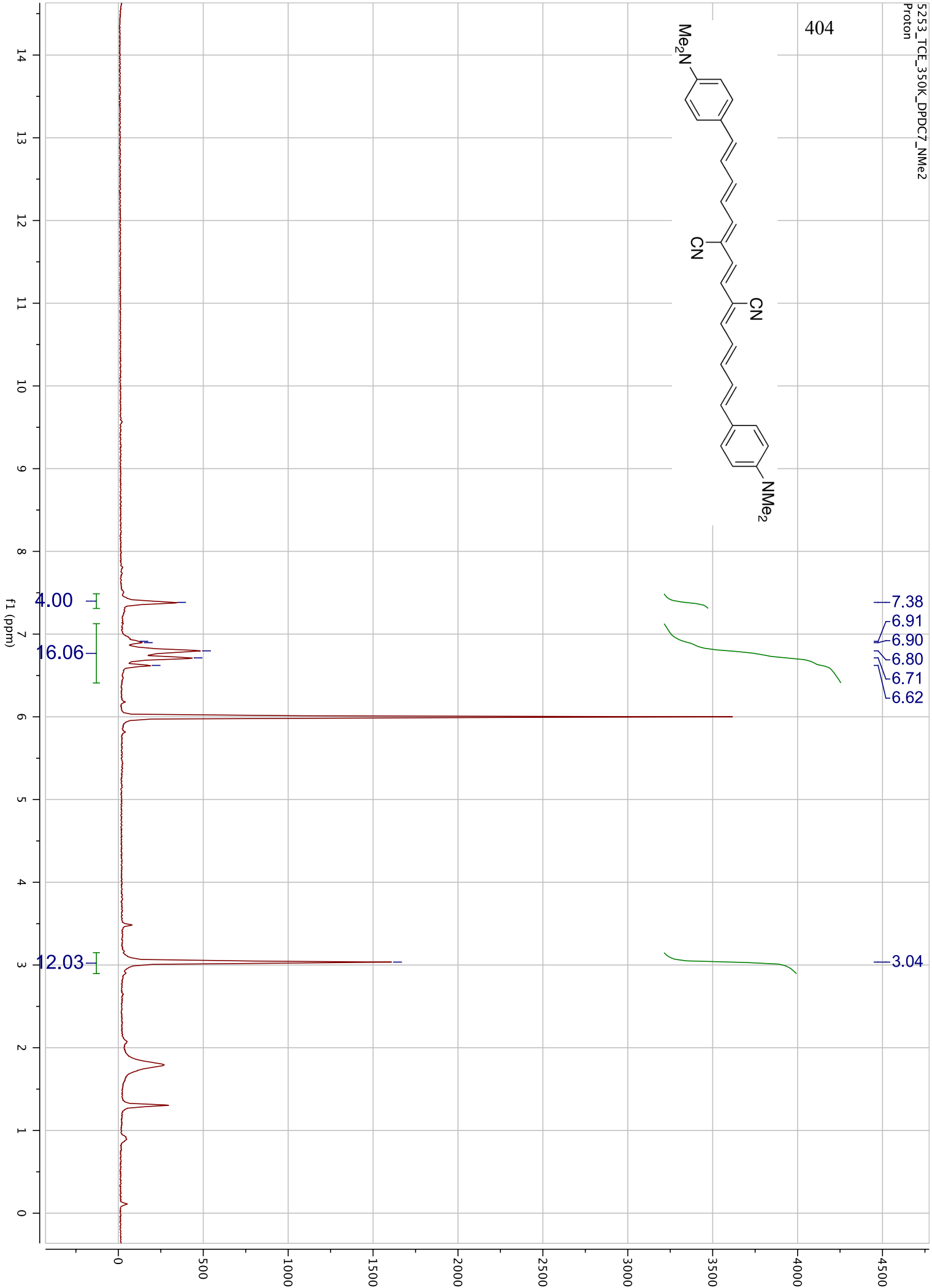
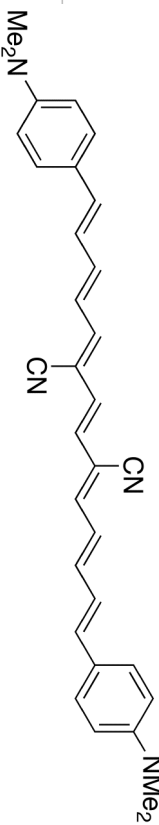




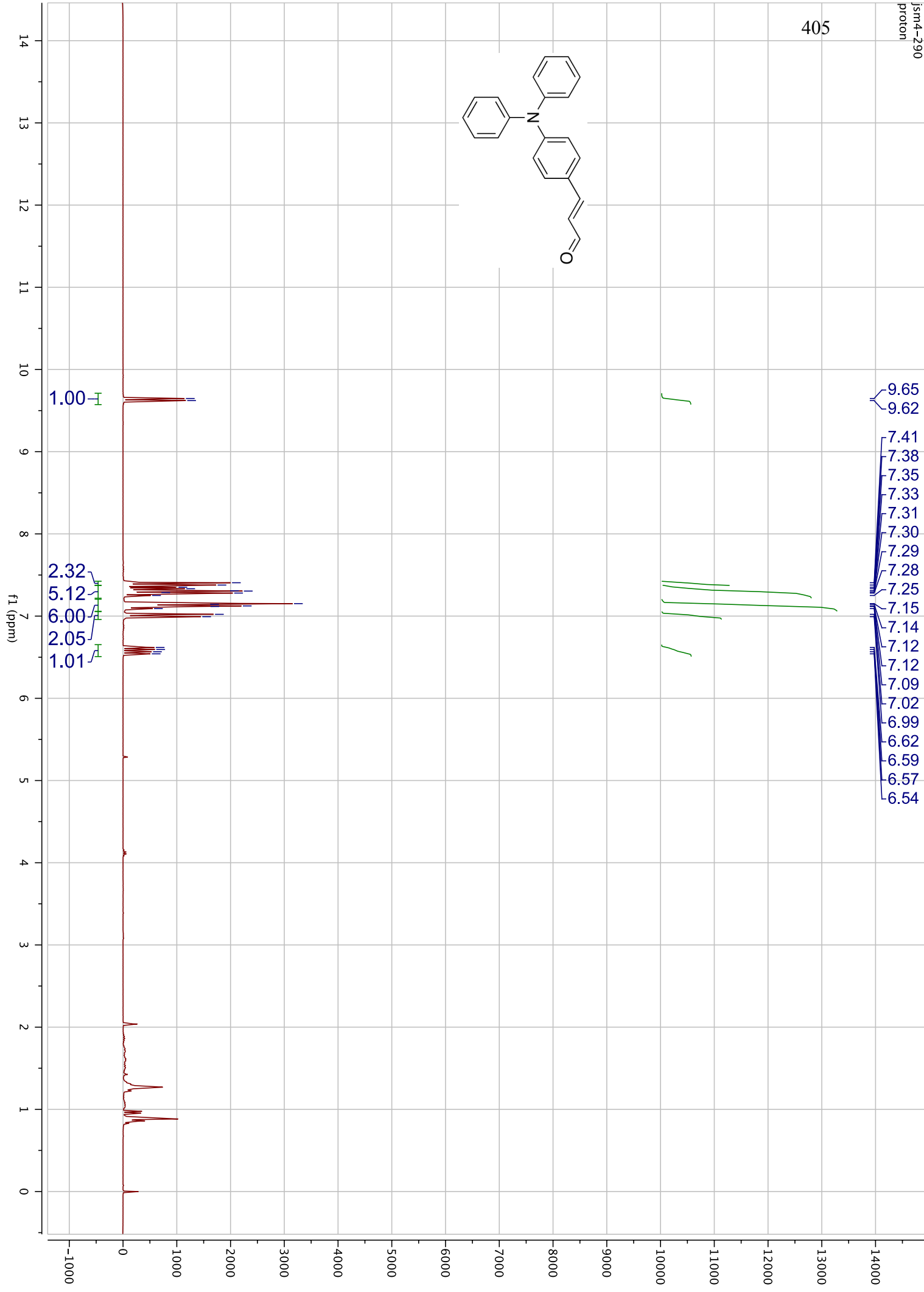
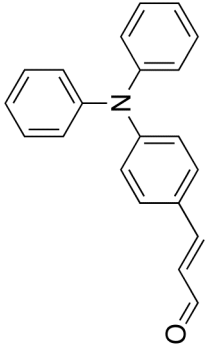
403

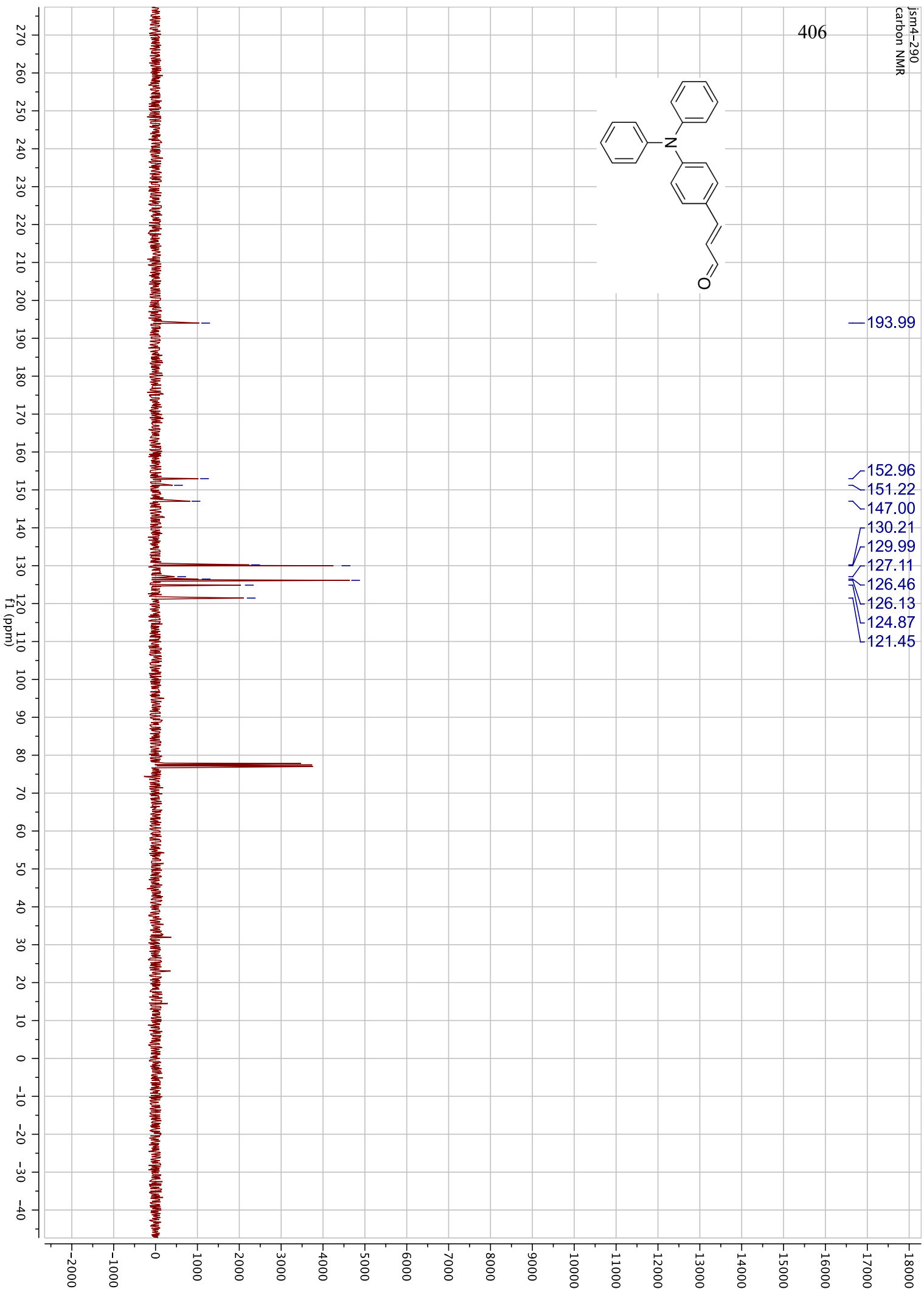
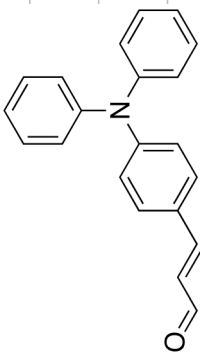


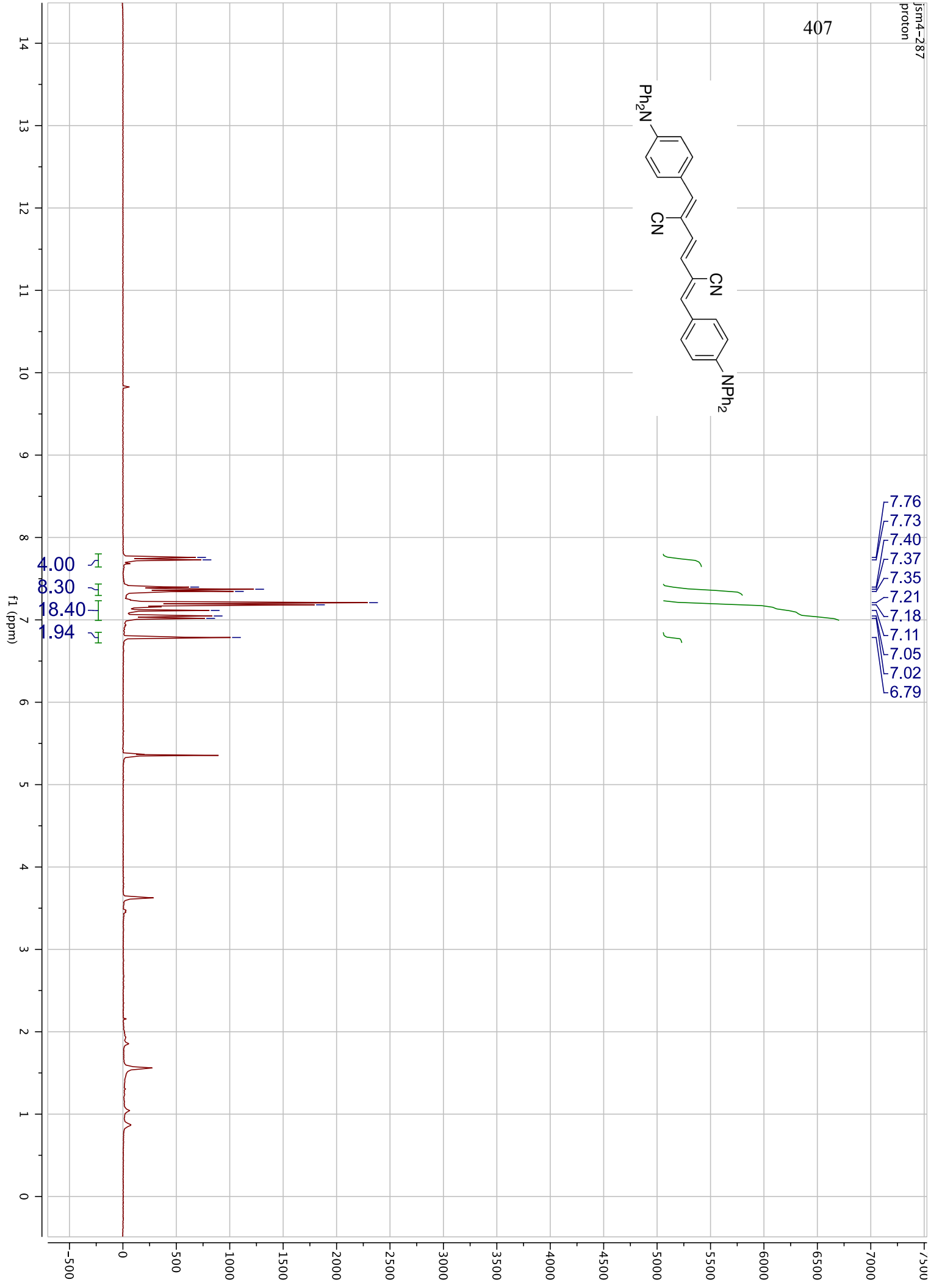
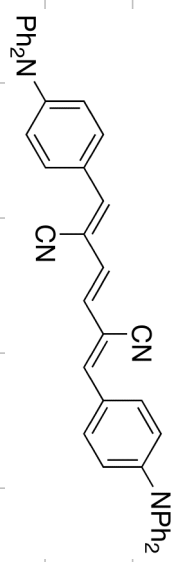
404



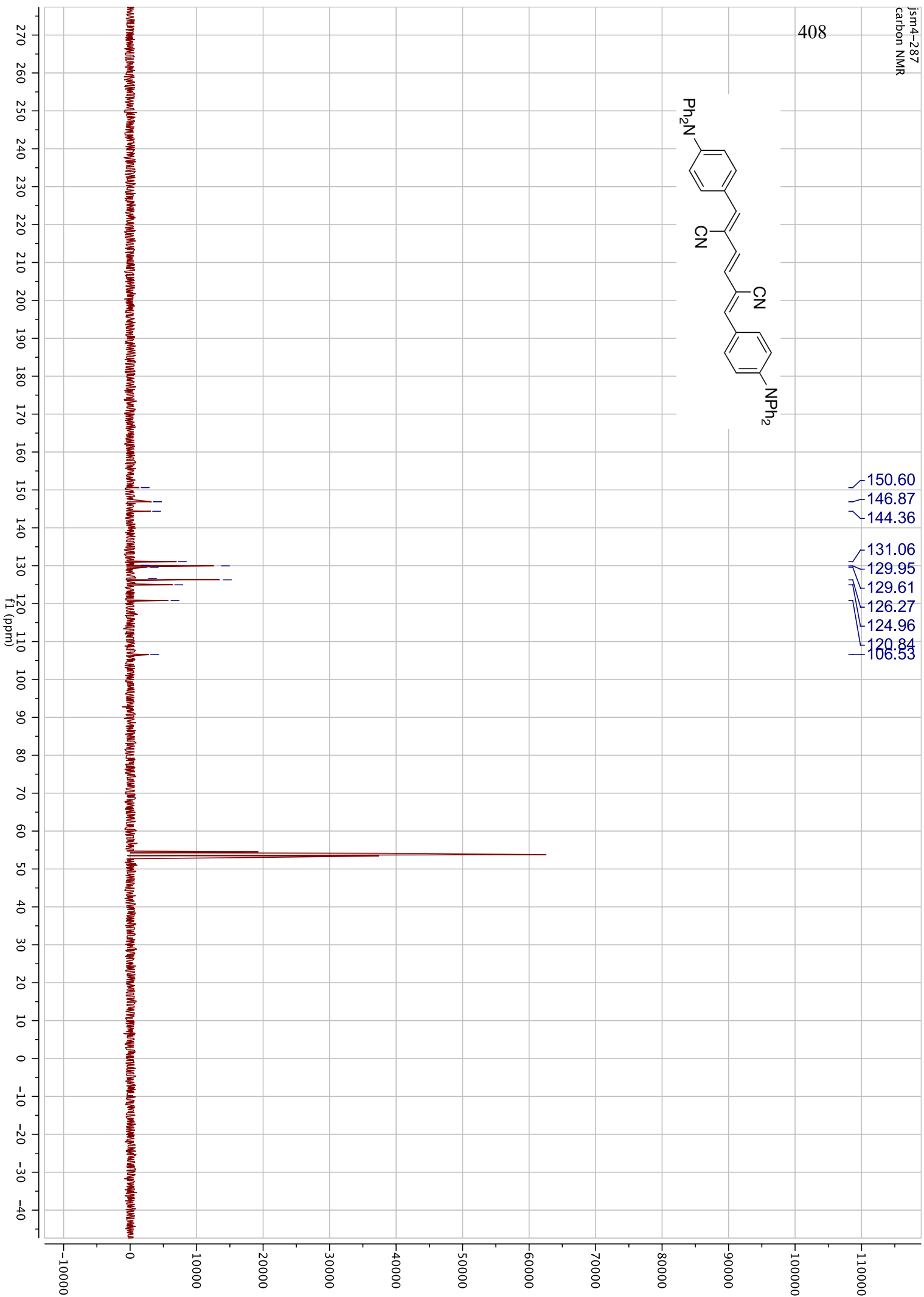
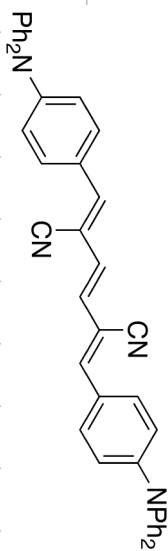


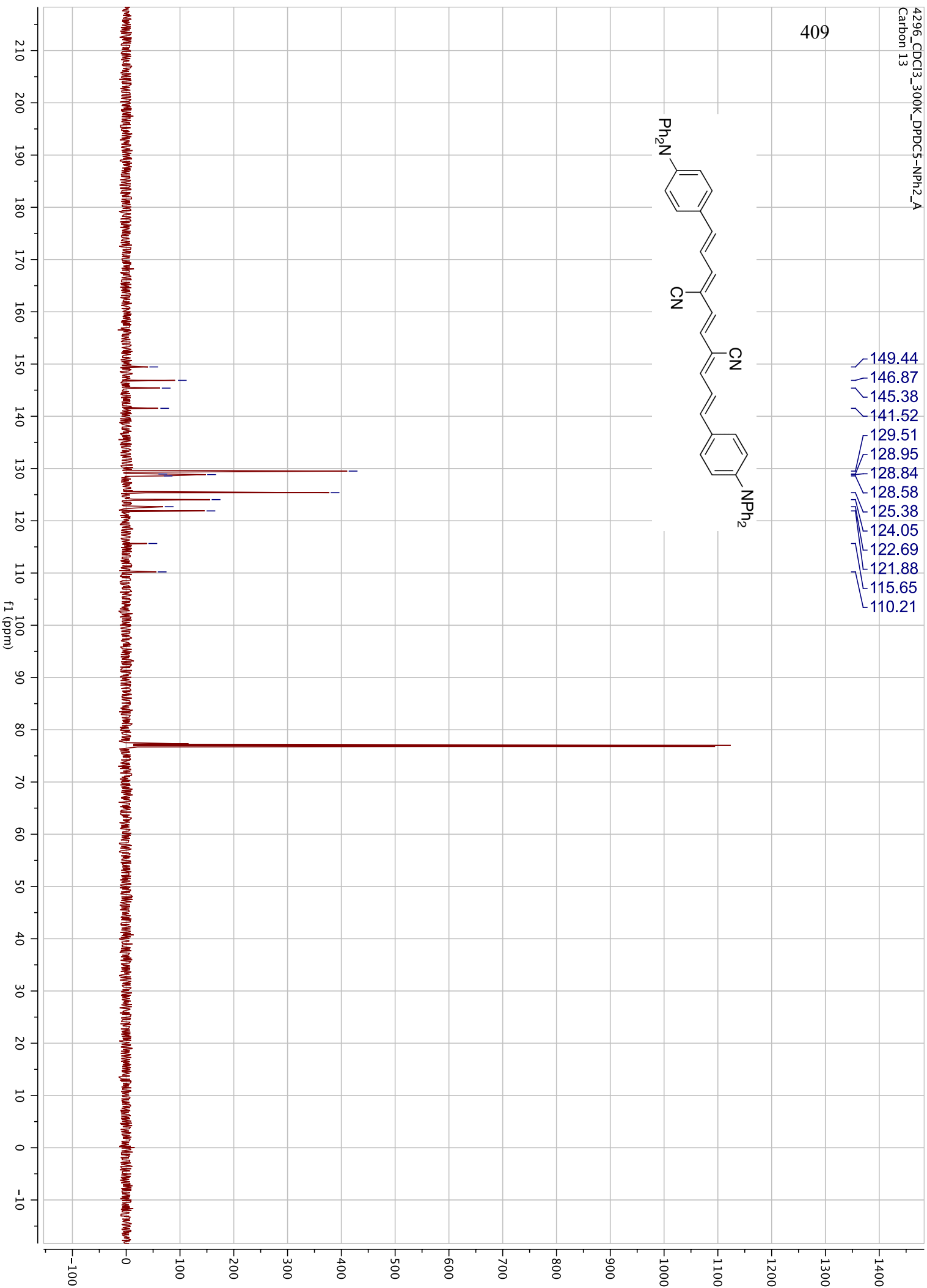
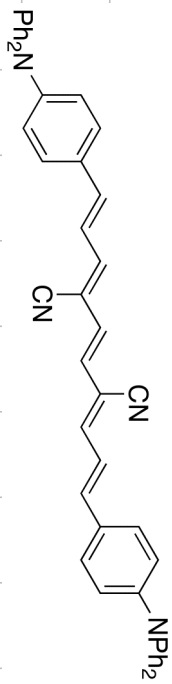




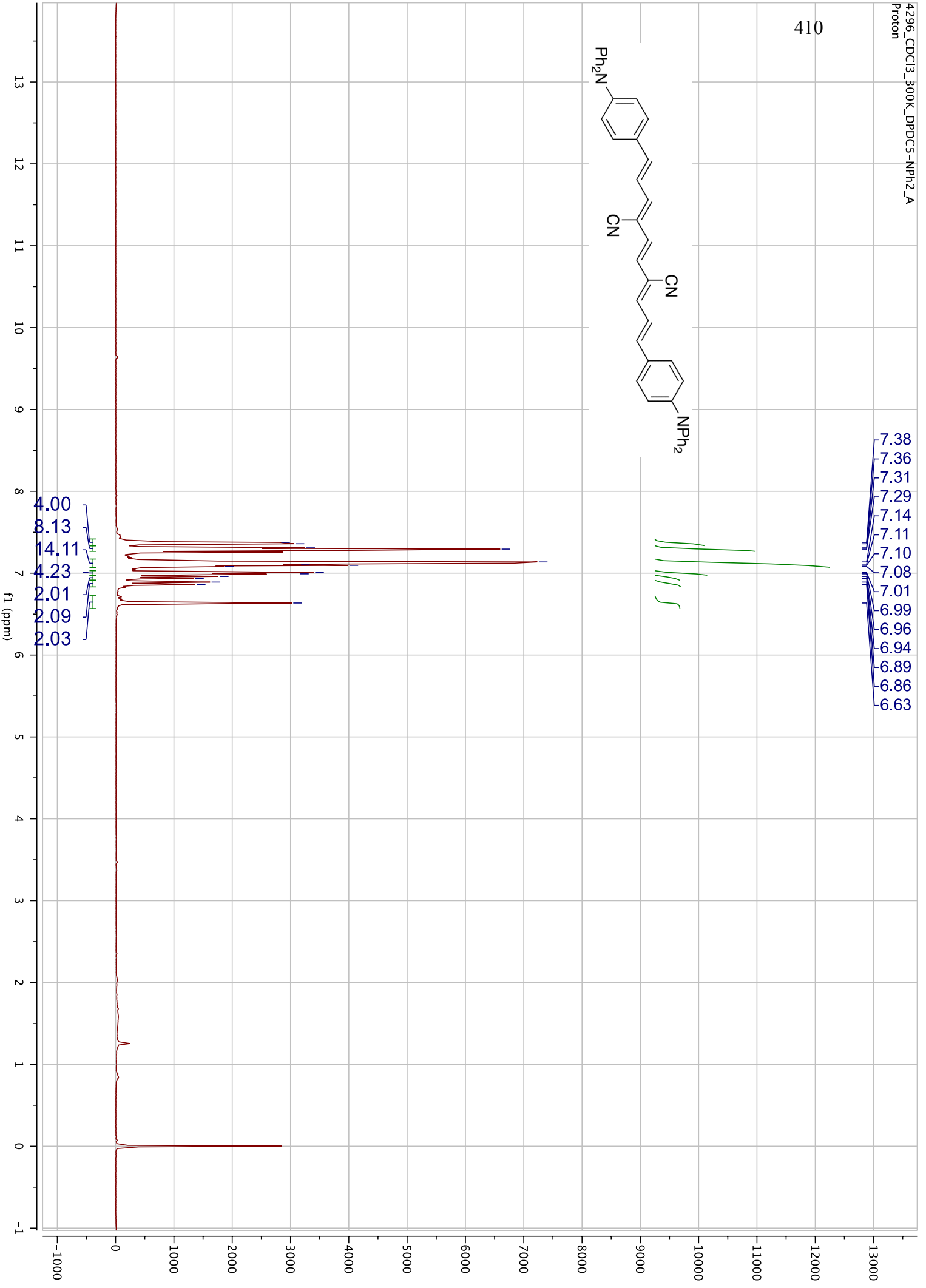
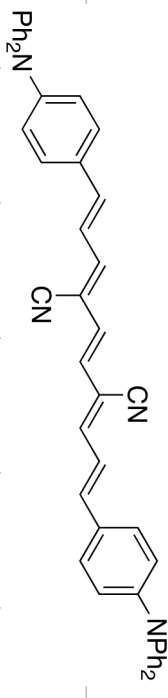


408



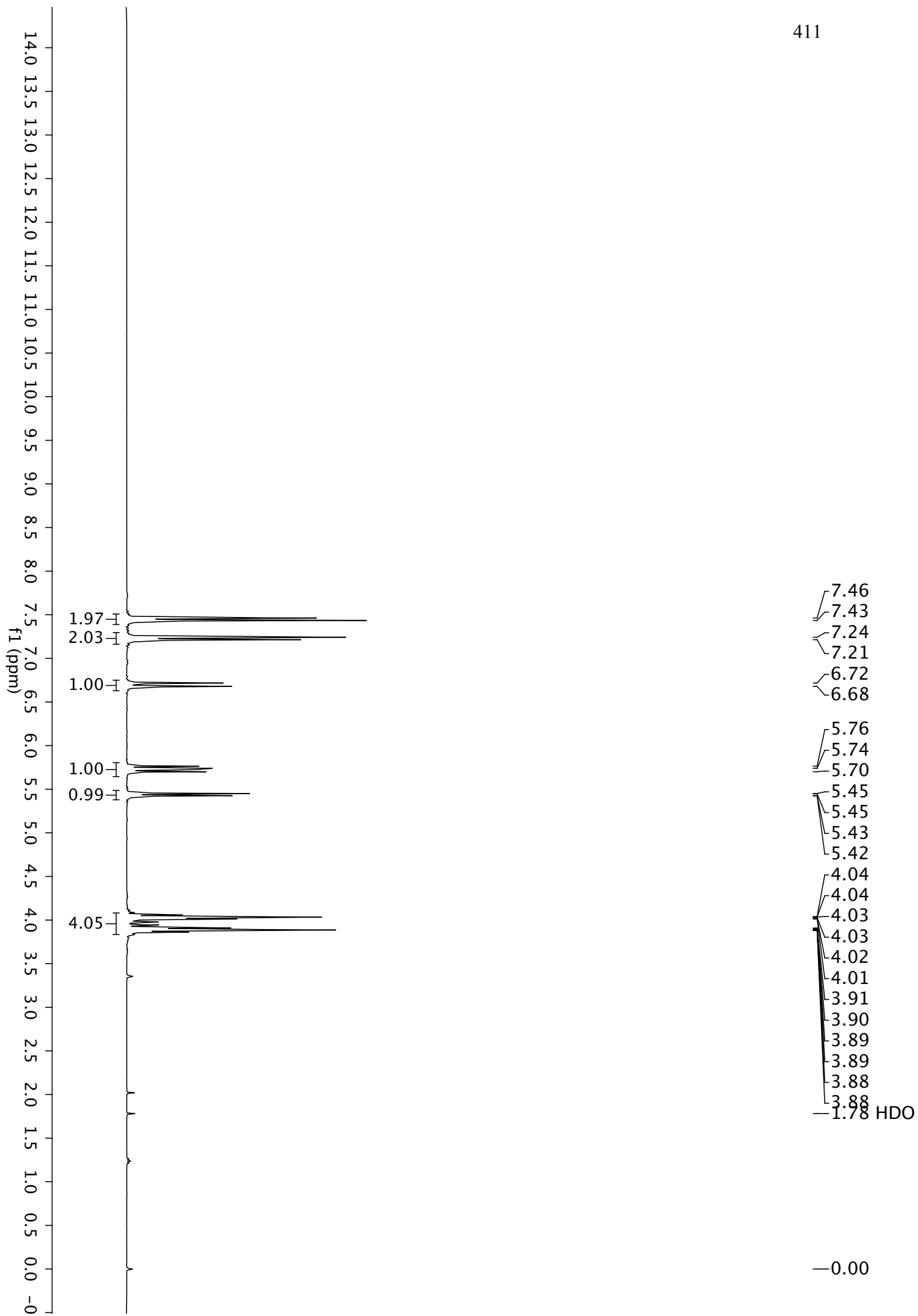


410

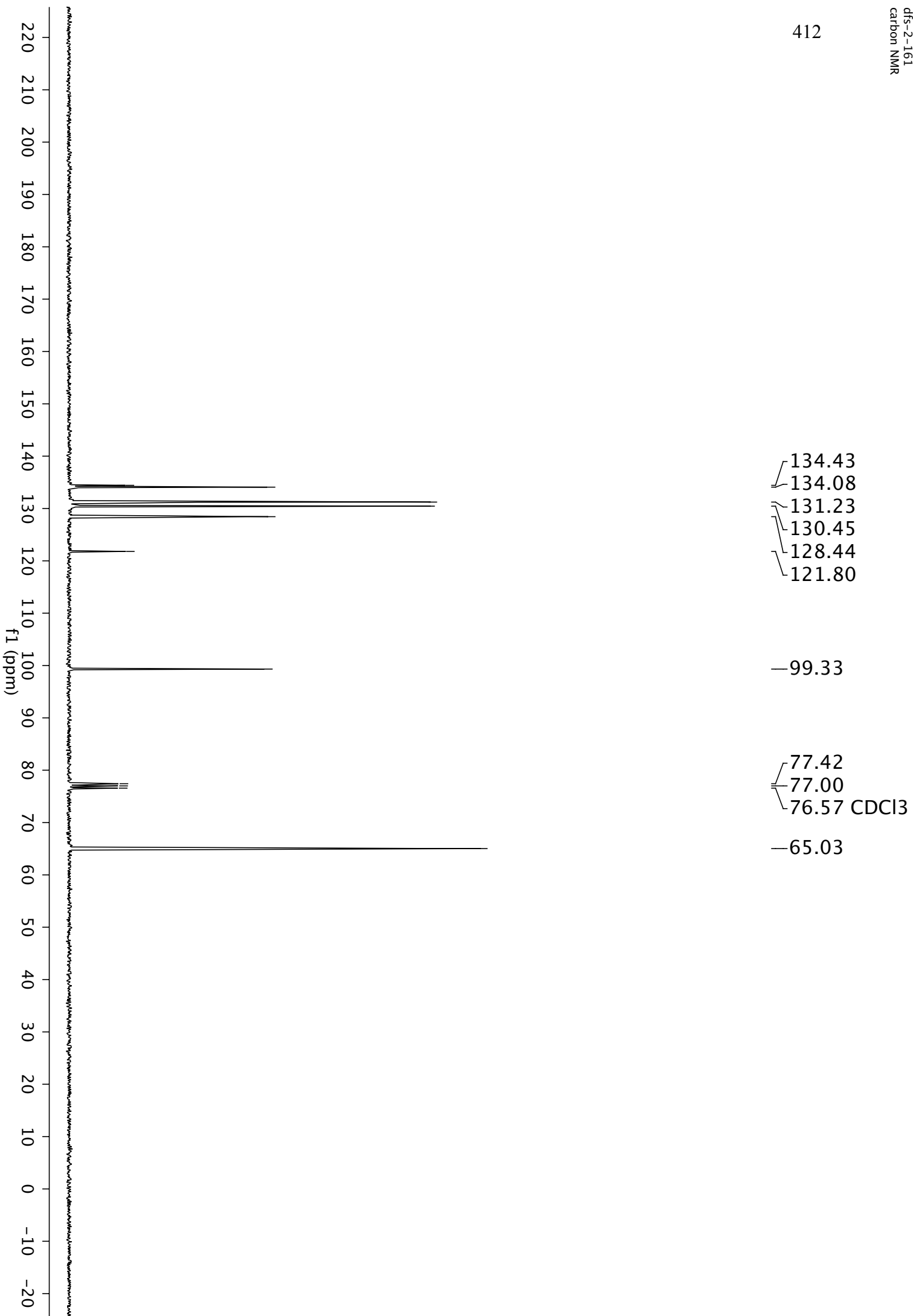


- 7.38
- 7.36
- 7.31
- 7.29
- 7.14
- 7.11
- 7.10
- 7.08
- 7.01
- 6.99
- 6.96
- 6.94
- 6.89
- 6.86
- 6.63

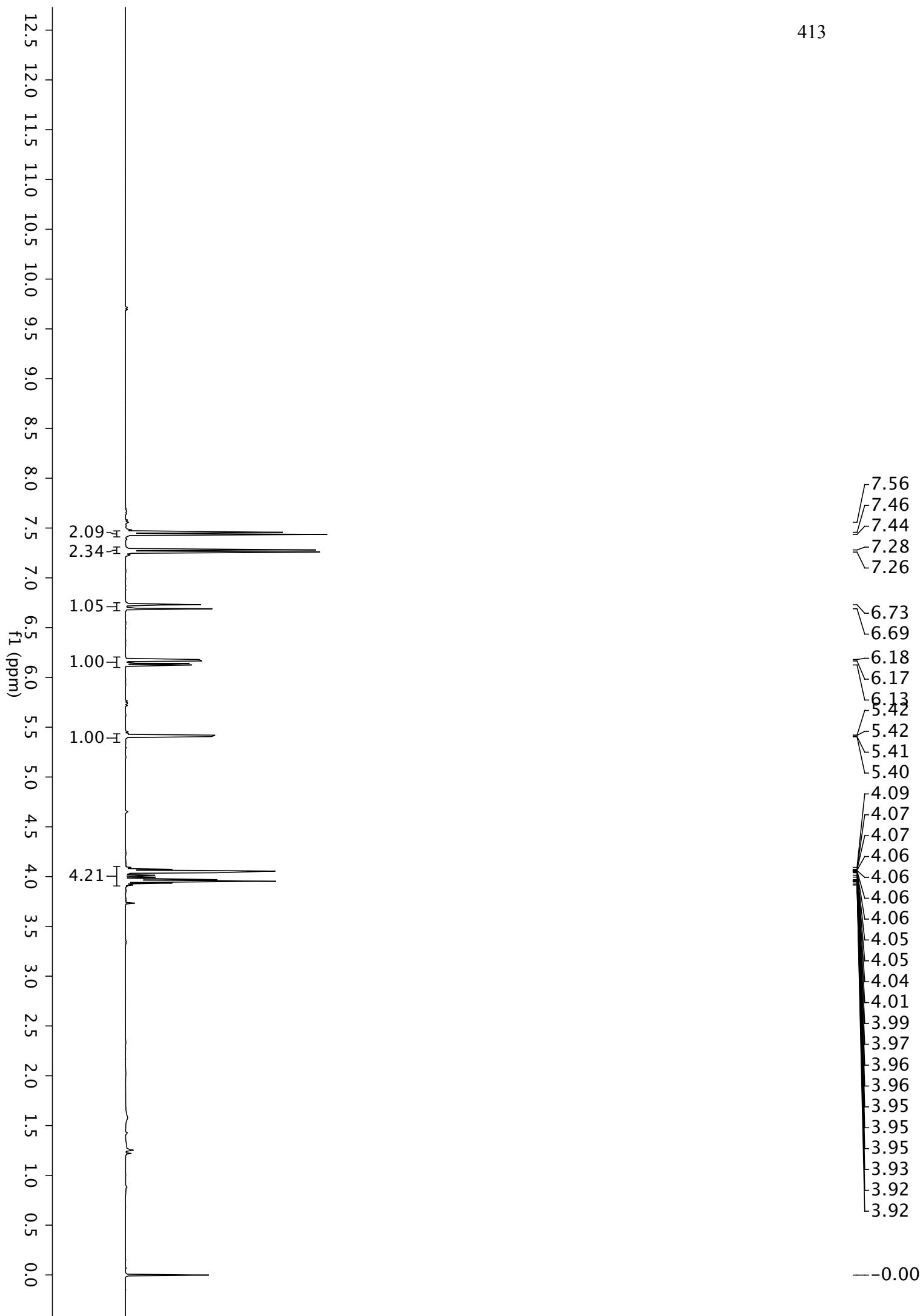
- 4.00
- 8.13
- 14.11
- 4.23
- 2.01
- 2.09
- 2.03



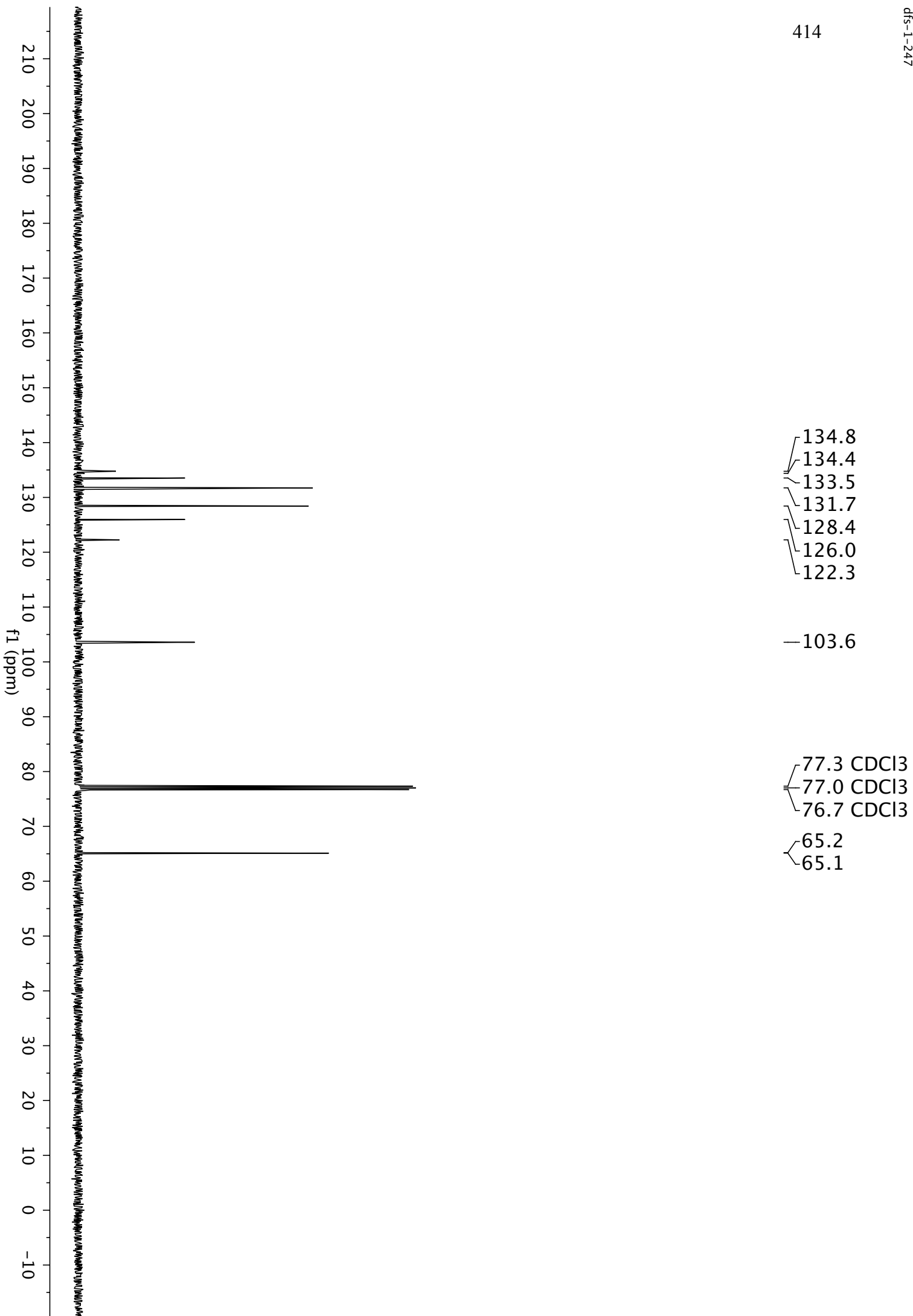
412

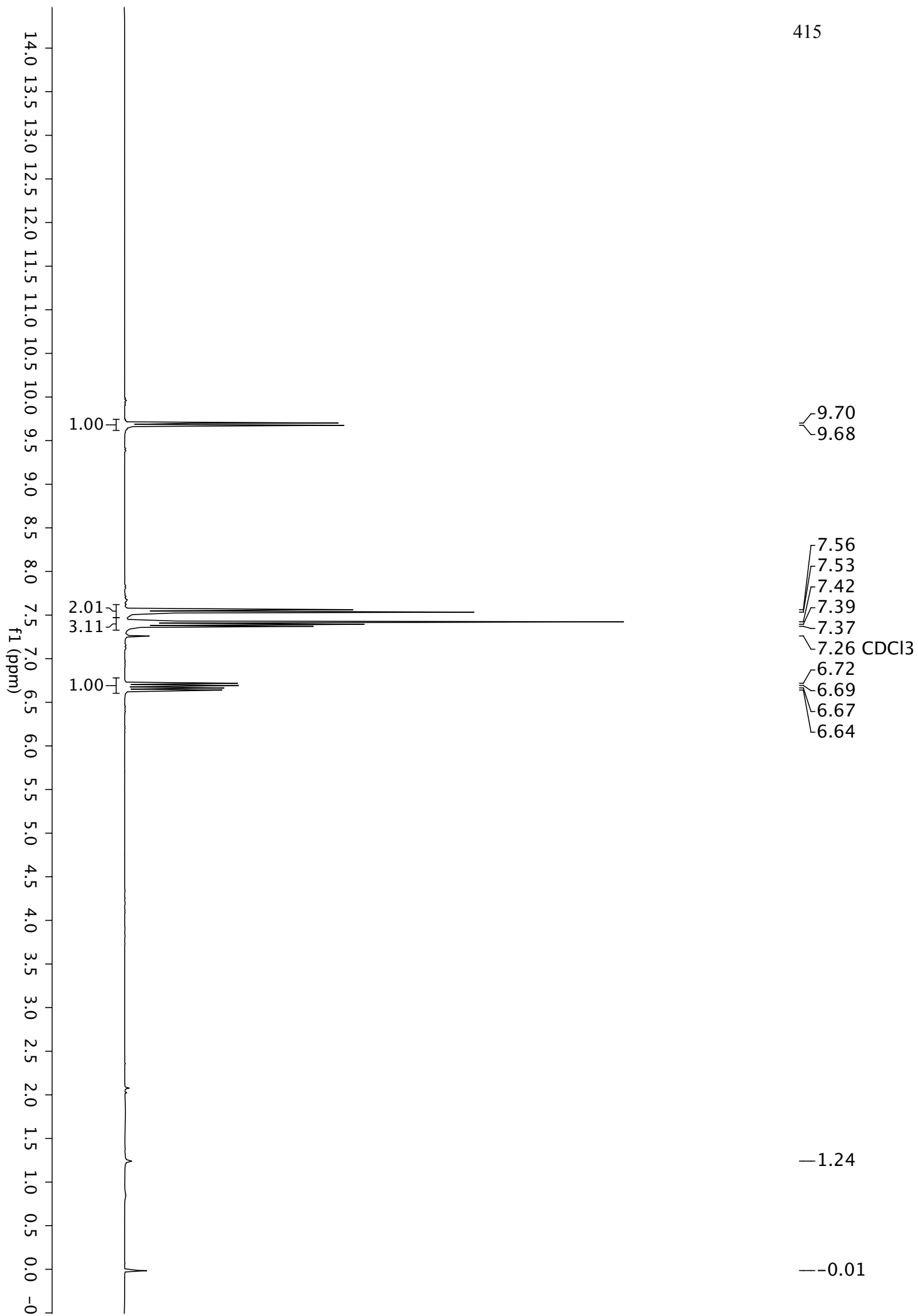


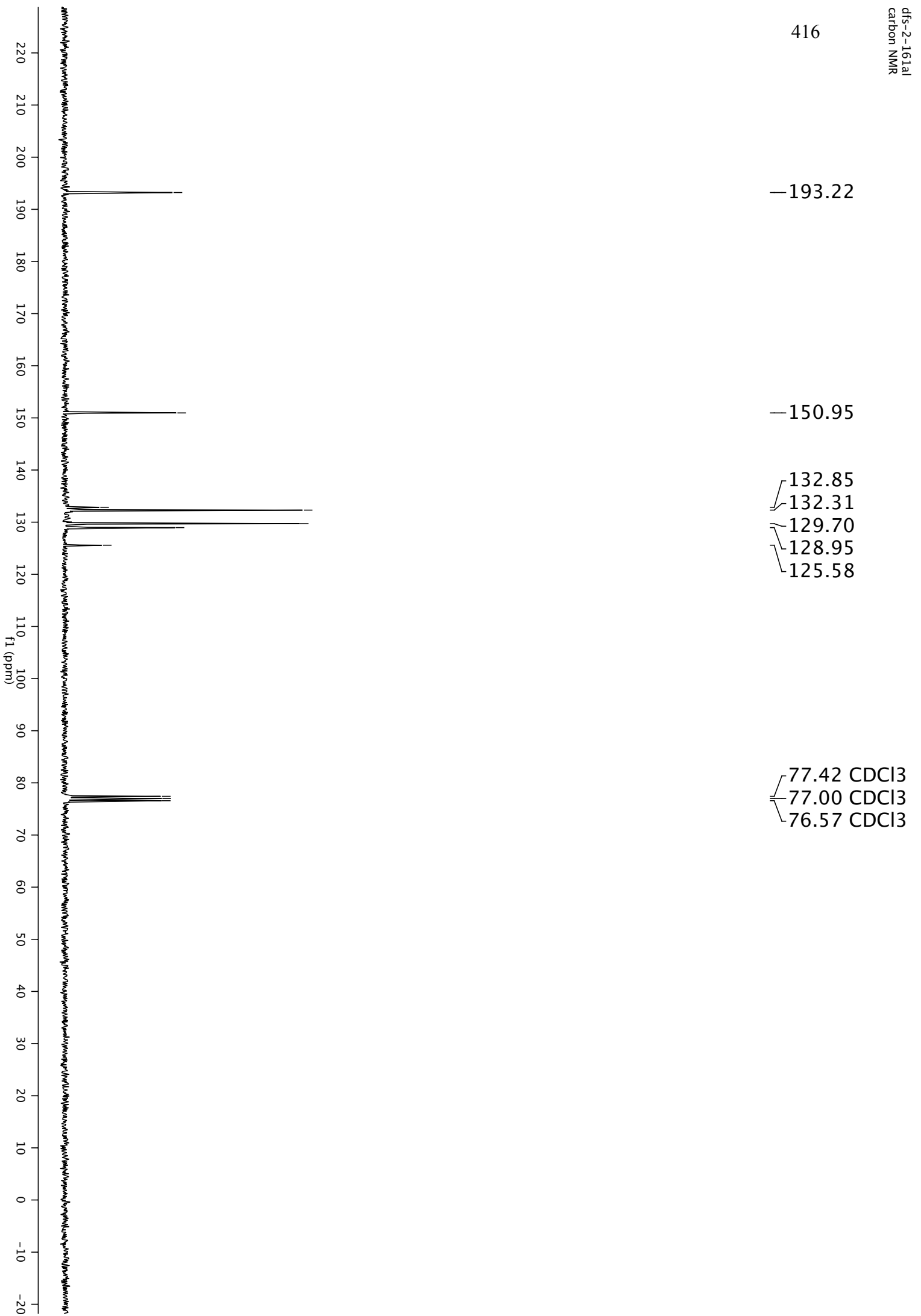


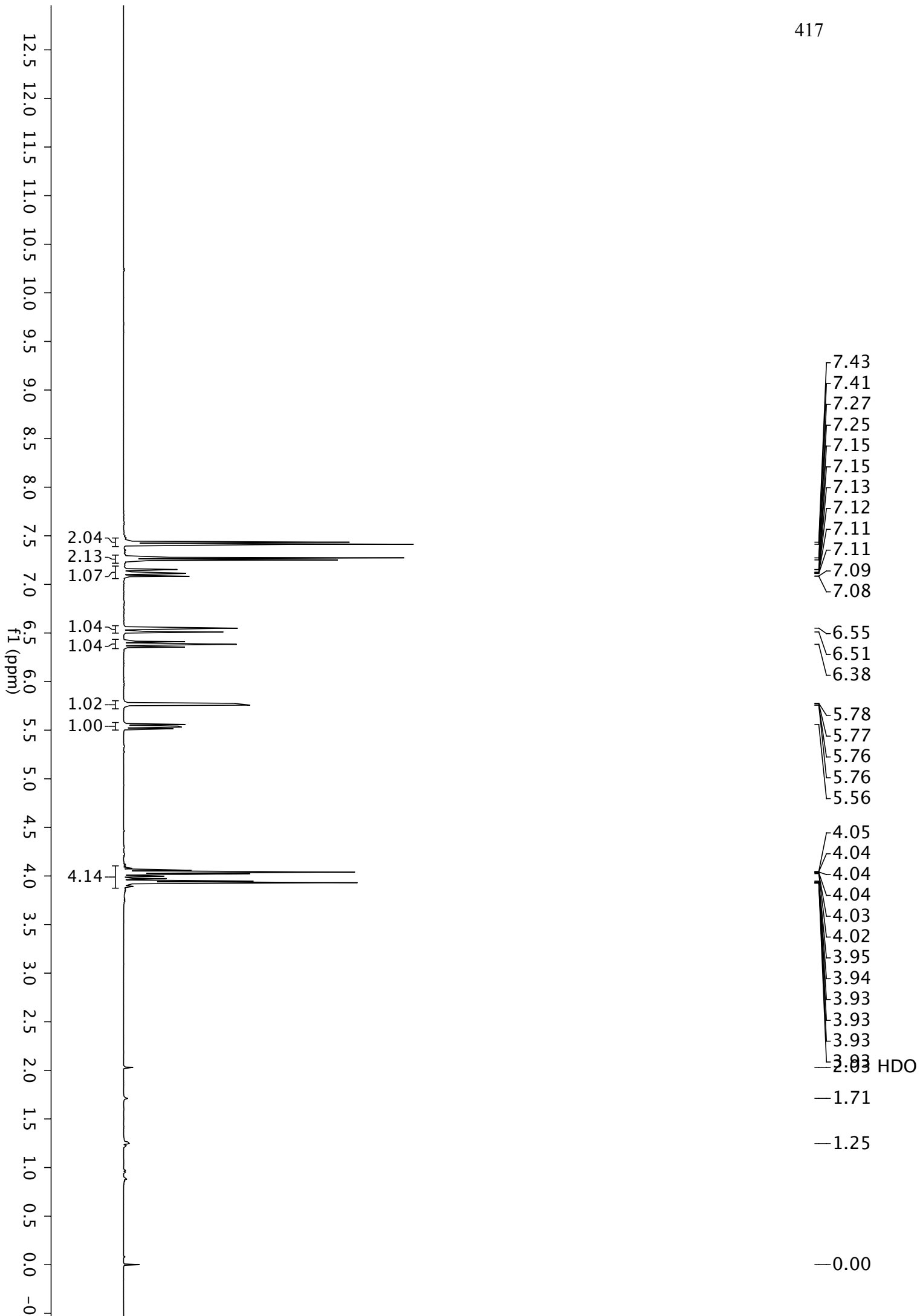


414

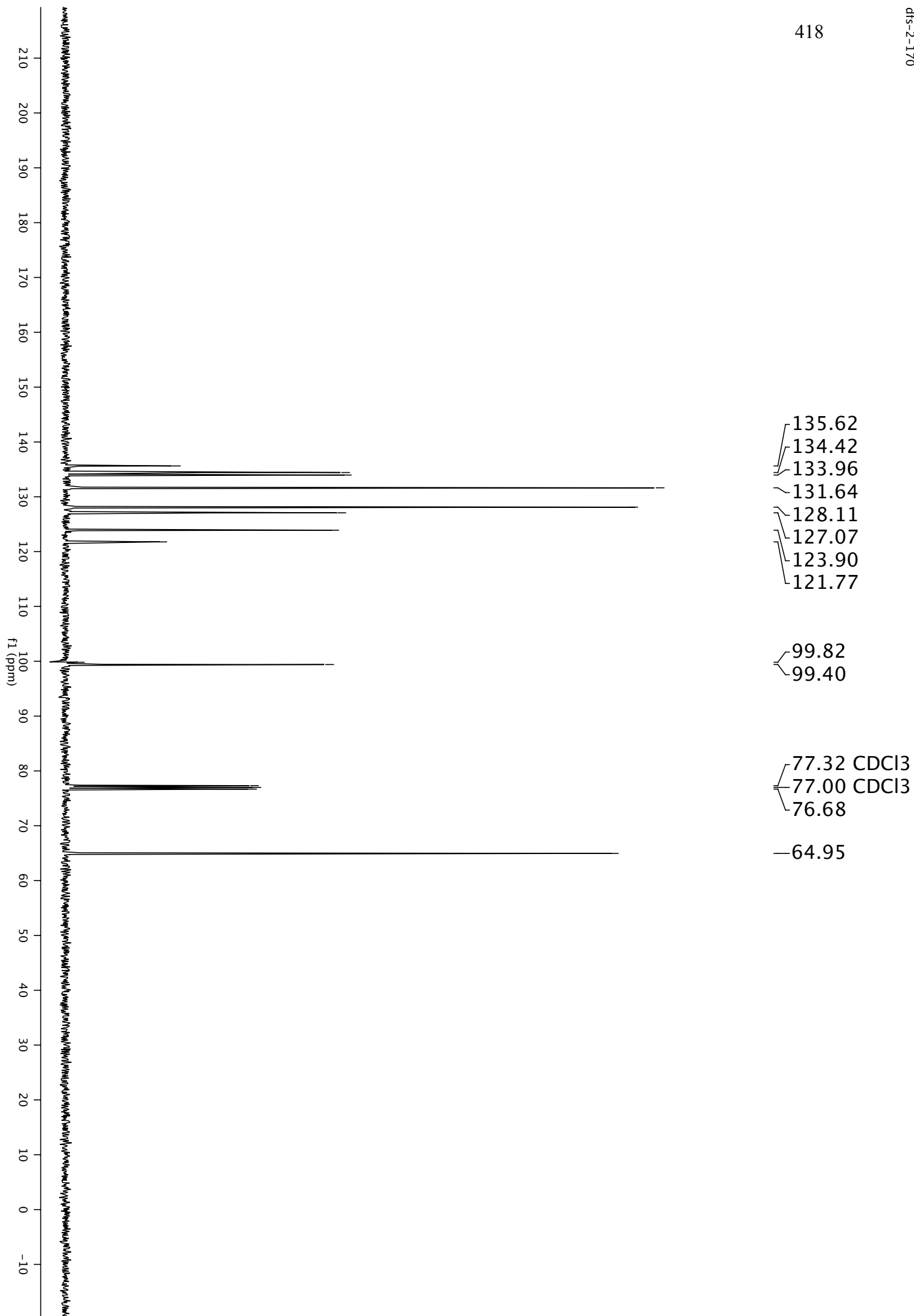


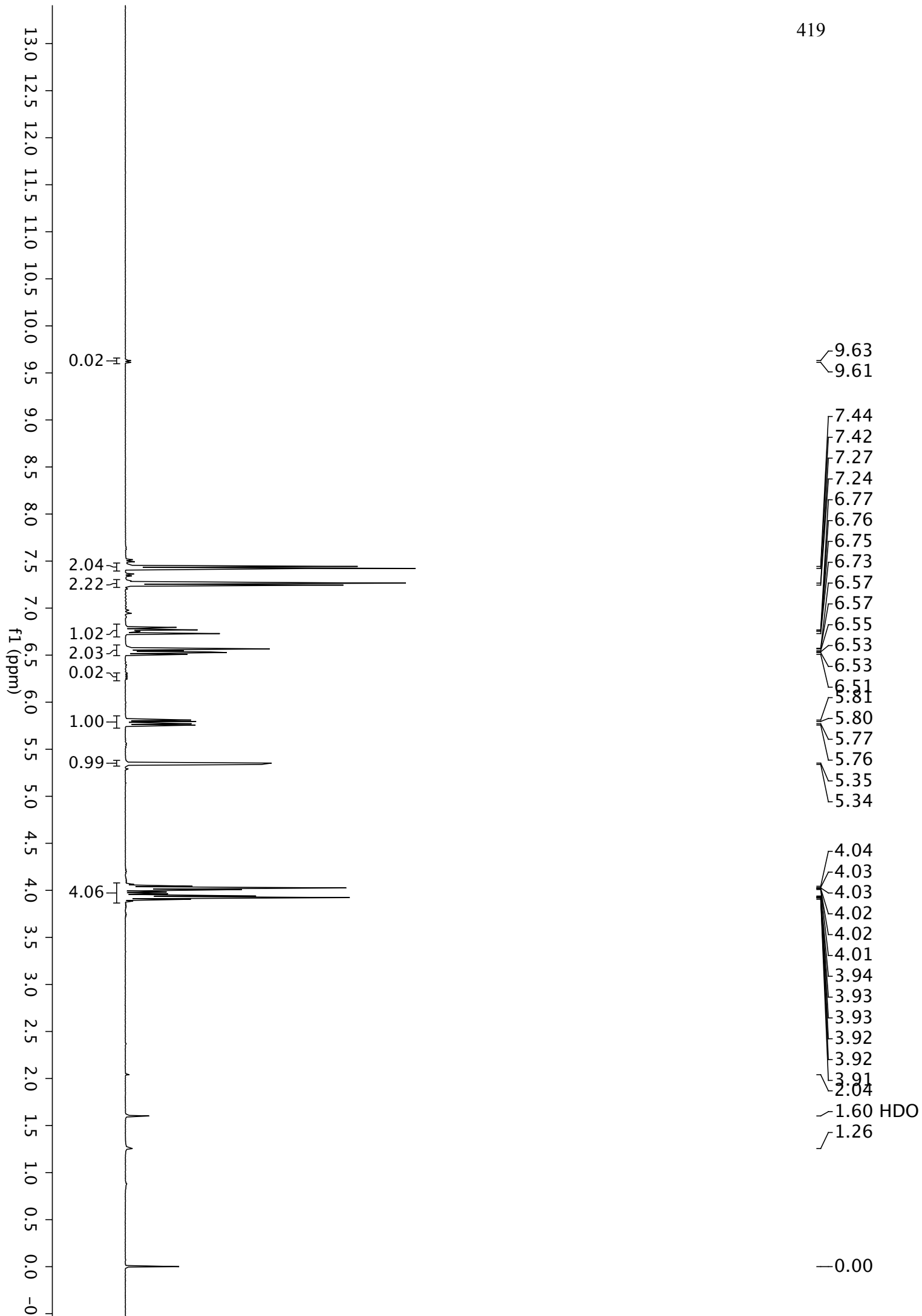


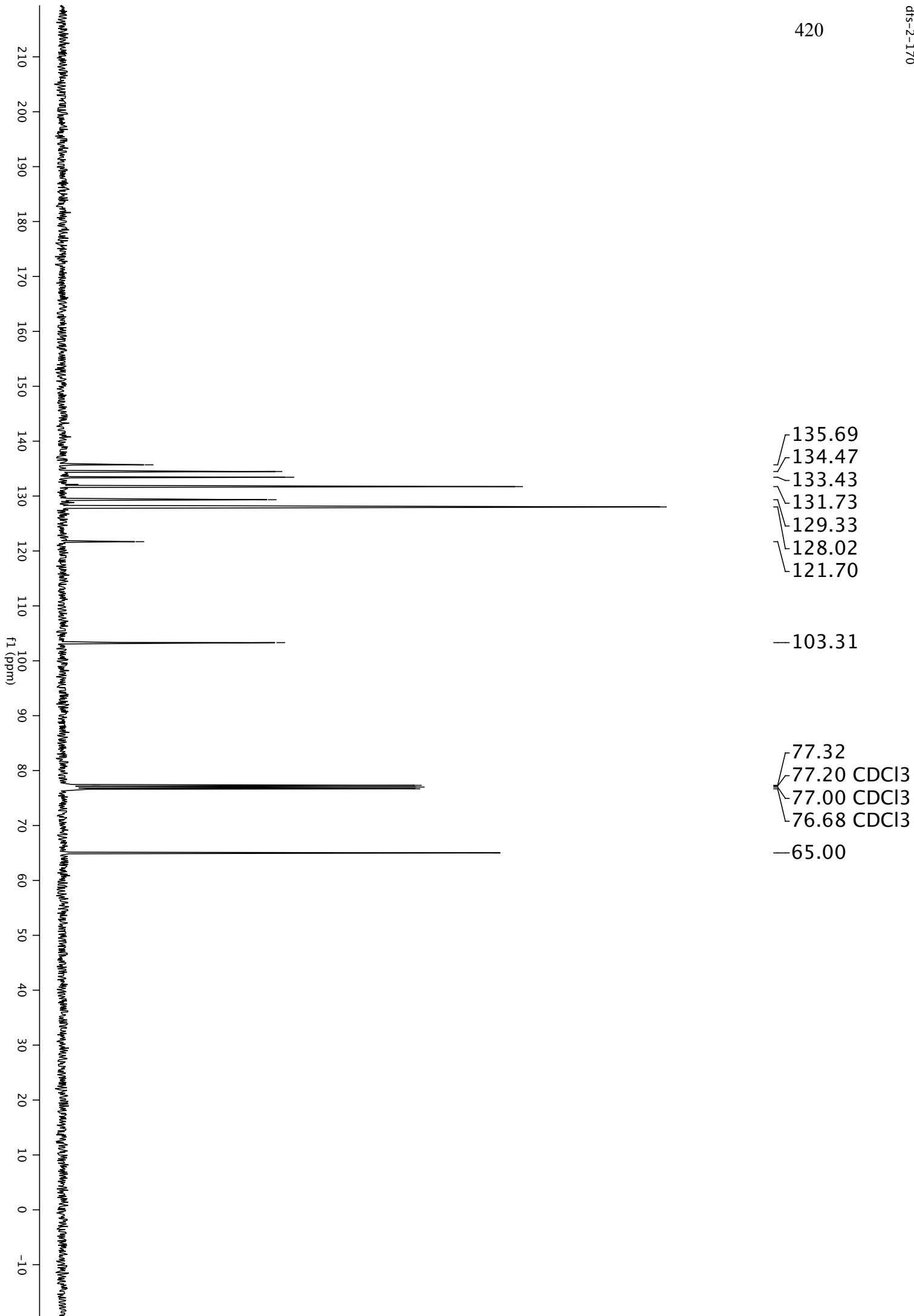




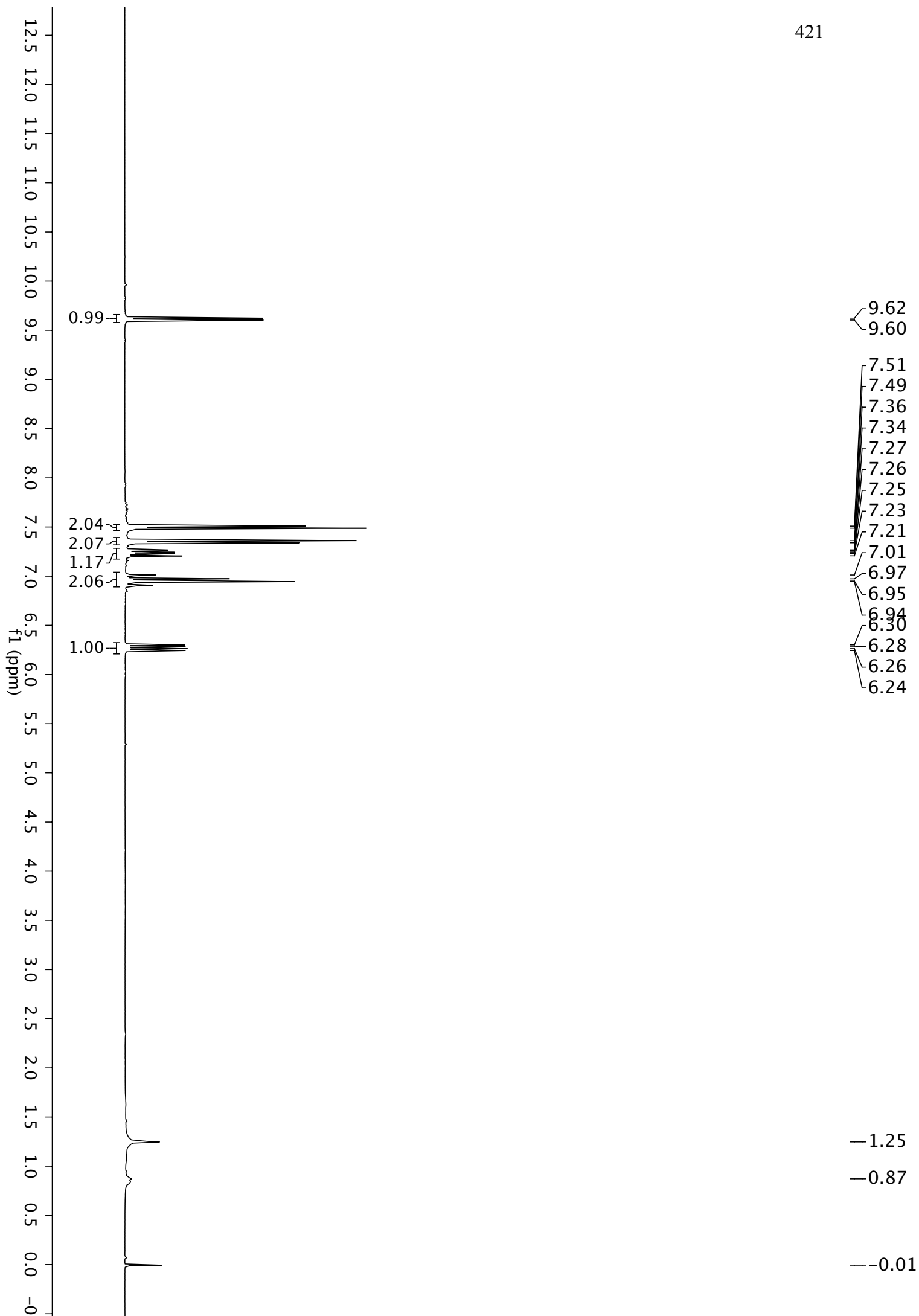
418



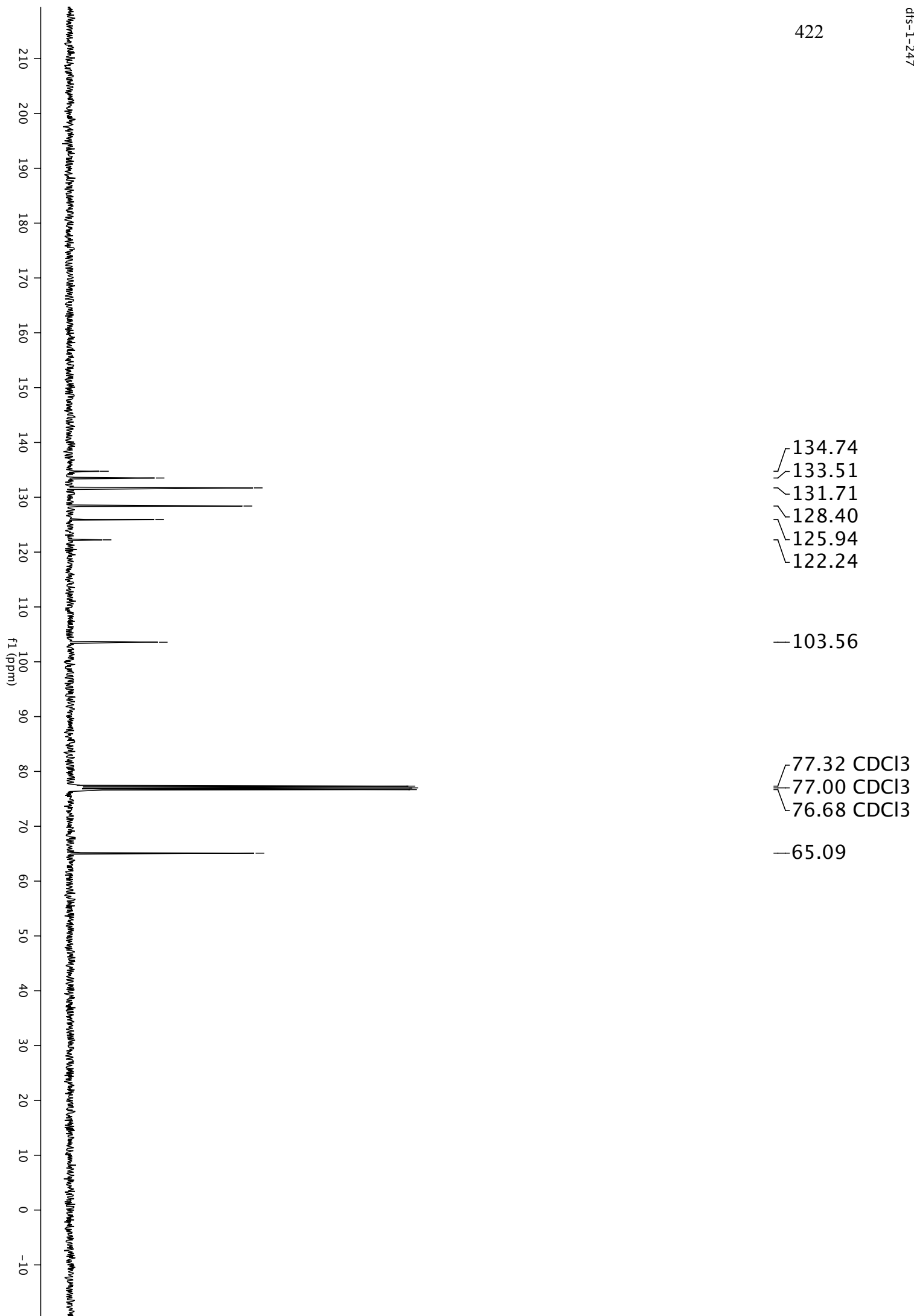


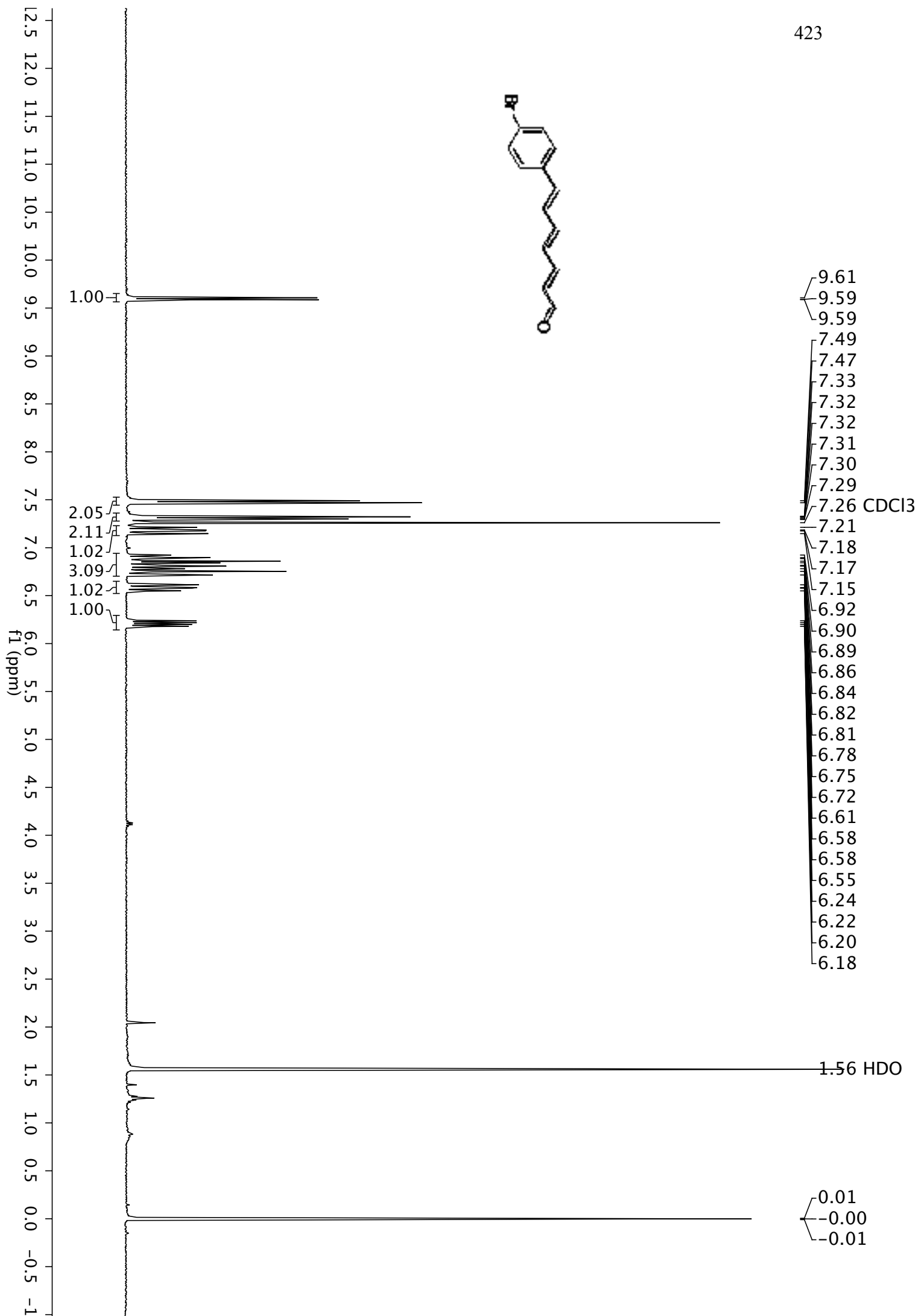


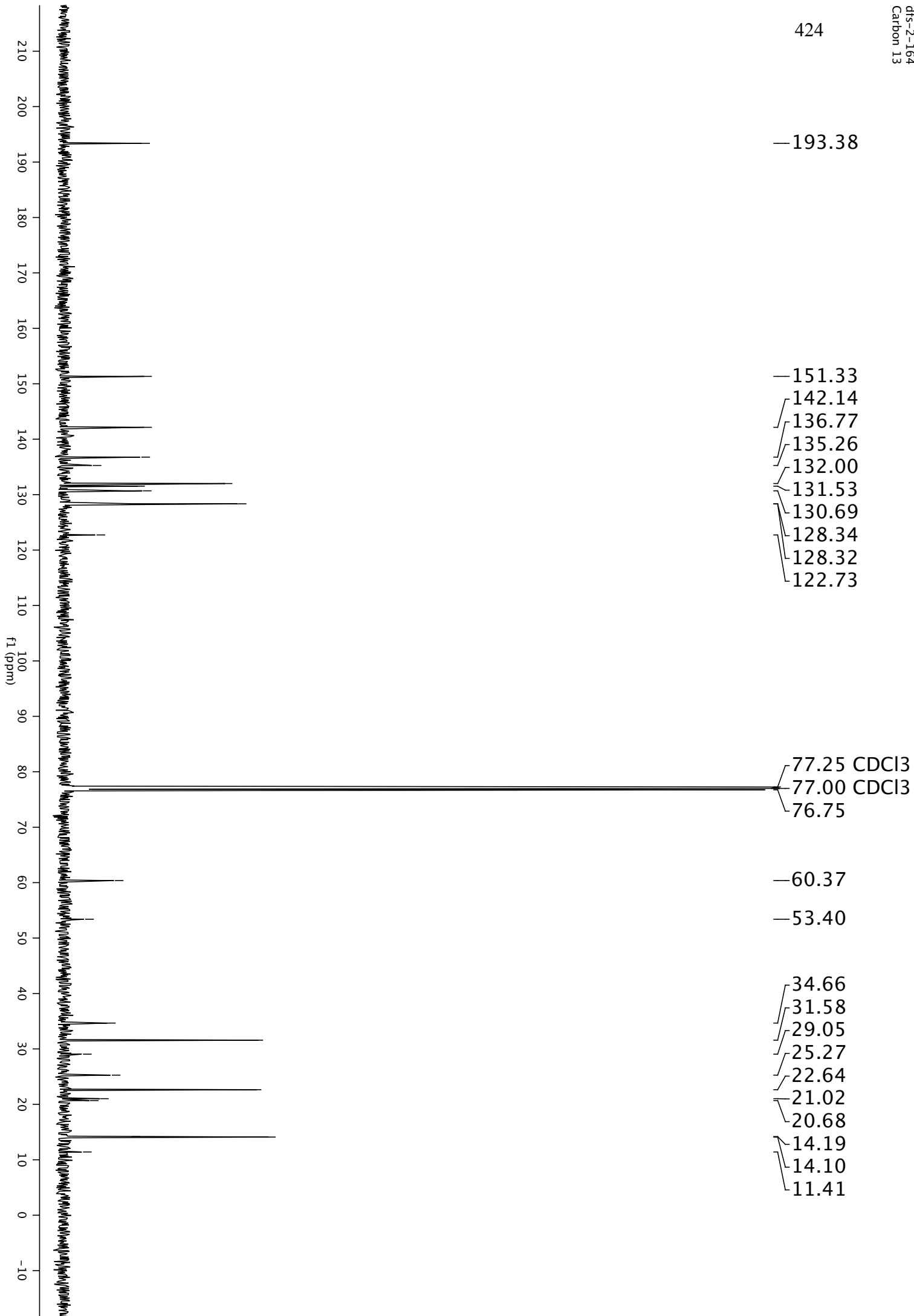


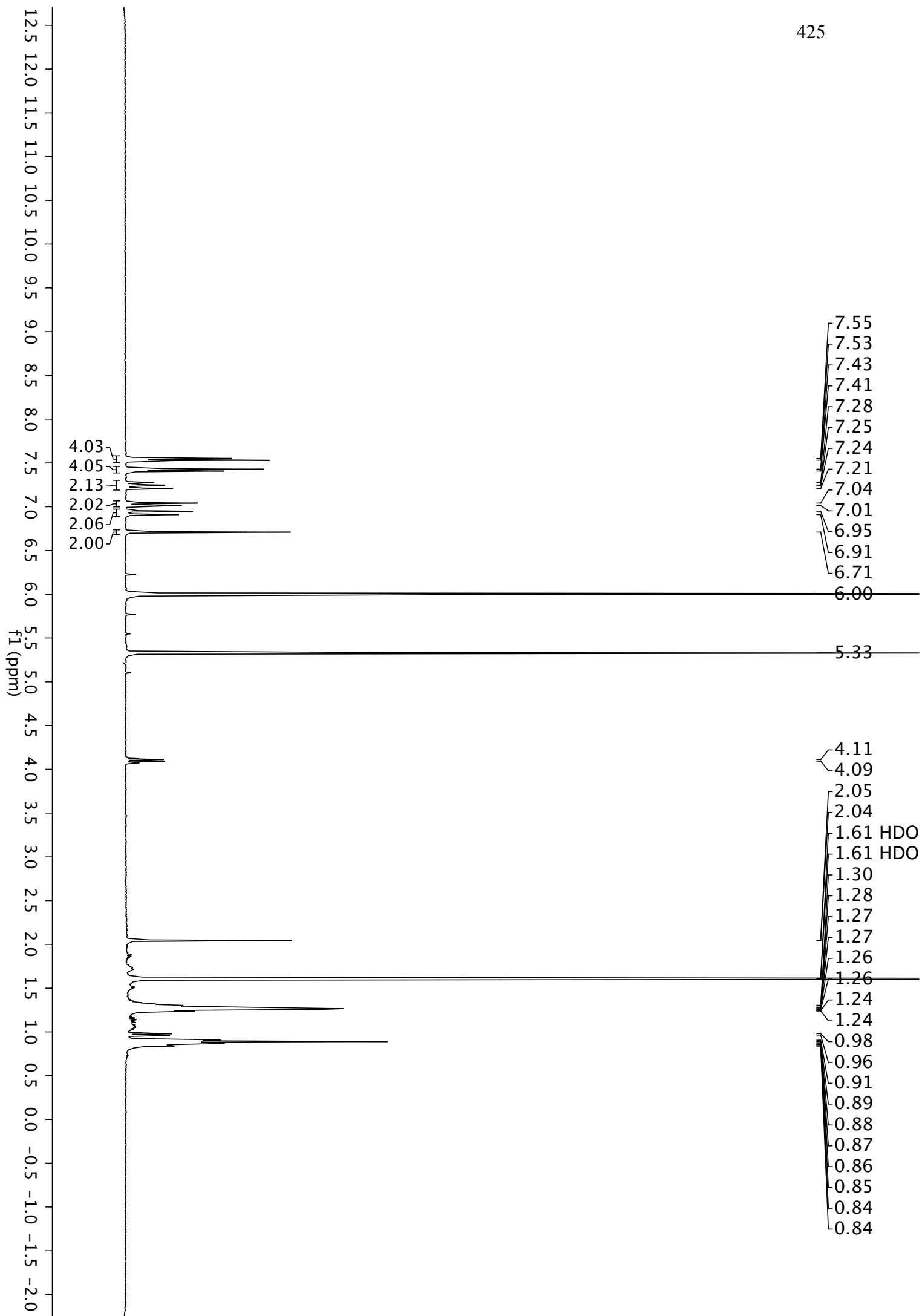


422

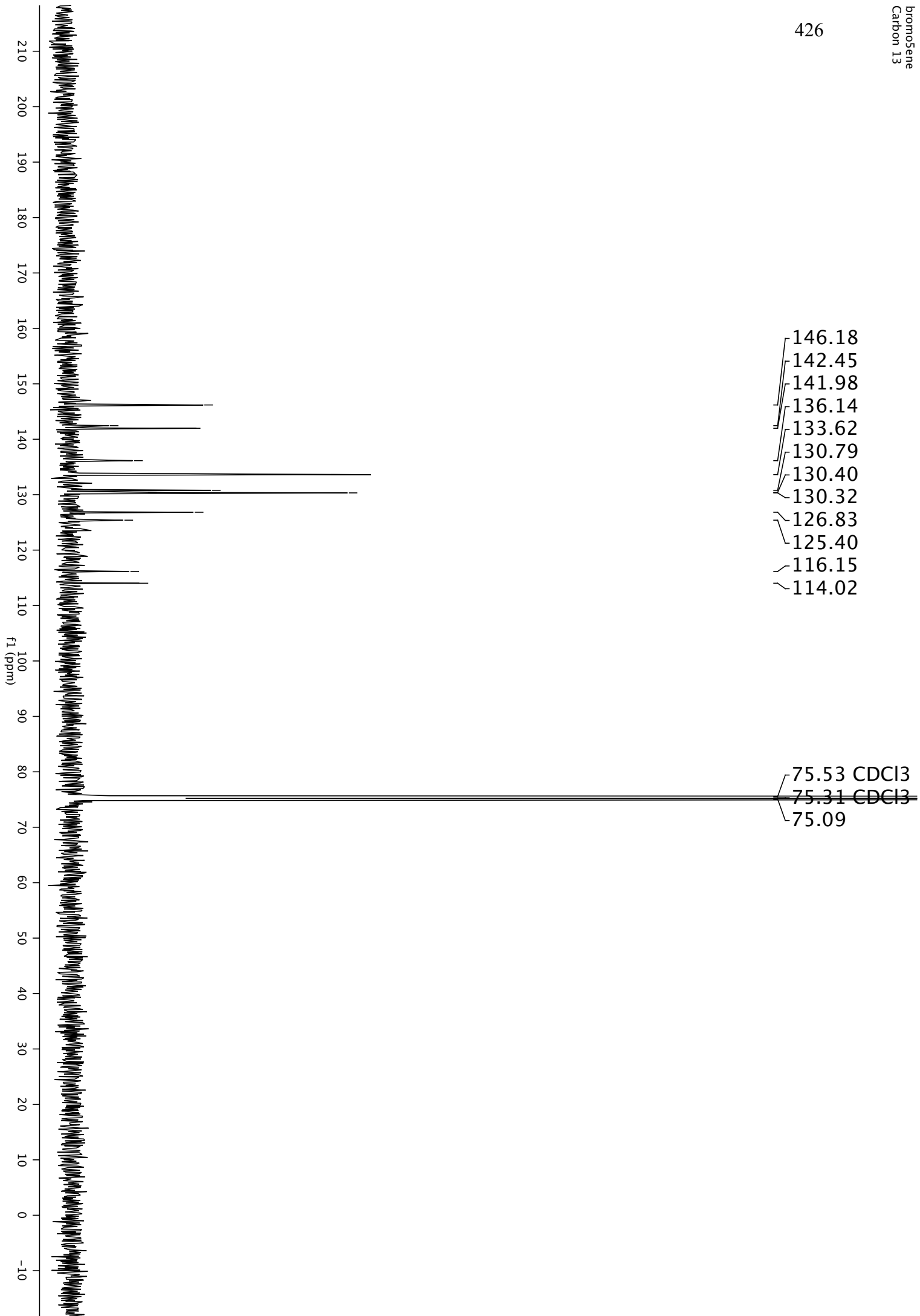


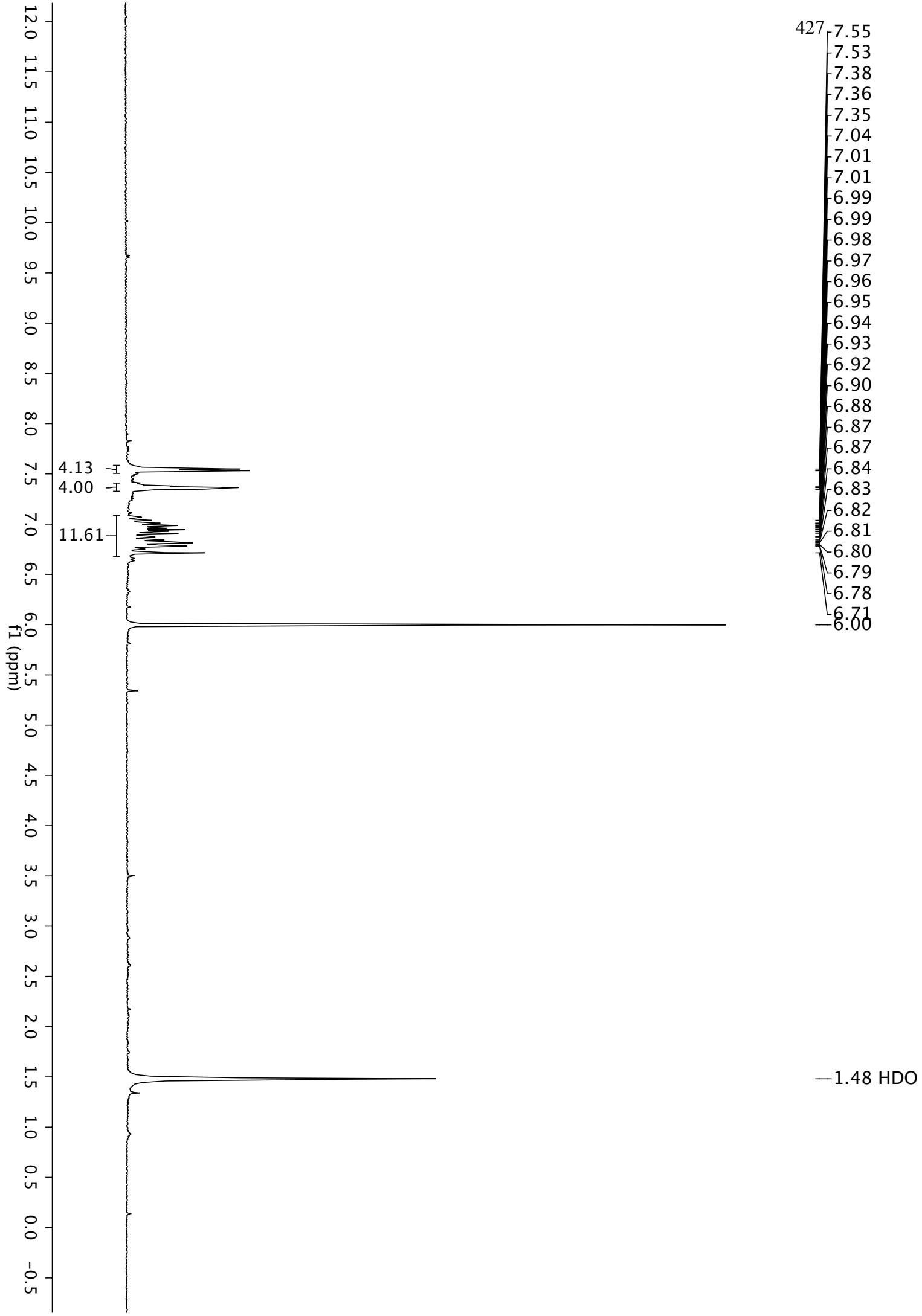




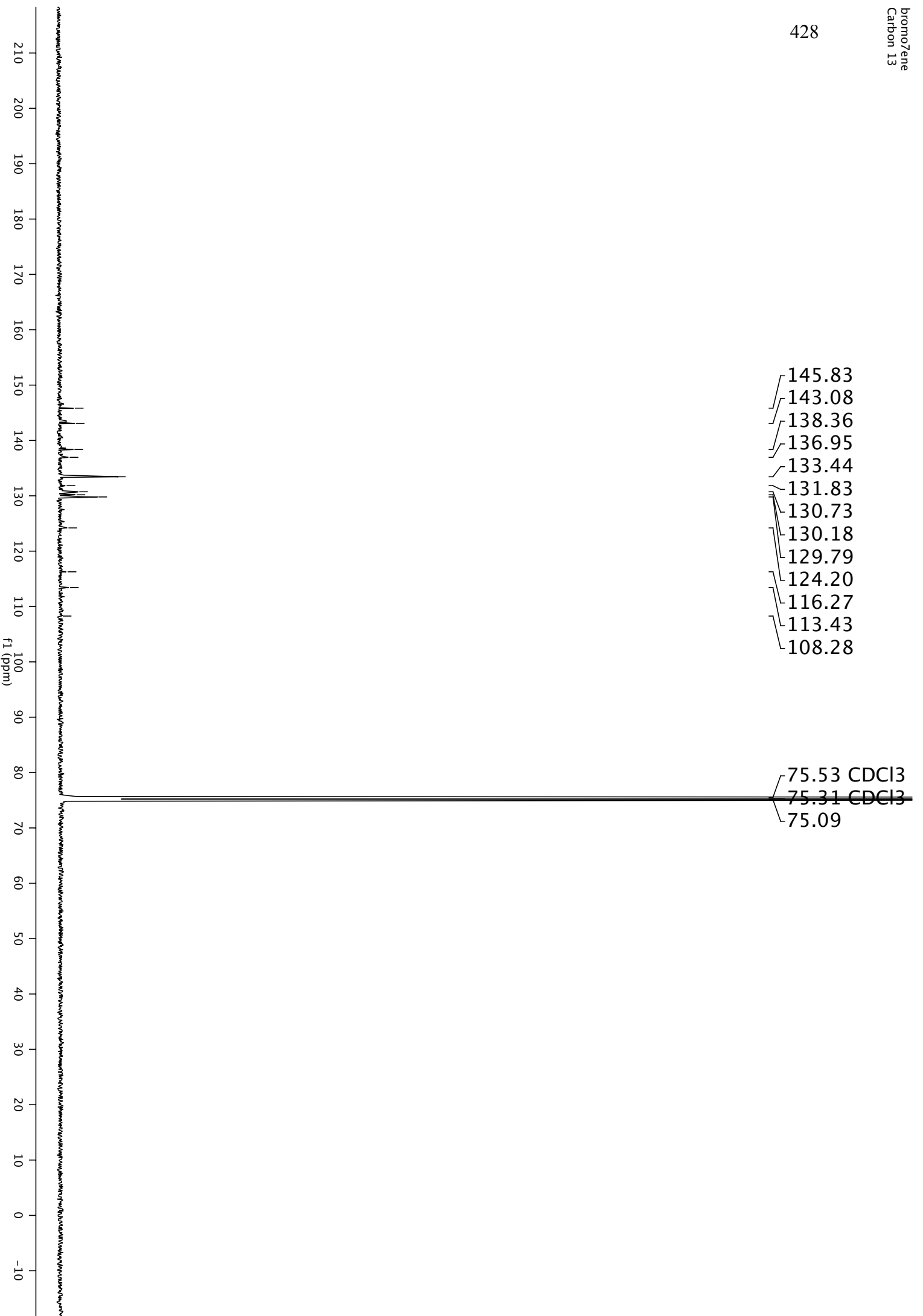


426

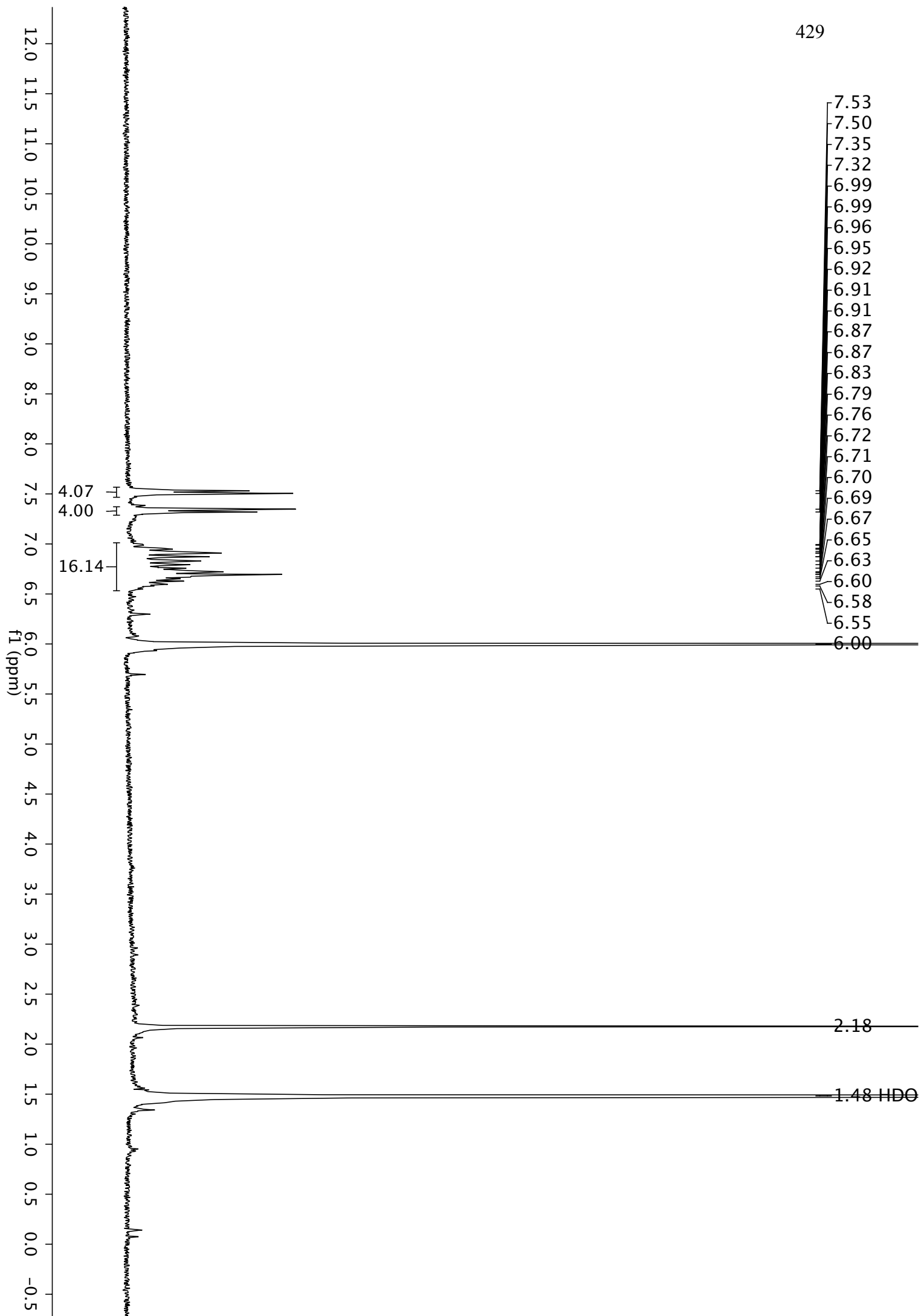


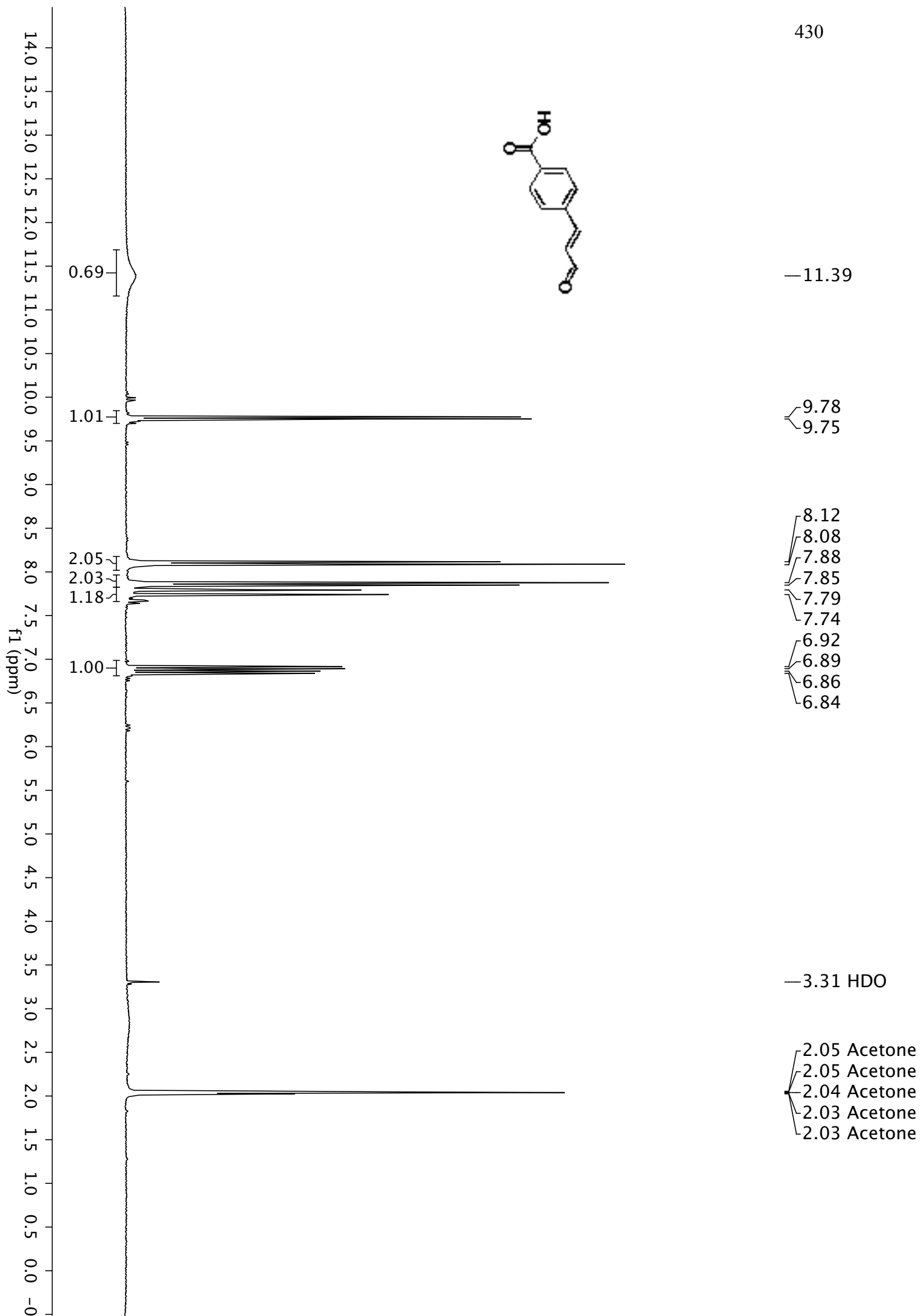


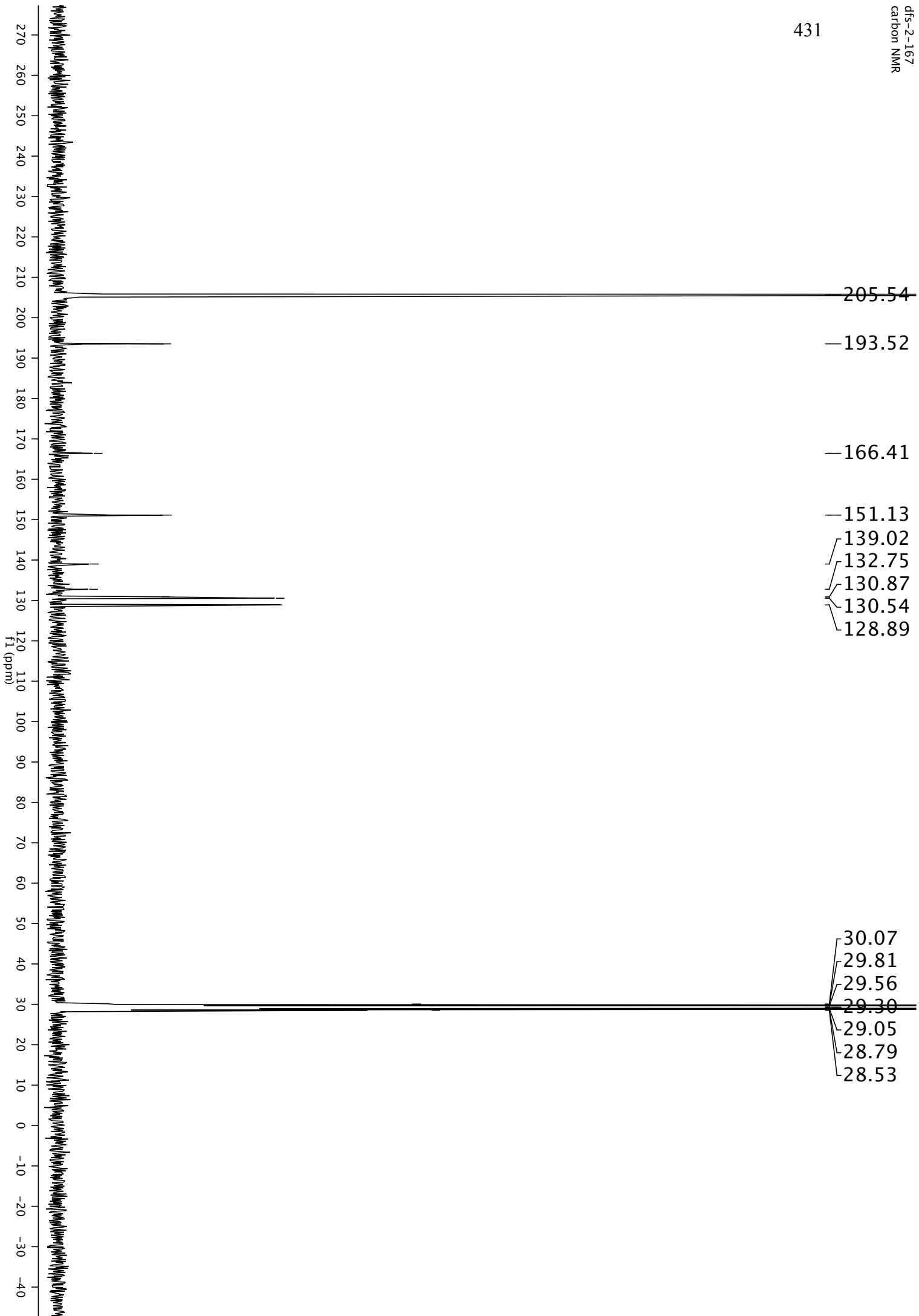
428

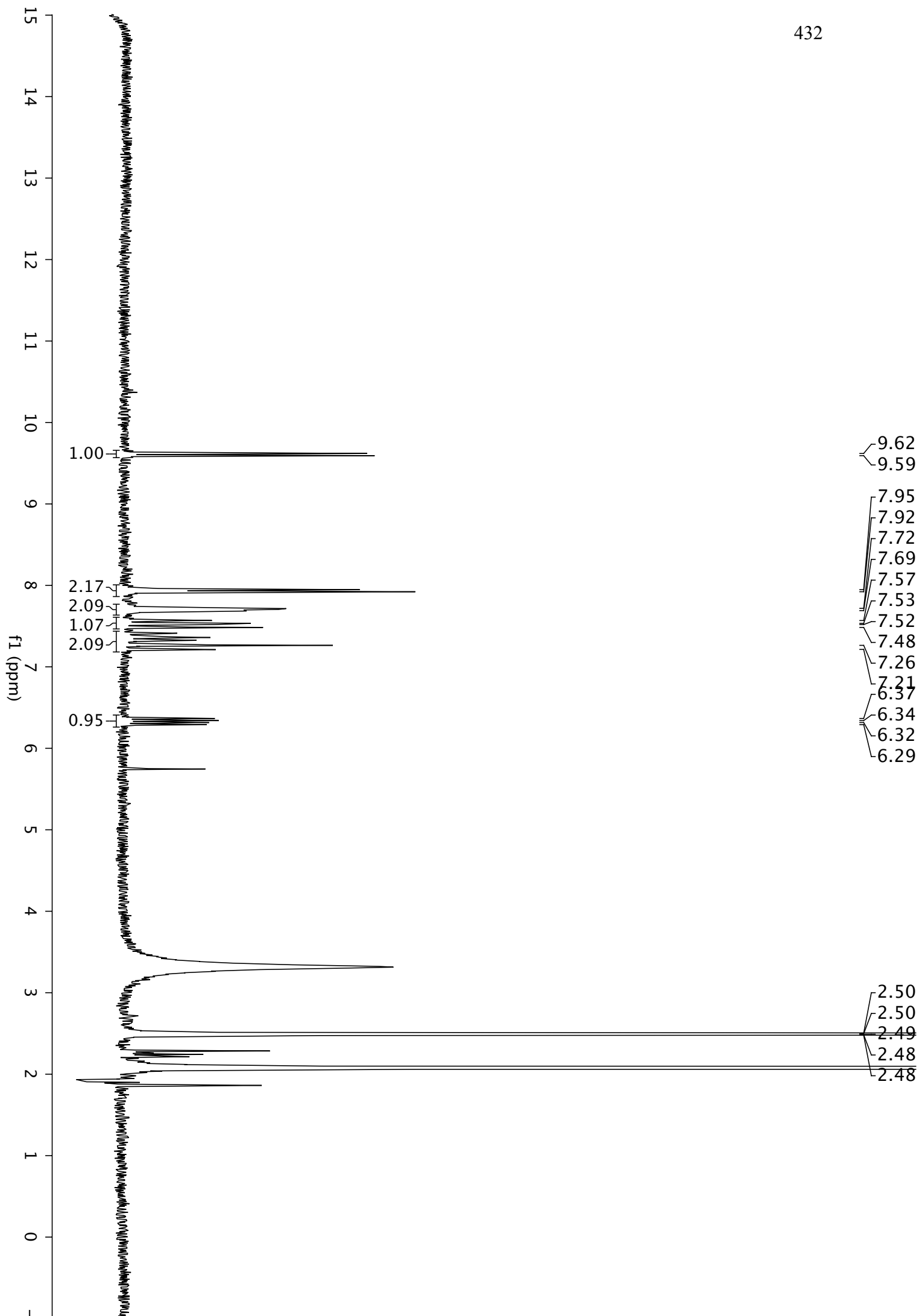


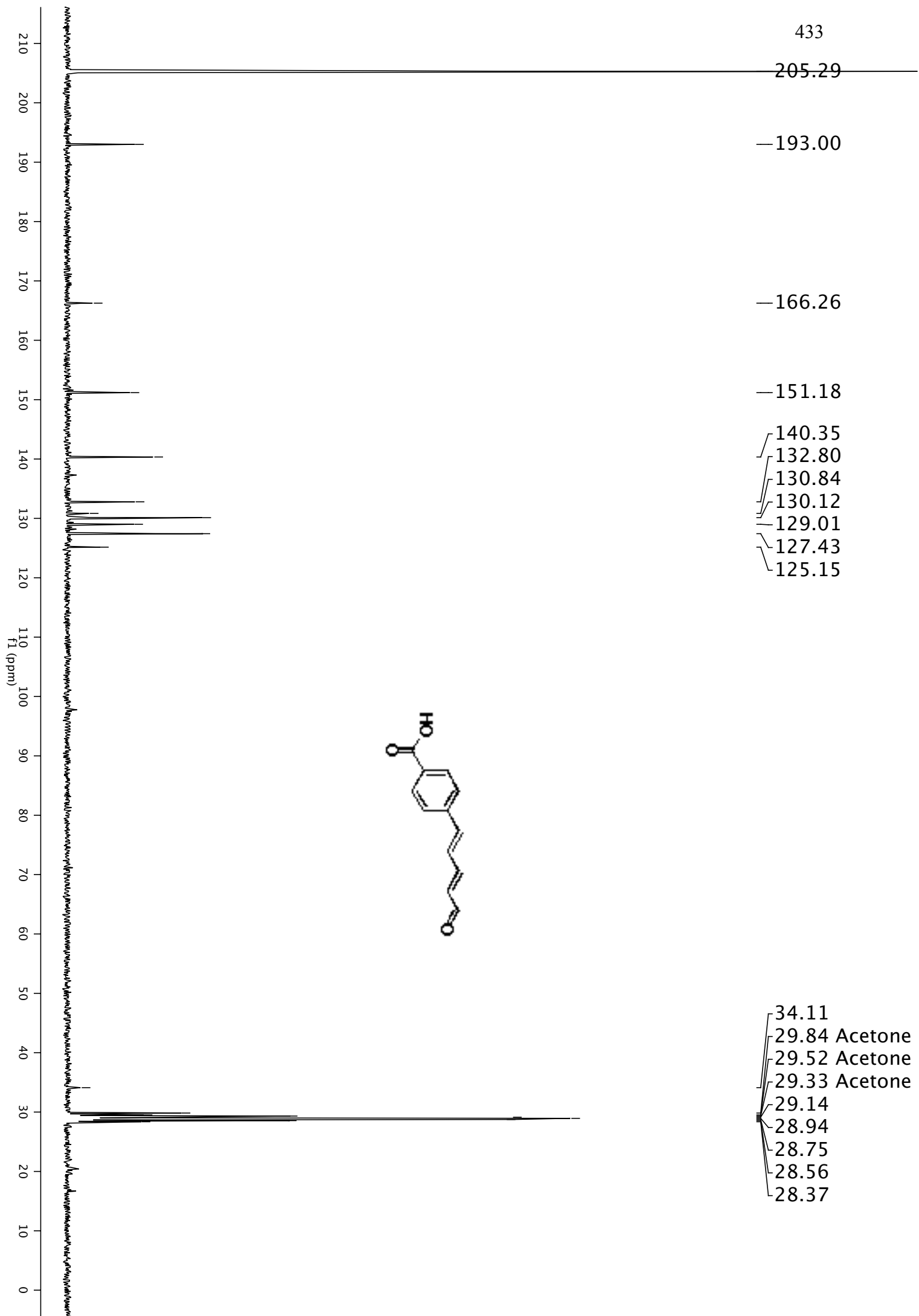


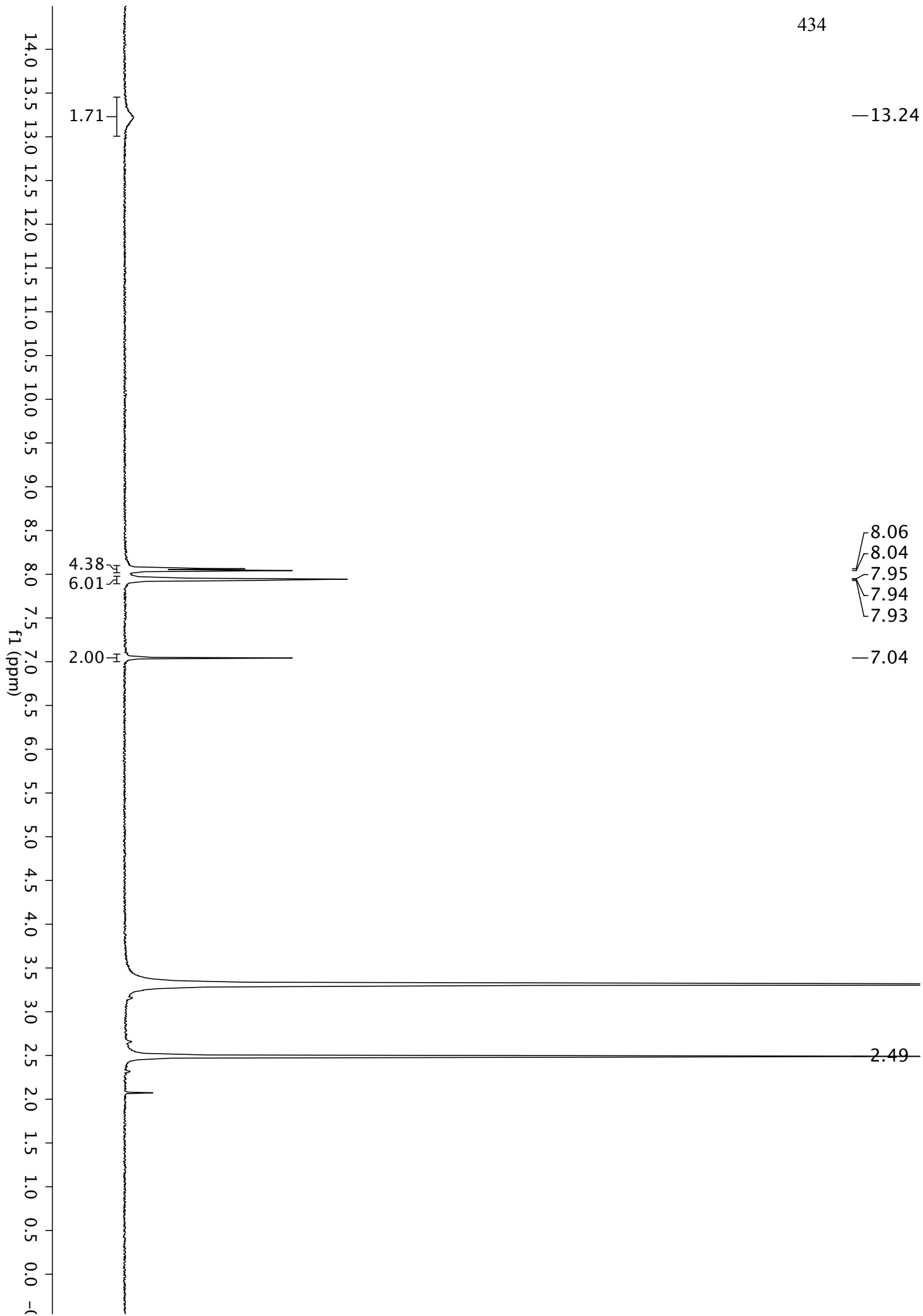


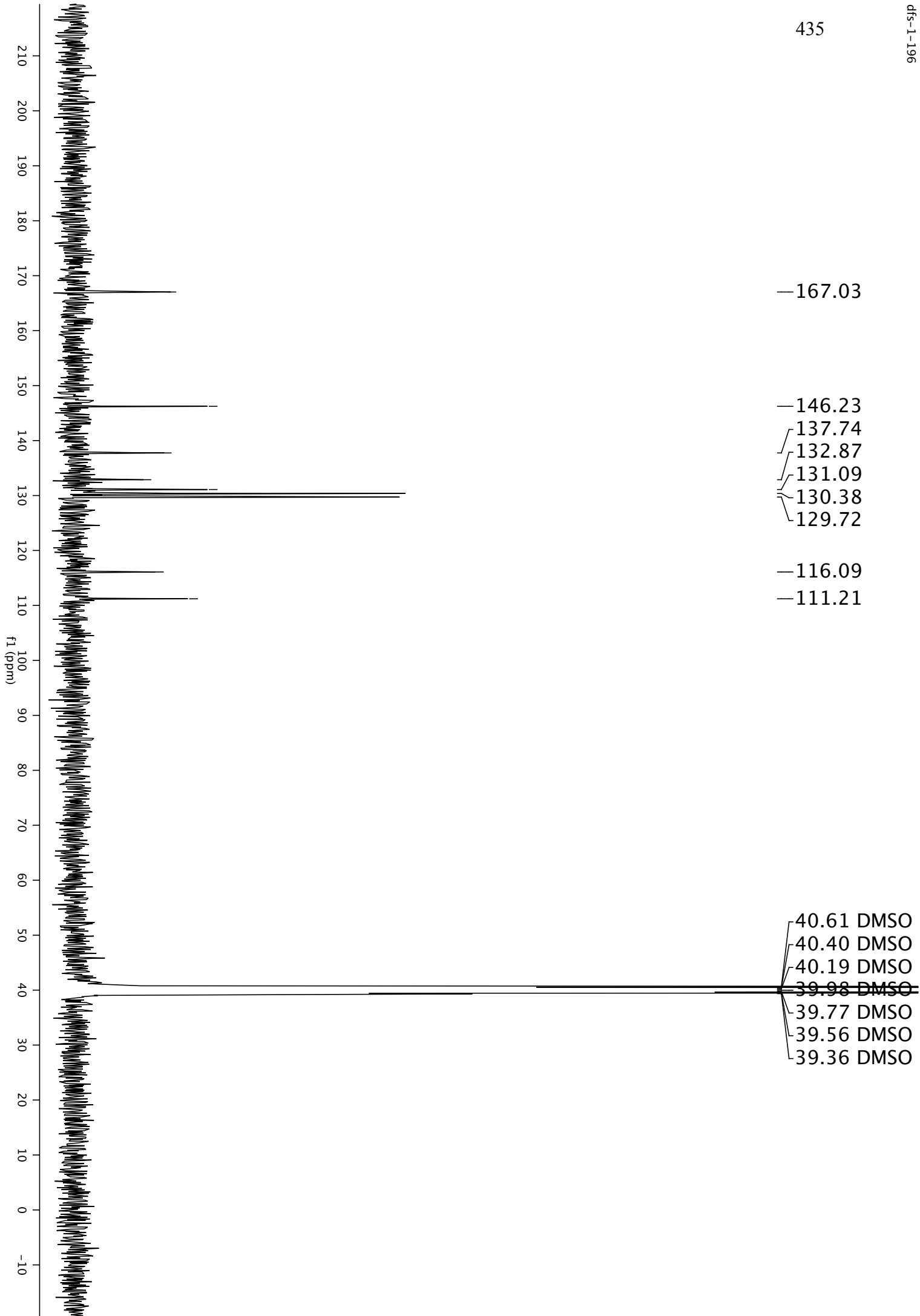


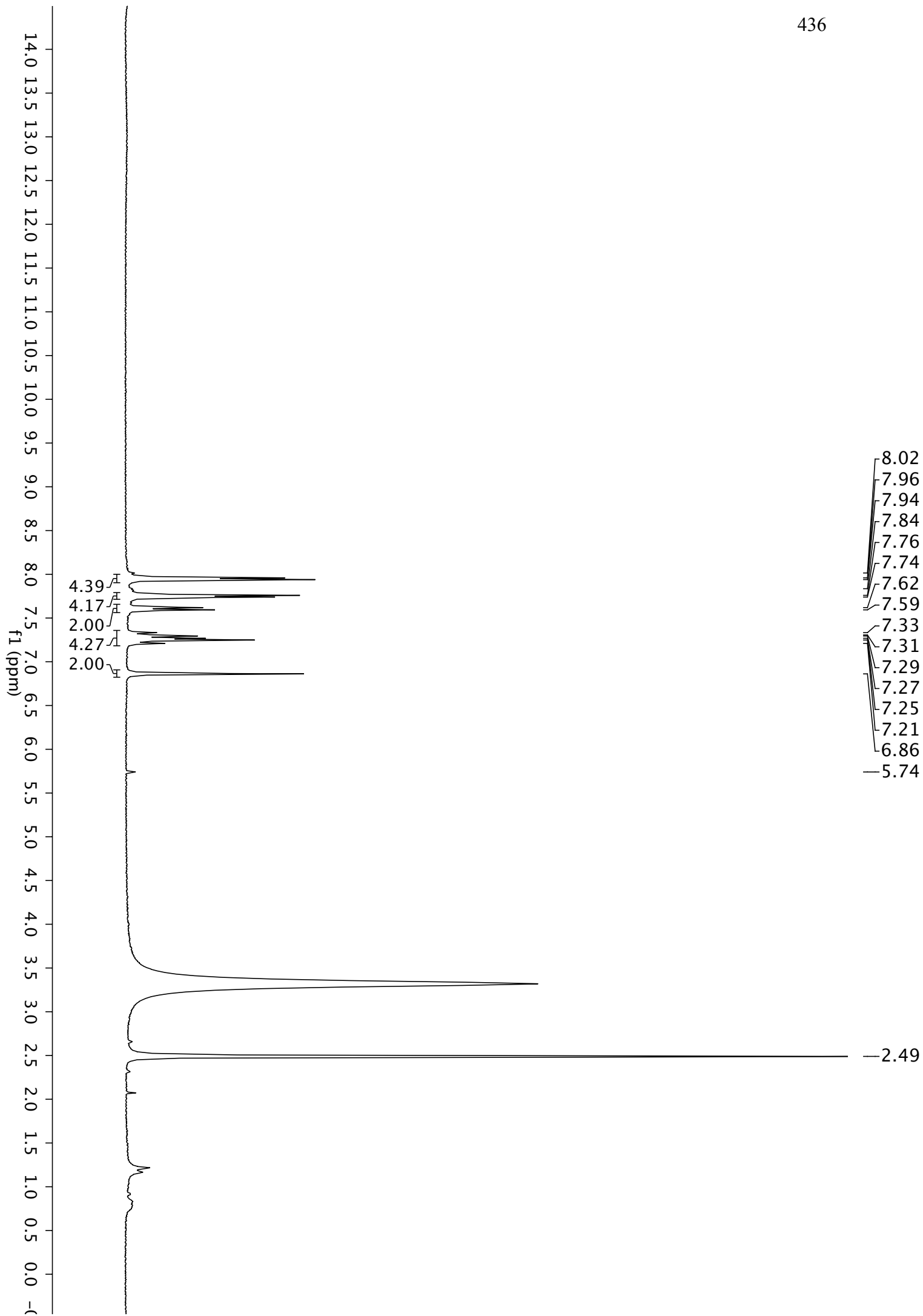






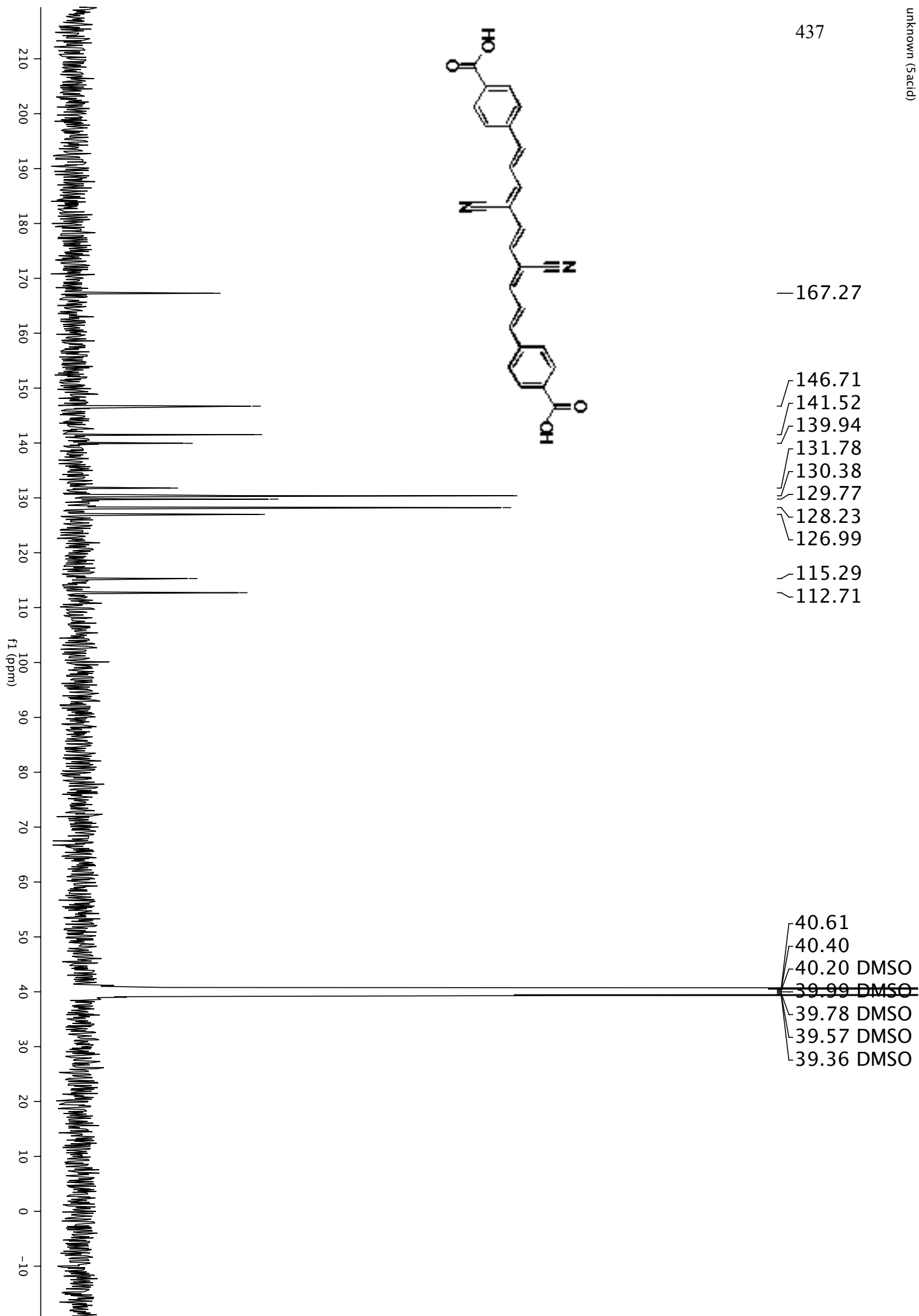


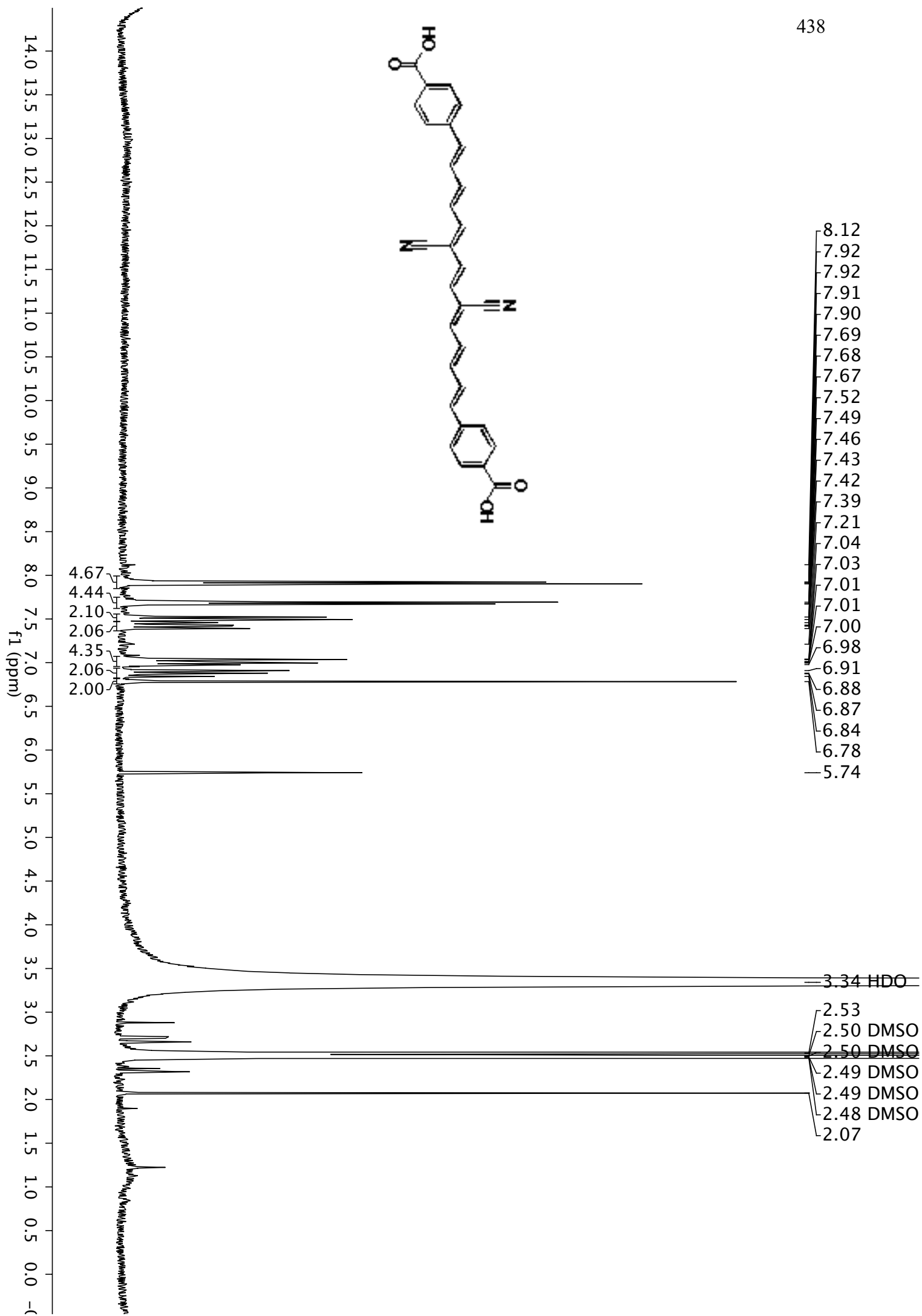


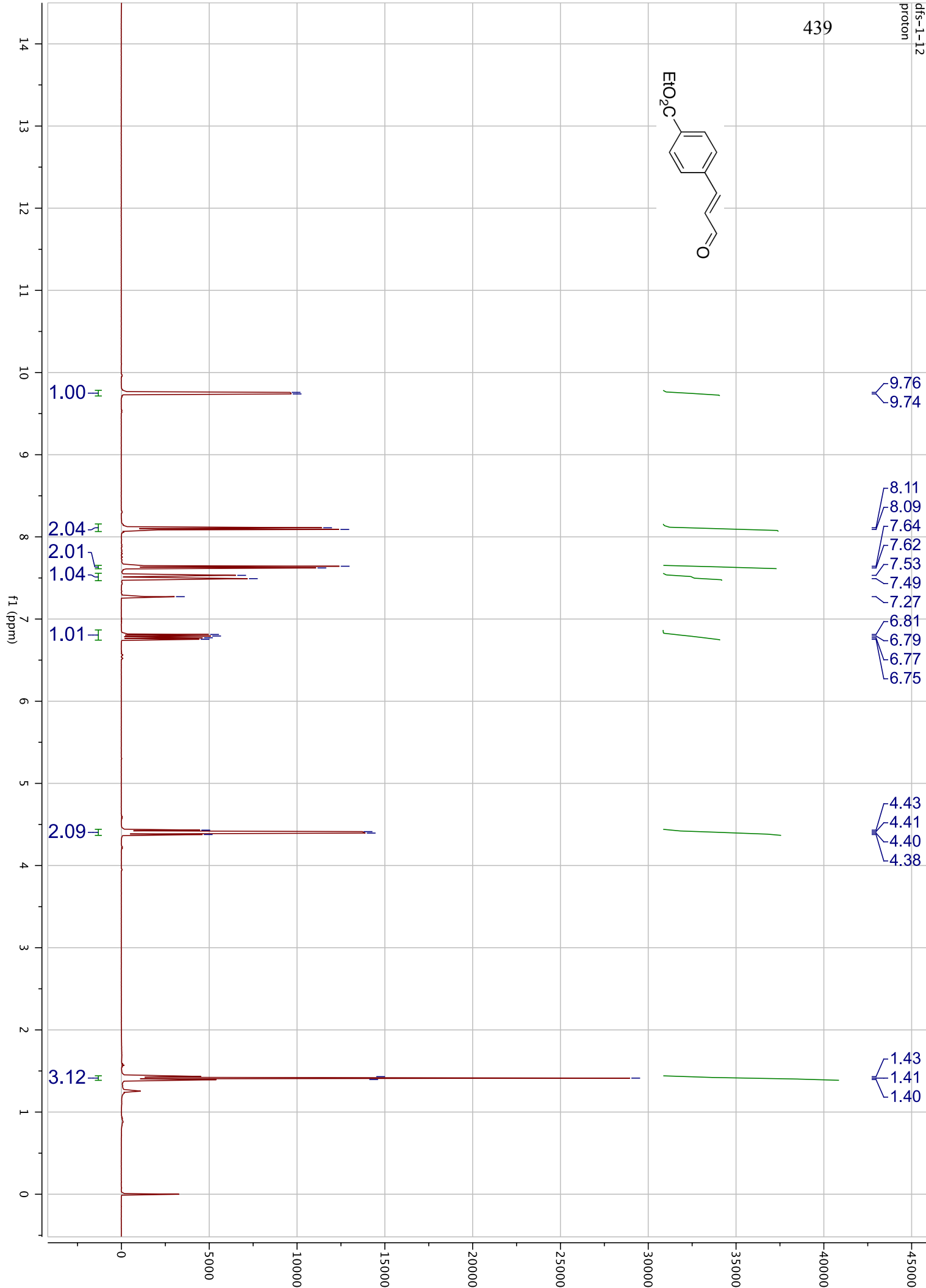
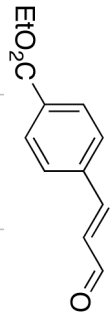




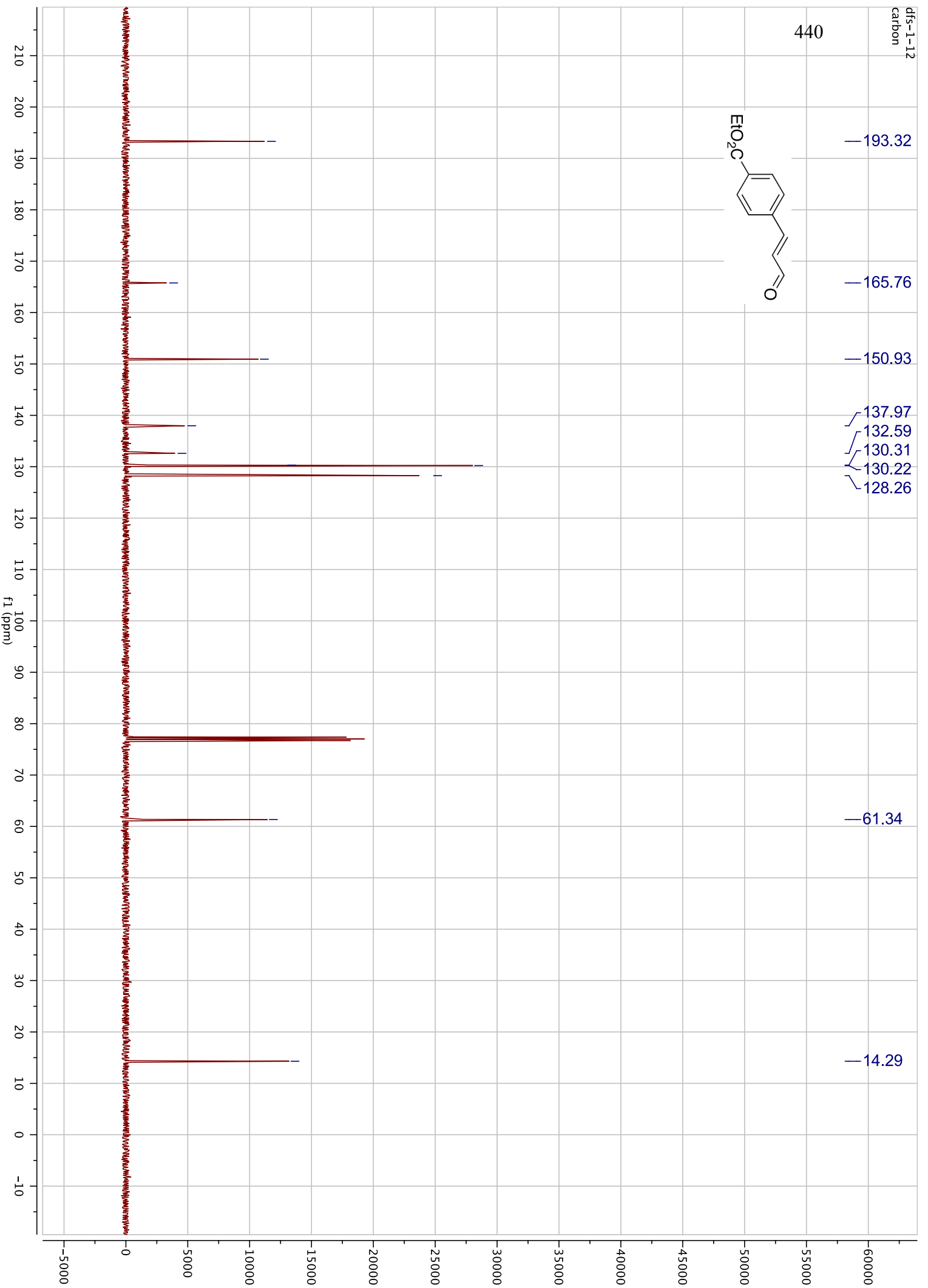
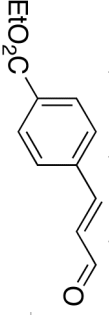
437

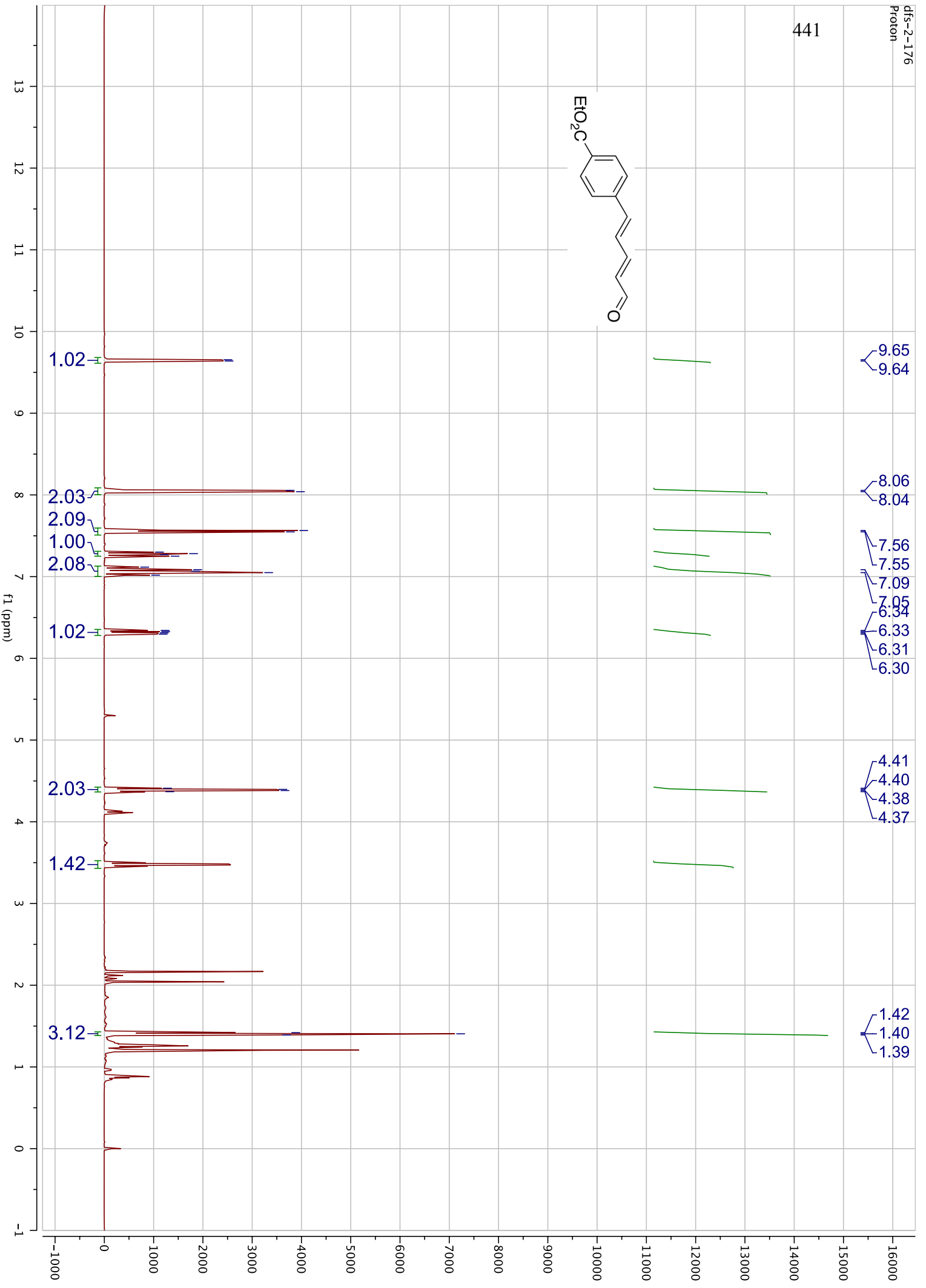
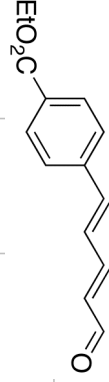




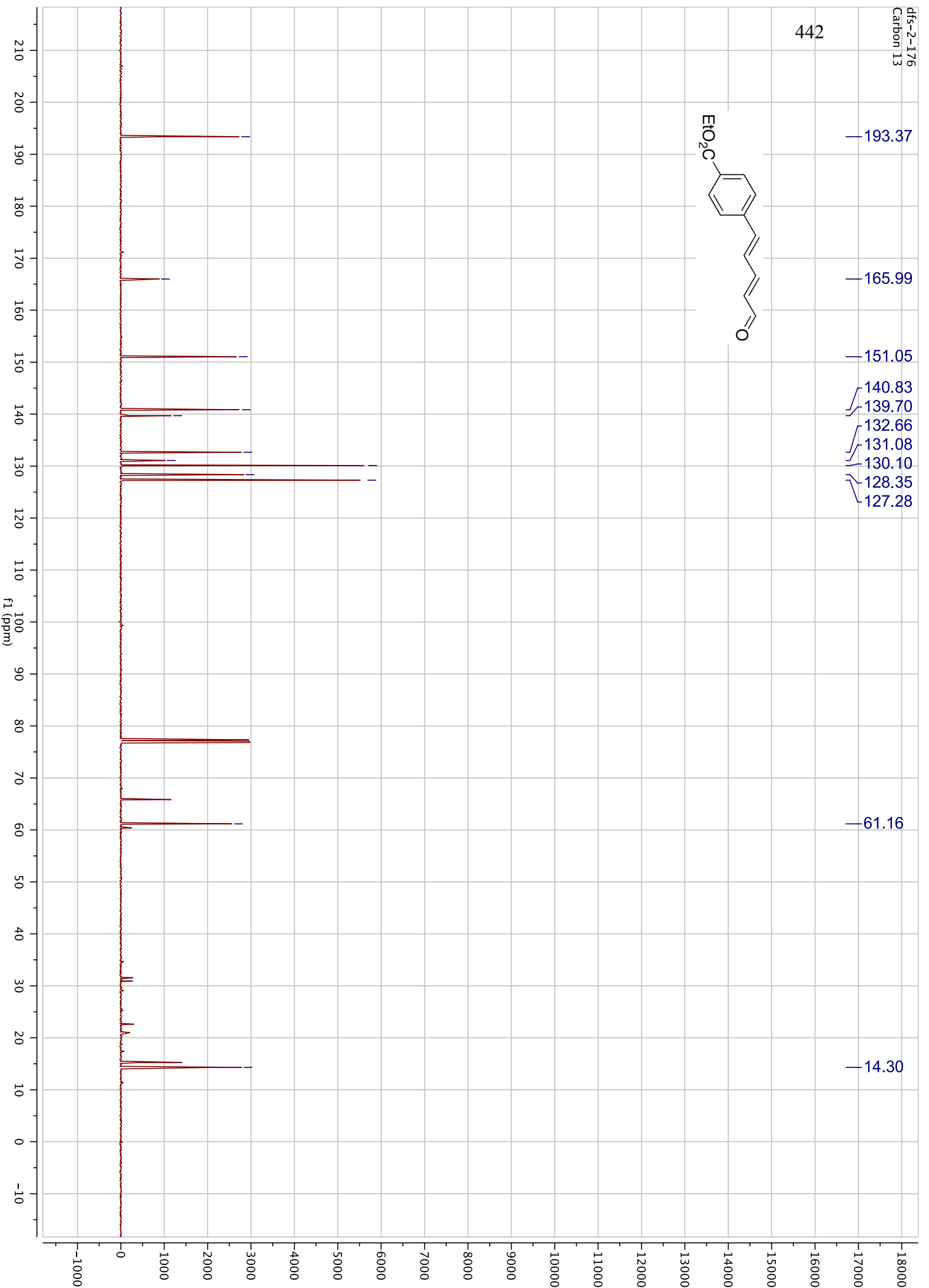
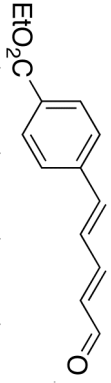


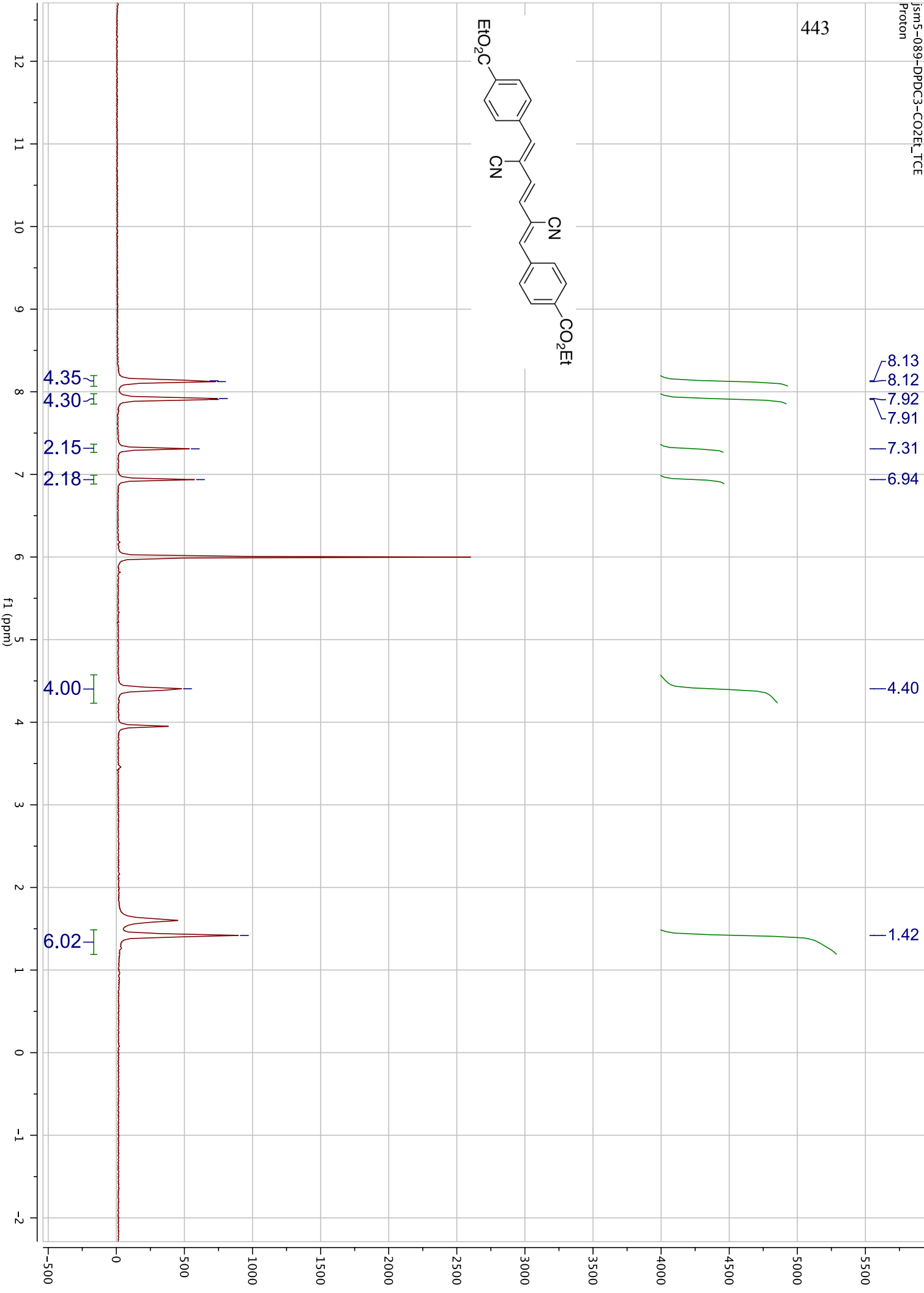
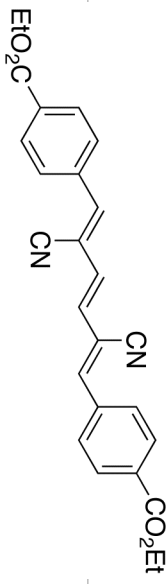
440



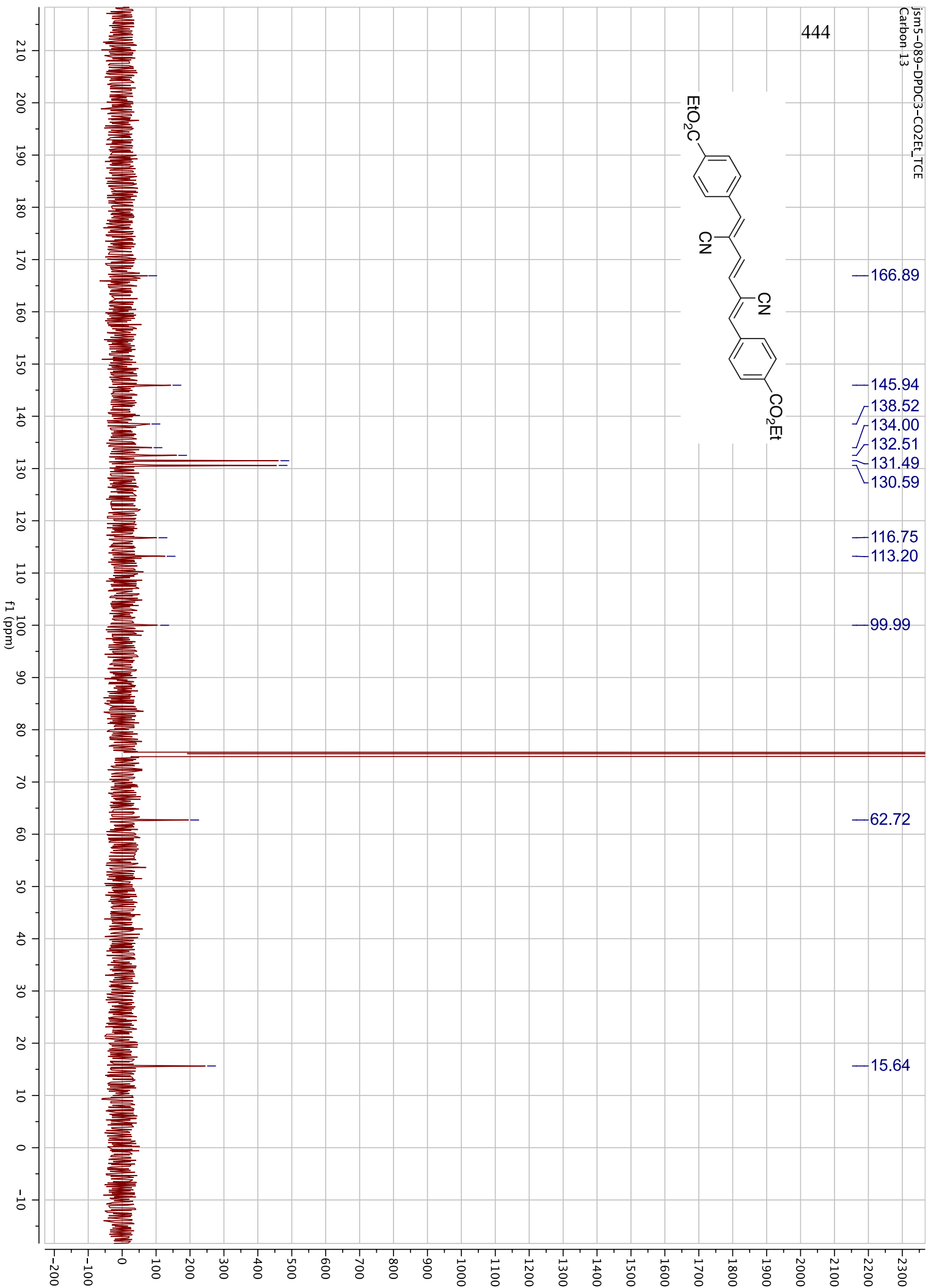
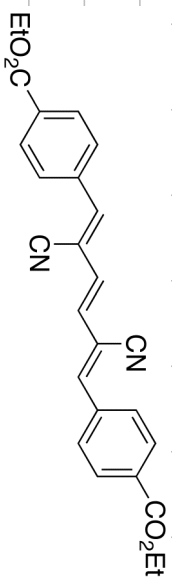


442

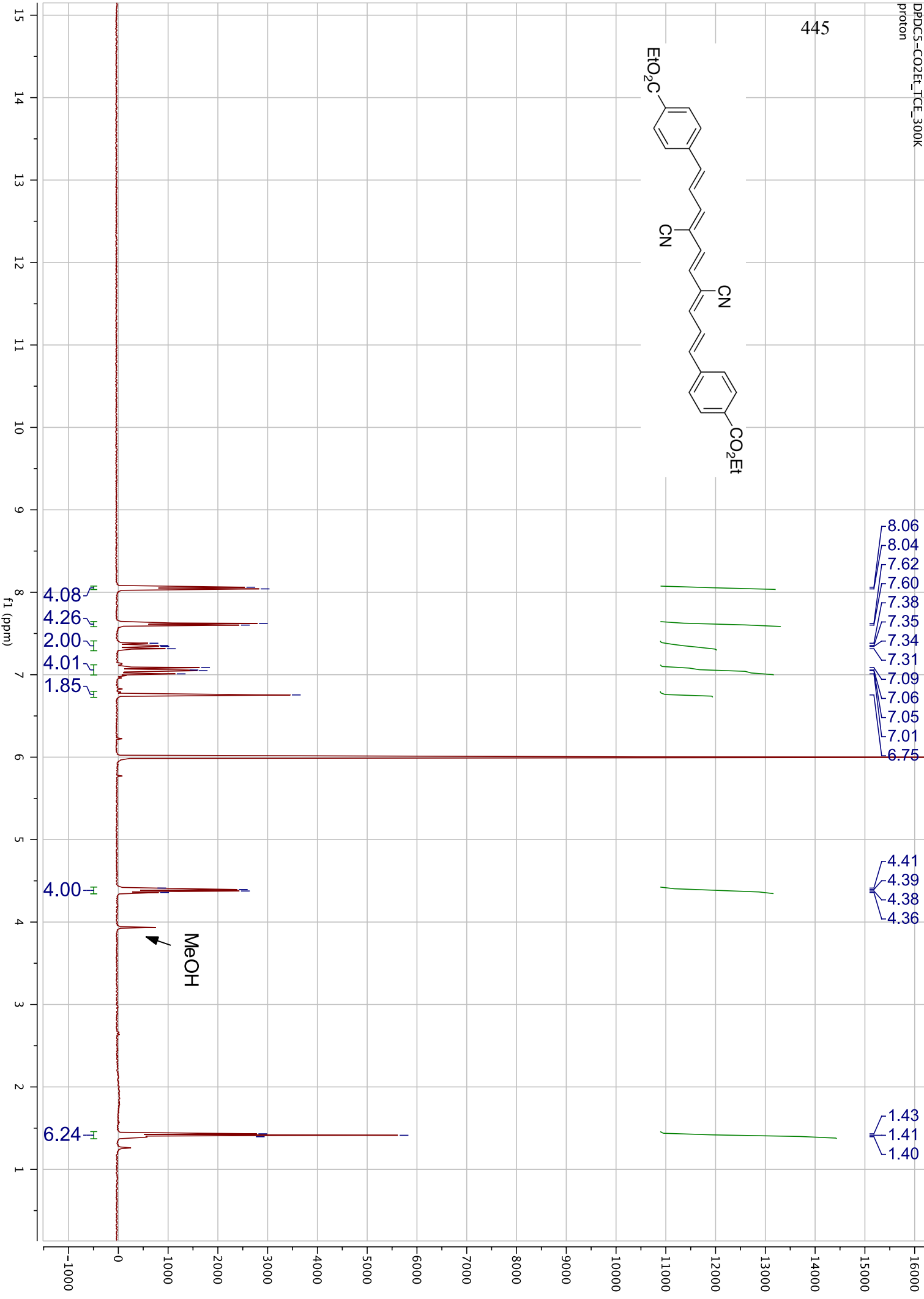
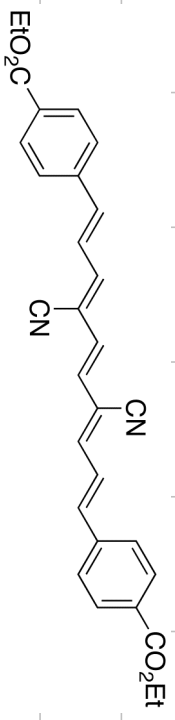


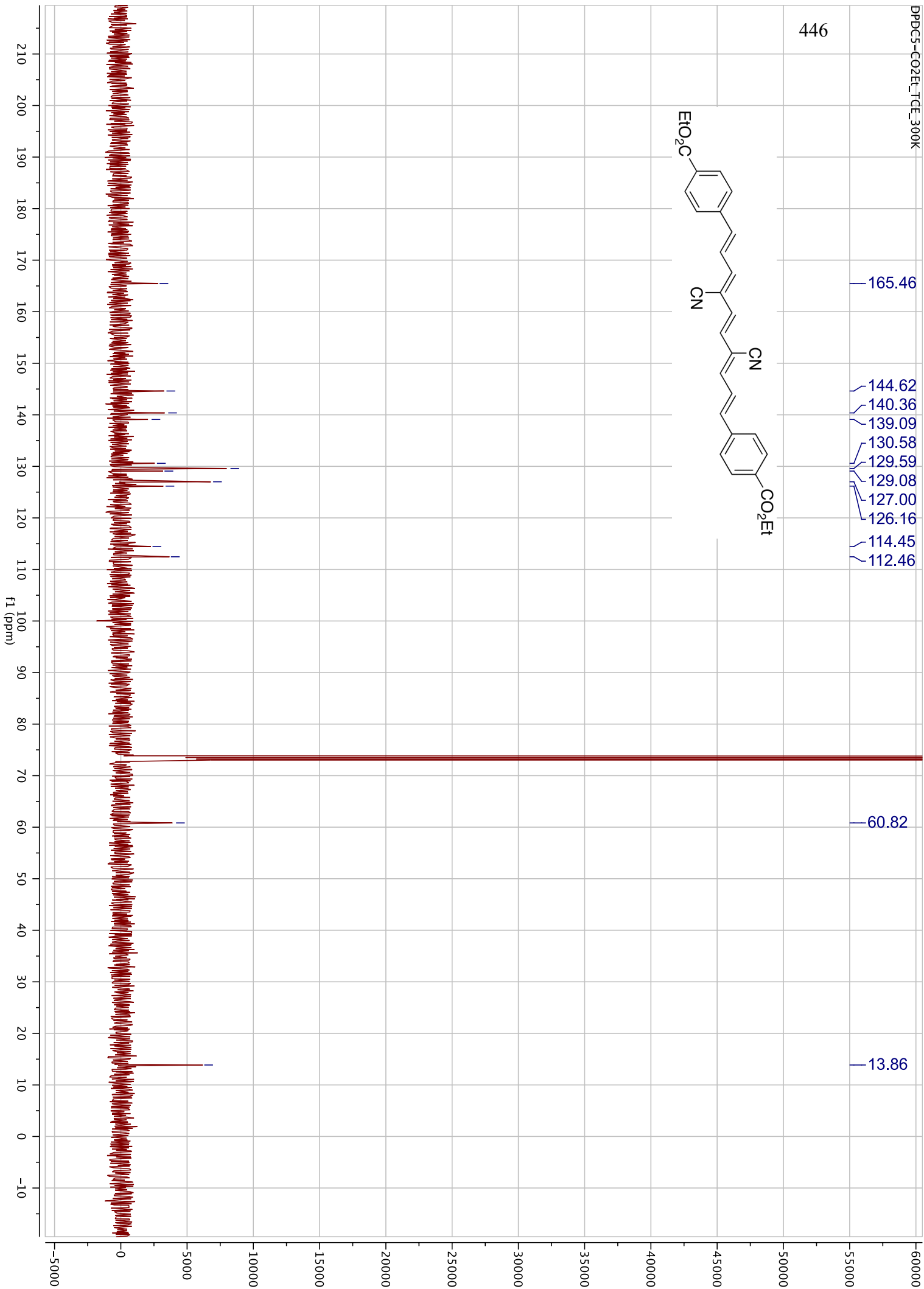
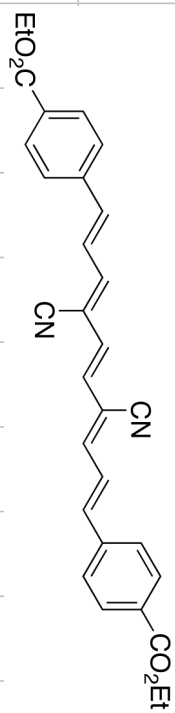


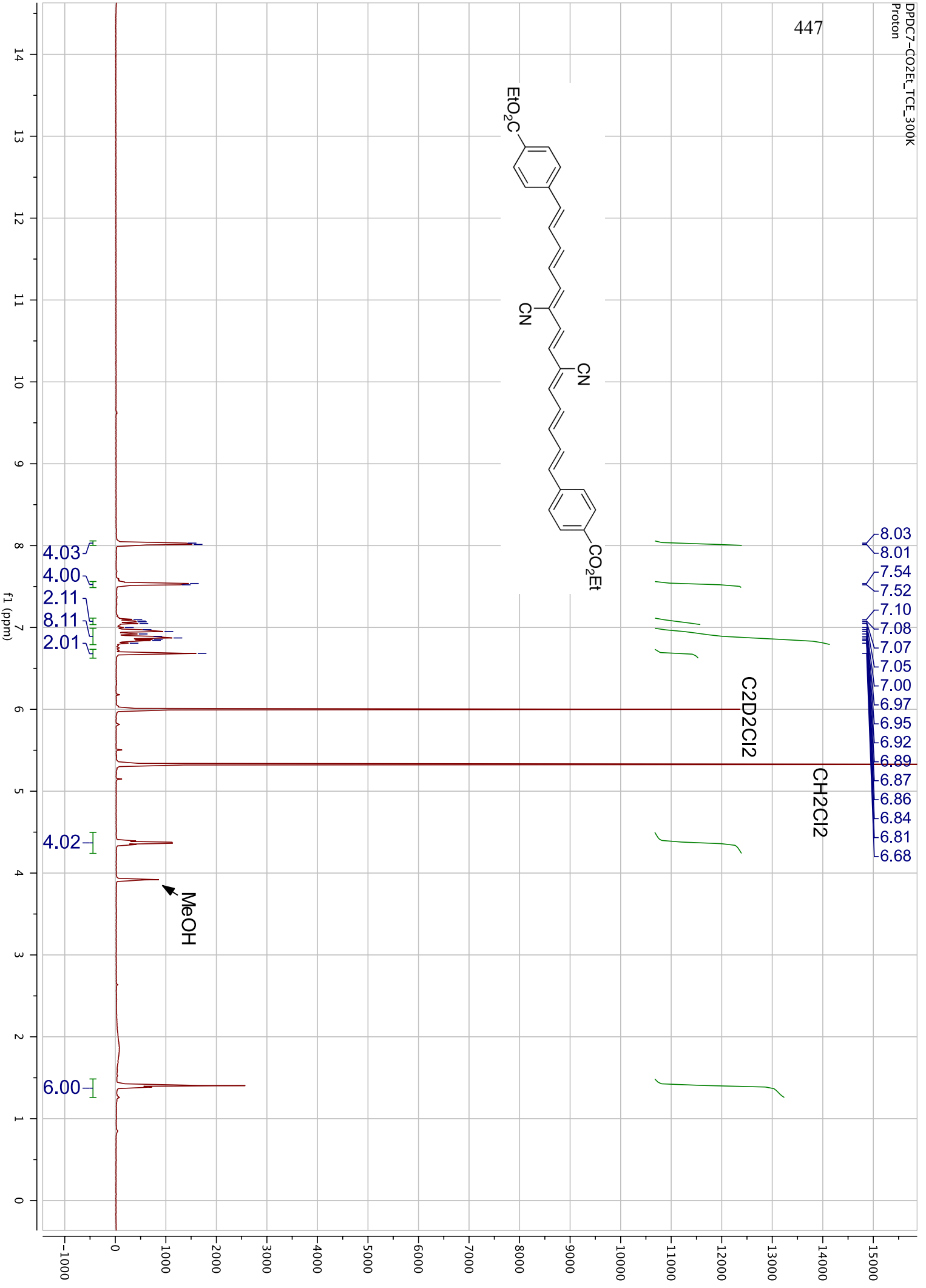
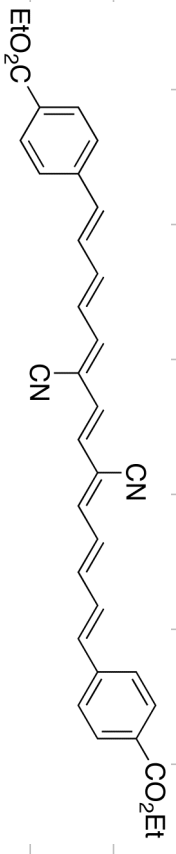
444



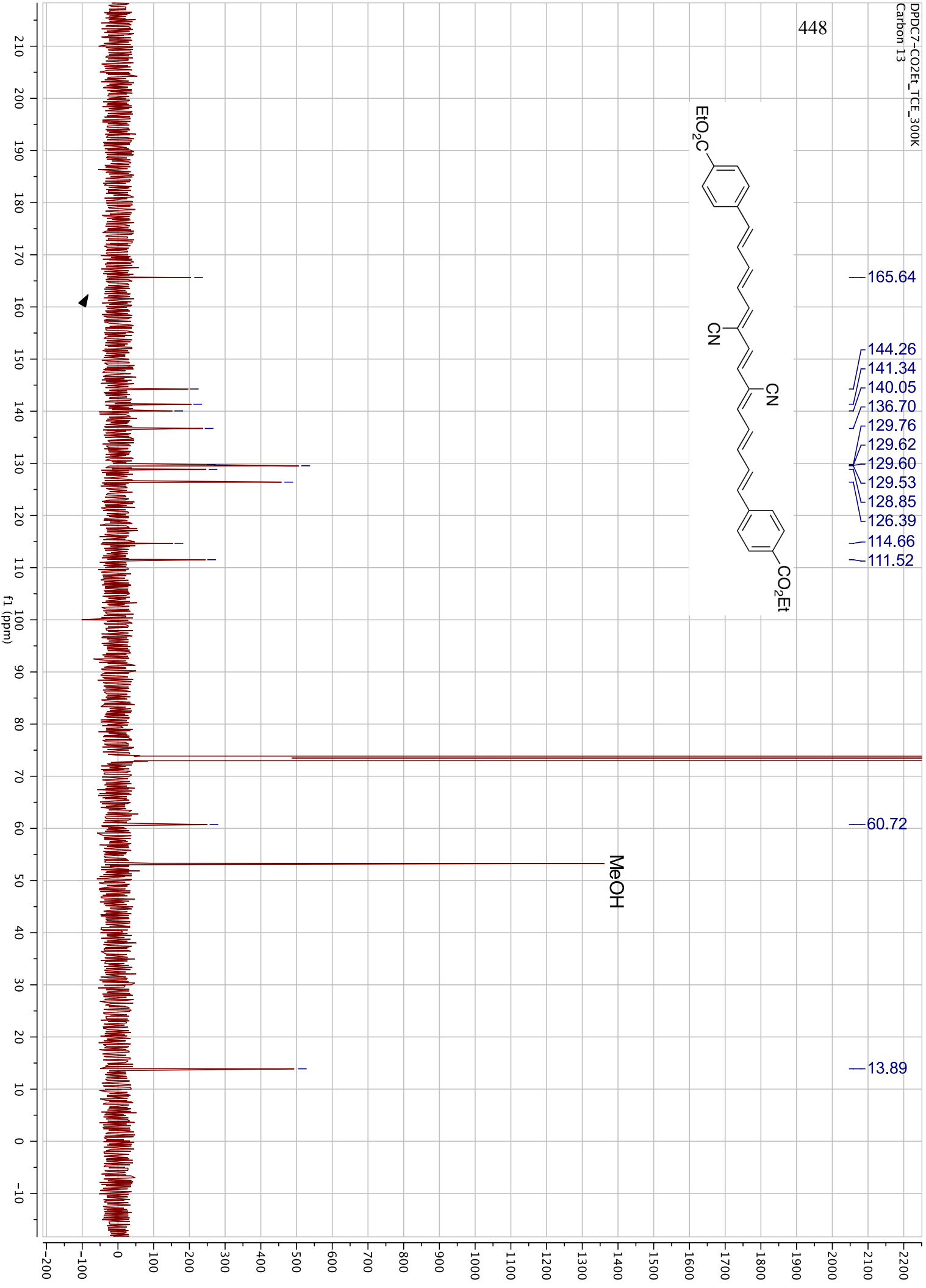
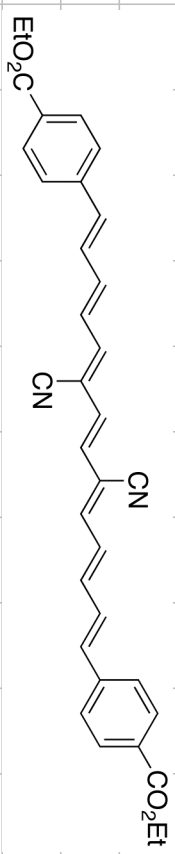


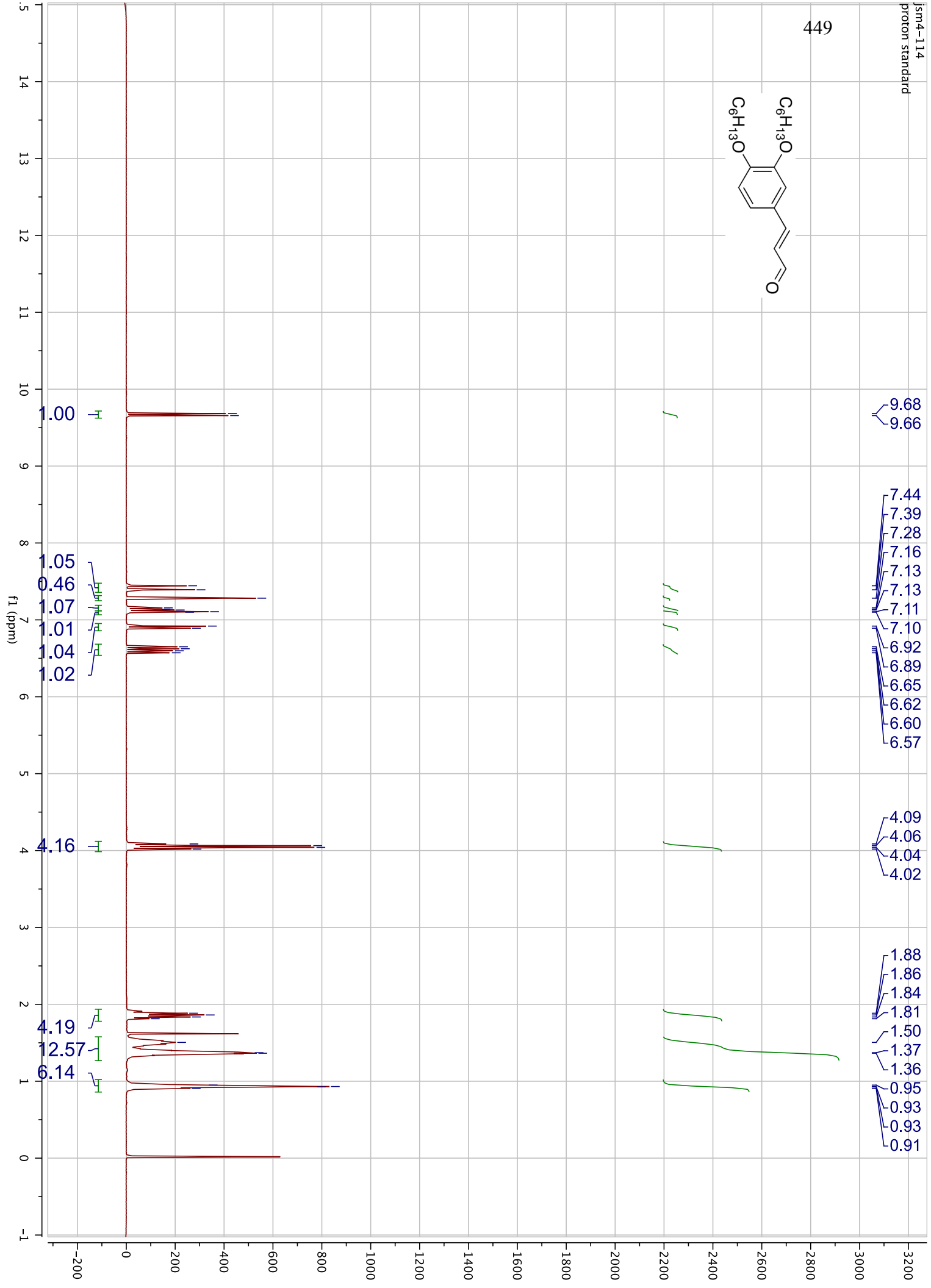
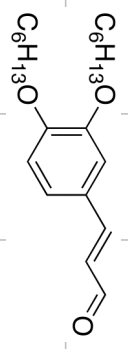




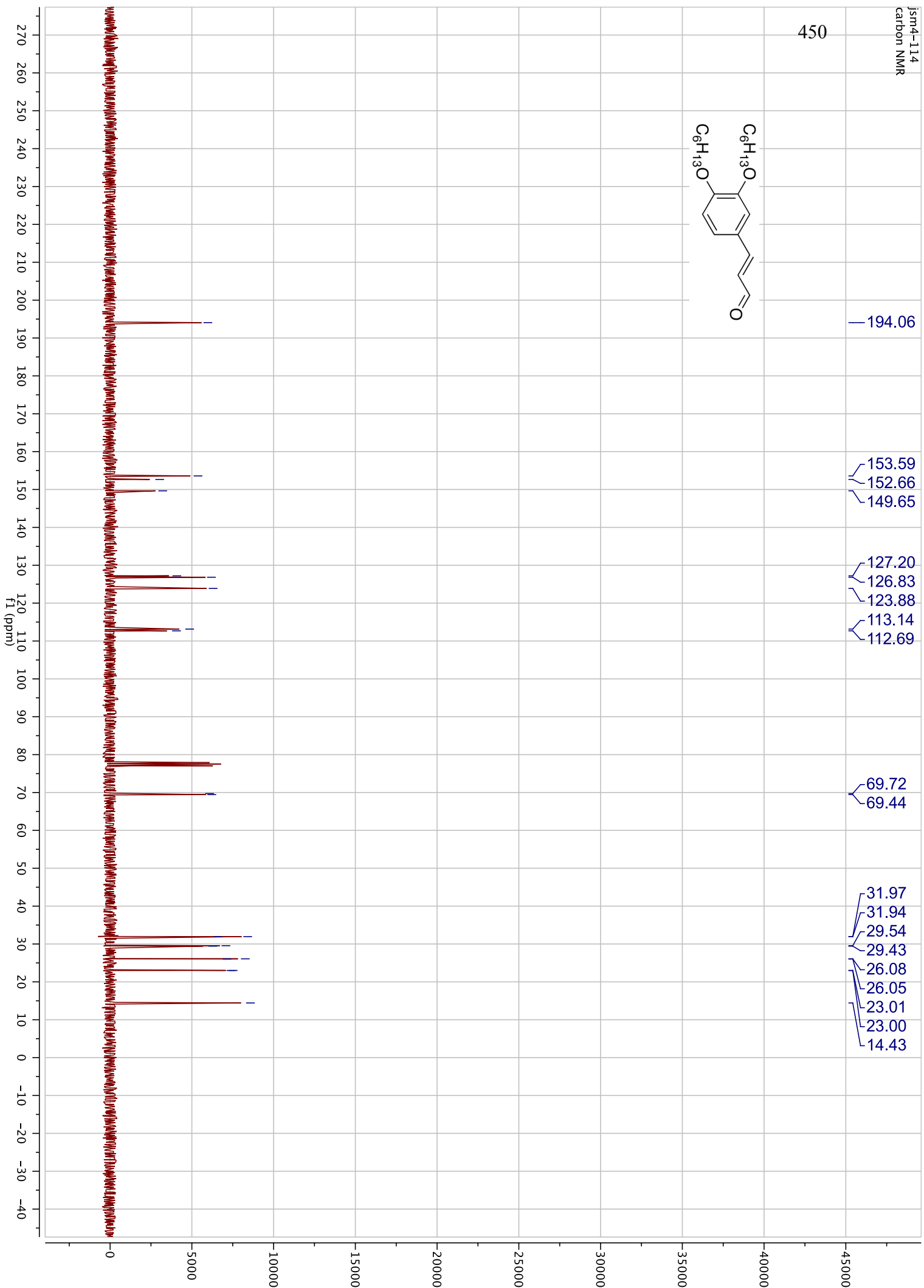
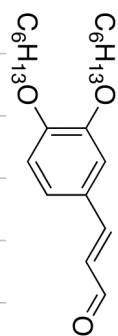


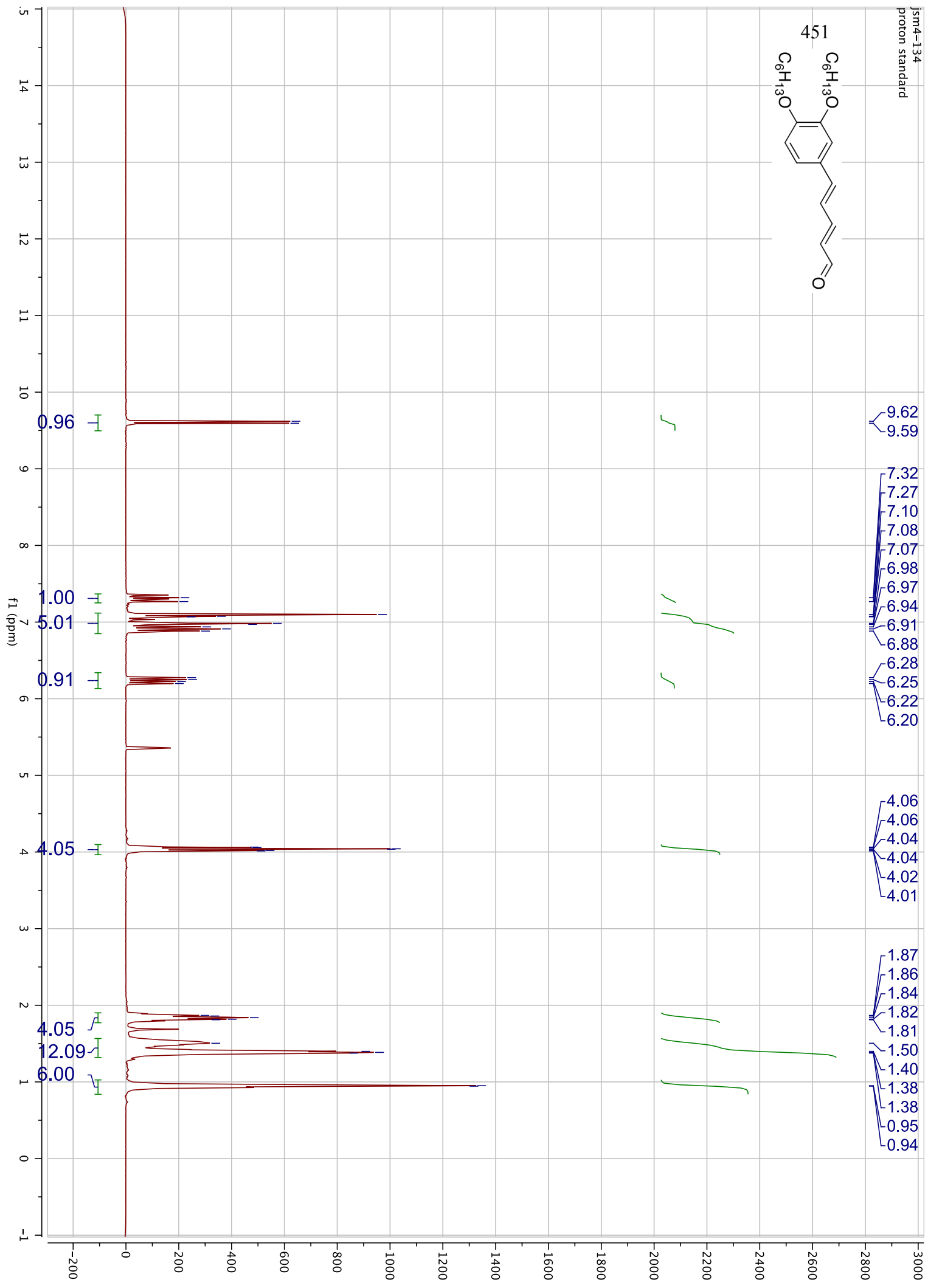
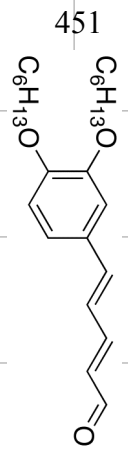
448

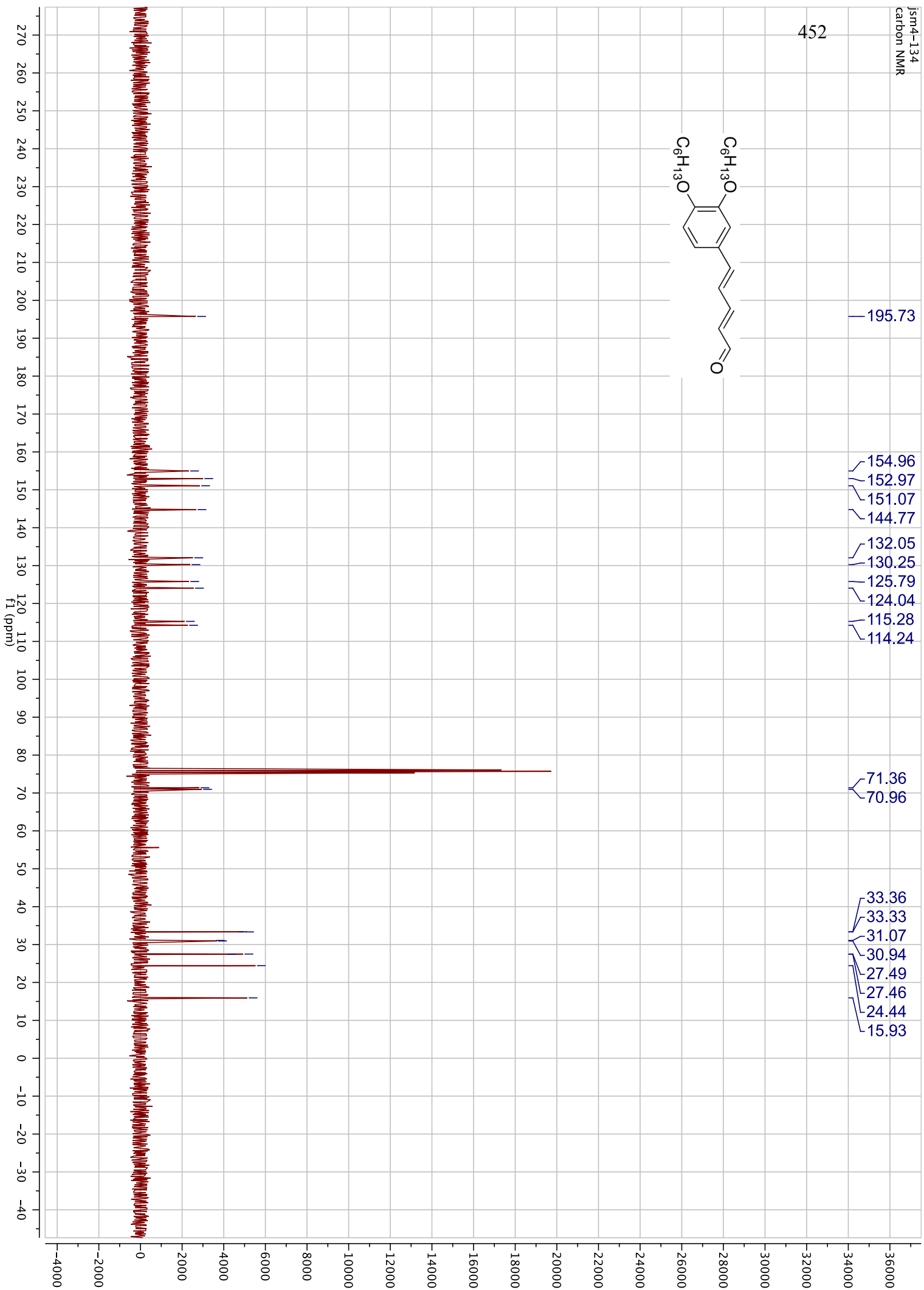
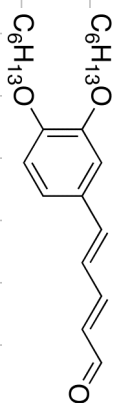




450

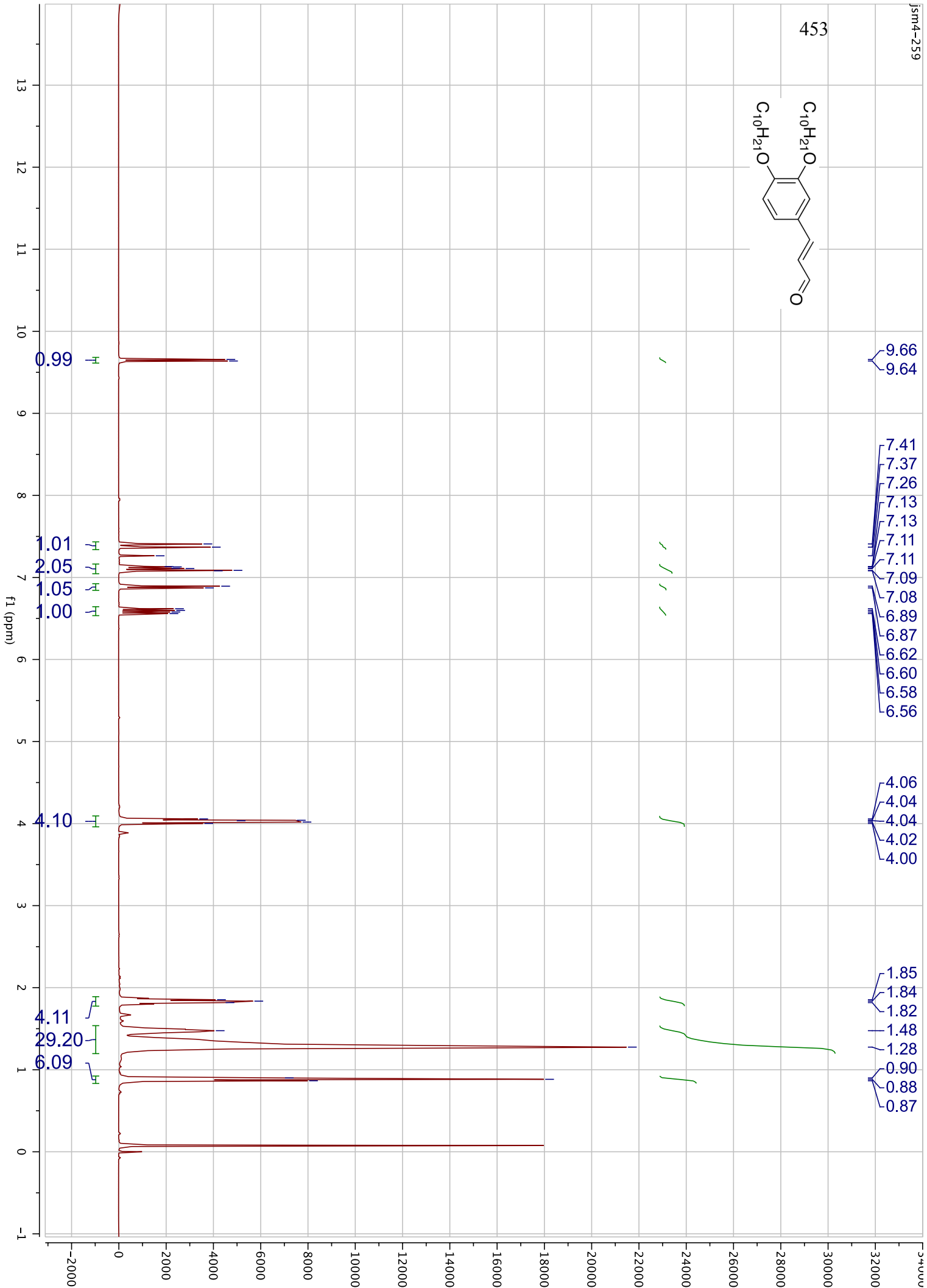
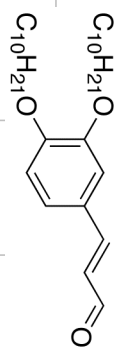




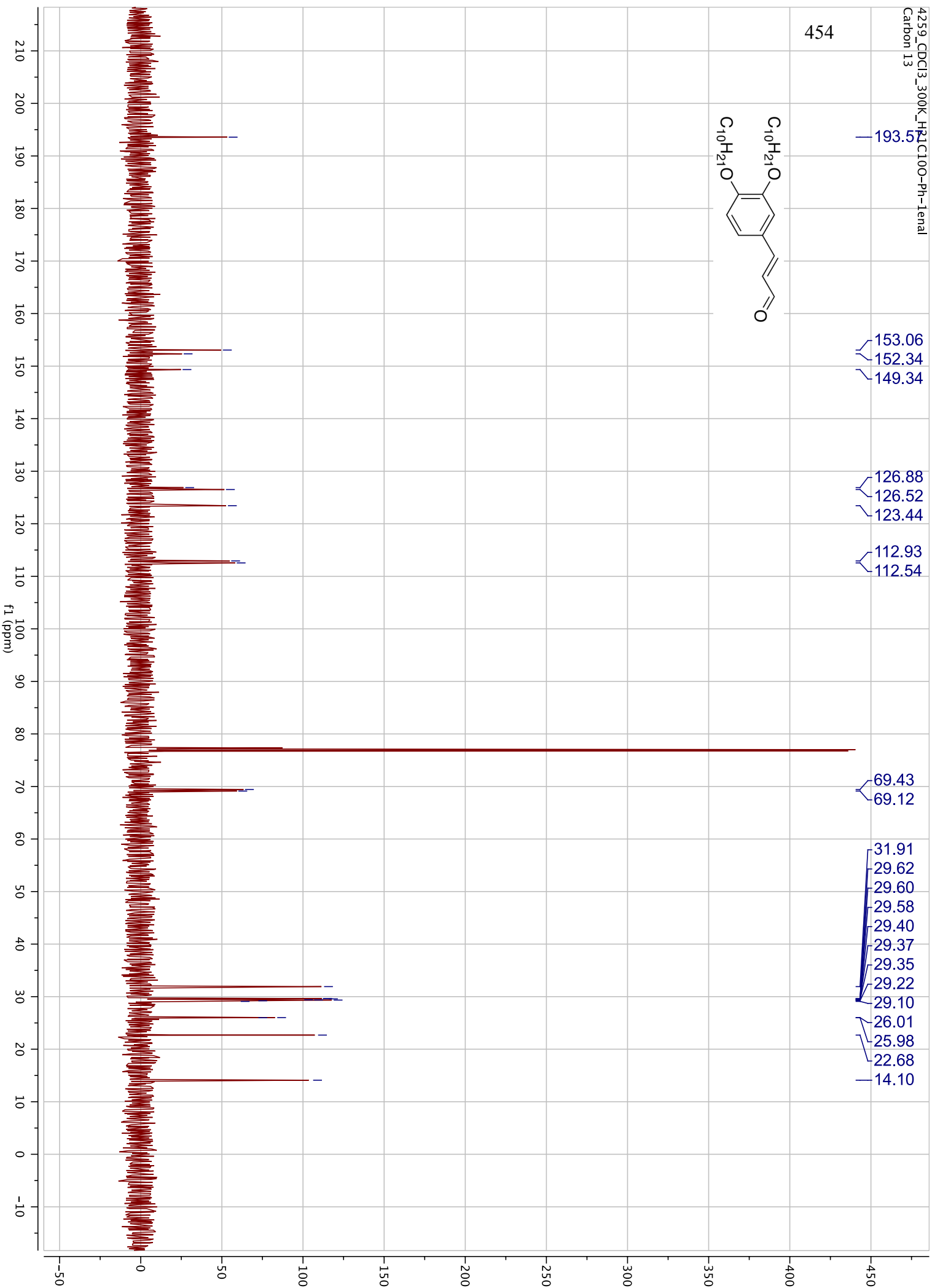
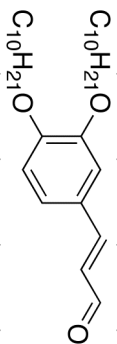




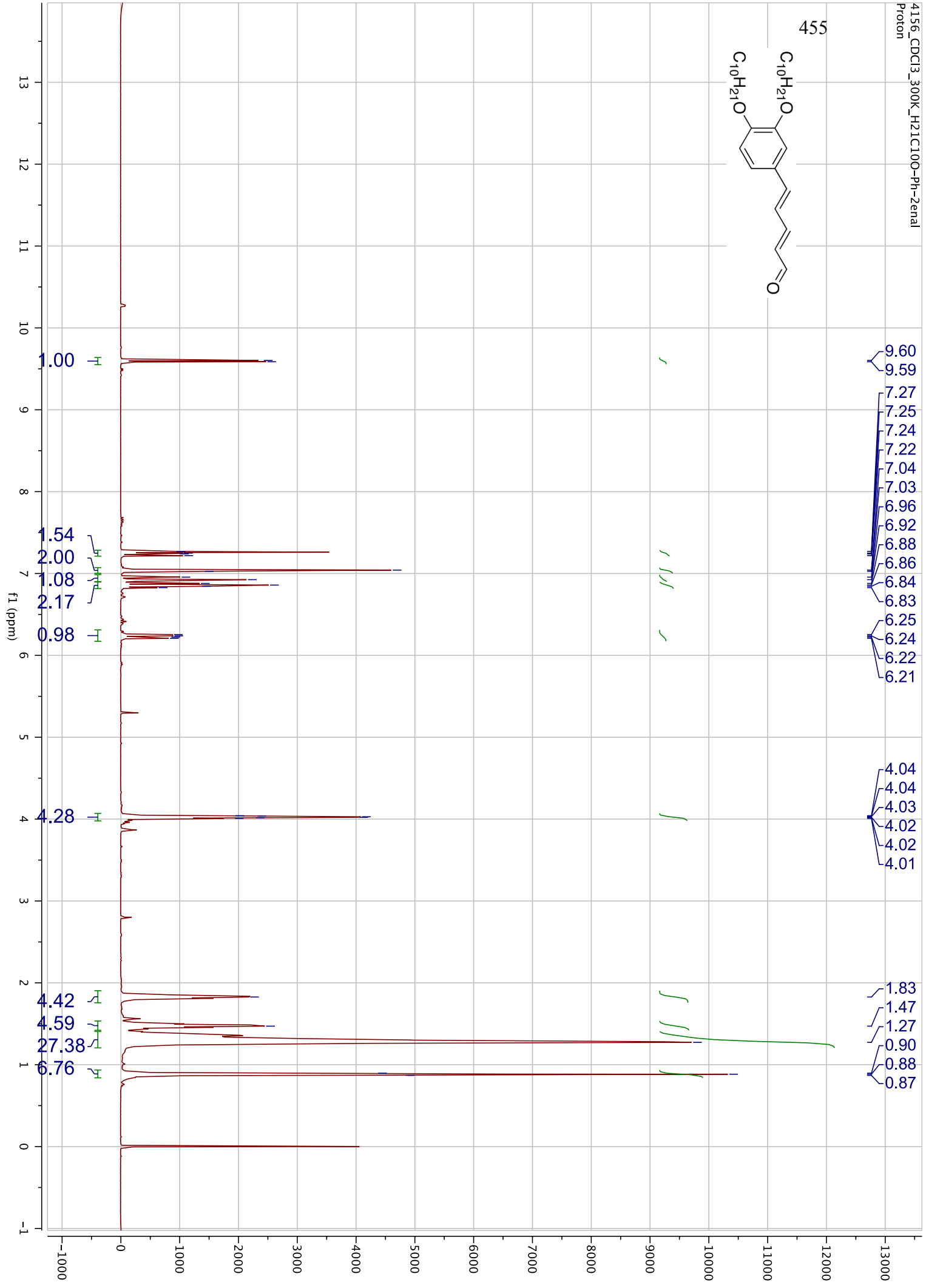
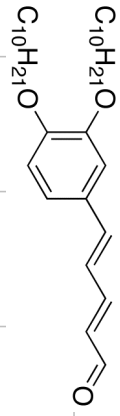
453



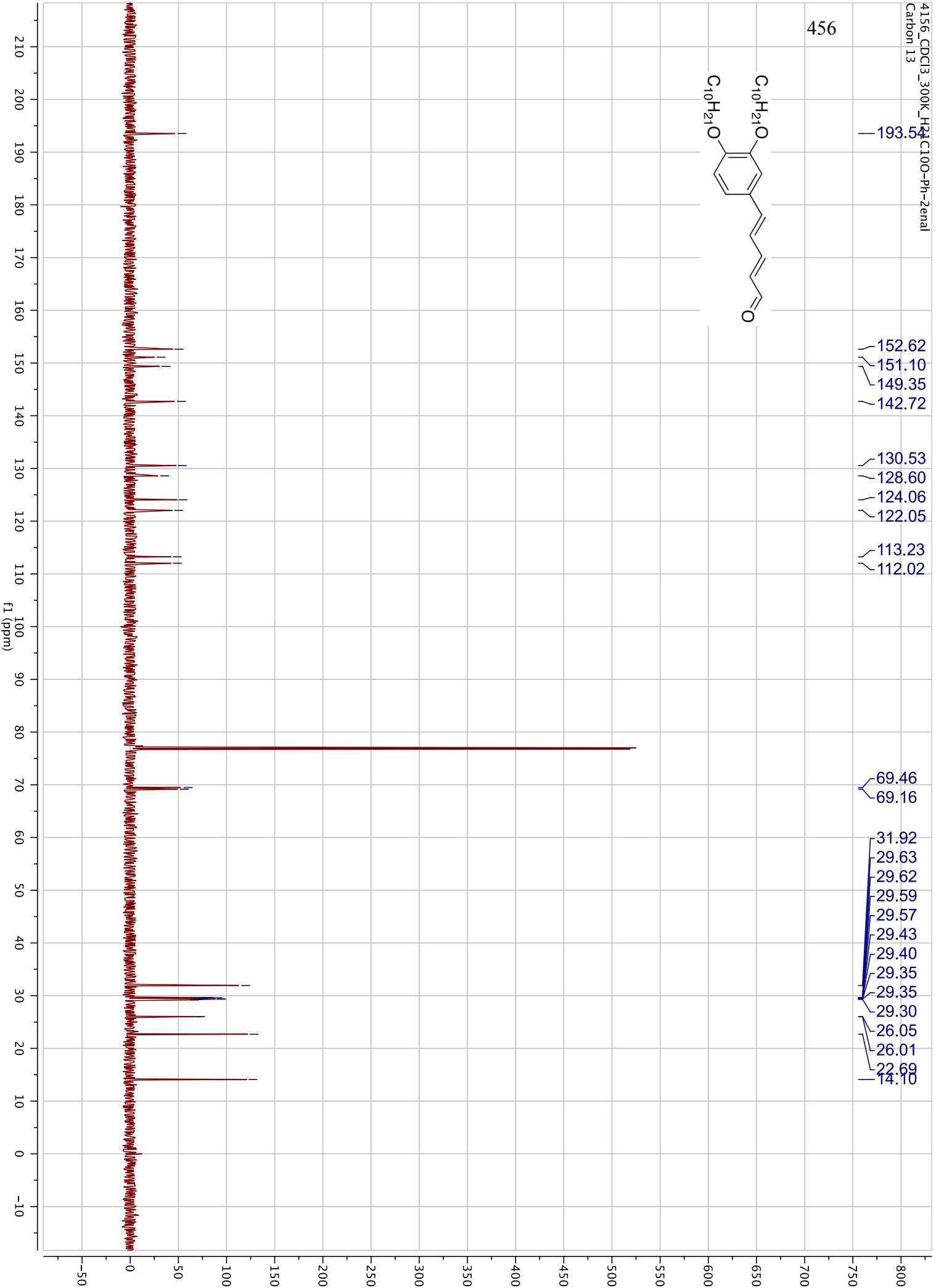
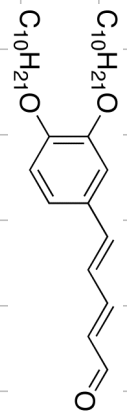
454

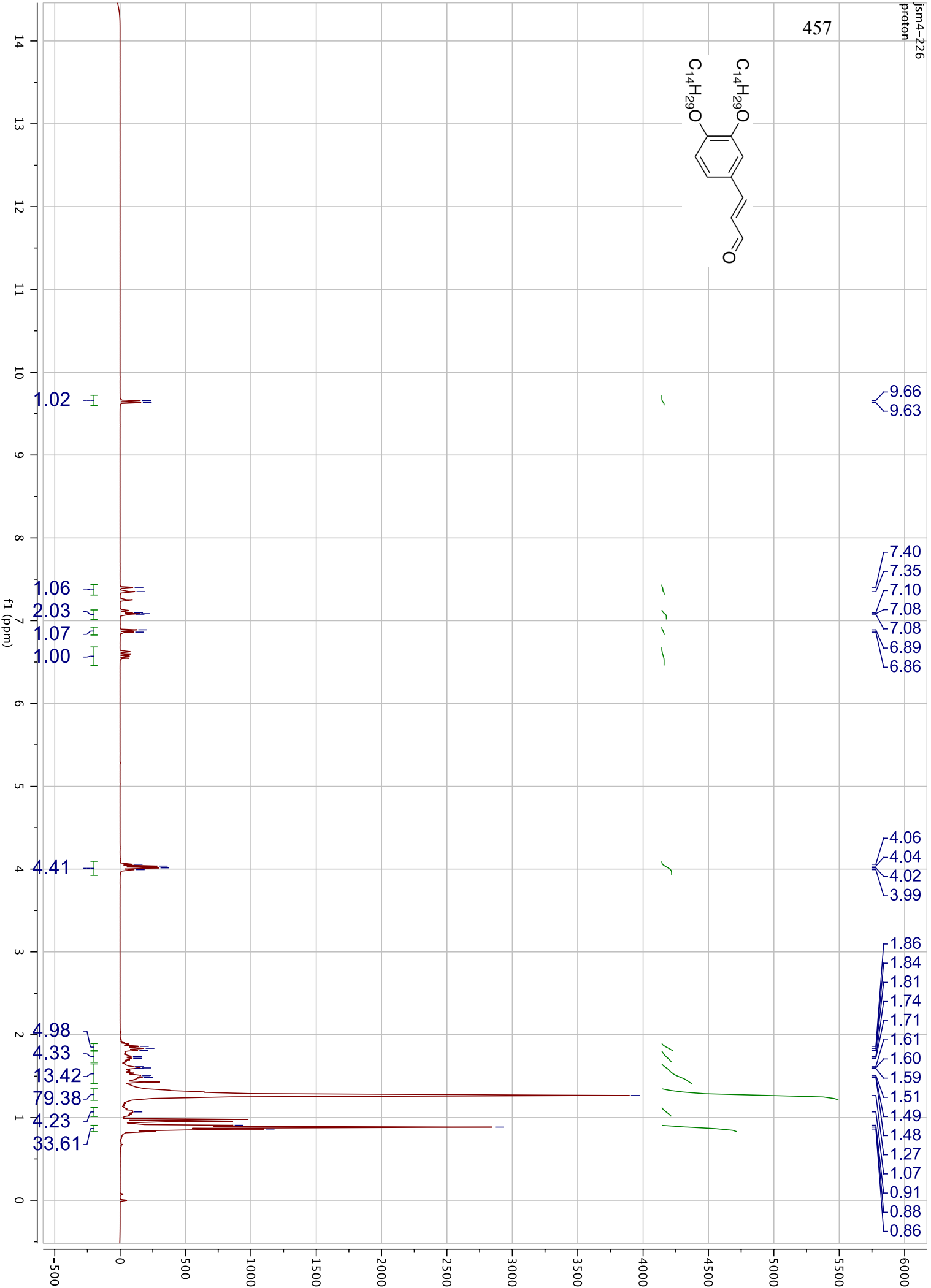
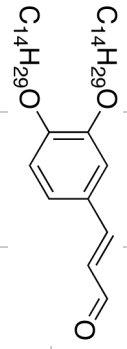


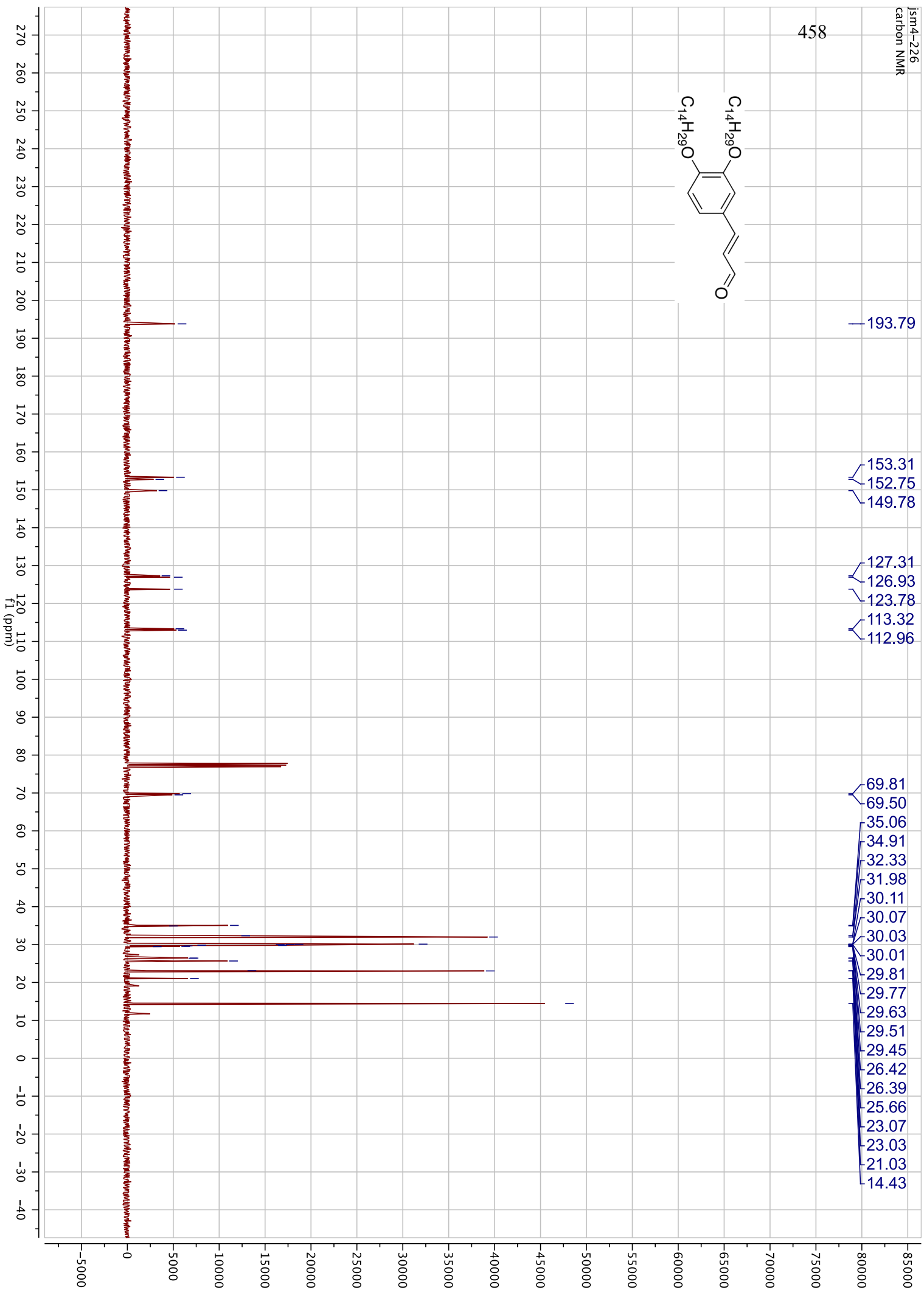
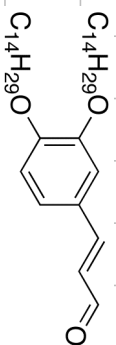
455

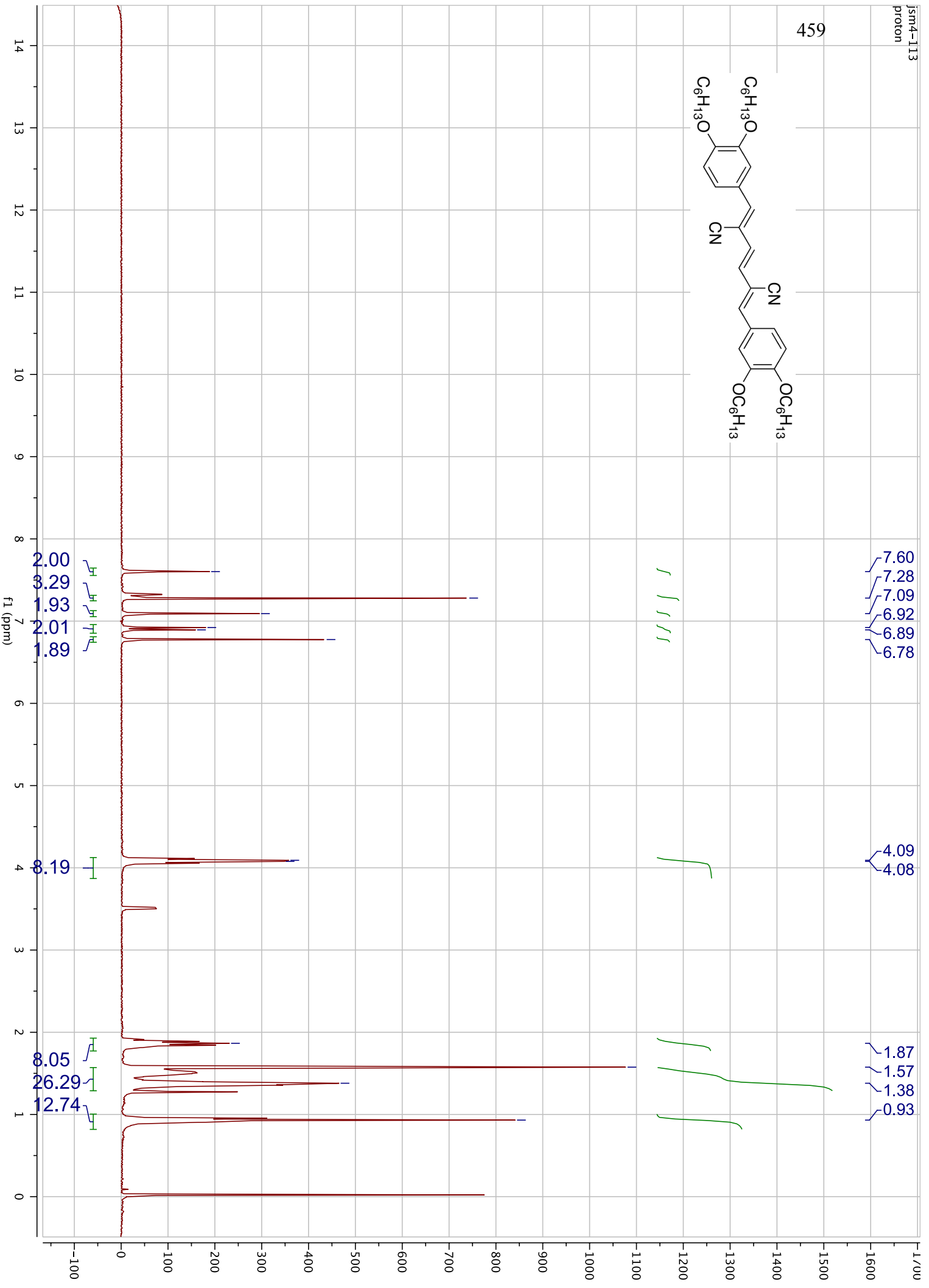
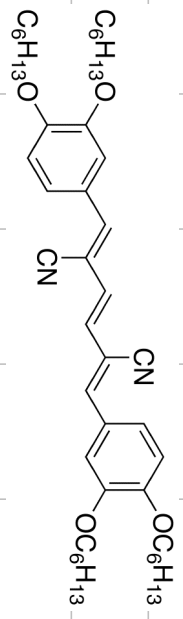


456

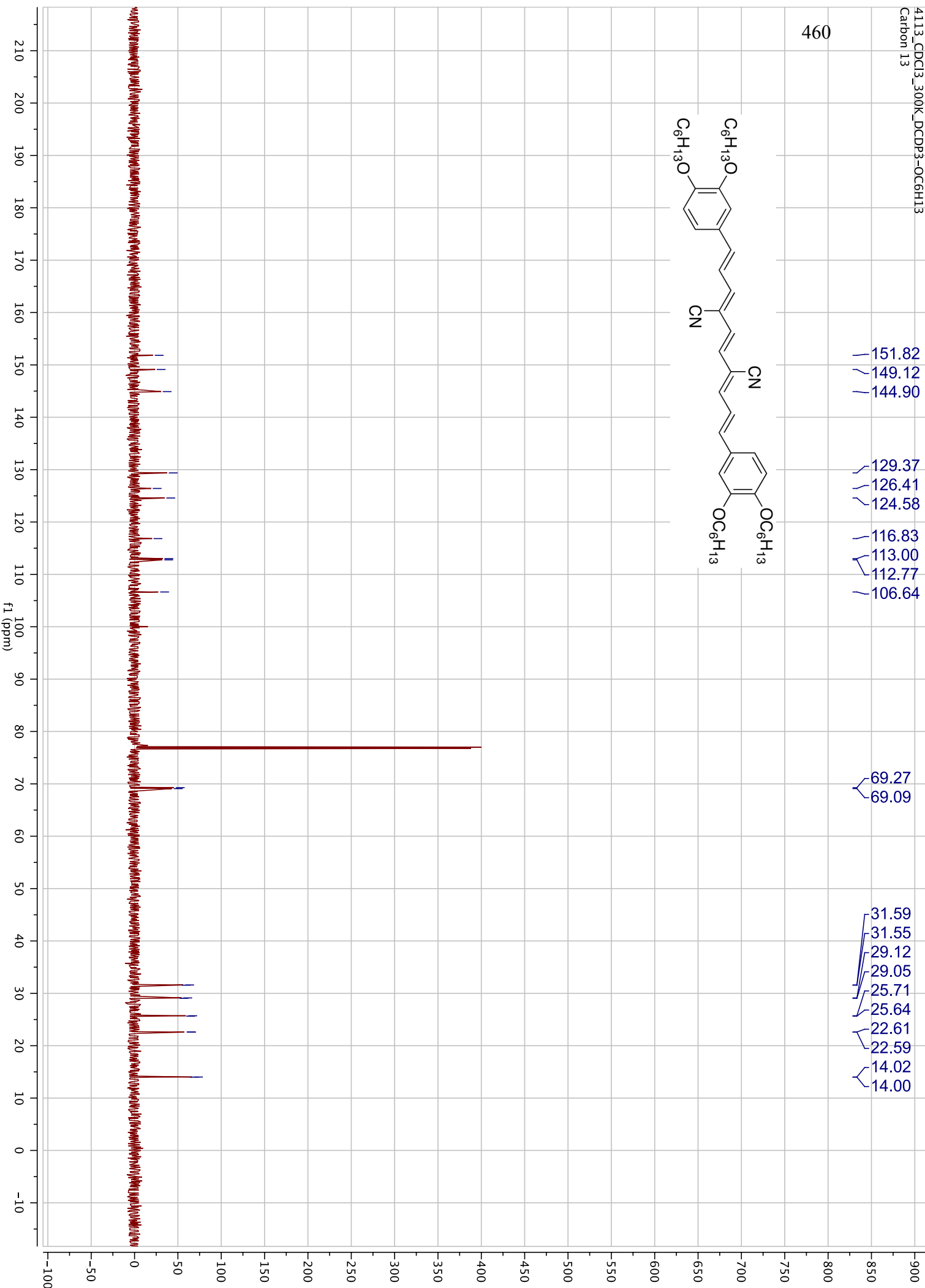
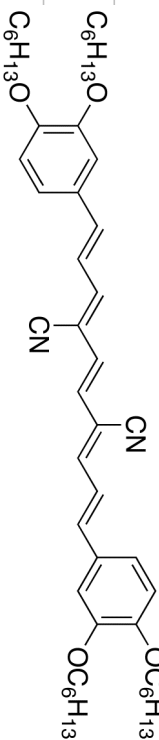






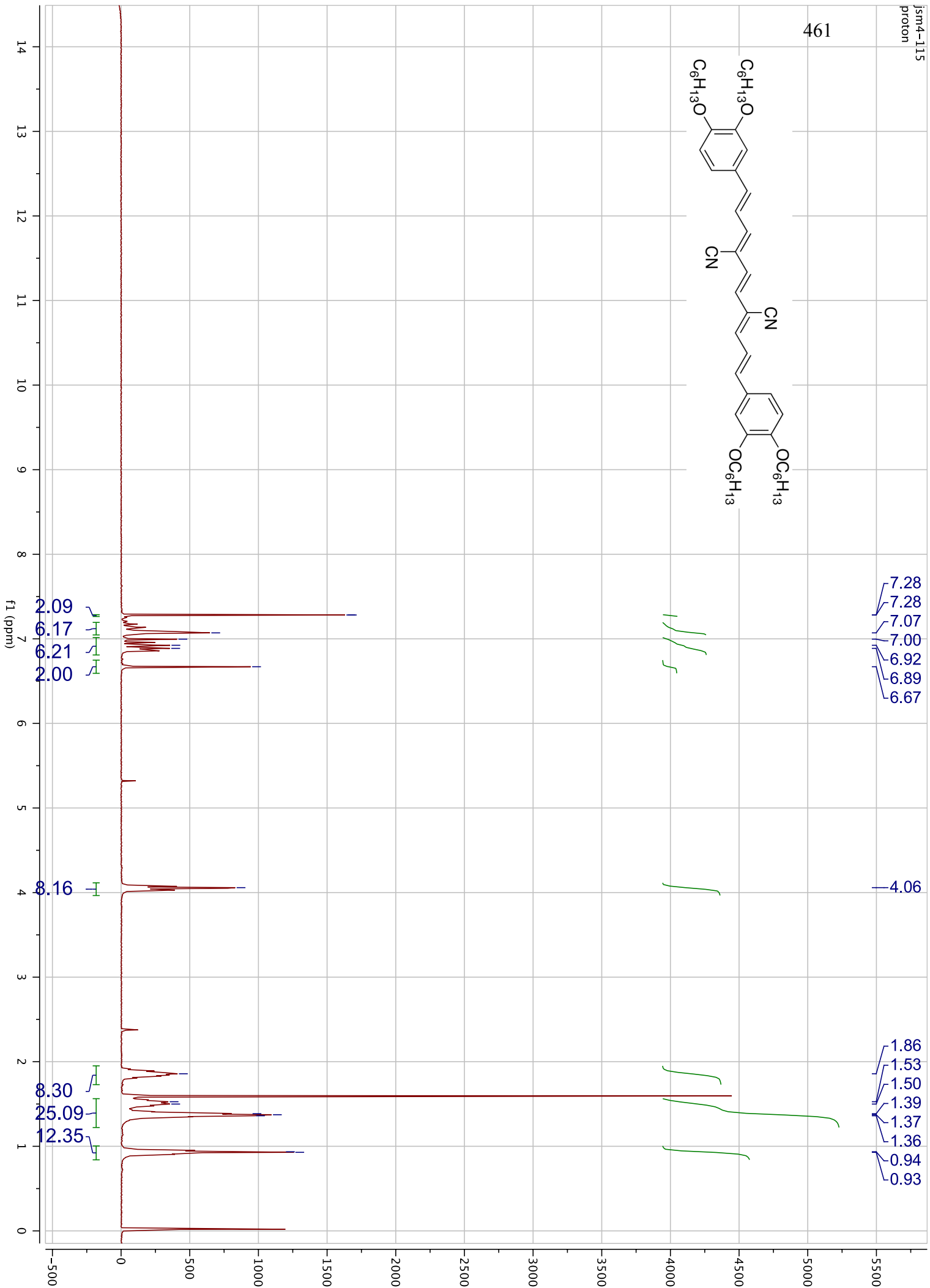
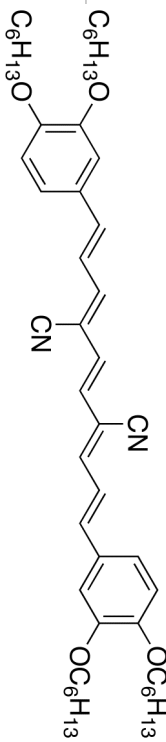


460

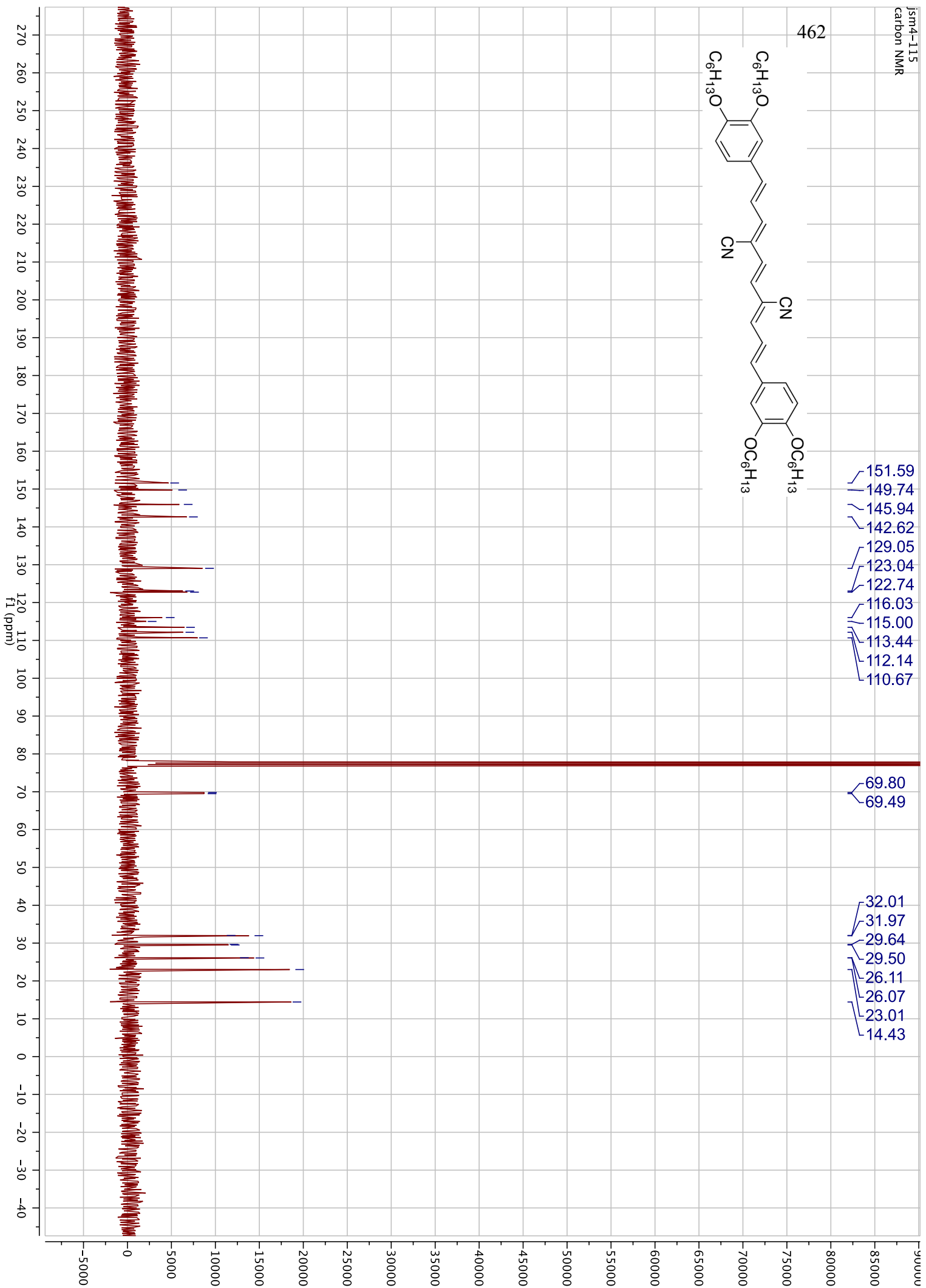
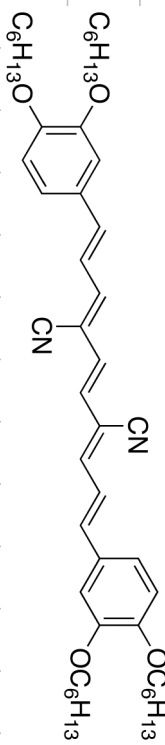




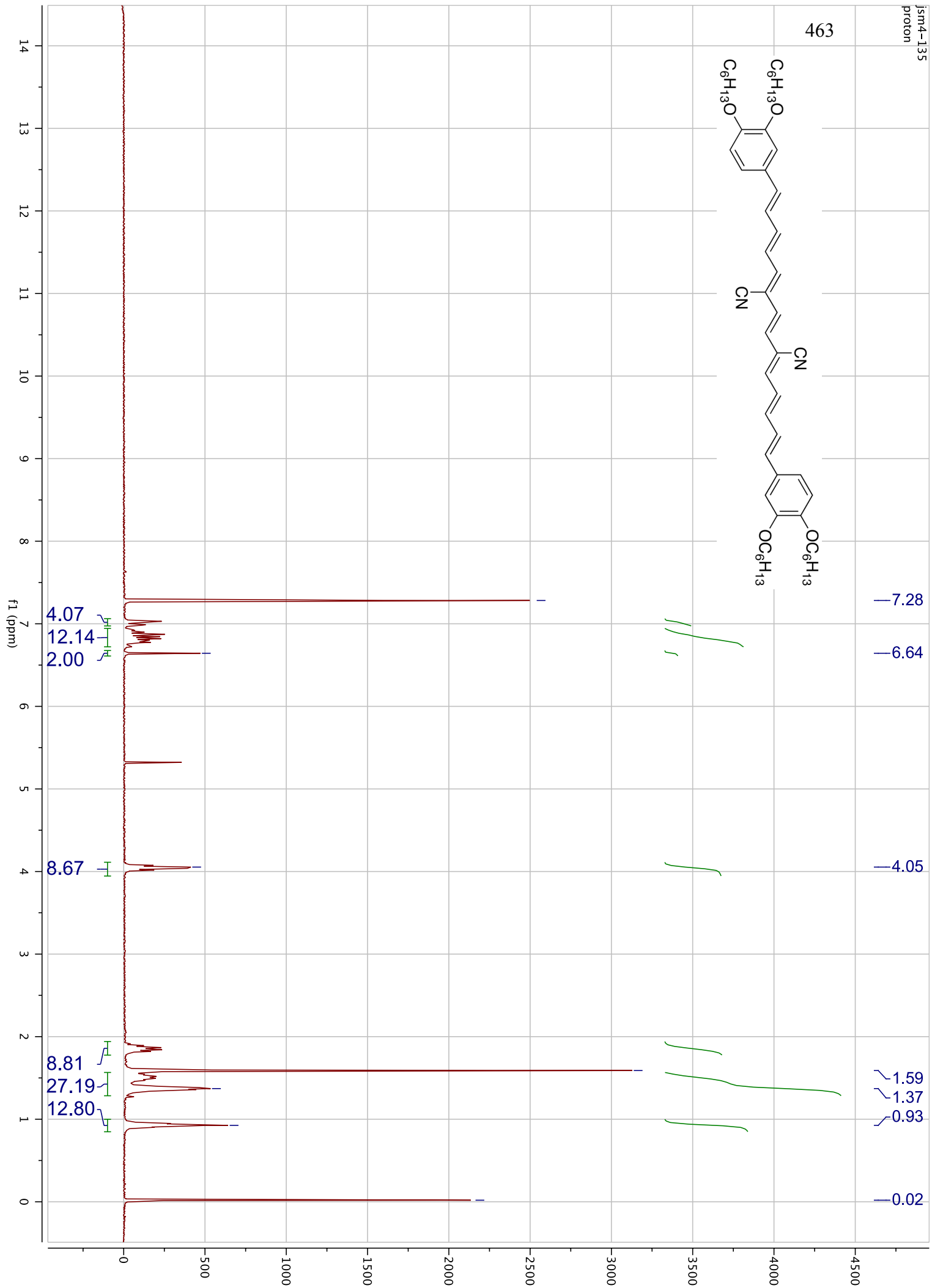
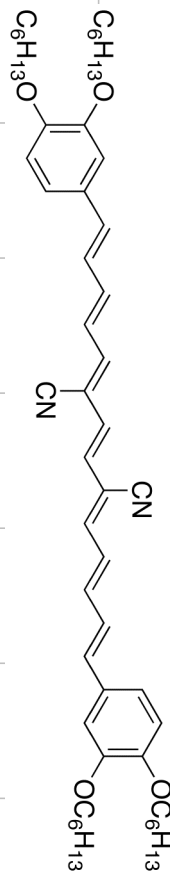
461



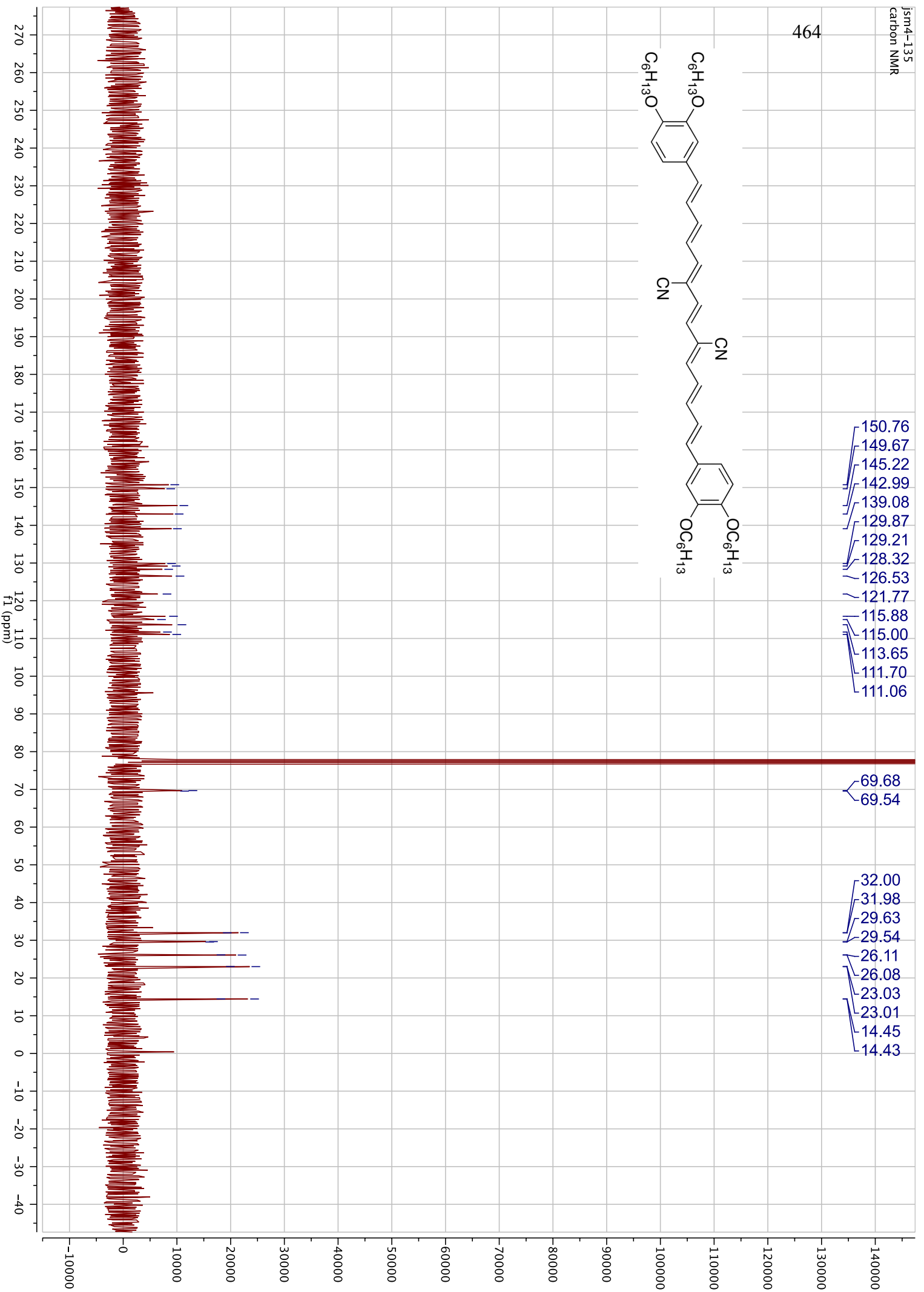
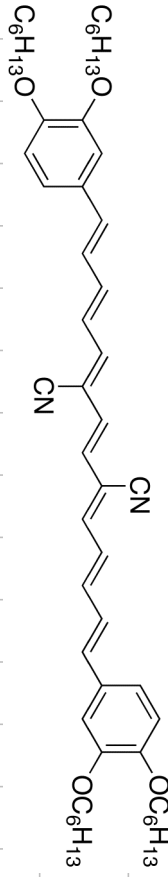
462



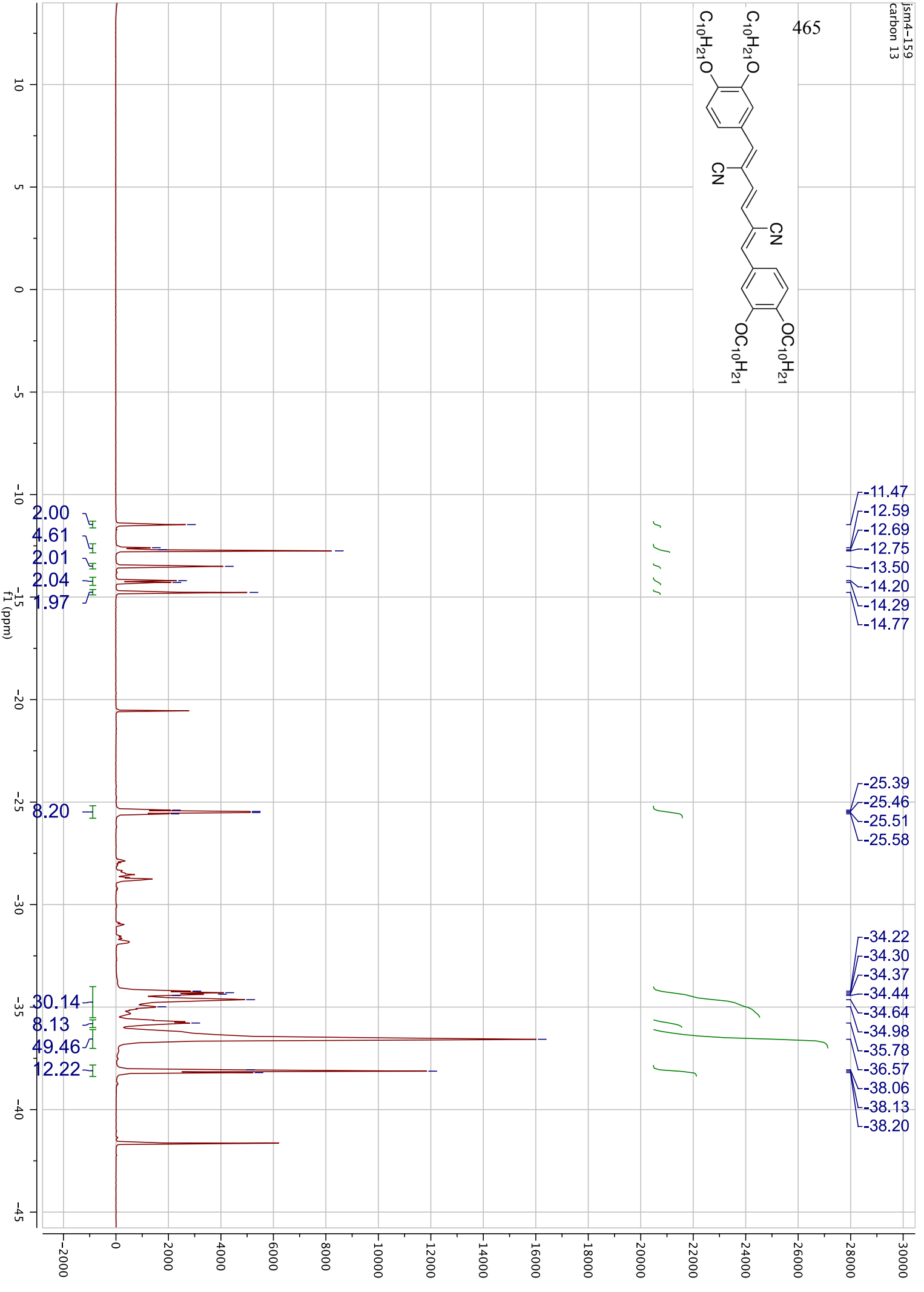
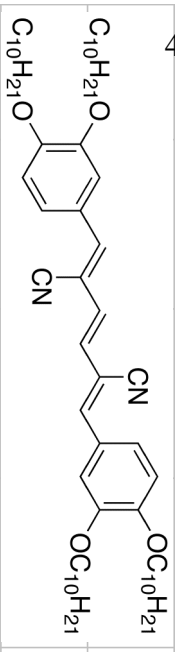
463

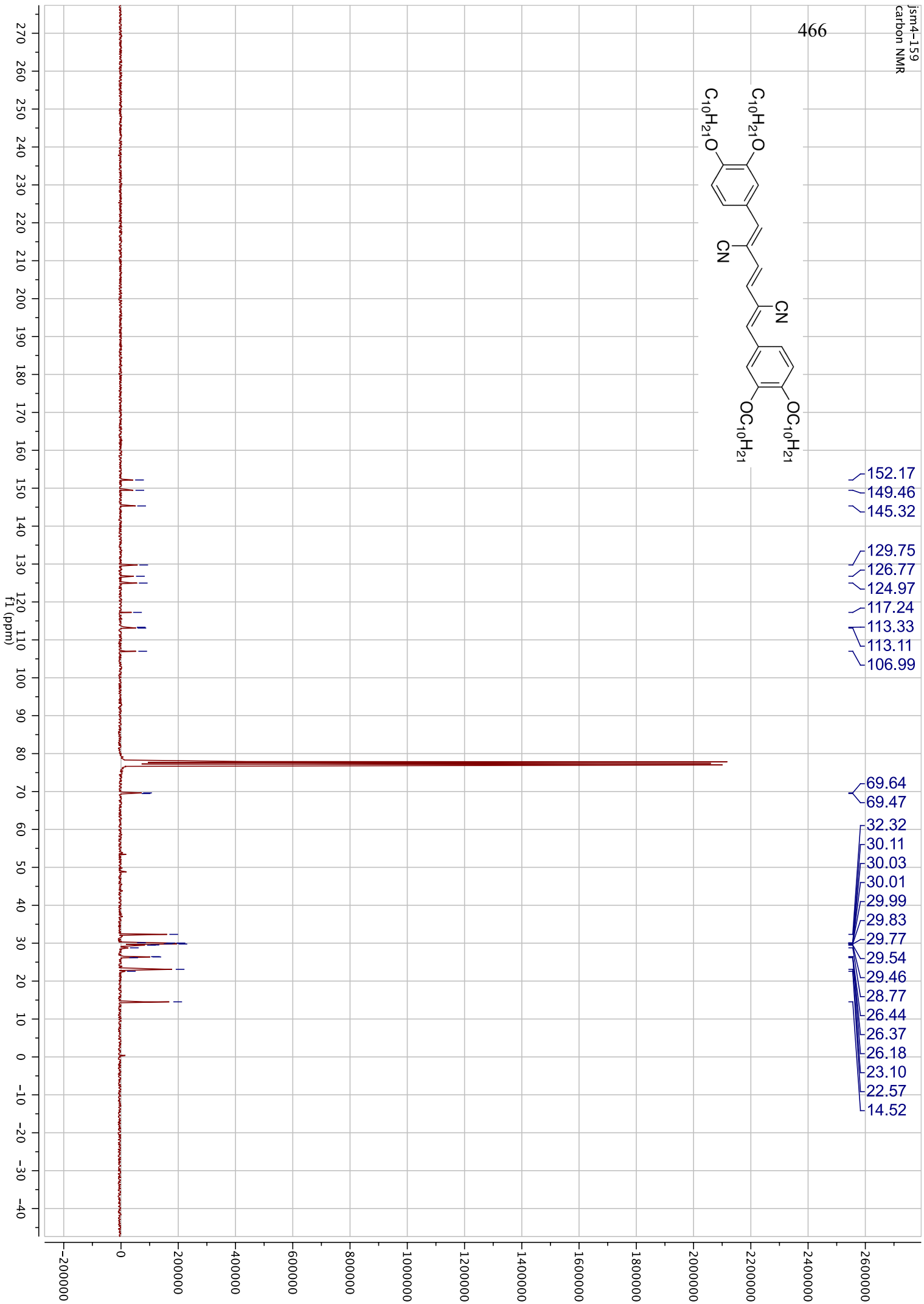
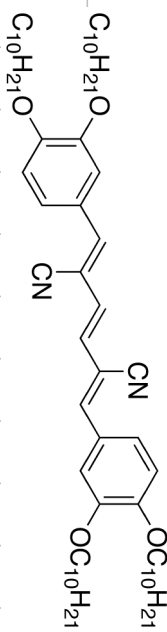


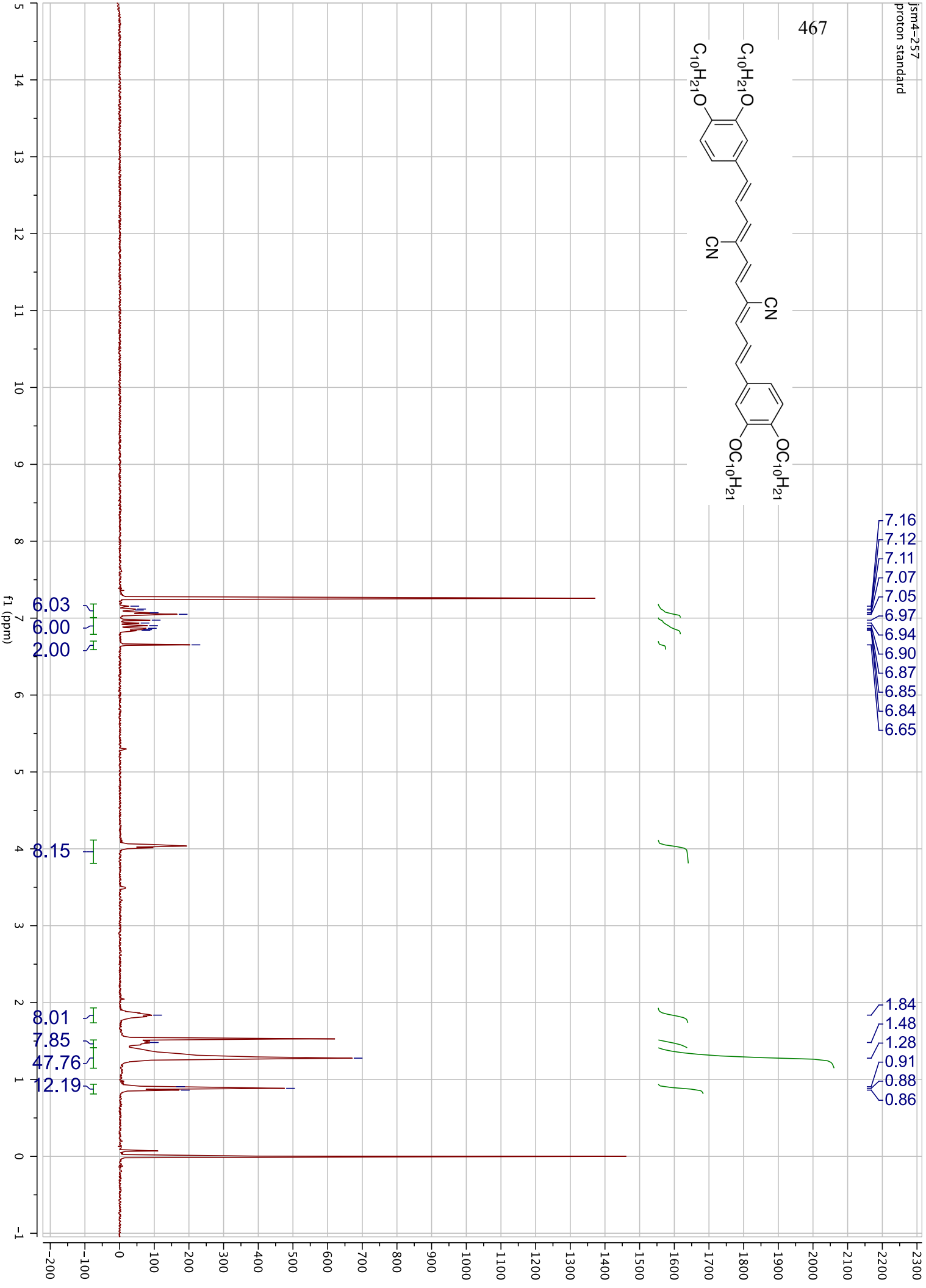
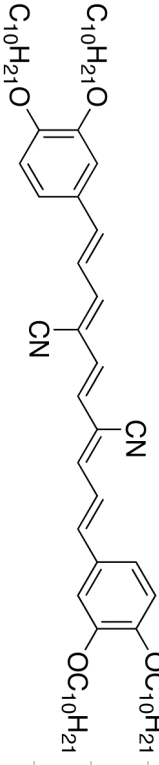
464

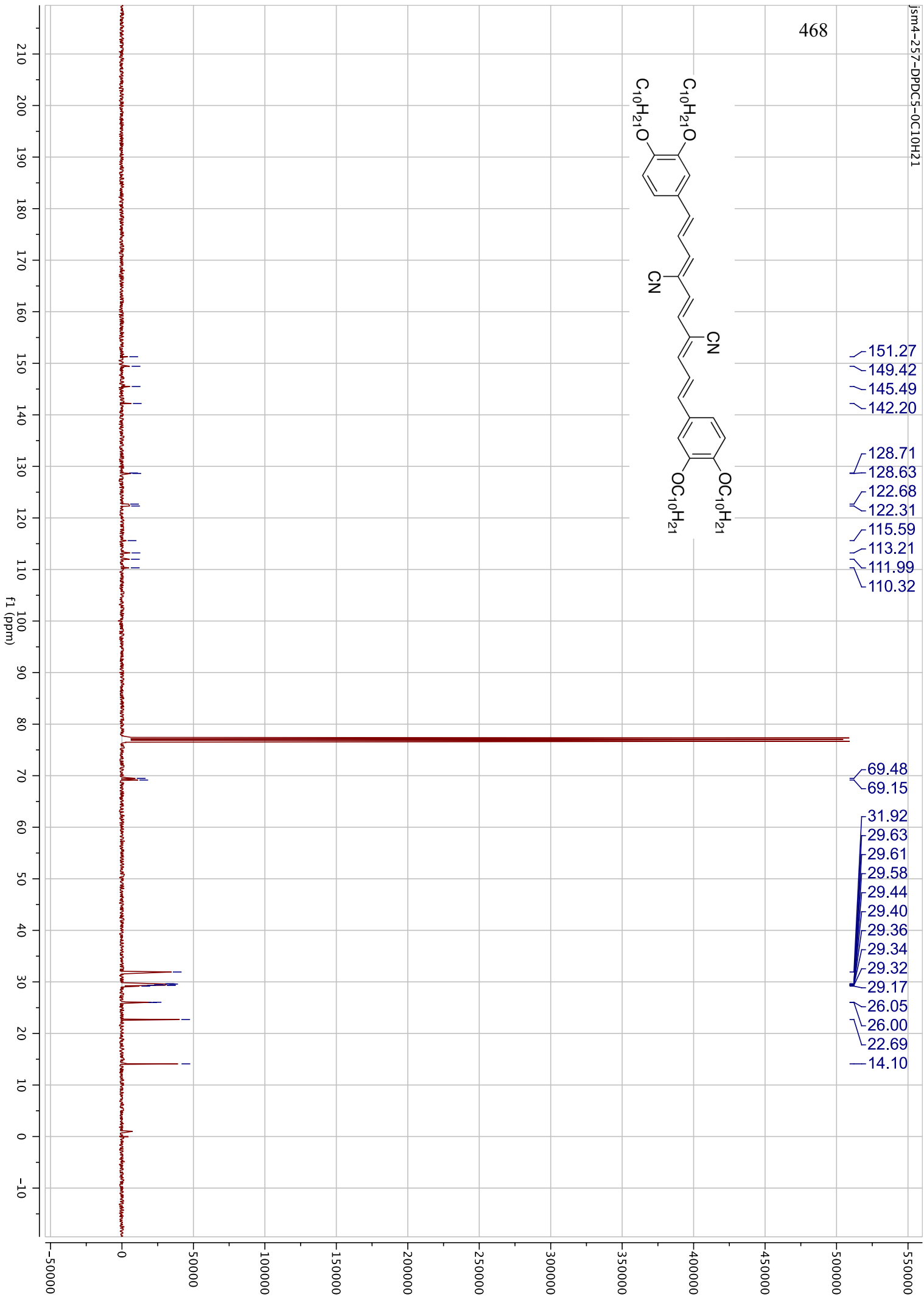


465

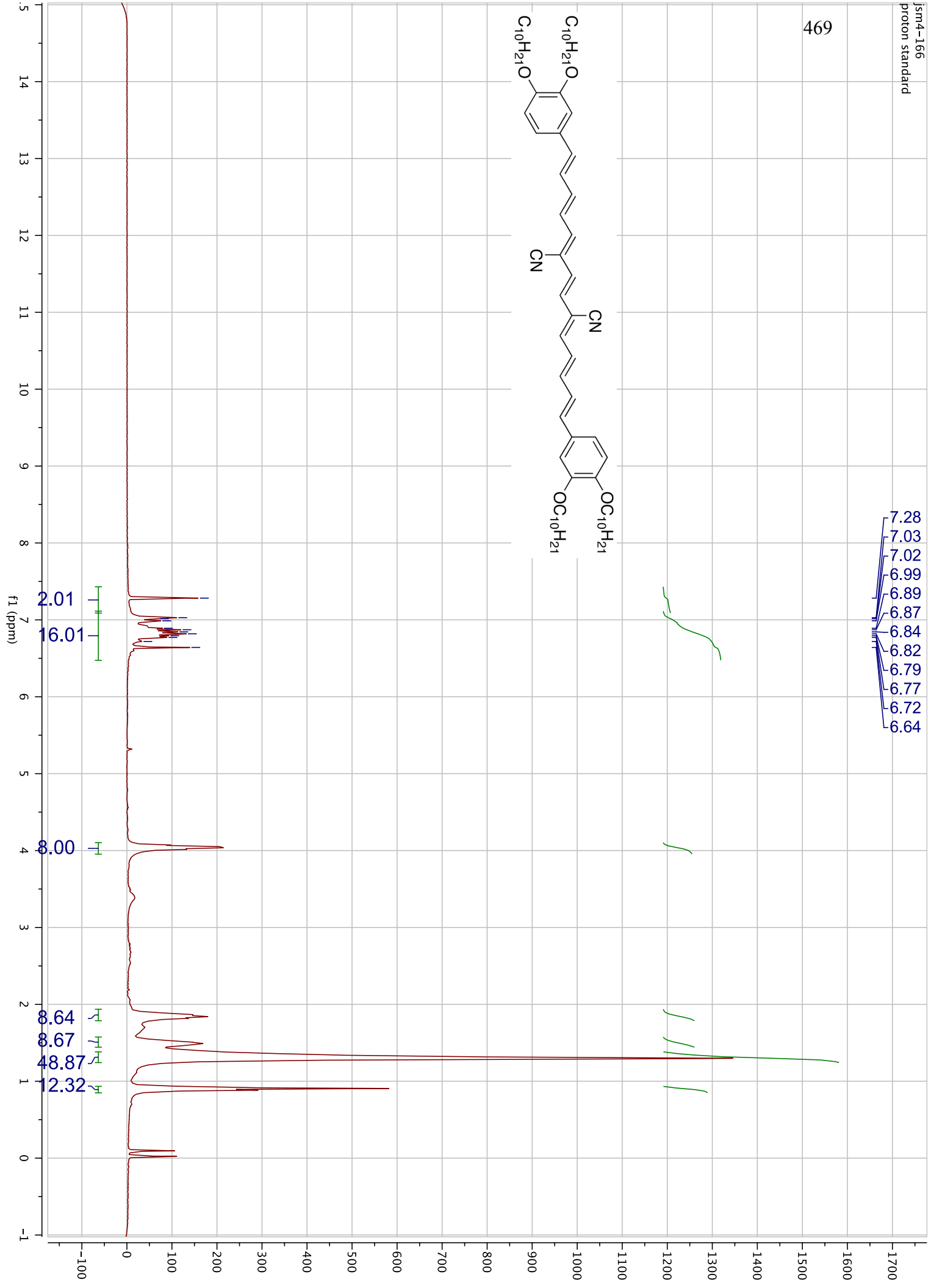
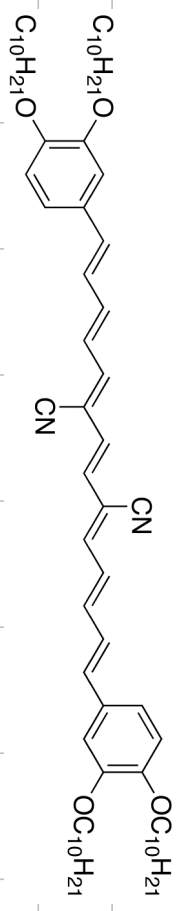




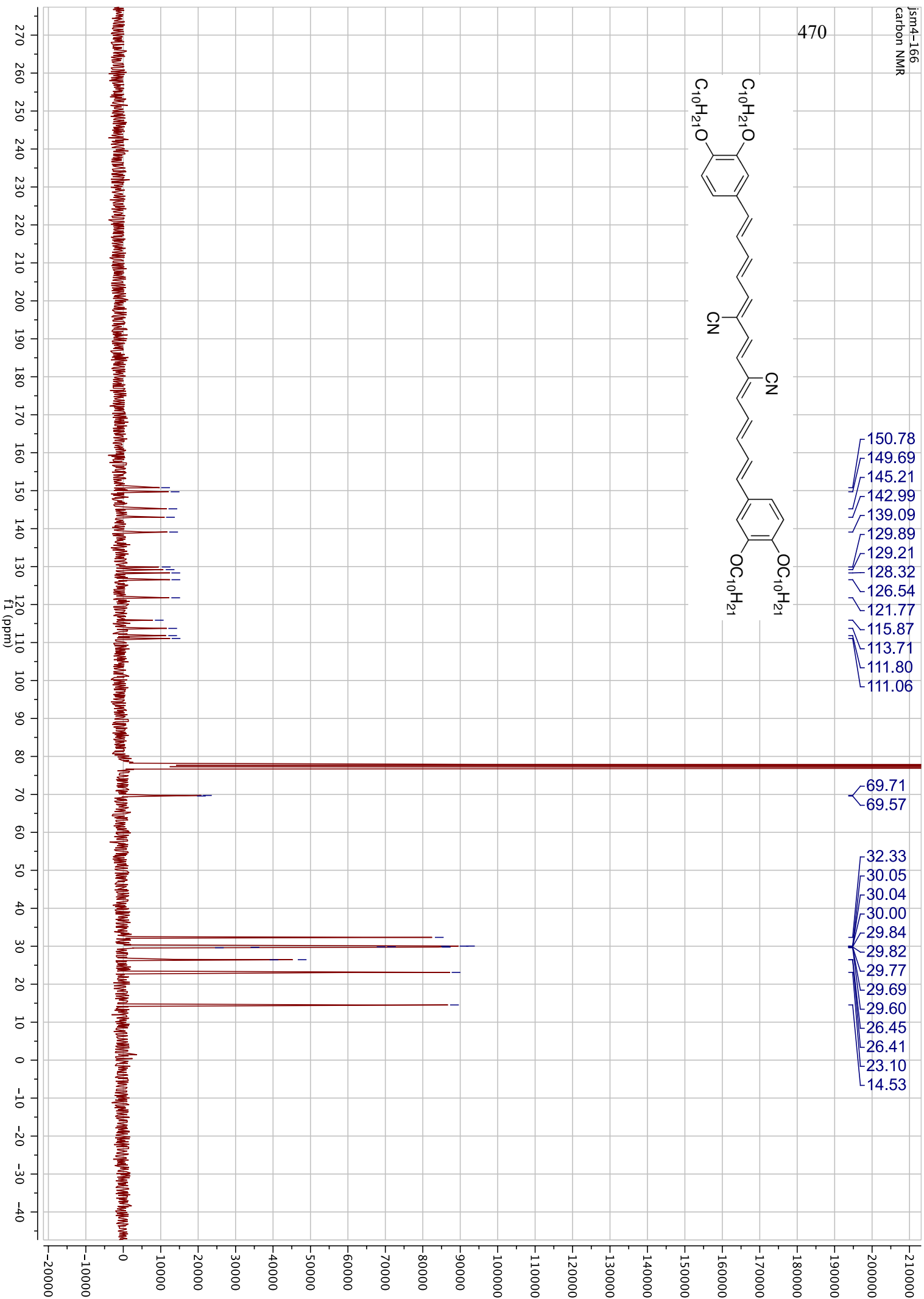
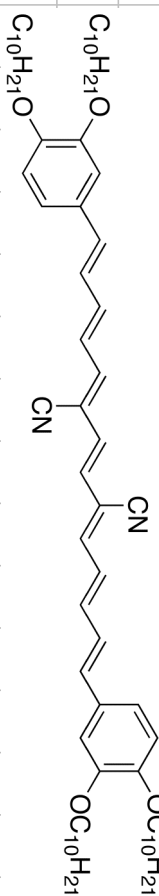




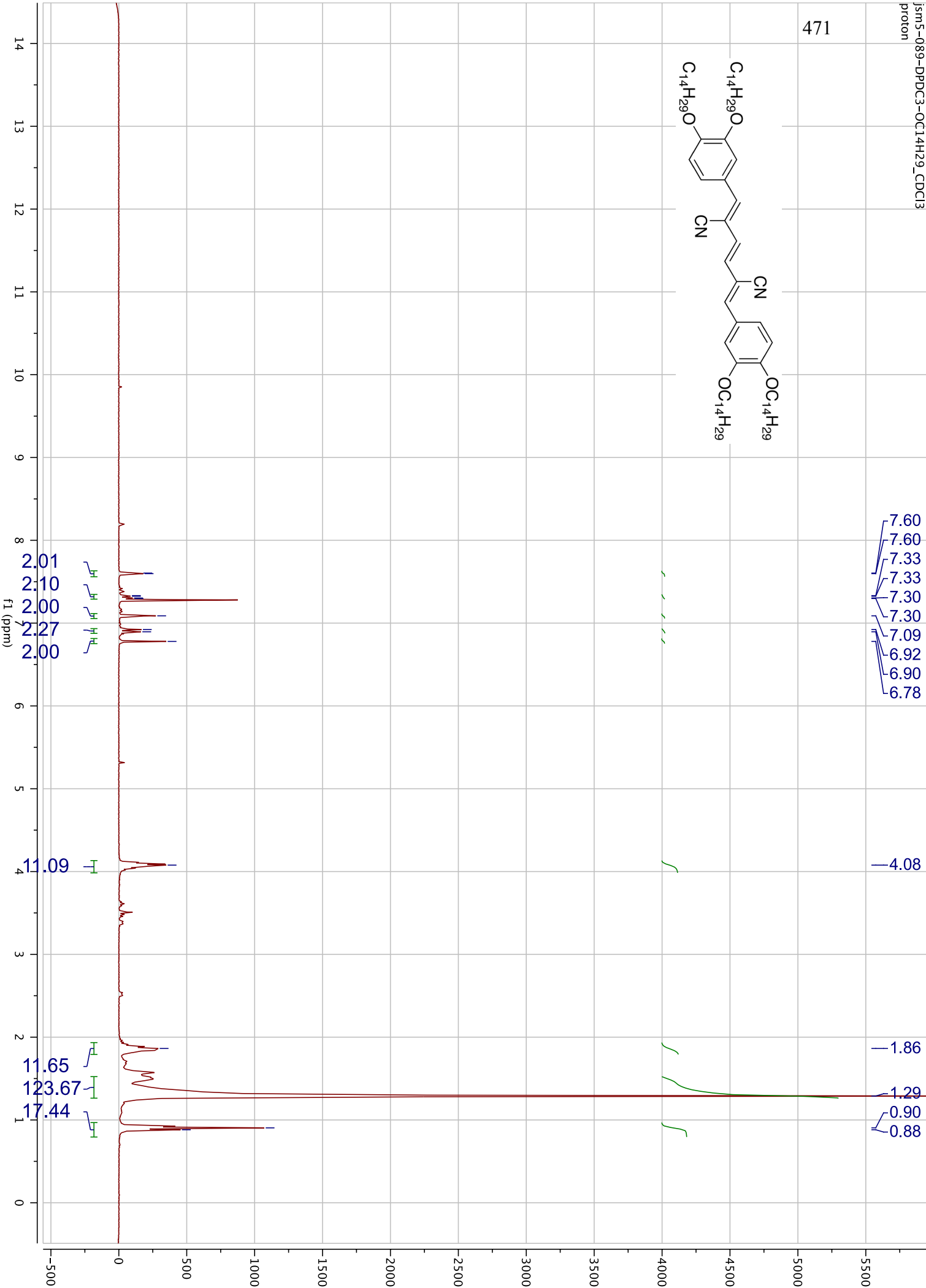
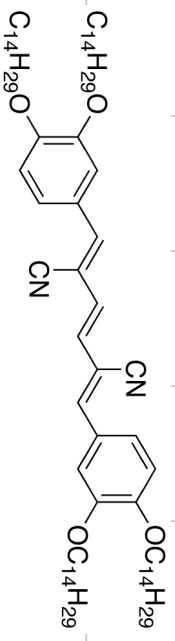


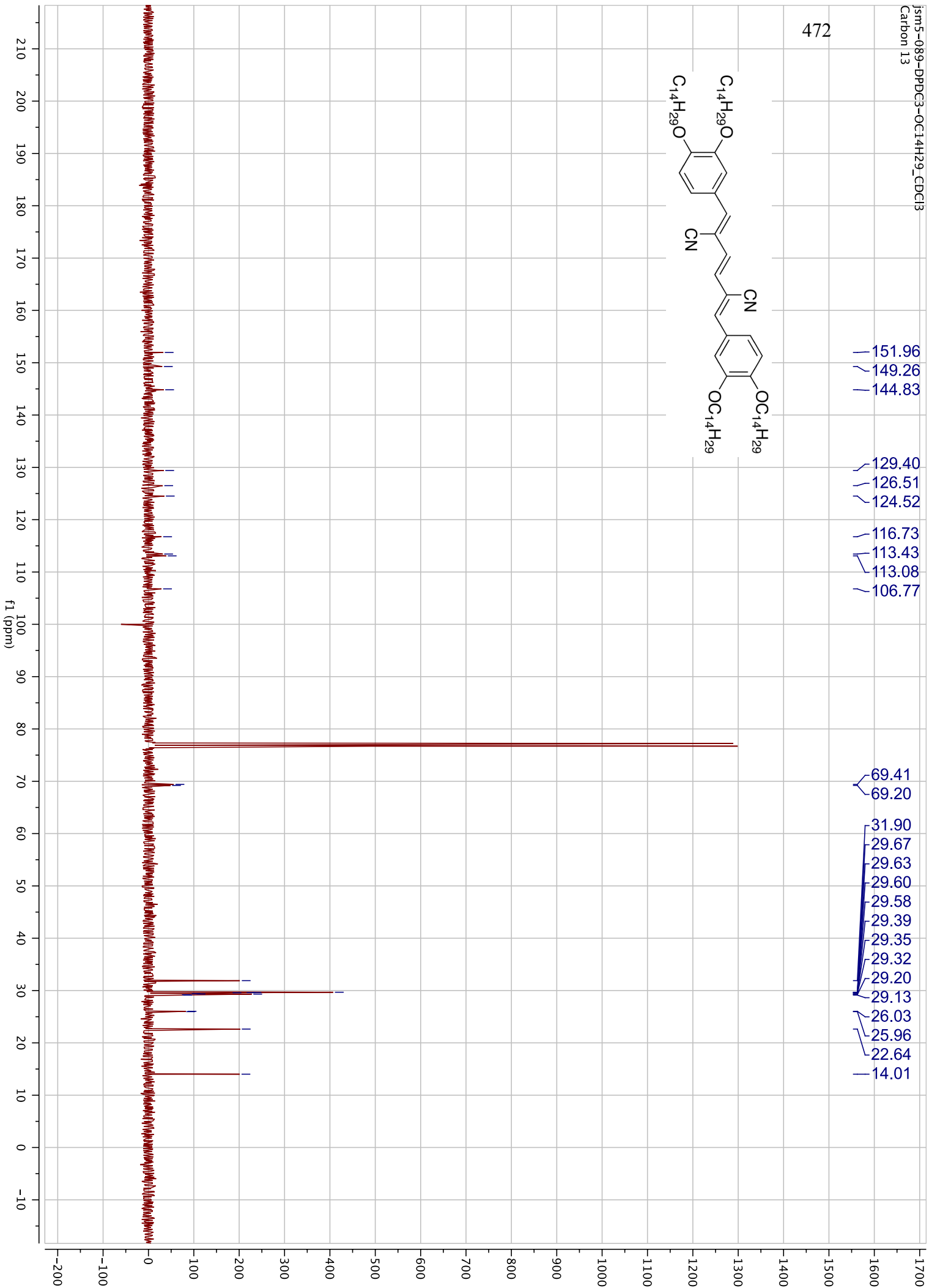
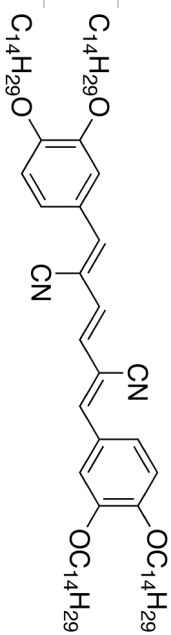


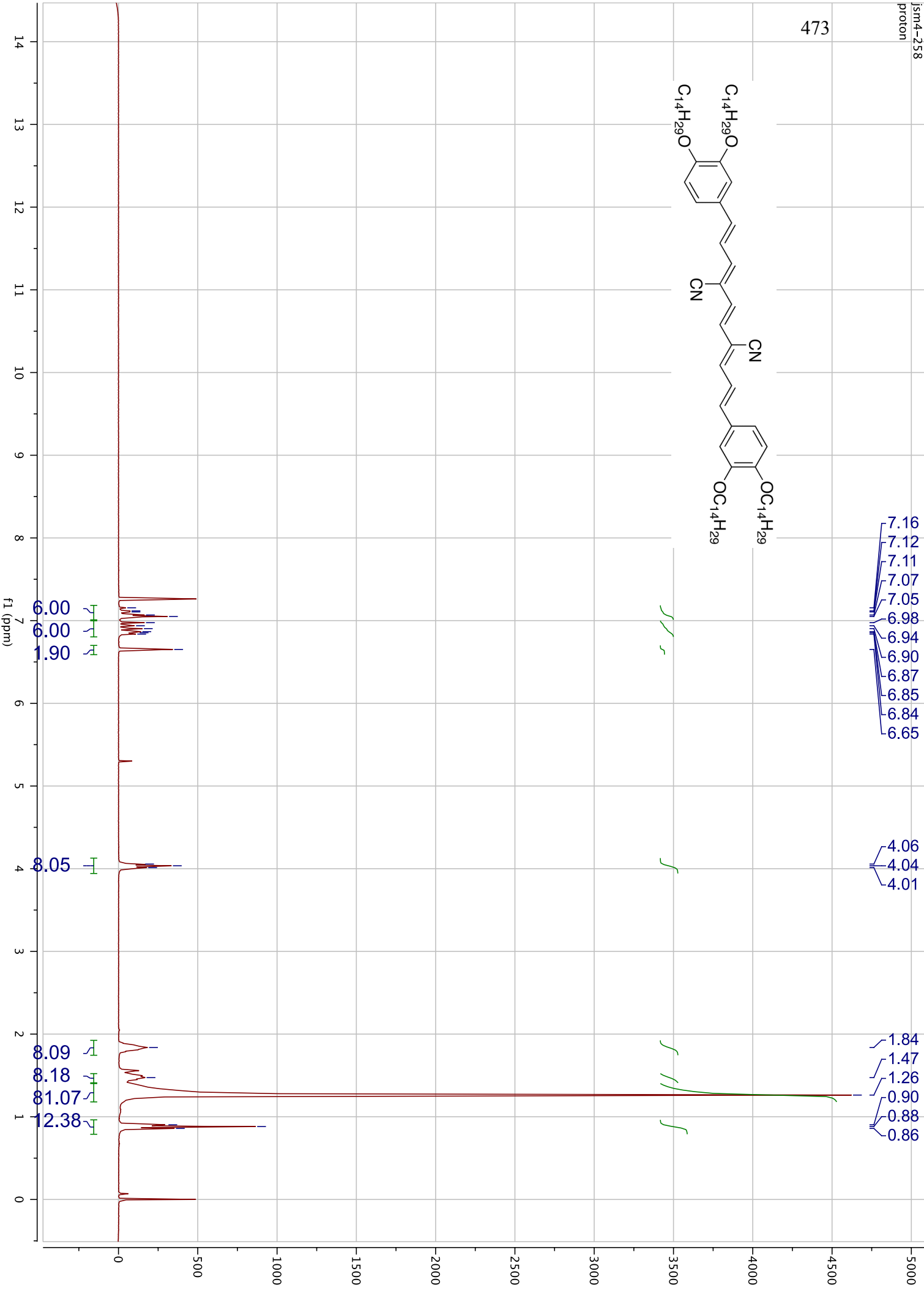
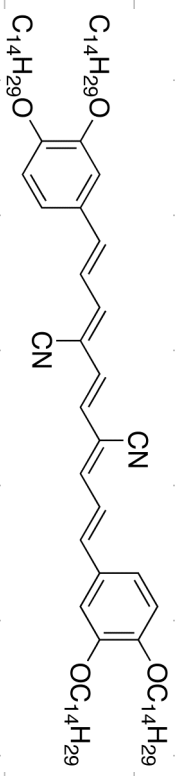
470



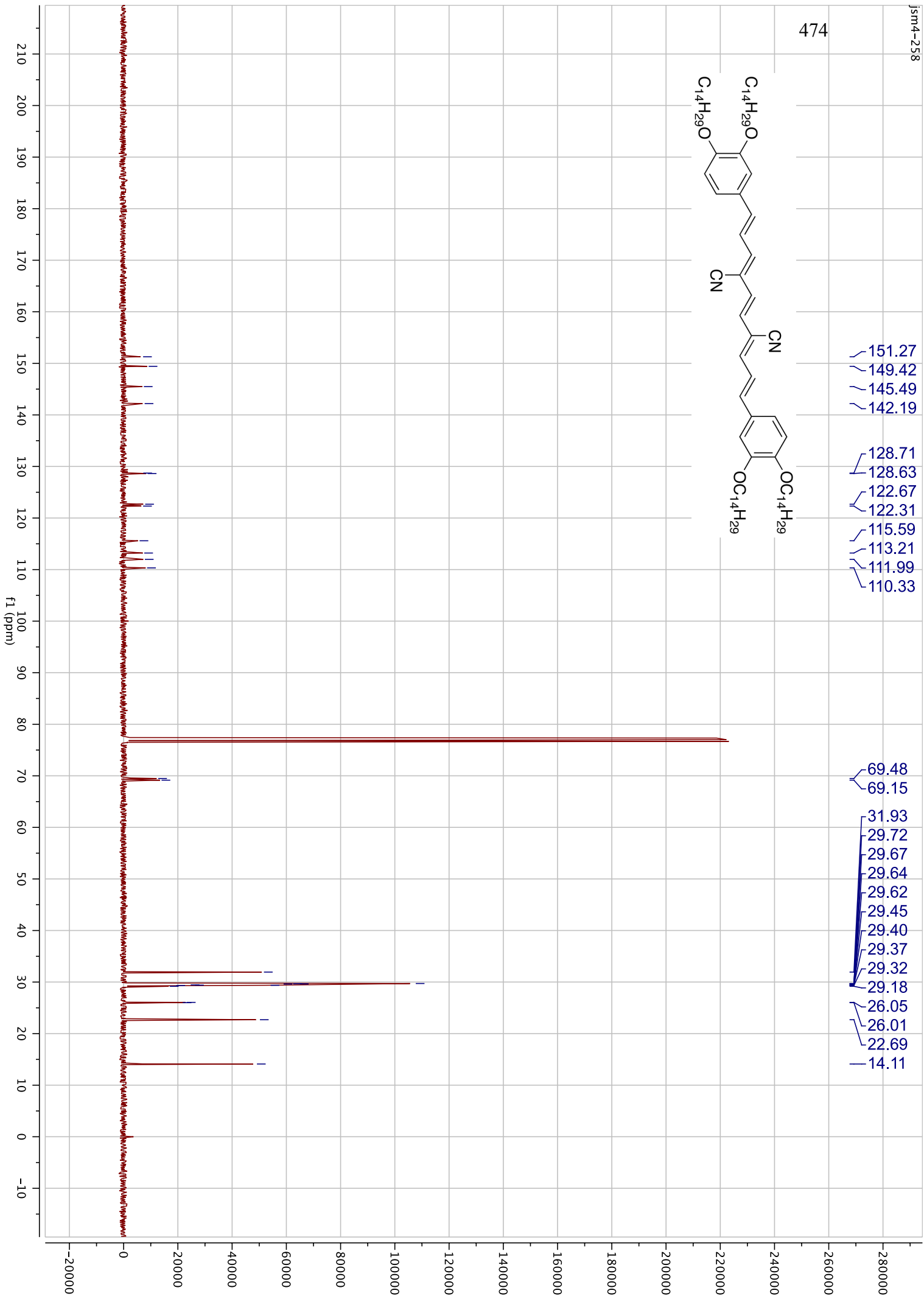
471

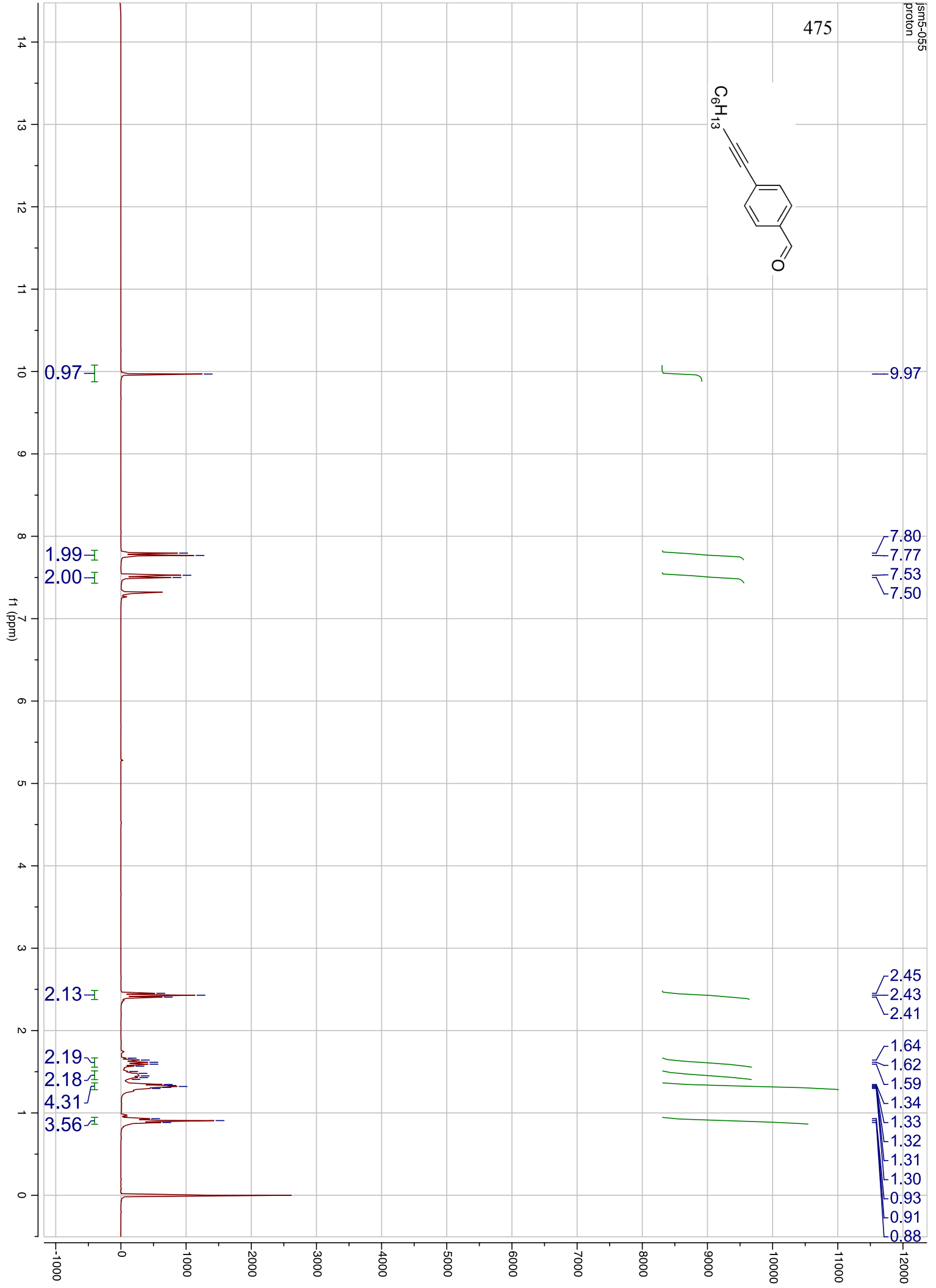
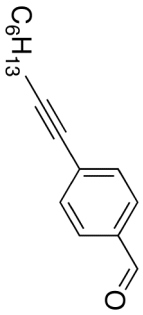




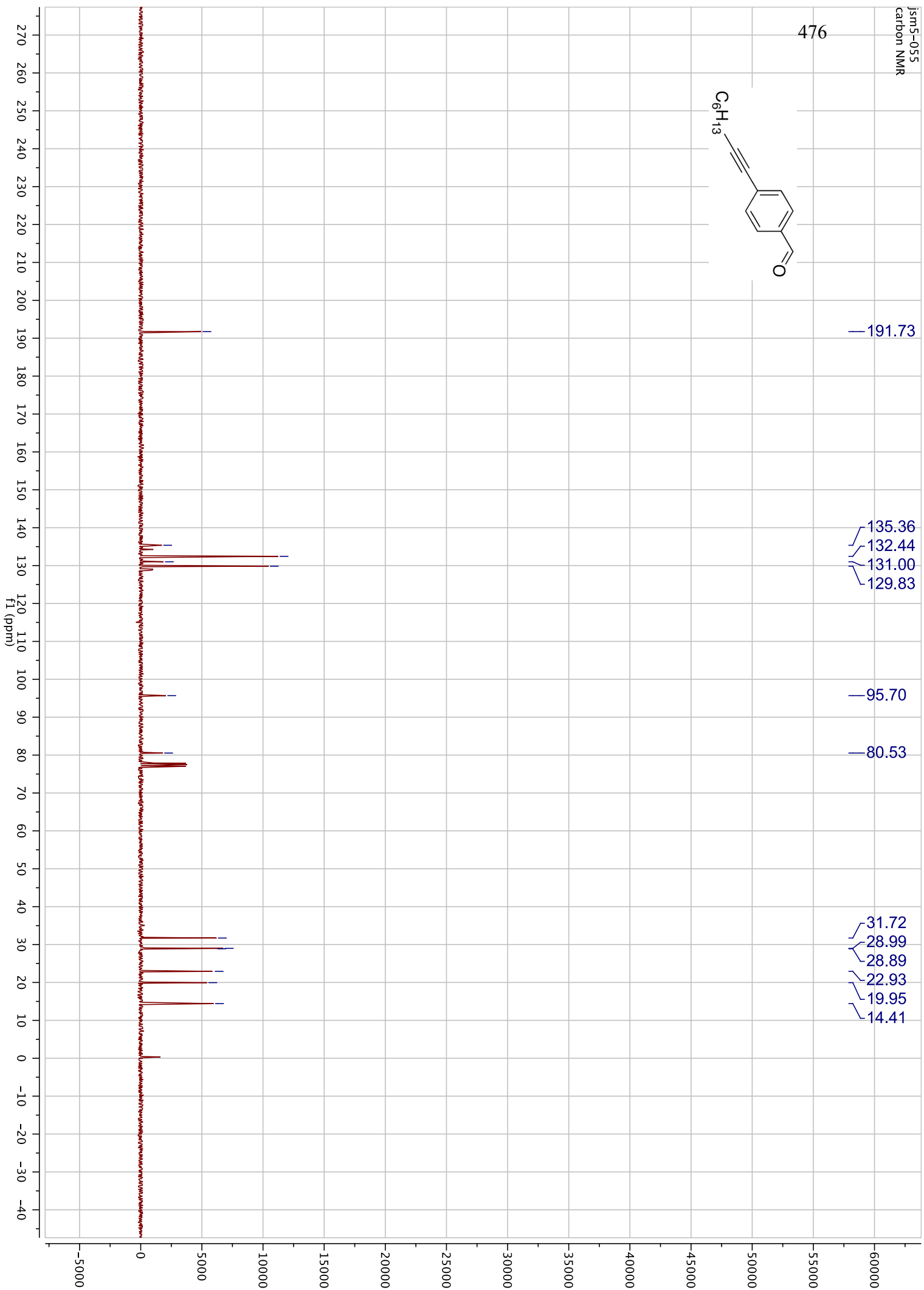
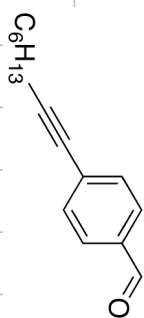


474

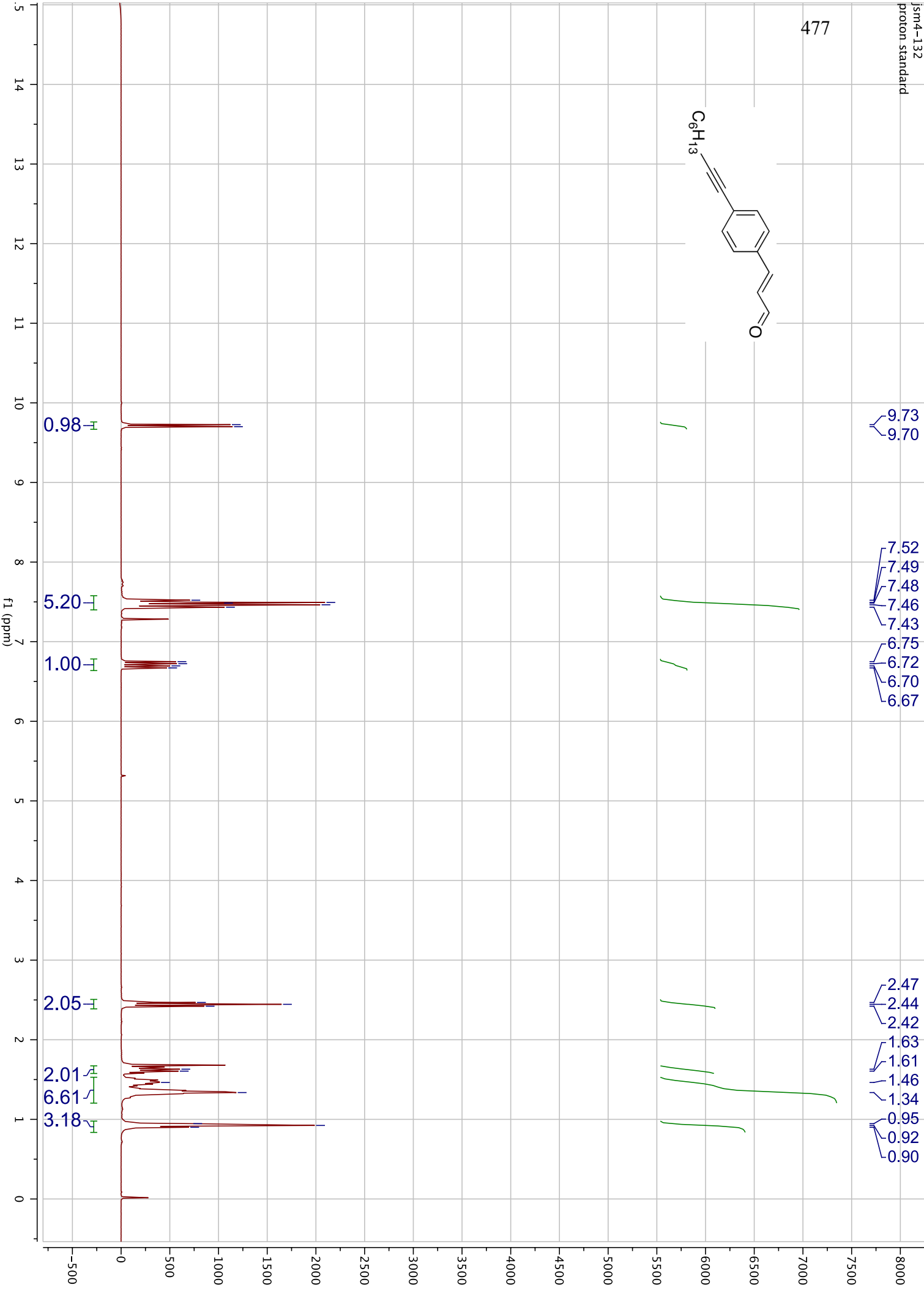
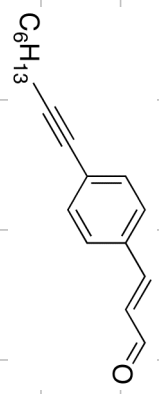




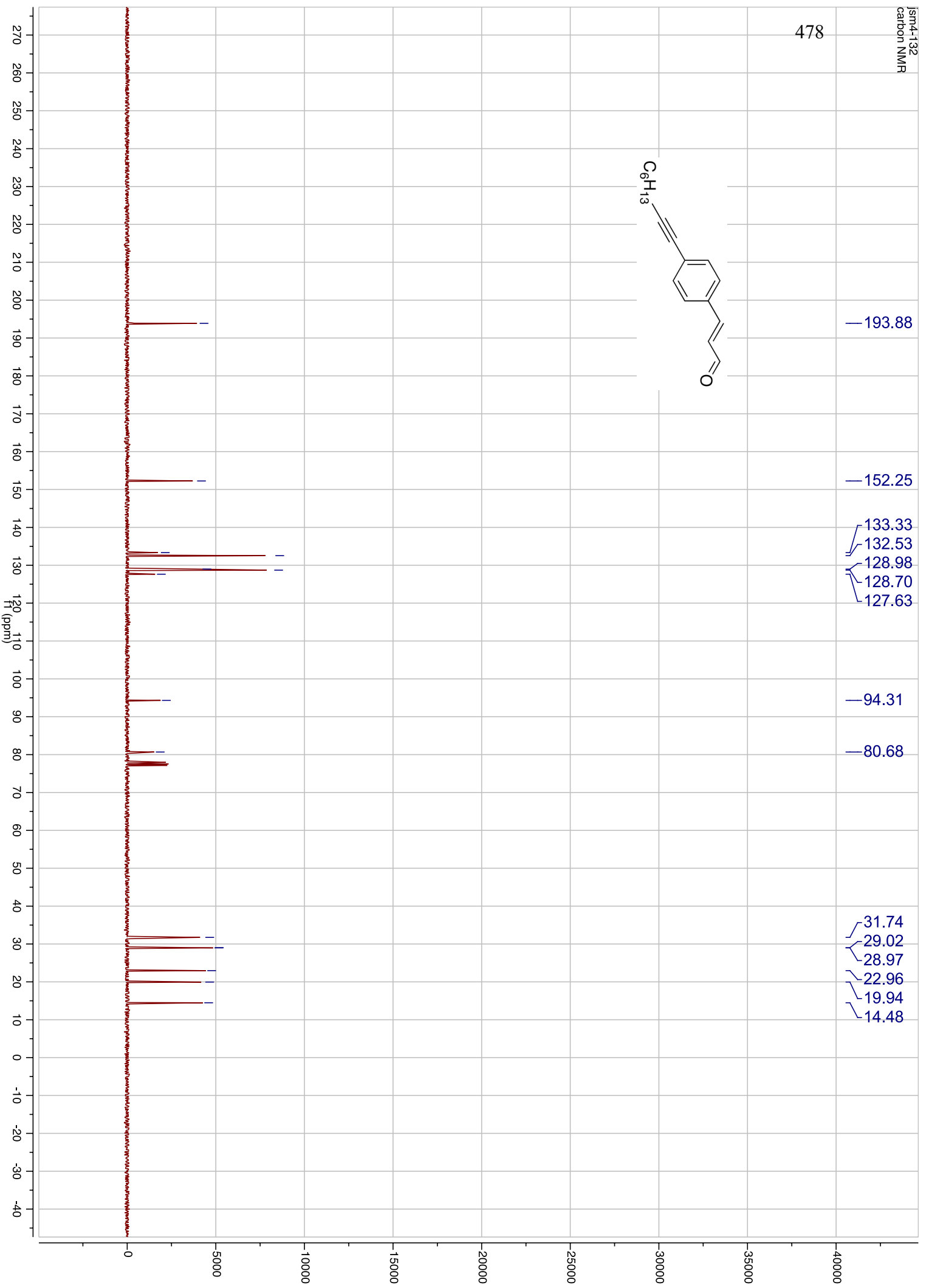
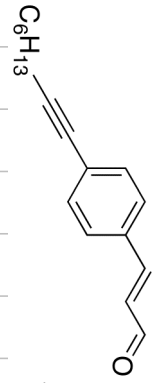
476

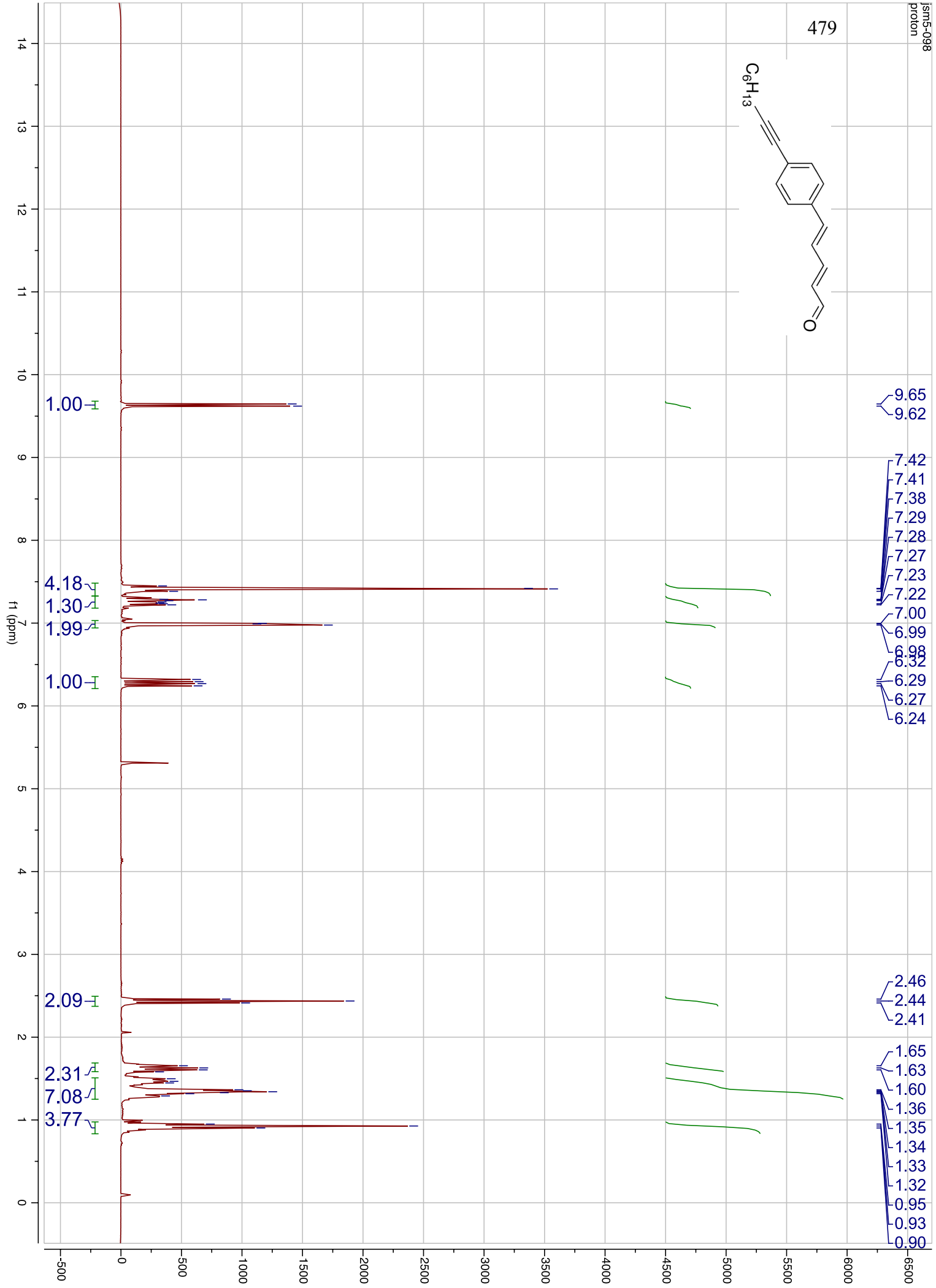
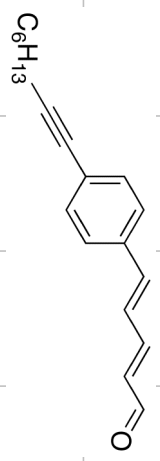




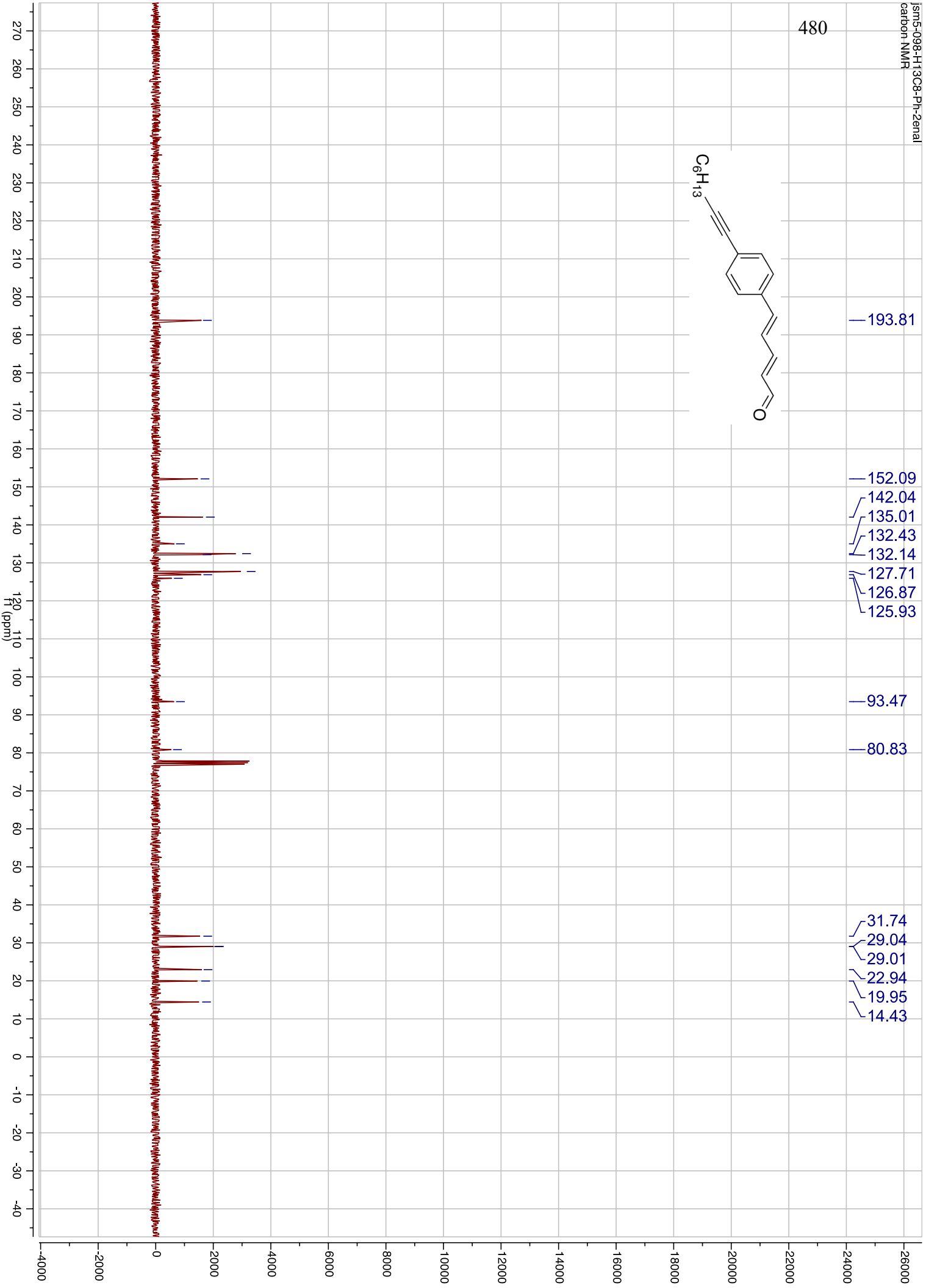
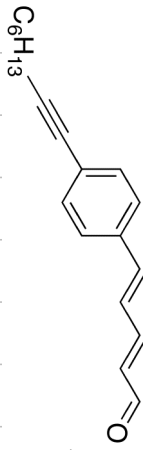


478

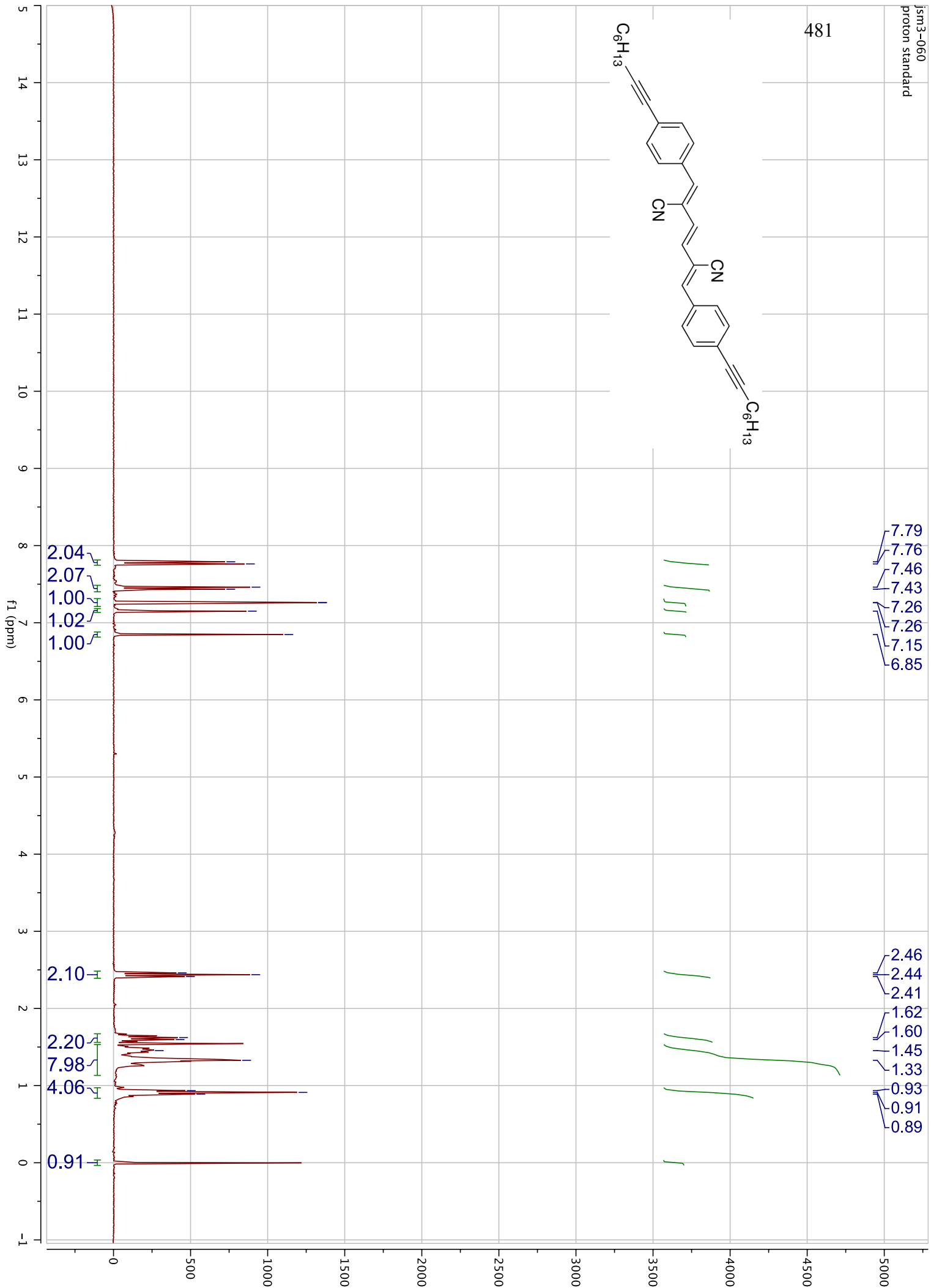
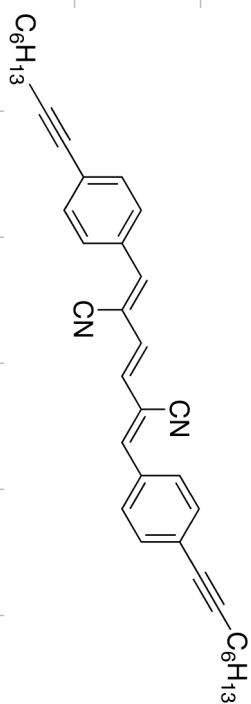


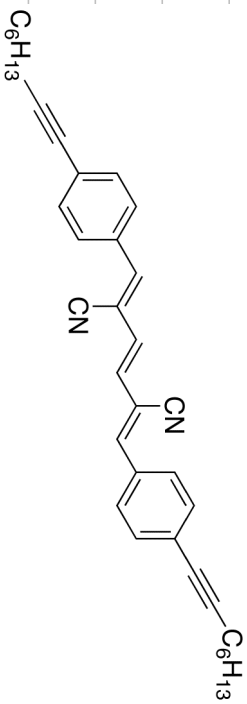


480

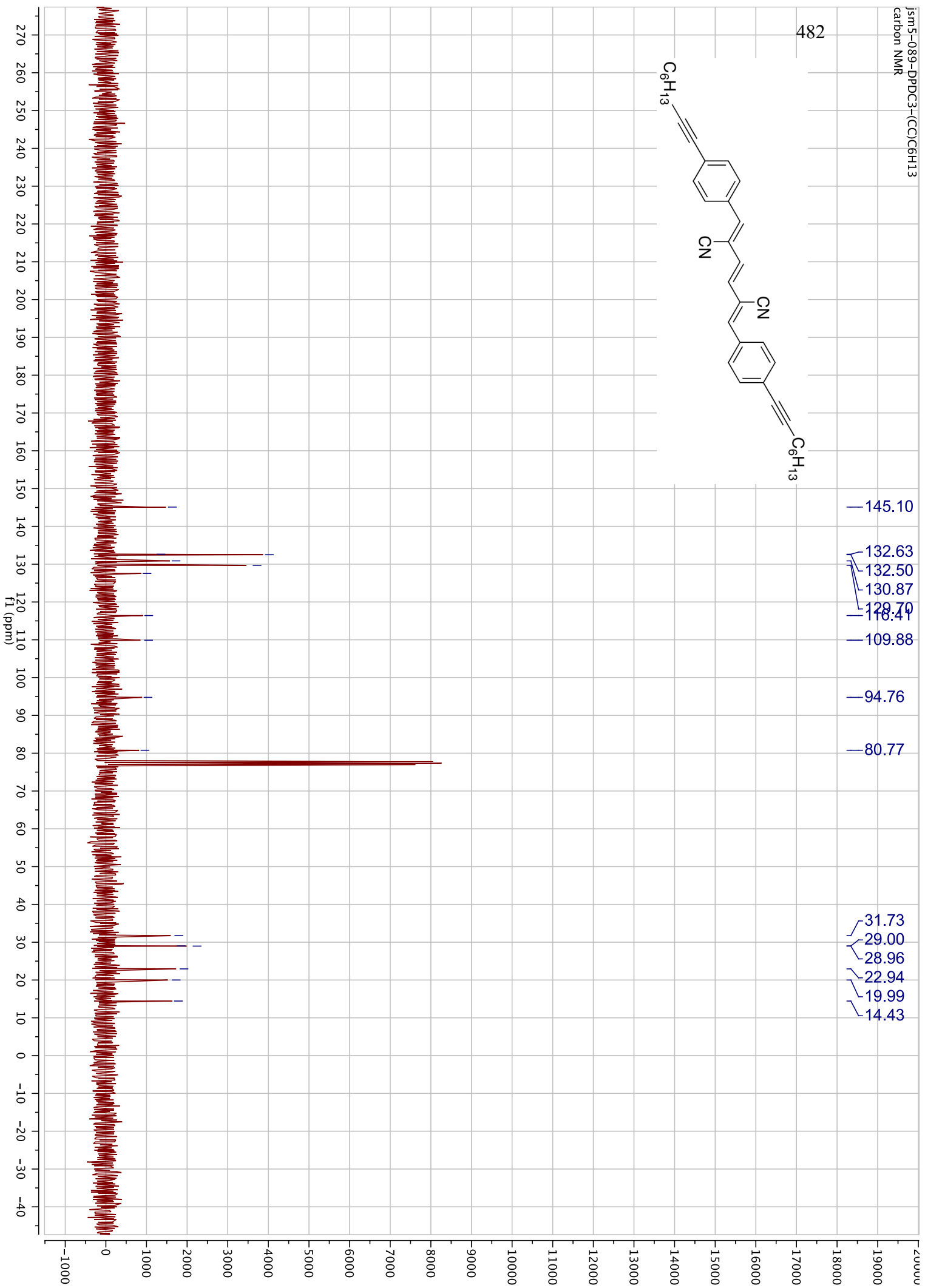


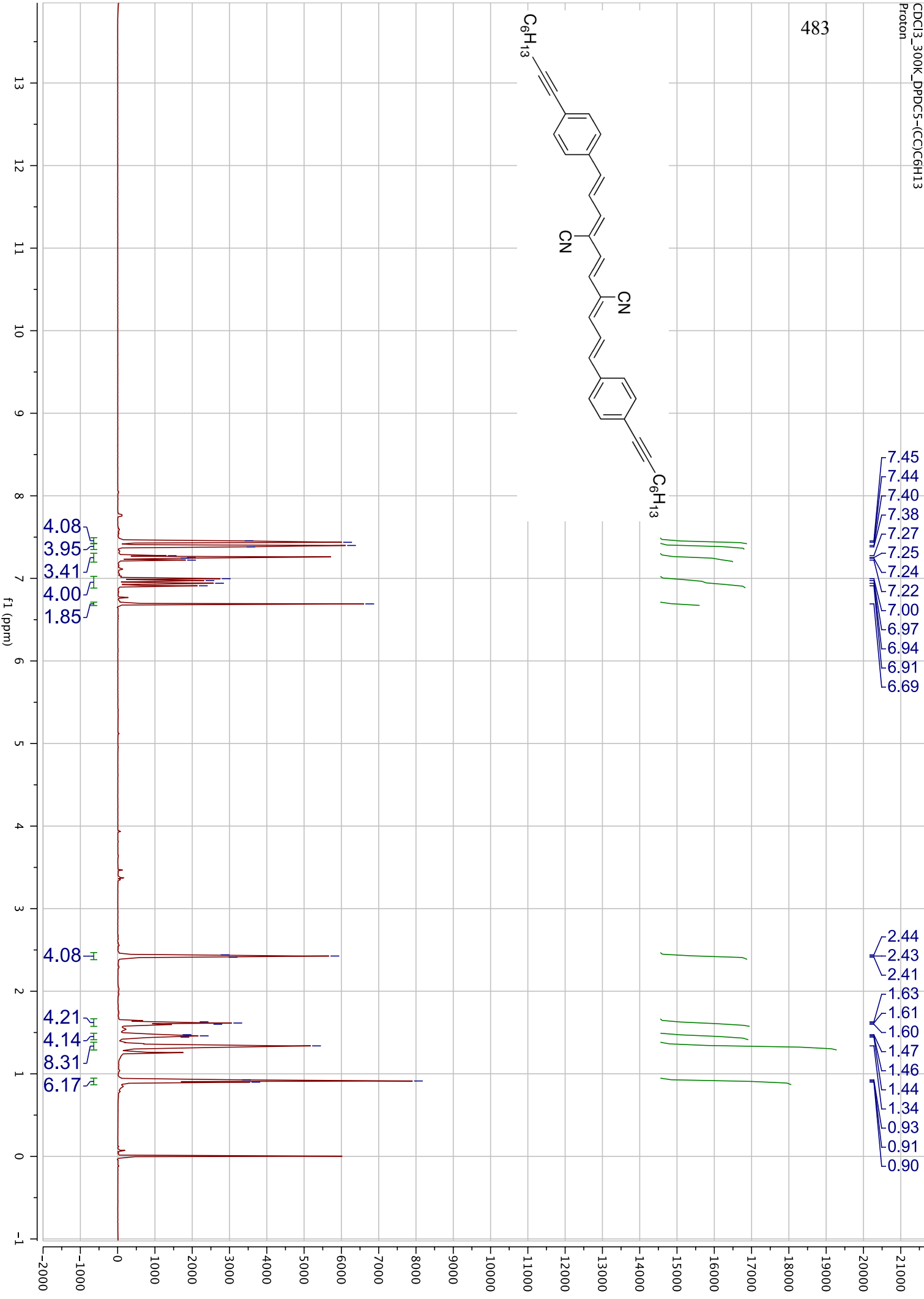
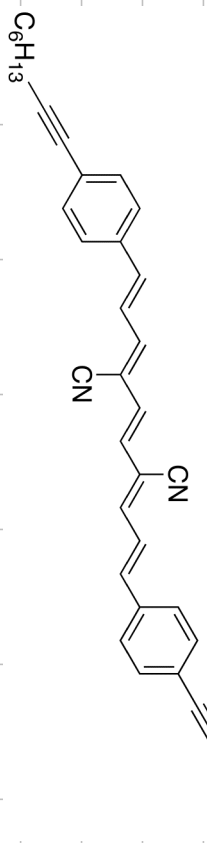
481



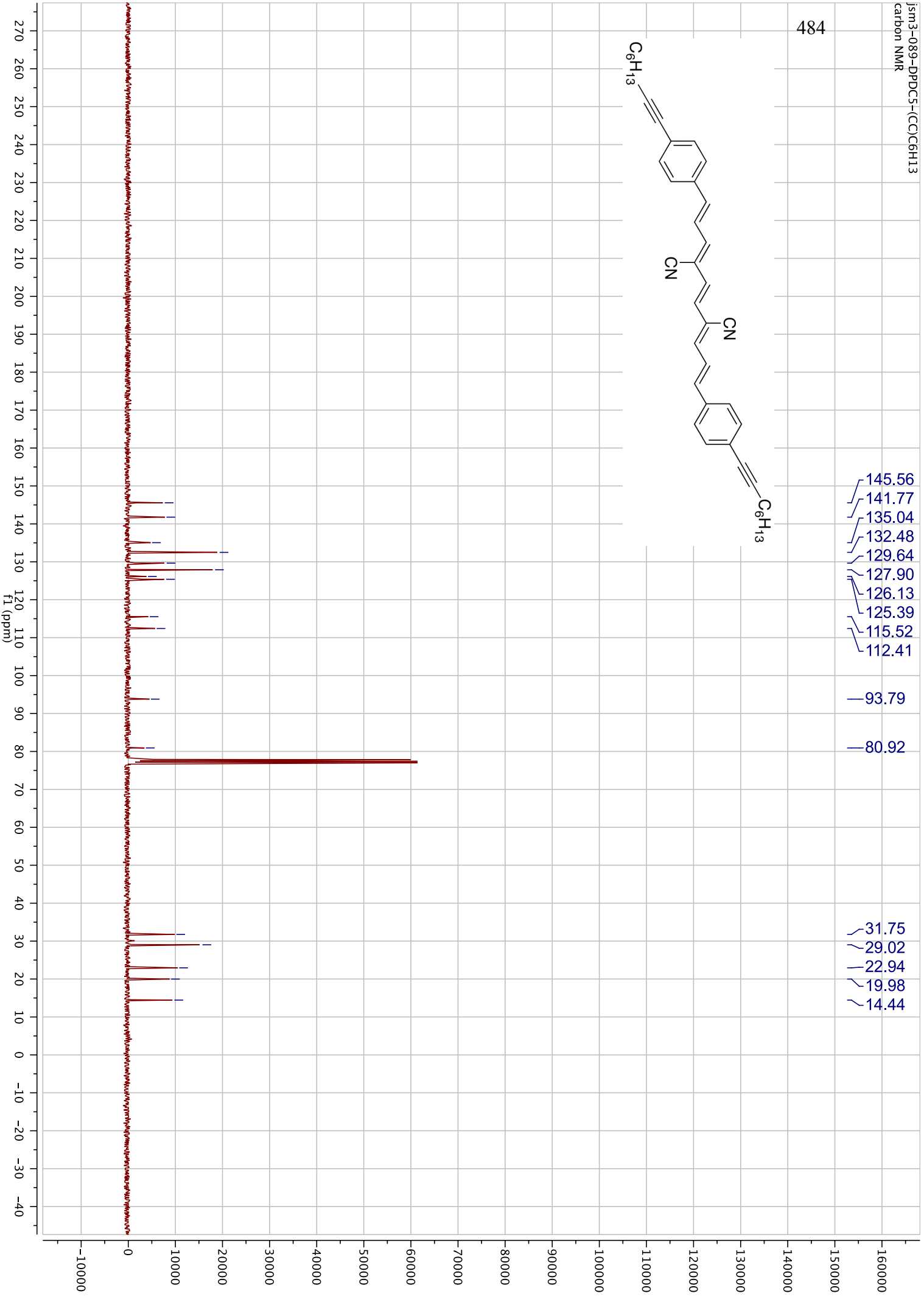
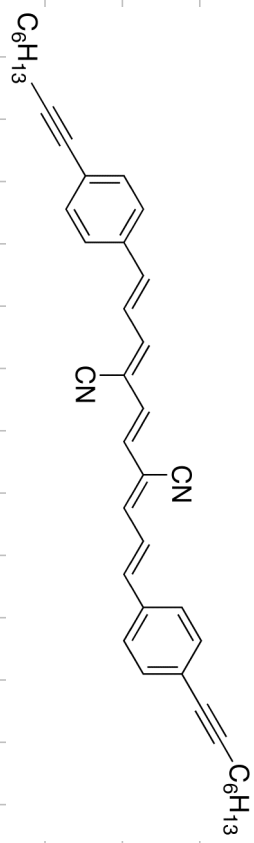


482

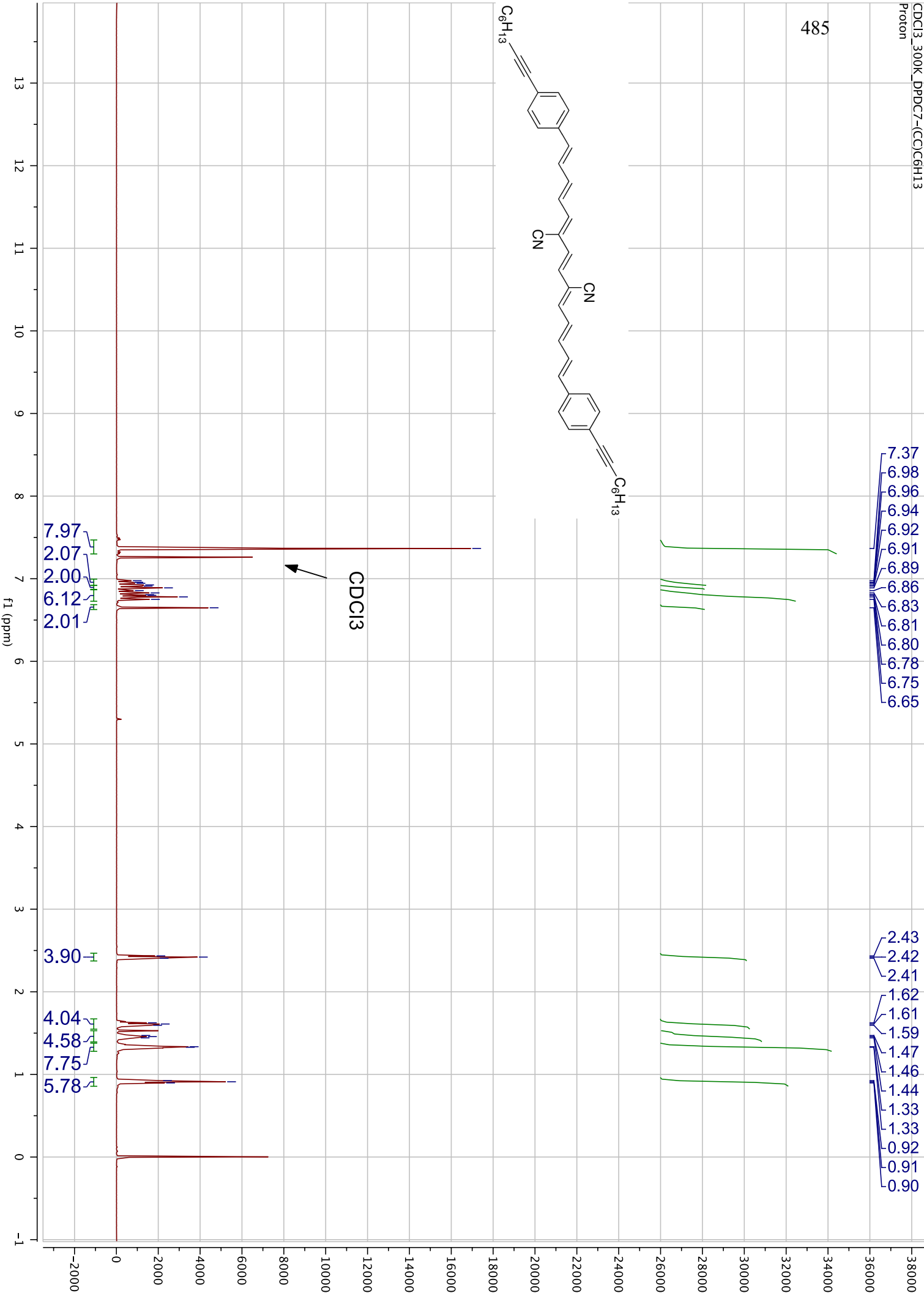
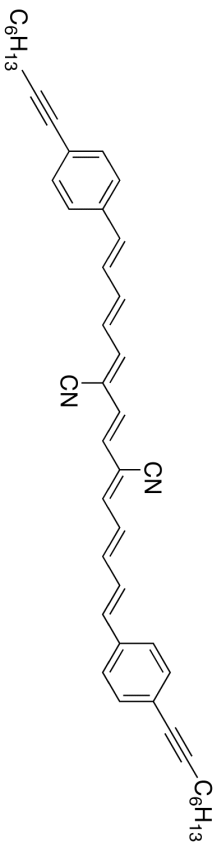


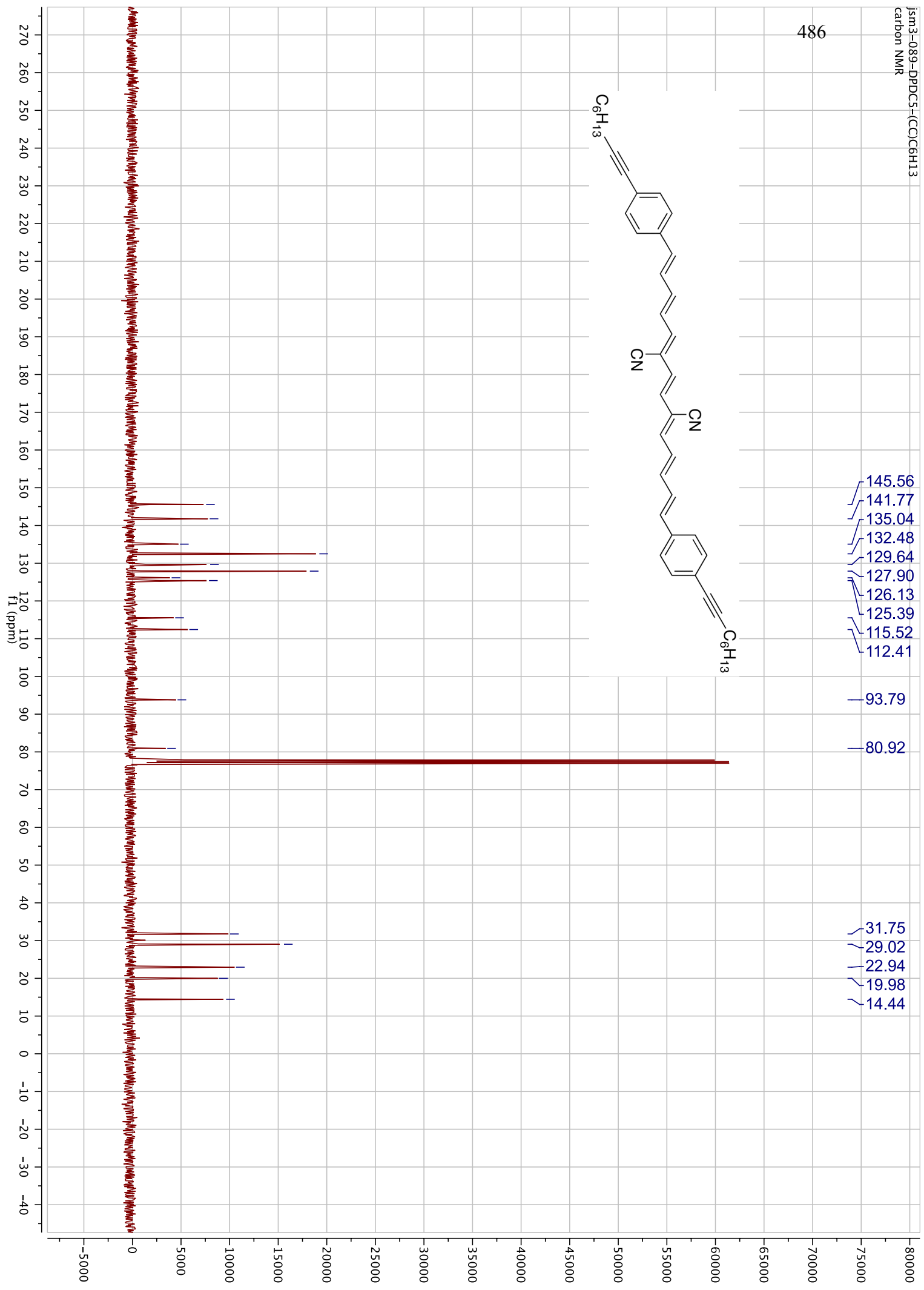
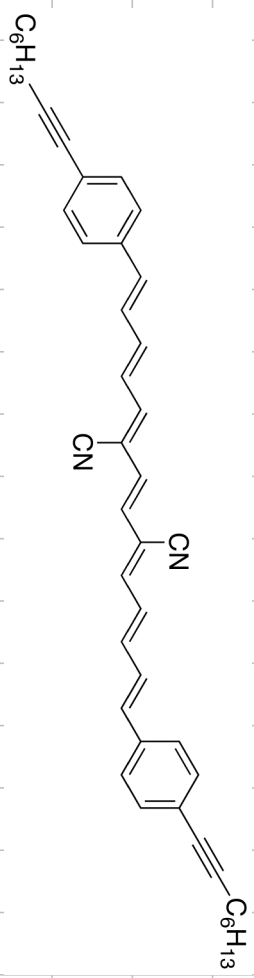


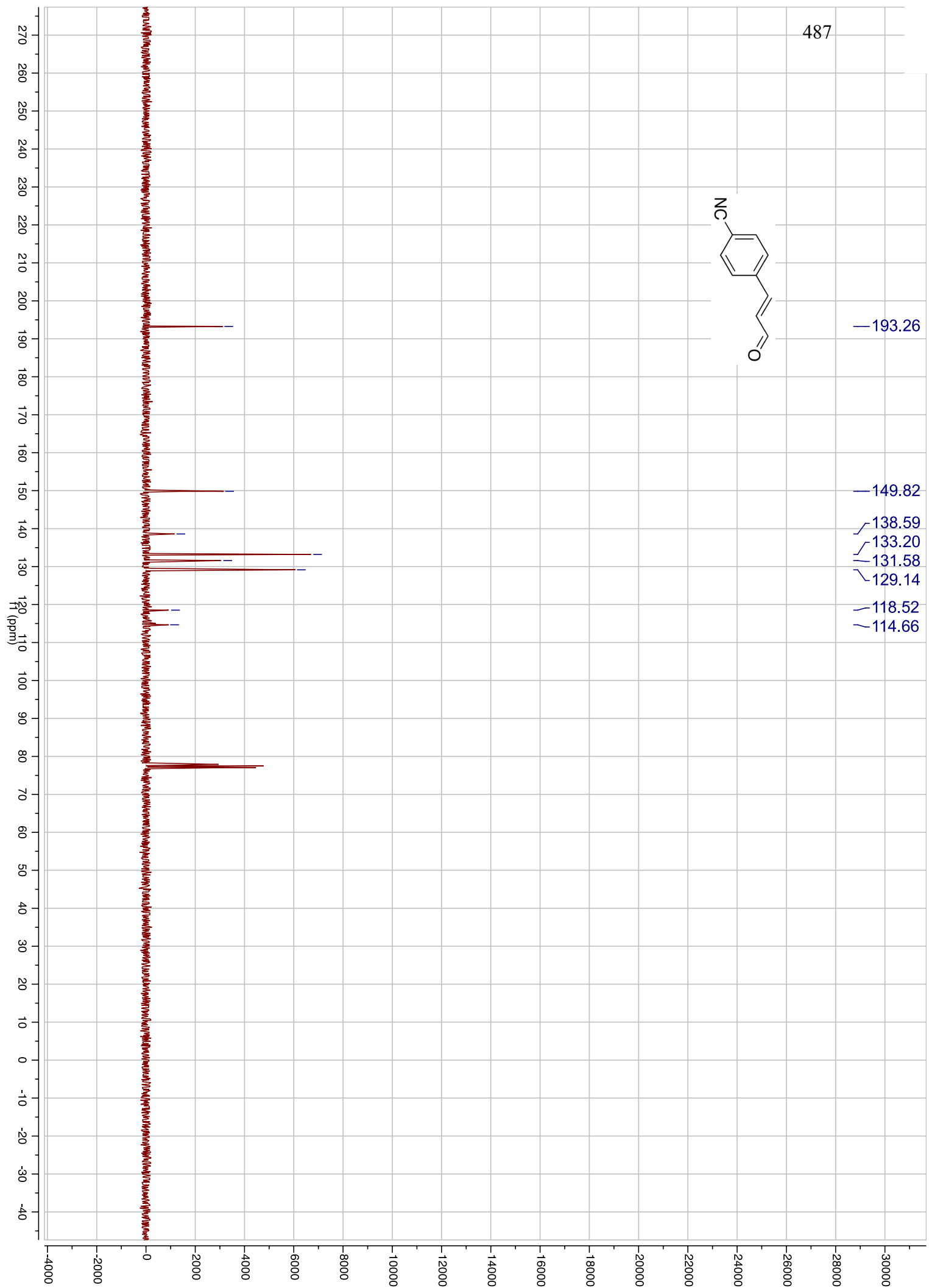
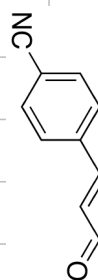
484

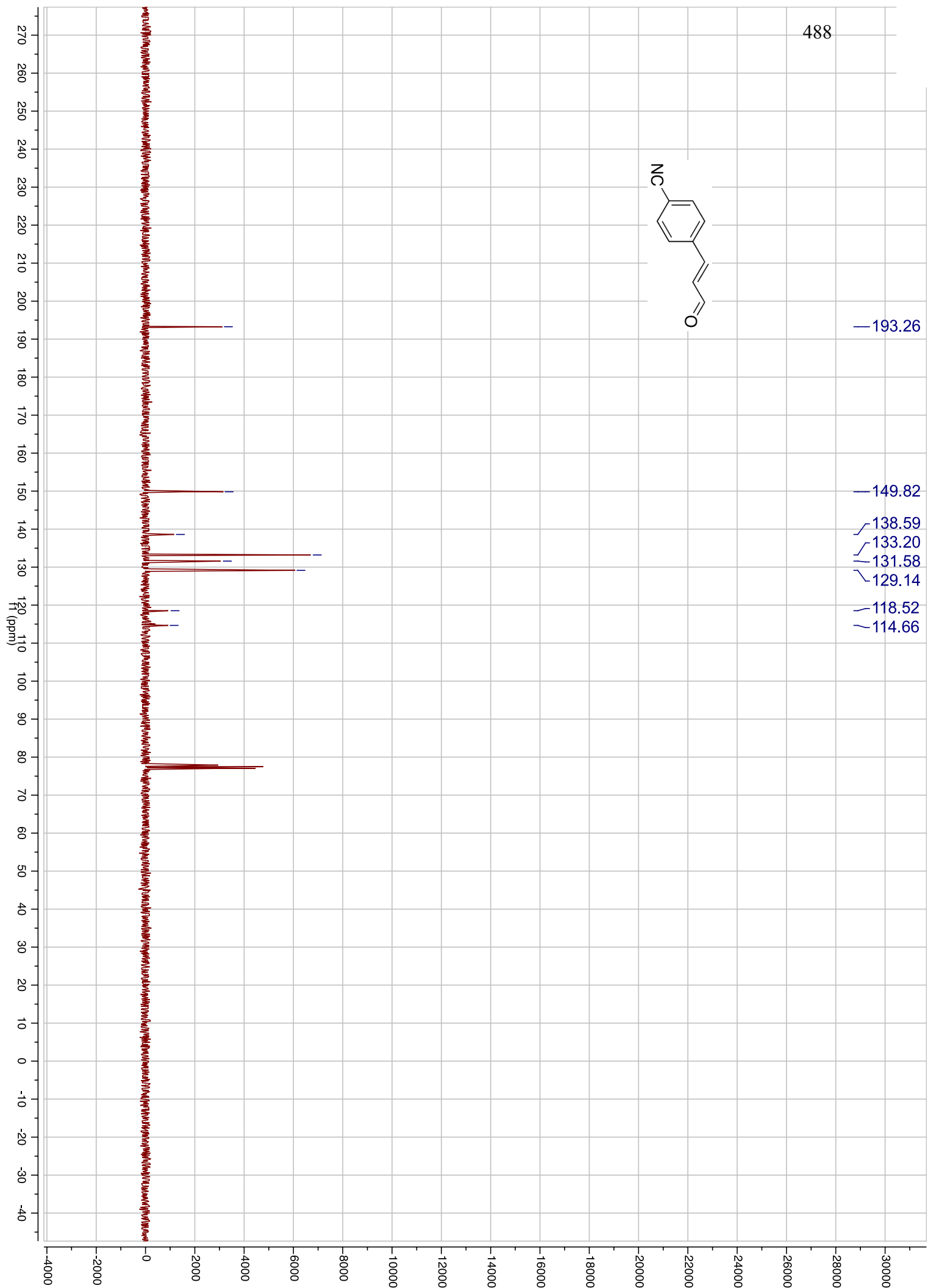
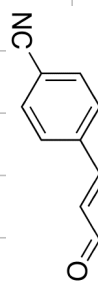


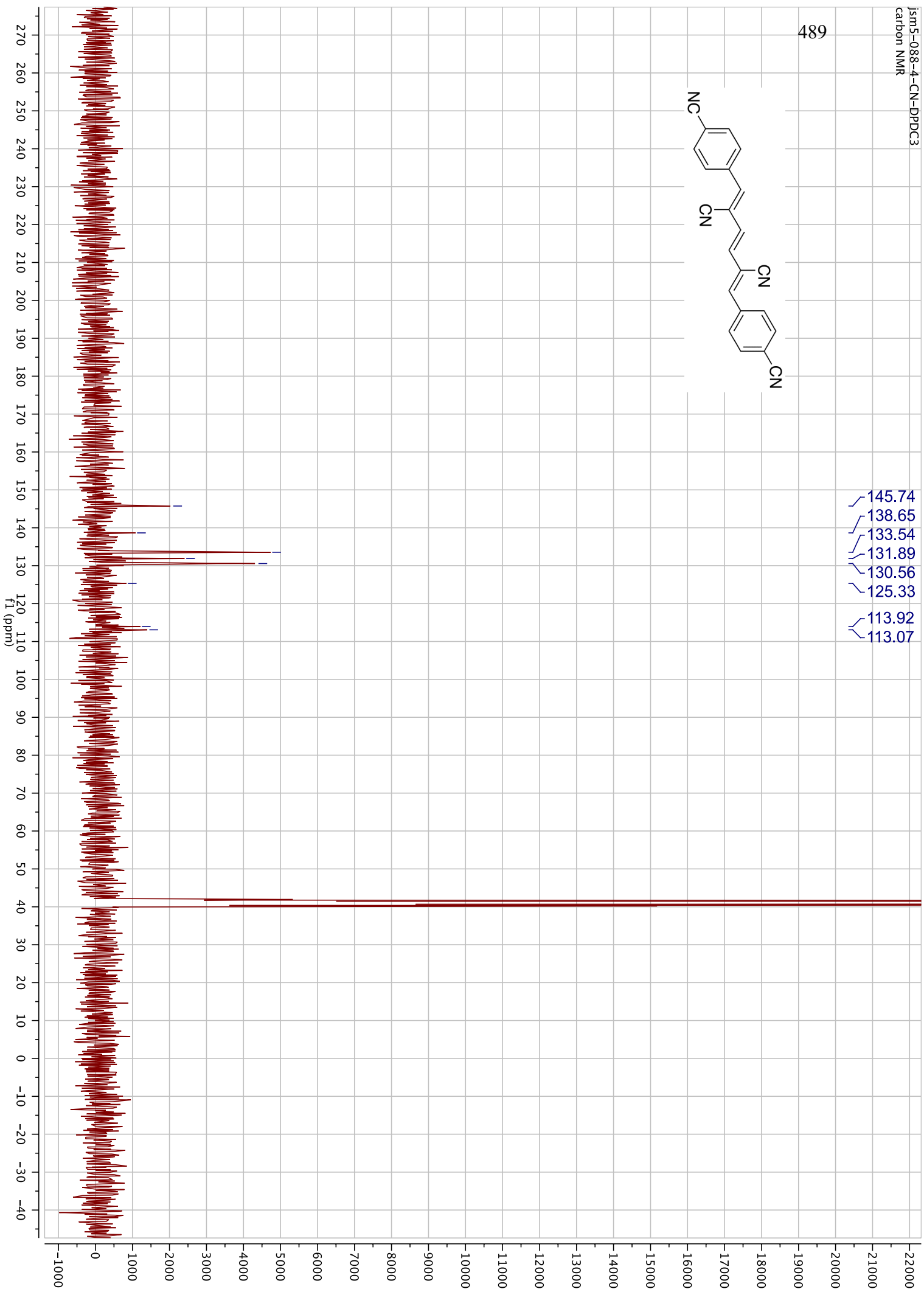
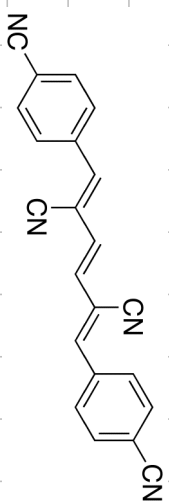




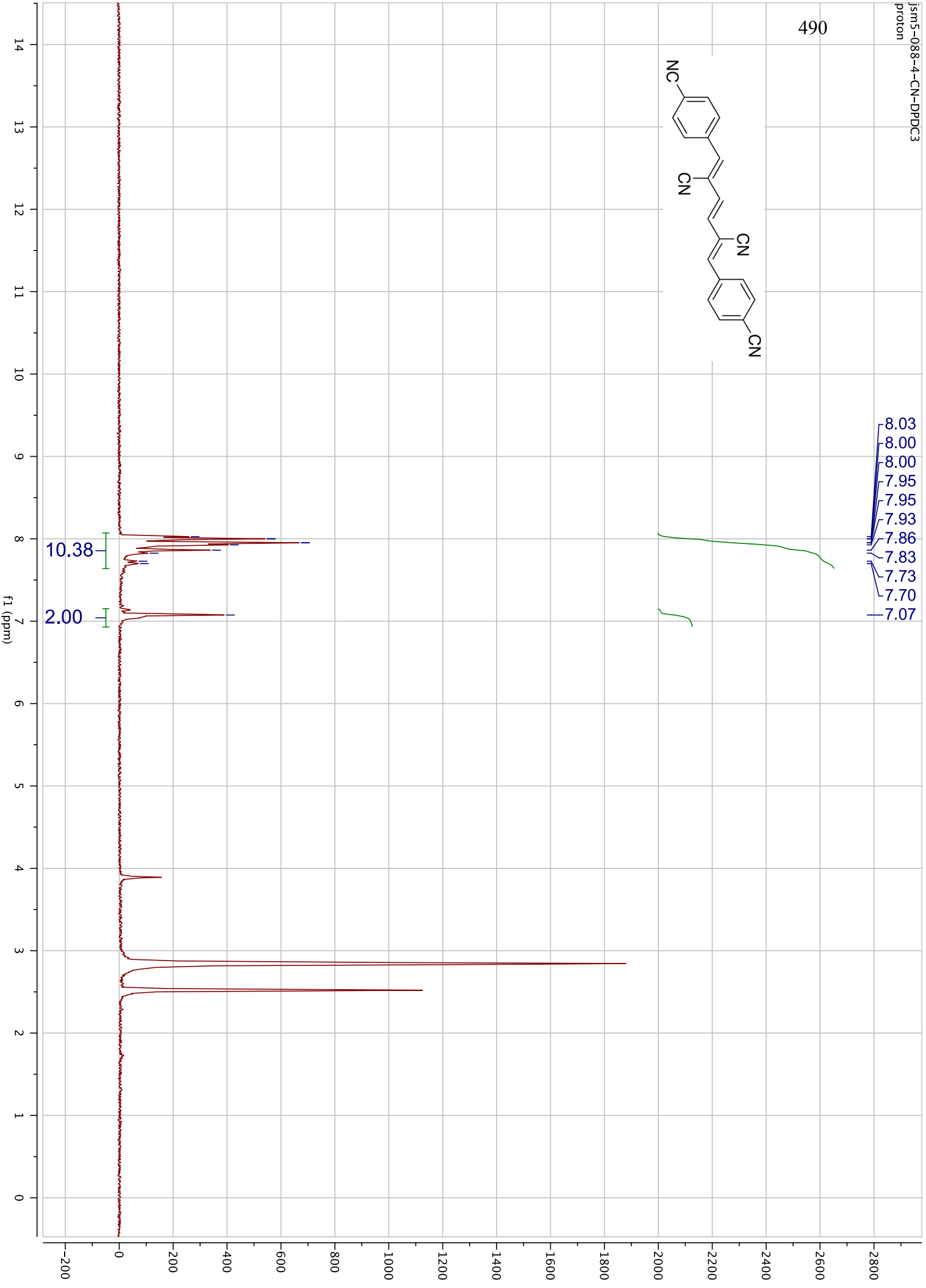
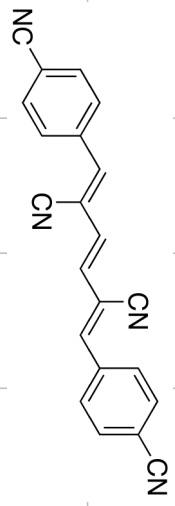


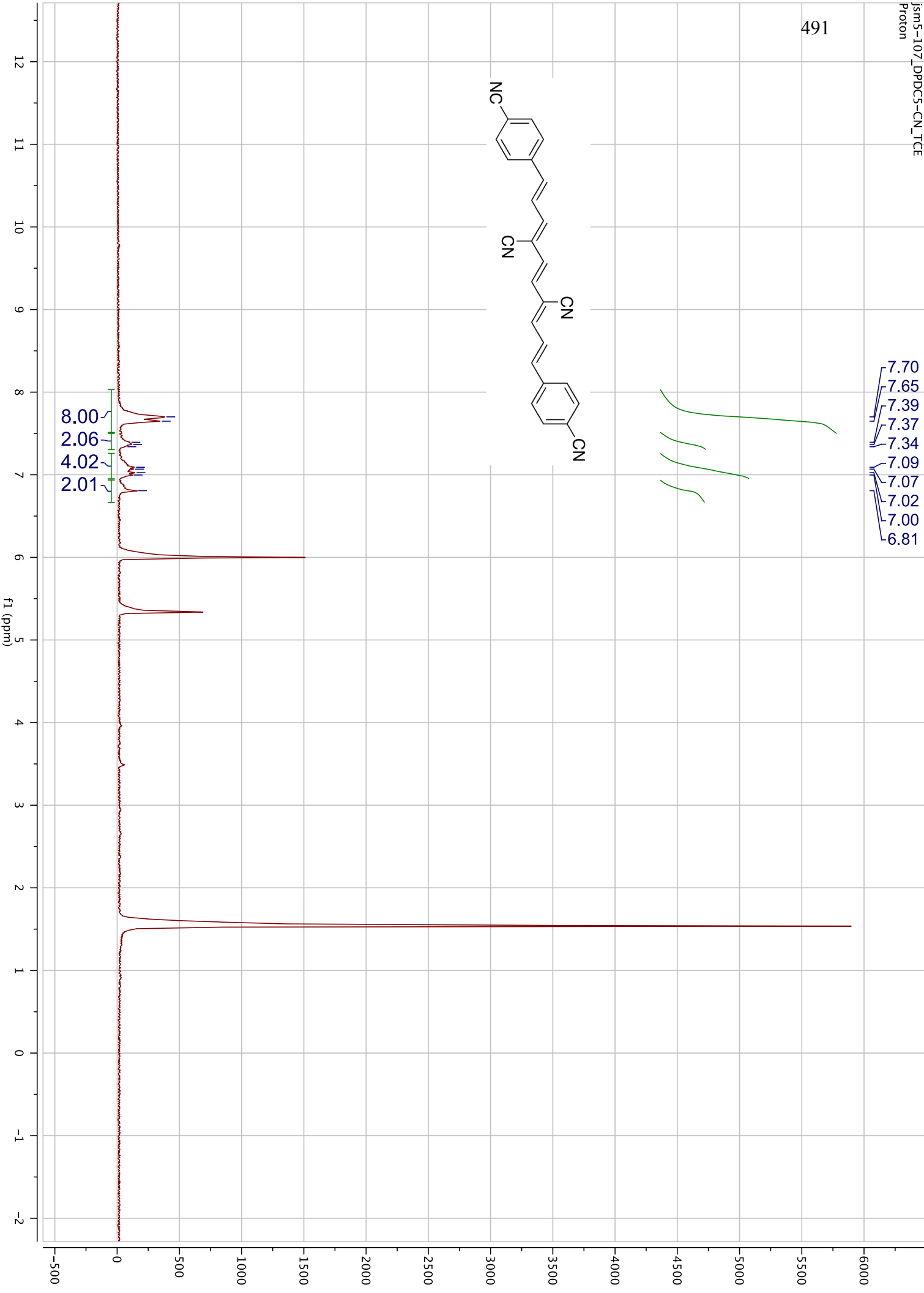
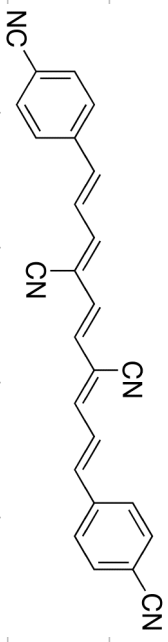


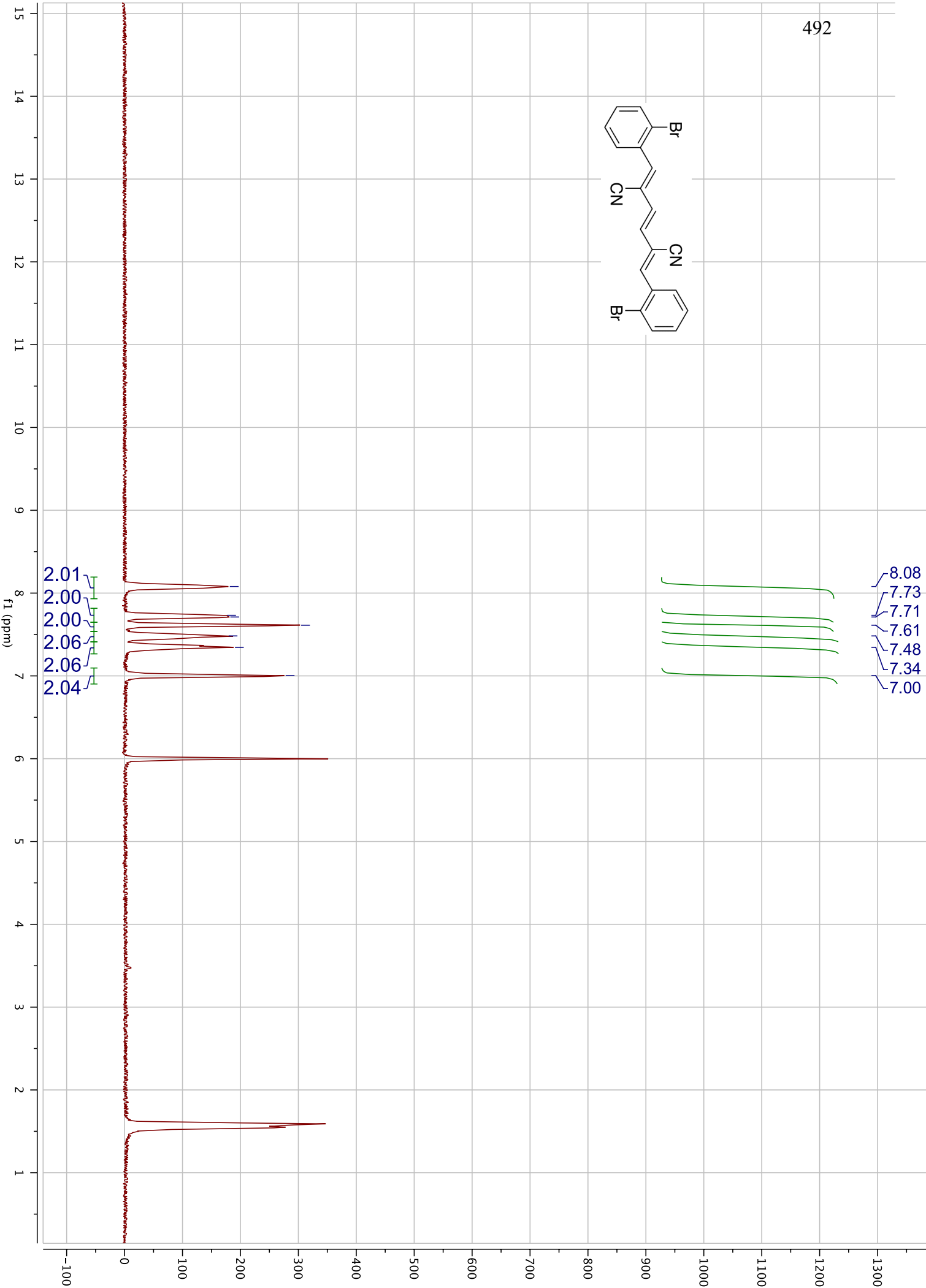
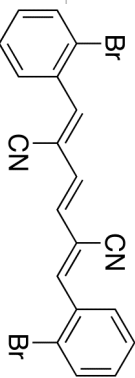




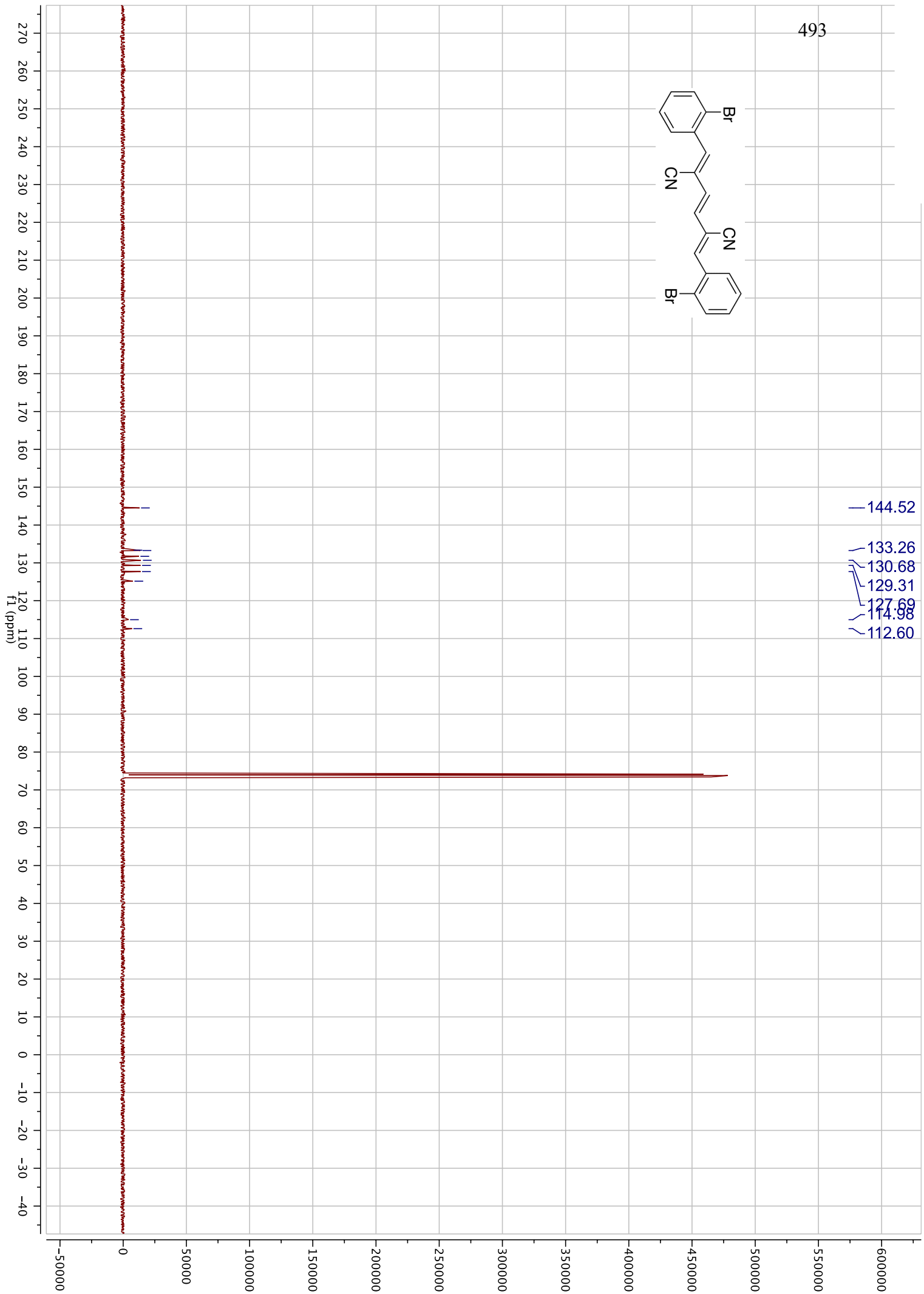
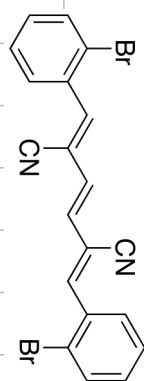
490



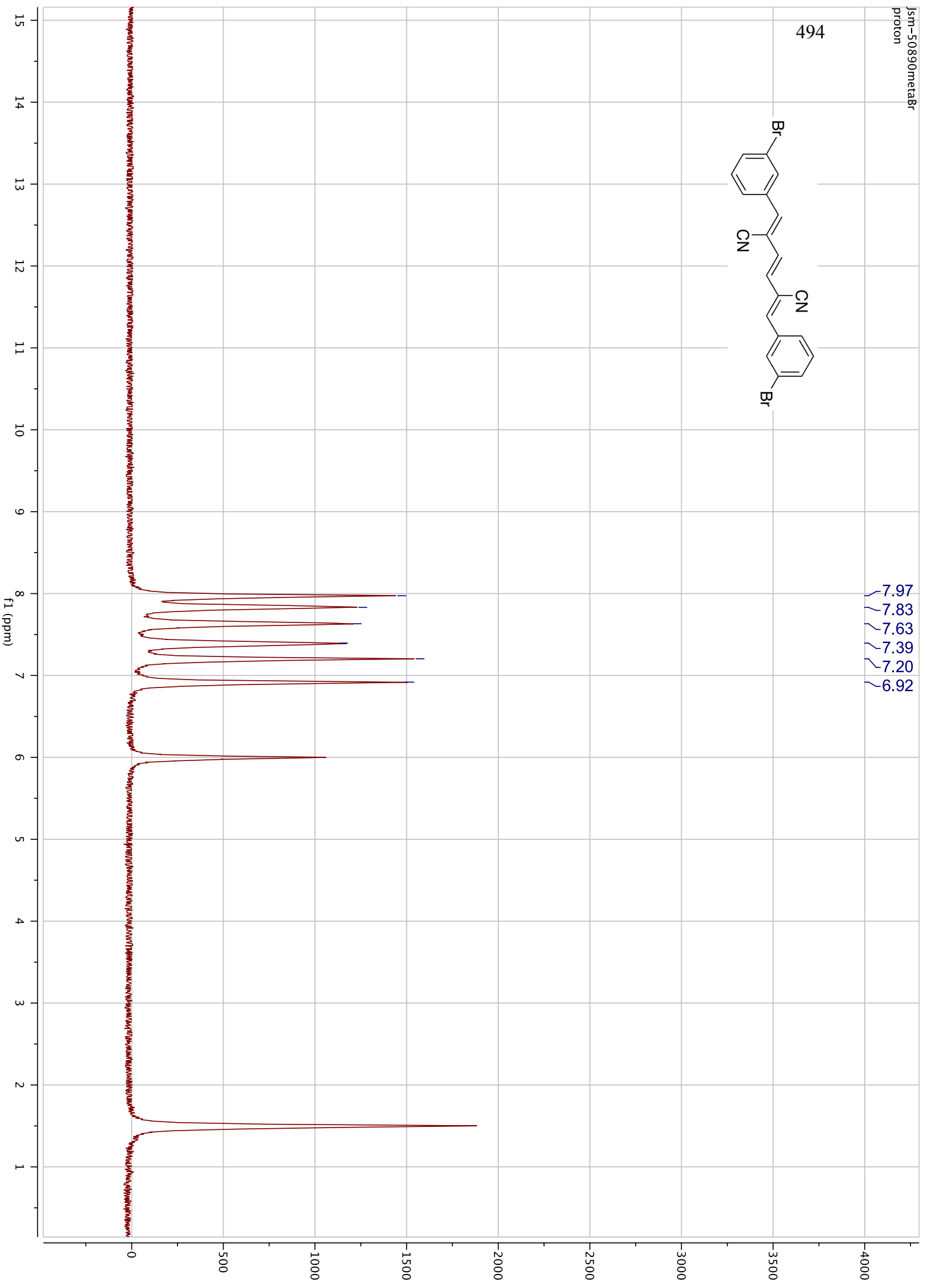
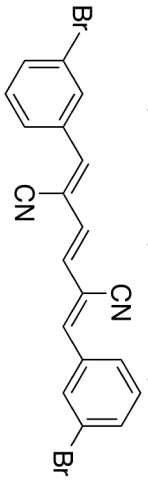


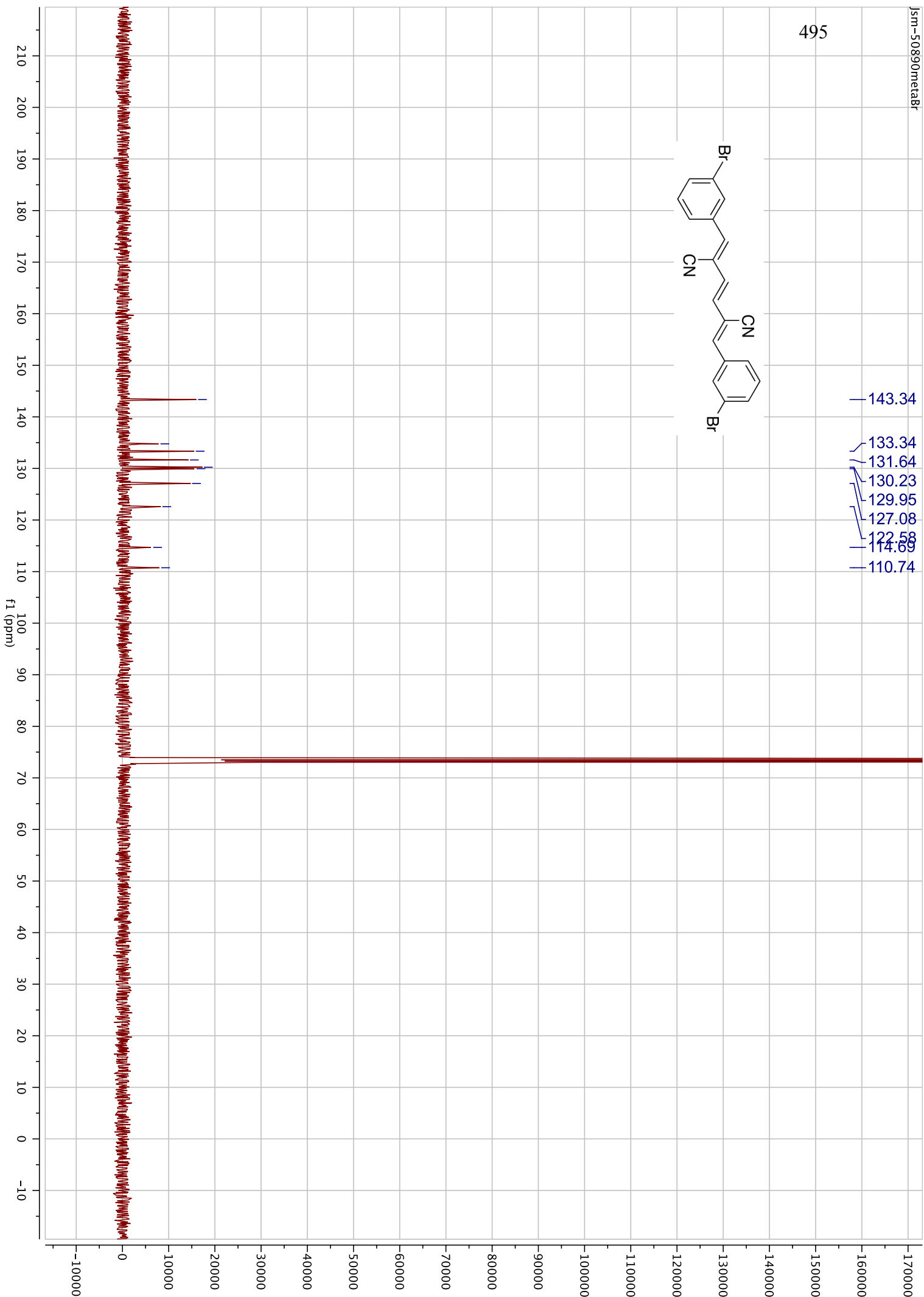
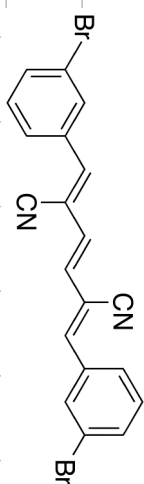


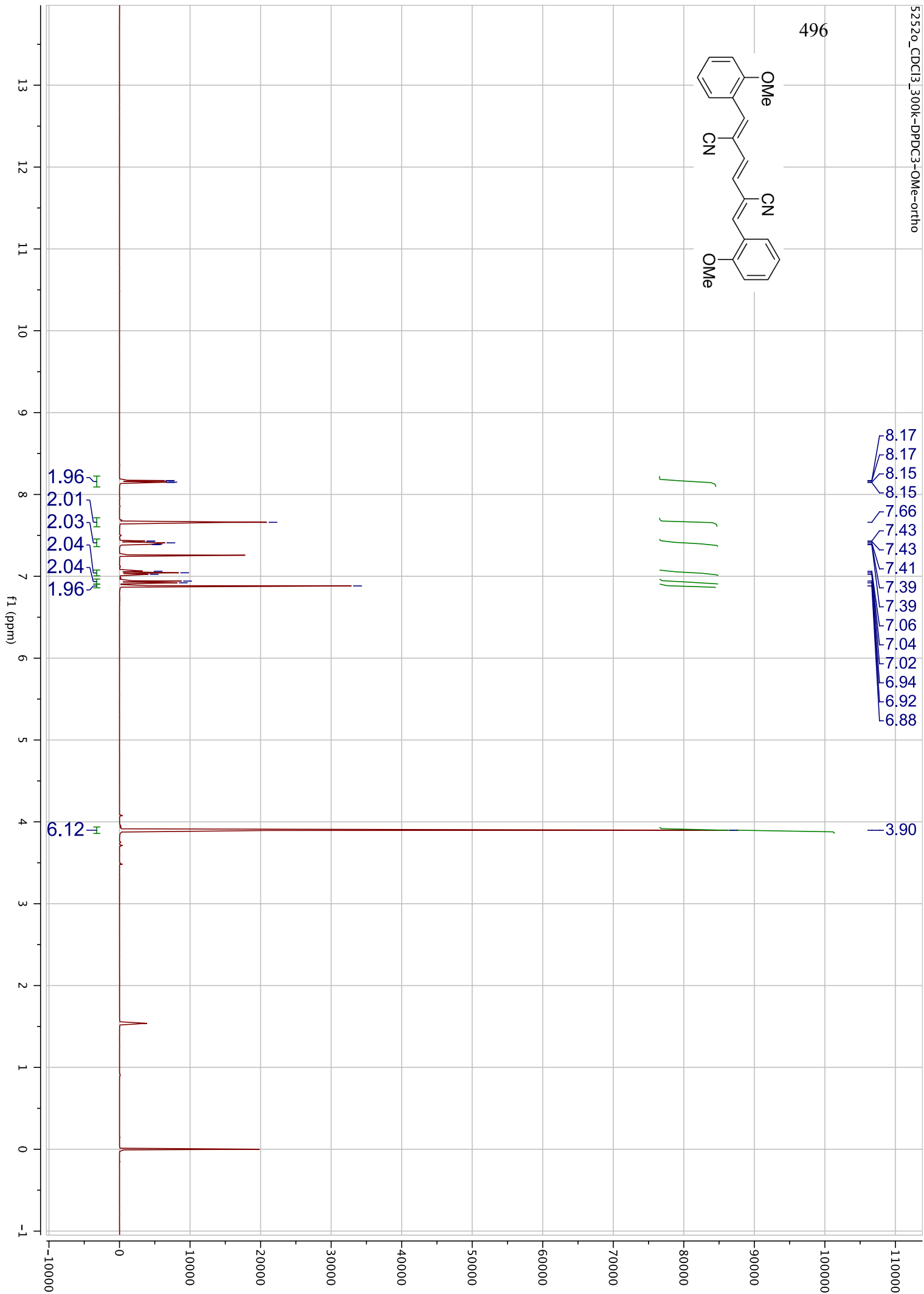
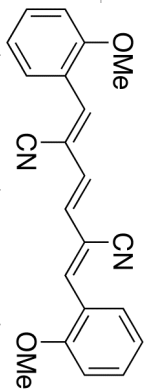


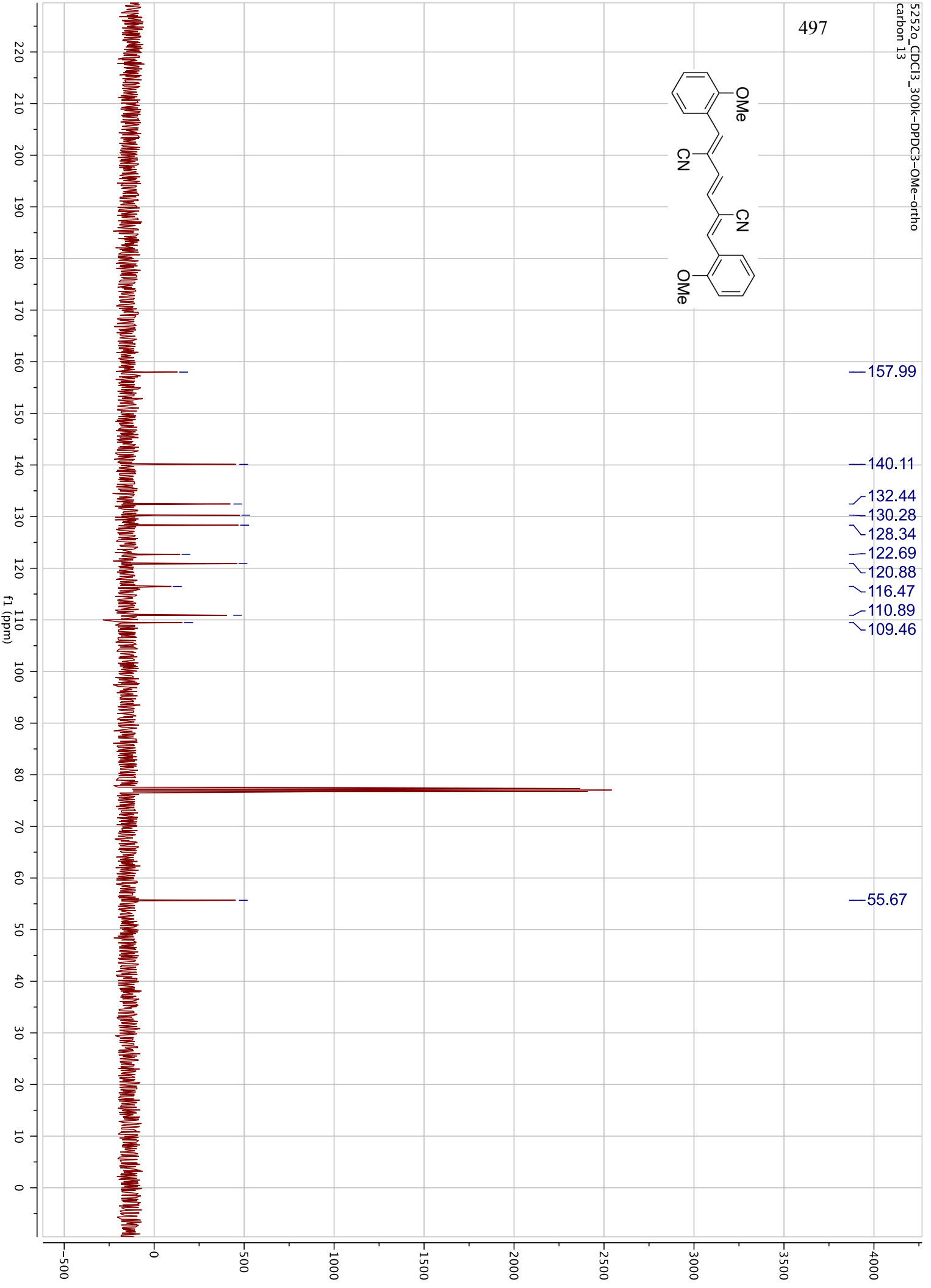
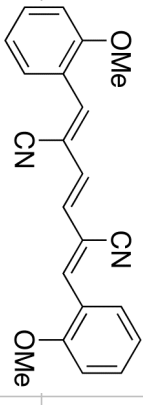


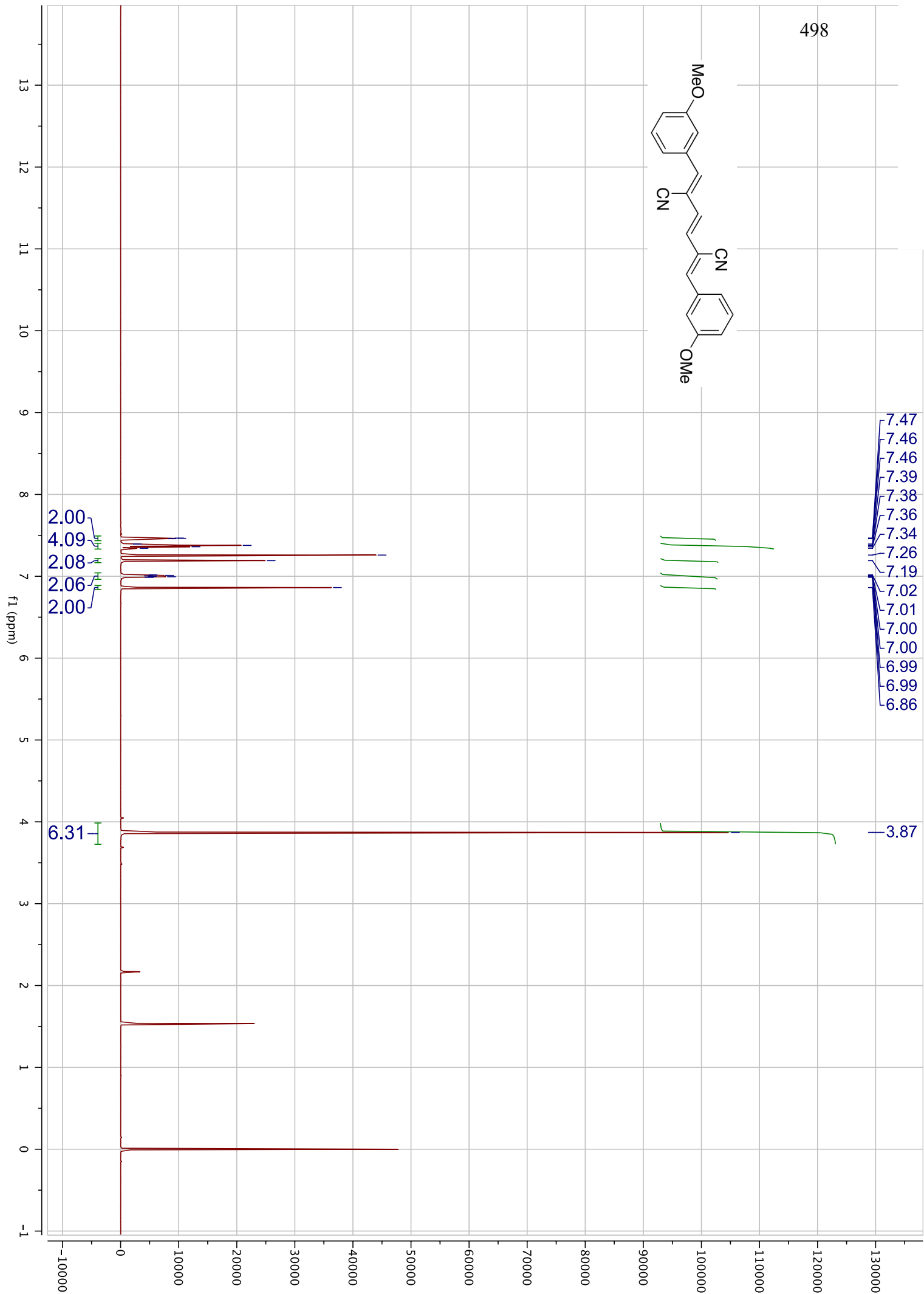
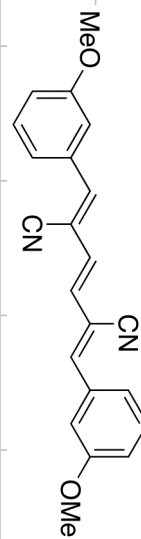
494

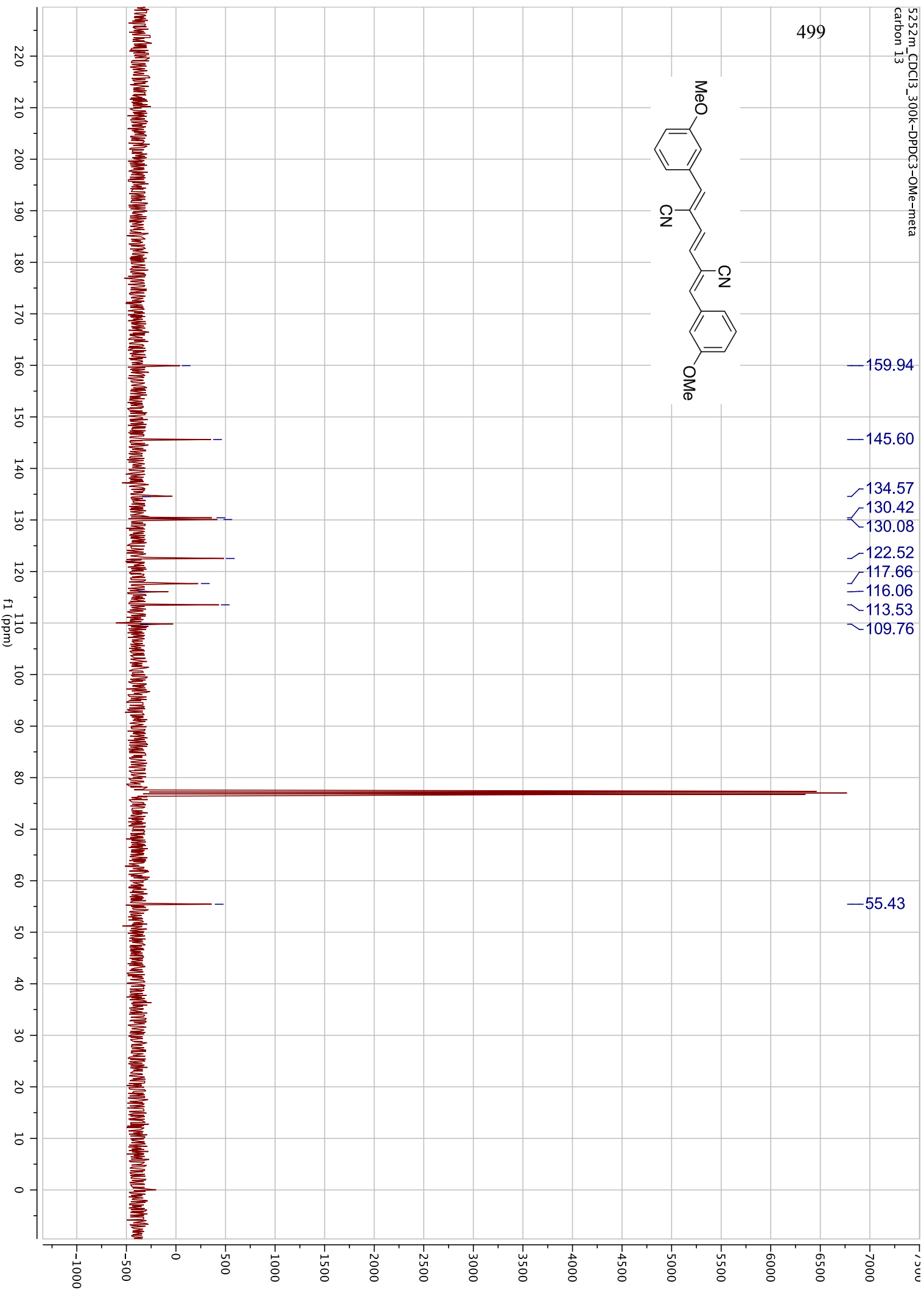
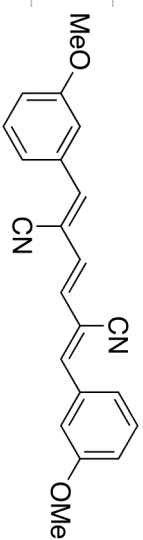




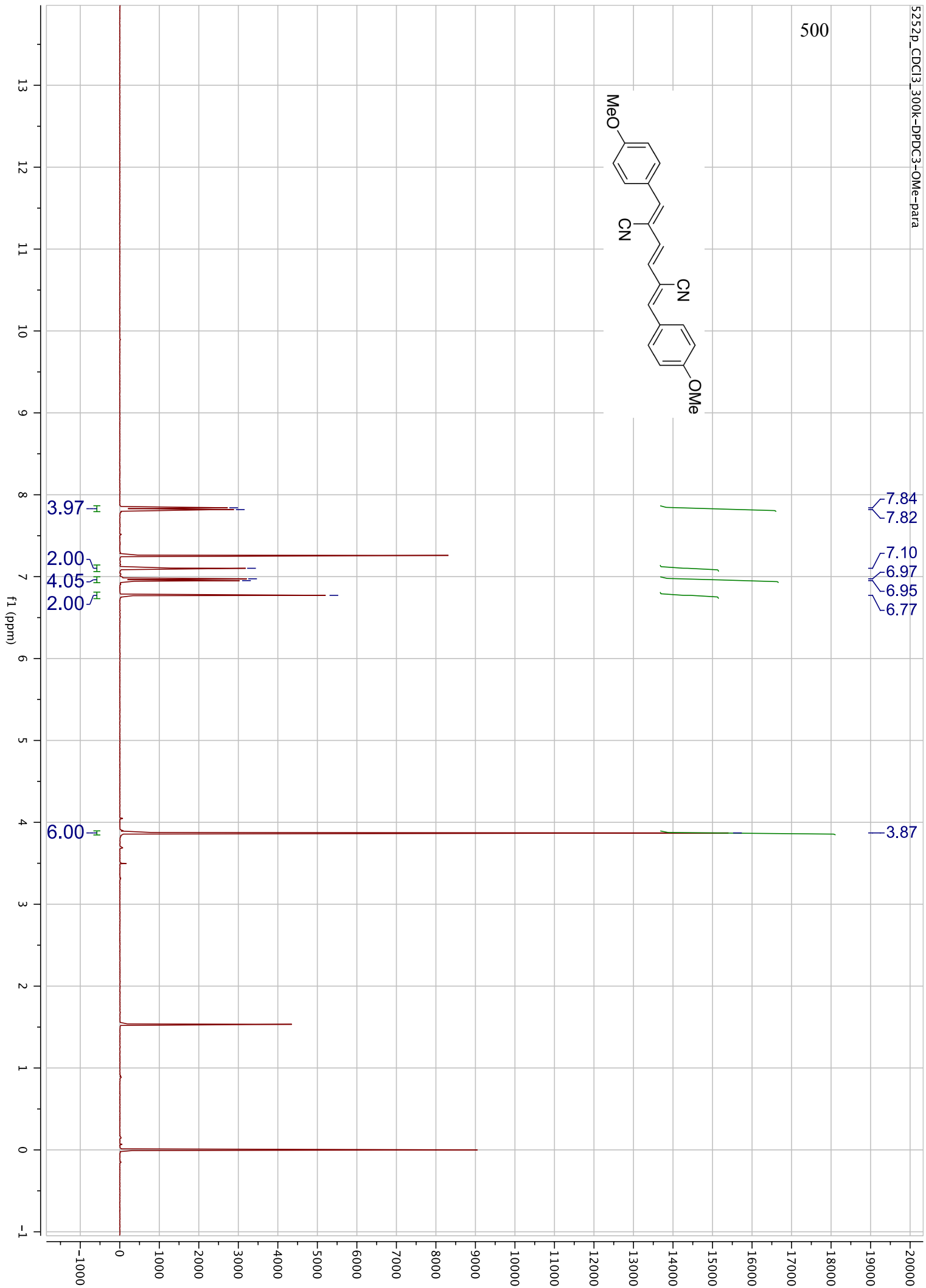
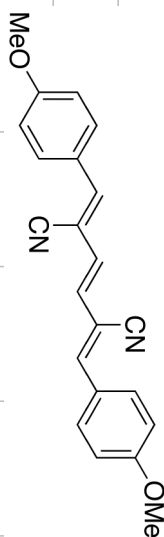




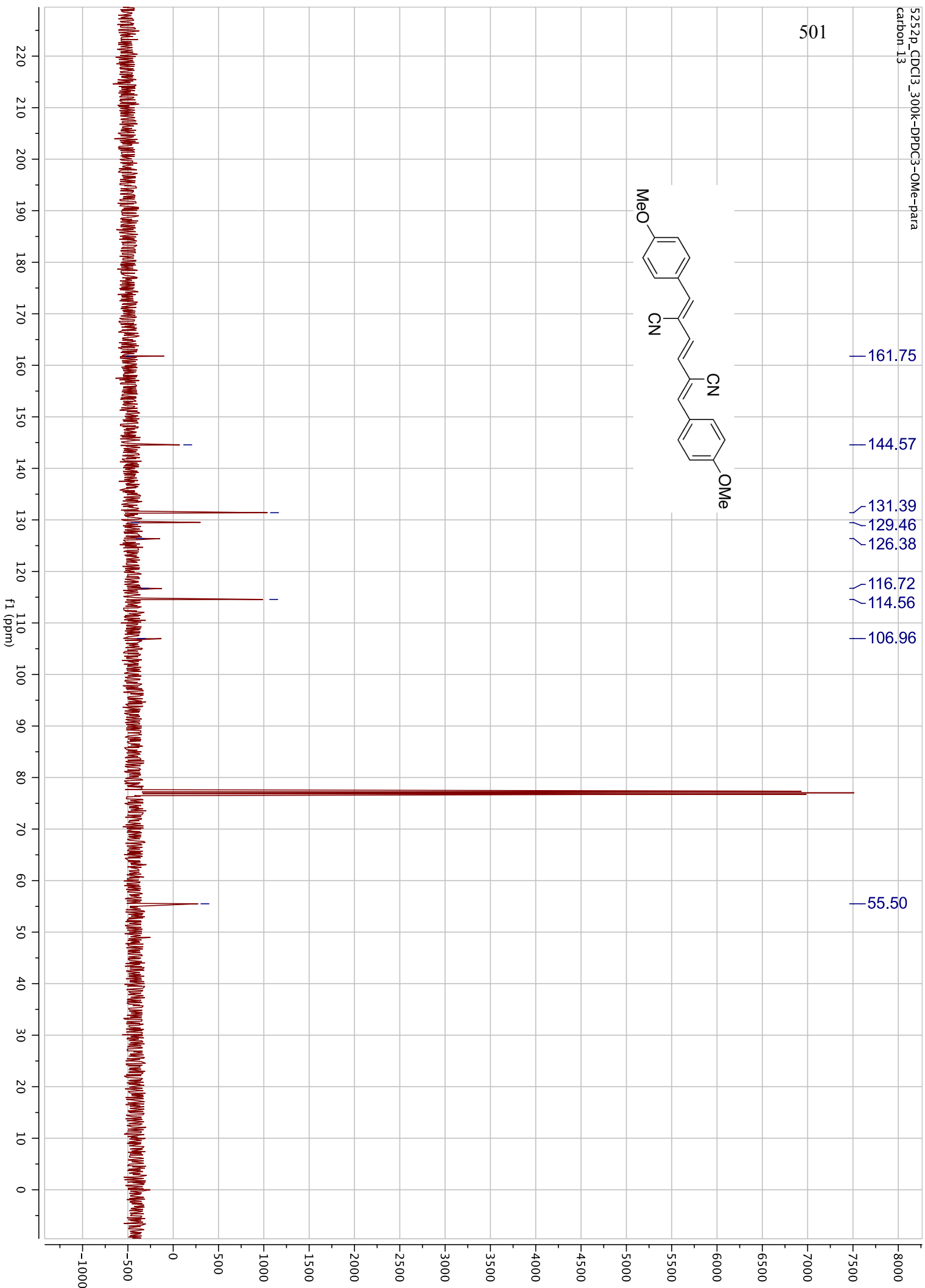
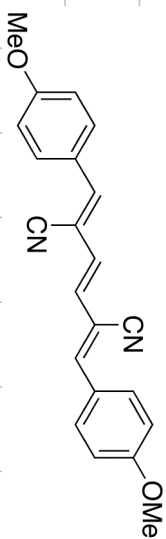


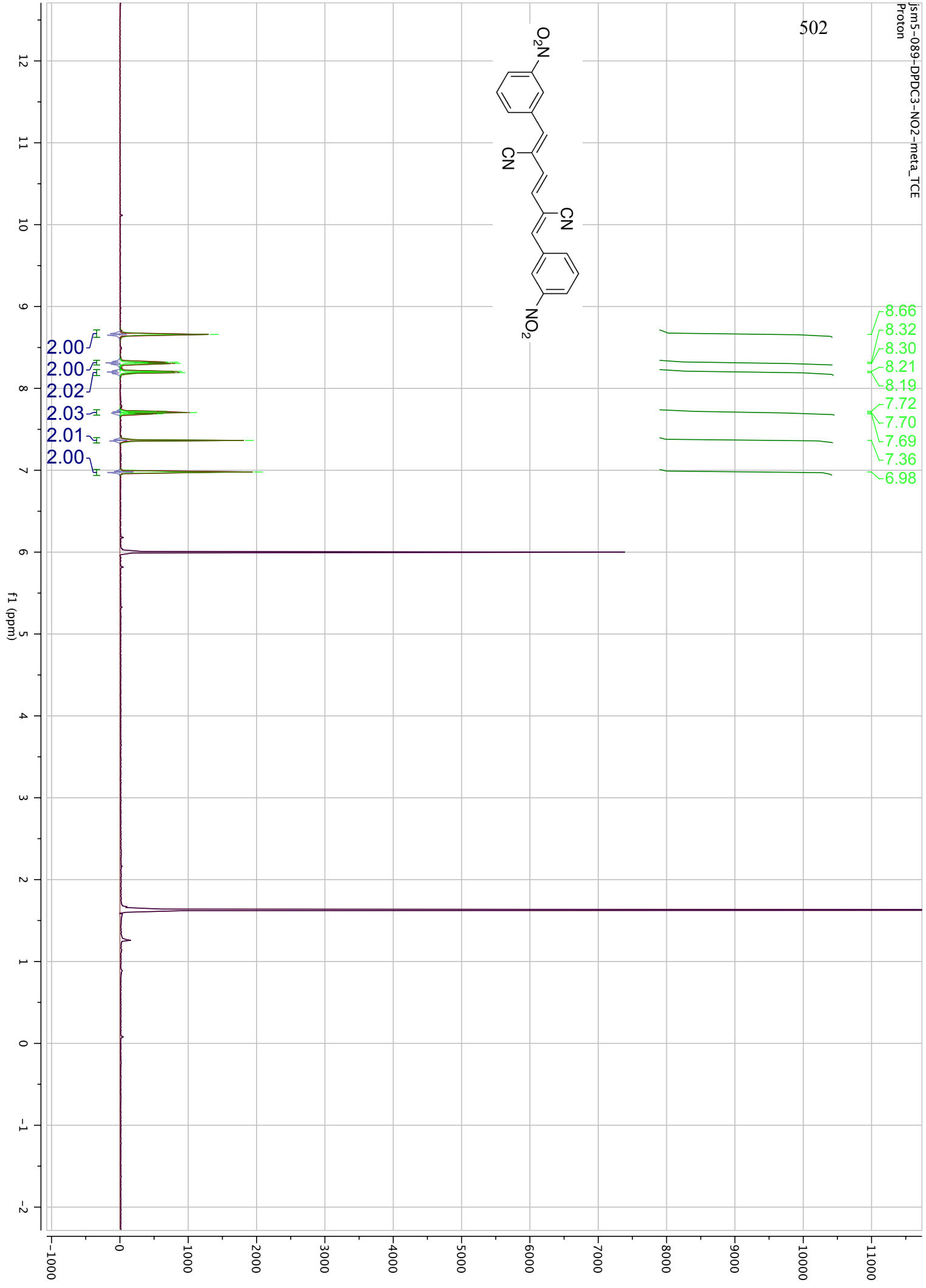
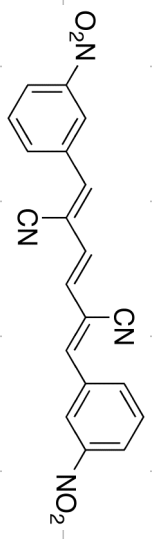


500

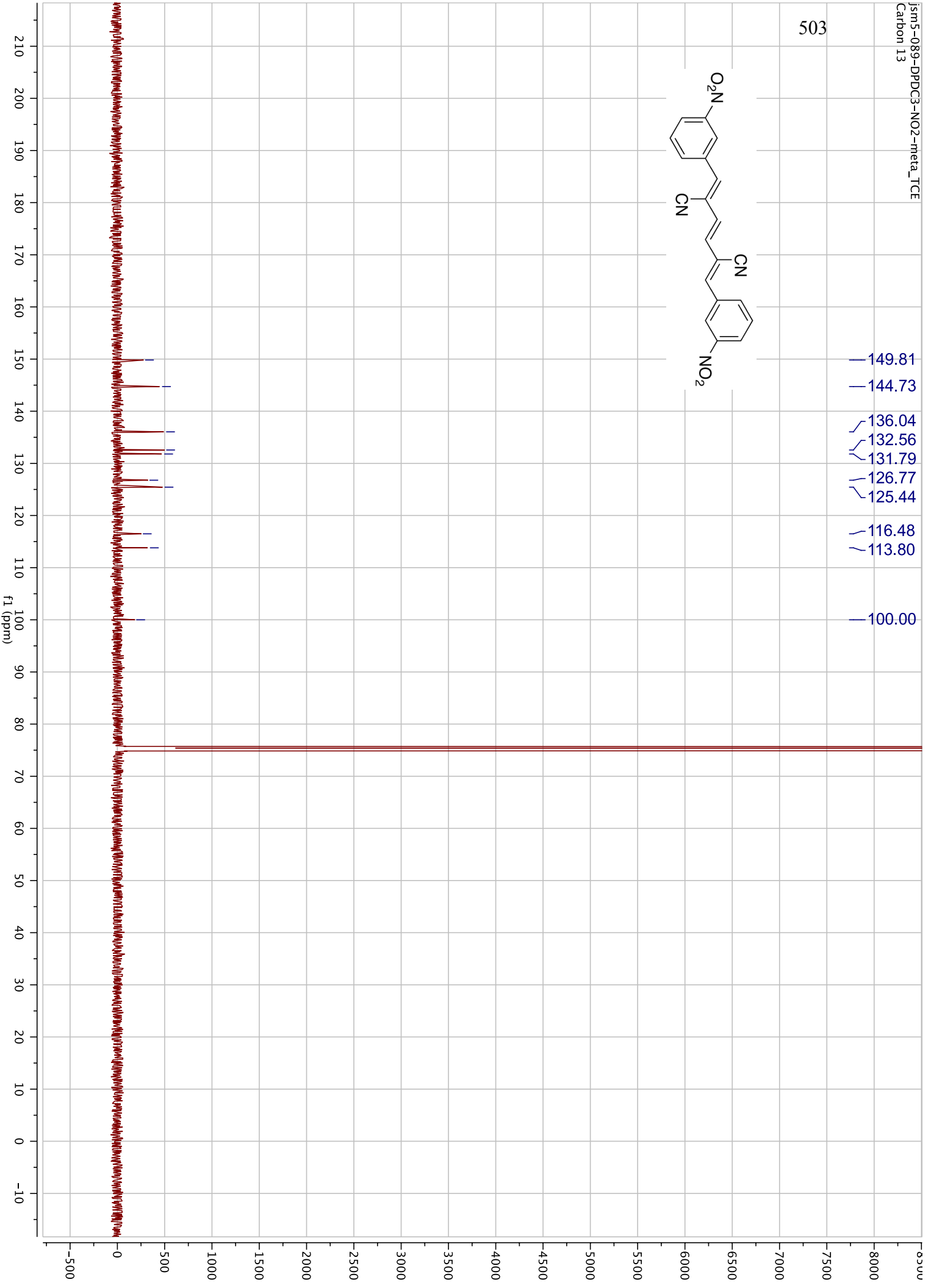
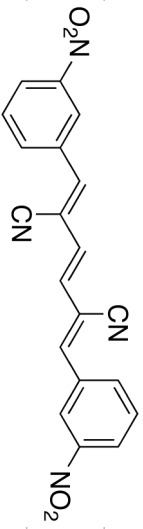


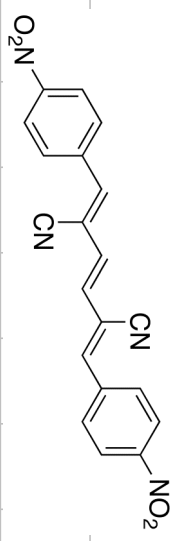




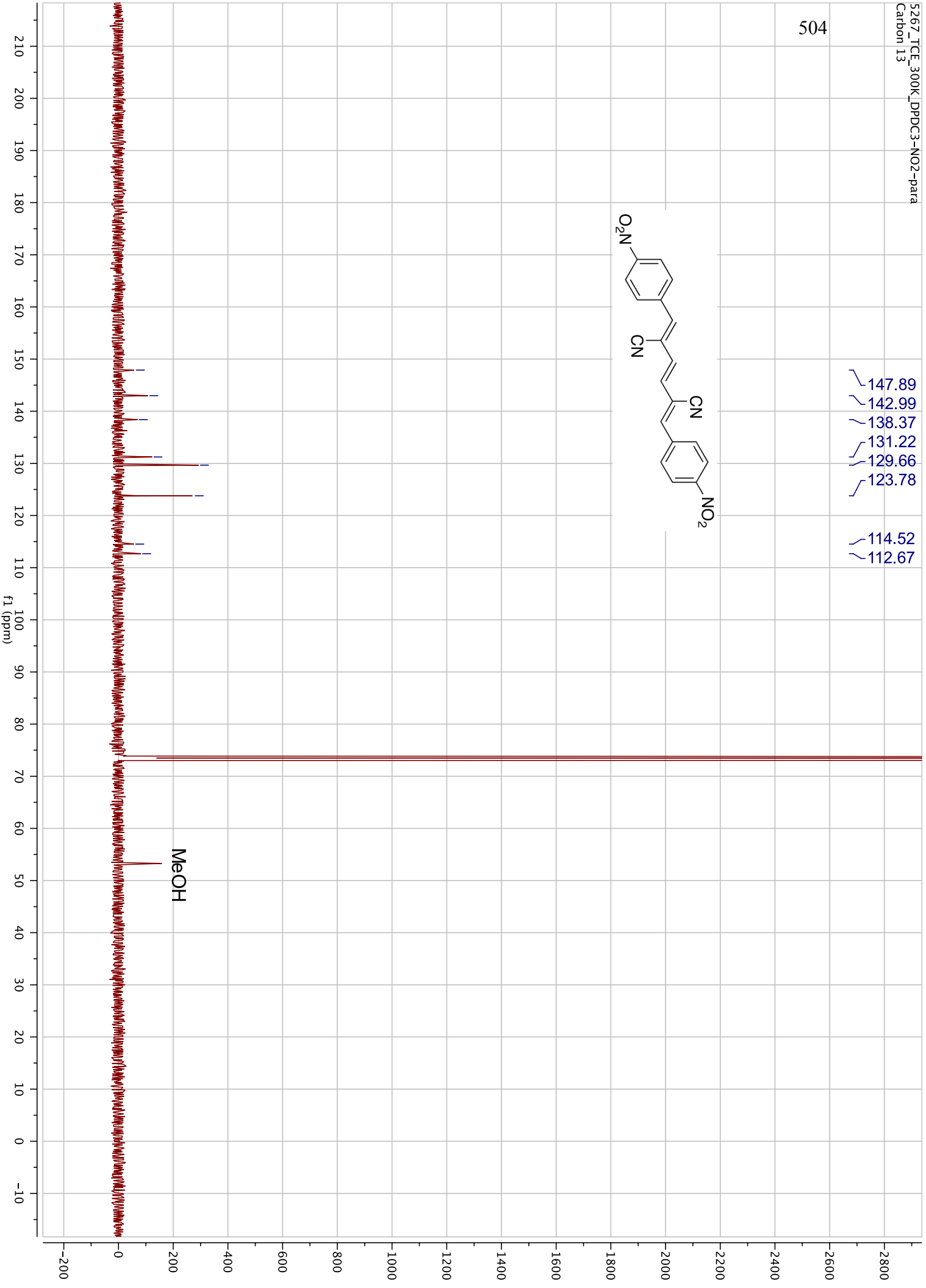


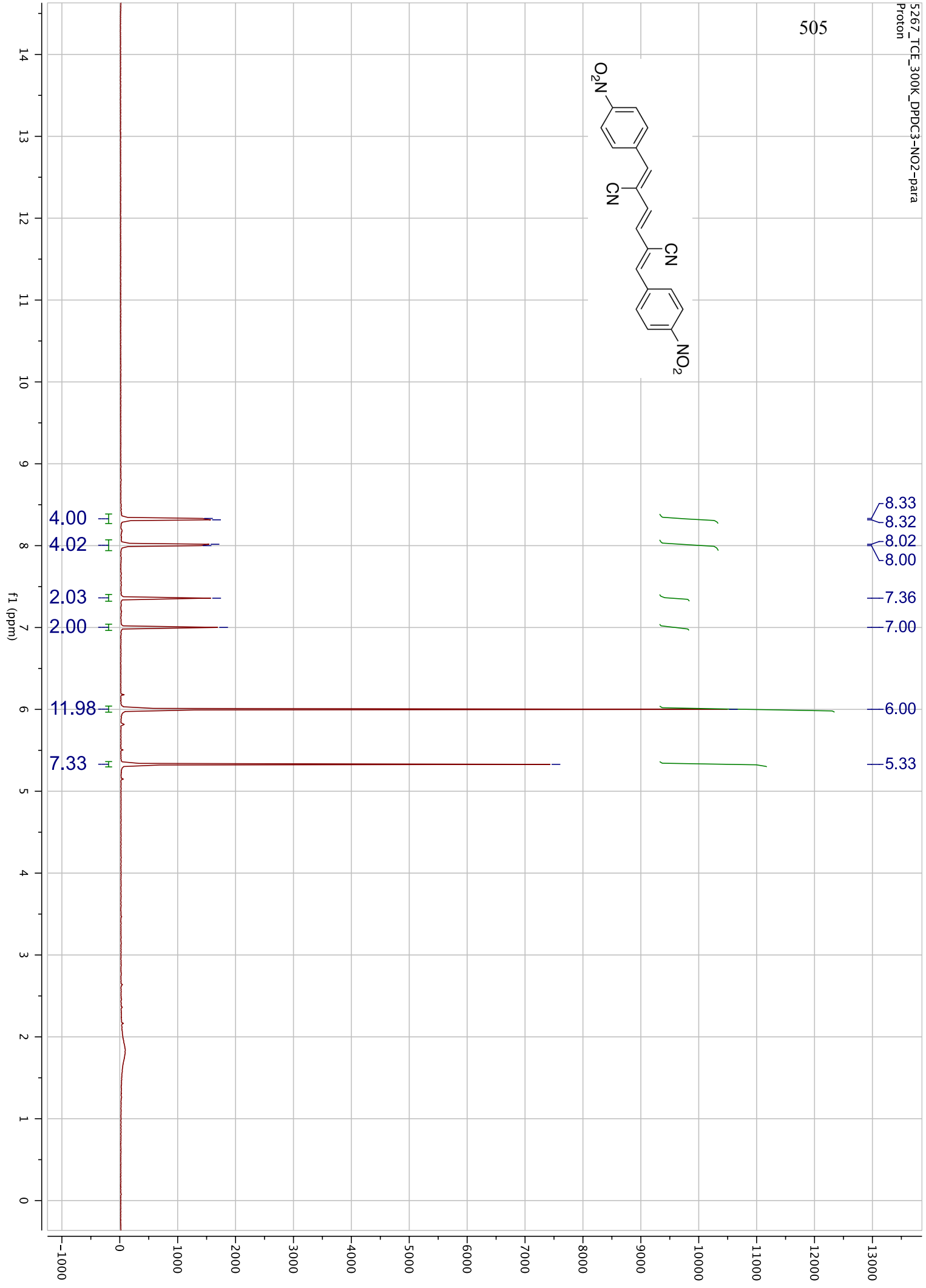
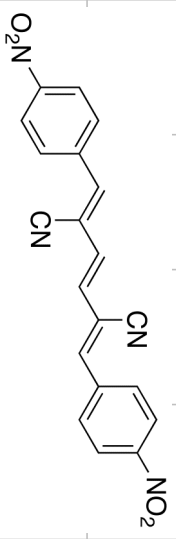
503



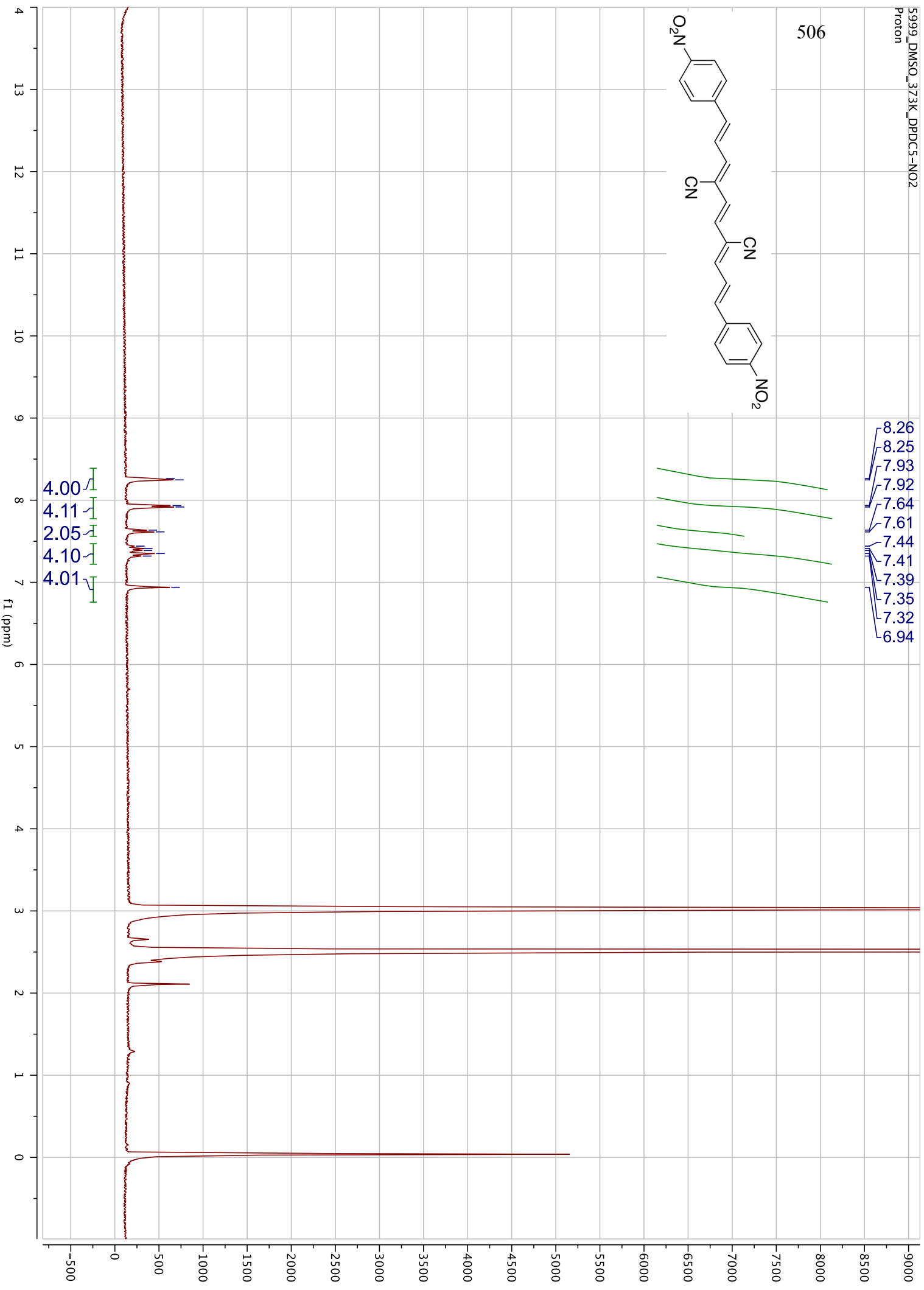
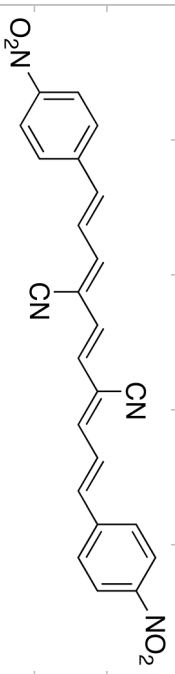


- 147.89
- 142.99
- 138.37
- 131.22
- 129.66
- 123.78
  
- 114.52
- 112.67

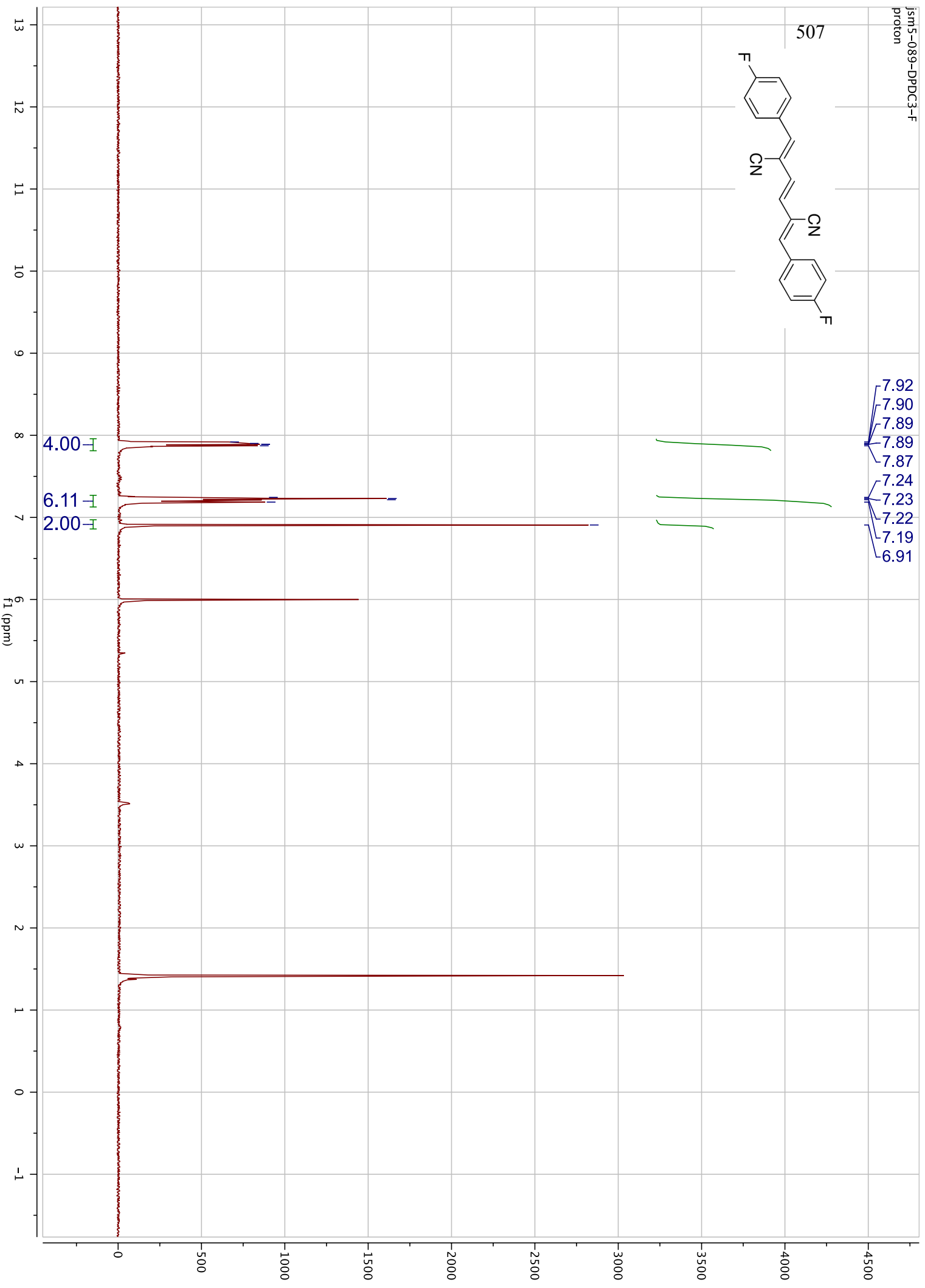
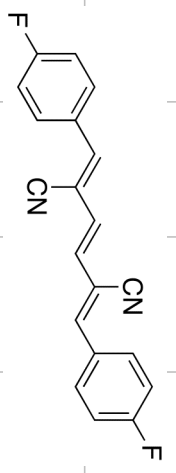




506



507



## Appendix B

### B1. General Information

The synthesis and characterization of molecules **An** and **Bn** can be found in Appendix A, as well as all absorption spectra and electrochemical. However, they conform to the naming scheme in Chapter 1. The key below describes the relationship.

Chapter 1 Name	Chapter 2 Name
<b>A0</b>	<b>DPDC3-SMe</b>
<b>A1</b>	<b>DPDC5-SMe</b>
<b>A2</b>	<b>DPDC7-SMe</b>
<b>A3</b>	<b>DPDC9-SMe</b>
<b>A4</b>	<b>DPDC11-SMe</b>
<b>B0</b>	<b>DPDC3-SC<sub>4</sub>H<sub>8</sub></b>
<b>B1</b>	<b>DPDC5- SC<sub>4</sub>H<sub>8</sub></b>
<b>B2</b>	<b>DPDC7- SC<sub>4</sub>H<sub>8</sub></b>
<b>B3</b>	<b>DPDC9- SC<sub>4</sub>H<sub>8</sub></b>
<b>B4</b>	<b>DPDC11- SC<sub>4</sub>H<sub>8</sub></b>



## **B2. Modified STM Break Junction Studies**

**Experimental Procedure and Data Analysis:** The details of our experimental setup have been described previously.<sup>1</sup> We prepare gold samples by evaporating 100 nm of gold onto freshly cleaved mica. During measurement, the sample is mounted on top of a single-axis piezoelectric positioner below a hand-cut gold tip in a home-built STM setup. The sample-tip junction is stretched and compressed with sub-nanometer precision by moving the substrate relative to the tip at a rate of 15 nm/s with the piezoelectric (Mad City Labs) while applying constant bias to the sample through a series resistor. The current in the tip is captured by a Keithly 428 current-voltage amplifier. The sample position is manipulated and data acquired at 40 kHz using a data acquisition board (National Instruments, PXI-4461) and custom-built software written in Igor (Wavemetrics, Inc). All position determinations were based on measurements with a built-in position sensor within our custom piezoelectric positioner. This position sensor was calibrated both by the manufacturer and by us using laser interference measurements. We found the absolute values of the measured displacements to be accurate to within 5%.

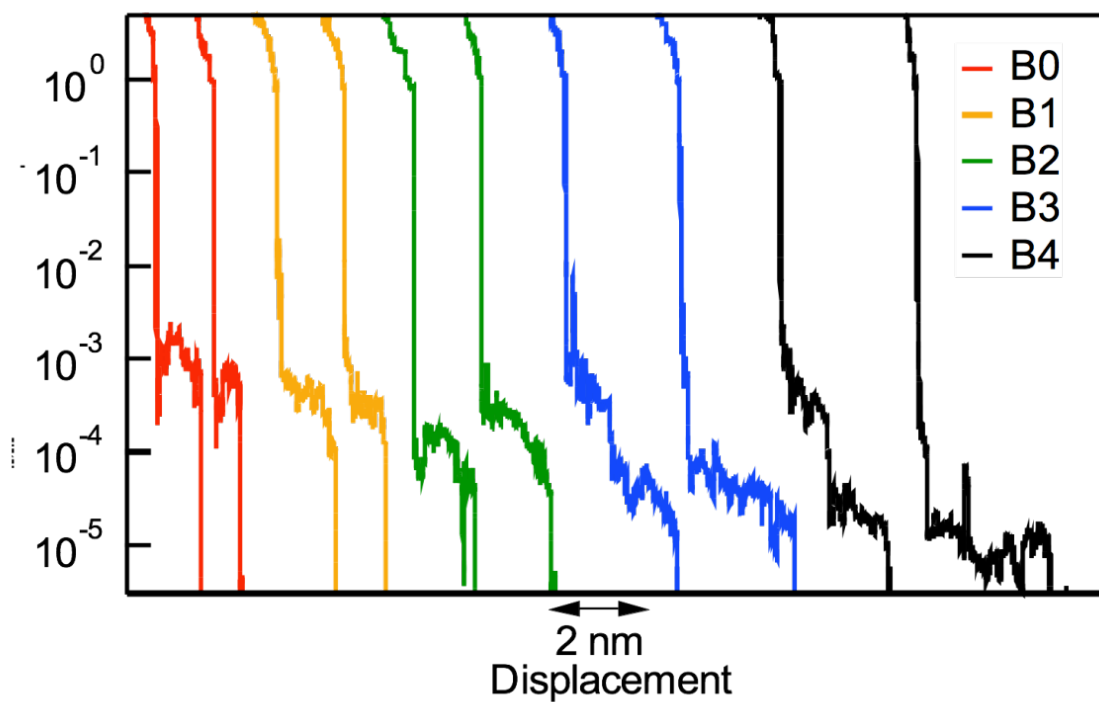


**Figure B1:** Sample conductance traces gained from STM-based break junction measurements on **B<sub>n</sub>** series. Step lengths become longer as molecular length increases, showing that conductive junctions are sustained at larger electrode separations with longer molecules.

We form metal-molecule-metal junctions by smashing the tip and substrate together until conductance exceeds  $5 G_0$  and then pulling them apart. All conductance traces acquired that reach a conductance below  $5 \times 10^{-6} G_0$  are then added to a linear binned histogram by an automated algorithm without any further data selection. Typically, 5000 traces are used to construct conductance histograms.

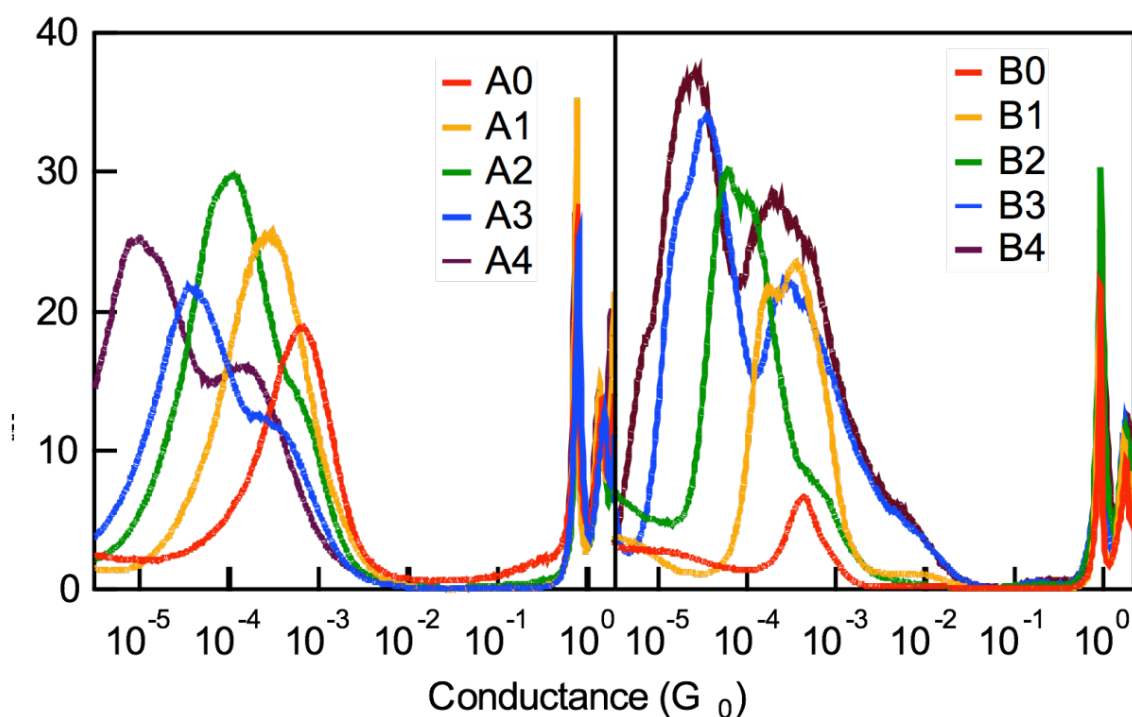


**Figure B2:** Logarithm binned conductance histograms for **A<sub>n</sub>** and **B<sub>n</sub>** series. Bin size is 100 per decade.

Two-dimensional (2D) conductance-displacement histograms are automatically generated<sup>2,3</sup> with the added requirement that a  $G_0$  break is clearly identifiable in the trace (more than 90% of traces that start with a conductance greater than  $1 G_0$  and break satisfy this requirement). In 2D histograms conductance is binned logarithmically with 100 bins per decade, while displacement is binned linearly for image clarity.

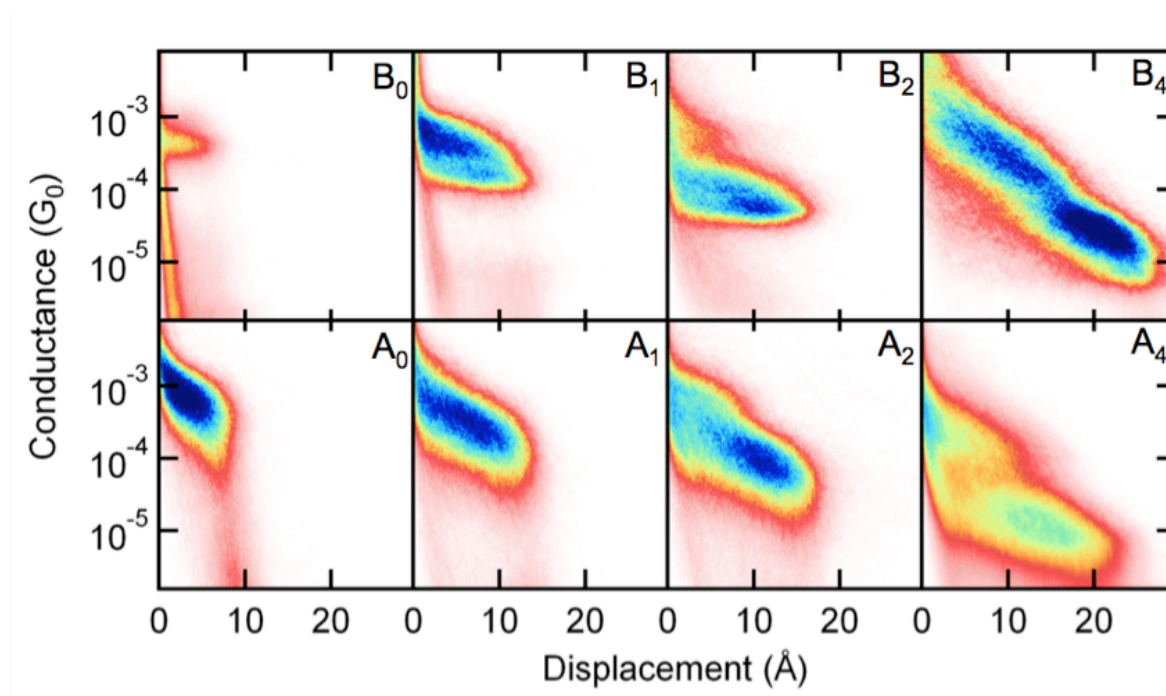


**Figure B3:** 2D conductance-displacement histograms for the  $A_n$  and  $B_n$  series. The displacement axis has linear bins while the conductance axis has logarithm bins (100 per decade). The higher conductance regime lengthens as the oligomer length increases.

We have not observed that cyano groups bind to gold. 1,4-dicyanobenzene, 1,4-dicyano-2-butene and oligoenes **DPDCn** do not show conductance peaks and likely do not form molecular junctions. Like the cyano-functionalized oligoenes, oligoenes without

cyano groups (**Cont-1**) contain 2 conductance peaks demonstrating that cyano groups do not play a direct role in junction formation.

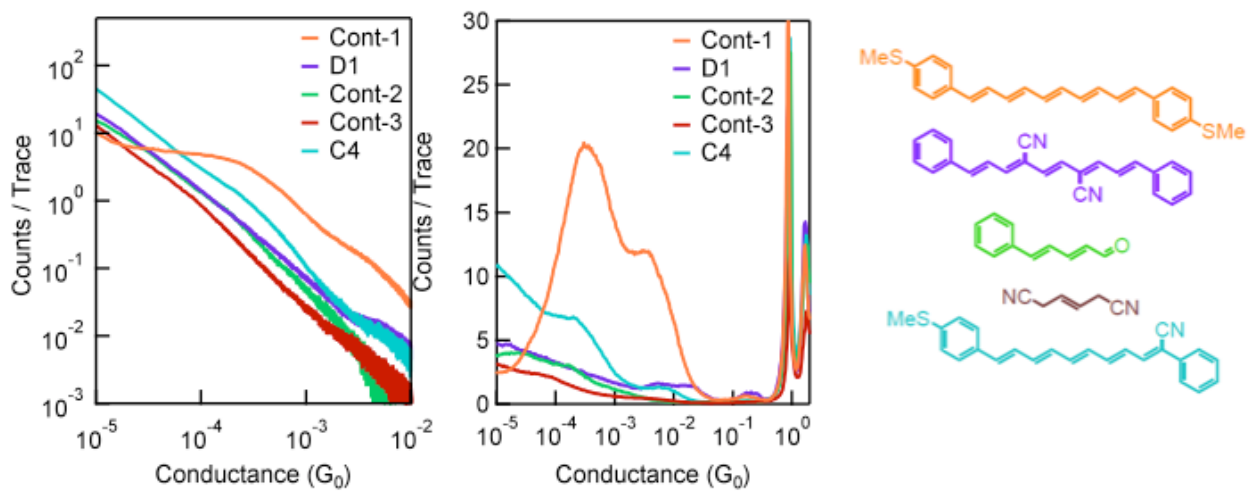


**Figure B4:** Linear and log binned conductance histograms of control compounds investigated. Structures are shown on the right.

### B3. Variable Resistance Measurements and Controls

Traces were selected from all measured traces using an automated algorithm. The number of data points in the initial "hold" region of each trace (starting at time  $t = 0$  s) that had a conductance within the required range was determined. Typically, 50% of all measured traces had a molecule during the initial "hold" region. All selected traces were used to construct a two-dimensional conductance vs. time histograms. Control measurements were carried out with 1,6-bis(methylsulfide)hexane, a saturated molecule. The zig-zag ramp used was chosen so that the proportional change in the in electrode-electrode separation relative to the length of the molecule was the same as in the ramp used in Figure 2.8 of Chapter 2. (Figure B5). The probability of having a junction start at the selected conductance with hexane is 15%, which is significantly lower than the 50% success rate with **B4**. In addition, no reproducible modulation in conductance during the ramp is observed. Traces collected without the presence of any molecules showed conductance oscillating between a closed and an open junction during the zig-zag ramp.

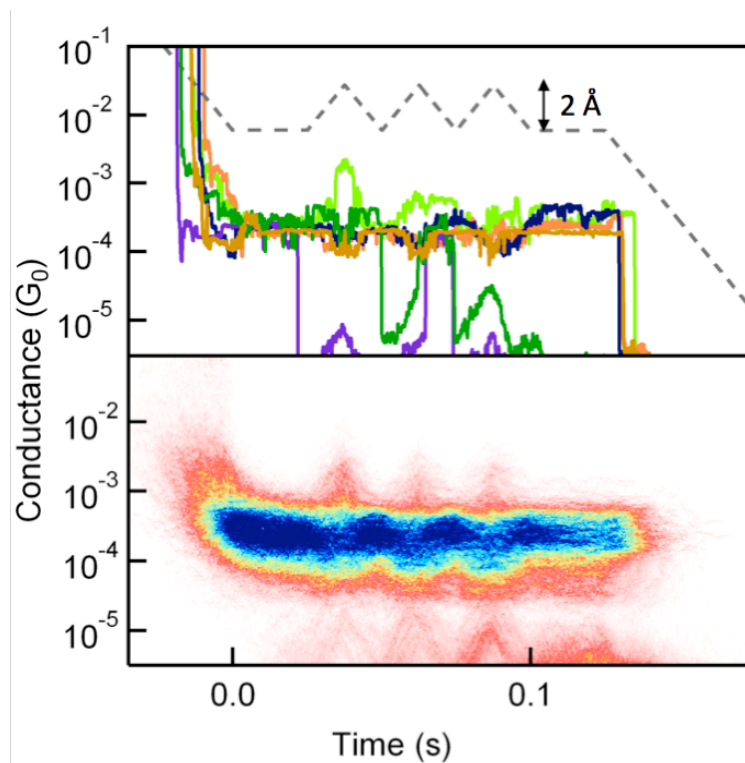


**Figure B5:** Upper panel: sample traces measured using the modified piezo ramp with a  $2 \text{ \AA}$  amplitude with 1,6-bis(methylsulfide)hexane. Lower panel: two-dimensional histograms of all selected traces (1477 out of 10000) measured with the zig-zag ramp.

#### **B4. Theoretical Methods and Details**

All electronic structure calculations used Jaguar (version 7.0, Schrodinger LLC, New York, NY, 2007) using the B3LYP hybrid functional and the 6-31G\*\* basis sets. The Au atoms were described using the LACVP local potentials. The geometries of **A1**, **C4**, **Au<sub>2</sub>-A1**, and **Au<sub>2</sub>-C4** were fully optimized. The final geometries and total energies are given below.



Molecule: **A1**

DFT: B3LYP, 6-31G\*\*

Final total energy: -1909.86419 hartrees

Final geometry:

	angstroms		
atom	x	y	z
C1	-0.0054586777	0.0160760258	-0.0169920773
C2	0.0027896249	0.0085385018	1.3914265084
C3	1.2617271719	0.0012497986	2.0283492339
C4	2.4438887757	0.0015085903	1.3053981250
C5	2.4188241032	0.0089772276	-0.0998196412
C6	1.1742433465	0.0163070722	-0.7499110173
C7	-1.2021440991	0.0072778950	2.2052531568
C8	-2.4927133813	0.0169740384	1.7749831566
C9	-3.6075929604	0.0127547254	2.6676183755
C10	-4.9334990519	0.0224029486	2.3021511411
C11	-5.2751397474	0.0392694232	0.9081509595
N12	-5.5621980629	0.0531364751	-0.2201717100
C13	-6.0101421145	0.0154862932	3.2699705747
C14	-7.3322358085	0.0233110312	2.9653261724
C15	-8.4151733561	0.0145807935	3.9266602800
C16	-8.0813278759	-0.0032513273	5.3218234957
N17	-7.7896758628	-0.0176148026	6.4488742453
C18	-9.7352003865	0.0222806138	3.5418266357
C19	-10.8782093540	0.0136783650	4.3994222849
C20	-12.1461860159	0.0220303112	3.9044895871
C21	-13.4021959869	0.0146818583	4.6351965919

C22	-14.6079289886	0.0263155388	3.9099862826
C23	-15.8483278911	0.0202660156	4.5387136047
C24	-15.9277001203	0.0017264220	5.9370020083
C25	-14.7299066618	-0.0103240334	6.6793230835
C26	-13.4999714035	-0.0041483078	6.0445455925
H27	-3.3938194979	0.0003963107	3.7351203893
H28	-9.9256264741	0.0358768554	2.4698511737
H29	-5.7046635080	0.0023889406	4.3139517264
H30	-7.6345826850	0.0364930545	1.9204393953
H31	-1.0316634905	-0.0025146717	3.2818925770
S32	3.9910988563	0.0084039910	-0.9274374134
H33	3.3957627930	-0.0044316048	1.8287255893
H34	1.3047841869	-0.0047694344	3.1145542437
H35	-0.9481970700	0.0214885691	-0.5550998814
H36	1.1158745968	0.0221111506	-1.8319398186
H37	-10.7015210857	-0.0001287768	5.4719983301
H38	-12.2526442300	0.0358262463	2.8196296730
S39	-17.4430232213	-0.0078399861	6.8645500296
H40	-16.7451674257	0.0300240106	3.9305929385
H41	-14.5699844983	0.0404738872	2.8235381871
H42	-12.6003534518	-0.0141466040	6.6514829712
H43	-14.7718464591	-0.0246611109	7.7647246498
H44	-2.7134702204	0.0283108250	0.7108404068
C45	-18.7342463992	0.0135341018	5.5795904309
H46	-19.6832765180	0.0068539840	6.1193210506
H47	-18.6792182189	0.9193772498	4.9717731839
H48	-18.6821711952	-0.8737282692	4.9446992281
C49	3.5500383513	0.0142213788	-2.6948981937
H50	4.5004270922	0.0121132100	-3.2322812278
H51	2.9861342170	-0.8798300083	-2.9698160773
H52	2.9926291711	0.9135017312	-2.9658734422

Molecule: C4

B3LYP, 6-31G\*\*

Final total energy: -1380.11453 hartrees

Final geometry:

	angstroms		
atom	x	y	z
C1	-0.0221616271	0.0305191350	0.0657841755
C2	0.0505512825	0.0074467812	1.4712469394
C3	1.3277432101	-0.0214717221	2.0644324619
C4	2.4824111277	-0.0279251694	1.2886342811
C5	2.3940480177	-0.0052338919	-0.1022654048
C6	1.1349232644	0.0236065508	-0.7067546243
C7	-1.1500491919	0.0210224430	2.3322139375
C8	-2.4642172798	0.0200794862	1.9282325595
C9	-3.5626572514	0.0607782631	2.8408985884
C10	-4.8923875129	0.0687414444	2.5311564879
C11	-5.8881283931	0.1410966200	3.5564740442
C12	-7.2395506329	0.1665423464	3.3755156381
C13	-8.1765498464	0.2718719279	4.4542673537
C14	-9.5285250050	0.3102243306	4.2922088751
C15	-10.4967098987	0.4474326670	5.3441060724
C16	-11.8299166562	0.4874863103	5.0879124803
C17	-12.9519267843	0.6487222766	6.0013380875
C18	-12.8435524243	0.8223418732	7.3944075692
C19	-13.9702420162	0.9877303016	8.1954721673
C20	-15.2552778560	0.9855665195	7.6300934672
C21	-15.3785559738	0.8073841152	6.2428590091
C22	-14.2523666593	0.6442161835	5.4547805575

H23	-7.7653337333	0.3339907054	5.4618309675
H24	-5.2159161072	0.0299975693	1.4910745619
H25	-9.9250838102	0.2437572817	3.2783197951
H26	-3.3058197567	0.0970533638	3.8970299195
H27	-7.6416884426	0.1163793456	2.3633494258
H28	-5.5136371922	0.1890132931	4.5791158155
H29	-12.1223322999	0.3951920445	4.0415861458
S30	-16.7774130997	1.1948086860	8.5286893528
H31	-16.3632711996	0.8015210691	5.7840625660
H32	-14.3719619379	0.5107655764	4.3826476703
H33	-11.8645342439	0.8327906750	7.8648242297
H34	-13.8376736657	1.1201628395	9.2633471263
H35	-2.6853256881	-0.0050533406	0.8644066396
C36	-0.9120067742	0.0384788820	3.7478490561
H37	3.2935780054	-0.0090819695	-0.7105257126
H38	3.4529261387	-0.0501423745	1.7755083334
H39	1.4134213558	-0.0385732287	3.1459155885
H40	-0.9857224925	0.0579577247	-0.4330746723
H41	1.0535213299	0.0430039393	-1.7896751657
H42	-10.1230897813	0.5277065949	6.3638829573
N43	-0.7363902581	0.0501750068	4.8991437366
C44	-16.2411684638	1.4463029825	10.2504037037
H45	-17.1591222690	1.5911879998	10.8236836060
H46	-15.7157666983	0.5714214952	10.6400607049
H47	-15.6177881406	2.3377946450	10.3492541465

Molecule: **Au<sub>2</sub>-A1**

B3LYP, 6-31G\*\*/LACVP

Final total energy: -2180.81428 hartrees

Final geometry:

	angstroms		
atom	x	y	z
C1	-0.1516373949	0.1679875211	-0.0920807598
C2	-0.1554448482	0.1426712864	1.3189390134
C3	1.0950682395	0.0959268006	1.9662913092
C4	2.2834179216	0.0722650893	1.2466190464
C5	2.2685631129	0.0939093271	-0.1578716415
C6	1.0283367266	0.1450026652	-0.8179739000
C7	-1.4298578120	0.1556168426	2.0175984357
C8	-1.6479765191	0.1579270279	3.3611422960
C9	-2.9622376371	0.1481850783	3.9206759664
C10	-3.2784332203	0.1451744227	5.2595695653
C11	-2.2256593264	0.1715243113	6.2341693894
N12	-1.3825923233	0.1950646990	7.0369549542
S13	3.7168477442	0.0609847888	-1.1863319944
C14	5.0901887530	-0.1068559426	-0.0023258630
C15	-4.6464451705	0.1045807583	5.7315867670
C16	-5.0255135231	0.0790647660	7.0345937175
C17	-6.3937433972	0.0239428273	7.5051142778
C18	-7.4441699552	-0.0080536046	6.5279112199
N19	-8.2840057906	-0.0353541022	5.7221000288
C20	-6.7115130661	-0.0132685978	8.8430009027
C21	-8.0256896009	-0.0812680369	9.4003620940
C22	-8.2437773535	-0.1239383696	10.7434470448

C23	-9.5174855466	-0.1938231748	11.4406077574
C24	-10.7729390874	-0.2106831967	10.7900000803
C25	-11.9527239137	-0.2787178759	11.5105828581
C26	-11.9345078346	-0.3325500112	12.9174044466
C27	-10.7015192229	-0.3151262038	13.5799404261
C28	-9.5202313733	-0.2476393486	12.8466948642
S29	-13.5277210425	-0.3528084540	13.7409995325
C30	-13.0603518622	-0.3164940106	15.5108257009
Au31	-14.5024901338	-2.6095863740	13.4571867019
H32	3.2218390586	0.0336526329	1.7879740759
H33	1.1452791694	0.0736161875	3.0507683321
H34	-1.0999330274	0.2039259268	-0.6228532913
H35	0.9941922861	0.1605641450	-1.9039558313
H36	-2.3072802772	0.1596859296	1.3702118362
H37	-0.8108994067	0.1618803954	4.0550936332
H38	-3.7981752710	0.1291394194	3.2228255261
H39	-5.4087535267	0.0872652434	4.9556374629
H40	-4.2630557325	0.0899286556	7.8105133488
H41	-5.8768160363	0.0099773858	9.5422295413
H42	-8.8616179730	-0.1007964511	8.7051387280
H43	-7.3670894811	-0.1046560205	11.3914968636
H44	-8.5712925854	-0.2372100081	13.3777291444
H45	-10.6450344931	-0.3569231448	14.6612106335
H46	-12.9045312944	-0.2987525020	10.9871035551
H47	-10.8253190860	-0.1688656503	9.7062787616
H48	5.1557753051	0.7553652430	0.6654996964
H49	5.0082487114	-1.0296409468	0.5767940192
H50	5.9958057167	-0.1510484786	-0.6111780022
H51	-12.4899264306	-1.2026905582	15.7924293051
H52	-14.0044300352	-0.3082362637	16.0571946543
H53	-12.5005591224	0.5952144728	15.7349863339

Au54    -15.6041498559    -4.9343391061    13.2321392566

Molecule: **Au<sub>2</sub>-C<sub>4</sub>**

B3LYP, 6-31G\*\*/LACVP

Final total energy: -1651.074011 hartrees

Final geometry:

	angstroms		
atom	x	y	z
C1	-0.0157017963	0.0713846205	0.0100088942
C2	-0.0118780466	0.0574814708	1.4167733522
C3	1.2404537151	0.0046851532	2.0705008407
C4	2.4275782274	0.0119996515	1.3502056867
C5	2.3943929024	0.0397774758	-0.0495957415
C6	1.1662093791	0.0546989829	-0.7199962650
C7	-1.2925818092	0.1475882933	2.1042742997
C8	-1.5445809720	0.0547421499	3.4348586239
C9	-2.8580297143	0.2437167487	3.9826887694
C10	-3.1844232823	0.1319396223	5.3000704689
C11	-4.4990801142	0.3756221425	5.8111019268
C12	-4.8574738253	0.2164532870	7.1164697956
C13	-6.1630000042	0.4864148915	7.6337069042
C14	-6.5143059703	0.2593894971	8.9324159169
C15	-7.8043499020	0.5445691560	9.4770163200
C16	-8.2013856165	0.2527364866	10.7570880070
C17	-7.2855822889	-0.4687689976	11.5941527484
N18	-6.5455373448	-1.0662493374	12.2662795552
S19	3.8714400398	0.2111589482	-1.0640110846
C20	4.9903736624	-1.0844467160	-0.4077782114
C21	-9.5126099593	0.6012157947	11.3377247039
C22	-10.3310782986	1.5966127061	10.7696238294



C23	-11.5618579051	1.9129444833	11.3374705296
C24	-12.0029360574	1.2502985388	12.4839933743
C25	-11.1987587534	0.2660184912	13.0606093806
C26	-9.9667531961	-0.0537118197	12.4969875873
H27	-2.4147493587	-0.1571741925	6.0159303128
H28	-6.9079680580	0.8887811008	6.9464122007
H29	-3.6437981061	0.5070433353	3.2738701458
H30	-5.7686471574	-0.1722184270	9.5981027247
H31	-5.2542664826	0.7082690098	5.0980360509
H32	-4.1091763819	-0.1462937171	7.8217503301
H33	-2.1424095822	0.3253711826	1.4455936853
H34	1.1353606077	0.0733025681	-1.8036737409
H35	-0.9674620536	0.1073238813	-0.5168104552
H36	1.2889975403	0.0083579577	3.1536287791
H37	3.3765622903	0.0336033088	1.8790898024
H38	-8.5304716919	1.0212860850	8.8235923062
H39	-12.9611702550	1.5060690611	12.9275935091
H40	-11.5281163260	-0.2545725451	13.9542156847
H41	-9.3493007561	-0.8221582988	12.9532240181
H42	-9.9947464398	2.1452441082	9.8961649563
H43	-12.1750177976	2.6907268560	10.8898848717
H44	-0.7430734747	-0.1635173370	4.1387137927
H45	5.9164448599	-0.9988878072	-0.9785381181
H46	5.2009031202	-0.9300127831	0.6503336885
H47	4.5364919704	-2.0624752090	-0.5760763271
Au48	4.7641825117	2.3655582803	-0.2666378145
Au49	5.5058118799	4.6126128264	0.7780153528

**B5. References**

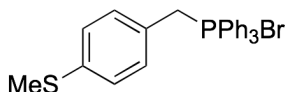
1. Ulrich, J.; Esrail, D.; Pontius, W.; Venkataraman, L.; Millar, D.; Doerrer, L. H., *J. Phys. Chem. B*, **2006**, *110*, 2462–2466.
2. Kamenetska, M.; Koentopp, M.; Whalley, A.; Park, Y. S.; Steigerwald, M.; Nuckolls, C.; Hybertsen, M.; Venkataraman, L. *Phys. Rev. Lett.*, **2009**, *102*, 126803.
3. Quek, S. Y.; Kamenetska, M.; Steigerwald, M. L.; Choi, H. J.; Louie, S. G.; Hybertsen, M. S.; Neaton, J. B.; Venkataraman, L. *Nature Nanotech.*, **2009**, *4*, 230–234.

## Appendix C

### C1. Synthetic Details

**General Information:** 4-(methylthio)benzaldehyde, 3-(methylthio)benzoic acid, 4-(methylthio)benzyl bromide, and all other starting materials and reagents were all purchased from Sigma-Aldrich. All reactions were carried out under nitrogen unless otherwise noted. (3-(methylthio)benzaldehyde,<sup>1</sup> (3-(methylthio)phenyl)methanol,<sup>1</sup> and (3-methylthio)benzyl chloride<sup>2</sup> were prepared according to the reported procedures. Sodium methoxide solution was made fresh by dissolving sodium metal into 5 mL of methanol. Flash column chromatography was performed on a Teledyne ISCO Combiflash RF using Redisep RF silica columns. All <sup>1</sup>H and <sup>13</sup>C NMR spectra were taken on a Bruker DRX300 (300MHz), DRX400 (400MHz) and DMX500 (500MHz).

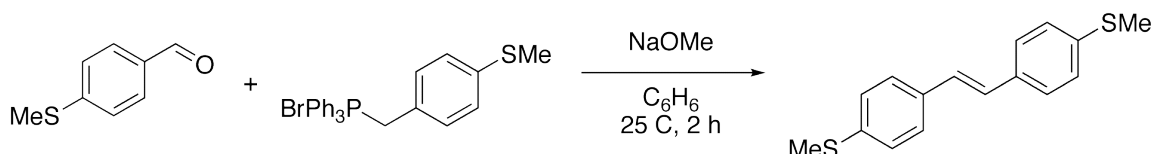
### Synthetic Experimentals:



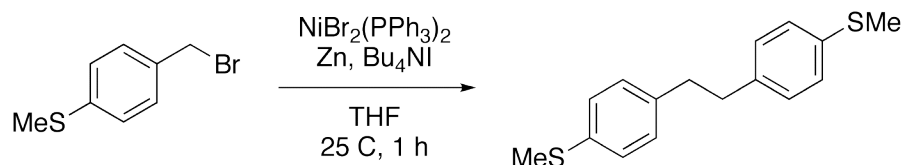
*4-(methylthio)benzyltriphenylphosphonium bromide:* Adapted from known procedure.<sup>3</sup>

To a flame dried 25-mL round-bottom flask was added triphenylphosphine (3.91 g, 14.9 mmol) and anhydrous benzene (10 mL). The reaction flask was purged with nitrogen gas and then heated to reflux, at which point a solution of (4-methylthio)benzyl bromide (3.23 g, 14.9 mmol) in 5 mL of anhydrous benzene was added to the reaction solution via syringe. The reaction was stirred at reflux for 12 hours as product precipitated out. The

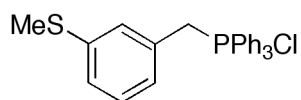
crude product was isolated by filtration, washed with benzene and recrystallized from CH<sub>2</sub>Cl<sub>2</sub>/benzene mixture. The product was isolated as white powder in quantitative yields. <sup>1</sup>H NMR (300 MHz, CDCl<sub>3</sub>): δ 7.81-7.74 (m, 9H), 7.69-7.62 (m, 6H), 7.08-6.98 (m, 4H), 5.45 (d, *J* = 14.4 Hz, 2H), 2.42 (s, 3H); <sup>13</sup>C NMR (300 MHz, DMSO-*d*<sub>6</sub>): δ 139.73, 139.68, 135.0, 134.9, 132.2, 132.1, 131.1, 130.9, 126.7, 124.8, 124.7, 119.3, 118.2, 28.9, 28.3, 15.2.



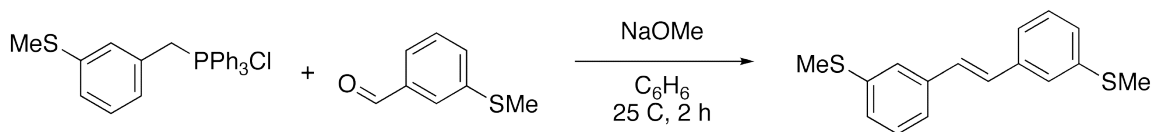
*(E)*-4,4'-*di*-(methylthio)stilbene (**1**): In a 100-mL round-bottom flask, (4-methylthio)benzaldehyde (0.100 g, 6.62 mmol) and (4-methylthio)benzyltriphenylphosphonium bromide (3.20 g, 6.62 mmol) were dissolved in 50 mL of anhydrous methanol under a nitrogen atmosphere. Sodium methoxide (13.2 mmol) in methanol solution was added to the reaction slowly over 10 min by syringe. An off-white precipitate forms while the reaction was stirred for an additional 2 hours at room temperature. The pure product was collected by vacuum filtration as pale yellow needles in 31.0% yield. No further purification was necessary. UV-vis: 223 nm ( $\epsilon = 1.38 \times 10^4 \text{ mol}^{-1} \cdot \text{cm}^{-1}$ ), 347 nm ( $\epsilon = 4.42 \times 10^4 \text{ mol}^{-1} \cdot \text{cm}^{-1}$ ), 362 nm (shoulder,  $\epsilon = 3.21 \times 10^4 \text{ mol}^{-1} \cdot \text{cm}^{-1}$ ); <sup>1</sup>H NMR (300 MHz, CDCl<sub>3</sub>): δ 7.44 (d, *J* = 8.4 Hz, 4H), 7.23 (d, *J* = 7.8 Hz, 4H), 7.02 (s, 2H), 2.50 (s, 6H); <sup>1</sup>H NMR (300 MHz, DMSO-*d*<sub>6</sub>): δ 7.54 (d, *J* = 8.4 Hz, 4H), 7.26 (d, *J* = 8.3 Hz, 4H), 7.18 (s, 2H), 2.50 (s, 6H); <sup>13</sup>C NMR (300 MHz, CDCl<sub>3</sub>): δ 138.2, 134.7, 127.8, 127.2, 127.1, 16.2; HR-MS: *m/z* calcd for (C<sub>16</sub>H<sub>16</sub>S<sub>2</sub>): 272.0693, found: 272.0686.



*1,2-bis(4-(methylthio)phenyl)ethane (2)*: This procedure was modified from the reported preparation of *1,2-bis(4-(methoxy)phenyl)ethane*.<sup>4</sup> In a 100-mL round-bottom flask, dibromobis(triphenylphosphine)nickel(II) (0.086 g, 0.12 mmol), zinc powder (0.112 g, 1.73 mmol) and tetrabutylammonium iodide (0.296 g, 1.15 mmol) were combined in a with 25 mL of tetrahydrofuran. The green slurry was stirred for 30 min at room temperature as the color changes to grey-brown. Then, a solution of 4-(methylthio)benzyl bromide (0.250 g, 1.15 mmol) in 5 mL of tetrahydrofuran was added dropwise to the reaction slurry. The reaction turns red and later dark purple. The reaction was monitored by TLC and finished in less than 1 hour. The zinc solid was filtered off and washed with dichloromethane. The organic solvents were removed by rotary evaporation and the product was isolated by flash column chromatography (hexanes) as a colorless crystalline solid in 46.2% yield. UV-vis: 261 nm ( $\epsilon = 2.66 \times 10^4 \text{ mol}^{-1} \cdot \text{cm}^{-1}$ ); <sup>1</sup>H NMR (300 MHz, CDCl<sub>3</sub>):  $\delta$  7.19 (d,  $J = 8.4$  Hz, 4H), 7.08 (d,  $J = 8.4$  Hz, 4H), 2.85 (s, 4H), 2.45 (s, 6H); <sup>13</sup>C NMR (300 MHz, CDCl<sub>3</sub>):  $\delta$  139.10, 135.91, 129.43, 127.53, 37.66, 16.71; HR-MS:  $m/z$  calcd for (C<sub>16</sub>H<sub>18</sub>S<sub>2</sub>): 274.0850, found: 274.0841.



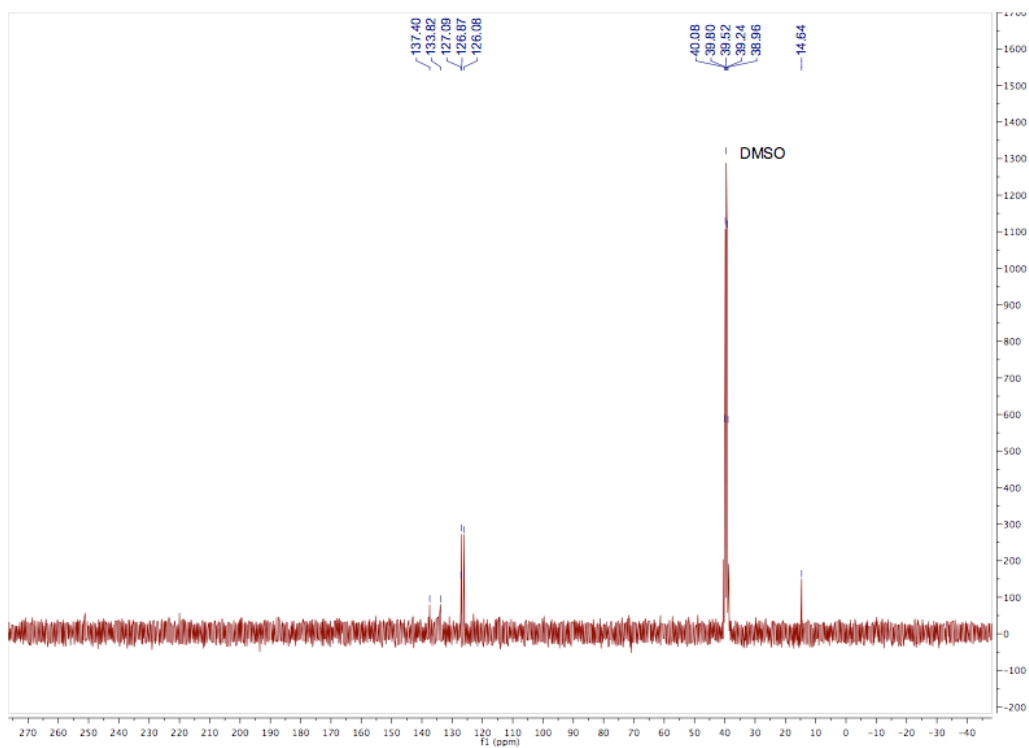
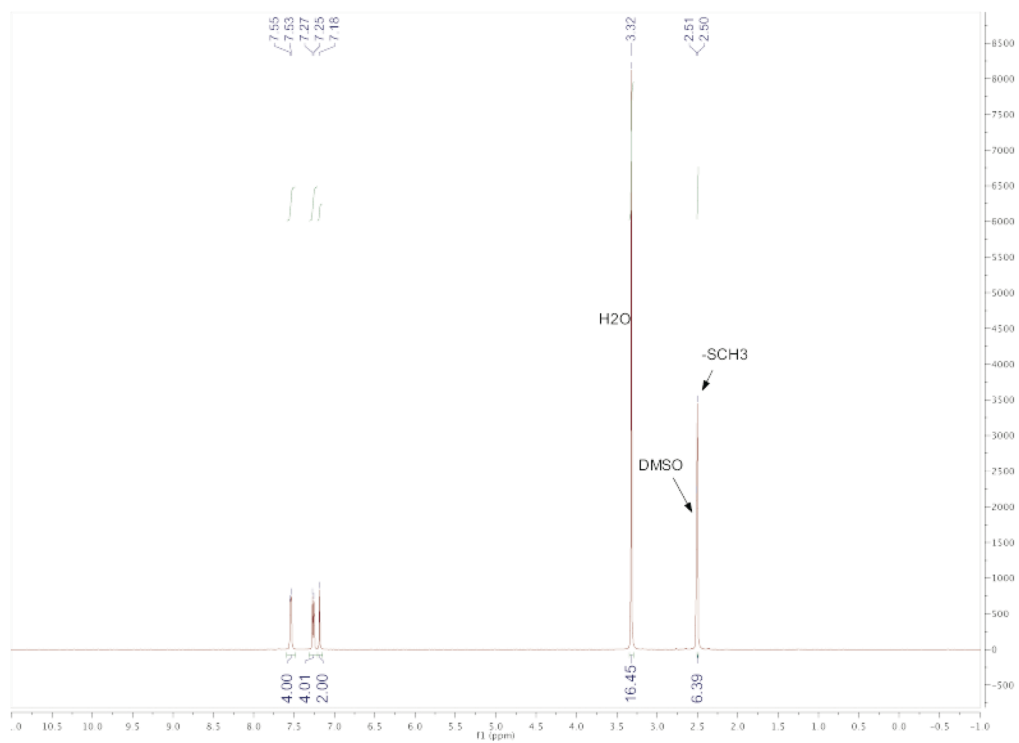
*3-(methylthio)benzyltriphenylphosphonium chloride*: Similar to the synthesis of *4-(methylthio)benzyltriphenylphosphonium bromide* above. *3-(methylthio)benzyl chloride* (0.230 g, 1.33 mmol) and triphenylphosphine (0.348 g, 1.33 mmol) were combined in anhydrous benzene (12 mL). The solution was refluxed for 24 hours. The reaction was cooled to room temperature, during which a white precipitate formed. The solid was isolated by vacuum filtration and washed with cold benzene. The white crystalline product (0.258 g, 45%) was dried in air.  $^1\text{H}$  NMR (300 MHz,  $\text{DMSO-}d_6$ ):  $\delta$  7.94 (t,  $J = 7.5$  Hz, 3H), 7.78-7.73 (m, 6H), 7.70-7.65 (m, 6H), 7.19 (m, 2H), 6.82 (bs, 1H), 6.74 (bs, 1H), 5.16 (d,  $J = 15.7$  Hz, 2H), 2.19 (s, 3H);  $^{13}\text{C}$  NMR (400 MHz,  $\text{DMSO-}d_6$ ):  $\delta$  139.43, 135.61, 135.58, 134.57, 134.47, 130.63, 130.51, 129.70, 129.28, 128.33, 127.58, 126.26, 118.59, 117.74, 28.81, 28.32, 14.75.



*(E)*-*3,3'*-*di-(methylthio)stilbene* (**3**): In a 50-mL round-bottom flask, *(3-methylthio)benzaldehyde* (0.10 g, 0.66 mmol) and *(3-methylthio)triphenyl-phosphonium chloride* (0.29 g, 0.66 mmol) were dissolved in 25 mL of anhydrous methanol under nitrogen. Sodium methoxide (1.32 mmol) was added to the solution slowly over 15 min via syringe. A colorful (usually yellow) precipitate forms while the reaction was stirred for an additional 2 hours at room temperature. The resultant *E/Z*-mixture of stereoisomers was collected by filtration and separated by flash column chromatography (25%  $\text{CH}_2\text{Cl}_2$

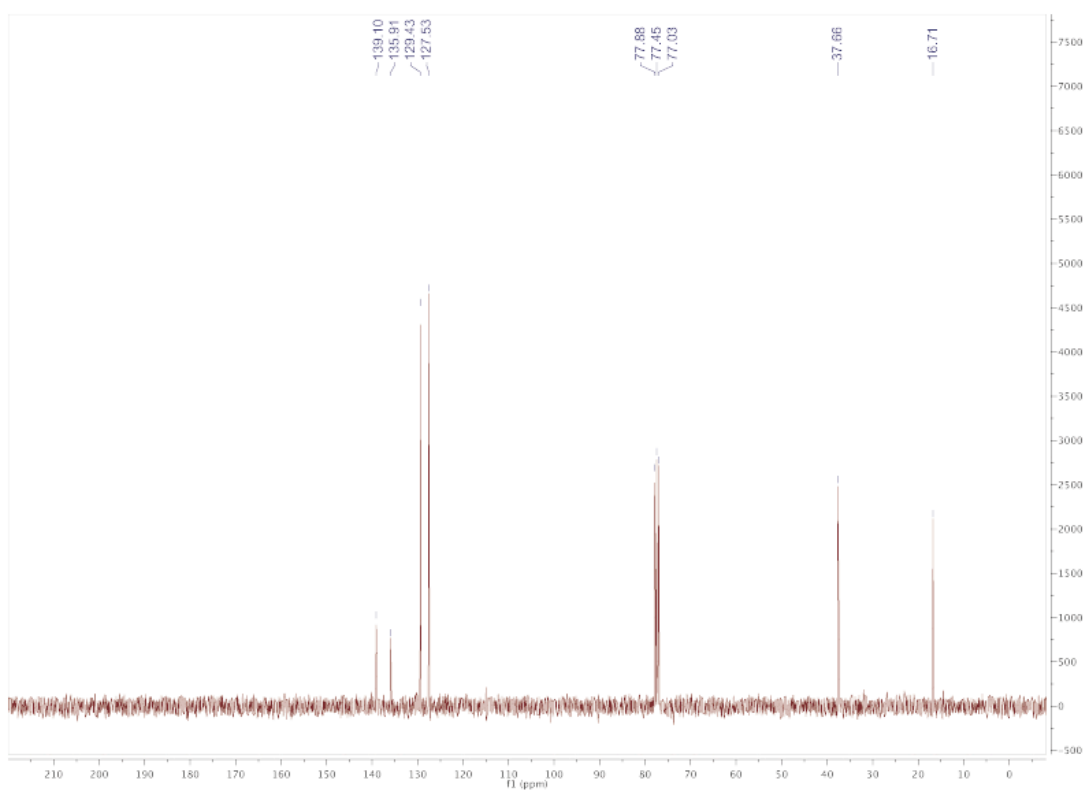
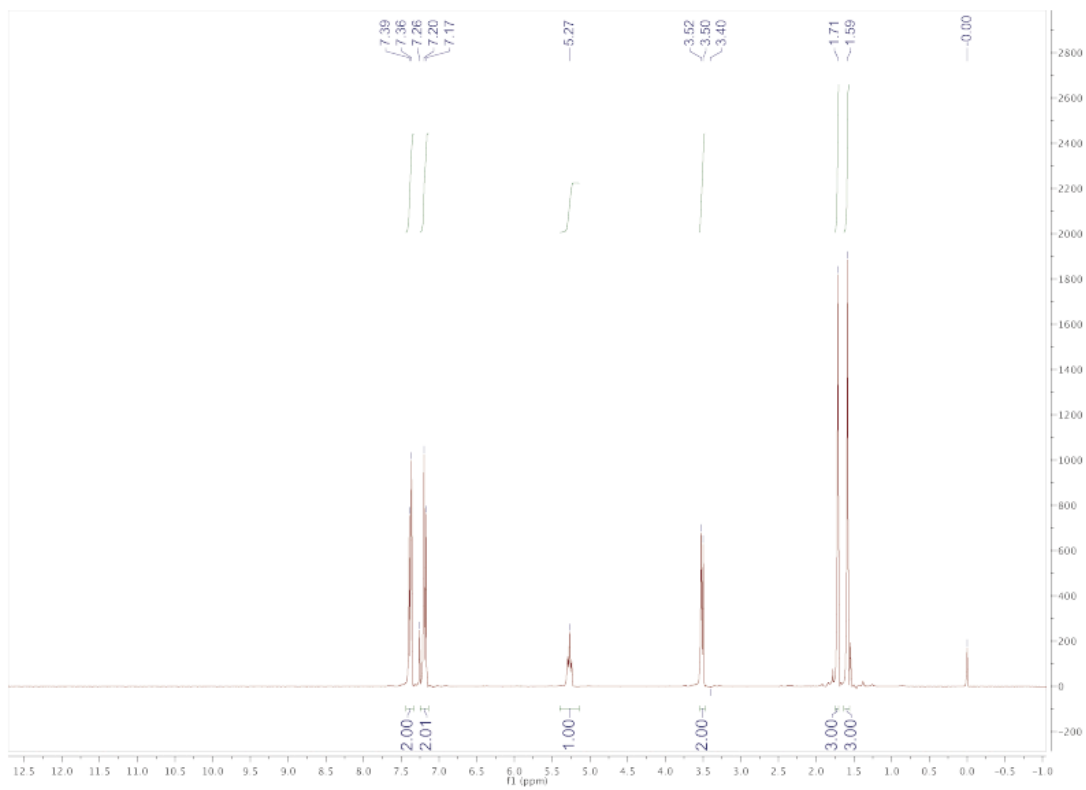
in hexanes). The (*E*)-stilbene was isolated as a white solid in overall 30% yield. UV-vis: 267 nm ( $\epsilon = 3.48 \times 10^4 \text{ mol}^{-1}\cdot\text{cm}^{-1}$ ), 302 nm ( $\epsilon = 2.68 \times 10^4 \text{ mol}^{-1}\cdot\text{cm}^{-1}$ );  $^1\text{H}$  NMR (300MHz,  $\text{CDCl}_3$ ):  $\delta$  7.39 (bs, 2H), 7.28-7.24 (m, 4H), 7.17-7.14 (m, 2H), 7.05 (s, 2H), 2.51 (s, 6H);  $^{13}\text{C}$  NMR (300 MHz,  $\text{CDCl}_3$ ):  $\delta$  139.46, 138.18, 129.49, 129.19, 126.34, 125.14, 123.81, 16.31; HR-MS:  $m/z$  calcd for ( $\text{C}_{16}\text{H}_{16}\text{S}_2$ ): 272.0693, found: 272.0692.

## C2. NMR Spectra

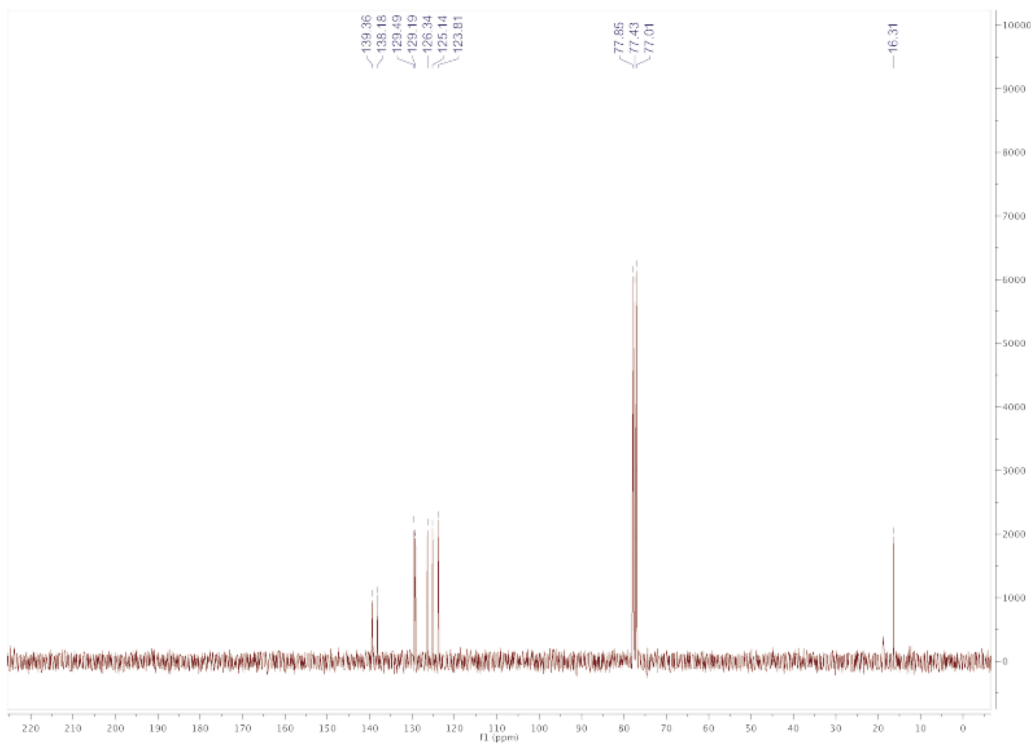
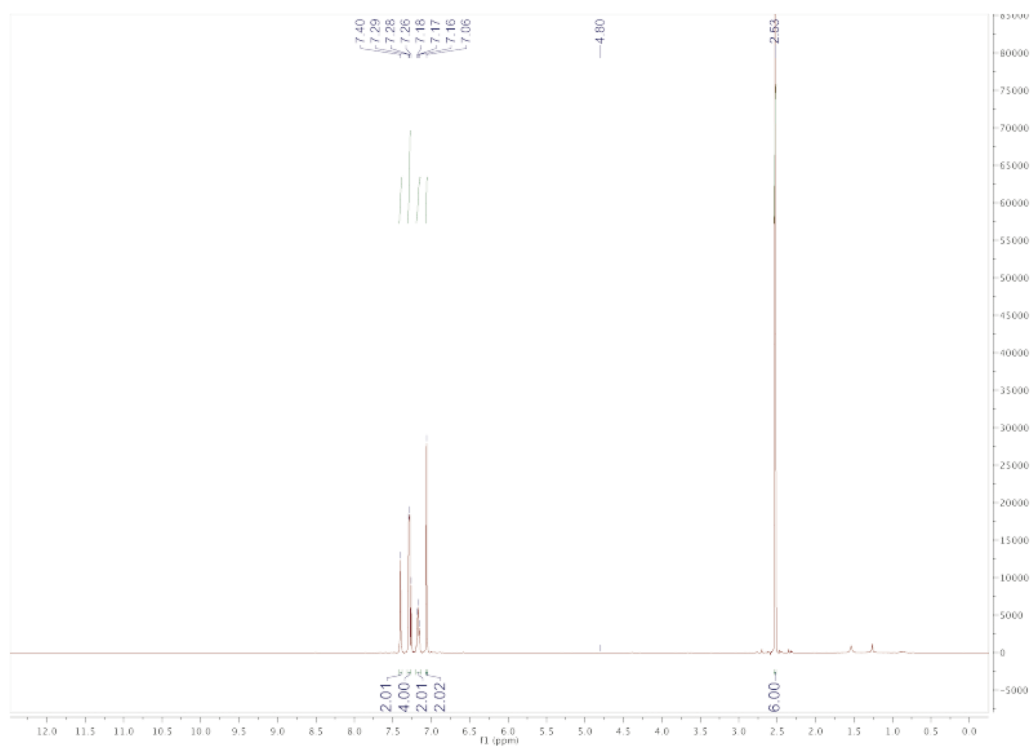


<sup>1</sup>H and <sup>13</sup>C NMR of (E)-4,4'-di-(methylthio)stilbene (1) in DMSO





$^1\text{H}$  and  $^{13}\text{C}$  NMR of *1,2-bis(4-(methylthio)phenyl)ethane* (**2**) in  $\text{CDCl}_3$



$^1\text{H}$  and  $^{13}\text{C}$  NMR of *(E)*-3,3'-di-(methylthio)stilbene (**3**) in  $\text{CDCl}_3$

### C3. Optical Absorption Spectroscopy

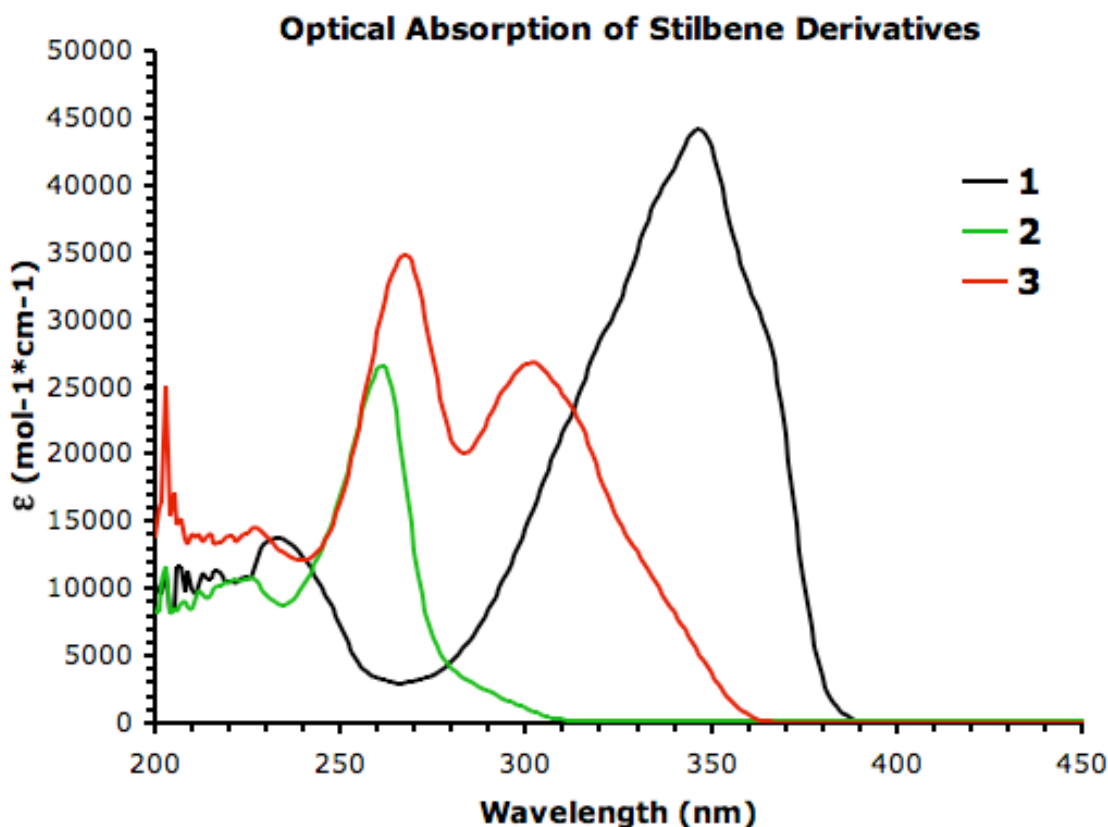


**Figure C1.** UV-vis spectra of each stilbene derivative (**1-3**) show conjugated molecules to have longest-wavelength absorption edges residing in the near UV spectrum (>350 nm), while molecule **2** (not fully conjugated) has an absorption edge at 310 nm. Absorption spectra were taken on an Agilent Technologies 8453 UV-Vis spectrophotometer using a quartz cuvette with path length equal to 1.0 cm. Solutions of oligoenes were prepared in CH<sub>2</sub>Cl<sub>2</sub> solution at a concentration of 5.00 x 10<sup>-5</sup> M. Solution optical band gaps,  $E_{OP}$ , are found to be 4.00, 3.42, 3.18 eV.

## C4. AFM-based Single-molecule Break Junction Studies

### Experimental Procedure

We use a custom-built conducting AFM to perform the simultaneous conductance and force measurements. All the experiments are performed in ambient and at room temperature. We use commercial tapping mode silicon AFM cantilevers (NanoAndMore) on which we sequentially thermally evaporate a  $\sim 10$  nm of chromium adhesion layer and an gold layer of  $\sim 100$  nm. Using the thermal spectrum method, we obtain nominal spring constants of  $\sim 50$  N/m (resonant frequency  $\sim 200$  kHz) after Au evaporation.<sup>5</sup> The substrates are cleaved mica surfaces coated with  $\sim 100$  nm of evaporated Au. The substrate is mounted on top of a single-axis piezoelectric stage (Mad City Labs). The substrate-tip junction is stretched and compressed with sub-angstrom precision by moving the substrate relative to the tip at a rate of 18 nm/s using the piezoelectric stage. A constant bias of 75 mV is applied to the substrate through a 10 k $\Omega$  series resistor. The current through the tip/substrate junction is measured by a current-voltage amplifier (Keithley 428). Both the conductance and force data are acquired at 100 kHz through data acquisition cards (National Instruments, PXI-4461 and PXI 6251) and custom-built software written in Igor Pro (Wavemetrics). All position determinations were based on measurements with a built-in position sensor within the piezoelectric positioner. This position sensor was calibrated both by the manufacturer and by us using laser interference measurements. We found the absolute values of the measured displacements to be accurate to within 5%. The details of our AFM based experimental setup have been described previously.<sup>6</sup>

## Analysis Technique

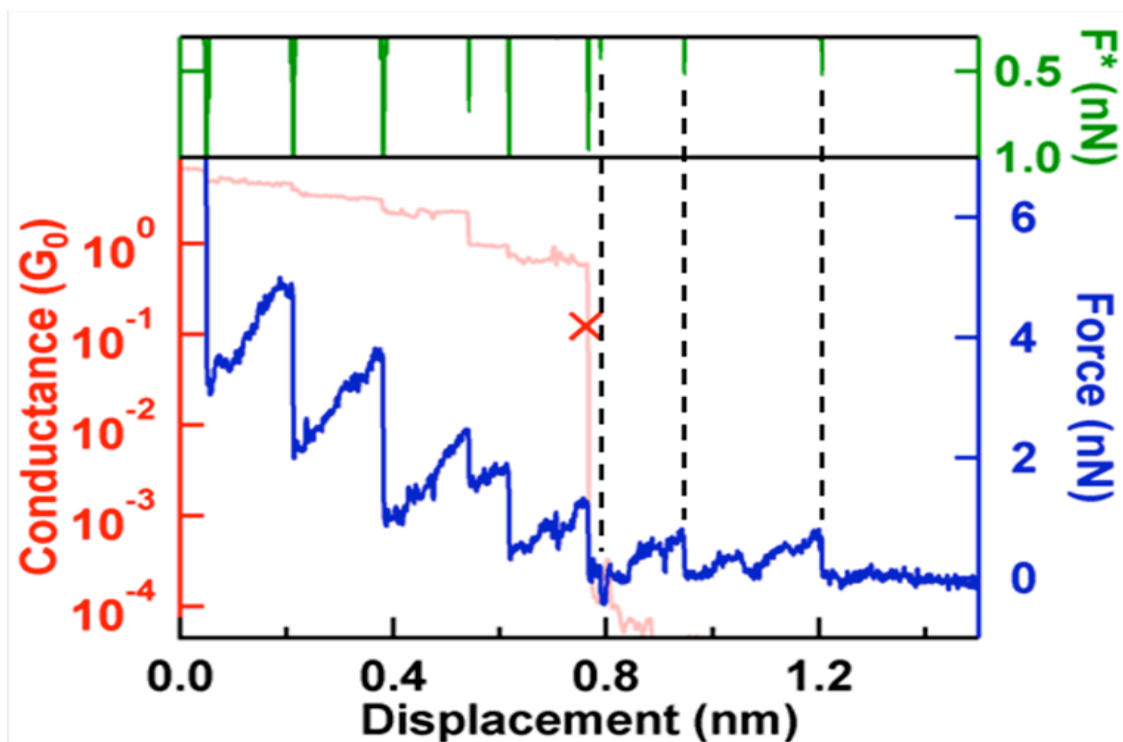
The measured conductance and force traces are analyzed using an automated algorithm (using Igor Pro software). The algorithm performs three sequential operations on every individual simultaneously measured conductance and force traces: (1) identifying the location of the end of the  $1G_0$  conductance plateau, (2) analyzing the force data beyond this point to find the last force event within 1 nm of this point and (3) setting the origin of conductance and force traces at this location and creating 2D histograms of force and conductance. Figure C2 demonstrates application of this technique on a sample individual elongation measurement of molecule **3**. The conductance drop from  $1 G_0$  is easily identified since the conductance decreases by more than two orders of magnitude upon the rupture of Au point-contacts. Analyzing the force data to identify significant events is carried out by the following procedure. First, the force trace  $F$  (Figure C2, blue trace) is transformed to a trace  $F^*$  (Figure S2, green trace) where every data point  $F^*[p]$  with index  $p$  is defined as:

$$F^*[p] = \sqrt{F[p]_{avg,10} \times F[p]_{avg,50}} \quad (\text{eq. C1})$$

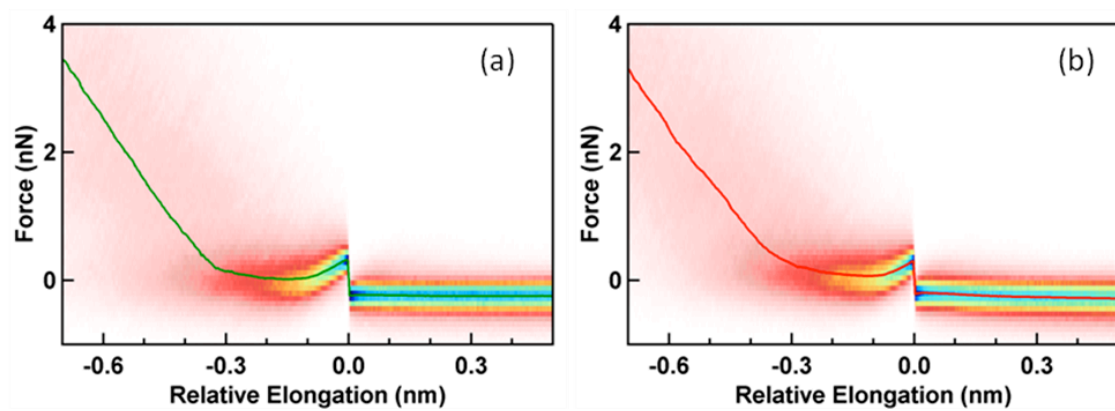
where,

$$F_{avg,n}[p] = \frac{1}{n} \left( \sum_{i=p-n}^p F[i] - \sum_{j=p}^{p+n} F[j] \right) \quad (\text{eq. C2})$$

$F^*$  shows clearly defined spikes at the positions where there are large changes in the force, and is much less sensitive to random noise compared to the original data, due to the averaging. We note that due to high frequency noise in the raw force trace, a simple numerical derivative cannot reliably identify the location of these sharp drops in force. We classify every spike of  $F^*$  that corresponds to a change in force greater than 0.3 nN (which is  $2\times$  the experimental noise level of the force data) as a significant force event, and use this threshold to consistently analyze all data collected here for all three molecule types.  $F^*$  is used to identify all the significant force events within a 1 nm elongation beyond the  $1 G_0$  point-contact rupture. Figure C2 demonstrates the high sensitivity of  $F^*$  to significant force events which are heuristically identified in the force data. It also demonstrates the insensitivity of  $F^*$  towards high frequency noise in the force data. The algorithm then identifies the last force event as the rupture of the molecular junction, irrespective of the conductance. This molecular rupture location is used as the origin to construct the displacement-preserving 2D histograms in (Figures 3.3 and 3.4 in Chapter 3).



**Figure C2.** Analysis technique applied to a sample pullout experiment. The rupture from  $1 G_0$  is shown by the red  $\times$ . Dashed lines are provided as visual guides to the force events identified through  $F^*$ , the auxiliary force trace (green) within a 1 nm displacement from the  $1 G_0$  rupture location.

**Force, Conductance and Elongation Length Histograms:**

**Figure C3.** 2D force histograms for molecule **2** (a) and **3** (b), with the statistically averaged force profiles overlaid.



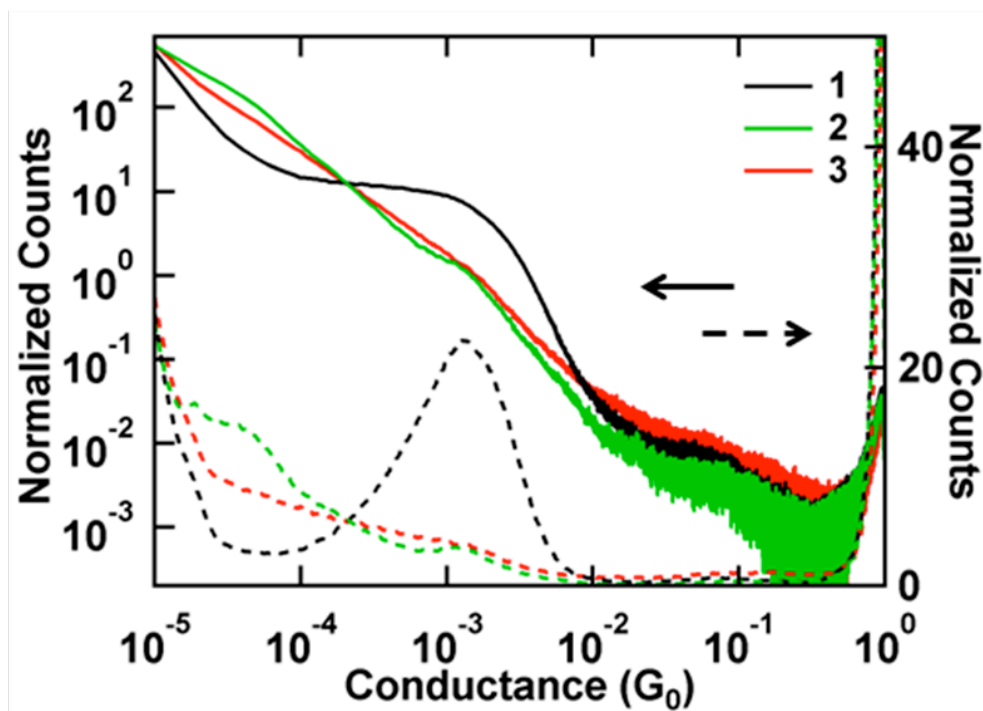


**Figure C4.** Histograms of conductance for all the measured traces for molecules **1-3**. Solid lines present a log-log plot of linearly binned conductance histograms with bin size =  $10^{-5} G_0$  and dashed lines present the logarithmically binned conductance histograms with 100 bins/decade. Conductance feature for **1** is prominent in both histograms, while **3** has no discernable feature in either representation.

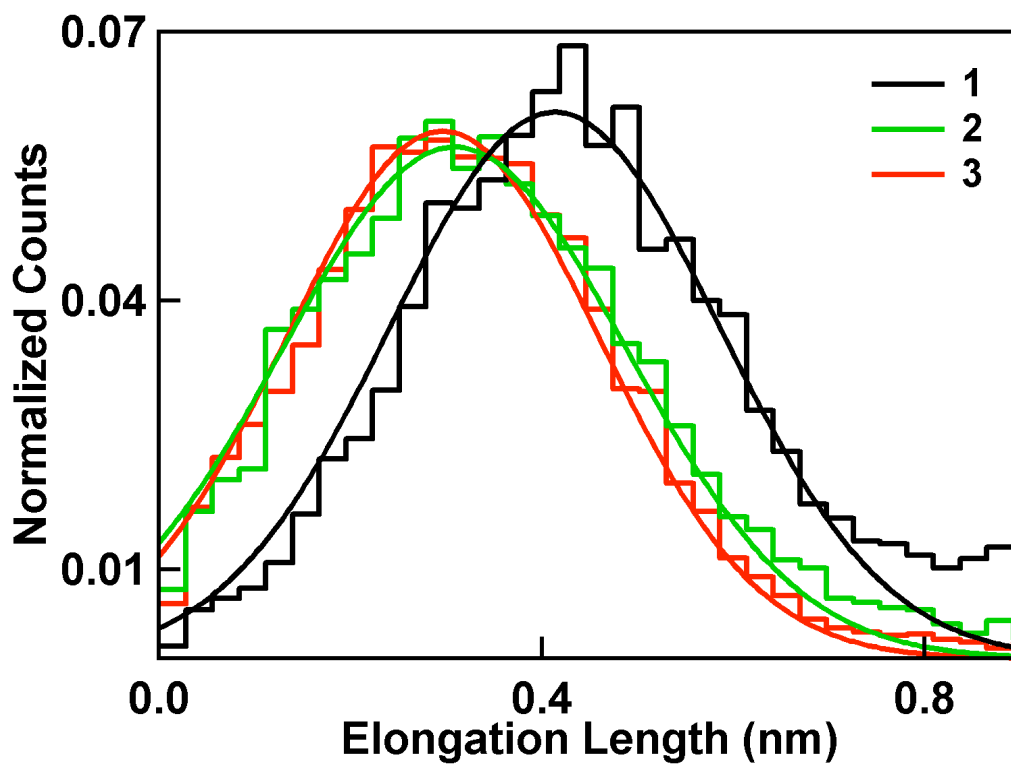


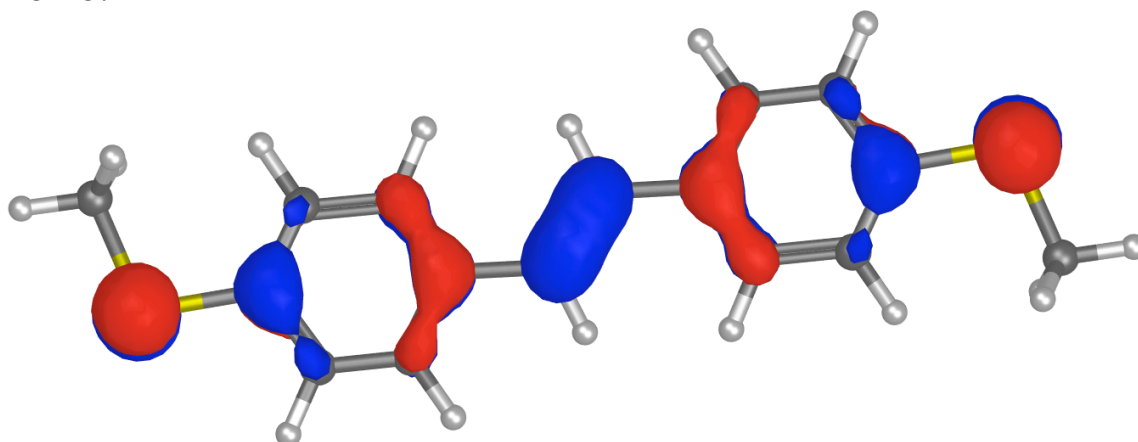
**Figure C5.** Elongation length distributions for molecules 1-3, normalized by total number of traces (1-6788, 2-6332 and 3-5965) for each case (0.03 nm/bin). Gaussian fits to the histograms are overlaid.

### C5. Theoretical Methods and Details

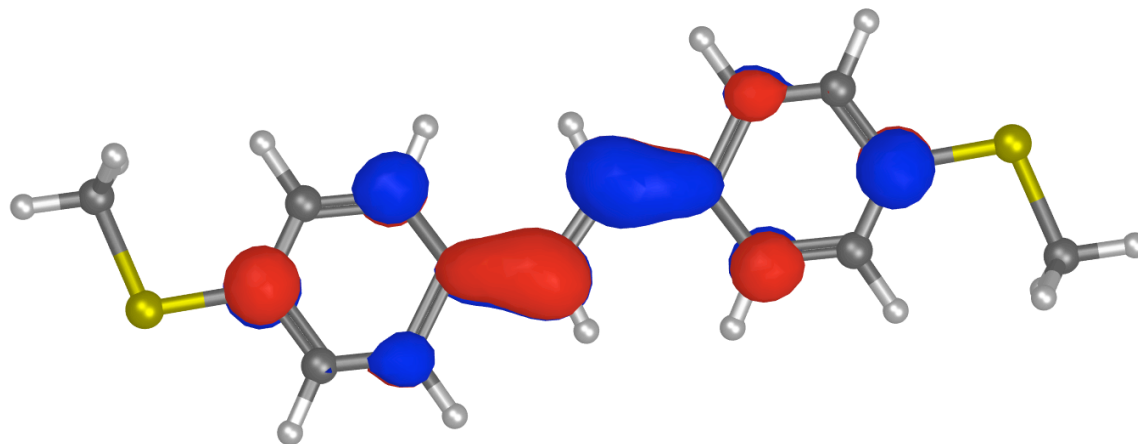
All electronic structure calculations used Jaguar (version 7.0, Schrodinger LLC, New York, NY, 2007) using the B3LYP hybrid functional and the 6-31G\*\* basis sets. The geometries of **1**, **2**, and **3** were fully optimized. The final geometries and total energies are given below.

*(E)*-4,4'-di-(methylthio)stilbene (**1**):

HOMO:



LUMO:



Final Geometry:

atom	x	y	z
C1	-3.8434657906	-1.8489488923	-0.0120387531

C2	-4.5597978043	-0.6660921203	-0.2805624712
C3	-5.9467255545	-0.6325681374	-0.2796433503
C4	-6.6855502592	-1.7937947552	-0.0064348986
C5	-5.9902287827	-2.9808488469	0.2650085261
C6	-4.5991963175	-3.0026449136	0.2621135588
H8	-4.0097134678	0.2469096457	-0.4949240973
H9	-6.4629515231	0.2996396986	-0.4916892543
H11	-6.5258516266	-3.8979328936	0.4823056343
H12	-4.0982714329	-3.9407699265	0.4812263322
C12	-1.5316801901	-2.8421871117	0.1511900371
C13	-2.3802636501	-1.8091183580	-0.0312521643
H15	-1.9652880229	-0.8205089096	-0.2198575523
H16	-1.9486865576	-3.8323927158	0.3259489543
C16	2.7734875957	-2.8774915889	0.1311408256
C17	2.0277379167	-4.0554884837	0.2888181918
C18	0.6411749301	-4.0140393968	0.2921141524
C19	-0.0682757996	-2.8065055585	0.1381972998
C20	0.6946137979	-1.6350753330	-0.0162369530
C21	2.0856456257	-1.6651369891	-0.0209750767
H23	2.5383213377	-5.0068558627	0.4096633569
H24	0.0856855673	-4.9404056715	0.4159550123
H25	0.1994174010	-0.6754224880	-0.1305297622
H26	2.6273682700	-0.7339753005	-0.1424063707
S26	-8.4609420801	-1.6384944700	-0.0311872223
C27	-9.0457398363	-3.3122035795	0.3862641249
H28	-10.1358266120	-3.2488756365	0.3880750438
H29	-8.7357642632	-4.0449031320	-0.3622958347
H30	-8.7077887729	-3.6191342554	1.3787457348
S30	4.5474530372	-3.0472519226	0.1422375258
C31	5.1465915681	-1.3400388869	-0.0658394496
H32	6.2362572697	-1.4100408636	-0.0593391970
H33	4.8255885854	-0.9149795515	-1.0193301512
H34	4.8286735152	-0.6998453415	0.7601083900

Total Energy (hartrees): -1415.73607449062

HOMO energy (hartrees): -0.18483

LUMO energy (hartrees): -0.04928

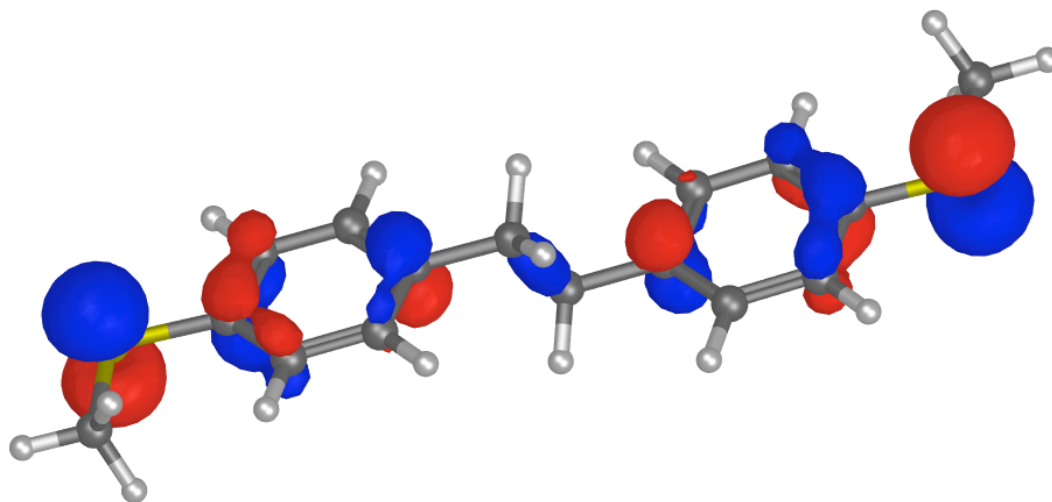
Orbital energies (hartrees):

-88.88533	-88.88533	-10.22391	-10.22390	-10.22024	-10.22022
-10.19744	-10.19727	-10.19490	-10.19484	-10.19299	-10.19283
-10.19270	-10.19270	-10.19168	-10.19162	-10.19059	-10.18982
-7.94627	-7.94626	-5.91154	-5.91154	-5.90741	-5.90741
-5.90116	-5.90115	-0.86678	-0.86337	-0.81690	-0.80337
-0.77646	-0.74930	-0.74811	-0.74693	-0.71289	-0.66634
-0.64406	-0.62146	-0.61013	-0.59317	-0.57536	-0.55401

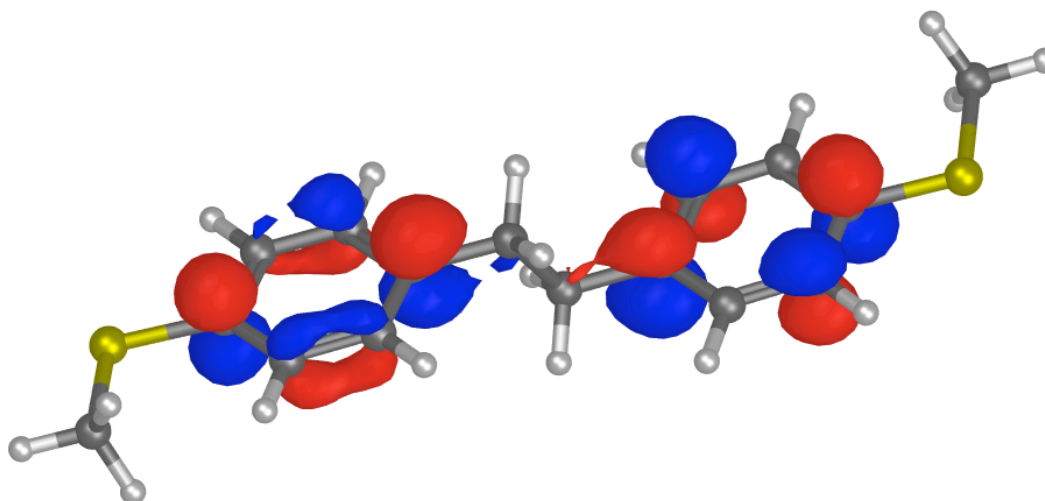
-0.50733	-0.50164	-0.46834	-0.46315	-0.45534	-0.44748
-0.44163	-0.43725	-0.43718	-0.43554	-0.42303	-0.41971
-0.40553	-0.40003	-0.38175	-0.37464	-0.36866	-0.36828
-0.35153	-0.34528	-0.33545	-0.32320	-0.32060	-0.31940
-0.29357	-0.25459	-0.25419	-0.25029	-0.21622	-0.18483
-0.04928	-0.00270	-0.00263	0.01549	0.03558	0.03569
0.07273	0.07408	0.07412	0.09542		

*1,2-bis(4-(methylthio)phenyl)ethane (2):*

HOMO:



LUMO:



Final geometry:

atom	x	y	z
C1	-2.0391223094	1.2619882597	0.2193244174
C2	-2.8429749263	2.0991273975	1.0072999068
C3	-4.2260745163	2.1113982422	0.8766424497
C4	-4.8599744865	1.2766399086	-0.0573181820
C5	-4.0717195107	0.4348307044	-0.8483758009
C6	-2.6821766960	0.4352886669	-0.7053876456
H8	-2.3772837900	2.7505411937	1.7431049756
H9	-4.8212531005	2.7681295433	1.5054024702
H11	-4.5246266736	-0.2287710339	-1.5762136209
H12	-2.0902480058	-0.2315183662	-1.3284610878

C12	-0.5318415897	1.2887850243	0.3460289145
H14	-0.2462663513	1.3803959869	1.4008232137
H15	-0.1086833348	0.3412859558	-0.0070304016
C15	0.1223094402	2.4539771393	-0.4433388058
H17	-0.1460269167	2.3543676346	-1.5018567924
H18	-0.3143949014	3.3992059037	-0.1011071460
C18	4.4402506542	2.5006518576	0.0495365811
C19	3.6205429879	3.2573621143	0.8934719110
C20	2.2352549305	3.2479458921	0.7187248637
C21	1.6265435738	2.4957170014	-0.2900060273
C22	2.4609976782	1.7451693037	-1.1306174682
C23	3.8415616660	1.7432791542	-0.9693360679
H25	4.0461817048	3.8612139509	1.6869369067
H26	1.6185232166	3.8478362191	1.3844878603
H27	2.0217598623	1.1530356593	-1.9303269106
H28	4.4615207037	1.1532452065	-1.6389004654
S28	6.2213643407	2.4242741773	0.1599858314
C29	6.6084822162	3.4853959305	1.5886467743
H30	7.6949071026	3.4507610684	1.6935820496
H31	6.3037293338	4.5200117629	1.4154965819
H32	6.1526080023	3.1062241112	2.5062533120
S32	-6.6416943423	1.3745702949	-0.1354578962
C33	-7.0820854404	0.1519479999	-1.4113037884
H34	-8.1712724770	0.1825905912	-1.4836298930
H35	-6.6561344384	0.4133711927	-2.3827759112
H36	-6.7752854926	-0.8563889808	-1.1236142931

Total Energy (hartrees): -1416.95778765468

HOMO energy: -0.20125

LUMO energy: -0.00500

Orbital energies (hartrees):

-88.88189 -88.88188 -10.22092 -10.22081 -10.21803 -10.21799  
-10.19190 -10.19182 -10.19161 -10.19157 -10.19084 -10.19078  
-10.18945 -10.18943 -10.18894 -10.18874 -10.18870 -10.18864  
-7.94285 -7.94284 -5.90816 -5.90814 -5.90404 -5.90402  
-5.89767 -5.89765 -0.86375 -0.86036 -0.81338 -0.79993  
-0.77341 -0.74710 -0.74495 -0.74232 -0.70947 -0.66622  
-0.64111 -0.61385 -0.60667 -0.60545 -0.57055 -0.56655  
-0.50044 -0.49205 -0.47815 -0.46031 -0.45356 -0.45022  
-0.44136 -0.43488 -0.43480 -0.43288 -0.42087 -0.41615  
-0.41266 -0.39824 -0.39736 -0.38188 -0.36915 -0.35851  
-0.35777 -0.35461 -0.34133 -0.33632 -0.32900 -0.31765  
-0.31515 -0.28134 -0.27265 -0.25091 -0.25046 -0.20663  
-0.20125 -0.00500 -0.00233 -0.00165 0.00757 0.03770

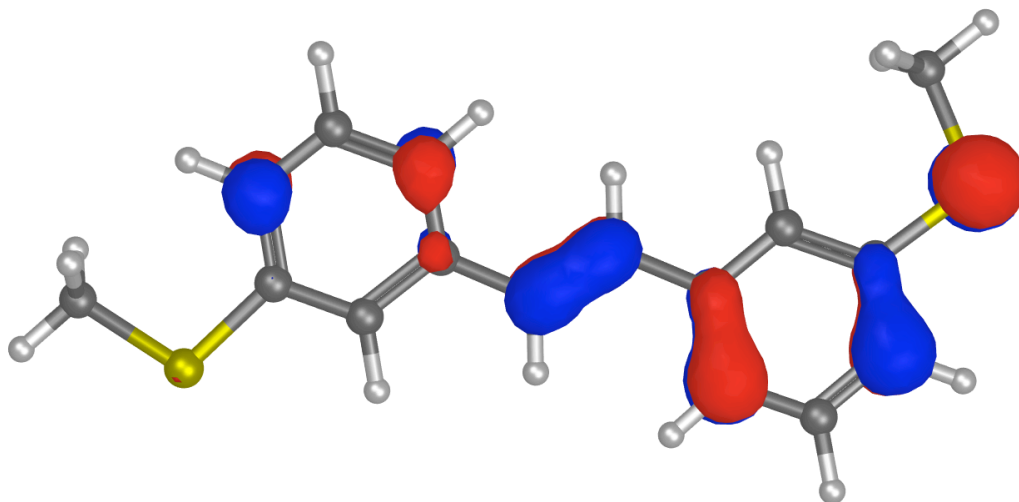
0.03789 0.07171 0.07587 0.10732 0.10821



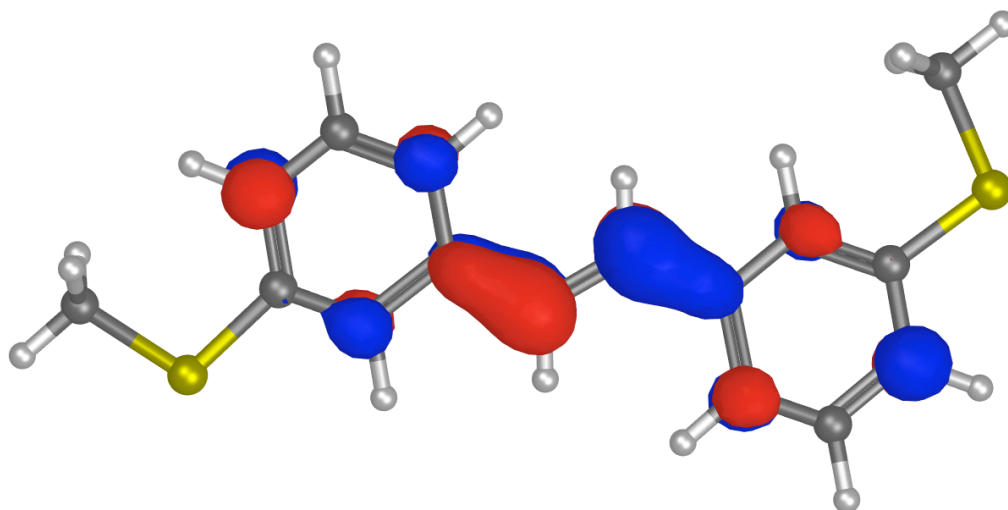


*(E)*-3,3'-di-(methylthio)stilbene (**3**):

HOMO:



LUMO:



Final Geometry:

atom	angstroms		
	x	y	z
C1	5.1445385010	-3.9313429181	2.2477499737
H2	6.0325375266	-4.4076372247	2.6682275355
H3	4.2585198521	-4.4739417722	2.5854357091
H4	5.1051384506	-2.8944674834	2.5891610324
S5	5.3426962042	-4.0349223237	0.4398560535
C6	1.5933339214	-2.1002631841	-1.3634677608
C7	1.7311136406	-2.1387232848	0.0161653010
C8	2.8529826542	-2.7171924821	0.6176900994
C9	3.8563150607	-3.2670897512	-0.1858178537
C10	3.7153360307	-3.2265107604	-1.5797833468
C11	2.5914510743	-2.6519535977	-2.1916495372

H12	0.7143541038	-1.6372538703	-1.7983644784
H13	0.9564255323	-1.7093655157	0.6454880562
H14	2.9299791236	-2.7292326065	1.6983686761
H15	4.4936068666	-3.6556800048	-2.2062883232
C16	1.4828296366	-2.2340023005	-4.4124944882
C17	2.5151314098	-2.6576279424	-3.6571012808
H19	3.3961469356	-3.0616085484	-4.1515398712
H20	0.5952018574	-1.8513909917	-3.9127592499
C20	1.0784016235	-2.1959102633	-8.6739565317
C21	2.2842817319	-2.5936219787	-8.1021572564
C22	2.4504008160	-2.6160642719	-6.7208510805
C23	1.3937985010	-2.2357263830	-5.8767761677
C24	0.1790943734	-1.8302158310	-6.4638104111
C25	0.0112666086	-1.8082598090	-7.8500840287
H26	0.9643853184	-2.1840800203	-9.7540838175
H27	3.1068042182	-2.8890971336	-8.7473788256
H28	3.4028447885	-2.9233262834	-6.3028848964
H29	-0.6324595076	-1.5343680030	-5.8077887956
S30	-1.4908402163	-1.3104803060	-8.6786025325
C31	-2.6280561353	-0.9139195680	-7.3125201402
H32	-3.5632991529	-0.6133465599	-7.7893867509
H33	-2.8172227925	-1.7856303585	-6.6817892623
H34	-2.2570580741	-0.0829439805	-6.7081032292

Total Energy (hartrees): -1415.73474599105

HOMO energy (hartrees): -0.20060

LUMO energy (hartrees): -0.05312

Orbital Energies (hartrees):

-88.88445 -88.88366 -10.22502 -10.22401 -10.21998 -10.21943  
-10.20369 -10.20330 -10.19514 -10.19484 -10.19435 -10.19402  
-10.19327 -10.19325 -10.19307 -10.19222 -10.18855 -10.18759  
-7.94541 -7.94459 -5.91071 -5.90990 -5.90660 -5.90577  
-5.90023 -5.89940 -0.86825 -0.86405 -0.81523 -0.80135  
-0.78538 -0.76030 -0.74202 -0.73738 -0.71284 -0.65842  
-0.65499 -0.63239 -0.60247 -0.59561 -0.57759 -0.53237  
-0.51613 -0.51053 -0.47476 -0.46933 -0.45154 -0.44594  
-0.44546 -0.43722 -0.43689 -0.43637 -0.42249 -0.41736  
-0.39871 -0.39539 -0.38344 -0.37850 -0.37529 -0.36254  
-0.35407 -0.34962 -0.33838 -0.32093 -0.31961 -0.31781  
-0.29000 -0.27703 -0.26241 -0.21845 -0.21000 -0.20060  
-0.05312 -0.00297 0.00009 0.01334 0.03529 0.03672  
0.07177 0.07260 0.07546 0.09345

## C6. References

1. Cody, J.; Fahrni, C. J. *Tetrahedron*, **2004**, *60*, 11099–11107.
2. Laufer, S. A.; Wergner, G. K. *J. Med. Chem.*, **2002**, *45*, 2733–2740.
3. Ngwendson, J. N.; Schultze, C. M.; Bollinger, J. C., Banerjee, A. *Can. J. Chem.*, **2008**, *86*, 7, 668–675.
4. Iyoda, M.; Sakaitani, M.; Otsuka, H.; Oda, M. *Chem. Lett.*, **1985**, *1*, 127–130.
5. Hutter, J. L.; Bechhoefer, J. *Rev. Sci. Instrum.*, **1993**, *64*, 1868–1873.
6. Frei, M.; Aradhya, S. V.; Koentopp, M.; Hybertsen, M. S.; Venkataraman, L. *Nano Lett.*, **2011**, *11*, 1518–1523.

## Appendix D

### D1. General Information

(*E*)-4-nitrostilbene, diethyl benzylphosphonate and (1,3-dioxolan-2-yl)methyltriphenylphosphonium bromide were purchased from TCI America and the latter was stored in a desiccator. 3-nitrobenzaldehyde, 4-nitrobenzaldehyde, 3-nitrobenzyl bromide, 4-nitrobenzyltriphenylphosphonium bromide, (*E*)-4,4'-diaminostilbene (**PP1A**), 4-nitrostilbene, 4-(methylthio)benzaldehyde, 4-(methylthio)benzyl bromide, 3-(methylthio)benzyl bromide, n-butyl lithium (1.6 M) in hexanes and all other reagents were purchased from Sigma-Aldrich. All reactions were carried out under nitrogen unless otherwise noted.

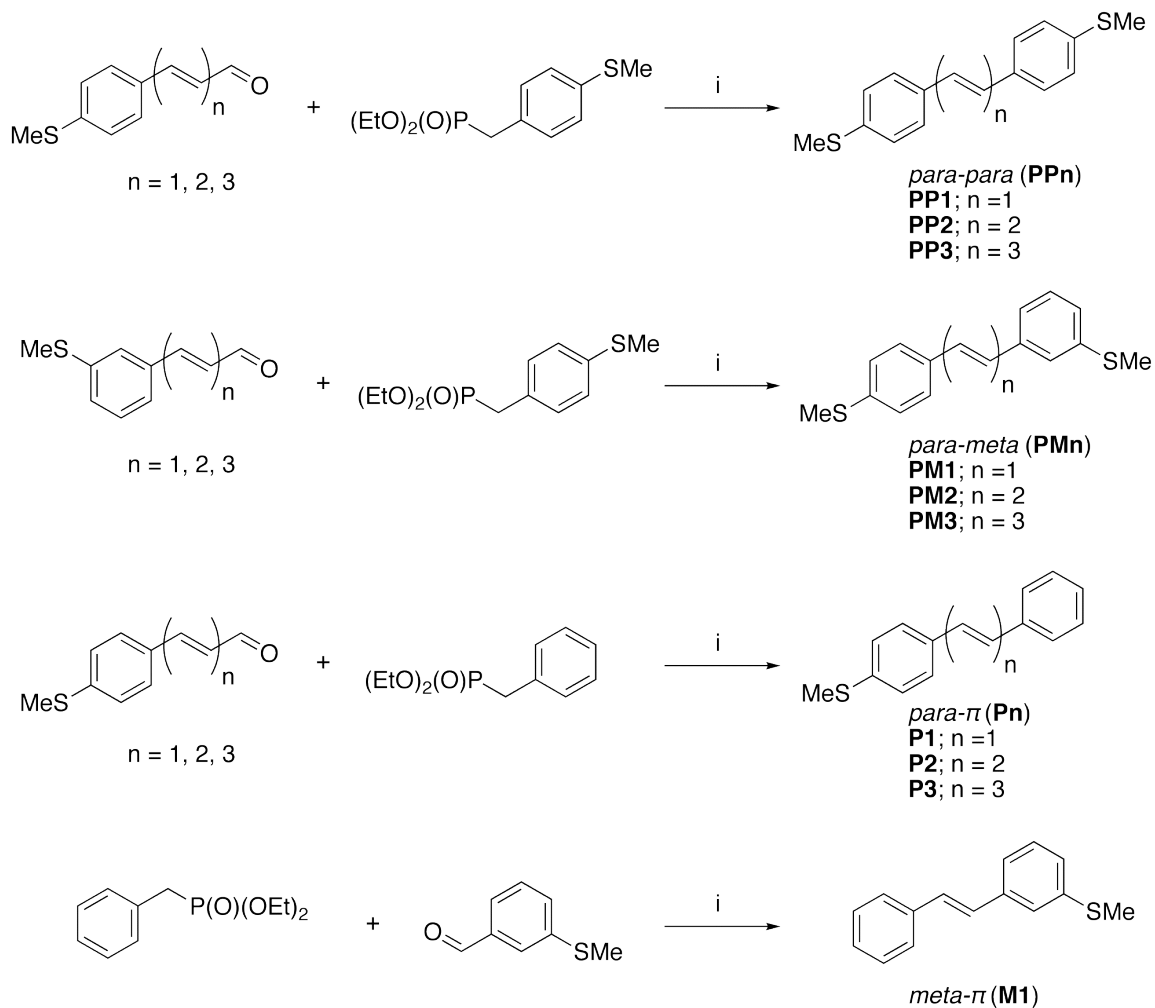
Compounds were prepared by the reported procedures: 3-(methylthio)benzaldehyde;<sup>1</sup> (*E*)-4-(methylthio)cinnamaldehyde and (2*E*,4*E*)-5-(4-(methylthio)phenyl)penta-2,4-dienal;<sup>2</sup> (*E*)-4,4'-di-(methylthio)stilbene (**PP1**);<sup>1</sup> 3-(dimethylamino)benzaldehyde;<sup>3</sup> (*E*)-methyl(4-styrylphenyl)sulfane (**P1**);<sup>4</sup> dimethyl 4-(methylthio)benzylphosphonate;<sup>5</sup> and (*E*)-4-aminostilbene (**P1A**).<sup>6</sup>

Chromatography was performed on a Teledyne ISCO Combiflash RF using Redisep RF silica columns. <sup>1</sup>H, <sup>13</sup>C and <sup>31</sup>P NMR spectra were taken on a Bruker DRX300 (300MHz), DRX400 (400MHz) and DMX500 (500MHz).

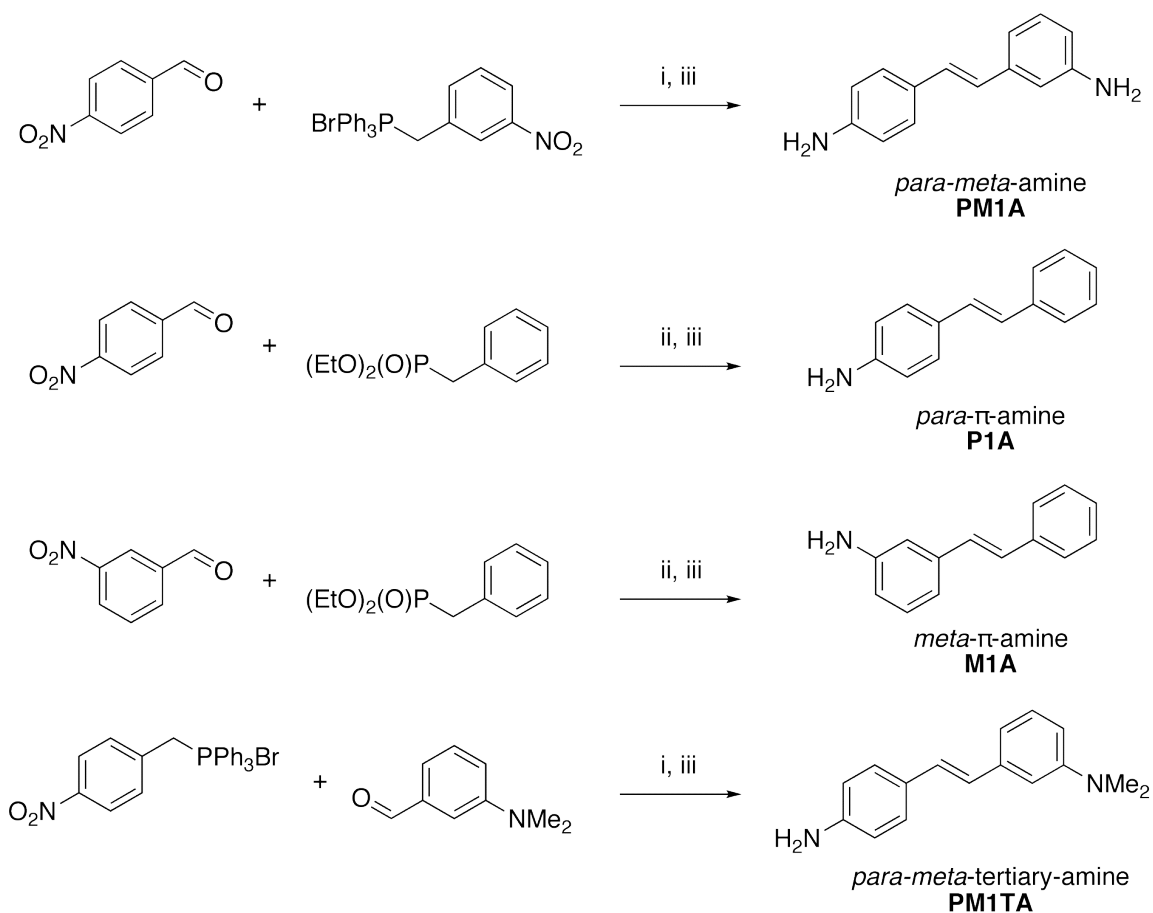
High resolution mass spectrometry (HR-MS) were obtained for all target molecules on a double focusing mass spectrometer (JMS-HX110A; JEOL, ltd.; Tokyo, Japan); Ionization method: FAB, High energy Xe\* beam (3 kV); Matix: *meta*-nitrobenzyl

alcohol (m-NBA); MS Acceleration-Voltage: 10 kJ; Resolution: 3,000/10,000 (Low-Res/High-Res).

## D2. Synthetic Experimentals

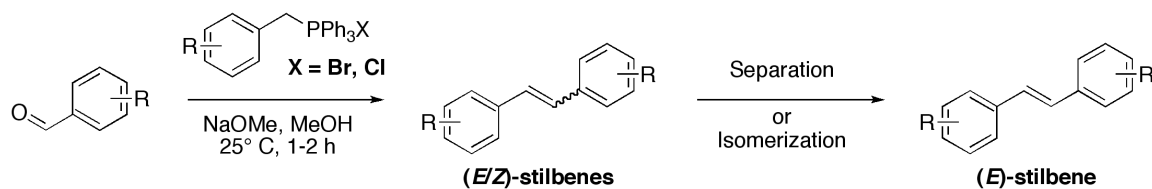


**Scheme D1:** Synthesis of *trans*- $\alpha,\omega$ -diphenyl- $\mu,\nu$ -oligoenes, where  $n = 1-3$ ; (i) General H.W.E. reaction: General H.W.E. reaction:  $^t\text{BuOK}$  (1.1 eq.), THF,  $0^\circ\text{C}$ , 1 h, let warm to room temperature overnight.

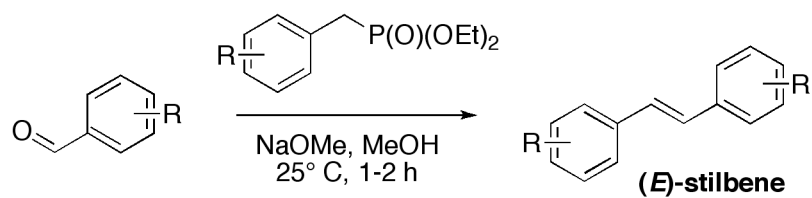


**Scheme D2:** Amine-functionalized stilbene derivative through Wittig Reaction or H.W.E. and  $\text{SnCl}_2$  reduction. Compound **M1A** was prepared as a control molecule to verify conductance trends found in the methylsulfide molecular wires; (i) NaOMe (1.2 eq.), MeOH, 1 h, produces a mixture of (E/Z)-stereoisomers that may be separated by flash column chromatography or by isomerization using  $\text{I}_2$ , acetone, reflux, 12 h; (ii) General H.W.E. reaction:  $^t\text{BuOK}$  (1.1 eq.), THF,  $0^\circ\text{C}$ , 1 h, let warm to room temperature overnight; (iii)  $\text{SnCl}_2 \cdot 2\text{H}_2\text{O}$ , EtOH (anhydrous),  $70^\circ\text{C}$ , 2 h (50-90%).

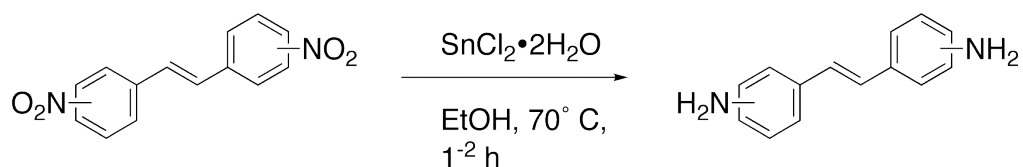




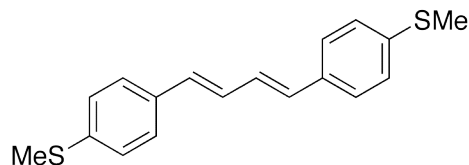
**General Wittig Procedure:** Adapted from the reported procedure.<sup>7</sup> In a 100-mL round-bottom flask, 3-nitrobenzaldehyde (0.100 g, 6.62 mmol) and 3-nitrobenzyltriphenylphosphonium bromide (3.20 g, 6.62 mmol) were dissolved in 50 mL of anhydrous methanol under nitrogen. Sodium methoxide (13.2 mmol) was added to the solution slowly over 15 min. A colorful (usually yellow) precipitate forms while the reaction was stirred for an additional 1-2 hours at room temperature. The resultant E/Z mixture of isomers was collected by filtration as a light yellow solid that was air-dried. The stereoisomers were separated (by chromatography or recrystallization) or where isomerized completely to the E isomer.



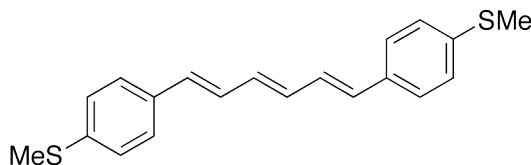
**General Hoerner-Wadsworth-Emmons (H.W.E.) Procedure:** Inside a flame-dried flask, aldehyde (0.150 g, 1.0 eq.) and phosphonate (1.1 eq.) were dissolved in 25 mL of dry THF. After being cooled to  $0^\circ\text{C}$ , a solution of tBuOK (1.1 eq.) in 5 mL of THF was slowly added to the stirred reaction solution. The reaction was left overnight and warmed to room temperature. The reaction was stopped by adding a large portion of water. Dichloromethane was added and the organic layer was extracted and then washed with brine and dried over magnesium sulfate. The product was isolated by column chromatography (usually 10% ethyl acetate in hexanes).



**General Reduction of Aryl-NO<sub>2</sub> Group to Aryl-NH<sub>2</sub> Group:** The dinitrostilbene (0.100 g, 0.370 mmol, 1.0 eq.), tin(II) chloride dihydrate (0.835 g, 3.70 mmol, 10.0 eq.), and 10 mL of anhydrous ethanol were added to a flame-dried, 25-mL RBF with stir bar and sealed with a septum. The suspension was purged with nitrogen for 10 minutes before heating to 80° C under an inert atmosphere. After 2-3 hours all solids dissolved and the reaction, which was monitored by TLC, was complete. The reaction solution was cooled to room temperature and water was added followed by extraction with ethyl acetate. The organic layers were combined, washed with aq. brine solution and dried with magnesium sulfate. Product was isolated by column chromatography on silica gel (usually in 50% ethyl acetate in hexanes).

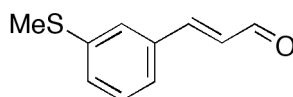


*(1E,3E)*-1,4-bis(4-(methylthio)phenyl)buta-1,3-diene (**PP2**): General H.W.E. Procedure. The product was prepared from (*E*)-3-(4-(methylthio)phenyl)acrylaldehyde<sup>2</sup> and dimethyl 4-(methylthio)benzylphosphonate and was isolated by column chromatography (10% ethyl acetate in hexanes) as a pale yellow solid in 67.7% yield. <sup>1</sup>H NMR (400MHz, C<sub>2</sub>D<sub>2</sub>C<sub>14</sub>): δ 7.38 (d, *J* = 8.4 Hz, 4H), 7.22 (d, *J* = 8.4 Hz, 4H), 6.97-6.87 (m, 2H), 6.68-6.52 (m, 2H), 2.51 (s, 6H); <sup>13</sup>C NMR (400MHz, C<sub>2</sub>D<sub>2</sub>C<sub>14</sub>): δ 137.18, 133.64, 131.43, 128.15, 126.28, 125.93, 15.17; HR-MS: *m/z* calcd for (C<sub>18</sub>H<sub>18</sub>S<sub>2</sub>): 298.0850, found: 298.0841.

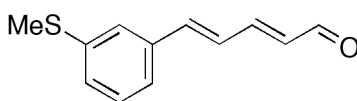


*(1E,3E,5E)*-1,6-bis(4-(methylthio)phenyl)hexa-1,3,5-triene (**PP3**): General H.W.E. Procedure. The product was prepared from (*2E,4E*)-5-(4-(methylthio)phenyl)penta-2,4-dienal<sup>2</sup> and dimethyl 4-(methylthio)benzylphosphonate and was isolated by column chromatography (10% ethyl acetate in hexanes) as a yellowish-green solid in 54.0% yield. This compound was previously prepared by Spangler and coworkers.<sup>8</sup> Our NMR characterization data agrees with their report. <sup>1</sup>H NMR (400MHz, 350K, C<sub>2</sub>D<sub>2</sub>C<sub>14</sub>): δ 7.36 (bs, 4H), 7.26 (bs, 4H), 7.35 (t, *J* = 7.5 Hz, 2H), 6.85 (bm, 2H), 6.72-6.33 (m, 4H), 2.53 (bs, 6H), note: spectral shifts appeared broad; <sup>13</sup>C NMR (400MHz, 350K, C<sub>2</sub>D<sub>2</sub>C<sub>14</sub>):

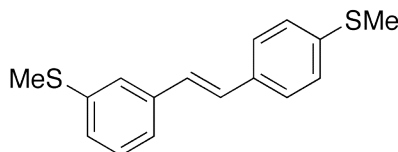
$\delta$  137.30, 137.04, 132.83, 131.43, 128.24, 126.56, 126.25, 15.46; HR-MS:  $m/z$  calcd for ( $C_{20}H_{20}S_2$ ): 324.1006, found: 324.1011.



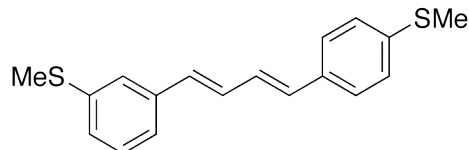
*(E)*-3-(methylthio)cinnamaldehyde: General Wittig homologation procedure. Product was prepared from 3-(methylthio)benzaldehyde and (1,3-dioxolan-2-yl)methyl-triphenylphosphonium bromide and isolated as a pale yellow solid (yield: 0.456 g, 38.9%).  $^1H$  NMR (300MHz,  $CDCl_3$ ):  $\delta$  9.70 (d,  $J = 7.8$  Hz, 1H), 7.44-7.30 (m, 5H), 6.70 (dd,  $J = 7.8$  Hz,  $J = 16.2$  Hz, 1H), 2.50 (s, 3H);  $^{13}C$  NMR (300MHz,  $CDCl_3$ ):  $\delta$  194.0, 152.5, 140.4, 135.0, 129.8, 129.4, 129.3, 126.3, 125.4, 15.9; HR-MS:  $m/z$  calcd for ( $C_{10}H_{10}OS$ ): 178.0452, found: 178.0460.



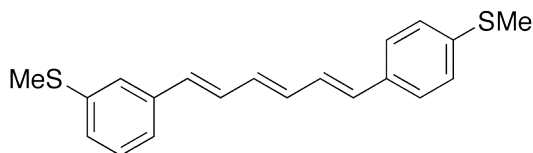
*(2E,4E)*-5-(3-(methylthio)phenyl)penta-2,4-dienal: General Wittig homologation procedure. Product was prepared from *(E)*-3-(methylthio)cinnamaldehyde and (1,3-dioxolan-2-yl)methyl-triphenylphosphonium bromide and isolated as a yellow solid (yield: 0.501 g, 96.2%).  $^1H$  NMR (300MHz,  $CDCl_3$ ):  $\delta$  9.59 (d,  $J = 8.1$  Hz, 1H), 7.32 (s, 1H), 7.28-7.14 (m, 4H), 6.98-6.86 (m, 2H), 6.23 (dd,  $J = 7.8$  Hz,  $J = 15.3$  Hz, 1H), 2.46 (s, 3H);  $^{13}C$  NMR (300MHz,  $CDCl_3$ ):  $\delta$  194.0, 152.2, 142.2, 139.9, 136.6, 132.2, 129.7, 127.8, 127.1, 125.7, 124.6, 16.1; HR-MS:  $m/z$  calcd for ( $C_{12}H_{12}OS$ ): 204.0609, found: 204.0636.



*(E)*-3,4'-di-(methylthio)stilbene (**PM1**): General Wittig Procedure. The product was prepared from 3-(methylthio)benzaldehyde and dimethyl 4-(methylthio)benzylphosphonate. Pure product as collected by filtration from the reaction suspension as a white solid (43.0%).  $^1\text{H}$  NMR (300MHz,  $\text{CDCl}_3$ ):  $\delta$  7.43 (d,  $J = 8.4$  Hz, 2H), 7.36 (bs, 1H), 7.30-7.20 (m, 5H), 7.20-7.09 (m, 1H), 7.04 (d,  $J = 16.4$  Hz, 1H), 7.03 (d,  $J = 16.4$  Hz, 1H), 2.52 (s, 3H), 2.51 (s, 3H);  $^{13}\text{C}$  NMR (400MHz,  $\text{CDCl}_3$ ):  $\delta$  138.9, 138.1, 138.0, 134.1, 129.1, 128.7, 127.5, 127.0, 126.7, 125.7, 124.6, 123.3, 15.9, 15.7; HR-MS:  $m/z$  calcd for ( $\text{C}_{16}\text{H}_{16}\text{S}_2$ ): 272.0693, found: 272.0686.

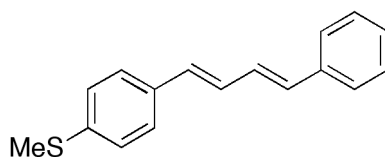


*(1E,3E)*-1-(3-(methylthio)phenyl)-4-(4-methylthio)phenyl)-buta-1,3-diene (**PM2**): General H.W.E. Procedure. The product was prepared from *(E)*-3-(methylthio)cinnamaldehyde and dimethyl 4-(methylthio)benzylphosphonate and isolated by column chromatography (10% ethyl acetate in hexanes) as an off-white solid in 86.5% yield.  $^1\text{H}$  NMR (500MHz,  $\text{CDCl}_3$ ):  $\delta$  7.36 (d,  $J = 8.4$  Hz, 2H), 7.32 (t,  $J = 1.6$  Hz, 1H), 7.29-7.15 (m, 4H), 7.13 (dt,  $J = 1.6$  Hz, 7.5 Hz, 1H), 7.00-6.84 (m, 2H), 6.68-6.53 (m, 2H), 2.51 (s, 3H), 2.50 (s, 3H);  $^{13}\text{C}$  NMR (500MHz,  $\text{CDCl}_3$ ):  $\delta$  138.97, 138.16, 138.12, 134.34, 132.78, 32.09, 130.02, 129.19, 128.60, 126.94, 126.78, 125.78, 124.58, 123.34, 16.02, 15.91; HR-MS:  $m/z$  calcd for ( $\text{C}_{18}\text{H}_{18}\text{S}_2$ ): 298.0850, found: 298.0848.



*(1E,3E,5E)-1-(3-(methylthio)phenyl)-6-(4-(methylthio)phenyl)-hexa-1,3,5-triene* (**PM3**):

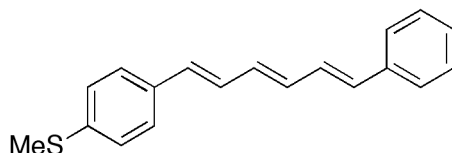
General H.W.E. Procedure. The product was prepared from *(2E,4E)-5-(3-(methylthio)phenyl)penta-2,4-dienal* and dimethyl 4-(methylthio)benzylphosphonate and isolated by column chromatography (10% ethyl acetate in hexanes) as a yellow solid in 40.5% yield.  $^1\text{H}$  NMR (300MHz,  $\text{CDCl}_3$ ):  $\delta$  7.34 (d,  $J = 8.4$  Hz, 2H), 7.30 (t,  $J = 1.5$  Hz, 1H), 7.24-7.18 (m, 4H), 7.12 (dt,  $J = 1.5$  Hz, 7.5 Hz, 1H), 6.91-6.81 (m, 2H), 6.75-6.40 (m, 4H), 2.51 (s, 3H), 2.49 (s, 3H);  $^{13}\text{C}$  NMR (500MHz,  $\text{CDCl}_3$ ):  $\delta$  138.96, 138.20, 138.07, 134.47, 134.17, 133.30, 132.49, 132.08, 129.93, 129.18, 128.63, 126.92, 126.82, 125.84, 124.66, 123.37, 16.05, 15.94; HR-MS:  $m/z$  calcd for  $(\text{C}_{20}\text{H}_{20}\text{S}_2)$ : 324.1006, found: 324.0997.



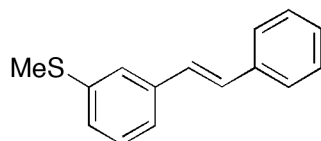
*(1E,3E)-1-(4-(methylthio)phenyl)-4-phenyl-but-1,3-diene* (**3b**): General H.W.E.

Procedure. The product was previously prepared from cyclopropyl carbinols through indium triflate catalyzed rearrangements by Ranu and Banerjee.<sup>9</sup> Our  $^1\text{H}$  and  $^{13}\text{C}$  NMR data agrees with their findings. We prepared the product from *(E)-4-(methylthio)cinnamaldehyde*<sup>2</sup> and diethyl benzylphosphonate and isolated it as a white solid in 45.0% yield.  $^1\text{H}$  NMR (300MHz,  $\text{CDCl}_3$ ):  $\delta$  7.51 (d,  $J = 7.5$  Hz, 2H), 7.44-7.35

(m, 4H), 7.30-7.24 (m, 3H), 7.07-6.94 (m, 2H), 6.74-6.66 (m, 2H), 2.53 (s, 3H);  $^{13}\text{C}$  NMR (300MHz,  $\text{CD}_2\text{Cl}_2$ ):  $\delta$  138.5, 137.8, 134.6, 132.9, 132.5, 130.8, 129.6, 129.0, 127.9, 127.1, 126.9, 126.7, 15.8; HR-MS:  $m/z$  calcd for ( $\text{C}_{17}\text{H}_{16}\text{S}$ ): 252.0973, found: 252.0979.



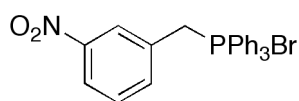
(*1E,3E,5E*)-1-(4-(methylthio)phenyl)-6-phenyl-hexaa-1,3,5-triene (**3c**): General H.W.E. Procedure. The product was prepared from (*2E,4E*)-5-(4-(methylthio)phenyl)penta-2,4-dienal<sup>2</sup> and diethyl benzylphosphonate and isolated as a yellow solid in 31.3% yield.  $^1\text{H}$  NMR (300MHz,  $\text{CDCl}_3$ ):  $\delta$  7.48 (d,  $J = 7.5$  Hz, 2H), 7.41-7.33 (m, 4H), 7.28-7.23 (m, 3H), 7.00-6.88 (m, 2H), 6.7-6.56 (m, 4H), 2.53 (s, 3H);  $^{13}\text{C}$  NMR (500MHz,  $\text{C}_2\text{D}_2\text{Cl}_4$ ):  $\delta$  137.36, 136.85, 133.81, 133.24, 133.02, 132.18, 131.66, 128.78, 128.35, 128.18, 127.27, 126.42, 126.10, 126.01, 15.32; HR-MS:  $m/z$  calcd for ( $\text{C}_{19}\text{H}_{18}\text{S}$ ): 278.1129, found: 278.1134.



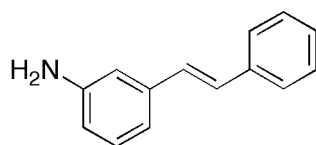
(*E*)-3-(methylthio)stilbene (**4**): The compound is known in the literature and was initially synthesized by cationic cycloaromatization of the respective styryl  $\beta,\beta$ -bis(methylthio)vinyl ketones.<sup>10</sup> General H.W.E. Procedure. The product was prepared from 3-(methylthio)benzaldehyde and diethyl benzylphosphonate and isolated by column



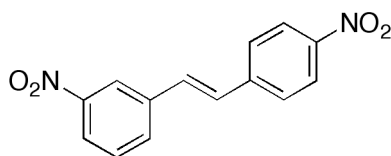
chromatography (5% ethyl acetate in hexanes) as a white solid in 98% yield.  $^1\text{H}$  NMR (400MHz,  $\text{CDCl}_3$ ):  $\delta$  7.52 (d,  $J = 7.6$  Hz, 2H), 7.40 (bs, 1H), 7.36 (t,  $J = 7.6$  Hz, 2H), 7.30-7.24 (m, 3H), 7.15 (m, 1H), 7.09 (d,  $J = 16.0$  Hz, 1H), 7.07 (d,  $J = 16.4$  Hz, 1H), 2.52 (s, 3H);  $^{13}\text{C}$  NMR (400MHz,  $\text{CDCl}_3$ ):  $\delta$  138.9, 138.0, 137.1, 129.3, 129.1, 128.7, 128.1, 127.8, 126.6, 125.7, 124.6, 123.4, 15.9; HR-MS:  $m/z$  calcd for ( $\text{C}_{15}\text{H}_{14}\text{S}$ ): 226.0816, found: 226.0808.



*3-nitrobenzyltriphenylphosphonium bromide*: This compound is known in the literature,<sup>11</sup> however detailed characterization was not given. General Synthesis of triphenylphosphonium Halide Salts (above). Product was prepared from 3-nitrobenzyl bromide and triphenylphosphine and isolated as a white powder in quantitative yields.  $^1\text{H}$  NMR (300MHz,  $\text{DMSO}-d_6$ ):  $\delta$  8.16 (d,  $J = 7.2$  Hz, 1H), 7.91 (t,  $J = 7.8$  Hz, 3H), 7.79-7.65 (m, 14H), 7.55 (t,  $J = 8.1$  Hz, 1H), 7.47 (bd,  $J = 7.8$  Hz, 2H), 5.36 (d,  $J = 15.9$  Hz, 2H);  $^{13}\text{C}$  NMR (300MHz,  $\text{DMSO}-d_6$ ):  $\delta$  138.2, 136.2, 135.0, 134.9, 131.2, 131.0, 126.4, 126.4, 124.1, 118.7, 117.5, 28.8, 28.2; HR-MS:  $m/z$  calcd for triphenylphosphonium cation ( $\text{C}_{25}\text{H}_{21}\text{NO}_2\text{P}$ ): 398.1310, found: 398.1301.

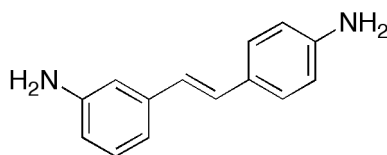


*(E)*-3-aminostilbene (**7**): This compound is known<sup>12</sup> and was synthesized as a control molecule to verify the trends in conductance found within the methylsulfide molecular wires. It was prepared by the General Reduction of Aryl-NO<sub>2</sub> to Aryl-NH<sub>2</sub> Group. *(E)*-3-dinitrostilbene<sup>13</sup> (0.100 g, 0.370 mmol), tin(II) chloride dihydrate (0.835 g), and 12 mL of anhydrous ethanol were added to a flame dried, 25-mL round-bottomed flask with stir bar and sealed with a septum. The suspension was purged with nitrogen for 10 minutes before heating to 70° C under an inert atmosphere. After 16 h the reaction was cooled to room temperature and the ethanol was removed under reduced pressure. Water was added followed by sat. aqueous NaHCO<sub>3</sub>. The aqueous layer was extracted three times with dichloromethane. The solvent was removed and leaving a off-white solid (0.059 g, 68%). <sup>1</sup>H NMR (400MHz, CDCl<sub>3</sub>): δ 7.54 (d, *J* = 8.0 Hz, 2H), 7.40 (t, *J* = 8.4 Hz, 2H), 7.29 (td, *J* = 1.6 Hz, 7.2 Hz, 1H), 7.19 (t, *J* = 8.0 Hz, 1H), 7.13 (d, *J* = 16.4 Hz, 1H), 7.07 (d, *J* = 16.4 Hz, 1H), 6.98 (d, *J* = 7.6 Hz, 1H), 6.87 (s, 1H), 6.64 (dd, *J* = 2.0 Hz, 8.0 Hz, 1H), 3.70 (bs, 2H); <sup>13</sup>C NMR (400MHz, CDCl<sub>3</sub>): δ 146.7, 138.4, 137.4, 129.6, 128.9, 128.7, 128.5, 127.6, 126.5, 117.3, 114.7, 112.9; HR-MS: *m/z* calcd for (C<sub>14</sub>H<sub>13</sub>N): 195.1048, found: 195.0461.

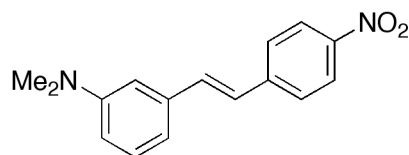


*(E)*-3,4'-dinitrostilbene: This compound is known in the literature,<sup>14</sup> however HR-MS, <sup>1</sup>H and <sup>13</sup>C NMR data was not provided. General Wittig Procedure. The product was prepared from 4-nitrobenzyltriposponium bromide and 3-nitrobenzaldehyde. A mixture

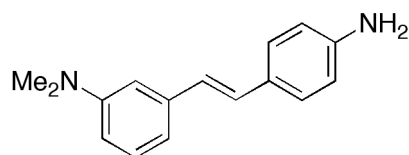
of E/Z isomers was collected by vacuum filtration from the reaction suspension as a pale yellow precipitate. The E/Z mixture was placed in a 50-mL round-bottom flask with 20 mL of acetone and a crystal of iodine. The mixture was heated at reflux under a nitrogen atmosphere for 12 hours. The solution was cooled, and the product was collected by filtration to give yellow needles in overall 29% yield.  $^1\text{H}$  NMR (300MHz,  $\text{CDCl}_3$ ):  $\delta$  8.43 (t,  $J = 1.9$  Hz, 1H), 8.27 (d,  $J = 8.9$  Hz, 2H), 8.18 (d,  $J = 6.9$  Hz, 1H), 7.88-7.81 (m, 1H), 7.69 (d,  $J = 8.9$  Hz, 2H), 7.59 (t,  $J = 8.0$  Hz, 1H), 7.29 (s, 2H);  $^{13}\text{C}$  NMR (300MHz,  $\text{CDCl}_3$ ):  $\delta$  148.5, 147.4, 142.6, 138.0, 132.7, 130.5, 129.9, 129.3, 127.3, 124.3, 123.1, 121.3; HR-MS:  $m/z$  calcd for ( $\text{C}_{14}\text{H}_{10}\text{N}_2\text{O}_4$ ): 270.0641, found: 270.0636.



(*E*)-3,4'-diaminostilbene (**5**): This compound is known in the literature.<sup>15</sup> General Reduction of Aryl- $\text{NO}_2$  to Aryl- $\text{NH}_2$  Group. The product was prepared from (*E*)-3,4'-dinitrostilbene and stannous chloride dihydrate and isolated by column chromatography (50% ethyl acetate in hexanes) as an off-white solid in 23.6% yield.  $^1\text{H}$  NMR (300MHz,  $\text{CDCl}_3$ ):  $\delta$  7.32 (d,  $J = 8.4$  Hz, 2H), 7.11 (t,  $J = 7.8$  Hz, 1H), 6.99 (d,  $J = 16.2$  Hz, 1H), 6.89 (d,  $J = 7.8$  Hz, 1H), 6.84 (d,  $J = 15.9$  Hz, 1H), 6.79 (s, 1H), 6.67 (d,  $J = 8.4$  Hz, 2H), 6.56 (d,  $J = 7.5$  Hz, 1H), 3.71 (bs, 4H);  $^{13}\text{C}$  NMR ( $\text{CDCl}_3$ ):  $\delta$  147.0, 146.5, 139.4, 129.8, 128.9, 128.5, 128.1, 125.7, 117.3, 115.6, 114.4, 112.9; HR-MS:  $m/z$  calcd for ( $\text{C}_{14}\text{H}_{14}\text{N}_2$ ): 210.1157, found: 210.1152.



*(E)*-3-dimethylamino-4'-nitrostilbene: The product was prepared from 3-dimethylaminobenzaldehyde and 4-nitrobenzyltriphenylphosphonium bromide using the General Wittig Procedure. Pure product was isolated by column chromatography (10% ethyl acetate in hexanes) as an orange solid in 20.0% yield.  $^1\text{H}$  NMR (300MHz,  $\text{CDCl}_3$ ):  $\delta$  8.22 (d,  $J = 8.7$  Hz, 2H), 7.63 (d,  $J = 8.7$  Hz, 2H), 7.29 (t,  $J = 7.8$  Hz, 1H), 7.22 (d,  $J = 16.2$  Hz, 1H), 7.13 (d,  $J = 16.2$  Hz, 1H), 6.95 (d,  $J = 7.5$  Hz, 1H), 6.85 (bs, 1H), 6.74 (dd,  $J = 2.4$  Hz, 8.1 Hz, 1H), 3.00 (s, 6H);  $^{13}\text{C}$  NMR (300MHz,  $\text{CDCl}_3$ ):  $\delta$  151.4, 147.1, 144.6, 137.3, 134.8, 129.9, 127.2, 126.2, 124.5, 115.7, 113.7, 111.5, 40.9; HR-MS:  $m/z$  calcd for ( $\text{C}_{16}\text{H}_{16}\text{N}_2\text{O}_2$ ): 268.1212, found: 268.1225.



*(E)*-3-dimethylamino-4'-aminostilbene (**8**): General Reduction of Aryl- $\text{NO}_2$  to Aryl- $\text{NH}_2$  Group. The product was prepared from *(E)*-3-dimethylamino-4'-nitrostilbene and tin(II) chloride dihydrate isolated by column chromatography (25% ethyl acetate in hexanes) as a off-white solid in 5.3% yield.  $^1\text{H}$  NMR (300MHz,  $\text{CDCl}_3$ ):  $\delta$  7.35 (d,  $J = 8.4$  Hz, 2H), 7.23 (d,  $J = 8.1$  Hz, 1H), 7.03 (d,  $J = 16.2$  Hz, 1H), 6.92 (d,  $J = 16.2$  Hz, 1H), 6.89 (d,  $J = 7.2$  Hz, 1H), 6.82 (bs, 1H), 6.67 (d,  $J = 8.4$  Hz, 2H), 6.62 (dd,  $J = 2.4$  Hz, 8.4 Hz, 1H), 3.62 (bs, 2H), 2.97 (s, 6H);  $^{13}\text{C}$  NMR (300MHz,  $\text{CDCl}_3$ ):  $\delta$  151.3, 146.4, 139.1, 129.6,

128.7, 128.6, 128.1, 126.5, 115.6, 115.2, 112.1, 111.0, 41.1; HR-MS: m/z calcd for (C<sub>16</sub>H<sub>18</sub>N<sub>2</sub>): 238.1470, found: 238.1480.

### D3. Optical Absorption Spectroscopy

The HOMO-LUMO gap of all our molecular wires was estimated using solution-phase UV-vis absorption spectroscopy. Absorption spectra were taken on an Agilent Technologies 8453 UV-Vis spectrophotometer using a quartz cuvette with path length equal to 1.0 cm. Solutions of molecular wires were prepared in  $\text{CH}_2\text{Cl}_2$  at concentrations of  $\sim 1$  mM. All spectra were normalized to 1.0 Abs for clarity.

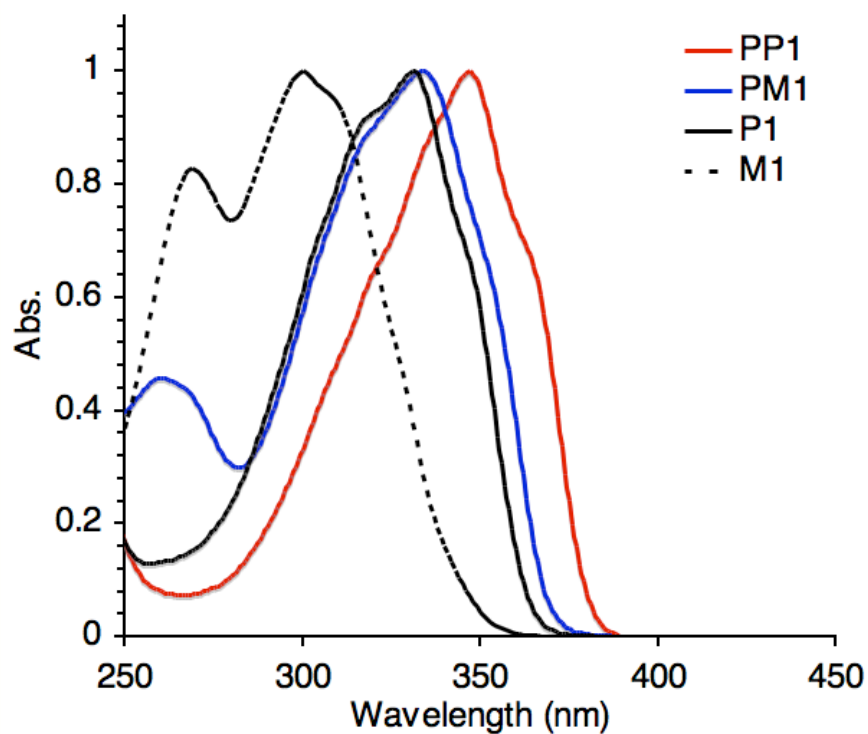


**Figure D1:** Optical absorption spectra of the methylsulfide-functionalized stilbenes.

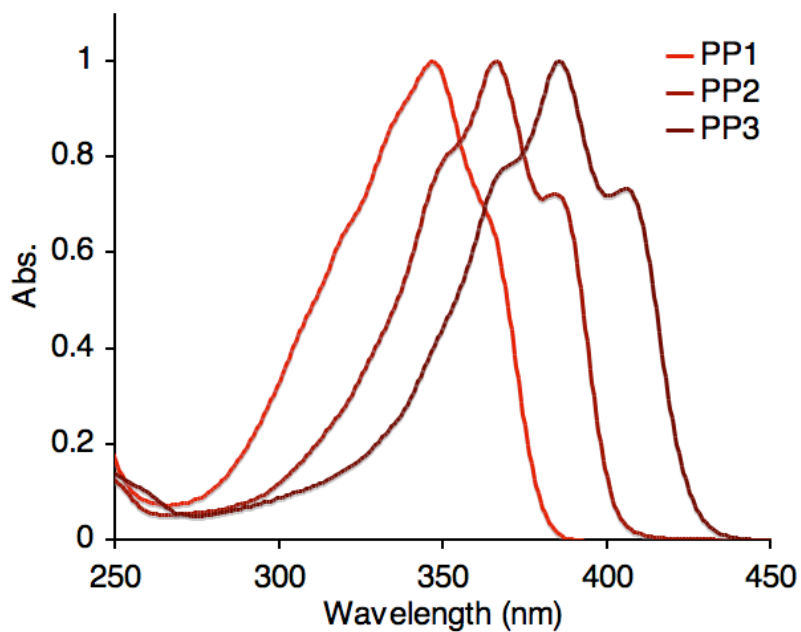


**Figure D2:** Optical absorption spectra of the *para-para* series (**PPn**).

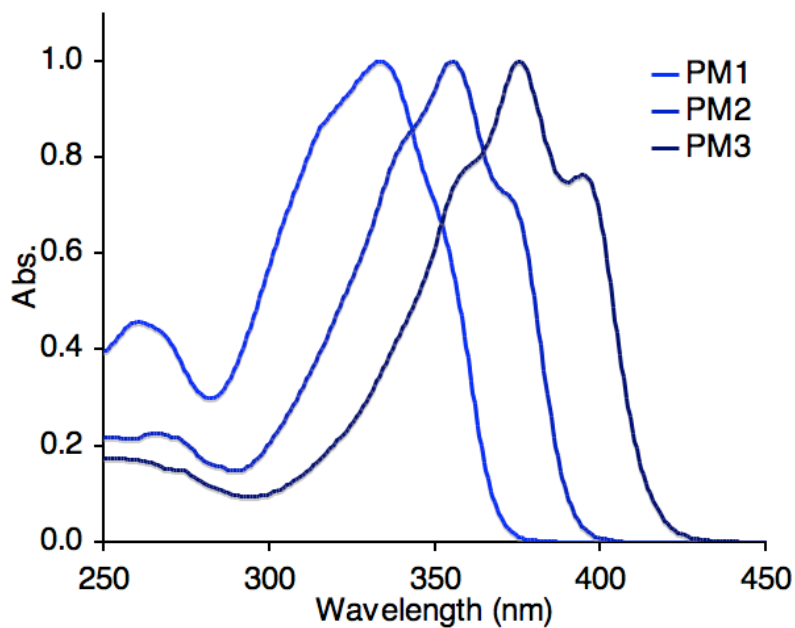


**Figure D3:** Optical absorption spectra of the *para-meta* series (**PMn**).

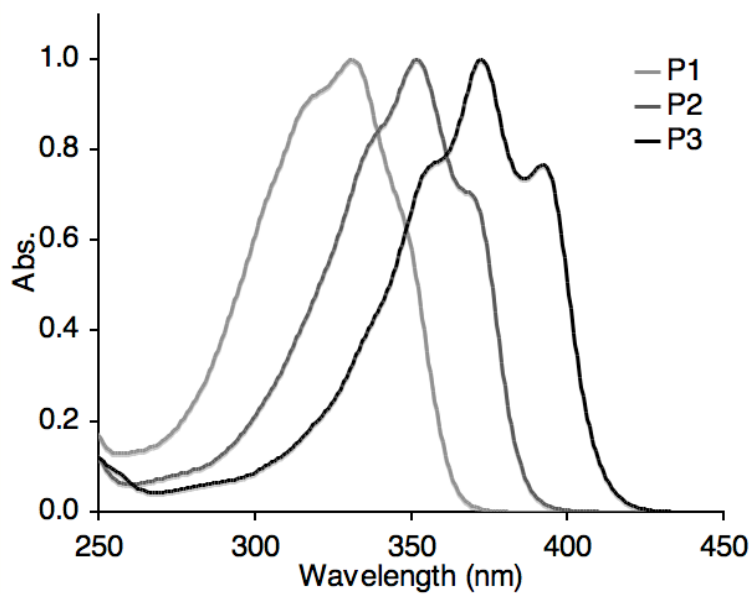


**Figure D4:** Optical absorption spectra of the *para*- $\pi$  series (**P<sub>n</sub>**).

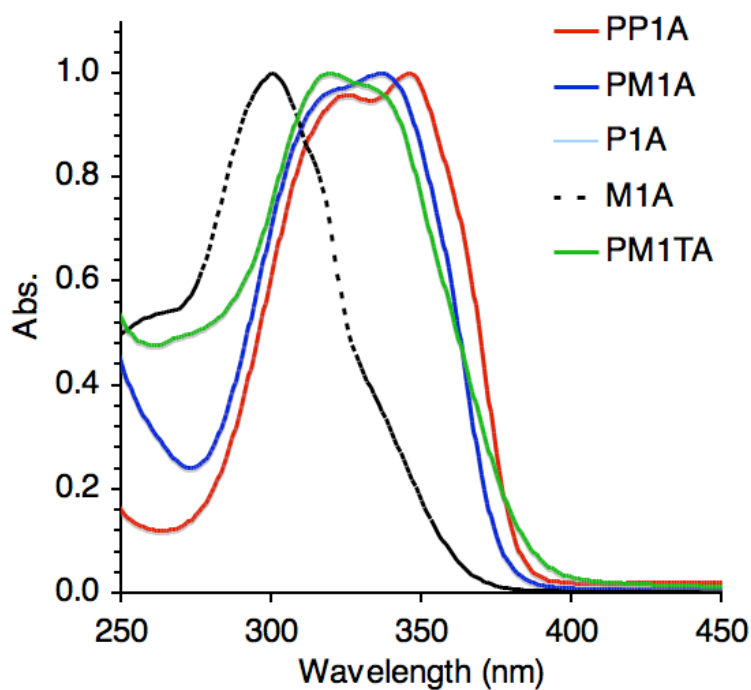


**Figure D5:** Optical absorption spectra of the amine-functionalized stilbene derivatives.



<b>Molecule</b>	<b><math>E_{OP}</math> (nm)</b>	<b><math>E_{OP}</math> (eV)</b>
<b>PP1</b>	389	3.19
<b>PP2</b>	416	2.98
<b>PP3</b>	435	2.85
<b>PM1</b>	380	3.26
<b>PM2</b>	403	3.08
<b>PM3</b>	430	2.88
<b>P1</b>	373	3.32
<b>P2</b>	395	3.14
<b>P3</b>	428	2.90
<b>M1</b>	358	3.46
<b>PM1A</b>	395	3.14
<b>P1A</b>	389	3.19
<b>PM1TA</b>	411	3.02

**Table D1:** Solution optical band gaps ( $E_{OP}$ ) for target molecules range from 2.88-3.46 eV.

#### D4. Single-molecule Conductance and Force Measurement and Analysis

**STM Break Junction Conductance Measurement.** Gold substrates were prepared by evaporating 100 nm of gold on freshly cleaved mica. A freshly cut gold wire was used as the STM tip. The junctions were repeatedly formed and broken in dilute solution of stilbene derivatives ( $1 \pm 0.1$  mM in 1,2,4-trichlorobenzene). The junction conductance (current/voltage) was measured at a constant bias of 500 mV. Over 5000 traces were used to construct 2D conductance-displacement (Figures D6 and D7) and 1D (Figure D8) conductance histograms.

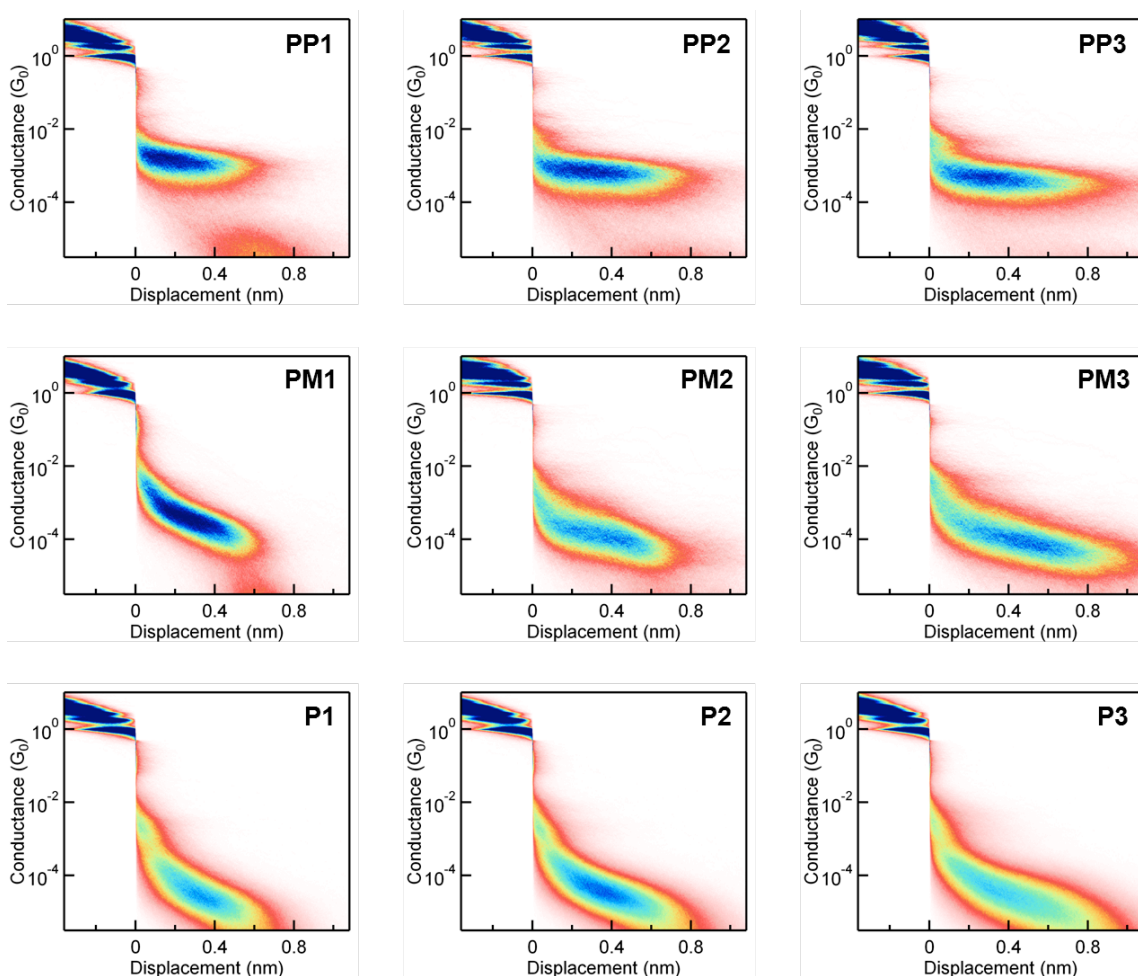


**Figure D6:** 2D conductance-displacement histograms for **PP<sub>n</sub>**, **PM<sub>n</sub>** and **P<sub>n</sub>** molecular junctions.

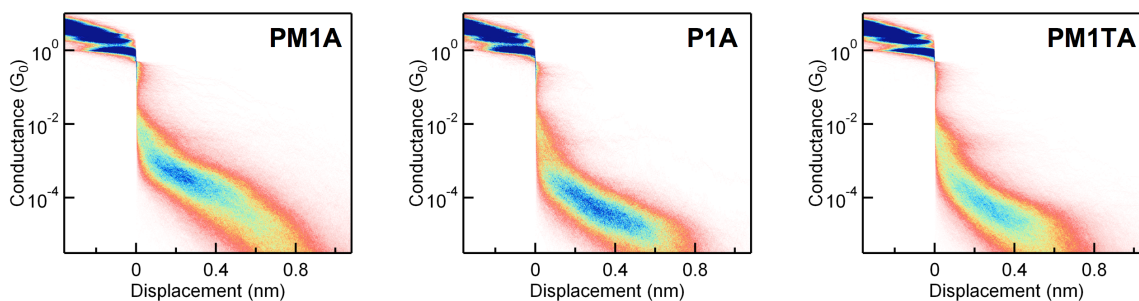


**Figure D7:** 2D conductance-displacement histograms for molecular junctions of amine-terminated molecular wires.

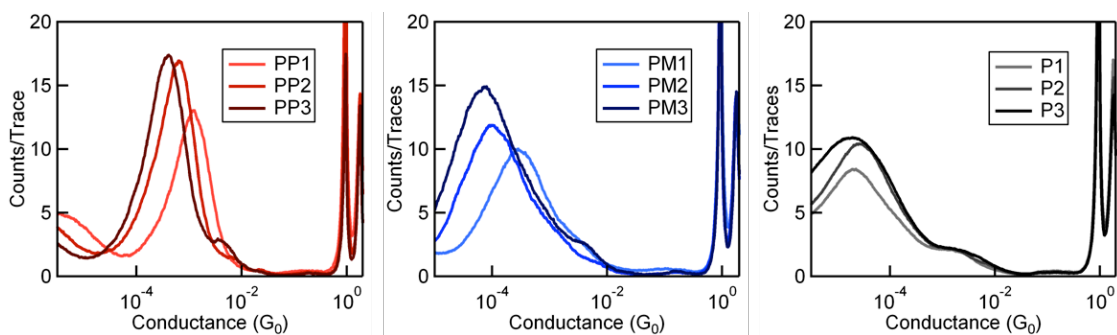


**Figure D8:** 1D conductance histograms of molecular junctions of **PP<sub>n</sub>**, **PM<sub>n</sub>** and **P<sub>n</sub>** series of molecular wires.

**Junction Variation Analysis.** The variability of the mono-substituted series, **P<sub>n</sub>**, is quantified in two steps. First, we construct separate (logarithmically binned) 1D histograms, 1000 traces at a time, for each molecule. The peak position of each of these histograms is well defined, and is extracted using a Gaussian fit in the neighborhood of

the molecular conductance feature. Then, peak values from these individual histograms are compiled from at least three separate experiments with different tip-sample combinations, totaling more than 30,000 individual measurements. The arithmetic mean as well as the 10<sup>th</sup>, 25<sup>th</sup>, 75<sup>th</sup> and 90<sup>th</sup> percentiles are computed from these peak positions, and are used to construct Figure 2 in the manuscript. Table D2 provides a summary of these statistics, along with the variation— defined as  $(75^{\text{th}} - 25^{\text{th}} \text{ percentile})/(\text{mean value})$  for **Pn** series. The largest variation among the difunctionalized compounds was observed in **PM3**, and is given in the table for comparison.

**Table D2:** Comparison of Conductance Variation in STM-BJ's.

Molecule	Mean	25th %ile	75th %ile	% variation
<b>P1</b>	$1.95 \times 10^{-5}$	$1.71 \times 10^{-5}$	$2.56 \times 10^{-5}$	44
<b>P2</b>	$2.74 \times 10^{-5}$	$1.56 \times 10^{-5}$	$3.39 \times 10^{-5}$	67
<b>P3</b>	$1.31 \times 10^{-5}$	$8.25 \times 10^{-6}$	$3.65 \times 10^{-5}$	216
<b>PM3</b>	$8.74 \times 10^{-5}$	$7.28 \times 10^{-5}$	$9.47 \times 10^{-5}$	25

**Sloping of 2D conductance histograms.** The slopes of the molecular

conductance features from 2D conductance histograms can be obtained from the “average conductance profile,” which corresponds to the maximum value of counts of conductance at each value of displacement in the 2D histogram. Figure S9 demonstrates this procedure for the 2D histogram of **PM1**, where the dashed white line is the average conductance profile, as obtained by fitting a Gaussian line shape at each displacement value. A line is then fitted to the linear section of this profile, which in turn yields the decay constant,  $\beta_s$ , such that where ‘G’ is the conductance and ‘L’ is the displacement.

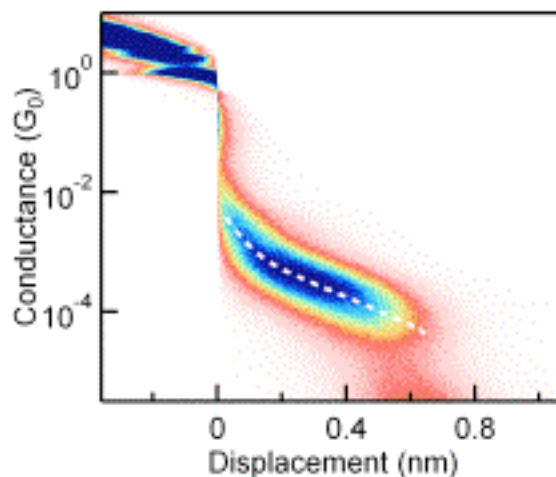


**Figure D9:** Maximum likelihood conductance profile overlaid on the 2D conductance histogram for **PM1**.

**AFM Simultaneous Force and Conductance Measurement:** A home-built conducting atomic force microscope (AFM) is used to simultaneously measure conductance and force across single molecule junctions. Au coated (100 nm) mica substrates and Au coated (100 nm) commercial AFM cantilevers ( $\sim 50$  N/m, NanoAndMore Inc.) are used as the two electrodes. Dilute solutions of the molecules (1 mM in 1,2,4-trichlorobenzene) are deposited on the substrates to perform single-molecule measurements. A constant voltage bias of 75 mV is used to obtain conductance measurements, while minimizing electrostatic tip-substrate interactions. The details of the experimental setup<sup>16</sup> and analysis technique<sup>1</sup> have been described in detail previously.

For junctions of **PP1** and **PM1**, the algorithm finds significant force fluctuations due to molecular junctions in more than 90% of the measured traces, in contrast to **P1** where only 12% of the measurements have such events. The rupture force for **PP1** and **PM1** are found to be 0.5 nN, whereas for **P1**, we obtain 0.3 nN, which is same as the threshold used to detect the force events (inset of Figure D10B). Together, the low probability of molecular force events, and the null value of the rupture force imply that the rupture force for **P1** is smaller than 0.3 nN.

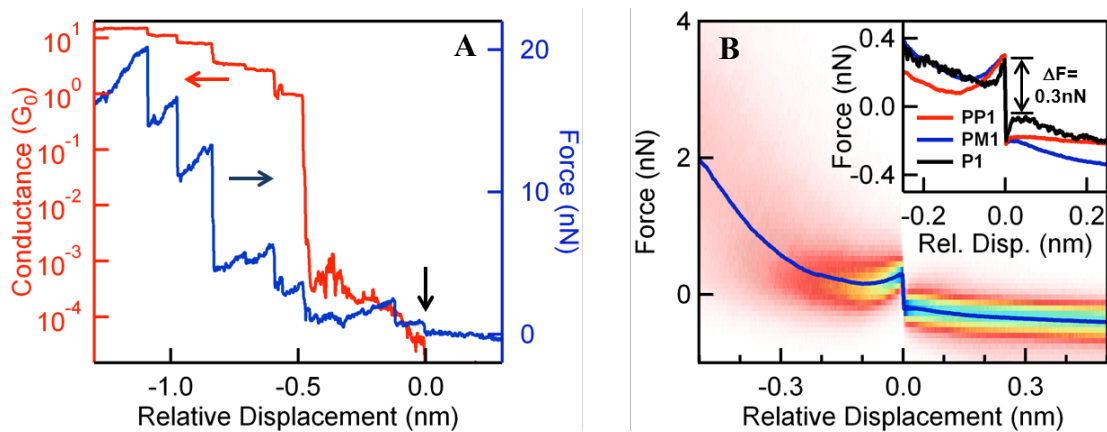


**Figure D10:** (A) A sample simultaneous measurement of conductance (red, left axis) and force (blue, right axis) with **PM1** molecule. The downward arrow indicates the rupture of the **PM1** molecular junction in force; a highly correlated drop in conductance is also observed in the conductance at the same location (zero of the displacement axis). (B) 2D force histogram for **PM1** constructed from 8242 traces. The averaged force profile is overlaid. Inset: Comparison of averaged force profiles for **PP1**, **PM1** and **P1**.

## D5. Theoretical Methods and Details

All electronic structure calculations used Jaguar (version 7.8, Schrodinger LLC, New York, NY, 2011) using the B3LYP hybrid functional and the 6-31G\*\* basis sets.

Final geometries and energies, as well as orbital energies are given below.

<b>Molecule</b>	<b>HOMO (eV)</b>	<b>LUMO (eV)</b>	<b><math>E_{DFT}</math> (eV)</b>
<b>PP1</b>	-5.03	-1.34	3.69
<b>PP2</b>	-4.89	-1.58	3.31
<b>PP3</b>	-4.79	-1.79	3.00
<b>PM1</b>	-5.22	-1.41	3.81
<b>PM2</b>	-5.06	-1.66	3.40
<b>PM3</b>	-4.93	-1.86	3.07
<b>P1</b>	-5.21	-1.35	3.85
<b>P2</b>	-5.04	-1.62	3.42
<b>P3</b>	-4.90	-1.82	3.08
<b>M1</b>	-5.47	-1.44	4.04
<b>PP1A</b>	-4.54	-0.75	3.79
<b>PM1A</b>	-4.82	-0.93	3.89
<b>P1A</b>	-4.93	-1.05	3.88
<b>M1A</b>	-5.11	-1.17	3.94
<b>PM1TA</b>	-4.98	-1.19	3.79

**Table D2:** Summary of DFT calculations. Energy of the HOMO ( $E_{HOMO}$ ) and LUMO ( $E_{LUMO}$ ) and the HOMO-LUMO energy gap ( $E_{DFT}$ ) energies of all derivatives.



**PP1**

Final total energy: -1415.73607449062 hartrees

Final geometry:

	angstroms		
atom	x	y	z
C1	-3.8434657906	-1.8489488923	-0.0120387531
C2	-4.5597978043	-0.6660921203	-0.2805624712
C3	-5.9467255545	-0.6325681374	-0.2796433503
C4	-6.6855502592	-1.7937947552	-0.0064348986
C5	-5.9902287827	-2.9808488469	0.2650085261
C6	-4.5991963175	-3.0026449136	0.2621135588
H8	-4.0097134678	0.2469096457	-0.4949240973
H9	-6.4629515231	0.2996396986	-0.4916892543
H11	-6.5258516266	-3.8979328936	0.4823056343
H12	-4.0982714329	-3.9407699265	0.4812263322
C12	-1.5316801901	-2.8421871117	0.1511900371
C13	-2.3802636501	-1.8091183580	-0.0312521643
H15	-1.9652880229	-0.8205089096	-0.2198575523
H16	-1.9486865576	-3.8323927158	0.3259489543
C16	2.7734875957	-2.8774915889	0.1311408256
C17	2.0277379167	-4.0554884837	0.2888181918
C18	0.6411749301	-4.0140393968	0.2921141524
C19	-0.0682757996	-2.8065055585	0.1381972998
C20	0.6946137979	-1.6350753330	-0.0162369530
C21	2.0856456257	-1.6651369891	-0.0209750767
H23	2.5383213377	-5.0068558627	0.4096633569
H24	0.0856855673	-4.9404056715	0.4159550123
H25	0.1994174010	-0.6754224880	-0.1305297622
H26	2.6273682700	-0.7339753005	-0.1424063707
S26	-8.4609420801	-1.6384944700	-0.0311872223
C27	-9.0457398363	-3.3122035795	0.3862641249
H28	-10.1358266120	-3.2488756365	0.3880750438
H29	-8.7357642632	-4.0449031320	-0.3622958347
H30	-8.7077887729	-3.6191342554	1.3787457348
S30	4.5474530372	-3.0472519226	0.1422375258
C31	5.1465915681	-1.3400388869	-0.0658394496
H32	6.2362572697	-1.4100408636	-0.0593391970
H33	4.8255885854	-0.9149795515	-1.0193301512
H34	4.8286735152	-0.6998453415	0.7601083900

HOMO energy: -0.18483 hartrees

LUMO energy: -0.04928 hartrees

Orbital energies (hartrees):

-88.88533	-88.88533	-10.22391	-10.22390	-10.22024	-10.22022
-10.19744	-10.19727	-10.19490	-10.19484	-10.19299	-10.19283
-10.19270	-10.19270	-10.19168	-10.19162	-10.19059	-10.18982
-7.94627	-7.94626	-5.91154	-5.91154	-5.90741	-5.90741
-5.90116	-5.90115	-0.86678	-0.86337	-0.81690	-0.80337
-0.77646	-0.74930	-0.74811	-0.74693	-0.71289	-0.66634
-0.64406	-0.62146	-0.61013	-0.59317	-0.57536	-0.55401
-0.50733	-0.50164	-0.46834	-0.46315	-0.45534	-0.44748
-0.44163	-0.43725	-0.43718	-0.43554	-0.42303	-0.41971
-0.40553	-0.40003	-0.38175	-0.37464	-0.36866	-0.36828
-0.35153	-0.34528	-0.33545	-0.32320	-0.32060	-0.31940
-0.29357	-0.25459	-0.25419	-0.25029	-0.21622	-0.18483
-0.04928	-0.00270	-0.00263	0.01549	0.03558	0.03569
0.07273	0.07408	0.07412	0.09542		

**PP2**

Final total energy: -1493.14718671261 hartrees

Final geometry:

	angstroms		
atom	x	y	z
C1	-2.3426775229	0.3995095608	0.2271635527
C2	-3.0478500144	1.6139813026	0.1671225268
C3	-4.4559283131	1.5375564676	0.2236024395
C4	-5.1094032871	0.3209868684	0.3336649073
C5	-4.3867386852	-0.8851527425	0.3925295337
C6	-2.9896899681	-0.8288809901	0.3374113222
H7	-1.2562442673	0.4182435637	0.1862575986
H9	-5.0508083675	2.4449004000	0.1812964131
H10	-6.1949642165	0.2986233620	0.3751764357
H12	-2.3939219123	-1.7334528963	0.3790083062
C12	-2.7918756553	4.1254521647	-0.0162133438
C13	-2.3021963745	2.8637794382	0.0524918686
H15	-1.2187522020	2.7464803418	0.0200902986
H16	-3.8676876486	4.2937979399	0.0125048882
C16	-2.4443747228	6.5643786043	-0.1968484366
C17	-1.9629571924	5.2996381087	-0.1280939073
H19	-0.8877721980	5.1271682639	-0.1565392351
H20	-3.5265966465	6.6919774791	-0.1654450995
C20	-0.3049851916	10.2844717219	-0.5322354923
C21	-1.7029789238	10.2492150939	-0.4815755756
C22	-2.3696077966	9.0306797560	-0.3725988926
C23	-1.6836926068	7.8052647531	-0.3103159240
C24	-0.2741033785	7.8611504965	-0.3626713669
C25	0.3985830592	9.0672098383	-0.4705632110
H27	-2.2844765369	11.1629551894	-0.5259612429
H28	-3.4563184210	9.0293368098	-0.3350256829
H29	0.3075175889	6.9454721734	-0.3173875929
H30	1.4845883058	9.0726916977	-0.5071149586
S30	0.6745435159	11.7661241977	-0.6714303558
S31	-5.3407273913	-2.3829791615	0.5323163287
C32	-0.5657889538	13.0994612142	-0.7048297948
H33	0.0037994124	14.0278260094	-0.7824793883
H34	-1.2232856043	13.0144143901	-1.5730491862
H35	-1.1548726080	13.1215346676	0.2148660257
C35	-4.0751165783	-3.6914743480	0.5912039609
H36	-4.6268065871	-4.6293897572	0.6814976262
H37	-3.4816895207	-3.7170720836	-0.3256451807
H38	-3.4230535777	-3.5792297134	1.4604472093

HOMO energy: -0.17989 hartrees

LUMO energy: -0.05819 hartrees

Orbital energies (hartrees):

-88.88601	-88.88588	-10.22447	-10.22425	-10.22057	-10.22050
-10.19725	-10.19723	-10.19413	-10.19405	-10.19398	-10.19375
-10.19270	-10.19268	-10.19246	-10.19226	-10.19081	-10.19078
-10.18983	-10.18946	-7.94694	-7.94681	-5.91220	-5.91207
-5.90808	-5.90794	-5.90186	-5.90172	-0.86558	-0.86476
-0.82047	-0.80901	-0.79180	-0.76513	-0.74978	-0.74851
-0.73865	-0.70716	-0.66780	-0.64956	-0.61125	-0.61004
-0.60663	-0.58150	-0.56194	-0.54973	-0.51334	-0.49343
-0.47655	-0.46312	-0.45779	-0.45268	-0.44704	-0.44006
-0.43752	-0.43742	-0.42570	-0.42117	-0.41798	-0.40503
-0.38873	-0.38726	-0.37988	-0.37744	-0.36963	-0.35834
-0.34567	-0.34181	-0.33736	-0.33359	-0.32096	-0.32057
-0.30755	-0.27847	-0.25434	-0.25395	-0.23881	-0.21178
-0.17989	-0.05819	-0.00481	-0.00258	0.00028	0.03521
0.03540	0.04919	0.07278	0.07419	0.09198	

**PP3**

Final total energy: -1570.55777722054 hartrees

Final geometry:

atom	angstroms		
	x	y	z
C1	-3.1551496645	-0.6879559967	0.0298618562
C2	-3.8331293924	0.5370730239	-0.0962281767
C3	-5.2228585531	0.6212940323	-0.0665630512
C4	-5.9934697400	-0.5356753780	0.0926084957
C5	-5.3320694910	-1.7712854312	0.2194653054
C6	-3.9494693277	-1.8440539426	0.1886412849
H8	-3.2545191227	1.4492428745	-0.2207461730
H9	-5.6921724636	1.5930939161	-0.1683384951
H11	-5.9135644082	-2.6807345772	0.3438048701
H12	-3.4783510527	-2.8169266177	0.2899312979
C12	-0.8723064740	-1.7732230234	0.1020687380
C13	-1.6969243605	-0.7019811848	-0.0077536449
H15	-1.2325168067	0.2754924195	-0.1391683053
H16	-1.2928066323	-2.7688387784	0.2351041179
C16	1.3962637767	-2.7598903379	0.1684609068
C17	0.5624780039	-1.6911897147	0.0564464166
H19	0.9972679888	-0.7000366234	-0.0767287034
H20	0.9581320534	-3.7497195073	0.3016018597
C20	3.6408452228	-3.7704801249	0.2427604174
C21	2.8316557782	-2.6880505007	0.1264906468
H23	3.2646124641	-1.6973844820	-0.0064163587
H24	3.1597096911	-4.7398825885	0.3743251359
C24	7.9335142822	-4.0201546780	0.1792768013
C25	7.1327097530	-5.1617697156	0.3418825608
C26	5.7503478782	-5.0538382762	0.3586689862
C27	5.0987091406	-3.8116301104	0.2154009235
C28	5.9166104051	-2.6782479235	0.0530805644
C29	7.3037137505	-2.7754150869	0.0348220496
H31	7.5981676516	-6.1369399235	0.4553998180
H32	5.1512769576	-5.9520865853	0.4860159106
H33	5.4664591196	-1.6972202701	-0.0620145632
H34	7.8884172616	-1.8716544615	-0.0931652146
S34	-7.7736393134	-0.5751673799	0.1480717571
S35	9.6970797157	-4.2727603815	0.1731346389
C36	10.3718983264	-2.5972341185	-0.0609335293
H37	11.4570840218	-2.7178796934	-0.0713936708
H38	10.0548913316	-2.1663199301	-1.0133891647
H39	10.0978857909	-1.9351469426	0.7636288567

C39	-8.2481010201	1.1731158198	-0.0402055755
H40	-9.3394650905	1.1862091481	-0.0087950934
H41	-7.8633221428	1.7833973846	0.7799505496
H42	-7.9170999999	1.5772378425	-0.9994620603

HOMO energy: -0.17597 hartrees

LUMO energy: -0.06587 hartrees

Orbital energies (hartrees):

-88.88634	-88.88628	-10.22501	-10.22480	-10.22090	-10.22087
-10.19776	-10.19755	-10.19555	-10.19457	-10.19420	-10.19363
-10.19339	-10.19328	-10.19277	-10.19231	-10.19152	-10.19150
-10.19055	-10.19003	-10.18975	-10.18953	-7.94727	-7.94721
-5.91253	-5.91248	-5.90840	-5.90834	-5.90219	-5.90212
-0.86588	-0.86569	-0.82335	-0.81312	-0.80103	-0.78040
-0.75762	-0.74938	-0.74891	-0.73375	-0.70373	-0.66695
-0.65086	-0.61964	-0.61114	-0.60818	-0.58537	-0.56898
-0.55545	-0.54884	-0.50969	-0.49922	-0.47893	-0.46574
-0.46033	-0.45538	-0.45073	-0.44285	-0.43786	-0.43786
-0.43428	-0.42655	-0.42086	-0.41497	-0.40402	-0.39260
-0.38555	-0.37971	-0.37888	-0.37037	-0.35954	-0.35813
-0.34697	-0.34081	-0.33968	-0.33928	-0.32118	-0.32075
-0.31813	-0.29534	-0.26489	-0.25488	-0.25449	-0.23099
-0.20760	-0.17597	-0.06587	-0.01572	-0.00322	-0.00218
0.03069	0.03496	0.03504	0.07243	0.07311	0.07326

**PM1**

Final total energy: -1415.73537949533 hartrees

Final geometry:

atom	angstroms		
	x	y	z
C1	-4.1841626791	1.5569152376	0.1876405253
H2	-4.8681849692	2.1476792536	0.8002559953
H4	-3.5310557600	2.2345545285	-0.3669654053
H5	-3.5926357479	0.9112819201	0.8407662029
S5	-5.2447620944	0.5862788618	-0.9305507327
C6	-2.3823785809	-1.9177229951	-3.5570237809
C7	-3.7844491201	-1.9666890719	-3.6834427426
C8	-4.6197022234	-1.2029753234	-2.8809826322
C9	-4.0829755879	-0.3486244001	-1.9053112009
C10	-2.6889818901	-0.2887247417	-1.7631528553
C11	-1.8610176290	-1.0591520904	-2.5731102603
H13	-4.2245698321	-2.6208744022	-4.4320987891
H14	-5.6965058426	-1.2683829515	-3.0096548134
H15	-2.2361014097	0.3563953038	-1.0191008976
H16	-0.7872595727	-0.9878255599	-2.4280142244
C16	-0.2166891382	-2.8021124764	-4.4961546441
C17	-1.5629807732	-2.7490076915	-4.4409475680
H19	-2.1367771807	-3.3756844631	-5.1215955134
H20	0.3582907936	-2.1623091605	-3.8287710090
C20	2.2951312176	-5.1603142055	-7.0404801091
C21	0.9139641993	-5.3366790344	-7.0833230429
C22	0.0675872953	-4.5900090945	-6.2688007359
C23	0.6001639505	-3.6354947902	-5.3846752709
C24	1.9986199116	-3.4671145401	-5.3448578342
C25	2.8479013190	-4.2165362547	-6.1615582525
H26	2.9419420299	-5.7526805353	-7.6810011348
H27	0.4938780097	-6.0732378099	-7.7625410961
H28	-1.0032460330	-4.7569812191	-6.3168710225
H29	2.4050003077	-2.7312507175	-4.6593427007
S30	4.6277835112	-4.0636045686	-6.1743032869
C31	4.9616803185	-2.7851081655	-4.9205730380
H32	6.0476767973	-2.6723956119	-4.9002796841
H33	4.5125037958	-1.8272913686	-5.1931900786
H34	4.6202373396	-3.0942580685	-3.9298415359

HOMO energy: -0.19201 hartrees

LUMO energy: -0.05198 hartrees

Orbital energies (hartrees):

-88.88746	-88.88300	-10.22661	-10.22306	-10.22202	-10.21902
-10.20222	-10.19962	-10.19723	-10.19551	-10.19498	-10.19406
-10.19377	-10.19234	-10.19214	-10.19182	-10.19105	-10.18648
-7.94839	-7.94393	-5.91366	-5.90953	-5.90924	-5.90511
-5.90329	-5.89874	-0.86837	-0.86348	-0.81707	-0.80198
-0.78236	-0.75441	-0.75061	-0.73640	-0.71449	-0.66063
-0.65402	-0.62388	-0.60948	-0.59341	-0.57814	-0.54317
-0.51293	-0.50491	-0.47107	-0.46640	-0.45517	-0.44585
-0.44386	-0.43904	-0.43713	-0.43586	-0.42558	-0.41866
-0.40479	-0.39467	-0.38316	-0.37503	-0.37209	-0.36662
-0.35597	-0.34634	-0.33625	-0.32313	-0.32257	-0.31755
-0.29178	-0.27053	-0.25646	-0.23700	-0.21015	-0.19201
-0.05198	-0.00496	0.00104	0.01355	0.03367	0.03727
0.07153	0.07222	0.07460	0.09410		



**PM2**

Final total energy: -1493.14628820380 hartrees

Final geometry:

	angstroms		
atom	x	y	z
C1	3.4309097782	-2.6742507232	-0.0445427170
C2	2.5858524868	-1.6221888849	0.0730163638
H3	3.0285750210	-0.6350856798	0.2075180118
H4	3.0323966266	-3.6783857411	-0.1798668317
C5	5.7072258229	-3.6165548353	-0.1211760795
C6	4.8672005688	-2.5614230687	-0.0029803294
H7	5.2693188189	-1.5585090740	0.1306008651
H8	5.2582754989	-4.6005685628	-0.2570214150
C9	9.9835303964	-3.7265535331	-0.0571460621
C10	9.2403428278	-4.9023263880	-0.2421129830
C11	7.8461417671	-4.8313837265	-0.2569875890
C12	7.1698681221	-3.6052080974	-0.0929508361
C13	7.9348211422	-2.4397050911	0.0908049013
C14	9.3242046084	-2.5106970002	0.1073491009
H15	11.0689058255	-3.7655739556	-0.0415250075
H16	7.2516000592	-5.7276615182	-0.3972100526
H17	7.4474516624	-1.4797181811	0.2249292723
H18	9.9072374063	-1.6052765001	0.2507602410
S19	10.1789174143	-6.4096989895	-0.4391533848
C20	8.9033085215	-7.6904505167	-0.6618136303
H21	9.4494681120	-8.6275149673	-0.7884150734
H22	8.2588917337	-7.7732585189	0.2163770056
H23	8.3024934736	-7.5084615313	-1.5558648984
C24	-1.7142516165	-1.5642160130	-0.0101675885
C25	-1.0213289917	-2.7807127837	-0.1512348766
C26	0.3624864690	-2.8167710817	-0.1258793556
C27	1.1265067181	-1.6421870324	0.0410959452
C28	0.4182519244	-0.4366410456	0.1809809238
C29	-0.9737426442	-0.3889636394	0.1573772335
H30	-1.5787877651	-3.7039888423	-0.2830047986
H31	0.8584053613	-3.7754774787	-0.2393656009
H32	0.9731481005	0.4892386087	0.3121587236
H33	-1.4680648502	0.5689931485	0.2707910000
S34	-3.4925301763	-1.6522694111	-0.0581361428
C35	-4.0137918152	0.0811330683	0.1413373017
H36	-5.1050381604	0.0648937336	0.1096878573
H37	-3.6938141556	0.4876739165	1.1032856899

H38      -3.6453074801    0.7064700900    -0.6748589477

HOMO energy: -0.18603 hartrees

LUMO energy: -0.06110 hartrees

Orbital energies (hartrees):

-88.88766 -88.88260 -10.22648 -10.22270 -10.22195 -10.21846  
-10.20187 -10.19941 -10.19614 -10.19587 -10.19501 -10.19453  
-10.19401 -10.19344 -10.19261 -10.19208 -10.19202 -10.19176  
-10.19093 -10.18662 -7.94861 -7.94353 -5.91386 -5.90973  
-5.90884 -5.90471 -5.90353 -5.89834 -0.86763 -0.86430  
-0.82173 -0.80760 -0.79356 -0.77168 -0.75197 -0.74474  
-0.73585 -0.70852 -0.66304 -0.65368 -0.62425 -0.61289  
-0.59445 -0.58687 -0.55923 -0.54472 -0.51379 -0.50050  
-0.48069 -0.46451 -0.45931 -0.45168 -0.44456 -0.44324  
-0.43901 -0.43533 -0.42895 -0.42279 -0.41729 -0.39707  
-0.39346 -0.38668 -0.38155 -0.37759 -0.36674 -0.36074  
-0.35206 -0.34196 -0.33836 -0.33488 -0.32264 -0.31764  
-0.30621 -0.28098 -0.26283 -0.25616 -0.22770 -0.20869  
-0.18603 -0.06110 -0.00628 -0.00268 0.00190 0.03379  
0.03776 0.04783 0.07179 0.07510 0.08987

**PM3**

Final total energy: -1570.55698523588 hartrees

Final geometry:

	angstroms		
atom	x	y	z
C1	-1.1214174131	-0.5496530163	-0.1421607584
C2	-1.9001919380	-1.7258257742	-0.1936817260
C3	-3.2834508741	-1.6741721547	-0.2293588137
C4	-3.9607073966	-0.4406197988	-0.2151470989
C5	-3.2054229588	0.7361770033	-0.1636312596
C6	-1.8147633186	0.6731104147	-0.1281622186
H8	-1.4163744755	-2.6976184912	-0.2061226513
H9	-3.8530224789	-2.5986170235	-0.2688857519
H11	-3.6874124894	1.7069506489	-0.1506857277
H12	-1.2478555418	1.6001010588	-0.0885594658
S12	-5.7395675213	-0.5083250317	-0.2654271733
C13	-6.2362483257	1.2435577975	-0.2344455922
H14	-7.3276436229	1.2395804495	-0.2646318884
H15	-5.9094981105	1.7365168155	0.6838635087
H16	-5.8602332270	1.7821032315	-1.1071461148
C16	1.1738665274	-1.6085319089	-0.1099699765
C17	0.3365626975	-0.5417718681	-0.1041437221
H19	0.7891279905	0.4492863493	-0.0673123014
H20	0.7664547045	-2.6175886665	-0.1457429997
C20	3.4565476790	-2.5642195597	-0.0772933417
C21	2.6070923235	-1.5026593544	-0.0715352384
H23	3.0277071992	-0.4971960234	-0.0356951856
H24	3.0359175572	-3.5696464281	-0.1127364341
C24	5.7237014967	-3.5284870603	-0.0454439044
C25	4.8902679352	-2.4599237635	-0.0396985916
H27	5.3007783018	-1.4521846187	-0.0052862828
H28	5.2673327592	-4.5177756381	-0.0808368635
C28	9.9985608557	-3.6650738906	0.0544182194
C29	9.2449052948	-4.8481614661	0.0049838393
C30	7.8516394427	-4.7671879714	-0.0266147217
C31	7.1852568012	-3.5244732234	-0.0100516582
C32	7.9600816236	-2.3514923509	0.0397254081
C33	9.3488468432	-2.4327556513	0.0712834146
H34	11.0833252990	-3.7111547758	0.0798298231
H36	7.2494542945	-5.6684899257	-0.0650609156
H37	7.4808841818	-1.3783068197	0.0544626917
H38	9.9396869824	-1.5219005612	0.1101052170
S38	10.1671572344	-6.3780466925	-0.0131781070

C39	8.8764800127	-7.6616286812	-0.0775953370
H40	9.4116810129	-8.6134289617	-0.0887541255
H41	8.2323539104	-7.6291314697	0.8042028085
H42	8.2763354500	-7.5834368827	-0.9871154871

HOMO energy: -0.18110 hartrees

LUMO energy: -0.06838 hartrees

Orbital energies (hartrees):

-88.88788	-88.88275	-10.22678	-10.22303	-10.22203	-10.21863
-10.20205	-10.19954	-10.19631	-10.19605	-10.19512	-10.19475
-10.19413	-10.19347	-10.19336	-10.19278	-10.19218	-10.19215
-10.19195	-10.19177	-10.19129	-10.18675	-7.94882	-7.94368
-5.91407	-5.90994	-5.90899	-5.90486	-5.90375	-5.89849
-0.86769	-0.86447	-0.82497	-0.81250	-0.80028	-0.78455
-0.76331	-0.75141	-0.73904	-0.73475	-0.70442	-0.66362
-0.65390	-0.62980	-0.61297	-0.59650	-0.59224	-0.56831
-0.55723	-0.53965	-0.51326	-0.50457	-0.47979	-0.47022
-0.46122	-0.45589	-0.44789	-0.44419	-0.43914	-0.43544
-0.43506	-0.43149	-0.42133	-0.41000	-0.39854	-0.39277
-0.38735	-0.38126	-0.37826	-0.37313	-0.36001	-0.35965
-0.35008	-0.34249	-0.34164	-0.33865	-0.32276	-0.31784
-0.31782	-0.29387	-0.27437	-0.25688	-0.25258	-0.22107
-0.20764	-0.18110	-0.06838	-0.01702	-0.00480	0.00133
0.02933	0.03363	0.03757	0.07122	0.07177	0.07498

**P1**

Final total energy: -978.23224126891 hartrees

Final geometry:

	angstroms		
atom	x	y	z
C1	2.0459081377	0.4276365722	-0.0033426950
C2	1.3357180151	1.6440195419	-0.0032010887
C3	-0.0509626423	1.6827516209	-0.0043976047
C4	-0.7949471235	0.4930725167	-0.0057504205
C5	-0.1054134668	-0.7279813582	-0.0058315340
C6	1.2853240827	-0.7547205650	-0.0047644557
H8	1.8906094781	2.5790452759	-0.0021160369
H9	-0.5626683380	2.6411109630	-0.0042185370
H11	-0.6448710554	-1.6681824002	-0.0067592443
H12	1.7820003632	-1.7199402003	-0.0049731160
C12	4.3565611442	-0.5836143713	-0.0031851937
C13	3.5091188302	0.4651646844	-0.0019358149
H15	3.9261363203	1.4704971079	0.0003770118
H16	3.9426085933	-1.5902623916	-0.0059349083
C16	8.6461496155	-0.5837977461	0.0026889973
C17	7.9253881781	-1.7773089379	-0.0017504087
C18	6.5331388321	-1.7519178731	-0.0036753571
C19	5.8216071913	-0.5376343723	-0.0012014785
C20	6.5674223129	0.6575897095	0.0031382380
C21	7.9575194646	0.6324310976	0.0050957687
H22	9.7321370603	-0.5981631253	0.0043013150
H23	8.4472423474	-2.7301744527	-0.0036965366
H24	5.9784854030	-2.6871478172	-0.0071477200
H25	6.0575640714	1.6160273577	0.0050404350
H26	8.5102615451	1.5677966082	0.0085199717
S26	-2.5692484006	0.6578768678	-0.0073705386
C27	-3.1620558017	-1.0642160476	0.0066487642
H28	-4.2519946798	-0.9987417114	0.0092229984
H29	-2.8427859704	-1.6057339193	-0.8866139095
H30	-2.8375598464	-1.5928114655	0.9057416875

HOMO energy: -0.19140 hartrees

LUMO energy: -0.04978 hartrees

Orbital energies (hartrees):

-88.88605 -10.22510 -10.22073 -10.19829 -10.19791 -10.19560  
 -10.19370 -10.19348 -10.19245 -10.19143 -10.18997 -10.18924  
 -10.18880 -10.18807 -10.18794 -10.18777 -7.94699 -5.91226

-5.90812	-5.90188	-0.86639	-0.85434	-0.81273	-0.78538
-0.75183	-0.74903	-0.74254	-0.71061	-0.65808	-0.62398
-0.60859	-0.60066	-0.57900	-0.55231	-0.51218	-0.50381
-0.46992	-0.46098	-0.45569	-0.44382	-0.43779	-0.43495
-0.42517	-0.41757	-0.41477	-0.40152	-0.38078	-0.36983
-0.36882	-0.36377	-0.34479	-0.34107	-0.33284	-0.32059
-0.31770	-0.27920	-0.25495	-0.24926	-0.23260	-0.19140
-0.04978	-0.00337	0.00157	0.01631	0.03503	0.07321
0.07500	0.09514	0.09722	0.10780		

**P2**

Final total energy: -1055.64297608260 hartrees

Final geometry:

	angstroms		
atom	x	y	z
C1	2.8973854205	-0.4443906152	-0.1831191150
H2	2.1970329203	0.1579681372	0.3989276309
H4	3.5114362165	0.2204662576	-0.7948510606
H5	3.5267705594	-1.0165161671	0.5023183332
S5	1.8644758597	-1.5374438418	-1.2111918286
C6	4.7999241016	-4.1456015661	-3.6511417726
C7	3.3992281022	-4.2782860333	-3.7351491977
C8	2.5419533889	-3.4816912974	-2.9900771823
C9	3.0523015305	-2.5062489895	-2.1187563074
C10	4.4437506303	-2.3589915839	-2.0223349818
C11	5.2939417983	-3.1632213857	-2.7732566971
H13	2.9790440950	-5.0269831043	-4.4022237057
H14	1.4677589366	-3.6160828947	-3.0814617644
H15	4.8772719135	-1.6172547051	-1.3615056586
H16	6.3647112429	-3.0185615614	-2.6692786264
C16	7.0013969925	-5.0313840855	-4.5188869564
C17	5.6483797033	-5.0154281452	-4.4602167591
H19	5.1105003154	-5.7294557356	-5.0841794250
H20	7.5793866300	-4.3344543659	-3.9140130575
C20	9.1127623910	-5.9437484210	-5.4039763198
C21	7.7600831444	-5.9320135220	-5.3493989552
H23	7.1848576830	-6.6309883102	-5.9544538115
H24	9.6455241721	-5.2264740881	-4.7794887427
C24	11.7293982254	-8.4357731511	-7.7080428338
C25	10.3458184511	-8.5964101881	-7.8237255724
C26	9.4784234639	-7.7989931974	-7.0861572139
C27	9.9706063371	-6.8133435733	-6.2072903554
C28	11.3672679908	-6.6665382750	-6.1053234127
C29	12.2357494690	-7.4652975610	-6.8438792508
H30	12.4032313170	-9.0609799261	-8.2863648288
H31	9.9419125411	-9.3492254975	-8.4948693297
H32	8.4080152396	-7.9420409230	-7.1944555221
H33	11.7694786509	-5.9120831771	-5.4336771646
H34	13.3090166275	-7.3296322298	-6.7446284783

HOMO energy: -0.18521 hartrees

LUMO energy: -0.05953 hartrees

Orbital energies (hartrees):

-88.88657	-10.22529	-10.22116	-10.19829	-10.19815	-10.19577
-10.19402	-10.19384	-10.19293	-10.19241	-10.19156	-10.19081
-10.19061	-10.18952	-10.18907	-10.18848	-10.18834	-10.18812
-7.94749	-5.91276	-5.90863	-5.90240	-0.86626	-0.85526
-0.81868	-0.80021	-0.77172	-0.74949	-0.74407	-0.74169
-0.70563	-0.65924	-0.62474	-0.61445	-0.60273	-0.58502
-0.56214	-0.54984	-0.51716	-0.49874	-0.47693	-0.46217
-0.45748	-0.45183	-0.43976	-0.43811	-0.43153	-0.42378
-0.41703	-0.41020	-0.39958	-0.38000	-0.37984	-0.37141
-0.36220	-0.35855	-0.34280	-0.33986	-0.33478	-0.33130
-0.32103	-0.29967	-0.26358	-0.25511	-0.24961	-0.22364
-0.18521	-0.05953	-0.00602	-0.00055	0.00305	0.03462
0.05007	0.07292	0.09114	0.09391	0.09629	



**P3**

Final total energy: -1133.05366167212 hartrees

Final geometry:

atom	angstroms		
	x	y	z
C1	-1.0698586648	2.1599637374	0.6695269374
H2	-1.8175361083	2.6015366693	1.3314113209
H4	-0.3339965142	2.9236838039	0.4079257627
H5	-0.5852566007	1.3292716903	1.1876646061
S5	-1.9908574827	1.5888324925	-0.7943259717
C6	1.1356252020	-0.3088822037	-3.6157988250
C7	-0.2390748395	-0.2447349763	-3.9213569268
C8	-1.1547952013	0.3320731935	-3.0548180697
C9	-0.7309406481	0.8751932235	-1.8316170211
C10	0.6332691168	0.8204321149	-1.5098262489
C11	1.5437782995	0.2400786071	-2.3860730676
H13	-0.5896129526	-0.6591269932	-4.8633469430
H14	-2.2066172740	0.3631751435	-3.3250485412
H15	0.9969667255	1.2286948988	-0.5738795252
H16	2.5911447770	0.2146165946	-2.1022017493
C16	3.3863725785	-1.0819427407	-4.4730796369
C17	2.0426602878	-0.9310210281	-4.5726489431
H19	1.5635581306	-1.3167731946	-5.4726854704
H20	3.9129159188	-0.7122485867	-3.5946824855
C20	5.5355100701	-1.8861293380	-5.4100089716
C21	4.1885764005	-1.7184344025	-5.4808218196
H23	3.6647102056	-2.0906768177	-6.3615791014
H24	6.0666624958	-1.5167344543	-4.5323777263
C24	7.6621111493	-2.6973203201	-6.3615524555
C25	6.3197093365	-2.5284338518	-6.4290881232
H27	5.7723220073	-2.8915284435	-7.2973913803
H28	8.1732332106	-2.3179259120	-5.4767153983
C28	10.3031827474	-4.5495930945	-9.1802564836
C29	8.9333816406	-4.4925851242	-9.4534648870
C30	8.0573712795	-3.8966378024	-8.5535216593
C31	8.5289099888	-3.3373048524	-7.3481763529
C32	9.9118569438	-3.4051393650	-7.0909529020
C33	10.7881291877	-4.0020630737	-7.9927142924
H34	10.9830803070	-5.0164784144	-9.8867791907
H35	8.5473810589	-4.9173414135	-10.3758883145
H36	6.9979789213	-3.8656061704	-8.7881527355
H37	10.2963869402	-2.9799883481	-6.1670738855
H38	11.8503309505	-4.0396795834	-7.7679459868

HOMO energy: -0.18009 hartrees

LUMO energy: -0.06687 hartrees

Orbital energies (hartrees):

-88.88700	-10.22598	-10.22145	-10.19843	-10.19825	-10.19648
-10.19474	-10.19425	-10.19327	-10.19284	-10.19172	-10.19129
-10.19089	-10.19072	-10.19042	-10.18957	-10.18909	-10.18853
-10.18841	-10.18811	-7.94794	-5.91320	-5.90907	-5.90285
-0.86688	-0.85527	-0.82293	-0.80842	-0.78740	-0.76206
-0.75016	-0.74318	-0.73537	-0.70171	-0.66041	-0.62883
-0.61596	-0.60444	-0.59077	-0.57028	-0.55649	-0.54740
-0.51387	-0.50383	-0.47753	-0.46843	-0.45777	-0.45518
-0.44779	-0.43850	-0.43451	-0.42968	-0.42184	-0.41693
-0.40891	-0.39453	-0.38622	-0.38040	-0.37184	-0.36646
-0.36026	-0.35364	-0.34278	-0.34010	-0.34009	-0.33480
-0.32164	-0.31361	-0.28521	-0.25606	-0.25084	-0.24947
-0.21680	-0.18009	-0.06687	-0.01596	-0.00333	0.00180
0.03138	0.03425	0.07264	0.07337	0.08889	0.09623

**M1**

Final total energy: -978.23150103717 hartrees

Final geometry:

atom	angstroms		
	x	y	z
C1	0.3642957432	0.8695936629	-0.2724815267
C2	-0.3381187969	2.0868137688	-0.2048729813
C3	-1.7284326436	2.1262271657	-0.2694616638
C4	-2.4550064930	0.9438346947	-0.4037590078
C5	-1.7749181289	-0.2752980164	-0.4717365436
C6	-0.3867561617	-0.3140860954	-0.4066117776
H8	0.2219301637	3.0129532474	-0.1005743682
H9	-2.2438677293	3.0808832409	-0.2149218739
H10	-3.5395052064	0.9690055540	-0.4545330883
H11	-2.3325348759	-1.2018725777	-0.5753061860
H12	0.1173585509	-1.2737648617	-0.4593138594
C12	2.6734725212	-0.1446155163	-0.2608163758
C13	1.8277462033	0.9025539758	-0.2001425573
H15	2.2421603871	1.9029215422	-0.0911925563
H16	2.2611696912	-1.1439588559	-0.3850426175
C16	6.9503433696	-0.1435051994	-0.0774355543
C17	6.2571340082	1.0659714963	0.1084786340
C18	4.8644337747	1.0772638636	0.0536671860
C19	4.1377404230	-0.1065255413	-0.1881644399
C20	4.8494776065	-1.3031338228	-0.3661164480
C21	6.2421032368	-1.3153577877	-0.3119856006
H22	8.0355382503	-0.1590426267	-0.0347459601
H24	4.3255761644	2.0040488248	0.2055571759
H25	4.3049859927	-2.2251287029	-0.5507944634
H26	6.7808340536	-2.2478945375	-0.4537809942
S26	7.2665089081	2.5086421731	0.4101439572
C27	6.0517307707	3.8484449315	0.6206949933
H28	6.6394484610	4.7491308494	0.8093946318
H29	5.4572603416	3.9974770632	-0.2837673200
H30	5.3983390158	3.6667585827	1.4773240499

HOMO energy: -0.20120 hartrees

LUMO energy: -0.05288 hartrees

Orbital energies (hartrees):

-88.88355 -10.22441 -10.21947 -10.20292 -10.20105 -10.19440  
-10.19361 -10.19288 -10.19243 -10.19231 -10.19192 -10.19159  
-10.19098 -10.19079 -10.19074 -10.18770 -7.94449 -5.90980

-5.90567	-5.89931	-0.86636	-0.85701	-0.80977	-0.79098
-0.75924	-0.74554	-0.73735	-0.71167	-0.65791	-0.63563
-0.60720	-0.59741	-0.57493	-0.55060	-0.51429	-0.51140
-0.47081	-0.46602	-0.45339	-0.44550	-0.43647	-0.43445
-0.43016	-0.41809	-0.41387	-0.39575	-0.38139	-0.37292
-0.37076	-0.36304	-0.34804	-0.34259	-0.33602	-0.31824
-0.31598	-0.28292	-0.26149	-0.25203	-0.21545	-0.20120
-0.05288	-0.00121	0.00022	0.01416	0.03646	0.07307
0.07421	0.09338	0.09535	0.10465		

**PP1A**

Final total energy: -651.44626208994 hartrees

Final geometry:

	angstroms		
atom	x	y	z
C1	1.1442166194	0.6818031711	0.0618402600
C2	0.4349865101	1.8927137851	0.1689828716
C3	-0.9528991953	1.9405994128	0.1511604126
C4	-1.7057625323	0.7628362013	0.0253036694
C5	-1.0120326688	-0.4561260144	-0.0799565693
C6	0.3743543041	-0.4917973466	-0.0604132470
H8	0.9920927291	2.8212882178	0.2697079892
H9	-1.4633079257	2.8975295717	0.2318308755
H11	-1.5739540019	-1.3820826899	-0.1790102014
H12	0.8672520333	-1.4560874434	-0.1350551349
C12	3.4507572035	-0.3347242966	-0.0676129751
C13	2.6071100538	0.7072413817	0.0880184901
H15	3.0299227942	1.6982830684	0.2464297822
H16	3.0279676494	-1.3229871983	-0.2425299026
C16	7.7635194306	-0.3900583980	-0.0031124859
C17	7.0675693135	0.8123219703	0.2168336693
C18	5.6811935930	0.8472179354	0.2002329020
C19	4.9134226630	-0.3097383282	-0.0380141590
C20	5.6246016162	-1.5042911189	-0.2559899793
C21	7.0125420231	-1.5517678536	-0.2403880042
H23	7.6279385954	1.7265065387	0.3992224210
H24	5.1864160518	1.7966641990	0.3794197770
H25	5.0689973284	-2.4206627025	-0.4409032259
H26	7.5246838985	-2.4947702672	-0.4170373943
N26	9.1589954654	-0.4144683407	-0.0422163230
H27	9.6148922453	0.3218547733	0.4793262979
H28	9.5749818376	-1.3169542279	0.1438104207
N28	-3.0990859751	0.8045346980	-0.0513485923
H29	-3.5690509264	-0.0478846485	0.2214319464
H30	-3.5258491168	1.6184497277	0.3699096669

HOMO energy: -0.16682 hartrees

LUMO energy: -0.02741 hartrees

Orbital energies (hartrees):

-14.33989 -14.33988 -10.22270 -10.22266 -10.18030 -10.18030  
-10.17989 -10.17988 -10.17948 -10.17947 -10.17801 -10.17799

-10.17661	-10.17659	-10.17467	-10.17391	-0.91473	-0.91467
-0.83818	-0.83074	-0.77372	-0.73657	-0.73578	-0.73112
-0.68527	-0.62017	-0.60580	-0.60412	-0.57896	-0.54415
-0.51525	-0.51354	-0.50521	-0.50081	-0.46685	-0.45835
-0.43572	-0.42778	-0.41410	-0.41278	-0.40881	-0.40461
-0.37820	-0.37768	-0.36580	-0.36324	-0.33713	-0.33155
-0.32841	-0.32026	-0.30882	-0.25769	-0.24196	-0.24180
-0.20944	-0.16682	-0.02741	0.00909	0.00941	0.03907
0.07807	0.08359	0.09919	0.10478	0.11036	0.11191

**PM1A**

Final total energy: -651.44579983956 hartrees

Final geometry:

	angstroms		
atom	x	y	z
C1	0.9022076285	-0.2088632304	0.0340343948
C2	0.2103317063	1.0127703760	0.0649771006
C3	-1.1901454641	1.0739459415	0.0677182325
C4	-1.9159794967	-0.1261423215	0.0375693172
C5	-1.2384644954	-1.3442607682	0.0064085838
C6	0.1503435750	-1.3998306379	0.0043269629
H8	0.7786545271	1.9408538365	0.0841512159
H10	-3.0028199342	-0.1012362234	0.0319223919
H11	-1.8111900401	-2.2675586331	-0.0173094659
H12	0.6467918854	-2.3635176622	-0.0213235811
C12	3.2089220325	-1.2294237409	0.0398884893
C13	2.3685416501	-0.1740592938	0.0367716031
H15	2.7915570935	0.8289790533	0.0392032070
H16	2.7827908732	-2.2312182216	0.0441252324
C16	7.5205416186	-1.2877533810	0.0458864424
C17	6.8292113899	-0.0622884967	0.0265702129
C18	5.4433046847	-0.0262257033	0.0242362819
C19	4.6716835614	-1.2048576484	0.0424279065
C20	5.3777833133	-2.4219712895	0.0615939482
C21	6.7653999535	-2.4710789936	0.0631663589
H23	7.3933157273	0.8673772614	0.0168130205
H24	4.9513554702	0.9411180787	0.0045770635
H25	4.8188390341	-3.3544002289	0.0729194637
H26	7.2740368978	-3.4320170201	0.0817409004
N26	8.9128575323	-1.3229776680	0.1055042654
H27	9.3821593327	-0.5083392571	-0.2655236629
H28	9.3355592761	-2.1826225310	-0.2170010959
N28	-1.8478638654	2.3087964095	0.0419166426
H29	-2.7868380898	2.2926346861	0.4167277742
H30	-1.3130472212	3.0780154316	0.4223007057

HOMO energy: -0.17707 hartrees

LUMO energy: -0.03402 hartrees

Orbital energies (hartrees):

-14.34379 -14.33452 -10.22729 -10.21882 -10.18742 -10.18437  
-10.18402 -10.18347 -10.18166 -10.18047 -10.18030 -10.17858  
-10.17696 -10.17264 -10.17217 -10.16792 -0.91893 -0.91017

-0.84042	-0.82975	-0.77832	-0.74110	-0.73925	-0.71731
-0.69156	-0.62481	-0.60965	-0.59486	-0.58379	-0.54488
-0.51744	-0.51327	-0.50094	-0.49536	-0.46837	-0.46434
-0.43791	-0.43371	-0.41513	-0.41425	-0.40815	-0.40146
-0.38172	-0.37485	-0.36849	-0.35375	-0.34407	-0.33194
-0.32892	-0.32334	-0.30678	-0.27095	-0.24580	-0.23147
-0.19817	-0.17707	-0.03402	0.00547	0.02108	0.03496
0.07692	0.08462	0.09737	0.10404	0.10784	0.11434



**P1A**

Final total energy: -596.08770091935 hartrees

Final geometry:

	angstroms		
atom	x	y	z
N1	1.6499256042	1.3024215562	0.0759396850
H2	2.5875266164	1.5499405815	-0.2085590009
H4	1.6409178744	0.7740372203	0.9374759812
C4	-0.9048579788	-0.1141201096	-3.0001118396
C5	-1.1300291782	-0.4309674901	-1.6475705049
C6	-0.2891079537	0.0125644342	-0.6357000029
C7	0.8308969524	0.8046424790	-0.9358688524
C8	1.0688507934	1.1302016844	-2.2842420818
C9	0.2224771102	0.6810707322	-3.2859608153
H11	-1.9894574321	-1.0440322485	-1.3866891314
H12	-0.4994882283	-0.2499493487	0.3984011830
H13	1.9280729193	1.7457455486	-2.5399878084
H14	0.4467559460	0.9538154821	-4.3126489929
C14	-1.7812695632	-0.4192687079	-5.3456986335
C15	-1.8313741330	-0.6192989618	-4.0124312702
H17	-2.6442358542	-1.2212163793	-3.6085737273
H18	-0.9718210368	0.1841606089	-5.7532560950
C18	-4.4401662431	-1.8527756973	-8.3966146760
C19	-4.6765175330	-2.1908790287	-7.0609769118
C20	-3.8293614819	-1.7386172488	-6.0550703804
C21	-2.7143561888	-0.9303684403	-6.3541008097
C22	-2.4934503819	-0.6011326144	-7.7048612068
C23	-3.3415606373	-1.0538386431	-8.7123229103
H24	-5.1045023940	-2.2085224623	-9.1785313246
H25	-5.5290522117	-2.8130583826	-6.8025782472
H26	-4.0369753093	-2.0177284883	-5.0265634792
H27	-1.6396182572	0.0215715110	-7.9610089553
H28	-3.1432629305	-0.7816128383	-9.7453092903

HOMO energy: -0.18127 hartrees

LUMO energy: -0.03876 hartrees

Orbital energies (hartrees):

-14.34584 -10.22964 -10.19214 -10.18691 -10.18649 -10.18597  
-10.18439 -10.18387 -10.18368 -10.18316 -10.18240 -10.18209  
-10.18178 -10.18145 -10.18056 -0.92097 -0.84952 -0.83981  
-0.78511 -0.74447 -0.74192 -0.73643 -0.69567 -0.62672  
-0.61119 -0.59808 -0.58244 -0.54702 -0.51911 -0.51521

-0.49903	-0.47489	-0.45330	-0.44502	-0.43067	-0.42272
-0.41483	-0.41136	-0.40529	-0.38410	-0.37200	-0.36437
-0.35708	-0.33620	-0.33531	-0.32728	-0.32529	-0.28412
-0.24805	-0.24345	-0.23330	-0.18127	-0.03876	0.00323
0.00747	0.02862	0.07488	0.08964	0.10011	0.10196
0.10559	0.12581				

**M1A**

Final total energy: -596.08503296076 hartrees

Final geometry:

	angstroms		
atom	x	y	z
C1	-0.2895692466	0.3590289273	-0.0932129658
C2	-0.9758155339	1.5196733895	-0.4804834983
C3	-2.3782522905	1.5942184994	-0.4606696530
C4	-3.1014732961	0.4661396360	-0.0359225663
C5	-2.4242053173	-0.6878562516	0.3522146310
C6	-1.0357932746	-0.7577054339	0.3290445405
H7	-0.4055143116	2.3872086762	-0.8067539301
H8	-4.1878056885	0.4992673269	-0.0115590031
H9	-2.9981123789	-1.5513089248	0.6776757863
H10	-0.5384096527	-1.6698535949	0.6400528411
C11	2.0153322259	-0.6341230807	0.1444437440
C12	1.1761636393	0.3779546906	-0.1502197804
H13	1.5985727958	1.3279701325	-0.4723044226
H14	1.5941438711	-1.5859748902	0.4625481972
C15	6.3034869834	-0.7001430455	0.0104189899
C16	5.6211943033	0.4671931991	-0.3427329346
C17	4.2320262224	0.5120021452	-0.3062046422
C18	3.4806837301	-0.6129945291	0.0854860142
C19	4.1857629553	-1.7788129174	0.4372752591
C20	5.5771321542	-1.8242450929	0.4012118348
H21	6.1773984575	1.3490813217	-0.6483351226
H22	3.7272259296	1.4313861870	-0.5853417944
H23	3.6269732208	-2.6601883963	0.7423518947
H24	6.0938000611	-2.7389034138	0.6781771323
N25	-3.0270859254	2.7469965583	-0.8480711070
H26	-4.0294972101	2.8060298144	-0.8344345723
H27	-2.5127276021	3.5515003032	-1.1592360387
H28	7.3887440385	-0.7305032580	-0.0196203385

HOMO energy: -0.18789 hartrees

LUMO energy: -0.04314 hartrees

Orbital energies (hartrees):

-14.34056 -10.22659 -10.19499 -10.19093 -10.18659 -10.18602  
-10.18577 -10.18535 -10.18505 -10.18497 -10.18471 -10.18150  
-10.17578 -10.17577 -10.16986 -0.91561 -0.85234 -0.83488  
-0.78791 -0.75019 -0.73974 -0.72299 -0.70038 -0.63027  
-0.60381 -0.59932 -0.58675 -0.54965 -0.51883 -0.50742

-0.50432	-0.47329	-0.45985	-0.44902	-0.43519	-0.42021
-0.41488	-0.40955	-0.40154	-0.38031	-0.36766	-0.36702
-0.35168	-0.34230	-0.33377	-0.32713	-0.32175	-0.28806
-0.25357	-0.24643	-0.20403	-0.18789	-0.04314	0.00441
0.01934	0.02852	0.07923	0.08719	0.09828	0.10294
0.11059	0.12577				

**PM1TA**

Final total energy: -1112.20499561224 hartrees

Final geometry:

atom	angstroms		
	x	y	z
C1	-1.2106703531	-0.5803126647	-0.0882786851
C2	-2.5315992428	-0.7769215720	0.0968129706
H3	-0.5826405231	-1.4358836992	-0.3302271185
H5	-3.1594587183	0.0884337127	0.3008329027
C6	1.0065903020	3.1119110051	0.0652895781
C7	1.6142701591	1.9032859301	-0.3082254053
C8	0.8780954871	0.7271329729	-0.3468227401
C9	-0.4916347679	0.6941654280	-0.0200035872
C10	-1.0831444844	1.9132458634	0.3570645407
C11	-0.3554237643	3.0984380091	0.3986410873
H13	2.6687498220	1.8864039324	-0.5698243125
H14	1.3728756392	-0.1952622666	-0.6411124325
H15	-2.1329392874	1.9447093059	0.6324677552
H16	-0.8607527293	4.0098336107	0.6974845644
C16	-4.7948221688	-4.4026172427	-0.0665453956
C17	-5.4162645425	-3.1636194629	0.0382833813
C18	-4.6747386462	-1.9881042634	0.0899227764
C19	-3.2713838379	-2.0427450682	0.0357666965
C20	-2.6446638477	-3.2957385709	-0.0622981972
C21	-3.3844839253	-4.4925966102	-0.1289696412
H22	-5.4061790136	-5.2956476214	-0.0931271049
H23	-6.5010183965	-3.1202451988	0.0858130036
H24	-5.1732972093	-1.0266602541	0.1731428798
H25	-1.5633908251	-3.3348378746	-0.0687436771
S26	2.0436697153	4.5620176615	0.0819697073
C27	0.9166304275	5.8915888591	0.6110378542
H28	1.5240096460	6.7988066879	0.6320303258
H29	0.0980484972	6.0307342358	-0.0988439203
H30	0.5210598526	5.7079511923	1.6126572514
N30	-2.7513271705	-5.7274952909	-0.2558076542
C32	-1.3105489286	-5.8035709535	-0.0957018341
H33	-0.8012074257	-5.1787148549	-0.8376362887
H34	-0.9684572779	-5.4896549681	0.9035131249
H35	-0.9867032585	-6.8329371841	-0.2592487188
C35	-3.5195254187	-6.9412737351	-0.0390624690
H36	-2.8690389293	-7.8054591714	-0.1844162616
H37	-3.9535168609	-7.0039917746	0.9717578671
H38	-4.3378348475	-7.0244896689	-0.7627696868

HOMO energy: -0.18301 hartrees

LUMO energy: -0.04357 hartrees

Orbital energies (hartrees):

-88.88330	-14.34937	-10.22178	-10.22152	-10.21848	-10.21639
-10.21602	-10.19420	-10.19224	-10.19032	-10.18976	-10.18963
-10.18891	-10.18571	-10.18416	-10.18029	-10.17593	-10.17380
-10.17100	-7.94422	-5.90949	-5.90537	-5.89910	-0.94253
-0.86235	-0.84047	-0.80813	-0.77960	-0.74803	-0.74518
-0.73967	-0.72400	-0.70260	-0.65666	-0.65304	-0.61832
-0.60381	-0.58084	-0.56618	-0.54628	-0.51733	-0.50076
-0.47559	-0.46971	-0.46293	-0.46078	-0.45053	-0.44481
-0.43532	-0.43190	-0.42110	-0.41878	-0.41245	-0.40522
-0.39469	-0.39209	-0.38150	-0.37624	-0.36514	-0.36185
-0.35829	-0.34668	-0.33404	-0.32831	-0.31762	-0.31509
-0.28555	-0.26348	-0.25127	-0.22856	-0.19273	-0.18301
-0.04357	0.00011	0.01637	0.02745	0.03748	0.07575
0.08155	0.08591	0.09984	0.10937		

## D6. References

---

1. Aradhya, S. V.; Meisner, J. S.; Krikorian, M.; Ahn, S.; Parameswaran, R.; Steigerwald, M. L.; Nuckolls, C.; Venkataraman, L. *Nano Lett.*, **2012**, *12*, 1643–1647.
2. Meisner, J. S.; Sedbrook, D. F.; Krikorian, M.; Chen, J.; Sattler, A.; Carnes, M. E.; Murray, C. B.; Steigerwald, M.; Nuckolls, C., *Chem. Sci.*, **2012**, *3*, 1007–1014.
3. Cody, J.; Fahrni, C. J.; *Tetrahedron*, **2004**, *60*, 11099–11107.
4. Marder, S., *Langmuir*, **2009**, *25*, 7967–7975
5. Xue, C.; Luo, F.-T., *J. Org. Chem.*, **2003**, *68*, 4417–4421.
6. Motoshima, K.; Noguchi-Yachide, T.; Sugita, K.; Hashimoto, Y.; Ishikawa, M. *Bioorg. Med. Chem.*, **2009**, *17*, 5001–5014.
7. Ling, C.; Minato, M.; Lahti, P. M.; Van Willigen, H. *J. Am. Chem. Soc.*, **1992**, *114*, 9959–9969.
8. Spangler, C. W.; Liu, P.-K.; Havelka, K. O., *J. Chem. Soc., Perkin's Trans. 2*, **1992**, *8*, 1207–1211.
9. Ranu, B. C.; Banerjee, S.; *Eur. J. Org. Chem.*, **2006**, 3012–3015.
10. Asokan, C. V.; Ila, H.; Junjappa, H., *Synthesis*, **1987**, 284–285.
11. (a) Jamey P. Weichert, Marc A. Longino, Susan W. Schwendner, and Raymond E. Counsell, *J. Med. Chem.*, **1986**, *29*, 1674–1682; (b) Clifford C. Leznoff, Wolodymyr Sywanyk., *J. Org. Chem.*, **1977**, *42*, 3203–3205.
12. Lewis, F. D.; Kalgutkar, R. S.; Kurth, T., *J. Phys. Chem. A*, **2004**, *108*, 1425–1434.
13. Saiyed, A. S.; Joshi, R. S.; Bedekar, A. V., *J. Chem. Res.*, **2011**, *35*, 408–411.
14. Ling, C.; Minato, M.; Lahti, P. M.; van Willigen, H., *J. Am. Chem. Soc.*, **1992**, *114*, 9959–9969.
15. Sun, B.; Hoshino, J.; Jermihov, K.; Marler, L.; Pezzuto, J. M.; Mesecar, A. D.; Cushman, M., *Bioorg. Med. Chem.*, **2010**, *18*, 5352–5366.
16. Frei, M.; Aradhya, S. V.; Koentopp, M.; Hybertsen, M. S.; Venkataraman, L. *Nano Lett.*, **2011**, *11*, 1518–1523.

## Appendix E

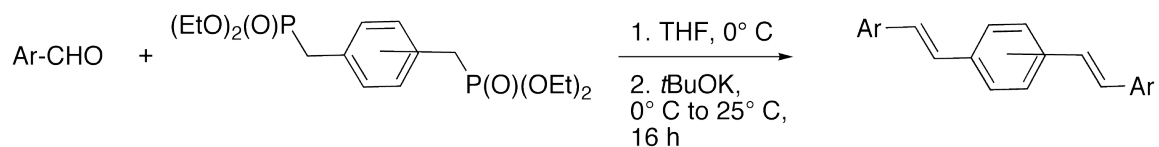
### E1. Synthetic Experimentals

**General Information:** 4-(diethoxymethyl)-benzaldehyde, triethyl phosphite, potassium *tert*-butoxide and all other starting materials and reagents were all purchased from Sigma-Aldrich. THF was freshly distilled under reduced pressure over an SG Water USA, LLC (formerly known as Contour Glass) purification column. Potassium *tert*-butoxide was stored in a glove box under an anhydrous argon atmosphere. Compounds **DPO1-DPO3** and dimethyl 4-(methylthio)benzyl phosphonate were prepared for in chapter 5 (see Appendix D). All reactions were carried out under nitrogen unless otherwise noted. 4,4-dimethylthiochroman-6-carbaldehyde (1),<sup>1</sup> (4,4'-dibromomethylstilbene, (*E*)-4,4'-bis(diethyl-phosphonatemethyl)stilbene,<sup>2</sup> and diethyl 4-(4,4,5,5-tetramethyl-1,3-dioxolan-2-yl)benzyl-phosphonate<sup>3</sup> were prepared according to the reported procedures.

Flash column chromatography was performed on a Teledyne ISCO Combiflash RF using Redisep RF silica columns. Spectra for <sup>1</sup>H and <sup>13</sup>C nuclear magnetic resonance spectroscopy (NMR) were taken on a Bruker DRX300 (300MHz), DRX400 (400MHz) and DMX500 (500MHz).

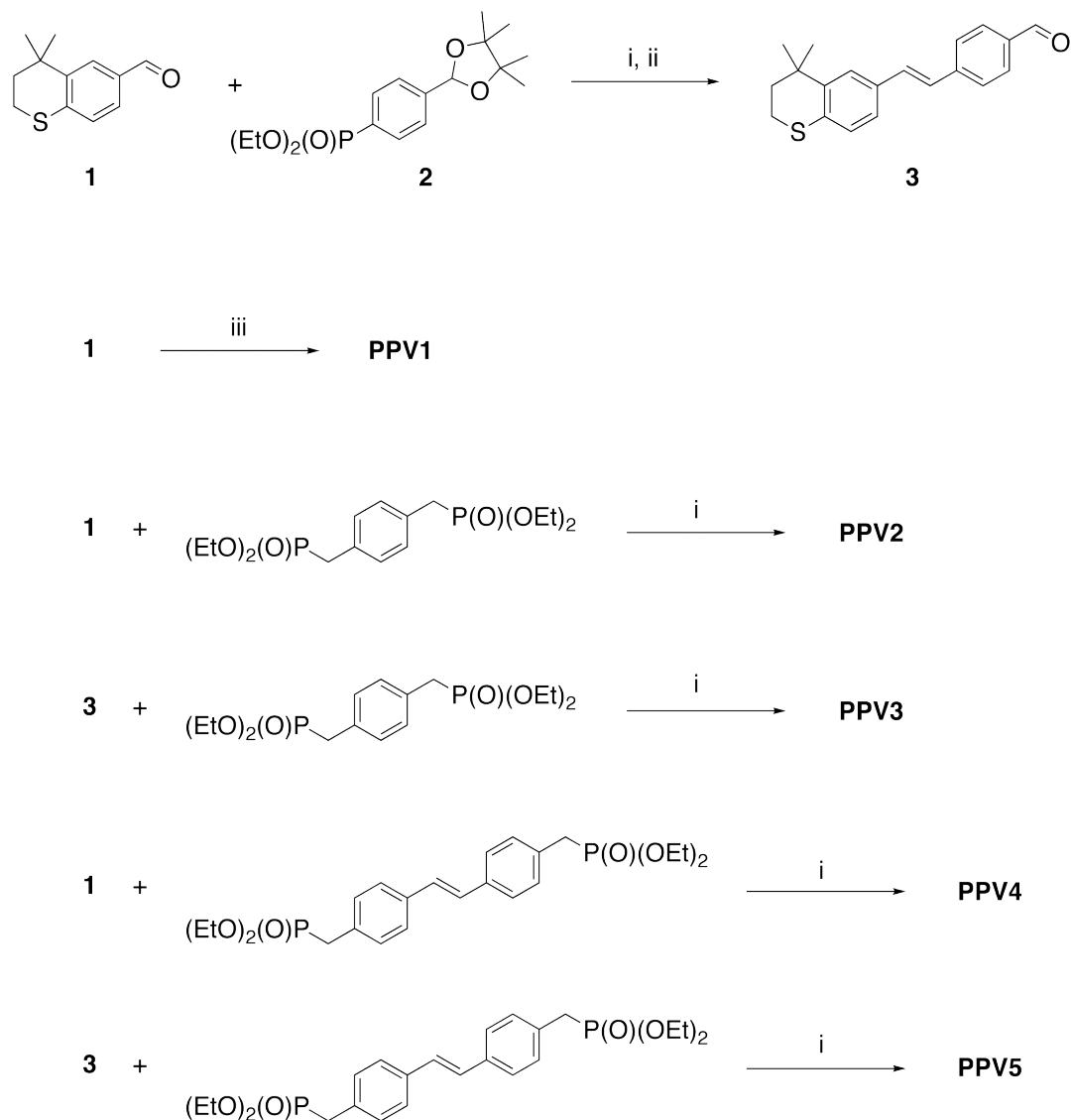
Low-resolution mass spectroscopy (LR-MS) and High-resolution mass spectrometry (HR-MS) was obtained on a double focusing mass spectrometer (JMS-HX110A; JEOL, Ltd.; Tokyo, Japan); Ionization method: FAB, High energy Xe\* beam (3 kV); Matrix: *meta*-nitrobenzyl alcohol (m-NBA); MS Acceleration-Voltage: 10 kJ; Resolution: 3,000/10,000 (Low-Res/High-Res).



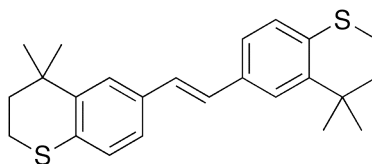


**General Horner-Wadsworth-Emmons (H.W.E.) Reaction Procedure:** In a 100-mL round-bottom flask 1.0 mmol of aryl-aldehyde was combined with a tetraethyl bisbenzylphosphonate (0.5 mmol) and dissolved in 50 mL of anhydrous tetrahydrofuran (THF). The solution was stirred while cooled in an ice bath for 25 min, at which time a solution of potassium *tert*-butoxide (1.1 mmol) in THF (5 mL) was added dropwise to the reaction solution. An immediate color is observed (usually yellow to orange in color) and followed by the precipitation of a colored solid. The reaction was left stirring overnight (16 h) as it warmed to room temperature. Water (50 mL) was added and the reaction was stirred vigorously for 30 min. The THF was removed under reduced pressure and the crude product was isolated by vacuum filtration. Lastly, the product was isolated by either flash column chromatography or recrystallized from THF/methanol. See specific experimentals for exact isolation procedure and characterization.

### Preparation of PPVn Oligomers

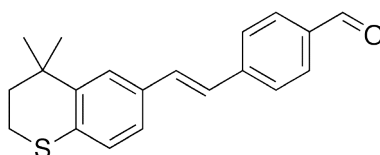


**Scheme E1:** Synthetic Route to end-functionalized oligo-*para*-phenylenevinylene (PPV<sub>n</sub>) molecular wires. Cyclic thioethers are more soluble than the methylthio derivatives due to the disruption of intermolecular attractive forces by distal out-of-plane methyl groups. For a comparison, **PPV4** and its 4-methylthio derivative, 1,4-bis(4-(4-(methylthio)styryl)styryl)benzene, have comparable solubilities in chlorinated organic solvents. An additional advantage to the cyclic thioether derivatives is that rotational freedom about the aryl-S bond is restricted in a cyclic system, as opposed to the linear alkylthio ether (i.e. MeS-Ar).<sup>4</sup>



*(E)*-1,2-bis(4,4-dimethylthiochroman-6-yl)ethane (**PPV1**): This experimental was modified from the reported McMurray coupling procedure.<sup>5</sup> Zinc powder (0.415 g, 6.35 mmol) was added to a flame dried 200-mL round-bottom flask under nitrogen atmosphere. Anhydrous THF (60 mL) was also added and the suspension was cooled in an ice bath while stirring vigorously for 30 min. Titanium(IV) chloride (0.600 g, 3.16 mmol) was added dropwise to the suspension during which a violently evolution of yellow gas occurs. This suspension was refluxed for 2 hours as the solution become dark. Next the reaction was cooled in an ice bath for 30 min. While stirring a solution of **1** (0.327 g, 1.59 mmol) in 10 mL of anhydrous THF was added slowly and the reaction was refluxed. After 16 h the reaction was cooled to room temperature and poured into saturated aq. sodium bicarbonate solution and left stirring for 30 min. The resulting suspension was filtered through a pad of celite and washed through with CH<sub>2</sub>Cl<sub>2</sub>. The organic layer was separate and aqueous layer was extracted with CH<sub>2</sub>Cl<sub>2</sub>, three times. The organic layers were combined, dried over magnesium sulfate and the solvent removed under reduced pressure. The product was isolate by flash column chromatography in 33% CH<sub>2</sub>Cl<sub>2</sub> in hexanes ( $R_f = 0.50$ ) as a white solid. Yield: 0.246 g (81%). <sup>1</sup>H NMR (300 MHz, C<sub>2</sub>D<sub>2</sub>Cl<sub>4</sub>): d 7.45 (d,  $J = 1.7$  Hz, 2H, Ph<sub>C</sub>), 7.25 (dd,  $J = 8.2$  Hz, 1.7 Hz, 2H, Ph<sub>B</sub>), 7.08 (d,  $J = 8.2$  Hz, 2H, Ph<sub>A</sub>), 6.97 (s, 2H, -CH=CH-), 3.12-3.10 (m, 4H, -SCH<sub>2</sub>-), 2.03-1.92 (m, 4H, -CH<sub>2</sub>-), 1.38 (s, 12H, -CH<sub>3</sub>); <sup>13</sup>C NMR (300 MHz, C<sub>2</sub>D<sub>2</sub>Cl<sub>4</sub>): d 141.53, 132.58,

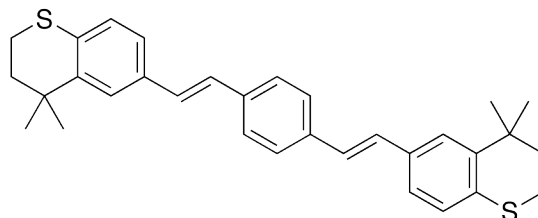
130.34, 126.35, 126.09, 124.40, 122.71, 36.75, 32.19, 29.42, 22.48; HR-MS: m/z calcd for (C<sub>24</sub>H<sub>28</sub>S<sub>2</sub>): 380.1632. Found: 380.1648; 380.1632 (100.0%), 381.1664 (28.7%), 382.1623 (12.8%), 383.1636 (2.8%), 384.1619 (0.6%), 385.1621 (0.1%).



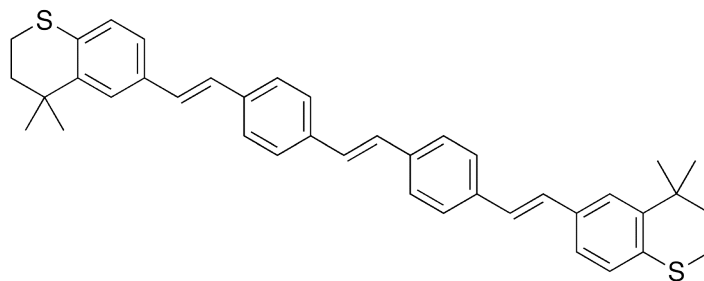
*(E)*-4-(2-(4,4-dimethylthiochroman-6-yl)vinyl)benzaldehyde (**3**): Using the general H.W.E. procedure from compound **1** and 4-(diethoxymethyl)benzaldehyde gives the acetal protected product, *(E)*-2-(4-(2-(4,4-dimethylthiochroman-6-yl)vinyl)phenyl)-4,4,5,5-tetramethyl-1,3-dioxolane, which may be isolated by column chromatography in 10% ethyl acetate in hexanes ( $R_f = 0.55$ ).  $^1\text{H}$  NMR (400 MHz,  $\text{CD}_2\text{Cl}_2$ ): d 7.56-7.41 (m, 5H), 7.25 (d,  $J = 8.1$  Hz, 1H, Ph), 7.15-7.01 (m, 3H), 5.95 (s, 1H,  $-\text{CH}^{\text{acetal}}$ ), 3.08-3.03 (m, 2H,  $-\text{CH}_2-$ ), 2.01-1.94 (m, 2H,  $-\text{CH}_2-$ ), 1.37 (s, 6H,  $-\text{CH}_3$ ), 1.32 (s, 6H,  $-\text{CH}_3^{\text{acetal}}$ ), 1.36 (s, 6H,  $-\text{CH}_3^{\text{acetal}}$ );  $^{13}\text{C}$  NMR (400 MHz,  $\text{CD}_2\text{Cl}_2$ ): d 142.32, 139.24, 137.84, 133.17, 131.80, 128.82, 126.68, 126.55, 126.05, 125.21, 123.65, 99.60, 82.57, 37.57, 32.96, 29.89, 24.14, 23.16, 21.99.

The acetal was dissolved in 10 mL of THF and conc. hydrochloric acid (4 mL) was added to the reaction solution and stirred for 3 h; the solution will immediately turn a darker color of yellow. Cleavage of the acetal protecting group may be easily monitored by TLC, where the product, a yellow spot, will emerge with a lower  $R_f$  than the acetal (blue spot). After completion the reaction solution was diluted with water (50 mL), extracted with  $\text{CH}_2\text{Cl}_2$  (3x 20 mL) and dried over magnesium sulfate. The solvent was removed under reduced pressure and the product was isolated by flash column chromatography in 5% ethyl acetate in hexanes ( $R_f = 0.30$ ) as a bright yellow solid in 59% overall yield.  $^1\text{H}$  NMR (400 MHz,  $\text{CD}_2\text{Cl}_2$ ): d. 9.97 (s, 1H, CHO), 7.85 (d,  $J = 8.1$  Hz, 2H, Ph), 7.66 (d,  $J = 8.1$  Hz, 2H, Ph), 7.53 (d,  $J = 1.0$  Hz, 1H,  $\text{Ph}_C$ ), 7.27 (dd,  $J = 8.2$

Hz, 1.0 Hz, 1H, Ph<sub>B</sub>), 7.23 (d,  $J = 16.4$  Hz, 1H, -C(H<sub>a</sub>)=CH<sub>b</sub>-), 7.10 (d,  $J = 16.3$  Hz, 1H, -CH<sub>a</sub>=C(H<sub>b</sub>-), 7.09 (d,  $J = 8.2$  Hz, 1H, Ph<sub>A</sub>), 3.10-3.01 (m, 2H, -SCH<sub>2</sub>-), 2.02-1.93 (m, 2H, -CH<sub>2</sub>-), 1.32 (s, 6H, -CH<sub>3</sub>); <sup>13</sup>C NMR (400 MHz, CD<sub>2</sub>Cl<sub>2</sub>): d 191.93, 144.25, 143.05, 135.82, 133.65, 133.12, 132.66, 130.65, 127.40, 127.21, 126.21, 126.17, 124.51, 38.03, 33.55, 30.41, 23.78; HR-MS:  $m/z$  calcd for (C<sub>20</sub>H<sub>20</sub>OS): 308.1235. Found: 308.1230; 308.1235 (100.0%), 309.1267 (23.4%), 310.1234 (7.2%), 311.1246 (1.2%), 312.1258 (0.2%).

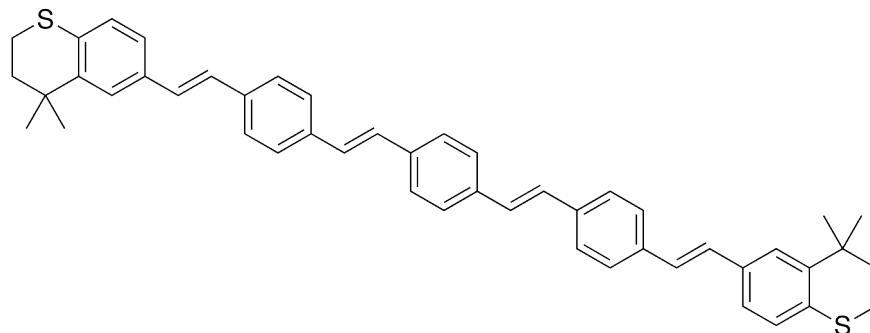


*1,4-bis((E)-2-(4,4-dimethylthiochroman-6-yl)vinyl)benzene (PPV2)*: This compound was prepared by the general H.W.E. procedure from **1** and tetraethyl 1,4-phenylenebis(methylene)diphosphonate. The product was isolated by flash column chromatography in ethyl acetate/hexanes (1:9;  $R_f = 0.50$ ) as a yellow solid in 91% yield.  $^1\text{H}$  NMR (300 MHz,  $\text{CDCl}_3$ ): d 7.47 (s, 4H, Ph), 7.46 (d,  $J = 1.8$  Hz, 2H, Ph<sub>C</sub>), 7.24 (dd,  $J = 8.2$  Hz, 1.8 Hz, 2H, Ph<sub>B</sub>), 7.24 (d,  $J = 8.2$  Hz, 2H, Ph<sub>A</sub>), 7.04 (d,  $J = 16.3$  Hz, 2H, -C(H<sub>a</sub>)=CH<sub>b</sub>-), 7.00 (d,  $J = 16.3$  Hz, 2H, -CH<sub>a</sub>=C(H<sub>b</sub>)-), 3.11-2.98 (m, 4H, -SCH<sub>2</sub>-), 2.03-1.89 (m, 4H -CH<sub>2</sub>-) 1.37 (s, 12H, -CH<sub>3</sub>);  $^{13}\text{C}$  NMR (300 MHz,  $\text{CDCl}_3$ ): d 136.84, 133.56, 128.60, 127.05, 126.95, 126.80 (2 peaks), 125.30, 123.84, 118.21, 37.82, 33.21, 30.33, 23.34; HR-MS:  $m/z$  calcd for ( $\text{C}_{32}\text{H}_{34}\text{S}_2$ ): 482.2102. Found: 482.2116; 482.2102 (100.0%), 483.2134 (37.7%), 484.2107 (15.8%), 485.2114 (4.1%), 486.2107 (0.9%), 487.2107 (0.2%).

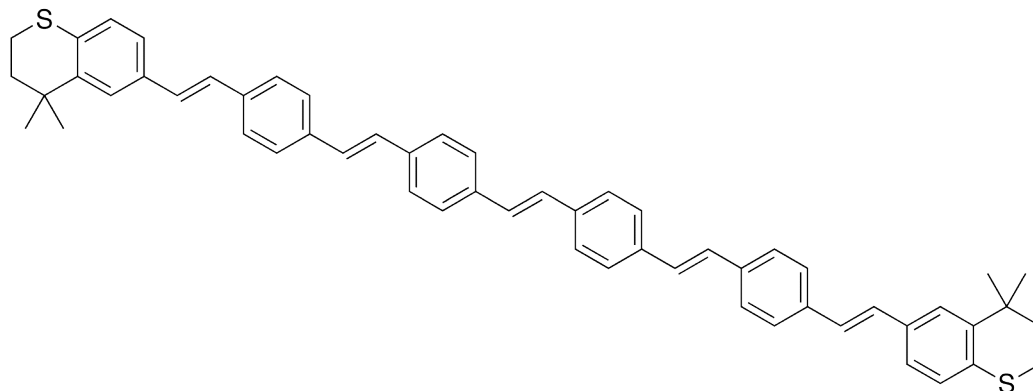


*(E)*-1,2-bis(4-((*E*)-2-(4,4-dimethylthiochroman-6-yl)vinyl)phenyl)ethane (**PPV3**): This compound was prepared by the general H.W.E. procedure from compound **1** and (*E*)-4,4'-bis(diethylphosphonatemethyl)stilbene. The product may be monitored by TLC (10% ethyl acetate in hexanes;  $R_f = 0.70$ ). Recrystallization from THF/methanol gave a bright yellow solid in 57% yield.  $^1\text{H}$  NMR (500 MHz,  $\text{C}_2\text{D}_2\text{Cl}_4$ ): d 7.53 (s, 8H, Ph), 7.48 (dd,  $J = 1.5$  Hz, 2H, Ph<sub>C</sub>), 7.28 (dd,  $J = 8.3$  Hz, 1.6 Hz, 2H, Ph<sub>B</sub>), 7.14 (s, 2H, -CH=), 7.13-7.07 (d,  $J = 16.5$  Hz, 2H, -C(H<sub>a</sub>)=CH<sub>b</sub>-), 7.10 (d,  $J = 8.2$  Hz, 2H, Ph<sub>C</sub>), 7.06-7.00 (d,  $J = 16.4$  Hz, 2H, -CH<sub>a</sub>=C(H<sub>b</sub>-), 3.14-2.97 (m, 4H, -SCH<sub>2</sub>-), 2.04-1.91 (m, 4H -CH<sub>2</sub>-) 1.39 (s, 12H, -CH<sub>3</sub>);  $^{13}\text{C}$  NMR (500 MHz, 320K,  $\text{C}_2\text{D}_2\text{Cl}_4$ ): d 141.83, 136.37, 135.90, 132.68, 131.11, 128.18, 127.58, 126.37 (2 peaks), 126.22, 126.18, 124.77, 123.09, 37.01, 32.44; 29.59, 22.73; HR-MS:  $m/z$  calcd for ( $\text{C}_{40}\text{H}_{40}\text{S}_2$ ): 584.2571. Found: 584.2593; 584.2571 (100.0%), 585.2604 (46.7%), 586.2588 (19.5%), 587.2592 (5.6%), 588.2591 (1.3%), 589.2592 (0.3%).





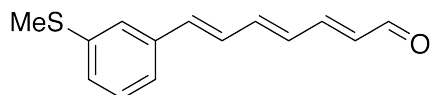
*1,4-bis(4-((E)-2-(4,4-dimethylthiochroman-6-yl)vinyl)styryl)benzene* (**PPV4**): This compound was prepared by the general H.W.E. procedure from compound **2** and (*E*)-4,4'-bis(diethylphosphonatemethyl)stilbene. The product was isolated by recrystallization from THF/methanol giving a sparingly soluble lemon-yellow solid in 74% yield.  $^1\text{H}$  NMR (500 MHz,  $\text{C}_2\text{D}_2\text{Cl}_4$ ): d 7.58-7.47 (m, 14H), 7.28 (d,  $J = 8.0$  Hz, 2H, Ph), 7.18-7.02 (m, 10H), 3.11-3.05 (m, 4H,  $-\text{CH}_2-$ ), 2.05-1.99 (m, 4H,  $-\text{CH}_2-$ ), 1.42 (s, 12H,  $-\text{CH}_3$ );  $^{13}\text{C}$  NMR (500 MHz, 373 K,  $\text{C}_2\text{D}_2\text{Cl}_4$ ): d 141.92, 136.60, 136.37, 136.04, 132.91, 131.24, 128.41, 127.94, 127.60, 126.42, 126.37 (3 overlapping C's signals), 126.22, 124.62, 123.19, 37.28, 32.51, 29.54, 22.74; HR-MS could not be obtained; LR-MS:  $m/z$  calcd for ( $\text{C}_{48}\text{H}_{46}\text{S}_2$ ): 686.3041. Found: 686.30.



*(E)-1,2-bis(4-(4-((E)-2-(4,4-dimethylthiochroman-6-yl)vinyl)styryl)phenyl)ethane*

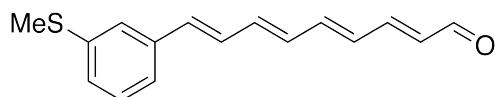
**(PPV5):** This compound was prepared by the general H.W.E. procedure from compound **2** and 1,4-phenylenebis(methylene)diphosphonate. The product may be monitored by TLC (10% ethyl acetate in hexanes;  $R_f = 0.55$ ). Recrystallization from THF/methanol gave a sparingly soluble lemon-yellow solid in 52% yield.  $^1\text{H}$  NMR (500 MHz, 300 K, 1000 scans,  $\text{C}_2\text{D}_2\text{Cl}_4$ ): d 7.58-7.46 (m, 14H), 7.31-7.00 (m, 20H), 3.09-3.04 (m, 4H, - $\text{CH}_2$ -), 2.03-1.96 (m, 4H, - $\text{CH}_2$ -), 1.38 (s, 12H, - $\text{CH}_3$ ); due to limited solubility the  $^{13}\text{C}$  NMR could not be obtained; due to limited solubility in methanol, LR and HR-MS could not be obtained.

## Preparation of Oligoenes (DPOn)



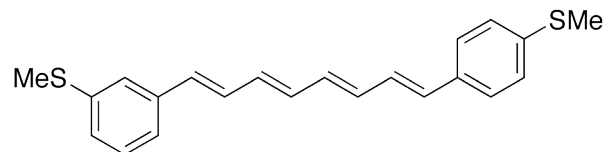
*7-(3-(methylthio)phenyl)hepta-2,4,6-trienal*: General Wittig Homologation Procedure.

HR-MS:  $m/z$  calcd for ( $C_{14}H_{14}OS$ ): 230.0765, found: 230.0754. See Appendix D for preparation and further characterization information.

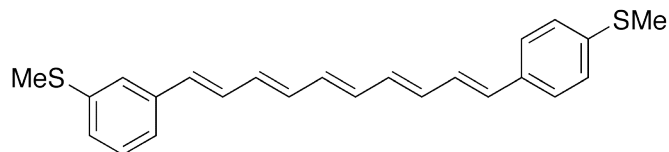


*9-(3-(methylthio)phenyl)nona-2,4,6,8-tetraenal*: General Wittig Homologation

Procedure. HR-MS:  $m/z$  calcd for ( $C_{16}H_{16}OS$ ): 256.0922, found: 256.0922. See Appendix D for preparation and further characterization information.

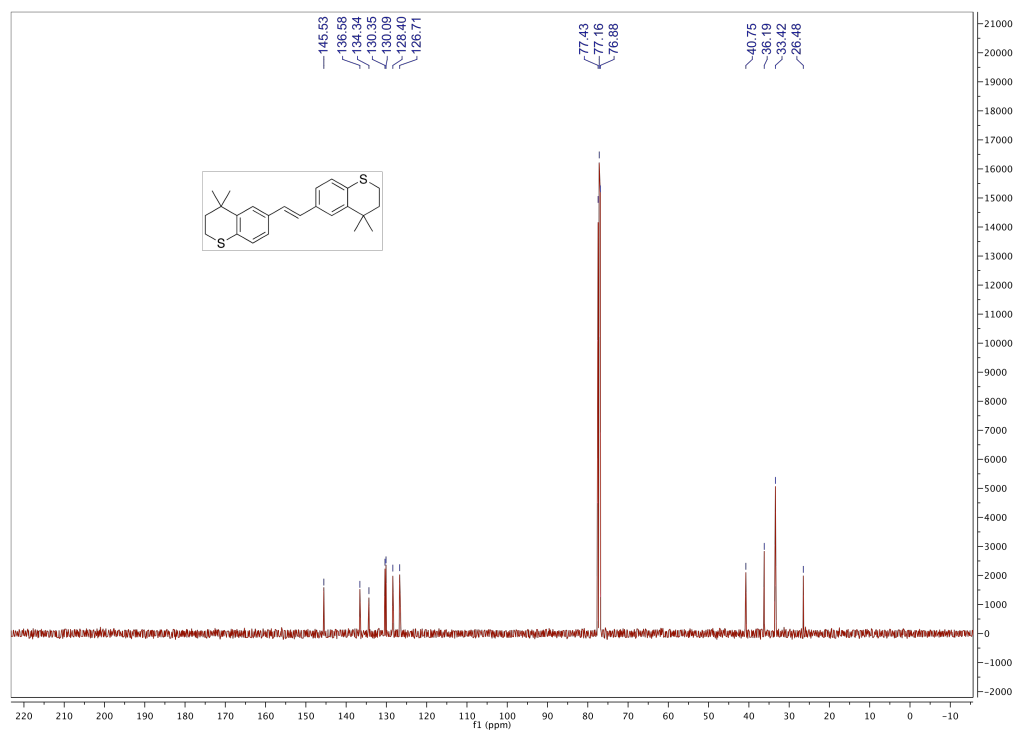
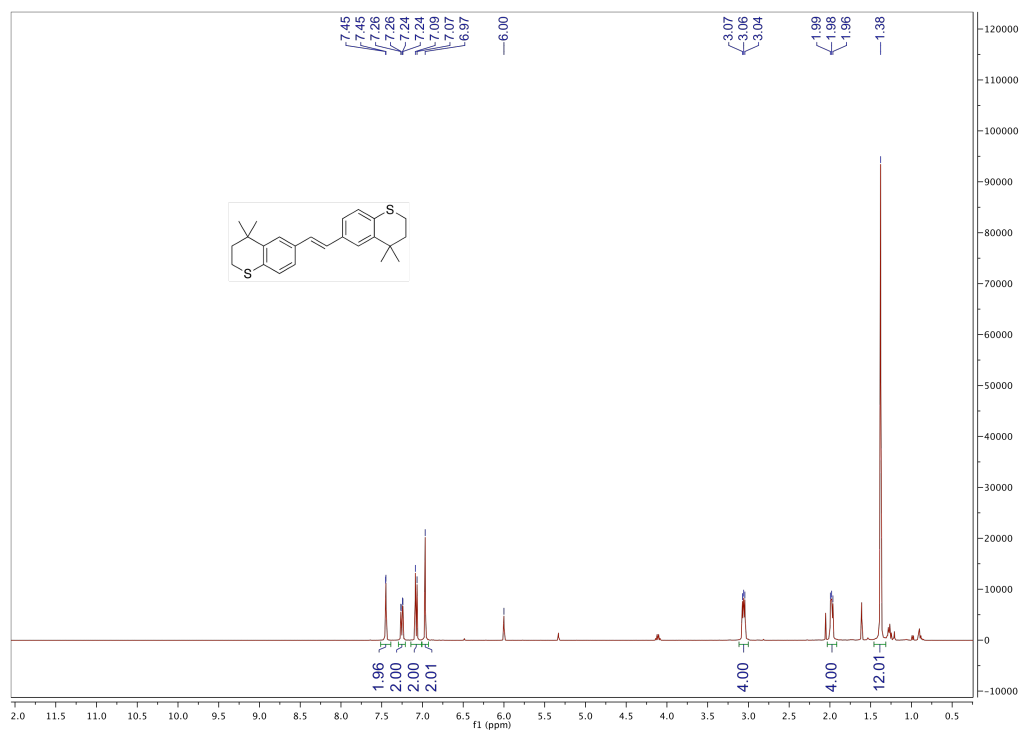


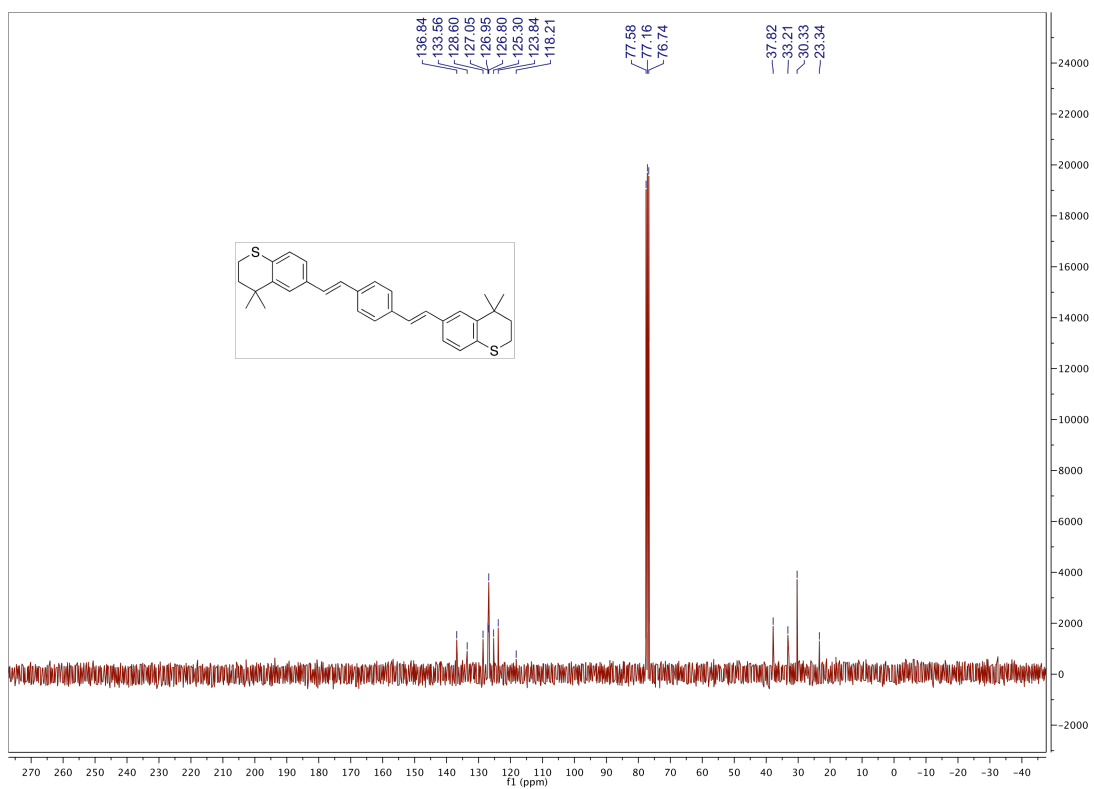
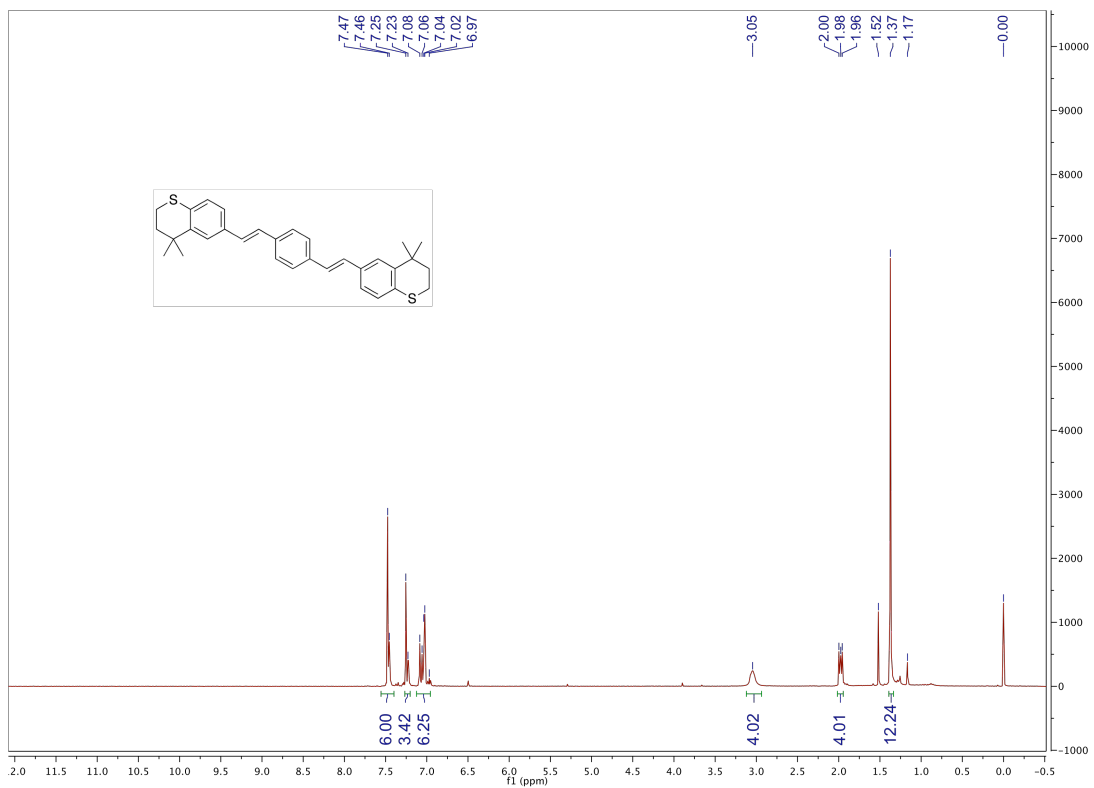
*1-(3-(methylthio)phenyl)-8-(4-(methylthio)phenyl)-octa-1,3,5,7-tetraene (4)*: The General HWE Procedure was followed (see Appendix D). The product was prepared from the corresponding trienal and dimethyl 4-(methylthio)benzyl phosphonate and was isolated by recrystallization from  $\text{CH}_2\text{Cl}_2/\text{MeOH}$  as a yellow solid in 49% yield.  $^1\text{H}$  NMR (500 MHz,  $\text{C}_2\text{D}_2\text{Cl}_4$ ):  $\delta$  7.35 (d,  $J = 8.4$  Hz, 2H), 7.28 (bs, 1H), 7.26 (d,  $J = 7.7$  Hz, 1H), 7.21 (m, 3H), 7.12 (d,  $J = 7.7$  Hz, 1H), 6.94-6.78 (m, 2H), 6.56 (d,  $J = 15.5$  Hz, 1H), 6.55 (d,  $J = 15.5$  Hz, 1H), 6.47 (m, 4H), 2.52 (s, 3H), 2.51 (s, 3H);  $^{13}\text{C}$  NMR (500 MHz,  $\text{C}_2\text{D}_2\text{Cl}_4$ ):  $\delta$  138.21, 137.43, 137.29, 133.66, 133.54, 133.33, 132.74, 132.69, 131.67, 131.35, 129.38, 128.64, 128.08, 126.30, 125.95, 124.93, 123.66, 122.68, 15.24, 15.17; HR-MS:  $m/z$  calcd for ( $\text{C}_{22}\text{H}_{22}\text{S}_2$ ): 350.1163, found: 350.1169.

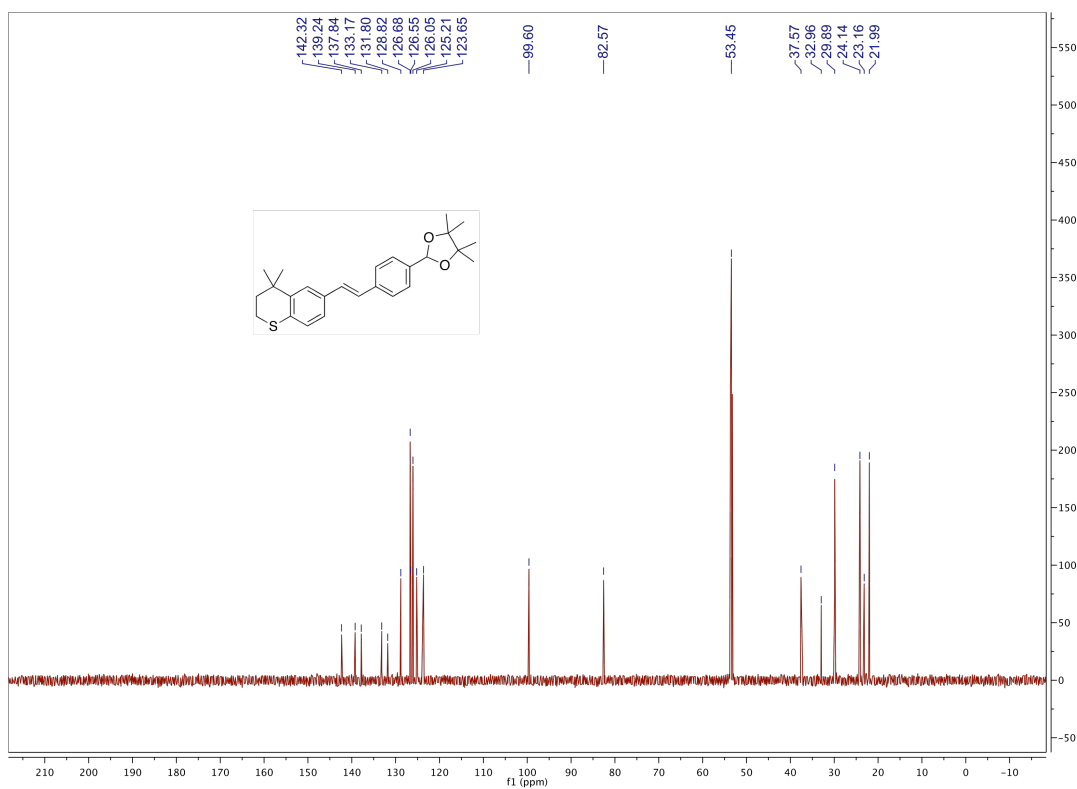
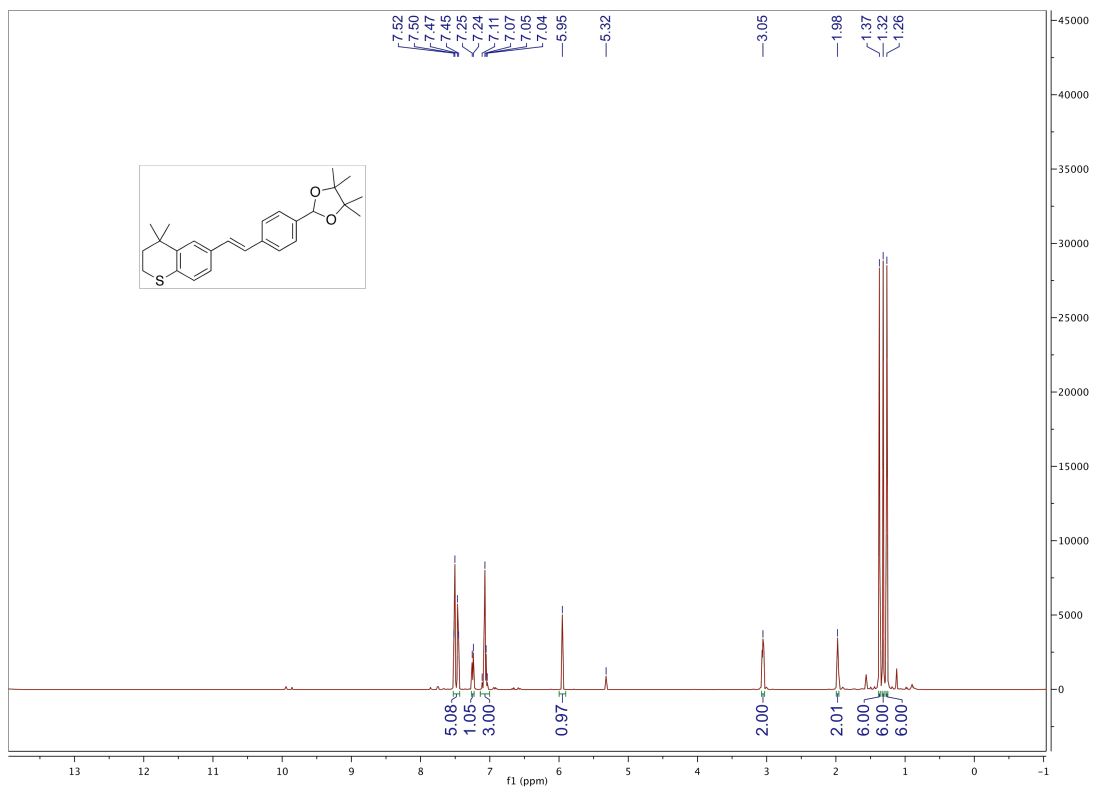


*1-(3-(methylthio)phenyl)-10-(4-(methylthio)phenyl)-deca-1,3,5,7,9-pentaene* (**5**): The General HWE Procedure was followed (see Appendix D). The product was prepared from the corresponding trienal and dimethyl 4-(methylthio)benzyl phosphonate and was isolated by recrystallization from CH<sub>2</sub>Cl<sub>2</sub>/MeOH as a light orange solid in 40% yield. <sup>1</sup>H NMR (500 MHz, C<sub>2</sub>D<sub>2</sub>C<sub>14</sub>): δ 7.34 (d, *J* = 8.3 Hz, 2H), 7.28 (bs, 1H), 7.25 (d, *J* = 7.7 Hz, 1H), 7.20 (m, 3H), 7.12 (d, *J* = 7.7 Hz, 1H), 6.91-6.79 (m, 2H), 6.54 (d, *J* = 15.5 Hz, 1H), 6.53 (d, *J* = 15.5 Hz, 1H), 6.49-6.37 (m, 6H), 2.51 (s, 3H), 2.50 (s, 3H); <sup>13</sup>C NMR (500 MHz, C<sub>2</sub>D<sub>2</sub>C<sub>14</sub>): δ 138.21, 137.44, 137.26, 133.69, 133.63, 133.31, 133.23, 132.90, 132.79, 132.73, 131.59, 131.35, 129.41, 128.64, 128.14, 126.29, 125.95, 124.94, 123.66, 122.68, 15.24, 15.18; HRMS could not be obtained due to insolubility in methanol.

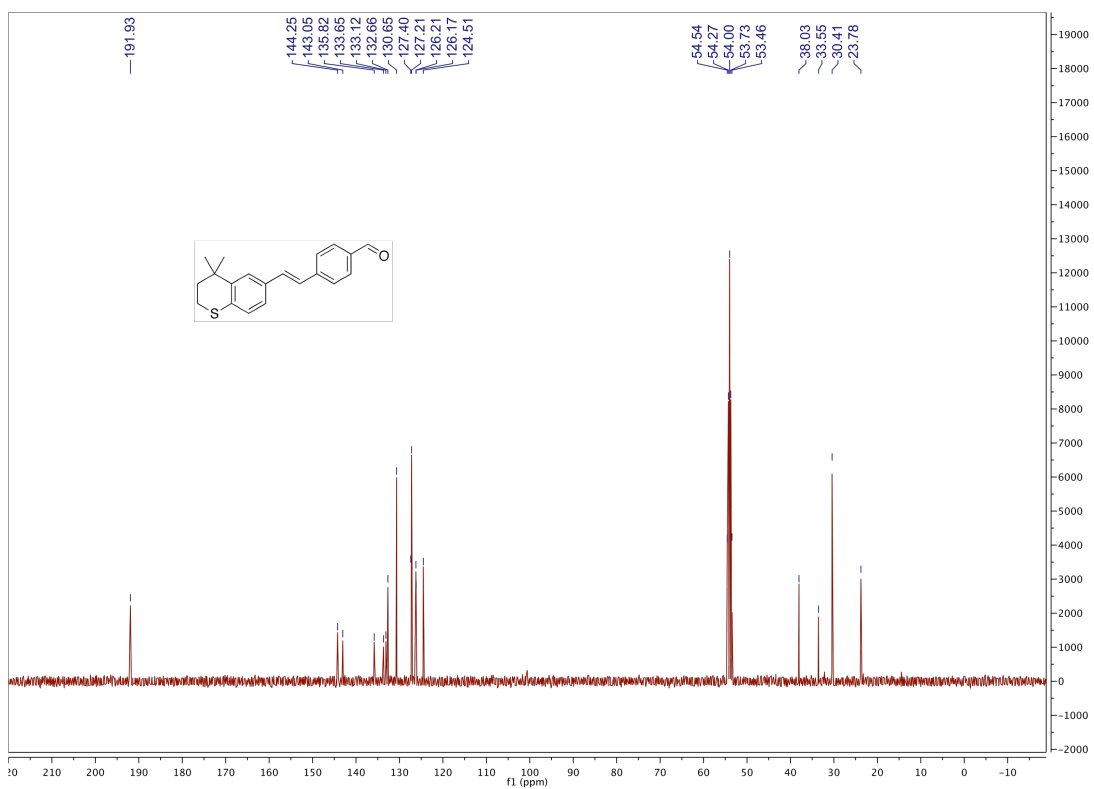
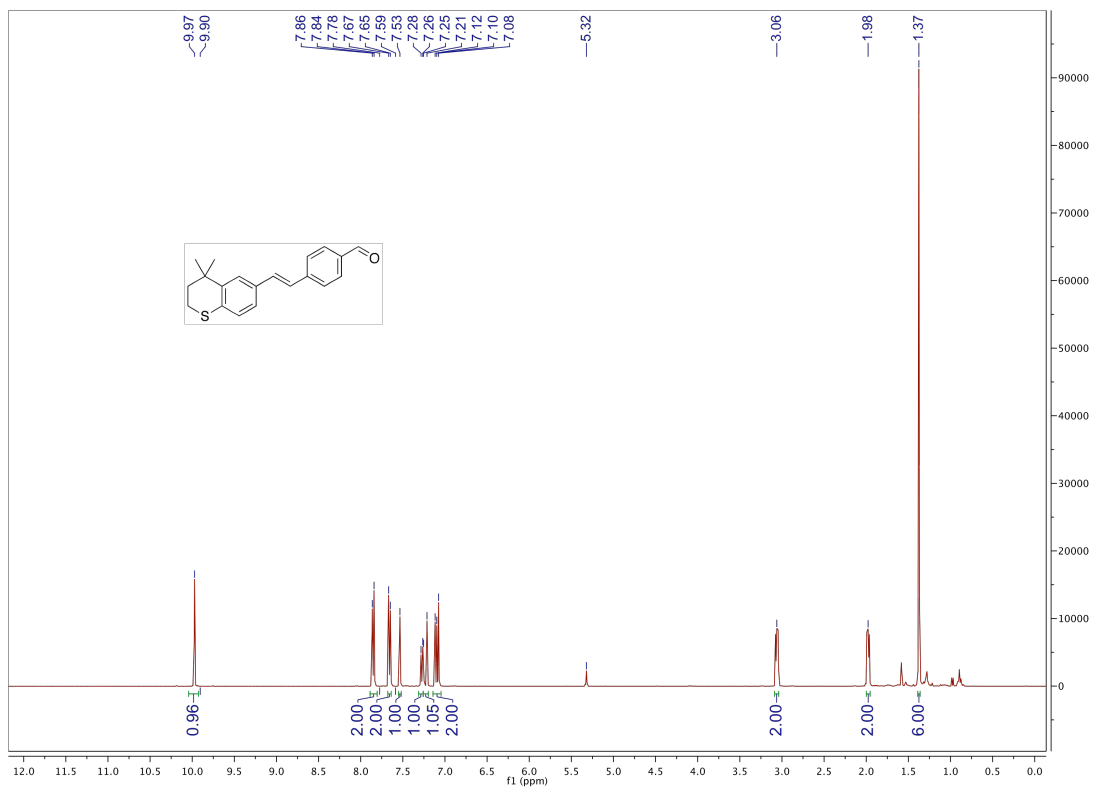
## E2. NMR Spectra

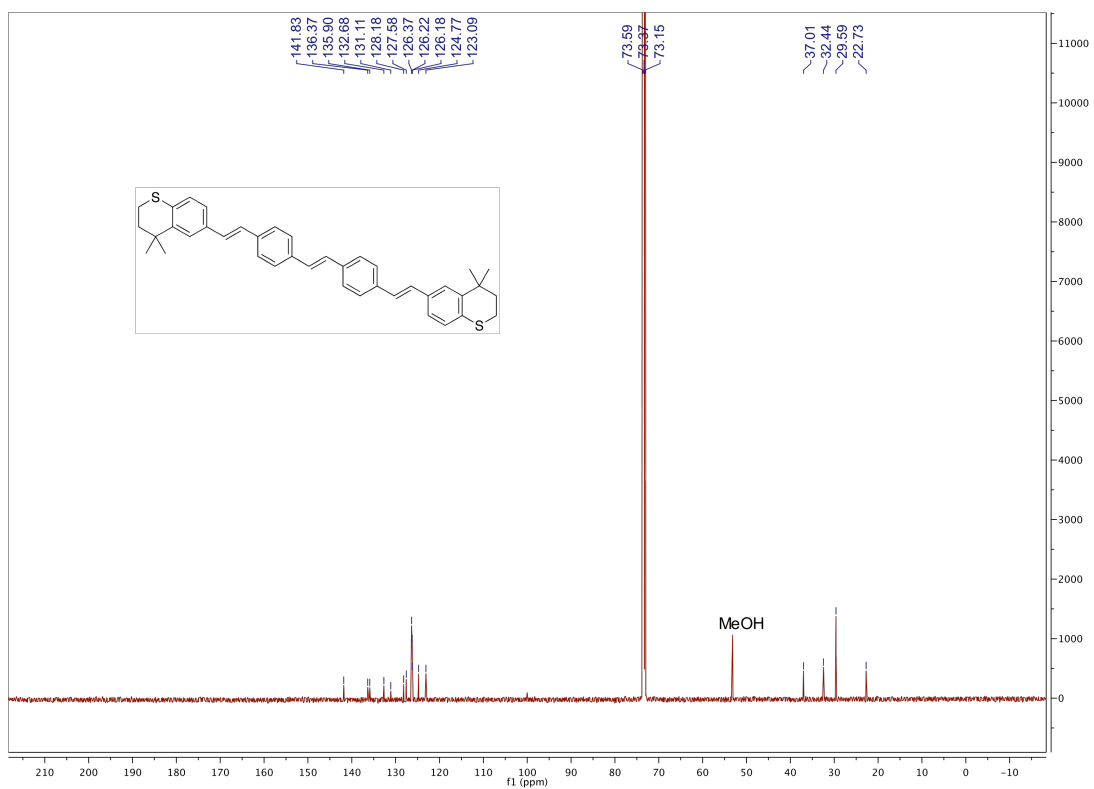
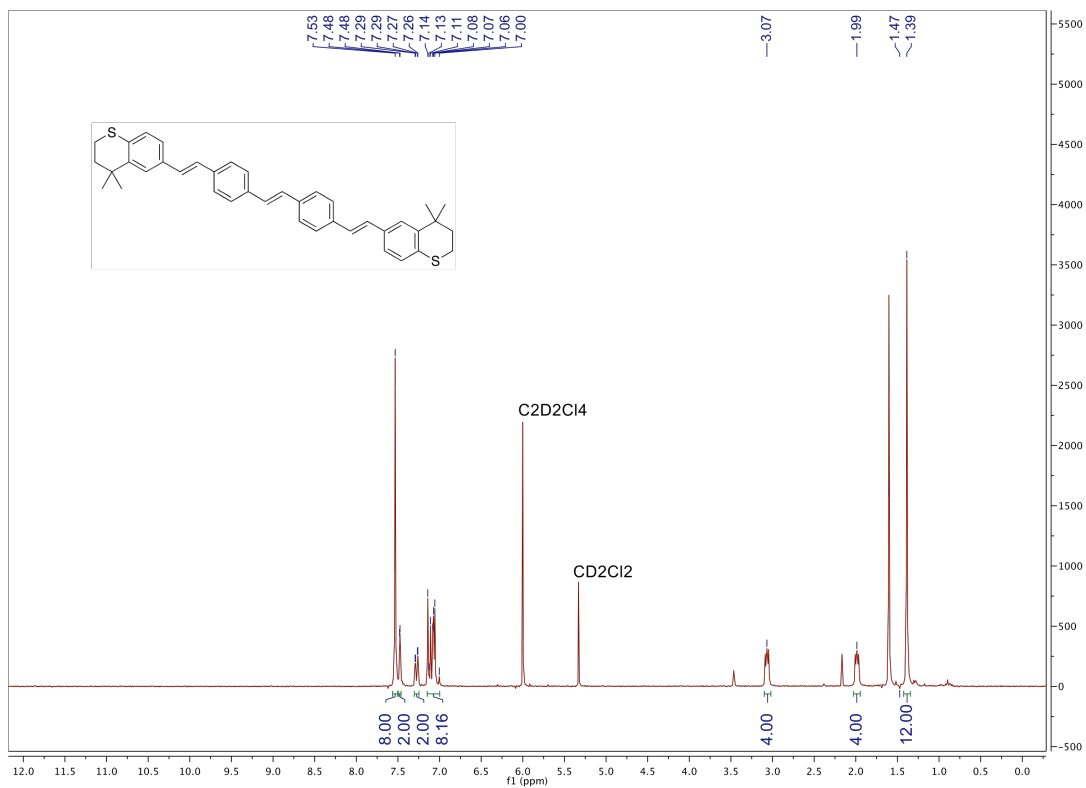


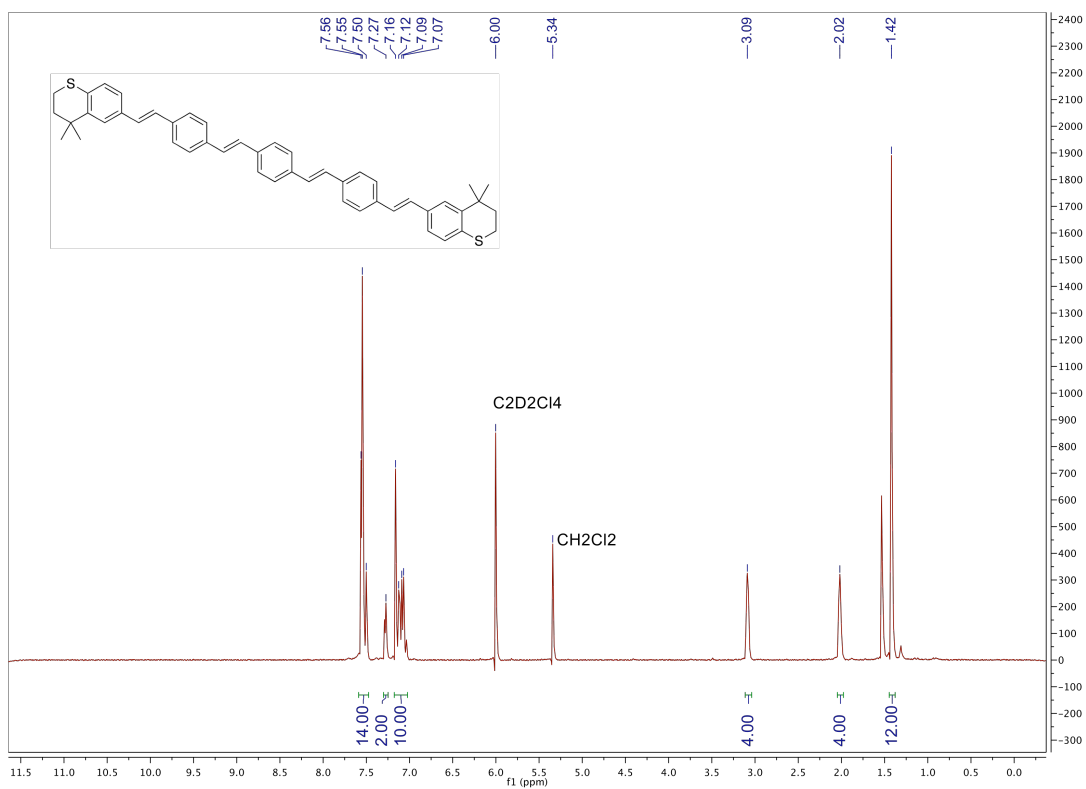
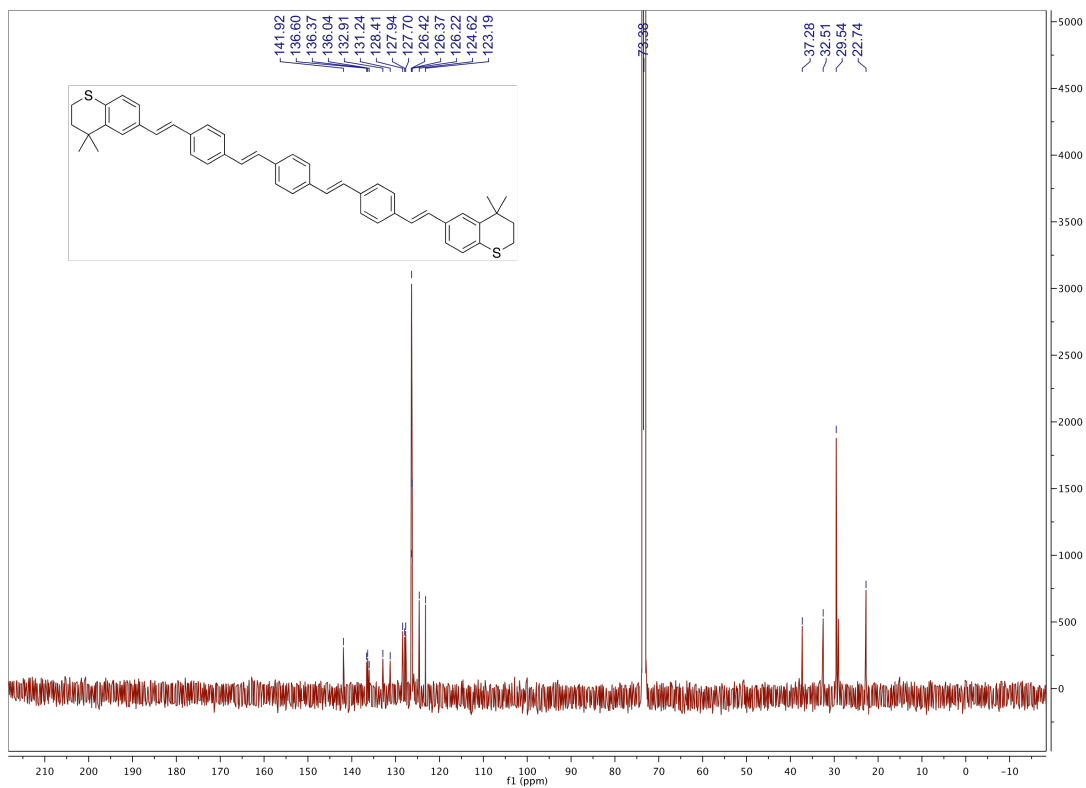


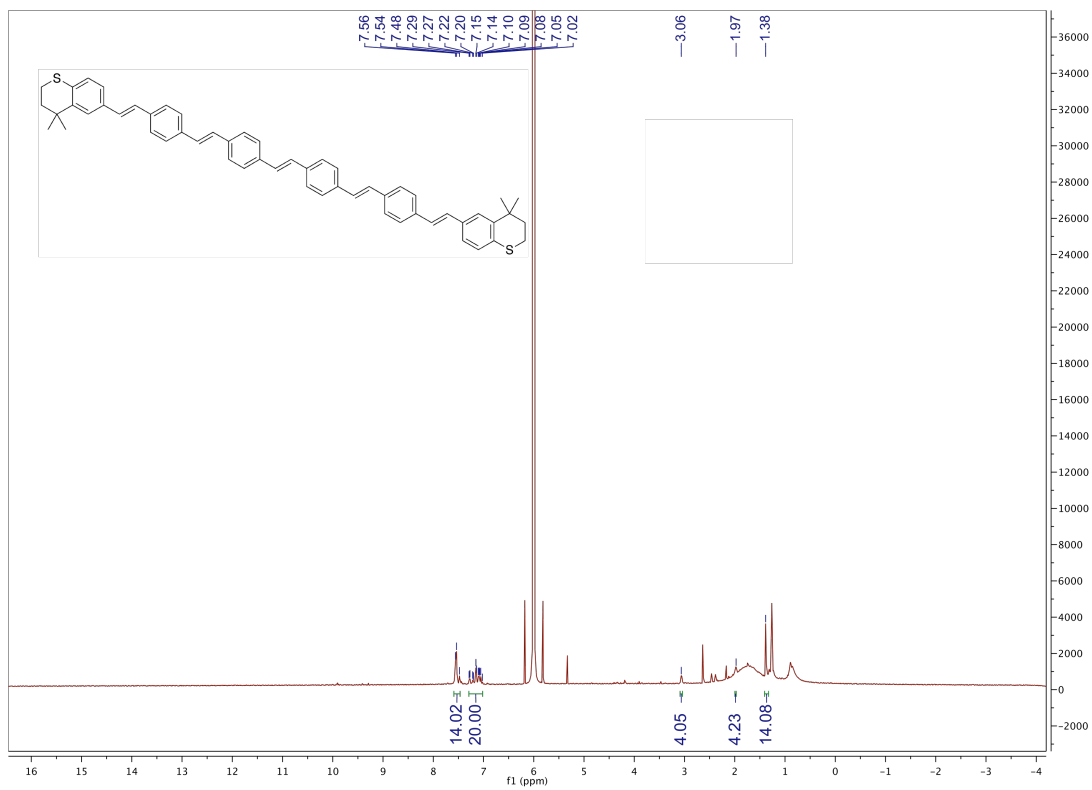


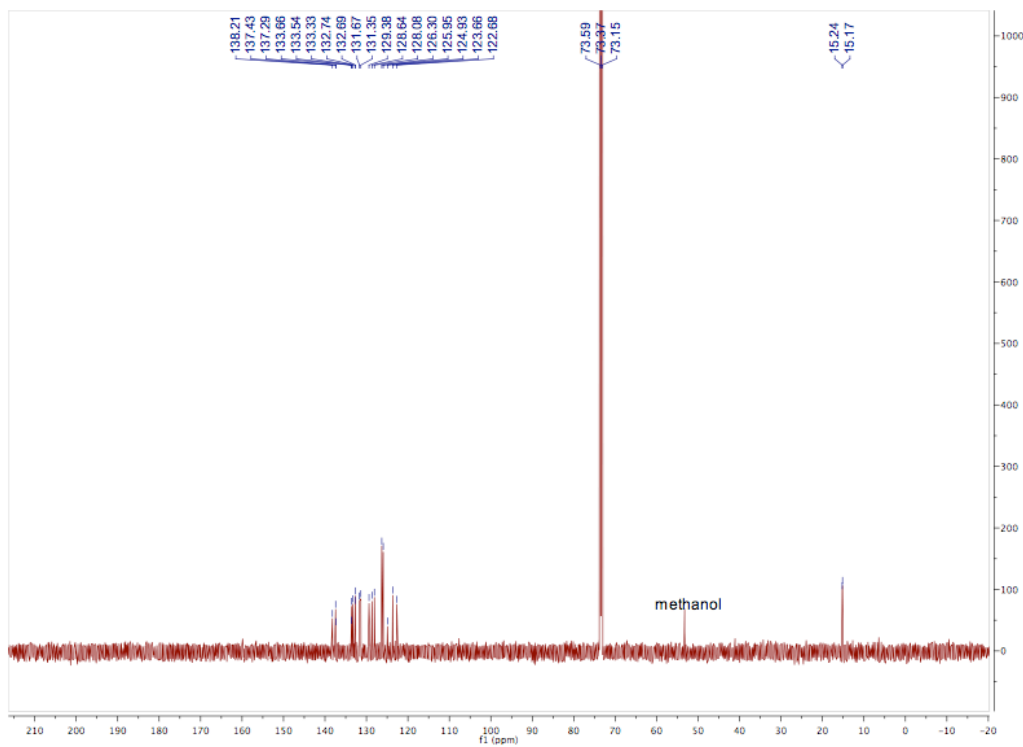
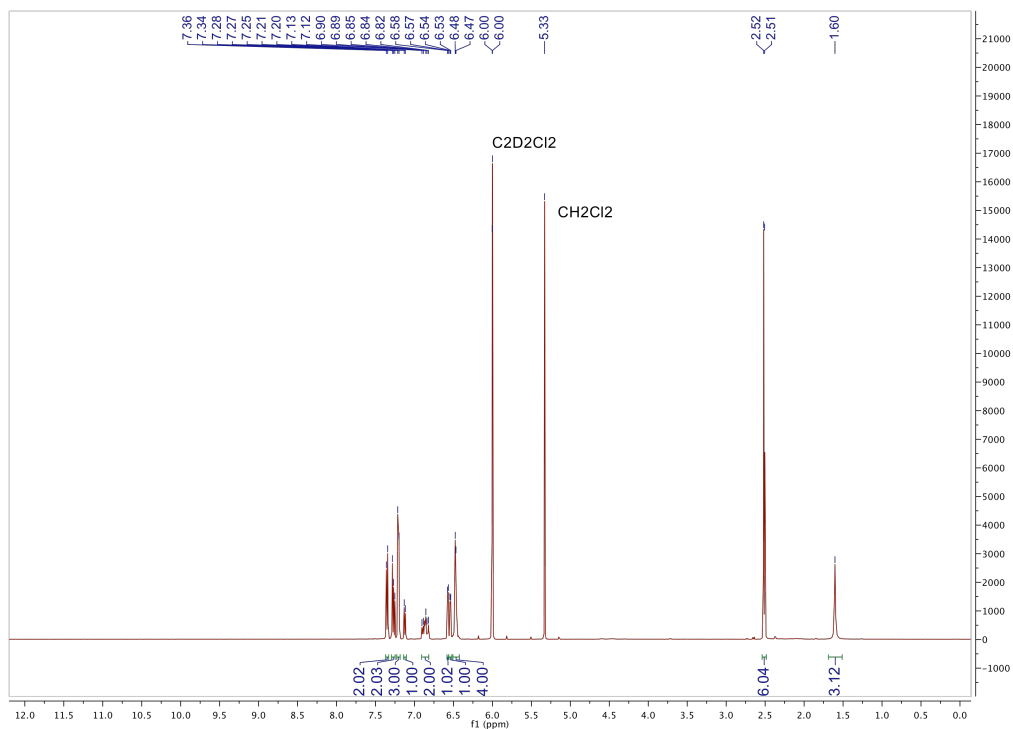




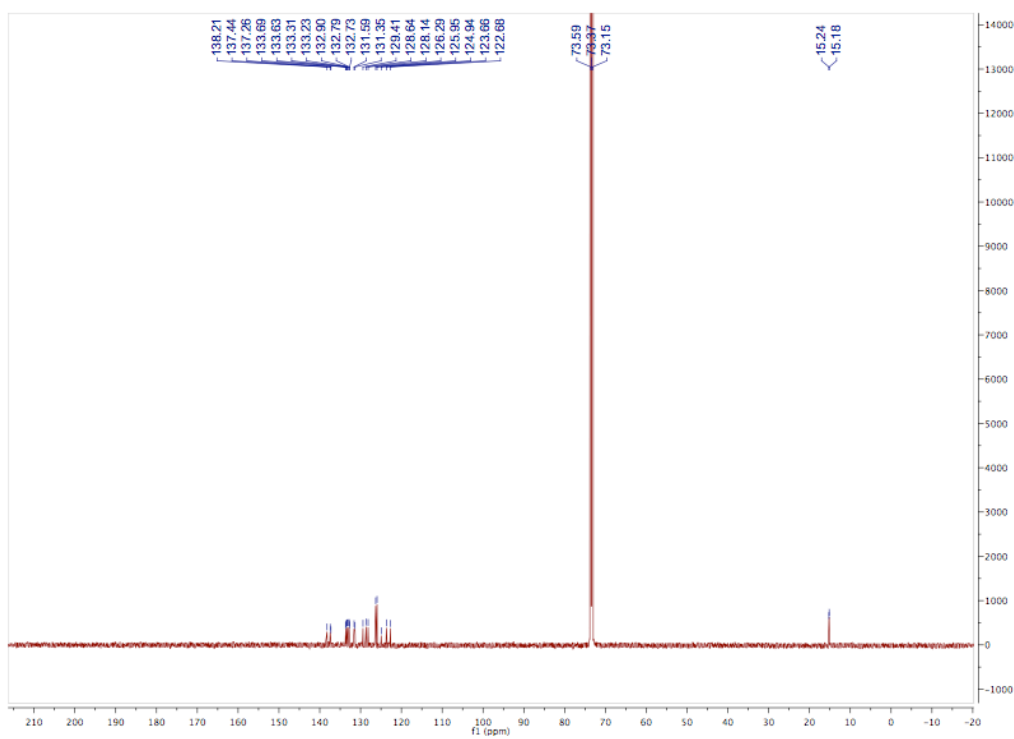
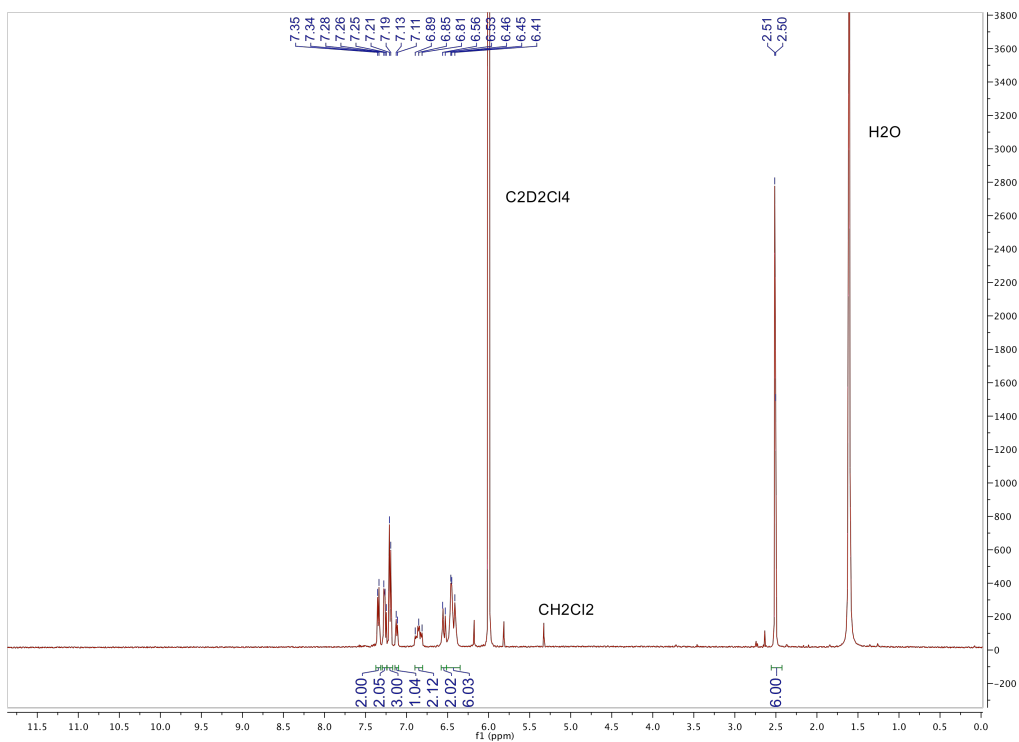








<sup>1</sup>H and <sup>13</sup>C NMR of 1-(3-(methylthio)phenyl)-8-(4-(methylthio)phenyl)-octa-1,3,5,7-tetraene (DPO4) in C<sub>2</sub>D<sub>2</sub>Cl<sub>4</sub>.



<sup>1</sup>H and <sup>13</sup>C NMR of 1-(3-(methylthio)phenyl)-10-(4-(methylthio)phenyl)-deca-1,3,5,7,9-pentaene (DPO5) in C<sub>2</sub>D<sub>2</sub>Cl<sub>4</sub>.

### E3. Optical Absorption Spectroscopy

Absorption spectra were taken on an Agilent Technologies 8453 UV-Vis spectrophotometer using a quartz cuvette with path length equal to 1.0 cm. Solutions of oligomers were prepared in  $\text{CH}_2\text{Cl}_2$  at concentrations between  $10^{-4}$  and  $10^{-5}$  M.

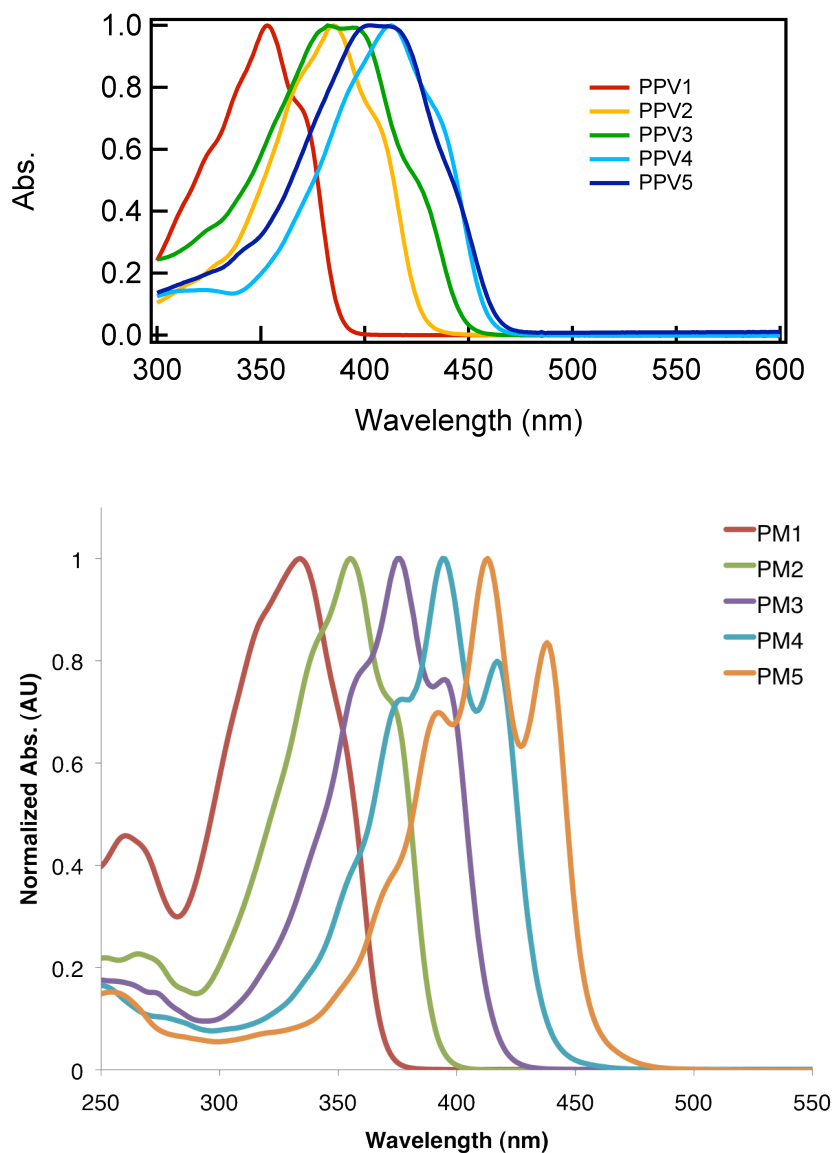


**Figure E1:** UV-vis optical absorption spectra of (top panel) **PPV<sub>n</sub>** series, from  $n = 1$  to 5. Due to increased conjugation the longest-wavelength absorptions shift to lower energies. (bottom panel) Spectra of Asymmetric Oligoenes (**DPO<sub>n</sub>**), from the stilbene to pentaene. For easy comparison, each spectrum was normalized to 1.0 abs.

## **E4. STM and AFM-BJ Measurement and Analysis**

### **Modified STM-BJ Technique**

Details on the experimental technique have been published before.<sup>6</sup> The setups consist of a gold substrate on top of a single axis piezoelectric nanopositioner equipped with a position sensor (Mad City Labs) below a hand-cut gold tip (Alfa-Aesar) with an accuracy of within 5%. During measurement, the conductance of the junction (current/voltage) is measured as a function of piezo displacement. This is done by applying a bias through the junction in series with a fixed resistor (either 100K $\Omega$  or 1M $\Omega$ ) while measuring the current through the junction and the voltage across the junction. The current through the junction is measured using a current amplifier (Keithley 428). A national instruments data acquisition board (PXI-4461) controlled by a Igor (Wavemetrics Inc.) software code controls the bias voltage and piezo position while recording the junction current, piezo position and voltage drop across the junction (sample rate = 40 kHz). The substrates are prepared by evaporating 100nm gold (Alfa-Aesar) on freshly-cleaved mica in a home-build thermal evaporator at a base pressure of  $1 \times 10^{-6}$  mbar. Sample and tip-holder are cleaned in a UV-ozone cleaner prior to measurement. For each tip-sample pair, the quality of the gold and the tunneling background is tested by recording the conductance histogram of typically 1000 traces in air and verifying the presence of (1) peaks at integer values of the conductance quantum and a (2) a featureless background out of contact. Subsequently, one or two droplets of freshly prepared  $10^{-5}$  M solutions of PPV1-PPV5 in 1,2,4-trichlorobenzene (SureSeal, Sigma-Aldrich) are added.

### **Two-Dimensional Conductance-Displacement Histograms for PPVn**



Two-dimensional conductance-displacement were generated by using an automated algorithm by setting the rupture of the  $G_0$  contact as the origin of the displacement axis on each trace; conductance and displacement relative to this origin are then binned to generate 2D maps. In all cases, the same traces used to create linear-binned conductance histograms in Figure 5.3D of Chapter 5 were used to create these histograms.

The most probable length shown in Figure 5.3C (Ch. 5) were determined from a displacement profile of each 2D histogram<sup>7</sup>. Displacement profiles (Figure E3) were created by adding all counts for each displacement along the conductance axis within 1 decade centered around the peak value of the 1D conductance histogram (see Figure E5). Each profile is normalized with respect to its maximum value. The most probable length was taken to be the length at which the profile has an amplitude of 20% of the maximum number of counts.

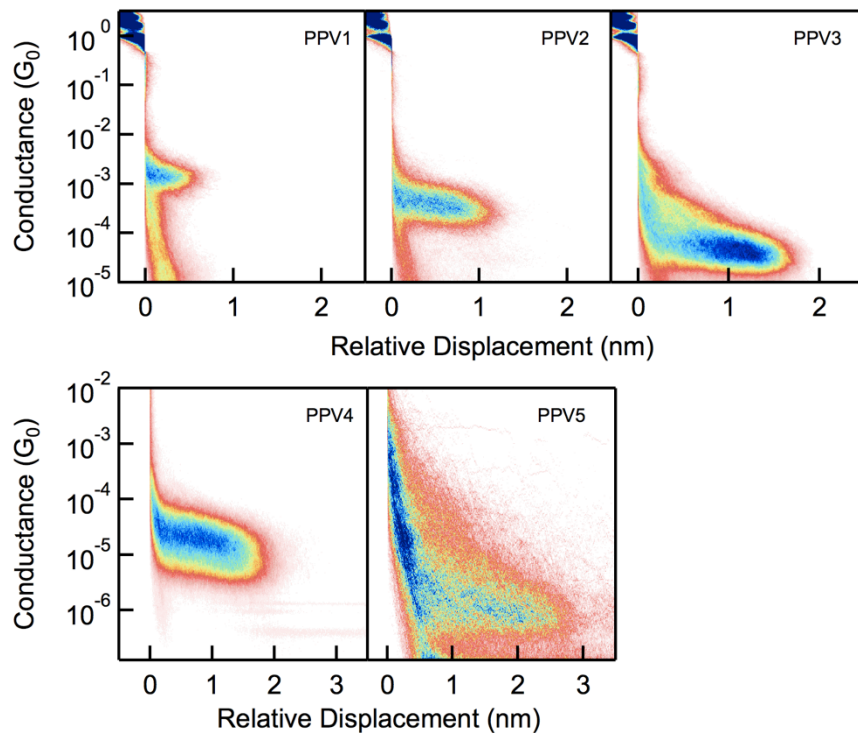


**Figure E2:** Two-dimensional conductance-displacement histograms for **PPV1-PPV5**.

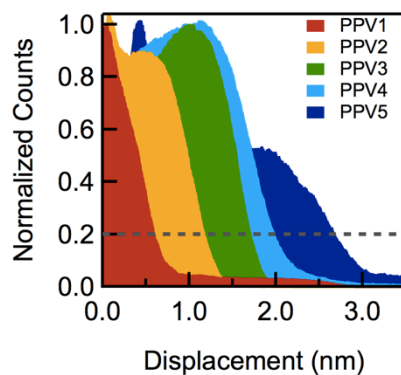


**Figure E3:** Length profiles of the 2D conductance histograms displayed in Figure E2.

## Most-probable conductance from conductance histograms

In the main text, we determined the most probable conductance value for each of the PPV molecules by determining the peak of the linear-binned conductance histograms after subtracting a background from the data and fitting the peak with a log-normal distribution. We show here the details of this method and two other methods that give comparable conductance and beta values for this series.

### Method A: Linearly Binned Histograms

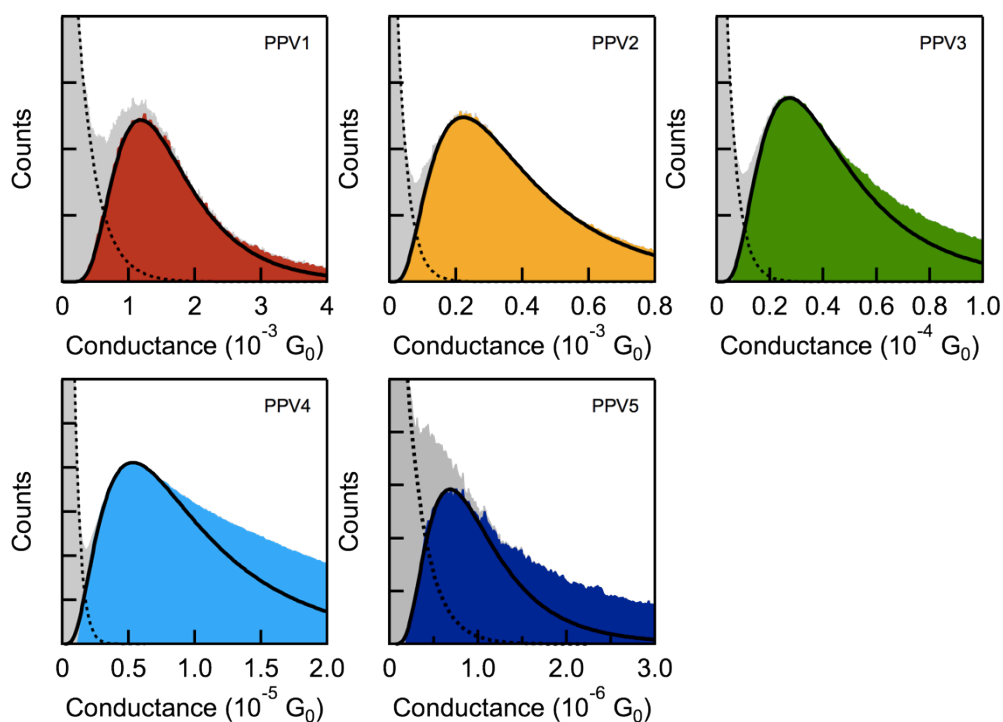
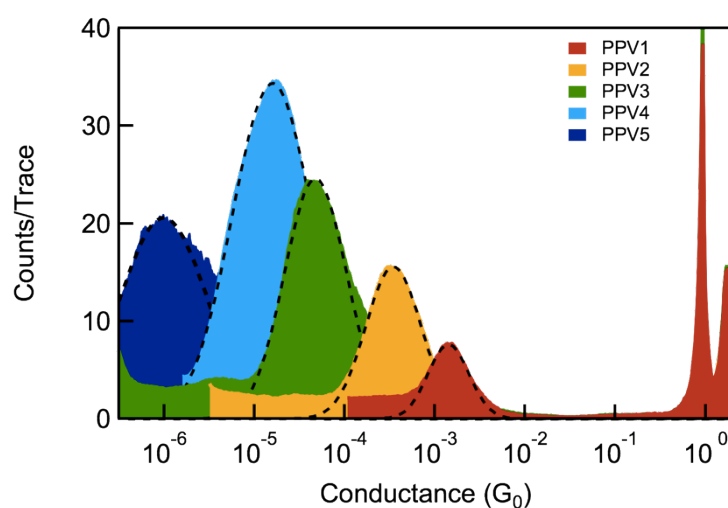


**Figure E4:** Linearly binned conductance histograms from Figure 5.3D showing the fits and conductance background. Conductance bin size varies from  $10^{-4} G_0$  for **PPV1** to  $10^{-7} G_0$  for **PPV5**.

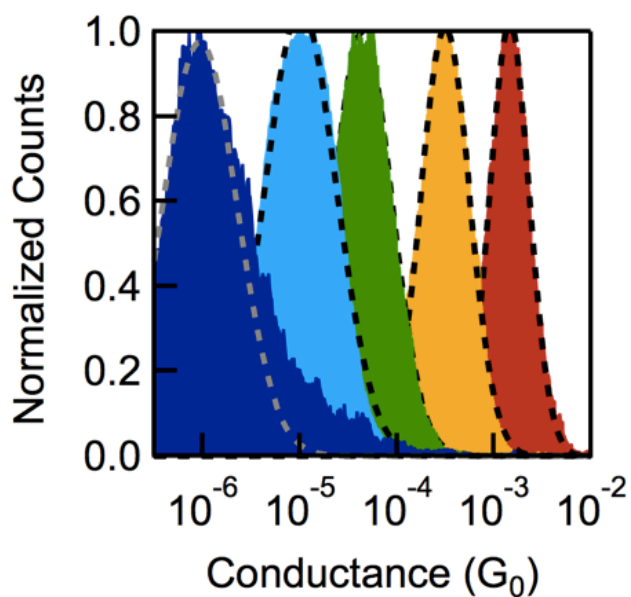
Figure E4 shows *linearly* binned 1D conductance histograms for all five compounds. The most probable conductance value,  $G_c$ , for each **PPVn** in the main text was determined by fitting the 1D *linearly* binned histogram (colored areas) with a lognormal distribution (black line) after subtracting an exponential tunneling background (dashed line) from the raw data (grey area).

### Method B: Log Binned Histograms

Alternatively, the most-probable conductance can be obtained from a Gaussian  $[Ng(g) = C \cdot \exp(-(g - g_c)^2/2w^2)]$  fit to the molecular peaks in *logarithmically* binned histograms (Figure E5). From  $g_c$  and  $w$ , the center of the conductance peak of a lognormal distribution in a linear histogram can be determined<sup>8</sup> as  $\log(G_c) = g_c - \ln(10)w^2$ .



**Figure E5:** Logarithmically binned conductance histograms with a bin size of 100/decade.

**Method C: 2D Histograms**

**Figure E6:** Conductance profiles of the 2D conductance histograms displayed in Figure E2 at two-thirds of the molecular plateau, averaged over 0.2 nm.

Finally, the most probable conductance can be determined from the conductance profile at a specific displacement in a 2D histogram. A displacement profile was created by adding all counts at roughly two thirds of the molecular plateau along the displacement axis for each of the 2D histograms shown in Figure E3. Figure E6 shows conductance profiles for all compounds, scaled to have the same maximum value. The most probable conductance was determined by fitting a Gaussian to these profiles and correcting their peak values as in method B.

Results from the three methods are summarized in Table E1.

	# of	Method A	Method B (Fig S5)			Method C (Fig S6)		
		$g_c$ [ $G_0$ ]	$\log(G_c)$	$w$	$g_c$ [ $G_0$ ]	$\log(G_c)$	$w$	$g_c$ [ $G_0$ ]
<b>PPV1</b>	5000	1.2e-3	-2.8	0.23	1.1e-3	-2.8	0.21	1.2e-3
<b>PPV2</b>	5000	2.2e-4	-3.5	0.31	2.2e-4	-3.5	0.25	2.2e-4
<b>PPV3</b>	5000	2.7e-5	-4.3	0.34	2.5e-5	-4.3	0.30	2.7e-5
<b>PPV4</b>	5000	5.3e-6	-4.8	0.45	5.5e-6	-5.0	0.37	5.0e-6
<b>PPV5</b>	2000	6.8e-7	-6.0	0.48	2.9e-7	-6.0	0.38	4.3e-7

**Table E1:** Comparison between the most-probable conductance value on a linear scale ( $g_c$ ) determined from a linearly binned histogram (Figure E3) and a logarithmically binned histogram using the conversion method proposed by Huber<sup>8</sup> (Figure E4 and Figure E6).

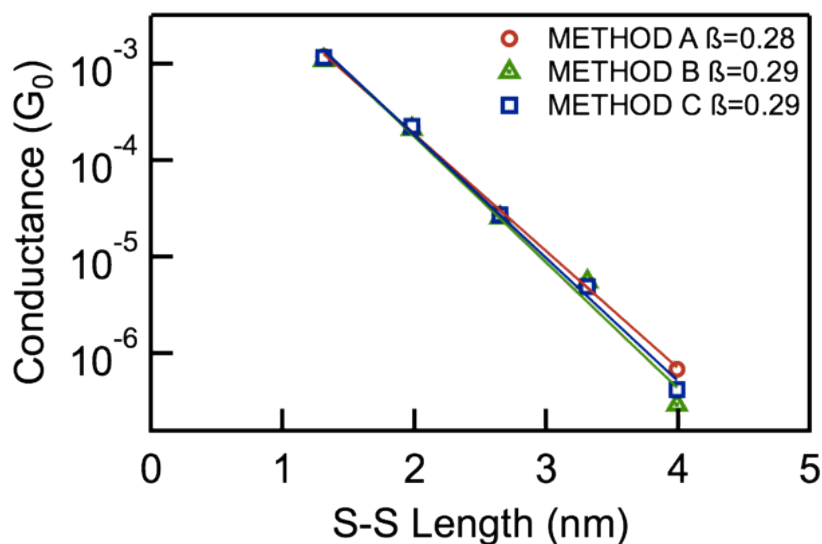


**Figure E7:** Conductance and corresponding  $\beta$ -values from 3 methods detailed above.

### Current-voltage Traces and Histograms

Figure E6 shows 2 sample current-voltage curves for each **PPV<sub>n</sub>** ( $n = 1-5$ ). Each trace was recorded after smashing the Au tip into the Au substrate until a conductance value of  $5 G_0$  was reached. Subsequently, the tip was retracted for 3 nm after which the bias was swept. Just before and after the bias sweep, the conductance was determined. Traces were added into a 2D histogram (see below) when the conductance before and after the bias sweep was found to be in between  $10^{-6}$  and  $1 G_0$  and differed by no more than 20%.

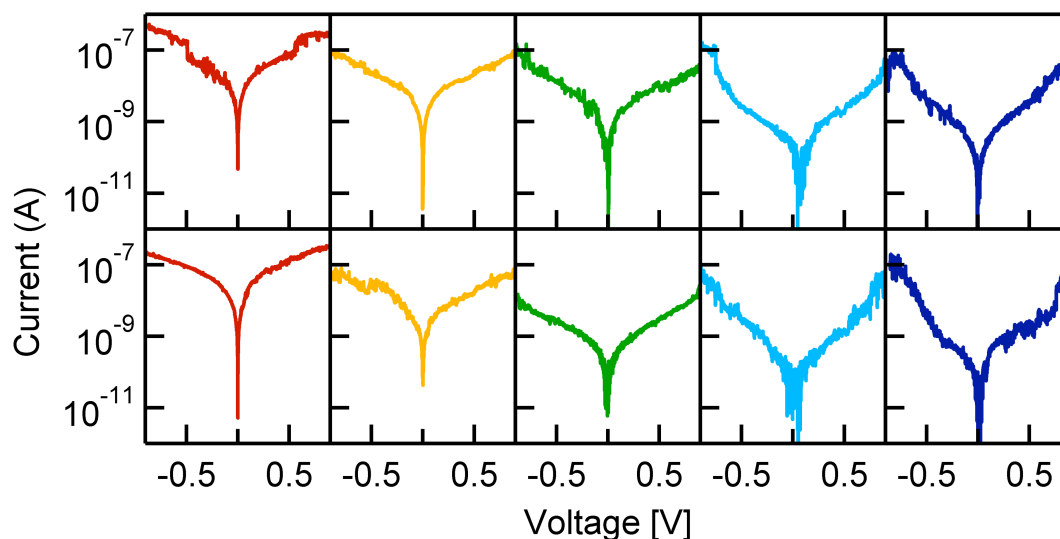


**Figure E8:** Sample current-voltage Curves for **PPV1-PPV5** (left to right). Only the down sweep is displayed for clarity.

Table E2 list the number of tip-sample pairs, the total number of traces that and the percentage those attempts that resulted in successful current-voltage traces for making



the 2D current-voltage histograms of the main text for each **PPVn**. Histograms were constructed by binning both the measured voltage (bin size = 0.01) and the logarithm of the current (bin size = 0.01) of all measurement points of a trace. The statistical IV curve was determined by fitting the 2D current/voltage map with a at each voltage was determined by fitting the logarithmically binned current distribution with a Gaussian and taking the center of this distribution as the most probable current value.

	#	Tip-Sample	Total Traces	% Selected
PPV1	3		68000	4
PPV2	3		90638	18
PPV3	4		120000	23
PPV4	4		120975	14
PPV5	4		80736	10

**Table E2:** Current-voltage analysis details. Number of tip-sample pairs, total number of traces analyzed and percentage of traces maintaining a molecular plateau during a voltage sweep.

Although the most probable current-voltage curve resulting from each histogram is close to perfectly symmetric with respect to the bias polarity, individual current-voltage characteristics can show some asymmetry with respect to the bias polarity. To give an impression of the spread in individually obtained IVs, we determined the rectification ratio for each individual current-voltage characteristic of **PPV2**. The rectification ratio is defined as  $^{10}\log(I(V=+0.7))/^{10}\log(I(V=-0.7))$ . Figure S7 displays the rectification ratio for each current-voltage trace and also shows the resulting histogram. The histogram is centered around 1 and no time dependence on the rectification ratio is observed.

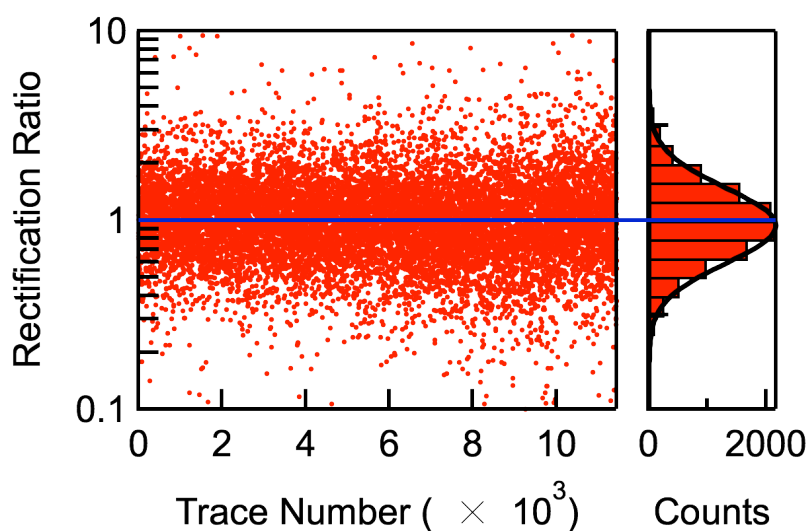


**Figure E9:** Rectification ratio as a number of the measured trace number for **PPV2**.

To check for any dependency of the most-probable IV on the sweep direction we constructed a 2D IV histogram for both positive and negative sweep direction: from 0 to 0.8 V and 0.8 to 0 V, respectively. Figure E10 shows the resulting histograms and most-probable IV curve for 11445 IV traces of **PPV2**. The traces are close to identical.

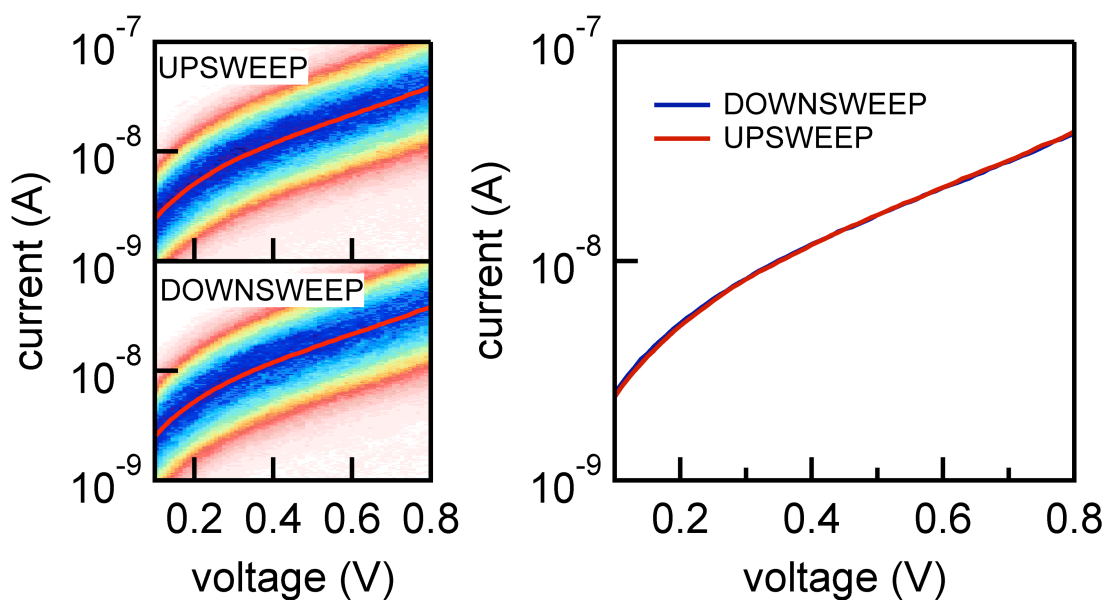


**Figure E10:** Dependence of sweep direction for 11455 IV traces of **PPV2**.

We find the number of selected IVs to decrease with the maximum amplitude of the bias voltage ramp. Figure E11 summarizes the bridging probability as a function of maximum applied bias voltage for **PPV4**.

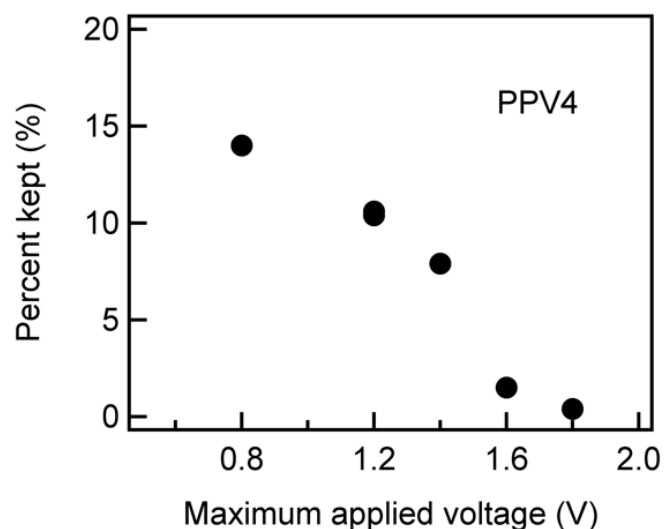


**Figure E11:** Bridging probability for **PPV4** as a function of applied maximum bias voltage in the ramp. For  $V = 1.2, 1.4, 1.6,$  and  $1.8$  V, a total of 1000 curves were recorded and traces were selected as described above. The data point at 1.2 was reproduced before and after ramping the maximum bias to 1.8 V. The data point at  $V = 0.8$  V was determined from the analysis described above using 120975 traces (solid data point).

### Current-voltage Fitting Procedure

The most-probable current-voltage characteristics were fit to equation 5.1 and 5.2 of the main text.

T [K]	$\epsilon$ [meV]					$\Gamma$ [meV]					Fit error [-]				
	PPV1	PPV2	PPV3	PPV4	PPV5	PPV1	PPV2	PPV3	PPV4	PPV5	PPV1	PPV2	PPV3	PPV4	PPV5
300	790	620	550	500	500	34.5	11.6	5.1	2.4	1.0	0.013	0.183	0.508	5.990	4.168
350	770	640	570	520	520	33.3	12.0	5.3	2.5	1.0	0.014	0.194	0.435	4.799	2.126
400	780	660	590	530	540	33.7	12.4	5.4	2.4	1.0	0.013	0.207	0.366	3.826	1.082
450	790	680	610	550	570	34.1	12.8	5.6	2.4	1.0	0.013	0.213	0.291	3.219	0.762
<b>500</b>	<b>800</b>	<b>690</b>	<b>630</b>	<b>560</b>	<b>590</b>	<b>34.5</b>	<b>12.8</b>	<b>5.7</b>	<b>2.3</b>	<b>0.9</b>	<b>0.014</b>	<b>0.217</b>	<b>0.218</b>	<b>3.098</b>	<b>0.688</b>
550	820	710	650	580	610	35.4	13.2	5.8	2.3	0.9	0.012	0.201	0.172	3.185	1.039
600	840	740	670	590	630	36.2	13.8	5.9	2.0	0.9	0.014	0.214	0.125	3.508	1.780
650	850	750	690	610	630	36.6	13.8	6.0	2.0	0.6	0.014	0.193	0.096	3.858	2.566
700	870	770	710	610	630	37.4	14.0	6.0	1.6	0.5	0.014	0.198	0.067	4.353	3.627
750	870	790	730	630	650	37.0	14.4	6.0	1.5	0.5	0.016	0.194	0.056	4.978	5.291
800	900	810	750	650	670	38.2	14.6	6.0	1.5	0.5	0.015	0.181	0.051	6.110	7.642

**Table E3:** Results from fits at different temperatures.

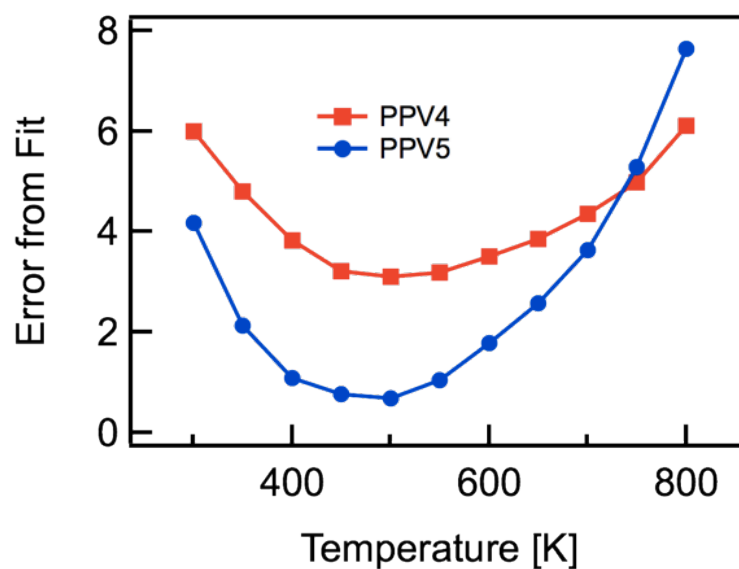


**Figure E12:** For **PPV4** and **PPV5**, the fit error parameter shows a clear minimum around  $T = 500$ . In this case,  $\Gamma \ll k_B T$ . Therefore, the width of the voltage range, over which the current increases, is determined by the electronic temperature of the leads (Fermi functions).

## C5. Theoretical Methods and Details

All electronic structure calculations used Jaguar (version 7.8, Schrodinger LLC, New York, NY, 2011) using the B3LYP hybrid functional and the 6-31G\*\* basis sets. The geometries of MeS-**PPV***n*, **PPV***n* and **DPO1-DPO5** were fully optimized. The final geometries, total energies, bond distances, bond angles and torsional angles may be found in the following sections. Below is a summary of the HOMO-LUMO energy differences (band gap) results of our calculations on methylthio-derivatives (**MeS-PPV***n*; *n* = 1 to 6) and our **PPV***n* series (from *n* = 1 to 5). **MeS-PPV***n* molecules are model compounds for our PPV series. Geometry optimizations of the longer **PPV***n* molecules (**PPV3**, **PPV4** and **PPV5**) were found to converge on a distribution of geometries, all of which were energetically similar. The geometries differed from each other by small degrees of twists and bends along the backbone. Incorporation of even the smallest twist and bend gave larger variations in the molecular length (i.e. S-S distance). **MeS-PPV***n*'s however converged on reliable linear geometries, which are expected during break junction experiments. In such cases, sulfur-to-sulfur (S-S) distances were taken from the **MeS-PPV***n* series calculations and not from the **PPV***n* calculations and are shown in Table E4.

<b>PPV<sub>n</sub></b>	S-S Length [nm]	HOMO [eV]	LUMO [eV]	HOMO-LUMO gap [eV]
n = 1	1.30	-4.90	-1.23	3.67
n = 2	1.97	-4.84	-1.68	3.16
n = 3	2.65 <sup>a</sup>	-4.82	-1.86	2.96
n = 4	3.31 <sup>a</sup>	-4.86	-2.06	2.80
n = 5	3.99 <sup>a</sup>	-4.79	-2.11	2.68
<b>MeS-PPV<sub>n</sub></b>	S-S Length [nm] <sup>a</sup>	HOMO [eV]	LUMO [eV]	HOMO-LUMO gap [eV]
n = 1	1.31	-5.03	-1.34	3.69
n = 2	1.98	-4.93	-1.75	3.18
n = 3	2.65	-4.88	-1.95	2.93
n = 4	3.31	-4.85	-2.06	2.79
n = 5	3.99	-4.84	-2.13	2.71
N = 6	4.65	-4.82	-2.18	2.64
<b>DPO<sub>n</sub></b>	S-S Length [nm]	HOMO [eV]	LUMO [eV]	HOMO-LUMO gap [eV]
n = 1	1.20	-5.22	-1.41	3.81
n = 2	1.45	-5.06	-1.66	3.40
n = 3	1.70	-4.93	-1.86	3.07
n = 4	1.95	-4.70	-1.95	2.75
n = 5	2.17	-4.62	-2.07	2.55

**Table E4:** DFT calculation results on **PPV<sub>n</sub>**, **MeS-PPV<sub>n</sub>** and **DPO<sub>n</sub>** series. <sup>a</sup>Due to unreliable geometry optimization convergence, sulfur-to-sulfur (S-S) distances for the longer oligomers, **PPV3-PPV5**, were estimated from DFT calculations performed on the model series **MeS-PPV**.



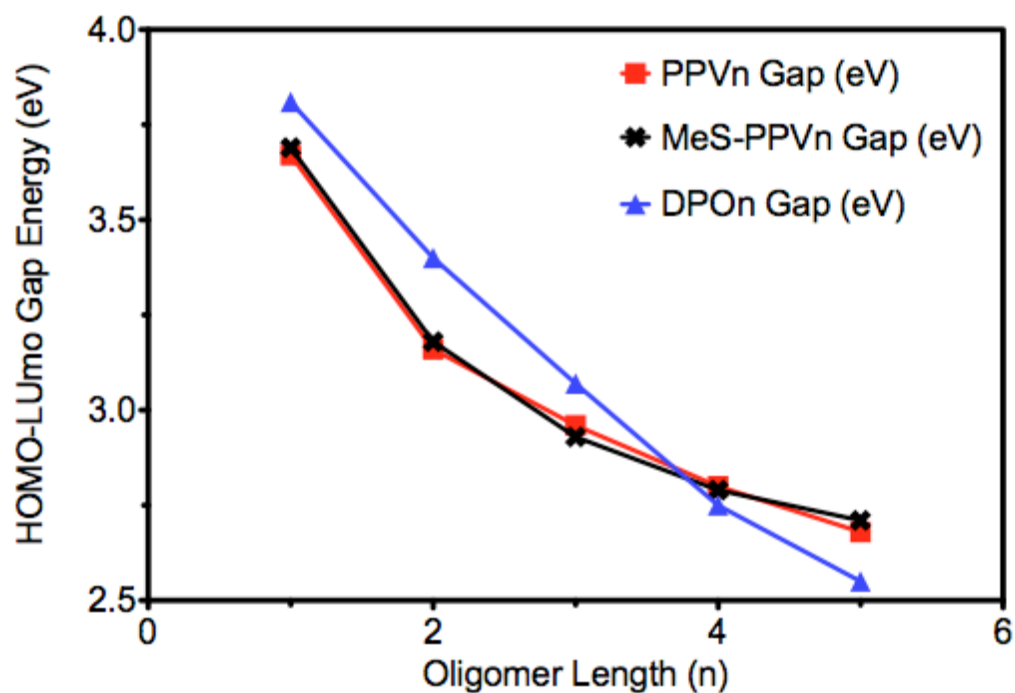
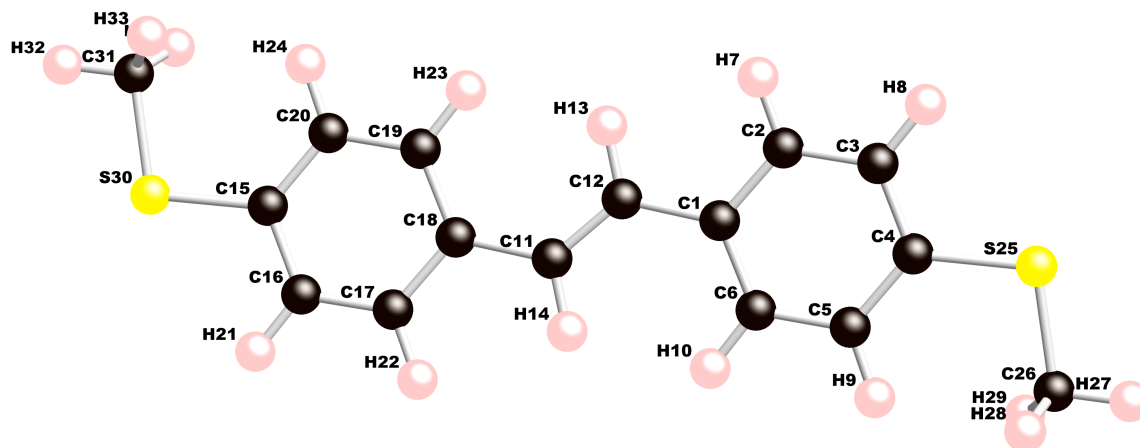


**Figure E13:** DFT estimations of the molecular band gap of **PPV $n$**  series. Molecular band gap converges as oligomer length ( $n$ ) increases. Simpler methylthio-derivatives (**MeS-PPV $n$** ) are an adequate model series for exploring our **PPV $n$**  series, since they predict very similar electronic properties. Length-dependent electronic properties of oligo-phenylenevinylene compounds have been previously studied. Experimental results have predicted the saturation of the electronic properties at oligomeric lengths of  $n \approx 10$ .<sup>2,6</sup>

## DFT Summary PPVn and MeS-PPVn Molecules:

### MeS-PPV1



Final geometry:

angstroms			
atom	x	y	z
C1	-3.8434660000	-1.8489490000	-0.0120390000
C2	-4.5597980000	-0.6660920000	-0.2805620000
C3	-5.9467260000	-0.6325680000	-0.2796430000
C4	-6.6855500000	-1.7937950000	-0.0064350000
C5	-5.9902290000	-2.9808490000	0.2650090000
C6	-4.5991960000	-3.0026450000	0.2621140000
H8	-4.0097130000	0.2469100000	-0.4949240000
H9	-6.4629520000	0.2996400000	-0.4916890000
H11	-6.5258520000	-3.8979330000	0.4823060000
H12	-4.0982710000	-3.9407700000	0.4812260000
C12	-1.5316800000	-2.8421870000	0.1511900000
C13	-2.3802640000	-1.8091180000	-0.0312520000
H15	-1.9652880000	-0.8205090000	-0.2198580000
H16	-1.9486870000	-3.8323930000	0.3259490000
C16	2.7734880000	-2.8774920000	0.1311410000
C17	2.0277380000	-4.0554880000	0.2888180000

C18	0.6411750000	-4.0140390000	0.2921140000
C19	-0.0682760000	-2.8065060000	0.1381970000
C20	0.6946140000	-1.6350750000	-0.0162370000
C21	2.0856460000	-1.6651370000	-0.0209750000
H23	2.5383210000	-5.0068560000	0.4096630000
H24	0.0856860000	-4.9404060000	0.4159550000
H25	0.1994170000	-0.6754220000	-0.1305300000
H26	2.6273680000	-0.7339750000	-0.1424060000
S26	-8.4609420000	-1.6384940000	-0.0311870000
C27	-9.0457400000	-3.3122040000	0.3862640000
H28	-10.1358270000	-3.2488760000	0.3880750000
H29	-8.7357640000	-4.0449030000	-0.3622960000
H30	-8.7077890000	-3.6191340000	1.3787460000
S30	4.5474530000	-3.0472520000	0.1422380000
C31	5.1465920000	-1.3400390000	-0.0658390000
H32	6.2362570000	-1.4100410000	-0.0593390000
H33	4.8255890000	-0.9149800000	-1.0193300000
H34	4.8286740000	-0.6998450000	0.7601080000

Total energy (hartrees): -1415.73607450152

HOMO energy (hartrees): -0.18483

LUMO energy (hartrees): -0.04926

Bond lengths (angstroms):

C1 -C2 : 1.408683 C1 -C6 : 1.406166

C1 -C13 : 1.463870 C2 -C3 : 1.387333

C2 -H8 : 1.087252 C3 -C4 : 1.403193  
 C3 -H9 : 1.086492 C4 -C5 : 1.402230  
 C4 -S26 : 1.782343 C5 -C6 : 1.391207  
 C5 -H11 : 1.084045 C6 -H12 : 1.085824  
 C12 -C13 : 1.349300 C12 -H16 : 1.088551  
 C12 -C19 : 1.463897 C13 -H15 : 1.088634  
 C16 -C17 : 1.403096 C16 -C21 : 1.402166  
 C16 -S30 : 1.782104 C17 -C18 : 1.387186  
 C17 -H23 : 1.086462 C18 -C19 : 1.408952  
 C18 -H24 : 1.087226 C19 -C20 : 1.406450  
 C20 -C21 : 1.391365 C20 -H25 : 1.085918  
 C21 -H26 : 1.084099 S26 -C27 : 1.821417  
 C27 -H28 : 1.091926 C27 -H29 : 1.092371  
 C27 -H30 : 1.092446 S30 -C31 : 1.821219  
 C31 -H32 : 1.091931 C31 -H33 : 1.092183  
 C31 -H34 : 1.092295

Bond angles:

C6 -C1 -C2 : 116.923317 C13 -C1 -C2 : 118.876979  
 C13 -C1 -C6 : 124.199617 C3 -C2 -C1 : 121.906029  
 H8 -C2 -C1 : 119.040098 H8 -C2 -C3 : 119.053871  
 C4 -C3 -C2 : 120.431514 H9 -C3 -C2 : 119.709051  
 H9 -C3 -C4 : 119.859433 C5 -C4 -C3 : 118.500734  
 S26 -C4 -C3 : 116.722201 S26 -C4 -C5 : 124.777037  
 C6 -C5 -C4 : 120.575007 H11 -C5 -C4 : 120.661252  
 H11 -C5 -C6 : 118.763685 C5 -C6 -C1 : 121.663176  
 H12 -C6 -C1 : 120.017019 H12 -C6 -C5 : 118.319632  
 H16 -C12 -C13 : 118.505622 C19 -C12 -C13 : 127.505200  
 C19 -C12 -H16 : 113.988445 C12 -C13 -C1 : 127.301743

H15 -C13 -C1 : 114.079178 H15 -C13 -C12 : 118.618703  
 C21 -C16 -C17 : 118.514128 S30 -C16 -C17 : 116.641084  
 S30 -C16 -C21 : 124.844764 C18 -C17 -C16 : 120.427320  
 H23 -C17 -C16 : 119.860759 H23 -C17 -C18 : 119.711915  
 C19 -C18 -C17 : 121.914514 H24 -C18 -C17 : 119.045577  
 H24 -C18 -C19 : 119.039873 C18 -C19 -C12 : 118.783561  
 C20 -C19 -C12 : 124.299272 C20 -C19 -C18 : 116.917000  
 C21 -C20 -C19 : 121.646087 H25 -C20 -C19 : 120.017018  
 H25 -C20 -C21 : 118.336142 C20 -C21 -C16 : 120.580679  
 H26 -C21 -C16 : 120.642222 H26 -C21 -C20 : 118.776986  
 C27 -S26 -C4 : 103.683925 H28 -C27 -S26 : 105.522306  
 H29 -C27 -S26 : 111.603754 H29 -C27 -H28 : 108.864039  
 H30 -C27 -S26 : 111.534903 H30 -C27 -H28 : 108.881948  
 H30 -C27 -H29 : 110.262660 C31 -S30 -C16 : 103.737140  
 H32 -C31 -S30 : 105.516675 H33 -C31 -S30 : 111.584580  
 H33 -C31 -H32 : 108.871487 H34 -C31 -S30 : 111.547237  
 H34 -C31 -H32 : 108.876169 H34 -C31 -H33 : 110.272905

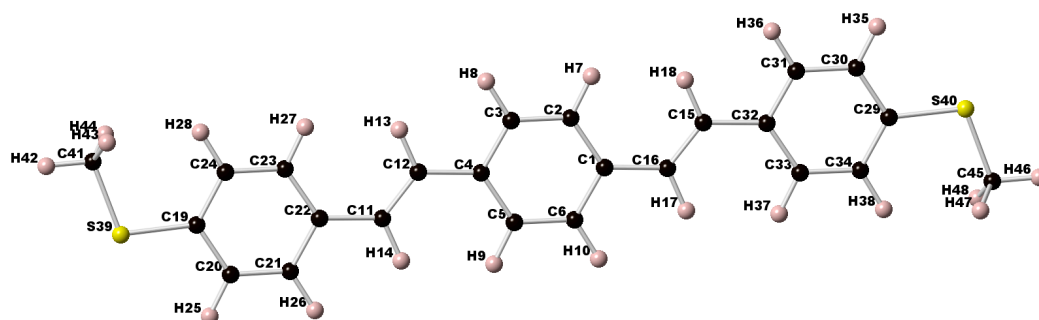
Torsional angles:

C1 -C2 -C3 -C4 : 0.027461  
 C1 -C2 -C3 -H9 : -179.992791  
 C1 -C6 -C5 -C4 : -0.100423  
 C1 -C6 -C5 -H11 : 179.984987  
 C1 -C13 -C12 -H16 : 0.596812  
 C1 -C13 -C12 -C19 : -179.734991  
 C2 -C1 -C6 -C5 : 0.177313  
 C2 -C1 -C6 -H12 : -179.668757  
 C2 -C1 -C13 -C12 : -177.369845  
 C2 -C1 -C13 -H15 : 2.401878

C2 -C3 -C4 -C5 : 0.055742  
C2 -C3 -C4 -S26 : 179.997672  
C3 -C2 -C1 -C6 : -0.141275  
C3 -C2 -C1 -C13 : 179.961316  
C3 -C4 -C5 -C6 : -0.020014  
C3 -C4 -C5 -H11 : 179.892947  
C3 -C4 -S26 -C27 :-179.158176  
C4 -C3 -C2 -H8 :-179.985191  
C4 -C5 -C6 -H12 : 179.748171  
C4 -S26 -C27 -H28 : 179.518535  
C4 -S26 -C27 -H29 : -62.388479  
C4 -S26 -C27 -H30 : 61.440312  
C5 -C4 -C3 -H9 :-179.923975  
C5 -C4 -S26 -C27 : 0.779693  
C5 -C6 -C1 -C13 :-179.931303  
C6 -C1 -C2 -H8 : 179.871376  
C6 -C1 -C13 -C12 : 2.740750  
C6 -C1 -C13 -H15 :-177.487527  
C6 -C5 -C4 -S26 :-179.956866  
H8 -C2 -C1 -C13 : -0.026033  
H8 -C2 -C3 -H9 : -0.005444  
H9 -C3 -C4 -S26 : 0.017955  
H11 -C5 -C4 -S26 : -0.043906  
H11 -C5 -C6 -H12 : -0.166419  
H12 -C6 -C1 -C13 : 0.222627  
C12 -C19 -C18 -C17 : 179.959990  
C12 -C19 -C18 -H24 : 0.029538  
C12 -C19 -C20 -C21 :-179.972064  
C12 -C19 -C20 -H25 : 0.349004  
C13 -C12 -C19 -C18 :-177.231741

C13 -C12 -C19 -C20 : 2.921653  
H15 -C13 -C12 -H16 :-179.165768  
H15 -C13 -C12 -C19 : 0.502429  
H16 -C12 -C19 -C18 : 2.449115  
H16 -C12 -C19 -C20 :-177.397491  
C16 -C17 -C18 -C19 : 0.071874  
C16 -C17 -C18 -H24 :-179.997678  
C16 -C21 -C20 -C19 : -0.065908  
C16 -C21 -C20 -H25 : 179.618242  
C16 -S30 -C31 -H32 : 179.794649  
C16 -S30 -C31 -H33 : -62.116894  
C16 -S30 -C31 -H34 : 61.720215  
C17 -C16 -C21 -C20 : -0.051328  
C17 -C16 -C21 -H26 : 179.824959  
C17 -C16 -S30 -C31 :-179.439229  
C17 -C18 -C19 -C20 : -0.182126  
C18 -C17 -C16 -C21 : 0.048406  
C18 -C17 -C16 -S30 : 179.994581  
C18 -C19 -C20 -C21 : 0.178712  
C18 -C19 -C20 -H25 :-179.500220  
C19 -C18 -C17 -H23 :-179.956366  
C19 -C20 -C21 -H26 :-179.944472  
C20 -C19 -C18 -H24 : 179.887422  
C20 -C21 -C16 -S30 :-179.992706  
C21 -C16 -C17 -H23 :-179.923311  
C21 -C16 -S30 -C31 : 0.503142  
H23 -C17 -C16 -S30 : 0.022863  
H23 -C17 -C18 -H24 : -0.025918  
H25 -C20 -C21 -H26 : -0.260322  
H26 -C21 -C16 -S30 : -0.116420

## MeS-PPV2



Final geometry:

atom	angstroms		
	x	y	z
C1	-2.8120865413	-0.2582606753	-0.3594449378
C2	-3.5789177950	0.9212626521	-0.2955934493
C3	-4.9617572948	0.8717848038	-0.2085965705
C4	-5.6656061523	-0.3501221241	-0.1788807713
C5	-4.8985048154	-1.5293881361	-0.2433538414
C6	-3.5162848113	-1.4796007215	-0.3306522037
H8	-3.0897152017	1.8897740262	-0.3150011667
H9	-5.5240094867	1.8012903938	-0.1614588915
H11	-5.3871056571	-2.4982075993	-0.2269536452
H12	-2.9547910301	-2.4090092701	-0.3794959964
C12	-7.9558096639	-1.3874909787	-0.0294016933
C13	-7.1247483046	-0.3246595101	-0.0859297329
H15	-7.5532792313	0.6756449293	-0.0601970325
H16	-7.5224192755	-2.3856209604	-0.0501838113
C16	-0.5139426978	0.7685180414	-0.4896095661
C17	-1.3533603872	-0.2885265498	-0.4539127556



H19	-0.9311097261	-1.2907886870	-0.4985582321
H20	-0.9379250567	1.7699235391	-0.4434744408
C20	-12.2502351860	-1.4978266518	0.2417106259
C21	-11.4824237091	-2.6723485360	0.2180381438
C22	-10.0998682827	-2.6062311244	0.1298982367
C23	-9.4157900535	-1.3762331780	0.0618191011
C24	-10.2003160884	-0.2093471765	0.0855677265
C25	-11.5876104606	-0.2637040073	0.1738384504
H27	-11.9731556314	-3.6403455158	0.2684473907
H28	-9.5271153592	-3.5301656680	0.1129167848
H29	-9.7254821113	0.7653593536	0.0330081940
H30	-12.1462449578	0.6652098869	0.1884459035
C30	3.7812981531	0.8377265105	-0.7726096544
C31	3.0285912502	2.0196087274	-0.6949183833
C32	1.6454787333	1.9672860188	-0.6041542497
C33	0.9459194360	0.7441402746	-0.5861118780
C34	1.7157461269	-0.4302757333	-0.6649436869
C35	3.1032567932	-0.3896100655	-0.7560680276
H37	3.5314225605	2.9826124709	-0.7062359104
H38	1.0846218680	2.8968158617	-0.5453872208
H39	1.2288903266	-1.4003950929	-0.6558917170
H40	3.6497981713	-1.3239891158	-0.8143002712
S40	-14.0168789273	-1.6998941581	0.3580277440
S41	5.5500783688	1.0219696634	-0.8858729748
C42	-14.6499483821	0.0077036231	0.3423750859
H43	-15.7361225956	-0.0824628134	0.4081729857
H44	-14.2900886943	0.5773342327	1.2019704126
H45	-14.3935808136	0.5219938068	-0.5864411626
C45	6.1593968022	-0.6921035646	-0.9751382788
H46	7.2458586524	-0.6127533886	-1.0497923991

H47 5.9073784973 -1.2553995148 -0.0739639793  
H48 5.7811336624 -1.2068103395 -1.8610583530

Total energy (hartrees): -1724.20777757151

HOMO energy (hartrees): -0.18125

LUMO energy (hartrees): -0.06433

Bond lengths (angstroms):

C1 -C2	: 1.408326	C1 -C6	: 1.410105
C1 -C17	: 1.462095	C2 -C3	: 1.386456
C2 -H8	: 1.085224	C3 -C4	: 1.410441
C3 -H9	: 1.087350	C4 -C5	: 1.408286
C4 -C13	: 1.462321	C5 -C6	: 1.385869
C5 -H11	: 1.085178	C6 -H12	: 1.086950
C12 -C13	: 1.350359	C12 -H16	: 1.088358
C12 -C23	: 1.462871	C13 -H15	: 1.088536
C16 -C17	: 1.350274	C16 -H20	: 1.088440
C16 -C33	: 1.463251	C17 -H19	: 1.088494
C20 -C21	: 1.403423	C20 -C25	: 1.402404
C20 -S40	: 1.781963	C21 -C22	: 1.386939
C21 -H27	: 1.086452	C22 -C23	: 1.409075
C22 -H28	: 1.087193	C23 -C24	: 1.406296
C24 -C25	: 1.391162	C24 -H29	: 1.085487
C25 -H30	: 1.084051	C30 -C31	: 1.403371
C30 -C35	: 1.402273	C30 -S41	: 1.781953
C31 -C32	: 1.387075	C31 -H37	: 1.086436
C32 -C33	: 1.409182	C32 -H38	: 1.087216

C33 -C34 : 1.406450 C34 -C35 : 1.391094  
C34 -H39 : 1.085469 C35 -H40 : 1.084049  
S40 -C42 : 1.821239 S41 -C45 : 1.821341  
C42 -H43 : 1.091895 C42 -H44 : 1.092191  
C42 -H45 : 1.092208 C45 -H46 : 1.091911  
C45 -H47 : 1.092214 C45 -H48 : 1.092182

## Bond angles:

C6 -C1 -C2 : 116.908895 C17 -C1 -C2 : 124.298913  
C17 -C1 -C6 : 118.792147 C3 -C2 -C1 : 121.066594  
H8 -C2 -C1 : 120.079352 H8 -C2 -C3 : 118.854030  
C4 -C3 -C2 : 122.003029 H9 -C3 -C2 : 119.205922  
H9 -C3 -C4 : 118.791048 C5 -C4 -C3 : 116.914273  
C13 -C4 -C3 : 118.959871 C13 -C4 -C5 : 124.125826  
C6 -C5 -C4 : 121.069175 H11 -C5 -C4 : 120.108796  
H11 -C5 -C6 : 118.821937 C5 -C6 -C1 : 122.038002  
H12 -C6 -C1 : 118.796755 H12 -C6 -C5 : 119.165220  
H16 -C12 -C13 : 118.421402 C23 -C12 -C13 : 127.645542  
C23 -C12 -H16 : 113.932960 C12 -C13 -C4 : 127.089035  
H15 -C13 -C4 : 114.225210 H15 -C13 -C12 : 118.685682  
H20 -C16 -C17 : 118.487064 C33 -C16 -C17 : 127.511908  
C33 -C16 -H20 : 114.001026 C16 -C17 -C1 : 127.281780  
H19 -C17 -C1 : 114.125629 H19 -C17 -C16 : 118.592591  
C25 -C20 -C21 : 118.499959 S40 -C20 -C21 : 116.653637  
S40 -C20 -C25 : 124.846401 C22 -C21 -C20 : 120.434013  
H27 -C21 -C20 : 119.851502 H27 -C21 -C22 : 119.714475  
C23 -C22 -C21 : 121.912888 H28 -C22 -C21 : 119.053929  
H28 -C22 -C23 : 119.033183 C22 -C23 -C12 : 118.738725  
C24 -C23 -C12 : 124.346991 C24 -C23 -C22 : 116.914248

C25 -C24 -C23 : 121.665980 H29 -C24 -C23 : 120.014973  
 H29 -C24 -C25 : 118.318990 C24 -C25 -C20 : 120.572862  
 H30 -C25 -C20 : 120.659256 H30 -C25 -C24 : 118.767868  
 C35 -C30 -C31 : 118.497051 S41 -C30 -C31 : 116.668934  
 S41 -C30 -C35 : 124.834014 C32 -C31 -C30 : 120.442855  
 H37 -C31 -C30 : 119.846370 H37 -C31 -C32 : 119.710771  
 C33 -C32 -C31 : 121.910290 H38 -C32 -C31 : 119.056888  
 H38 -C32 -C33 : 119.032821 C32 -C33 -C16 : 118.794090  
 C34 -C33 -C16 : 124.311708 C34 -C33 -C32 : 116.894169  
 C35 -C34 -C33 : 121.682119 H39 -C34 -C33 : 120.021110  
 H39 -C34 -C35 : 118.296767 C34 -C35 -C30 : 120.573511  
 H40 -C35 -C30 : 120.663349 H40 -C35 -C34 : 118.763137  
 C42 -S40 -C20 : 103.752842 C45 -S41 -C30 : 103.761529  
 H43 -C42 -S40 : 105.535740 H44 -C42 -S40 : 111.574502  
 H44 -C42 -H43 : 108.868621 H45 -C42 -S40 : 111.543557  
 H45 -C42 -H43 : 108.882206 H45 -C42 -H44 : 110.265933  
 H46 -C45 -S41 : 105.535432 H47 -C45 -S41 : 111.575827  
 H47 -C45 -H46 : 108.873516 H48 -C45 -S41 : 111.555335  
 H48 -C45 -H46 : 108.868542 H48 -C45 -H47 : 110.261541

Torsional angles:

C1 -C2 -C3 -C4 : 0.043587  
 C1 -C2 -C3 -H9 : -179.968951  
 C1 -C6 -C5 -C4 : -0.009391  
 C1 -C6 -C5 -H11 : 179.880607  
 C1 -C17 -C16 -H20 : 0.085776  
 C1 -C17 -C16 -C33 : -179.898358  
 C2 -C1 -C6 -C5 : -0.018650  
 C2 -C1 -C6 -H12 : 179.925637

C2 -C1 -C17 -C16 : 0.295902  
C2 -C1 -C17 -H19 :-179.701660  
C2 -C3 -C4 -C5 : -0.069537  
C2 -C3 -C4 -C13 : 179.990681  
C3 -C2 -C1 -C6 : 0.001852  
C3 -C2 -C1 -C17 : 179.922822  
C3 -C4 -C5 -C6 : 0.052242  
C3 -C4 -C5 -H11 :-179.836351  
C3 -C4 -C13 -C12 :-179.108931  
C3 -C4 -C13 -H15 : 0.790835  
C4 -C3 -C2 -H8 : 179.987654  
C4 -C5 -C6 -H12 :-179.953479  
C4 -C13 -C12 -H16 : 0.210726  
C4 -C13 -C12 -C23 :-179.909614  
C5 -C4 -C3 -H9 : 179.942950  
C5 -C4 -C13 -C12 : 0.955933  
C5 -C4 -C13 -H15 :-179.144300  
C5 -C6 -C1 -C17 :-179.944153  
C6 -C1 -C2 -H8 :-179.941534  
C6 -C1 -C17 -C16 :-179.784513  
C6 -C1 -C17 -H19 : 0.217925  
C6 -C5 -C4 -C13 : 179.988594  
H8 -C2 -C1 -C17 : -0.020565  
H8 -C2 -C3 -H9 : -0.024884  
H9 -C3 -C4 -C13 : 0.003168  
H11 -C5 -C4 -C13 : 0.100001  
H11 -C5 -C6 -H12 : -0.063481  
H12 -C6 -C1 -C17 : 0.000134  
C12 -C23 -C22 -C21 : 179.991169  
C12 -C23 -C22 -H28 : -0.003375

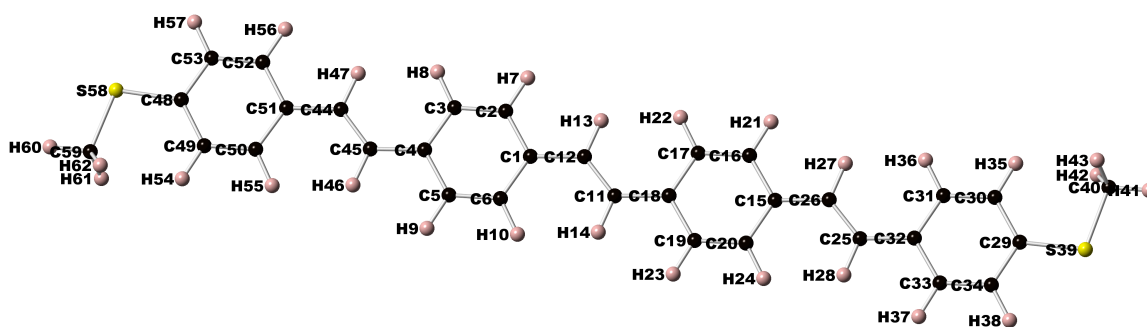
C12	-C23	-C24	-C25	:-179.991536
C12	-C23	-C24	-H29	: 0.096972
C13	-C12	-C23	-C22	:-179.073363
C13	-C12	-C23	-C24	: 0.998462
H15	-C13	-C12	-H16	:-179.685079
H15	-C13	-C12	-C23	: 0.194582
H16	-C12	-C23	-C22	: 0.810847
H16	-C12	-C23	-C24	:-179.117329
C16	-C33	-C32	-C31	:-179.948657
C16	-C33	-C32	-H38	: 0.040738
C16	-C33	-C34	-C35	: 179.954595
C16	-C33	-C34	-H39	: -0.024478
C17	-C16	-C33	-C32	:-179.750829
C17	-C16	-C33	-C34	: 0.318819
H19	-C17	-C16	-H20	:-179.916758
H19	-C17	-C16	-C33	: 0.099107
H20	-C16	-C33	-C32	: 0.264435
H20	-C16	-C33	-C34	:-179.665917
C20	-C21	-C22	-C23	: 0.024720
C20	-C21	-C22	-H28	:-179.980737
C20	-C25	-C24	-C23	: -0.032606
C20	-C25	-C24	-H29	: 179.880337
C20	-S40	-C42	-H43	: 179.749034
C20	-S40	-C42	-H44	: -62.159868
C20	-S40	-C42	-H45	: 61.657952
C21	-C20	-C25	-C24	: -0.021011
C21	-C20	-C25	-H30	: 179.935864
C21	-C20	-S40	-C42	:-179.372075
C21	-C22	-C23	-C24	: -0.075335
C22	-C21	-C20	-C25	: 0.024867

C22	-C21	-C20	-S40	:-179.955584
C22	-C23	-C24	-C25	: 0.079091
C22	-C23	-C24	-H29	:-179.832401
C23	-C22	-C21	-H27	: 179.989192
C23	-C24	-C25	-H30	:-179.990287
C24	-C23	-C22	-H28	: 179.930121
C24	-C25	-C20	-S40	: 179.957699
C25	-C20	-C21	-H27	:-179.939556
C25	-C20	-S40	-C42	: 0.648859
H27	-C21	-C20	-S40	: 0.079993
H27	-C21	-C22	-H28	: -0.016266
H29	-C24	-C25	-H30	: -0.077344
H30	-C25	-C20	-S40	: -0.085425
C30	-C31	-C32	-C33	: 0.005338
C30	-C31	-C32	-H38	:-179.984054
C30	-C35	-C34	-C33	: -0.025224
C30	-C35	-C34	-H39	: 179.954198
C30	-S41	-C45	-H46	: 179.775833
C30	-S41	-C45	-H47	:-62.126695
C30	-S41	-C45	-H48	: 61.695094
C31	-C30	-C35	-C34	: 0.016246
C31	-C30	-C35	-H40	: 179.997338
C31	-C30	-S41	-C45	:-179.720486
C31	-C32	-C33	-C34	: -0.013162
C32	-C31	-C30	-C35	: -0.006495
C32	-C31	-C30	-S41	:-179.997613
C32	-C33	-C34	-C35	: 0.023034
C32	-C33	-C34	-H39	:-179.956039
C33	-C32	-C31	-H37	: 179.981774
C33	-C34	-C35	-H40	: 179.993330

C34	-C33	-C32	-H38	: 179.976232
C34	-C35	-C30	-S41	:-179.993425
C35	-C30	-C31	-H37	:-179.982900
C35	-C30	-S41	-C45	: 0.289025
H37	-C31	-C30	-S41	: 0.025983
H37	-C31	-C32	-H38	: -0.007618
H39	-C34	-C35	-H40	: -0.027248
H40	-C35	-C30	-S41	: -0.012333



## MeS-PPV3



Final geometry:

atom	angstroms		
	x	y	z
C1	-2.7675470000	-0.4598810000	-0.3083940000
C2	-3.4299300000	0.7854490000	-0.2887840000
C3	-4.8119210000	0.8827600000	-0.3002390000
C4	-5.6206460000	-0.2699890000	-0.3323540000
C5	-4.9584140000	-1.5156030000	-0.3513080000
C6	-3.5752520000	-1.6135290000	-0.3396710000
H8	-2.8340650000	1.6945860000	-0.2644080000
H9	-5.2673370000	1.8675260000	-0.2845130000
H11	-5.5545020000	-2.4246280000	-0.3758760000
H12	-3.1176970000	-2.5980190000	-0.3551430000
C12	-0.4917440000	-1.5512220000	-0.3124910000
C13	-1.3069830000	-0.4738430000	-0.2961390000
H15	-0.8558160000	0.5161660000	-0.2719540000
H16	-0.9377880000	-2.5437100000	-0.3371680000
C16	3.8264650000	-1.6822310000	-0.2863260000
C17	3.1398730000	-0.4505140000	-0.2637720000
C18	1.7562020000	-0.3798810000	-0.2711970000
C19	0.9697080000	-1.5479350000	-0.3017970000

C20	1.6558880000	-2.7802180000	-0.3237380000
C21	3.0404710000	-2.8504780000	-0.3164480000
H23	3.7171930000	0.4700770000	-0.2400640000
H24	1.2820150000	0.5959230000	-0.2529910000
H25	1.0779090000	-3.7008930000	-0.3472950000
H26	3.5159940000	-3.8257450000	-0.3342550000
C26	6.1164640000	-2.7372140000	-0.2953690000
C27	5.2882330000	-1.6708520000	-0.2775230000
H29	5.7243060000	-0.6738740000	-0.2543660000
H30	5.6799670000	-3.7340060000	-0.3183310000
C30	10.4200850000	-2.8458330000	-0.2764770000
C31	9.7531850000	-1.6122850000	-0.2565900000
C32	8.3632420000	-1.5592500000	-0.2623210000
C33	7.5795580000	-2.7267780000	-0.2876290000
C34	8.2677370000	-3.9562040000	-0.3072770000
C35	9.6533040000	-4.0210870000	-0.3019160000
H37	10.3106590000	-0.6827590000	-0.2367040000
H38	7.8856240000	-0.5847200000	-0.2468310000
H39	7.6959560000	-4.8806810000	-0.3275830000
H40	10.1471530000	-4.9886670000	-0.3180970000
S40	12.1909730000	-3.0451890000	-0.2715710000
C41	12.8192900000	-1.3357620000	-0.2456140000
H42	13.9076190000	-1.4240630000	-0.2450630000
H43	12.5103260000	-0.7810590000	-1.1342880000
H44	12.5073700000	-0.8069920000	0.6577060000
C44	-7.8768560000	0.8477580000	-0.3320930000
C45	-7.0827620000	-0.2445480000	-0.3477610000
H47	-7.5473750000	-1.2285110000	-0.3752410000
H48	-7.4065600000	1.8288250000	-0.3039450000
C48	-12.1719730000	1.1253600000	-0.3826410000

C49	-11.5548720000	-0.1336470000	-0.4069580000
C50	-10.1680510000	-0.2426020000	-0.3907570000
C51	-9.3389140000	0.8925630000	-0.3495720000
C52	-9.9777850000	2.1484690000	-0.3252700000
C53	-11.3593230000	2.2687840000	-0.3412840000
H55	-12.1490250000	-1.0398000000	-0.4388260000
H56	-9.7290170000	-1.2351410000	-0.4109940000
H57	-9.3697530000	3.0491980000	-0.2936600000
H58	-11.8141540000	3.2552740000	-0.3220520000
S58	-13.9328430000	1.3971210000	-0.3999710000
C59	-14.6306490000	-0.2840350000	-0.4625930000
H60	-15.7142770000	-0.1503580000	-0.4780600000
H61	-14.3265990000	-0.8110110000	-1.3696680000
H62	-14.3591770000	-0.8649550000	0.4215760000

Total energy (hartrees): -2032.67948856201

HOMO energy (hartrees): -0.17933

LUMO energy (hartrees): -0.07150

Bond lengths (angstroms):

C1	-C2	: 1.410667	C1	-C6	: 1.408641
C1	-C13	: 1.460682	C2	-C3	: 1.385460
C2	-H8	: 1.087281	C3	-C4	: 1.408509
C3	-H9	: 1.085088	C4	-C5	: 1.410838
C4	-C45	: 1.462418	C5	-C6	: 1.386673
C5	-H11	: 1.087314	C6	-H12	: 1.085733

C12 -C13	: 1.351158	C12 -H16	: 1.088392
C12 -C19	: 1.461495	C13 -H15	: 1.088235
C16 -C17	: 1.410335	C16 -C21	: 1.408366
C16 -C27	: 1.461839	C17 -C18	: 1.385493
C17 -H23	: 1.086898	C18 -C19	: 1.408495
C18 -H24	: 1.085071	C19 -C20	: 1.410619
C20 -C21	: 1.386384	C20 -H25	: 1.087316
C21 -H26	: 1.085166	C26 -C27	: 1.350338
C26 -H30	: 1.088417	C26 -C33	: 1.463152
C27 -H29	: 1.088421	C30 -C31	: 1.402424
C30 -C35	: 1.403504	C30 -S40	: 1.782081
C31 -C32	: 1.390966	C31 -H37	: 1.084062
C32 -C33	: 1.406386	C32 -H38	: 1.085388
C33 -C34	: 1.409065	C34 -C35	: 1.387096
C34 -H39	: 1.087200	C35 -H40	: 1.086444
S40 -C41	: 1.821427	C41 -H42	: 1.091905
C41 -H43	: 1.092198	C41 -H44	: 1.092190
C44 -C45	: 1.350542	C44 -H48	: 1.088330
C44 -C51	: 1.462849	C45 -H47	: 1.088487
C48 -C49	: 1.402321	C48 -C53	: 1.403399
C48 -S58	: 1.781802	C49 -C50	: 1.391189
C49 -H55	: 1.084042	C50 -C51	: 1.406330
C50 -H56	: 1.085493	C51 -C52	: 1.409272
C52 -C53	: 1.386860	C52 -H57	: 1.087205
C53 -H58	: 1.086464	S58 -C59	: 1.821302
C59 -H60	: 1.091952	C59 -H61	: 1.092216
C59 -H62	: 1.092209		

Bond angles:

C6 -C1 -C2 : 117.004542 C13 -C1 -C2 : 118.544198  
 C13 -C1 -C6 : 124.451245 C3 -C2 -C1 : 122.023522  
 H8 -C2 -C1 : 118.759641 H8 -C2 -C3 : 119.216831  
 C4 -C3 -C2 : 121.026756 H9 -C3 -C2 : 118.834232  
 H9 -C3 -C4 : 120.139004 C5 -C4 -C3 : 116.960051  
 C45 -C4 -C3 : 124.059587 C45 -C4 -C5 : 118.980347  
 C6 -C5 -C4 : 122.034979 H11 -C5 -C4 : 118.756953  
 H11 -C5 -C6 : 119.208068 C5 -C6 -C1 : 120.950129  
 H12 -C6 -C1 : 120.085051 H12 -C6 -C5 : 118.964820  
 H16 -C12 -C13 : 118.693131 C19 -C12 -C13 : 126.974798  
 C19 -C12 -H16 : 114.332051 C12 -C13 -C1 : 127.649879  
 H15 -C13 -C1 : 113.956524 H15 -C13 -C12 : 118.393565  
 C21 -C16 -C17 : 116.942559 C27 -C16 -C17 : 118.679592  
 C27 -C16 -C21 : 124.377847 C18 -C17 -C16 : 122.047839  
 H23 -C17 -C16 : 118.782228 H23 -C17 -C18 : 119.169931  
 C19 -C18 -C17 : 121.030724 H24 -C18 -C17 : 118.828696  
 H24 -C18 -C19 : 120.140580 C18 -C19 -C12 : 124.083517  
 C20 -C19 -C12 : 118.969643 C20 -C19 -C18 : 116.946832  
 C21 -C20 -C19 : 122.005251 H25 -C20 -C19 : 118.780512  
 H25 -C20 -C21 : 119.214235 C20 -C21 -C16 : 121.026783  
 H26 -C21 -C16 : 120.085556 H26 -C21 -C20 : 118.887660  
 H30 -C26 -C27 : 118.523764 C33 -C26 -C27 : 127.417912  
 C33 -C26 -H30 : 114.058323 C26 -C27 -C16 : 127.379711  
 H29 -C27 -C16 : 114.072106 H29 -C27 -C26 : 118.548174  
 C35 -C30 -C31 : 118.489309 S40 -C30 -C31 : 124.813329  
 S40 -C30 -C35 : 116.697360 C32 -C31 -C30 : 120.574787  
 H37 -C31 -C30 : 120.658158 H37 -C31 -C32 : 118.767054  
 C33 -C32 -C31 : 121.684672 H38 -C32 -C31 : 118.287417  
 H38 -C32 -C33 : 120.027910 C32 -C33 -C26 : 124.279243  
 C34 -C33 -C26 : 118.821192 C34 -C33 -C32 : 116.899555

C35 -C34 -C33 : 121.911898 H39 -C34 -C33 : 119.033801  
 H39 -C34 -C35 : 119.054298 C34 -C35 -C30 : 120.439776  
 H40 -C35 -C30 : 119.847223 H40 -C35 -C34 : 119.712991  
 C41 -S40 -C30 : 103.759270 H42 -C41 -S40 : 105.541714  
 H43 -C41 -S40 : 111.559674 H43 -C41 -H42 : 108.870990  
 H44 -C41 -S40 : 111.569958 H44 -C41 -H42 : 108.868072  
 H44 -C41 -H43 : 110.260036 H48 -C44 -C45 : 118.378630  
 C51 -C44 -C45 : 127.755810 C51 -C44 -H48 : 113.865540  
 C44 -C45 -C4 : 126.999504 H47 -C45 -C4 : 114.286192  
 H47 -C45 -C44 : 118.714298 C53 -C48 -C49 : 118.501374  
 S58 -C48 -C49 : 124.865494 S58 -C48 -C53 : 116.633132  
 C50 -C49 -C48 : 120.583094 H55 -C49 -C48 : 120.650098  
 H55 -C49 -C50 : 118.766808 C51 -C50 -C49 : 121.658023  
 H56 -C50 -C49 : 118.332036 H56 -C50 -C51 : 120.009939  
 C50 -C51 -C44 : 124.394191 C52 -C51 -C44 : 118.697058  
 C52 -C51 -C50 : 116.908722 C53 -C52 -C51 : 121.918205  
 H57 -C52 -C51 : 119.031460 H57 -C52 -C53 : 119.050325  
 C52 -C53 -C48 : 120.430579 H58 -C53 -C48 : 119.860474  
 H58 -C53 -C52 : 119.708943 C59 -S58 -C48 : 103.779453  
 H60 -C59 -S58 : 105.527573 H61 -C59 -S58 : 111.546430  
 H61 -C59 -H60 : 108.878313 H62 -C59 -S58 : 111.585292  
 H62 -C59 -H60 : 108.858831 H62 -C59 -H61 : 110.272684

Torsional angles:

C1 -C2 -C3 -C4 : -0.003839  
 C1 -C2 -C3 -H9 : -179.972973  
 C1 -C6 -C5 -C4 : -0.013831  
 C1 -C6 -C5 -H11 : 179.980668  
 C1 -C13 -C12 -H16 : -0.040714

C1	-C13	-C12	-C19	: 179.904696
C2	-C1	-C6	-C5	: 0.043388
C2	-C1	-C6	-H12	:-179.960964
C2	-C1	-C13	-C12	:-179.921512
C2	-C1	-C13	-H15	: 0.011622
C2	-C3	-C4	-C5	: 0.033871
C2	-C3	-C4	-C45	:-179.921537
C3	-C2	-C1	-C6	: -0.034959
C3	-C2	-C1	-C13	: 179.923555
C3	-C4	-C5	-C6	: -0.025306
C3	-C4	-C5	-H11	: 179.980171
C3	-C4	-C45	-C44	: -0.118360
C3	-C4	-C45	-H47	: 179.854224
C4	-C3	-C2	-H8	: 179.967265
C4	-C5	-C6	-H12	: 179.990473
C4	-C45	-C44	-H48	: -0.068512
C4	-C45	-C44	-C51	: 179.875982
C5	-C4	-C3	-H9	:-179.997394
C5	-C4	-C45	-C44	: 179.927075
C5	-C4	-C45	-H47	: -0.100341
C5	-C6	-C1	-C13	:-179.912417
C6	-C1	-C2	-H8	: 179.993810
C6	-C1	-C13	-C12	: 0.033663
C6	-C1	-C13	-H15	: 179.966797
C6	-C5	-C4	-C45	: 179.932463
H8	-C2	-C1	-C13	: -0.047676
H8	-C2	-C3	-H9	: -0.001870
H9	-C3	-C4	-C45	: 0.047198
H11	-C5	-C4	-C45	: -0.062060
H11	-C5	-C6	-H12	: -0.015027

H12	-C6	-C1	-C13	:	0.083230
C12	-C19	-C18	-C17	:	-179.945533
C12	-C19	-C18	-H24	:	0.052858
C12	-C19	-C20	-C21	:	179.939676
C12	-C19	-C20	-H25	:	-0.045850
C13	-C12	-C19	-C18	:	0.035694
C13	-C12	-C19	-C20	:	-179.932822
H15	-C13	-C12	-H16	:	-179.971252
H15	-C13	-C12	-C19	:	-0.025842
H16	-C12	-C19	-C18	:	179.983140
H16	-C12	-C19	-C20	:	0.014623
C16	-C17	-C18	-C19	:	0.005302
C16	-C17	-C18	-H24	:	-179.993110
C16	-C21	-C20	-C19	:	0.009595
C16	-C21	-C20	-H25	:	179.995060
C16	-C27	-C26	-H30	:	-0.048525
C16	-C27	-C26	-C33	:	179.948208
C17	-C16	-C21	-C20	:	0.019474
C17	-C16	-C21	-H26	:	-179.971639
C17	-C16	-C27	-C26	:	179.983377
C17	-C16	-C27	-H29	:	-0.052164
C17	-C18	-C19	-C20	:	0.023568
C18	-C17	-C16	-C21	:	-0.026950
C18	-C17	-C16	-C27	:	179.958610
C18	-C19	-C20	-C21	:	-0.031073
C18	-C19	-C20	-H25	:	179.983401
C19	-C18	-C17	-H23	:	179.991951
C19	-C20	-C21	-H26	:	-179.999189
C20	-C19	-C18	-H24	:	-179.978041
C20	-C21	-C16	-C27	:	-179.965177

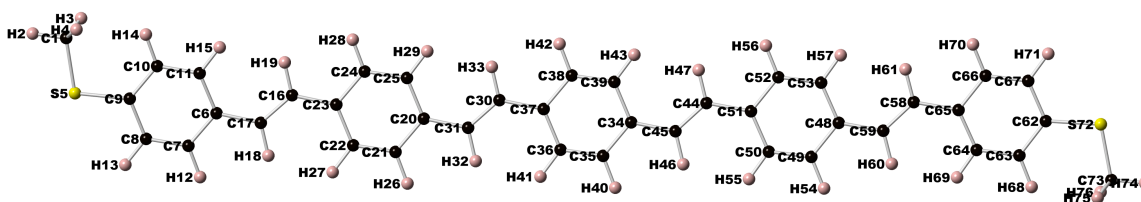


C21	-C16	-C17	-H23	: 179.986351
C21	-C16	-C27	-C26	: -0.032220
C21	-C16	-C27	-H29	: 179.932239
H23	-C17	-C16	-C27	: -0.028088
H23	-C17	-C18	-H24	: -0.006462
H25	-C20	-C21	-H26	: -0.013724
H26	-C21	-C16	-C27	: 0.043710
C26	-C33	-C32	-C31	:-179.976985
C26	-C33	-C32	-H38	: 0.012538
C26	-C33	-C34	-C35	: 179.972841
C26	-C33	-C34	-H39	: -0.005078
C27	-C26	-C33	-C32	: -0.144134
C27	-C26	-C33	-C34	: 179.893352
H29	-C27	-C26	-H30	: 179.988416
H29	-C27	-C26	-C33	: -0.014850
H30	-C26	-C33	-C32	: 179.852723
H30	-C26	-C33	-C34	: -0.109791
C30	-C31	-C32	-C33	: 0.017236
C30	-C31	-C32	-H38	:-179.972463
C30	-C35	-C34	-C33	: -0.004671
C30	-C35	-C34	-H39	: 179.973244
C30	-S40	-C41	-H42	:-179.840460
C30	-S40	-C41	-H43	: -61.750765
C30	-S40	-C41	-H44	: 62.067927
C31	-C30	-C35	-C34	: 0.007400
C31	-C30	-C35	-H40	: 179.972862
C31	-C30	-S40	-C41	: -0.297310
C31	-C32	-C33	-C34	: -0.013813
C32	-C31	-C30	-C35	: -0.013564
C32	-C31	-C30	-S40	:-179.997118

C32	-C33	-C34	-C35	:	0.007574
C32	-C33	-C34	-H39	:	-179.970345
C33	-C32	-C31	-H37	:	-179.996514
C33	-C34	-C35	-H40	:	-179.970179
C34	-C33	-C32	-H38	:	179.975711
C34	-C35	-C30	-S40	:	179.992286
C35	-C30	-C31	-H37	:	-179.999552
C35	-C30	-S40	-C41	:	179.718869
H37	-C31	-C30	-S40	:	0.016894
H37	-C31	-C32	-H38	:	0.013786
H39	-C34	-C35	-H40	:	0.007735
H40	-C35	-C30	-S40	:	-0.042251
C44	-C51	-C50	-C49	:	-179.931703
C44	-C51	-C50	-H56	:	0.054625
C44	-C51	-C52	-C53	:	179.926432
C44	-C51	-C52	-H57	:	-0.035534
C45	-C44	-C51	-C50	:	-0.193940
C45	-C44	-C51	-C52	:	179.869721
H47	-C45	-C44	-H48	:	179.959981
H47	-C45	-C44	-C51	:	-0.095525
H48	-C44	-C51	-C50	:	179.752659
H48	-C44	-C51	-C52	:	-0.183680
C48	-C49	-C50	-C51	:	0.011435
C48	-C49	-C50	-H56	:	-179.975115
C48	-C53	-C52	-C51	:	0.006537
C48	-C53	-C52	-H57	:	179.968496
C48	-S58	-C59	-H60	:	-179.795566
C48	-S58	-C59	-H61	:	-61.712499
C48	-S58	-C59	-H62	:	62.124252
C49	-C48	-C53	-C52	:	0.010792

C49	-C48	-C53	-H58	: 179.986369
C49	-C48	-S58	-C59	: -0.292713
C49	-C50	-C51	-C52	: 0.005675
C50	-C49	-C48	-C53	: -0.019608
C50	-C49	-C48	-S58	: 179.990834
C50	-C51	-C52	-C53	: -0.014659
C50	-C51	-C52	-H57	:-179.976625
C51	-C50	-C49	-H55	:-179.995324
C51	-C52	-C53	-H58	:-179.969076
C52	-C51	-C50	-H56	: 179.992004
C52	-C53	-C48	-S58	:-179.998792
C53	-C48	-C49	-H55	: 179.987279
C53	-C48	-S58	-C59	: 179.717553
H55	-C49	-C48	-S58	: -0.002279
H55	-C49	-C50	-H56	: 0.018126
H57	-C52	-C53	-H58	: -0.007117
H58	-C53	-C48	-S58	: -0.023216

## MeS-PPV4



Final geometry:

angstroms

atom	x	y	z
C1	-7.8000230000	2.6608420000	0.1427530000
H2	-8.4725620000	3.2839440000	0.7358560000
H4	-6.9699760000	3.2758070000	-0.2125690000
H5	-7.4270090000	1.8476990000	0.7696240000
S5	-8.8081710000	2.0326510000	-1.2385040000
C6	-5.9947040000	-0.6160170000	-3.7762290000
C7	-7.3523910000	-0.4113990000	-4.0927460000
C8	-8.1739020000	0.3899950000	-3.3129560000
C9	-7.6687400000	1.0267410000	-2.1686920000
C10	-6.3206940000	0.8319690000	-1.8353550000
C11	-5.5065890000	0.0266730000	-2.6241790000
H13	-7.7676390000	-0.8936680000	-4.9743030000
H14	-9.2156860000	0.5239330000	-3.5906720000
H15	-5.8943360000	1.3028450000	-0.9569560000
H16	-4.4710870000	-0.1049270000	-2.3268980000
C16	-3.8603290000	-1.7183240000	-4.5339430000
C17	-5.1832880000	-1.4703710000	-4.6423340000
H19	-5.7361020000	-1.9359060000	-5.4566230000
H20	-3.3043700000	-1.2376020000	-3.7306990000
C20	-1.3443290000	-4.2164840000	-7.0028960000

C21	-2.7314960000	-4.1268780000	-7.2428660000
C22	-3.5616610000	-3.3336310000	-6.4660990000
C23	-3.0490730000	-2.5754950000	-5.3949460000
C24	-1.6623160000	-2.6670580000	-5.1533900000
C25	-0.8323420000	-3.4600770000	-5.9299120000
H27	-3.1594570000	-4.7007100000	-8.0613440000
H28	-4.6232370000	-3.3069520000	-6.6920710000
H29	-1.2351450000	-2.0963110000	-4.3323340000
H30	0.2275580000	-3.4931810000	-5.6974660000
C30	0.8040330000	-5.2685160000	-7.7854890000
C31	-0.5312050000	-5.0748750000	-7.8603030000
H33	-1.0919990000	-5.5995170000	-8.6320240000
H34	1.3638440000	-4.7388060000	-7.0166130000
C34	3.3437170000	-7.7673520000	-10.2288110000
C35	1.9514660000	-7.7166210000	-10.4507750000
C36	1.1132140000	-6.9238220000	-9.6822260000
C37	1.6220680000	-6.1274940000	-8.6369840000
C38	3.0142050000	-6.1794100000	-8.4140370000
C39	3.8520200000	-6.9716430000	-9.1825630000
H41	1.5263780000	-8.3196910000	-11.2494640000
H42	0.0487680000	-6.9252600000	-9.8959620000
H43	3.4390240000	-5.5776820000	-7.6141700000
H44	4.9156580000	-6.9719780000	-8.9655650000
C44	5.5063230000	-8.7877890000	-11.0082110000
C45	4.1667720000	-8.6249790000	-11.0779000000
H47	3.6116010000	-9.1751880000	-11.8357970000
H48	6.0566270000	-8.2350030000	-10.2494230000
C48	8.1112970000	-11.2473430000	-13.4216590000
C49	6.7202480000	-11.2240100000	-13.6556240000
C50	5.8598600000	-10.4459860000	-12.8959350000

C51	6.3445970000	-9.6372500000	-11.8489760000
C52	7.7355140000	-9.6612230000	-11.6146040000
C53	8.5947820000	-10.4390020000	-12.3739780000
H55	6.3138310000	-11.8364610000	-14.4569070000
H56	4.7975930000	-10.4665420000	-13.1196950000
H57	8.1422450000	-9.0477350000	-10.8142520000
H58	9.6564510000	-10.4146320000	-12.1510650000
C58	10.2964380000	-12.2514670000	-14.1671700000
C59	8.9590390000	-12.0892650000	-14.2634660000
H61	8.4219660000	-12.6307090000	-15.0405080000
H62	10.8300980000	-11.7154350000	-13.3840940000
C62	12.9188110000	-14.6704120000	-16.5796930000
C63	11.5469760000	-14.6240830000	-16.8676030000
C64	10.6875730000	-13.8480170000	-16.0971960000
C65	11.1521530000	-13.0864770000	-15.0095580000
C66	12.5333000000	-13.1456700000	-14.7357250000
C67	13.3998560000	-13.9163980000	-15.4976510000
H69	11.1360780000	-15.1910000000	-17.6951170000
H70	9.6334650000	-13.8377930000	-16.3557510000
H71	12.9316090000	-12.5706020000	-13.9033410000
H72	14.4585300000	-13.9348040000	-15.2541330000
S72	14.1164890000	-15.6230380000	-17.4918630000
C73	13.1265400000	-16.4264100000	-18.7930180000
H74	13.8351270000	-17.0184380000	-19.3758990000
H75	12.3725150000	-17.0938990000	-18.3696760000
H76	12.6554910000	-15.6915790000	-19.4499210000

Total energy (hartrees): -2341.15120336664

HOMO energy (hartrees): -0.17817

LUMO energy (hartrees): -0.07571

Bond lengths (angstroms):

C1 -H2	: 1.091941	C1 -H4	: 1.092435
C1 -H5	: 1.092386	C1 -S5	: 1.821773
S5 -C9	: 1.781967	C6 -C7	: 1.409030
C6 -C11	: 1.406601	C6 -C17	: 1.462346
C7 -C8	: 1.387510	C7 -H13	: 1.087270
C8 -C9	: 1.403558	C8 -H14	: 1.086453
C9 -C10	: 1.402240	C10 -C11	: 1.390508
C10 -H15	: 1.084016	C11 -H16	: 1.085338
C16 -C17	: 1.350352	C16 -H20	: 1.088754
C16 -C23	: 1.460892	C17 -H19	: 1.088757
C20 -C21	: 1.410619	C20 -C25	: 1.409105
C20 -C31	: 1.460532	C21 -C22	: 1.386283
C21 -H27	: 1.087355	C22 -C23	: 1.408860
C22 -H28	: 1.085688	C23 -C24	: 1.410613
C24 -C25	: 1.385901	C24 -H29	: 1.087364
C25 -H30	: 1.085594	C30 -C31	: 1.351279
C30 -H34	: 1.088647	C30 -C37	: 1.460160
C31 -H33	: 1.088711	C34 -C35	: 1.410746
C34 -C39	: 1.409312	C34 -C45	: 1.460786
C35 -C36	: 1.386313	C35 -H41	: 1.087335
C36 -C37	: 1.409114	C36 -H42	: 1.085694
C37 -C38	: 1.410832	C38 -C39	: 1.385713
C38 -H43	: 1.087352	C39 -H44	: 1.085548
C44 -C45	: 1.351207	C44 -H48	: 1.088194

C44 -C51 : 1.459854 C45 -H47 : 1.088739  
 C48 -C49 : 1.410780 C48 -C53 : 1.408832  
 C48 -C59 : 1.461553 C49 -C50 : 1.386620  
 C49 -H55 : 1.087348 C50 -C51 : 1.408952  
 C50 -H56 : 1.085773 C51 -C52 : 1.410729  
 C52 -C53 : 1.385616 C52 -H57 : 1.087364  
 C53 -H58 : 1.085092 C58 -C59 : 1.350636  
 C58 -H62 : 1.088729 C58 -C65 : 1.462569  
 C59 -H61 : 1.088762 C62 -C63 : 1.402487  
 C62 -C67 : 1.403836 C62 -S72 : 1.781568  
 C63 -C64 : 1.390820 C63 -H69 : 1.083979  
 C64 -C65 : 1.406675 C64 -H70 : 1.085403  
 C65 -C66 : 1.409275 C66 -C67 : 1.387614  
 C66 -H71 : 1.087298 C67 -H72 : 1.086476  
 S72 -C73 : 1.821650 C73 -H74 : 1.091945  
 C73 -H75 : 1.092389 C73 -H76 : 1.092422

Bond angles:

H4 -C1 -H2 : 108.869679 H5 -C1 -H2 : 108.867641  
 H5 -C1 -H4 : 110.256848 S5 -C1 -H2 : 105.530692  
 S5 -C1 -H4 : 111.590863 S5 -C1 -H5 : 111.554078  
 C9 -S5 -C1 : 103.684741 C11 -C6 -C7 : 116.872293  
 C17 -C6 -C7 : 119.107626 C17 -C6 -C11 : 124.019907  
 C8 -C7 -C6 : 121.879207 H13 -C7 -C6 : 119.059752  
 H13 -C7 -C8 : 119.060928 C9 -C8 -C7 : 120.471590  
 H14 -C8 -C7 : 119.688084 H14 -C8 -C9 : 119.840298  
 C8 -C9 -S5 : 116.841212 C10 -C9 -S5 : 124.682635  
 C10 -C9 -C8 : 118.476109 C11 -C10 -C9 : 120.559509  
 H15 -C10 -C9 : 120.690733 H15 -C10 -C11 : 118.749422



C10 -C11 -C6 : 121.740605 H16 -C11 -C6 : 120.001293  
 H16 -C11 -C10 : 118.256962 H20 -C16 -C17 : 118.582505  
 C23 -C16 -C17 : 127.191549 C23 -C16 -H20 : 114.224792  
 C16 -C17 -C6 : 127.110495 H19 -C17 -C6 : 114.270036  
 H19 -C17 -C16 : 118.618008 C25 -C20 -C21 : 116.919636  
 C31 -C20 -C21 : 119.008673 C31 -C20 -C25 : 124.071402  
 C22 -C21 -C20 : 121.999640 H27 -C21 -C20 : 118.787639  
 H27 -C21 -C22 : 119.212553 C23 -C22 -C21 : 121.067888  
 H28 -C22 -C21 : 118.880181 H28 -C22 -C23 : 120.051239  
 C22 -C23 -C16 : 124.179906 C24 -C23 -C16 : 118.887118  
 C24 -C23 -C22 : 116.932745 C25 -C24 -C23 : 122.001164  
 H29 -C24 -C23 : 118.779395 H29 -C24 -C25 : 119.219436  
 C24 -C25 -C20 : 121.078658 H30 -C25 -C20 : 120.093791  
 H30 -C25 -C24 : 118.827421 H34 -C30 -C31 : 118.522093  
 C37 -C30 -C31 : 127.272085 C37 -C30 -H34 : 114.205740  
 C30 -C31 -C20 : 127.001976 H33 -C31 -C20 : 114.366596  
 H33 -C31 -C30 : 118.631411 C39 -C34 -C35 : 116.900825  
 C45 -C34 -C35 : 119.058681 C45 -C34 -C39 : 124.040489  
 C36 -C35 -C34 : 122.010514 H41 -C35 -C34 : 118.779853  
 H41 -C35 -C36 : 119.209617 C37 -C36 -C35 : 121.068012  
 H42 -C36 -C35 : 118.877113 H42 -C36 -C37 : 120.054752  
 C36 -C37 -C30 : 124.243163 C38 -C37 -C30 : 118.836226  
 C38 -C37 -C36 : 116.920542 C39 -C38 -C37 : 122.005056  
 H43 -C38 -C37 : 118.776583 H43 -C38 -C39 : 119.218355  
 C38 -C39 -C34 : 121.094976 H44 -C39 -C34 : 120.107302  
 H44 -C39 -C38 : 118.797706 H48 -C44 -C45 : 118.430758  
 C51 -C44 -C45 : 127.565862 C51 -C44 -H48 : 114.003297  
 C44 -C45 -C34 : 126.822293 H47 -C45 -C34 : 114.457471  
 H47 -C45 -C44 : 118.720203 C53 -C48 -C49 : 116.886199  
 C59 -C48 -C49 : 119.073034 C59 -C48 -C53 : 124.040617

C50 -C49 -C48 : 122.021340 H55 -C49 -C48 : 118.779257  
 H55 -C49 -C50 : 119.199399 C51 -C50 -C49 : 121.044372  
 H56 -C50 -C49 : 118.916203 H56 -C50 -C51 : 120.039407  
 C50 -C51 -C44 : 124.360616 C52 -C51 -C44 : 118.708947  
 C52 -C51 -C50 : 116.930303 C53 -C52 -C51 : 121.999738  
 H57 -C52 -C51 : 118.783104 H57 -C52 -C53 : 119.217023  
 C52 -C53 -C48 : 121.117980 H58 -C53 -C48 : 120.094630  
 H58 -C53 -C52 : 118.787075 H62 -C58 -C59 : 118.523363  
 C65 -C58 -C59 : 127.361482 C65 -C58 -H62 : 114.115120  
 C58 -C59 -C48 : 127.046132 H61 -C59 -C48 : 114.293576  
 H61 -C59 -C58 : 118.660228 C67 -C62 -C63 : 118.402444  
 S72 -C62 -C63 : 124.758919 S72 -C62 -C67 : 116.838626  
 C64 -C63 -C62 : 120.605672 H69 -C63 -C62 : 120.678416  
 H69 -C63 -C64 : 118.715866 C65 -C64 -C63 : 121.755739  
 H70 -C64 -C63 : 118.255279 H70 -C64 -C65 : 119.988797  
 C64 -C65 -C58 : 124.137781 C66 -C65 -C58 : 119.042932  
 C66 -C65 -C64 : 116.819134 C67 -C66 -C65 : 121.915389  
 H71 -C66 -C65 : 119.048881 H71 -C66 -C67 : 119.035729  
 C66 -C67 -C62 : 120.501614 H72 -C67 -C62 : 119.838373  
 H72 -C67 -C66 : 119.659997 C73 -S72 -C62 : 103.662108  
 H74 -C73 -S72 : 105.529816 H75 -C73 -S72 : 111.578478  
 H75 -C73 -H74 : 108.874632 H76 -C73 -S72 : 111.542190  
 H76 -C73 -H74 : 108.876344 H76 -C73 -H75 : 110.268675

Torsional angles:

C1 -S5 -C9 -C8 : 179.615450  
 C1 -S5 -C9 -C10 : -0.306620  
 H2 -C1 -S5 -C9 : -179.957530  
 H4 -C1 -S5 -C9 : 61.944508

H5 -C1 -S5 -C9 : -61.881357  
S5 -C9 -C8 -C7 : -179.990905  
S5 -C9 -C8 -H14 : -0.051795  
S5 -C9 -C10 -C11 : 179.986255  
S5 -C9 -C10 -H15 : 0.199757  
C6 -C7 -C8 -C9 : -0.120496  
C6 -C7 -C8 -H14 : 179.940301  
C6 -C11 -C10 -C9 : 0.117422  
C6 -C11 -C10 -H15 : 179.908010  
C6 -C17 -C16 -H20 : -0.673589  
C6 -C17 -C16 -C23 : 179.741608  
C7 -C6 -C11 -C10 : -0.289389  
C7 -C6 -C11 -H16 : 179.315409  
C7 -C6 -C17 -C16 : 176.177937  
C7 -C6 -C17 -H19 : -3.372414  
C7 -C8 -C9 -C10 : -0.063808  
C8 -C7 -C6 -C11 : 0.291340  
C8 -C7 -C6 -C17 : -179.854305  
C8 -C9 -C10 -C11 : 0.065359  
C8 -C9 -C10 -H15 : -179.721139  
C9 -C8 -C7 -H13 : -179.996490  
C9 -C10 -C11 -H16 : -179.494024  
C10 -C9 -C8 -H14 : 179.875302  
C10 -C11 -C6 -C17 : 179.864140  
C11 -C6 -C7 -H13 : -179.832664  
C11 -C6 -C17 -C16 : -3.978809  
C11 -C6 -C17 -H19 : 176.470840  
H13 -C7 -C6 -C17 : 0.021690  
H13 -C7 -C8 -H14 : 0.064307  
H15 -C10 -C11 -H16 : 0.296564

H16	-C11	-C6	-C17	:	-0.531062
C16	-C23	-C22	-C21	:	-179.998850
C16	-C23	-C22	-H28	:	-0.305063
C16	-C23	-C24	-C25	:	-179.989890
C16	-C23	-C24	-H29	:	-0.015079
C17	-C16	-C23	-C22	:	-2.755979
C17	-C16	-C23	-C24	:	177.424573
H19	-C17	-C16	-H20	:	178.859455
H19	-C17	-C16	-C23	:	-0.725348
H20	-C16	-C23	-C22	:	177.643823
H20	-C16	-C23	-C24	:	-2.175625
C20	-C21	-C22	-C23	:	0.062969
C20	-C21	-C22	-H28	:	-179.634333
C20	-C25	-C24	-C23	:	-0.063450
C20	-C25	-C24	-H29	:	179.961847
C20	-C31	-C30	-H34	:	-0.279898
C20	-C31	-C30	-C37	:	179.830364
C21	-C20	-C25	-C24	:	-0.055910
C21	-C20	-C25	-H30	:	179.811618
C21	-C20	-C31	-C30	:	179.236750
C21	-C20	-C31	-H33	:	-0.714423
C21	-C22	-C23	-C24	:	-0.176168
C22	-C21	-C20	-C25	:	0.056174
C22	-C21	-C20	-C31	:	179.868389
C22	-C23	-C24	-C25	:	0.177648
C22	-C23	-C24	-H29	:	-179.847541
C23	-C22	-C21	-H27	:	179.912463
C23	-C24	-C25	-H30	:	-179.932621
C24	-C23	-C22	-H28	:	179.517618
C24	-C25	-C20	-C31	:	-179.857650

C25	-C20	-C21	-H27	:-179.793938
C25	-C20	-C31	-C30	: -0.965386
C25	-C20	-C31	-H33	: 179.083441
H27	-C21	-C20	-C31	: 0.018277
H27	-C21	-C22	-H28	: 0.215161
H29	-C24	-C25	-H30	: 0.092675
H30	-C25	-C20	-C31	: 0.009878
C30	-C37	-C36	-C35	:-179.983413
C30	-C37	-C36	-H42	: -0.112234
C30	-C37	-C38	-C39	:-179.992903
C30	-C37	-C38	-H43	: -0.021357
C31	-C30	-C37	-C36	: -1.173722
C31	-C30	-C37	-C38	: 178.924843
H33	-C31	-C30	-H34	: 179.669429
H33	-C31	-C30	-C37	: -0.220310
H34	-C30	-C37	-C36	: 178.932497
H34	-C30	-C37	-C38	: -0.968938
C34	-C35	-C36	-C37	: 0.010563
C34	-C35	-C36	-H42	:-179.862103
C34	-C39	-C38	-C37	: -0.046312
C34	-C39	-C38	-H43	: 179.982264
C34	-C45	-C44	-H48	: 0.024060
C34	-C45	-C44	-C51	:-179.864548
C35	-C34	-C39	-C38	: -0.026155
C35	-C34	-C39	-H44	: 179.926751
C35	-C34	-C45	-C44	: 179.700303
C35	-C34	-C45	-H47	: -0.232156
C35	-C36	-C37	-C38	: -0.080250
C36	-C35	-C34	-C39	: 0.043834
C36	-C35	-C34	-C45	:-179.978964

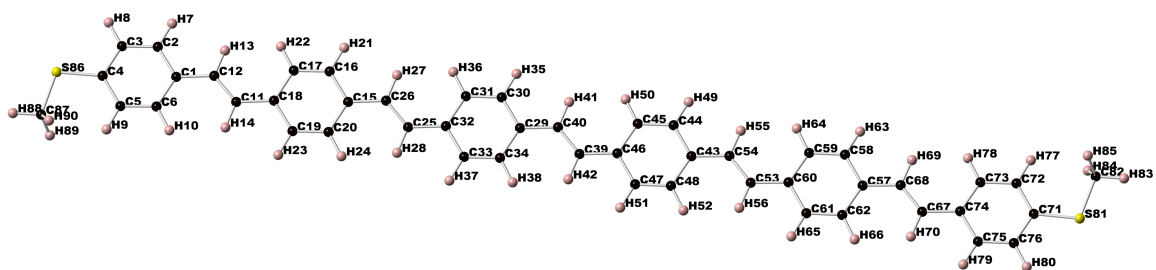
C36 -C37 -C38 -C39 : 0.098479  
C36 -C37 -C38 -H43 :-179.929975  
C37 -C36 -C35 -H41 : 179.964319  
C37 -C38 -C39 -H44 :-179.999822  
C38 -C37 -C36 -H42 : 179.790929  
C38 -C39 -C34 -C45 : 179.997894  
C39 -C34 -C35 -H41 :-179.910114  
C39 -C34 -C45 -C44 : -0.324233  
C39 -C34 -C45 -H47 : 179.743308  
H41 -C35 -C34 -C45 : 0.067088  
H41 -C35 -C36 -H42 : 0.091653  
H43 -C38 -C39 -H44 : 0.028754  
H44 -C39 -C34 -C45 : -0.049200  
C44 -C51 -C50 -C49 : 179.770172  
C44 -C51 -C50 -H56 : -0.180136  
C44 -C51 -C52 -C53 :-179.784500  
C44 -C51 -C52 -H57 : 0.080455  
C45 -C44 -C51 -C50 : -0.147711  
C45 -C44 -C51 -C52 : 179.714761  
H47 -C45 -C44 -H48 : 179.953955  
H47 -C45 -C44 -C51 : 0.065347  
H48 -C44 -C51 -C50 : 179.959520  
H48 -C44 -C51 -C52 : -0.178009  
C48 -C49 -C50 -C51 : 0.062909  
C48 -C49 -C50 -H56 :-179.986236  
C48 -C53 -C52 -C51 : -0.048434  
C48 -C53 -C52 -H57 :-179.912821  
C48 -C59 -C58 -H62 : 0.406067  
C48 -C59 -C58 -C65 :-179.666674  
C49 -C48 -C53 -C52 : 0.011355

C49 -C48 -C53 -H58 :-179.782015  
C49 -C48 -C59 -C58 :-178.723701  
C49 -C48 -C59 -H61 : 1.182467  
C49 -C50 -C51 -C52 : -0.094535  
C50 -C49 -C48 -C53 : -0.018814  
C50 -C49 -C48 -C59 :-179.883409  
C50 -C51 -C52 -C53 : 0.088161  
C50 -C51 -C52 -H57 : 179.953117  
C51 -C50 -C49 -H55 :-179.957823  
C51 -C52 -C53 -H58 : 179.747580  
C52 -C51 -C50 -H56 : 179.955158  
C52 -C53 -C48 -C59 : 179.868537  
C53 -C48 -C49 -H55 :-179.998167  
C53 -C48 -C59 -C58 : 1.422043  
C53 -C48 -C59 -H61 :-178.671789  
H55 -C49 -C48 -C59 : 0.137238  
H55 -C49 -C50 -H56 : -0.006967  
H57 -C52 -C53 -H58 : -0.116807  
H58 -C53 -C48 -C59 : 0.075167  
C58 -C65 -C64 -C63 : 179.883903  
C58 -C65 -C64 -H70 : 0.043029  
C58 -C65 -C66 -C67 :-179.887894  
C58 -C65 -C66 -H71 : 0.101880  
C59 -C58 -C65 -C64 : 1.319734  
C59 -C58 -C65 -C66 :-178.827417  
H61 -C59 -C58 -H62 :-179.496469  
H61 -C59 -C58 -C65 : 0.430790  
H62 -C58 -C65 -C64 :-178.750289  
H62 -C58 -C65 -C66 : 1.102560  
C62 -C63 -C64 -C65 : -0.027616

C62	-C63	-C64	-H70	: 179.815918
C62	-C67	-C66	-C65	: 0.020108
C62	-C67	-C66	-H71	:-179.969667
C62	-S72	-C73	-H74	: 179.786408
C62	-S72	-C73	-H75	:-62.116740
C62	-S72	-C73	-H76	: 61.706590
C63	-C62	-C67	-C66	: -0.017943
C63	-C62	-C67	-H72	:-179.971688
C63	-C62	-S72	-C73	: 0.513166
C63	-C64	-C65	-C66	: 0.028057
C64	-C63	-C62	-C67	: 0.021628
C64	-C63	-C62	-S72	:-179.938191
C64	-C65	-C66	-C67	: -0.024369
C64	-C65	-C66	-H71	: 179.965404
C65	-C64	-C63	-H69	:-179.950594
C65	-C66	-C67	-H72	: 179.973935
C66	-C65	-C64	-H70	:-179.812817
C66	-C67	-C62	-S72	: 179.945061
C67	-C62	-C63	-H69	: 179.943087
C67	-C62	-S72	-C73	:-179.447223
H69	-C63	-C62	-S72	: -0.016733
H69	-C63	-C64	-H70	: -0.107060
H71	-C66	-C67	-H72	: -0.015840
H72	-C67	-C62	-S72	: -0.008684



## MeS-PPV5



Final geometry:

angstroms

atom	x	y	z
C1	-1.2260462267	0.3579924365	-1.1912687316
C2	-1.9451433869	1.5143222637	-1.5543536908
C3	-3.3321508011	1.5410139852	-1.5701760686
C4	-4.0705439251	0.4000316963	-1.2183763534
C5	-3.3721415961	-0.7601042313	-0.8529060455
C6	-1.9811820900	-0.7754703468	-0.8407813309
H8	-1.3969118741	2.4116030011	-1.8309148448
H9	-3.8491786577	2.4527437179	-1.8563300523
H11	-3.9053294589	-1.6612156475	-0.5724085057
H12	-1.4797458221	-1.6922188305	-0.5472549862
C12	1.0918339132	-0.6041957352	-0.9198185506
C13	0.2368338773	0.4039955776	-1.1969272103
H15	0.6485756540	1.3761171091	-1.4618195927
H16	0.6806413772	-1.5794524541	-0.6641081912
C16	5.4147608938	-0.6024479784	-0.8876820356
C17	4.6945115194	0.5740241529	-1.1831882778
C18	3.3084940056	0.6026909642	-1.2009440220
C19	2.5536688516	-0.5535371990	-0.9222683998
C20	3.2740981866	-1.7296689250	-0.6263111559

C21	4.6597629397	-1.7584708977	-0.6087400194
H23	5.2466793137	1.4847742903	-1.4021966151
H24	2.8073417747	1.5370630217	-1.4321623078
H25	2.7217603493	-2.6398725301	-0.4056319262
H26	5.1606415211	-2.6919616033	-0.3739334541
C26	7.7273579553	-1.5733739918	-0.6332940222
C27	6.8760813399	-0.5544614498	-0.8859579157
H29	7.2903618256	0.4250637935	-1.1173247246
H30	7.3103555804	-2.5517566025	-0.4027266921
C30	12.0483092562	-1.6091203386	-0.5823905903
C31	11.3401213969	-0.4247293994	-0.8763946008
C32	9.9545642494	-0.3831413110	-0.8998252667
C33	9.1883728472	-1.5336974394	-0.6282465483
C34	9.8967456999	-2.7179317532	-0.3341162049
C35	11.2817554598	-2.7594374319	-0.3107023479
H37	11.9017745401	0.4811894066	-1.0911462125
H38	9.4624516558	0.5556206204	-1.1326924229
H39	9.3351303207	-3.6238936863	-0.1196959966
H40	11.7732093934	-3.6985422157	-0.0784892773
C40	14.3498606676	-2.6031632798	-0.3209317082
C41	13.5099421846	-1.5757599180	-0.5775211892
H43	13.9348931399	-0.6012550486	-0.8105032772
H44	13.9218363060	-3.5759942567	-0.0870903932
C44	18.6696625864	-2.6920840947	-0.2749081179
C45	17.9760221626	-1.5007583110	-0.5759388410
C46	16.5911274781	-1.4414686036	-0.5971138743
C47	15.8112028399	-2.5804297775	-0.3163186010
C48	16.5053392926	-3.7710522034	-0.0149223257
C49	17.8895204012	-3.8304733906	0.0065107307
H51	18.5489258936	-0.6038380058	-0.7984274229

H52	16.1104119800	-0.4984508817	-0.8363063024
H53	15.9333805736	-4.6683356002	0.2062712880
H54	18.3694690216	-4.7743136979	0.2436745257
C54	20.9615160980	-3.7095949664	-0.0072326084
C55	20.1312303931	-2.6771027434	-0.2747767119
H57	20.5663642354	-1.7108060607	-0.5222479947
H58	20.5260926786	-4.6750287705	0.2433465503
C58	25.2815426443	-3.8174408025	0.0099915749
C59	24.5893847811	-2.6301538937	-0.3082450180
C60	23.2049436103	-2.5666037726	-0.3198601524
C61	22.4232061833	-3.6970160140	-0.0117781507
C62	23.1151581254	-4.8845527265	0.3066618195
C63	24.5000564114	-4.9479121473	0.3185374567
H65	25.1633298329	-1.7394486312	-0.5519656294
H66	22.7259778238	-1.6265495444	-0.5735709569
H67	22.5412729936	-5.7758907869	0.5485455237
H68	24.9792664616	-5.8889739753	0.5684347970
C68	27.5790772656	-4.8231292481	0.2879227543
C69	26.7437724510	-3.8024106347	-0.0026686605
H71	27.1744191668	-2.8424490759	-0.2812172855
H72	27.1495525946	-5.7814216884	0.5741504797
C72	31.8859560224	-4.9072791869	0.2699393884
C73	31.2079833664	-3.7363717980	-0.0997563201
C74	29.8175832205	-3.6922896216	-0.0989498611
C75	29.0426988532	-4.8067246313	0.2692217275
C76	29.7414098694	-5.9739374486	0.6372478416
C77	31.1277083091	-6.0292793946	0.6399566537
H79	31.7570144202	-2.8489471369	-0.3931520683
H80	29.3325697853	-2.7676958613	-0.3953734722
H81	29.1775722988	-6.8571197957	0.9274591397

H82	31.6286179231	-6.9488666468	0.9296047283
S82	33.6579830330	-5.0872275326	0.3077330446
C83	34.2675575354	-3.4661305320	-0.2565826101
H84	35.3565051829	-3.5466357272	-0.2552257079
H85	33.9306148517	-3.2424404176	-1.2713734128
H86	33.9716979743	-2.6657485909	0.4254238860
S86	-5.8453208476	0.5448123940	-1.2711008498
C87	-6.4278390181	-1.0922097916	-0.7247303911
H88	-7.5181066773	-1.0338043504	-0.7375546737
H89	-6.1081631481	-1.8813738382	-1.4090783883
H90	-6.0976724341	-1.3164478165	0.2921755196

Total energy (hartrees): -2649.62277737387

HOMO energy (hartrees): -0.17781

LUMO energy (hartrees): -0.07821

Bond lengths (angstroms):

C1	-C2	: 1.409266	C1	-C6	: 1.406346
C1	-C13	: 1.463614	C2	-C3	: 1.387354
C2	-H8	: 1.087270	C3	-C4	: 1.403862
C3	-H9	: 1.086487	C4	-C5	: 1.402587
C4	-S86	: 1.781453	C5	-C6	: 1.391097
C5	-H11	: 1.083960	C6	-H12	: 1.085368
C12	-C13	: 1.350653	C12	-H16	: 1.088849
C12	-C19	: 1.462714	C13	-H15	: 1.088448
C16	-C17	: 1.410734	C16	-C21	: 1.408623
C16	-C27	: 1.462109	C17	-C18	: 1.386428

C17	-H23	: 1.087345	C18	-C19	: 1.408646
C18	-H24	: 1.085203	C19	-C20	: 1.410636
C20	-C21	: 1.386075	C20	-H25	: 1.087312
C21	-H26	: 1.085089	C26	-C27	: 1.351552
C26	-H30	: 1.088249	C26	-C33	: 1.461562
C27	-H29	: 1.088406	C30	-C31	: 1.410940
C30	-C35	: 1.408776	C30	-C41	: 1.462022
C31	-C32	: 1.386379	C31	-H37	: 1.087318
C32	-C33	: 1.408753	C32	-H38	: 1.085208
C33	-C34	: 1.410927	C34	-C35	: 1.385829
C34	-H39	: 1.087269	C35	-H40	: 1.085066
C40	-C41	: 1.351613	C40	-H44	: 1.088249
C40	-C47	: 1.461526	C41	-H43	: 1.088358
C44	-C45	: 1.411033	C44	-C49	: 1.408456
C44	-C55	: 1.461645	C45	-C46	: 1.386325
C45	-H51	: 1.087284	C46	-C47	: 1.408673
C46	-H52	: 1.085165	C47	-C48	: 1.410761
C48	-C49	: 1.385622	C48	-H53	: 1.086821
C49	-H54	: 1.085095	C54	-C55	: 1.351664
C54	-H58	: 1.088323	C54	-C61	: 1.461751
C55	-H57	: 1.088261	C58	-C59	: 1.410676
C58	-C63	: 1.408505	C58	-C69	: 1.462362
C59	-C60	: 1.385948	C59	-H65	: 1.087276
C60	-C61	: 1.408496	C60	-H66	: 1.085117
C61	-C62	: 1.410831	C62	-C63	: 1.386398
C62	-H67	: 1.087352	C63	-H68	: 1.085213
C68	-C69	: 1.350572	C68	-H72	: 1.088459
C68	-C75	: 1.463833	C69	-H71	: 1.088381
C72	-C73	: 1.402621	C72	-C77	: 1.403829
C72	-S82	: 1.781541	C73	-C74	: 1.391099

C73 -H79 : 1.083992 C74 -C75 : 1.406400  
 C74 -H80 : 1.085347 C75 -C76 : 1.409264  
 C76 -C77 : 1.387405 C76 -H81 : 1.087266  
 C77 -H82 : 1.086484 S82 -C83 : 1.821535  
 C83 -H84 : 1.091920 C83 -H85 : 1.092414  
 C83 -H86 : 1.092372 S86 -C87 : 1.821453  
 C87 -H88 : 1.091906 C87 -H89 : 1.092385  
 C87 -H90 : 1.092424

Bond angles:

C6 -C1 -C2 : 116.841992 C13 -C1 -C2 : 118.896035  
 C13 -C1 -C6 : 124.261814 C3 -C2 -C1 : 121.928502  
 H8 -C2 -C1 : 119.037847 H8 -C2 -C3 : 119.033635  
 C4 -C3 -C2 : 120.487250 H9 -C3 -C2 : 119.663210  
 H9 -C3 -C4 : 119.849517 C5 -C4 -C3 : 118.401629  
 S86 -C4 -C3 : 116.777841 S86 -C4 -C5 : 124.820494  
 C6 -C5 -C4 : 120.617027 H11 -C5 -C4 : 120.671187  
 H11 -C5 -C6 : 118.711653 C5 -C6 -C1 : 121.723513  
 H12 -C6 -C1 : 120.005352 H12 -C6 -C5 : 118.270699  
 H16 -C12 -C13 : 118.535385 C19 -C12 -C13 : 127.333322  
 C19 -C12 -H16 : 114.131105 C12 -C13 -C1 : 127.477848  
 H15 -C13 -C1 : 114.023196 H15 -C13 -C12 : 118.498690  
 C21 -C16 -C17 : 116.886946 C27 -C16 -C17 : 118.891401  
 C27 -C16 -C21 : 124.221582 C18 -C17 -C16 : 122.027370  
 H23 -C17 -C16 : 118.778846 H23 -C17 -C18 : 119.193747  
 C19 -C18 -C17 : 121.076872 H24 -C18 -C17 : 118.829175  
 H24 -C18 -C19 : 120.093782 C18 -C19 -C12 : 124.352847  
 C20 -C19 -C12 : 118.762368 C20 -C19 -C18 : 116.884708  
 C21 -C20 -C19 : 122.042337 H25 -C20 -C19 : 118.757211

H25	-C20	-C21	: 119.200452	C20	-C21	-C16	: 121.081745
H26	-C21	-C16	: 120.096609	H26	-C21	-C20	: 118.821611
H30	-C26	-C27	: 118.426490	C33	-C26	-C27	: 127.574705
C33	-C26	-H30	: 113.998803	C26	-C27	-C16	: 127.228066
H29	-C27	-C16	: 114.186692	H29	-C27	-C26	: 118.585240
C35	-C30	-C31	: 116.904374	C41	-C30	-C31	: 118.903298
C41	-C30	-C35	: 124.192314	C32	-C31	-C30	: 122.027859
H37	-C31	-C30	: 118.768726	H37	-C31	-C32	: 119.203409
C33	-C32	-C31	: 121.050884	H38	-C32	-C31	: 118.867153
H38	-C32	-C33	: 120.081956	C32	-C33	-C26	: 124.414870
C34	-C33	-C26	: 118.672916	C34	-C33	-C32	: 116.912211
C35	-C34	-C33	: 122.034181	H39	-C34	-C33	: 118.760263
H39	-C34	-C35	: 119.205556	C34	-C35	-C30	: 121.070490
H40	-C35	-C30	: 120.100675	H40	-C35	-C34	: 118.828832
H44	-C40	-C41	: 118.417422	C47	-C40	-C41	: 127.597929
C47	-C40	-H44	: 113.984641	C40	-C41	-C30	: 127.195857
H43	-C41	-C30	: 114.208954	H43	-C41	-C40	: 118.595185
C49	-C44	-C45	: 116.919766	C55	-C44	-C45	: 118.876490
C55	-C44	-C49	: 124.203651	C46	-C45	-C44	: 122.035410
H51	-C45	-C44	: 118.757727	H51	-C45	-C46	: 119.206845
C47	-C46	-C45	: 121.028475	H52	-C46	-C45	: 118.885677
H52	-C46	-C47	: 120.085788	C46	-C47	-C40	: 124.439553
C48	-C47	-C40	: 118.653709	C48	-C47	-C46	: 116.906626
C49	-C48	-C47	: 122.074075	H53	-C48	-C47	: 118.771375
H53	-C48	-C49	: 119.154535	C48	-C49	-C44	: 121.035633
H54	-C49	-C44	: 120.113367	H54	-C49	-C48	: 118.850942
H58	-C54	-C55	: 118.517534	C61	-C54	-C55	: 127.376855
C61	-C54	-H58	: 114.105601	C54	-C55	-C44	: 127.331500
H57	-C55	-C44	: 114.135919	H57	-C55	-C54	: 118.532577
C63	-C58	-C59	: 116.916487	C69	-C58	-C59	: 118.685993

C69 -C58 -C63 : 124.397384 C60 -C59 -C58 : 122.046418  
H65 -C59 -C58 : 118.753633 H65 -C59 -C60 : 119.199940  
C61 -C60 -C59 : 121.049555 H66 -C60 -C59 : 118.855251  
H66 -C60 -C61 : 120.095090 C60 -C61 -C54 : 124.234358  
C62 -C61 -C54 : 118.848225 C62 -C61 -C60 : 116.917184  
C63 -C62 -C61 : 122.027583 H67 -C62 -C61 : 118.773446  
H67 -C62 -C63 : 119.198931 C62 -C63 -C58 : 121.042763  
H68 -C63 -C58 : 120.094739 H68 -C63 -C62 : 118.862315  
H72 -C68 -C69 : 118.548578 C75 -C68 -C69 : 127.385494  
C75 -C68 -H72 : 114.065850 C68 -C69 -C58 : 127.502497  
H71 -C69 -C58 : 114.011617 H71 -C69 -C68 : 118.485825  
C77 -C72 -C73 : 118.398594 S82 -C72 -C73 : 124.798496  
S82 -C72 -C77 : 116.802909 C74 -C73 -C72 : 120.625160  
H79 -C73 -C72 : 120.659968 H79 -C73 -C74 : 118.714795  
C75 -C74 -C73 : 121.717721 H80 -C74 -C73 : 118.260845  
H80 -C74 -C75 : 120.021188 C74 -C75 -C68 : 124.271496  
C76 -C75 -C68 : 118.888636 C76 -C75 -C74 : 116.839672  
C77 -C76 -C75 : 121.934561 H81 -C76 -C75 : 119.036801  
H81 -C76 -C77 : 119.028637 C76 -C77 -C72 : 120.484268  
H82 -C77 -C72 : 119.849136 H82 -C77 -C76 : 119.666549  
C83 -S82 -C72 : 103.673985 H84 -C83 -S82 : 105.529686  
H85 -C83 -S82 : 111.518704 H85 -C83 -H84 : 108.895943  
H86 -C83 -S82 : 111.593478 H86 -C83 -H84 : 108.865567  
H86 -C83 -H85 : 110.267371 C87 -S86 -C4 : 103.691339  
H88 -C87 -S86 : 105.529431 H89 -C87 -S86 : 111.577921  
H89 -C87 -H88 : 108.873836 H90 -C87 -S86 : 111.533994  
H90 -C87 -H88 : 108.886347 H90 -C87 -H89 : 110.269075

Torsional angles:



C1 -C2 -C3 -C4 : 0.063144  
C1 -C2 -C3 -H9 :-179.991645  
C1 -C6 -C5 -C4 : -0.045624  
C1 -C6 -C5 -H11 :-179.913486  
C1 -C13 -C12 -H16 : 0.380777  
C1 -C13 -C12 -C19 :-179.787230  
C2 -C1 -C6 -C5 : 0.100505  
C2 -C1 -C6 -H12 :-179.655226  
C2 -C1 -C13 -C12 :-177.916404  
C2 -C1 -C13 -H15 : 1.891823  
C2 -C3 -C4 -C5 : -0.003120  
C2 -C3 -C4 -S86 : 179.930595  
C3 -C2 -C1 -C6 : -0.109467  
C3 -C2 -C1 -C13 :-179.970634  
C3 -C4 -C5 -C6 : -0.005453  
C3 -C4 -C5 -H11 : 179.859806  
C3 -C4 -S86 -C87 :-178.776849  
C4 -C3 -C2 -H8 :-179.984271  
C4 -C5 -C6 -H12 : 179.714196  
C4 -S86 -C87 -H88 : 179.517230  
C4 -S86 -C87 -H89 : -62.387394  
C4 -S86 -C87 -H90 : 61.429977  
C5 -C4 -C3 -H9 :-179.948229  
C5 -C4 -S86 -C87 : 1.152127  
C5 -C6 -C1 -C13 : 179.953438  
C6 -C1 -C2 -H8 : 179.937951  
C6 -C1 -C13 -C12 : 2.233479  
C6 -C1 -C13 -H15 :-177.958295  
C6 -C5 -C4 -S86 :-179.933369  
H8 -C2 -C1 -C13 : 0.076783

H8	-C2	-C3	-H9	:	-0.039060
H9	-C3	-C4	-S86	:	-0.014514
H11	-C5	-C4	-S86	:	-0.068110
H11	-C5	-C6	-H12	:	-0.153666
H12	-C6	-C1	-C13	:	0.197706
C12	-C19	-C18	-C17	:	179.941395
C12	-C19	-C18	-H24	:	0.093370
C12	-C19	-C20	-C21	:	-179.958011
C12	-C19	-C20	-H25	:	0.041138
C13	-C12	-C19	-C18	:	1.232000
C13	-C12	-C19	-C20	:	-178.872310
H15	-C13	-C12	-H16	:	-179.419910
H15	-C13	-C12	-C19	:	0.412083
H16	-C12	-C19	-C18	:	-178.929731
H16	-C12	-C19	-C20	:	0.965960
C16	-C17	-C18	-C19	:	-0.021387
C16	-C17	-C18	-H24	:	179.828521
C16	-C21	-C20	-C19	:	0.042144
C16	-C21	-C20	-H25	:	-179.957003
C16	-C27	-C26	-H30	:	0.049204
C16	-C27	-C26	-C33	:	-179.936114
C17	-C16	-C21	-C20	:	-0.016463
C17	-C16	-C21	-H26	:	-179.947612
C17	-C16	-C27	-C26	:	-179.722401
C17	-C16	-C27	-H29	:	0.296968
C17	-C18	-C19	-C20	:	0.043916
C18	-C17	-C16	-C21	:	0.006444
C18	-C17	-C16	-C27	:	-179.900947
C18	-C19	-C20	-C21	:	-0.054562
C18	-C19	-C20	-H25	:	179.944588

C19	-C18	-C17	-H23	:-179.951398
C19	-C20	-C21	-H26	: 179.974152
C20	-C19	-C18	-H24	:-179.804110
C20	-C21	-C16	-C27	: 179.885477
C21	-C16	-C17	-H23	: 179.936734
C21	-C16	-C27	-C26	: 0.377492
C21	-C16	-C27	-H29	:-179.603139
H23	-C17	-C16	-C27	: 0.029343
H23	-C17	-C18	-H24	: -0.101489
H25	-C20	-C21	-H26	: -0.024994
H26	-C21	-C16	-C27	: -0.045672
C26	-C33	-C32	-C31	:-179.972614
C26	-C33	-C32	-H38	: -0.003315
C26	-C33	-C34	-C35	: 179.974086
C26	-C33	-C34	-H39	: -0.028083
C27	-C26	-C33	-C32	: -0.166887
C27	-C26	-C33	-C34	: 179.852790
H29	-C27	-C26	-H30	:-179.970918
H29	-C27	-C26	-C33	: 0.043765
H30	-C26	-C33	-C32	: 179.847247
H30	-C26	-C33	-C34	: -0.133076
C30	-C31	-C32	-C33	: -0.000876
C30	-C31	-C32	-H38	:-179.970541
C30	-C35	-C34	-C33	: 0.000136
C30	-C35	-C34	-H39	:-179.997685
C30	-C41	-C40	-H44	: -0.100490
C30	-C41	-C40	-C47	: 179.863889
C31	-C30	-C35	-C34	: 0.007064
C31	-C30	-C35	-H40	: 179.986039
C31	-C30	-C41	-C40	:-179.976856

C31	-C30	-C41	-H43	: -0.001257
C31	-C32	-C33	-C34	: 0.008025
C32	-C31	-C30	-C35	: -0.006736
C32	-C31	-C30	-C41	: 179.951227
C32	-C33	-C34	-C35	: -0.007710
C32	-C33	-C34	-H39	: 179.990120
C33	-C32	-C31	-H37	: 179.969705
C33	-C34	-C35	-H40	: -179.979102
C34	-C33	-C32	-H38	: 179.977325
C34	-C35	-C30	-C41	: -179.948446
C35	-C30	-C31	-H37	: -179.977441
C35	-C30	-C41	-C40	: -0.022175
C35	-C30	-C41	-H43	: 179.953424
H37	-C31	-C30	-C41	: -0.019477
H37	-C31	-C32	-H38	: 0.000040
H39	-C34	-C35	-H40	: 0.023077
H40	-C35	-C30	-C41	: 0.030529
C40	-C47	-C46	-C45	: -179.835521
C40	-C47	-C46	-H52	: 0.074371
C40	-C47	-C48	-C49	: 179.853327
C40	-C47	-C48	-H53	: -0.102317
C41	-C40	-C47	-C46	: -0.394904
C41	-C40	-C47	-C48	: 179.730906
H43	-C41	-C40	-H44	: 179.924856
H43	-C41	-C40	-C47	: -0.110764
H44	-C40	-C47	-C46	: 179.570807
H44	-C40	-C47	-C48	: -0.303382
C44	-C45	-C46	-C47	: -0.017734
C44	-C45	-C46	-H52	: -179.928687
C44	-C49	-C48	-C47	: -0.003802

C44 -C49 -C48 -H53 : 179.951677  
C44 -C55 -C54 -H58 : -0.215402  
C44 -C55 -C54 -C61 : 179.747062  
C45 -C44 -C49 -C48 : 0.027439  
C45 -C44 -C49 -H54 : 179.938996  
C45 -C44 -C55 -C54 : 179.687812  
C45 -C44 -C55 -H57 : -0.333506  
C45 -C46 -C47 -C48 : 0.040673  
C46 -C45 -C44 -C49 : -0.016927  
C46 -C45 -C44 -C55 : 179.877254  
C46 -C47 -C48 -C49 : -0.030318  
C46 -C47 -C48 -H53 :-179.985961  
C47 -C46 -C45 -H51 : 179.931161  
C47 -C48 -C49 -H54 :-179.916454  
C48 -C47 -C46 -H52 : 179.950565  
C48 -C49 -C44 -C55 :-179.860521  
C49 -C44 -C45 -H51 :-179.966043  
C49 -C44 -C55 -C54 : -0.426273  
C49 -C44 -C55 -H57 : 179.552410  
H51 -C45 -C44 -C55 : -0.071862  
H51 -C45 -C46 -H52 : 0.020208  
H53 -C48 -C49 -H54 : 0.039024  
H54 -C49 -C44 -C55 : 0.051036  
C54 -C61 -C60 -C59 :-179.785513  
C54 -C61 -C60 -H66 : 0.095572  
C54 -C61 -C62 -C63 : 179.809879  
C54 -C61 -C62 -H67 : -0.115960  
C55 -C54 -C61 -C60 : -0.651823  
C55 -C54 -C61 -C62 : 179.529244  
H57 -C55 -C54 -H58 : 179.806741

H57	-C55	-C54	-C61	:	-0.230795
H58	-C54	-C61	-C60	:	179.312044
H58	-C54	-C61	-C62	:	-0.506889
C58	-C59	-C60	-C61	:	-0.032274
C58	-C59	-C60	-H66	:	-179.914804
C58	-C63	-C62	-C61	:	0.002569
C58	-C63	-C62	-H67	:	179.928103
C58	-C69	-C68	-H72	:	-0.374722
C58	-C69	-C68	-C75	:	179.733348
C59	-C58	-C63	-C62	:	0.003497
C59	-C58	-C63	-H68	:	179.846325
C59	-C58	-C69	-C68	:	179.049823
C59	-C58	-C69	-H71	:	-0.858350
C59	-C60	-C61	-C62	:	0.036620
C60	-C59	-C58	-C63	:	0.011239
C60	-C59	-C58	-C69	:	179.882908
C60	-C61	-C62	-C63	:	-0.022236
C60	-C61	-C62	-H67	:	-179.948076
C61	-C60	-C59	-H65	:	179.933786
C61	-C62	-C63	-H68	:	-179.842160
C62	-C61	-C60	-H66	:	179.917705
C62	-C63	-C58	-C69	:	-179.860066
C63	-C58	-C59	-H65	:	-179.954966
C63	-C58	-C69	-C68	:	-1.088855
C63	-C58	-C69	-H71	:	179.002972
H65	-C59	-C58	-C69	:	-0.083297
H65	-C59	-C60	-H66	:	0.051255
H67	-C62	-C63	-H68	:	0.083374
H68	-C63	-C58	-C69	:	-0.017237
C68	-C75	-C74	-C73	:	-179.890689

C68 -C75 -C74 -H80 : -0.074502  
C68 -C75 -C76 -C77 : 179.892672  
C68 -C75 -C76 -H81 : -0.098125  
C69 -C68 -C75 -C74 : -1.650358  
C69 -C68 -C75 -C76 : 178.516120  
H71 -C69 -C68 -H72 : 179.529844  
H71 -C69 -C68 -C75 : -0.362086  
H72 -C68 -C75 -C74 : 178.453609  
H72 -C68 -C75 -C76 : -1.379913  
C72 -C73 -C74 -C75 : 0.044902  
C72 -C73 -C74 -H80 :-179.774407  
C72 -C77 -C76 -C75 : -0.030221  
C72 -C77 -C76 -H81 : 179.960577  
C72 -S82 -C83 -H84 :-179.405003  
C72 -S82 -C83 -H85 : -61.314152  
C72 -S82 -C83 -H86 : 62.501182  
C73 -C72 -C77 -C76 : 0.018154  
C73 -C72 -C77 -H82 : 179.939215  
C73 -C72 -S82 -C83 : -1.072894  
C73 -C74 -C75 -C76 : -0.054049  
C74 -C73 -C72 -C77 : -0.025364  
C74 -C73 -C72 -S82 : 179.961637  
C74 -C75 -C76 -C77 : 0.046855  
C74 -C75 -C76 -H81 :-179.943942  
C75 -C74 -C73 -H79 : 179.945158  
C75 -C76 -C77 -H82 :-179.951425  
C76 -C75 -C74 -H80 : 179.762138  
C76 -C77 -C72 -S82 :-179.969887  
C77 -C72 -C73 -H79 :-179.923670  
C77 -C72 -S82 -C83 : 178.914295

H79 -C73 -C72 -S82 : 0.063331

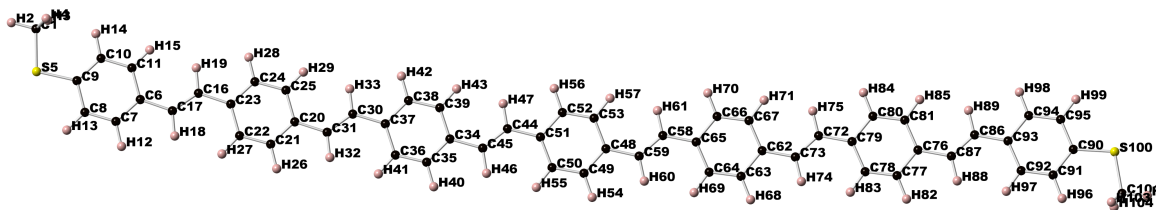
H79 -C73 -C74 -H80 : 0.125849

H81 -C76 -C77 -H82 : 0.039373

H82 -C77 -C72 -S82 : -0.048826



## MeS-PPV6



Final geometry:

atom	angstroms		
	x	y	z
C1	-5.0888493610	-0.5592865372	0.9740341311
H2	-5.6962096409	0.0665081993	1.6310116332
H4	-4.4338883222	0.0826632153	0.3806170836
H5	-4.4954173951	-1.2427496108	1.5857124329
S5	-6.2739682755	-1.4596185847	-0.0763442714
C6	-3.7296418350	-4.1362479476	-2.8590503940
C7	-5.1380682033	-4.1111001234	-2.8913718687
C8	-5.8766021681	-3.2971388435	-2.0442254446
C9	-5.2326992161	-2.4636911649	-1.1160752228
C10	-3.8310436829	-2.4765478519	-1.0683647756
C11	-3.1011376883	-3.2960263789	-1.9222904745
H13	-5.6613468548	-4.7466379316	-3.6016434991
H14	-6.9615435525	-3.3065022925	-2.1006809015
H15	-3.2953224731	-1.8494059207	-0.3650649260
H16	-2.0183770143	-3.2774179959	-1.8503103874
C16	-1.6738260256	-5.1447720259	-3.9079411331
C17	-3.0118912883	-5.0160260509	-3.7809200835
H19	-3.6569779252	-5.6146004004	-4.4214008757
H20	-1.0312957026	-4.5398715915	-3.2703194140
C20	0.6147028985	-7.6700408501	-6.5650935163

C21	-0.7957861219	-7.6983142780	-6.5819365092
C22	-1.5575763944	-6.9006239966	-5.7406140255
C23	-0.9476051528	-6.0194690848	-4.8253985362
C24	0.4625353126	-5.9924420499	-4.8086991312
C25	1.2227073824	-6.7892392673	-5.6488785843
H27	-1.2979431556	-8.3671429724	-7.2768960926
H28	-2.6394054899	-6.9642322531	-5.7964572435
H29	0.9651850265	-5.3236416429	-4.1142342553
H30	2.3041891561	-6.7243218640	-5.5919647671
C30	2.7025592895	-8.6295149892	-7.5855258832
C31	1.3586722811	-8.5349327166	-7.4784903841
H33	0.7364594770	-9.1515369440	-8.1245011595
H34	3.3164263730	-8.0096756997	-6.9344667324
C34	5.1263209065	-11.0802138269	-10.1919741447
C35	3.7178421500	-11.1408978818	-10.2520747893
C36	2.9117351178	-10.3679382231	-9.4285675970
C37	3.4726140724	-9.4805584186	-8.4880815779
C38	4.8810224318	-9.4203294271	-8.4290163065
C39	5.6848554994	-10.1920448118	-9.2512175957
H41	3.2529345819	-11.8153486505	-10.9672227179
H42	1.8337436201	-10.4545663699	-9.5187483601
H43	5.3465695560	-8.7451652999	-7.7151592956
H44	6.7620772271	-10.1008170623	-9.1611611776
C44	7.2695625369	-11.9828442681	-11.1425179714
C45	5.9205874277	-11.9201356134	-11.0871682746
H47	5.3369089996	-12.5445335489	-11.7611010912
H48	7.8411746625	-11.3551304407	-10.4612920234
C48	9.8737851915	-14.3492186184	-13.6518370175
C49	8.4711944684	-14.4473300314	-13.7771263240
C50	7.6063857604	-13.7012582027	-12.9881179629

C51	8.0995810159	-12.8053952657	-12.0178649026
C52	9.5017709499	-12.7078783122	-11.8939935672
C53	10.3634815031	-13.4523022279	-12.6816424121
H55	8.0583890241	-15.1300524938	-14.5160155346
H56	6.5357071211	-13.8166957493	-13.1273048701
H57	9.9155603692	-12.0263808349	-11.1547274102
H58	11.4324752057	-13.3355820670	-12.5382546686
C58	12.0853244874	-15.1767798142	-14.5140185129
C59	10.7332308015	-15.1641343261	-14.5097741514
H61	10.1997354772	-15.8155406489	-15.2002311173
H62	12.6085739794	-14.5206021016	-13.8207588761
C62	14.8447572743	-17.4962627794	-16.8980780286
C63	13.4503677744	-17.6380599990	-17.0660186632
C64	12.5390566040	-16.9067228494	-16.3183054924
C65	12.9741671304	-15.9808085120	-15.3488245347
C66	14.3687075714	-15.8373852904	-15.1831316200
C67	15.2788463210	-16.5682374027	-15.9301185628
H69	13.0825939365	-18.3459802025	-17.8049126700
H70	11.4774669064	-17.0584188412	-16.4880115801
H71	14.7372668632	-15.1311531109	-14.4430513190
H72	16.3392277087	-16.4175697803	-15.7567908699
C72	17.0961719172	-18.3061544886	-17.6883301656
C73	15.7444988108	-18.3070736863	-17.7160945208
H75	15.2386738178	-18.9764243077	-18.4100076649
H76	17.6015595980	-17.6357392009	-16.9951213785
C76	19.8797514592	-20.6660299625	-20.0057434247
C77	18.4871881906	-20.8113191975	-20.1797863644
C78	17.5720557355	-20.0661297665	-19.4522400250
C79	17.9993098215	-19.1216406875	-18.4975598141
C80	19.3922746895	-18.9753485131	-18.3242176469

C81	20.3074859786	-19.7208283640	-19.0518687067
H83	18.1238837646	-21.5330874525	-20.9073680377
H84	16.5127094322	-20.2228981722	-19.6266331320
H85	19.7561714970	-18.2557967599	-17.5946569213
H86	21.3668823799	-19.5681196020	-18.8735485822
C86	22.1308163918	-21.4877425073	-20.7860190758
C87	20.7804284125	-21.4926885071	-20.8072361959
H89	20.2730822193	-22.1770492679	-21.4853029958
H90	22.6376398040	-20.7999482226	-20.1117491460
C90	24.9018826383	-23.8661794432	-23.0696395741
C91	23.5210780672	-24.0500865077	-23.2350173614
C92	22.6120130266	-23.2898860113	-22.5058137752
C93	23.0355960273	-22.3161975994	-21.5826650511
C94	24.4264283360	-22.1469749248	-21.4296006617
C95	25.3414502451	-22.8989127138	-22.1521011770
H97	23.1419831346	-24.7888474443	-23.9319824292
H98	21.5525990865	-23.4661047496	-22.6619012877
H99	24.7936148973	-21.4044841437	-20.7252929591
H100	26.4058129406	-22.7369242951	-22.0056545201
S100	26.1626877725	-24.7767222561	-23.9387710010
C101	25.2189824348	-25.9036640257	-25.0144532173
H102	25.9677240215	-26.4768507713	-25.5651093236
H103	24.6037054881	-26.5936925196	-24.4326187125
H104	24.6003356684	-25.3533869219	-25.7269841404

Total energy (hartrees): -2958.09426200184

HOMO energy (hartrees): -0.17724

LUMO energy (hartrees): -0.08011

## Bond lengths (angstroms):

C1 -H2	: 1.091845	C1 -H4	: 1.092345
C1 -H5	: 1.092444	C1 -S5	: 1.821647
S5 -C9	: 1.781416	C6 -C7	: 1.409022
C6 -C11	: 1.406595	C6 -C17	: 1.462539
C7 -C8	: 1.387668	C7 -H13	: 1.087297
C8 -C9	: 1.403819	C8 -H14	: 1.086450
C9 -C10	: 1.402526	C10 -C11	: 1.390502
C10 -H15	: 1.083944	C11 -H16	: 1.085310
C16 -C17	: 1.350233	C16 -H20	: 1.088720
C16 -C23	: 1.460897	C17 -H19	: 1.088413
C20 -C21	: 1.410873	C20 -C25	: 1.408876
C20 -C31	: 1.461445	C21 -C22	: 1.387248
C21 -H27	: 1.087411	C22 -C23	: 1.409297
C22 -H28	: 1.085135	C23 -C24	: 1.410498
C24 -C25	: 1.385153	C24 -H29	: 1.087305
C25 -H30	: 1.084922	C30 -C31	: 1.351457
C30 -H34	: 1.088536	C30 -C37	: 1.460091
C31 -H33	: 1.088430	C34 -C35	: 1.411066
C34 -C39	: 1.409194	C34 -C45	: 1.462088
C35 -C36	: 1.387602	C35 -H41	: 1.087410
C36 -C37	: 1.409447	C36 -H42	: 1.085220
C37 -C38	: 1.410932	C38 -C39	: 1.384813
C38 -H43	: 1.087278	C39 -H44	: 1.084822
C44 -C45	: 1.351566	C44 -H48	: 1.088501
C44 -C51	: 1.460052	C45 -H47	: 1.088457
C48 -C49	: 1.411589	C48 -C53	: 1.409092

C48	-C59	: 1.462460	C49	-C50	: 1.388183
C49	-H55	: 1.087417	C50	-C51	: 1.409682
C50	-H56	: 1.085841	C51	-C52	: 1.411025
C52	-C53	: 1.384595	C52	-H57	: 1.087279
C53	-H58	: 1.084865	C58	-C59	: 1.352159
C58	-H62	: 1.088562	C58	-C65	: 1.460618
C59	-H61	: 1.088889	C62	-C63	: 1.411606
C62	-C67	: 1.409472	C62	-C73	: 1.461540
C63	-C64	: 1.387234	C63	-H69	: 1.087370
C64	-C65	: 1.409444	C64	-H70	: 1.085718
C65	-C66	: 1.411654	C66	-C67	: 1.385816
C66	-H71	: 1.087345	C67	-H72	: 1.084966
C72	-C73	: 1.351959	C72	-H76	: 1.088766
C72	-C79	: 1.461345	C73	-H75	: 1.088763
C76	-C77	: 1.410898	C76	-C81	: 1.409340
C76	-C87	: 1.461839	C77	-C78	: 1.386398
C77	-H83	: 1.087343	C78	-C79	: 1.409262
C78	-H84	: 1.084990	C79	-C80	: 1.411311
C80	-C81	: 1.386661	C80	-H85	: 1.087398
C81	-H86	: 1.085099	C86	-C87	: 1.350564
C86	-H90	: 1.088380	C86	-C93	: 1.462740
C87	-H89	: 1.088818	C90	-C91	: 1.402780
C90	-C95	: 1.403817	C90	-S100	: 1.781602
C91	-C92	: 1.391417	C91	-H97	: 1.084085
C92	-C93	: 1.407016	C92	-H98	: 1.085253
C93	-C94	: 1.409425	C94	-C95	: 1.387329
C94	-H99	: 1.087275	C95	-H100	: 1.086533
S100	-C101	: 1.821447	C101	-H102	: 1.091961
C101	-H103	: 1.092354	C101	-H104	: 1.092350

## Bond angles:

H4 -C1 -H2 : 108.879857 H5 -C1 -H2 : 108.895622  
H5 -C1 -H4 : 110.251238 S5 -C1 -H2 : 105.565133  
S5 -C1 -H4 : 111.548702 S5 -C1 -H5 : 111.533502  
C9 -S5 -C1 : 103.582189 C11 -C6 -C7 : 116.824138  
C17 -C6 -C7 : 119.132214 C17 -C6 -C11 : 124.043643  
C8 -C7 -C6 : 121.900959 H13 -C7 -C6 : 119.052765  
H13 -C7 -C8 : 119.046205 C9 -C8 -C7 : 120.514559  
H14 -C8 -C7 : 119.649678 H14 -C8 -C9 : 119.835756  
C8 -C9 -S5 : 116.898706 C10 -C9 -S5 : 124.713067  
C10 -C9 -C8 : 118.388217 C11 -C10 -C9 : 120.604459  
H15 -C10 -C9 : 120.710098 H15 -C10 -C11 : 118.685407  
C10 -C11 -C6 : 121.767575 H16 -C11 -C6 : 120.012439  
H16 -C11 -C10 : 118.219813 H20 -C16 -C17 : 118.475261  
C23 -C16 -C17 : 127.502496 C23 -C16 -H20 : 114.022034  
C16 -C17 -C6 : 127.084224 H19 -C17 -C6 : 114.259465  
H19 -C17 -C16 : 118.655896 C25 -C20 -C21 : 116.854568  
C31 -C20 -C21 : 119.314613 C31 -C20 -C25 : 123.830798  
C22 -C21 -C20 : 122.020665 H27 -C21 -C20 : 118.791328  
H27 -C21 -C22 : 119.188007 C23 -C22 -C21 : 121.044025  
H28 -C22 -C21 : 118.851966 H28 -C22 -C23 : 120.104009  
C22 -C23 -C16 : 124.543992 C24 -C23 -C16 : 118.559568  
C24 -C23 -C22 : 116.896410 C25 -C24 -C23 : 122.036348  
H29 -C24 -C23 : 118.784736 H29 -C24 -C25 : 119.178892  
C24 -C25 -C20 : 121.147949 H30 -C25 -C20 : 120.113039  
H30 -C25 -C24 : 118.738977 H34 -C30 -C31 : 118.265503  
C37 -C30 -C31 : 127.893660 C37 -C30 -H34 : 113.840837  
C30 -C31 -C20 : 126.664652 H33 -C31 -C20 : 114.532005  
H33 -C31 -C30 : 118.803322 C39 -C34 -C35 : 116.818316

C45 -C34 -C35 : 119.436708 C45 -C34 -C39 : 123.744959  
C36 -C35 -C34 : 122.048465 H41 -C35 -C34 : 118.779366  
H41 -C35 -C36 : 119.172168 C37 -C36 -C35 : 121.033861  
H42 -C36 -C35 : 118.899976 H42 -C36 -C37 : 120.066123  
C36 -C37 -C30 : 124.720307 C38 -C37 -C30 : 118.404925  
C38 -C37 -C36 : 116.874645 C39 -C38 -C37 : 122.058270  
H43 -C38 -C37 : 118.777102 H43 -C38 -C39 : 119.164602  
C38 -C39 -C34 : 121.166436 H44 -C39 -C34 : 120.132079  
H44 -C39 -C38 : 118.701385 H48 -C44 -C45 : 118.147622  
C51 -C44 -C45 : 128.176548 C51 -C44 -H48 : 113.675759  
C44 -C45 -C34 : 126.436222 H47 -C45 -C34 : 114.666242  
H47 -C45 -C44 : 118.897490 C53 -C48 -C49 : 116.786269  
C59 -C48 -C49 : 119.546302 C59 -C48 -C53 : 123.667236  
C50 -C49 -C48 : 122.086933 H55 -C49 -C48 : 118.760383  
H55 -C49 -C50 : 119.152683 C51 -C50 -C49 : 120.983617  
H56 -C50 -C49 : 118.965753 H56 -C50 -C51 : 120.050621  
C50 -C51 -C44 : 124.874337 C52 -C51 -C44 : 118.252577  
C52 -C51 -C50 : 116.873060 C53 -C52 -C51 : 122.097537  
H57 -C52 -C51 : 118.763672 H57 -C52 -C53 : 119.138752  
C52 -C53 -C48 : 121.172561 H58 -C53 -C48 : 120.127657  
H58 -C53 -C52 : 118.699652 H62 -C58 -C59 : 118.230481  
C65 -C58 -C59 : 127.984719 C65 -C58 -H62 : 113.784647  
C58 -C59 -C48 : 126.490895 H61 -C59 -C48 : 114.670879  
H61 -C59 -C58 : 118.838076 C67 -C62 -C63 : 116.876355  
C73 -C62 -C63 : 119.064190 C73 -C62 -C67 : 124.058895  
C64 -C63 -C62 : 122.129372 H69 -C63 -C62 : 118.707579  
H69 -C63 -C64 : 119.162921 C65 -C64 -C63 : 120.949122  
H70 -C64 -C63 : 118.974451 H70 -C64 -C65 : 120.076277  
C64 -C65 -C58 : 124.534058 C66 -C65 -C58 : 118.564576  
C66 -C65 -C64 : 116.900889 C67 -C66 -C65 : 122.136731



H71 -C66 -C65 : 118.732587 H71 -C66 -C67 : 119.130558  
C66 -C67 -C62 : 121.007304 H72 -C67 -C62 : 120.142133  
H72 -C67 -C66 : 118.850343 H76 -C72 -C73 : 118.527458  
C79 -C72 -C73 : 127.310655 C79 -C72 -H76 : 114.161768  
C72 -C73 -C62 : 127.128926 H75 -C73 -C62 : 114.316065  
H75 -C73 -C72 : 118.554567 C81 -C76 -C77 : 116.879103  
C87 -C76 -C77 : 118.832696 C87 -C76 -C81 : 124.287862  
C78 -C77 -C76 : 122.101288 H83 -C77 -C76 : 118.729592  
H83 -C77 -C78 : 119.169022 C79 -C78 -C77 : 121.038429  
H84 -C78 -C77 : 118.846677 H84 -C78 -C79 : 120.114635  
C78 -C79 -C72 : 124.177782 C80 -C79 -C72 : 118.955193  
C80 -C79 -C78 : 116.866302 C81 -C80 -C79 : 122.090125  
H85 -C80 -C79 : 118.770058 H85 -C80 -C81 : 119.139697  
C80 -C81 -C76 : 121.024709 H86 -C81 -C76 : 120.127253  
H86 -C81 -C80 : 118.847734 H90 -C86 -C87 : 118.532288  
C93 -C86 -C87 : 127.433524 C93 -C86 -H90 : 114.034118  
C86 -C87 -C76 : 127.254854 H89 -C87 -C76 : 114.191252  
H89 -C87 -C86 : 118.553889 C95 -C90 -C91 : 118.398785  
S100 -C90 -C91 : 124.895247 S100 -C90 -C95 : 116.705741  
C92 -C91 -C90 : 120.643216 H97 -C91 -C90 : 120.620378  
H97 -C91 -C92 : 118.736277 C93 -C92 -C91 : 121.684755  
H98 -C92 -C91 : 118.274274 H98 -C92 -C93 : 120.040710  
C92 -C93 -C86 : 124.267584 C94 -C93 -C86 : 118.897435  
C94 -C93 -C92 : 116.834835 C95 -C94 -C93 : 121.952928  
H99 -C94 -C93 : 119.051617 H99 -C94 -C95 : 118.995422  
C94 -C95 -C90 : 120.485421 H100 -C95 -C90 : 119.838297  
H100 -C95 -C94 : 119.676281 C101 -S100 -C90 : 103.748113  
H102 -C101 -S100 : 105.504902 H103 -C101 -S100 : 111.598412  
H103 -C101 -H102 : 108.858767 H104 -C101 -S100 : 111.528931  
H104 -C101 -H102 : 108.894344 H104 -C101 -H103 : 110.282998

## Torsional angles:

C1 -S5 -C9 -C8 : 179.415273  
C1 -S5 -C9 -C10 : -0.547750  
H2 -C1 -S5 -C9 :-179.756075  
H4 -C1 -S5 -C9 : 62.135424  
H5 -C1 -S5 -C9 : -61.636705  
S5 -C9 -C8 -C7 :-179.990916  
S5 -C9 -C8 -H14 : -0.020309  
S5 -C9 -C10 -C11 :-179.997632  
S5 -C9 -C10 -H15 : 0.073064  
C6 -C7 -C8 -C9 : -0.052013  
C6 -C7 -C8 -H14 : 179.977326  
C6 -C11 -C10 -C9 : 0.022667  
C6 -C11 -C10 -H15 : 179.953382  
C6 -C17 -C16 -H20 : -0.143611  
C6 -C17 -C16 -C23 :-179.966213  
C7 -C6 -C11 -C10 : -0.095827  
C7 -C6 -C11 -H16 : 179.750664  
C7 -C6 -C17 -C16 : 178.403494  
C7 -C6 -C17 -H19 : -1.357113  
C7 -C8 -C9 -C10 : -0.025466  
C8 -C7 -C6 -C11 : 0.110597  
C8 -C7 -C6 -C17 :-179.913926  
C8 -C9 -C10 -C11 : 0.039852  
C8 -C9 -C10 -H15 :-179.889453  
C9 -C8 -C7 -H13 :-179.954178  
C9 -C10 -C11 -H16 :-179.826476  
C10 -C9 -C8 -H14 : 179.945141

C10 -C11 -C6 -C17 : 179.930024  
C11 -C6 -C7 -H13 :-179.987244  
C11 -C6 -C17 -C16 : -1.622917  
C11 -C6 -C17 -H19 : 178.616476  
H13 -C7 -C6 -C17 : -0.011767  
H13 -C7 -C8 -H14 : 0.075161  
H15 -C10 -C11 -H16 : 0.104239  
H16 -C11 -C6 -C17 : -0.223484  
C16 -C23 -C22 -C21 : 179.867650  
C16 -C23 -C22 -H28 : -0.137238  
C16 -C23 -C24 -C25 :-179.877429  
C16 -C23 -C24 -H29 : 0.065437  
C17 -C16 -C23 -C22 : -0.603026  
C17 -C16 -C23 -C24 : 179.332275  
H19 -C17 -C16 -H20 : 179.607672  
H19 -C17 -C16 -C23 : -0.214930  
H20 -C16 -C23 -C22 : 179.567697  
H20 -C16 -C23 -C24 : -0.497001  
C20 -C21 -C22 -C23 : 0.033899  
C20 -C21 -C22 -H28 :-179.961273  
C20 -C25 -C24 -C23 : -0.021061  
C20 -C25 -C24 -H29 :-179.963709  
C20 -C31 -C30 -H34 : 0.121628  
C20 -C31 -C30 -C37 :-179.877689  
C21 -C20 -C25 -C24 : -0.016394  
C21 -C20 -C25 -H30 :-179.947383  
C21 -C20 -C31 -C30 :-179.842973  
C21 -C20 -C31 -H33 : 0.210967  
C21 -C22 -C23 -C24 : -0.068631  
C22 -C21 -C20 -C25 : 0.009999

C22	-C21	-C20	-C31	:-179.939812
C22	-C23	-C24	-C25	: 0.062816
C22	-C23	-C24	-H29	:-179.994318
C23	-C22	-C21	-H27	:-179.972502
C23	-C24	-C25	-H30	: 179.910855
C24	-C23	-C22	-H28	: 179.926480
C24	-C25	-C20	-C31	: 179.930924
C25	-C20	-C21	-H27	:-179.983625
C25	-C20	-C31	-C30	: 0.210929
C25	-C20	-C31	-H33	:-179.735131
H27	-C21	-C20	-C31	: 0.066564
H27	-C21	-C22	-H28	: 0.032327
H29	-C24	-C25	-H30	: -0.031793
H30	-C25	-C20	-C31	: -0.000064
C30	-C37	-C36	-C35	: 179.877187
C30	-C37	-C36	-H42	: -0.049290
C30	-C37	-C38	-C39	:-179.885013
C30	-C37	-C38	-H43	: 0.056390
C31	-C30	-C37	-C36	: 0.227438
C31	-C30	-C37	-C38	:-179.904340
H33	-C31	-C30	-H34	:-179.934371
H33	-C31	-C30	-C37	: 0.066312
H34	-C30	-C37	-C36	:-179.771904
H34	-C30	-C37	-C38	: 0.096318
C34	-C35	-C36	-C37	: 0.010633
C34	-C35	-C36	-H42	: 179.937951
C34	-C39	-C38	-C37	: -0.012035
C34	-C39	-C38	-H43	:-179.953219
C34	-C45	-C44	-H48	: 0.074328
C34	-C45	-C44	-C51	: 179.970456

C35 -C34 -C39 -C38 : 0.028667  
C35 -C34 -C39 -H44 :-179.854897  
C35 -C34 -C45 -C44 :-179.439886  
C35 -C34 -C45 -H47 : 0.480737  
C35 -C36 -C37 -C38 : 0.007134  
C36 -C35 -C34 -C39 : -0.028168  
C36 -C35 -C34 -C45 :-179.981542  
C36 -C37 -C38 -C39 : -0.006441  
C36 -C37 -C38 -H43 : 179.934962  
C37 -C36 -C35 -H41 :-179.980894  
C37 -C38 -C39 -H44 : 179.873157  
C38 -C37 -C36 -H42 :-179.919343  
C38 -C39 -C34 -C45 : 179.979832  
C39 -C34 -C35 -H41 : 179.963392  
C39 -C34 -C45 -C44 : 0.610157  
C39 -C34 -C45 -H47 :-179.469220  
H41 -C35 -C34 -C45 : 0.010018  
H41 -C35 -C36 -H42 : -0.053576  
H43 -C38 -C39 -H44 : -0.068027  
H44 -C39 -C34 -C45 : 0.096268  
C44 -C51 -C50 -C49 :-179.882132  
C44 -C51 -C50 -H56 : 0.082567  
C44 -C51 -C52 -C53 : 179.897795  
C44 -C51 -C52 -H57 : -0.029604  
C45 -C44 -C51 -C50 : 0.152574  
C45 -C44 -C51 -C52 :-179.786036  
H47 -C45 -C44 -H48 :-179.843279  
H47 -C45 -C44 -C51 : 0.052850  
H48 -C44 -C51 -C50 :-179.947431  
H48 -C44 -C51 -C52 : 0.113960

C48	-C49	-C50	-C51	:	-0.035019
C48	-C49	-C50	-H56	:	179.999906
C48	-C53	-C52	-C51	:	0.010726
C48	-C53	-C52	-H57	:	179.937862
C48	-C59	-C58	-H62	:	-0.237434
C48	-C59	-C58	-C65	:	179.610905
C49	-C48	-C53	-C52	:	0.013801
C49	-C48	-C53	-H58	:	179.881318
C49	-C48	-C59	-C58	:	179.622308
C49	-C48	-C59	-H61	:	-0.520993
C49	-C50	-C51	-C52	:	0.057244
C50	-C49	-C48	-C53	:	-0.001744
C50	-C49	-C48	-C59	:	179.843916
C50	-C51	-C52	-C53	:	-0.045742
C50	-C51	-C52	-H57	:	-179.973141
C51	-C50	-C49	-H55	:	179.955800
C51	-C52	-C53	-H58	:	-179.858640
C52	-C51	-C50	-H56	:	-179.978057
C52	-C53	-C48	-C59	:	-179.824870
C53	-C48	-C49	-H55	:	-179.992598
C53	-C48	-C59	-C58	:	-0.543238
C53	-C48	-C59	-H61	:	179.313461
H55	-C49	-C48	-C59	:	-0.146938
H55	-C49	-C50	-H56	:	-0.009275
H57	-C52	-C53	-H58	:	0.068496
H58	-C53	-C48	-C59	:	0.042647
C58	-C65	-C64	-C63	:	-179.632105
C58	-C65	-C64	-H70	:	0.225939
C58	-C65	-C66	-C67	:	179.638494
C58	-C65	-C66	-H71	:	-0.232156

C59	-C58	-C65	-C64	:	-0.053281
C59	-C58	-C65	-C66	:	-179.793443
H61	-C59	-C58	-H62	:	179.911222
H61	-C59	-C58	-C65	:	-0.240440
H62	-C58	-C65	-C64	:	179.800695
H62	-C58	-C65	-C66	:	0.060533
C62	-C63	-C64	-C65	:	0.012969
C62	-C63	-C64	-H70	:	-179.846613
C62	-C67	-C66	-C65	:	0.004644
C62	-C67	-C66	-H71	:	179.874796
C62	-C73	-C72	-H76	:	-0.331551
C62	-C73	-C72	-C79	:	179.535336
C63	-C62	-C67	-C66	:	0.119900
C63	-C62	-C67	-H72	:	179.947496
C63	-C62	-C73	-C72	:	-179.809170
C63	-C62	-C73	-H75	:	-0.056728
C63	-C64	-C65	-C66	:	0.111993
C64	-C63	-C62	-C67	:	-0.129405
C64	-C63	-C62	-C73	:	179.609481
C64	-C65	-C66	-C67	:	-0.121481
C64	-C65	-C66	-H71	:	-179.992131
C65	-C64	-C63	-H69	:	179.881242
C65	-C66	-C67	-H72	:	-179.825137
C66	-C65	-C64	-H70	:	179.970038
C66	-C67	-C62	-C73	:	-179.604610
C67	-C62	-C63	-H69	:	-179.998255
C67	-C62	-C73	-C72	:	-0.090304
C67	-C62	-C73	-H75	:	179.662137
H69	-C63	-C62	-C73	:	-0.259369
H69	-C63	-C64	-H70	:	0.021659

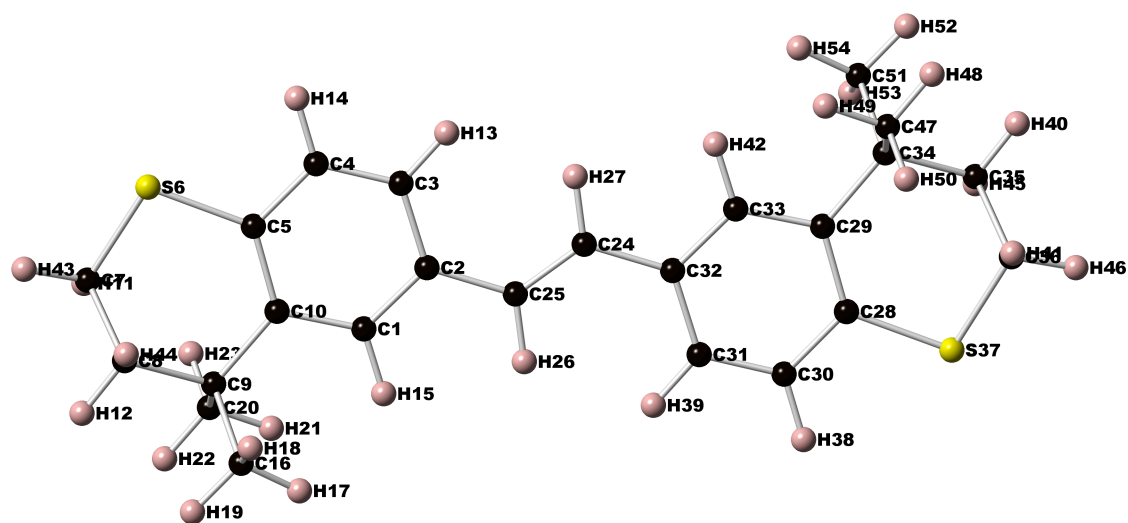
H71 -C66 -C67 -H72 : 0.045016  
H72 -C67 -C62 -C73 : 0.222986  
C72 -C79 -C78 -C77 :-179.630542  
C72 -C79 -C78 -H84 : 0.182275  
C72 -C79 -C80 -C81 : 179.640641  
C72 -C79 -C80 -H85 : -0.232361  
C73 -C72 -C79 -C78 : -0.407372  
C73 -C72 -C79 -C80 : 179.912206  
H75 -C73 -C72 -H76 : 179.925287  
H75 -C73 -C72 -C79 : -0.207826  
H76 -C72 -C79 -C78 : 179.464447  
H76 -C72 -C79 -C80 : -0.215975  
C76 -C77 -C78 -C79 : -0.000949  
C76 -C77 -C78 -H84 :-179.816093  
C76 -C81 -C80 -C79 : 0.014329  
C76 -C81 -C80 -H85 : 179.886876  
C76 -C87 -C86 -H90 : -0.333408  
C76 -C87 -C86 -C93 : 179.769114  
C77 -C76 -C81 -C80 : 0.041485  
C77 -C76 -C81 -H86 : 179.838366  
C77 -C76 -C87 -C86 : 179.524173  
C77 -C76 -C87 -H89 : -0.502025  
C77 -C78 -C79 -C80 : 0.055993  
C78 -C77 -C76 -C81 : -0.048322  
C78 -C77 -C76 -C87 : 179.749009  
C78 -C79 -C80 -C81 : -0.062983  
C78 -C79 -C80 -H85 :-179.935984  
C79 -C78 -C77 -H83 : 179.883636  
C79 -C80 -C81 -H86 :-179.785101  
C80 -C79 -C78 -H84 : 179.868810



C80 -C81 -C76 -C87 :-179.743628  
C81 -C76 -C77 -H83 :-179.933395  
C81 -C76 -C87 -C86 : -0.694623  
C81 -C76 -C87 -H89 : 179.279179  
H83 -C77 -C76 -C87 : -0.136063  
H83 -C77 -C78 -H84 : 0.068491  
H85 -C80 -C81 -H86 : 0.087446  
H86 -C81 -C76 -C87 : 0.053253  
C86 -C93 -C92 -C91 :-179.912175  
C86 -C93 -C92 -H98 : -0.101189  
C86 -C93 -C94 -C95 : 179.959825  
C86 -C93 -C94 -H99 : -0.106871  
C87 -C86 -C93 -C92 : -1.101143  
C87 -C86 -C93 -C94 : 179.042723  
H89 -C87 -C86 -H90 : 179.693798  
H89 -C87 -C86 -C93 : -0.203679  
H90 -C86 -C93 -C92 : 178.997478  
H90 -C86 -C93 -C94 : -0.858656  
C90 -C91 -C92 -C93 : -0.003626  
C90 -C91 -C92 -H98 :-179.817836  
C90 -C95 -C94 -C93 : -0.075721  
C90 -C95 -C94 -H99 : 179.990938  
C90 -S100 -C101 -H102 : 179.860644  
C90 -S100 -C101 -H103 : -62.065879  
C90 -S100 -C101 -H104 : 61.781086  
C91 -C90 -C95 -C94 : 0.014914  
C91 -C90 -C95 -H100 :-179.987527  
C91 -C90 -S100 -C101 : 0.366027  
C91 -C92 -C93 -C94 : -0.053328  
C92 -C91 -C90 -C95 : 0.023915

C92 -C91 -C90 -S100 : 179.844604  
C92 -C93 -C94 -C95 : 0.093066  
C92 -C93 -C94 -H99 :-179.973629  
C93 -C92 -C91 -H97 : 179.866514  
C93 -C94 -C95 -H100 : 179.926716  
C94 -C93 -C92 -H98 : 179.757659  
C94 -C95 -C90 -S100 :-179.820453  
C95 -C90 -C91 -H97 :-179.843768  
C95 -C90 -S100 -C101 :-179.810541  
H97 -C91 -C90 -S100 : -0.023080  
H97 -C91 -C92 -H98 : 0.052304  
H99 -C94 -C95 -H100 : -0.006625  
H100 -C95 -C90 -S100 : 0.177106

## PPV1



Final geometry:

atom	angstroms		
	x	y	z
C1	1.1804350000	-1.8512460000	0.0196610000
C2	2.4748730000	-1.3095190000	0.0337080000
C3	2.5819370000	0.0944610000	0.0305200000
C4	1.4449970000	0.8798280000	-0.0009440000
C5	0.1554660000	0.3154630000	-0.0191090000
S6	-1.1712080000	1.5074060000	-0.0471810000
C7	-2.6210960000	0.4380600000	-0.3550130000
C8	-2.5176350000	-0.8769010000	0.4075670000
C9	-1.3595510000	-1.8041640000	-0.0361400000
C10	0.0050010000	-1.0858070000	0.0061380000
H11	-2.7348350000	0.2770070000	-1.4305930000
H12	-3.4586720000	-1.4279710000	0.2812820000
H13	3.5544880000	0.5759530000	0.0435830000
H14	1.5438160000	1.9619600000	-0.0189260000

H15	1.0945400000	-2.9336650000	0.0192170000
C16	-1.3823630000	-3.0151080000	0.9247300000
H17	-0.6928870000	-3.8059010000	0.6188140000
H18	-1.1230970000	-2.7156230000	1.9450280000
H19	-2.3858650000	-3.4543360000	0.9437840000
C20	-1.6107060000	-2.3108440000	-1.4773470000
H21	-0.8343990000	-3.0209610000	-1.7776490000
H22	-2.5800680000	-2.8192580000	-1.5453940000
H23	-1.6005990000	-1.4948520000	-2.2057600000
C24	4.9300340000	-1.8797280000	0.0493290000
C25	3.6232500000	-2.2174060000	0.0502510000
H26	3.3579900000	-3.2730080000	0.0647050000
H27	5.1940270000	-0.8238650000	0.0338610000
C28	8.4056110000	-4.4015780000	0.1323610000
C29	8.5509440000	-3.0003290000	0.0912470000
C30	7.1181050000	-4.9704180000	0.1221700000
C31	5.9792070000	-4.1886920000	0.0847680000
C32	6.0806640000	-2.7845390000	0.0690180000
C33	7.3731250000	-2.2387270000	0.0746720000
C34	9.9109180000	-2.2723870000	0.1157100000
C35	11.0792750000	-3.2042190000	-0.2894150000
C36	11.1730250000	-4.5035150000	0.5009240000
S37	9.7378920000	-5.5864950000	0.1748100000
H38	7.0222750000	-6.0525170000	0.1522850000
H39	5.0078490000	-4.6732560000	0.0778730000
H40	12.0159120000	-2.6466210000	-0.1594530000
H41	11.2569500000	-4.3220600000	1.5760900000
H42	7.4557020000	-1.1560300000	0.0652730000
H43	-3.4827510000	1.0187610000	-0.0145910000
H44	-2.4197420000	-0.6583580000	1.4775390000

H45	10.9999800000	-3.4459030000	-1.3559210000
H46	12.0467150000	-5.0847890000	0.1939730000
C47	10.1508130000	-1.7137580000	1.5393550000
H48	11.1125800000	-1.1895240000	1.5922290000
H49	9.3638170000	-1.0052570000	1.8145990000
H50	10.1506350000	-2.5052430000	2.2945060000
C51	9.9268570000	-1.0959880000	-0.8877770000
H52	10.9261490000	-0.6479330000	-0.9191410000
H53	9.6743160000	-1.4348870000	-1.8973890000
H54	9.2278850000	-0.3019460000	-0.6134220000

bond lengths (angstroms):

C1	-C2	: 1.403294	C1	-C10	: 1.402756
C1	-H15	: 1.085822	C2	-C3	: 1.408060
C2	-C25	: 1.464002	C3	-C4	: 1.382181
C3	-H13	: 1.085293	C4	-C5	: 1.407739
C4	-H14	: 1.086783	C5	-S6	: 1.783698
C5	-C10	: 1.409551	S6	-C7	: 1.827686
C7	-C8	: 1.523599	C7	-H11	: 1.093502
C7	-H43	: 1.093412	C8	-C9	: 1.548500
C8	-H12	: 1.097805	C8	-H44	: 1.096442
C9	-C10	: 1.542669	C9	-C16	: 1.546020
C9	-C20	: 1.548186	C16	-H17	: 1.092847
C16	-H18	: 1.094494	C16	-H19	: 1.095582
C20	-H21	: 1.094121	C20	-H22	: 1.096712
C20	-H23	: 1.093860	C24	-C25	: 1.349708
C24	-H27	: 1.088475	C24	-C32	: 1.463906
C25	-H26	: 1.088516	C28	-C29	: 1.409365

C28	-C30	: 1.407606	C28	-S37	: 1.783481
C29	-C33	: 1.402701	C29	-C34	: 1.542734
C30	-C31	: 1.381877	C30	-H38	: 1.086751
C31	-C32	: 1.407902	C31	-H39	: 1.085535
C32	-C33	: 1.402996	C33	-H42	: 1.085882
C34	-C35	: 1.548385	C34	-C47	: 1.548025
C34	-C51	: 1.546336	C35	-C36	: 1.523678
C35	-H40	: 1.097768	C35	-H45	: 1.096419
C36	-S37	: 1.827239	C36	-H41	: 1.093596
C36	-H46	: 1.093358	C47	-H48	: 1.096637
C47	-H49	: 1.094119	C47	-H50	: 1.093939
C51	-H52	: 1.095592	C51	-H53	: 1.094507
C51	-H54	: 1.092856			

Total energy (hartrees): -1727.85570961920

HOMO energy (hartrees): -0.18021

LUMO energy (hartrees): -0.04525

bond angles:

C10	-C1	-C2	: 124.221386	H15	-C1	-C2	: 117.245450
H15	-C1	-C10	: 118.533164	C3	-C2	-C1	: 117.067279
C25	-C2	-C1	: 118.965020	C25	-C2	-C3	: 123.967698
C4	-C3	-C2	: 120.269527	H13	-C3	-C2	: 120.695586
H13	-C3	-C4	: 119.032599	C5	-C4	-C3	: 121.735349
H14	-C4	-C3	: 119.429925	H14	-C4	-C5	: 118.833452
S6	-C5	-C4	: 114.432798	C10	-C5	-C4	: 119.742220

C10 -C5 -S6 : 125.817302 C7 -S6 -C5 : 101.636755  
 C8 -C7 -S6 : 111.517982 H11 -C7 -S6 : 109.533118  
 H11 -C7 -C8 : 111.854982 H43 -C7 -S6 : 105.187450  
 H43 -C7 -C8 : 110.857675 H43 -C7 -H11 : 107.607181  
 C9 -C8 -C7 : 115.098885 H12 -C8 -C7 : 108.508807  
 H12 -C8 -C9 : 107.910210 H44 -C8 -C7 : 108.812132  
 H44 -C8 -C9 : 109.402731 H44 -C8 -H12 : 106.788723  
 C10 -C9 -C8 : 112.013777 C16 -C9 -C8 : 106.254659  
 C16 -C9 -C10 : 111.146451 C20 -C9 -C8 : 109.961681  
 C20 -C9 -C10 : 108.747879 C20 -C9 -C16 : 108.652657  
 C5 -C10 -C1 : 116.948324 C9 -C10 -C1 : 119.167602  
 C9 -C10 -C5 : 123.838492 H17 -C16 -C9 : 112.550084  
 H18 -C16 -C9 : 111.196050 H18 -C16 -H17 : 108.029138  
 H19 -C16 -C9 : 109.775889 H19 -C16 -H17 : 107.016172  
 H19 -C16 -H18 : 108.086959 H21 -C20 -C9 : 110.659292  
 H22 -C20 -C9 : 110.662592 H22 -C20 -H21 : 108.012750  
 H23 -C20 -C9 : 111.978563 H23 -C20 -H21 : 107.147481  
 H23 -C20 -H22 : 108.220119 H27 -C24 -C25 : 118.523637  
 C32 -C24 -C25 : 127.326712 C32 -C24 -H27 : 114.149593  
 C24 -C25 -C2 : 127.178853 H26 -C25 -C2 : 114.229123  
 H26 -C25 -C24 : 118.592024 C30 -C28 -C29 : 119.729206  
 S37 -C28 -C29 : 125.748001 S37 -C28 -C30 : 114.516620  
 C33 -C29 -C28 : 116.973899 C34 -C29 -C28 : 124.026447  
 C34 -C29 -C33 : 118.960093 C31 -C30 -C28 : 121.697486  
 H38 -C30 -C28 : 118.871355 H38 -C30 -C31 : 119.429470  
 C32 -C31 -C30 : 120.338239 H39 -C31 -C30 : 119.021326  
 H39 -C31 -C32 : 120.637593 C31 -C32 -C24 : 124.051902  
 C33 -C32 -C24 : 118.925735 C33 -C32 -C31 : 117.022304  
 C32 -C33 -C29 : 124.218174 H42 -C33 -C29 : 118.529380  
 H42 -C33 -C32 : 117.252445 C35 -C34 -C29 : 112.151811

C47 -C34 -C29 : 108.751736 C47 -C34 -C35 : 109.929259  
 C51 -C34 -C29 : 110.962998 C51 -C34 -C35 : 106.276051  
 C51 -C34 -C47 : 108.703597 C36 -C35 -C34 : 115.080821  
 H40 -C35 -C34 : 107.887716 H40 -C35 -C36 : 108.616460  
 H45 -C35 -C34 : 109.426110 H45 -C35 -C36 : 108.725477  
 H45 -C35 -H40 : 106.787862 S37 -C36 -C35 : 111.377124  
 H41 -C36 -C35 : 111.912783 H41 -C36 -S37 : 109.516708  
 H46 -C36 -C35 : 110.909605 H46 -C36 -S37 : 105.213182  
 H46 -C36 -H41 : 107.631809 C36 -S37 -C28 : 101.372515  
 H48 -C47 -C34 : 110.656089 H49 -C47 -C34 : 110.705573  
 H49 -C47 -H48 : 108.007977 H50 -C47 -C34 : 111.945363  
 H50 -C47 -H48 : 108.223782 H50 -C47 -H49 : 107.142106  
 H52 -C51 -C34 : 109.822239 H53 -C51 -C34 : 111.141407  
 H53 -C51 -H52 : 108.099987 H54 -C51 -C34 : 112.534941  
 H54 -C51 -H52 : 107.062243 H54 -C51 -H53 : 107.997266

torsional angles:

C1 -C2 -C3 -C4 : -0.724231  
 C1 -C2 -C3 -H13 : 179.831336  
 C1 -C2 -C25 -C24 : 179.162595  
 C1 -C2 -C25 -H26 : -0.840167  
 C1 -C10 -C5 -C4 : -1.340328  
 C1 -C10 -C5 -S6 : 179.726451  
 C1 -C10 -C9 -C8 : 161.564451  
 C1 -C10 -C9 -C16 : 42.872326  
 C1 -C10 -C9 -C20 : -76.693365  
 C2 -C1 -C10 -C5 : 1.188476  
 C2 -C1 -C10 -C9 : 178.827749  
 C2 -C3 -C4 -C5 : 0.548539



C2	-C3	-C4	-H14	:-179.036050
C2	-C25	-C24	-H27	: -0.063155
C2	-C25	-C24	-C32	: 179.843325
C3	-C2	-C1	-C10	: -0.160854
C3	-C2	-C1	-H15	: 179.830209
C3	-C2	-C25	-C24	: -0.819990
C3	-C2	-C25	-H26	: 179.177248
C3	-C4	-C5	-S6	: 179.578129
C3	-C4	-C5	-C10	: 0.528241
C4	-C3	-C2	-C25	: 179.258659
C4	-C5	-S6	-C7	: 170.687783
C4	-C5	-C10	-C9	:-178.858488
C5	-C4	-C3	-H13	:-179.997845
C5	-S6	-C7	-C8	: 38.901741
C5	-S6	-C7	-H11	: -85.463017
C5	-S6	-C7	-H43	: 159.140352
C5	-C10	-C1	-H15	:-178.802481
C5	-C10	-C9	-C8	: -20.969202
C5	-C10	-C9	-C16	:-139.661327
C5	-C10	-C9	-C20	: 100.772982
S6	-C5	-C4	-H14	: -0.834879
S6	-C5	-C10	-C9	: 2.208291
S6	-C7	-C8	-C9	:-65.433396
S6	-C7	-C8	-H12	: 173.574297
S6	-C7	-C8	-H44	: 57.736099
C7	-S6	-C5	-C10	:-10.329567
C7	-C8	-C9	-C10	: 54.535693
C7	-C8	-C9	-C16	: 176.083151
C7	-C8	-C9	-C20	:-66.507769
C8	-C9	-C16	-H17	: 172.003957

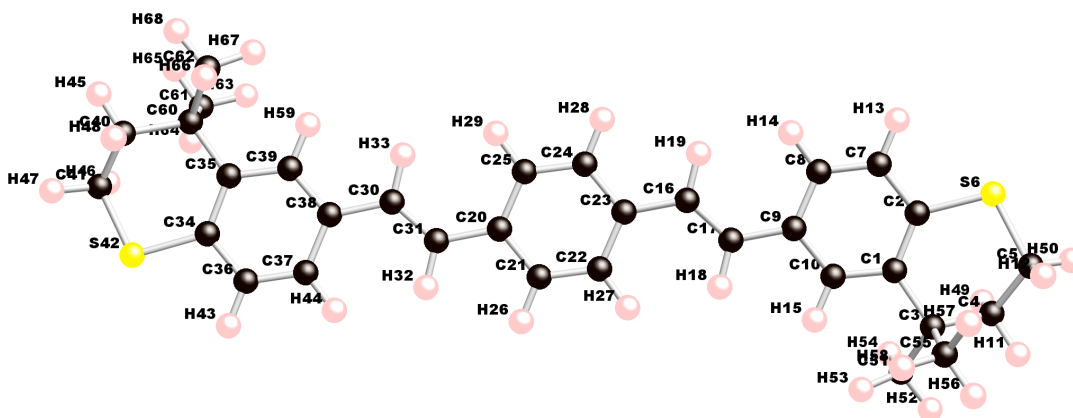
C8	-C9	-C16	-H18	: -66.632507
C8	-C9	-C16	-H19	: 52.924343
C8	-C9	-C20	-H21	: -176.140195
C8	-C9	-C20	-H22	: -56.444294
C8	-C9	-C20	-H23	: 64.389940
C9	-C8	-C7	-H11	: 57.616472
C9	-C8	-C7	-H43	: 177.721636
C9	-C10	-C1	-H15	: -1.163207
C10	-C1	-C2	-C25	: 179.855365
C10	-C5	-C4	-H14	: -179.884767
C10	-C9	-C8	-H12	: 175.853728
C10	-C9	-C8	-H44	: -68.318890
C10	-C9	-C16	-H17	: -65.895809
C10	-C9	-C16	-H18	: 55.467727
C10	-C9	-C16	-H19	: 175.024577
C10	-C9	-C20	-H21	: 60.875319
C10	-C9	-C20	-H22	: -179.428780
C10	-C9	-C20	-H23	: -58.594547
H11	-C7	-C8	-H12	: -63.375835
H11	-C7	-C8	-H44	: -179.214033
H12	-C8	-C7	-H43	: 56.729329
H12	-C8	-C9	-C16	: -62.598814
H12	-C8	-C9	-C20	: 54.810267
H13	-C3	-C2	-C25	: -0.185774
H13	-C3	-C4	-H14	: 0.417567
H15	-C1	-C2	-C25	: -0.153572
C16	-C9	-C8	-H44	: 53.228567
C16	-C9	-C20	-H21	: -60.233052
C16	-C9	-C20	-H22	: 59.462849
C16	-C9	-C20	-H23	: -179.702918

H17	-C16	-C9	-C20	: 53.726634
H18	-C16	-C9	-C20	: 175.090170
H19	-C16	-C9	-C20	: -65.352980
C20	-C9	-C8	-H44	: 170.637648
C24	-C32	-C31	-C30	:-179.075000
C24	-C32	-C31	-H39	: 0.305728
C24	-C32	-C33	-C29	:-179.908880
C24	-C32	-C33	-H42	: 0.076066
C25	-C24	-C32	-C31	: 0.384068
C25	-C24	-C32	-C33	:-179.525151
H26	-C25	-C24	-H27	: 179.939713
H26	-C25	-C24	-C32	: -0.153806
H27	-C24	-C32	-C31	:-179.705981
H27	-C24	-C32	-C33	: 0.384801
C28	-C29	-C33	-C32	: -1.349962
C28	-C29	-C33	-H42	: 178.665271
C28	-C29	-C34	-C35	: 19.428740
C28	-C29	-C34	-C47	:-102.365032
C28	-C29	-C34	-C51	: 138.115664
C28	-C30	-C31	-C32	: -0.635304
C28	-C30	-C31	-H39	: 179.974030
C28	-S37	-C36	-C35	: -40.253839
C28	-S37	-C36	-H41	: 84.074877
C28	-S37	-C36	-H46	:-160.494195
C29	-C28	-C30	-C31	: -0.595518
C29	-C28	-C30	-H38	: 179.880056
C29	-C28	-S37	-C36	: 11.291322
C29	-C33	-C32	-C31	: 0.175553
C29	-C34	-C35	-C36	: -53.435085
C29	-C34	-C35	-H40	:-174.863058

C29 -C34 -C35 -H45 : 69.310528  
C29 -C34 -C47 -H48 : 179.935847  
C29 -C34 -C47 -H49 : -60.348388  
C29 -C34 -C47 -H50 : 59.124026  
C29 -C34 -C51 -H52 :-175.080629  
C29 -C34 -C51 -H53 : -55.512071  
C29 -C34 -C51 -H54 : 65.760158  
C30 -C28 -C29 -C33 : 1.523989  
C30 -C28 -C29 -C34 : 179.206693  
C30 -C28 -S37 -C36 :-169.620753  
C30 -C31 -C32 -C33 : 0.835806  
C31 -C30 -C28 -S37 :-179.743089  
C31 -C32 -C33 -H42 :-179.839501  
C32 -C31 -C30 -H38 : 178.886532  
C32 -C33 -C29 -C34 :-179.155028  
C33 -C29 -C28 -S37 :-179.431638  
C33 -C29 -C34 -C35 :-162.931635  
C33 -C29 -C34 -C47 : 75.274593  
C33 -C29 -C34 -C51 : -44.244711  
C33 -C32 -C31 -H39 :-179.783466  
C34 -C29 -C28 -S37 : -1.748935  
C34 -C29 -C33 -H42 : 0.860205  
C34 -C35 -C36 -S37 : 65.945423  
C34 -C35 -C36 -H41 : -57.021835  
C34 -C35 -C36 -H46 :-177.232944  
C35 -C34 -C47 -H48 : 56.798173  
C35 -C34 -C47 -H49 : 176.513938  
C35 -C34 -C47 -H50 : -64.013648  
C35 -C34 -C51 -H52 : -52.905717  
C35 -C34 -C51 -H53 : 66.662841

C35	-C34	-C51	-H54	:-172.064930
C36	-C35	-C34	-C47	: 67.683066
C36	-C35	-C34	-C51	:-174.852379
S37	-C28	-C30	-H38	: 0.732485
S37	-C36	-C35	-H40	:-173.022980
S37	-C36	-C35	-H45	:-57.174241
H38	-C30	-C31	-H39	: -0.504134
H40	-C35	-C34	-C47	:-53.744907
H40	-C35	-C34	-C51	: 63.719648
H40	-C35	-C36	-H41	: 64.009762
H40	-C35	-C36	-H46	:-56.201347
H41	-C36	-C35	-H45	: 179.858501
H43	-C7	-C8	-H44	:-59.108869
H45	-C35	-C34	-C47	:-169.571320
H45	-C35	-C34	-C51	:-52.106765
H45	-C35	-C36	-H46	: 59.647392
C47	-C34	-C51	-H52	: 65.371261
C47	-C34	-C51	-H53	:-175.060182
C47	-C34	-C51	-H54	:-53.787952
H48	-C47	-C34	-C51	:-59.145631
H49	-C47	-C34	-C51	: 60.570134
H50	-C47	-C34	-C51	:-179.957452

## PPV2



Final geometry:

angstroms				
atom	x	y	z	
C1	-0.7269977200	-1.5243657451	-0.1496497698	
C2	0.4835853395	-0.8027626381	-0.1162801904	
C3	-0.8082881727	-3.0642958000	-0.1553707709	
C4	0.5082005310	-3.7098469442	-0.6528757114	
C5	1.7609304718	-3.2869395643	0.1041302030	
S6	2.1204585923	-1.5097019823	-0.1291171863	
C7	0.4576818391	0.6048875893	-0.0914759975	
C8	-0.7309113706	1.3101648368	-0.0885060441	
C9	-1.9614099095	0.6253722108	-0.0993718438	
C10	-1.9129511542	-0.7768395614	-0.1271968181	
H11	0.4032449139	-4.7994070638	-0.5699120157	
H12	1.6841892248	-3.5066382262	1.1725118185	
H13	1.3997370927	1.1461792383	-0.0682832674	
H14	-0.7004229487	2.3948688282	-0.0695802166	
H15	-2.8605450179	-1.3067486302	-0.1328725647	
C16	-3.5094207236	2.6140801378	-0.0654957701	

C17	-3.2661323636	1.2859180360	-0.0865924300
H18	-4.1131877298	0.6019036009	-0.1000686853
H19	-2.6629645195	3.2987033764	-0.0531758253
C20	-7.2971139943	4.6902965505	-0.0703046137
C21	-7.2457117365	3.2803474169	-0.0752802385
C22	-6.0453526225	2.5875120856	-0.0719077875
C23	-4.8145818170	3.2728362964	-0.0624455644
C24	-4.8658888640	4.6828233983	-0.0529505950
C25	-6.0668285645	5.3760495025	-0.0563197756
H26	-8.1796526538	2.7235018512	-0.0843807827
H27	-6.0652319626	1.5021336238	-0.0779643686
H28	-3.9318318206	5.2393858546	-0.0430026595
H29	-6.0482377495	6.4615520266	-0.0466860755
C30	-8.8680690857	6.6659609057	-0.1162872968
C31	-8.6051168832	5.3417997685	-0.0809655757
H32	-9.4434920992	4.6481486478	-0.0635818821
H33	-8.0335626841	7.3648968865	-0.1468914333
C34	-12.6735406129	8.6538582842	-0.1869241137
C35	-11.4836662108	9.4076230417	-0.2399058221
C36	-12.6076500742	7.2512332814	-0.0873778450
C37	-11.3993602156	6.5821148019	-0.0516019940
C38	-10.1883254619	7.2969364036	-0.1271434194
C39	-10.2763589331	8.6942468619	-0.2190119162
C40	-12.7746434512	11.5938289587	0.0908346289
C41	-14.0264985093	11.0713078745	-0.6025891414
S42	-14.3301213478	9.3130257200	-0.2061199477
H43	-13.5336181670	6.6840620915	-0.0428712442
H44	-11.3996233960	5.5003640164	0.0293279006
H45	-12.7024571412	12.6742400127	-0.0895518662
H46	-13.9729753807	11.1966620606	-1.6874913590

H47	-14.9160080437	11.6015478429	-0.2517929659
H48	-12.8872837509	11.4600387706	1.1732571181
H49	0.6443247813	-3.4847294737	-1.7173097174
H50	2.6418310425	-3.8094821582	-0.2785153595
C51	-1.9211779678	-3.5613836086	-1.1063626893
H52	-1.8994695815	-4.6552434707	-1.1622743889
H53	-2.9204698721	-3.2786734427	-0.7659501366
H54	-1.7834104044	-3.1665108386	-2.1178288404
C55	-1.1286391417	-3.5509015197	1.2789130120
H56	-1.1821240002	-4.6457370925	1.3134026976
H57	-0.3754711357	-3.2221905309	2.0008431945
H58	-2.0915990028	-3.1543524887	1.6145864707
H59	-9.3446936401	9.2485424623	-0.2787414951
C60	-11.4478859808	10.9433605629	-0.3717742181
C61	-11.1644760360	11.3087854339	-1.8491263030
C62	-10.3353742119	11.5529232003	0.5115278136
H63	-10.1959483757	10.9102170506	-2.1658178825
H64	-11.9191770935	10.8961782423	-2.5249317031
H65	-11.1432691884	12.3972000748	-1.9818718610
H66	-10.4454380421	11.2445131784	1.5558775627
H67	-9.3343296228	11.2685051501	0.1784956304
H68	-10.3876252895	12.6464324366	0.4721161069

Total energy (hartrees): -2036.32737837009

HOMO energy (hartrees): -0.17772

LUMO energy (hartrees): -0.06158

Bond lengths (angstroms):



C1	-C2	: 1.409729	C1	-C3	: 1.542085
C1	-C10	: 1.402065	C2	-S6	: 1.783054
C2	-C7	: 1.408107	C3	-C4	: 1.548351
C3	-C51	: 1.545964	C3	-C55	: 1.548089
C4	-C5	: 1.523562	C4	-H11	: 1.097743
C4	-H49	: 1.096461	C5	-S6	: 1.828179
C5	-H12	: 1.093433	C5	-H50	: 1.093368
C7	-C8	: 1.382092	C7	-H13	: 1.086739
C8	-C9	: 1.408256	C8	-H14	: 1.085297
C9	-C10	: 1.403325	C9	-C17	: 1.462458
C10	-H15	: 1.085712	C16	-C17	: 1.350425
C16	-H19	: 1.088737	C16	-C23	: 1.461990
C17	-H18	: 1.088834	C20	-C21	: 1.410895
C20	-C25	: 1.408565	C20	-C31	: 1.461315
C21	-C22	: 1.385963	C21	-H26	: 1.087385
C22	-C23	: 1.408743	C22	-H27	: 1.085577
C23	-C24	: 1.410952	C24	-C25	: 1.386661
C24	-H28	: 1.087347	C25	-H29	: 1.085704
C30	-C31	: 1.350479	C30	-H33	: 1.088967
C30	-C38	: 1.463327	C31	-H32	: 1.088268
C34	-C35	: 1.409528	C34	-C36	: 1.407696
C34	-S42	: 1.783011	C35	-C39	: 1.402474
C35	-C60	: 1.541804	C36	-C37	: 1.381653
C36	-H43	: 1.086775	C37	-C38	: 1.408290
C37	-H44	: 1.084774	C38	-C39	: 1.403092
C39	-H59	: 1.085731	C40	-C41	: 1.523485
C40	-H45	: 1.097742	C40	-H48	: 1.096461
C40	-C60	: 1.548354	C41	-S42	: 1.827821
C41	-H46	: 1.093431	C41	-H47	: 1.093362

C51 -H52 : 1.095503 C51 -H53 : 1.092882  
C51 -H54 : 1.094517 C55 -H56 : 1.096684  
C55 -H57 : 1.093845 C55 -H58 : 1.094175  
C60 -C61 : 1.548039 C60 -C62 : 1.545792  
C61 -H63 : 1.094165 C61 -H64 : 1.093861  
C61 -H65 : 1.096685 C62 -H66 : 1.094485  
C62 -H67 : 1.092655 C62 -H68 : 1.095466

Bond angles:

C3 -C1 -C2 : 123.815066 C10 -C1 -C2 : 116.941529  
C10 -C1 -C3 : 119.201738 S6 -C2 -C1 : 125.818266  
C7 -C2 -C1 : 119.757311 C7 -C2 -S6 : 114.416248  
C4 -C3 -C1 : 111.883278 C51 -C3 -C1 : 111.181248  
C51 -C3 -C4 : 106.281486 C55 -C3 -C1 : 108.745114  
C55 -C3 -C4 : 110.034490 C55 -C3 -C51 : 108.656311  
C5 -C4 -C3 : 115.070296 H11 -C4 -C3 : 107.953416  
H11 -C4 -C5 : 108.455735 H49 -C4 -C3 : 109.383191  
H49 -C4 -C5 : 108.861554 H49 -C4 -H11 : 106.799365  
S6 -C5 -C4 : 111.601669 H12 -C5 -C4 : 111.839138  
H12 -C5 -S6 : 109.499013 H50 -C5 -C4 : 110.849171  
H50 -C5 -S6 : 105.159604 H50 -C5 -H12 : 107.606043  
C5 -S6 -C2 : 101.769452 C8 -C7 -C2 : 121.734887  
H13 -C7 -C2 : 118.839346 H13 -C7 -C8 : 119.424795  
C9 -C8 -C7 : 120.217492 H14 -C8 -C7 : 119.071199  
H14 -C8 -C9 : 120.709457 C10 -C9 -C8 : 117.120576  
C17 -C9 -C8 : 124.044186 C17 -C9 -C10 : 118.835078  
C9 -C10 -C1 : 124.212548 H15 -C10 -C1 : 118.551608  
H15 -C10 -C9 : 117.235785 H19 -C16 -C17 : 118.591870  
C23 -C16 -C17 : 127.158649 C23 -C16 -H19 : 114.248964

C16 -C17 -C9 : 127.234888 H18 -C17 -C9 : 114.216801  
 H18 -C17 -C16 : 118.547826 C25 -C20 -C21 : 117.047738  
 C31 -C20 -C21 : 118.562633 C31 -C20 -C25 : 124.389608  
 C22 -C21 -C20 : 122.080102 H26 -C21 -C20 : 118.717491  
 H26 -C21 -C22 : 119.202252 C23 -C22 -C21 : 120.896939  
 H27 -C22 -C21 : 118.942350 H27 -C22 -C23 : 120.160665  
 C22 -C23 -C16 : 124.106383 C24 -C23 -C16 : 118.865637  
 C24 -C23 -C22 : 117.027772 C25 -C24 -C23 : 122.077059  
 H28 -C24 -C23 : 118.706828 H28 -C24 -C25 : 119.216111  
 C24 -C25 -C20 : 120.869709 H29 -C25 -C20 : 120.119073  
 H29 -C25 -C24 : 119.011171 H33 -C30 -C31 : 118.740862  
 C38 -C30 -C31 : 126.773761 C38 -C30 -H33 : 114.484158  
 C30 -C31 -C20 : 127.706617 H32 -C31 -C20 : 113.907817  
 H32 -C31 -C30 : 118.384504 C36 -C34 -C35 : 119.734556  
 S42 -C34 -C35 : 125.888039 S42 -C34 -C36 : 114.368973  
 C39 -C35 -C34 : 117.008420 C60 -C35 -C34 : 123.742750  
 C60 -C35 -C39 : 119.206004 C37 -C36 -C34 : 121.689065  
 H43 -C36 -C34 : 118.882767 H43 -C36 -C37 : 119.427432  
 C38 -C37 -C36 : 120.319934 H44 -C37 -C36 : 118.990100  
 H44 -C37 -C38 : 120.688949 C37 -C38 -C30 : 123.820533  
 C39 -C38 -C30 : 119.111434 C39 -C38 -C37 : 117.067995  
 C38 -C39 -C35 : 124.162818 H59 -C39 -C35 : 118.566944  
 H59 -C39 -C38 : 117.270168 H45 -C40 -C41 : 108.469720  
 H48 -C40 -C41 : 108.848344 H48 -C40 -H45 : 106.802295  
 C60 -C40 -C41 : 115.089244 C60 -C40 -H45 : 107.940348  
 C60 -C40 -H48 : 109.372991 S42 -C41 -C40 : 111.573649  
 H46 -C41 -C40 : 111.842963 H46 -C41 -S42 : 109.489173  
 H47 -C41 -C40 : 110.863167 H47 -C41 -S42 : 105.175612  
 H47 -C41 -H46 : 107.611726 C41 -S42 -C34 : 101.749341  
 H52 -C51 -C3 : 109.766475 H53 -C51 -C3 : 112.546821

H53 -C51 -H52 : 106.996391 H54 -C51 -C3 : 111.214171  
 H54 -C51 -H52 : 108.093783 H54 -C51 -H53 : 108.035862  
 H56 -C55 -C3 : 110.672523 H57 -C55 -C3 : 111.995432  
 H57 -C55 -H56 : 108.229714 H58 -C55 -C3 : 110.635970  
 H58 -C55 -H56 : 108.013336 H58 -C55 -H57 : 107.133224  
 C40 -C60 -C35 : 111.901426 C61 -C60 -C35 : 108.723388  
 C61 -C60 -C40 : 110.049927 C62 -C60 -C35 : 111.137921  
 C62 -C60 -C40 : 106.278844 C62 -C60 -C61 : 108.692221  
 H63 -C61 -C60 : 110.627312 H64 -C61 -C60 : 111.978094  
 H64 -C61 -H63 : 107.127479 H65 -C61 -C60 : 110.691260  
 H65 -C61 -H63 : 108.021227 H65 -C61 -H64 : 108.235148  
 H66 -C62 -C60 : 111.208021 H67 -C62 -C60 : 112.491800  
 H67 -C62 -H66 : 108.035867 H68 -C62 -C60 : 109.800504  
 H68 -C62 -H66 : 108.108336 H68 -C62 -H67 : 107.011764

Torsional angles:

C1 -C2 -S6 -C5 : -9.545939  
 C1 -C2 -C7 -C8 : 0.505920  
 C1 -C2 -C7 -H13 : -179.854882  
 C1 -C3 -C4 -C5 : 55.149222  
 C1 -C3 -C4 -H11 : 176.412105  
 C1 -C3 -C4 -H49 : -67.734586  
 C1 -C3 -C51 -H52 : 174.920991  
 C1 -C3 -C51 -H53 : -66.032742  
 C1 -C3 -C51 -H54 : 55.350282  
 C1 -C3 -C55 -H56 : -179.332405  
 C1 -C3 -C55 -H57 : -58.467547  
 C1 -C3 -C55 -H58 : 60.979656  
 C1 -C10 -C9 -C8 : -0.252001

C1	-C10	-C9	-C17	: 179.608876
C2	-C1	-C3	-C4	: -21.658242
C2	-C1	-C3	-C51	: -140.321304
C2	-C1	-C3	-C55	: 100.089034
C2	-C1	-C10	-C9	: 1.238310
C2	-C1	-C10	-H15	: -178.852042
C2	-S6	-C5	-C4	: 38.099196
C2	-S6	-C5	-H12	: -86.279194
C2	-S6	-C5	-H50	: 158.355973
C2	-C7	-C8	-C9	: 0.527313
C2	-C7	-C8	-H14	: -179.964152
C3	-C1	-C2	-S6	: 2.140900
C3	-C1	-C2	-C7	: -178.959892
C3	-C1	-C10	-C9	: 178.980603
C3	-C1	-C10	-H15	: -1.109749
C3	-C4	-C5	-S6	: -65.211041
C3	-C4	-C5	-H12	: 57.844342
C3	-C4	-C5	-H50	: 177.931585
C4	-C3	-C1	-C10	: 160.764318
C4	-C3	-C51	-H52	: 52.942698
C4	-C3	-C51	-H53	: 171.988965
C4	-C3	-C51	-H54	: -66.628010
C4	-C3	-C55	-H56	: -56.465181
C4	-C3	-C55	-H57	: 64.399678
C4	-C3	-C55	-H58	: -176.153120
C5	-C4	-C3	-C51	: 176.679974
C5	-C4	-C3	-C55	: -65.853860
C5	-S6	-C2	-C7	: 171.503552
S6	-C2	-C1	-C10	: 179.768811
S6	-C2	-C7	-C8	: 179.525656

S6 -C2 -C7 -H13 : -0.835146  
S6 -C5 -C4 -H11 : 173.799647  
S6 -C5 -C4 -H49 : 57.951026  
C7 -C2 -C1 -C10 : -1.331980  
C7 -C8 -C9 -C10 : -0.650085  
C7 -C8 -C9 -C17 : 179.496998  
C8 -C9 -C10 -H15 : 179.837259  
C8 -C9 -C17 -C16 : 0.128064  
C8 -C9 -C17 -H18 : 179.869021  
C9 -C8 -C7 -H13 : -179.109825  
C9 -C17 -C16 -H19 : -0.199151  
C9 -C17 -C16 -C23 : 179.522951  
C10 -C1 -C3 -C51 : 42.101256  
C10 -C1 -C3 -C55 : -77.488406  
C10 -C9 -C8 -H14 : 179.849526  
C10 -C9 -C17 -C16 : -179.722497  
C10 -C9 -C17 -H18 : 0.018460  
H11 -C4 -C3 -C51 : -62.057143  
H11 -C4 -C3 -C55 : 55.409023  
H11 -C4 -C5 -H12 : -63.144970  
H11 -C4 -C5 -H50 : 56.942273  
H12 -C5 -C4 -H49 : -178.993591  
H13 -C7 -C8 -H14 : 0.398709  
H14 -C8 -C9 -C17 : -0.003391  
H15 -C10 -C9 -C17 : -0.301864  
C16 -C23 -C22 -C21 : -179.662820  
C16 -C23 -C22 -H27 : 0.258919  
C16 -C23 -C24 -C25 : 179.670089  
C16 -C23 -C24 -H28 : -0.310455  
C17 -C16 -C23 -C22 : 0.486828

C17	-C16	-C23	-C24	:-179.341802
H18	-C17	-C16	-H19	:-179.930205
H18	-C17	-C16	-C23	: -0.208103
H19	-C16	-C23	-C22	:-179.780793
H19	-C16	-C23	-C24	: 0.390577
C20	-C21	-C22	-C23	: 0.039199
C20	-C21	-C22	-H27	:-179.883478
C20	-C25	-C24	-C23	: -0.037240
C20	-C25	-C24	-H28	: 179.943209
C20	-C31	-C30	-H33	: 0.384658
C20	-C31	-C30	-C38	: 179.959161
C21	-C20	-C25	-C24	: 0.241443
C21	-C20	-C25	-H29	:-179.678664
C21	-C20	-C31	-C30	:-177.971126
C21	-C20	-C31	-H32	: 1.644162
C21	-C22	-C23	-C24	: 0.168702
C22	-C21	-C20	-C25	: -0.244362
C22	-C21	-C20	-C31	: 179.705268
C22	-C23	-C24	-C25	: -0.170620
C22	-C23	-C24	-H28	: 179.848835
C23	-C22	-C21	-H26	: 179.893640
C23	-C24	-C25	-H29	: 179.883738
C24	-C23	-C22	-H27	:-179.909559
C24	-C25	-C20	-C31	:-179.704948
C25	-C20	-C21	-H26	: 179.900517
C25	-C20	-C31	-C30	: 1.974512
C25	-C20	-C31	-H32	:-178.410200
H26	-C21	-C20	-C31	: -0.149853
H26	-C21	-C22	-H27	: -0.029037
H28	-C24	-C25	-H29	: -0.135813

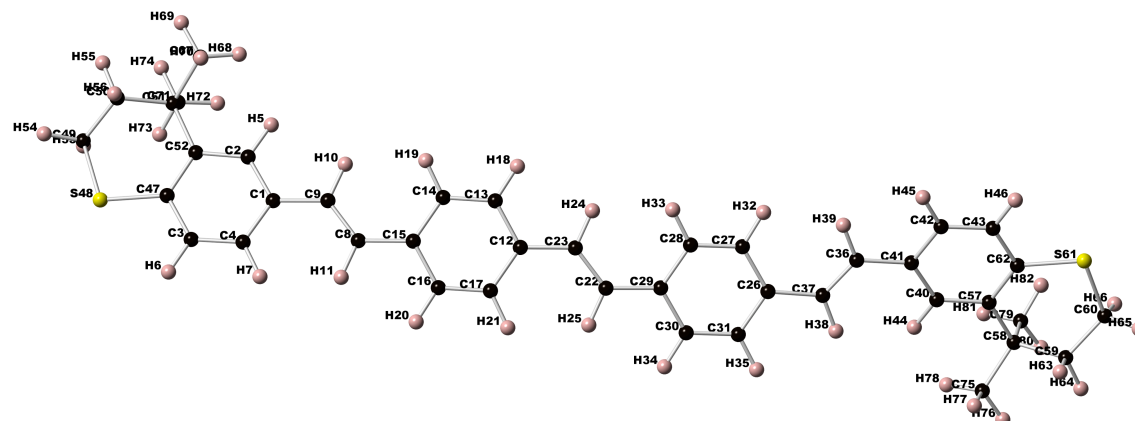
H29	-C25	-C20	-C31	:	0.374945
C30	-C38	-C37	-C36	:	-179.051929
C30	-C38	-C37	-H44	:	0.577549
C30	-C38	-C39	-C35	:	179.911630
C30	-C38	-C39	-H59	:	0.009870
C31	-C30	-C38	-C37	:	2.434062
C31	-C30	-C38	-C39	:	-177.492682
H32	-C31	-C30	-H33	:	-179.215578
H32	-C31	-C30	-C38	:	0.358925
H33	-C30	-C38	-C37	:	-177.975879
H33	-C30	-C38	-C39	:	2.097377
C34	-C35	-C39	-C38	:	-1.104260
C34	-C35	-C39	-H59	:	178.796314
C34	-C35	-C60	-C40	:	21.645723
C34	-C35	-C60	-C61	:	-100.117887
C34	-C35	-C60	-C62	:	140.288431
C34	-C36	-C37	-C38	:	-0.583993
C34	-C36	-C37	-H44	:	179.780280
C34	-S42	-C41	-C40	:	-38.105792
C34	-S42	-C41	-H46	:	86.250808
C34	-S42	-C41	-H47	:	-158.374044
C35	-C34	-C36	-C37	:	-0.593383
C35	-C34	-C36	-H43	:	179.720524
C35	-C34	-S42	-C41	:	9.562991
C35	-C39	-C38	-C37	:	-0.020025
C35	-C60	-C40	-C41	:	-55.168956
C35	-C60	-C40	-H45	:	-176.452692
C35	-C60	-C40	-H48	:	67.703093
C35	-C60	-C61	-H63	:	-60.933203
C35	-C60	-C61	-H64	:	58.489436



C35	-C60	-C61	-H65	: 179.362458
C35	-C60	-C62	-H66	: -55.295102
C35	-C60	-C62	-H67	: 66.044577
C35	-C60	-C62	-H68	: -174.902182
C36	-C34	-C35	-C39	: 1.382733
C36	-C34	-C35	-C60	: 178.978210
C36	-C34	-S42	-C41	: -171.503212
C36	-C37	-C38	-C39	: 0.876197
C37	-C36	-C34	-S42	: -179.598611
C37	-C38	-C39	-H59	: -179.921785
C38	-C37	-C36	-H43	: 179.100431
C38	-C39	-C35	-C60	: -178.813655
C39	-C35	-C34	-S42	: -179.735753
C39	-C35	-C60	-C40	: -160.808606
C39	-C35	-C60	-C61	: 77.427785
C39	-C35	-C60	-C62	: -42.165897
C39	-C38	-C37	-H44	: -179.494325
C40	-C60	-C61	-H63	: 176.181360
C40	-C60	-C61	-H64	: -64.396000
C40	-C60	-C61	-H65	: 56.477022
C40	-C60	-C62	-H66	: 66.678294
C40	-C60	-C62	-H67	: -171.982027
C40	-C60	-C62	-H68	: -52.928787
C41	-C40	-C60	-C61	: 65.829315
C41	-C40	-C60	-C62	: -176.655466
S42	-C34	-C35	-C60	: -2.140277
S42	-C34	-C36	-H43	: 0.715296
S42	-C41	-C40	-H45	: -173.776361
S42	-C41	-C40	-H48	: -57.923785
S42	-C41	-C40	-C60	: 65.228063

H43	-C36	-C37	-H44	: -0.535296
H45	-C40	-C41	-H46	: 63.198880
H45	-C40	-C41	-H47	: -56.907729
H45	-C40	-C60	-C61	: -55.454420
H45	-C40	-C60	-C62	: 62.060798
H46	-C41	-C40	-H48	: 179.051457
H46	-C41	-C40	-C60	: -57.796696
H47	-C41	-C40	-H48	: 58.944848
H47	-C41	-C40	-C60	: -177.903305
H48	-C40	-C60	-C61	: -171.298635
H48	-C40	-C60	-C62	: -53.783417
H49	-C4	-C3	-C51	: 53.796166
H49	-C4	-C3	-C55	: 171.262332
H49	-C4	-C5	-H50	: -58.906348
C51	-C3	-C55	-H56	: 59.516434
C51	-C3	-C55	-H57	: -179.618707
C51	-C3	-C55	-H58	: -60.171505
H52	-C51	-C3	-C55	: -65.436467
H53	-C51	-C3	-C55	: 53.609800
H54	-C51	-C3	-C55	: 174.992824
H59	-C39	-C35	-C60	: 1.086920
C61	-C60	-C62	-H66	: -174.907361
C61	-C60	-C62	-H67	: -53.567682
C61	-C60	-C62	-H68	: 65.485559
C62	-C60	-C61	-H63	: 60.173873
C62	-C60	-C61	-H64	: 179.596512
C62	-C60	-C61	-H65	: -59.530466

## PPV3



Final geometry:

angstroms

atom	x	y	z
C1	-1.7503402346	0.1387931046	0.3811012728
C2	-2.4134342473	1.2997925062	-0.0448516430
C3	-3.9271411774	-0.8936947218	0.6118315532
C4	-2.5516750933	-0.9666523341	0.7230921189
H5	-1.7993179132	2.1553933212	-0.3066403970
H6	-4.5304468549	-1.7593866220	0.8718134368
H7	-2.0998621518	-1.8860806443	1.0805223035
C8	0.5164512012	-0.9262464533	0.6584752786
C9	-0.2878208970	0.1363266177	0.4384355124
H10	0.1710655141	1.1059713774	0.2535228970
H11	0.0590375119	-1.9038344289	0.7987758960
C12	4.8328726426	-1.1068520189	0.7156104152
C13	4.1624036209	0.1340757648	0.6948137618
C14	2.7788555925	0.2212654021	0.6834949584
C15	1.9785691723	-0.9373989478	0.6952793661
C16	2.6489786935	-2.1777580195	0.7428375886
C17	4.0325685162	-2.2651699690	0.7505466850

H18	4.7521311410	1.0475240779	0.6840736477
H19	2.3136974143	1.2017138485	0.6746663524
H20	2.0592725007	-3.0908756128	0.7687721967
H21	4.4974223091	-3.2449391164	0.7913840404
C22	7.1057963304	-2.1896579037	0.5620215821
C23	6.2943432380	-1.1172645935	0.6952459118
H24	6.7470581842	-0.1304663749	0.7704018333
H25	6.6548184592	-3.1735772257	0.4473231340
C26	11.4232968023	-2.2832485256	0.3334491473
C27	10.7420630536	-1.0904848652	0.6608963965
C28	9.3614414105	-1.0447427509	0.7507469954
C29	8.5665223273	-2.1873768522	0.5135890505
C30	9.2459520101	-3.3784279340	0.1972213202
C31	10.6309362345	-3.4231681282	0.1039142922
H32	11.3051032003	-0.1794189559	0.8363557629
H33	8.8883791120	-0.1031111048	1.0102326652
H34	8.6698021836	-4.2815696835	0.0112623395
H35	11.1173381935	-4.3614199090	-0.1497055569
C36	13.7853091607	-1.4449270308	0.5608415409
C37	12.8778586670	-2.3842036578	0.2169855271
H38	13.2337948186	-3.3354046834	-0.1749402520
H39	13.4271003389	-0.5194590438	1.0081864592
C40	15.9137932678	-2.5012447163	-0.3124786623
C41	15.2416480965	-1.5196414154	0.4349251698
C42	16.0303658400	-0.5563765317	1.0873461911
C43	17.4117725431	-0.5969951538	1.0067376570
H44	15.3176709709	-3.2318938489	-0.8449621558
H45	15.5505670018	0.2235210973	1.6731876377
H46	18.0031292727	0.1493757167	1.5302197341
C47	-4.5712713728	0.2756988567	0.1663226180

S48	-6.3491825706	0.1566092668	0.1038227552
C49	-6.8079790578	1.7284658503	-0.7103189459
C50	-5.9023713220	2.8734158114	-0.2744107457
C51	-4.4162760320	2.7287042965	-0.6845843390
C52	-3.8060600840	1.4137565958	-0.1604608786
H53	-6.7985204721	1.5937477474	-1.7952165145
H54	-7.8422070418	1.9150828279	-0.4086865766
H55	-6.2861120699	3.8042055386	-0.7116997304
H56	-5.9684622788	2.9835044599	0.8142501828
C57	17.3065393285	-2.5672935235	-0.4236926787
C58	17.9736984959	-3.6356141475	-1.3064951080
C59	19.3467427727	-4.0411218324	-0.7114502805
C60	20.3890220701	-2.9306512074	-0.6863559734
S61	19.8439097063	-1.4631795276	0.2707298950
C62	18.0650054747	-1.5880851372	0.2578248194
H63	19.1968455175	-4.4272802269	0.3038012305
H64	19.7541307565	-4.8664467823	-1.3092078363
H65	21.3049103097	-3.2735285422	-0.1976076633
H66	20.6519847500	-2.6127124056	-1.6983164473
C67	-3.6848318205	3.9588558318	-0.1015743320
H68	-2.6508892728	4.0349801038	-0.4472610681
H69	-4.1951255747	4.8762694387	-0.4144439021
H70	-3.6756097548	3.9311283946	0.9923215448
C71	-4.2835920777	2.7583203573	-2.2265768241
H72	-3.2304032424	2.7313807132	-2.5221162551
H73	-4.7722082775	1.8999214517	-2.6964242430
H74	-4.7281670662	3.6733277929	-2.6363952127
C75	17.1290483601	-4.9235960812	-1.3919896205
H76	17.6750848979	-5.6870014584	-1.9559921102
H77	16.9129695982	-5.3258178386	-0.3972478465

H78	16.1791497971	-4.7650092407	-1.9092746339
C79	18.1474295549	-3.0633782577	-2.7341891647
H80	18.6847377078	-3.7722845687	-3.3758761876
H81	17.1697254962	-2.8703976588	-3.1861047656
H82	18.6958743041	-2.1171751599	-2.7332042923

Total energy (hartrees): -2344.79833221306

HOMO energy (hartrees): -0.17726

LUMO energy (hartrees): -0.06852

Bond lengths (angstroms):

C1	-C2	: 1.403228	C1	-C4	: 1.407517
C1	-C9	: 1.463645	C2	-H5	: 1.085230
C2	-C52	: 1.402056	C3	-C4	: 1.381886
C3	-H6	: 1.086734	C3	-C47	: 1.407431
C4	-H7	: 1.085007	C8	-C9	: 1.350679
C8	-H11	: 1.088389	C8	-C15	: 1.462624
C9	-H10	: 1.088568	C12	-C13	: 1.410625
C12	-C17	: 1.408335	C12	-C23	: 1.461650
C13	-C14	: 1.386339	C13	-H18	: 1.087328
C14	-C15	: 1.408226	C14	-H19	: 1.085232
C15	-C16	: 1.410745	C16	-C17	: 1.386370
C16	-H20	: 1.087295	C17	-H21	: 1.085221
C22	-C23	: 1.351382	C22	-H25	: 1.088409
C22	-C29	: 1.461530	C23	-H24	: 1.088288
C26	-C27	: 1.412086	C26	-C31	: 1.407103
C26	-C37	: 1.462705	C27	-C28	: 1.384298

C27	-H32	: 1.085284	C28	-C29	: 1.412003
C28	-H33	: 1.085261	C29	-C30	: 1.407237
C30	-C31	: 1.388845	C30	-H34	: 1.087288
C31	-H35	: 1.086842	C36	-C37	: 1.350535
C36	-H39	: 1.088541	C36	-C41	: 1.463680
C37	-H38	: 1.088614	C40	-C41	: 1.404969
C40	-H44	: 1.082935	C40	-C57	: 1.398740
C41	-C42	: 1.405563	C42	-C43	: 1.384353
C42	-H45	: 1.087041	C43	-H46	: 1.086649
C43	-C62	: 1.403511	C47	-S48	: 1.782991
C47	-C52	: 1.409791	S48	-C49	: 1.828675
C49	-C50	: 1.523500	C49	-H53	: 1.093271
C49	-H54	: 1.093360	C50	-C51	: 1.548439
C50	-H55	: 1.097656	C50	-H56	: 1.096207
C51	-C52	: 1.541479	C51	-C67	: 1.545375
C51	-C71	: 1.547974	C57	-C58	: 1.538100
C57	-C62	: 1.413714	C58	-C59	: 1.550408
C58	-C75	: 1.542608	C58	-C79	: 1.547885
C59	-C60	: 1.523194	C59	-H63	: 1.096505
C59	-H64	: 1.097470	C60	-S61	: 1.834839
C60	-H65	: 1.093294	C60	-H66	: 1.092840
S61	-C62	: 1.783331	C67	-H68	: 1.092855
C67	-H69	: 1.095415	C67	-H70	: 1.094286
C71	-H72	: 1.094201	C71	-H73	: 1.093778
C71	-H74	: 1.096739	C75	-H76	: 1.095008
C75	-H77	: 1.094524	C75	-H78	: 1.093179
C79	-H80	: 1.096818	C79	-H81	: 1.094246
C79	-H82	: 1.093660			

Bond angles:

C4 -C1 -C2 : 117.034879 C9 -C1 -C2 : 119.043316  
 C9 -C1 -C4 : 123.920767 H5 -C2 -C1 : 117.266195  
 C52 -C2 -C1 : 124.170187 C52 -C2 -H5 : 118.561668  
 H6 -C3 -C4 : 119.423255 C47 -C3 -C4 : 121.660815  
 C47 -C3 -H6 : 118.915801 C3 -C4 -C1 : 120.374667  
 H7 -C4 -C1 : 120.563898 H7 -C4 -C3 : 119.061123  
 H11 -C8 -C9 : 118.512941 C15 -C8 -C9 : 127.254019  
 C15 -C8 -H11 : 114.206666 C8 -C9 -C1 : 127.064034  
 H10 -C9 -C1 : 114.397909 H10 -C9 -C8 : 118.516312  
 C17 -C12 -C13 : 116.987829 C23 -C12 -C13 : 118.770505  
 C23 -C12 -C17 : 124.241302 C14 -C13 -C12 : 121.991197  
 H18 -C13 -C12 : 118.775843 H18 -C13 -C14 : 119.232645  
 C15 -C14 -C13 : 121.019865 H19 -C14 -C13 : 118.989447  
 H19 -C14 -C15 : 119.988259 C14 -C15 -C8 : 124.167441  
 C16 -C15 -C8 : 118.855660 C16 -C15 -C14 : 116.976745  
 C17 -C16 -C15 : 121.997825 H20 -C16 -C15 : 118.779655  
 H20 -C16 -C17 : 119.221695 C16 -C17 -C12 : 121.005973  
 H21 -C17 -C12 : 120.004726 H21 -C17 -C16 : 118.987845  
 H25 -C22 -C23 : 118.617528 C29 -C22 -C23 : 127.024732  
 C29 -C22 -H25 : 114.332838 C22 -C23 -C12 : 127.402825  
 H24 -C23 -C12 : 114.111628 H24 -C23 -C22 : 118.461792  
 C31 -C26 -C27 : 116.772912 C37 -C26 -C27 : 123.814651  
 C37 -C26 -C31 : 119.411434 C28 -C27 -C26 : 121.608487  
 H32 -C27 -C26 : 119.755136 H32 -C27 -C28 : 118.632161  
 C29 -C28 -C27 : 121.589910 H33 -C28 -C27 : 118.615495  
 H33 -C28 -C29 : 119.794594 C28 -C29 -C22 : 123.942446  
 C30 -C29 -C22 : 119.253490 C30 -C29 -C28 : 116.798999  
 C31 -C30 -C29 : 121.590054 H34 -C30 -C29 : 119.054508  
 H34 -C30 -C31 : 119.352090 C30 -C31 -C26 : 121.634138



H35 -C31 -C26 : 119.039487 H35 -C31 -C30 : 119.326132  
 H39 -C36 -C37 : 118.347498 C41 -C36 -C37 : 127.672316  
 C41 -C36 -H39 : 113.964709 C36 -C37 -C26 : 126.863048  
 H38 -C37 -C26 : 114.463635 H38 -C37 -C36 : 118.663700  
 H44 -C40 -C41 : 118.008993 C57 -C40 -C41 : 123.479886  
 C57 -C40 -H44 : 118.499798 C40 -C41 -C36 : 123.878536  
 C42 -C41 -C36 : 118.908447 C42 -C41 -C40 : 117.212033  
 C43 -C42 -C41 : 120.851170 H45 -C42 -C41 : 119.614727  
 H45 -C42 -C43 : 119.529625 H46 -C43 -C42 : 119.659205  
 C62 -C43 -C42 : 121.079521 C62 -C43 -H46 : 119.261267  
 S48 -C47 -C3 : 114.328020 C52 -C47 -C3 : 119.714804  
 C52 -C47 -S48 : 125.946520 C49 -S48 -C47 : 102.026821  
 C50 -C49 -S48 : 111.682445 H53 -C49 -S48 : 109.494042  
 H53 -C49 -C50 : 111.801703 H54 -C49 -S48 : 105.141886  
 H54 -C49 -C50 : 110.797800 H54 -C49 -H53 : 107.636659  
 C51 -C50 -C49 : 115.116839 H55 -C50 -C49 : 108.389824  
 H55 -C50 -C51 : 108.013658 H56 -C50 -C49 : 108.892186  
 H56 -C50 -C51 : 109.288203 H56 -C50 -H55 : 106.822305  
 C52 -C51 -C50 : 111.689727 C67 -C51 -C50 : 106.255868  
 C67 -C51 -C52 : 111.309120 C71 -C51 -C50 : 110.141932  
 C71 -C51 -C52 : 108.728787 C71 -C51 -C67 : 108.663174  
 C47 -C52 -C2 : 117.026547 C51 -C52 -C2 : 119.378476  
 C51 -C52 -C47 : 123.543268 C58 -C57 -C40 : 120.685819  
 C62 -C57 -C40 : 117.591870 C62 -C57 -C58 : 121.673173  
 C59 -C58 -C57 : 110.213257 C75 -C58 -C57 : 111.976894  
 C75 -C58 -C59 : 106.726420 C79 -C58 -C57 : 108.741444  
 C79 -C58 -C59 : 110.566321 C79 -C58 -C75 : 108.602706  
 C60 -C59 -C58 : 114.937901 H63 -C59 -C58 : 109.050591  
 H63 -C59 -C60 : 109.574782 H64 -C59 -C58 : 108.444707  
 H64 -C59 -C60 : 107.651345 H64 -C59 -H63 : 106.870587

S61 -C60 -C59 : 112.853548 H65 -C60 -C59 : 110.607333  
 H65 -C60 -S61 : 105.457493 H66 -C60 -C59 : 111.192062  
 H66 -C60 -S61 : 108.773103 H66 -C60 -H65 : 107.675159  
 C62 -S61 -C60 : 103.683637 C57 -C62 -C43 : 119.778328  
 S61 -C62 -C43 : 114.264644 S61 -C62 -C57 : 125.956916  
 H68 -C67 -C51 : 112.576184 H69 -C67 -C51 : 109.781128  
 H69 -C67 -H68 : 106.980744 H70 -C67 -C51 : 111.158278  
 H70 -C67 -H68 : 108.058891 H70 -C67 -H69 : 108.099149  
 H72 -C71 -C51 : 110.553588 H73 -C71 -C51 : 111.999480  
 H73 -C71 -H72 : 107.135581 H74 -C71 -C51 : 110.698027  
 H74 -C71 -H72 : 108.046045 H74 -C71 -H73 : 108.249735  
 H76 -C75 -C58 : 109.730660 H77 -C75 -C58 : 111.380108  
 H77 -C75 -H76 : 108.080677 H78 -C75 -C58 : 112.388349  
 H78 -C75 -H76 : 106.900659 H78 -C75 -H77 : 108.169099  
 H80 -C79 -C58 : 110.833795 H81 -C79 -C58 : 110.233003  
 H81 -C79 -H80 : 108.063575 H82 -C79 -C58 : 112.042740  
 H82 -C79 -H80 : 108.303465 H82 -C79 -H81 : 107.208980

Torsional angles:

C1 -C2 -C52 -C47 : -0.521918  
 C1 -C2 -C52 -C51 : -177.999720  
 C1 -C4 -C3 -H6 : 179.467950  
 C1 -C4 -C3 -C47 : -0.400360  
 C1 -C9 -C8 -H11 : 0.917163  
 C1 -C9 -C8 -C15 : 178.931891  
 C2 -C1 -C4 -C3 : 1.149801  
 C2 -C1 -C4 -H7 : -178.645386  
 C2 -C1 -C9 -C8 : -171.052848  
 C2 -C1 -C9 -H10 : 7.211397

C2 -C52 -C47 -C3 : 1.292473  
C2 -C52 -C47 -S48 :-179.965516  
C2 -C52 -C51 -C50 :-159.359843  
C2 -C52 -C51 -C67 :-40.771743  
C2 -C52 -C51 -C71 : 78.894114  
C3 -C4 -C1 -C9 :-178.475008  
C3 -C47 -S48 -C49 :-172.758745  
C3 -C47 -C52 -C51 : 178.655416  
C4 -C1 -C2 -H5 : 179.821481  
C4 -C1 -C2 -C52 : -0.695112  
C4 -C1 -C9 -C8 : 8.564890  
C4 -C1 -C9 -H10 :-173.170866  
C4 -C3 -C47 -S48 :-179.755041  
C4 -C3 -C47 -C52 : -0.872694  
H5 -C2 -C1 -C9 : -0.534636  
H5 -C2 -C52 -C47 : 178.955263  
H5 -C2 -C52 -C51 : 1.477461  
H6 -C3 -C4 -H7 : -0.733808  
H6 -C3 -C47 -S48 : 0.376000  
H6 -C3 -C47 -C52 : 179.258348  
H7 -C4 -C1 -C9 : 1.729805  
H7 -C4 -C3 -C47 : 179.397882  
C8 -C15 -C14 -C13 :-178.765774  
C8 -C15 -C14 -H19 : 1.806981  
C8 -C15 -C16 -C17 : 178.586174  
C8 -C15 -C16 -H20 : -1.080719  
C9 -C1 -C2 -C52 : 178.948771  
C9 -C8 -C15 -C14 : 9.136954  
C9 -C8 -C15 -C16 :-170.715773  
H10 -C9 -C8 -H11 :-177.283814

H10 -C9 -C8 -C15 : 0.730914  
H11 -C8 -C15 -C14 :-172.775670  
H11 -C8 -C15 -C16 : 7.371603  
C12 -C13 -C14 -C15 : 0.137043  
C12 -C13 -C14 -H19 : 179.569907  
C12 -C17 -C16 -C15 : 0.228878  
C12 -C17 -C16 -H20 : 179.894344  
C12 -C23 -C22 -H25 : 0.485535  
C12 -C23 -C22 -C29 : 178.559404  
C13 -C12 -C17 -C16 : 1.002225  
C13 -C12 -C17 -H21 :-178.554458  
C13 -C12 -C23 -C22 :-172.083016  
C13 -C12 -C23 -H24 : 6.100266  
C13 -C14 -C15 -C16 : 1.089490  
C14 -C13 -C12 -C17 : -1.188964  
C14 -C13 -C12 -C23 : 178.601295  
C14 -C15 -C16 -C17 : -1.277095  
C14 -C15 -C16 -H20 : 179.056013  
C15 -C14 -C13 -H18 : 179.930440  
C15 -C16 -C17 -H21 : 179.789990  
C16 -C15 -C14 -H19 :-178.337756  
C16 -C17 -C12 -C23 :-178.775379  
C17 -C12 -C13 -H18 : 179.016728  
C17 -C12 -C23 -C22 : 7.690896  
C17 -C12 -C23 -H24 :-174.125822  
H18 -C13 -C12 -C23 : -1.193014  
H18 -C13 -C14 -H19 : -0.636695  
H20 -C16 -C17 -H21 : -0.544545  
H21 -C17 -C12 -C23 : 1.667938  
C22 -C29 -C28 -C27 :-178.437526

C22 -C29 -C28 -H33 : 1.554462  
C22 -C29 -C30 -C31 : 178.316042  
C22 -C29 -C30 -H34 : -1.013783  
C23 -C22 -C29 -C28 : 7.340950  
C23 -C22 -C29 -C30 :-171.812993  
H24 -C23 -C22 -H25 :-177.628255  
H24 -C23 -C22 -C29 : 0.445614  
H25 -C22 -C29 -C28 :-174.514697  
H25 -C22 -C29 -C30 : 6.331360  
C26 -C27 -C28 -C29 : -0.280808  
C26 -C27 -C28 -H33 : 179.727112  
C26 -C31 -C30 -C29 : 0.611793  
C26 -C31 -C30 -H34 : 179.939669  
C26 -C37 -C36 -H39 : 2.449838  
C26 -C37 -C36 -C41 :-179.075434  
C27 -C26 -C31 -C30 : -0.116252  
C27 -C26 -C31 -H35 :-179.935735  
C27 -C26 -C37 -C36 : 9.189756  
C27 -C26 -C37 -H38 :-171.962492  
C27 -C28 -C29 -C30 : 0.735496  
C28 -C27 -C26 -C31 : -0.045951  
C28 -C27 -C26 -C37 : 179.586581  
C28 -C29 -C30 -C31 : -0.897615  
C28 -C29 -C30 -H34 : 179.772560  
C29 -C28 -C27 -H32 : 178.970165  
C29 -C30 -C31 -H35 :-179.569229  
C30 -C29 -C28 -H33 :-179.272516  
C30 -C31 -C26 -C37 :-179.765773  
C31 -C26 -C27 -H32 :-179.288676  
C31 -C26 -C37 -C36 :-171.186859

C31	-C26	-C37	-H38	:	7.660893
H32	-C27	-C26	-C37	:	0.343856
H32	-C27	-C28	-H33	:	-1.021915
H34	-C30	-C31	-H35	:	-0.241353
H35	-C31	-C26	-C37	:	0.414744
C36	-C41	-C40	-H44	:	1.453580
C36	-C41	-C40	-C57	:	-179.790829
C36	-C41	-C42	-C43	:	179.330449
C36	-C41	-C42	-H45	:	0.103927
C37	-C36	-C41	-C40	:	12.889168
C37	-C36	-C41	-C42	:	-167.482273
H38	-C37	-C36	-H39	:	-176.354870
H38	-C37	-C36	-C41	:	2.119858
H39	-C36	-C41	-C40	:	-168.579821
H39	-C36	-C41	-C42	:	11.048738
C40	-C41	-C42	-C43	:	-1.016308
C40	-C41	-C42	-H45	:	179.757170
C40	-C57	-C58	-C59	:	-148.394320
C40	-C57	-C58	-C75	:	-29.754077
C40	-C57	-C58	-C79	:	90.258082
C40	-C57	-C62	-C43	:	-0.192745
C40	-C57	-C62	-S61	:	179.936509
C41	-C40	-C57	-C58	:	-177.472586
C41	-C40	-C57	-C62	:	0.020055
C41	-C42	-C43	-H46	:	-179.147536
C41	-C42	-C43	-C62	:	0.881488
C42	-C41	-C40	-H44	:	-178.180796
C42	-C41	-C40	-C57	:	0.574795
C42	-C43	-C62	-C57	:	-0.251949
C42	-C43	-C62	-S61	:	179.633287

C43 -C62 -C57 -C58 : 177.273596  
C43 -C62 -S61 -C60 : 176.533930  
H44 -C40 -C57 -C58 : 1.277262  
H44 -C40 -C57 -C62 : 178.769904  
H45 -C42 -C43 -H46 : 0.079637  
H45 -C42 -C43 -C62 :-179.891339  
H46 -C43 -C62 -C57 : 179.776962  
H46 -C43 -C62 -S61 : -0.337802  
C47 -S48 -C49 -C50 : -36.567986  
C47 -S48 -C49 -H53 : 87.815334  
C47 -S48 -C49 -H54 :-156.795884  
C47 -C52 -C51 -C50 : 23.335960  
C47 -C52 -C51 -C67 : 141.924060  
C47 -C52 -C51 -C71 : -98.410084  
S48 -C47 -C52 -C51 : -2.602573  
S48 -C49 -C50 -C51 : 64.666846  
S48 -C49 -C50 -H55 :-174.284049  
S48 -C49 -C50 -H56 : -58.427513  
C49 -S48 -C47 -C52 : 8.440287  
C49 -C50 -C51 -C52 : -56.418668  
C49 -C50 -C51 -C67 :-177.975934  
C49 -C50 -C51 -C71 : 64.508428  
C50 -C51 -C67 -H68 :-171.993934  
C50 -C51 -C67 -H69 : -52.938623  
C50 -C51 -C67 -H70 : 66.612898  
C50 -C51 -C71 -H72 : 175.800007  
C50 -C51 -C71 -H73 : -64.802809  
C50 -C51 -C71 -H74 : 56.108118  
C51 -C50 -C49 -H53 : -58.414035  
C51 -C50 -C49 -H54 :-178.479921

C52	-C51	-C50	-H55	:-177.672402
C52	-C51	-C50	-H56	: 66.464550
C52	-C51	-C67	-H68	: 66.205856
C52	-C51	-C67	-H69	:-174.738833
C52	-C51	-C67	-H70	:-55.187313
C52	-C51	-C71	-H72	:-61.515132
C52	-C51	-C71	-H73	: 57.882052
C52	-C51	-C71	-H74	: 178.792979
H53	-C49	-C50	-H55	: 62.635071
H53	-C49	-C50	-H56	: 178.491606
H54	-C49	-C50	-H55	:-57.430815
H54	-C49	-C50	-H56	: 58.425720
H55	-C50	-C51	-C67	: 60.770332
H55	-C50	-C51	-C71	:-56.745306
H56	-C50	-C51	-C67	:-55.092716
H56	-C50	-C51	-C71	:-172.608354
C57	-C58	-C59	-C60	:-64.621458
C57	-C58	-C59	-H63	: 58.845961
C57	-C58	-C59	-H64	: 174.874792
C57	-C58	-C75	-H76	:-175.189097
C57	-C58	-C75	-H77	:-55.552823
C57	-C58	-C75	-H78	: 66.010170
C57	-C58	-C79	-H80	: 176.021081
C57	-C58	-C79	-H81	:-64.385469
C57	-C58	-C79	-H82	: 54.916817
C57	-C62	-S61	-C60	:-3.589128
C58	-C57	-C62	-S61	:-2.597151
C58	-C59	-C60	-S61	: 58.560220
C58	-C59	-C60	-H65	: 176.430904
C58	-C59	-C60	-H66	:-63.985574



C59 -C58 -C57 -C62 : 34.216850  
C59 -C58 -C75 -H76 : -54.503535  
C59 -C58 -C75 -H77 : 65.132739  
C59 -C58 -C75 -H78 : -173.304268  
C59 -C58 -C79 -H80 : 54.889836  
C59 -C58 -C79 -H81 : 174.483286  
C59 -C58 -C79 -H82 : -66.214428  
C59 -C60 -S61 -C62 : -22.759653  
C60 -C59 -C58 -C75 : 173.571570  
C60 -C59 -C58 -C79 : 55.632811  
S61 -C60 -C59 -H63 : -64.627836  
S61 -C60 -C59 -H64 : 179.498995  
C62 -C57 -C58 -C75 : 152.857093  
C62 -C57 -C58 -C79 : -87.130748  
C62 -S61 -C60 -H65 : -143.611688  
C62 -S61 -C60 -H66 : 101.129549  
H63 -C59 -C58 -C75 : -62.961011  
H63 -C59 -C58 -C79 : 179.100230  
H63 -C59 -C60 -H65 : 53.242848  
H63 -C59 -C60 -H66 : 172.826369  
H64 -C59 -C58 -C75 : 53.067820  
H64 -C59 -C58 -C79 : -64.870939  
H64 -C59 -C60 -H65 : -62.630321  
H64 -C59 -C60 -H66 : 56.953200  
C67 -C51 -C71 -H72 : 59.785688  
C67 -C51 -C71 -H73 : 179.182872  
C67 -C51 -C71 -H74 : -59.906200  
H68 -C67 -C51 -C71 : -53.498951  
H69 -C67 -C51 -C71 : 65.556360  
H70 -C67 -C51 -C71 : -174.892120

C75 -C58 -C79 -H80 : -61.894222

C75 -C58 -C79 -H81 : 57.699229

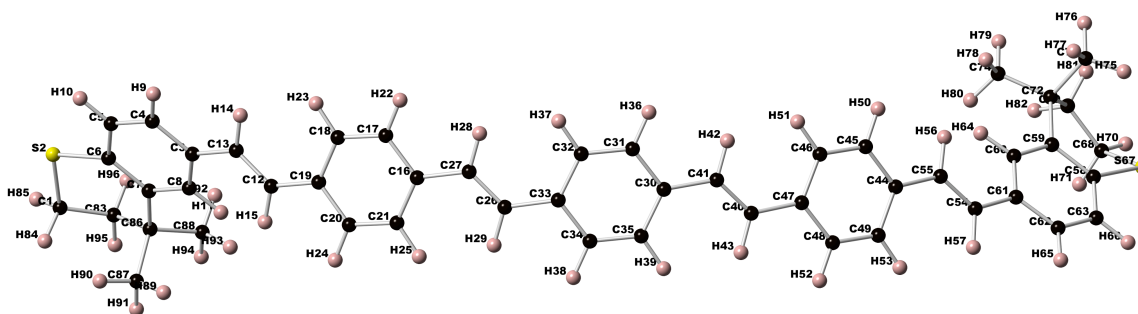
C75 -C58 -C79 -H82 : 177.001515

H76 -C75 -C58 -C79 : 64.717709

H77 -C75 -C58 -C79 : -175.646017

H78 -C75 -C58 -C79 : -54.083024

## PPV4



Final geometry:

atom	x	y	z
C1	0.1311759001	-4.8233740321	1.4399943570
S2	-0.9890420911	-4.3641105345	0.0698979678
C3	1.6580420060	-4.0156632387	-3.6837177687
C4	0.2925651842	-3.6829789008	-3.6670074669
C5	-0.4444921163	-3.7924394563	-2.5001795780
C6	0.1355228307	-4.2634152201	-1.3098970055
C7	1.4962042125	-4.6455218474	-1.2972765329
C8	2.2177456374	-4.4905926153	-2.4868594269
H9	-0.1870697937	-3.3260759650	-4.5748137483
H10	-1.4947215977	-3.5134239266	-2.5009360953
H11	3.2565520563	-4.7972966951	-2.5013596546
C12	3.7701423245	-3.8967026348	-5.0263730297
C13	2.4238894138	-3.9249560804	-4.9282922064
H14	1.8251189494	-3.8989081426	-5.8377398164
H15	4.3469499557	-3.8470089357	-4.1038683134
C16	6.3214375181	-4.4362718062	-8.4603722525
C17	4.9175032206	-4.4686350670	-8.5972176616
C18	4.0700547648	-4.2494966753	-7.5209240575

C19	4.5837393494	-3.9831692690	-6.2361536865
C20	5.9853146105	-3.8855063064	-6.1151584374
C21	6.8309888425	-4.1011771326	-7.1903733964
H22	4.4912725235	-4.7126309537	-9.5673759684
H23	2.9983975874	-4.3326020761	-7.6700862346
H24	6.4122928717	-3.6648601823	-5.1398197563
H25	7.9028339584	-4.0477694320	-7.0314022839
C26	8.5036465354	-4.9671990367	-9.5903093500
C27	7.1568284422	-4.8518903029	-9.5847543647
H28	6.6009723305	-5.1714012355	-10.4641285912
H29	9.0544660957	-4.6444994437	-8.7086852474
C30	11.0076317524	-7.1610955887	-12.3242428398
C31	9.6550623189	-6.9064778181	-12.6372080706
C32	8.8393060693	-6.1491522716	-11.8105338918
C33	9.3338831274	-5.6009952338	-10.6100572752
C34	10.7067649175	-5.7844468154	-10.3413864126
C35	11.5213406605	-6.5404877645	-11.1684606827
H36	9.2331091596	-7.3508079277	-13.5349678465
H37	7.7967819242	-6.0163068121	-12.0804164888
H38	11.1244511709	-5.3550195272	-9.4339784502
H39	12.5596776579	-6.6862764057	-10.8891329569
C40	13.0197504572	-8.5514201002	-12.9244824431
C41	11.7542235268	-8.1234582926	-13.1309231382
H42	11.1726836148	-8.5821463434	-13.9282208061
H43	13.6115705098	-8.0743142010	-12.1451424981
C44	14.9875759823	-12.0507673095	-14.4968600814
C45	13.6726760266	-11.7249540376	-14.8905082989
C46	13.0364862768	-10.5762959660	-14.4465993670
C47	13.6842483765	-9.6808586208	-13.5720992456
C48	15.0192058561	-9.9777671188	-13.2257444298

C49	15.6564611713	-11.1257146527	-13.6722110739
H50	13.1331314573	-12.4157148055	-15.5339516028
H51	12.0090021282	-10.3986841535	-14.7459604852
H52	15.5486866754	-9.3046751325	-12.5565273697
H53	16.6682937239	-11.3307695883	-13.3374978510
C54	16.7841375028	-13.8187358957	-14.6631758770
C55	15.5360861940	-13.3506145645	-14.8763336595
H56	14.8185967060	-14.0117687876	-15.3590480454
H57	17.5425232882	-13.1508418805	-14.2583695928
C58	18.1196925823	-17.8328441977	-15.3300325468
C59	16.7329974114	-17.5890246393	-15.1935798692
C60	16.3300062022	-16.2696597034	-14.9739737376
C61	17.2333267675	-15.1909289168	-14.9187326338
C62	18.6013873763	-15.4713268663	-15.0684126080
C63	19.0352628803	-16.7767471159	-15.2650190003
H64	15.2795312438	-16.0608339288	-14.8151330875
H65	19.3267552358	-14.6636808275	-15.0147559102
H66	20.0963751346	-16.9920632477	-15.3474995786
S67	18.7368927211	-19.4965405212	-15.5245009274
C68	17.5983695271	-20.2476885976	-14.2942171550
C69	16.1125393370	-20.0390398110	-14.6145201573
H70	17.8468433317	-21.3114587414	-14.2527495718
H71	17.8551648959	-19.8092023059	-13.3263549210
C72	15.7110543368	-18.7244406595	-15.3729780168
C73	15.6113978289	-19.0195106031	-16.8951064867
C74	14.3027610960	-18.3357360639	-14.8816723561
H75	16.5638310376	-19.3640900916	-17.3025773186
H76	14.8605214861	-19.7965969833	-17.0791221320
H77	15.3101488177	-18.1185816215	-17.4389564079
H78	13.8608270376	-17.5357335699	-15.4833121635

H79	13.6378591363	-19.2020318827	-14.9608623683
H80	14.3123317839	-18.0158609950	-13.8344174606
H81	15.7436773510	-20.8839589516	-15.2063898629
H82	15.5742478065	-20.0745222520	-13.6592874282
C83	1.2199254274	-5.7833844435	0.9783704079
H84	0.5511509823	-3.9186465296	1.8877071942
H85	-0.5116818836	-5.2951510987	2.1880497128
C86	2.2173742473	-5.1974034315	-0.0507206029
C87	3.0406978736	-4.0567189724	0.5950943297
C88	3.1787109640	-6.3495953829	-0.4247362875
H89	3.7971752139	-3.6861974547	-0.1034038374
H90	2.4135505118	-3.2045638581	0.8726221168
H91	3.5553251350	-4.4119394414	1.4960293734
H92	2.6562006803	-7.1410385739	-0.9711255417
H93	4.0185909080	-6.0136562998	-1.0380938162
H94	3.6030306827	-6.7875596844	0.4852654702
H95	1.7918007363	-6.1081536374	1.8571890388
H96	0.7490240011	-6.6799402055	0.5577915813

Total energy (hartrees): -2653.25687824603

HOMO energy (hartrees): -0.17849

LUMO energy (hartrees): -0.07562

Bond lengths (angstroms):

C1 -S2 : 1.828381    C1 -C83 : 1.523185

C1 -H84 : 1.093324    C1 -H85 : 1.093356

S2	-C6	: 1.782868	C3	-C4	: 1.405519
C3	-C8	: 1.404028	C3	-C13	: 1.464143
C4	-C5	: 1.384457	C4	-H9	: 1.086987
C5	-C6	: 1.405350	C5	-H10	: 1.086661
C6	-C7	: 1.413371	C7	-C8	: 1.399904
C7	-C86	: 1.542258	C8	-H11	: 1.083234
C12	-C13	: 1.350117	C12	-H15	: 1.089124
C12	-C19	: 1.460475	C13	-H14	: 1.089174
C16	-C17	: 1.410959	C16	-C21	: 1.408839
C16	-C27	: 1.461113	C17	-C18	: 1.387299
C17	-H22	: 1.087388	C18	-C19	: 1.409055
C18	-H23	: 1.085175	C19	-C20	: 1.410174
C20	-C21	: 1.384834	C20	-H24	: 1.087327
C21	-H25	: 1.084885	C26	-C27	: 1.351757
C26	-H29	: 1.088484	C26	-C33	: 1.459752
C27	-H28	: 1.088284	C30	-C31	: 1.411461
C30	-C35	: 1.408859	C30	-C41	: 1.460916
C31	-C32	: 1.386503	C31	-H36	: 1.086944
C32	-C33	: 1.409336	C32	-H37	: 1.085054
C33	-C34	: 1.410901	C34	-C35	: 1.385346
C34	-H38	: 1.087317	C35	-H39	: 1.085091
C40	-C41	: 1.351787	C40	-H43	: 1.088693
C40	-C47	: 1.461710	C41	-H42	: 1.088240
C44	-C45	: 1.410700	C44	-C49	: 1.408253
C44	-C55	: 1.460981	C45	-C46	: 1.386076
C45	-H50	: 1.087326	C46	-C47	: 1.409310
C46	-H51	: 1.084844	C47	-C48	: 1.410754
C48	-C49	: 1.386799	C48	-H52	: 1.086855
C49	-H53	: 1.085304	C54	-C55	: 1.349891
C54	-H57	: 1.088623	C54	-C61	: 1.466286

C55	-H56	: 1.088545	C58	-C59	: 1.414564
C58	-C63	: 1.399227	C58	-S67	: 1.785116
C59	-C60	: 1.396908	C59	-C72	: 1.538090
C60	-C61	: 1.408084	C60	-H64	: 1.082745
C61	-C62	: 1.404499	C62	-C63	: 1.389613
C62	-H65	: 1.086890	C63	-H66	: 1.085874
S67	-C68	: 1.836861	C68	-C69	: 1.534216
C68	-H70	: 1.093191	C68	-H71	: 1.093147
C69	-C72	: 1.569911	C69	-H81	: 1.095563
C69	-H82	: 1.097035	C72	-C73	: 1.553664
C72	-C74	: 1.541351	C73	-H75	: 1.091740
C73	-H76	: 1.096148	C73	-H77	: 1.094622
C74	-H78	: 1.094203	C74	-H79	: 1.094913
C74	-H80	: 1.095059	C83	-C86	: 1.548324
C83	-H95	: 1.097651	C83	-H96	: 1.096561
C86	-C87	: 1.547934	C86	-C88	: 1.546481
C87	-H89	: 1.094278	C87	-H90	: 1.093848
C87	-H91	: 1.096680	C88	-H92	: 1.094505
C88	-H93	: 1.092914	C88	-H94	: 1.095428

## Bond angles:

C83	-C1	-S2	: 111.663131	H84	-C1	-S2	: 109.532871
H84	-C1	-C83	: 111.782338	H85	-C1	-S2	: 105.119899
H85	-C1	-C83	: 110.834284	H85	-C1	-H84	: 107.622597
C6	-S2	-C1	: 101.985576	C8	-C3	-C4	: 117.207568
C13	-C3	-C4	: 120.239038	C13	-C3	-C8	: 122.482983
C5	-C4	-C3	: 120.565196	H9	-C4	-C3	: 119.766679
H9	-C4	-C5	: 119.664604	C6	-C5	-C4	: 121.372510
H10	-C5	-C4	: 119.580357	H10	-C5	-C6	: 119.046648



C5 -C6 -S2 : 114.461563 C7 -C6 -S2 : 125.807735  
 C7 -C6 -C5 : 119.702664 C8 -C7 -C6 : 117.303204  
 C86 -C7 -C6 : 123.651087 C86 -C7 -C8 : 119.040033  
 C7 -C8 -C3 : 123.803195 H11 -C8 -C3 : 117.817386  
 H11 -C8 -C7 : 118.315222 H15 -C12 -C13 : 117.873022  
 C19 -C12 -C13 : 127.909809 C19 -C12 -H15 : 114.160398  
 C12 -C13 -C3 : 125.776151 H14 -C13 -C3 : 115.068169  
 H14 -C13 -C12 : 119.144571 C21 -C16 -C17 : 116.921286  
 C27 -C16 -C17 : 119.192338 C27 -C16 -C21 : 123.680876  
 C18 -C17 -C16 : 121.934733 H22 -C17 -C16 : 118.796692  
 H22 -C17 -C18 : 119.221023 C19 -C18 -C17 : 120.967343  
 H23 -C18 -C17 : 118.980757 H23 -C18 -C19 : 119.988330  
 C18 -C19 -C12 : 124.290301 C20 -C19 -C12 : 118.587899  
 C20 -C19 -C18 : 116.978766 C21 -C20 -C19 : 121.974413  
 H24 -C20 -C19 : 118.770987 H24 -C20 -C21 : 119.226054  
 C20 -C21 -C16 : 121.069698 H25 -C21 -C16 : 120.075145  
 H25 -C21 -C20 : 118.808923 H29 -C26 -C27 : 118.396856  
 C33 -C26 -C27 : 127.342733 C33 -C26 -H29 : 113.999157  
 C26 -C27 -C16 : 126.661614 H28 -C27 -C16 : 114.412274  
 H28 -C27 -C26 : 118.720217 C35 -C30 -C31 : 116.862535  
 C41 -C30 -C31 : 119.085794 C41 -C30 -C35 : 123.836346  
 C32 -C31 -C30 : 122.014713 H36 -C31 -C30 : 118.776913  
 H36 -C31 -C32 : 119.165917 C33 -C32 -C31 : 120.920430  
 H37 -C32 -C31 : 118.938437 H37 -C32 -C33 : 120.094094  
 C32 -C33 -C26 : 124.355855 C34 -C33 -C26 : 118.480088  
 C34 -C33 -C32 : 116.943055 C35 -C34 -C33 : 121.966451  
 H38 -C34 -C33 : 118.774078 H38 -C34 -C35 : 119.202316  
 C34 -C35 -C30 : 121.049284 H39 -C35 -C30 : 120.060498  
 H39 -C35 -C34 : 118.835534 H43 -C40 -C41 : 118.652656  
 C47 -C40 -C41 : 127.053157 C47 -C40 -H43 : 114.120287

C40 -C41 -C30 : 127.060424 H42 -C41 -C30 : 114.148996  
 H42 -C41 -C40 : 118.602637 C49 -C44 -C45 : 117.027082  
 C55 -C44 -C45 : 118.878289 C55 -C44 -C49 : 123.931787  
 C46 -C45 -C44 : 121.995111 H50 -C45 -C44 : 118.745483  
 H50 -C45 -C46 : 119.224557 C47 -C46 -C45 : 120.951046  
 H51 -C46 -C45 : 118.817360 H51 -C46 -C47 : 120.167853  
 C46 -C47 -C40 : 123.842703 C48 -C47 -C40 : 118.948502  
 C48 -C47 -C46 : 116.972184 C49 -C48 -C47 : 122.005428  
 H52 -C48 -C47 : 118.804614 H52 -C48 -C49 : 119.144135  
 C48 -C49 -C44 : 120.931205 H53 -C49 -C44 : 119.954243  
 H53 -C49 -C48 : 119.046296 H57 -C54 -C55 : 119.343743  
 C61 -C54 -C55 : 125.467638 C61 -C54 -H57 : 115.185290  
 C54 -C55 -C44 : 127.925599 H56 -C55 -C44 : 114.085829  
 H56 -C55 -C54 : 117.956216 C63 -C58 -C59 : 120.455655  
 S67 -C58 -C59 : 120.669474 S67 -C58 -C63 : 118.833031  
 C60 -C59 -C58 : 117.436477 C72 -C59 -C58 : 120.853431  
 C72 -C59 -C60 : 121.592806 C61 -C60 -C59 : 123.001924  
 H64 -C60 -C59 : 119.019917 H64 -C60 -C61 : 117.962559  
 C60 -C61 -C54 : 121.819635 C62 -C61 -C54 : 120.251918  
 C62 -C61 -C60 : 117.888612 C63 -C62 -C61 : 120.447737  
 H65 -C62 -C61 : 119.765625 H65 -C62 -C63 : 119.779878  
 C62 -C63 -C58 : 120.751333 H66 -C63 -C58 : 119.092882  
 H66 -C63 -C62 : 120.140943 C68 -S67 -C58 : 95.385122  
 C69 -C68 -S67 : 113.880346 H70 -C68 -S67 : 106.406545  
 H70 -C68 -C69 : 111.123549 H71 -C68 -S67 : 106.461860  
 H71 -C68 -C69 : 110.965098 H71 -C68 -H70 : 107.658819  
 C72 -C69 -C68 : 117.543045 H81 -C69 -C68 : 109.510126  
 H81 -C69 -C72 : 107.378999 H82 -C69 -C68 : 106.799153  
 H82 -C69 -C72 : 108.800413 H82 -C69 -H81 : 106.275820  
 C69 -C72 -C59 : 113.071470 C73 -C72 -C59 : 107.282623

C73 -C72 -C69 : 109.310450 C74 -C72 -C59 : 112.564714  
 C74 -C72 -C69 : 106.908128 C74 -C72 -C73 : 107.551863  
 H75 -C73 -C72 : 111.693392 H76 -C73 -C72 : 110.062451  
 H76 -C73 -H75 : 108.131300 H77 -C73 -C72 : 110.370749  
 H77 -C73 -H75 : 108.326459 H77 -C73 -H76 : 108.152832  
 H78 -C74 -C72 : 112.218374 H79 -C74 -C72 : 109.406020  
 H79 -C74 -H78 : 107.063732 H80 -C74 -C72 : 111.747367  
 H80 -C74 -H78 : 108.409221 H80 -C74 -H79 : 107.793737  
 C86 -C83 -C1 : 115.047759 H95 -C83 -C1 : 108.435585  
 H95 -C83 -C86 : 107.967963 H96 -C83 -C1 : 108.940986  
 H96 -C83 -C86 : 109.339083 H96 -C83 -H95 : 106.792286  
 C83 -C86 -C7 : 111.802235 C87 -C86 -C7 : 108.798187  
 C87 -C86 -C83 : 110.135391 C88 -C86 -C7 : 111.211037  
 C88 -C86 -C83 : 106.214622 C88 -C86 -C87 : 108.620214  
 H89 -C87 -C86 : 110.542169 H90 -C87 -C86 : 112.023387  
 H90 -C87 -H89 : 107.128802 H91 -C87 -C86 : 110.710569  
 H91 -C87 -H89 : 108.038743 H91 -C87 -H90 : 108.237118  
 H92 -C88 -C86 : 111.267097 H93 -C88 -C86 : 112.608150  
 H93 -C88 -H92 : 107.997215 H94 -C88 -C86 : 109.740204  
 H94 -C88 -H92 : 108.090789 H94 -C88 -H93 : 106.943866

Torsional angles:

C1 -S2 -C6 -C5 :-174.131013  
 C1 -S2 -C6 -C7 : 7.813344  
 C1 -C83 -C86 -C7 :-55.860997  
 C1 -C83 -C86 -C87 : 65.224637  
 C1 -C83 -C86 -C88 :-177.337314  
 S2 -C1 -C83 -C86 : 65.084267  
 S2 -C1 -C83 -H95 :-173.937759

S2	-C1	-C83	-H96	: -58.065829
S2	-C6	-C5	-C4	: -178.695051
S2	-C6	-C5	-H10	: 1.050263
S2	-C6	-C7	-C8	: 179.964275
S2	-C6	-C7	-C86	: -0.912508
C3	-C4	-C5	-C6	: -1.385404
C3	-C4	-C5	-H10	: 178.870618
C3	-C8	-C7	-C6	: -1.747213
C3	-C8	-C7	-C86	: 179.087593
C3	-C13	-C12	-H15	: -5.838516
C3	-C13	-C12	-C19	: 171.244222
C4	-C3	-C8	-C7	: -0.063728
C4	-C3	-C8	-H11	: 176.967863
C4	-C3	-C13	-C12	: 162.981345
C4	-C3	-C13	-H14	: -18.248636
C4	-C5	-C6	-C7	: -0.510374
C5	-C4	-C3	-C8	: 1.648410
C5	-C4	-C3	-C13	: 178.672384
C5	-C6	-C7	-C8	: 2.001861
C5	-C6	-C7	-C86	: -178.874922
C6	-S2	-C1	-C83	: -36.955848
C6	-S2	-C1	-H84	: 87.417167
C6	-S2	-C1	-H85	: -157.203648
C6	-C5	-C4	-H9	: 179.298800
C6	-C7	-C8	-H11	: -178.765007
C6	-C7	-C86	-C83	: 21.772342
C6	-C7	-C86	-C87	: -100.085475
C6	-C7	-C86	-C88	: 140.317304
C7	-C6	-C5	-H10	: 179.234939
C7	-C8	-C3	-C13	: -177.015731

C7 -C86 -C83 -H95 :-177.093813  
C7 -C86 -C83 -H96 : 67.076699  
C7 -C86 -C87 -H89 :-61.210923  
C7 -C86 -C87 -H90 : 58.185716  
C7 -C86 -C87 -H91 : 179.105608  
C7 -C86 -C88 -H92 :-54.927505  
C7 -C86 -C88 -H93 : 66.487320  
C7 -C86 -C88 -H94 :-174.510917  
C8 -C3 -C4 -H9 :-179.036490  
C8 -C3 -C13 -C12 :-20.156438  
C8 -C3 -C13 -H14 : 158.613581  
C8 -C7 -C86 -C83 :-159.118794  
C8 -C7 -C86 -C87 : 79.023389  
C8 -C7 -C86 -C88 :-40.573832  
H9 -C4 -C3 -C13 : -2.012516  
H9 -C4 -C5 -H10 : -0.445178  
H11 -C8 -C3 -C13 : 0.015860  
H11 -C8 -C7 -C86 : 2.069799  
C12 -C19 -C18 -C17 :-172.524606  
C12 -C19 -C18 -H23 : 4.546292  
C12 -C19 -C20 -C21 : 172.908980  
C12 -C19 -C20 -H24 : -5.131646  
C13 -C12 -C19 -C18 : -6.706481  
C13 -C12 -C19 -C20 : 177.780366  
H14 -C13 -C12 -H15 : 175.437115  
H14 -C13 -C12 -C19 : -7.480146  
H15 -C12 -C19 -C18 : 170.467192  
H15 -C12 -C19 -C20 : -5.045961  
C16 -C17 -C18 -C19 : 0.009326  
C16 -C17 -C18 -H23 :-177.090578

C16 -C21 -C20 -C19 : -0.294607  
C16 -C21 -C20 -H24 : 177.737371  
C16 -C27 -C26 -H29 : -5.626922  
C16 -C27 -C26 -C33 : 168.119645  
C17 -C16 -C21 -C20 : 3.343803  
C17 -C16 -C21 -H25 :-179.158716  
C17 -C16 -C27 -C26 :-175.172876  
C17 -C16 -C27 -H28 : -0.494423  
C17 -C18 -C19 -C20 : 3.054588  
C18 -C17 -C16 -C21 : -3.219227  
C18 -C17 -C16 -C27 : 171.764727  
C18 -C19 -C20 -C21 : -2.931935  
C18 -C19 -C20 -H24 : 179.027439  
C19 -C18 -C17 -H22 : 177.470292  
C19 -C20 -C21 -H25 :-177.823132  
C20 -C19 -C18 -H23 :-179.874515  
C20 -C21 -C16 -C27 :-171.393245  
C21 -C16 -C17 -H22 : 179.309395  
C21 -C16 -C27 -C26 : -0.548542  
C21 -C16 -C27 -H28 : 174.129910  
H22 -C17 -C16 -C27 : -5.706651  
H22 -C17 -C18 -H23 : 0.370388  
H24 -C20 -C21 -H25 : 0.208846  
H25 -C21 -C16 -C27 : 6.104236  
C26 -C33 -C32 -C31 :-170.404769  
C26 -C33 -C32 -H37 : 7.074343  
C26 -C33 -C34 -C35 : 170.741479  
C26 -C33 -C34 -H38 : -6.485864  
C27 -C26 -C33 -C32 : 3.237468  
C27 -C26 -C33 -C34 :-171.185263

H28	-C27	-C26	-H29	: 179.899248
H28	-C27	-C26	-C33	: -6.354185
H29	-C26	-C33	-C32	: 177.216802
H29	-C26	-C33	-C34	: 2.794071
C30	-C31	-C32	-C33	: -0.175937
C30	-C31	-C32	-H37	:-177.683691
C30	-C35	-C34	-C33	: 0.118426
C30	-C35	-C34	-H38	: 177.334255
C30	-C41	-C40	-H43	: -6.956239
C30	-C41	-C40	-C47	: 167.947794
C31	-C30	-C35	-C34	: 3.813173
C31	-C30	-C35	-H39	:-178.907586
C31	-C30	-C41	-C40	:-175.416936
C31	-C30	-C41	-H42	: -0.512127
C31	-C32	-C33	-C34	: 4.096248
C32	-C31	-C30	-C35	: -3.805225
C32	-C31	-C30	-C41	: 171.068948
C32	-C33	-C34	-C35	: -4.094765
C32	-C33	-C34	-H38	: 178.677891
C33	-C32	-C31	-H36	: 177.424221
C33	-C34	-C35	-H39	:-177.193484
C34	-C33	-C32	-H37	:-178.424639
C34	-C35	-C30	-C41	:-170.793262
C35	-C30	-C31	-H36	: 178.585608
C35	-C30	-C41	-C40	: -0.923175
C35	-C30	-C41	-H42	: 173.981634
H36	-C31	-C30	-C41	: -6.540220
H36	-C31	-C32	-H37	: -0.083533
H38	-C34	-C35	-H39	: 0.022345
H39	-C35	-C30	-C41	: 6.485979

C40 -C47 -C46 -C45 :-171.488710  
C40 -C47 -C46 -H51 : 5.573523  
C40 -C47 -C48 -C49 : 171.879389  
C40 -C47 -C48 -H52 : -5.636367  
C41 -C40 -C47 -C46 : -5.783805  
C41 -C40 -C47 -C48 : 179.981686  
H42 -C41 -C40 -H43 : 178.339870  
H42 -C41 -C40 -C47 : -6.756097  
H43 -C40 -C47 -C46 : 169.316959  
H43 -C40 -C47 -C48 : -4.917551  
C44 -C45 -C46 -C47 : -0.173183  
C44 -C45 -C46 -H51 :-177.274357  
C44 -C49 -C48 -C47 : -0.069162  
C44 -C49 -C48 -H52 : 177.438424  
C44 -C55 -C54 -H57 : -7.257325  
C44 -C55 -C54 -C61 : 172.045468  
C45 -C44 -C49 -C48 : 2.753721  
C45 -C44 -C49 -H53 : 179.720624  
C45 -C44 -C55 -C54 : 176.060407  
C45 -C44 -C55 -H56 : -6.072128  
C45 -C46 -C47 -C48 : 2.850761  
C46 -C45 -C44 -C49 : -2.650836  
C46 -C45 -C44 -C55 : 172.894957  
C46 -C47 -C48 -C49 : -2.748718  
C46 -C47 -C48 -H52 : 179.735526  
C47 -C46 -C45 -H50 : 177.651905  
C47 -C48 -C49 -H53 :-177.063163  
C48 -C47 -C46 -H51 : 179.912994  
C48 -C49 -C44 -C55 :-172.544879  
C49 -C44 -C45 -H50 : 179.514020



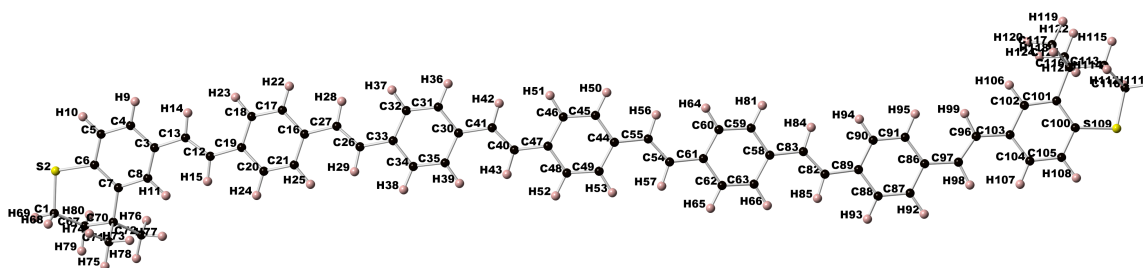
C49 -C44 -C55 -C54 : -8.722490  
C49 -C44 -C55 -H56 : 169.144975  
H50 -C45 -C44 -C55 : -4.940186  
H50 -C45 -C46 -H51 : 0.550731  
H52 -C48 -C49 -H53 : 0.444423  
H53 -C49 -C44 -C55 : 4.422024  
C54 -C61 -C60 -C59 :-178.905969  
C54 -C61 -C60 -H64 : -0.358626  
C54 -C61 -C62 -C63 : 177.785836  
C54 -C61 -C62 -H65 : -1.266290  
C55 -C54 -C61 -C60 : -22.452850  
C55 -C54 -C61 -C62 : 159.891602  
H56 -C55 -C54 -H57 : 174.946777  
H56 -C55 -C54 -C61 : -5.750429  
H57 -C54 -C61 -C60 : 156.875555  
H57 -C54 -C61 -C62 : -20.779993  
C58 -C59 -C60 -C61 : 1.640443  
C58 -C59 -C60 -H64 :-176.892273  
C58 -C59 -C72 -C69 : 45.924558  
C58 -C59 -C72 -C73 : -74.669828  
C58 -C59 -C72 -C74 : 167.211613  
C58 -C63 -C62 -C61 : 0.598954  
C58 -C63 -C62 -H65 : 179.650945  
C58 -S67 -C68 -C69 : 58.412878  
C58 -S67 -C68 -H70 :-178.821360  
C58 -S67 -C68 -H71 : -64.192111  
C59 -C58 -C63 -C62 : -0.129584  
C59 -C58 -C63 -H66 : 178.470911  
C59 -C58 -S67 -C68 : -40.659734  
C59 -C60 -C61 -C62 : -1.197235

C59 -C72 -C69 -C68 : -23.402957  
C59 -C72 -C69 -H81 : -147.314032  
C59 -C72 -C69 -H82 : 98.055276  
C59 -C72 -C73 -H75 : 62.262631  
C59 -C72 -C73 -H76 : -177.615839  
C59 -C72 -C73 -H77 : -58.313846  
C59 -C72 -C74 -H78 : 65.660286  
C59 -C72 -C74 -H79 : -175.657248  
C59 -C72 -C74 -H80 : -56.359408  
C60 -C59 -C58 -C63 : -0.952677  
C60 -C59 -C58 -S67 : 176.667323  
C60 -C59 -C72 -C69 : -138.114027  
C60 -C59 -C72 -C73 : 101.291587  
C60 -C59 -C72 -C74 : -16.826972  
C60 -C61 -C62 -C63 : 0.039665  
C60 -C61 -C62 -H65 : -179.012460  
C61 -C60 -C59 -C72 : -174.453326  
C61 -C62 -C63 -H66 : -177.986908  
C62 -C61 -C60 -H64 : 177.350107  
C62 -C63 -C58 -S67 : -177.792817  
C63 -C58 -C59 -C72 : 175.171576  
C63 -C58 -S67 -C68 : 136.998341  
H64 -C60 -C59 -C72 : 7.013959  
H65 -C62 -C63 -H66 : 1.065082  
H66 -C63 -C58 -S67 : 0.807677  
S67 -C58 -C59 -C72 : -7.208425  
S67 -C68 -C69 -C72 : -31.035529  
S67 -C68 -C69 -H81 : 91.796340  
S67 -C68 -C69 -H82 : -153.523177  
C68 -C69 -C72 -C73 : 96.030655

C68	-C69	-C72	-C74	:-147.833706
C69	-C72	-C73	-H75	:-60.686565
C69	-C72	-C73	-H76	: 59.434965
C69	-C72	-C73	-H77	: 178.736959
C69	-C72	-C74	-H78	:-169.599732
C69	-C72	-C74	-H79	:-50.917266
C69	-C72	-C74	-H80	: 68.380575
H70	-C68	-C69	-C72	:-151.180501
H70	-C68	-C69	-H81	:-28.348632
H70	-C68	-C69	-H82	: 86.331851
H71	-C68	-C69	-C72	: 89.064845
H71	-C68	-C69	-H81	:-148.103286
H71	-C68	-C69	-H82	:-33.422803
C73	-C72	-C69	-H81	:-27.880419
C73	-C72	-C69	-H82	:-142.511112
C73	-C72	-C74	-H78	:-52.299681
C73	-C72	-C74	-H79	: 66.382785
C73	-C72	-C74	-H80	:-174.319375
C74	-C72	-C69	-H81	: 88.255220
C74	-C72	-C69	-H82	:-26.375473
C74	-C72	-C73	-H75	:-176.411616
C74	-C72	-C73	-H76	:-56.290085
C74	-C72	-C73	-H77	: 63.011908
C83	-C86	-C87	-H89	: 175.923144
C83	-C86	-C87	-H90	:-64.680218
C83	-C86	-C87	-H91	: 56.239674
C83	-C86	-C88	-H92	: 66.926518
C83	-C86	-C88	-H93	:-171.658656
C83	-C86	-C88	-H94	:-52.656893
H84	-C1	-C83	-C86	:-58.018789

H84	-C1	-C83	-H95	:	62.959185
H84	-C1	-C83	-H96	:	178.831115
H85	-C1	-C83	-C86	:	-178.078730
H85	-C1	-C83	-H95	:	-57.100756
H85	-C1	-C83	-H96	:	58.771174
C87	-C86	-C83	-H95	:	-56.008179
C87	-C86	-C83	-H96	:	-171.837667
C87	-C86	-C88	-H92	:	-174.630608
C87	-C86	-C88	-H93	:	-53.215783
C87	-C86	-C88	-H94	:	65.785980
C88	-C86	-C83	-H95	:	61.429870
C88	-C86	-C83	-H96	:	-54.399618
C88	-C86	-C87	-H89	:	59.986551
C88	-C86	-C87	-H90	:	179.383189
C88	-C86	-C87	-H91	:	-59.696919

## PPV5



Final geometry:

angstroms

atom	x	y	z
C1	-0.8228682975	-2.1534157401	1.3720545370
S2	-1.8090592213	-1.9925479834	-0.1584315924
C3	0.9859230210	-3.2186652657	-3.6107066183
C4	-0.2940248788	-2.6707657077	-3.8054971413
C5	-1.0824531648	-2.3122876158	-2.7260180642
C6	-0.6396747609	-2.4963894231	-1.4063935059
C7	0.6312393404	-3.0681630824	-1.1672011581
C8	1.4084979114	-3.3985972057	-2.2834340028
H9	-0.6656410410	-2.5174552357	-4.8154573410
H10	-2.0625485147	-1.8759729689	-2.8985677822
H11	2.3860638694	-3.8320499632	-2.1117777595
C12	3.0677406988	-4.0254391290	-4.7679625093
C13	1.7928851553	-3.5830149818	-4.7768066173
H14	1.2802295216	-3.4752668858	-5.7317420426
H15	3.5769514209	-4.1035888405	-3.8087861224
C16	5.6169915369	-5.3765978543	-7.9803662542
C17	4.3013159013	-4.9421944961	-8.2471312468
C18	3.4588214031	-4.4856153982	-7.2421504898
C19	3.8894495078	-4.4428078427	-5.9010369544

C20	5.2099177854	-4.8615522932	-5.6384401784
C21	6.0486998761	-5.3157957829	-6.6403791807
H22	3.9362371515	-4.9760243589	-9.2709850331
H23	2.4516912339	-4.1724191121	-7.5003924034
H24	5.5718803393	-4.8377698672	-4.6134530123
H25	7.0472692772	-5.6465385898	-6.3735680202
C26	7.7250463999	-6.3228989220	-8.9440784258
C27	6.4473279621	-5.9008401623	-9.0635860596
H28	5.9528136678	-5.9671064964	-10.0315607526
H29	8.2040066542	-6.2362845994	-7.9707988231
C30	10.3406313668	-8.2806674458	-11.7651499110
C31	9.0685289794	-7.8209854680	-12.1698770247
C32	8.2092017424	-7.1673209817	-11.2970135939
C33	8.5785358652	-6.9374821244	-9.9561777147
C34	9.8597562832	-7.3741795007	-9.5600261877
C35	10.7142930205	-8.0284696885	-10.4305201662
H36	8.7511553609	-7.9955494293	-13.1952165938
H37	7.2374867533	-6.8440754346	-11.6577528971
H38	10.1755395807	-7.2051733411	-8.5334695191
H39	11.6787206218	-8.3647554827	-10.0627703468
C40	12.4133153887	-9.5113376068	-12.4666779607
C41	11.1809567060	-9.0138339915	-12.7098373799
H42	10.7287543251	-9.1731040041	-13.6870904892
H43	12.8553494888	-9.3397164992	-11.4873401243
C44	15.0098013228	-11.9118002323	-14.9497930828
C45	13.7895959512	-11.4132115412	-15.4562516998
C46	12.9381656336	-10.6317014056	-14.6889795095
C47	13.2613753521	-10.2971766067	-13.3587213379
C48	14.4893647433	-10.7788115257	-12.8597153375
C49	15.3378584868	-11.5615410664	-13.6254357466

H50	13.5076700733	-11.6586026193	-16.4772860931
H51	12.0085385240	-10.2820864559	-15.1277875194
H52	14.7742453828	-10.5297635841	-11.8402977768
H53	16.2669907342	-11.9094780560	-13.1857956828
C54	17.0049038518	-13.3644380382	-15.4587885040
C55	15.8456264949	-12.7581828106	-15.7983142589
H56	15.4514679588	-12.9086886376	-16.8021022875
H57	17.3953732081	-13.2214071993	-14.4525024887
C58	19.5111216333	-15.9698112103	-17.8254484967
C59	18.3441784586	-15.3950868922	-18.3717236074
C60	17.5261072437	-14.5522648144	-17.6376435562
C61	17.8291669371	-14.2299909803	-16.3007032542
C62	19.0002582789	-14.7976179862	-15.7549068119
C63	19.8194433721	-15.6419577201	-16.4896048251
H64	16.6379348405	-14.1447215475	-18.1089805241
H65	19.2652297514	-14.5642952986	-14.7264007629
H66	20.7056715373	-16.0557763598	-16.0180492049
C67	0.0992546031	-3.3645898140	1.3202894020
H68	-0.2685527238	-1.2277842882	1.5493530838
H69	-1.5574344106	-2.2578627845	2.1751954221
C70	1.2103336869	-3.2971596418	0.2439734198
C71	2.1952429316	-2.1475602091	0.5687697496
C72	1.9733143004	-4.6391961233	0.3257970439
H73	3.0229431045	-2.1365425499	-0.1468210581
H74	1.7126848228	-1.1672295980	0.5176017667
H75	2.6168211616	-2.2701481604	1.5737884481
H76	1.3397904220	-5.4753846331	0.0136605926
H77	2.8744654473	-4.6482645758	-0.2924987060
H78	2.2926968029	-4.8210417885	1.3577994543
H79	0.5825832783	-3.4747678956	2.2996767718

H80	-0.5057834528	-4.2653996794	1.1626905319
H81	18.0793777934	-15.6273858621	-19.4003899327
C82	21.4447924204	-17.5110188558	-18.3260013500
C83	20.3088975090	-16.8618634258	-18.6603215959
H84	19.9083602873	-17.0009358004	-19.6629909013
H85	21.8573803310	-17.3751248984	-17.3276083489
C86	23.8118961556	-20.1680562267	-20.7751414055
C87	24.1847454901	-19.8214955254	-19.4629600150
C88	23.4107632141	-18.9672497414	-18.6892450973
C89	22.2182822402	-18.4060157612	-19.1823114455
C90	21.8456155338	-18.7536410790	-20.4998580987
C91	22.6166860085	-19.6039951085	-21.2727956918
H92	25.0993084011	-20.2368619638	-19.0469147597
H93	23.7306590039	-18.7244431236	-17.6786495615
H94	20.9335188299	-18.3483574353	-20.9272319390
H95	22.2877437525	-19.8349403934	-22.2811517604
C96	24.4406254028	-21.5579663946	-22.7791381214
C97	24.6663195791	-21.0758544914	-21.5376650278
H99	25.5723231538	-21.3797459853	-21.0171219119
H100	23.5264007155	-21.2629732966	-23.2917842522
C100	26.8293259834	-24.2288502195	-25.1425621316
C101	25.5991608935	-23.7534476121	-25.6405958817
C102	24.8677359319	-22.8909772209	-24.8118894296
C103	25.2957813393	-22.4635400935	-23.5461417304
C104	26.5403621197	-22.9424417878	-23.0944546152
C105	27.2801881591	-23.8079961930	-23.8770700342
H108	23.9072193645	-22.5251443839	-25.1614283398
H109	26.9306490826	-22.6424110219	-22.1270522215
H110	28.2324757038	-24.1798644416	-23.5084931512
S110	27.9424738943	-25.3324685941	-25.9914687496



C111	26.9229257126	-25.8642277886	-27.4118290490
H112	27.6371318462	-26.2207947376	-28.1589254724
H113	26.3005710176	-26.7135603124	-27.1170170523
C114	26.0894996511	-24.7142050368	-27.9630689214
H116	26.7611989173	-23.8976067710	-28.2534305599
H117	25.5892296102	-25.0543309452	-28.8789717157
C117	25.0051703821	-24.1700033337	-27.0010667840
C120	24.3545935056	-22.9647771267	-27.7180548154
H121	25.0660754501	-22.1408494723	-27.8322809705
H122	24.0182222748	-23.2645406885	-28.7165771606
H123	23.4787436786	-22.5838800713	-27.1868201352
C123	23.9211256285	-25.2483725043	-26.7583695284
H124	23.4837014118	-25.5794175601	-27.7079869777
H125	24.3246057576	-26.1250635191	-26.2433673560
H126	23.1149266848	-24.8511118780	-26.1342525335

Total energy (hartrees): -3270.21268240747

HOMO energy (hartrees): -0.17622

LUMO energy (hartrees): -0.07934

Bond lengths (angstroms):

C1	-S2	: 1.827796	C1	-C67	: 1.523133
C1	-H68	: 1.093387	C1	-H69	: 1.093404
S2	-C6	: 1.782898	C3	-C4	: 1.405846
C3	-C8	: 1.404492	C3	-C13	: 1.464147
C4	-C5	: 1.383980	C4	-H9	: 1.087025

C5	-C6	: 1.404050	C5	-H10	: 1.086614
C6	-C7	: 1.413988	C7	-C8	: 1.399748
C7	-C70	: 1.542467	C8	-H11	: 1.083043
C12	-C13	: 1.349472	C12	-H15	: 1.088771
C12	-C19	: 1.460568	C13	-H14	: 1.089186
C16	-C17	: 1.410983	C16	-C21	: 1.409125
C16	-C27	: 1.462072	C17	-C18	: 1.388614
C17	-H22	: 1.087522	C18	-C19	: 1.409205
C18	-H23	: 1.085860	C19	-C20	: 1.409943
C20	-C21	: 1.383392	C20	-H24	: 1.087282
C21	-H25	: 1.085228	C26	-C27	: 1.350918
C26	-H29	: 1.088199	C26	-C33	: 1.459624
C27	-H28	: 1.088995	C30	-C31	: 1.411863
C30	-C35	: 1.408710	C30	-C41	: 1.461545
C31	-C32	: 1.388384	C31	-H36	: 1.087437
C32	-C33	: 1.409636	C32	-H37	: 1.085749
C33	-C34	: 1.410378	C34	-C35	: 1.384228
C34	-H38	: 1.087245	C35	-H39	: 1.085564
C40	-C41	: 1.351053	C40	-H43	: 1.088095
C40	-C47	: 1.460305	C41	-H42	: 1.088521
C44	-C45	: 1.412088	C44	-C49	: 1.408625
C44	-C55	: 1.461149	C45	-C46	: 1.387227
C45	-H50	: 1.087295	C46	-C47	: 1.409240
C46	-H51	: 1.085813	C47	-C48	: 1.410297
C48	-C49	: 1.385256	C48	-H52	: 1.087379
C49	-H53	: 1.085187	C54	-C55	: 1.351572
C54	-H57	: 1.088823	C54	-C61	: 1.461989
C55	-H56	: 1.088854	C58	-C59	: 1.410844
C58	-C63	: 1.409620	C58	-C83	: 1.459184
C59	-C60	: 1.385086	C59	-H81	: 1.087307

C60	-C61	: 1.408231	C60	-H64	: 1.084943
C61	-C62	: 1.411223	C62	-C63	: 1.386995
C62	-H65	: 1.087416	C63	-H66	: 1.085823
C67	-C70	: 1.548386	C67	-H79	: 1.097700
C67	-H80	: 1.096525	C70	-C71	: 1.548263
C70	-C72	: 1.545929	C71	-H73	: 1.094203
C71	-H74	: 1.093859	C71	-H75	: 1.096731
C72	-H76	: 1.094529	C72	-H77	: 1.092907
C72	-H78	: 1.095492	C82	-C83	: 1.350344
C82	-H85	: 1.088800	C82	-C89	: 1.460333
C83	-H84	: 1.088631	C86	-C87	: 1.407459
C86	-C91	: 1.412215	C86	-C97	: 1.461362
C87	-C88	: 1.388315	C87	-H92	: 1.087220
C88	-C89	: 1.407163	C88	-H93	: 1.087470
C89	-C90	: 1.412676	C90	-C91	: 1.383866
C90	-H94	: 1.085736	C91	-H95	: 1.085505
C96	-C97	: 1.350787	C96	-H100	: 1.088868
C96	-C103	: 1.462754	C97	-H99	: 1.088190
C100	-C101	: 1.409735	C100	-C105	: 1.407787
C100	-S110	: 1.782614	C101	-C102	: 1.401996
C101	-C117	: 1.541825	C102	-C103	: 1.402869
C102	-H108	: 1.085635	C103	-C104	: 1.407959
C104	-C105	: 1.381671	C104	-H109	: 1.085454
C105	-H110	: 1.086732	S110	-C111	: 1.827476
C111	-H112	: 1.093336	C111	-H113	: 1.093437
C111	-C114	: 1.523488	C114	-H116	: 1.096505
C114	-H117	: 1.097649	C114	-C117	: 1.548345
C117	-C120	: 1.545928	C117	-C123	: 1.548204
C120	-H121	: 1.094583	C120	-H122	: 1.095468
C120	-H123	: 1.092889	C123	-H124	: 1.096679

C123 -H125 : 1.093897 C123 -H126 : 1.094210

Bond angles:

C67 -C1 -S2 : 111.603373 H68 -C1 -S2 : 109.560864  
H68 -C1 -C67 : 111.824672 H69 -C1 -S2 : 105.128284  
H69 -C1 -C67 : 110.838155 H69 -C1 -H68 : 107.598897  
C6 -S2 -C1 : 101.966982 C8 -C3 -C4 : 117.051939  
C13 -C3 -C4 : 119.236914 C13 -C3 -C8 : 123.706687  
C5 -C4 -C3 : 120.766471 H9 -C4 -C3 : 119.666513  
H9 -C4 -C5 : 119.564248 C6 -C5 -C4 : 121.296351  
H10 -C5 -C4 : 119.602829 H10 -C5 -C6 : 119.100412  
C5 -C6 -S2 : 114.455054 C7 -C6 -S2 : 125.830602  
C7 -C6 -C5 : 119.700121 C8 -C7 -C6 : 117.365078  
C70 -C7 -C6 : 123.520958 C70 -C7 -C8 : 119.081654  
C7 -C8 -C3 : 123.799968 H11 -C8 -C3 : 118.204809  
H11 -C8 -C7 : 117.988357 H15 -C12 -C13 : 118.108262  
C19 -C12 -C13 : 128.322644 C19 -C12 -H15 : 113.565926  
C12 -C13 -C3 : 126.658095 H14 -C13 -C3 : 114.471376  
H14 -C13 -C12 : 118.870466 C21 -C16 -C17 : 116.883300  
C27 -C16 -C17 : 119.991724 C27 -C16 -C21 : 123.093693  
C18 -C17 -C16 : 122.014459 H22 -C17 -C16 : 118.779511  
H22 -C17 -C18 : 119.203585 C19 -C18 -C17 : 120.886961  
H23 -C18 -C17 : 119.041586 H23 -C18 -C19 : 120.065890  
C18 -C19 -C12 : 125.103344 C20 -C19 -C12 : 117.857601  
C20 -C19 -C18 : 117.027320 C21 -C20 -C19 : 122.037452  
H24 -C20 -C19 : 118.741526 H24 -C20 -C21 : 119.215806  
C20 -C21 -C16 : 121.140471 H25 -C21 -C16 : 120.168578  
H25 -C21 -C20 : 118.679715 H29 -C26 -C27 : 118.069722  
C33 -C26 -C27 : 128.554276 C33 -C26 -H29 : 113.348331

C26 -C27 -C16 : 125.706036 H28 -C27 -C16 : 114.990770  
 H28 -C27 -C26 : 119.282597 C35 -C30 -C31 : 116.890841  
 C41 -C30 -C31 : 119.741028 C41 -C30 -C35 : 123.344439  
 C32 -C31 -C30 : 122.055389 H36 -C31 -C30 : 118.750115  
 H36 -C31 -C32 : 119.191248 C33 -C32 -C31 : 120.837411  
 H37 -C32 -C31 : 119.026918 H37 -C32 -C33 : 120.131057  
 C32 -C33 -C26 : 125.099857 C34 -C33 -C26 : 117.826331  
 C34 -C33 -C32 : 117.045774 C35 -C34 -C33 : 122.040689  
 H38 -C34 -C33 : 118.745517 H38 -C34 -C35 : 119.205048  
 C34 -C35 -C30 : 121.109003 H39 -C35 -C30 : 120.075600  
 H39 -C35 -C34 : 118.805542 H43 -C40 -C41 : 118.324479  
 C47 -C40 -C41 : 128.165815 C47 -C40 -H43 : 113.500572  
 C40 -C41 -C30 : 126.358403 H42 -C41 -C30 : 114.509038  
 H42 -C41 -C40 : 119.119514 C49 -C44 -C45 : 116.785552  
 C55 -C44 -C45 : 119.376644 C55 -C44 -C49 : 123.834388  
 C46 -C45 -C44 : 122.066549 H50 -C45 -C44 : 118.761959  
 H50 -C45 -C46 : 119.169365 C47 -C46 -C45 : 121.001629  
 H51 -C46 -C45 : 118.904431 H51 -C46 -C47 : 120.093087  
 C46 -C47 -C40 : 124.832093 C48 -C47 -C40 : 118.249265  
 C48 -C47 -C46 : 116.912804 C49 -C48 -C47 : 122.054308  
 H52 -C48 -C47 : 118.791178 H52 -C48 -C49 : 119.153994  
 C48 -C49 -C44 : 121.167786 H53 -C49 -C44 : 120.037667  
 H53 -C49 -C48 : 118.793921 H57 -C54 -C55 : 118.740010  
 C61 -C54 -C55 : 127.191477 C61 -C54 -H57 : 114.066825  
 C54 -C55 -C44 : 127.199675 H56 -C55 -C44 : 114.101128  
 H56 -C55 -C54 : 118.690145 C63 -C58 -C59 : 116.942826  
 C83 -C58 -C59 : 118.666566 C83 -C58 -C63 : 124.388973  
 C60 -C59 -C58 : 122.086016 H81 -C59 -C58 : 118.732431  
 H81 -C59 -C60 : 119.180868 C61 -C60 -C59 : 121.017946  
 H64 -C60 -C59 : 118.805474 H64 -C60 -C61 : 120.175668

C60 -C61 -C54 : 124.116132 C62 -C61 -C54 : 118.899372  
C62 -C61 -C60 : 116.982162 C63 -C62 -C61 : 122.012877  
H65 -C62 -C61 : 118.796928 H65 -C62 -C63 : 119.190184  
C62 -C63 -C58 : 120.956231 H66 -C63 -C58 : 120.095028  
H66 -C63 -C62 : 118.947786 C70 -C67 -C1 : 115.050824  
H79 -C67 -C1 : 108.424850 H79 -C67 -C70 : 107.975839  
H80 -C67 -C1 : 108.910322 H80 -C67 -C70 : 109.378640  
H80 -C67 -H79 : 106.782020 C67 -C70 -C7 : 111.901862  
C71 -C70 -C7 : 108.694313 C71 -C70 -C67 : 110.058977  
C72 -C70 -C7 : 111.259733 C72 -C70 -C67 : 106.233662  
C72 -C70 -C71 : 108.633626 H73 -C71 -C70 : 110.578129  
H74 -C71 -C70 : 112.024282 H74 -C71 -H73 : 107.102963  
H75 -C71 -C70 : 110.718239 H75 -C71 -H73 : 108.038051  
H75 -C71 -H74 : 108.217035 H76 -C72 -C70 : 111.250753  
H77 -C72 -C70 : 112.594537 H77 -C72 -H76 : 108.033926  
H78 -C72 -C70 : 109.745999 H78 -C72 -H76 : 108.094426  
H78 -C72 -H77 : 106.928643 H85 -C82 -C83 : 119.063722  
C89 -C82 -C83 : 126.512689 C89 -C82 -H85 : 114.423185  
C82 -C83 -C58 : 127.744189 H84 -C83 -C58 : 113.823101  
H84 -C83 -C82 : 118.431955 C91 -C86 -C87 : 117.025791  
C97 -C86 -C87 : 118.982334 C97 -C86 -C91 : 123.991872  
C88 -C87 -C86 : 121.560650 H92 -C87 -C86 : 119.047394  
H92 -C87 -C88 : 119.391620 C89 -C88 -C87 : 121.505229  
H93 -C88 -C87 : 119.425833 H93 -C88 -C89 : 119.068938  
C88 -C89 -C82 : 119.198106 C90 -C89 -C82 : 123.916151  
C90 -C89 -C88 : 116.885692 C91 -C90 -C89 : 121.677989  
H94 -C90 -C89 : 119.793573 H94 -C90 -C91 : 118.528412  
C90 -C91 -C86 : 121.344016 H95 -C91 -C86 : 119.923094  
H95 -C91 -C90 : 118.732862 H100 -C96 -C97 : 118.443856  
C103 -C96 -C97 : 127.243324 C103 -C96 -H100 : 114.311968

C96 -C97 -C86 : 127.127251 H99 -C97 -C86 : 114.246639  
H99 -C97 -C96 : 118.625529 C105 -C100 -C101 : 119.750770  
S110 -C100 -C101 : 125.834536 S110 -C100 -C105 : 114.404204  
C102 -C101 -C100 : 116.992991 C117 -C101 -C100 : 123.834616  
C117 -C101 -C102 : 119.129135 C103 -C102 -C101 : 124.164326  
H108 -C102 -C101 : 118.591642 H108 -C102 -C103 : 117.244009  
C102 -C103 -C96 : 118.904534 C104 -C103 -C96 : 123.996271  
C104 -C103 -C102 : 117.099155 C105 -C104 -C103 : 120.310768  
H109 -C104 -C103 : 120.646464 H109 -C104 -C105 : 119.042132  
C104 -C105 -C100 : 121.665801 H110 -C105 -C100 : 118.896220  
H110 -C105 -C104 : 119.437261 C111 -S110 -C100 : 101.647689  
H112 -C111 -S110 : 105.161979 H113 -C111 -S110 : 109.512124  
H113 -C111 -H112 : 107.620975 C114 -C111 -S110 : 111.516629  
C114 -C111 -H112 : 110.872601 C114 -C111 -H113 : 111.871816  
H116 -C114 -C111 : 108.836419 H117 -C114 -C111 : 108.501921  
H117 -C114 -H116 : 106.798113 C117 -C114 -C111 : 115.063005  
C117 -C114 -H116 : 109.376566 C117 -C114 -H117 : 107.948727  
C114 -C117 -C101 : 111.924822 C120 -C117 -C101 : 111.145447  
C120 -C117 -C114 : 106.294250 C123 -C117 -C101 : 108.639405  
C123 -C117 -C114 : 110.056257 C123 -C117 -C120 : 108.727213  
H121 -C120 -C117 : 111.204464 H122 -C120 -C117 : 109.793649  
H122 -C120 -H121 : 108.086033 H123 -C120 -C117 : 112.552570  
H123 -C120 -H121 : 108.016967 H123 -C120 -H122 : 106.999169  
H124 -C123 -C117 : 110.719772 H125 -C123 -C117 : 111.947872  
H125 -C123 -H124 : 108.231633 H126 -C123 -C117 : 110.635879  
H126 -C123 -H124 : 108.035816 H126 -C123 -H125 : 107.109322

Torsional angles:

C1 -S2 -C6 -C5 :-172.480496

C1 -S2 -C6 -C7 : 8.904530  
C1 -C67 -C70 -C7 : -55.821384  
C1 -C67 -C70 -C71 : 65.146552  
C1 -C67 -C70 -C72 : -177.428358  
S2 -C1 -C67 -C70 : 65.101758  
S2 -C1 -C67 -H79 : -173.916049  
S2 -C1 -C67 -H80 : -58.078563  
S2 -C6 -C5 -C4 : -179.202866  
S2 -C6 -C5 -H10 : 1.030589  
S2 -C6 -C7 -C8 : -179.995419  
S2 -C6 -C7 -C70 : -2.085893  
C3 -C4 -C5 -C6 : -0.722216  
C3 -C4 -C5 -H10 : 179.043175  
C3 -C8 -C7 -C6 : -1.308835  
C3 -C8 -C7 -C70 : -179.314667  
C3 -C13 -C12 -H15 : -1.676205  
C3 -C13 -C12 -C19 : 177.630466  
C4 -C3 -C8 -C7 : 0.145710  
C4 -C3 -C8 -H11 : 179.171689  
C4 -C3 -C13 -C12 : 174.839515  
C4 -C3 -C13 -H14 : -5.253751  
C4 -C5 -C6 -C7 : -0.495588  
C5 -C4 -C3 -C8 : 0.889013  
C5 -C4 -C3 -C13 : -179.850653  
C5 -C6 -C7 -C8 : 1.456040  
C5 -C6 -C7 -C70 : 179.365567  
C6 -S2 -C1 -C67 : -37.465073  
C6 -S2 -C1 -H68 : 86.940638  
C6 -S2 -C1 -H69 : -157.690201  
C6 -C5 -C4 -H9 : 179.884994



C6 -C7 -C8 -H11 : 179.663223  
C6 -C7 -C70 -C67 : 22.279883  
C6 -C7 -C70 -C71 : -99.475544  
C6 -C7 -C70 -C72 : 140.947362  
C7 -C6 -C5 -H10 : 179.737868  
C7 -C8 -C3 -C13 :-179.078418  
C7 -C70 -C67 -H79 :-177.048264  
C7 -C70 -C67 -H80 : 67.109119  
C7 -C70 -C71 -H73 : -61.107342  
C7 -C70 -C71 -H74 : 58.281525  
C7 -C70 -C71 -H75 : 179.181739  
C7 -C70 -C72 -H76 : -55.159486  
C7 -C70 -C72 -H77 : 66.281364  
C7 -C70 -C72 -H78 :-174.740848  
C8 -C3 -C4 -H9 :-179.718814  
C8 -C3 -C13 -C12 : -5.952351  
C8 -C3 -C13 -H14 : 173.954383  
C8 -C7 -C70 -C67 :-159.844496  
C8 -C7 -C70 -C71 : 78.400077  
C8 -C7 -C70 -C72 : -41.177017  
H9 -C4 -C3 -C13 : -0.458480  
H9 -C4 -C5 -H10 : -0.349615  
H11 -C8 -C3 -C13 : -0.052439  
H11 -C8 -C7 -C70 : 1.657392  
C12 -C19 -C18 -C17 :-177.736766  
C12 -C19 -C18 -H23 : 1.397041  
C12 -C19 -C20 -C21 : 177.844464  
C12 -C19 -C20 -H24 : -1.317765  
C13 -C12 -C19 -C18 : -1.722206  
C13 -C12 -C19 -C20 : 179.564712

H14	-C13	-C12	-H15	: 178.420732
H14	-C13	-C12	-C19	: -2.272598
H15	-C12	-C19	-C18	: 177.610593
H15	-C12	-C19	-C20	: -1.102489
C16	-C17	-C18	-C19	: -0.231729
C16	-C17	-C18	-H23	:-179.374273
C16	-C21	-C20	-C19	: 0.190654
C16	-C21	-C20	-H24	: 179.349033
C16	-C27	-C26	-H29	: -2.478728
C16	-C27	-C26	-C33	: 175.467260
C17	-C16	-C21	-C20	: 0.583745
C17	-C16	-C21	-H25	: 179.348208
C17	-C16	-C27	-C26	: 178.666559
C17	-C16	-C27	-H28	: -3.005850
C17	-C18	-C19	-C20	: 0.985966
C18	-C17	-C16	-C21	: -0.564699
C18	-C17	-C16	-C27	: 177.463642
C18	-C19	-C20	-C21	: -0.973625
C18	-C19	-C20	-H24	: 179.864146
C19	-C18	-C17	-H22	: 179.192244
C19	-C20	-C21	-H25	:-178.591789
C20	-C19	-C18	-H23	:-179.880227
C20	-C21	-C16	-C27	:-177.377922
C21	-C16	-C17	-H22	:-179.991029
C21	-C16	-C27	-C26	: -3.432596
C21	-C16	-C27	-H28	: 174.894996
H22	-C17	-C16	-C27	: -1.962689
H22	-C17	-C18	-H23	: 0.049700
H24	-C20	-C21	-H25	: 0.566590
H25	-C21	-C16	-C27	: 1.386541

C26	-C33	-C32	-C31	:-176.720561
C26	-C33	-C32	-H37	: 2.490482
C26	-C33	-C34	-C35	: 176.701310
C26	-C33	-C34	-H38	: -2.213749
C27	-C26	-C33	-C32	: 2.073725
C27	-C26	-C33	-C34	:-175.937570
H28	-C27	-C26	-H29	: 179.259196
H28	-C27	-C26	-C33	: -2.794816
H29	-C26	-C33	-C32	:-179.900304
H29	-C26	-C33	-C34	: 2.088400
C30	-C31	-C32	-C33	: -0.120975
C30	-C31	-C32	-H37	:-179.340603
C30	-C35	-C34	-C33	: 0.436620
C30	-C35	-C34	-H38	: 179.346850
C30	-C41	-C40	-H43	: -1.730384
C30	-C41	-C40	-C47	: 177.091986
C31	-C30	-C35	-C34	: 0.773625
C31	-C30	-C35	-H39	: 179.617947
C31	-C30	-C41	-C40	: 179.973246
C31	-C30	-C41	-H42	: -1.361737
C31	-C32	-C33	-C34	: 1.304756
C32	-C31	-C30	-C35	: -0.931897
C32	-C31	-C30	-C41	: 177.356794
C32	-C33	-C34	-C35	: -1.471910
C32	-C33	-C34	-H38	: 179.613030
C33	-C32	-C31	-H36	: 179.215038
C33	-C34	-C35	-H39	:-178.422073
C34	-C33	-C32	-H37	:-179.484200
C34	-C35	-C30	-C41	:-177.447658
C35	-C30	-C31	-H36	: 179.729266

C35	-C30	-C41	-C40	:	-1.853820
C35	-C30	-C41	-H42	:	176.811197
H36	-C31	-C30	-C41	:	-1.982043
H36	-C31	-C32	-H37	:	-0.004590
H38	-C34	-C35	-H39	:	0.488156
H39	-C35	-C30	-C41	:	1.396665
C40	-C47	-C46	-C45	:	-178.332760
C40	-C47	-C46	-H51	:	1.327448
C40	-C47	-C48	-C49	:	178.245151
C40	-C47	-C48	-H52	:	-1.490234
C41	-C40	-C47	-C46	:	2.717911
C41	-C40	-C47	-C48	:	-176.373761
H42	-C41	-C40	-H43	:	179.660065
H42	-C41	-C40	-C47	:	-1.517566
H43	-C40	-C47	-C46	:	-178.412480
H43	-C40	-C47	-C48	:	2.495848
C44	-C45	-C46	-C47	:	0.148315
C44	-C45	-C46	-H51	:	-179.515859
C44	-C49	-C48	-C47	:	0.142489
C44	-C49	-C48	-H52	:	179.876944
C44	-C55	-C54	-H57	:	-0.645095
C44	-C55	-C54	-C61	:	178.852073
C45	-C44	-C49	-C48	:	0.774690
C45	-C44	-C49	-H53	:	-179.516550
C45	-C44	-C55	-C54	:	-176.857531
C45	-C44	-C55	-H56	:	2.023763
C45	-C46	-C47	-C48	:	0.769914
C46	-C45	-C44	-C49	:	-0.922330
C46	-C45	-C44	-C55	:	178.431152
C46	-C47	-C48	-C49	:	-0.918715

C46	-C47	-C48	-H52	: 179.345900
C47	-C46	-C45	-H50	: 179.611036
C47	-C48	-C49	-H53	:-179.569814
C48	-C47	-C46	-H51	:-179.569878
C48	-C49	-C44	-C55	:-178.547063
C49	-C44	-C45	-H50	: 179.612839
C49	-C44	-C55	-C54	: 2.447654
C49	-C44	-C55	-H56	:-178.671052
H50	-C45	-C44	-C55	: -1.033680
H50	-C45	-C46	-H51	: -0.053138
H52	-C48	-C49	-H53	: 0.164641
H53	-C49	-C44	-C55	: 1.161697
C54	-C61	-C60	-C59	:-179.106022
C54	-C61	-C60	-H64	: 0.542470
C54	-C61	-C62	-C63	: 179.113074
C54	-C61	-C62	-H65	: -0.848635
C55	-C54	-C61	-C60	: 0.778546
C55	-C54	-C61	-C62	:-178.648044
H56	-C55	-C54	-H57	:-179.480986
H56	-C55	-C54	-C61	: 0.016181
H57	-C54	-C61	-C60	:-179.704318
H57	-C54	-C61	-C62	: 0.869093
C58	-C59	-C60	-C61	: 0.032995
C58	-C59	-C60	-H64	:-179.620220
C58	-C63	-C62	-C61	: 0.011054
C58	-C63	-C62	-H65	: 179.972616
C58	-C83	-C82	-H85	: -0.663430
C58	-C83	-C82	-C89	: 179.581323
C59	-C58	-C63	-C62	: 0.351047
C59	-C58	-C63	-H66	: 179.991814

C59	-C58	-C83	-C82	:-179.657743
C59	-C58	-C83	-H84	: 0.017758
C59	-C60	-C61	-C62	: 0.330656
C60	-C59	-C58	-C63	: -0.375350
C60	-C59	-C58	-C83	: 179.180009
C60	-C61	-C62	-C63	: -0.354212
C60	-C61	-C62	-H65	: 179.684079
C61	-C60	-C59	-H81	: 179.728024
C61	-C62	-C63	-H66	:-179.633764
C62	-C61	-C60	-H64	: 179.979148
C62	-C63	-C58	-C83	:-179.176184
C63	-C58	-C59	-H81	: 179.928303
C63	-C58	-C83	-C82	: -0.138073
C63	-C58	-C83	-H84	: 179.537427
H64	-C60	-C59	-H81	: 0.074810
H65	-C62	-C63	-H66	: 0.327799
H66	-C63	-C58	-C83	: 0.464584
C67	-C70	-C71	-H73	: 176.019898
C67	-C70	-C71	-H74	:-64.591235
C67	-C70	-C71	-H75	: 56.308979
C67	-C70	-C72	-H76	: 66.856945
C67	-C70	-C72	-H77	:-171.702205
C67	-C70	-C72	-H78	:-52.724417
H68	-C1	-C67	-C70	:-58.024882
H68	-C1	-C67	-H79	: 62.957311
H68	-C1	-C67	-H80	: 178.794797
H69	-C1	-C67	-C70	:-178.085803
H69	-C1	-C67	-H79	:-57.103610
H69	-C1	-C67	-H80	: 58.733876
C71	-C70	-C67	-H79	:-56.080329

C71	-C70	-C67	-H80	:-171.922946
C71	-C70	-C72	-H76	:-174.772672
C71	-C70	-C72	-H77	:-53.331822
C71	-C70	-C72	-H78	: 65.645966
C72	-C70	-C67	-H79	: 61.344762
C72	-C70	-C67	-H80	:-54.497855
C72	-C70	-C71	-H73	: 60.095042
C72	-C70	-C71	-H74	: 179.483909
C72	-C70	-C71	-H75	:-59.615877
H81	-C59	-C58	-C83	: -0.516338
C82	-C89	-C88	-C87	:-179.856652
C82	-C89	-C88	-H93	: 0.148535
C82	-C89	-C90	-C91	: 179.790151
C82	-C89	-C90	-H94	: -0.149749
C83	-C82	-C89	-C88	: 177.793217
C83	-C82	-C89	-C90	: -2.122043
H84	-C83	-C82	-H85	: 179.674138
H84	-C83	-C82	-C89	: -0.081109
H85	-C82	-C89	-C88	: -1.971825
H85	-C82	-C89	-C90	: 178.112916
C86	-C87	-C88	-C89	: -0.122340
C86	-C87	-C88	-H93	: 179.872455
C86	-C91	-C90	-C89	: 0.247584
C86	-C91	-C90	-H94	:-179.811780
C86	-C97	-C96	-H100	: -0.546134
C86	-C97	-C96	-C103	: 179.810479
C87	-C86	-C91	-C90	: -0.288995
C87	-C86	-C91	-H95	: 179.649313
C87	-C86	-C97	-C96	: 177.072060
C87	-C86	-C97	-H99	: -2.644631

C87 -C88 -C89 -C90 : 0.064504  
C88 -C87 -C86 -C91 : 0.227497  
C88 -C87 -C86 -C97 :-179.789916  
C88 -C89 -C90 -C91 : -0.126911  
C88 -C89 -C90 -H94 : 179.933189  
C89 -C88 -C87 -H92 :-179.909633  
C89 -C90 -C91 -H95 :-179.691439  
C90 -C89 -C88 -H93 :-179.930309  
C90 -C91 -C86 -C97 : 179.729378  
C91 -C86 -C87 -H92 :-179.984496  
C91 -C86 -C97 -C96 : -2.946650  
C91 -C86 -C97 -H99 : 177.336659  
H92 -C87 -C86 -C97 : -0.001910  
H92 -C87 -C88 -H93 : 0.085162  
H94 -C90 -C91 -H95 : 0.249197  
H95 -C91 -C86 -C97 : -0.332314  
C96 -C103 -C102 -C101 : 179.834506  
C96 -C103 -C102 -H108 : -0.222202  
C96 -C103 -C104 -C105 : 179.305830  
C96 -C103 -C104 -H109 : -0.401246  
C97 -C96 -C103 -C102 : 177.917773  
C97 -C96 -C103 -C104 : -2.157510  
H99 -C97 -C96 -H100 : 179.159578  
H99 -C97 -C96 -C103 : -0.483810  
H100 -C96 -C103 -C102 : -1.738149  
H100 -C96 -C103 -C104 : 178.186567  
C100 -C101 -C102 -C103 : 1.153281  
C100 -C101 -C102 -H108 :-178.789299  
C100 -C101 -C117 -C114 : -21.278043  
C100 -C101 -C117 -C120 :-139.960723



C100 -C101 -C117 -C123 : 100.451351  
C100 -C105 -C104 -C103 : 0.543131  
C100 -C105 -C104 -H109 :-179.745125  
C100 -S110 -C111 -H112 : 158.981524  
C100 -S110 -C111 -H113 : -85.628959  
C100 -S110 -C111 -C114 : 38.741320  
C101 -C100 -C105 -C104 : 0.564806  
C101 -C100 -C105 -H110 :-179.745501  
C101 -C100 -S110 -C111 : -10.192601  
C101 -C102 -C103 -C104 : -0.095381  
C101 -C117 -C114 -C111 : 54.811614  
C101 -C117 -C114 -H116 : -68.028602  
C101 -C117 -C114 -H117 : 176.125656  
C101 -C117 -C120 -H121 : 55.526037  
C101 -C117 -C120 -H122 : 175.098609  
C101 -C117 -C120 -H123 : -65.829597  
C101 -C117 -C123 -H124 :-179.272836  
C101 -C117 -C123 -H125 : -58.405054  
C101 -C117 -C123 -H126 : 60.980491  
C102 -C101 -C100 -C105 : -1.357881  
C102 -C101 -C100 -S110 : 179.889215  
C102 -C101 -C117 -C114 : 161.189180  
C102 -C101 -C117 -C120 : 42.506500  
C102 -C101 -C117 -C123 : -77.081426  
C102 -C103 -C104 -C105 : -0.768203  
C102 -C103 -C104 -H109 : 179.524722  
C103 -C102 -C101 -C117 : 178.853428  
C103 -C104 -C105 -H110 :-179.144922  
C104 -C103 -C102 -H108 : 179.847910  
C104 -C105 -C100 -S110 : 179.454594

C105 -C100 -C101 -C117 :-178.939245  
C105 -C100 -S110 -C111 : 170.996338  
H108 -C102 -C101 -C117 : -1.089152  
H109 -C104 -C105 -H110 : 0.566822  
H110 -C105 -C100 -S110 : -0.855713  
S110 -C100 -C101 -C117 : 2.307851  
S110 -C111 -C114 -H116 : 57.655798  
S110 -C111 -C114 -H117 : 173.514444  
S110 -C111 -C114 -C117 : -65.472717  
C111 -C114 -C117 -C120 : 176.331180  
C111 -C114 -C117 -C123 : -66.100167  
H112 -C111 -C114 -H116 : -59.166103  
H112 -C111 -C114 -H117 : 56.692543  
H112 -C111 -C114 -C117 : 177.705382  
H113 -C111 -C114 -H116 :-179.310358  
H113 -C111 -C114 -H117 : -63.451712  
H113 -C111 -C114 -C117 : 57.561127  
C114 -C117 -C120 -H121 : -66.490192  
C114 -C117 -C120 -H122 : 53.082380  
C114 -C117 -C120 -H123 : 172.154173  
C114 -C117 -C123 -H124 : -56.409169  
C114 -C117 -C123 -H125 : 64.458613  
C114 -C117 -C123 -H126 :-176.155843  
H116 -C114 -C117 -C120 : 53.490964  
H116 -C114 -C117 -C123 : 171.059618  
H117 -C114 -C117 -C120 : -62.354778  
H117 -C114 -C117 -C123 : 55.213876  
C120 -C117 -C123 -H124 : 59.640330  
C120 -C117 -C123 -H125 :-179.491887  
C120 -C117 -C123 -H126 : -60.106343

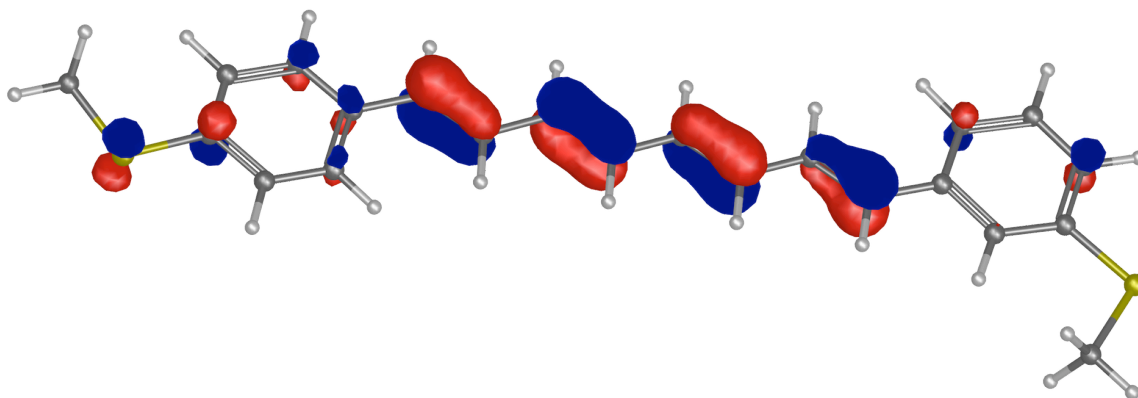
H121 -C120 -C117 -C123 : 175.061613

H122 -C120 -C117 -C123 : -65.365815

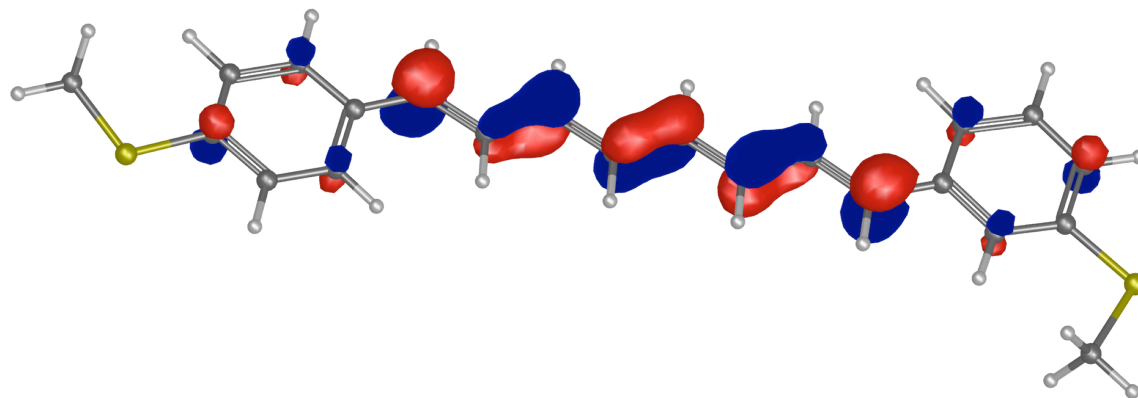
H123 -C120 -C117 -C123 : 53.705978

*1-(3-(methylthio)phenyl)-8-(4-(methylthio)phenyl)-octa-1,3,5,7-tetraene (4):*

HOMO:



LUMO:



Final Geometry:

angstroms

atom	x	y	z
------	---	---	---

C1	-1.2605521880	-0.4962683601	-0.1191088892
C2	-1.9538433705	-1.7182240942	-0.2579329767
C3	-3.3365392714	-1.7607597597	-0.3195444052
C4	-4.0996515448	-0.5807181456	-0.2449482062
C5	-3.4301443195	0.6402080296	-0.1067259292
C6	-2.0393160783	0.6720275557	-0.0461478384
H8	-1.4024684241	-2.6513865681	-0.3192516582
H9	-3.8386263780	-2.7183155838	-0.4274013595
H11	-3.9797141188	1.5724932972	-0.0451705165
H12	-1.5403396498	1.6321307884	0.0611036738
S12	-5.8686673613	-0.7685443637	-0.3353438500
C13	-6.4884814759	0.9396624444	-0.2129311912
H14	-7.5761777657	0.8620698582	-0.2678254642
H15	-6.2143169538	1.3985048215	0.7396240983
H16	-6.1352214210	1.5541502391	-1.0439655102
C16	1.1029942636	-1.3942191944	-0.1025609568
C17	0.1921182013	-0.3895794093	-0.0500588096
H19	0.5732255851	0.6261970978	0.0558515889
H20	0.7664305408	-2.4244307406	-0.2074964697
C20	3.4434997660	-2.1983118598	-0.0793651802
C21	2.5236277311	-1.1953648736	-0.0282084495
H23	2.8756200757	-0.1685724459	0.0758176978
H24	3.0877212716	-3.2239916122	-0.1829814042
C24	5.7734087193	-3.0221304909	-0.0572229441
C25	4.8633706520	-2.0102726502	-0.0068286890
H27	5.2244682489	-0.9864486731	0.0952269604
H28	5.4068985561	-4.0438636448	-0.1586742033
C28	8.0781508215	-3.8833566022	-0.0363976940
C29	7.1976518354	-2.8517538885	0.0137019870
H31	7.5611085395	-1.8301808272	0.1137404017

H32	7.6625386545	-4.8864355673	-0.1338539002
C32	12.3739261651	-3.8635756886	0.1395336134
C33	11.6469478444	-5.0597750945	0.0301587784
C34	10.2619694336	-5.0374521767	-0.0253615249
C35	9.5338067431	-3.8308544196	0.0260545726
C36	10.2778659591	-2.6413128560	0.1353921365
C37	11.6676295188	-2.6527142071	0.1911782669
H39	12.1725632384	-6.0097400616	-0.0118652338
H40	9.7208392961	-5.9764527444	-0.1106858901
H41	9.7666307144	-1.6842097787	0.1765828384
H42	12.1944873684	-1.7090119925	0.2748030860
S42	14.1481946616	-4.0114674541	0.2030153987
C43	14.7225183988	-2.2885504765	0.3393138682
H44	15.8122750001	-2.3455258762	0.3768638010
H45	14.4292893835	-1.6975352611	-0.5311705939
H46	14.3614996069	-1.8170025635	1.2559703467

bond lengths (angstroms):

C1	-C2	: 1.411772	C1	-C6	: 1.405956
C1	-C17	: 1.458219	C2	-C3	: 1.384721
C2	-H8	: 1.085618	C3	-C4	: 1.407268
C3	-H9	: 1.086572	C4	-C5	: 1.399288
C4	-S12	: 1.781254	C5	-C6	: 1.392510
C5	-H11	: 1.083961	C6	-H12	: 1.087326
S12	-C13	: 1.821298	C13	-H14	: 1.091841
C13	-H15	: 1.092275	C13	-H16	: 1.092248
C16	-C17	: 1.357112	C16	-H20	: 1.088863
C16	-C21	: 1.436409	C17	-H19	: 1.090074

C20 -C21 : 1.361868 C20 -H24 : 1.090566  
 C20 -C25 : 1.434104 C21 -H23 : 1.090423  
 C24 -C25 : 1.361824 C24 -H28 : 1.090211  
 C24 -C29 : 1.436150 C25 -H27 : 1.090423  
 C28 -C29 : 1.357200 C28 -H32 : 1.090137  
 C28 -C35 : 1.457941 C29 -H31 : 1.088908  
 C32 -C33 : 1.404049 C32 -C37 : 1.402750  
 C32 -S42 : 1.781553 C33 -C34 : 1.386271  
 C33 -H39 : 1.086495 C34 -C35 : 1.410228  
 C34 -H40 : 1.087117 C35 -C36 : 1.407334  
 C36 -C37 : 1.390929 C36 -H41 : 1.085866  
 C37 -H42 : 1.084042 S42 -C43 : 1.821227  
 C43 -H44 : 1.091891 C43 -H45 : 1.092257  
 C43 -H46 : 1.092223

bond angles:

C6 -C1 -C2 : 116.893257 C17 -C1 -C2 : 123.861918  
 C17 -C1 -C6 : 119.244814 C3 -C2 -C1 : 121.421060  
 H8 -C2 -C1 : 120.009053 H8 -C2 -C3 : 118.569882  
 C4 -C3 -C2 : 120.887593 H9 -C3 -C2 : 119.531042  
 H9 -C3 -C4 : 119.581359 C5 -C4 -C3 : 118.517792  
 S12 -C4 -C3 : 116.578863 S12 -C4 -C5 : 124.903341  
 C6 -C5 -C4 : 120.140352 H11 -C5 -C4 : 120.895293  
 H11 -C5 -C6 : 118.964355 C5 -C6 -C1 : 122.139939  
 H12 -C6 -C1 : 118.990601 H12 -C6 -C5 : 118.869460  
 C13 -S12 -C4 : 103.630941 H14 -C13 -S12 : 105.604197  
 H15 -C13 -S12 : 111.542401 H15 -C13 -H14 : 108.889818  
 H16 -C13 -S12 : 111.497010 H16 -C13 -H14 : 108.900451  
 H16 -C13 -H15 : 110.243445 H20 -C16 -C17 : 119.779904

C21 -C16 -C17 : 124.009494 C21 -C16 -H20 : 116.210600  
 C16 -C17 -C1 : 127.780628 H19 -C17 -C1 : 114.901757  
 H19 -C17 -C16 : 117.317608 H24 -C20 -C21 : 118.414572  
 C25 -C20 -C21 : 124.769911 C25 -C20 -H24 : 116.815517  
 C20 -C21 -C16 : 124.342122 H23 -C21 -C16 : 117.036396  
 H23 -C21 -C20 : 118.621481 H28 -C24 -C25 : 118.368204  
 C29 -C24 -C25 : 124.941111 C29 -C24 -H28 : 116.690682  
 C24 -C25 -C20 : 124.216492 H27 -C25 -C20 : 117.110778  
 H27 -C25 -C24 : 118.672729 H32 -C28 -C29 : 117.087870  
 C35 -C28 -C29 : 128.227929 C35 -C28 -H32 : 114.684105  
 C28 -C29 -C24 : 123.462152 H31 -C29 -C24 : 116.541699  
 H31 -C29 -C28 : 119.996117 C37 -C32 -C33 : 118.527801  
 S42 -C32 -C33 : 116.596697 S42 -C32 -C37 : 124.875497  
 C34 -C33 -C32 : 120.443670 H39 -C33 -C32 : 119.830439  
 H39 -C33 -C34 : 119.725883 C35 -C34 -C33 : 121.882580  
 H40 -C34 -C33 : 119.113197 H40 -C34 -C35 : 119.004220  
 C34 -C35 -C28 : 118.892103 C36 -C35 -C28 : 124.169229  
 C36 -C35 -C34 : 116.938664 C37 -C36 -C35 : 121.630939  
 H41 -C36 -C35 : 119.936837 H41 -C36 -C37 : 118.432152  
 C36 -C37 -C32 : 120.576313 H42 -C37 -C32 : 120.636124  
 H42 -C37 -C36 : 118.787557 C43 -S42 -C32 : 103.780057  
 H44 -C43 -S42 : 105.541924 H45 -C43 -S42 : 111.566703  
 H45 -C43 -H44 : 108.879489 H46 -C43 -S42 : 111.530837  
 H46 -C43 -H44 : 108.878101 H46 -C43 -H45 : 110.273983

torsional angles:

C1 -C2 -C3 -C4 : -0.019270  
 C1 -C2 -C3 -H9 : 179.952208  
 C1 -C6 -C5 -C4 : -0.019994

C1 -C6 -C5 -H11 : 179.978892  
C1 -C17 -C16 -H20 : -0.057732  
C1 -C17 -C16 -C21 : 179.922182  
C2 -C1 -C6 -C5 : -0.002422  
C2 -C1 -C6 -H12 : 179.995642  
C2 -C1 -C17 -C16 : -0.057154  
C2 -C1 -C17 -H19 : 179.913073  
C2 -C3 -C4 -C5 : -0.003602  
C2 -C3 -C4 -S12 :-179.983260  
C3 -C2 -C1 -C6 : 0.021964  
C3 -C2 -C1 -C17 :-179.941003  
C3 -C4 -C5 -C6 : 0.022787  
C3 -C4 -C5 -H11 :-179.976078  
C3 -C4 -S12 -C13 :-179.816063  
C4 -C3 -C2 -H8 :-179.990871  
C4 -C5 -C6 -H12 : 179.981939  
C4 -S12 -C13 -H14 : 179.858723  
C4 -S12 -C13 -H15 : -62.000858  
C4 -S12 -C13 -H16 : 61.729518  
C5 -C4 -C3 -H9 :-179.975065  
C5 -C4 -S12 -C13 : 0.205732  
C5 -C6 -C1 -C17 : 179.962334  
C6 -C1 -C2 -H8 : 179.993163  
C6 -C1 -C17 -C16 : 179.980699  
C6 -C1 -C17 -H19 : -0.049074  
C6 -C5 -C4 -S12 :-179.999396  
H8 -C2 -C1 -C17 : 0.030196  
H8 -C2 -C3 -H9 : -0.019394  
H9 -C3 -C4 -S12 : 0.045277  
H11 -C5 -C4 -S12 : 0.001740



H11	-C5	-C6	-H12	:	-0.019174
H12	-C6	-C1	-C17	:	-0.039602
C16	-C21	-C20	-H24	:	-0.037579
C16	-C21	-C20	-C25	:	179.959503
C17	-C16	-C21	-C20	:	179.957591
C17	-C16	-C21	-H23	:	-0.052278
H19	-C17	-C16	-H20	:	179.972663
H19	-C17	-C16	-C21	:	-0.047424
H20	-C16	-C21	-C20	:	-0.061841
H20	-C16	-C21	-H23	:	179.928290
C20	-C25	-C24	-H28	:	-0.031995
C20	-C25	-C24	-C29	:	179.986715
C21	-C20	-C25	-C24	:	179.902312
C21	-C20	-C25	-H27	:	-0.091657
H23	-C21	-C20	-H24	:	179.972435
H23	-C21	-C20	-C25	:	-0.030483
H24	-C20	-C25	-C24	:	-0.100564
H24	-C20	-C25	-H27	:	179.905467
C24	-C29	-C28	-H32	:	-0.118673
C24	-C29	-C28	-C35	:	-179.999315
C25	-C24	-C29	-C28	:	179.841297
C25	-C24	-C29	-H31	:	-0.093279
H27	-C25	-C24	-H28	:	179.961887
H27	-C25	-C24	-C29	:	-0.019404
H28	-C24	-C29	-C28	:	-0.140276
H28	-C24	-C29	-H31	:	179.925147
C28	-C35	-C34	-C33	:	-179.954093
C28	-C35	-C34	-H40	:	0.027746
C28	-C35	-C36	-C37	:	179.987583
C28	-C35	-C36	-H41	:	-0.111035

C29	-C28	-C35	-C34	: 179.111485
C29	-C28	-C35	-C36	: -0.914905
H31	-C29	-C28	-H32	: 179.813747
H31	-C29	-C28	-C35	: -0.066896
H32	-C28	-C35	-C34	: -0.771563
H32	-C28	-C35	-C36	: 179.202046
C32	-C33	-C34	-C35	: -0.059216
C32	-C33	-C34	-H40	: 179.958964
C32	-C37	-C36	-C35	: -0.004766
C32	-C37	-C36	-H41	: -179.907584
C32	-S42	-C43	-H44	: -179.801580
C32	-S42	-C43	-H45	: -61.697886
C32	-S42	-C43	-H46	: 62.115255
C33	-C32	-C37	-C36	: 0.018070
C33	-C32	-C37	-H42	: -179.953984
C33	-C32	-S42	-C43	: 179.944840
C33	-C34	-C35	-C36	: 0.070399
C34	-C33	-C32	-C37	: 0.013291
C34	-C33	-C32	-S42	: 179.989975
C34	-C35	-C36	-C37	: -0.038335
C34	-C35	-C36	-H41	: 179.863047
C35	-C34	-C33	-H39	: 179.974618
C35	-C36	-C37	-H42	: 179.967798
C36	-C35	-C34	-H40	: -179.947761
C36	-C37	-C32	-S42	: -179.956517
C37	-C32	-C33	-H39	: 179.979421
C37	-C32	-S42	-C43	: -0.080130
H39	-C33	-C32	-S42	: -0.043894
H39	-C33	-C34	-H40	: -0.007202
H41	-C36	-C37	-H42	: 0.064980

H42 -C37 -C32 -S42 : 0.071428

Nuclear repulsion energy: 1764.727438154 hartrees

Total energy: -1647.96862312329 hartrees

HOMO energy: -0.17263 hartrees

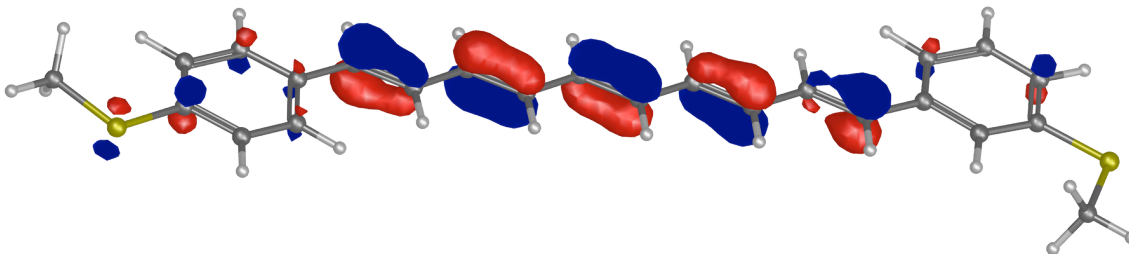
LUMO energy: -0.07160 hartrees

Orbital energies (hartrees):

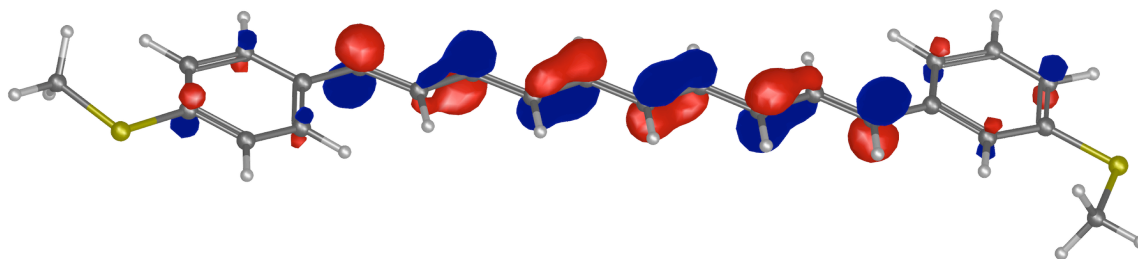
-88.88664 -88.88662 -10.22527 -10.22501 -10.22118 -10.22107  
-10.19802 -10.19782 -10.19596 -10.19474 -10.19449 -10.19425  
-10.19373 -10.19341 -10.19296 -10.19273 -10.19207 -10.19169  
-10.19104 -10.19085 -10.19036 -10.19017 -10.18991 -10.18980  
-7.94756 -7.94755 -5.91283 -5.91280 -5.90869 -5.90867  
-5.90248 -5.90247 -0.86617 -0.86596 -0.82532 -0.81635  
-0.80658 -0.79180 -0.77116 -0.75242 -0.74954 -0.74811  
-0.72855 -0.70079 -0.66686 -0.65277 -0.62254 -0.61230  
-0.61121 -0.59016 -0.57428 -0.55961 -0.55540 -0.54615  
-0.50806 -0.50232 -0.47652 -0.47483 -0.45956 -0.45770  
-0.45357 -0.44797 -0.43818 -0.43805 -0.43702 -0.43520  
-0.42319 -0.41986 -0.41123 -0.40515 -0.39266 -0.38400  
-0.37977 -0.37941 -0.37565 -0.36327 -0.35838 -0.35448  
-0.34608 -0.34527 -0.33997 -0.33958 -0.32650 -0.32139  
-0.32112 -0.30656 -0.28375 -0.25593 -0.25513 -0.25235  
-0.22517 -0.20365 -0.17263 -0.07160 -0.02598 -0.00359  
-0.00300 0.01629 0.03479 0.03483 0.05453 0.07291  
0.07298

*1-(3-(methylthio)phenyl)-10-(4-(methylthio)phenyl)-deca-1,3,5,7,9-pentaene (5)*:

HOMO:



LUMO:



Final Geometry:

	angstroms		
atom	x	y	z
C1	-1.2685483096	-0.5232818274	-0.1741804875
C2	-1.9792472266	-1.7432042485	-0.1844324071
C3	-3.3634919748	-1.7718377283	-0.2091844483
C4	-4.1108090872	-0.5794189701	-0.2251672053
C5	-3.4239587808	0.6397315968	-0.2157256438
C6	-2.0318917221	0.6576095905	-0.1907349026
H8	-1.4405272218	-2.6857048685	-0.1723392490
H9	-3.8792507160	-2.7281728092	-0.2159774678
H11	-3.9609761890	1.5812642582	-0.2275377093
H12	-1.5192734494	1.6165106158	-0.1836371183
S12	-5.8835248777	-0.7502446407	-0.2563815512

C13	-6.4808669862	0.9703004921	-0.2670290909
H14	-7.5705258724	0.9025396510	-0.2832936138
H15	-6.1732570339	1.5069041237	0.6332445861
H16	-6.1465420406	1.5052968932	-1.1586961432
C16	1.0868017945	-1.4448560680	-0.1272563633
C17	0.1859789246	-0.4294491090	-0.1469668459
H19	0.5794399871	0.5871869929	-0.1415554208
H20	0.7397658423	-2.4769632963	-0.1316328835
C20	3.4247501182	-2.2612294771	-0.0765768600
C21	2.5092387323	-1.2521600868	-0.0989909199
H23	2.8687413565	-0.2226526971	-0.0943353152
H24	3.0643009576	-3.2904989360	-0.0808128156
C24	5.7571122792	-3.0837785610	-0.0206874179
C25	4.8443015169	-2.0711175217	-0.0459816170
H27	5.2069098775	-1.0427175989	-0.0416767966
H28	5.3913840367	-4.1112041210	-0.0245118238
C28	8.0799698726	-3.9230528956	0.0410882561
C29	7.1778311343	-2.9023551393	0.0124775555
H31	7.5481279425	-1.8766666767	0.0159794904
H32	7.7037093103	-4.9463791481	0.0381457785
C32	10.3764267035	-4.8018392175	0.1097661505
C33	9.5058659047	-3.7606539435	0.0770503314
H35	9.8798085368	-2.7379206284	0.0793874495
H36	9.9497691694	-5.8050633092	0.1093730483
C36	14.6741269991	-4.8154937179	0.2343456067
C37	13.9331904083	-6.0081172814	0.2419424167
C38	12.5479587435	-5.9749037572	0.1999921573
C39	11.8330545021	-4.7602023439	0.1499237255
C40	12.5913207418	-3.5743975337	0.1421839950
C41	13.9814010569	-3.5967948788	0.1833030027

H43	14.4481426442	-6.9640684011	0.2808573413
H44	11.9960805730	-6.9115444231	0.2066884962
H45	12.0913223329	-2.6117557189	0.1014487585
H46	14.5191223146	-2.6555017915	0.1745415410
S46	16.4471948646	-4.9771965985	0.2918107100
C47	17.0407481622	-3.2556403314	0.2671630450
H48	18.1301269227	-3.3212820239	0.3027989976
H49	16.7474293982	-2.7431686699	-0.6517371552
H50	16.6915822130	-2.6983545951	1.1392099966

bond lengths (angstroms):

C1	-C2	: 1.411881	C1	-C6	: 1.406226
C1	-C17	: 1.457805	C2	-C3	: 1.384762
C2	-H8	: 1.085667	C3	-C4	: 1.407338
C3	-H9	: 1.086568	C4	-C5	: 1.399350
C4	-S12	: 1.781201	C5	-C6	: 1.392406
C5	-H11	: 1.083979	C6	-H12	: 1.087345
S12	-C13	: 1.821320	C13	-H14	: 1.091885
C13	-H15	: 1.092273	C13	-H16	: 1.092275
C16	-C17	: 1.357542	C16	-H20	: 1.088898
C16	-C21	: 1.435708	C17	-H19	: 1.090133
C20	-C21	: 1.362676	C20	-H24	: 1.090567
C20	-C25	: 1.432552	C21	-H23	: 1.090481
C24	-C25	: 1.363578	C24	-H28	: 1.090585
C24	-C29	: 1.432640	C25	-H27	: 1.090463
C28	-C29	: 1.362533	C28	-H32	: 1.090311
C28	-C33	: 1.435565	C29	-H31	: 1.090490
C32	-C33	: 1.357576	C32	-H36	: 1.090181

C32 -C39 : 1.457776 C33 -H35 : 1.088955  
 C36 -C37 : 1.404064 C36 -C41 : 1.402748  
 C36 -S46 : 1.781353 C37 -C38 : 1.386265  
 C37 -H43 : 1.086523 C38 -C39 : 1.410353  
 C38 -H44 : 1.087157 C39 -C40 : 1.407537  
 C40 -C41 : 1.390869 C40 -H45 : 1.085512  
 C41 -H46 : 1.084091 S46 -C47 : 1.821172  
 C47 -H48 : 1.091936 C47 -H49 : 1.092264  
 C47 -H50 : 1.092223

bond angles:

C6 -C1 -C2 : 116.888481 C17 -C1 -C2 : 123.916812  
 C17 -C1 -C6 : 119.194694 C3 -C2 -C1 : 121.411311  
 H8 -C2 -C1 : 120.015947 H8 -C2 -C3 : 118.572734  
 C4 -C3 -C2 : 120.897205 H9 -C3 -C2 : 119.524871  
 H9 -C3 -C4 : 119.577921 C5 -C4 -C3 : 118.519710  
 S12 -C4 -C3 : 116.578604 S12 -C4 -C5 : 124.901686  
 C6 -C5 -C4 : 120.133933 H11 -C5 -C4 : 120.897117  
 H11 -C5 -C6 : 118.968950 C5 -C6 -C1 : 122.149356  
 H12 -C6 -C1 : 118.984457 H12 -C6 -C5 : 118.866186  
 C13 -S12 -C4 : 103.645498 H14 -C13 -S12 : 105.590831  
 H15 -C13 -S12 : 111.524984 H15 -C13 -H14 : 108.893780  
 H16 -C13 -S12 : 111.535979 H16 -C13 -H14 : 108.886445  
 H16 -C13 -H15 : 110.243985 H20 -C16 -C17 : 119.829722  
 C21 -C16 -C17 : 123.871368 C21 -C16 -H20 : 116.298887  
 C16 -C17 -C1 : 127.894108 H19 -C17 -C1 : 114.849542  
 H19 -C17 -C16 : 117.256339 H24 -C20 -C21 : 118.474271  
 C25 -C20 -C21 : 124.599124 C25 -C20 -H24 : 116.926568  
 C20 -C21 -C16 : 124.511643 H23 -C21 -C16 : 116.963454

H23 -C21 -C20 : 118.524868 H28 -C24 -C25 : 118.364825  
 C29 -C24 -C25 : 124.766705 C29 -C24 -H28 : 116.868430  
 C24 -C25 -C20 : 124.415362 H27 -C25 -C20 : 117.048794  
 H27 -C25 -C24 : 118.535799 H32 -C28 -C29 : 118.330023  
 C33 -C28 -C29 : 124.989506 C33 -C28 -H32 : 116.680420  
 C28 -C29 -C24 : 124.209170 H31 -C29 -C24 : 117.124690  
 H31 -C29 -C28 : 118.666092 H36 -C32 -C33 : 117.051720  
 C39 -C32 -C33 : 128.280687 C39 -C32 -H36 : 114.667344  
 C32 -C33 -C28 : 123.420874 H35 -C33 -C28 : 116.575908  
 H35 -C33 -C32 : 120.003098 C41 -C36 -C37 : 118.525948  
 S46 -C36 -C37 : 116.613787 S46 -C36 -C41 : 124.860262  
 C38 -C37 -C36 : 120.450955 H43 -C37 -C36 : 119.829470  
 H43 -C37 -C38 : 119.719575 C39 -C38 -C37 : 121.885900  
 H44 -C38 -C37 : 119.106059 H44 -C38 -C39 : 119.008021  
 C38 -C39 -C32 : 118.873444 C40 -C39 -C32 : 124.208439  
 C40 -C39 -C38 : 116.918117 C41 -C40 -C39 : 121.646985  
 H45 -C40 -C39 : 119.945422 H45 -C40 -C41 : 118.407494  
 C40 -C41 -C36 : 120.572027 H46 -C41 -C36 : 120.643956  
 H46 -C41 -C40 : 118.784006 C47 -S46 -C36 : 103.777716  
 H48 -C47 -S46 : 105.538537 H49 -C47 -S46 : 111.554266  
 H49 -C47 -H48 : 108.879179 H50 -C47 -S46 : 111.550758  
 H50 -C47 -H48 : 108.877805 H50 -C47 -H49 : 110.270375

torsional angles:

C1 -C2 -C3 -C4 : 0.007500  
 C1 -C2 -C3 -H9 : -179.969577  
 C1 -C6 -C5 -C4 : -0.000414  
 C1 -C6 -C5 -H11 : 179.994003  
 C1 -C17 -C16 -H20 : 0.034584



C1	-C17	-C16	-C21	:-179.907696
C2	-C1	-C6	-C5	: 0.017837
C2	-C1	-C6	-H12	:-179.992710
C2	-C1	-C17	-C16	: -0.003863
C2	-C1	-C17	-H19	:-179.964052
C2	-C3	-C4	-C5	: 0.010565
C2	-C3	-C4	-S12	:-179.993057
C3	-C2	-C1	-C6	: -0.021285
C3	-C2	-C1	-C17	: 179.936793
C3	-C4	-C5	-C6	: -0.014008
C3	-C4	-C5	-H11	: 179.991684
C3	-C4	-S12	-C13	: 179.875659
C4	-C3	-C2	-H8	: 179.976460
C4	-C5	-C6	-H12	:-179.989879
C4	-S12	-C13	-H14	:-179.840667
C4	-S12	-C13	-H15	: -61.712667
C4	-S12	-C13	-H16	: 62.034318
C5	-C4	-C3	-H9	: 179.987630
C5	-C4	-S12	-C13	: -0.128222
C5	-C6	-C1	-C17	:-179.942313
C6	-C1	-C2	-H8	:-179.989803
C6	-C1	-C17	-C16	: 179.953307
C6	-C1	-C17	-H19	: -0.006882
C6	-C5	-C4	-S12	: 179.989942
H8	-C2	-C1	-C17	: -0.031725
H8	-C2	-C3	-H9	: -0.000617
H9	-C3	-C4	-S12	: -0.015992
H11	-C5	-C4	-S12	: -0.004366
H11	-C5	-C6	-H12	: 0.004538
H12	-C6	-C1	-C17	: 0.047141

C16	-C21	-C20	-H24	:	0.043409
C16	-C21	-C20	-C25	:	-179.884434
C17	-C16	-C21	-C20	:	179.876611
C17	-C16	-C21	-H23	:	-0.054652
H19	-C17	-C16	-H20	:	179.993947
H19	-C17	-C16	-C21	:	0.051667
H20	-C16	-C21	-C20	:	-0.067535
H20	-C16	-C21	-H23	:	-179.998798
C20	-C25	-C24	-H28	:	0.047017
C20	-C25	-C24	-C29	:	-179.878284
C21	-C20	-C25	-C24	:	179.850764
C21	-C20	-C25	-H27	:	-0.070070
H23	-C21	-C20	-H24	:	179.973680
H23	-C21	-C20	-C25	:	0.045837
H24	-C20	-C25	-C24	:	-0.078095
H24	-C20	-C25	-H27	:	-179.998929
C24	-C29	-C28	-H32	:	0.038357
C24	-C29	-C28	-C33	:	-179.876036
C25	-C24	-C29	-C28	:	179.819944
C25	-C24	-C29	-H31	:	-0.099669
H27	-C25	-C24	-H28	:	179.966761
H27	-C25	-C24	-C29	:	0.041460
H28	-C24	-C29	-C28	:	-0.106370
H28	-C24	-C29	-H31	:	179.974017
C28	-C33	-C32	-H36	:	-0.080228
C28	-C33	-C32	-C39	:	-179.887491
C29	-C28	-C33	-C32	:	179.756688
C29	-C28	-C33	-H35	:	-0.116626
H31	-C29	-C28	-H32	:	179.956817
H31	-C29	-C28	-C33	:	0.042424

H32	-C28	-C33	-C32	: -0.158978
H32	-C28	-C33	-H35	: 179.967708
C32	-C39	-C38	-C37	:-179.904109
C32	-C39	-C38	-H44	: 0.043578
C32	-C39	-C40	-C41	: 179.938720
C32	-C39	-C40	-H45	: -0.177299
C33	-C32	-C39	-C38	: 179.060366
C33	-C32	-C39	-C40	: -0.941122
H35	-C33	-C32	-H36	: 179.788940
H35	-C33	-C32	-C39	: -0.018324
H36	-C32	-C39	-C38	: -0.750747
H36	-C32	-C39	-C40	: 179.247765
C36	-C37	-C38	-C39	: -0.062086
C36	-C37	-C38	-H44	: 179.990277
C36	-C41	-C40	-C39	: -0.006753
C36	-C41	-C40	-H45	:-179.892460
C36	-S46	-C47	-H48	: 179.936747
C36	-S46	-C47	-H49	: -61.968495
C36	-S46	-C47	-H50	: 61.845478
C37	-C36	-C41	-C40	: 0.044662
C37	-C36	-C41	-H46	:-179.916491
C37	-C36	-S46	-C47	:-179.978756
C37	-C38	-C39	-C40	: 0.097271
C38	-C37	-C36	-C41	: -0.010908
C38	-C37	-C36	-S46	: 179.970810
C38	-C39	-C40	-C41	: -0.062742
C38	-C39	-C40	-H45	: 179.821239
C39	-C38	-C37	-H43	: 179.943677
C39	-C40	-C41	-H46	: 179.955114
C40	-C39	-C38	-H44	:-179.955042

C40 -C41 -C36 -S46 :-179.935418  
C41 -C36 -C37 -H43 : 179.983323  
C41 -C36 -S46 -C47 : 0.001668  
H43 -C37 -C36 -S46 : -0.034960  
H43 -C37 -C38 -H44 : -0.003960  
H45 -C40 -C41 -H46 : 0.069407  
H46 -C41 -C36 -S46 : 0.103429

Nuclear repulsion energy: 1926.234326193 hartrees

Total energy: -1725.37955583703 hartrees

HOMO energy: -0.16991 hartrees

LUMO energy: -0.07610 hartrees

Orbital energies (hartrees):

-88.88692 -88.88690 -10.22570 -10.22547 -10.22135 -10.22125  
-10.19836 -10.19823 -10.19624 -10.19509 -10.19478 -10.19444  
-10.19401 -10.19379 -10.19335 -10.19308 -10.19260 -10.19226  
-10.19139 -10.19122 -10.19088 -10.19062 -10.19036 -10.19021  
-10.19009 -10.18994 -7.94785 -7.94783 -5.91311 -5.91308  
-5.90897 -5.90895 -5.90277 -5.90275 -0.86647 -0.86629  
-0.82666 -0.81906 -0.81048 -0.79944 -0.78284 -0.76403  
-0.75067 -0.74976 -0.74469 -0.72404 -0.69844 -0.66682  
-0.65437 -0.62594 -0.61470 -0.61160 -0.59506 -0.57878  
-0.56292 -0.56148 -0.54998 -0.54567 -0.50899 -0.50119  
-0.48304 -0.47122 -0.46694 -0.45680 -0.45507 -0.45203  
-0.44373 -0.43838 -0.43825 -0.43812 -0.42736 -0.42209  
-0.41913 -0.41268 -0.39867 -0.39735 -0.38070 -0.37998

-0.37979	-0.37962	-0.36778	-0.35993	-0.35684	-0.35226
-0.34807	-0.34559	-0.34021	-0.34000	-0.33304	-0.32165
-0.32138	-0.31525	-0.29654	-0.27289	-0.25563	-0.25525
-0.24411	-0.22058	-0.19992	-0.16991	-0.07610	-0.03471
-0.00442	-0.00349	0.00485	0.03458	0.03461	0.03961
0.07179	0.07269				

## C6. References

---

1. Meisner, J. S.; Sedbrook, D.; Krikorian, M.; Chen, J.; Carnes, M.; Steigerwald, M. L.; Murray, C. B.; Nuckolls, C. *Chem. Sci.*, **2012**, *3*, 1007–1014.
2. Garner, L. E.; Park, J.; Dyar, S. M.; Chworos, A.; Sumner, J. J.; Bazan, G. C. *J. Am. Chem. Soc.*, **2010**, *132*, 10042–10052.
3. Bartholomew, G. P.; Rumi, M.; Pond, S. J. K.; Perry, J. W.; Tretiak, S.; Bazan, G. C. *J. Am. Chem. Soc.*, **2004**, *126*, 11529–11542.
4. Park, Y. S.; Widawsky, J. R.; Kamenetska, M.; Steigerwald, M. L.; Hybertsen, M. S.; Nuckolls, C.; Venkataraman, L. *J. Am. Chem. Soc.*, **2009**, *131*, 10820–10821.
5. Uddin, M. J.; Rao, P. N. P.; Knaus, E. E. *Bioorg. Med. Chem.*, **2004**, *12*, 5929–5940.
6. (a) Geerts, Y.; Klaerner, G.; Muellen, K. in *Electronic materials: The Oligomeric Approach*, Ed. Muellen, K.; Wegner, G., Wiley-VHC, New York, **1998**, p. 74-75 and 414-424; and references therein; (b) Meier, H.; Stalmach, U.; Kolshorn, H. *Acta Polym.*, **1997**, *48*, 379–384.